Bioconjugate Chemistry

JANUARY/FEBRUARY 1991
Volume 2, Number 1

© Copyright 1991 by the American Chemical Society

REVIEW

Sequence-Selective DNA Recognition by Synthetic Ligands

Peter E. Nielsen

Research Center for Medical Biotechnology, Department of Biochemistry B, The Panum Institute, Blegdamsvej 3c, DK-2200 Copenhagen N, Denmark. Received December 13, 1990

Table of Contents

1. Introduction
2. Protein–DNA Recognition
3. Drug–DNA Recognition
4. Minor-Groove Interaction
   4.1 Lexitropsins
   4.2 Oligodistamycins
   4.3 Intercalator–Peptide Conjugates
5. Major-Groove Recognition
   5.1 Peptides
   5.2 Triple Helix
6. DNA-Modifying Ligands
7. Future Prospects

1. INTRODUCTION

For more than a decade it has been a dream and a goal for organic chemists interested in DNA recognition to design reagents that bind to DNA selectively at desired sequences. Such reagents eventually equipped with a chemical or photochemical tag capable of modifying or cleaving DNA at the site of binding should have great prospects as "synthetic restriction enzymes" and not least as gene-selective drugs.

Giant steps toward this goal are being taken these years and reaching it within the not so distant future does not appear as wishful thinking anymore, but is rapidly approaching reality.

In the present paper I shall briefly review the principles exploited by nature for the sequence-selective recognition of DNA by proteins (mostly involved in gene regulation) and by drugs. Next I describe how organic chemists have followed the paths devised by nature to construct synthetic DNA-sequence-selective ligands. Finally I shall try to foresee and suggest new approaches to reach the ultimate goal, e.g., the ability to construct ligands designed to bind specifically to any chosen DNA sequence (up to ~20 bp).

2. PROTEIN–DNA RECOGNITION

The DNA double helix—and I shall limit the discussion to the B-form, although similar arguments apply to other forms such as A or Z—presents three areas of recognition, the phosphate backbone and the two grooves (major and minor), and all three features are exploited by nature in protein–DNA recognition (see refs 1–6 for recent reviews on DNA structure and protein–DNA interaction). The most detailed sequence information is available on the "floor" of the major groove. Four recognition sites are present in the major groove of AT base pairs (Figure 1). These are the adenine-N7 (hydrogen acceptor), the adenine amino group (N6) (hydrogen donor), the thymine-O4 (hydrogen acceptor), and the thymine methyl group (van der Waal interaction). Similarly, the recognition sites available at GC base pairs are two hydrogen acceptors (guanine-N7 and guanine O6) and one hydrogen donor (the cytosine amino group at C4). Thus the DNA sequence can be unambigously read from the major groove as a "two-dimensional grid" of hydrogen-donor and -acceptor and van der Waals contact sites (Figure 2). Especially, it should be noticed that ApT versus TpA (and GpC versus CpG) base pairs are easily distinguishable. Since the floor of the groove is not planer, the corresponding sites of the DNA binding ligand furthermore have to be positioned correctly in space in much the same way as the key–lock principle of the substrate–enzyme recognition.

Considerably less sequence information is present in the DNA helix when read from the minor groove. The GC base pair presents two hydrogen-acceptor (guanine-N3 and cytosine-O2) and one hydrogen-donor site (guanine-C2–NH_2) while only two hydrogen-acceptor sites (adenine-N3 and thymine-O2) are available at AT base pairs. Distinguishing GpC from CpG and especially TpA from ApT sites is furthermore much more difficult from the minor groove compared to the major groove (cf. Figure 2). Indeed, efficient discrimination between AT and TA base pairs may not be possible since the recognition in both

1043-1802/91/2902-0001$02.50/0 © 1991 American Chemical Society

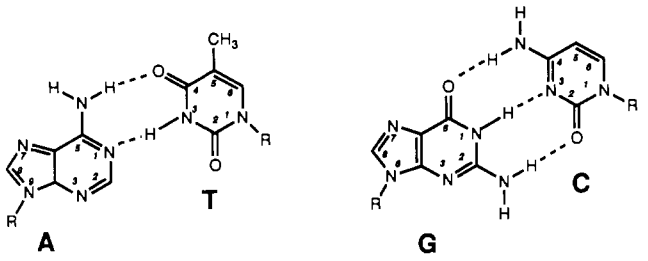


Figure 1. Chemical structures of GC and AT base pairs.

cases is a hydrogen-acceptor acceptor site quite symmetrically positioned in the groove.

How much sequence information is available in the phosphate backbone in terms of interphosphate distances (groove widths), deoxyribose conformation, and electronegative potential and to what extent this is exploited by nature is still not clear. There is no doubt, however, that the DNA conformation in terms of the above parameters as well as the twist, roll, etc. and angles of the base pairs is strongly influenced by the DNA base sequence (*7–10*). Likewise, the biological function of the DNA is also to some degree governed by the DNA conformation (*11–13*). Furthermore, the electrostatic potential of the DNA grooves is strongly dependent on the DNA conformation, in particular the groove width. Specifically, it has been calculated that the deepest electronegative potential is in the minor groove of AT sequences (*14*). The electronegative potential of DNA most likely also serves as a "biological-recognition parameter".

The majority of the sequence-selective DNA-binding proteins studied so far recognize the DNA from the major groove (*3, 5*) and four types of structural oligopeptide motifs (the helix–turn–helix, the Zn-fingers, the Leu-zipper, and the antiparallel β-sheets) are primarily responsible for the DNA recognition. Of these only members of the helix–turn–helix and β-sheet groups have been studied at atomic resolution and the results show that the recognition exploits hydrogen bonding, hydrophobic interaction, and ionic interactions. The recognition is in other words based on a three-dimensional grid more than on a "digital readout" of the bases by the protein. Thus a direct base pair–amino acid residue(s) code for recognition does not seem to exist, although certain "base pair–amino acid rules" can be visualized at least in the case of lac repressor (*15*).

The amino acid residues which are determinant for DNA-sequence recognition by the "helix–turn–helix proteins" reside in the α_3-helix of this motif and are found on the side of the helix facing the floor of the major groove. The second helix of the motif together with a third α-helix helps position the α_3-helix in the groove and interact with the backside of the α_3-helix, which is very lipophilic. Although X-ray structures are not yet available for Zn-fingers and Leu-zippers, it is almost certain that DNA recognition by Leu-zipper proteins is also mediated by α-helices. In this case two helices—turning away from each other and held together by a Leu-zipper in the middle—are placed in the DNA major groove in a scissorlike grip (*16*). An α-helix motif has also been implicated in the DNA recognition by the glucocorticoid-type Zn-fingers (*5*).

Recently it has been found that some prokaryotic repressors (Met and Arc repressors) recognize DNA by way of two antiparallel β-strands positioned in the DNA major groove (*17, 18*).

Recognition of DNA via the minor groove has been suggested for a few proteins of which IHF (integration host factor) binds sequence specifically to DNA (*19*). The mechanism of this recognition is still not known in detail.

An X-ray crystallographic study of the Trp–repressor–DNA (*20*) complex indicated that in this case the recognition was predominantly due to contacts with the DNA backbone and thus determined by the conformation of the DNA. It appears, however, that the DNA used in this study was not the optimal operator sequence (*21*). Thus an example where the DNA conformation is determinant for protein recognition is still lacking.

3. DRUG–DNA RECOGNITION

Several drugs bind to DNA with remarkable sequence selectivity (*22*). On the basis of their mode of binding, they can be divided into intercalators and groove binders. However, most intercalators exploit groove interaction for DNA binding as well, and some groove binders at some DNA sequences bind to DNA in an intercalationlike fashion (*23*).

It is widely agreed that DNA intercalation, per se, does not contribute much sequence discrimination. Thus, the sequence selectivity exhibited by certain intercalators, such as echinomycin and actinomycin, is governed primarily by hydrogen bonding and hydrophobic interactions in the minor groove (*24*). However, the sequence preference is very "soft". Echinomycin (Figure 3), for example, binds preferentially to GC-rich DNA sequences and especially to the GpC step, and the binding constant ratio between high-affinity and low-affinity sites is of the order of 10–20 (*25*). For comparison lac-repressor (a helix–turn–helix protein) binds to the operator sequence with $K_a \approx 10^{13}$ M^{-1} while the affinity for random DNA is $\sim 10^8$ M^{-1} (*26*), i.e., a ratio of 10^5.

Most minor groove DNA binding drugs, such as distamycin, netropsin, Hoechst 33258 (Figure 4), and DAPI (4′,6-diamidino-2-phenylindole) bind with significant preference (10–10^2 times) to AT-rich sequences, and the preferred binding sites contain a run of at least four A/T's (*27–30*). Several models explaining this preference for runs of A/T's have been proposed (*28, 29, 31*), but most researchers now agree that a major contribution stems from the large electronegative potential of the narrow minor groove of A/T sequences which attracts the positively charged drugs (*31*) and also neatly accommodates these flat curved molecules snugly in the minor groove (Figure 5).

One family of drugs, the chromomycins, which bind selectively to GC-rich sequences via minor-groove interactions have also been identified (*32*), and NMR results (*33*) indicate that drug dimer formation and significant widening of the minor groove are involved.

4. MINOR-GROOVE INTERACTION

4.1 Lexitropsins. From early X-ray studies on the binding of netropsin to AT-rich DNA sequence a model based on specific hydrogen bonding between the amide protons of netropsin and the hydrogen-acceptor sites in the AT minor groove was developed in which the amide protons of netropsin form bifurcated hydrogen bonds to the adenine-N7 and thymine-O4 of two adjacent AT base pairs (*34*). On the basis of this model it was suggested that switching of the sequence preference from AT to GC should be possible by designing analogues of netropsin with hydrogen-bonding donor/acceptor properties complementary to the GC base pair steps (*35, 36*). Specifically, the pyrrole moieties of the netropsin were replaced by imidazole (**1**, Figure 5), which due to the nitrogen lone pair positioned in the minor groove was predicted to

hydrogen bond to the H_2N group of guanine. The experiments with these new reagents termed lexitropsins were rather disappointing, however. Although an increased relative binding to GC-containing sequences was obtained, this was achieved by decreased affinity for AT sequences rather than by increased affinity for GC sequences (*34, 35*). After it became clear that the cationic character of the ligand was a significant factor for conferring AT specificity, lexitropsin derivatives with only one positive charge containing imidazoles, furans, thiophenes, or thiazoles moieties (*36–50*) (e.g. **2–5**, Figure 5) were synthesized (*38–40*) by Lown and co-workers, the immediate aim being GC acceptance by the lexitropsin and the ultimate goal controlling the sequence specificity of these reagents. The results so far have shown that the introduction of hydrogen-bonding acceptor groups (=N— or —O—) pointing into the minor groove (compounds **2**, **3**) results in lexitropsins which no longer exhibit the pronounced $(A/T)_4$ specificity typical for netropsin (and distamycin) but which bind to AT–GC mixed sequences as probed by DNase I footprinting. Proton NMR studies of complexes of these lexitropsins with self-complementary oligonucleotides indicate that hydrogen bonding between the guanine-NH_2 and the lexitropsin acceptor moiety (imidazole or furan) may indeed take place. Somewhat unexpectedly the analogous thiazoles (*e.g.*, compound **5**) exhibit an AT preference which is even stronger than that of netropsin (*49*). This finding (termed GC avoidance) has been rationalized on the basis of the sulfur atom which sterically clashes with guanine-NH_2.

Model studies reveal that phasing between the hydrogen-bonding-donor/-acceptor sites in the minor groove of DNA and those of the lexitropsins becomes a problem for longer lexitropsins. It may therefore be necessary to connect such "oligolexitropsins" with linkers which both bring the individual lexitropsin units in phase with the DNA helix and at the same time make them follow the helical path of the groove (*51*).

In an analogous approach Wade and Dervan have made distamycin derivatives containing a hydrogen-bond-accepting moiety (a pyridine) (*52*) and found that one of these (**6**: X, Y, Z = N, CH, CH) in contrast to distamycin binds preferentially to a GC–AT mixed sequence.

Several other analogues of distamycin have also been prepared (*53–56*), but the detailed sequence preference of these reagents has not been studied yet.

Finally, a few analogues of Hoechst 33258 with altered sequence preference have been described (*57*). In analogy to the hydrogen-bonding-acceptor lexitropsins, these drugs (e.g. **7**) also bind to GC containing sequences as analyzed by footprinting and ^1H NMR studies (*57*).

It must be emphasized, however, that the binding mode of these new lexitropsins is far from fully understood and that it is not yet possible to design reagents specifically targeted to desired sequences by this approach. (For recent reviews on lexitropsins, see refs 37 and 128.)

4.2 Oligodistamycins. From statistical considerations of base contents and genomic sizes, it can be calculated that a unique sequence in *Escherichia coli* consists of ~12 base pairs, while the corresponding number in a human cell is ~15–19 base pairs (*58*). One goal is therefore to be able to target ligands selectivily to sequences of this size. Targeting $(A/T)_n$ sequences—although without discrimination of the positions of the A's and T's—is a relatively simple task and has been accomplished by distamycin-type oligomers (*59–63*). The DNA binding site of these oligomers usually obey an emperical/theoretical rule stating that an oligomer with *n* pyrrole units, i.e. *n* peptide bonds, binds to an $(A/T)_{n+1}$ sequence. This behavior is consistent with the binding mode in which each amide proton forms bifurcated hydrogen bonds with the two hydrogen-acceptor sites of two adjacent AT base pairs. The largest reagent constructed so far is a "distamycin trimer" connected head to tail by β-alanine linkers and it recognizes ~16 bp (*64*). Some of these reagents were equipped with an EDTA ligand which functions as a DNA-cleaving reagent upon complexing with Fe^{2+}.

Finally, it has been very elegantly demonstrated that it is possible to design metal ion inducible DNA binding ligands by tethering individual distamycin units with metal ion (e.g. Mg^{2+}) chelators in such a way that only the chelated form has the right conformation for DNA binding. These reagents therefore bind much more strongly to their target oligo-TA sequence in the presence of chelated divalent metal ions (*65*). Likewise, it is also possible to use optically active linkers. In the one case examined (tartaric acid), identical binding specificities were observed for the two forms (*66*). The *R,R* form binds 10 times less efficiently to DNA than the *S,S* form, however, showing that steric fit is an important parameter for DNA recognition by these compounds. For recent reviews on oligodistamycins, see refs 58 and 67.

4.3 Intercalator–Peptide Conjugates. Echinomycin is a naturally occurring intercalator–peptide conjugate in which two quinoxaline ligands are connected via a cyclic depsipeptide (Figure 3). Removal of the *N*-methyl groups (and exchanging the thioacetal bridge with a disulfide) gives the analogue TANDEM (*68*), which binds preferentially to AT-rich sequences in contrast to echinomycin which prefers the GpC step. An echinomycin analogue in which the quinoxaline moieties are replaced with acridinyl have also been synthesized (*69*), but the sequence-binding preference of this compound has not been reported.

These results show that the sequence recognition by echinomycin is determined by the depsipeptide moiety. Thus, it could be interesting to explore the possibility of constructing sequence-selective DNA-recognizing ligands by tethering peptides to intercalators in general and in particular by using peptides as linkers for bis-intercalators.

Finally, acridine–distamycin-like conjugates have been described (*70, 71*) which retain the AT preference of the distamycin ligand in accord with the lack of sequential DNA binding usually exhibited by simple intercalators like 9-aminoacridine.

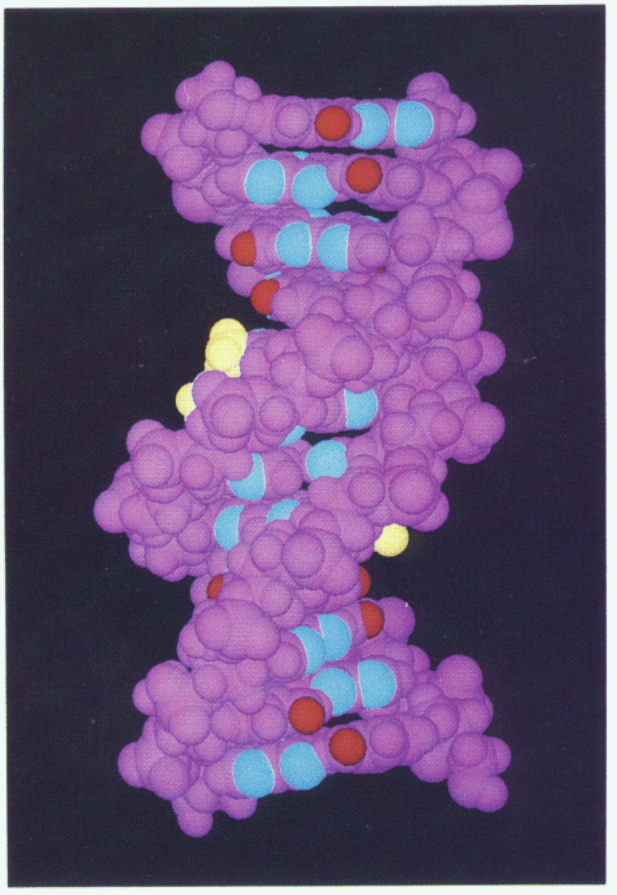
5. MAJOR-GROOVE RECOGNITION

5.1 Peptides. Although it is not yet possible to design peptide α-helices—analogous to those found for instance in λ-repressor, crolac repressor, CRP, etc. (*72*)—for recognition of predetermined DNA sequences, it is feasible to exploit the peptide–DNA recognition exhibited by these proteins. A pertinent question is how much of the protein is required for sequence-selective DNA binding, i.e., how large is the DNA binding domain. Recent results using the *Hin* recombinase indicate that three α-helices (α_1, α_2, and the DNA-recognizing α_3) corresponding to ~50 amino acids are sufficient for efficient DNA recognition. Specifically the 51-mer oligopeptide (residues 139–190) was chemically synthesized and conjugated to various DNA-cleaving ligands, such as EDTA (*73*) or the Cu(I) binding tripeptide Gly-Gly-His (*74–75*) and thus converted to a sequence-selective DNA-cleaving reagent. Analogously, by conjugation of phenanthroline to the catabolite gene regulatory protein (CRP) (*76*) or of staphylococcal nu-









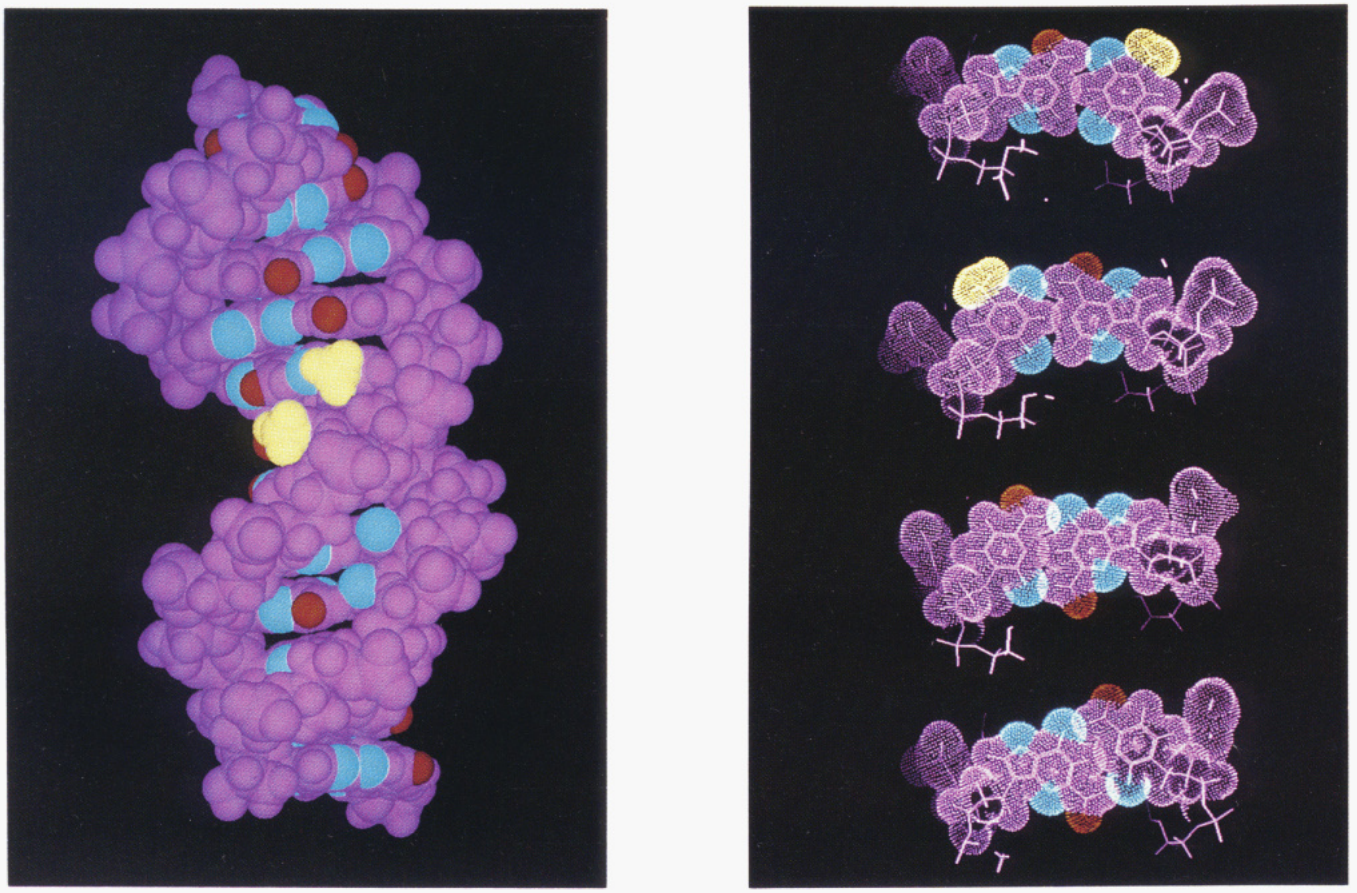
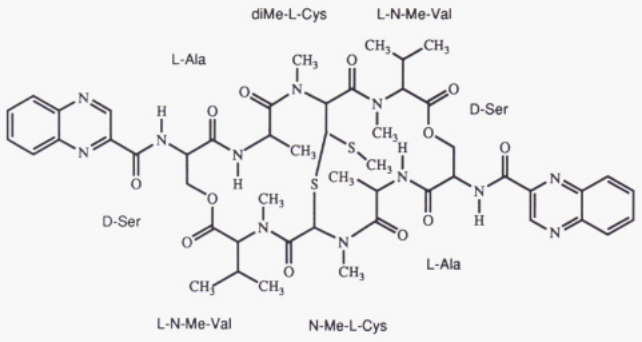


Figure 2. Three-dimensional structure of the Drew–Dickerson dodecamer (5′-CGCGAATTCGCG)$_2$ (refs 9 and 10) part a (previous page, upper left) shows molecular graphics model colored according to atoms; parts b–e (previous page, upper right; previous page, lower left; previous page, lower right; this page, left, respectively) are the same as a, but colored according to recognition sites: hydrogen acceptor (cyan), hydrogen donor (red), and van der Waals (thymine methyl groups) (yellow). The dodecamer is shown from four angles at 90° intervals. Part f (this page, right) shows surface models of the four base pairs (from above; AT, TA, CG, and GC) colored as in b–e. The major groove is facing upward. Models were constructed on a "Personal Iris" using "Insight/Discover" software.



Echinomycin

Figure 3. Chemical structure of echinomycin.

clease to a truncated λ-repressor (*77*), these peptides have been converted to sequence-selective DNA-cleaving reagents.

Recently the putative DNA binding domain (50 amino acids) of a Leu-zipper DNA-binding protein (GCN4) containing an EDTA ligand was synthesized and shown to recognize and cleave the GCN4 recognition sequence (*78*).

Peptide–DNA cleaver conjugates can also be used to study the DNA-binding mode of the peptide and thus the protein from which the DNA-binding domain originates. This was elegantly exploited in the studies of the DNA binding of GCN4 transcription factor (*78*) and *Hin* recombinase (*79*, *80*) using the appropriate peptide–EDTA-(Fe^{II}) conjugates.

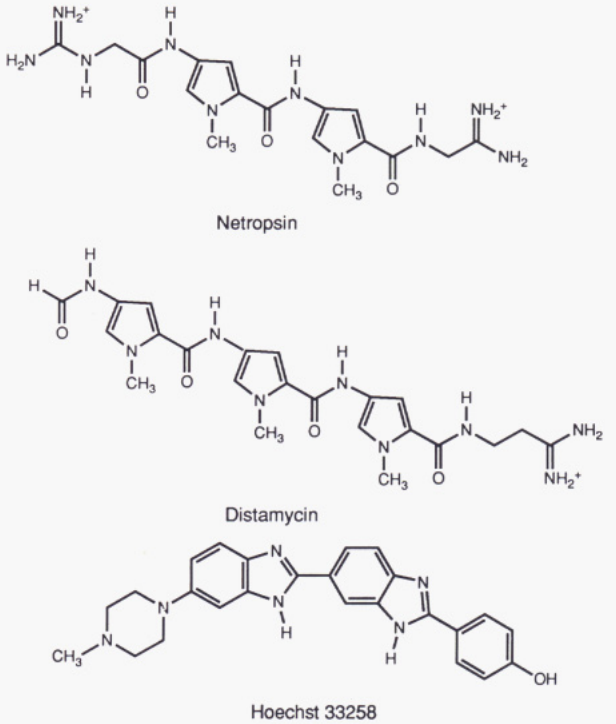


Figure 4. Chemical structures of the minor-groove binders netropsin, distamycin, and Hoechst 33258.

All available genetic and biochemical data indicate that mainly the α_3-helix of the helix–turn–helix proteins is

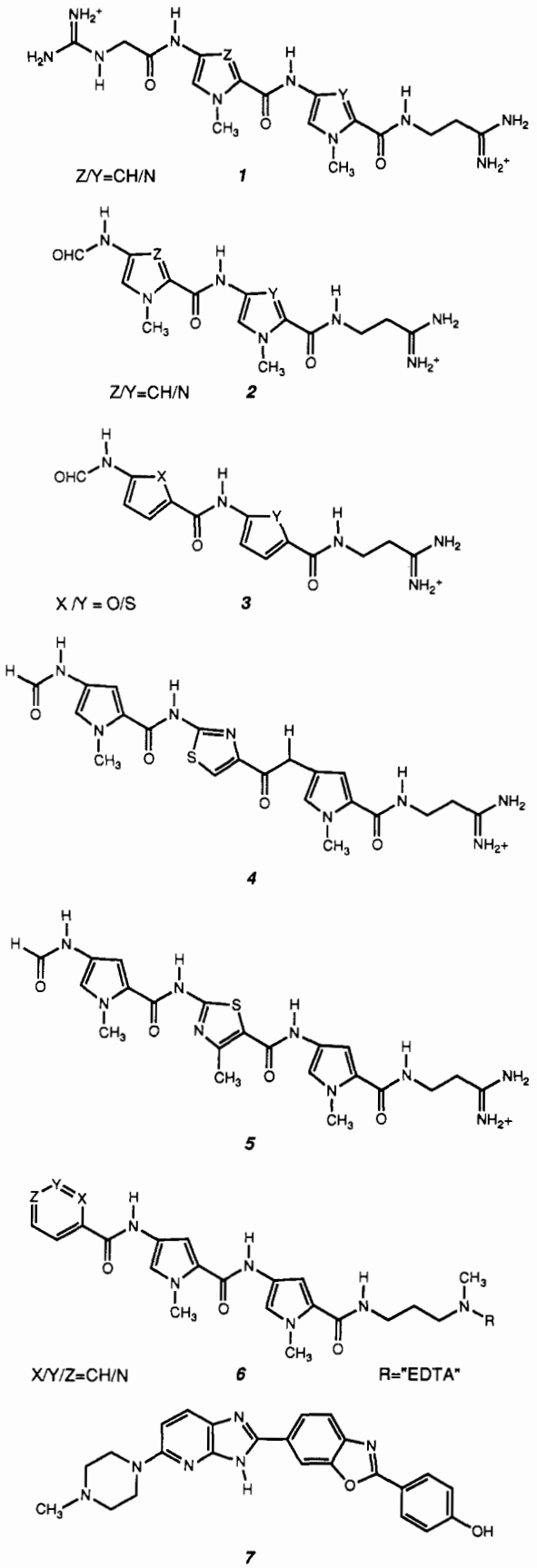


Figure 5. Chemical structures of various lexitropsins and analogues of distamycin and Hoechst 33258.

responsible for DNA recognition (*81*, *82*). It should therefore be a major goal to synthesize such modified "α_3-helices"—probably in a "helix-stabilized" from—which bind sequence specifically to DNA.

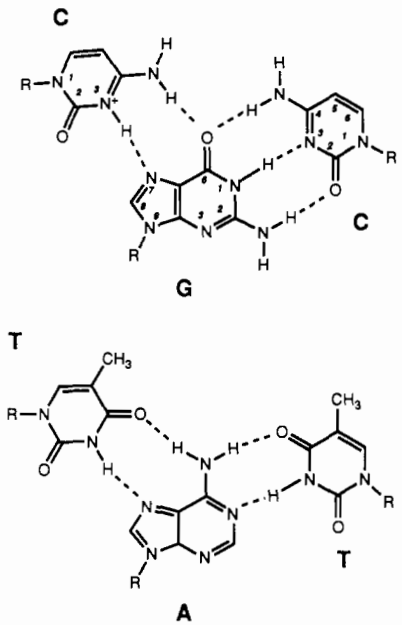
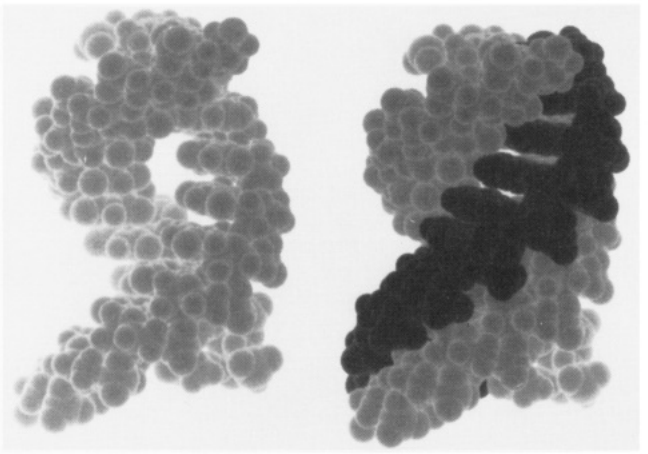


Figure 6. Chemical structures of helix base triplets with Watson–Crick/Hoogsteen base pairing.

5.2 Triple Helix. The exploitation of DNA triple helix formation is for the time being the most versatile and rational approach to sequence-selective DNA recognition although severe limitations for a general application still exist. RNA triple helices were discovered 3 decades ago (*83*) in the 2:1 poly(U)–poly(A) complex and several triple helix structures have been described since then (e.g. refs 84, 85). Triple-helix formation relies in most cases on Hoogsteen hydrogen bonds in the major groove between adenines, or guanines, of the second strand, and thymines, or protonated cytosines, of the third strand (Figure 6), and stable triple helices are thus formed between oligopyrimidine–oligonucleotides and "Hoogsteen-complementary" homopurine–homopyrimidine DNA sequences where the two pyrimidine strands have antiparallel orientation (Figure 7).

Triple-helix formation is promoted by a high concentration of cations (e.g., 1 M Na^+), which are necessary for shielding of the negative phosphate backbone, and by acidic pH if cytosines are involved. However, triple helices can be formed at physiological salt concentrations and neutral pH if spermidine (1 mM) is included in the medium and they are furthermore stabilized by moderate concentrations of organic solvents (*86*). Triple helices can be further stabilized if an intercalator is conjugated to the third strand oligonucleotide (87–92). For example, the T_m of an 11-mer (6T + 5C) triple helix was measured to 19.3 °C (at pH 6.0, 1 mM spermidine). The corresponding 5′-acridine conjugate triple helix melted at 37.4 °C while the 3′-acridine conjugate melted at 25.5 °C. (Oligonucleotide conjugated with ethidium, ellipticine, or daunorubicin showed similar stabilization (*90–92*).) The results also indicate that triple-helix formation induces a conformational change in the DNA double helix (e.g. to an A-like conformation) which results in a strong intercalation site at the 5′-junction. Independent experiments have confirmed this (*92*).

In order to be able to study the triple-helix formation by affinity cleavage as well as with the goal of making sequence-targeted DNA-modifying and -cleavage reagents (artificial restriction enzymes) a large variety of DNA-cleaving ligands have been conjugated to "triple-helix oligonucleotides". These include EDTA–Fe(II) (*86*, *89*),



5'-TTTTTTTTTTTTTTT

5'-....AGCTTATATATATATAAAAAAAAAAAAAAAATCGATAGGATC....

3'-....TCGAATATATATATATTTTTTTTTTTTTTTTAGCTATCCTAG....

5'-TTTTTCTCTCTCTCT

5'-....AGCTTATATATATATAAAAAGAGAGAGAGATCGATAGGATC....

3'-....TCGAATATATATATATTTTTCTCTCTCTCTAGCTATCCTAG....

Figure 7. Space-filling molecular graphics model of DNA triple helix (top). The A-form double helix is shown in grey while the third strand is in black; sequence of a typical "Hoogsteen" triple helix is shown (bottom).

azidoproflavine (*87*), phenanthroline–Cu(I) (93–95), or porphyrin (96–98). Analogously, oligonucleotides capable of cross-linking to the target DNA have been designed by conjugation to psoralens (*99*) or alkylating agents (*100*).

The major and far from trivial challenge in the triple-helix approach is to target purine/pyrimidine mixed DNA sequence. Molecular modeling reveals that the third helix is asymmetrically positioned in the major groove, since it is only reading the information of one side of the groove, the purine side. Thus in order to read mixed sequences two possibilities appear. Either the reading base (which in principle could be any aromatic ligand) must switch from one side of the groove to the other when encountering a purine–pyrimidine step or it must read the information of the pyrimidine half of the base pair. Both approaches have been tried without yet reaching a general solution. It has been shown that 5′-Pu_mPy_n (Pu = purine, Py = pyrimidine) sequences may be recognized by third strand oligonucleotides of the type 5′-Pu_m–linker–3′-Py_{n-1} in which the linker couples the two Py oligonucleotides in a tail to tail fashion which allows for a "groove switch" over one base pair (which is not read) in the Pu–Py junction of the double helix (*101*). In this way both the Pu sequence and the Py sequence is read by conventional Hoogsteen base pairing. Finally, it has been shown that a single T A base pair in a purine sequence can be read by a guanine in the triple strand (G·TA) (*102*), but whether this finding can be extended to additional T A interruptions or interrupting T A runs is not yet known and probably doubtful.

The "Hoogsteen-type" triple helix may only be one out of a family of mutually incompatible triple helices since it has been reported that G·GC triplets combined with occasional T·AT and T·TA triplets may be formed in triple-helix structures in which the two G strands are antiparallel (*103*, *104*).

It is thus pertinent that the basic physicochemical properties of oligonucleotide triple helices be explored in terms of possible structures, their stabilities, rate of formation, and the relative stability of individual triplets in various environments.

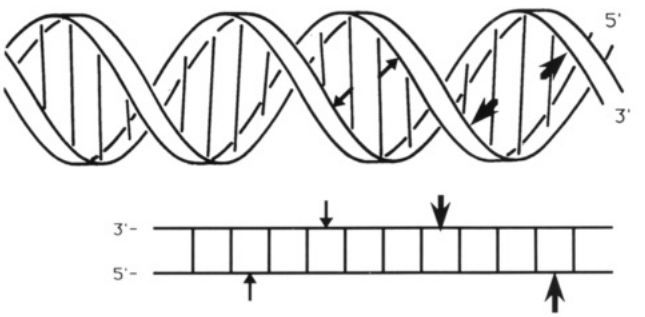


Figure 8. Schematic models of B-DNA helix showing attack from the major (large arrows) and the minor (small arrows) groove.

The biological and potential clinical prospects for triple-helix-based ligands (drugs) seem very bright judging from recent reports of efficient blockage of protein–DNA interaction and restriction enzyme DNA cleavage by sequence-directed triple-helix formation (*105*, *106*). Even more interesting, preliminary results indicate that oligonucleotides targeted to regulatory sequences via triple-helix formation exhibit the predicted biological effect in vivo. Specifically it was shown that a $(dT)_8$ acridine conjugate targeted to the origin of replication of SV40 inhibits virus replication in CV-1 cells (*107*).

One of the arguments against the feasibility of using oligonucleotides as drugs has been their presumed inability to cross cell membranes due to their polyanionic character. This seems not to be a problem. Acridine-conjugated oligonucleotides are taken up by cells quite efficiently (*108*) and recent results have indicated that even natural oligonucleotides are taken up by cells in a receptor-mediated transport (*109*).

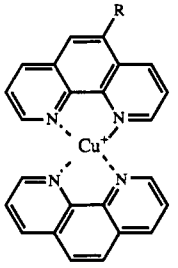
The possible use of "triple-helix DNA cutters" as "rare-cutter restriction enzymes", e.g., in connection with the human genome sequencing project, is also close to reality. It has been demonstrated that a single sequence-specific cut can be introduced in DNA molecules of more than 10^5 base pairs in length, although the cleavage efficiency is still only 25–70% at best (*94*, *110–112*) (see refs 67, 112, 113 for more specific reviews on the triple-helix approach).

6. DNA-MODIFYING LIGANDS

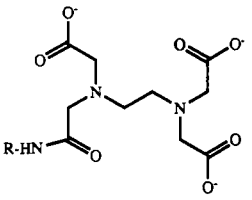
A DNA-cleaving ligand is often included in the design of sequence-directed reagents. This serves two purposes. Primarily, these reagents are designed to cleave DNA sequences selectively either with the aim of constructing "synthetic restriction enzymes" or with the aim of deactivating specific DNA sequence in vivo in the course of "gene-directed chemotherapy". Additionally, however, the presence of a DNA-cleaving ligand in the reagent also provides a convenient means by which the sequence selectivity and DNA-binding mode of the reagent may be analyzed by "affinity cleavage" or "autofootprinting".

The cleavage pattern of the two DNA strands even reveals if the cleaving ligand is bound in the minor or in the major groove. Due to the asymmetry of the B-DNA helix, cleavage from the major groove will result in a 2 or 3 base pair stagger in the 3′-direction between the two DNA strands whereas major-groove cleavage will result in a 4 or 5 base pair stagger in the 5′-direction (Figure 8).

A large variety of DNA-cleaving ligands have been used for this purpose, and virtually all of them have been chosen from the broad selection of footprinting reagents which are now at hand (*116*) (Figures 9 and 10). Dervan and co-workers have used the versatile EDTA–Fe(II) complex

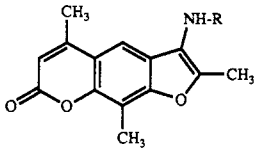


Cu(I)-Phenanthroline

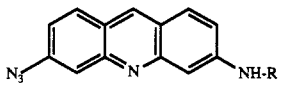


EDTA

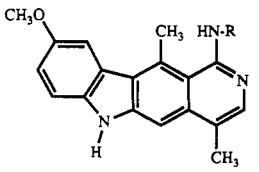
Figure 9. DNA-cleaving ligands. R denotes the site of conjugation. It should be noted that when phenanthroline is conjugated to oligonucleotides, only one phenanthroline moiety seems to be involved (*94*).



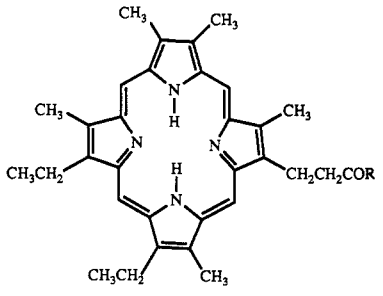
Trimethylpsoralen



Azidoproflavin



Ellipticine



Porphyrine

Figure 10. DNA photocleaving and photo-cross-linking ligands. R as in Figure 9.

in most reagents (*58*, *67*) and have obtained cleavage efficiences—defined as yield of cleaved target under a set of optimized conditions—of ~25% (*110*).

Hélène and co-workers have tried a larger selection of ligands (*117*) including photochemically activated azidoproflavin, azidophenacyl, porphyrin, and recently ellipticin (*91*). The Cu(I) complex of phenanthroline has also proven very versatile (*76*, *94*, *118*, *119*) and a DNA double strand cleavage yield of 70% has been reported for this ligand conjugated to an oligonucleotide (*112*).

Photo-cross-linking of the reagent to the DNA target has been obtained with the above mentioned azidoproflavin and azidophenacyl ligands as well as with psoralens (ref 99 and refs cited in 120) and quinones (*121*). Chemical cross-linking was accomplished by various alkylating ligands, such as alkyl halides (*123–125*) and nitrogen mustards (*122*). Ideally, one would require a DNA-cleaving ligand with catalytic activity (one ligand cleaving more than one target). This is probably to some extent the case with the EDTA–Fe(II) and the phenanthroline–Cu(I) complexes. Furthermore, the mechanism should preferentially be hydrolytic—at least in the case where "synthetic restriction enzymes" are the goal—in order for the products to be processable by conventional enzymes. In other words, a synthetic analogue of the catalytic site of a DNase like DNase I or micrococcus nuclease would be "handy".

7. FUTURE PROSPECTS

As discussed above the efforts to create sequence-selective DNA-binding and -cleaving ligands have so far been centered around three principles, namely minor groove recognizing "lexitropsins", polypeptides constituting the DNA-recognizing domains of known sequence-selective DNA-binding proteins, and last but not least, oligonucleotides capable of forming triple helices.

It is difficult to judge the prospects of the lexitropsin approach at the present stage if the goal is to design ligands targeted to predetermined DNA sequences since the principle of recognition is rather poorly understood. On the other hand, there is little doubt that ligands capable of selectively recognizing mixed sequences are not far away by combining the lexitropsin and the oligodistamycin approaches. The chemistry in the lexitropsin approach is, furthermore, extremely well developed, giving a comfortably high degree of freedom in the chemical design (see ref 126 for an extensive review of the chemistry of lexitropsins). Therefore as soon as the understanding of the recognition principle is advanced the prospects appear bright. Finally, these compounds could quickly find their way into clinical tests, since availability (large-quantity synthesis) solubility, and cell/tissue penetration/distribution does not seem to pose a problem as judged from the behavior of distamycin, netropsin, and the analogues already synthesized (e.g. refs 127, 128).

Several apparently severe obstacles have to be overcome before peptides analogous to the DNA-recognizing domains of natural proteins can be exploited to target predetermined DNA sequences. First of all, principles for reduction of the size of the peptides (from ~50 to ~10–20) without jeopardizing the sequence-recognition properties must be developed. These will most probably include chemical modification of the peptides in order to stabilize the conformation involved in DNA recognition. In this connection it is very interesting that recent studies have shown that the DNA-recognizing domain in several DNA-binding proteins is stabilized considerably in terms of the α-helical conformation upon association with the DNA-recognition sequence (*129–132*). Secondly, techniques must be developed to choose the peptide sequences required to recognize the desired DNA sequence. This may not be as insurmountable a task as judged by first appearance since it should be possible to persuade nature to perform the job. In the course of genetic analysis of the lac repressor/operator system Müller-Hill et al. have developed a technique by which repressors binding to mutant operator sequences can be selected (*133*). By

further refinement and expansion of this procedure an "α-helix-selection kit" could be developed in which the target DNA sequence is placed in the operator box and the α-helix can be deduced from sequencing of the biologically selected repressor. Similar systems could be developed based on Leu-zipper, Zn-finger, and other DNA-recognizing proteins.

Although some nontrivial obstacles still have to be overcome in the triple-helix approach, this has been met with the most success so far and it is also the one in which there appears to be most confidence for the immediate future. The shortcomings of this approach in terms of the type of sequence which can be targeted at the present stage have already been discussed as well as the possible ways of overcoming these. Especially, the employment of "new bases" would be interesting. The four natural bases are not necessarily optimal for triple-helix formation as already indicated by the improved stability at neutral pH of triple helices containing 5-methylcytosine·GC, 5-bromouracil·TA triplets (*134*). Thus it should be possible on the basis of computer modeling to design heterocycles ("bases") that fit either of the four possible base pair sites both in terms of hydrogen donor and acceptor sites as well as their spatial positions. Naturally, the synthetic problems in this approach are huge, but thus also challenging. It is worth recalling that much of the experience obtained in the rapidly developing field of antisense gene regulation (see refs 113, 117, 135 for excellent reviews) can be adapted immediately in the triple-helix approach. This includes the many efforts to modify the deoxyribose phosphate backbone of the oligonucleotides using, e.g., methylphosphonates or thio- and dithiophosphates in order to increase the biostability of the oligonucleotides. More radical changes of the backbone have also been accomplished (see refs 121, 135 for reviews), most recently by using morpholino linkages (*136*). The pursuit of such alternative ways connecting DNA major groove recognizing bases (or more generally, ligands) appears worthwhile and could lead to the ultimate goal of a general recognition principle.

Likewise, more untraditional approaches should be explored. These include conjugation of oligonucleotides with peptides (*137*, *138*) and one could even imagine conjugation of oligonucleotides with lexitropsins if these are connected via a "groove-switching intercalator" like the acridine derivatives recently developed for cancer chemotherapy by Denny et al. (*139*).

The number of unexplored routes is still large, and new principles of sequence-specific DNA recognition are still being discovered from the ongoing studies of DNA-binding proteins and natural drugs and thereby opened as a means for synthetic design and ingenuity.

The coming of the age of sequence-targeted designer drugs is close and only time and experiments will tell if it lives up to our (maybe too) optimistic expectations and produces valuable molecular tools, and hopefully also efficient and specific drugs for treating, e.g., virus infections and cancer.

ACKNOWLEDGMENT

The financial support of the Alfred Benzon Foundation is gratefully acknowledged. I also want to thank Drs. P. Dervan, C. Hélène, and W. Lown for supplying re- and preprints of their recent work and Dr. O. Buchardt for critically reading the manuscript. Finally thanks are due to Mrs. Else Uhrenfeldt for typing the manuscript.

LITERATURE CITED

(1) Zimmerman, S. B. (1982) The three-dimensional structure of DNA. *Annu. Rev. Biochem. 51*, 395–427.
(2) Rich, A., Nordheim, A., and Wang, A. H.-J. (1984) The chemistry and biology of left-handed Z-DNA. *Annu. Rev. Biochem. 53*, 791–846.
(3) Ollis, D. L., and White, S. W. (1987) Structural basis of protein–nucleic acid interactions. *Chem. Rev. 87*, 981–995.
(4) Travers, A. A. (1989) DNA conformation and protein binding. *Annu. Rev. Biochem. 58*, 427–52.
(5) Schleif, R. (1988) DNA binding by proteins. *Science 241*, 1182–1187.
(6) Hélène, C., and Lancelot, G (1982) Interactions between functional groups in protein–nucleic acid association. *Prog. Biophys. Mol. Biol. 39*, 1–68.
(7) Trifonov, E. N. (1985) Curved DNA. *CRC Crit. Rev. Biochem. 19*, 89–106.
(8) Fujimoto, B. S., and Schurr, J. M. (1990) Dependence of the torsional rigidity of DNA on base composition. *Nature 344*, 175–178.
(9) Wing, R., Drew, H., Takano, T., Broka, C., Tanaka, S., Itakura, K., and Dickerson, R. E. (1980) Crystal structure analysis of a complete turn of B-DNA. *Nature 287*, 755–758.
(10) Dickerson, R. E., and Drew, H. R. (1981) Structure of a B-DNA dodecamer II. Influence of base sequence on helix structure. *J. Mol. Biol. 149*, 761–786.
(11) Drew, H. R., and Travers, A. A. (1984) DNA structural variations in the E. coli tyrT promoter. *Cell 37*, 491–502.
(12) Rhodes, D., and Klug, A. (1986) An underlying repeat in some transcriptional control sequences corresponding to half a double helical turn of DNA. *Cell 46*, 123–132.
(13) Goodman, S. D., and Nash, H. A. (1989) Functional replacement of a protein-induced bend in a DNA recombination site. *Nature 341*, 251–254.
(14) Lavery, R., and Pullman, B. (1981) Molecular electrostatic potential on the surface envelopes of macro molecules: B-DNA. *Int. J. Quantum Chem. 20*, 259–272.
(15) Lehming, N., Sartorius, J., Kister-Woike, B., Wilcken-Bergmann, B., and Müller-Hill, B. (1990) Mutant lac repressors with new specificities hint at rules for protein-DNA recognition. *EMBO J. 9*, 615–621.
(16) Sauer, R. T. (1990) Scissors and helical forks. *Nature 347*, 514–515.
(17) Rafferty, J. B., Somers, W. S., Saint-Girons, I., and Phillips, S. E. V. (1989) Three-dimensional crystal structure of *Escherichia coli* met repressor with and without corepressor. *Nature 341*, 705–710.
(18) Breg, J. N., van Opheusdan, J. H. J., Burgering, M. J. M., Boelens, R., and Kaptein, R. (1990) Structure of Arc repressor in solution: evidence for a family of β-sheet DNA-binding proteins. *Nature 346*, 586–589.
(19) Yang, C.-C., and Nash, H. A. (1989) The interaction of *E. coli* IHF protein with its specific binding sites. *Cell 57*, 869–880.
(20) Otwinowski, Z., Schevitz, R. W., Zhang, R.-G., Lawson, C. L., Joachimiak, A., Marmorstein, R. Q., Luisi, B. F., and Sigler, P. B. (1988) Crystal structure of trp repressor/operator complex at atomic resolution. *Nature 335*, 321–329.
(21) Staacke, D., Walter, B., Kister-Woike, B., Wilcken-Bergmann, B., and Miler-Hill, B. (1990) How Trp repressor binds to its operator. *EMBO J. 9*, 1963–1967.
(22) Neidle, S., and Abraham, Z. (1984) Structural and sequence-dependent aspects of drug intercalation into nucleic acids. *CRC Crit. Rev. Biochem. 17*, 73–121.
(23) Wilson, W. D., Tanious, F. A., Barton, H. J., Strekowski, L., and Boykin, D. W. (1989) Binding of 4,6-diamidino-2-phenylindole (DAPI) to GC and mixed sequences in DNA: Intercalation of a classical groove-binding molecule. *J. Am. Chem. Soc. 111*, 5008–5010.
(24) Ughetto, G., Wang, A. H.-J., Quigley, G. J., Marel der van, G. A., van Boom, J. H., and Rich, A. (1985) A comparison of the structure of echinomycin and triostin A complexed to a DNA fragment. *Nucleic Acids Res. 13*, 2305–2323.
(25) Wakelin, L. P. G., and Waring, M. J. (1976) The binding of echinomycin to deoxyribonucleic acid. *Biochem. J. 157*, 721–740.
(26) Riggs, A. D., Suzuki, H., and Bourgeois, S. (1970) lac repressor–operator interaction. I. Equilibrium studies. *J. Mol. Biol. 48*, 67–83.

(27) Pjura, P. E., Grzeskowiak, K., and Dickerson, R. E. (1987) Binding of Hoechst 33258 to the minor groove of B-DNA. *J. Mol. Biol. 197*, 257–271.
(28) Coll, M., Aymami, J., Marel van der, J. A., van Boom, J. H., Rich, A., and Wang, A. H.-J. (1989) Molecular structure of the netropsin–d(CGCGATATCGCG) complex DNA conformation in an alternating AT segment. *Biochemistry 28*, 310–320.
(29) Coll, M., Frederick, C. A., Wang, A. H.-J., and Rich, A. (1987) A bifurcated hydrogen-bonded conformation in the d(A·T) base pairs of the DNA dodecamer d(CGCAAATTTGCG) and its complex with distamycin. *Proc. Natl. Acad. Sci. U.S.A. 84*, 8385–8389.
(30) Portugal, J., and Waring, M. J. (1987) Comparison of binding sites in DNA for berenil, netropsin and distamycin. A footprinting study. *Eur. J. Biochem. 167*, 281–289.
(31) Zakrzewska, K., Lavery, R., and Pullman, B. (1984) Theoretical studies of the selective binding to DNA of two nonintercalating ligands: netropsin and SN 18071. *Nucleic Acids Res. 11*, 8825–8839.
(32) Gao, X., and Patel, D. J. (1989) Solution structure of the chromamycin–DNA complex. *Biochemistry 28*, 751–762.
(33) Cons, B., and Fox, K. R. (1989) High resolution hydroxyl radical footprinting of the binding of mithramycin and related antibiotic to DNA. *Nucleic Acids Res. 17*, 5447–5459.
(34) Kopka, M. L., Yoon, C., Goodsell, D., Pjura, P., and Dickerson, R. E. (1985) The molecular origin of DNA–drug specificty in netropsin and distamycin. *Proc. Natl. Acad. Sci. U.S.A. 82*, 1376–1380.
(35) Krowicki, K., Lee, M., Hartley, J. A., Ward, B., Kissinger, K., Skorobogaty, A., Dabrowiak, J. C., and Lown, J. W. (1988) Molecular recognition between oligopeptides and nucleic acids—Rational design of sequence specific DNA binding agents. *Struct. Expression. 2*, 251–271.
(36) Lown, J. W., Krowicki, K., Bhat, U. G., Skorobogaty, A., Ward, B., and Dabrowiak, J. C. (1986) Molecular recognition between oligopeptides and nucleic acids: novel imidazole-containing oligopeptides related to netropsin that exhibit altered DNA sequence specificity. *Biochemistry 25*, 7408–7416.
(37) Lown, J. W. (1988) Lexitropsins: rational design of DNA sequence reading agents as novel anti-cancer agents and potential cellular probes. *Anti-Cancer Drug Des. 3*, 25–40.
(38) Kissinger, K., Krowicki, K., Dabrowiak, J. C., and Lown, J. W. (1987) Molecular recognition between oligopeptides and nucleic acids. Monocationic imidazole lexitropsins that display enhanced GC sequence dependent DNA binding. *Biochemistry 26*, 5590.
(39) Lee, M., Hartley, J. A., Pon, R. T., Krowicki, K., and Lown, J. W. (1988) Sequence specific molecular recognition by a monocationic lexitropsin of the decadeoxyribonucleotide d-[CATGGCCATG 2: Structural and dynamic aspects deduced from high field ^{1}H-NMR studies. *Nucleic Acids Res. 16*, 665–684.
(40) Lee, M., Pon, R. T., Krowicki, K., and Lown, J. W. (1988) Structural and dynamic aspects of the sequence specific binding of netropsin and its bis-imidazole analogue on the decadeoxyribonucleotide d-[CGCAATTGCG]2. *J. Biomol. Struct. Dyn. 5*, 939–949.
(41) Rao, K. E., Shea, R. G., Yadagiri, B., and Lown, J. W. (1990) Molecular recognition between oligopeptides and nucleic acids: DNA sequence specificity and binding properties of thiazole–lexitropsins incorporating the concepts of base site acceptance and avoidance. *Anti-Cancer Drug Des. 5*, 3–20.
(42) Lee, M., Krowicki, K., Shea, R. G., Lown, J. W., and Pon, R. T. (1989) Molecular recognition between oligopeptides and nucleic acids. Specificity of binding of a monocationic bis-furan lexitropsin to DNA deduced from footprinting and ^{1}H NMR studies. *J. Mol. Recognit. 2*, 84–93.
(43) Kissinger, K. L., Dabrowiak, J. C., and Lown, J. W. (1990) Molecular recognition between oligopeptides and nucleic acids: DNA binding specificity of a series of bis netropsin analogues deduced from footprinting analysis. *Chem. Res. Toxicol. 3*, 162–168.
(44) Burckhardt, G., Luck, G., Zimmer, C., Storl, J., Krowicki, K., and Lown, J. W. (1989) Variation of DNA sequence specificity of DNA–oligopeptide binding ligands related to netropsin: imidazole-containing lexitropsins. *Biochim. Biophys. Acta* 11–18.
(45) Lown, J. W., Krowicki, K., Balzarini, J., Newman, R. A., and De Clercq, E. (1989) Novel linked antiviral and antitumor agents related to netropsin and distamycin: Synthesis and biological evaluation. *J. Med. Chem. 32*, 2368–2375.
(46) Rao, K. E., Bathini, Y., and Lown, J. W. (1990) Synthesis of novel thiazole-containing DNA minor groove binding oligopeptides related to the antibiotic distamycin. *J. Org. Chem. 55*, 728.
(47) Lee, M., Chang, D.-K., Hartley, J. A., Pon, R. T., Krowicki, K., and Lown, J. W. (1988) Structural and dynamic aspects of binding of a prototype lexitropsin to the decadeoxyribonucleotide d(CGCAATTGCG)$_2$ deduced from high-resolution ^{1}H NMR studies. *Biochemistry 27*, 445–455.
(48) Lee, M., Pon, R. T., Krowicki, K., and Lown, J. W. (1988) Sequence specific molecular recognition and binding of a monocationic bis-imidazole lexitropsin to the decadeoxyribonucleotide d-[(GATCCGTATG)$_x$ (CATACGGATC)]: Structural and dynamic aspects of intermolecular exchange studied by ^{1}H-NMR. *J. Biomol. Struct. Dyn. 5*, 1059–1087.
(49) Kumar, S., Jaseja, M., Zimmermann, J., Yadagiri, B., Pon, R. T., Sapse, A.-M., and Lown, J. W. (1990) Molecular recognition and binding of a GC site-avoiding thiazole-lexitropsin to the decadeoxyribonucleotide d-[CGCAATTGCG]$_2$: ^{1}H-NMR evidence for thiazole interaction. *J. Biomol. Struct. Dyn. 8*, 331–358.
(50) Lee, M., Krowicki, K., Hartley, J. A., Pon, R. T., and Lown, J. W. (1988) Molecular recognition between oligopeptides and nucleic acids: Influence of van der Waals contacts in determining the 3′-terminus of DNA Sequences read by monocationic lexitropsins. *J. Am. Chem. Soc. 110*, 3641.
(51) Rao, K. E., Zimmermann, J., and Lown, J. W. (1991) Sequence selective DNA binding by linked bis-*N*-methylpyrrole dipeptides: An analysis by MPE footprinting and force field calculations. *J. Org. Chem. 56*, 786–797.
(52) Wade, W. S., and Dervan, P. B. (1987) Alteration of the sequence specificity of distamycin on DNA by replacement of an *N*-methylpyrrolecarboxamide with pyridine-2-carboxamide. *J. Am. Chem. Soc. 109*, 1574–1575.
(53) Bailly, C., Houssin, R., Bernier, J.-L., and Henichart, J.-P. (1988) Depsipeptide analogs of the antitumor drug distamycin containing thiazole amino acids residues. *Tedrahedron 44*, 5833–5843.
(54) Dasgupta, D., Parrack, P., and Sasisekharan, V. (1987) Interaction of synthetic analogues of distamycin with poly(dA-dT): Role of the conjugated *N*-methylpyrrole system. *Biochemistry 26*, 6381–6386.
(55) Rao, K. E., Dasgupta, D., and Sasisekharan, V. (1988) Interaction of synthetic analogues of distamycin and netropsin with nucleic acids. Does curvature of ligand play a role in distamycin-DNA interactions? *Biochemistry 27*, 3018–3024.
(56) Dasgupta, D., Rajagopalan, M., and Sasisekharan, V. (1986) DNA-binding characteristics of a synthetic analogue of distamycin. *Biochem. Biophys. Res. Commun. 140*, 626–631.
(57) Bathini, Y., Rao, K. E., Shea, R. G., and Lown, J. W. (1990) Molecular recognition between ligands and nucleic acids: pyridine- and benzoxaxzole-containing agents related to Hoechst 33258 that exhibit altered DNA sequence specificity deduced from footprinting analysis and spectroscopic studies. *Chem. Res. Toxicol. 3*, 268–280.
(58) Dervan, P. B. (1986) Design of sequence-specific DNA-binding molecules. *Science 232*, 464–471.
(59) Schultz, P. G., Taylor, J. S., and Dervan, P. B. (1982) Design and synthesis of a sequence-specific DNA cleaving molecule. (Distamycin–EDTA)iron(II). *J. Am. Chem. Soc. 104*, 6861–6863.
(60) Schultz, P. G., and Dervan, P. B. (1983) Sequence-specific double-strand cleavage of DNA by bis(EDTA-bis(distamycin)×Fe^{II}) and EDTA–bis(distamycin)×Fe^{II}. *J. Am. Chem. Soc. 105*, 7748–7750.
(61) Taylor, J. S., Schultz, P. G., and Dervan, P. B. (1984) DNA affinity cleaving. Sequence specific cleavage of DNA by distamycin-EDTA×Fe(II) and EDTA–distamycin×Fe(II). *Tedrahedron 40*, 457–465.

(62) Youngquist, R. S., and Dervan, P. B. (1985) Sequence-specific recognition of B-DNA by oligo(*N*-methylpyrrolecarboxamide)s. *Proc. Natl. Acad. Sci. U.S.A. 82*, 2565–2569.
(63) Youngquist, R. S., and Dervan, P. B. (1985) Sequence-specific recognition of B DNA by bis(EDTA-distamycin)fumaramide. *J. Am. Chem. Soc. 107*, 5528–5529.
(64) Youngquist, R. S., and Dervan, P. B. (1987) A synthetic peptide binds 16 base pairs of A,T double helical DNA. *J. Am. Chem. Soc. 109*, 7564–7566.
(65) Griffin, J. H., and Dervan, P. B. (1987) Metalloregulation in the sequence specific binding of synthetic molecules to DNA. *J. Am. Chem. Soc. 109*, 6840–6842.
(66) Griffin, J. H., and Dervan, P. B. (1986) Sequence-specific chiral recognition of right-handed double-helical DNA by (2*S*,3*S*)- and (2*R*,3*R*)-dihydroxybis(netropsin)succinamide. *J. Am. Chem. Soc. 108*, 5008–5009.
(67) Dervan, P. B. (1990) Chemical methods for the site-specific cleavage of genomic DNA. *Struct. Methods 1*, 37–49.
(68) Low, C. M. L., Fox, K. R., and Waring, M. J. (1986) DNA sequence recognition by under-methylated analogues of triostin A. *Nucl. Acids Res. 14*, 2015–2033.
(69) Helbecque, N., Bernier, J.-L., and Henichart, J.-P. (1985) Design of a new DNA-polyintercalating drug, a bisacridinyl peptidic analogue of triostin A. *Biochem. J. 225*, 829–832.
(70) Bailly, C., Helbecque, N., Henichart, J.-P., Colson, P., Houssier, C., Rao, K. E., Shea, R. G., and Lown, J. W. (1990) Molecular recognition between oligopeptides and nucleic acids. DNA sequence specificity and binding properties of an acridine-linked netropsin hybrid ligand. *J. Mol. Recognit. 3*, 26–35.
(71) Eliadis, A., Phillips, D. R., Reiss, J. A., and Skorobogaty, A. (1988) The synthesis and DNA footprinting of acridine-linked netropsin and distamycin bifunctional mixed ligands. *J. Chem. Soc. Chem. Commun.* 1049–1052.
(72) Brennan, R. G., and Matthews, B. W. (1989) The Helix–Turn–Helix DNA Binding Motif. *J. Biol. Chem. 264*, 1903–1906.
(73) Sluka, J. P., Horvath, S. J., Bruist, M. F., Simon, M. I., and Dervan, P. B. (1987) Synthesis of a sequence-specific DNA-cleaving peptide. *Science 238*, 1129–1132.
(74) Mack, D. P., Iverson, B. L., and Dervan, P. B. (1988) Design and chemical synthesis of a sequence-specific DNA-cleaving protein. *J. Am. Chem. Soc. 110*, 7572–7574.
(75) Mack, D. P., and Dervan, P. B. (1990) Nickel-mediated sequence-specific oxidative cleavage of DNA by a desingned metalloprotein. *J. Amer. Chem. Soc. 112*, 4604–4606.
(76) Ebright, R. H., Ebright, Y. W., Pendergrast, P. S., and Gunasekera, A. (1990) Conversion of a helix–turn–helix motif sequence-specific DNA binding protein into a site-specific DNA cleavage agent. *Proc. Natl. Acad. Sci. U.S.A. 87*, 2882–2886.
(77) Pei, D., and Schultz, P. G. (1990) Site-specific cleavage of duplex DNA with a lambda repressor–staphylococcal nuclease hybrid. *J. Am. Chem. Soc. 112*, 4579–4580.
(78) Oakley, M. G., and Dervan, P. B. (1990) Structural motif of the GCN4 DNA binding domain characterized by affinity cleaving. *Science 248*, 847–850.
(79) Sluka, J. P., Horvath, S. J., Glasgow, A. C., Simon, M. I., and Dervan, P. B. (1990) Importance of minor-groove contacts for recognition of DNA by the binding domain of *Hin* recombinase. *Biochemistry 29*, 6551–6561.
(80) Mack, D. P., Sluka, J. P., Shin, J. A., Griffin, J. H., Simon, M. I., and Dervan, P. B. (1990) Orientation of the putative recognition helix in the DNA binding domain of *Hin* recombinase complexed with the *Hix* site. *Biochemistry 29*, 6562–6567.
(81) Pabo, C. O., and Sauer, R. T. (1984) Protein–DNA recognition. *Annu. Rev. Biochem. 53*, 293–321.
(82) Wharton, R. P., and Ptashne, M. (1986) An α-helix determines the DNA-binding specificity of a repressor. *Trends Biochem. Sci. 11*, 71–73.
(83) Felsenfeld, G., Davies, D. R., and Rich, A. (1957) Formation of a three-stranded polynucleotide molecule. *J. Am. Chem. Soc. 79*, 2023.
(84) Hoogsteeen, K. (1959) The structure of crystals containing a hydrogen-bonded complex of 1-methylthymine and 9-methyladenine. *Acta Crystallogr. 12*, 822–823.
(85) Felsenfeld, G., and Miles, H. T. (1967) The physical and chemical properties of nucleic acids. *Annu. Rev. Bichem. 36*, 407–448.
(86) Moser, H. E., and Dervan, P. B. (1987) Sequence-specific cleavage of double helical DNA by triple helix formation. *Science 238*, 645–650.
(87) Le Doan, T., Perrouault, L., Praseuth, D., Habhoub, N., Decout, J. L., Thuong, N. T., Lhomme, J., and Hélène, C. (1987) Sequence-specific recognition, photocrosslinking and cleavage of the DNA double helix by an oligo-[α]-thymidylate covalently linked to an azidoproflavine derivative. *Nucleic Acids Res. 15*, 7749–7760.
(88) Francois, J. C., Saison-Behmoaras, T., and Hélène, C. (1988) Sequence-specific recognition of the major groove of DNA by oligodeoxynucleotides via triple helix formation. Footprinting studies. *Nucleic Acids Res. 16*, 11431–11440.
(89) Boidot-Forget, M., Chassignol, M., Takasugi, M., Thuong, N. T., and Hélène, C. (1988) Site-specific cleavage of single-stranded and double-stranded DNA sequences by oligodeoxyribonucleotides covalently linked to an intercalating agent and an EDTA–Fe chelate. *Genome 72*, 361–371.
(90) Sun, J. S., Francois, J. C., Montenay-Garestier, T., Saison-Behmoaras, T., Roig, V., Thuong, N. T., and Hélène, C. (1989) Sequence-specific intercalating agents: intercalation at specific sequences on duplex DNA via major groove recognition by oligonucleotide–intercalator conjugates. *Proc. Natl. Acad. Sci. U.S.A. 86*, 9198–9202.
(91) Perrouault, L., Asseline, U., Rivalle, C., Thuong, N. T., Bisagni, E., Giovannangeli, C., Le Doan, T., and Hélène, C. (1990) Sequence-specific artificial photo-induced endonucleases based on triple helix-forming oligonucleotides. *Nature 344*, 358–360.
(92) Montenay-Garestier, T., Sun, J. S., Chomilier, J., Mergny, J. L., Takasugi, M., Asseline, U., Thuong, N. T., Rougee, M., and Hélène, C. (1990) Design of bifunctional nucleic acid ligands. In *Molecular Basis of Specificity in Nucleic Acid–Drug Interactions* (B. Pullman, and J. Jortner, Eds.) pp 275–290, Kluwer Academic Publishers, Dordrecht.
(93) Francois, J. C., Saison-Behmoaras, T., Chassignol, M., Thuong, N. T., Sun, J. S., and Hélène, C. (1988) Periodic cleavage of poly(dA) by oligothymidylates covalently linked to 1,10-phenanthroline–copper complex. *Biochemistry 27*, 2272–2276.
(94) Francois, J. C Saison-Behmoaras, T., Barbier, C., Chassignol, M., Thuong, N. T., and Hélène, C. (1989) Sequence-specific recognition and cleavage of duplex DNA via triple-helix formation by oligonucleotides covalently linked to a phenanthroline–copper chelate. *Proc. Natl. Acad. Sci. U.S.A. 86*, 9702–9706.
(95) Francois, J. C., Saison-Behmoaras, T., Chassignol, M., Thuong, N. T., and Hélène, C. (1989) Sequence-targeted cleavage of single- and double-stranded DNA by oligothymidylates covalently linked to 1,10-phenanthroline. *J. Biol. Chem. 264*, 5891–5898.
(96) Le Doan, T., Perrouault, L., Hélène, C., Chassignol, M., and Thuong, N. T. (1986) Targeted cleavage of polynucleotides by complementary oligonucleotides covalently linked to iron–porphyrins. *Biochemistry 25*, 6736–6739.
(97) Le Doan, T., Perrouault, L., Chassignol, M., Thuong, N. T., and Hélène, C. (1987) Sequence-targeted chemical modifications of nucleic acids by complementary oligonucleotides covalently linked to porphyrins. *Nucleic Acids Res. 15*, 8643–8659.
(98) Le Doan, T., Praseuth, D., Perrouault, L., Chassignol, M., Thuong, N. T., and Hélène, C. (1990) Sequence-targeted photochemical modifications of nucleic acids by complementary oligonucleotides covalently linked to porphyrins. *Bioconjugate Chem. 1*, 108–113.
(99) Lee, B. L., Murakami, A., Blake, K. R., Lin, S. B., and Miller, P. S. (1988) Interaction of psoralen-derivatized oligodeoxyribonucleoside methylphosphonates with single-stranded DNA. *Biochemistry 27*, 3197–3203.
(100) Fedorova, O. S., Knorre, D. G., Podust, L. M., and Zarytova, V. F. (1988) Complementary addressed modification of double-stranded DNA within a ternary complex. *FEBS Lett. 228*, 273–276.

(101) Horne, D. A., and Dervan, P. B. (1990) Recognition of mixed-sequence duplex DNA by alternate-strand triple-helix formation. *J. Am. Chem. Soc. 112*, 2435–2437.

(102) Griffin, L. C., and Dervan, P. B. (1989) Recognition of thymine adenine base pairs by guanine in a pyrimidine triple helix motif. *Science 245*, 967–971.

(103) Durland, R. H., Kessler, D. J., Duvic, M., and Hogan, M. (1990) Triplex forming oligonucleotide reagents: rationalization of DNA site selectivity and applications in a pharmaceutical context. In *Molecular Basis of Specificity in Nucleic Acid–Drug Interactions* (B. Pullman, and J. Jortner, Eds.) pp 565–578, Kluwer Academic Publishers, Dordrecht.

(104) Kohwi, Y., and Kohwi-Shigematsu, T. (1988) Magnesium ion dependent triple-helix structure formed by homopurine–homopyrimidine sequences in supercoiled plasmid DNA. *Proc. Natl. Acad. Sci. U.S.A. 85*, 3781–3785.

(105) Maher, L. J., III, Wold, B., and Dervan, P. B. (1989) Inhibition of DNA binding proteins by oligonucleotide-directed triple helix formation. *Science 245*, 725–730.

(106) Francois, J. C., Saison-Behmoaras, T., Thuong, N. T., and Hélène, C. (1989) Inhibition of restriction endonuclease cleavage via triple helix formation by homopyrimidine oligonucleotides. *Biochemistry 28*, 9617–9619,

(107) Birg, F., Praseuth, D., Zerial, A., Thuong, N. T., Asseline, U., Le Doan, T., and Hélène, C. (1990) Inhibition of Simian virus 40 DNA replication in CV-1 cells by an oligodeoxynucleotide covalently linked to an intercalating agent. *Nucleic Acids Res. 18*, 2901–2907.

(108) Hélène, C., Montenay-Garestier, T., Saison, T., Takasugi, M., Toulme, J. J., Asseline, U., Lancelot, G., Maurizot, J. C., Toulme, F., and Thoung, N. T. (1985) Oligodeoxynucleotides covalently linked to intercalating agents: A new class of gene regulatory substances. *Biochimie 67*, 777–783.

(109) Yakubov, L. A., Deeva, E. A., Zarytova, V. F., Ivanova, E. M., Ryte, A. S., Yurchenko, L. V., and Vlassov, V. V. (1989) Mechanism of oligonucleotide uptake by cells: Involvement of specific receptors? *Proc. Natl. Acad. Sci. U.S.A. 86*, 6454–6458.

(110) Strobel, S. A., Moser, H. E., and Dervan, P. B. (1988) Double-strand cleavage of genomic DNA at a single site by triple-helix formation. *J. Am. Chem. Soc. 110*, 7927–7929.

(111) Strobel, S. A., and Dervan, P. B. (1990) Site-specific cleavage of a yeast chromosome by oligonucleotide-directed triple-helix formation. *Science 249*, 73–75.

(112) Hélène, C., Sun, J. S., Francois, J. C., Saison-Behmoaras, T., Montenay-Garestier, T., Asseline, U., and Thuong, N. T. (1990) Sequence-specific recognition and cleavage of the DNA double-helix by triple helix formation and intercalation. *Struct. Methods 1*, 51–59.

(113) Hélène, C., and Toulm, J.-J. (1990) Specific regulation of gene expression by antisense, sense and antigene nucleic acids. *Biochim. Biophys. Acta 1049*, 99–125.

(114) Hélène, C. (1989) Artificial control of gene expression by oligodeoxynucleotides covalently linked to intercalating agents. *Br. J. Cancer 60*, 157–160.

(115) Hélène, C., and Thuong, N. T. (1989) Control of gene expression by oligonucleotides covalently linked to intercalating agents. *Genome 31*, 413–421.

(116) Nielsen, P. E. (1990) Chemical and Photochemical Probing of DNA Complexes. *J. Mol. Recognit. 3*, 1–25.

(117) Chen, C.-h. B., and Sigman, D. S. (1988) Sequence-specific scission of RNA by 1,10-phenanthroline–copper linked to deoxyoligonucleotides. *J. Am. Chem. Soc. 110*, 6570–6572.

(118) Chi-hong, B., and Sigman, D. (1986) Nuclease activity of 1,10-phenantroline–copper: sequence-specific targeting. *Proc. Natl. Acad. Sci. U.S.A. 83*, 7147–7151.

(119) Hélène, C., Le Doan, T., and Thuong, N. T. (1989) Sequence-Targeted Photochemical Reactions in Single-Stranded and Double-Stranded Nucleic Acids by Oligonucleotide-Photosensitizer Conjugates. In *Photochemical Probes in Biochemistry* (P. E. Nielsen, Ed.) pp 219–230, Kluwer Academic Press, Dordrect.

(120) Goodchild, J. (1990) Conjugates of oligonucleotides and modified oligonucleotides: A review of their synthesis and properties. *Bioconjugate Chem. 1*, 165–187.

(121) Chatterjee, M., and Rokita, S. E. (1990) Inducible alkylation of DNA using an oligonucleotide–quinone conjugate. *J. Am. Chem. Soc. 112*, 6397–6399.

(122) Knorre, D. G., and Vlassov, V. V. (1985) Complementary-addressed (sequence-specific) modification of nucleic acids. *Prog. Nucl. Acid Res.* 291–320.

(123) Baker, B. F., and Dervan, P. B. (1985) Sequence-specific cleavage of double-helical DNA. *N*-bromoacetyldistamycin. *J. Am. Chem. Soc. 107*, 8266.

(124) Baker, B. F., and Dervan, P. B. (1989) Sequence-specific cleavage of DNA by N-bromoacetyldistamycin. Product and kinetic analyses. *J. Am. Chem. Soc. 111*, 2700.

(125) Krowicki, K., Balzarini, J., De Clercq, E., Newman, R. A., and Lown, J. W. (1988) Novel DNA groove binding alkylators: Design, synthesis and biological evaluation. *J. Med. Chem. 31*, 341–345.

(126) Lown, J. W. (1989) Synthetic chemistry of naturally occurring oligopeptide antibiotics and related lexitropsins. *Org. Prep. Proc. Int. 21*, 1–46.

(127) Bailly, C., Catteau, J.-P., Henichart, J.-P., Reszka, K., Shea, R. G., Krowicki, K., and Lown, J. W. (1989) Subcellular distribution of a nitroxide spin-labeled netropsin in living KB cells. *Biochem. Pharmacol. 38*, 1625–1630.

(128) Lown, J. W. (1990) Molecular mechanisms of DNA sequence recognition by groove binding ligands: biochemical and biological consequences. In *Molecular Basis of Specificity in Nucleic Acid–Drug Interaction* (B. Pullman, and J. Jortner Eds.) pp 103–122, Kluwer Academic Publishers, Dordrecht.

(129) Weiss, M. A., Ellenberger, T., Wobbe, C. R., Lee, J. P., Harrison, S. C., and Struhl, K. (1990) Folding transition in the DNA-binding domain of GCN4 on specific binding to DNA. *Nature, 347*, 575–578.

(130) Patel, L., Abate, C., and Curran, T. (1990) Altered protein conformation on DNA binding by Fos and Jun. *Nature 347*, 572–575.

(131) O'Neil, K. T., Hoess, R. H., and DeGrado, W. F. (1990) Design of DNA-binding peptides based on the leucine zipper motif. *Science 249*, 774–778.

(132) Talanian, R. V., McKnight, C. J., and Kim, P. S. (1990) Sequence-specific DNA binding by a short peptide dimer. *Science 249*, 769–771.

(133) Sartorius, J., Lehming, N., Kisters, B., von Wilcken-Bergmann, B., and Müller-Hill, B. (1989) Lac repressor mutants with double or triple exchanges in the recognition helix bind specifically to lac operator variants with multiple exchanges. *EMBO J. 8*, 1265–1270.

(134) Povsic, T. J., and Dervan, P. B. (1989) Triple helix formation by oligonucleotides on DNA extended to the physiological pH range. *J. Am. Chem. Soc. 111*, 3059–3061.

(135) Stein, C. A., and Cohen, J. S. (1988) Oligodeoxynucleotides as inhibitors of gene expression: a review. *Cancer Res. 48*, 2659–2668.

(136) Stirchak, P., Summerton, J. E., and Weller, D. D. (1989) Uncharged stereoregular nucleic acid analogs: 2. Morpholino nucleoside oligomers with carbamate internucleoside linkages. *Nucleic Acids Res. 17*, 6129–6141.

(137) Haralambidis, J., Angus, K., Pownall, S., Duncan, L., Chai, M., and Tregear, G. W. (1990) The preparation of polyamide–oligonucleotide probes containing multiple non-radioactive labels. *Nucleic Acids Res. 18*, 501–505.

(138) Haralambidis, J., Duncan, J., Angus, K., and Tregear, G. W. (1990) The synthesis of polyamide–oligonucleotide conjugate molecules. *Nucleic Acids Res. 18*, 493–499.

(139) Wakelin, L. P. G., Chetcutl, P., and Denny, W. A. (1990) Kinetic and equilibrium binding studies of asymmetrical DNA intercalating agents which bind by threading through the DNA helix. *J. Med. Chem. 33*, 2039.

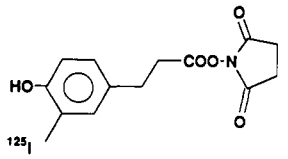
LETTERS

(*N*-Succinimidyl 4-pentynoate)hexacarbonyldicobalt: A Transition-Metal Carbonyl Complex Having Similar Uses to the Bolton–Hunter Reagent

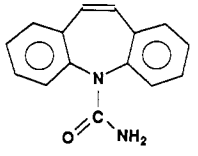
Michèle Salmain, Anne Vessières, Ian S. Butler,† and Gérard Jaouen*
Ecole Nationale Supérieure de Chimie de Paris, U.A. C.N.R.S 403, 11 rue Pierre et Marie Curie, 75231 Paris Cedex 05, France. Received November 27, 1990

The synthesis of the transition-metal carbonyl complex (*N*-succinimidyl 4-pentynoate)hexacarbonyldicobalt [$[(C_4H_4O_2N)O(CO)CH_2CH_2C{\equiv}CH]Co_2(CO)_6$] is described. This cobalt carbonyl complex is structurally similar to the Bolton–Hunter conjugation reagent and has been successfully employed as a *nonradioactive* tracer for labeling the drug carbamazepine. The metal carbonyl tracer can be detected at extremely low concentrations (ca. 1 pmol) by FT-IR spectroscopy in the ν(CO) region (2150–1800 cm^{-1}). The cobalt carbonyl labeled carbamazepine retains good recognition for anti-carbamazepine antibodies. This novel labeling procedure, which can be broadly termed *carbonylmetalloimmunoassay* (CMIA), has considerable potential for assaying a wide range of biological materials.

The labeling of biomolecules with radionuclides and other conjugates is an extremely important field for clinical diagnosis and there is a constant search for new and more sensitive analytical techniques for the detection of biological tracers (*1*). The Bolton–Hunter reagent, ^{125}I-labeled *N*-succinimidyl 3-(4-hydroxyphenyl)propionate (1), was the first conjugation species to be used extensively



1



4

to prepare high-activity, high-specificity, radiolabeled tracers for immunoassay (*2, 3*). However, chiefly because of the attendant legal and technical problems associated with ^{125}I and other radioisotopes (*4*), considerable effort is being placed nowadays into the development of *nonradioactive* tracers for clinical diagnosis.

In 1977, Cais et al. (*5*) introduced a nonradioactive *metalloimmunoassay* procedure in which bioligands labeled with organometallic groups were used for assaying the free bioligands. Several such studies have now been reported in which the metallic species are detected by atomic absorption (*6*) or electrochemically (*7*). Unfortunately, these detection techniques are often hampered by metal contamination of the biological materials being examined.

In our approach, biomolecules such as hormonal steroids (*8–10*) and mycotoxines (*11*) are labeled with various metal carbonyl fragments which can then be unambiguously detected by FT-IR spectroscopy in the ν(CO) region (2150–1800 cm^{-1}). The FT-IR sensitivity can be increased markedly by incorporating a liquid-nitrogen cooled, indium antimonide detector and by employing an ultralow-volume, gold light-pipe, solution cell (*12*). Our overall objective is to develop a new analytical technique for immunoassay, which we term *carbonylmetalloimmunoassay* (CMIA).

Labeled biomolecules that exhibit good molecular-recognition properties are usually synthesized by direct complexation of a reactive precursor (*13*). Indirect labeling of hormonal steroids with $Co_2(CO)_6$ fragments has been successful in certain cases due to the alkylating properties of carbenium ions (*10, 14*). At the present time, there are no direct or indirect methods of labeling polyfunctional molecules, such as proteins, with metal carbonyl fragments. We report here the synthesis of a cobalt carbonyl complex that is structurally similar to the Bolton–Hunter reagent (**3**) and describe its use in labeling the antiepileptic drug carbamazepine (**4**).

Compound **3** was prepared by reaction of *N*-succinimidyl 4-pentynoate (**2**) with $Co_2(CO)_8$ (Scheme I). Carbamazepine (**4**) was labeled as shown in Scheme II. This labeling can be done in various solvents, including water. In most direct-labeling experiments, the solvent is THF, in which many biological substances, especially proteins, are insoluble. There are three characteristic ν(CO) peaks for $Co_2(CO)_6$-labeled carbamazepine (**6**) in CCl_4 solution (Figure 1). The best correlation between the quantity of the marker injected into the IR cell (in the range 10^{-7}–10^{-5} M) and the intensities of the ν(CO) peaks is obtained for the 2052 cm^{-1} peak ($r = 0.998$), supporting the possibility of quantitative work. Approximately 1 pmol of **6** can be detected by the CMIA technique and this detection level

† Permanent address: Department of Chemistry, McGill University, 801 Sherbrooke St. West, Montreal, Quebec, Canada H3A 2K6.

1043-1802/91/2902-0013$02.50/0 © 1991 American Chemical Society

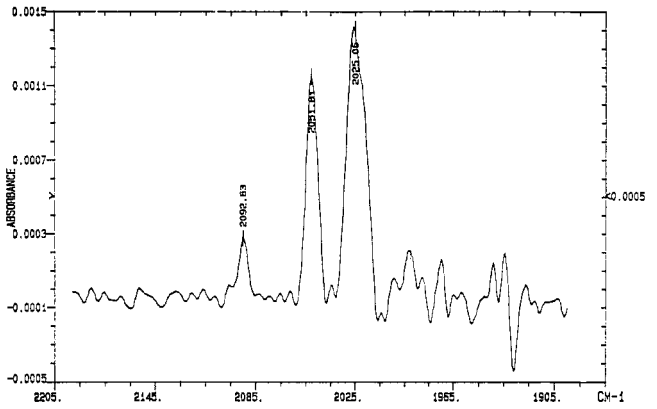
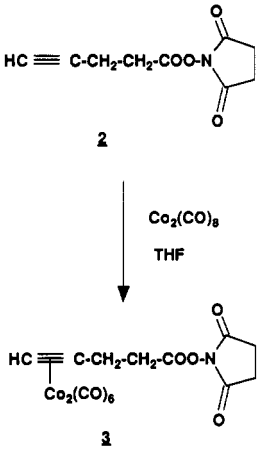
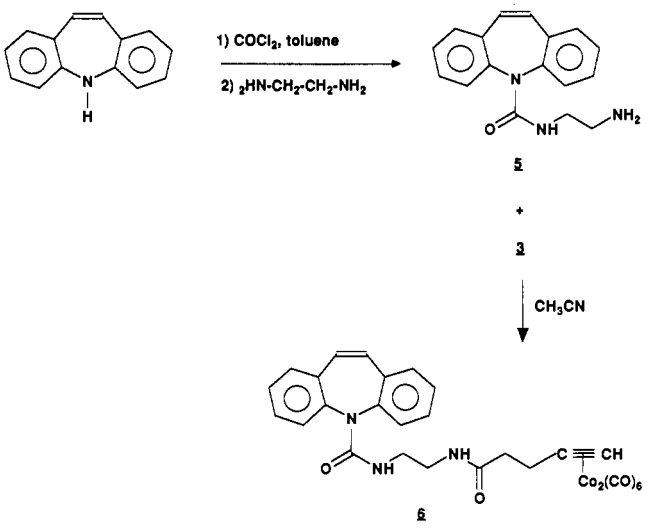


Figure 1. Expansion of the ν(CO) region of the FT-IR spectrum of **6** ($c = 10^{-7}$ M; 1.6 pmol injected; CCl_4 solution; 20-mm gold light-pipe cell; 10 scans; 4 cm^{-1} resolution).

Scheme I. Synthetic Scheme for the Preparation of 3



Scheme II. Synthetic Scheme for the Preparation of 6



appears to be the lowest ever reported for a solution-phase FT-IR experiment over such a short time period (10 scans, 4 cm^{-1} resolution, 66 s).

In a preliminary CMIA study using rabbit anti-carbamazepine antibodies, $Co_2(CO)_6$-labeled carbamazepine (**6**) as the tracer, and FT-IR detection of the ν(CO) mode at 2052 cm^{-1}, we have established that it is possible to perform a high-sensitivity immunoassay of carbamazepine (*15*). A typical standard immunoassay curve is obtained in the presence of 10 pmol of **6** and of 0–80 pmol of carbamazepine per tube. Under these conditions, 32 pmol of carbamazepine are required to displace 50% of the binding of **6** to the antibodies. For a physiological level of carbamazepine (*16*), only 2.5 μL of serum is necessary to perform the immunoassay. The affinity constant of the antibodies for **6** is 4.5×10^7 M^{-1}, while the number of binding sites is estimated to be 2.6×10^{-8} M. These results confirm the feasibility of a FT-IR immunoassay of carbamazepine. Finally, we have found that other methods can be used to label peptides with organometallic units, such as the complexation of norleucine acetylenic fragments (*17*), but the herein described conjugation procedure is particularly straightforward.

Experimental Procedures. All solvents were freshly distilled under argon. Infrared spectra were recorded on a Bomem Michelson 100 FT spectrometer equipped with an In/Sb detector and a beam condensor (to produce the required 1.0-mm IR microbeam). The NMR, UV–visible, and mass spectra were measured on a 250-MHz Bruker, a Kontron Uvikon 860, and a Nermag spectrometer, respectively.

(*N*-Succinimidyl 4-pentynoate)hexacarbonyldicobalt (3). 4-Pentynoic acid (200 mg, 2.0 mmol) and *N*-hydroxysuccinimide (230 mg, 2.0 mmol) were added to a solution of dicyclohexylcarbodiimide (DCC, 500 mg, 2.4 mmol) in THF (5 mL) at −10 °C. The mixture was stirred at −10 °C for 2 h and was then allowed to warm up to ambient temperature overnight. Acetic acid (25 μL) was added and the dicyclohexylurea which formed was removed by filtration. The filtrate was stripped down to give a white product, *N*-succinimidyl 4-pentynoate (**2**) (ca. 400 mg): IR (KBr) $\nu(CH_2)$ 2933 (s), 2853 (s), ν(C≡C) 2114, ν(CO) 1815 (s), 1786 (s), 1728 (s) cm^{-1}. Two-hundred milligrams (1.0 mmol) of **2** was dissolved in THF (7 mL), and $Co_2(CO)_8$ (350 mg, 1.2 mmol) was added. The reaction mixture was stirred at room temperature for 1 h. The solvent was almost completely evaporated off under reduced pressure, and the residue remaining was chromatographed on a silica gel TLC plate (Kieselgel 60 GF 254) using ether/pentane (1/1) as eluent. The crude product ($R_f = 0.4$) recovered from the TLC plate was recrystallized from the same solvent mixture at −20 °C to yield bright-purple crystals of **3** (150 mg, 31%; mp 62 °C): ^{1}H NMR (acetone-d_6) δ 2.90 (s, 4 H of cycle), 3.05 (t, 2 H, ^3J = 7.3 Hz, $C(O)CH_2$), 3.39 (t, 2 H, ^3J = 7.3 Hz, CCH_2), 6.52 ppm (t, 1 H, ^4J = 1.0 Hz, HC≡C); IR (KBr) ν(CO) 2099 (s), 2046 (s), 2006 (s), 1996 (sh) cm^{-1}; UV–vis (MeOH) 406 (ϵ_{max} = 640), 347 (ϵ_{max} = 3070), 207 nm (ϵ_{max} = 23 600); MS (DCI/NH_3) base peak m/e = 499 (MNH_4^+).

5-[*N*-(2-Aminoethyl)carbamoyl]-5*H*-dibenz[*b,f*]azepine (5) was prepared essentially according to the literature method (*18*), except that a 4-fold excess of ethylenediamine was added. Compound **5** was obtained as a beige powder (1.31 g, 47% yield): ^{1}H NMR (CD_3OD) δ 2.61 (t, 2 H, ^3J = 5.0 Hz, H_2NCH_2), 3.10 (t, 2 H, ^3J = 5.0 Hz, CH_2NH), 6.93 (s, 2 H, vinylic), 7.39 ppm (s, 8 H, aromatic); IR (KBr) ν(NH) 3360, ν(CO) (ketone) 1660, ν[amide(II)] 1510, ν(CN) 1319, 798 cm1–1; UV–vis (EtOH) 282 (ϵ_{max} = 8910), 238 (ϵ_{max} = 12 360), 216 nm (ϵ_{max} = 24 540); MS (DCI/NH_3) base peak m/e = 280 (MH^+).

[5-[*N*-[2-(4-Pentynamido)ethyl]carbamoyl]-5*H*-dibenz[*b,f*]azepine]hexacarbonyldicobalt (6). Acetonitrile solutions of **3** (48 mg, 0.1 mmol, 1.0 mL) and **5** (30 mg, 0.1 mmol, 4 mL) were stirred together at 4 °C for 3.5 h. The reaction mixture was chromatographed on silica preparative TLC plates with ether/ethyl acetate (2/1) as eluent. The product ($R_f = 0.67$) was scraped off the TLC plate and was recrystallized from CH_2Cl_2/hexane (7/1) as a brick-red powder (22 mg, 50% yield): ^{1}H NMR (CD_3COCD_3) δ 1.28 and 5.46 (s, large, NH), 2.50 (t, 2 H, ^3J =

7.9 Hz, CH_2), 3.20 (m, 6 H, CH_2), 6.98 (s, 2 H, vinylic), 7.39 ppm (m, 8 H, aromatic); IR (KBr disk) ν(NH) 3310, ν(CO) 2092 (s), 2050 (vs), 2017 (vs), ν(CO) (ketone) 1650, ν[amide-(II)] 1510, ν[amide(VI)] 518 cm^{-1}; UV–vis (EtOH) 347 (ϵ_{max} = 2130), 225 (ϵ_{max} = 28 290).

ACKNOWLEDGMENT

This research was performed in part under the auspices of a France–Quebec Exchange (Biotechnology). Operating grants in partial support of the research from ANVAR, CNRS, and Région Bourgogne are also acknowledged.

LITERATURE CITED

(1) Schall, R. F., and Tenoso, H. J. (1981) Alternatives to Radioimmunoassay Labels and Methods. *Clin. Chem. 27*, 1157–1164.

(2) Bolton, A. E., and Hunter, W. M. (1973) The Labelling of Proteins to High Specific Activities by Conjugation to a ^{125}I-containing Acylating Agent. *Biochem. J. 133*, 529–539.

(3) Langone, J. J. (1980) Radioiodination by the Use of the Bolton–Hunter and Related Reagents. *Methods Enzymol. 70*, 221–243.

(4) Gosling, J. P. (1990) A Decade of Development in Immunoassay Methodology. *Clin. Chem. 36*, 1408–1427.

(5) Cais, M., Dani, S., Eden, Y., Gandolfi, O., Horn, M., Isaacs, E. E., Josephy, Y., Saar, Y., Slovin, E., and Snarsky, L. (1977) Metalloimmunoassay. *Nature 270*, 534–535.

(6) (a) Cais, M., Slovin, E., and Snarsky, L. (1978) Iron-Metallohaptens from Estrogen Steroids. *J. Organomet. Chem. 160*, 223–230. (b) Cais, M. (1983) Metalloimmunoassay: Principles and Practice. *Methods Enzymol. 92*, 445–458. (c) Cheret, P. (1987) Ph.D. Thesis, Université de Bourgogne.

(7) Kricka, L. J. (1985) Ligand-Binder Assays: Labels and Analytical Strategies, Marcel-Dekker, New York and Basel.

(8) Butler, I. S., Vessières, A., and Jaouen, G. (1989) Application of Organotransition Metal Carbonyl Complexes as Infrared Markers for Hormonal Steroids in Biological Processes. *Comments Inorg. Chem. 8*, 269–286.

(9) Vessières, A., Top, S., Ismail, A. A., Butler, I. S., Loüer, M., and Jaouen, G. (1988) Organometallic Estrogens: Synthesis, Interaction with Lamb Uterine Estrogen Receptor, and Detection by Infrared Spectroscopy. *Biochemistry 27*, 6659–6666.

(10) Vessières, A., Jaouen, G., Gruselle, M., Rossignol, J. L., Savignac, M., Top, S., and Greenfield, S. (1988) Synthesis and Receptor Binding of Polynuclear Organometallic Estradiol Derivatives. *J. Steroid Biochem. 30*, 301–305.

(11) Gruselle, M., Deprez, P., Vessières, A., Greenfield, S., Jaouen, G., Larue, J.-P., and Thouvenot, D. (1989) Cobalt and Molybdenum Carbonyl Clusters in Immunology. Synthesis and Binding Properties of Mycotoxin Derivatives of Zearalenone. *J. Organomet. Chem. 359*, C53–C56.

(12) Vessières, A., Jaouen, G., Salmain, M., and Butler, I. S. (1990) An Ultra-low Volume, Gold Light-pipe Cell for the IR Analysis of Dilute Organic Solutions. *Appl. Spectrosc. 44*, 1091–1094.

(13) See, for example: Zalutsky, M. R., Noska, M. A., Colapinto, E. V., Garg, P. K., and Bigner, D. D. (1989) Enhanced Tumor Localization and in Vivo Stability of a Monoclonal Antibody Radioiodinated Using *N*-Succinimidyl 3-(Tri-*n*-stannyl)benzoate. *Cancer Res. 49*, 5543–5549.

(14) Gruselle, M., Greenfield, S., and Jaouen, G. (1987) The Selective Introduction of Organometallic Markers into Oestrogens. C-16 prop-2-ynylation of Oestrone. *J. Chem. Soc. Chem. Commun.* 1353–1355.

(15) Salmain, M. (1990) Ph.D. Thesis, Université de Paris VI.

(16) Kutt, K. Clinical Pharmocology of Carbamazepine. In Pippenger, C. E., Penry, J. K., and Kutt, K. (Eds.) (1978) *Antiepileptic Drugs: Quantitative Analysis and Interpretation*, pp 297–305, Raven Press, New York.

(17) (a) Sasaki, N. A., Potier, P., Savignac, M., and Jaouen, G. (1988) Organometallic Derivatives of Peptides: Application to Peptide Receptor Analysis *Tetrahedron Lett. 29*, 5759–5762. (b) Le Borgne, F., and Beaucourt, J. P. (1988) Cobalt Carbonyl Complexes of Some Peptides as Infrared Markers. *Tetrahedron Lett. 29*, 5649–5652.

(18) Sidki, A. M., Landon, J., and Rowell, F. (1984) Influence of the Hapten-Fluorophore Bridge on Binding Parameters in a Fluoroimmunoassay for Carbamazepine. *Clin. Chem. 30*, 1348–1352.

ARTICLES

Production of Macrophage-Derived Cytotoxic Factor by *N*-[3-[(Carbamoylmethyl)thio]propionylated] Neoglycoproteins

Pascal Breton, Patrick Midoux, Claire Petit, Marie-Thérèse Bousser, Annie Claude Roche, Roger Mayer, and Michel Monsigny*

Laboratoire de Biochimie des Glycoconjugués et Lectines Endogènes, Centre de Biophysique Moléculaire CNRS, INSERM and Université d'Orléans, 1 Rue Haute, F-45071 Orléans Cedex 2, France. Received December 28, 1990

6-Phosphomannosylated bovine serum albumin (Man6P-BSA), a neoglycoprotein endocytosed by macrophages, bearing either 3-(2-pyridyldithio)propionyl or 3-[(carbamoylmethyl)thio]propionyl residues coming from alkylation of thiol residues by iodoacetamide were prepared and tested for their immunomodulator properties. The supernatants of mouse peritoneal macrophages incubated with Man6P-BSA bearing 3-[(carbamoylmethyl)thio]propionyl groups, and by a lesser extent 3-(2-pyridyldithio)-propionyl groups, were cytotoxic to L929 cells, suggesting the presence of a tumor necrosis factor like compound. This macrophage-activation process is linked to the capacity of Man6P-BSA to be endocytosed via membrane lectins of macrophages, because the supernatants of macrophages incubated with unglycosylated conjugates were not cytotoxic. The cytotoxic activity induced by 3-[(carbamoylmethyl)thio]propionyl groups bound onto Man6P-BSA was similar to that induced by Man6P-BSA bearing muramyl dipeptide, indicating that endocytosed neoglycoproteins bearing 3-[(carbamoylmethyl)-thio]propionyl residues are potent macrophage activators.

INTRODUCTION

Muramyl dipeptide[1] (MDP) is the smallest fragment of the bacterial cell wall known to render macrophages cytostatic and cytotoxic against tumorigenic target cells (*1*). Recently we synthesized a series of acyl pseudopeptide analogues of muramyl dipeptide (*2, 3*). We have studied their capacity to activate macrophages inducing the release of cytotoxic factors and we found that some derivatives without the muramyl moiety were more active than MDP (*2*). Because macrophages are devoid of cell surface receptors for MDP (*4, 5*) and knowing that MDP is at least 100 times more efficient when it is coupled to a macromolecular carrier (mannosylated serum albumin and polymer) recognized by membrane lectins of macrophages (*6-8*) than when it is free, the selected pseudopeptides were targeted to macrophages after coupling them onto 6-phosphomannosylated bovine serum albumin (Man6P-BSA). The pseudopeptides which possess an amino group instead of a carboxylic group were coupled onto glycosylated carriers via a disulfide bridge by using the heterobifunctional reagent SPDP (*9*). Surprisingly, an inactive pseudopeptide bound to Man6P-BSA by using this method was found as efficient as the active one bound to the same ligand. Man6P-BSA modified by PDP groups (introduced to allow conjugation with the pseudopeptide) was also found to induce the release of cytotoxic factors by macrophages. These surprising results prompt us to examine the effect of the carrier modifications introduced for the coupling of the pseudopeptide onto its carrier on the macrophage activation.

We showed that Man6P-BSA bearing *N*-[3-[(carbamoylmethyl)thio]propionyl] (CMTP, $COCH_2CH_2SCH_2CONH_2$) groups generated after alkylation of thiol functions by iodoacetamide was a potent macrophage activator when the conjugates are efficiently internalized by the membrane lectins of macrophages.

EXPERIMENTAL PROCEDURES

Chemicals. Bovine serum albumin (BSA) and Trisacryl GF05 were purchased from IBF-Biotechnics (Villeneuve-la-Garenne, France); *N*-succinimidyl 3-(2-pyridyldithio)-propionate (SPDP) and iodoacetamide were from Pierce (Rockford, IL, USA); dithiothreitol (DTT) was from Serva (Heidelberg, FRG); all buffers were extemporaneously prepared and abundantly outgassed under reduced pressure. BSA bearing 16 *N*-[[*p*-(*O*-6-phospho-α-D-mannopyranosyl)phenyl]thioamidyl] residues ($Man6P_{16}$-BSA) was prepared as previously described (*10*). Muramyl dipeptide (MDP) was synthesized according to ref 11 and $(Man6P)_{16}$-BSA bearing eight MDP residues [$(Man6P)_{16}$-,-$(MDP)_8$-BSA] was prepared as previously described (*6*).

Preparation of *N*-[3-(2-Pyridyldithio)propionylated] Protein and Neoglycoprotein [$(Man6P)_{16}$-,-$(PDP)_{15}$-BSA and of $(PDP)_{15}$-BSA]. To 20 mg of $(Man6P)_{16}$-BSA or BSA in 1 mL of 0.1 M borate buffer (pH 8.6) was added SPDP (4 mg; 12.8 μmol) in 130 μL of ethanol and the mixture was stirred for 20 h at 20 °C. $(Man6P)_{16}$-,$(PDP)_{15}$-BSA was purified by gel filtration on Trisacryl GF05 eluted by PBS followed by gel purification on Trisacryl GF05 in H_2O/1-butanol (95:5; v/v) and then freeze-dried. $(PDP)_{15}$-BSA was purified by gel filtration on Trisacryl GF05 in H_2O/1-butanol (95:5; v/v) and then freeze-dried. Fifteen PDP groups were coupled to $(Man6P)_{16}$-BSA and BSA as determined from absorbance at 343 nm in the presence of DTT (*9*).

* To whom reprint request should be addressed.

[1] Abbreviations: CMTP, 3-[(carbamoylmethyl)thio]propanoyl; BSA, bovine serum albumin; DTT, dithiothreitol; LDL, low-density lipoprotein; LPS, lipopolysaccharide; Man6P, *N*-[[*p*-(*O*-6-phospho-α-D-mannopyranosyl)phenyl]thioamidyl]; MDP, muramyl dipeptide; PBS, phosphate-buffered saline; PDP, 3-(2-pyridylthio)propionyl; SPDP, *N*-succinimidyl 3-(2-pyridyldithio)propionate; TNF, tumor necrosis factor.

1043-1802/91/2902-0016$02.50/0 © 1991 American Chemical Society

Preparation of *N*-[3-[(Carbamoylmethyl)thio]-propionylated] Protein and Neoglycoprotein [$(Man6P)_{16}$–,$(CMTP)_{15}$–BSA and $(CMTP)_{15}$–BSA)]. Ten milligrams of $(Man6P)_{16}$–,$(PDP)_{15}$–BSA or $(PDP)_{15}$–BSA in 0.1 M citrate–phosphate buffer (pH 5.3) was treated with DTT (25 mM final concentration) at 20 °C for 30 min. DTT and other small molecules were eliminated by gel filtration on Trisacryl GF05 eluted by the same citrate–phosphate buffer outgassed by bubbling nitrogen. Free thiol groups of proteins reacted with iodoacetamide (1% final concentration) for 1 h at 20 °C, the pH being adjusted to 7.5 with a 0.2 M sodium carbonate solution. The solution volume was reduced by freeze-drying. $(Man6P)_{16}$–,-$(CMTP)_{15}$–BSA and $(CMTP)_{15}$–BSA were finally purified on Trisacryl GF05 columns as described above.

Macrophage Supernatants. (C57BL/6 × Balb/c) F_1 mice (6–7 weeks old) purchased from CSEAL (Orléans, France) were injected ip with 2 mL of thioglycolate medium (Institut Pasteur, Paris, France). Four days later, peritoneal macrophages were harvested by lavages of the peritoneal cavity and identified by neutral red uptake, as previously described (*6*). Thioglycolate-elicited peritoneal macrophages (2.5×10^5) were plated in 16 mm diameter well of multiwell plates (Falcon, Becton-Dickinson, Sunnyvale, CA) in serum-free RPMI medium. Upon 2-h incubation at 37 °C in a humidified atmosphere containing 5% CO_2, nonadherent cells were discarded; adherent cells were cultured in 0.5 mL of serum-free RPMI medium supplemented with antibiotics and L-glutamine and in the presence or absence of 100 μg/mL stimulating agents; incubations were conducted in the presence of 10 μg/mL polymyxin B (Sigma, St. Louis, MO). Culture supernatants were collected after 24-h incubation at 37 °C. Before testing, supernatants were rendered cell-free by centrifugation at 2000*g* for 10 min.

Cytotoxic Factor Assay. The cytotoxic activity of macrophage culture supernatants was determined according to ref 12. Briefly, L929 cells (kindly given by Dr. C. De Chastellier, Institut Pasteur, Paris, France) in exponential phase growth were pretreated with 2 μg/mL actinomycin D (Calbiochem, La Jolla, CA) for 2 h at 37 °C in a humidified atmosphere containing 5% CO_2 (*13*). Actinomycin D pretreated L929 (actD-L929) cells were collected after trypsin treatment, and seeded in 96-well microplates (4×10^4 cells suspended in 0.05 mL serum-free RPMI medium per well). After 3–4 h at 37 °C, diluted supernatants from stimulated macrophages were added (0.05 mL) and the actD-L929 cells were further incubated at 37 °C for 18–20 h in a humidified atmosphere with 5% CO_2. Three wells containing cells treated under identical conditions were used. Microplates were washed with PBS and the percentage of cell lysis was determined after staining the cells with 0.05 mL of crystal violet (0.2% in 2% ethanol). The plates were then washed with tap water and the dye was solubilized by adding 0.05 mL/well of 0.3% sodium dodecyl sulfate. Absorbance of each well was read at 570 nm on Dinatech Micro-Elisa autoreader (Artek System Corp., Farmingdale, NY). Percent cytotoxicity was calculated according to

$$(A_{NS} - A_S)/A_{NS} \times 100$$

where A_{NS} and A_S were the absorbances of wells containing target cells incubated with supernatant dilutions of non-stimulated and stimulated macrophages, respectively. All experiments were conducted four times under identical conditions. Results from single experiments were expressed as mean values of triplicate determinations. Results from different experiments were very similar. All cell lines were regularly checked under fluorescence microscope to detected putative mycoplasma contamination by using either bisbenzimidazole (*14*) or a benzoxazinone derivative (*15*).

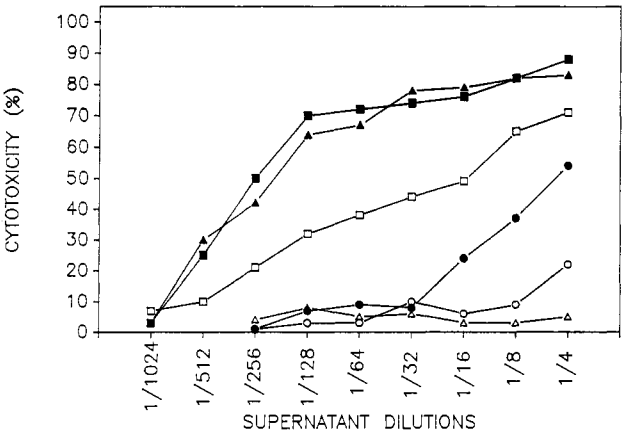


Figure 1. Thioglycolate-elicited peritoneal macrophages were incubated at 37 °C for 24 h in the presence of polymyxin B with either 100 μg/mL $(Man6P)_{16}$–,$(MDP)_8$–BSA (■), $(Man6P)_{16}$–$(CMTP)_{16}$–BSA (▲), $(Man6P)_{16}$–,$(PDP)_{15}$–BSA (□), $(CMTP)_{15}$–BSA (○), $(PDP)_{15}$–BSA (●), or $(Man6P)_{16}$–BSA (△). Cytotoxic activity was then tested with the corresponding supernatants incubated 18–20 h with actD-L929 cells. Cytolysis was assessed by counting viable cells upon crystal violet coloration. Supernatants were collected from two wells and a triplicate cytolysis assay was performed (mean deviation < 10%).

RESULTS

Effects of PDP and CMTP Conjugates on the Macrophage Cytotoxicity. $(Man6P)_{16}$–BSA and BSA were substituted upon reaction with SPDP by 15 3-(2-pyridyldithio)propionyl groups [$(Man6P)_{16}$–,$(PDP)_{15}$–BSA and $(PDP)_{15}$–BSA]. These conjugates, after treatment with DTT to generate thiol groups, were reacted at neutral pH with iodoacetamide to give $(Man6P)_{16}$–BSA and BSA bearing 15 3-[(carbamoylmethyl)thio]propionyl groups $(Man6P)_{16}$–,$(CMTP)_{15}$–BSA and $(CMTP)_{15}$–BSA, respectively. Mouse thioglycolate-elicited peritoneal macrophages were incubated at 37 °C in the presence of 100 μg/mL of each conjugate. The incubations were performed in the presence of polymyxin B to avoid side effects due to LPS contamination in serum, medium, or sample preparations. The culture supernatants were collected after 24 h and their cytotoxicity activities were tested on a tumor necrosis factor (TNF) sensitive L929 cell line. Supernatants from macrophages incubated with $(Man6P)_{16}$–,$(CMTP)_{15}$–BSA were found as cytotoxic as $(Man6P)_{16}$–,$(MDP)_8$–BSA on actD-L929 cells: 50% cytotoxicity dose was obtained at $^1/_{200}$ supernatant dilution (Figure 1). Supernatants from macrophages incubated with $(Man6P)_{16}$–,$(PDP)_{15}$–BSA were found to be less cytotoxic: 50% cytotoxicity dose was obtained at $^1/_{16}$ supernatant dilution (Figure 1). Under the same conditions, supernatants from macrophages incubated with $(Man6P)_{16}$–BSA or $(PDP)_{15}$–BSA or $(CMTP)_{15}$–BSA did not induce cytotoxicity against actD-L929 cells (Figure 1). The viability and the growth of L929 cells were not affected when they were cultured in medium containing 100 μg/mL of either $(Man6P)_{16}$–,$(PDP)_{15}$–BSA or $(Man6P)_{16}$–,$(CMTP)_{15}$–BSA (data not shown). As a further control, $(Man6P)_{16}$–BSA was incubated with iodoacetamide and purified by gel filtration under the same conditions described for the preparation of $(Man6P)_{16}$–,$(CMTP)_{15}$–BSA. The culture supernatants of macrophages collected after incubation with this iodoacetamide-treated $(Man6P)_{16}$–BSA were tested on actD-L929 cells and the cytotoxicity was as low as that obtained

with supernatants from macrophages incubated in the presence of $(Man6P)_{16}$–BSA or $(PDP)_{15}$–BSA or $(CMTP)_{15}$–BSA (data not shown). This result indicated that the cytotoxic effect of $(Man6P)_{16}$–,$(CMTP)_{15}$–BSA was not due to traces of iodoacetamide nor to modifications of $Man6P_{16}$–BSA in the presence of iodoacetamide.

DISCUSSION

These results demonstrated that supernatants from macrophages incubated with 6-phosphomannosylated BSA bearing 3-[(carbamoylmethyl)thio]propionyl (CMTP) and in a less extent 3-(2-pyridyldithio)propionyl(PDP) groups can provide a signal to render macrophages cytotoxic for actD-L929 cells. The cytotoxic effect was due to 3-[(carbamoylmethyl)thio]propionyl or 3-(2-pyridyldithio)propionyl groups linked to lysine residues of BSA bearing Man6P residues, a neoglycoprotein endocytosed by macrophages via membrane lectins. Macrophages did not possess receptor for *N*-[3-[(carbamoylmethyl)thio]propionyl] groups as evidenced by the inefficiency of BSA bearing *N*-[3-[(carbamoylmethyl)thio]propionyl] groups to render macrophages cytotoxic for L929 cells. Modified proteins such as LDL in which lysine residues have been modified by acetylation, maleylation, or succinylation bind to the scavanger receptor of macrophages (*16*) and specially maleylated BSA which binds to this receptor were effective in rending macrophages cytotoxic (*17*). In this case a specific cell surface receptor was implicated. Like MDP, macrophage activation by 3-[(carbamoylmethyl)thio]propionyl group required its internalization into macrophages which was performed with specific carrier such as BSA bearing mannose 6-phosphate residues specifically recognized by membrane lectins whereas unglycosylated BSA was totally ineffective. Recently, Petit et al. reported that MDP linked to Man6P–BSA or Man–BSA induced the release of tumor necrosis factor (TNF) by macrophages (*18*). The cytotoxic effect of macrophages incubated with $(Man6P)_{16}$–,$(CMTP)_{15}$–BSA (50% cytotoxicity at $^1/_{200}$ supernatant dilution) was close to that obtained with $(Man6P)_{40}$–,$(MDP)_8$–BSA (50% cytotoxicity at $^1/_{256}$ supernatant dilution) (*18*). As in the case of MDP, the cytotoxic factor released by peritoneal macrophages stimulated by $(Man6P)_{16}$–,$(CMTP)_{15}$–BSA could be TNF.

In conclusion, proteins bearing 3-(2-pyridyldithio)propionyl or 3-[(carbamoylmethyl)thio]propionyl groups can induced the release by macrophages of cytotoxic factors if they are internalized by macrophages. Thereby, the heterobifunctional reagent SPDP used to link active molecules or drugs onto macromolecular carriers must be taken with care. This activation process is linked to the capacity of the carrier to be endocytosed. A 3-[(carbamoylmethyl)thio]propionyl group linked on the ϵ-amino group of lysine of BSA bearing mannose 6-phosphate residues is an immunoactivator much less expensive than but as efficient as MDP bound to the same carrier.

ACKNOWLEDGEMENT

P.B. received a fellowship from MRT. P.M. and A.C.R. are Chargé and Directeur de Recherche INSERM, respectively.

LITERATURE CITED

(1) Adam A., Petit, J.-F., Lefrancier, P., and Lederer, E. (1981) Muramylpeptides: chemical structure, biological activity and mechanism of action. *Mol. Cell. Biochem. 41*, 27–47.
(2) Breton, P. (1989) Synthesis and characterization of putative macrophage activators: pseudopeptide analogues of muramyl dipeptide. Thesis, Orléans, France.
(3) Breton, P., Monsigny, M., and Mayer, R. (1990) Synthesis of new acylpseudopeptides analogous to N-acetylmuramyl dipeptide (MDP). *Tetrahedron 46*, 4265–4276.
(4) Tenu, J. P., Roche, A. C., Yapo, A., Kieda, C., Monsigny, M., and Petit, J. F. (1982) Absence of cell surface receptors for muramylpeptides in mouse peritoneal macrophages. *Biol. Cell 44*, 157–164.
(5) Fogler, W. E., and Figler, I. J. (1986) The activation of tumoricidal properties in human blood monocytes by muramyl dipeptide requires specific intracellular interaction. *J. Immunol. 136*, 2311–2317.
(6) Monsigny, M., Roche, A. C., and Bailly, P. (1984) Tumoricidal activation of murine alveolar macrophages by muramyldipeptide substituted mannosylated serum albumin. *Biochem. Biophys. Res. Commun. 121*, 579–584.
(7) Roche, A. C., Bailly, P., and Monsigny, M. (1985) Macrophage activation by MDP bound to neoglycoproteins: metastasis eradication in mice. *Invasion Metastasis 5*, 218–232.
(8) Derrien, D., Midoux, P., Petit, C., Nègre, E., Mayer, R., Monsigny, M., and Roche, A. C. (1989) Muramyl Dipeptide Bound to Poly-L-Lysine Substituted with Mannose and Gluconoyl Residues as Macrophage Activators. *Glycoconjugates J. 6*, 241–255.
(9) Carlsson, J., Drevin, H., and Axen, R. (1978) Protein thiolation and reversible protein-conjugation. *N*-succinimidyl 3-(2-pyridyldithio)propionate, a new heterobifunctional reagent. *Biochem. J. 173*, 723–737.
(10) Roche, A. C., Midoux, P., Bouchard, P., and Monsigny, M. (1985) Membrane lectins on human monocytes. Maturation-dependent modulation of 6-phosphomannose and mannose receptors. *FEBS Letters 193*, 63–68.
(11) Merser, C., Sinay, P., and Adam, A. (1975) Total synthesis and adjuvant activity of bacterial peptidoglycan derivatives. *Biochem. Biophys. Res. Commun. 66*, 1316–1322.
(12) Fish, H., and Gifford, G. E. (1983) A photometric and plaque assay for macrophage mediated tumor cell cytotoxicity. *J. Immunol. Methods 57*, 311–325.
(13) Ostrove, J. M., and Gifford, G. E. (1979) Stimulation of RNA synthesis in L929 cells by rabbit tumor necrosis factor. *Proc. Soc. Exp. Biol. Med. 160*, 354–358.
(14) Chen, T. R. (1977) In situ detection of mycoplasma contamination in cell cultures by fluorescent Hoescht 33258 stain. *Exp. Cell Res. 104*, 255–262.
(15) Monsigny, M., Midoux, P., Depierreux, C., Le Bris, M. T., and Valeur, B. Benzoxazinone kanamycin A conjugate. A new fluorescent probe suitable to detect mycoplasma in cell culture. *Biol. Cell*, in press.
(16) Brown, M. S., and Goldstein, J. L. (1983) Lipoprotein metabolism in the macrophage: implications for cholesterol deposition in atherosclerosis. *Annu. Rev. Biochem. 52*, 223–261.
(17) Somers, S. D., Hamilton, T. A., and Adams, D. O. (1987) Maleylated bovine serum albumin triggers cytolytic function in selected populations of primed murine macrophages. *J. Immunol. 139*, 1361–1368.
(18) Petit, C., Monsigny, M., and Roche, A. C. (1990) Macrophages activation by muramyldipeptide bound to neoglycoproteins and glycosylated polymers: Cytotoxic factor production. *J. Biol. Response Modif. 9*, 33–43.

Highly Fluorochrome Labeled Gene Probes for Quantitative Tracing of RNA in Individual Cells by in Situ Hybridization

Katharina Pachmann,*,† Klaus Reinecke,‡ Bertold Emmerich,† and Eckhard Thiel§

Medizinische Klinik Innenstadt, University of München, München, Germany, GSF Institute for Immunology, München, Germany, and Klinikum Steglitz, Berlin, Germany. Received June 1, 1990

A new method is presented for preparing highly fluorochrome labeled gene probes suitable for in situ hybridization. For this purpose fluorochromes were attached to a synthetic polypeptide, which was then coupled covalently to various gene probes. The advantage of the reported method is its high labeling efficiency and the easy coupling procedure. The method allows rapid and quantitative detection of homologous RNA at the single cell level. Optimal conditions for the hybridization of fluorochrome-labeled gene probes were established microfluorimetrically, and the specificity and sensitivity of the method were tested. Quantitation of the RNA with a fluorochrome-labeled gene probe in situ in individual cells allows determination of the degree of gene activation in individual cells and may thus provide a new tool for investigation of normal and malignant cells with respect to activation of genes controlling differentiation and proliferation.

INTRODUCTION

Transcriptional processes play a central part in cell proliferation and differentiation. Quantification of the transcription product, the mRNA, may supply important information concerning maturation of normal and malignant cells. Biochemical methods routinely used for investigation of such processes (*1*) require large and uniform populations for analysis. In addition, by blot hybridization, mRNA content can be determined only from whole populations.

In situ hybridization, in contrast, is applicable to relatively small cell populations and can also yield results in heterogeneous populations. Moreover, it allows for identification and location of the RNA of interest in individual cells. Conventional methods (*2*, *3*) using radioactively labeled gene probes are hazardous to handle, time consuming, require special precautions, and do not provide quantitative results. Attempts have been made to develop alternative methods (*4–10*). Here we present a method employing spacer molecules by which an amplification effect is obtained, allowing attachment of many fluorochromes to a gene probe, in contrast to a method previously published by us (*11*) which only allowed attachment of one fluorochrome molecule per probe molecule by end labeling. The labeling procedure is rapid and easy and can be traced by fluorescence microscopy immediately and, in addition, offers the possibility of quantifying the results. Quantitation of the RNA of genes coding for receptor molecules, as well as oncogenes, and even viral RNA may thus be performed at the single-cell level.

EXPERIMENTAL PROCEDURES

Buffers and Solutions. For fluorochrome coupling a 0.5 M carbonate buffer, adjusted to pH 9.5, was used; other solutions and buffers used were PBS[1] containing 0.14 M NaCl and 0.01 M sodium phosphate, pH 7.4; 1 × SSC containing 0.15 M NaCl, 0.015 M sodium citrate, pH 7.5; and TE buffer consisting of 10 mM Tris, 1 mM EDTA, pH 7.4. The hybridization buffer consisted of a mixture of 10 mM Tris HCl (Sigma), pH 7.5, 1 mM EDTA (Sigma), 600 mM NaCl, 0.02% Ficoll (Sigma), and 0.02% polyvinylpyrollidone (Sigma), and according to the experimental conditions, 50% deionized formamide (Merck, Darmstadt) was added or omitted.

Labeling of the Spacer Molecule with FITC.[2] The principle of the method for labeling is shown in Figure 1a. Fluorochrome molecules are attached to a spacer and amplifier molecule, a synthetic polypeptide PEI[3] (Serva, median molecular weight 30 000–40 000), by using a method described by Goldman for conjugating proteins with fluorochromes (*12*) (see step 1 in Figure 1). The fluorochrome FITC was obtained from Fluka (Buchs); 1 mL of polypeptide solution (5 mg/mL) in carbonate buffer was incubated with 7.5–20 μg of FITC dissolved in 1 mL of carbonate buffer for 1 h at room temperature. To remove excess fluorochrome, the conjugated polypeptide was purified over a 0.6 × 25 cm Sephadex G25 (Pharmacia) column which had been equilibrated with PBS. Elution was performed with PBS and the first yellow fraction containing the fluorochrome-labeled PEI was collected. With measurement of the absorbance at 280 nm for the peptide and 490 nm for FITC, the degree of labeling could be deduced from a nomograph (*13*).

Since high labeling of the polypeptide results in nonspecific binding of the labeled complex to cellular components via electrostatic forces (*14*), the concentration of FITC at which no visible binding of the FITC–PEI[4] conjugate to cell preparations occurred was determined. We found that if FITC was added to the reaction mixture at concentrations exceeding 2 μg/mg of PEI, leading to a

* Address correspondence to Katharina Pachmann, Med Klinik Innenstadt, Ziemssenstr 1, D-8000 München 2, Germany.
† Medizinische Klinik Innenstadt.
‡ GSF Institute for Immunology.
§ Klinikum Steglitz.

[1] PBS: phosphate-buffered salt solution.
[2] FITC: fluorescein isothiocyanate.
[3] PEI: polyethylenimine.
[4] FITC–PEI: fluorescein isothiocyanate conjugated to polyethylenimine.

1043-1802/91/2902-0019$02.50/0 © 1991 American Chemical Society

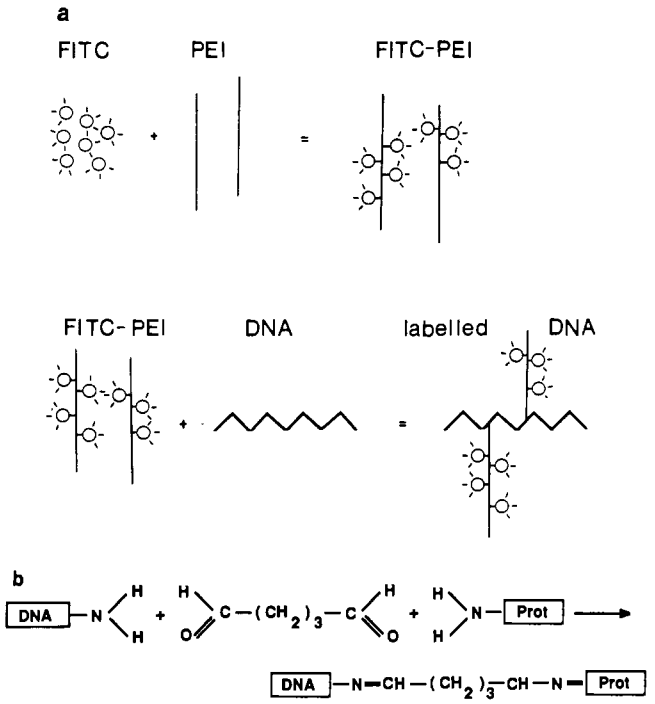


Figure 1. (a) Schematic drawing of the principle for labeling gene probes. Step 1: fluorochrome (FITC) is coupled to the polypeptide (PEI). Step 2: the fluorochrome-labeled polypeptide is attached to the DNA probe. (b) Assumed coupling mechanism with the glutaraldehyde is shown.

binding of more than four molecules FITC/PEI molecule, this resulted in visually observable nonspecific fluorescence.

In a second step the fluorescinated PEI was coupled to the DNA probe (see step 2 in Figure 1a), modifying a method described by Renz and Kurz (*15*) using glutaraldehyde as a coupling reagent. The possible mechanism of the cross-linking reaction is shown in Figure 1b.

DNA coding for the immunoglobulin μ constant fragment[5] (80 base pairs of domain C3 and all of domain C4 plus intervening sequences) was kindly provided by Dr. M. Pech (Institute for Physiological Chemistry, University of München) and produced according to the sequence published by Rabbitts et al. (*16*). The 920 nucleotide fragment was used for hybridization. For tracing mRNA of the TCR[6] α and β chains, we used cDNA specific for the constant regions of the TCR chains derived from poly-(A) + RNA of the MOLT-3 T cell line (*17*), Salmon sperm DNA used as negative control probe was obtained from Boehringer (Mannheim), sonicated, and electrophoresed, and fragments were sheared to the same size as the probe, cut out, and eluted from the gel. The DNA probe was denatured by boiling for 5 min and rapid cooling on ice, and between 1 mg and 10 ng of DNA in 10 μL of hybridization buffer was added to 10 μL of the FITC–PEI and incubated together with 3 μL of glutaraldehyde at different concentrations for 10 min at 37 °C. Excess binding capacity of the glutaraldehyde was saturated by adding 5 μL of 2% bovine serum albumin. The probe was then diluted 1:1 (v/v) with hybridization buffer. For calculation of the amount of fluorochrome molecules bound per base pair, the labeled DNA probe was separated over a G-100 column from the unbound polypeptide with PBS as elution buffer. Again, monitoring was facilitated by the fact that both the fraction of unbound polypeptide and the DNA-bound polypeptide were yellow, and the first yellow fraction was collected. The fluorescence intensity of a defined volume of labeled probe solution was then compared to the fluorescence intensity of a known FITC solution microfluorimetrically.

Cytological Preparations. Lymphoid cells from peripheral blood of patients with ALL[7] were isolated by Ficoll Isopaque separation and washed twice in PBS pH 7.4, and 10^6 cells sedimented in 10 μL of PBS. The Jurkat and the K562 cell lines were cultured in our laboratory. IgM-producing cells of a mouse hybridoma cell line were kindly provided by Dr. U. Kummer (GSF Institut für Hämatologie). Cultured cells were harvested and washed twice in PBS.

The cell membrane was permeabilized in suspension by adding 500 μL of hypotonic medium (0.9% trisodium citrate) to the sediment. At different times (0–5 min) thereafter the cells were fixed by adding 500 μL of ultrapure acetone. After 2-h fixation the cells were cytocentrifuged directly onto slides at 520 rpm (8*g*) at a density allowing at least three cell diameters of free space between the individual cells or allowed to sediment onto adhesion slides (Bio-Rad).

In Situ Hybridization. Hybridization reactions were carried out by modifying a method of Fournier et al. (*18*). Ten microliters of the reaction mixture was added to each slide and sealed under a coverslip with a vulcanizing glue, and the slides were incubated for 24–96 h in a moist chamber at 37 °C. The slides were then unsealed in 1 × SSC buffer and washed once in the hybridization buffer with 50% formamide for 30 min at 47 °C and once in the hybridization buffer without formamide. They were then washed again in 1 × SSC at room temperature, covered with one drop of glycerine, and inspected or measured. Measurements were performed on a Leitz Orthoplan microscope photometer MPV 2 equipped with a Ploem optique for fluorescein and rhodamin illumination. Each cell was adjusted into a measuring diaphragm under visual control and excited individually for 0.5 s. Fluorescence intensity was measured through a phototube, and values were recorded, transferred to a Commodore CM 8032 and stored on a floppy disk. Relative intensity values were related to an external fluorescence standard. Fluorochrome-labeled beads (Becton and Dickinson) were used as external standard. Background measurements were performed on a cell-free space adjacent to the cells and subtracted automatically from the total value. Corrected net values were plotted as frequency-distribution diagrams (*19*).

RESULTS

Determination of Optimal Labeling Conditions. The positive signal of a specific DNA probe labeled with the FITC–PEI and the background signal of only the FITC–PEI complex reacted with a cell preparation were compared microfluorimetrically at different F/P[8] ratios. The specific signal, as well as the nonspecific signal, increased simultaneously over the whole range of the applied concentrations, but since the signal-to-background ratio remained constant, increasing the concentration of FITC did not provide a better signal-to-noise ratio. Therefore 2 μg of FITC/mg of PEI, a concentration at which no visually observable unspecific binding was detected, was usually employed in the subsequent work.

[5] μ constant fragment: gene segment of the gene coding for the immunoglobulin M constant chain.

[6] TCR: T-cell receptor.

[7] ALL: acute lymphatic leukemia.

[8] F/P ratio: fluorescein to protein ratio.

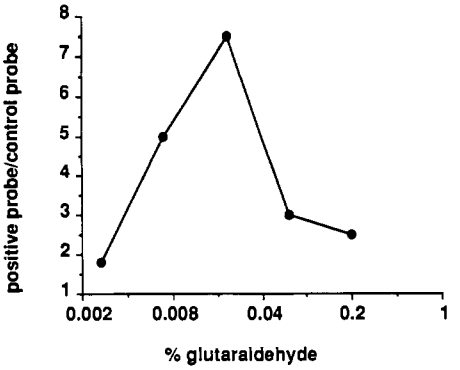


Figure 2. Relation between the mean values of the fluorescence intensities of 100 hybridoma cells hybridized with either the specific cμ probe or the sheared salmon sperm DNA, at different glutaraldehyde concentrations.

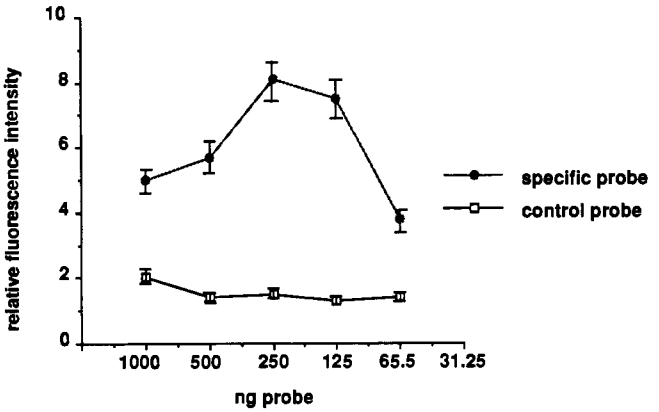


Figure 3. Mean values of the fluorescence intensities of 100 hybridoma cells hybridized with either a specific cμ probe (●) or a control probe (□), sheared salmon sperm DNA, at different probe concentrations (values + SEM).

The optimal amount of glutaraldehyde for cross-linking the fluorochrome-labeled polypeptide to the gene probe was determined with the hybridoma cell line.

The signal of the μ-specific probe, as compared to sheared salmon sperm DNA of the same chain length as control probe, was highest at 0.04% glutaraldehyde (Figure 2). Further increase in glutaraldehyde concentration increased unspecific binding of both the control and the μ-specific probe, thus reducing the ratio between the specific and the nonspecific signal.

The dependence of the signal on probe concentration was tested in the hybridoma cell line with the FITC–PEI conjugate (5 mg/mL of PEI) at a glutaraldehyde concentration of 0.04%. Starting from 1 μg/10 μL, specific probe and control probe (sheared salmon sperm DNA) were diluted in log 2 steps to the same final concentration. Intensity peaked between 3 and 4 × log 2 dilution (Figure 3) and therefore 100 ng/10 μL was used in the further experiments.

At the probe concentration thus determined, the optimal concentration of the PEI–FITC complex for discrimination between specific and control probe was tested. Although there was a decrease in absolute intensity (Figure 4a), the ratio between specific and nonspecific binding increased plateauing over about three dilution steps (Figure 4b).

Cell Preparation. Having established the optimal conditions for probe labeling, different cell preparation conditions for hybridization were tested. For accessibility of the RNA, the cells were made porous by hypotonic treatment with trisodium citrate before fixation. Increasing the time of hypotonic treatment lead to an increase

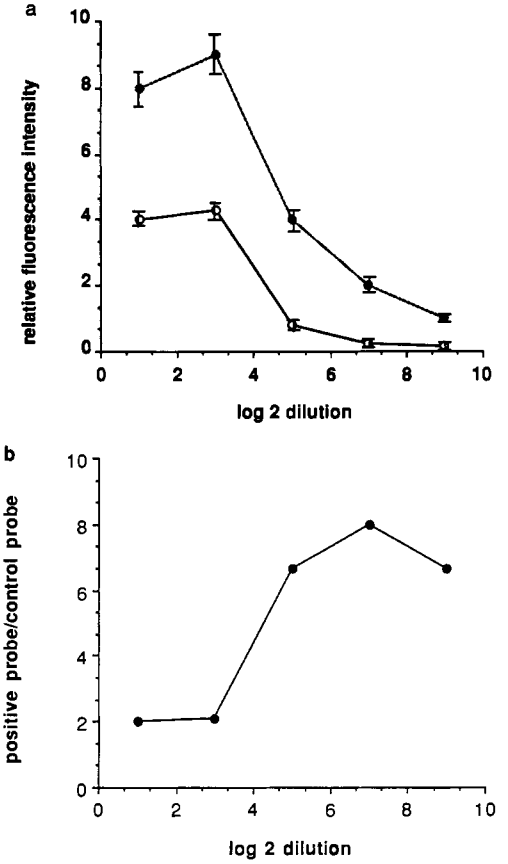


Figure 4. Mean values of the fluorescence intensities of 100 cells hybridized with a specific (●) and a control probe (○) coupled to different concentrations of PEI–FITC: (a) decrease in fluorescence of both specific and control probe (values + SEM) (b) relation between specific probe and control probe at the different concentrations of PEI–FITC.

in fluorescence signal, approaching a plateau at 3–4 min. Three minutes of hypotonic treatment were therefore usually chosen before addition of the fixative.

Among different fixatives, most of them leading to high autofluorescence, the best results were obtained with acetone. It was added 1:1 (v/v) to the cell suspension in hypotonic medium immediately after 3 min of treatment and could be left until use of the cells. Cells can be stored under these conditions for at least 2 weeks in a stoppered vial. They were then either cytocentrifuged or applied to adhesion slides.

Determination of Optimal Hybridization Conditions. Two hybridization temperatures, 37 and 45 °C, were assayed. Hybridization was performed with a cocktail with 50% deionized formamide or without formamide in the hybridization buffer. Fluorescence intensity increased continually over time, but cells disintegrated at 45 °C; therefore 37 °C was used in further studies.

A microfluorograph of cells reacted with the specific probe is shown in Figure 5.

Cell preparations were measured at different times, and frequency histograms established (Figure 6a). The height of the signal was lower under conditions including formamide, and it may be assumed that only the more specific hybrids are formed; however, the plateau was reached 24 h earlier without formamide (Figure 6b). In order to reduce nonspecific hybrid formation, the slides in the subsequent experiments were incubated without formamide but were routinely washed after hybridization in a buffer containing 50% formamide at 47 °C for 30 min.

Under these conditions a significant difference between a specific probe (μ) and a nonspecific probe (salmon sperm

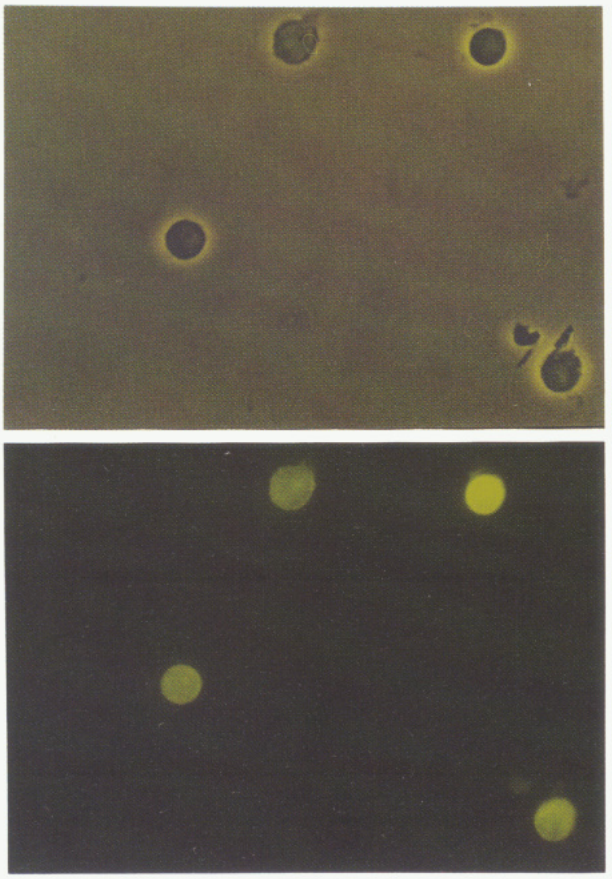


Figure 5. Microfluorograph of cells in transmitted light (top) and in incident light when reacted with the specific probe (bottom).

DNA) could be detected in an ALL after only 6 h of hybridization, but the plateau of the reaction was reached at 48 h (Figure 7).

To control the specificity of binding of the fluorochrome-labeled probe, digestion of cellular RNA with ribonuclease and hybridization inhibition by preincubation with unlabeled homologous probe were performed (Figure 8).

After digestion of the cell preparations of an ALL for 1 h at 37 °C with 20 μL of a solution of 10 mg/mL RNase A, the specific signal with the Tα probe was decreased to the level of that of the nonspecific signal.

Fluorescence of the ALL cells hybridized with the fluorochrome-labeled Tα probe could be reduced almost to control background levels by preincubation with unlabeled Tα but not with Tβ probe, with which the signal was comparable to that of the untreated control.

Quantification of mRNA. To obtain a quantitative measure of the amount of nucleic acid measurable by our method, the amount of labeled probe which can be discerned from background was determined. In a dilution series, as few as 10 labeled probe molecules included in the measuring diaphragm could clearly by detected, resulting in a fluorescence intensity of 1 relative units as compared to the background of 0.2 relative units.

In addition, a dilution series of unlabeled denatured probe was prepared, and defined volumes (5 μL) were applied to defined 5-mm areas of adhesion slides which bind cells or molecules via electrostatic forces. These areas were then immersed in 2% BSA to coat remnant binding sites and subsequently reacted with the fluorochrome-labeled probe. They were washed as described for the cells and the fluorescence intensity in the measuring area (10 μm diameter) determined. Assuming that the applied

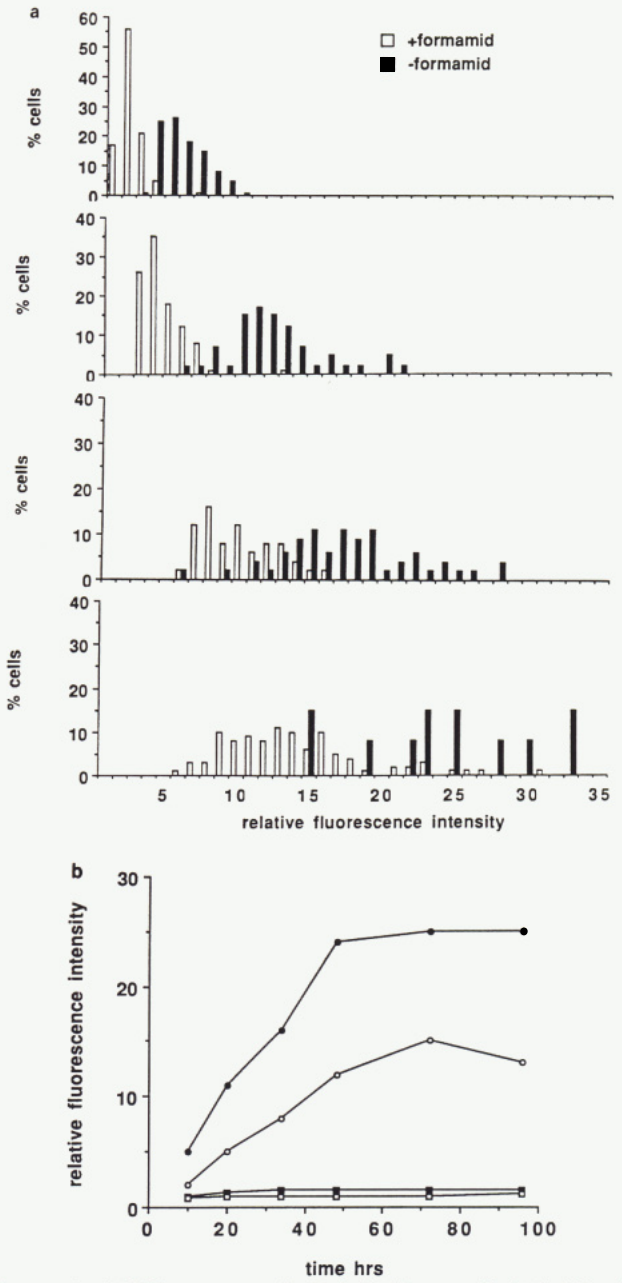


Figure 6. (a) Histograms of 100 hybridoma cells hybridized with a fluorochrome-labeled μ probe in a hybridization medium with (empty columns) or without (filled columns) 50% formamide for 10, 20, 36, and 44 h; (b) mean values, circles, μ-specific probe; squares, control probe; filled symbols, without formamide; empty symbols, with formamide.

nucleic acids were quantitatively bound to the test areas, we calculated that between 2 and 20 nucleic acid molecules can be distinguished from the background fluorescence with this method (Figure 9).

DISCUSSION

Refined methods have recently been developed to study differentiation and proliferation of normal and malignant cells at the molecular level. They allow us to shed light on the steps that occur during activation at the transcriptional and the translational levels and their presumable deviation during malignant transformation.

At the DNA level, the Southern blot hybridization method (*20*) lead to the detection of rearrangement of DNA sequences coding for lymphocyte antigen receptors (*17*, *21*). Moreover, oncogene rearrangements including

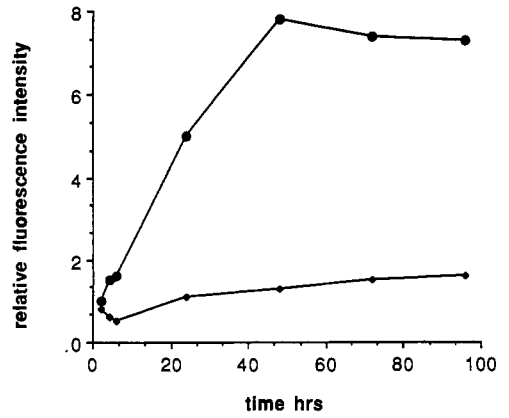


Figure 7. Mean values of common acute leukemia cells hybridized for different times with either the fluorochrome-labeled specific cμ probe (●) or the control salmon sperm DNA probe (◆).

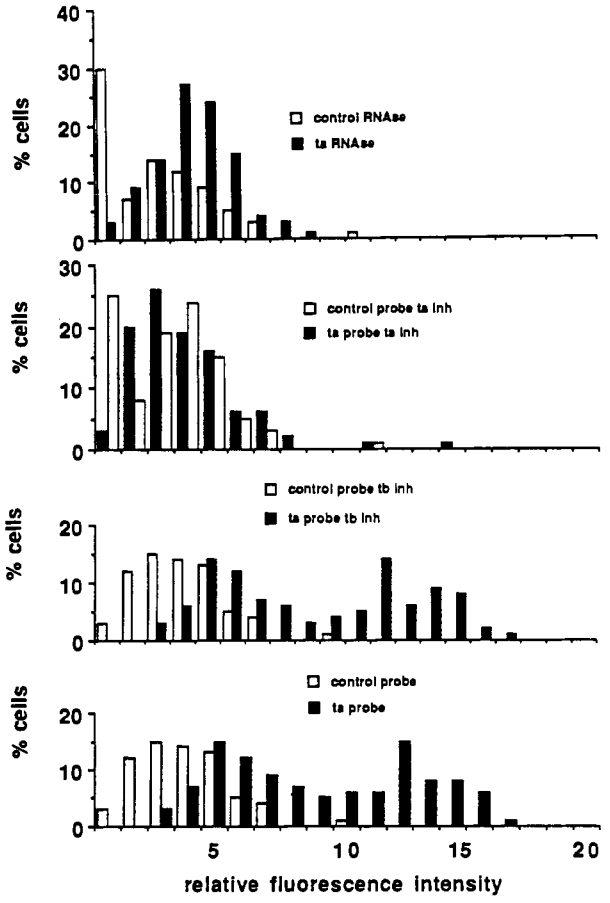


Figure 8. Frequency-distribution histograms of cells from a common acute leukemia hybridized with either control probe or a Tα probe previously treated with RNase or prehybridized with either unlabeled Tα or unlabeled Tβ probe.

chromosome translocations eventually leading to growth stimulation have been detected by this method (*22*).

Whether or not such genes then become activated can be studied at the mRNA level by Northern blot hybridization (*1*), but with this method only whole cell populations can be studied and one cannot discriminate between cells of high and low RNA content in heterogeneous populations.

This is, however, possible by in situ hybridization (*2*), which allows analysis of mRNA content at the single-cell level. But, whereas in situ hybridization using radiolabeled gene probes is hampered by difficulties in quantifying the results, labeling with fluorochromes has the advantage of being immediately detectable and quantifyable.

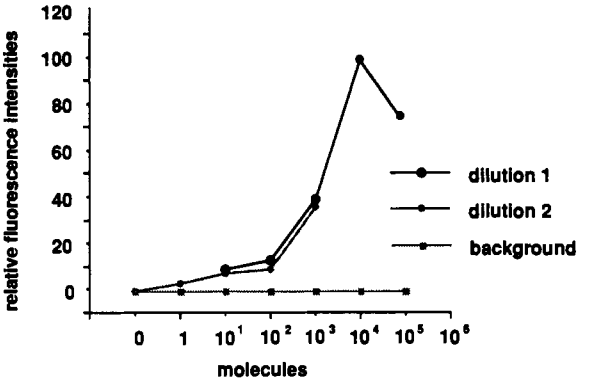


Figure 9. Fluorescence intensities measured on a dilution series of plasmid DNA of defined concentrations reacted with the same fluorochrome-labeled plasmid under the same conditions as for the cells.

With the new fluorochrome-labeling method described here, we can calculate the amount of probe molecules bound per cell from the fluorescence intensity measured fluorimetrically due to the direct binding of fluorochrome molecules to the probe.

A limiting factor for the detection of fluorescence is the amount of fluorochrome molecules attached per probe molecule. Although high labeling will lead to nonspecific binding of the FITC–PEI complex to cellular components via electrostatic forces (*14*), this does not play a role in microfluorimetry where nonspecific fluorescence can be corrected for. Still in the present report a concentration of FITC leading to no nonspecific direct binding of the complex to the cells was used since increasing the FITC–PEI ratio did not further increase the signal to background ratio.

The concentration of glutaraldehyde, in contrast, may influence the hybridization properties of the DNA probe by modifying the DNA structure. As shown, this concentration reached an optimum providing the highest binding of a specific versus a nonspecific probe treated in the same way.

Also, for probe concentration an optimum was obtained. After the optimum was reached there was no further increase in fluorescence with increasing probe concentration. This indicates that at higher probe concentrations, the PEI–FITC complex was no longer present in excess and less PEI–FITC complex per probe molecule was available.

Since the probe–FITC–PEI complex forms a quite large molecule, the porosity of the cell membrane necessary to allow entering of the complex is of importance. In our hands a hypotonic shock as used for chromosome preparation (*23*) and immediate fixation after 3 min of treatment gave the best results. Prolonged treatment did not lead to increase in fluorescence and resulted in cell loss, obviously due to disruption. The cells were then additionally spread onto slides. Probe size was not a limiting factor for entering the cells and access to the RNA molecules, since we found only a borderline improvement of hybridization with reduced probe length, in contrast to reports by others (*24*). This may be due to the fact that the longer the strand the more FITC–PEI molecules can be attached, thus improving the detectability of bound molecules. As a fixative, acetone was chosen, because it induced the least autofluorescence. Paraformaldehyde, which was only tested recently, may give comparable results (*25*).

Completion of the hybridization reaction in our hands took 48 h, even if significant differences between control probe and specific probe were already seen after 6 h of incubation. This length of time has been reported as the optimal incubation period (*26*). Differences in hybridization conditions (temperature and salt concentrations) as well as reannealing of the probe strands and thus exhaustion of the single-stranded probe available for hybridization to cellular nucleic acids may contribute to different extents to the termination of the reaction. Use of unidirectional probes may help to overcome this problem.

To avoid further prolongation of hybridization times formamide was omitted from the hybridization mixture, but washing was performed in 50% formamide at 45 °C to reduce low-stringency binding.

We can detect down to 10 probe molecules, a number that has been calculated directly from the minimal amount of fluorescent molecules which can be discriminated from autofluorescence of cells. The amount of fluorochrome-labeled probe reacting with a slide area was correlated to the amount of homologous probe attached to this area over the range of 4 log dilution steps. Work is in progress to directly control whether the unlabeled nucleic acid strands remain completely bound to the test area in order to establish a standard curve.

So far we have not seen any other report describing a comparable quantitative method where an exact discrimination at the individual cell level between background and specific fluorescence is possible. The advantage of the method appears especially in instances where low amounts of RNA are to be detected since any fluorescence intensity exceeding control fluorescence (autofluorescence of the cells plus unspecific binding) is indicative for specific binding. We are able to discriminate at least 10 bound probe molecules from background fluorescence. This number is directly calculated from the fluorescence intensity, in contrast to indirect calculation from northern blots, which may be hampered by the heterogeneous expression of specific mRNA in the investigated population (*27*)

Quantitative in situ hybridization with fluorochrome-labeled probes may thus contribute to improvement of our knowledge concerning activation of differentiation genes (*28*) and oncogenes (*29*) and in microbiology of the virus load of individual cells (*30*) and the presented method may increase the sensitivity of the hybridization procedure.

ACKNOWLEDGMENT

The skillful technical help of Mrs. Sabine Blieninger is gratefully acknowledged. This work was supported by the Deutsche Forschungsgemeinschaft (Projekt Em 20/6-2,3) and by the Deutsche Krebshilfe (W25/84/Th1).

LITERATURE CITED

(1) Alwine, J. C., Kemp, D. J., and Stark, G. R. (1977) Method for detection of specific RNAs in agarose gels by transfer to diazobenzylmethyl-paper and hybridization with DNA probes. *Proc. Natl. Acad. Sci. U.S.A. 74*, 5350–5354.

(2) Gall, J. G., and Pardue, M. L. (1969) Formation and detection of RNA–DNA hybrid molecules in cytological preparations. *Proc. Natl. Acad. Sci. U.S.A. 63*, 378–383.

(3) Gerhard, D. S., Kawasaki, E. S., Bancroft, F. C., and Szabo, P. (1981) Localization of a unique gene by direct hybridization in situ. *Proc. Natl. Acad. Sci. U.S.A. 78*, 3755–3759.

(4) Baumann, J. G. J., Wiegant, J., and van Duijn, P. (1983) The development, using poly(Hg-U) in a model system, of a new method to visualize cytochemical hybridization in fluorescence microscopy. *J. Histochem. Cytochem. 31*, 571–578.

(5) Baumann, J. G. J., Wiegant, J., and van Duijn, P. (1981) Cytochemical hybridization with fluorochrome-labeled RNA. I. Development of a method using nucleic acids bound to agarose beads as a model. *J. Histochem. Cytochem. 29*, 227–237.

(6) Baumann, J. G. J., Wiegant, J., Borst, P., and van Duijn, P. (1980) A new method for fluorescence microscopical localization of specific DNA sequences by in situ hybridization of fluorochrome-labeled RNA. *Exp. Cell Res. 128*, 485–490.

(7) Hopman, A. H. N., Wiegand, J., and van Duijn, P. (1986) A new hybrid–cytochemical method based on mercurated nucleic acid probes and sulfhydryl-hapten ligands. I. Stability of the mercury–sulfhydryl bond and influence of the ligand structure on immunochemical detection of the hapten. *Histochem. 84*, 169–175.

(8) Landegent, J. E., in de Wal, N. J., van Ommen, G.-J. B., Baas, F., de Vijlder, J. J. M., van Dujin, P., and van der Ploeg, M. (1985) Chromosomal localization of a unique gene by nonautoradiographic in situ hybridization. *Nature 317*, 175–177.

(9) Tchen, P., Fuchs, R. P. P., Sage, E., and Leng, M. (1984) Chemically modified nucleic acids as immunodetectable probes in hybridization experiments. *Proc. Natl. Acad. Sci. U.S.A. 81*, 3466–3470.

(10) van Prooijen-Knegt, A. C., van Hoek, J. F. M., Baumann, J. G. J., van Duijn, P., Wool, I. G., and van der Ploeg, M. (1982) In situ hybridization of DNA sequences in human metaphase chromosomes visualized by an indirect fluorescent immunocytochemical procedure. *Exp. Cell Res. 141*, 397–407.

(11) Pachmann, K. (1987) In situ hybridization with fluorochrome-labeled cloned DNA for quantitative determination of the homologous mRNA in individual cells. *J. Mol. Cell Immunol. 3*, 13–19.

(12) Goldman, M. (1969) In *Fluorescent Antibody Methods*, p 101 ff, Academic Press, New York and London.

(13) Goldman, M. (1969) In *Fluorescent Antibody Methods*, p 125, Academic Press, New York and London.

(14) Brandtzaeg, P. (1975) Rhodamine conjugates: specific and nonspecific binding properties in immunochemistry. In Fifth International Conference on Immunofluorescence and Related Staining Techniques (W. Hijmans, Ed.) *Ann. N.Y. Acad. Sci. 245*, 35–53.

(15) Renz, M., and Kurz, C. (1984) A colorimetric method for DNA hybridization. *Nucleic Acids Res. 12*, 3435–3444.

(16) Rabbitts, T. H., Forster, A., and Milstein, C. P. (1981) Human immunoglobulin heavy chain genes: evolutionary comparisons of cμ, cδ and cγ genes and associated sequences. *Nucleic Acids Res. 18*, 4509–4524.

(17) Yanagi, Y., Chan, A., Chin, B., Minden, M., and Mak, T. W. (1985) Analysis of cDNA clones specific for human T cells and the α and β chains of the T-cell heterodimer from a human T-cell line. *Proc. Natl. Acad. Sci. U.S.A. 82*, 3430–3434.

(18) Fournier, J. G., Kessous, A., Richer, G., Brechot, C., and Simard, R. (1982) Detection of hepatitis B viral RNAs in human liver tissues by in situ hybridization. *Biol. Cell 43*, 225–228.

(19) Pachmann, K., Dörken, B., Emmerich, B., and Thiel, E. (1988) Quantitation of μ mRNA by in situ hydridization reveals a correlation between B-maturation associated antigens and IgM gene activation in acute lymphatic leukemias. *Med. Oncol. Tumor Pharmacol. 5*, 33–39.

(20) Southern, B. M. (1975) Detection of specific sequences among DNA fragments separated by gel electrophoresis. *J. Mol. Biol. 98*, 503–517.

(21) Hozumi, N., and Tonegawa, S. (1976) Evidence for somatic rearrangement of immunoglobulin genes coding for variable and constant regions. *Proc. Natl. Acad. Sci. U.S.A. 73*, 3628–3632.

(22) Finger, L. R., Harvey, R. C., Moore, R. C. A., Showe, L. C., and Croce, C. M. (1986) A common mechanism of chromosomal translocation in T- and B-cell neoplasia. *Science 234*, 982–985.

(23) Gall, J. G. (1963) Chromosome fibers from an interphase nucleus. *Science 139*, 120–121.

(24) Singer, R. H., and Ward, D. C. (1982) Actin gene expression visualized in chicken muscle tissue culture by using in situ hybridization with a biotinated nucleotide analog. *Proc. Natl. Acad. Sci. U.S.A. 79*, 7331–7335.

(25) Lawrence, J. B., and Singer, R. H. (1985) Quantitative analysis of in situ hybridization methods for the detection of actin gene expression. *Nucleic Acid Res. 13*, 1777–1799.

(26) Bresser, J., and Evinger-Hodges, M. J. (1987) Comparison and optimization of in situ hybridization procedures yielding rapid sensitive mRNA detections. *Gene Anal. Tech. 4*, 89–104.

(27) Evinger-Hodges, M.-J., Bresser, J., Brouwer, R., Cox, I., Spitzer, G., and Dicke, K. (1988) myc and sis expression in acute myelogenous leukemia. *Leukemia 2*, 45–49.

(28) Pachmann, K., Raghavachar, A., Bartram, C., Emmerich, B., Thiel, E., and Ziegler-Heitbrock, H. W. L. (1989) T cell receptor alpha expression in B-type chronic lymphatic leukemia. *Leukemia 3*, 497–500.

(29) Ascione, R., Sacchi, N., Watson, D. K., Fischer, R. J., Fujiwara, S., Seth, A., and Papas, T. S. (1986) Oncogenes: molecular probes for clinical application in malignant diseases. *Gene Anal. Tech. 3*, 25–39.

(30) Neumann, R., Genersch, E., and Eggers, H. J. (1987) Detection of adenovirus nucleic acid sequences in human tonsils in the absence of infectious virus. *Virus Res. 7*, 93–97.

Registry No. Glutaraldehyde; 111-30-8

Carboxymethyl-Substituted Bifunctional Chelators: Preparation of Aryl Isothiocyanate Derivatives of 3-(Carboxymethyl)-3-azapentanedioic Acid, 3,12-Bis(carboxymethyl)-6,9-dioxa-3,12-diazatetradecanedioic Acid, and 1,4,7,10-Tetraazacyclododecane-*N,N',N'',N'''*-tetraacetic Acid for Use as Protein Labels

Steven J. Kline, David A. Betebenner, and David K. Johnson*

Abbott Laboratories, Department 90M, Abbott Park, Illinois 60064. Received September 5, 1990

3-(Carboxymethyl)-3-azapentanedioic acid (NTA), 3,12-bis(carboxymethyl)-6,9-dioxa-3,12-diazatetradecanedioic acid (EGTA), and 1,4,7,10-tetraazacyclododecane-*N,N',N'',N'''*-tetraacetic acid (DOTA) structures having a 4-nitrophenyl substituent attached via an alkyl spacer to the methylene carbon atom of one carboxymethyl arm of the chelator were obtained by alkylation of 4-nitrophenylalanine with bromoacetic acid (NTA), by reductive alkylation of 1,8-diamino-3,6-dioxaoctane with (4-nitrophenyl)-pyruvic acid followed by alkylation with bromoacetic acid (EGTA), and by alkylation of the trimethyl ester of 1,4,7,10-tetraazacyclododecane-*N,N',N''*-triacetic acid with the methyl ester of α-bromo-4-(4-nitrophenyl)pentanoic acid and subsequent saponification (DOTA). The nitrophenyl-substituted chelators were converted to the corresponding amines by hydrogenation then reacted with thiophosgene to give the protein-reactive aryl isothiocyanate derivatives.

Labeling of proteins and other biologically active molecules with metal ions is often accomplished with synthetic chelating agents that contain a bioreactive substituent (*1*, *2*). The first such bifunctional chelators to find widespread use were EDTA[1] analogues derivatized at a methylene carbon atom of the diamine backbone with phenyl (*3*), benzyl (*4*), or phenethyl (*5*) moieties bearing a protein-reactive substituent on the aromatic ring. In recent years, interest in tumor targeting using radiometal-labeled antibody–chelator conjugates has prompted the development of alternative bifunctional ligands (*6–15*). As in vivo stability of the chelate label is of paramount importance in such applications, these efforts have concentrated on the design and synthesis of bifunctional chelating agents that impart enhanced kinetic and/or thermodynamic stability to their chelates with radiometals of interest. Systems of this type include analogues of DTPA (*6–8*) and HBED (*9*, *10*) and ligands based on tetraaza (*11–13*) and triaza (*14*) macrocyclic polyaminopolycarboxylates and their polyamine precursors (*15*), once again derivatized at methylene carbon atoms of the polyamine backbone with various protein-reactive side chains.

Although the recent focus of bifunctional chelator development has been on high stability, future applications of these potentially versatile agents may emphasize additional properties. For example, metal ion selectivity will be important if bifunctional chelators are to be used to target endogenous metal pools that are implicated in producing tissue damage in some disease states (*16*). While stability and selectivity are often maximized through the use of high-denticity ligands, applications in which biomolecules are labeled with metal complexes that possess catalytic activity are likely to require bifunctional chelators that do not completely saturate the coordination sphere, in order to avoid blocking substrate access to the metal ion. Before any such uses can be systematically investigated, a spectrum of bifunctional chelators spanning a range of metal-binding properties will be required, so that structure–activity relationships can be established empirically. To this end, we are expanding a series of bifunctional polyaminopolycarboxylates in which an aryl isothiocyanate side chain is incorporated into one carboxymethyl arm of the chelator. The preparation of EDTA and DTPA systems of this type has been previously described (*17*). This report presents syntheses of three additional analogues (**4**, **10**, **20**; Schemes I–III).

[1] The following abbreviations are used: DK, a β-diketone; DOTA, 1,4,7,10-tetraazacyclododecane-*N,N',N'',N'''*-tetraacetic acid; DTPA, diethylenetriaminepentaacetic acid; EDTA, ethylenediaminetetraacetic acid; EGTA: 3,12-bis(carboxymethyl)-6,9-dioxa-3,12-diazatetradecanedioic acid; HBED, *N,N'*-bis(2-hydroxybenzyl)ethylenediamine-*N,N'*-diacetic acid; NTA, 3-(carboxymethyl)-3-azapentanedioic acid; TMS, trimethylsilane; TSP, 3-(trimethylsilyl)-1-propanesulfonic acid.

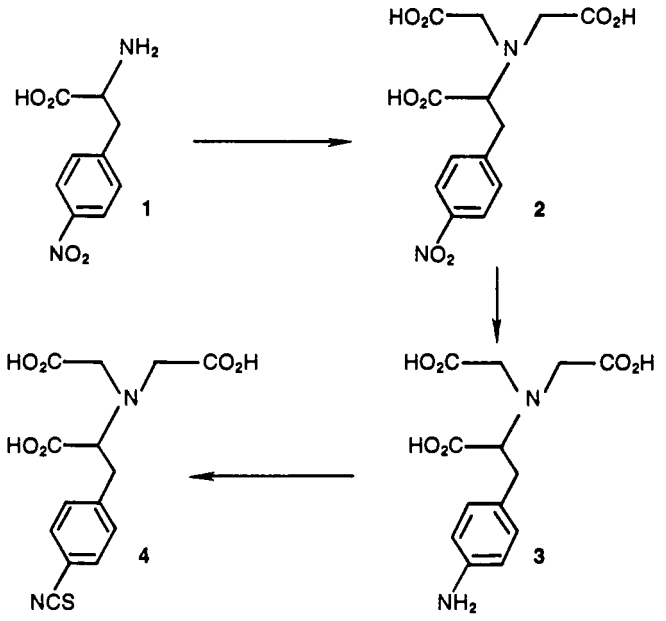
EXPERIMENTAL PROCEDURES

(4-Nitrophenyl)pyruvic acid (**5**) was synthesized as previously described (*17*). 1,8-Diamino-3,6-dioxaoctane (**6**) was prepared from 1,8-dichloro-3,6-dioxaoctane via 1,8-diphthaloyl-3,6-dioxaoctane following the procedure of Sun et al. (*18*). 1,4,7,10-Tetraazacyclododecane (**16**) was prepared as described by Richman et al. (*19*). All other starting materials and reagents were purchased from Aldrich Chemical Co., Milwaukee, WI. ^{1}H NMR and ^{13}C NMR spectra were recorded on a General Electric QE-300 spectrometer, operating at 300.23 and 75.5 MHz, respectively. Chemical shifts are given in ppm relative to TMS as internal standard, unless otherwise specified, and coupling constants are reported in hertz. Mass spectra were obtained with a Kratos MS-50 spectrometer by either the fast atom bombardment technique using a thioglycerol or glycerol/thioglycerol matrix or by direct ionization. Elemental analyses were performed by Galbraith Laboratories, Knoxville, TN.

***N,N*-Bis(carboxymethyl)-4-nitrophenylalanine Hydrochloride (2).** A solution of bromoacetic acid (4.99 g,

1043-1802/91/2902-0026$02.50/0 © 1991 American Chemical Society

Scheme I



35 mmol) in H_2O (20 mL) was added to a suspension of 4-nitro-*dl*-phenylalanine (1; 3.02 g, 14 mmol) in H_2O (50 mL) and the pH of the resulting solution was raised to 12 by addition of 6 M NaOH. The reaction mixture was then stirred at 45 °C for 2 days, the pH being maintained in the range of 11–12 by periodic addition of 6 M NaOH. After cooling to room temperature, the reaction solution was evaporated to dryness under vacuum to give a yellow oil, which was redissolved in H_2O (10 mL), adjusted to pH 10 with 6 M NaOH, and applied to a Bio-Rad AG1-X4 anion-exchange column (formate form, column weight 100 g). The column was eluted successively with H_2O (1 L), 4 M formic acid (500 mL), and 5 M formic acid (500 mL), fractions being evaluated by TLC on silica plates developed in 25% concentrated aqueous NH_4OH/75% EtOH (95%) (R_f for 1 = 0.60; R_f for 2 = 0.21; R_f for monoalkylation product = 0.38). The desired product, contaminated with some higher R_f material, eluted in the 5 M formic acid fractions. These were combined, evaporated to dryness, redissolved in H_2O (10 mL), readjusted to pH 10, and applied to a second Bio-Rad AG1-X4 anion-exchange column (formate form, column weight 70 g) that was eluted successively with H_2O (500 mL), 4 M formic acid (500 mL), 4.25 M formic acid (500 mL), 4.5 M formic acid (500 mL), and 4.75 M formic acid (500 mL), and 10-mL fractions were collected. The desired product eluted slowly in the 4.75 M formic acid fractions and these were combined, evaporated to dryness under vacuum, and redissolved in 4 M HCl (100 mL). The resulting solution was again evaporated to dryness under vacuum and the residue was repeatedly redissolved in water and reevaporated to dryness until a solid residue was obtained. This was then dried under vacuum over P_2O_5 to afford **2** in the form of a pale yellow powder (3.64 g, 72%): ^1H NMR (D_2O, TSP standard) δ 3.29–3.48 (m, 2 H), 3.95–4.08 (m, 4 H), 4.32 (t, 1 H, J = 7.7), 7.54 (d, 2 H, J = 8.4), 8.22 (d, 2 H, J = 8.8); mass spectrum (FAB$^+$, thioglycerol/glycerol), m/e 349 (M + Na)$^+$, 327 (M + H)$^+$.

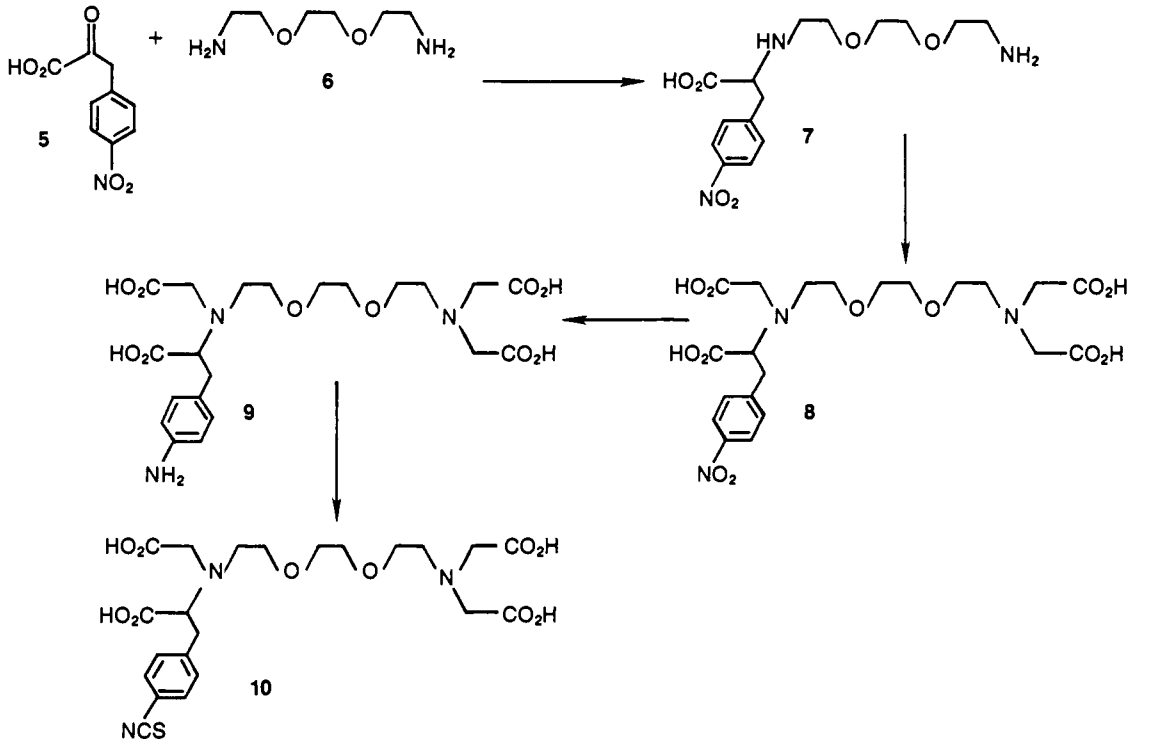
***N,N*-Bis(carboxymethyl)-4-aminophenylalanine Dihydrochloride (3).** A solution of **2** (0.60 g, 1.65 mmol) in H_2O (150 mL) was hydrogenated in a Parr apparatus at room temperature and 35 psi H_2 over 10% palladium on carbon (60 mg) for 2 h. The catalyst was removed by filtration and the filtrate evaporated to dryness under vacuum. The resulting residue was dissolved in 4 M HCl (50 mL) and reevaporated to dryness, followed by four cycles of redissolution in H_2O (200 mL) and reevaporation to dryness. The oil thus obtained was dissolved in H_2O (10 mL), lyophilized, then dried under vacuum over P_2O_5 to give 0.55 g (99%) of **3** in the form of a yellow solid: ^1H NMR (D_2O, TSP standard) δ 3.28 (dd, 1 H, J = 14.3, 8.1), 3.42 (dd, 1 H, J = 14.3, 7.4), 4.01–4.15 (m, 4 H), 4.36 (t, 1 H, J = 7.7), 7.40 (d, 2 H, J = 8.8), 7.48 (d, 2 H, J = 8.5); mass spectrum (glycerol/thioglycerol), m/e 319 (M + Na)$^+$, 297 (M + H)$^+$.

***N,N*-Bis(carboxymethyl)-4-isothiocyanatophenylalanine Hydrochloride (4).** An 80% (v:v) solution of thiophosgene in CCl_4 (0.18 mL, 1.87 mmol) was added to a solution of **3** (45 mg, 0.13 mmol) in 3 M HCl (1.2 mL) and the resulting solution was vigorously stirred at room temperature for 6 h. The solvents and residual thiophosgene were then removed under vacuum in a fume hood, and the residue was dried further over P_2O_5 under vacuum to yield 47 mg (97%) of **4** as a pale beige powder: ^1H NMR (DMSO-d_6, TMS standard) δ 2.89–3.04 (m, 2 H), 3.49–3.62 (m, 4 H), 3.72 (t, 1 H, J = 7.7), 7.33 (s, 4 H); mass spectrum (glycerol/thioglycerol), m/e 339 (M + H)$^+$.

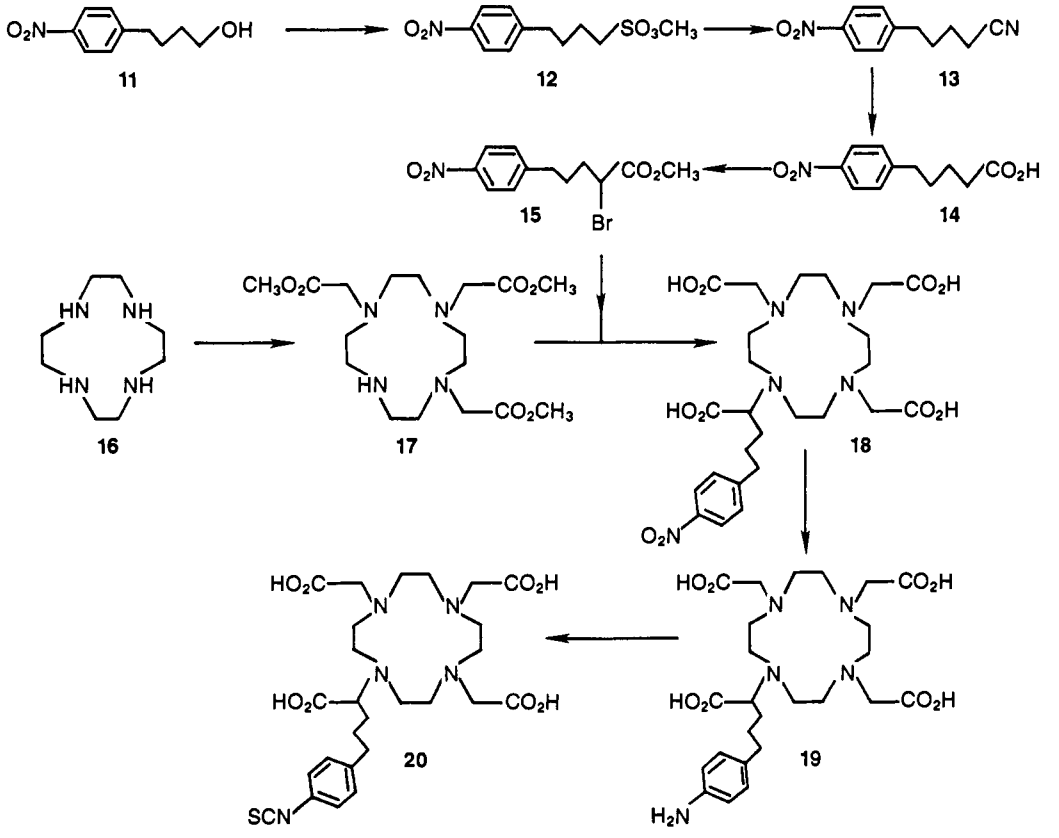
***N*-(1-Amino-3,6-dioxaoctyl)-3-(4-nitrophenyl)alanine Dihydrochloride (7).** A solution of **5** (3.57 g, 17 mmol) in MeOH (70 mL) was added to a solution of **6** (2.53 g, 17 mmol) in H_2O (15 mL) and the pH of the resulting dark red solution was adjusted to 6 by addition of 4 M HCl. Sodium cyanoborohydride (1.13 g, 17 mmol) was then added and the reaction mixture stirred at pH 6 and room temperature for 5 days. The resulting yellow solution was then acidified to pH 1 by addition of concentrated HCl and evaporated to dryness under vacuum. The residue was extracted with a mixture of H_2O (250 mL) and EtOAc (200 mL), the organic phase being subsequently discarded. The aqueous phase was extracted with EtOAc (2 × 200 mL) then concentrated to a volume of ca. 5 mL and adjusted to pH 3 by addition of 6 M NaOH. This solution was applied to a Dowex 50X-2-200 column (H^+ form, column weight 300 g) which was eluted sequentially with H_2O, 1 M HCl, 2 M HCl, and 4 M HCl. Unreacted **6** eluted in the 2 M HCl, whereas the desired product was isolated from the 4 M HCl eluate. Fractions containing the product were identified by TLC on silica plates developed in 20% concentrated aqueous NH_4OH/80% EtOH (95%) and treated with ninhydrin (R_f = 0.5). These were combined, evaporated to dryness under vacuum, redissolved in H_2O (250 mL), and again evaporated to dryness. A further four cycles of dissolution in 250-mL aliquots of H_2O followed by reevaporation to dryness gave a residue that upon lyophilization afforded 2.68 g (38%) of **7** in the form of a pale yellow solid: ^1H NMR (D_2O, TSP standard) δ 3.21 (t, 2 H, J = 5.0), 3.33–3.42 (m, 3 H), 3.50 (dd, 1 H, J = 14.2, 6.1), 3.67–3.86 (m, 8 H), 4.31 (dd, 1 H, J = 7.5, 6.1), 7.55 (d, 2 H, J = 8.4), 8.24 (d, 2 H, J = 8.4); ^{13}C NMR (D_2O, TSP standard) δ 37.72, 41.99, 49.23, 63.57, 68.38, 69.33, 72.47, 72.53, 126.97, 133.42, 144.93, 150.01, 173.08; mass spectrum (glycerol/thioglycerol), m/e 342 (M + H)$^+$; high-resolution mass spectrum calcd for $C_{15}H_{24}N_3O_6$ 342.1665, found 342.1667. Anal. Calcd for $C_{15}H_{25}Cl_2N_3O_6$: C, 43.49; H, 6.08; N, 10.14. Found: C, 43.16; H, 6.07; N, 9.93.

2-(4-Nitrobenzyl)-3,12-bis(carboxymethyl)-6,9-dioxa-3,12-diazatetradecanedioic Acid Dihydrochloride (8). Solid **7** (1.29 g, 3 mmol) was added to a solution of bromoacetic acid (1.74 g, 12.0 mmol) in H_2O (10 mL) and the pH of the resulting yellow solution was adjusted to 12 by addition of 6 M NaOH. The solution was then stirred at 45 °C for 7 days, the pH being maintained at 12 by

Scheme II



Scheme III



periodic addition of 6 M NaOH. The orange solution thus obtained was applied to a Bio-Rad AG1-X4 anion-exchange column (formate form, column weight 40 g), which was eluted successively with H_2O (200 mL), 0.1 M formic acid (350 mL), 0.5 M formic acid (350 mL), and 0.7 M formic acid (1.5 L). The desired product eluted in the 0.7 M formic acid, product-containing fractions being identified by TLC on silica plates developed in 20% concentrated aqueous NH_4OH/80% EtOH (95%) (R_f for 8 = 0.6). Fractions containing the product were combined, and 4 M HCl (5 mL) was added, then the solution was evaporated to dryness under vacuum and the residue was lyophilized. Trituration of the lyophilized material with CH_2Cl_2 produced a yellow solid that was dried under vacuum to afford 1.20 g (67%) of 8: ^1H NMR (D_2O, TSP standard) δ 3.43–3.73 (m, 10 H), 3.82–3.89 (m, 4 H), 4.12–4.31 (m, 6 H), 4.61 (t, 1 H, J = 7.2), 7.60 (d, 2 H, J = 8.4), 8.25 (d, 2 H, J = 8.4); ^{13}C NMR (D_2O, TSP standard) δ 35.23,

56.39, 58.24, 58.33, 58.80, 67.79, 70.22, 72.43, 72.53, 126.97, 133.39, 145.54, 149.91, 170.88, 171.49, 172.04; mass spectrum (thioglycerol), m/e 516 $(M + H)^+$; high-resolution mass spectrum calcd for $C_{21}H_{30}N_3O_{12}$ 516.1830, found 516.1830. Anal. Calcd for $C_{21}H_{31}Cl_2N_3O_{12}$: C, 42.87; H, 5.31; N, 7.14. Found: C, 42.60; H, 5.13; N, 7.06.

2-(4-Aminobenzyl)-3,12-bis(carboxymethyl)-6,9-dioxa-3,12-diazatetradecanedioic Acid Trihydrochloride (9). A solution of **8** (404 mg, 0.69 mmol) in H_2O (100 mL) was hydrogenated in a Parr apparatus at room temperature and 35 psi H_2 over 10% palladium on carbon (40 mg) for 2 h. The catalyst was removed by filtration and 4 M HCl (5 mL) was added to the filtrate, which was then evaporated to dryness under vacuum. The resulting oil was dissolved in H_2O (10 mL) and lyophilized to give 399 mg (97%) of **9** in the form of a hygroscopic white solid: ^1H NMR (D_2O, TSP standard) δ 3.35–3.77 (m, 10 H), 3.81–3.92 (m, 4 H), 4.22 (m, 4 H), 4.25 (s, 4 H), 4.57 (t, 1 H, J = 7.6), 7.43 (d, 2 H, J = 8.3), 7.53 (d, 2 H, J = 8.3); ^{13}C NMR (D_2O, TSP standard) δ 35.12, 56.48, 58.00, 58.48, 58.74, 67.71, 67.81, 70.82, 72.50, 72.60, 126.60, 132.21, 133.91, 138.84, 171.12, 171.79, 172.58; mass spectrum (thioglycerol), m/e 486 $(M + H)^+$; high-resolution mass spectrum calcd for $C_{21}H_{32}N_3O_{10}$ 486.2088, found 486.2084. Anal. Calcd for $C_{21}H_{34}Cl_3N_3O_{10}$: C, 42.40; H, 5.76; N, 7.06. Found: C, 42.52; H, 5.58; N, 6.71.

2-(4-Isothiocyanatobenzyl)-3,12-bis(carboxymethyl)-6,9-dioxa-3,12-diazatetradecanedioic Acid Dihydrochloride (10). An 80% (v:v) solution of thiophosgene in CCl_4 (50 μL, 0.52 mmol) was added to a solution of **9** (22 mg, 0.037 mmol) in 3 M HCl (330 μL) and the resulting reaction mixture was stirred vigorously at room temperature for 6 h. Evaporation to dryness under vacuum followed by vacuum drying over P_2O_5 gave 21.9 mg (99%) of **10** in the form of a light beige powder: ^1H NMR (DMSO-d_6, TSP standard) δ 3.06–3.26 (m, 5 H), 3.40–3.53 (m, 6 H), 3.55–3.64 (m, 2 H), 3.72–3.80 (m, 2 H), 3.88 (br s, 2 H), 4.08 (t, 1 H), 4.21 (s, 3 H), 7.39 (s, 4 H); mass spectrum (thioglycerol), m/e 528 $(M + H)^+$; high-resolution mass spectrum calcd for $C_{22}H_{30}N_3O_{10}S$ 528.1652, found 528.1647. Anal. Calcd for $C_{22}H_{31}Cl_2N_3O_{10}S$: C, 44.00; H, 5.20; N, 7.00. Found: C, 43.81; H, 5.19; N, 6.87.

4-(4-Nitrophenyl)butyl Methanesulfonate (12). 4-(4-Nitrophenyl)-1-butanol (19.44 g, 99.6 mmol) and triethylamine (15.2 g, 151 mmol) were dissolved in dry CH_2Cl_2 (250 mL), and the resulting solution was stirred under N_2 at 0 °C while a solution of methanesulfonyl chloride (17.1 g, 149 mmol) in CH_2Cl_2 (100 mL) was added dropwise over 30 min. After stirring at 0 °C for a further 45 min, the reaction mixture was extracted sequentially with cold H_2O (2 × 100 mL), cold 2 M HCl (2 × 100 mL), cold 1 M NaOH (2 × 100 mL), and cold H_2O (2 × 100 mL). The organic phase was dried over anhydrous Na_2SO_4 then evaporated to dryness under vacuum to give a yellow oil that solidified on standing at 0 °C. This crude product was extracted at reflux with Et_2O (600 mL), giving a colorless extract and leaving an insoluble orange tar. Evaporation to dryness of the ether extract gave 26.12 g (96%) of **12** in the form of a tan solid: ^1H NMR ($CDCl_3$) δ 1.78–1.85 (m, 4 H), 2.75–2.82 (m, 2 H), 3.01 (s, 3 H), 4.24–4.29 (m, 2 H), 7.34 (d, 2 H, J = 9.0), 8.16 (d, 2 H, J = 9.0); ^{13}C NMR ($CDCl_3$) δ 26.67, 28.46, 34.90, 37.19, 69.43, 123.50, 123.60, 129.08, 146.25, 149.37; mass spectrum (DCI), m/e 291 $(M + NH_4)^+$. Anal. Calcd for $C_{11}H_{15}NO_5S$: C, 48.34; H, 5.53; N, 5.13. Found: C, 48.25; H, 5.59; N, 5.15.

4-(4-Nitrophenyl)pentanenitrile (13). A mixture of **12** (5.0 g, 18.3 mmol) and NaCN (2.8 g, 57 mmol) in dry DMSO (40 mL) was stirred at 60 °C for 30 min under N_2. After cooling to room temperature, the reaction mixture was poured into Et_2O (300 mL) and the resulting suspension was filtered. The filtrate was extracted with H_2O (4 × 150 mL), dried over anhydrous Na_2SO_4, and evaporated to dryness. The resulting residue was chromatographed on a silica gel column eluted with CH_2Cl_2 to give 3.31 g (89%) of **13** in the form of a yellow oil: ^1H NMR ($CDCl_3$) δ 1.66–1.90 (m, 4 H), 2.40 (t, 2 H, J = 7.5), 2.79 (t, 2 H, J = 7.5), 7.35 (d, 2 H, J = 9.0), 8.17 (d, 2 H, J = 9.0); ^{13}C NMR ($CDCl_3$) δ 17.04, 24.80, 29.77, 34.89, 119.43, 123.71, 129.18, 146.45, 149.18; mass spectrum (DEI), m/e 204 $(M)^+$.

4-(4-Nitrophenyl)pentanoic Acid (14). A solution of **13** (10.26 g, 50.2 mmol) in 6 M HCl (500 mL) was refluxed for 60 h. After cooling to room temperature, the reaction mixture was extracted with CH_2Cl_2 (2 × 150 mL), and the organic extracts were combined and extracted with 5% aqueous $NaHCO_3$ (10 × 100 mL). The aqueous extracts were combined, acidified to pH 2 by addition of concentrated HCl at 0 °C, then extracted with CH_2Cl_2 (4 × 150 mL). The combined organic extracts were dried over anhydrous Na_2SO_4 then evaporated to dryness to give a white solid. Recrystallization from H_2O gave 10.24 g (91%) of **14** in the form of colorless prisms: ^1H NMR ($CDCl_3$) δ 1.62–1.79 (m, 4 H), 2.35–2.45 (m, 2 H), 2.70–2.80 (m, 2 H), 7.33 (d, 2 H, J = 9.0), 8.15 (d, 2 H, J = 9.0); ^{13}C NMR ($CDCl_3$) δ 24.04, 30.13, 33.67, 35.38, 123.61, 129.11, 146.30, 149.78, 179.80; mass spectrum (DEI), m/e 223 $(M)^+$. Anal. Calcd for $C_{11}H_{13}NO_4$: C, 59.19; H, 5.87; N, 6.27. Found: C, 58.96; H, 5.98; N, 6.20.

α-Bromo-4-(4-nitrophenyl)pentanoic Acid Methyl Ester (15). A mixture of **14** (3.97 g, 17.8 mmol) and thionyl chloride (16.3 g, 137 mmol) in dry CCl_4 (40 mL) was refluxed for 45 min under N_2. The reaction mixture was cooled to room temperature and *N*-bromosuccinimide (3.97 g, 22.3 mmol) and HBr (10 drops of a 47–49% aqueous solution) were added, then the mixture was stirred at reflux for a further 2 h. After cooling to room temperature, the reaction mixture was evaporated to dryness, redissolved in MeOH (100 mL), and refluxed under N_2 for a further 1.5 h. After again cooling to room temperature, the reaction mixture was evaporated to dryness under vacuum and the residue was dissolved in CH_2Cl_2 (150 mL) and extracted with H_2O (2 × 75 mL). The organic phase was dried over anhydrous Na_2SO_4 and evaporated to dryness to give a dark brown oil which was chromatographed on a silica gel column eluted with CH_2Cl_2. The eluate was evaporated to dryness and the residue recrystallized from hexane to give 2.2 g (39%) of **15** as colorless prisms: ^1H NMR ($CDCl_3$) δ 1.65–2.19 (m, 4 H), 2.77 (t, 2 H, J = 7.5), 3.78 (s, 3 H), 4.24 (m, 1 H), 7.34 (d, 2 H, J = 9.0), 8.16 (d, 2 H, J = 9.0); mass spectrum (DCI), m/e 333 $(M + NH_4)^+$. Anal. Calcd for $C_{12}H_{14}NO_4Br$: C, 45.59; H, 4.46; N, 4.43. Found: C, 45.63; H, 4.49; N, 4.38.

1,4,7,10-Tetraazacyclododecane-*N*,*N*′,*N*″-triacetic Acid Trimethyl Ester (17). A mixture of 1,4,7,10-tetraazacyclododecane (1.0 g, 5.8 mmol), methyl bromoacetate (3.55 g, 23.2 mmol), and triethylamine (1.69 g, 16.7 mmol) in dry MeOH (25 mL) was refluxed for 16 h under N_2. After cooling to room temperature, the reaction mixture was evaporated to dryness and the residue was triturated with 2-propanol (5 mL). The resulting white solid was filtered off and washed with additional 2-propanol (5 mL), then the filtrate plus washings were evaporated to dryness. The resulting oil was further purified by preparative TLC on silica gel plates developed in 10% *i*-PrOH/90% CH_2Cl_2 to give 1.21 g (54%) of **17** in the form of a pale brown oil: ^1H NMR ($CDCl_3$) δ 2.72–

2.99 (m, 17 H), 3.40–3.49 (m, 6 H), 3.66–3.75 (m, 9 H); mass spectrum (DCI), m/e 389 $(M + H)^+$. Anal. Calcd for $C_{17}H_{32}H_4O_6 \cdot CH_2Cl_2$: C, 45.67; H, 7.24; N, 11.84. Found: C, 45.91; H, 7.43; N, 11.93.

***N*-[4-(4-Nitrophenyl)-1-carboxybutyl]-1,4,7,10-tetraazacyclododecane-*N*′,*N*″,*N*‴-triacetic Acid (18).** A mixture of **17** (2.43 g, 6.26 mmol), **15** (3.94 g, 12.5 mmol) and triethylamine (636 mg, 6.28 mmol) in dry MeOH (21 mL) was refluxed under N_2 for 6 days. After cooling to room temperature, the reaction mixture was evaporated to dryness and the residue was dissolved in CH_2Cl_2 (100 mL) and extracted with saturated aqueous $NaHCO_3$ (75 mL) and H_2O (75 mL). The organic phase was then dried over anhydrous Na_2SO_4 and evaporated to dryness under vacuum to give an oil. This was chromatographed on a silica gel column eluted first with CH_2Cl_2 then with 20% MeOH/80% CH_2Cl_2, fractions eluting in the latter being combined and evaporated to dryness to give a brown oil, which was used in the next step without further purification. The oil was dissolved in EtOH (40 mL) and the resulting solution stirred at room temperature while 0.5 M NaOH (80 mL) was slowly added. After stirring at room temperature for a further 18 h, the reaction mixture was applied directly to a Bio-Rad AG1-X4 anion-exchange column (formate form, 50-mequiv capacity). The column was eluted successively with H_2O (500 mL), 0.05 M formic acid (500 mL), 0.1 M formic acid (500 mL), and 0.2 M formic acid (1 L). The 0.2 M formic acid fractions were combined and evaporated to dryness to give 0.80 g (36%) of **18** in the form of a tan solid: ^1H NMR (D_2O) δ 1.55–1.63 (m, 4 H), 2.62–4.01 (m, 25 H), 7.45 (d, 2 H, J = 9.0), 8.17 (d, 2 H, J = 9.0); mass spectrum (FAB), m/e 568 $(M + H)^+$. Anal. Calcd for $C_{25}H_{37}N_5O_{10} \cdot H_2O$: C, 51.28; H, 6.71; N, 11.96. Found: C, 50.90; H, 6.53; N, 11.71.

***N*-[4-(4-Aminophenyl)-1-carboxybutyl]-1,4,7,10-tetraazacyclododecane-*N*′,*N*″,*N*‴-triacetic Acid (19).** A mixture of **18** (199 mg, 0.35 mmol) and 10% palladium on carbon (20 mg) in H_2O (50 mL) was hydrogenated in a Parr apparatus at room temperature and 35 psi H_2 for 3 h. The catalyst was removed by filtration and the filtrate evaporated to dryness to give 179 mg (95%) of **19** in the form of a white solid: ^1H NMR (D_2O) δ 1.55–1.90 (m, 4 H), 2.57–4.08 (m, 25 H), 7.36 (m, 4 H); mass spectrum (FAB), m/e 538 $(M + H)^+$.

***N*-[4-(4-Isothiocyanatophenyl)-1-carboxybutyl]-1,4,7,10-tetraazacyclododecane-*N*′,*N*″,*N*‴-triacetic Acid (20).** An 85% (v:v) solution of thiophosgene (223 mg, 1.94 mmol) in CCl_4 was added to a solution of **19** (81 mg, 0.15 mmol) in 3 M HCl (3.5 mL) and the mixture stirred at room temperature for 6 h. The residue obtained on evaporation of the reaction mixture to dryness was dissolved in 4 M HCl (10 mL) and reevaporated to dryness under vacuum to give 88 mg (89%) of **20** in the form of a tan powder: ^1H NMR (D_2O) δ 1.55–1.89 (m, 4 H), 2.57–4.04 (m, 25 H), 7.28 (s, 4 H); mass spectrum (FAB), m/e 580 $(M + H)^+$.

RESULTS AND DISCUSSION

Syntheses of these bifunctional chelators were for the most part straightforward. Carboxymethylation of 4-nitrophenylalanine and subsequent conversion to **4** by standard methods was a simple, high-yield procedure. The absence of competing lactam-forming reactions, which had been a major obstacle in preparing the EDTA and DTPA systems (*17*), facilitated carboxymethylation of **7** and permitted synthesis of the EGTA analogue **10** in relatively high overall yield [24% based on (4-nitrophenyl)pyruvic acid]. In the case of the macrocyclic system, introduction of the protein-reactive side chain was achieved by direct alkylation rather than reductive alkylation, as the polyamine precursor contained only secondary amino groups. The synthetic strategy that was adopted required controlled carboxymethylation of this polyamine, **16**, such that trisubstituted species **17** was the major product. Reaction conditions were optimized empirically and it was determined that an input stoichiometry of methyl bromoacetate:**16** of 4:1 provided a maximal yield of **17** (54%), with the tetrasubstituted side product being isolated in yields of 9–20%. The remainder of the synthetic route to **20** was unremarkable.

Formation constants for 1:1 trivalent metal complexes of NTA (typically 10^8–10^{12}) are inadequate for in vivo applications, but an ability to form protein–NTA–metal–NTA–protein linkages may provide a nondenaturing and readily reversible means for cross-linking two proteins, such as an antibody and an enzyme, for in vitro use. The bifunctional NTA ligand may also prove useful for tethering ternary metal complexes to proteins, e.g. an [(NTA)Eu(DK)] label might allow direct observation of europium fluorescence without needing to release the metal from the protein with excess DK, as is presently done (*20*). EGTA is an octadentate chelator best known for its selectivity for Ca^{2+} relative to Mg^{2+}, which exceeds that of most calcium-binding proteins (*21*). Applications ranging from novel chromatographic matrices for the removal of Ca^{2+}, through selective probes of intracellular calcium metabolism, to constructs for intervening in calcium-dependent processes in vivo can be envisioned with use of the bifunctional version of this ligand. DOTA is a recently described macrocyclic chelator that forms very stable complexes with radioactive ($^{90}Y^{3+}$, $^{212}Bi^{2+}$) and paramagnetic (Gd^{3+}) metals that are of interest for radiotherapy (*12*, *13*, *22*) and MRI contrast (*23*) applications, respectively. All of these potential uses remain speculative at this point, but access to appropriate bifunctional ligand systems is an essential first step in evaluating such possibilities. The ability to introduce a protein-reactive substituent into any polyaminopolycarboxylate chelator, either by reductive alkylation with **5** (Scheme II and ref 17), in the case of polyamine precursors that contain a primary amine, or by direct alkylation with **15** (Scheme III), for polyamine frameworks that contain only secondary amino groups, should facilitate the identification of additional areas where an interface between coordination chemistry and protein biochemistry may bear fruit.

LITERATURE CITED

(1) Meares, C. F., and Wensel, T. G. (1984) Metal chelates as probes of biological systems. *Acc. Chem. Res. 17*, 209–214.
(2) Meares, C. F., and Goodwin, D. A. (1984) Linking radiometals to proteins with bifunctional chelating agents. *J. Protein Chem. 3*, 215–228.
(3) Sundberg, M. W., Meares, C. F., Goodwin, D. A., and Diamanti, C. I. (1974) Selective binding of metal ions to macromolecules using bifunctional analogues of EDTA. *J. Med. Chem. 17*, 1304–1307.
(4) Yeh, S. M., Sherman, D. G., and Meares, C. F. (1979) A new route to "bifunctional" chelating agents: conversion of amino acids to analogs of ethylenediaminetetra-acetic acid. *Anal. Biochem. 100*, 152–159.
(5) Altman, J., Shoef, N., Wilchek, M., and Warshawsky, A. (1983) Bifunctional chelating agents. Part 1. 1-(*p*-aminophenethyl)-ethylenediaminetetra-acetic acid. *J. Chem. Soc. Perkin Trans.* 365–368.
(6) Brechbiel, M. W., Gansow, O. A., Atcher, R. W., Schlom, J., Esteban, J., Simpson, D. E., and Colcher, D. (1986) Synthesis of 1-(*p*-isothiocyanatobenzyl) derivatives of DTPA and EDTA.

Antibody labeling and tumor imaging studies. *Inorg. Chem. 25*, 2772–2781.
(7) Esteban, J. M., Schlom, J., Gansow, O. A., Atcher, R. W., Brechbiel, M. W., Simpson, D. E., and Colcher, D. (1987) New method for the chelation of indium-111 to monoclonal antibodies: biodistribution and imaging of athymic mice bearing human colon carcinoma xenografts. *J. Nucl. Med. 28*, 861–870.
(8) Kozak, R. W., Raubitschek, A., Mirzadeh, S., Brechbiel, M. W., Junghaus, R., Gansow, O. A., and Waldman, T. A. (1989) Nature of the bifunctional chelating agent used for radioimmunotherapy with yttrium-90 monoclonal antibodies: critical factors in determining in vivo survival and organ toxicity. *Cancer Res. 49*, 2639–2644.
(9) Mathias, C. J., Sun, Y., Connett, J. M., Philpott, G. W., Welch, M. J., and Martell, A. E. (1990) A new bifunctional chelate, $BrMe_2HBED$: an effective conjugate for radiometals and antibodies. *Inorg. Chem. 29*, 1475–1480.
(10) Mathias, C. J., Sun, Y., Welch, M. J., Connett, J. M., Philpott, G. W., and Martell, A. E. (1990) *N,N'*-Bis(2-hydroxybenzyl)-1-(4-bromoacetamidobenzyl)-1,2-ethylenediamine-*N,N'*-diacetic acid: a new bifunctional chelate for radiolabeling antibodies. *Bioconjugate Chem. 1*, 204–211.
(11) Moi, M. K., Meares, C. F., McCall, M. J., Cole, W. C., and DeNardo, S. J. (1985) Copper chelates as probes of biological systems: stable copper complexes with a macrocyclic bifunctional chelating agent. *Anal. Biochem. 148*, 249–253.
(12) Moi, M. K., Meares, C. F., and DeNardo, S. J. (1988) The peptide way to macrocyclic bifunctional chelating agents: synthesis of 2-(p-nitrobenzyl)-1,4,7,10-tetraazacyclododecane-*N,N',N'',N'''*-tetraacetic acid and study of its yttrium(III) complex. *J. Am. Chem. Soc. 110*, 6266–6267.
(13) Cox, J. P. L., Jankowski, K. J., Kataky, R., Parker, D., Beeley, N. R. A., Boyce, B. A., Eaton, M. A. W., Millar, K., Millican, A. T., Harrison, A., and Walker, C. (1989) Synthesis of a kinetically stable yttrium-90 labelled macrocycle–antibody conjugate. *J. Chem. Soc. Chem. Commun.* 797–798.
(14) Craig, A. S., Helps, I. M., Jankowski, K. J., Parker, D., Beeley, N. R. A., Boyce, B. A., Eaton, M. A. W., Millican, A. T., Millar, K., Phipps, A., Rhind, S. K., Harrison, A., and Walker, C. (1989) Towards tumour imaging with indium-111 labelled macrocycle-antibody conjugates. *J. Chem. Soc. Chem. Commun.* 794–796.
(15) Morphy, J. R., Parker, D., Kataky, R., Harrison, A., Eaton, M. A. W., Millican, A., Phipps, A., and Walker, C. (1989) Towards tumour targeting with copper-radiolabelled macrocycle-antibody conjugates. *J. Chem. Soc. Chem. Commun.* 792–794.
(16) Braughler, J. M., Burton, P. S., Chase, R. L., Pregenzer, J. F., Jacobsen, E. J., VanDoornik, F. J., Tustin, J. M., Ayer, D. E., and Bundy, G. L. (1988) Novel membrane localized iron chelators as inhibitors of iron-dependent lipid peroxidation. *Biochem. Pharmacol. 37*, 3853–3860.
(17) Westerberg, D. A., Carney, P. L., Rogers, P. E., Kline, S. J., and Johnson, D. K. (1989) Synthesis of novel bifunctional chelators and their use in preparing monoclonal antibody conjugates for tumor targeting. *J. Med. Chem. 32*, 236–243.
(18) Sun, Y., Martell, A. E., and Motekaitis, R. J. (1985) New multidentate ligands. 27. Synthesis and evaluation of metal ion affinities of new endocyclic hydroxamate macrocycles. *Inorg. Chem. 24*, 4343–4350.
(19) Richman, J. E., and Atkins, T. J. (1974) Nitrogen analogues of crown ethers. *J. Am. Chem. Soc. 96*, 2268–2270.
(20) Hemmilä, I, Dakubu, S., Mukkala, V-M., Siitari, H, and Lövgren, T. (1984) Europium as a label in time-resolved immunofluorometric assays. *Anal. Biochem. 137*, 335–343.
(21) Schauer, C. K., and Anderson, O. P. (1987) Calcium-selective ligands. 2. Structural and spectroscopic studies on calcium and cadmium complexes of $EGTA^{4-}$. *J. Am. Chem. Soc. 109*, 3646–3656.
(22) Gansow, O. A., Kumar, K., Brechbiel, M. W., Mirzadeh, S., Anderson-Berg, W. T., Ruegg, C. L., and Strand, M. (1990) Bismuth complexes of the bifunctional DTPA's and of the polyazacycloalkane-*N*-acetic acid DOTA. *J. Nucl. Med. 31*, 824.
(23) Magerstadt, M., Gansow, O. A., Brechbiel, M. W., Colcher, D., Baltzer, L., Knop, R. H., Girton, M. E., and Naegele, M. (1986) Gd(DOTA): An alternative to Gd(DTPA) as a T1,2 relaxation agent for NMR imaging or spectroscopy. *Magn. Reson. Med. 3*, 808–812.

Immunoadsorbents with Synthetic Oligosaccharide Hapten Representing Blood Group A Substances

M. Abdul Mazid* and Marie Kaplan†

CHEMBIOMED LTD., Edmonton Research Park, 2011-94 Street, Edmonton, Alberta, Canada T6H 4N9.
Received October 10, 1990

Immunoadsorbents with a synthetic oligosaccharide hapten representing human blood group A specific substances are prepared. The synthetic hapten, known as A-trisaccharide, which carries a space arm, is chemically attached to various solid supports, either directly through a suitable functional group at the end of the spacer arm or indirectly via a protein conjugated to the hapten. The preparation involves simple and mild procedures for the activation and/or derivatization of the supports. The latter includes naturally occurring polyhydroxy materials such as agarose, cellulose, or cellulose derivatives, and other particulate materials such as inorganic diatomites and a synthetic organic copolymer. The methods used for the coupling concern specifically the preparation of controlled-capacity and high-efficiency immunoadsorbents, with limited incorporations, which may be prepared easily and used for the selective removal, or affinity chromatographic separation, of specific antibodies from plasma environment or blood. It has been found that while hapten incorporation to the support may be varied rather easily, the physical nature of the support as well as the form of the hapten is important in determining the efficiency of an immunoadsorbent.

INTRODUCTION

Selective removal of specific substances from blood has been described variously since therapeutic intervention with an immunoadsorbent was first reported in the mid-1970s. Considerable attention has been devoted to the development of adsorbents for the removal of unwanted plasma protein components, especially for the treatment of autoimmune disorders. Several experimental in vivo systems for the elimination of specific antigens or antibodies have been reported. In one example, blood flows through a tube coated with entrapped immunoadsorbents (*1*). In another, antigen is bound to a derivatized nylon tube which is used to remove specific antibody during blood circulation (*2*). Yet, in a different system, antigen is immobilized on collodion adherent to activated charcoal particles and placed into a column to remove antibodies from dogs by perfusion of plasma through the column (*3*).

The feasibility of the foregoing approach has been demonstrated for the removal of anti-A and anti-B antibodies using formalin-fixed erythrocytes as immunoadsorbents (*4*). Subsequently, synthetic trisaccharides representing blood group A and B substances chemically coupled to silica particles have been used in a number of studies (*5–16*) for the selective removal of A and B isoagglutinins directed against the corresponding blood groups. Some of these studies have been applied in humans and it has been possible to successfully avoid the effects of ABO incompatibility in bone marrow and renal transplants. Another therapeutic approach has been the use of protein A bound to charcoal–collodion for the treatment of solid tumors (*17*) and heat-killed *Staphylococcus aureus* sorbent to remove serum IgG in autoimmune hemolytic anemia syndrome (*18*). Recently, Behm et al. (*19*) reviewed selective and specific adsorbents for medical therapy, while Margel and Marcus (*20*) described the potential uses of a specific sorbent system consisting of cross-linked agarose–polyacrolein microsphere beads (so called agarose acrobeads) for specific hemoperfusion in various systems.

Affinity adsorbents using agarose as a carrier have been prepared mostly by two methods: the cyanogen bromide (CNBr) method and the epoxy method. Immunoadsorbents with blood group substance A, in particular, coupled to cross-linked agarose by the CNBr method has been described by Kristiansen (*21*). The adsorbent prepared by this method is reported to have a number of disadvantages, including low ligand concentration, instability, nonspecific adsorption, and excess chemical reactivity (*22*). With the epoxy method, nonderivatized sugars have been used directly to obtain a stable linkage, a higher degree of substitution, and an adsorbent with less nonspecific adsorption (*22–25*). However, this method has some disadvantages such as the requirement of high pH and a large excess of ligand during the coupling step. Therefore, some epimerization and degradation of sugars are considered inevitable in this step (*24*, *26*). To avoid these severe conditions for coupling, the conversion of epoxy groups on agarose gel into more reactive groups has been reported (*27*).

Matsumoto et al. (*22*) described the derivatization of amino and carboxyl agarose, prepared from epoxy-activated agarose by simple procedures, with a variety of sugars under mild conditions. Two types of affinity adsorbents for the purification of lectins were prepared. These include coupling of oligosaccharide ligands (lactose and maltose) by reductive amination with cyanoborohydride to amino-Sepharose 4B prepared by amination of epoxy-activated Sepharose 4B. The second type of affinity adsorbent involves coupling of hexosamines (GalN and GlcN) by the aid of carbodiimide to carboxy-Sepharose 4B prepared by succinylation of amino-Sepharose 4B. Both types of adsorbents have high ligand concentrations and chemically stable linkage between ligand and Sepharose 4B; however, the coupling of oligosaccharides to amino-

* Author to whom all correspondence should be addressed.
† Present address: Department of Medical Microbiology, University of Alberta, Edmonton, Alberta, Canada.

1043-1802/91/2902-0032$02.50/0 © 1991 American Chemical Society

Sepharose 4B by reductive amination is very slow, while the coupling of amino sugars with carboxy-Sepharose-4B via succinylation also requires a large excess of ligand during the coupling step and does not necessarily produce a good adsorbent with high capacity. This fact alone is a major drawback to the use of synthetic oligosaccharides such as the blood group determinants for the removal of specific antibodies by extracorporeal immunoadsorption.

It is notable that most immunoadsorbents so far have been reported with arbitrary amounts of ligands contained therein or coupled thereto, possibly limited by the efficiency or conditions of the coupling method used and, perhaps, without due consideration to the utilization of optimum capacity of the immunoadsorbents. We have recently reported on the flow-rate dependence of in vitro removal of anti-A and anti-B antibodies by immunoadsorbents with synthetic oligosaccharides representing blood group substances (*28*). However, a systematic study of the relationship between ligand density and specific binding or selective removal capacity of an immunoadsorbent during therapeutic intervention is not possible, nor is it easy to evaluate the efficacy of different immunoadsorbents using various solid supports even with the same ligand. This paper attempts to describe a comparative study of a number of immunoadsorbents under laboratory conditions. The immunoadsorbents are prepared by covalently linking chemically synthesized A-trisaccharide hapten with a spacer arm (abbreviated together as ATS), representing human blood group A substances, to a variety of commercially available support materials, their capacities being evaluated by in vitro hemagglutination techniques following batch absorptions. In particular, the methods used for the chemical coupling of the synthetic hapten concern its limited incorporation to the support material and relate specifically to the preparation of controlled-capacity and efficient immunoadsorbents for the selective removal of anti-A antibodies from human plasma.

EXPERIMENTAL PROCEDURES

Materials and Methods. General. Immunoadsorbents with chemically synthesized human blood group A-trisaccharide, an 8-(azidocarbonyl)octyl derivative of αGalNAc1,3[αFuc1,2]βGal or a similar derivative of the trisaccharide but with another functional group at the end of the spacer arm, covalently attached to natural polyhydroxy supports and other particulate materials, including inorganic silica and a synthetic copolymer, are prepared by published methods. The natural polyhydroxy supports are of the types of agarose and cellulose, which include commercially available Sepharose 4B (Pharmacia), (aminoethyl)cellulose, (carboxymethyl)cellulose (AE- and CM-cellulose, Sigma), beaded Excellulose (Pierce), and ordinary cotton. The synthetic support material used is the aminomethylated styrene/divinylbenzene (DVB) copolymer, available under the trade name of Lewatit (Bayer), while the inorganic silica particle is of the diatomaceous type Chromosorb P (30/60 mesh) obtained from Manville Corp.

The synthetic blood group substance, i.e. the A-trisaccharide with the linking spacer arm, and the trisaccharide-derivatized silica particles, known as Synsorb A, are the products of Chembiomed Ltd. (Edmonton, Canada). The latter is surface-modified with a synthetic polymeric membrane-type coating by a proprietary technique (*29*) to provide a better surface resistance and therefore adequate physical and mechanical stability to the immunoadsorbent particles (otherwise known as Biosynsorb A). This coating prevents the release of potentially harmful fines during clinical application, while the original biological activity and efficacy is maintained. The derivatization of silica particles follows the introduction of reactive amino groups using (3-aminopropyl)triethoxysilane under standard conditions (*30*) as described elsewhere (*29, 31, 32*). The silane-treated diatomite itself containing approximately 5–10 μmol of NH_2/g, also coated by the above mentioned proprietary technique, are additionally coupled to the synthetic trisaccharide indirectly via a conjugated protein such as bovine serum albumin (BSA) in various amounts.

The aminoethyl and carboxymethyl derivatives of cellulose and aminomethylated styrene/divinylbenzene supports are used without further derivatization. In general, the coupling procedure involves treatment of the carboxyl derivative of the support or the synthetic ligand with di-*N*-succinimidyl carbonate (DSC), followed by reaction with an amino-terminated ligand or support, respectively. The coupling of amino groups is performed via activation with glutaraldehyde and that of amino groups and carboxyl groups between the support and the ligand are achieved in the presence of a water-soluble carbodiimide, while underivatized polyhydroxy supports are utilized after activation with divinyl sulfone or epoxy reagents.

Immobilization of A-Trisaccharide. Di-*N*-succinimidyl Carbonate Activation. Di-*N*-succinimidyl carbonate is dissolved in 0.2–0.5 mL of dimethylformamide (DMF) to which is added a molar equivalent of carboxyl-terminated A-trisaccharide (ATS-acid). Alternatively, the solution of DSC in DMF is added to a suspension of the carboxyl-derivatized support CM-cellulose (thoroughly washed and preswelled) in DMF. The activation of the ligand or the support is carried out for 2–3 h, followed by addition of the amino-derivatized support AE-cellulose or the ligand ethylenediamine (EDA) terminated A-trisaccharide, ATS-EDA, or ATS–BSA conjugate. The coupling reaction is continued overnight (12–16 h) at room temperature with gentle agitation, and then the support is washed thoroughly with water, the washings being saved for the estimation of the trisaccharide and therefore its incorporation to the support. Finally, the haptenated support is treated with a solution of 10% glycine in 0.5 M Na_2CO_3 to block any residual activated carboxyl group on the support.

1-Ethyl-3-[3′-(dimethylamino)propyl]carbodiimide Activation. The covalent attachment of amino group and carboxyl group between the support and the ligand is performed in the presence of a water-soluble carbodiimide such as 1-ethyl-3-[3′-(dimethylamino)propyl]carbodiimide hydrochloride (EDAC). About 10 mg of the reagent is dissolved initially in a buffer under acidic conditions, 0.1 M phosphate at pH between 4.0 and 5.0, and the carboxyl group containing ligand ATS-acid or the support CM-cellulose is mixed to it. The mixture is rotated for 30 min at room temperature, and then the support AE-cellulose or the ligand containing an amino group is added. The coupling reaction is continued for 3–4 h at room temperature after which the haptenated support is washed thoroughly with water.

Glutaraldehyde Activation. The coupling reaction between amino groups in supports, including the silane-treated and surface-modified diatomite, and ligands via activation with glutaraldehyde is carried out under the following conditions. The support is suspended in a buffer, 0.1 M borate or phosphate at a pH in the range of 7–9, containing 1–10% glutaraldehyde, which is precooled to

a temperature below 10 °C. The activation of the support is carried out at this temperature for 1 h with gentle stirring, and then washed extensively with water or buffer until a negative Schiff's test is obtained. The washed support is kept suspended in the same buffer, pH ~7, to which the amino-terminated ligand ATS-EDA or ATS-BSA conjugate is added. The coupling reaction is carried out initially at room temperature for 1 h and then continued overnight at temperatures between 0 and 4 °C. The haptenated support is washed thoroughly with cold water, followed by washing with phosphate buffer containing 1 M NaCl in the case of coupling with ATS-BSA conjugate, and finally suspended in water or the buffer after washing off the NaCl. The washings are saved for the estimation of trisaccharide by the phenol-sulfuric acid assay (*33*) or protein by the standard Bio-Rad procedures (*34*).

Epoxy Activation. The hydroxyl groups occurring in agarose and cellulose are utilized for chemical coupling of the A-trisaccharide, following initial activation and functionalization by published methods (*22, 26*). These involve the formation of epoxy derivatives with epichlorohydrin (ECH) or the long-chain bisoxirane 1,4-*n*-butanediol diglycidyl ether (BDDE) under basic conditions, e.g. 5% (v/v) in 0.4 N NaOH solution containing 20% dioxane, to provide for a covalently linked epoxide. The epoxide group is then opened with 6 M ammonia or 5% ethylenediamine to provide for terminal primary amines. This, in turn, is utilized for coupling of carboxyl-terminated hapten using methods previously described, involving di-*N*-succinimidyl carbonate activated ATS-acid in DMF. After washing with methanol, the remaining amine groups are blocked by acetylation in 5% acetic anhydride in methanol.

Divinyl Sulfone Activation. The activation of hydroxyl group containing natural polymers (agarose and cellulose) is performed with divinyl sulfone (DVS) in alkaline solutions (*35*). The reaction is carried out for 3 h at room temperature or 1 h at 40 °C using 0.1–0.5 mL of the reagent in a suspension of 5–10 g suction-dried support in 10–20 mL solution of 0.5 M Na_2CO_3. The amino-terminated ATS-EDA or ATS-BSA conjugate is coupled by mixing overnight at room temperature, also in 0.5 M Na_2CO_3, but after washing the activated support free of divinyl sulfone. Any unreacted vinyl group is blocked by reaction with a solution of glycine (10% w/v) in 0.5 M Na_2CO_3 or 1.5 M 2-mercaptoethanol or sodium thiosulfate (*35*).

Determination of Biological Activity of Immunoadsorbents. The immunoadsorbents prepared by various methods are tested for their biological activity by in vitro hemagglutination technique. Generally, 25 mg of the immunoadsorbent material (suction-dried) is incubated with 0.5 mL of O-plasma or O-serum by rotating in a hematology mixer for 1 h at room temperature (21 °C). The supernatant is then removed, and antibody titers of IgM and IgG are determined by saline agglutination and indirect antiglobulin (Coombs) tests, respectively, at 37 °C from serial dilutions with human A_1RBC (red blood cells) by using standard procedures (*36*). The titers are expressed as the reciprocal of the highest dilution that produces macroscopically visible agglutination. It is to be noted that some of the antibody titers (indicated with a footnote in tables of results) have been obtained with O-serum/plasma of which preadsorption titers are lower by a factor of 2 or 4 (one or two reciprocal dilutions) than the most commonly observed preadsorption titers shown in the top of a table. These titers are therefore multiplied by the corresponding factor for the purpose of a more direct comparison.

Table I. Biological Activity of Immunoadsorbents Based on Agarose Coupled with A-Trisaccharide

material tested	hapten incorporated, μmol/g of suction-dried support	human A_1 titers IgM	IgG
O-serum	–	32	256
agarose control, ECH/EDA treated and acetylated	0	32	128
agarose–ATS-acid	0.12	8	32
	0.36	8	16
	0.68	4	8
	1.26	2	4
	3.02	1	4
agarose–(ATS–BSA)	0.46	4	32[a]

[a] Titer multiplied by four to conform with that of the starting serum.

Table II. Biological Activity of Immunoadsorbents Based on Cellulosic Supports Coupled with A-Trisaccharide

material tested	hapten incorporated, μmol/g of suction-dried support	human A_1 titers IgM	IgG
O-plasma		64	128
cellulose fiber, untreated control	0	64	64
cellulose–ATS-acid	1.84	32	64
cellulose–(ATS–BSA)	0.14	64	128
beaded cellulose, untreated control	0	32	64
beaded cellulose–(ATS–EDA)	0.46	32	64
beaded cellulose–ATS-acid	0.51	32	64
beaded cellulose–(ATS–BSA)	0.07	16	32[a]

[a] Titer multiplied by two to conform with that of the starting plasma.

Table III. Biological Activity of Immunoadsorbents Based on Derivatized Cellulosic Supports with A-Trisaccharide

material tested	hapten incorporated, μmol/g of suction-dried support	human A_1 titers IgM	IgG
O-plasma		64	128
AE-cellulose, washed control	0	64	128
AE-cellulose–ATS-acid	1.67	8	32
AE-cellulose–(ATS–BSA)	0.19	2	4
CM-cellulose, washed control	0	64	64
CM-cellulose–(ATS–BSA)	0.31	8	16

RESULTS AND DISCUSSION

The biological activity of various immunoadsorbents as well as the amount of hapten incorporated therein are shown in Tables I–V. Included in Tables I and V are also the results for agarose- and diatomite-based immunoadsorbents at different levels of haptenation with ATS-acid and ATS–BSA conjugates, respectively.

Table I shows that the efficiency of antibody removal with the agarose-based immunoadsorbents increases significantly as the amount of hapten incorporation is increased. This would suggest that a certain amount of hapten may be attached to a smaller quantity of agarose gel and yet obtain the same level of efficiency. There is, however, no significant advantage in coupling an antigen such as ATS–BSA conjugate to agarose-type supports since the efficiencies of these immunoadsorbents with equivalent amounts of A-trisaccharide hapten are about the same. This may be accounted for by the fact that the porosity of the agarose beads (exclusion limit of 20×10^6 Da) is sufficient to allow equally efficient interaction of antibodies with haptens coupled to the support either directly or

Table IV. Biological Activity of Immunoadsorbents Based on Synthetic Styrene/DVB Copolymers Coupled with A-Trisaccharide

material tested	hapten incorporated, μmol/g of suction-dried support	human A_1 titers IgM	IgG
O-plasma		64	128
aminomethylated (AM) styrene/DVB control	0	32[a]	128[a]
AM-styrene/DVB, acetylated	0	32	32
AM-styrene/DVB-ATS-acid	1.13	64[a]	128[a]
AM-styrene/DVB-ATS-acid, acetylated	0.38	64[a]	128[a]
AM-styrene/DVB-(ATS-BSA)	0.13	8[a]	16[a]
AM-styrene/DVB-BSA (0.44 mg/g)	0	64	128

[a] Titers multiplied by a factor of 4 to conform with that of the starting plasma.

Table V. Biological Activity of Immunoadsorbents Based on Inorganic Diatomaceous Supports (30/60 Mesh) Coupled with A-Trisaccharides

material tested	hapten incorporated, μmol/g of suction-dried support	human A_1 titers IgM	IgG
O-plasma	–	128	256
0.5% polystyrene-coated diatomite	0	64	128
precoated diatomite coupled with ATS-BSA after glutaraldehyde activation	0.05	32	64
	0.10	16	32
	0.20	16	32
	0.30	16	32
	0.40	16	32
precoated diatomite coupled with ATS-BSA in the presence of glutaraldehyde	0.05	16	64
	0.10	8	32
	0.20	8	16
uncoated diatomite–ATS	0.7	16	32
uncoated diatomite–(ATS–BSA)	0.6	8[a]	8[a]

[a] Titer adjusted by a factor of 2 to conform with that of the starting plasma.

with conjugated ATS–BSA. It is also possible that the small size of agarose beads (50–140 μm) provides a relatively larger external surface area which is readily available for hapten incorporation and, therefore, more amenable or predisposed to interaction with neutralizing antibodies present in the plasma.

In contrast to agarose-based immunoadsorbents, chemical coupling of haptens to other polyhydroxy supports such as the cellulosic materials in various forms show different results. These supports include fibrous and beaded cellulose as well as cellulose functionalized with aminoethyl and carboxymethyl groups (Tables II and III). Haptenation of cellulose fibers with EDA-terminated A-trisaccharide via activation with the long-chain bisoxirane 1,4-*n*-butanediol diglycidyl ether appeared unsuccessful (data not shown), while ATS–BSA incorporation yields an equivalent of 0.14 μmol of ATS/g of suction-dried support (1 g dry weight corresponds to 2 g of suction-dried support). Also, incorporation of DSC-treated ATS-acid to ECH-activated cotton fiber gives an immunoadsorbent with 1.84 μmol of ATS/g of suction-dried support. However, none of these immunoadsorbents shows any considerable biological activity (see Table II) despite the fact that reasonable levels of hapten incorporation is achieved. Thus, it would appear that small oligosaccharide haptens attached to cellulose are not accessible to the antibodies since cellulose in its fibrous form is relatively nonporous.

Alternatively, haptenation of beaded cellulose was achieved both with ATS–EDA (0.46 μmol/g of suction-dried support) via DVS activation and also with DSC-treated ATS-acid (0.51 μmol/g of suction-dried support) via ECH activation. Again, there is little biological activity as noted in Table II, suggesting that the physical nature of the support is not appropriate or suitable for obtaining an efficient immunoadsorbent. On the other hand, haptenation of beaded cellulose with ATS–BSA conjugate via ECH activation (0.07 μmol of ATS/g of suction-dried support) shows some biological activity, which is consistent with the specified exclusion limit of 5000 Da for this support. However, the overall performance of all the beaded cellulosic supports is generally poor, indicating that the porosity of the beads is not sufficient to permit interaction of antibodies with haptens which may be attached to the interior of the support, similar to the fibrous cellulose.

The effect of the nature of immunoadsorbents on biological activity is more pronounced with derivatized cellulosic supports (see Table III). For instance, haptenation with ATS–BSA was achieved both for AE-cellulose via glutaraldehyde activation (0.19 μmol of ATS/g of suction-dried support) and for CM-cellulose via EDAC activation (0.31 μmol of ATS/g of suction-dried support) or via DSC activation (0.11 μmol of ATS/g of suction-dried support). In terms of biological activity, however, both CM-cellulose supports coupled with ATS–BSA conjugate appear to be equally efficient as the AE-cellulose coupled with DSC-treated ATS-acid which contains about 6–15 times more hapten (1.67 μmol of ATS/g of suction-dried support), while the best efficiency is observed with AE-cellulose–(ATS–BSA) containing only 0.19 μmol of ATS/g of suction-dried support. This implies that the physical nature of the support, including its morphology, as well as the form of the hapten is important in determining the efficiency of an immunoadsorbent.

It would seem that haptenation of an appropriate support with an antigen such as ATS–BSA conjugate is a logical approach to the preparation of an efficient immunoadsorbent. This fact is also corroborated by the results obtained with immunoadsorbents based on styrene/divinylbenzene copolymer coupled with the hapten. Table IV shows that aminomethylated styrene/divinylbenzene copolymer haptenated with ATS–BSA conjugate (0.13 μmol of ATS/g) via glutaraldehyde activation has reasonably good biological activity, while the untreated control support or the one haptenated with a considerable amount of ATS-acid (0.38 μmol/g) has practically no activity. It is also notable that increasing the level of haptenation does not necessarily yield an improved immunoadsorbent, as evident from the results of another styrene/divinylbenzene support coupled with ATS-acid via DSC activation which yields an incorporation of 1.13 μmol/g.

Tests were carried out to determine if acetylation of aminomethylated styrene/DVB copolymer itself or blocking of residual amino groups after haptenation and BSA incorporation alone would show any difference in activity. Incorporation of BSA was done chemically via glutaraldehyde activation of unacetylated support. The results of biological activity assays for styrene/DVB-based immunoadsorbents are shown in Table IV, which includes an untreated support as well. It would appear that there is very little or no effect of the various treatments, in general, while acetylation of the supports, haptenated or

not, enhances the reduction of IgG titers to some extent. This may be explained by increased nonspecific interactions due to blocking of amino groups which would increase the hydrophobicity of the support. However, considering the level of hapten incorporation, this effect is not an important factor in determining the overall efficiency of the immunoadsorbent. It may be noted that the use of different blocking reagents following immobilization of ATS via DVS activation would not influence the immunoadsorbent activity considerably since the blocking involves similar inactivation of otherwise same reactive group on the support.

Table V shows results for immunoadsorbents prepared with aminosilated diatomite (30/60 mesh) which was precoated with a polymer, as described elsewhere (*29*). Haptenation was done by coupling of various amounts of ATS–BSA conjugate via glutaraldehyde activation. Included in the table are also results for an immunoadsorbent prepared by the same procedure but using uncoated diatomite and for one that is haptenated with ATS-acyl azide. The results indicate that a saturating level of efficiency could be reached with a hapten incorporation equivalent to 0.1 μmol of ATS/g of immunoadsorbent, and that haptenation of the coated support in presence of glutaraldehyde (in situ coupling) shows relatively better activity than the support preactivated with glutaraldehyde. In both cases, however, the maximum activity appears to be observed with immunoadsorbents containing only a fraction of the hapten compared to the uncoated supports haptenated either with ATS-acyl azide or with ATS–BSA conjugate, all of which show more or less similar activities. Further work along this line would seem necessary to confirm this finding.

The improved efficiency with precoated immunoadsorbents may be accounted for by the fact that the activation of the supports with glutaraldehyde, and therefore chemical coupling of the ATS–BSA conjugate thereto, would occur rather preferentially on the coated surface and also involve simultaneous intramolecular cross-linking of the protein on the surface of the coated support. This implies that the protein portion of the antigen may be unfolded and hence the haptens are more completely or better exposed to yield maximum biological activity. The significance of these results is that physically stable immunoadsorbents with improved efficiency may be prepared by coating the support first with a suitable polymeric membrane-type film (*29*) followed by chemical attachment or immobilization of an antigenic determinant such as a hapten-protein conjugate by an appropriate method.

ACKNOWLEDGMENT

We wish to thank Dr. R. M. Ippolito for valuable discussion and for his interest in the work.

LITERATURE CITED

(1) Schenkein, I., Bystryn, J.-C., and Uhr, J. W. (1971) Specific removal of in vivo antibody by extracorporeal circulation over an immunoadsorbent in gel. *J. Clin. Invest. 50*, 1864–1868.

(2) Lyle, L. R., Parker, B. M., and Parker, C. W. (1974) The use of protein-substituted nylon catheters for selective immunoadsorption in vivo. *J. Immunol. 113*, 517–521.

(3) Terman, D. S., Tavel, T., Petty, D., Racic, M. R., and Buffaloe, G. (1977) Specific removal of antibody by extracorporeal circulation over antigen immobilized in collodion–charcoal. *Clin. Exp. Immunol. 28*, 180–188.

(4) Buskard, N. A., Williams, B., Terman, D. S., Buckner, C. D., Clift, R. A., Gray, M., and Thomas, E. D. (1978) Antibody adsorption on formalinized red cell ghosts: A potential method for the in vivo removal of isohemagglutinins. *Blood 52 (suppl. 1)*, 296.

(5) Bensinger, W. I. (1981) Plasma exchange and immunoadsorption for removal of antibodies prior to ABO-incompatible bone marrow transplantation. *Int. Soc. Artif. Organs 51*, 254–258.

(6) Bensinger, W. I., Baker, D. A., Buckner, C. D., Clift, R. A., and Thomas, E. D. (1981) Immunoadsorption for removal of A and B blood group antibodies. *N. Engl. J. Med. 304*, 160–162.

(7) Bensinger, W. I., Baker, D. A., Buckner, C. D., Clift, R. A., and Thomas, E. D. (1981) In vitro and in vivo removal of anti-A erythrocyte antibody by adsorption to a synthetic immunoadsorbent. *Transfusion 21*, 335–342.

(8) Bensinger, W. I., Buckner, C. D., Baker, D. A., Clift, R. A., and Thomas, E. D. (1982) Removal of specific antibody in vivo by whole blood immunoadsorption: Preliminary results in dogs. *J. Clin. Apheresis 1*, 2–5.

(9) Bensinger, W. I., Buckner, C. D., Williams, B., and Clift, R. A. (1982) Immune adsorption of anti-A and anti-B antibodies. In *Cytapheresis and Plasma Exchange: Clinical Indications* (W. R. Volger, Ed.) pp 295–300, Alan R. Liss, Inc., New York.

(10) Watanabe, K., Kobayaski, N., Nakamura, K., Kate, S., Hosi, N., Hisazumi, T., and Hida, M. (1983) An example of ABO-incompatible bone marrow transplant by use of immunoadsorbent. *Jpn. Clin. Haematol. Conf. Abstr.* 219.

(11) Bensinger, W. I. (1984) Selective removal of A and B isoagglutinins. In *Selective Plasma Component Removal* (A. A. Pineda, Ed.) pp 43–70, Futura Publishing Co., Mount Kisco, NY.

(12) Bensinger, W. I., Buckner, C. D., and Clift, R. A. (1985) Whole blood immunoadsorption of anti-A or anti-B antibodies. *Vox Sang 48*, 357–361.

(13) Bussel, A., Schenmetzler, C., Gluckman, E., and Reviron, J. (1985) Removal of recipient allo-agglutinins in ABO-incompatible bone marrow transplantation: Comparative study between plasma exchange and immunoadsorption. *Plasma Ther. Transfus. Technol. 6*, 461–464.

(14) Osterwalder, B., Gratwohl, A., Nissen, C., and Speck, B. (1986) Immunoadsorption for removal of anti-A and anti-B blood group antibodies in ABO-incompatible bone marrow transplantation. *Blut 53*, 379–390.

(15) Raja, R., Bannett, A., Caruana, R., and Baquero, A. (1986) Removal of antibodies with immunoadsorption from an ABO-incompatible recipient prior to renal transplant. *Trans. Am. Soc. Artif. Intern. Organs 32*, 102–103.

(16) Bannett, A. D., Bensinger, W. I., Raja, R., Baquero, A., and McAlack, R. F. (1987) Immunoadsorption and renal transplant in two patients with a major ABO-incompatibility. *Transplantation 43*, 909–910.

(17) Terman, D. S., Young, J. B., Shearer, W. T., Ayus, C., Lehane, D., Mattioli, C., Espada, R., Howell, J. F., Yamamoto, T., Zaleski, H. I., Miller, L., Frommer, P., Feldman, L., Henry, J. F., Tillquist, R., Cook, G., and Daskal, Y. (1981) Preliminary observations of the effects on breast adenocarcinoma of plasma perfusion over immobilized protein A. *N. Engl. J. Med. 305*, 1195–1200.

(18) Besa, E. C., Ray, P. K., Swami, V. K., Idiculla, A., Rhoades, J. E., Jr., Bassett, J. G., Joseph, R. R., and Cooper, D. R. (1981) Specific immunoadsorption of IgG antibody in a patient with chronic lymphocytic leukemia and autoimmune hemolytic anemia: A new form of therapy for the acute critical stage. *Am. J. Med. 71*, 1035–1040.

(19) Behm, E., Ivanovich, P., and Klinkmann, H. (1989) Selective and specific adsorbents for medical therapy. *Int. J. Artif. Organs 12*, 1–10.

(20) Margel, S., and Marcus, L. (1986) Specific Hemoperfusion through agarose acrobeads. *Appl. Biochem. Biotechnol. 12*, 37–66.

(21) Kristiansen, T. (1974) Studies on blood group substances. V. Blood group substance A coupled to agarose as an immunosorbent. *Biochim. Biophys. Acta 263*, 567–574.

(22) Matsumoto, I., Kitagaki, H., Akai, Y., Ito, Y., and Seno, N. (1981) Derivatization of epoxy-activated agarose with various carbohydrates for the preparation of stable and high-capacity

affinity adsorbents: Their use for affinity chromatography of carbohydrate-binding proteins. *Anal. Biochem. 116*, 103–110.

(23) Vretblad, P. (1979) Purification of lectins by biospecific affinity chromatography. *Biochim. Biophys. Acta 434*, 169–176.

(24) Uy, R., and Wold, F. (1977) 1,4-Butanediol diglycidyl ether coupling of carbohydrates to Sepharose: Affinity adsorbents for lectins and glycosidases. *Anal. Biochem. 81*, 98–107.

(25) Gurtler, L. G. (1978) The fucosyl specific lectins of *Ulex europaeus* and *Sarothamnus scoparius*: Biochemical characterization and binding properties to human B-lymphocytes. *Biochim. Biophys. Acta 544*, 593–604.

(26) Matsumoto, I., Mizuno, Y., and Seno, N. (1979) Activation of Sepharose with epichlorohydrin and subsequent immobilization of ligand for affinity adsorbent. *J. Biochem. 85*, 1091–1098.

(27) Matsumoto, I., Seno, N., Golovtchenko-Matsumoto, A. M., and Osawa, T. (1980) *J. Biochem. 87*, 535–540.

(28) Kaplan, M., and Mazid, M. A. (1989) Flow rate dependence of in vitro removal of anti-A and anti-B antibodies by immunoadsorbents with synthetic oligosaccharides representing blood group substances. *Int. J. Artif. Organs 12*, 799–804.

(29) Mazid, M. A. (1990) Improved affinity supports for hemoperfusion. European Pat. Appln. EP 0 371 636 A2.

(30) Weetall, H. H., and Filbert, A. M. (1974) Porous glass for affinity chromatography applications. *Methods Enzymol. 34B*, 59–72.

(31) Lemieux, R. U., Bundle, D. R., and Baker, D. A. (1979) Glycoside-ether-ester compounds. U.S. Patent 4 137 401.

(32) Lemieux, R. U., Bundle, D. R., and Baker, D. A. (1980) Artificial oligosaccharide antigenic determinants. U.S. Patent 4 238 473.

(33) Dubois, M., Gilles, K., Hamilton, J. K., Rebers, P. A., and Smith, F. (1956) Colorimetric method for determination of sugars and related substances. *Anal. Chem. 28*, 350–356.

(34) Bradford, M. M. (1979) A rapid and sensitive method for the quantitation of microgram quantities of protein utilizing the principle of protein–dye binding. *Anal. Biochem. 72*, 248–254.

(35) Porath, J., Låås, T., and Janson, J.-C. (1975) Agar derivatives for chromatography, electrophoresis and gel-bound enzymes. III. Rigid agarose gels cross-linked with divinyl sulfone (DVS). *J. Chromatogr. 103*, 49–62.

(36) Issitt, P. D. (1970) *Applied Blood Group Serology*, Chapter 4, Spectra Biologicals, Oxnard, CA.

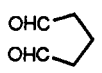
Diazo- and Azido-Functionalized Glutaraldehydes as Cross-Linking Reagents and Potential Fixatives for Electron Microscopy

Sui Xiong Cai and John F. W. Keana*

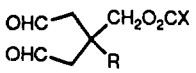
Department of Chemistry, University of Oregon, Eugene, Oregon 97403. Received October 16, 1990

The synthesis of diazo and perfluorophenyl azide (PFPA) functionalized glutaraldehydes **7** and **13a–d** as new cross-linking reagents for bioconjugation and potential fixatives for electron microscopy is reported. A key step is the generation of the 1,5-dialdehyde structures by oxidative cleavage of the corresponding cyclopentene epoxide using HIO_4 in aqueous tetrahydrofuran. A model reaction between 3-substituted glutaraldehyde **14** and 6-aminohexanoic acid resulted in the formation of pyridinium ion containing products with UV spectra comparable to those observed with glutaraldehyde itself. Thus modification of glutaraldehyde in the 3-position most probably did not significantly change its reactivity with amines under chemical-fixation conditions. Fixation of red blood cells by **7** demonstrates that as a fixative, **7** is comparable to glutaraldehyde.

Bifunctional reagents are widely used for the cross-linking of biomolecules such as membrane components (*1*, *2*). Glutaraldehyde (**1**) has been used as a cross-linking



1



2a, R = H
2b, R = CH_2O_2CX

reagent for protein-protein (*3*) and drug–antibody conjugation (*4*) as well as a fixative (*5*) of biological specimens for electron microscopy (EM) (*6*). Glutaraldehyde fixation chemistry is thought to involve a reaction with free amino groups of proteins resulting in the formation of pyridinium and polypyridinium ions (*7*, *8*). Glutaraldehyde generally does not react with lipids (*9*) and no reagent has been reported to be an efficient fixative for saturated lipids (*10*). Herein we report the development of a family of photoactive glutaraldehydes **2** as new cross-linking reagents and potential fixatives for EM preparations. The 3-position of glutaraldehyde was chosen for modification since the protons in the 3-position are not involved in the condensation reaction leading to the formation of pyridinium ions in the proposed mechanism (*7*, *8*). Photolysis of the diazo or azido group X generates a highly reactive carbene or nitrene intermediate which is capable of insertion into unreactive CH bonds with concomitant formation of a stable covalent linkage (*11*).

EXPERIMENTAL PROCEDURES

General Chemical Procedure. Solvents and chemicals were reagent grade and used as received unless otherwise specified. Red blood cells were from fresh human blood of a healthy volunteer. ^1H NMR spectra were measured on a QE-300 NMR spectrometer in $CDCl_3$. IR spectra were recorded on a Nicolet 5DXB FTIR spectrometer in $CDCl_3$. UV spectra were measured on a Beckman DU-7 spectrometer. All reactions involving diazo or azido compounds were run under subdued light by wrapping the flasks with aluminum foil. Reactions were routinely monitored by TLC or ^1H NMR. $MgSO_4$ was used as the drying agent for organic solutions. Photolysis was carried out in a Rayonet photochemical reactor with 254-nm lamps and quartz reaction tubes.

3-Cyclopentene-1-methanol 2′-Diazo-3′,3′,3′-trifluoropropionate (6). (a) A solution of 1.54 g of acyl chloride **5** (*12*) (8.93 mmol) in CH_2Cl_2 (10 mL) was added dropwise to a stirred solution of 0.767 g (7.8 mmol) of alcohol **3a** (*13*) and 1.22 g (12 mmol) of Et_3N in ether (5 mL). It was stirred for 1 h then filtered. The filtrate was washed with water (2 × 15 mL), dried, and evaporated and the residue was distilled to give 1.14 g of **6** as a yellow oil: bp 52–53 °C (0.8 mm); ^1H NMR δ 2.10 (m, 2), 2.50 (m, 2), 2.65 (m, 1), 4.18 (d, 2, J = 7.2 Hz), 5.65 (s, 2); IR 2140, 1720 cm^{-1}; UV λ_{max} = 236 nm, log ϵ = 3.92. Anal. Calcd for $C_9H_9F_3N_2O_2$: C, 46.16; H, 3.87; N, 11.96. Found: C, 45.94; H, 3.84; N, 11.72.

(b) A solution of 57.3 mg (0.192 mmol) of anhydride **8** and 18.2 mg (0.186 mmol) of alcohol **3a** with 39.4 mg (0.498 mmol) of pyridine in THF (2 mL) was heated at 50 °C for 12 h. It was diluted by ether (3 mL), washed by 5% Na_2CO_3 (1 mL) and water (2 × 2 mL). The organic phase was dried and evaporated to leave 32.4 mg of **6** as a pale yellow oil (74%).

1,5-Dioxopentane-3-methanol 2′-Diazo-3′,3′,3′-trifluoropropionate (7). To a stirred mixture of 111 mg (0.475 mmol) of **6** in water (1.5 mL) and ether (1.5 mL) was added 350 μL of 2.5 wt% OsO_4 (6.82 mg, 0.026 mmol)–*tert*-butyl alcohol solution, followed by addition of 236 mg (1.20 mmol) of $NaIO_4$ portionwise and the mixture was stirred for 2 h. The mixture was filtered and the filtrate was extracted with ethyl acetate (2 × 1.5 mL). The extract was dried and evaporated to leave 147 mg of crude **7** as a dark-brown oil: ^1H NMR δ 2.60 (m), 2.98 (m), 4.28 (m), 9.75 (s), also 1.8, 2.5, 4.1, 5.5–5.0 (integral 5.5–5.0:9.75 = 11:2) [After the sample in the NMR tube had been kept at 25 °C in the dark for 2 days, retaking of the ^1H NMR showed a relative increase in the peaks at δ 2.60 (m), 2.98 (m), 4.28 (d), and 9.75 (s) (5.5–5.0:9.75 = 3.5:2).]; MS m/z 274 ($M^+ + 2H_2O - N_2$), 238 ($M^+ - N_2$); IR 2130, 1720 cm^{-1}; UV λ_{max} = 239 nm, log ϵ = 3.92. On one occasion, a 22-mg sample was separated by preparative TLC (1:2:2 acetone–ether–CH_2Cl_2) to give 2 mg of quite pure dial **7** (R_f = 0.45–0.60): ^1H NMR δ 2.60 (m, 4), 2.98 (m, 1), 4.28 (d, 2, J = 5.4 Hz), 9.77 (s, 2). The structure assignment was supported by proton decoupling. Irradiation at δ 2.98 transformed the multiplets at both δ 4.28 and 2.60 to singlets.

1043-1802/91/2902-0038$02.50/0 © 1991 American Chemical Society

2-Diazo-3,3,3-trifluoropropionic Anhydride (8). Water (0.2 mL, 11 mmol) was added dropwise to a vigorously stirred solution of 1.0 g (5.8 mmol) of acyl chloride **5** in CH_2Cl_2 (10 mL), dioxane (5 mL), and pyridine (1.4 mL). The mixture was stirred for 0.5 h, then poured into a mixture of 2 N HCl (35 mL) and ice (10 g). It was stirred for 10 min and extracted with CH_2Cl_2 (3 × 25 mL). The extract was dried and evaporated to leave 0.62 g (73%) of solid which was purified by chromatography (silica gel, 1:4 ether–hexane) followed by crystallization ($CHCl_3$–hexane) to give **8** as large colorless needles: mp 55–56 °C; IR 2148, 1789, 1720 cm^{-1}. Anal. Calcd for $C_6F_6N_4O_3$: C, 24.84; N, 19.31. Found: C, 24.43, N, 19.81.

3-Cyclopentane-1,1-bis[2-[2-(2-methoxyethoxy)-ethoxy]ethanol] (3d). A mixture of 0.64 g (0.081 mol) of LiH with 4.0 g (0.031 mol) of diol **3b** (*14*) in di-*n*-butyl ether (80 mL) was refluxed overnight. To the mixture was added 19.4 g of 2-[2-[2-(2-chloroethoxy)ethoxy]ethoxy]tetrahydropyran (**9**) (*15*) at room temperature and it was heated at 100 °C for 10 days. To the mixture was then added 0.45 g of LiH and it was heated at 100 °C for 7 days. The mixture was filtered and the filtrate was washed with water (3 × 60 mL), dried, and evaporated to leave a red oil which was dissolved in MeOH (60 mL) and $CHCl_3$ (60 mL), then 3 mL of concentrated HCl was added. The mixture was refluxed for 2 h, then 17 g of $NaHCO_3$ was added portionwise at room temperature. The mixture was stirred for 15 min and filtered. The filtrate was evaporated to leave an oil which was distilled (0.005 mm, 90.0 °C) to give 9.1 g of yellow oil residue. The residue was purified by chromatography (silica gel, ether–ethanol = 20:1, 20:2, 20:3, and 20:4, 400 mL of each) to give 6.47 g (53%) of **3d** as a pale yellow oil: ^1H NMR δ 2.185 (s, 4), 3.001 (s, 2), 3.393 (s, 4), 3.621 (m, 12), 3.665 (s, 8), 3.714 (d, 4, J = 3.6 Hz), 5.568 (s, 2). Anal. Calcd for $C_{19}H_{36}O_8 \cdot 0.5H_2O$: C, 56.83; H, 9.28. Found: C, 56.72; H, 9.38.

2-[2-[2-(3-Cyclopentenylmethoxy)ethoxy]ethoxy]-ethanol (3c). Alcohol **3c** was prepared from **3a** in a manner similar to that for **3d**. From 3.04 g (31.0 mmol) of **3a** and 18.2 g (72.2 mmol) of **9** there was obtained 5.70 g (80%) of **3c** as an almost colorless thick oil: ^1H NMR δ 2.0–2.5 (m, 6), 3.362 (d, 2, J = 7.2 Hz), 3.67 (m, 12), 5.636 (s, 2). Anal. Calcd for $C_{12}H_{22}O_4 \cdot 0.1H_2O$: C, 62.09; H, 9.64. Found: C, 61.96; H, 9.28.

3-Cyclopentene-1-methanol 4′-Azido-2′,3′,5′,6′-tetrafluorobenzoate (11a). Ester **11a** was prepared from alcohol **3a** and acyl chloride **10** (*16*) in a manner similar to that of **6**. From 250 mg (0.985 mmol) of **10** and 42.0 mg (0.428 mmol) of **3a** there was obtained 120 mg (89%) of **11a** as a yellow oil after purification by preparative TLC (1:2 ether–hexane): ^1H NMR δ 2.16 (m, 2), 2.52 (m, 2), 2.73 (m, 1), 4.289 (d, 2, J = 7.2 Hz), 5.67 (s, 2); IR 2935, 2119, 1732, 1648, 1490 cm^{-1}. A neat sample of **11a** was stored at 25 °C in the dark for 1 day. An ^1H NMR of the resulting yellow solid showed a complicated spectrum in which the δ 5.67 singlet due to **11a** had decreased. The intensity of the 2119 cm^{-1} peak (azide) in the IR spectrum also decreased. The sample in the NMR tube ($CDCl_3$) however showed no change after 10 days in the dark.

3,4-Epoxycyclopentane-1-methanol 4′-Azido-2′,3′,5′,6′-tetrafluorobenzoate (12a). To a solution of **11a** [freshly prepared from 330 mg (1.30 mmol) of **10** and 127 mg (1.29 mmol) of **3a**] in ether (15 mL) was added 352 mg (1.73 mmol) of 85% *m*-chloroperbenzoic acid and it was stirred at 25 °C for 1 h. To the solution was added 0.5 g of anhydrous Na_2CO_3 and the mixture was stirred for 1 h and filtered. The filtrate was washed with 5% aqueous Na_2CO_3 (2 × 10 mL) and water (2 × 10 mL), dried, and evaporated to leave a liquid which was purified by preparative TLC (5:5:1 CH_2Cl_2–hexane–methanol) to give 206 mg (48%) of **12a** as a colorless solid (mp 38–40 °C): ^1H NMR δ 1.516 (m, 2), 2.220 (m, 3), 3.514 (s, 2), 4.328 (d, 2, J = 4.78 Hz); and 1.948 (m, 4), 2.49 (m, 1), 3.532 (s, 2), 4.213 (d, 2, J = 8.10 Hz); IR 3000, 2129, 1733, 1648, 1490, 1421 cm^{-1}; UV λ_{max} = 264 nm, log ϵ = 4.27. Anal. Calcd for $C_{13}H_9F_4N_3O_3$: C, 47.14; H, 2.73; N, 12.69. Found: C, 47.29; H, 2.61; N, 12.53.

1,5-Dioxopentane-3-methanol 4′-Azido-2′,3′,5′,6′-tetrafluorobenzoate (13a). A solution of 17.7 mg (0.053 mmol) of **12a** and 20 mg (1.0 mmol) of HIO_4 in water (0.5 mL) and THF (0.5 mL) was heated at 50 °C for 1 h. The solution was extracted with $CHCl_3$ (3 × 1 mL) and the extract was dried and evaporated to leave 18.6 mg of **13a** as a pale yellow oil (100%): ^1H NMR δ 2.67 (m, 4), 3.021 (m, 1), 4.386 (d, 2, J = 5.1 Hz), 9.775 (s, 2); also 5.5–5.0 (m), 4.2 (m) [^1H NMR of the sample in the NMR tube after being kept at 25 °C in dark for 6 h showed an increase of the signals for **13a** and a decrease of the δ 5.5–5.0 signals.]; IR 2957, 2129, 1734, 1648, 1490, 1420 cm^{-1}; UV λ_{max} = 267 nm, log ϵ = 4.25; MS m/z 347 (14, M^+), 319 (3, $M^+ - N_2$), 276 (25, $M^+ - N_2 - CH_2CHO$), 218 (30, $N_3C_6F_4CO$), 190 (5, NC_6F_4CO), 162 (80, NC_6F_4), 69 (100); high-resolution MS calcd for $C_{13}H_9F_4N_3O_4$ 347.0526, found 347.0531.

3,4-Epoxycyclopentane-1,1-dimethanol Bis(4-azido-2,3,5,6-tetrafluorobenzoate) (12b). To a solution of 38.6 mg (0.301 mmol) of diol **3b** and 130 mg (1.29 mmol) of Et_3N in 10 mL of ether was added 213 mg (0.840 mmol) of **10** and the mixture was stirred for 8 h. It was filtered and the filtrate was evaporated to leave **11b** as a liquid: ^1H NMR δ 2.376 (s, 4), 4.371 (s, 4), 5.663 (s, 2). The liquid was dissolved in CH_2Cl_2 (15 mL) and to the solution was added 400 mg of *m*-chloroperbenzoic acid. The solution was heated at 50 °C for 2.5 h then 3 mL of 10% aqueous Na_2SO_3 was added and the mixture stirred for 30 min. It was washed with 5% aqueous $NaHCO_3$ (3 × 10 mL) and water (2 × 10 mL), dried, and evaporated to leave 260 mg of residue which was separated by preparative TLC (1:1:0.4 $CHCl_3$–hexane–acetone) to give 60 mg (34%) of **12b** as a pale yellow oil: ^1H NMR δ 1.800 (d, 2, J = 15.14 Hz), 2.183 (d, 2, J = 15.14 Hz), 3.598 (s, 2), 4.236 (s, 2), 4.339 (s, 2); IR, 3000, 2129, 1737, 1647, 1490 cm^{-1}. Anal. Calcd for $C_{21}H_{10}F_8N_6O_5$: C, 43.61; H, 1.74; N, 14.53. Found: C, 43.82; H, 1.64; N, 14.53.

1,5-Dioxopentane-3,3-dimethanol Bis(4-azido-2,3,5,6-tetrafluorobenzoate) (13b). The oxidation of **12b** by HIO_4 was carried out in a manner similar to that of **12a**. From 24 mg (0.042 mmol) of **12b** and 40 mg (0.21 mmol) of HIO_4 there was obtained 24.2 mg (98%) of dial **13b** as a thick oil: ^1H NMR δ 2.960 (m), 4.512 (m), 9.759 (s); also 1.5–2.0, 2.80, 4.32, 5.0–6.0; IR 3000, 2129, 1737, 1647, 1490 cm^{-1}.

2-[2-[2-[(3,4-Epoxycyclopentanyl)methoxy]ethoxy]-ethoxy]ethanol 4′-Azido-2′,3′,5′,6′-tetrafluorobenzoate (12c). Epoxide **12c** was prepared from alcohol **3c** and **10** in a manner similar to that of epoxide **12a**. From 152 mg (0.663 mmol) of **3c** and 176 mg (0.697 mmol) of **10** there was obtained **11c** as a colorless oil: ^1H NMR δ 2.065 (m, 2), 2.441 (m, 3), 3.355 (d, 2, J = 7.2 Hz), 3.587 (m, 2), 3.649 (m, 2), 3.676 (s, 4), 3.813 (t, 2, J = 4.80 Hz), 4.515 (t, 2, J = 4.80 Hz), 5.638 (s, 2); IR 2868, 2129, 1737, 1648, 1491 cm^{-1}. Epoxidation of the colorless oil gave 278 mg (94%) of **12c** as a pale yellow oil after purification by preparative TLC (5:5:1 $CHCl_3$–hexane–methanol): ^1H NMR δ 1.856 (m, 4), 2.340 (m, 1), 3.263 (d, 2, J = 7.80 Hz), 3.459 (s, 2), 3.659 (m, 8), 3.808 (t, 2, J = 4.80 Hz), 4.509 (t, 2, J = 4.80

Hz); and 1.430 (m, 2), 2.096 (m, 3), 3.380 (d, 2, J = 5.40 Hz), 3.451 (s, 2), 3.659 (m, 8), 3.808 (t, 2, J = 4.80 Hz), 4.509 (t, 2, J = 4.80 Hz); IR 2871, 2129, 1736, 1648, 1490 cm^{-1}; UV, λ_{max} = 264 nm, log ϵ = 4.30. Anal. Calcd for $C_{19}H_{21}F_4N_3O_6$: C, 49.25; H, 4.57; N, 9.07. Found: C, 49.11; H, 4.68; N, 9.25.

2-[2-[2-[(1,5-Dioxopentan-3-yl)methoxy]ethoxy]-ethoxy]ethanol 4'-Azido-2',3',5',6'-tetrafluorobenzoate (13c). The oxidation of epoxide **12c** by HIO_4 was carried out in a manner similar to that of **12a**. From 40 mg (0.086 mmol) of **12c** and 40 mg (0.21 mmol) of HIO_4 there was obtained 41 mg (99%) of dial **13c** as an colorless oil: ^1H NMR (fresh sample in $CDCl_3$) δ 2.5 (m, 4), 2.85 (m, 1), 3.42 (m, 2), 3.6 (m, 8), 3.809 (m, 2), 4.519 (m, 2), 9.751 (s, 2); also 3.33, 2.70; IR 2129, 1735, 1648, 1490 cm^{-1}. ^1H NMR of the sample as a $CDCl_3$ solution after three days showed increasing intensity of 2.5 (m), 2.85 (m), 3.42 (d), and 9.75 (s) and decreasing intensity of 3.33 and 2.70; IR 2129, 1733, 1726, 1652, 1647, 1490 cm^{-1}; UV λ_{max} = 267 nm, log ϵ = 4.31.

(3,4-Epoxycyclopentane-1,1-diyl)bis[2-[2-(2-methoxyethoxy)ethoxy]ethanol] Bis(4-azido-2,3,5,6-tetrafluorobenzoate) (12d). Ester **12d** was prepared from **3d** and **10** in a manner similar to that of **12a**. From 265 mg (1.05 mmol) of **10** and 195 mg (0.498 mmol) of diol **3d** there was obtained **11d** as a colorless oil: ^1H NMR δ 2.174 (s, 4), 3.364 (s, 4), 3.58 (m, 8), 3.662 (s, 8), 3.182 (t, 4), 4.509 (t, 4), 5.552 (s, 2). Epoxidation of the colorless oil gave 206 mg (49%) of **12d** as a pale yellow oil: ^1H NMR δ 1.694 (d, 2, J = 15.0 Hz), 1.862 (d, 2, J = 15.0 Hz), 3.277 (s, 2), 3.289 (s, 2), 3.454 (s, 2), 3.7–3.5 (m, 16), 3.813 (m, 4), 4.513 (t, 4, J = 4.63 Hz); IR 3000, 2129, 1736, 1648, 1490 cm^{-1}. Anal. Calcd for $C_{33}H_{34}F_8N_6O_{11}$: C, 47.04; H, 4.07; N, 9.97. Found: C, 47.10; H, 4.06; N, 9.57.

(1,5-Dioxopentane-3,3-diyl)bis[2-[2-(2-methoxyethoxy)ethoxy]ethanol] Bis(4-azido-2,3,5,6-tetrafluorobenzoate) (13d). Epoxide **12d** was oxidized in a manner similar to that of **12a**. From 48 mg (0.057 mmol) of **12d** and 40 mg (0.21 mmol) of HIO_4 there was obtained 48 mg (99%) of dial **13d** as an oil: ^1H NMR δ 2.0–1.6 (m, 4), 3.5–3.2 (m, 4), 3.505 (s, 2), 3.7–3.6 (m, 16), 3.806 (m, 4), 4.511 (t, 4), 9.777 (s, 2); also δ 5.0 and 1.8; IR 2876, 2129, 1735, 1649, 1490 cm^{-1}.

1,5-Dioxopentane-3-methanol Propionate (14). A solution of 0.392 g (4.00 mmol) of alcohol **3a** in 1.50 g (11.5 mmol) of propionic anhydride was heated at 100 °C for 15 h. It was cooled to 25 °C and diluted with ether (15 mL). The solution was washed with 5% aqueous Na_2CO_3 (2 × 6 mL) and water (2 × 10 mL), dried, and evaporated to give 0.507 g (82%) of a pale yellow oil which was purified by chromatography (silica gel, 1:1 hexane–ether) to give 0.48 g of ester as colorless liquid: ^1H NMR δ 1.14 (t, 3, J = 7.50 Hz), 2.08 (m, 2), 2.33 (q, 2, J = 7.50 Hz), 2.48 (m, 2), 2.60 (m, 1), 3.99 (d, 2, J = 6.90 Hz), 5.65 (s, 2). Anal. Calcd for $C_9H_{14}O_2 \cdot 0.3H_2O$: C, 67.72; H, 9.22. Found: C, 67.77; H, 9.08. The ester was oxidized by $OsO_4/NaIO_4$ in a manner similar to that of ester **6**. From 201 mg of the ester there was obtained 180 mg (74%) of dial **14** as a pale brown oil: ^1H NMR δ 1.14 (m), 2.37 (m), 2.56 (m), 2.95 (m), 4.063 (m), 9.759 (s); also 2.50, 3.90, and 5.0–6.0.

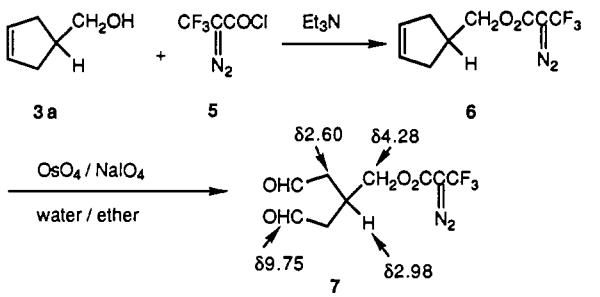
Reaction of Glutaraldehyde (1) and 1,5-Dioxopentane-3-methanol Propionate (14) with 6-Aminohexanoic Acid (15). To a solution of 0.1 mL of 0.1 M glutaraldehyde in phosphate buffer (pH = 7.4) was added 1.8 mL of buffer and 0.1 mL of 0.05 M amine **15** in buffer. The UV absorption of the solution was monitored at 265 nm (absorption maximum). A straight line absorption increase (ΔOD/min = 0.061) was observed. The reaction of dialdehyde **14** with amine **15** was carried out in the same manner under the same conditions and a similar absorption increase was observed (ΔOD/min = 0.059).

Table I. Fixation of Red Blood Cells by Dialdehyde 7 and Glutaraldehyde 1 at 25 °C in PBS Buffer (pH = 8.0)

dial	[dial]	incub[a]	photo[b]	color[c]
7	0.05	15	45	colorless
1	0.05	15	45	colorless
none		15	45	red
7	0.05	60	no	colorless
1	0.05	60	no	colorless
none		60	no	red
7	0.002	51	9	colorless
1	0.002	51	9	colorless
1	0.002	60	no	colorless
7	0.0004	55	4.5	red
1	0.0004	55	4.5	red
1	0.0004	60	no	red

[a] Incubation time (min). [b] Photolysis time (min). [c] Color of the supernatant solution, water + buffer (1:1).

Scheme I



Fixation of Red Blood Cells by Dialdehydes 1 and 7. Red blood cells were prepared according to Steck (*17*). A sample (10 mL) of fresh blood from a healthy donor was mixed with pH 8.0 phosphate-buffered saline (PBS) (10 mL) and centrifuged at 4 °C for 5 min. The supernatant solution and "buffy coat" were removed by aspirator through a Pasteur pipet. The pelleted red cells were washed by PBS (10 mL). The pellet was then diluted with PBS (2 mL) and kept at 4 °C.

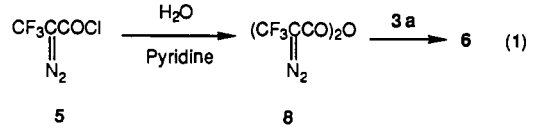
A mixture of 1 mL of 0.05 M of **7** (PBS) and 0.1 mL of the above red blood cells was incubated at 25 °C for 15 min. The sample was photolyzed (Rayonet reactor, 254 nm) in a quartz tube for 45 min. The sample was then mixed with 5 mL of PBS and centrifuged. The pellet was mixed with 1 mL of PBS and 1 mL of water and centrifuged. The supernatant solution was clear and colorless. The pellet was mixed with 1 mL of PBS and observed under an optical microscope and photographed. Other experiments were carried out in the same manner. Representative conditions and results are collected in Table I.

RESULTS AND DISCUSSION

Our plan called for the masking of the glutaraldehyde moiety in the form of the cyclopentenyl group in alcohol **3a** (*13*) (Scheme I) and the attachment of photoactive agents to the hydroxyl group. Two photoactive acylating agents, 2-diazo-3,3,3-trifluoropropionyl chloride (**5**) and 4-azido-2,3,5,6-tetrafluorobenzoyl chloride (**10**) were selected for these studies. The strongly electron-withdrawing CF_3 group in **5** both stabilizes the diazo function and suppresses Wolff rearrangement of the corresponding carbene (*12*). Another advantage of this photoactive group is its relatively small size, which should not cause drastic reduction of the aqueous solubility of the modified glutaraldehyde.

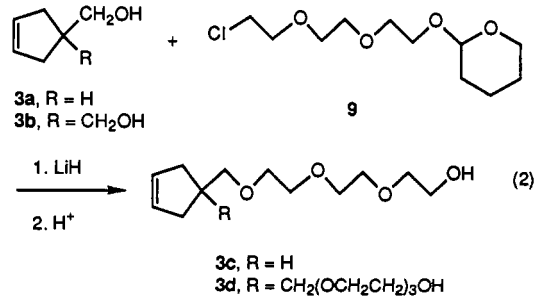
Acylation of alcohol **3a** by **5** gave ester **6**, which was subjected to oxidation of the cyclopentene moiety with osmium tetroxide and sodium periodate (*18*). A strong diazo absorption peak at 2130 cm^{-1} in the IR spectrum of the product mixture indicated that the diazo function was stable under the oxidation conditions. An ^1H NMR spectrum of the products showed the presence of the expected dialdehyde **7**, as evidenced by characteristic peaks at δ 9.75, 4.28, 2.98, and 2.60, together with other peaks at δ 5.0–5.5, 4.1, 2.5, and 1.8. Korn et al. (*19*) reported a similar complicated ^1H NMR spectrum for glutaraldehyde in water. They proposed that aqueous glutaraldehyde exists as a mixture of free monomer, cyclic hydrate, and oligomers. The signals of **7** increased at the expense of the other signals after the sample was kept as a $CDCl_3$ solution in the dark, corresponding to a relative increase of the dial form. A pure (by NMR) sample of **7** was obtained by preparative TLC. The solubility of crude **7** in aqueous buffer was measured by UV absorption at 239 nm (λ_{max}) to be 0.17 M, which is in the range of concentrations (1–4 wt%, 0.1–0.4 M) of glutaraldehyde employed for EM applications.

Anhydride **8** was prepared from **5** via reaction with water (eq 1). Acylation of alcohol **3a** by **8** gave ester **6**. Since



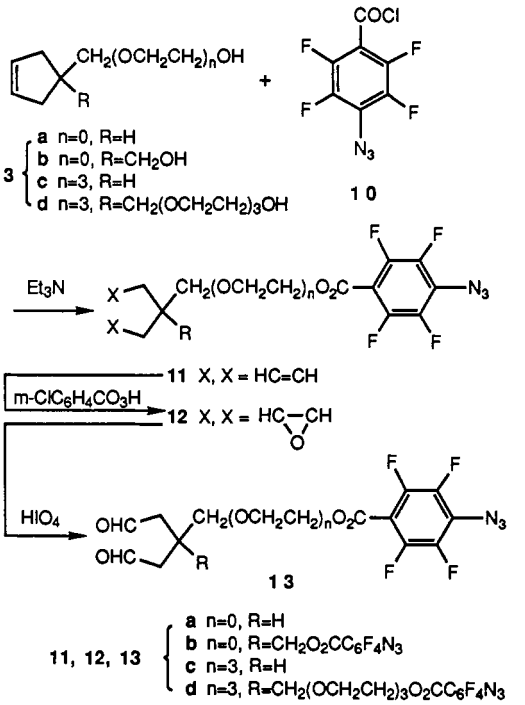
acyl chloride **5** is a low-boiling liquid, crystalline anhydride **8** constitutes a convenient alternative reagent for introduction of the diazotrifluoropropionyl group into another molecule.

4-Azido-2,3,5,6-tetrafluorobenzoyl chloride (**10**) is among the functionalized perfluorophenyl azides (PFPAs) recently developed in our laboratory as photolabeling agents showing improved CH insertion efficiency when photolyzed in hydrocarbon solvents (*16*). Before the acylation reaction, three ethyleneoxy units were inserted into alcohol **3a** and diol **3b**, serving both to increase the aqueous solubility of the final products and as a spacer arm connecting the dial function and the azido function. The chain extension was carried out by coupling of diol **3b** with an excess of THP-protected chloro ether **9** in the presence of LiH. Hydrolysis of the THP protecting group (eq 2) then gave alcohol **3d**. Alcohol **3c** was similarly prepared.



The mono PFPA modified dialdehyde **13a** was prepared first. Reaction of alcohol **3a** with acyl chloride **10** gave ester **11a** (Scheme II). The ^1H NMR and IR spectra suggested that possibly an azido olefin [3 + 2] cycloaddition (*20*) had taken place during storage of a neat sample at room temperature in the dark for 1 day. Since a dilute solution of freshly prepared **11a** in $CDCl_3$ was stable under

Scheme II



the same conditions, the cycloaddition reaction was probably intermolecular.

Dialdehydes in the glutaraldehyde series are generally difficult to obtain in analytical pure form due to the presence of different hydrated forms and oligomers (*19*). For example, several 3,3-disubstituted glutaraldehydes such as 3,3-dimethylglutaraldehyde (*21*) and 3,3-diphenylglutaraldehyde (*22*) were reported without elemental analysis characterization. Therefore, it was important that the precursor to dialdehyde **13a** should be fully characterized. Owing to the tendency of the cyclopentene double bond and the azido group to undergo a cycloaddition reaction, alkene **11a** was converted to epoxide **12a** with *m*-chloroperbenzoic acid (MCPBA). Epoxide **12a** was isolated as a colorless low-melting solid and was fully characterized. The ^1H NMR spectrum of **12a** revealed the presence of two stereoisomers in a ratio of about 2:1. Epoxidation of alcohol **3a** under similar conditions was reported to produce the corresponding epoxide as a mixture of cis–trans isomers (*14*).

Treatment of **12a** with HIO_4 (*23*) gave dialdehyde **13a** as a mixture of hydrated forms which behaved similarly to that of dialdehyde **7**. The ^1H NMR spectrum showed that the signals corresponding to **13a** (δ 2.67, 3.021, 4.386, 9.775) increased after the sample was allowed to stand as a solution in $CDCl_3$. High-resolution mass spectrum confirmed the molecular ion to be $C_{13}H_9F_4N_3O_4$. The solubility of dialdehyde **13a** in aqueous solution was found to be lower (4.4×10^{-4} M) than that of dialdehyde **7** (0.17 M).

Diester **11b** was prepared from diol **3b** and acyl chloride **10**. Epoxidation of **11b** by MCPBA was carried out at 50 °C to give epoxide **12b**, which was oxidized with HIO_4 to give dialdehyde **13b** as a thick oil. The ^1H NMR spectrum of **13b** showed peaks at δ 2.960 and 9.759 for the CH_2CHO moiety and 4.512 for the CH_2O_2C moiety, as well as signals around δ 1.5–2.0 and 5.0–6.0. This can be compared with the reported ^1H NMR spectrum for 3,3-dimethylglutaraldehyde which showed δ 2.6 and 10.0 for the CH_2CHO moiety as well as δ 5.1 and 1.7 for the hydrate forms (*21*).

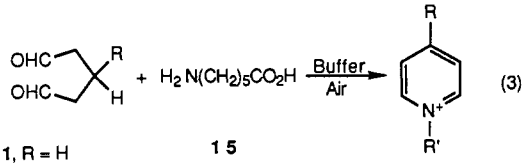
Acylation of alcohol **3c** by **10** gave ester **11c** which was unstable in the pure form (cf. **11a**). Epoxidation of **11c**

by MCPBA produced a stereoisomeric mixture of epoxides **12c** which gave a satisfactory elemental analysis. Oxidative cleavage of epoxide **12c** by HIO_4 gave a mixture containing dialdehyde **13c** and various hydrated forms as observed from the ^1H NMR spectrum. The signals corresponding to **13c** increased after the sample was kept in $CDCl_3$ for several days. The IR spectrum of a freshly prepared sample of **13c** in $CDCl_3$ showed a single peak in the carbonyl region at 1735 cm^{-1} corresponding to the carbonyl of the ester group, whereas after 3 days the IR spectrum of the solution showed a new peak at 1726 cm^{-1} corresponding to the aldehyde group and 1733 cm^{-1} for the ester. The solubility of **13c** in aqueous solution was found to be 0.010 M, a value significantly higher than that of **13a**.

Bis-PFPA-modified dialdehyde **13d** was prepared similarly. Esterification of diol **3d** by **10** gave diester **11d**, which was epoxidized by MCPBA to give **12d**. Oxidation with HIO_4 then gave dialdehyde **13d**, which showed spectral properties similar to those of **13c**.

The next series of experiments were designed to determine whether the new 3-substituted glutaraldehydes behaved similarly to glutaraldehyde under conditions related to EM fixation. Hardy et al. (*8*) reported that glutaraldehyde reacted with amines in aqueous solution to form polypyridinium type polymers which were characterized by a UV maximum at 265 nm. However, dialdehydes **7** and **13a–d** all had strong absorption at 265 nm due to the diazo and azido groups, respectively, thus making it difficult to monitor their reaction with amines in aqueous solution by UV spectroscopy. Therefore dialdehyde **14** was synthesized from alcohol **3a** and propionic anhydride followed by oxidation as a representative 3-substituted glutaraldehyde for our model studies.

Parallel reactions of dialdehyde **14** and glutaraldehyde with 6-aminohexanoic acid (*8*) in aqueous buffer (pH = 7.4) were monitored at 265 nm (eq 3). The absorption



(3)

1, R = H
14, R = $CH_2O_2CCH_2CH_3$

15

and / or other pyridinium ions with UV absorption maxima at 265 nm

increased linearly in both cases and at comparable rate (ΔOD/min for **14**, 0.059; for glutaraldehyde, 0.061). As judged by UV criteria, the 3-substituted glutaraldehyde **14** reacts with amine **15** in a manner similar to that of glutaraldehyde.

Dialdehyde **7** was chosen as a representative among the new cross-linking reagents for comparison to glutaraldehyde in terms of its ability to effect biological fixation using red blood cells (erythrocytes) as a model system. Erythrocytes swell in hypotonic buffers, and depending on the ionic strength, hemolysis can occur (*17*). Hemolysis results in a red buffer solution due to the released hemoglobin and is easily observable. Since glutaraldehyde fixation stabilizes the cell against hemolysis (*17*), fixation of erythrocytes by **7** was used to assess its fixative properties (Table I). Under all conditions examined, the behavior of dialdehyde **7** was similar to that of glutaraldehyde as a fixative for red blood cells. Cells fixed by dialdehyde **7** and glutaraldehyde appeared identical under optical microscopy. Interestingly, photolysis of the diazo moiety had no observable effect on the fixation properties of **7** (Table I). Since little is known as to whether cross-linking of membrane proteins to lipids stabilizes red cells toward hemolysis, studies with other membrane protein systems will be needed in order to determine the protein–lipid cross-linking properties of these new heterobifunctional cross-linking reagents.

In conclusion, a series of 3-substituted glutaraldehydes **7** and **13a–d** were synthesized. A representative of the series, dialdehyde **14** reacted with amine **15** in a manner similar to that of glutaraldehyde as monitored by UV spectroscopy. Another representative, dialdehyde **7**, showed fixative properties toward red blood cells similar to that of glutaraldehyde in hypotonic solution. These photoactive glutaraldehydes (**7** and **13a–d**) employ a novel combination of reactive groups and constitute a new approach to bioconjugation and EM fixation. The reagents may also find application in protein-to-protein and protein-to-nucleic acid cross-linking studies.

ACKNOWLEDGMENT

This work was supported by NIH Grant GM-27137. We thank Professor O. H. Griffith for his suggestions and Dr. Karen Hedberg for her assistance with the red blood cells experiments.

LITERATURE CITED

(1) Han, K.-K., Claude, R., and Delacourte, A. (1984) Chemical cross-links of proteins by using bifunctional reagents. *Int. J. Biochem. 16*, 129.

(2) Gaffney, B. J. (1985) Chemical and biochemical crosslinking of membrane components. *Biochim. Biophys. Acta 822*, 289.

(3) Means, G. E., and Feeney, R. E. (1990) Chemical modification of proteins: History and applications. *Bioconjugate Chem. 1*, 2.

(4) Pietersz, G. A. (1990) The linkage of cytotoxic drugs to monoclonal antibodies for the treatment of cancer. *Bioconjugate Chem. 1*, 89.

(5) Hayat, M. A. (1986) Glutaraldehyde: Role in electron microscopy. *Micron Microsc. Acta 17*, 115.

(6) Hayat, M. A. (1981) *Priciples and Techniques of Electron Microscopy*, 2nd ed., Vol. 1, University Park Press, Baltimore.

(7) Johnson, T. J. A. (1984) Glutaraldehyde fixation chemistry. *The Science of Biological Specimen Preparation* (J.-P. Revel, T. Barnard, G. H. Haggis, Eds.) p 51, SEM Inc. AMF, O'Hare, IL.

(8) (a) Hardy, P. M., Nicholls, A. C., and Rydon, H. N. (1976) The nature of the cross-linking of proteins by glutaraldehyde. Part 1. Interaction of glutaraldehyde with the amino-group of 6-aminohexanoic acid and of α-*N*-acetyl-lysine. *J. Chem. Soc. Perkin Trans. 1*, 958. (b) Hardy, P. M., Hughes, G. J., and Rydon, H. N. (1979) The nature of the cross-linking of proteins by glutarldehyde. Part 2. The formation of quaternary pyridinium compounds by the action of glutaraldehyde on proteins and the identification of a 3-(2-piperidyl)-pyridinium derivative, anabilysine, as a cross-linking entity. *J. Chem. Soc. Perkin Trans. 1*, 2282.

(9) (a) Korn, E. D., and Weisman, R. A. (1966) I. Loss of lipids during preparation of amoebae for electron microscopy. *Biochim. Biophys. Acta 116*, 309. (b) Jost, P., Brooks, U. H., and Griffith, O. H. (1973) Fluidity of phospholipid bilayers and membranes after exposed to osmium tetroxide and glutaraldehyde. *J. Mol. Biol. 76*, 313.

(10) Lawton, J. R. (1989) An investigation of the fixation and staining of lipids by a combination of malachite green or other triphenylmethane dyes with glutaraldehyde. *J. Microsc. 154*, 83.

(11) (a) Bayley, H. (1983) *Photogenerated Reagents in Biochemistry and Molecular Biology*, Elsevier, New York. (b) Schuster, D. I., Probst, W. C., Ehrlich, G. K., and Singh, G. (1989) Photoaffinity labeling. *Photochem. Photobiol. 49*, 785.

(12) Chowdhry, V., Vaughan, R., and Westheimer, F. H. (1976) 2-Diazo-3,3,3-trifluoropropionyl chloride: Reagent for photoaffinity labeling. *Proc. Natl. Acad. Sci. U.S.A. 73*, 1406.

(13) (a) Depres, J.-P., and Greene, A. E. (1984) Improved selectivity in the preparation of some 1,1-difunctionalized 3-cyclopentenes. High yield synthesis of 3-cyclopentenecarboxylic acid. *J. Org. Chem. 49*, 928. (b) Meinwald, J., Gassman, P. G., and Crandall, J. K. (1962) The synthesis of 4-substituted cyclopentenes from 1,4-dibromobutane-2. *J. Org. Chem. 27*, 3366.

(14) Paulsen, H., and Maass, U. (1981) Cyclitol reactions, II. Preparation of building units for synthesis of carbocyclic furanose analogs. *Chem. Ber. 114*, 346.

(15) Van Boom, J. H., and Herschied, J. D. M. (1973) *p*-Toluenesulfonic acid as a catalyst for the rapid tetrahydropyranylation and methoxytetrahydropyranylation of steroidal alcohols. *Synthesis* 169.

(16) Keana, J. F. W., and Cai, S. X. (1990) New reagents for photoaffinity labeling: Synthesis and photolysis of functionalized perfluorophenyl azides. *J. Org. Chem. 55*, 3640.

(17) Steck, T. L. (1974) In *Methods in Membrane Biology* (E. D. Korn, Ed.) Vol. II. Chapter 4, Plenum Press, New York.

(18) Pappo, R., Allen, D. S., Jr., Lemieux, R. U., and Johnson, W. S. (1956) Osmium tetroxide-catalyzed periodate oxidation of olefinic bonds. *J. Org. Chem. 21*, 478.

(19) Korn, A. H., Feairheller, S. H., and Filachione, E. M. (1972) Glutaraldehyde: Nature of the reagent. *J. Mol. Biol. 65*, 525.

(20) Hassner, A., Amarasekara, A. S., and Andisik, D. (1988) Intramolecular azide-olefin cycloaddition. A novel synthesis of 2,5-dihydrooxazoles. *J. Org. Chem. 53*, 27.

(21) Foos, J., Steel, F., Rizvi, S. Q. A., and Fraenkel, G. (1979) Synthesis and nuclear magnetic resonance spectra of *N*-carboethoxy-4-spiro-1,4-dihydropyridines. *J. Org. Chem. 44*, 2522.

(22) Kukla, M. J., and Breslin, H. J. (1987) Polycyclic heterocycles from glutaraldehyde in one reaction. *J. Org. Chem. 52*, 5046.

(23) Nagarkatti, J. P., and Ashley, K. R. (1973) Periodic acid cleavage of epoxides in aqueous medium. *Tetrahedron Lett.* 4599.

Fluorine-18 Labeling of Monoclonal Antibodies and Fragments with Preservation of Immunoreactivity

Pradeep K. Garg, Sudha Garg, and Michael R. Zalutsky*

Duke University Medical Center, Department of Radiology, Box 3808, Durham, North Carolina 27710.
Received November 5, 1990

A new method is reported for labeling proteins with the positron-emitting nuclide ^{18}F. Initially, 4-[^{18}F]-fluorobenzylamine was prepared in two steps from aqueous [^{18}F]fluoride in high yield. The ^{18}F acylation agent was formed by reaction of this product with disuccinimidyl suberate. Overall yields for the 4-[^{18}F]fluorobenzylamine succinimidyl ester ([^{18}F]SFBS), decay corrected to the end of cyclotron bombardment, were about 30% in a synthesis time of 60 min. After a 15-min reaction, 30–45% (decay corrected) of the [^{18}F]SFBS could be coupled to intact antibodies and their F(ab')$_2$ and Fab fragments. Coupling yields were dependent on protein concentration but not reaction time. HPLC purification of [^{18}F]SFBS was necessary to obtain optimal coupling efficiency and immunoreactivity. The immunoreactivities of ^{18}F-labeled F(ab')$_2$ and Fab fragments of an antimyosin antibody were 89 ± 5% and 75 ± 9%, respectively. Biodistribution studies in normal mice demonstrated similar in vivo behavior of ^{18}F-labeled antibody fragments and those labeled with ^{125}I by using *N*-succinimidyl 3-[^{125}I]iodobenzoate. These results indicate that this method may be useful for labeling monoclonal antibodies and other proteins and peptides with ^{18}F.

Positron-emission tomography (PET)[1] is a functional imaging modality which permits quantitative evaluation of physiology in the living human. Considering the ubiquitousness of proteins and peptides and their role in many disease processes, the development of a method for labeling proteins with a positron-emitting nuclide could provide valuable diagnostic tools. For example, serial PET scans of a monoclonal antibody (MAb) labeled with a positron emitter could be used to quantitate their three-dimensional distribution in vivo. In addition to its diagnostic utility, this information could be used to generate accurate dosimetry data from which a radiolabeled MAb therapy procedure could be planned more rationally.

Methods for labeling proteins with positron-emitting nuclides have been described in only a few published reports. Proteins have been labeled with 20-min half-life ^{11}C by ^{11}C methylation (*1*, *2*), and methods for labeling proteins with 68-min ^{68}Ga have also been reported (*3–5*). Of the commonly available positron emitters, 110-min ^{18}F appears to be the nuclide of choice for labeling MAbs and their fragments. The longer half-life of ^{18}F would facilitate imaging at later time points, a feature which may be important because of the relatively slow clearance of MAbs from nontarget tissues (*6*). In addition, Kilbourn and coworkers (*7*) have reported that because of the lower positron energy of ^{18}F compared to ^{68}Ga, the radiation dose received by critical normal organs would be as much as 40% lower per mCi of administered activity with ^{18}F.

A number of approaches for labeling proteins with ^{18}F have been described. Müller-Platz et al. (*8*) utilized a water-soluble carbodiimide to label urokinase with ^{18}F via a 2-[^{18}F]fluoroacetate intermediate. In another preliminary report, the synthesis of the potential protein labeling agents *N*-(*p*-[^{18}F]fluorophenyl)maleimide and *m*-maleimido-*N*-(*p*-[^{18}F]fluorobenzyl)benzamide have been described (*9*). Two approaches for labeling proteins with ^{18}F have been reported by Kilbourn et al. (*7*). In the first, methyl 3-[^{18}F]fluoro-5-nitrobenzimidate was synthesized by nucleophilic substitution of [^{18}F]fluoride for nitro in 3,5-dinitrobenzonitrile, followed by reaction with sodium methoxide in anhydrous methanol. In the second, 4-[^{18}F]-fluorophenacyl bromide was synthesized from [^{18}F]fluoride ion in three steps beginning with fluoro for nitro exchange on 4-nitrobenzonitrile. Several proteins could be labeled by incubation with either reagent at near-physiological pH.

Of critical importance is the demonstration that proteins can be labeled with ^{18}F without compromising their biological integrity; however, little data is available concerning the effect of ^{18}F labeling on protein function. The blood clearance of ^{18}F-labeled human serum albumin has been shown to be similar to that observed when ^{125}I was used as the label (*7*), but as these authors point out, human serum albumin cannot be denatured easily.

This paper describes a new method for labeling MAb and other proteins with ^{18}F that utilizes *N*-succinimidyl 8-[(4'-[^{18}F]fluorobenzyl)amino]suberate ([^{18}F]SFBS) as the ^{18}F-labeled acylation agent. MAb F(ab')$_2$ and Fab fragments maintained immunoreactivity after labeling with ^{18}F. The results of biodistribution studies in normal mice suggest that these MAb fragments retain their ^{18}F-label after administration in vivo.

EXPERIMENTAL PROCEDURES

General Procedures. ^1H NMR spectra were obtained in $CDCl_3$ and recorded on a General Electric midfield GN-300 spectrometer. Proton chemical shifts are reported in ppm downfield from internal TMS (0.00 ppm). Mass spectral data were obtained on a Finigan 4500 single quadrupole mass spectrometer. Melting points were deter-

[1] Abbreviations used: PET, positron-emission tomography; MAb, monoclonal antibody; [^{18}F]SFBS, *N*-succinimidyl 8-[(4'-[^{18}F]fluorobenzyl)amino]suberate; DSS, disuccinimidyl suberate; PBS, phosphate-buffered saline; SFBS, *N*-succinimidyl 8-[(4'-fluorobenzyl)amino]suberate; ID, injected dose.

1043-1802/91/2902-0044$02.50/0 © 1991 American Chemical Society

mined on a Haake Buchler variable-heat apparatus and are uncorrected.

Lithium aluminum hydride, 4-nitrobenzonitrile, *tert*-butylammonium hydroxide, 4-fluorobenzylamine, and dimethyl sulfoxide were obtained from Aldrich (Milwaukee, WI). Disuccinimidyl suberate (DSS) was purchased from Pierce (Rockford, IL). Sodium [^{125}I]iodide was obtained from Du Pont-New England Nuclear (North Billerica, MA).

The generation and purification of the murine MAb R11D10 directed against cardiac myosin have been described (*10*). The Fab and F(ab')$_2$ fragments of this antmyosin MAb were provided as gifts from Dr. David Shealy from Centocor (Malvern, PA). Mel-14 F(ab')$_2$ (*11*) is reactive with the tumor-associated chondroitin sulfate antigen present in melanomas and has no known reactivity with cardiac myosin. MAb 81C6 is a murine IgG reactive with the extracellular matrix antigen tenascin (*12*). Both Mel-14 F(ab')$_2$ and 81C6 IgG were obtained as gifts from Dr. Darell D. Bigner of the Department of Pathology, Duke University Medical Center.

Radioactivity levels were assessed with an LKB 1282 dual-channel γ-counter. High-pressure liquid chromatography was performed in isocratic mode with an LKB Model 2150 pump, 2151 variable-wavelength UV detector, and a Beckman Model 170 radioisotope detector. A Nelson Analytical software package was used for peak analysis. The separation system used for analysis of aryl fluorides was a Partisil 10 silica 10 μm, 250 × 4.6 mm column (Alltech) eluted with ethyl acetate (or ethyl acetate–hexane) at a flow rate of 0.8 mL/min. For size-exclusion HPLC, a 300 × 7.5 mm Biosil TSK 250 column (Bio-Rad) eluted with phosphate-buffered saline (PBS, pH 7.4) at a flow rate of 1 mL/min was used.

Preparation of *N*-Succinimidyl 8-[(4'-Fluorobenzyl)amino]suberate (SFBS). DSS (368 mg) was dissolved in 400 μL of dimethyl formamide. To the resultant clear solution was added 115 mg of 4-fluorobenzylamine and the reaction mixture was stirred at room temperature for 2 h. After the addition of 10 mL of diethyl ether, the precipitate was removed. The filtrate was washed with 1 mL of 0.5 N HCl followed by 2 mL of water and then dried over Na_2SO_4. After removing the ether by rotary evaporation, the product (205 mg, 55% yield) was isolated by flash chromatography on a silica gel column using 10% hexane in ethyl acetate as the eluant (melting point 110 °C). Purity was greater than 95% by TLC [silica gel; ethyl acetate–hexane (9:1); R_f 0.6]. The assigned structure for SFBS was in agreement with its NMR and mass spectral data. ^{1}H NMR: ($CDCl_3$, δ) 1.4 (m, 4 H, alkyl), 1.72 (m, 4 H, alkyl), 2.25 (t, 2 H, CH_2COO), 2.6 (t, 2 H, $NHCOCH_2CH_2$), 2.78 (s, 4 H, *N*-succ), 4.15 (d, 2 H, $ArCH_2NH$), 7.00–7.24 (m, 4 H, aryl). MS: *m/e* 378 (M^+, 6), 264 ($M^+ - 114$, 44), 235 ($M^+ - 143$, 27). Anal. Calcd for $C_{19}H_{23}N_2O_5F \cdot {}^1/_2H_2O$: C, 58.91; H, 6.2; N, 7.20. Found: C, 59.13; H, 5.4; N, 7.05.

Preparation of 4-[^{18}F]Fluorobenzonitrile. Aqueous [^{18}F]fluoride was produced with the ^{18}O(p,n)^{18}F reaction by irradiating [^{18}O]H_2O in a small-volume silver target (*13*). The synthesis of this compound was achieved by using a modification of the method of Kilbourn et al. (*7*). The conversion of aqueous [^{18}F]fluoride ion to tetrabutylammonium [^{18}F]fluoride and the fluoro for nitro exchange were performed in the same vessel in order to reduce vessel-to-vessel transfer losses. Briefly, 300 μL of [^{18}O]H_2O containing 5–100 mCi of [^{18}F]fluoride was added by a remote handling system (*14*) to a glass tube containing 1 mL of acetonitrile and 2–10 μmol of tetrabutylammonium hydroxide. The mixture was evaporated by heating at 110 °C and using a gentle stream of nitrogen. Any remaining water was removed azeotropically with 2 × 1 mL of acetonitrile. To the dried tube was added 800 μg of 4-nitrobenzonitrile in 100 μL of DMSO, and the solution was heated at 140–150 °C for 15 min. The resultant 4-[^{18}F]-fluorobenzonitrile was separated from the reaction mixture with a C_{18} Sep-Pak (Millipore) eluted with 0.5 mL of diethyl ether. Decay-corrected yields were 60–80%. A radiochemical purity of 95–99% was determined by HPLC [silica column; ethyl acetate–hexane (1:9); t_R = 8.8 min]. The crude product was used for the next step. HPLC analyses revealed the presence of less than 50 μg of 4-nitrobenzonitrile (t_R = 12.7 min) in the 4-[^{18}F]fluorobenzonitrile preparation.

Synthesis of 4-[^{18}F]Fluorobenzylamine. Lithium aluminum hydride (50 mg) was added to the above product and the mixture was allowed to stand at room temperature for 5 min. The reaction was quenched with 2 mL of aqueous saturated ammonium chloride followed by 2 drops of 1 N NaOH. The ether layer was separated and washed with 1 mL of H_2O and dried over Na_2SO_4. The decay-corrected yield for this step was 80–95% and the radiochemical purity was determined to be 95–99% by TLC (silica; ethyl acetate).

Preparation of [^{18}F]SFBS. DSS is a homobifunctional agent that reacts with primary amino groups (*15, 16*). To 150 μg of DSS in 15 μL of DMF was added 5–50 mCi of 4-[^{18}F]fluorobenzylamine. The mixture was incubated for 5 min at room temperature, then the ether was evaporated slowly under a stream of nitrogen. In preliminary studies, the residue was used in unpurified form for protein labeling. Subsequently, [^{18}F]SFBS was purified by HPLC using a silica gel column eluted with ethyl acetate at 0.8 mL/min (t_R = 12.5 min).

General Method for Labeling Proteins with [^{18}F]-SFBS. The organic solvent (ether, nonpurified; ethyl acetate, HPLC purified) containing the [^{18}F]SFBS was evaporated, and 200–1100 μg of the protein of interest in 100–200 μL of pH 8.5 borate buffer was added. The mixture was incubated for 15 min at room temperature and the reaction terminated by addition of 300 μL of 0.2 M glycine in 0.1 M borate. The [^{18}F]SFBS–protein conjugate was isolated from lower molecular weight impurities with a 1 × 10 cm Sephadex G-25 column eluted with PBS. Protein-associated radioactivity, determined by precipitation with 20% trichloroacetic acid, was greater than 96% for all preparations. Selected batches of labeled proteins were analyzed by size-exclusion HPLC.

Effect of Incubation Time and Protein Concentration. Because of the short half-life of ^{18}F, the time dependence of the [^{18}F]SFBS coupling reaction was of interest. Antimyosin Fab fragment (500 μg in 200 μL) was added to about 1 mCi of [^{18}F]SFBS and incubated at room temperature for 15, 30, 60, 90, or 120 min. To study the effect of protein concentration on coupling efficiency, 100–150 μL of MAb fragment at 2.5, 5.5, and 8.5 mg/mL was reacted with about 1 mCi of [^{18}F]SFBS for 30 min. HPLC-purified [^{18}F]SFBS was used. Protein coupling efficiency was determined by dividing the ^{18}F activity eluting in the void volume of the Sephadex G-25 column by the total ^{18}F activity added to the column. Fluorine-18 activity levels were measured with a Capintec CRC-7 dose calibrator. Two or three determinations were performed at each set of reaction conditions.

Immunoreactivity Assay. The immunoreactivity of ^{18}F-labeled antimyosin Fab and F(ab')$_2$ fragments was determined with a 1-mL myosin Sepharose column, which

was obtained as a gift from Dr. David Shealy of Centocor. Approximately 10 ng of ^{18}F-labeled antimyosin fragment was added to the column; the column was then washed with PBS containing 0.5% human serum albumin and stripped with 8 mL of 0.1 M glycine (pH 2.5). Aliquots (100–250 μL) in triplicate from both the PBS wash and the glycine stripping solution were counted for ^{18}F activity in an automated γ-counter. Percent immunoreactivity was calculated from the ratio of activity in glycine to activity in glycine plus PBS. In some cases, nonspecific binding to the myosin Sepharose column was measured using ^{18}F-labeled Mel-14 F(ab')$_2$.

Biodistribution Measurements. Initially, the effect of HPLC purification of the [^{18}F]SFBS coupling agent on the tissue distribution of ^{18}F-labeled antimyosin Fab was studied. With both HPLC-purified and unpurified [^{18}F]-SFBS, ^{18}F-labeled antimyosin Fab was prepared as described above. Normal BALB/c mice weighing 20–25 g were injected with 1–2 μg (8 μCi) of each preparation and groups of five animals were sacrificed by ether overdose at 0.5, 1, and 2 h. Following dissection, tissues of interest were removed, weighed, washed with PBS, and counted for ^{18}F activity. In the second experiment, antimyosin F(ab')$_2$ was labeled with ^{125}I by using *N*-succinimidyl 3-[^{125}I]iodobenzoate as described (*17*) and with ^{18}F by using HPLC-purified [^{18}F]SFBS. Mice were injected with 3 μg (3 μCi) of ^{125}I-labeled Fab and 2 μg (4 μCi) of ^{18}F-labeled Fab, and the tissue distribution of both nuclides was determined at 0.5, 1, and 2 h. Counting data for ^{125}I were corrected for crossover of ^{18}F into the ^{125}I counting window. The percent injected dose (ID) in each tissue was calculated by comparison to injection standards of appropriate count rate. Blood was assumed to represent 6% of total body weight.

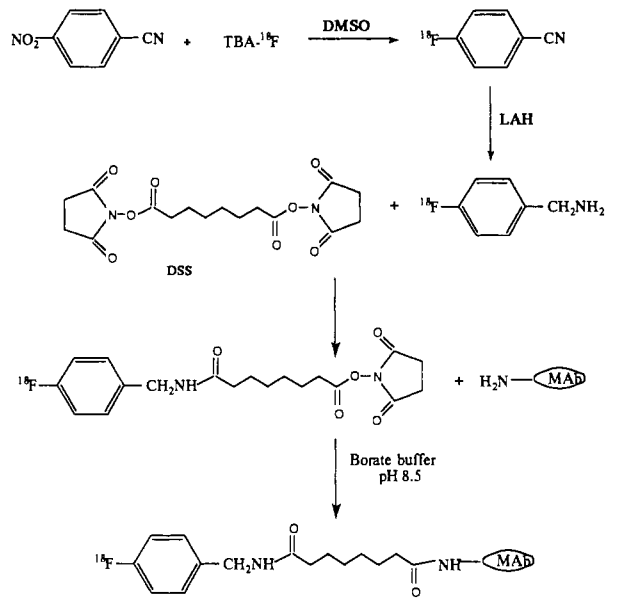
Statistical Analysis. Comparisons between the tissue distribution of Fab labeled by reaction with HPLC-purified and unpurified [^{18}F]SFBS were made by using the Student's *t* test (*18*). Since the experiment comparing F(ab')$_2$ labeled with ^{18}F and ^{125}I was performed in paired-label format, with each animal serving as its own control, a paired *t* test was used (*18*). Only results having $P < 0.05$ have been considered to be statistically significant.

RESULTS AND DISCUSSION

Strategies for labeling proteins with ^{18}F must be compatible with the 110-min half-life of this nuclide. In addition, the radiofluorination method should produce a labeled protein which retains the ^{18}F label after in vivo administration. Of critical importance is the ability of the ^{18}F-labeled protein to maintain its biological function after labeling. Because of their sensitivity to losses in immunoreactivity as a consequence of radiolabeling procedures, MAb fragments were chosen as model proteins for this study. In addition, there is considerable interest in the clinical application of radiolabeled MAbs, making the development of a method for labeling MAbs with ^{18}F of potential practical utility.

Scheme I outlines the four-step approach for labeling MAbs with ^{18}F. Yields for the production of 4-[^{18}F]fluorobenzonitrile, corrected to the end of cyclotron bombardment, were 60–80% and comparable to those reported in the literature for the synthesis of this compound by aromatic nucleophilic substitution for the nitro group of 4-nitrobenzonitrile (*7*, *19*). Reduction with lithium aluminum hydride gave 4-[^{18}F]fluorobenzylamine in an end of bombardment overall yield of 65–75%, a range which is considerably higher than that reported previously for the synthesis of 4-[^{18}F]fluorobenzylamine from [^{18}F]fluoride (*19*).

Scheme I. Fluorine-18 Labeling of Antibodies



Overall yields for the synthesis of [^{18}F]SFBS were between 25 and 40% in a synthesis time of 55–60 min, including HPLC purification. Omitting HPLC purification decreased synthesis time by nearly 20 min, increasing available activity by more than 10%; however, because of difficulties described below with the crude [^{18}F]SFBS preparation, this approach was not pursued after initial investigations.

Conjugation efficiencies with [^{18}F]SFBS were similar for 81C6 IgG, Mel-14 F(ab')$_2$, antimyosin F(ab')$_2$, and antimyosin Fab, suggesting the versatility of this method. Decay-corrected coupling efficiencies were dependent on protein concentration, increasing from 29 ± 3% at 2.5 mg/mL to 32 ± 4% at 5.5 mg/mL to 47 ± 5% at 8.5 mg/mL. Other *N*-succinimidyl ester radiohalogenation agents exhibit similar concentration-dependent protein labeling (*20*, *21*). However, compared to those of [^{18}F]SFBS, yields for *N*-succinimidyl iodobenzoates are higher, and yields with the Bolton–Hunter agent are lower (*20*, *21*), suggesting that manipulation of the spacer between the aryl fluoride and the active ester might be an approach for increasing protein-labeling efficiency.

Because of the short half-life of ^{18}F, minimizing the incubation time for the [^{18}F]SFBS protein-coupling reaction is critical. Significant differences in protein-coupling efficiency were not observed between 15 and 120 min. For example, in one set of experiments with 500 μg (2.5 mg/mL) of antimyosin Fab, coupling efficiencies were 34, 37, 36, 36, and 38% at 15, 30, 60, 90, and 120 min, respectively. On the basis of these results, a 15–20-min reaction period was adopted in order to minimize losses of available ^{18}F-labeled protein due to isotopic decay.

The ability to achieve acceptable protein labeling yields in shorter reaction times is an advantage of using SFBS for labeling proteins. In contrast, labeling proteins by reaction with either 3-[^{18}F]fluorobenzimidate or 4-[^{18}F]-fluorophenacyl bromide appears to require at least 120–240 min to obtain reasonable yields (*7*). Both of these methods also involve prolonged heating at 47 °C. Since the biologic integrity of some proteins may be compromised at elevated temperatures, an additional advantage of SFBS is that the reaction is carried out at 25 °C.

Comparison of the current method with those described previously is complicated by the fact that in most cases, reaction time, protein concentration, and the nature of

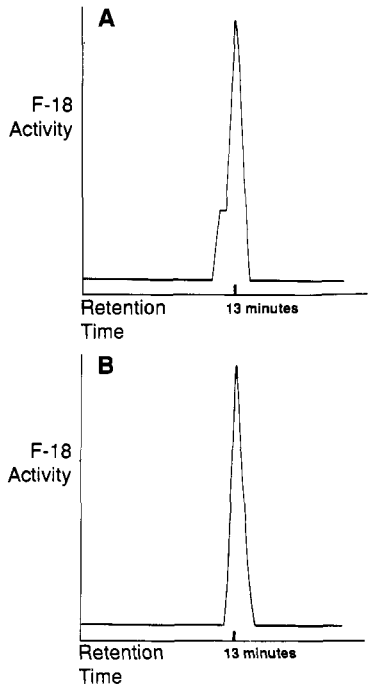


Figure 1. Size-exclusion HPLC of ^{18}F-labeled antimyosin Fab fragment prepared with (A) crude [^{18}F]SFBS and (B) [^{18}F]SFBS purified by HPLC prior to reaction with Fab fragment. The peak appearing with a retention time of ca. 13 min corresponds to Fab. The shoulder observed in A presumably reflects cross-linked Fab.

the protein are all important variables. With [^{18}F]SFBS, about 8–10 mCi of three different ^{18}F-labeled proteins could be prepared from 100 mCi of [^{18}F]fluoride in a synthesis time of 80–90 min. These yields are more than twice those reported for ^{18}F labeling of human serum albumin using 3-[^{18}F]fluorobenzimidate (*7*). The available protein activity per mCi [^{18}F]fluoride for [^{18}F]SFBS is similar to that reported for labeling human serum albumin using 4-[^{18}F]fluorophenacyl bromide. However, when the later reagent was used to label an IgA immunoglobulin, labeling yields were considerably lower, and only about half those seen at similar protein concentrations with SFBS.

Despite decreasing preparation time, omitting the HPLC purification of [^{18}F]SFBS is not recommended. In paired experiments, use of HPLC increased protein coupling yields by 15–40%, presumably by decreasing competition of unlabeled active ester byproducts for reaction with free amino groups on the protein. As shown in Figure 1, size-exclusion HPLC analysis of ^{18}F-labeled antimyosin Fab indicates that use of crude [^{18}F]SFBS results in a shoulder on the Fab peak accounting for about 15% of ^{18}F activity. It is presumed that this reflects cross-linked Fab resulting from exposure to unreacted bifunctional DSS.

HPLC purification of [^{18}F]SFBS also had a significant effect on tissue distribution (Figure 2). With ^{18}F-labeled antimyosin F(ab')$_2$, omitting the HPLC purification of [^{18}F]SFBS significantly increased liver and spleen uptake and decreased blood-pool activity at all time points ($P <$ 0.005). For example, at 1 h, use of HPLC resulted in more than 2-fold lower liver uptake (6.7 ± 0.9 vs 17.1 ± 1.4% ID) and nearly 2-fold higher blood-pool activity (20.9 ± 1.5 vs 11.6 ± 1.3% ID). These differences are consistent with those reported for MAbs labeled with ^{111}In when methods with and without a propensity for causing protein cross-linking were compared (*22*, *23*).

Because of the rapid clearance of MAb F(ab')$_2$ and Fab fragments from the blood pool and normal tissues (*24*–*26*), their pharmacokinetics appear to be more compatible with the 110-min half-life of ^{18}F. The tissue distribution of ^{18}F-labeled antimyosin Fab in normal mice at 0.5–2 h is summarized in Table I. Fluorine-18 activity cleared rapidly from the blood pool, reaching a level of 8.15 ± 0.63% ID/g at 2 h. After 0.5 h, Fab uptake in the kidneys was higher than that observed in other tissues. Although little data at early time points is available for comparison,

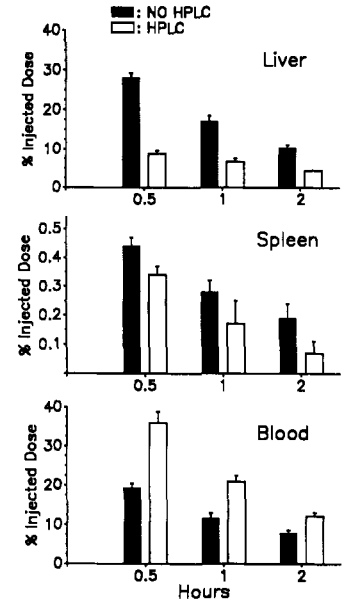


Figure 2. Tissue distribution of ^{18}F activity in normal mice injected with ^{18}F-labeled antimyosin Fab. Purification of the [^{18}F]SFBS intermediate results in significant reduction in liver and spleen uptake and higher activity remaining in blood pool.

Table I. Biodistribution of ^{18}F-Labeled Antimyosin Fab Fragment in Normal Mice (HPLC-Purified Intermediate)

	% ID/g[a]		
tissue	0.5 h	1 h	2 h
liver	5.63 ± 0.94	4.92 ± 0.44	3.04 ± 0.26
spleen	3.65 ± 0.52	2.22 ± 0.24	0.75 ± 0.20
lungs	14.13 ± 3.09	8.62 ± 1.97	5.81 ± 0.88
kidneys	17.89 ± 3.16	17.54 ± 1.54	12.48 ± 0.94
stomach	1.44 ± 0.30	1.32 ± 0.35	1.10 ± 0.37
muscle	0.99 ± 0.27	0.97 ± 0.16	0.64 ± 0.11
bone	2.08 ± 0.34	0.99 ± 0.15	0.76 ± 0.14
blood	24.13 ± 3.31	14.89 ± 0.94	8.15 ± 0.63
brain	0.51 ± 0.08	0.27 ± 0.06	0.02 ± 0.02
heart	5.24 ± 0.97	3.70 ± 0.33	1.59 ± 0.53

[a] Mean ± standard deviation; n = 5.

Table II. Paired-Label Biodistribution of Antimyosin F(ab')$_2$ Fragment Labeled with ^{18}F by Using DSS and ^{125}I by Using *N*-Succinimidyl 3-[^{125}I]Iodobenzoate

	% ID/g[a]			
	1 h postinjection		2 h postinjection	
tissue	^{18}F	^{125}I	^{18}F	^{125}I
liver	9.35 ± 1.12	7.27 ± 0.89[b]	8.39 ± 0.88	6.00 ± 0.91[b]
spleen	4.53 ± 0.36	4.20 ± 0.31	3.47 ± 0.49	3.33 ± 0.26
lungs	17.84 ± 5.79	18.18 ± 5.93	13.94 ± 3.06	14.29 ± 2.95
kidneys	13.99 ± 1.25	11.79 ± 0.62[b]	15.55 ± 1.32	9.95 ± 0.86[b]
stomach	1.68 ± 0.76	1.83 ± 0.81	2.02 ± 0.30	2.21 ± 0.31
muscle	0.80 ± 0.07	0.86 ± 0.09	0.73 ± 0.09	0.80 ± 0.08
bone	1.69 ± 0.30	1.85 ± 0.17	1.40 ± 0.18	1.96 ± 0.18[b]
blood	32.09 ± 1.94	31.80 ± 2.00	27.48 ± 0.99	27.44 ± 1.12
brain	0.71 ± 0.05	0.76 ± 0.05	0.62 ± 0.10	0.65 ± 0.05
heart	6.33 ± 0.47	6.66 ± 0.49	5.55 ± 0.67	6.12 ± 0.68

[a] Mean ± standard deviation; n = 5. [b] Significance of difference $P < 0.01$ determined by two-sided paired t test; all other differences not significant.

the tissue distribution of ^{18}F-labeled antimyosin Fab is similar to that reported for other Fab fragments radioiodinated by using the Iodogen method (*25*, *26*).

A paired-label biodistribution study was performed in normal mice to compare the pharmacokinetics of antimyosin F(ab')$_2$ labeled by reaction with [^{18}F]SFBS and *N*-succinimidyl 3-[^{125}I]iodobenzoate. This radioiodination method was used because it has been shown to decrease the dehalogenation of MAbs and F(ab')$_2$ fragments in vivo (*27*, *28*). As summarized in Table II, in most tissues the uptake of ^{18}F and ^{125}I was nearly identical at 1 and 2 h. Small but significant differences were observed in the liver at both time points and in the bone at 2 h. Increased liver uptake of ^{18}F may be related to a small degree of cross-linking. However, the data presented in Figure 2 would suggest that if this were a major factor, differences in spleenic and blood-pool uptake of ^{18}F and ^{125}I would also be seen, and this was not the case. The most significant difference between ^{18}F and ^{125}I activity was noted in the kidneys where 19–56% higher levels of ^{18}F were observed. Complementary differences in bladder activity were seen (^{125}I, 17.8 ± 1.9% ID; ^{18}F, 11.9 ± 1.4% ID at 2 h), suggesting that the excretion rates of ^{18}F- and ^{125}I-labeled Fab (or their labeled catabolites) are slightly different.

Of critical importance is the demonstration that a protein-labeling method does not destroy the immunoreactivity of the MAb or MAb fragment. Although methods for labeling proteins with ^{18}F have been described previously (*7–9*), retention of immunocompetence of a MAb or MAb fragment after radiofluorination has not been reported. Initially, the effect of HPLC purification of the [^{18}F]SFBS acylation agent on the binding of ^{18}F-labeled antimyosin Fab was investigated with a myosin affinity column. In two paired preparations, immunoreactivity with HPLC-purified [^{18}F]SFBS was 82 and 84%, compared with 49 and 67% when crude [^{18}F]SFBS was used. Immunoreactivity of 11 batches of ^{18}F-labeled antimyosin Fab using HPLC-purified [^{18}F]SFBS was 75 ± 9%. Binding of ^{18}F-labeled antimyosin F(ab')$_2$ to the myosin affinity column was 89 ± 5% compared to less than 5% for ^{18}F-labeled control Mel-14 F(ab')$_2$.

The higher immunoreactivity of divalent F(ab')$_2$ compared to monovalent Fab is consistent with the results reported for other MAbs (*24*, *25*, *29*). No published data are available for the binding of antimyosin fragments to myosin affinity columns after other radiolabeling procedures. Nevertheless, the immunoreactivities measured for ^{18}F-labeled antimyosin Fab and F(ab')$_2$ compare favorably with those reported in the literature for other radiolabeled MAb fragments (*24–26*, *29*). For example, the binding of ^{125}I-labeled anti-CEA MAb fragments to carcinoembryonic antigen affinity columns ranged between 50 and 65% for two Fab fragments and 54–77% for four F(ab')$_2$ fragments (*29*).

In summary, we have described a method for labeling proteins with ^{18}F in good yield at specific activities of up to 11 mCi/mg in a synthesis time of about 80–90 min, nearly 1 h shorter than previously published methods. HPLC purification of the [^{18}F]SFBS intermediate is required to achieve optimal protein coupling efficiency, in vivo tissue distribution, and immunoreactivity of ^{18}F-labeled MAb fragments. The results from the immunoreactivity and in vivo stability measurements suggest that [^{18}F]SFBS may be a valuable reagent for labeling MAbs and their fragments with ^{18}F for use with PET. To this end, we have initiated an investigation (to be reported in a subsequent publication) of the pharmacokinetics of ^{18}F-labeled antimyosin F(ab')$_2$ and Fab in a canine myocardial infarct model. In five animals studied to date, ^{18}F-labeled MAb fragments were observed to selectively accumulate in myosin-rich infarcted myocardium.

ACKNOWLEDGMENT

The excellent technical assistance of Susan Slade is greatly appreciated. Ann Tamariz provided editorial assistance. This research was supported by National Institutes of Health Grants CA 42324, NS 20023, CA 14236 and by Grant DEFG05-89ER60789 from the Department of Energy.

LITERATURE CITED

(1) Straatmann, M. G., and Welch, M. J. (1975) A general method for labeling proteins with ^{11}C. *J. Nucl. Med. 16*, 425–428.
(2) Turton, D. R., Brady, F., Pike, V. N., Selwyn, A. P., Shea, M. J., Wilson, R. A., and DeLandsheere, C. M. (1984) Preparation of human serum [methyl-^{11}C]methylalbumin microspheres and human serum [methyl-^{11}C]methylalbumin for clinical use. *Int. J. Appl. Radiat. Isot. 35*, 337–344.
(3) Hnatowich, D. J. (1975) Labeling of tin-soaked albumin microspheres with ^{68}Ga. *J. Nucl. Med. 17*, 57–60.
(4) Wagner, S. J., and Welch, M. J. (1979) Gallium-68 labeling of albumin and albumin microspheres. *J. Nucl. Med. 20*, 428–433.
(5) Khaw, B. A., Fallon, J. T., Katus, H., Elmaleh, D., Strauss, H. W., Locke, E., Pohost, G. M., and Haber, E. (1979) Positron imaging of experimental myocardial infarction with ^{68}Ga-DTPA-anti-myosin antibody. *Circulation 135*, 1527–1531.
(6) Carasquillo, J. A. (1989) Radioimmunoscintigraphy with Polyclonal and Monoclonal Antibodies. In *Antibodies in Radioimmunodiagnosis and Therapy* (M. R. Zalutsky, Ed.) pp 169–198, CRC Press, Boca Raton, FL.
(7) Kilbourn, M. R., Dence, C. S., Welch, M. J., and Mathias, C. J. (1987) Fluorine-18 labeling of proteins. *J. Nucl. Med. 28*, 462–470.
(8) Müller-Platz, C. M., Kloster, G., Leger, G., Stöcklin, G. (1982) ^{18}F-fluoroacetate: An agent for introducing no-carrier-added fluorine-18 into urokinase without loss of biological activity. *J. Labelled Compd. Radiopharm. 19*, 1645–1646 (abstr.).
(9) Shiue, C.-Y., Wolf, A. P., and Hainfeld, J. F. (1988) Synthesis of ^{18}F-labeled *N*-(*p*-[^{18}F]fluorophenyl)maleimide and its derivatives for labelling monoclonal antibody with ^{18}F. *J. Labelled Compds. Radiopharm. 26*, 287–289 (abstr.).
(10) Khaw, B. A., Mattis, J. A., Melincoff, G., Strauss, H. W., Gold, H. K., and Haber, E. (1984) Monoclonal antibody to cardiac myosin: imaging of experimental myocardial infarction. *Hybridoma 3*, 11–23.
(11) Carrel, S., Accolla, R. S., Carmagnola, A. L., and Mach, J.-P. (1980) Common human melanoma-associated antigen(s) detected by monoclonal antibodies. *Cancer Res. 40*, 2523–2528.
(12) Bourdon, M. A., Wikstrand, C. J., Furthmayr, H., Matthews, T. J., and Bigner, D. D. (1983) Human glioma-mesenchymal extracellular matrix antigen defined by monoclonal antibody. *Cancer Res. 43*, 2796–2805.
(13) Wieland, B. W., Hendry, G. O., Schmidt, D. G., Bida, G., and Ruth, T. J. (1986) Efficient small-volume O-18 water targets for producing F-18 fluoride with low energy protons. *J. Labelled Compd. Radiopharm. 23*, 1202–1204.
(14) Padgett, H., Schmidt, D. G., Luxen, A., Bida, G. T., Satyamurthy, N. H., and Barrio, J. R. (1989) Computer-controlled radiochemical synthesis: A chemistry process control unit for the automated production of radiochemicals. *Int. J. Appl. Radiat. Isot. 40*, 433–445.
(15) Montesano, L., Cawley, D., and Herschman, H. R. (1982) Disuccinimidyl suberate cross-linked ricin does not inhibit cell-free protein synthesis. *Biochem. Biophys. Res. Commun. 109*, 7–13.
(16) Giedroc, D. P., Puett, D., Ling, N., and Staros, J. V. (1983) Demonstration by covalent crosslinking of a specific interaction between β-endorphin and calmodulin. *J. Biol. Chem. 258*, 16–19.

(17) Garg, P. K., Archer, G. E., Jr., Bigner, D. D., and Zalutsky, M. R. (1989) Synthesis of radioiodinated *N*-succinimidyl iodobenzoate: Optimization for use in antibody labelling. *Appl. Radiat. Isot. 40*, 485–490.

(18) Remington, R. D., and Schork, M. A. (1985) *Statistics with Applications to the Biological Sciences* pp 135–190, Prentice-Hall, Englewood Cliffs, NJ.

(19) Attinà, M., Cacace, F., and Wolf, A. P. (1983) Labeled aryl fluorides from the nucleophilic displacement of activated nitro groups by ^{18}F–F^-. *J. Labelled Compd. Radiopharm. 20*, 501–514.

(20) Wilbur, D. S., Hadley, S. W., Hylarides, M. D., Abrams, P. G., Beaumier, P. A., Morgan, A. C., Reno, J. M., and Fritzberg, A. R. (1989) Development of a stable radioiodinating reagent to label monoclonal antibodies for radiotherapy of cancer. *J. Nucl. Med. 30*, 216–226.

(21) Vaidyanathan, G., and Zalutsky, M. R. (1990) Protein radiohalogenation observations on the design of *N*-succinimidyl ester acylation agents. *Bioconjugate Chem. 1*, 269–273.

(22) Brechbiel, M. W., Gansow, O. A., Atcher, R. W., Schlom, J., Esteban, J., Simpson, D. E., and Colcher, D. (1986) Synthesis of 1-(*p*-isothiocyanatobenzyl) derivatives of DTPA and EDTA. Antibody labeling and tumor imaging studies. *Inorg. Chem. 25*, 2772–2781.

(23) Esteban, J. M., Schlom, J., Gansow, O. A., Atcher, R. A., Brechbiel, M. W., Simpson, D. E., and Colcher, D. (1987) New method for the chelation of indium-111 to monoclonal antibodies: biodistribution and imaging of athymic mice bearing human colon carcinoma xenografts. *J. Nucl. Med. 28*, 861–870.

(24) Colcher, D., Zalutsky, M., Kaplan, W., Kufe, D., Austin, F., and Schlom, J. (1983) Radiolocalization of human mammary tumors in athymic mice by monoclonal antibody. *Cancer Res. 43*, 736–742.

(25) Holton, O. D., Black, C. D. V., Parker, R. J., Covell, D. G., Barney, J., Sieber, S. M., Talley, M. J., and Weinstein, J. N. (1987) Biodistribution of monoclonal IgGl, $F(ab')_2$ and Fab' in mice after iv injection: a comparison between anti-B-cell (anti-LyB8.2) and irrelevant (MOPC-21) antibodies. *J. Immunol. 139*, 3041–3049.

(26) Colapinto, E. V., Lee, Y., Humphrey, P. A., Zalutsky, M. R., Friedman, H. S., Bullard, D. E., and Bigner, D. D. (1988) The localisation of radiolabelled murine monoclonal antibody 81C6 and its Fab fragment in human glioma xenografts in athymic mice. *Br. J. Neurosurg. 2*, 179–191.

(27) Zalutsky, M. R., and Narula, A. S. Radiohalogenation of a monoclonal antibody using a *N*-succinimidyl-3-(tri-*n*-butylstannyl)benzoate intermediate. *Cancer Res. 48*, 1446–1450.

(28) Zalutsky, M. R., Noska, M. A., Colapinto, E. V., Garg, P. K., and Bigner, D. D. (1989) Enhanced tumor localization and in vivo stability of a monoclonal antibody radioiodinated using *N*-succinimidyl-3-(tri-*n*-butylstannyl)benzoate. *Cancer Res. 49*, 5543–5549.

(29) Buchegger, F., Haskell, C. M., Schreyer, M., Scazziga, B. R., Randin, S., Carrel, S., and Mach, J.-P. (1983) Radiolabeled fragments of monoclonal antibodies against carcinoembryonic antigen for localization of human colon carcinoma grafted into nude mice. *J. Exp. Med. 158*, 413–427.

Registry No. SFBS, 131865-53-7; [^{18}F]SFBS, 131865-55-9; 4-[^{18}F]fluorobenzonitrile, 81755-10-4; 4-nitrobenzonitrile, 619-72-7; 4-[^{18}F]fluorobenzylamine, 131865-54-8.

N-Succinimidyl 5-(Trialkylstannyl)-3-pyridinecarboxylates: A New Class of Reagents for Protein Radioiodination

Sudha Garg, Pradeep K. Garg, and Michael R. Zalutsky*

Department of Radiology, Duke University Medical Center, Box 3808, Durham, North Carolina 27710.
Received November 26, 1990

N-Succinimidyl 5-(trialkylstannyl)-3-pyridinecarboxylates (alkyl = Me, Bu) have been prepared and used as a precursor to label *N*-succinimidyl 5-[^{131}I]iodo-3-pyridinecarboxylate (SIPC). SIPC was obtained in greater than 80% yield from either the methyl or butyl precursor with *N*-chlorosuccinimide and heating at 60–65 °C. Significantly lower yields were observed with *tert*-butyl hydroperoxide. After a 30-min incubation with [^{131}I]SIPC at pH 8.5, goat IgG, an intact monoclonal antibody (MAb), and a MAb F(ab')$_2$ fragment were labeled in 60–65% yield. Specific binding of the MAb and MAb fragment after SIPC labeling was identical with that observed with *N*-succinimidyl 3-iodobenzoate and higher than that reported previously for these MAbs after labeling by using the Iodogen method. When 5-[^{131}I]iodonicotinic acid was injected into normal mice, thyroid uptake was less than 0.2% of the injected dose, reflecting the inertness of this compound to deiodination. Paired-label biodistribution studies indicate that for both the MAb and the F(ab')$_2$ labeled by using SIPC, accumulation of activity in the thyroid and other tissues is comparable to that observed when these proteins were labeled by using *N*-succinimidyl 3-iodobenzoate. The results of this study suggest that SIPC may be a reagent for labeling MAbs with halogen nuclides.

Compared with labeling monoclonal antibodies (MAbs)[1] with metallic nuclides, radioiodination offers certain advantages (*1*), particularly when therapeutic applications are envisioned. Radioimmunoscintigraphic studies utilizing ^{123}I-labeled MAb fragments and single-photon tomographic imaging (*2, 3*) have been most encouraging and suggest that this approach may permit an accurate evaluation of tumor- and normal-tissue dosimetry prior to therapy. The therapeutic potential of ^{131}I-labeled MAbs has been under active investigation by a number of groups (*4–9*), with positive responses noted most frequently in protocols utilizing nonintravenous routes of MAb delivery. Nevertheless, as is the case with radiometal-labeled MAbs, tumor uptake of radioiodinated MAbs is quite low (*10*).

Loss of radioiodine (dehalogenation) from MAbs occurs extensively in vivo (*11, 12*) and appears to play a significant role in decreasing the tumor uptake of radioiodinated MAbs. To date, clinical investigations have utilized MAbs labeled via conventional methods that primarily substitute iodine ortho to hydroxyl groups of tyrosine residues found on a MAb (*13*). Dehalogenation of these MAbs is presumably related to the presence of multiple deiodinases in the liver, kidney, and other tissues (*14–16*) and the structural similarity between iodotyrosines on the MAb and the endogenous substrates for these enzymes. For this reason, alternative strategies for protein radioiodination have been sought to provide iodination sites on the MAb which should have high C–I bond strengths while being dissimilar in structure to iodotyrosines and thyroxine.

Our initial efforts in this area have involved labeling MAbs via conjugation with *N*-succinimidyl 3-iodobenzoate (SIB), which is prepared by the iododestannylation of *N*-succinimidyl 3-(tri-*n*-butylstannyl)benzoate (ATE) (*17–19*). Compared with MAbs and fragments labeled by using the Iodogen method, thyroid uptake (reflecting the presence of free iodide) for MAbs labeled with SIB was up to 100-fold lower, and tumor accumulation was significantly higher. Promising results have also been reported by other investigators who have used the 4-iodobenzoate analogue for labeling MAbs (*20, 21*).

Other aryl iodide acylation agents including 2-hydroxy-5-iodo-3-methylbenzoic acid hydrazide (*22*), *N*-succinimidyl 2,4-dimethoxy-3-iodobenzoate (*23*), and the Bolton–Hunter reagent (*24*) have all been shown to result in decreased dehalogenation of MAbs in vivo, albeit to a lesser extent than SIB. Despite the chemical stability of vinyl iodides, iodovinyl–MAb conjugates are only marginally more inert to loss of label than MAbs labeled by using chloramine-T (*25*), suggesting that a better understanding of the structural features necessary for minimizing dehalogenation clearly is needed.

This investigation explores the feasibility of labeling MAbs by reaction with *N*-succinimidyl 5-iodo-3-pyridinecarboxylate (SIPC), obtained by the iododestannylation of *N*-succinimidyl 5-(trialkylstannyl)-3-pyridinecarboxylates (SPC) (Schemes I and II). Little, if any, data exists concerning the radiosynthesis or the in vivo stability of iodopyridines. However, since the recognition of iodinated heterocycles by endogenous deiodinases might be less likely than aryl iodides, the goal of this study was to determine whether an iodinated, electron-deficient heterocycle would be inert to dehalogenation in vivo. Our results indicate that both 5-iodonicotinic acid and its MAb and F(ab')$_2$ conjugates retain their radioiodine label after in vivo administration.

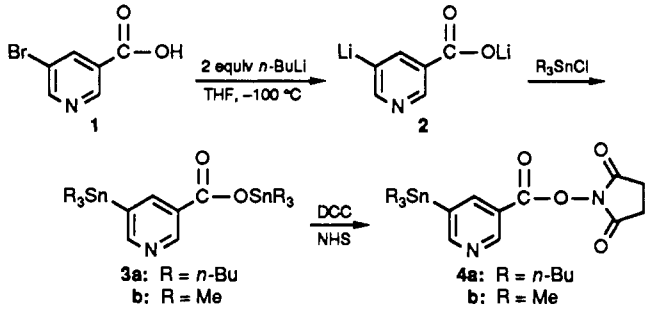
EXPERIMENTAL PROCEDURES

Materials. *N*-hydroxysuccinimide, *N*-chlorosuccinimide, 90% *tert*-butyl hydroperoxide, 5-bromonicotinic acid,

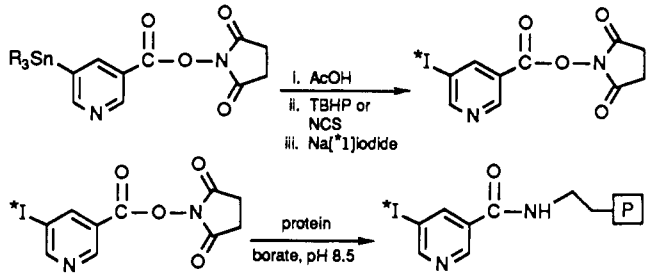
[1] Abbreviations used: MAbs, monoclonal antibodies; SIB, *N*-succinimidyl 3-iodobenzoate; ATE, *N*-succinimidyl 3-(tri-*n*-butylstannyl)benzoate; SIPC, *N*-succinimidyl 5-iodo-3-pyridinecarboxylate; SPC, *N*-succinimidyl 5-(trialkylstannyl)-3-pyridinecarboxylate; % ID, percent injected dose.

1043-1802/91/2902-0050$02.50/0 © 1991 American Chemical Society

Scheme I. Synthesis of *N*-Succinimidyl 5-(Trialkylstannyl)-3-pyridinecarboxylate [SPC]



Scheme II. Radioiodination of Proteins Using SPC



n-butyllithium, trimethyltin chloride, tri-*n*-butyltin chloride, and dicyclohexylcarbodiimide were purchased from Aldrich. Hexane, acetic acid, tetrahydrofuran, ethyl acetate, and dichloromethane were of HPLC grade and were obtained from Fisher Scientific. Sodium [^{131}I]iodide (8–10 Ci/mg) and sodium [^{125}I]iodide (17 Ci/mg), both in pH 7–11 NaOH, were purchased from Du pont-New England Nuclear (North Billerica, MA).

Goat IgG was obtained from Sigma. MAb 81C6 is a murine IgG2b reactive with the extracellular matrix antigen tenascin found in gliomas and other tumors (*26*). MAb Mel-14 is a murine IgG2a which reacts with the tumor-associated chondroitin sulfate antigen present in gliomas and melanomas (*27*). Generation of Mel-14 F(ab′)$_2$ fragments was performed by using a previously published procedure (*28*). Both 81C6 IgG and Mel-14 F(ab′)$_2$ were obtained as gifts from Dr. Darell D. Bigner, Department of Pathology, Duke University Medical Center.

General Procedures. Thin-layer chromatography was performed on analytical silica gel, precoated on plastic plates (Merck). Flash chromatography was done with 60–240 mesh silica gel (VWR Scientific, Marietta, GA). For high-pressure liquid chromatography, a system consisting of LKB Model 2150 pumps, an LKB 2151 variable-wavelength UV detector, and a Beckman Model 170 radioisotope detector was used. A Nelson Analytical software package was used for peak analysis. Compounds were separated on a silica column (Alltech, 10 μm, 300 mm × 4.6 mm) eluted with hexane–EtOAc–AcOH (70:30:2) at a flow rate of 1 mL/min.

Mass spectral data were obtained on a Finigan 4500 single quadrapole mass spectrometer. ^{1}H NMR were acquired in $CDCl_3$ and recorded on a GE Nicolet 300 MHz FT-NMR. Proton chemical shifts are reported in ppm downfield from internal TMS (0.00 ppm). Elemental analyses were performed by Oneida Research Services (Whitesboro, NY). Melting points were determined on a Haake-Buchler variable-heat apparatus and are uncorrected.

Synthesis of Tri-*n*-butylstannyl 5-(Tri-*n*-butylstannyl)-3-pyridinecarboxylate (3a). A solution of 5-bromonicotinic acid (2.02 g, 10 mmol) in 100 mL of anhydrous tetrahydrofuran was placed in a 250-mL flask, maintained under an argon atmosphere, and cooled to −100 °C with an ether–liquid nitrogen bath. To the above was added 12.5 mL of 1.6 M *n*-butyllithium in hexane slowly over 10–15 min while the temperature was maintained at −100 °C. After an additional 15 min of stirring, 2.2 equiv of tri-*n*-butyltin chloride (7.16 g, 22 mmol) was added. The cooling bath was removed and the reaction mixture was stirred for an additional 1.5 h. The reaction mixture was diluted with 250 mL of ethyl acetate and then washed with 2 × 100 mL of water, 2 × 25 mL of 5% $NaHCO_3$, and 2 × 25 mL of water. The organic layer was extracted, dried over anhydrous Na_2SO_4, and concentrated on a rotary evaporator. Routine flash chromatography on a silica gel column furnished an oil in 40% yield which had spectral data in agreement with the assigned structure. ^{1}H NMR: ($CDCl_3$, δ) 0.8–1.7 (m, 54 H, typical 6 × *n*-C_4H_9), 8.36 (s, 1 H, C-4H), 8.69 (s, 1 H, C-6H), 9.12 (s, 1 H, C-2H).

Preparation of *N*-Succinimidyl 5-(Tri-*n*-butylstannyl)-3-pyridinecarboxylate (4a). To a solution of 2.2 g of **3a** in 150 mL of methylene chloride were added 1.0 equiv of dicyclohexylcarbodiimide and 1.2 equiv of *N*-hydroxysuccimimide, and the reaction mixture was stirred for 4 h at room temperature. After filtering off the precipitated dicyclohexylurea, the solvent was removed on a rotary evaporator to furnish an oil. Routine flash chromatography (ethyl acetate–hexane, 35:65) provided the required compound in 80% yield. The HPLC retention time of **4a** was 10.7 min. NMR and mass spectral data of this product were consistent with the assigned structure. ^{1}H NMR: ($CDCl_3$, δ) 0.8–1.6 (m, 27 H, typical 3 × *n*-C_4H_9), 2.93 (s, 4 H, $COCH_2CH_2CO$), 8.42 (s, 1 H, C-4H), 8.86 (s, 1 H, C-6H), 9.2 (s, 1 H, C-2H). MS: *m/e* calcd 510.4, 511 (M^+, 4.4), 453 (M^+ − 57, 92), 397 (M^+ − 114, 47.1), 226 (100).

Synthesis of Trimethylstannyl 5-(Trimethylstannyl)-3-pyridinecarboxylate (3b). Synthesis of **3b** was accomplished as described above for **3a** except that trimethyltin chloride was used instead of tri-*n*-butyltin chloride. The solid product was crystallized from an ethyl acetate–hexane mixture in 45% yield (mp 159–160 °C). ^{1}H NMR: ($CDCl_3$, δ) 0.36 (s, 18 H, 6 × CH_3), 8.4 (s, 1 H, C-4H), 8.73 (s, 1 H, C-6H), 9.14 (s, 1 H, C-2H). MS: *m/e* calcd 448.68, 449 (M^+, 3), 434 (M^+ − 15, 100).

Synthesis of *N*-Succinimidyl 5-(Trimethylstannyl)-3-pyridinecarboxylate (4b). Reaction of **3b** with *N*-hydroxysuccinimide and dicyclohexylcarbodiimide, as described above for **4a**, gave the required product in 70% yield. Flash chromatography (ethyl acetate–hexane, 40:60) yielded a white solid with mp 114–115 °C. The HPLC retention time of **4b** was 18.7 min. Spectral data is in complete agreement with the assigned structure. ^{1}H NMR: ($CDCl_3$, δ) 0.4 (s, 9 H, 3 × CH_3), 2.93 (s, 4 H, $-COCH_2CH_2CO-$), 8.44 (s, 1 H, C-4H), 8.87 (s, 1 H, C-6H), 9.22 (s, 1 H, C-2H). MS: *m/e* calcd 383, 384 (M^+ + 1, 17.2), 369 (M^+ − 15, 100). Anal. Calcd for $C_{13}H_{16}N_2O_4Sn$: C, 40.77; H, 4.21; N, 7.31. Found: C, 40.64; H, 4.11; N, 7.27.

Preparation of *N*-Succinimidyl 5-Bromo-3-pyridinecarboxylate. This compound was synthesized for use as a reference standard in the development of the desired iodo analogue. To a solution of 2.1 g of 5-bromonicotinic acid in 100 mL of CH_2Cl_2 were added 2.06 g of dicyclohexylcarbodiimide and 1.15 g of *N*-hydroxysuccinimide, and the mixture was stirred at room temperature for 2 h. After filtering off the precipitated dicyclohexylurea, the solvent was evaporated. The resulting solid was purified by flash chromatography using ethyl acetate–hexane (60:

40) and was obtained in 82% yield (mp 165–166 °C). Retention time on HPLC was 14.5 min. ^{1}H NMR: ($CDCl_3$, δ) 2.93 (s, 4 H, $-COCH_2CH_2CO-$), 8.52 (s, 1 H, C-4H), 8.96 (s, 1 H, C-6H), 9.23 (s, 1 H, C-2H). MS: m/e calcd 299.08, 300 ($M^+ + 1$, 5.3), 186 ($M^+ - 114$, 100).

Synthesis of *N*-Succinimidyl 5-Iodo-3-pyridinecarboxylate (SIPC). To a solution of 250 mg of **4b** in 10 mL of CH_2Cl_2 were added 100 μL of 9% TBHP and 250 mg of molecular iodine. The reaction mixture was stirred at 55–60 °C for 15 min and cooled to room temperature. The organic layer was washed with aqueous $Na_2S_2O_3$ followed by water, dried over Na_2SO_4, and evaporated on a rotary evaporator. The required compound was isolated by flash chromatography on a silica gel column and recrystallized from CH_2Cl_2–hexane. A white crystalline solid was isolated in 89% yield (mp 175 °C) with a retention time on HPLC of 14.5 min, identical with the bromo analogue. Spectral data were consistent with the assigned structure. ^{1}H NMR: ($CDCl_3$, δ) 2.9 (s, 4 H, $-COCH_2CH_2CO-$), 8.7 (s, 1 H, C-4H), 9.1 (s, 1 H, C-6H), 9.26 (s, 1 H, C-2H). MS: m/e calcd 346.08, 347 (M + 1, 100), 250 ($M^+ - 96$, 7.4), 232 ($M^+ - 114$, 60). Anal. Calcd for $C_{10}H_7IN_2O_4$: C, 34.70; H, 2.04; N, 8.09. Found: C, 35.01; H, 1.82; N, 7.98.

Radioiodination of 4a and 4b. The following solutions were prepared: (a) 5 μL of glacial acetic acid in 95 μL of CH_2Cl_2, (b) 45 μL of *tert*-butyl hydroperoxide in 450 μL of CH_2Cl_2 containing a few crystals of anhydrous Na_2SO_4, (c) 13.3 mg of *N*-chlorosuccinimide in 1 mL of CH_2Cl_2, (d) 51 mg of **4a** in 1 mL of CH_2Cl_2, and (e) 38 mg of **4b** in 1 mL of CH_2Cl_2. To 100–800 μCi of sodium [^{125}I or ^{131}I]-iodide in a 1-mL glass vial was added a sufficient amount of reagent a to adjust the pH to 5–5.5. To this solution was added 5 μL of either TBHP (b) or NCS (c) followed by 5 μL of either **4a** (d) or **4b** (e). The following reaction conditions were investigated: room temperature for 0–60 min, heating at 60–65 °C for 5–30 min, and heating at 60–65 °C for 5 min followed by incubation at room temperature for 5–30 min. Radioiodination yields were determined with HPLC by calculating the fraction of radioactivity that eluted with a retention time corresponding to that of authentic, cold SIPC. Each set of reaction conditions was run three to five times.

For some of the biological studies, 5-[^{131}I]iodonicotinic acid was prepared by hydrolyzing [^{131}I]SIPC for 16 h in phosphate-buffered saline. Conversion to the free acid was confirmed by HPLC (iodonicotinic acid t_R = 10.2 min).

Protein Labeling. The HPLC fractions containing [^{131}I]SIPC were evaporated with a gentle stream of nitrogen, and the residue was taken up in 100–150 μL of CH_2Cl_2 and transferred to a 0.5-dram glass vial. After evaporation of the organic solvent, 50–150 μL of either goat IgG, 81C6 IgG, or Mel-14 F(ab')$_2$ (2–10 mg/mL) in pH 8.5 0.1 M borate buffer was added and incubated at room temperature for 15–45 min. The coupling reaction was terminated by the addition of 300 μL of 0.2 M glycine. Labeled proteins were isolated by gel filtration on a Sephadex G-25 column eluted with phosphate-buffered saline.

Determination of Specific Binding. The immunoreactivities of MAb 81C6 IgG and Mel-14 F(ab')$_2$, after labeing with [^{131}I]SIPC were compared to those for the same proteins after labeling with [^{125}I]SIB. MAb 81C6 and Mel-14 F(ab')$_2$ were labeled with ^{125}I by using the ATE method as described previously (*19*, *29*) and were also labeled with ^{131}I by using **4b** as described above. This assay was performed in paired-label format using D-54 MG human glioma homogenates. For example, 100 ng of both ^{131}I- and ^{125}I-labeled 81C6 in 1 mL of phosphate-buffered saline containing 1% human serum albumin was incubated at room temperature for 2–5 h in triplicate with about 250 mg of D-54 MG glioma and antigen-negative rat liver homogenates. After centrifugation, the homogenates were washed three times with 500 μL of phosphate-buffered saline and counted for both ^{125}I and ^{131}I with an LKB 1282 automated γ-counter. A correction was applied for crossover of ^{131}I into the ^{125}I counting window. Specific binding was calculated by subtracting the percentage radioiodine bound to rat liver from the percentage bound to D-54 MG tumor.

Table I. Electrophilic Iododestannylation of 4a and 4b Using *N*-Chlorosuccinimide and *tert*-Butyl Hydroperoxide

reaction time,[b] min	% yield of SIPC[a]			
	N-chlorosuccinimide		*tert*-butyl hydroperoxide	
	4a	**4b**	**4a**	**4b**
5	78 ± 7	82 ± 7	50 ± 5	52 ± 3
10	81 ± 5	84 ± 5	48 ± 4	53 ± 2
30	84 ± 6	84 ± 4	47 ± 5	66 ± 4

[a] Mean ± SD for three to five experiments. [b] Heating at 60–65 °C for 5 min followed by incubation for specified time at room temperature.

Tissue-Distribution Measurements. BALB/c mice weighing between 24 and 30 g were used for the three sets of paired-label protocols. In the first, animals received 7 μCi of 5-[^{131}I]iodonicotinic acid and 8 μCi of [^{125}I]iodide and groups of six animals were sacrificed by halothane overdose at 1, 2, 4, and 6 h. In the second, mice were injected with 6 μg of 81C6 IgG, with half of the MAb labeled with ^{125}I by using ATE (6 μCi) and half labeled with ^{131}I by using **4b** (5 μCi), and groups of five animals were sacrificed 1, 2, 3, 4, and 7 days later. In the last, animals received 5 μg of ^{131}I-labeled Mel-14 F(ab')$_2$ (5 μCi) and 5 μg of ^{125}I-labeled Mel-14 F(ab')$_2$ (6 μCi) prepared with **4b** and ATE, respectively. Groups of five animals were sacrificed at 1, 2, 3, and 4 days. Animals were dissected and tissues of interest were removed, washed with PBS, and weighed. The percent injected dose (% ID) of both nuclides was calculated by comparison to 5% ID counting standards.

Statistical Analyses. Comparisons between different sets of radioiodination conditions were performed by using the Student's *t* test (*30*). Because of the paired-label nature of the biodistribution studies, each animal served as its own control, permitting the use of a paired *t* test with a one-sided alternative (*30*). Only a P of < 0.05 was considered statistically significant.

RESULTS

The radioiodination of **4a** and **4b** was investigated with either *tert*-butyl hydroperoxide or *N*-chlorosuccinimide in chloroform–acetic acid (pH 5–5.5) (Scheme I). When the reaction was performed at room temperature, unsatisfactory yields of SIPC were obtained (generally <20%, *tert*-butyl hydroperoxide; 35–50%, *N*-chlorosuccinimide). Heating at 60–65 °C increased the efficiency of iododestannylation; however, when the reaction was run at elevated temperature for more than 5 min, a peak on HPLC corresponding to iodonicotinic acid (t_R = 10.2 min) was observed. The iodonicotinic acid peak increased from less than 5% of total activity at 5 min to up to 50% after 30 min of heating when **4b** and *N*-chlorosuccinimide were used.

Subsequent experiments utilized a 5-min heating period at 60–65 °C followed by incubation at room temperature for various times prior to HPLC analysis (Table I). With *N*-chlorosuccinimide, radioiodination yields were greater than 80% for all reaction periods with **4b**; no significant

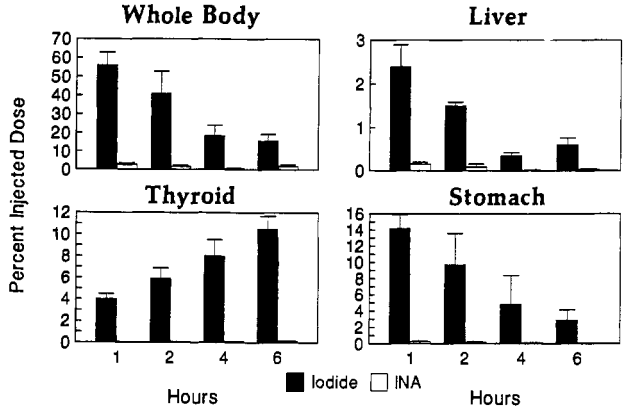


Figure 1. Comparison of the tissue distribution of radioiodine following the injection of 5-[^{131}I]iodonicotinic acid (INA) and [^{125}I]iodide into normal mice.

differences between **4b** and **4a** were seen. Yields with *tert*-butyl hydroperoxide were significantly lower than those obtained with *N*-chlorosuccinimide at all time points ($P < 0.001$). With *tert*-butyl hydroperoxide, radioiodination efficiencies for **4b** were higher than those for **4a** (differences not significant, 5 min; $P < 0.02$, 10 min; $P < 0.001$, 30 min). Synthesis of SIPC is now performed routinely with **4b** and *N*-chlorosuccinimide, with the reaction mixture heated at 60–65 °C for 5 min followed by incubation at room temperature for 5 min to permit cooling prior to HPLC purification.

The efficiency for the coupling of SIPC to goat IgG (3.5 mg/mL) at pH 8.5 increased from 55.6 ± 0.9% (mean ± SD) at 15 min to 62.0 ± 2.9% at 30 min ($P < 0.001$). No significant increase in coupling yields occurred with longer reaction periods. Yields for the conjugation of SIPC to 81C6 IgG and Mel-14 F(ab′)$_2$ were similar.

The specific binding of 81C6 IgG and Mel-14 F(ab′)$_2$ labeled with SIPC was compared with that for SIB with D-54 MG human glioma homogenates as the antigen-positive target. With 81C6 IgG, binding to D-54 MG (87.5 ± 2.2%, SIPC; 87.5 ± 1.1%, SIB) and rat liver (4.1 ± 1.0%, SIPC; 3.9 ± 1.0%, SIB) for the two labeling methods was nearly identical, resulting in specific binding values of 83.4 ± 2.4% for SIPC and 83.6 ± 1.5% for SIB. Specific binding percentages for Mel-14 F(ab′)$_2$ were 71.2 ± 3.3% for SIPC and 71.3 ± 3.2% for SIB.

The tissue distribution of 5-[^{131}I]iodonicotinic acid, a potential catabolite of MAbs labeled with [^{131}I]SIPC, was compared with that of [^{125}I]iodide in normal mice. The thyroid uptake of ^{131}I ranged from 0.05 ± 0.02% ID at 1 h to 0.16 ± 0.04% ID at 6 h, compared with 4.0 ± 0.5% ID to 10.5 ± 1.2% ID for ^{125}I (Figure 1). Clearance of 5-iodonicotinic acid was considerably more rapid than that of iodide from all tissues. At 1 h, total body retention of 5-[^{131}I]iodonicotinic acid was 2.7 ± 0.8% compared with 56 ± 7% for [^{125}I]iodide. Although total urine collection was not attempted, the urine obtained from the 1- and 2-h groups sometimes contained over 80% of the ^{131}I dose, indicating that this was the primary route of iodonicotinic acid elimination.

Paired-label studies were performed with both a MAb (81C6) and a F(ab′)$_2$ fragment (Mel-14) to compare the tissue distribution of proteins labeled with [^{131}I]SIPC and [^{125}I]SIB. As shown in Figures 3 and 4, uptake of ^{131}I was not significantly different than that of ^{125}I in blood, lung, kidney, spleen, liver, stomach, or muscle for both 81C6 IgG and Mel-14 F(ab′)$_2$. For the 81C6–[^{131}I]SIPC conjugate, thyroid accumulation ranged from 0.51 ± 0.08% ID at 4 days to 0.27 ± 0.08% ID at 7 days (Figure 2). These

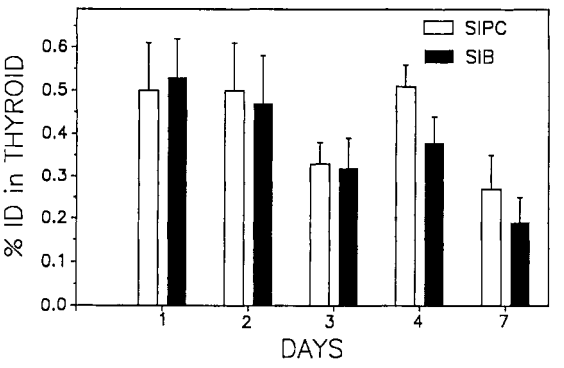


Figure 2. Comparison of the percent injected dose of radioiodine taken up by the thyroids of normal mice injected with MAb 81C6 IgG labeled with ^{131}I and ^{125}I by using SPIC and SIB, respectively.

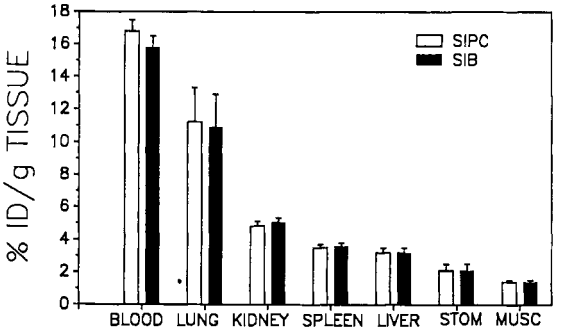


Figure 3. Comparative tissue distribution of ^{131}I and ^{125}I 2 days after injection of MAb 81C6 IgG labeled with [^{131}I]SPIC and [^{125}I]SIB.

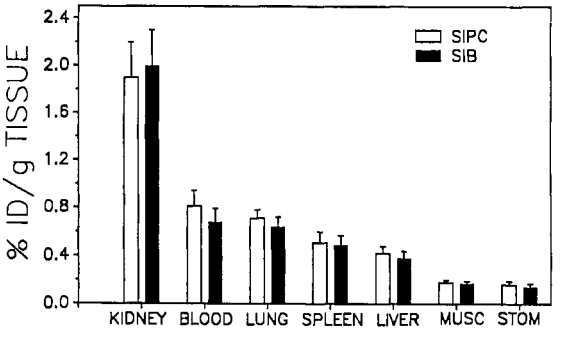


Figure 4. Tissue distribution in normal mice of radioiodine 1 day after injection of F(ab′)$_2$ fragment of Mel-14 labeled with [^{131}I]SPIC and [^{125}I]SIB.

Table II. Thyroid Uptake of Radioiodine in Normal Mice Injected with Mel-14 F(ab′)$_2$ Labeled With ^{125}I by Using [^{125}I]SIB and with ^{131}I by Using [^{131}I]SIPC

	thyroid uptake (% ID)[a]		
time, days	[^{125}I]SIB	[^{131}]SIPC	significance
1	0.07 ± 0.02	0.15 ± 0.03	<0.005
2	0.05 ± 0.02	0.19 ± 0.07	<0.02
3	0.07 ± 0.02	0.26 ± 0.09	<0.01
4	0.04 ± 0.01	0.09 ± 0.05	<0.05

[a] Mean ± SD.

values were not significantly different from those observed for 81C6 labeled with [^{125}I]SIB except at day 4 (0.38 ± 0.06% ID, $P < 0.001$). As shown in Table II, thyroid uptake for Mel-14 F(ab′)$_2$ fragment labeled by using SIPC was quite low, ranging from 0.26 ± 0.09% ID at day 3 to 0.09 ± 0.05% ID at day 4. Nevertheless, these values are significantly higher than those observed for fragment labeled by using SIB at all time points.

DISCUSSION

At least two factors must be considered in the design of acylation reagents for MAb iodination. From a chemical perspective, the method should result in the formation of an aromatic or vinyl C–I bond because their bond strengths are higher than aliphatic iodides (*31*). In addition, because of the presence of numerous deiodinases involved in the metabolism of thyroid hormones (*14–16*), structures dissimilar to iodotyrosine and thyroxine would appear to be advantageous. In this study, we have explored the feasability of using a 5-iodopyridine template for labeling proteins. This approach was attractive because the aromatic stability of the pyridine ring is well-established (*32*), permitting the exploitation of the higher bond strengths of aromatic iodides while further decreasing the similarity in structure to the thyroid hormones, which all contain aryl templates.

Although the pyridine ring is present in many natural products, little information is available concerning its regiospecific halogenation, particularly at position 3 or 5. This is not surprising, considering the electron-deficient nature of the pyridine ring. Methods for the synthesis of iodopyridines have been reported (*33, 34*), but their yields are low and/or involve a large excess of iodide and prolonged heating. These methods thus are not suitable for the regiospecific radioiodination of a pyridine ring, particularly when an easily hydrolyzed functionality is attached to the pyridine ring. The synthesis of 3-[^{131}I]-iodopyridine via isotopic exchange using a CuCl catalyst has been described (*35*); however, the specific activity of the product was quite low, making this method of little utility for labeling MAbs.

The rationale for the labeling approach outlined in Schemes I and II is as follows: On the basis of our experience (*17–19, 29*) and that of others (*20, 21*), electrophilic iododestannylation of trialkylstannyl precursors has been shown to be a facile method for the radiosynthesis of *N*-succinimidyl iodobenzoates. And second, from the extensive literature describing halogen–metal exchange reactions on pyridine rings (*36*), it appeared that the synthesis of **4b** and **4a** should be straightforward. Yields for the synthesis of these compounds were 30–35% and were comparable to those reported for the corresponding ATE esters (*17, 20, 37*).

Unlike the trialkylstannyl benzoates, radioiodination of SPC did not proceed in high yield at room temperature. This is presumably related to the lower nucleophilicity of the pyridine ring, and since the reaction is run at pH 5–5.5, protonation of the heteroatom would further increase the deactivation of the pyridine ring toward electrophilic substitution. The radioiodination of both **4b** and **4a** could be accomplished with *N*-chlorosuccinimide in greater than 80% yield by heating at 60–65 °C for 5 min. Unlike the results of a previous study using trialkylstannyl benzoates (*37*), yields with *tert*-butyl hydroperoxide were significantly lower than those observed with *N*-chlorosuccinimide at all sets of reaction conditions. This could be related to the slow decomposition of *tert*-butyl hydroperoxide at elevated temperatures (*38*) or the generation of a stronger electrophilic species, ICl, with *N*-chlorosuccinimide (*39, 40*).

The results of previous studies using trialkylstannyl benzoates (*23, 37*) suggested that higher radioiodination yields might be obtainable with **4b** compared with **4a**; however, this was not the case. Decreasing the bulk of the alkyltin substituent appears to have a greater effect for electrophilic astatodestannylation (*29*), and experiments are in progress using **4b** and **4a** and ^{211}At to address this question.

Running the iodination reaction for more than 5 min at elevated temperature resulted in decreased yields of SIPC due to hydrolysis of the iodinated product to 5-iodonicotinic acid. An additional problem associated with extended heating when *N*-chlorosuccinimide was used as the oxidant was the appearance of a nonradioactive peak on HPLC with an elution time of 15.1 min. This peak could be from the generation of *N*-succinimidyl 5-chloro-3-pyridinecarboxylate. The formation of chlorinated side products when *N*-chlorosuccinimide is used at elevated temperatures has been reported previously (*40*).

No attempt was made to quantitate or further analyze this chlorinated product since it was not observed on HPLC for reaction periods of 5 min or less. From a practical perspective, the lack of appreciable levels of this potential byproduct can be inferred from the high degree of specific binding observed for a MAb and a MAb F(ab')$_2$ fragment labeled with NCS and **4b**. Indeed, the specific binding values for radioiodinated 81C6 and Mel-14 F(ab')$_2$ were considerably higher than the values reported for the same proteins labeled by using Iodogen (*19, 28*) and identical with those seen by using the ATE method.

Although iodopyridine-containing compounds retain their iodine substituent to sufficient degree to permit their use as heavy atom labels for in vitro studies (*41*), the inertness to dehalogenation of iodopyridines and their in vivo distribution is unknown. When 5-iodonicotinic acid was injected into normal mice, thyroid uptake was less than 0.2% ID at all time points, suggesting minimal loss of iodine from this compound in vivo. This level of thyroid uptake is comparable to that observed previously for *m*-iodobenzoic acid (*19*). 5-iodonicotinic acid is cleared rapidly from the body via urinary excretion with uptake of activity in all organs less than 1% ID by 1 h. Its clearance appears to be even more rapid than that of *m*-iodobenzoic acid, presumably reflecting the higher water solubility of 5-iodonicotinic acid (octanol–water partition coefficient: 0.05, 5-iodonicotinic acid; 0.48, *m*-iodobenzoic acid; data not shown). Since 5-iodonicotinic acid should be a catabolic product of proteins labeled with SIPC, the rapid excretion of 5-iodonicotinic acid could be advantageous in helping to decrease normal tissue background.

When 81C6 IgG and Mel-14 F(ab')$_2$ were labeled by using SIPC, their tissue distributions in normal mice were nearly identical with that observed when the same proteins were labeled by using SIB. Of particular importance is the observation that thyroid uptake for MAbs labeled by using SIPC was quite low. In some cases, the thyroid uptake associated with SIPC labeling was significantly higher than that observed when SIB was used; however, the differences were small and suggest that both methods yield proteins whose inertness to dehalogenation is nearly identical. Experiments are in progress comparing the tumor retention and in vivo stability of 81C6 IgG and Mel-14 G(ab')$_2$ labeled with SIPC and SIB in athymic mice bearing human glioma xenografts.

In summary, the results of this study indicate that *N*-succimimidyl 5-(trialkylstannyl)-3-pyridinecarboxylates may be a valuable new class of reagents for use in protein radiohalogenation. In addition, because of the inertness to dehalogenation of 5-iodonicotinic acid, it may be possible to use radioiodinated pyridine analogues for the in vivo investigation of some of the numerous natural products containing pyridine rings in their structure.

ACKNOWLEDGMENT

The excellent technical assistance of Susan Slade and the editorial assistance of Ann Tamariz are greatly appreciated. This research was supported by National

Institutes of Health Grants CA 42324, NS 20023, CA 14236, and by Grant DEFG05-89ER60789 from the Department of Energy.

LITERATURE CITED

(1) Larson, S. M., and Carrasquillo, J. A. (1988) Advantages of radioiodine over radioindium labeled monoclonal antibodies for imaging solid tumors. *Nucl. Med. Biol. 15*, 231–233.

(2) Delaloye, B., Bischof-Delaloye, A., Buchegger, F., von Fliedner, V., Grob, J.-P., Volant, J.-C., Pettavel, J., and Mach, J.-P. (1986) Detection of colorectal carcinoma by emission-computerized tomography after injection of ^{123}I-labeled Fab or F(ab')$_2$ fragments from monoclonal anti-carcinoembryonic antigen antibodies. *J. Clin. Invest. 77*, 301–311.

(3) Bischof-Delaloye, A., Delaloye, B., Buchegger, F., Gilgien, W., Studer, A., Curchod, S., Givel, J-C., Mosimann, F., Pettavel, J., and Mach, J.-P. (1989) Clinical value of immunoscintigraphy in colorectal carcinoma patients: A prospective study. *J. Nucl. Med. 30*, 1646–1656.

(4) Carrasquillo, J. A., Krohn, K. A., Beaumier, P., McGuffin, R. W., Brown, J. P., Hellstrom, K. E., Hellstrom, I., and Larson, S. M. (1984) Diagnosis of and therapy for solid tumors with radiolabeled antibodies and immune fragments. *Cancer Treat. Rep. 68*, 317–328.

(5) Bernstein, I. D., Eary, J. F., Badger, C. C., Press, O. W., Appelbaum, F. R., Martin, P. J., Krohn, K. A., Nelp, W. B., Porter, B., Fisher, D., Miller, R., Brown, S., Levy, R., and Thomas, E. D. (1990) High dose radiolabeled antibody therapy of lymphoma. *Cancer Res. 50 (Suppl.)*, 1017s–1021s.

(6) Epenetos, A. A., Munro, A. J., Stewart, S., Rampling, R., Lambert, H. E., McKenzie, C. G., Soutter, P. A., Rahemtulla, G., Hooker, G., Sivolapenko, G. B., Snook, D., Courtenay-Luck, N., Dhokia, B., Krausz, T., Taylor-Papadimitriou, J., Durbin, H., and Bodmer, W. F. (1987) Antibody-guided irradiation of advanced ovarian cancer with intraperitoneally administered radiolabeled monoclonal antibodies. *J. Clin. Oncol. 5*, 1890–1899.

(7) Lashford, L. S., Davies, A. G., Richardson, R. B., Bourne, S. P., Bullimore, J. A., Eckhert, H., Kemshead, J. T., and Coakham, H. B. (1988) A pilot study of ^{131}I monoclonal antibodies in the therapy of leptomeningeal tumors. *Cancer 61*, 857–868.

(8) Pectasides, D., Courtenay-Luck, N., Rampling, R., Munro, A. J., Krausz, T., Dhokia, B., Snook, D., Hooker, G., Durbin, H., Taylor-Papadimitriou, J., Bodmer, W. F., and Epenetos, A. A. (1986) Antibody-guided irradiation of malignant pleural and pericardial effusions. *Br. J. Cancer 53*, 727–732.

(9) Moseley, R. P., Davies, A. G., Richardson, R. B., Zalutsky, M., Carrel, S., Fabre, J., Slack, N., Bullimore, J., Pizer, B., Papanastassiou, V., Kemshead, J. T., Coakham, H. B., and Lashford, L. S. (1990) Intrathecal administration of ^{131}I radiolabelled monoclonal antibody as a treatment for neoplastic meningitis. *Br. J. Cancer 62*, 637–642.

(10) Larson, S. M. (1990) Clinical radioimmunodetection, 1978–1988: Overview and suggestions for standardization of clinical trials. *Cancer Res. 50 (Suppl.)*, 892s–898s.

(11) Hayes, D. F., Zalutsky, M. R., Kaplan, W., Noska, M., Thor, A., Colcher, D., Schlom, J., and Kufe, D. (1986) Pharmacokinetics of radiolabeled monoclonal antibody B6.2 in patients with metastatic breast cancer. *Cancer Res. 46*, 3157–3163.

(12) Carasquillo, J. A. (1989) Radioimmunoscintigraphy with polyclonal and monoclonal antibodies. In *Antibodies in Radiodiagnosis and Therapy* (M. R. Zalutsky, Ed.) pp 169–198, CRC Press, Boca Raton, FL.

(13) Eary, J. F., Krohn, K. A., Koshore, R., and Nelp, W. B. (1989) Radiochemistry of halogenated antibodies. In *Antibodies in Radiodiagnosis and Therapy* (M. R. Zalutsky, Ed.) pp 83–102, CRC Press, Inc., Boca Raton, FL.

(14) Leonard, J. L., and Rosenberg, I. N. (1978) Subcellular distribution of thyroxine 5'-deiodinase in the rat kidney: A plasma membrane location. *Endocrinology 103*, 274–280.

(15) Koehrle, J., Auf'mkolk, M., Rokos, H., Hesch, R.-D., and Cody, V. (1986) Rat liver iodothyronine ligand-binding site. *J. Biol. Chem. 261*, 11613–11622.

(16) Gershengorn, M. C., Glinoer, D., and Robbins, J. (1980) Transport and metabolism of thyroid hormones. In *The Thyroid Gland* (M. DeVisscher, Ed.) pp 81–121, Raven Press, New York.

(17) Zalutsky, M. R., and Narula, A. S. (1987) A method for the radiohalogenation of proteins resulting in decreased thyroid uptake of radioiodine. *Appl. Radiat. Isot. 38*, 1051–1055.

(18) Zalutsky, M. R., and Narula, A. S. Radiohalogenation of a monoclonal antibody using a *N*-succinimidyl-3-(tri-*n*-butylstannyl)benzoate intermediate. *Cancer Res. 48*, 1446–1450.

(19) Zalutsky, M. R., Noska, M. A., Colapinto, E. V., Garg, P. K., and Bigner, D. D. (1989) Enhanced tumor localization and in vivo stability of a monoclonal antibody radioiodinated using *N*-succinimidyl-3-(tri-*n*-butylstannyl)benzoate. *Cancer Res. 49*, 5543–5549.

(20) Wilbur, D. S., Hadley, S. W., Hylarides, M. D., Abrams, P. G., Beaumier, P. A., Morgan, A. C., Reno, J. M., and Fritzberg, A. R. (1989) Development of a stable radioiodinating reagent to label monoclonal antibodies for radiotherapy of cancer. *J. Nucl. Med. 30*, 216–226.

(21) Khawli, L. A., and Kassis, A. I. (1989) Synthesis of ^{125}I labeled *N*-succinimidyl *p*-iodobenzoate for use in radiolabeling antibodies. *Nucl. Med. Biol. 16*, 727–733.

(22) Rea, D. W., Ultee, M. E., Belinka, B. A., Jr., Coughlin, D. J., and Alvarez, V. L. (1990) Site-specifically radioiodinated antibody for targeting tumors. *Cancer Res. 50 (Suppl.)*, 857s–861s.

(23) Vaidyanathan, G., and Zalutsky, M. R. (1990) Radioiodination of antibodies via *N*-succinimidyl 2,4-dimethoxy-3-(trialkylstannyl)benzoates *Bioconjugate Chem. 1*, 387–393.

(24) Vaidyanathan, G., and Zalutsky, M. R. (1990) Protein radiohalogenation observations on the design of *N*-succinimidyl ester acylation agents. *Bioconjugate Chem. 1*, 269–273.

(25) Hadley, S. W., and Wilbur, D. S. (1990) Evaluation of iodovinyl antibody conjugates: Comparison with a *p*-iodobenzoyl conjugate and direct iodination. *Bioconjugate Chem. 1*, 154–161.

(26) Bourdon, M. A., Wikstrand, C. J., Furthmayr, H., Matthews, T. J., and Bigner, D. D. (1983) Human glioma-mesenchymal extracellular matrix defined by monoclonal antibody. *Cancer Res. 43*, 2796–2805.

(27) Carrel, S., Accolla, R. S., Carmagnola, A. L., and Mach, J.-P. (1980) Common human melanoma-associated antigen(s) detected by monoclonal antibodies. *Cancer Res. 40*, 2523–2528.

(28) Colapinto, E. V., Humphrey, P. A., Zalutsky, M. R., Groothuis, D. R., Friedman, H. S., de Tribolet, N., Carrel, S., and Bigner, D. D. (1988) Comparative localization of murine monoclonal antibody Mel-14 F(ab')$_2$ fragment and whole IgGa2 in human glioma xenografts. *Cancer Res. 48*, 5701–5707.

(29) Zalutsky, M. R., Garg, P. K., Friedman, H. S., and Bigner, D. D. (1989) Labeling monoclonal antibodies and F(ab')$_2$ fragments with the α-particle emitting nuclide astatine-211: Preservation of immunoreactivity and in vivo localizing capacity. *Proc. Natl. Acad. Sci. U.S.A. 86*, 7149–7153.

(30) Remington, R. D., and Schork, M. A. (1985) *Statistics with Applications to the Biological Sciences*, pp 135–190, Prentice-Hall, Englewood Cliffs, NJ.

(31) Coenen, H. H., Moerlein, S. M., and Stöcklin, G. (1983) No-carrier-added radiohalogenation methods with heavy halogens. *Radiochim. Acta 34*, 47–68.

(32) Wheland, G. W., and Pauling, L. (1935) A quantum mechanical discussion of substituents in aromatic molecules. *J. Am. Chem. Soc. 57*, 2086–2095.

(33) Uemura, S., Tanaka, S., Okano, M., and Hamana, M. (1983) Decarboxylative ipso halogenation of mercury(II) pyridinecarboxylates. Facile formation of 3-iodo- and 3-bromopyridines. *J. Org. Chem. 48*, 3297–3301.

(34) Newkome, G. R., Moorfield, C. N., and Sabbaghian, B. (1986) Reductive dehalogenation of electron-poor heterocycles. Nicotinic acid derivatives. *J. Org. Chem. 51*, 953–954.

(35) Iroshnikova, N. G., and Stanko, V. I. (1985) Isotope exchange of iodine in inactivated iodine derivatives of benzene, catalyzed by copper salts. *J. Org. Chem. (U.S.S.R.) 21*, 514–520.

(36) Lukevics, E., and Segal, I. D. (1988) Pyridine and quinoline derivatives of Group IVB elements. In *Organometallic*

Chemistry Reviews (A. G. Davies, E. O. Fischer, and O. A. Reutov, Eds.) pp 71–195, Elsevier, New York.
(37) Garg, P. K., Archer, G. E., Jr., Bigner, D. D., and Zalutsky, M. R. (1989) Synthesis of radioiodinated *N*-succinimidyl iodobenzoate: Optimization for use in antibody labeling. *Appl. Radiat. Isot. 40*, 485–490.
(38) Milas, N. A., and Sussman, S. (1937) The hydroxylation of unsaturated substances IV. The catalytic hydroxylation of unsaturated hydrocarbons. *J. Am. Chem. Soc. 59*, 2345–2347.
(39) Wilbur, D. S., and Anderson, K. W. (1982) Bromine chloride from *N*-chlorosuccinimide oxidation of bromide ion. Electrophilic addition reactions in protic and aprotic solvents. *J. Org. Chem. 47*, 358–359.
(40) Wilbur, D. S., Anderson, K. W., Stone, W. E., and O'Brien, H. A. Jr., (1982) Radiohalogenation of nonactivated aromatic compounds via aryltrimethylstannyl intermediates. *J. Labelled Compd. Radiopharm. 19*, 1171–1188.
(41) Abdallah, M. A., and Biellmann, J.-F. (1980) Activity determination of 3-iodopyridineadenine dinucleotide and its phosphate as hydride acceptors in the presence of dehydrogenases using a coupled redox system. *Eur. J. Biochem. 112*, 331–333.

Registry No. **1**, 20826-04-4; **2**, 131865-56-0; **3a**, 131865-57-1; **3b**, 131865-58-2; **4a**, 131865-59-3; **4b**, 131865-60-6; SIPC, 131865-61-7; [^{131}I]SIPC, 131865-63-9; [^{125}I]SIB, 125215-73-8; *N*-succinimidyl 5-bromo-3-pyridinecarboxylate, 107293-80-1; 5-[^{131}I]-iodonicotinic acid, 131865-62-8.

Photolytic Cleavage of DNA by Nitrobenzamido Ligands Linked to 9-Aminoacridines Gives DNA Polymerase Substrates in a Wavelength-Dependent Reaction

Peter E. Nielsen,*,† Michael Egholm,‡ Troels Koch,‡ Jørn B. Christensen,‡ and Ole Buchardt*,‡

Research Center for Medical Biotechnology, University of Copenhagen, Department of Biochemistry B, The Panum Institute, Blegdamsvej 3c, DK-2200 Copenhagen N, Denmark, and Chemical Laboratory II, The H. C. Ørsted Institute, Universitetsparken 5, DK-2100 Copenhagen Ø, Denmark. Received December 13, 1990

A series of reagents containing 3- or 4-nitrobenzamido ligands tethered to 9-aminoacridine via variable-length linkers have been prepared and their properties as photochemical DNA cleavers (photonucleases) examined. When irradiated with ~300-nm light, where the nitrobenzamido ligand can absorb, they cleave DNA in an oxygen-independent reaction presumably involving oxygen transfer from the nitro group to the deoxyribose units of the DNA backbone (Nielsen et al., 1988b). This reaction is pH independent and only slightly affected by the linker length, and the DNA fragments are not substrates for DNA polymerase. When ~420-nm light is used, were only the 9-aminoacridinyl ligands absorb, the DNA cleavage is also oxygen-independent but pH dependent, requires DNA saturation with the reagent (base pair:reagent ≤ 2), and is most efficient with the longer linkers. The cleavage is specific for guanine residues and results in 5′-phosphate termini and heterogeneous (more than four products) 3′-termini. One of the products is presumably 3′-hydroxy since DNA photocleaved with nitrobenzamido acridine reagents and 420-nm radiation are substrates for DNA polymerase in a nick translation assay as well as for the Klenow fragment. An electron-transfer mechanism is suggested.

INTRODUCTION

Synthetic DNA cleaving reagents ("synthetic nucleases") (Sigman, 1990) are of interest in molecular biology and medicinal chemistry for designing DNA-cleaving molecules directed at specific sequences (see, e.g., Dervan, 1986; Moser & Dervan, 1987; Chi-hong & Sigman, 1986; Chen & Sigman, 1988; Le Doan et al., 1987; Praseuth et al., 1988a,b) and as molecular probes (for a recent review on DNA probes, see Nielsen, 1990). In most cases the cleaving principle involves oxidation of the DNA (RNA) backbone deoxyriboses by transition-metal complexes (e.g., Fe(II), Cu(I), Ru(II), etc.) (Hertzberg & Dervan, 1984; Tullius & Dombroski, 1985; Sigman, 1986; Barton, 1986; Stubbe & Kozarich, 1987; Goyne & Sigman, 1987; Tullius, 1989). In some cases photochemical activation of the cleavage reaction has also been exploited (see, e.g., Freifelder et al., 1961; Friedman & Brown, 1978; Subramanian & Meares, 1985, 1986; Fleisher et al., 1986; Blacker et al., 1986; Ward et al., 1986; Buchardt et al., 1987; Nielsen et al., 1988a–c; Jeppesen et al., 1988; Behr, 1989; Veal & Kill, 1988; Jeppesen & Nielsen, 1989a,b; Uchida et al., 1989).

From a biological point of view, cleavage mechanisms which result in products that can be processed directly by conventional DNA-metabolizing enzymes would be advantageous, and metal-activated hydrolytic cleavage of DNA has been reported with Zn(II)), Cd(II), and Pb(II) complexes of trisphenanthroline derivatives (Basile et al., 1987). Thus the development of more efficient DNA-cleaving ligands is warranted and preferably with a catalytic cleavage mechanism.

We have recently found that nitrobenzamido ligands linked to 9-aminoacridine photocleave DNA (Buchardt et al., 1987; Nielsen et al., 1988b) presumably via a hydrogen-abstraction/oxygen-transfer mechanism. We also found that 4-nitrobenzamido derivatives are 10–30 times as efficient as the corresponding 2- or 3-substituted reagents, and that the reaction is induced by light absorbed by the nitrobenzimido chromophore (Nielsen et al., 1988b). Furthermore, it was recently shown that nitrooligopyrroles (distamycin analogues) photocleave DNA (Nishiwaki et al., 1990).

We now report that a different DNA photocleavage mechanism is in operation for the nitrobenzamido acridine reagents with light absorbed by the aminoacridine chromophore, and that one or more of the DNA products are substrates for *Escherichia coli* DNA polymerase. A mechanism involving electron transfer between the acridine and the nitrobenzamido ligands is suggested.

EXPERIMENTAL PROCEDURES

Chemistry. General Remarks.[1] All solvents used for chromatography were distilled prior to use. NMR spectra were recorded on a JEOL FX 90Q spectrometer. Mass spectrometry was performed on a MassLab VG 12-250 quadrupole instrument fitted with a VG FAB source and probe. Melting points were determined on a Büchi melting point apparatus and are uncorrected.

Methyl 6-aminohexanoate hydrochloride was prepared according to the procedure given by Garmaise et al. (1958).

† The Panum Institute.
‡ The H. C. Ørsted Institute.

[1] Abbreviations: BSA, bovine serum albumin; DMF, dimethylformamide; DMSO, dimethyl sulfoxide; DTT, dithiothreitol; HMPA, hexamethylphosphorotriamide; THF, tetrahydrofuran; Boc, *tert*-butoxycarbonyl; DhbtOH, 3,4-dihydro-3-hydroxy-4-oxo-1,2,3-benzotriazine; DCC, dicyclohexylcarbodiimide; SDS, sodium dodecyl sulfate; NMR, nuclear magnetic resonance; s, singlet; d, doublet; dd, doublet of doublets; t, triplet; q, quartet; m, multiplet; b, broad; δ, chemical shift.

1043-1802/91/2902-0057$02.50/0 © 1991 American Chemical Society

Table I. Data for Boc-NH$(CH_2)_n$NH$_2$·HCl

n	formula	% found (% calcd) C	H	N	Cl	recrystallized from	mp, °C
3	$C_8H_{19}N_2O_2Cl$	45.44 (45.60)	9.21 (9.09)	13.40 (13.30)	16.98 (16.83)	EtOAc/absolute EtOH 4:1	153–154.5
5	$C_{10}H_{23}N_2O_2Cl$	49.93 (50.30)	9.75 (9.71)	11.69 (11.73)	14.23 (14.85)	EtOAc	110–111
7	$C_{12}H_{27}N_2O_2Cl$	53.40 (54.02)	10.30 (10.20)	10.54 (10.50)	13.80 (13.29)	EtOAc/absolute EtOH 4:1, precipitated with *n*-hexane	124–125

6-Benzamidohexanoic acid was prepared according to the method of Eck and Marvel (1959), starting from 6-aminohexanoic acid.

Mono-Boc-diamine hydrochlorides (Boc-NH-$(CH_2)_n$NH$_2$·HCl) were all prepared analogous to mono-Boc-hexanediamine hydrochloride (Hansen et al., 1982); compounds with n = 3, 5, and 7 have not been prepared earlier, and their data are outlined in Table I.

The reaction is easily followed by TLC. The eluent should be 2-propanol/concentrated ammonia/water in the ratio 6:3:1. After elution the TLC plate is dried at 120 °C for 5 min and subsequently sprayed with a 0.2% ninhydrin solution in ethanol. After heating to 120 °C for 5 min, both unprotected, mono-Boc- and di-Boc-diamine are visualized.

1,5-Bis(Boc-amino)-3-azapentane Hydrochloride. 1,5-Bis(Boc-amino)-3-azapentane hydrochloride was prepared analogously to 1,7-bis(Boc-amino)-4-azaheptane hydrochloride (Hansen et al., 1982). It was recrystallized from ethyl acetate/absolute ethanol (4:1). Mp: 183.5–184.5 °C. ^{1}H NMR (D_2O): δ 3.40–3.17 ppm (m, 8 H), 1.42 (s, 18 H). Anal. Calcd for $C_{14}H_{30}N_3O_4Cl$: C, 49.47; H, 8.90; N, 12.37; Cl, 10.43. Found: C, 49.48; H, 8.92; N, 12.40; Cl, 10.57.

3-Methoxy-5-nitrobenzoic Acid. We have modified the procedure of Herlt et al. (1981). To a solution of 3,5-dinitrobenzoic acid (7.0 g, 30 mmol) in HMPA (160 mL) was added lithium methoxide (Talalaeva et al., 1964) (5.0 g, 30 mmol) with stirring. The mixture was heated to 90 °C for 4 h. The dark solution was cooled to room temperature and poured into a mixture of ice water (1500 mL) and concentrated sulfuric acid (120 mL). The resulting precipitate was collected by filtration and dissolved in 40% sodium hydroxide and water (250 mL), treated with activated carbon (1 g), and filtered. The filtrate was extracted with methylene chloride (2 × 100 mL) and subsequently acidified by addition of concentrated hydrochloric acid (100 mL). The product was isolated by filtration and dried. Yield: 4.5 g (69%). Mp: 188–190 °C (lit. mp 189–191 °C). ^{1}H NMR ($CDCl_3$): δ 8.2 ppm (m, 1 H), 7.9 (m, 1 H), 7.8 (m, 1 H), 3.9 (s, 3 H).

3-Hydroxy-5-nitrobenzoic acid was obtained from 3-methoxy-5-nitrobenzoic acid by the procedure given by Herlt et al. (1981).

***N*-Succinimidyl 3-Hydroxy-5-nitrobenzoate (Ie).** 3-Hydroxy-5-nitrobenzoic acid (1.0 g, 5.5 mmol) and *N*-hydroxysuccinimide (0.63 g, 5.5 mmol) were dissolved in dry tetrahydrofuran, cooled to −10 °C, and added to a solution of dicyclohexylcarbodiimide (1.24 g, 6.0 mmol) in dry tetrahydrofuran. The temperature of the reaction mixture was kept at −10 °C for 4 h, and subsequently at 4 °C overnight. The precipitated dicyclohexylurea was filtered off and the filtrate was evaporated to dryness, in vacuo. The product was dissolved in a minimum of boiling ethyl acetate and cooled to 0 °C, and the precipitated dicyclohexylurea was filtered off. The filtrate was evaporated; the resulting crystalline material was washed with boiling chloroform (50 mL) and recrystallized from ethyl acetate/hexane. Yield: 1.04 g (68%). Mp: 207–209 °C. ^{1}H NMR (DMSO-d_6) δ 9.88 ppm (b s, 1 H, OH), 8.36–8.33 (m, 1 H, H-6), 8.06–7.90 (m, 2 H), 2.99 (s, 4 H). Anal. Calcd for $C_{11}H_8N_2O_7$: C, 47.15; H, 2.88; N, 10.00. Found: C, 47.12; H, 2.96; N, 9.84.

***N*-Succinimidyl 3-methoxy-5-nitrobenzoate** was prepared analogously to Ie. The product was recrystallized from 2-propanol. Mp: 140–141 °C. ^{1}H NMR ($CDCl_3$): δ 8.5 ppm (m, 1 H), 7.9 (m, 2 H), 4.0 (m, 3 H), 2.9 (s, 4 H). Anal. Calcd for $C_{10}H_{10}N_2O_7$: C, 48.98; H, 3.43; N, 9.52. Found: C, 49.10; H, 3.34; N, 9.69.

Compounds IIa, IIc, IId, and IIg. The mono-Boc-diamine hydrochloride (1 equiv) was dissolved in water. Ethyl acetate and four equiv of sodium hydrogen carbonate were added. The appropriate acid chloride (1.2 equiv) was added slowly with stirring, which was continued overnight. The organic layer was isolated and washed once with a 5% sodium hydrogen carbonate solution and twice with water, dried over magnesium sulfate, and evaporated to dryness, in vacuo. The residue was recrystallized from either ethyl acetate or toluene. Yields were typically 75–85%. The identity of the products was established by elemental analysis and IR and ^{1}H NMR spectroscopy.

Compounds IIe. One equivalent of *N*-succinimidyl 3-hydroxy-5-nitrobenzoate was dissolved in dry tetrahydrofuran. The mono-Boc-diamine (1.1 equiv) was added, and after 1 h the solution was evaporated to dryness, in vacuo. The product was purified by chromatography on a silica gel column with chloroform/acetone (4:1) (the products have R_f values between 0.45 and 0.55), followed by recrystallization from either toluene or ethyl acetate/hexane. Yields were typically 70–80%. The identity of the products was established by elemental analysis and IR and ^{1}H NMR spectroscopy.

Compounds IIf. One equivalent of *N*-succinimidyl 3-methoxy-5-nitrobenzoate was dissolved in dry tetrahydrofuran and 1 equiv of the mono-Boc-diamine was added. After 1 h the mixture was evaporated to dryness, in vacuo, subsequently dissolved in ethyl acetate, and washed twice with 5% sodium hydrogen carbonate and once with water. The ethyl acetate solution was dried over anhydrous magnesium sulfate and evaporated to dryness, in vacuo, and recrystallized from toluene. Yields were between 65 and 75%. The identity was established by elemental analysis and ^{1}H NMR and IR spectroscopy.

Compounds IIIa–g and VId. Compounds II or V were dissolved in a solution of 1 M hydrogen chloride in acetic acid, left for 30 min, and evaporated to dryness, in vacuo. The product was used without further purification. Yield: ~100%. The resulting hydrochloride was dissolved in phenol at 80 °C, 9-phenoxyacridine (1 equiv) was added, and the temperature was raised to 120 °C. After 1.5 h at this temperature the reaction mixture was cooled and treated with ether which caused crystallization of the product. The product was isolated by filtration and washed thoroughly with ether, dissolved in boiling methanol, filtered, cooled, and poured into cold ether. The precipitate was filtered off and again thoroughly washed with ether. The recrystallization from methanol/ether was repeated from two to six times. Yields were typically 55–65%. The identity of the products was established by

elemental analysis and IR, FAB-MS, and ^{1}H NMR spectroscopy.

^{1}H NMR spectra of representative examples of compounds II and III are given below. They were all recorded in DMSO-d_6 with tetramethylsilane as internal standard unless otherwise stated.

IIc8 ^{1}H NMR: δ 8.76 ppm (b t, 1 H, ArCONH), 8.32 (d, J = 8.85 Hz, 2 H, Ar H-3 and H-5), 8.06 (d, J = 8.85 Hz, 2 H, Ar H-2 and H-6), 6.76 (b t, 1 H, BocN*H*), 2.92 (m, 4 H), 1.71–1.26 (m, 17 H).

IId6 ^{1}H NMR: δ 8.84 ppm (b t, 1 H, ArCON*H*), 8.70 (t, 1 H, Ar H-2), 8.35 (m, 2 H, Ar H-4 and H-6), 7.76 (t, J = 7.94 Hz, 1 H, Ar H-5), 6.96 (b t, 1 H, BocN*H*), 3.28 (m, 2 H, ArCONHCH_2), 2.97 (m, 2 H, BocNHCH_2), 1.72–1.38 (m, 17 H).

IIe6 ^{1}H NMR: δ 10.66 ppm (b, 1 H, ArO*H*), 8.70 (b t, 1 H, ArCON*H*), 8.13 (m, 1 H, Ar H-6), 7.66 (m, 2 H, Ar H-2 and H-4), 6.71 (b t, 1 H, BocN*H*), 3.21 (m, 2 H, ArCONHCH_2), 2.89 (m, 2 H, BocNHCH_2), 1.36 (m, 17 H).

IIIc8 ^{1}H NMR: δ 8.89 ppm (b t, 1 H, ArCON*H*), 8.63 (d, J = 8.54 Hz, 2 H, Acr H-1 and H-8), 8.28 (d, J = 8.85 Hz, 2 H, Ar H-3 and H-5), 8.09–7.94 (m, 6 H), 7.60–7.46 (m, 2 H, Acr H-3 and H-6), 4.10 (t, AcrNHCH_2), 1.98 (m, 2 H, AcrNHCH$_2$CH_2), 1.61 (m, 6 H). The missing ArCONHCH_2 signal is hidden under a huge water peak from 3.73 to 3.01 ppm.

IIId6 ^{1}H NMR: δ 9.3 ppm (b t, 1 H, ArCON*H*), 8.64–8.50 (m, 3 H, Ar H-2 and Acr H-1 and H-8), 8.42–8.22 (m, 2 H, Ar H-4 and H-6), 7.95–7.46 (m, 7 H), 4.14 (t, 2 H, AcrNHCH_2), 1.99–1.65 (m, 8 H). The missing ArCONHCH_2 signal is hidden under a huge water peak from 3.63 to 3.01 ppm.

IIIe6 ^{1}H NMR: δ 8.56 ppm (d, J = 8.54 Hz, 2 H, Acr H-1 and H-8), 8.10 (m, 1 H, Ar H-6), 7.9 (m, 4 H, Acr H-2, H-4, H-5, and H-7), 7.70–7.34 (m, 4 H), 4.11 (m, 2 H, AcrNHCH_2), 3.35 (m, 2 H, ArCONHCH_2), 1.93 (m, 2 H, AcrNHCH$_2$CH_2), 1.65 (m, 6 H).

IIIf6 ^{1}H NMR: δ 8.79 ppm (b t, 1 H, ArCON*H*), 8.54 (d, J = 8.54 Hz, 2 H), 8.24 (s, 1 H, Ar H-6), 7.99–7.82 (m, 6 H), 7.62–7.44 (m, 2 H, Acr H-3 and H-6), 3.91 (s, 3 H, CH_3O), 1.90 (m, 2 H, AcrNHCH$_2$CH_2), 1.43 (m, 6 H). The missing ArCONHCH_2 signal is hidden under a huge water peak from 3.63 to 3.01 ppm.

VId ^{1}H NMR: δ 9.00–8.26 ppm (m, 8 H), 8.02–7.26 (m, 13 H), 4.64–3.68 (m, 8 H), 3.20 (m, 2 H, ArCONHCH_2), 2.37 (m, 2 H, –CH_2CO–), 1.3 m (m, 6 H).

6-Benzamidohexanoic Acid Dhbt Ester. To a cold (–10 °C) solution of 6-benzamidohexanoic acid (IVa, 6.0 g, 25 mmol) in methylene chloride (100 mL) was added DCC (5.2 g, 25 mmol) and the solution was stirred at –10 °C for 30 min after which 3,4-dihydro-3-hydroxy-4-oxo-1,2,3-benzotriazine (4.2 g, 25 mmol) was added with continuous stirring for 6 h at –10 °C. The precipitated dicyclohexylurea was removed by filtration and the filtrate was evaporated to dryness, in vacuo. The residue was dissolved in methylene chloride (100 mL) and filtered, and the ester was precipitated by addition of pentane (100 mL). Yield: 5.5 g (57%). Mp: 128–130 °C. ^{1}H NMR ($CDCl_3$): δ 8.32–7.23 ppm (m, 9 H), 6.95 (b, 1 H), 3.44 (t, 2 H), 2.74 (t, 2 H), 1.94–1.60 (m, 6 H). ^{13}C NMR ($CDCl_3$): δ 169.4 ppm, 167.7, 150.4, 144.3, 135.5, 134.8, 132.8, 131.2, 129.0, 128.4, 127, 125.6, 122.1, 39.6, 31.2, 28.9, 25.9, 23.3. Anal. Calcd for $C_{20}H_{20}N_4O_4$: C, 63.07; H, 5.41; N, 14.82. Found: C, 63.15; H, 5.30; N, 14.37.

Methyl 6-(3-Methoxy-5-nitrobenzamido)hexanoate. To a solution of *N*-succinimidyl 3-methoxy-5-nitrobenzoate (9.0 g, 35 mmol) and methyl 6-aminohexanoate hydrochloride (6.3 g, 35 mmol) in methylene chloride (225 mL) was added triethylamine (5 mL, 68.1 mmol). The solution was stirred overnight and extracted with 6 *N* hydrochloric acid (2 × 75 mL) followed by 10% aqueous sodium hydrogen carbonate (4 × 75 mL). The organic phase was dried over sodium sulfate and evaporated to dryness, in vacuo. The residue was recrystallized from methanol/water. Yield: 5.9 g (57%). Mp: 82–83 °C. ^{1}H NMR ($CDCl_3$): δ 8.16 ppm (m, 1 H), 7.80 (m, 2 H), 6.95 (b, NH), 3.92 (s, 3 H), 3.53 (s, 3 H), 2.34 (m, 2 H), 1.59 (m, 6 H). ^{13}C NMR ($CDCl_3$): 174.2 ppm, 165.4, 160.2, 149.0, 137.3, 119.7, 114.0, 110.8, 56.1, 51.5, 40.2, 33.8, 29.0, 26.5, 24.5. Anal. Calcd for $C_{15}H_{20}N_2O_6$: C, 55.62; H, 6.27; N, 8.71. Found: C, 55.44; H, 6.22; N, 8.64.

6-(3-Methoxy-5-nitrobenzamido)hexanoic Acid (IVf). Aqueous sodium hydroxide (10 mL, 2 M, 20 mmol) was added to a solution of methyl 6-(3-methoxy-5-nitrobenzamido)hexanoate (5.0 g, 15 mmol) in methanol (100 mL). The solutiion was refluxed for 5 h and evaporated to dryness, in vacuo. The residue was dissolved in water and acidified with concentrated hydrochloric acid. The precipitated acid was filtered off and recrystallized from chloroform. Yield: 3.8 g (80%). Mp: 112–113 °C. Anal. Calcd for $C_{14}H_{18}N_2O_6$: C, 54.00; H, 5.90; N, 9.16. Found: C, 54.19; H, 5.85; N, 9.03.

6-(3-Methoxy-5-nitrobenzamido)hexanoic Acid Dhbt Ester. The ester was prepared analogously to that described for 6-benzamidohexanoic acid Dhbt ester. Yield: 38%. ^{1}H NMR ($CDCl_3$): δ 8.30–7.74 ppm (m, 7 H), 6.95 (b, NH), 3.88 (s, 3 H), 3.75 (m, 2 H), 2.82 (m, 2 H), 1.78 (m, 6 H).

6-(3-Nitrobenzamido)hexanoic Acid (IVd). 6-Aminohexanoic acid (5.00 g, 38.1 mmol) and triethylamine (1.14 mL, 2.2 equiv) were mixed with dioxane (100 mL), and water was added until a clear solution resulted. The solution was cooled to 0 °C, and 3-nitrobenzoyl chloride (7.07 g, 38.1 mmol) dissolved in dry dioxane (30 mL) was added dropwise. The solution was stirred overnight. The reaction mixture was brought to pH 1 with 4 M HCl, and water (300 mL) was added to precipitate the product, which was filtered off and washed thoroughly with water. Drying gave 6.4 g (60%). Mp: 115–118 °C. ^{1}H NMR (DMSO-d_6): δ 8.83 ppm (b t, 1 H, N*H*), 8.69 (t, 1 H, Ar H-2), 8.44–8.25 (m, 3 H, Ar H-2, H-4 and H-6), 7.77 (t, J = 7.94 Hz, 1 H, Ar H-5), 3.34–3.20 (m, 2 H, ArCONHCH_2), 2.31–2.16 (m, 2 H, CH_2CO$_2$H), 1.72–1.28 (m, 6 H). Anal. Calcd for $C_{13}H_{16}N_2O_5 \cdot {}^1/_4H_2O$: C, 54.82; H, 5.83; N, 9.83. Found: C, 55.08; H, 5.83; N, 9.84.

6-(3-Nitrobenzamido)hexanoyl Chloride. 6-(3-Nitrobenzamido)hexanoic acid (1.0 g, 3.63 mmol) was dissolved in thionyl chloride (5 mL) and stirred for 4 h under nitrogen at room temperature, evaporated to dryness, in vacuo, and used without further purification.

1,5-Bis(Boc-amino)-3-[6-(3-nitrobenzamido)hexanoyl]-3-azapentane (Vd). The acid chloride from above was dissolved in dry ethyl acetate. The resulting solution was filtered and added dropwise to a stirred mixture of 1,5-bis(Boc-amino)-3-azapentane hydrochloride (0.8 g, 2.35 mmol), sodium hydrogen carbonate (1.18 g, 14.0 mmol) in water (50 mL), and ethyl acetate (100 mL). The reaction mixture was stirred overnight. The organic layer was washed once with 5% sodium hydrogen carbonate solution and twice with water, dried, and evaporated to dryness, in vacuo. A pure sample was obtained by column chromatography (silica gel 60). The target compound was eluted with methylene chloride/acetone (1:1) (R_f = 0.75). Only the fractions containing the product as the only constituent were collected. Evaporation of the collected fractions gave 850 mg (43%) of an oily substance. When

dissolved in diethyl ether and evaporated to dryness, in vacuo, it became a very voluminous powder. Mp: 50–54 °C. ^{1}H NMR (DMSO-d_6): δ 8.81 ppm (b t, 1 H, ArCONH), 8.67 (t, 1 H, Ar H-2), 8.43–8.25 (m, 2 H, Ar H-4 and H-6), 7.7 m (t, J = 7.94 Hz, 1 H, Ar H-5), 6.9 (b t, 1 H, BocNH), 6.75 (b t, 1 H, BocNH), 3.31 (s, 8 H), 3.04 (m, 2 H, ArCONHCH$_2$), 2.27 (m, 2), 1.79–1.09 (m, 24 H). Anal. Calcd for $C_{27}H_{43}N_5O_8$: C, 57.33; H, 7.66; N, 12.38. Found: C, 56.54; H, 7.77; N, 12.13.

1,5-Bis(Boc-amino)-3-(6-benzamidohexanoyl)-3-azapentane (Va). A solution of 1,5-bis(Boc-amino)-3-azapentane (398 mg, 1.31 mmol) in DMF (5 mL) was mixed with a solution of 6-benzamidohexanoic acid Dhbt ester (500 mg, 1.31 mmol) in DMF (5 mL). After 3 days at room temperature the DMF was removed in vacuo (the temperature of the water bath did not exceed 40 °C). The residue was taken up in a mixture of water (25 mL) and diethyl ether (100 mL). The ether phase was washed with saturated sodium hydrogen carbonate (3 × 25 mL), dried, and evaporated to dryness, in vacuo. Yield: 590 mg (87%). ^{1}H NMR ($CDCl_3$): δ 7.86–7.39 ppm (m, 5 H), 6.92 (b, ArCONH), 5.48 (b, BocNH), 5.15 (b, BocNH), 3.49–3.22 (m, 10 H), 2.68 (t, 2 H), 1.67–1.42 (m, 24 H). FAB-MS: 521 (MH), 421 (MH – Boc), 321 (MH – 2 Boc). Anal. Calcd for $C_{26}H_{44}N_4O_6$: C, 59.57; H, 8.00; N, 10.42. Found: C, 61.39; H, 8.72; N, 11.10.

1,5-Bis(Boc-amino)-3-[6-(3-methoxy-5-nitrobenzamido)hexanoyl]-3-azapentane (Vf). The title compound was prepared analogously to the method described for 1,5-bis(Boc-amino)-3-(6-benzamidohexanoyl)-3-azapentane (Va). Yield: ~100%. ^{1}H NMR ($CDCl_3$): δ 8.29–7.77 ppm (m, 3 H), 5.65 (b, Boc-NH), 5.38 (b, Boc-NH), 3.91 (d, 3 H), 3.44–3.05 (m, 1 H), 2.35 (m, 2 H), 1.90–0.99 (m, 24 H).

3-(6-Benzamidohexanoyl)-1,5-bis(9-acridinylamino)-3-azapentane Dihydrochloride 3.5-Hydrate (VIa). 1,5-Bis(Boc-amino)-3-[6-(3-methoxy-5-nitrobenzamido)hexanoyl]-3-azapentane (590 mg, 1.13 mmol) was added to a 1 N solution of hydrogen chloride in glacial acetic acid (25 mL). The resulting solution was stirred for 30 min and evaporated to dryness, in vacuo. Phenol (12 g) and 9-phenoxyacridine (1.2 g, 4.4 mmol) were added, and the mixture was heated to 120 °C for 2 h with stirring. The resulting dark solution was cooled to ca. 40 °C, poured on 2 N sodium hydroxide (100 mL), and extracted with chloroform (3 × 100 mL). The combined chloroform extract was washed with water (5 × 100 mL), dried over magnesium sulfate, and concentrated, in vacuo. The title compound was isolated from the residue by chromatography on silica, first eluting with 5% triethylamine in diethyl ether followed by methanol. The methanolic solution was evaporated to dryness and redissolved in diethyl ether, whereafter the title compound precipitated by the addition of hydrogen chloride (as an ethereal solution). The precipitate was dried overnight at 50 °C over phosphorus pentoxide, in vacuo. Yield: 620 mg (73%). ^{1}H NMR (DMSO-d_6): δ 10.19 ppm (m, 4 H), 8.72–8.04 (m, 4 H), 7.95–7.40 (m, 17 H), 4.28–3.84 (m, 8 H), 3.23 (m, 2 H), 2.47 (m, 2 H), 1.37 (m, 6 H). FAB-MS: 675 (M + 1). Anal. Calcd for $C_{43}H_{44}N_5Cl_2O_2 \cdot 2.25H_2O$: C, 65.28; H, 6.40; N, 10.67; Cl, 8.60. Found: C, 65.52; H, 6.20; N, 10.66; Cl, 8.99.

3-[6-(3-Methoxy-5-nitrobenzamido)hexanoyl]-1,5-bis(9-acridinylamino)-3-azapentane Dihydrochloride 3.5-Hydrate (VIf). The title compound was prepared according to the protocol for 3-(6-benzamidohexanoyl)-1,5-bis(9-acridinylamino)-3-azapentane dihydrochloride 3.5-hydrate. Yield: 56%. ^{1}H NMR (DMSO-d_6): δ 10.27 ppm (m, 4 H), 8.65–7.42 (m, 19 H), 4.82–2.89 (m, 13 H), 2.51 (m, 2 H), 1.33 (m, 6 H). FAB-MS: 750 (M + 1). Anal. Calcd for $C_{44}H_{45}N_7Cl_2O_5 \cdot 3.5H_2O$: C, 60.52; H, 6.35; N, 11.07; Cl, 8.48. Found: C, 59.66; H, 5.92; N, 11.07; Cl, 8.00.

Photocleavage. Irradiations were performed with Philips fluorescent light tubes with emission peaks (20–30-nm band widths) at 300 (TL 20W/12), 365 (TL 20W/09 N), or 420 nm (TL 40 W/03). The samples were contained in open Eppendorf tubes and irradiated from above at a distance of 20 cm from the lamp. The light intensity at this distance was 20 J·m^{-2}·s^{-1} measured by actinometry.

Plasmid Relaxation. Supercoiled plasmid DNA (0.5 μg; pUC 19) dissolved in 10 μL of 10 mM sodium phosphate buffer with the warranted pH was used for each assay. The desired amount of reagent dissolved in 1 μL of DMSO was added and the sample was irradiated. The DNA was subsequently analyzed by electrophoresis in 1% agarose in TBE buffer (90 mM Tris borate, 1 mM EDTA, pH 8.3). The gel was stained with ethidium bromide, photographed, and the amount of supercoiled, relaxed, and linear plasmid DNA determined by densitometric scanning (Shimadzu CS 930 scanner).

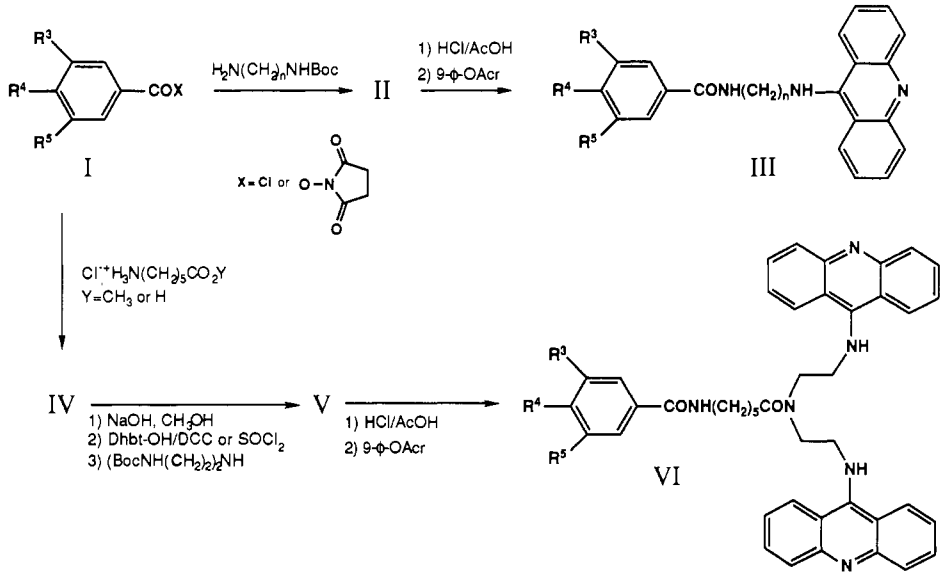
DNA Polymerase, DNA Ligase, and Polynucleotide Kinase Reactions. Plasmid DNA to be used as DNA polymerase or DNA ligase substrates was photonicked as described above and subsequently purified by extraction with phenol (in 0.5% SDS, 0.1 M sodium acetate, pH 8) and precipitation with 66% ethanol. A typical DNA polymerase reaction mixture contained 0.5 μg DNA, 0.1 mM dCTP, 0.1 mM dGTP, 0.1 mM dTTP, 0.1 μCi [α-^{32}P]dATP, and 0.1 unit of DNA polymerase (either the Kornberg holoenzyme or the Klenow fragment (Gibco-BRL)) in 20 μL of buffer (50 mM Tris-HCl, pH 7.2, 10 mM MgCl, 0.1 mM DTT, 50 μg/mL BSA). The mixture was incubated at 16 °C for 30 min, precipitated with ethanol, redissolved in TBE buffer, and analyzed by electrophoresis in a 1% agarose gel TBE buffer which was subsequently stained with ethidium bromide, dried, and subjected to autoradiography.

The ligation mixture contained 0.5 μg of DNA, 1 mM ATP, and 1 unit of T_4-DNA ligase (Gibco-BRL) in 5 μL of buffer (50 mM Tris-HCl, pH 7.4, 10 mM $MgCl_2$, 0.1 mM DTT, 1 mM spermidine, 100 μg/mL BSA). After incubation at 37 °C for 60 min, 1 μL of 5 × application buffer (50% glycerol, 5 × TBE, 5 μg/mL ethidium bromide) was added, and the sample was analyzed by electrophoresis in a 1% agarose gel in TBE buffer containing 0.5 μg/mL ethidium bromide.

The 5′-^{32}P-exchange reaction mixture contained 0.5 μg of DNA in 40 μL of buffer (10 mM $MgCl_2$, 5 mM DTT, 0.1 mM spermidine, 0.1 mM EDTA, 50 mM imidazole hydrochloride, pH 6.5). After heating to 100 °C (5 min) and cooling in ice ADP (to a final concentration of 1 mM), 0.1 μCi [^{32}P]ATP and 0.1 unit of T_4 polynucleotide kinase (Gibco-BRL) was added. The sample was incubated at 37 °C for 30 min, 1 vol 20 × SSC (1.5 M NaCl, 0.15 M sodium citrate, pH 7) was added, and the sample was dot blotted onto nitrocellulose which was washed in 2 × SSC and subjected to autoradiography.

Photocleavage of ^{32}P-End-Labeled DNA. The mixture for this reaction contained 0.5 μg of calf thymus DNA, 500 cps of the small (90 bp) *Eco*RI/*Pvu*II fragment of pUC 19 (labeled either at the 3′- or 5′-end at the EcoRI site) in 10 μL of buffer. The desired amount of reagent dissolved in 1 μL of DMSO was added and the mixiture was irradiated. Following addition of 90 μL of H_2O, the DNA was precipitated with 250 μL of ethanol, 0.2 M

Scheme I



No.	X	n	R^3	R^4	R^5
a	Cl	6	H	H	H
b	NHS	6	OH	H	H
c	Cl	6	H	NO_2	H
d	Cl	4,6,8	NO_2	H	H
e	NHS	3-8	NO_2	H	OH
f	NHS	4,6,8	NO_2	H	OMe
g	Cl	6	NO_2	H	NO_2

potassium acetate, taken up in 4 μL of 80% formamide loading buffer, and analyzed on a 10% polyacrylamide/7 M urea sequencing gel run in TBE buffer.

RESULTS

The reagents were prepared as shown in Scheme I and are summarized in Table II, which also summarizes the cleaving results. Originally, we attempted to exploit the strong acidity of the excited state of nitrophenols (Martynov et al., 1977) as a means for photohydrolytic cleavage of DNA by attaching a 3-hydroxy-5-nitrobenzamido ligand to the DNA intercalator 9-aminoacridine (Table II, reagents IIIe3–e8). The acridinyl moiety should assure high affinity for DNA while the presence of the nitro group shifts the ultraviolet absorption of the phenol 86 nm toward the visible.[2] As contemplated, these compounds do photocleave DNA (Table II). It soon became clear, however, that our presumptive cleavage mechanism was incorrect, since the DNA cleavage activity (using 300-nm radiation) was hardly influenced by the exchange of the hydroxy group for a methoxy group or by removing it altogether (Table II, reagents IIIf4–f8 and IIId4–d8). The nitro group turned out to be the crucial moiety for DNA photocleavage, and subsequent experiments showed that 4-nitrobenzamido ligands resulted in the most efficient DNA photocleaving reagents (Nielsen et al., 1988b).

DNA Nicking/Plasmid Relaxation. Although the 3-nitrobenzamido derivatives are rather poor DNA cleaving reagents (~30 times less efficient than the 4-nitro analogues when irradiated at 300 nm), their DNA-cleaving properties encouraged us to pursue the matter. The DNA photocleavage by the 5-methoxy- (and 5-hydroxy-) 3-nitrobenzoylamine derivatives is most efficient at wavelengths corresponding to absorption by the acridine ligand ($\lambda \approx 420$ nm, Figure 1), in contrast to the 4-nitro derivatives, which show highest efficiency at shorter wavelengths corresponding to absorption by the nitrobenzamido moiety (Nielsen et al., 1988b). Furthermore, the photocleavage is most efficient at low pH (Figure 2), and the cleavage efficiency is also distinctly influenced by the distance between the nitrobenzamido and the acridine moieties. Longer linkers result in the most efficient reagents (Table II, reagents IIIe3–e8 and IIIf4–f8). Finally, it was found that a threshold concentration of the reagent is required to observe DNA cleavage (Figure 4), and this concentration corresponds to intercalation saturation of the DNA with the reagent.

Nick Translation. Since we initially expected hydrolytic cleavage, we tested the photocleaved DNA molecules for their activity as substrates for *E. coli* DNA polymerase in a nick translation assay using the holoenzyme, or in a 3′-labeling assay using the Klenow fragment. These results (Figure 3) show that plasmid DNA nicked by nitrobenzamido acridine derivatives and 300-nm ra-

[2] Compared by recording the spectra of IIIb6, IIIe6, and IIId6 in ethanolic solution. The 3-hydroxy derivative (IIIb6) shows a peak at 216 nm with a shoulder at 246 nm, while the 3-hydroxy-5-nitro derivative (IIIe6) shows approximately the same spectrum but with an additional peak at 332 nm (ϵ = 2750 M^{-1}). The 3-nitro derivative (IIId6) again shows a spectrum similar to that of IIIe6 but with the n,π^* transition giving rise to absorption at 292 nm.

Table II. DNA Photonicking Activity of (Nitrobenzoyl)amino Reagents

reagent	R^3	R^4	R^5	linker (n)	relative photonicking activity[b] 420[c]	365[c]	300[d]
IIId4	NO_2	H	H	4	15	50	3
IIId6	NO_2	H	H	6	15	50	3
IIId8	NO_2	H	H	8	52	50	3
IIIe3	NO_2	H	OH	3		<5	
IIIe4	NO_2	H	OH	4	43	5	1
IIIe5	NO_2	H	OH	5		7	
IIIe6	NO_2	H	OH	6	54	10	1
IIIe7	NO_2	H	OH	7		15	
IIIe8	NO_2	H	OH	8	79	20	1
IIIf4	NO_2	H	OCH_3	4	44	25	
IIIf6	NO_2	H	OCH_3	6	60	30	
IIIf8	NO_2	H	OCH_3	8	100	100	1
IIIc4	H	NO_2	H	4	25		90
IIIc6	H	NO_2	H	6	40		100
IIIc8	H	NO_2	H	8	71		80
IIIb6	OH	H	H	6	17	<1	<0.1
IIIa6	H	H	H	6	<5	<1	<0.1
VId	NO_2	H	H	6	50		3

[a] The code is made of three parts: the Roman numeral signifies the reagent type, the letter the substitution of the benzoylamino ligand, and the Arabic numeral the length of the polymethylene linker. [b] Photonicking activity relative to reagent IIIf8 (420 and 365 nm) or reagent IIIc6 (300 nm). The values at different wavelenths cannot be directly compared, but for reagent IIIf8 the relative efficiencies at the wavelengths 420 (pH 5.5), 365 (pH 7.5), and 300 nm (pH 7.5) were determined as 1:0.2:0.5. [c] pH 5.5. [d] pH 7.5.

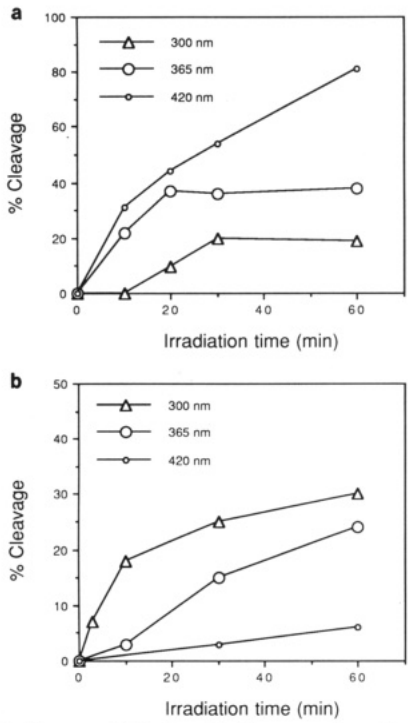


Figure 1. Influence of the irradiation wavelength of the DNA photonicking by reagents IIIf8 (A) and IIId8 (B). A: a mixture of 0.5 μg of pUC 19 DNA and 1 μg of reagent IIIf8 in 10 μL of 10 mM potassium phosphate, pH 5.5, 10% DMSO, was irradiated for the times indicated at 420 (o), 365 (O), or 300 nm (Δ). The DNA was analyzed by gel electrophoresis in 1% agarose (TBE). The gel was stained with ethidium bromide and the ratio of supercoiled versus relaxed (nicked) DNA determined by densitometric scanning (reflection in the fluorescent mode) of the photographic positive. B: a mixture of 0.5 μg of plasmid and 0.5 μg of reagent IIId8 in 10 μL of 10 mM Tris-HCl pH 7.4, 10% DMSO was irradiated and analyzed as above.

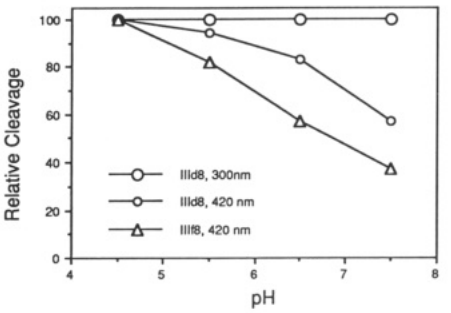


Figure 2. Influence of pH on the photonicking of DNA by reagents IIId8 and IIIf8. A mixture of 0.5 μg of pUC 19 DNA and 0.5 μg of reagent IIId8 (o, O) or IIIf8 (Δ) in 10 μL of 10 mM potassium phosphate of the indicated pH, 10% DMSO, was irradiated for 30 min at 300 (O) or 420 nm (o, Δ) and the DNA nicking analyzed as described in the legend to Figure 1.

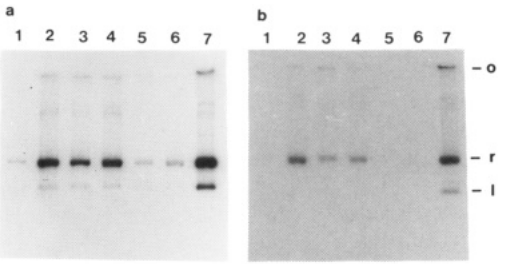


Figure 3. DNA polymerase substrate assay of photonicked plasmid DNA. pUC 19 DNA was nicked with reagents IIId8, IIIf8, or IIIc8 or with DNase I to ~80% relaxed plasmid and used as substrate for DNA polymerase (a, holoenzyme; b, Klenow fragment) as described in the Experimental Procedures. The conditions for DNA nicking were as follows: lane 1, nontreated control; lane 2, reagent IIIf8, 420 nm, pH 5.5; lane 3, reagent IIId8, 420 nm, pH 5.5; lane 4, reagent IIIc8, 420 nm, pH 5.5; lane 5, reagent IIId8, 300 nm, pH 7.5; lane 6, reagent IIIc8, 300 nm, pH 7.5; lane 7, DNase I. Plasmid relaxed by methylene blue and white light gave a result identical with that of lane 5, i.e., no substrate activity (o, origin; r, relaxed; l, linear).

diation is not a DNA polymerase substrate, whereas plasmid nicked by nitrobenzamido acridine derivatives and 420-nm radiation is a substrate. In particular, DNA nicking by reagent IIId8 results in nick translation substrates when the irradiation is performed with 420-nm light, whereas this is not the case when 300-nm irradiation is employed (Figure 3, lanes 4 and 6). The DNA photonicking by 3-nitrobenzamides at 300 nm is not pH dependent ($4.5 \leq pH \leq 7.5$, Figure 2) and does not exhibit the threshold concentration dependency (Figure 4).

DNA Ligation. As a rigorous test of photohydrolysis the photonicked plasmids were treated with DNA ligase and analyzed by electrophoresis in agarose containing ethidium bromide. These results (Figure 5) show that

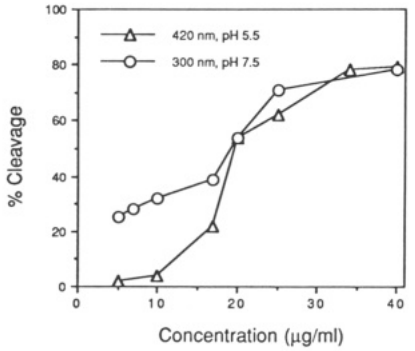


Figure 4. Influence of reagent concentration on DNA photonicking by reagent IIId8: O, 300-nm irradiation at pH 7.5: Δ, 420-nm irradiation at pH 5.5.

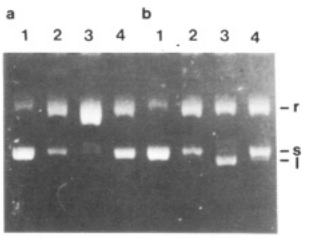


Figure 5. Religation of nicked plasmids. DNA nicked by reagent IIId6, 420 nm, pH 5.5 (lane 2); DNase I (lane 3); or reagent IIIf8, 420 nm, pH 5.5 (lane 4) or control DNA (lane 1) was incubated under ligation conditions (see the Experimental Procedures) with (lanes b) or without (lanes a) ligase and analyzed by gel electrophoresis in 1% agarose (TBE, 0.5 μg/μL ethidium bromide) (r, relaxed; s, supercoiled; l, ligated).

Table III. 5′-^{32}P Exchange of Nicked Plasmid DNA[a] by Polynucleotide Kinase

reagent used for nicking	relative ^{32}P incorporation	reagent used for nicking	relative ^{32}P incorporation
DNase I	100	IIIf8	86
IIId8	38	none	13
IIIe8	49		

[a] All photocleavage reactions were performed in 10 mM sodium phosphate buffer, pH 5.5, using 420-nm radiation, and except for the control equal amounts (±20%) of relaxed (nicked) plasmid DNA, were obtained with all four reagents.

plasmid nicked by DNase I is readily religated while plasmid photonicked by reagents IIIf8 or IIIc6 is not.

5′-^{32}P Exchange by Kinase. Treatment of photocleaved plasmid with T_4-kinase and [γ-^{32}P]ATP in the presence of ADP resulted in ^{32}P labeling of the DNA to an extent comparable to that obtained with plasmid DNA nicked by DNaseI (Table III).

Cleavage of ^{32}P-End-Labeled DNA. Photocleavage of ^{32}P-end-labeled DNA restriction fragments with some of the reagents was undertaken in order to study the sequence specificity of the reaction as well as to obtain further information of the nature of the termini of the cleavage products. Photocleavage of 3′-end-labeled DNA resulted predominantly in fragments that comigrate with those cleaved specifically at G residues by the Maxam–Gilbert sequencing protocol (Figure 6). Furthermore, quantitatively and qualitatively identical results were obtained whether the samples were treated with hot piperidine or not prior to to gel electrophoretic analysis. These results confirm the plasmid-relaxation results with respect to the increased photocleavage activity at lower pH (lanes 4 and 7) and the importance of the nitro group (Figure 6d). The very different photoreactions taking place as a function of wavelength are also reflected in the sequence dependence of the photocleavage. The DNA photocleavage by IIIc8 and 300-nm radiation show the complex

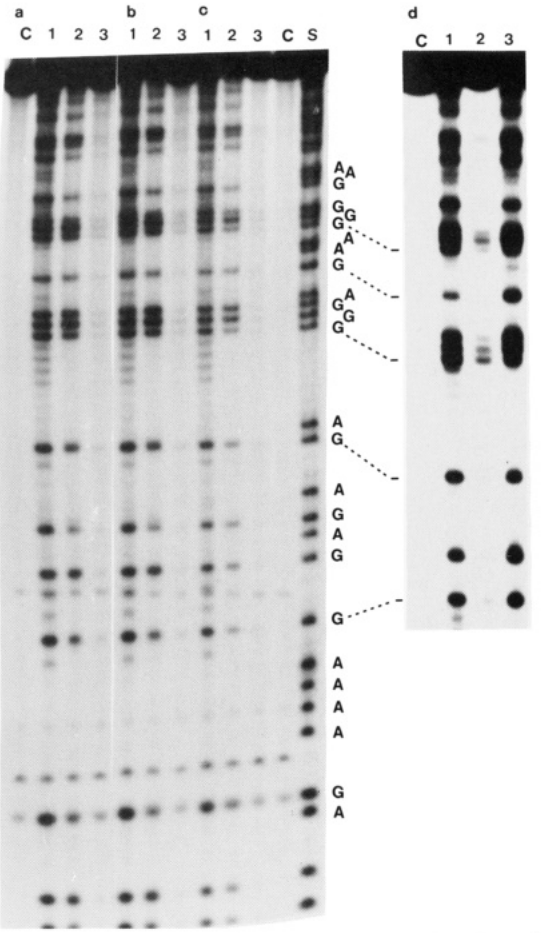


Figure 6. Sequence specificity (5′-termini) of the photocleavage of DNA. The small *Eco*RI/*Pvu*II fragment (90 bp) of pUC19 (3′-^{32}P end labeled at the 3′ *Eco*RI site was photocleaved with IIIf8 (420-nm radiation) (lanes 1), methylene blue (1 mM, white light) (lanes 2), or acridine orange (1 mM, 420 nm) (lanes 3) in 10 mM NaP, pH 5.5, (a, b) or TE buffer (c). The samples of b and c were treated with piperidine prior to gel analysis. Lane S is an A + G sequence marker while lanes c are no-reagent, irradiated controls. (d) Photocleavage with IIIf8 (lane 1), IIIa6 (lane 2), or methylene blue (lane 3) (the samples were not treated with piperidine prior to gel electrophoresis) is shown.

sequence dependence (Figure 8, lane b2) reported previously (Nielsen et al., 1988b) whereas virtually complete G selectivity is observed when 420-nm radiation is employed (Figure 8, lane a2).

A 5′-end-labeled DNA fragment was used to study the cleavage products at the 3′-end. In this case (Figure 7) blurred bands resulted which were converted to distinct G-cleavage bands upon treatment of the DNA with warm piperidine. Thus multiple (at least four) products which are converted to 3′-phosphate are formed at the 3′-end of the photocleavage site.

DISCUSSION

It is clear from these observations that two different DNA photocleaving mechanisms are in operation for the nitrobenzamido 9-aminoacridine reagents.

Nitrobenzamides linked to 9-aminoacridine cleave DNA when irradiated at 300 nm (absorption by the nitrobenzamido chromophore) in an oxygen-independent reaction presumably involving hydrogen abstraction from the deoxyriboses of DNA and subsequent oxygen transfer by the nitro group as previously discussed (Buchardt et al., 1987; Nielsen et al., 1988b). This mechanism is consistent with 3-nitrobenzamido derivatives being significantly less ef-

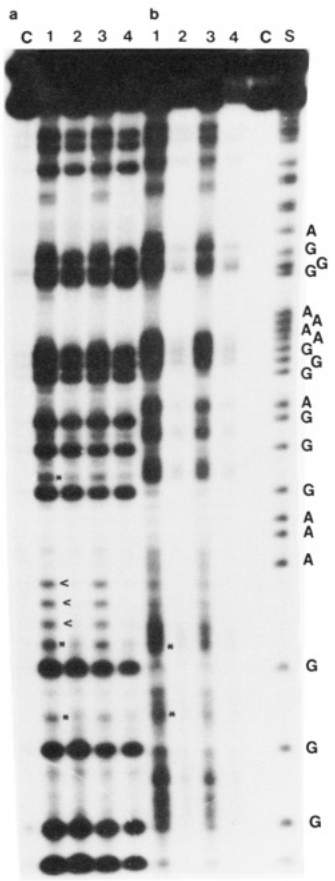


Figure 7. Sequence specificity (3′-termini) of the photocleavage of DNA. The small *Eco*RI/*Pvu*II fragment of pUC19 (5′-^{32}P end labeled at the *Eco*RI site) was photocleaved with IIIf8 (4 mM) and 420-nm radiation (lanes 1 and 3) or with methylene blue (1 mM) and white light (lanes 2 and 4) in either NaP, pH 5.5 (lanes 1 and 2), or TE buffer (lanes 3 and 4). The samples of lanes a were treated with piperidine prior to gel analysis while the samples of b were not. Lanes c are no-reagent, 420-nm-radiation controls, and lane S is an A + G sequence marker. The apparently significant increase in cleavage upon piperidine treatment of the methylene blue samples is mainly due to differences in gel loading (lanes a2,4 versus b2,4).

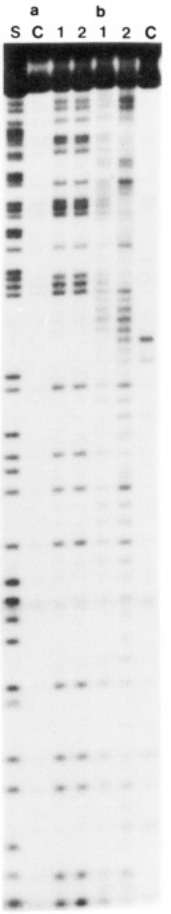


Figure 8. Influence of the wavelength on the sequence specificity of DNA photocleavage. The small *Eco*RI/*Pvu*II fragment of pUC19 (3′-^{32}P end labeled at the *Eco*RI site) was photocleaved with reagent IIIf8 (4 mM) (lanes 1) or reagent IIIc8 (4 mM) (lanes 2) with (a) 420-nm radiation in 10 mM NaP, pH 5.5, or (b) 300-nm radiation in TE buffer. C are irradiated controls without reagent, S is an A + G sequence marker, and all samples were treated with piperidine prior to gel analysis. The prominent band seen in lane bc is due to a "hot-spot" pyrimidine photoreaction (probably a 6-4 adduct) (cf. Nielsen et al., 1988b).

ficient than their corresponding 4-nitrobenzamido analogues, since it is well-known that hydrogen abstraction is less efficient with nitrobenzenes having an electron-withdrawing group in the 3-position rather than in the 4-position (Mattison et al., 1979; Döpp, 1975). This photocleavage reaction is independent of pH and only slightly influenced by the distance between the nitrobenzamido and the acridinyl moiety of the reagent. The DNA products are not substrates for DNA polymerase (or DNA ligase) and the sequence dependence is complex.

When irradiation of the nitrobenzamido acridine reagents is conducted at 420 nm, corresponding to the absorption maximum of the acridinyl moiety, the DNA photocleavage reaction is heavily dependent on pH. It only takes place when the DNA is saturated with reagent (base pair:reagent ≤ 2), and it is most efficient for reagents with long linkers between the nitrobenzamido ligand and the acridinyl moiety. Finally, at least some of the DNA cleavage products are substrates for DNA polymerase both in the case of the holoenzyme in a nick translation assay and for the Klenow fragment (Figure 3). The DNA labeling by the Klenow fragment could be due to addition of one nucleotide at the 3′-terminal if the cleavage reaction results in removal of one or more nucleotides, but is more likely a result of the 3′-editing activity of the enzyme which causes replacement of the 3′-nucleotide. These results show that *some* of the products contain a free 3′-OH group.

In order to distinguish between phosphodiester hydrolysis and other possibilities we treated the nicked plasmids with DNA ligase. These results (Figure 5) unequivocally show that DNA photocleaved by the nitrobenzamido reagents and 420 nm radiation cannot be ligated by T_4 DNA ligase. The major photocleavage is therefore not simply a phosphodiester hydrolysis. The possibility remains that the 5′-termini are hydroxyl or that one or more nucleoside/-tide units have been removed in the DNA photocleavage reaction, or that photohydrolysis only accounts for a minor fraction of the photocleavage. We estimate that less than 10% photohydrolysis cannot be detected in the ligation assay.

Experiments using polynucleotide kinase for 5′-^{32}P-phosphate exchange clearly indicate that the 5′-termini are similar to those produced by DNaseI, i.e., 5′-phosphate (Table III). This conclusion is consistent with the sequence analysis results with 3′-end-labeled DNA (Figure 6), which also show that 5′-phosphate termini are produced. The results are more ambiguous for the 3′-end of the cleavage products. Clearly multiple products are formed, but since the majority of these are converted to 3′-phosphate upon alkaline treatment, it is most likely that they are modified 3′-phosphates where oxidized deoxyribose units such as

glycolate, etc., still are attached to the phosphate. The 3′-OH products indicated to be present by the nick translation assay migrate slower than the corresponding 3′-phosphates and should be unaffected by the piperidine treatment. As can be seen from the results in Figure 7, such bands are present (marked by asterisks) in the samples from DNA photocleaved with reagent IIIf8 (lanes 1,3) but not in those from DNA photocleaved with methylene blue (lanes 2, 4). This is in accordance with the observation that plasmid DNA photocleaved with methylene blue is not a nick translation substrate for DNA polymerase (data not shown).

The experiments with DNA polymerase (Figure 3) indicate that ~50% of the strand scissions induced by IIIf8 contain a 3′-OH group (and a 5′-phosphate with an entire nucleotide unit missing). This number seems to be somewhat in contrast to the sequence gel analysis results (Figure 7). The band tentatively identified as the 3′-OH product (marked by asterisks) accounts for 20% of the cleavage at the most. However, there are other bands (marked by arrowheads) which could be 3′-OH cleavage sites at other bands than G and thus make up for the remaining 30%.

Due to the apparent need for saturation of the DNA by reagent and the preferential cleavage at G residues, the cleavage might be induced at abasic sites inherent in the plasmid DNA, analogous to the recent results obtained with acridines tethered to purines (Constant et al., 1988). In order to test this, plasmid DNA depurinated by formic acid treatment (50%, 30 s; inducing ~1 depurination/200 base pairs) was photocleaved with reagent IIIf8, but no significant increase in cleavage susceptibility was observed. We therefore conclude that abasic sites do not play any significant role in the photocleavage mechanism.

The results indicate that the nitrobenzamido ligand is important for the DNA photocleavage, but the light is absorbed by the acridinyl ligand with >420-nm radiation. Therefore an energy-transfer mechanism must be involved. The necessity of DNA saturation by the reagent and the pronounced effect of the linker length indicate intermolecular energy transfer between the acridine ligand of a nonintercalated reagent and the nitrobenzamido moiety of another reagent molecule (where the acridine is probably bound to the DNA by intercalation). With subsaturating concentrations of reagent IIIf8 it was found that DNA-saturating concentrations of another intercalator (9-aminoacridine) did not increase the photocleavage. Thus it is not the intercalation saturation of the DNA, per se, that is responsible for the "saturation effect", e.g., by way of a DNA conformational change.

As an attempt to circumvent the necessity of saturating the DNA by reagent, we prepared reagents VI containing two acridine ligands in a configuration that does not allow bis-intercalation; the idea being that one of the acridine moieties should be responsible for DNA association by intercalation, while the other should serve as the antenna for energy transfer to the nitrobenzamido ligand. Although these reagents did not show enhanced DNA nicking activity at subsaturating concentrations, our proposed mechanism may still be correct, since the geometry of the DNA-bound reagents VIc or VIf could be unfavorable for energy transfer.

It is striking that (apart from the presence of some alkaline-resistant 3′-termini in the case of IIIf8) the sequence analysis gives virtually identical results for DNA photocleaved by IIIf8 and by methylene blue (and acridine orange), i.e., G-specific cleavage yielding 5′-phosphates and a multitude (at least four) of 3′-products which all yield 3′-phosphate upon alkaline hydrolysis (Figure 7). This could indicate identical mechanisms of cleavage.

Table IV. Effect of NaN_3 of Photocleavage of DNA by IIIf8

mM NaN_3	% ccDNA	rcDNA	rel cleavage
0	69	31	1
1	47	53	1.7
3	41	59	1.9
10	24	76	2.5
30	15	85	2.7
control	100	0	0

At least two mechanisms are responsible for the methylene blue mediated photocleavage of DNA. Either direct electron transfer between methylene blue and guanines in the DNA causes guanine oxidation or methylene blue–oxygen (O_2) energy transfer produces singlet oxygen which in turn oxidizes guanines (OhUigin et al., 1987).

Since the DNA photocleavage by nitrobenzamido acridine conjugates is indifferent to the oxygen content of the medium (O_2 versus N_2 saturation, data not shown) and is not inhibited by azide ion (Table IV), an efficient quencher of singlet oxygen, we conclude that a singlet-oxygen mechanism is not a major pathway. We therefore suggest an electron-transfer mechanism in which the electron is transferred from guanine to the acridine and possibly further to the nitrobenzamide. However, this mechanism does not readily account for the dramatic effect of pH on the cleavage efficiency since this is not observed with methylene blue. In fact, the DNA photocleavage with methylene blue is decreased at low pH (as assayed by plasmid relaxation, results not shown). Thus, although methylene blue (and acridine orange) and (nitrobenzoyl)amine acridine conjugates both give rise to G-preferential DNA photocleavage (oxidation), somewhat different mechanisms must be involved.

We also find it noteworthy that both in the case of IIIf8 and methylene blue, predominantly frank strand breaks are produced with only little additional cleavage upon piperidine treatment (Figure 6). This is somewhat in contrast to previous studies in which alkaline hydrolysis had to be included in the cleavage procedure (Friedman & Brown, 1978; Fox & Waring, 1988; OhUigin et al., 1987; Schneider et al., 1990). We cannot at present account for this discrepancy, but we consistently find that at least 50% of the methylene blue induced DNA scissions are frank strand breaks, eventually induced by the heating (90 °C, 5 min) in formamide prior to gel loading.

Finally, we have presented a, from a photochemical point of view, rare example of a photochemical reaction that proceeds via two apparently independent pathways as a function of wavelength. This is most dramatically illustrated by the completely different sequence dependence of the DNA photocleavage by reagents IIIc8 and IIIf8 when irradiated at 300 nm as compared to 420 nm (Figure 8).

CONCLUSIONS

The present results indicate that DNA photocleavage mediated by nitrobenzamido 9-aminoacridine reagents and 420-nm radiation proceeds partly via a novel (electron transfer) mechanism which, inter alia, results in generation of 3′-hydroxy termini. The photocleavage with the presently described reagents is too inefficient for the reaction to be of immediate use in biological molecular tools. However, the observation that the electron transfer (oxidation) properties of a DNA-binding ligand—in this case 9-aminoacridine—can be strongly modulated by ligands tethered to it suggests a new way of constructing more efficient molecular tools.

LITERATURE CITED

Barton, J. (1986) Metals and DNA: Molecular left-hand complements. *Science 233*, 727–734.

Basile, L. A., Raphael, A. L., and Barton, J. K. (1987) Metal-activated hydrolytic cleavage of DNA. *J. Am. Chem. Soc. 109*, 7550–7551.

Behr, J. P. (1989) Photohydrolysis of DNA by polyaminobenzenediazonium salts. *J. Chem. Soc., Chem. Commun.* 101–103.

Blacker, A. J., Jazwinski, J., Lehn, J.-M., et al. (1986) Photochemical cleavage of DNA by 2,7-diazapyrenium cations. *J. Chem. Soc., Chem. Commun.* 1035–1037.

Buchardt, O., Egholm, M., Karup, G., et al. (1987) 9-(4-Nitrobenzamidopolymethylene)aminoacridines and their Photochemical Cleavage of DNA. *J. Chem. Soc., Chem. Commun.* 1696–1697.

Chen, C.-H. B., and Sigman, D. S. (1988) Sequence-specific scission by 1,10-phenanthroline–copper linked to deoxyoligonucleotides. *J. Am. Chem. Soc. 110*, 6570–6572.

Chi-hong, B., and Sigman, D. (1986) Nuclease activity of 1,10-phenanthroline–copper: Sequence-specific targeting. *Proc. Natl. Acad. Sci. USA 83*, 7145–7151.

Constant, J. F., O'Connor, T. R., Lhomme, J., et al. (1988) 9-[(10-(aden-9-yl)-4,8-diazadecyl)amino]-6-chloro-2-methoxy-acridine incises DNA at apurinic sites. *Nucl. Acids Res. 16*, 2691.

Dervan, P. B. (1986) Design of sequence-specific DNA-binding molecules. *Science 232*, 464–471.

Döpp, D. (1975) Reactions of aromatic nitro compounds via excited triplet states. *Top. Curr. Chem. 55*, 49–85.

Eck, J. C., and Marvel, C. S. (1959) ϵ-Benzylaminocaproic acid, in Organic Syntheses (A. H. Blatt, Ed.) Coll. Vol. 2, 9th printing, p 76–78, John Wiley and Sons, New York.

Fleisher, M. B., Waterman, K. C., Turro, N. J., et al. (1986) Light-induced cleavage of DNA by metal complexes. *Inorg. Chem. 25*, 3549–3551.

Fox, U., and Waring, M. (1986) Nucleotide sequence binding preferences of nogalamycin investigated by DNase I footprinting. *Biochemistry 25*, 4349–4356.

Freifelder, D., Davidson, P. F., and Geiduschek, E. P. (1961) Damage by visible light to the acridine orange–DNA complex. *Biophys. J. 1*, 389–400.

Friedman, T., and Brown, D. M. (1978) Base-specific reactions useful for DNA sequencing: methylene blue-sensitized photooxidation of guanine and osmium tetraoxide modification of thymine. *Nucl. Acids Res. 5*, 615–622.

Garmaise, D. L., Schwartz, R., and McKay, A. F. (1958) Amino acids. VI. Preparation and chemistry of ω-carbalkoxyalkyl isothiocuanates. *J. Am. Chem. Soc.*, 3332–3334.

Goyne, T. E., and Sigman, D. S. (1987) Nuclease activity of 1,10-phenanthroline–copper ion. Chemistry of deoxyribose oxidation. *J. Am. Chem. Soc. 109*, 2846–2848.

Hansen, J. B., Nielsen, M. C., Ehrbar, U., et al. (1982) Partially Protected Polyamines. *Synthesis* 404.

Herlt, A. J., Kibby, J. J., and Rickards, R. W. (1981) Synthesis of unlabelled and carboxyl-labelled 3-amino-5-hydroxybenzoic acid. *Aust. J. Chem. 34*, 1319–1324.

Hertzberg, R. P., and Dervan, P. B (1984) Cleavage of DNA with methidiumpropyl–EDTA–iron(II): Reaction conditions and product analyses. *Biochemistry 23*, 3934–3945.

Jeppesen, C., and Nielsen, P. E. (1989a) Photofootprinting of drug-binding sites on DNA using diazo- and azido-9-aminoacridine derivatives. *Eur. J. Biochem. 182*, 437–444.

Jeppesen, C., and Nielsen, P. E. (1989b) Uranyl mediated photofootprinting reveals strong E. coli polymerase–DNA backbone contacts in the +10 region of the deoP1 protomer open complex. *Nucl. Acids Res. 17*, 4947–4956.

Jeppesen, C., Buchardt, O., Henriksen, U., et al. (1988) Photocleavage of DNA and photofootprinting of *E. coli* RNA polymerase bound to protomer DNA by azido-9-acridinylamines. *Nucl. Acids Res. 16*, 5755–5770.

LeDoan, T., Perrouault, L., Praseuth, D., et al. (1987) Sequence-targeted chemical modification of nucleic acids by complementary oligonucleotides covalently linked to porphyrins. *Nucl. Acids Res. 15*, 7749–7760.

Mattison, L., and O'Dell, D. (1979) *Mol. Photochem. 9*, 213–216.

Moser, H. E., and Dervan, P. B. (1987) Sequence-specific cleavage of double helican DNA by triple helix formation. *Science 238*, 645–650.

Nielsen, P. E. (1990) Chemical and photochemical probing of DNA complexes. *J. Mol. Recognit. 3*, 1–25.

Nielsen, P. E., Jeppesen, C., and Buchardt, O. (1988a) Uranyl salts as photochemical agents for cleavage of DNA and probing of protein-DNA contacts. *FEBS Lett. 235*, 122–124.

Nielsen, P. E., Jeppesen, C., Egholm, M., et al. (1988b) Photochemical Cleavage of DNA by Nitrobenzamides Linked to 9-Aminoacridines. *Biochemistry 27*, 6338–6343.

Nielsen, P. E., Jeppesen, C., Egholm, M., et al. (1988c) Adenine-guanosine preferential photocleavage of DNA by azido-benzoyl- and diazocyclopentadienyloxy derivatives of 9-aminoacridine. *Nucl. Acids Res. 16*, 3877–3888.

Nishiwaki, E., Lee, H., Matsumoto, T., et al. (1990) Synthesis of nitrated oligo-*N*-methylpyrrole carboxamide derivatives and their photochemical DNA cleaving activities. *Tetrahedron Lett. 31*, 1299–1302.

OhUigin, C., McConnell, D. J., Kelly, J. M., et al. (1987) Methylene blue photosensitized strand cleavage of DNA: effects of dye binding and oxygen. *Nucl. Acids Res. 15*, 7411–7427.

Praseuth, D., LeDoan, T., Chassignol, M., et al. (1988a) Sequence-targeted photosensitized reactions in nucleic acids by oligo-α-deoxynucleotides and oligo-β-deoxynucleotides covalently linked to proflavin. *Biochemistry 27*, 3031–3038.

Praseuth, D., Perrouault, L., LeDoan, T., et al. (1988b) Sequence-specific binding and photocrosslinking of α and β oligodeoxynucleotides to the major groove of DNA via triple-helix formation. *Proc. Natl. Acad. Sci. U.S.A. 85*, 1345–1353.

Schneider, J. E., Price, S., Maidt, L., et al. (1990) Methylene blue plus light mediates 8-hydroxy-2′-deoxy-guanosine formation in DNA preferentially over strand breakage. *Nucl. Acids Res. 18*, 631–635.

Sigman, D. S. (1986) Nuclease activity of 1,10-phenanthroline–copper ion. *Acc. Chem. Res. 19*, 180–186.

Sigman, D. S. (1990) Chemical nucleases. *Biochemistry 29*, 9097–9105.

Stubbe, J., and Kozarich, J. W. (1987) Mechanism of bleomycin-induced DNA degradation. *Chem. Rev. 87*, 1107–1136.

Subramanian, R., and Meares, C. F. (1985) Photo-induced nicking of deoxyribonucleic acid by ruthenium(II)–bleomycin in the presence of air. *Biochem. Biophys. Res. Commun. 133*, 1145–1151.

Subramanian, R., and Meares, C. F. (1986) Photosensitization of cobalt bleomycin. *J. Am. Chem. Soc. 108*, 6427–6429.

Talalaeva, T. V., Tsareva, G. V., Simonov, A. P., et al. (1964) Synthesis and structure of lithium alcoholates. *Isv. Akad. Nauk SSSR, Ser. Khim. 4*, 638–644 [Chem. Abstr. (1964) *61*, 2957*g*].

Tullius, T. D. (1989) Physical studies of protein–DNA complexes by footprinting. *Annu. Rev. Biophys. Chem. 18*, 213–237.

Tullius, T. D., and Dombroski, B. A. (1985) Iron(II) EDTA used to measure the helix twist along any DNA molecule. *Science 230*, 679–681.

Uchida, K., Pyle, A. M., Morii, T., et al. (1989) High resolution footprinting of *Eco*RI and distiamycin with $Rh(phi)_2(bpy)^{3+}$, a new photofootprinting reagent. *Nucl. Acids Res. 17*, 10259–10279.

Veal, J. M., and Rill, R. L. (1988) Sequence specificity of DNA cleavage by bis(1,10-phenanthroline)copper(I). *Biochemistry 27*, 1822–1827.

Ward, B., Skorobogaty, A., and Dabrowiak, J. C. (1986) DNA cleavage specificity of a group of cationic metalloporphyrins. *Biochemistry 25*, 6875–6883.

TECHNICAL NOTE

Characterization of Antibody–Chelator Conjugates: Determination of Chelator Content by Terbium Fluorescence Titration

Kimberly D. Brandt, Karen E. Schnobrich, and David K. Johnson*

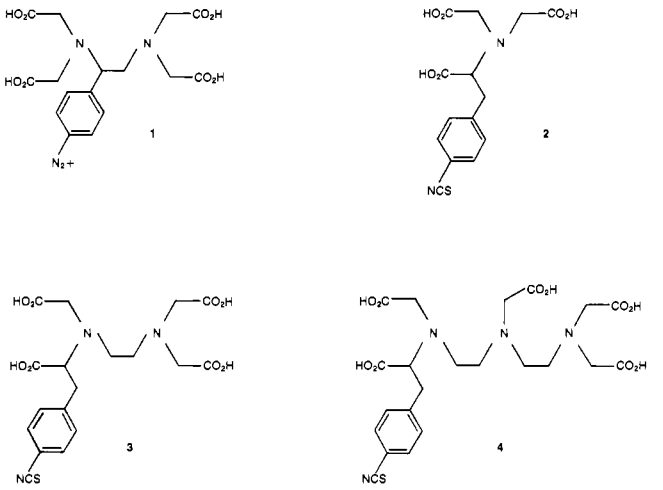
Abbott Laboratories, Department 90M, Abbott Park, Illinois 60064. Received September 17, 1990

Fluorescence titrations were performed by adding varying mole ratios of terbium(III) to antibody conjugates formed by benzyl isothiocyanate derivatives of three different polyaminopolycarboxylate chelators (NTA, EDTA, and DTPA) and the results compared to values for average chelator content obtained by cobalt-57 binding assays. For two different murine monoclonal antibodies, the average chelator content obtained by terbium fluorescence titration correlated closely with that measured by the cobalt-57 binding assay. It is concluded that lanthanide fluorescence titrations provide a useful alternative to radiometal binding assays for the determination of chelator content in protein–chelator conjugates.

Monoclonal antibodies derivatized with polyaminopolycarboxylate chelates of a variety of radiometals are finding increasing use in the detection (*1–5*) and potential treatment (*6–8*) of a number of cancers. Among many parameters that influence the behavior of such chelate immunoconjugates, the average level of substitution (i.e. the number of chelating groups incorporated into each antibody molecule) is a fundamental characteristic that has nevertheless been poorly defined in many of the preparations used clinically. In our laboratory, the ^{57}Co binding assay (*9*) has been the method of choice for measuring the average chelator substitution of EDTA[1] and DTPA immunoconjugates. In contrast to the use of ^{14}C-labeled chelators (*10*, *11*), the ^{57}Co binding assay provides functional information as to the available metal binding capacity of a conjugate and is sufficiently simple that it can be performed routinely on every preparation that is produced. However, as with any assay, equivocal results are sometimes obtained and, in the course of efforts to develop an independent technique by which to confirm chelator substitution levels measured by the ^{57}Co assay, we evaluated the use of terbium fluorescence titrations.

Binding of lanthanide metals such as terbium(III) and europium(III) to chelating agents that contain an aromatic moiety held close to the coordination sphere can lead to "sensitized" fluorescence, in which light is absorbed through the aromatic system and the energy transferred to the metal, which then produces emissions characterized by a very large Stokes shift and fluorescence lifetimes of up to several seconds (*12*). Earlier studies (*13*) of an albumin conjugate of a bifunctional EDTA derivative (**1**, Chart I) had shown that the phenyl moiety present in that chelator was able to sensitize europium and terbium fluorescence at micromolar concentrations. As each chelating site in the conjugate bound one lanthanide ion, and as a lanthanide ion had to be in a chelate site if energy transfer was to occur, this technique could be used to quantitate the number of chelating groups present (*13*).

Chart I



Similarly, we observed that the phenyl group in the bifunctional EDTA derivative **3** (Chart I) produced sensitized terbium fluorescence (Figure 1). Conjugates of an anti-CEA monoclonal antibody (C110) with a homologous series of bifunctional polyaminopolycarboxylates of varying denticity (**2–4**, Chart I) were therefore prepared and terbium fluorescence titrations performed, in order to assess the extent of correlation with ^{57}Co binding assay data and the applicability of this technique to different chelate structures.

Chelating agents **3** and **4** were synthesized as previously reported (*14*). The synthesis of compound **2** will be presented elsewhere. The generation and characterization of the anti-CEA antibody used in these studies has been previously described (*15*). C110 is an IgG_1 murine monoclonal antibody that is presently in clinical trials in the form of an indium-111-labeled conjugate of compound **4** (*16*). All glassware used in these studies was washed sequentially with 3 M HCl, deionized water, and methanol. Deionized water was obtained from a MILLI-Q system (Millipore Corp., Bedford, MA), and all buffer salts were reagent grade or better. Antibody concentrations were determined from the absorbance at 280 nm, using a

[1]The following abbreviations are used: CEA, carcinoembryonic antigen; DTPA, diethylenetriaminepentaacetic acid; EDTA, ethylenediaminetetraacetic acid; NTA, nitrilotriacetic acid.

1043-1802/91/2902-0067$02.50/0 © 1991 American Chemical Society

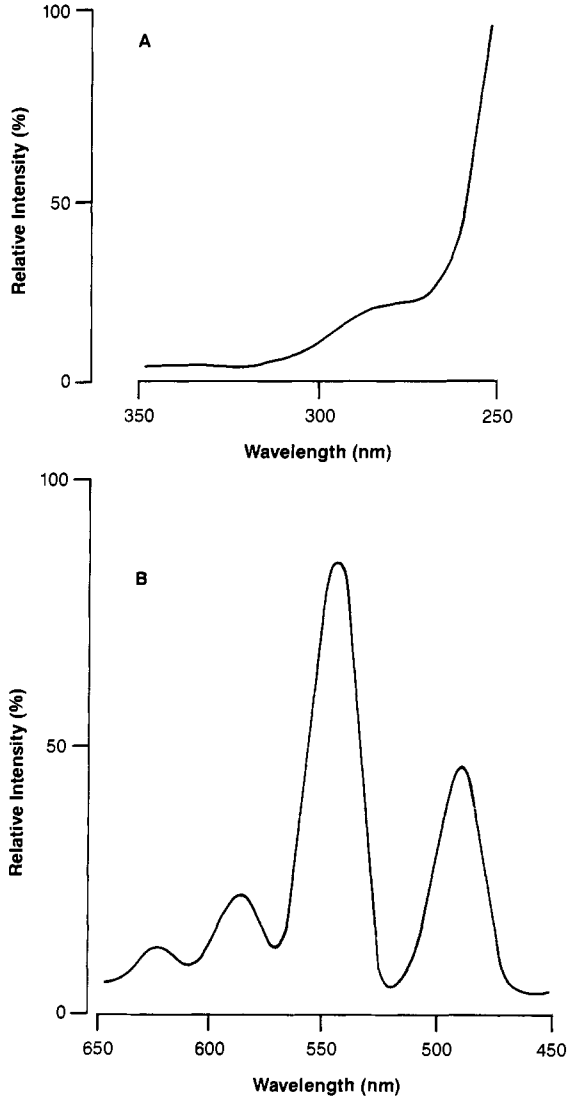


Figure 1. Excitation (A) and emission (B) scans, obtained as described in the text, for an antibody conjugate of compound 3 that had been exposed to a 6-fold molar excess of terbium(III) then subjected to size-exclusion chromatography by spin column to remove unbound terbium.

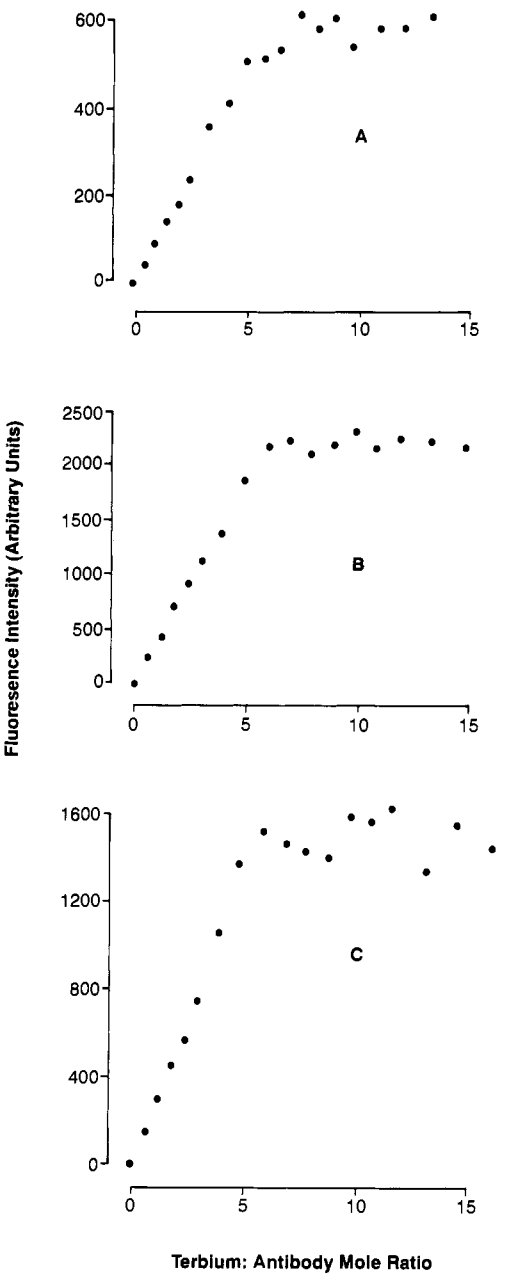


Figure 2. Fluorescence intensity at 548 nm as a function of terbium:antibody input mole ratio for C110 conjugates of (A) compound 2, (B) compound 3, and (C) compound 4. Each data point shown is the mean of 10 fluorimeter readings, the standard deviation from the mean being less than 1% in all cases. Underivatized C110 antibody at the same concentration as the conjugates gave fluorescence intensities of less than 20 units (same scale) when exposed to terbium under the same conditions at Tb:antibody input mole ratios up to 10:1.

correlation coefficient previously established for that particular antibody from plots of A_{280} vs antibody concentration as measured by the Bradford dye binding assay (Bio-Rad Laboratories, Richmond, CA). Conjugates of C110 with each of the chelators were prepared as previously described (*15*), using a 40:1 input mole ratio of chelator: antibody at an antibody concentration of 10 mg/mL.

Each conjugate was diluted into 0.05 M citrate buffer, pH 6.0, to a final concentration of 2.8–4.2 × 10^{-5} M. To aliquots of this stock solution (100 μL) were then added terbium(III) citrate solutions (10 μL per aliquot) obtained by dissolving $TbCl_3 \cdot 6H_2O$ (99.999%, Aldrich Chemical Co., Milwaukee, WI) in 0.05 M citrate, pH 6.0. Terbium solutions of varying molarity were used so as to span a range of Tb:antibody input mole ratios. After incubation in the presence of terbium for 30 min at room temperature, each aliquot was centrifuged through a Sephadex G-25 spin column to remove non-antibody-bound terbium. The eluate (100 μL) was then diluted into 0.05 M Tris/0.9% NaCl/5% ethylene glycol, pH 7.5, to a final volume of 2.0 mL and transferred to a cuvette. Fluorescence measurements were made with a Perkin-Elmer LS-5 fluorimeter operating in time-resolved mode, exciting at 268, 271, and 283 nm, respectively, for the NTA, DTPA, and EDTA conjugates and monitoring emission at 548 nm. A 200-μs delay time was employed, with a 1.0-s gate and excitation and emission slit widths of 15 and 20 nm, respectively.

Fluorescence titration curves for the three C110–chelator conjugates are shown in Figure 2. In each case there was a distinct break in the curve at a terbium:antibody ratio of ca. 6, with no further increase in fluorescence intensity observed beyond that ratio. This indicated that each conjugate contained an average of six chelators per antibody molecule, a value identical with that previously obtained from ^{57}Co binding assays performed on C110 conjugates of 4 (*15*). The similarity in results obtained with three different chelators suggests that this method may also be applicable to other bifunctional ligands that contain phenyl groups (*4–6*, *10*).

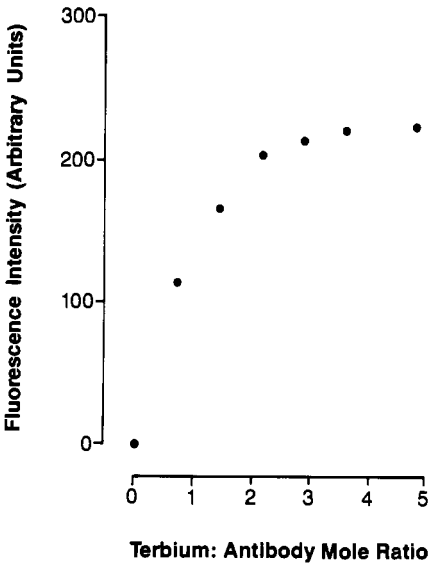


Figure 3. Fluorescence intensity at 548 nm as a function of terbium:antibody input mole ratio for a B72.3 conjugate of compound **4**. Each data point shown is the mean of 10 fluorimeter readings, the standard deviation from the mean being less than 1% in all cases.

To further confirm the correspondence between substitution levels measured by ^{57}Co binding assays and those obtained by terbium fluorescence titration, the latter method was applied to a conjugate of **4** with a second IgG_1 murine monoclonal antibody, B72.3. This antibody is directed against a high molecular weight tumor-associated mucin (*17*) and its production and conjugation to **4** have been described elsewhere (*14*, *18*). The conjugate used in the fluorescence study was obtained at an input mole ratio of 4:B72.3 of 3:1 and contained approximately two chelators per antibody by ^{57}Co binding assay (*18*). The corresponding fluorescence titration curve (Figure 3) showed a plateau in intensity at a terbium:antibody mole ratio of ca. 2, again demonstrating good correlation between the two methods.

The primary constraints on configuring fluorescence assays of this type appear to be related to adventitious metal contamination of samples and materials used in the assay. The practical limit of detection of terbium in these systems is well below nanomolar and the Tris/ethylene glycol/salt buffer minimizes physical trapping and adsorption of proteins (to columns, cuvettes, etc.) at such low conjugate concentrations. Thus, in principle, an assay could be performed at antibody concentrations some 4–5 log units lower than are used here, making it a sensitive procedure requiring very small sample sizes. However, in practice, conjugate concentrations of at least micromolar are needed to obtain reasonable assay precision in the face of ambient levels of metal contaminants. When replicate titrations were performed on a single C110 conjugate of **4** under the conditions described earlier, the break point in the titration curve was reasonably reproducible, but given samples at a particular (but apparently random) mole ratio sometimes gave intensities that fell substantially below the curve. We attribute this to contamination of individual spin columns, sample vials, or cuvettes with metals that were able to compete with terbium for protein-bound chelating sites. This level of variability in the assay, plus the cumbersome nature of a procedure requiring separate processing of samples at each mole ratio, led us to investigate an alternative, simplified configuration that employed a single aliquot of conjugate, a single buffer, and a single cuvette.

A 1.0×10^{-6} M solution of a C110 conjugate of **4** in 0.05 M Tris, pH 7.5, was prepared and a 2.5-mL aliquot

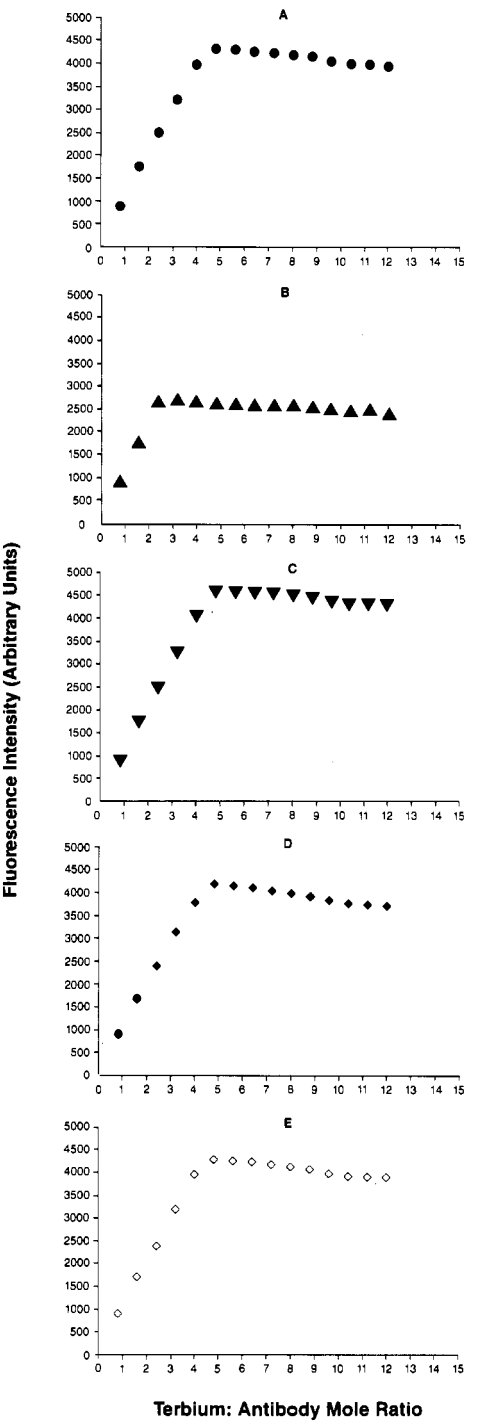


Figure 4. Fluorescence intensity at 548 nm as a function of terbium:antibody input mole ratio for a C110 conjugate of compound **4**. Each data point shown is the mean of 10 fluorimeter readings, the standard deviation from the mean being less than 1% in all cases. Each panel (A–E) represents a single titration experiment performed on an aliquot of a single conjugate stock solution.

transferred to a 5-mL cuvette. A 2×10^{-5} M stock solution of terbium in 0.05 M Tris, pH 7.5, was prepared by dissolving $TbCl_3 \cdot 6H_2O$ in 0.1 M HCl to give a 0.01 M stock, which was then diluted with 0.05 M Tris, pH 7.5. A 100-μL aliquot of the 2×10^{-5} M terbium solution was added to the cuvette containing the conjugate and the resulting solution stirred at room temperature for 10 min, using a small magnetic stir bar placed in the cuvette. Fluorescence measurements were then performed with instrument settings identical with those described earlier. This procedure was repeated until a total of 15 100-μL aliquots of the terbium solution had been added serially to the

cuvette, fluorescence readings being made after each addition. A dilution correction was applied to the fluorescence intensity measured at each mole ratio, to compensate for the change in volume of the test solution. Replicate fluorescence titrations of this type were performed on five aliquots of the 1.0×10^{-6} M conjugate stock, the results of these assays appearing in Figure 4. The scatter in the data in the plateau region of the curve was consistently less than that evident in Figure 2. However, although four of the five replicates agreed very closely (panels A, C, D, E, Figure 4), the fifth (panel B, Figure 4) gave a completely disparate substitution level (2.5 chelators/antibody vs. 5). Again, the most likely explanation for this variability in the data is metal contamination of either the cuvette, the stir bar, or the pipet used to transfer aliquot B. In this assay configuration, such contamination affects all data points, as opposed to the individual data points that are affected when the spin column procedure is used. Thus, the choice of a particular configuration depends upon the type of variability that is easiest to deal with in a given application.

For routine analysis of DTPA immunoconjugates that are available in quantities permitting the generation of micromolar stock solutions, the single cuvette titration in Tris buffer is the preferred procedure. However, given the data in Figure 4, it is recommended that assays be run in duplicate and that, if duplicate measured substitution levels differ by more than 20%, the titration should be repeated. With these precautions, the procedure is relatively straightforward to perform, given access to a fluorimeter with time-resolution capabilities. Attempts to measure terbium fluorescence without time gating are generally confounded by interfering short-lived fluorescent signals from buffers, etc. However, any fluorimeter with a ratio mode that permits intensities to be compared at at least two different time points after exciting the sample can be used to perform this assay.

The average substitution level of a chelator immuno conjugate affects performance characteristics, such as theease of labeling with a radiometal (*19*), and may also influence the disposition of such radiometal labeled conjugates in vivo. We conclude that lanthanide fluorescence titrations offer an independent, nonisotopic method for quantitating this basic parameter in conjugates that incorporate a sensitizing moiety.

LITERATURE CITED

(1) Siccardi, A. G., Buraggi, G. L., Callegaro, L., Colella, A. C., De Filippi, P. G., Galli, G., Mariani, G., Masi, R., Palumbo, R., Riva, P., Salvatore, M., Scassellati, G. A., Scheidhauer, K., Turco, G. L., Zaniol, P., Benini, S., Deleide, G., Gasparini, M., Lastoria, S., Mansi, L., Paganelli, G., Salvischiani, E., Seregni, E., Viale, G., and Natali, P. G. (1989) Immunoscintigraphy of adenocarcinomas by means of radiolabeled $F(ab')_2$ fragments of an anti-carcinoembryonic antigen monoclonal antibody: A multicenter study. *Cancer Res. 49*, 3095–3103.

(2) Chatal, J-F., Saccavani, J-C., Gestin, J-F., Thédrez, P., Curtet, C., Kremer, M., Guerreau, D., Nolibé, D., Fumoleau, P., and Guillard, Y. (1989) Biodistribution of indium-111 labeled OC 125 monoclonal antibody intraperitoneally injected into patients operated on for ovarian carcinomas. *Cancer Res. 49*, 3087–3094.

(3) Beatty, J. D., Hyams, D. M., Morton, B. A., Beatty, B. G., Williams, L. E., Yamauchi, D., Merchant, B., Paxton, R. J., and Shively, J. E. (1989) Impact of radiolabeled antibody imaging on management of colon cancer. *Am. J. Surg. 157*, 13–19.

(4) Craig, A. S., Helps, I. M., Jankowski, K. J., Parker, D., Beeley, N. R. A., Boyce, B. A., Eaton, M. A. W., Millican, A. T., Millar, K., Phipps, A., Rhind, S. K., Harrison, A., and Walker, C. (1989) Towards tumor imaging with indium-111 labelled macrocycle-antibody conjugates. *J. Chem. Soc. Chem. Commun.* 794–796.

(5) Mathias, C. J., Sun, Y., Welch, M. J., Connett, J. M., Philpott, G. W., and Martell, A. E. (1989) BrΦHBED: an improved bifunctional chelate for radiolabeling antibodies. *J. Nucl. Med. 30*, 763.

(6) Deshpande, S. V., DeNardo, S. J., Kukis, D. L., Moi, M. K., McCall, M. J., DeNardo, G. L., and Meares, C. F. (1990) Yttrium-90 labeled monoclonal antibody for therapy: labeling by a new macrocyclic bifunctional chelating agent. *J. Nucl. Med. 31*, 473–479.

(7) Macklis, R. M., Kinsey, B. M., Kassis, A. I., Ferrara, J. L. M., Atcher, R. W., Hines, J. J., Coleman, C. N., Adelstein, S. J., and Burakoff, S. J. (1988) Radioimmunotherapy with alpha-particle-emitting immunoconjugates. *Science 240*, 1024–1026.

(8) Boniface, G. R., Izard, M. E., Walker, K. Z., McKay, D. R., Sorby, P. J., Turner, J. H., and Morris, J. G. (1989) Labeling of monoclonal antibodies with samarium-153 for combined radioimmunoscintigraphy and radioimmunotherapy. *J. Nucl. Med. 30*, 683–691.

(9) Meares, C. F., McCall, M. J., Reardon, D. T., Goodwin, D. A., Diamanti, C. I., and McTigue, M. (1984) Conjugation of antibodies with bifunctional chelating agents: isothiocyanate and bromoacetamide reagents, methods of analysis and subsequent addition of metal ions. *Anal. Biochem. 142*, 68–78.

(10) Brechbiel, M. W., Gansow, O. A., Atcher, R. W., Schlom, J., Esteban, J., Simpson, D. E., and Colcher, D. (1986) "Synthesis of 1-(*p*-isothiocyanatobenzyl) derivatives of DTPA and EDTA. Antibody labeling and tumor imaging studies. *Inorg. Chem. 25*, 2772–2781.

(11) Mirzadeh, S., Brechbiel, M. W., Atcher, R. W., and Gansow, O. A. (1990) Radiometal labeling of immunoproteins: Covalent linkage of 2-(4-isothiocyanatobenzyl)diethylenetriaminepentaacetic acid ligands to immunoglobulin. *Bioconjate Chem. 1*, 59–65.

(12) Richardson, F. S. (1982) Terbium(III) and europium(III) as luminescent probes and stains for biomolecular systems. *Chem. Rev. 82*, 541–552.

(13) Leung, C. S-H., and Meares, C. F. (1977) Attachment of fluorescent metal chelates to macromolecules using "bifunctional" chelating agents. *Biochem. Biophys. Res. Commun. 75*, 149–155.

(14) Westerberg, D. A., Carney, P. L., Rogers, P. E., Kline, S. J., and Johnson, D. K. (1989) Synthesis of novel bifunctional chelators and their use in preparing monoclonal antibody conjugates for tumor targeting. *J. Med. Chem. 32*, 236–243.

(15) Sumerdon, G. A., Rogers, P. E., Lombardo, C. M., Schnobrich, K. E., Melvin, S. L., Hobart, E. D., Tribby, I. I. E., Stroupe, S. D., and Johnson, D. K. (1990) An optimized antibody–chelator conjugate for imaging of carcinoembryonic antigen with indium-111. *Nucl. Med. Biol. 17*, 247–254.

(16) Griffin, T., Brill, B., Bokhari, F., Collins, J., Stochl, M., Gionet, M., Ruschowski, M., Stroupe, S., Kiefer, H., Sumerdon, G., Johnson, D., and Hnatowich, D. (1989) Radioimmunodetection of recurrent colorectal cancer with an ^{111}In labeled anti-CEA antibody. Fourth International Conference on Monoclonal Antibody Immunoconjugates for Cancer, San Diego, CA, March 30–April 1, Abstract 23.

(17) Nuti, M., Teramoto, Y. A., Mariani-Costantini, R., Horan Hand, P., Colcher, D., and Schlom, J. (1982) A monoclonal antibody (B72.3) defines patterns of distribution of a novel tumor-associated antigen in human mammary carcinoma cell populations. *Int. J. Cancer 29*, 539–545.

(18) Carney, P. L., Rogers, P. E., and Johnson, D. K. (1989) Dual isotope study of iodine-125 and indium-111 labeled antibody in athymic mice. *J. Nucl. Med. 30*, 374–384.

(19) Rogers, P. E., Schnobrich, K. E., and Johnson, D. K. (1988) Correlation of radiochemical yield with chelator concentration in indium-111 labeled antibody-chelator conjugates. *J. Nucl. Med. 29*, 924.

Registry No. 1, 53641-65-9; 2, 131322-70-8; 3, 117499-22-6; 4, 117499-23-7; terbium, 7440-27-9.

A Novel Bifunctional Metabolizable Linker for the Conjugation of Antibodies with Radionuclides

Yasushi Arano,† Hiroshi Matsushima,† Masaaki Tagawa,† Mitsuru Koizumi,‡ Keigo Endo,‡ Junji Konishi,‡ and Akira Yokoyama*,†

Faculty of Pharmaceutical Sciences, and School of Medicine, Kyoto University, Sakyo-ku, Kyoto 606, Japan.
Received October 23, 1990

A novel heterogeneous bifunctional reagent containing an ester bond, *N*-[[4-(2-maleimidoethoxy)-succinyl]oxy]succinimide (MESS), was designed and synthesized for the conjugation of antibodies with the gallium-67 (^{67}Ga) chelate of succinyldeferoxamine (SDF) via the ester bond. MESS was synthesized by the acylation of *N*-(2-hydroxyethyl)maleimide with succinic anhydride, followed by the activation of the resulting carboxylic acid to a succinimido ester. MESS possesses a maleimide group for protein conjugation and an active ester group for deferoxamine (DFO) coupling, and the two functional groups are linked via ester bonding. Conjugation of ^{67}Ga-SDF with nonspecific human IgG was performed by reacting freshly thiolated IgG with the reaction product of MESS and DFO, followed by ^{67}Ga labeling of the resulting conjugate using $GaCl_3$ (^{67}Ga-DFO-MESS-IgG). For comparison, ^{67}Ga-DFO conjugated nonspecific human IgG with a nonmetabolizable linkage was synthesized under the same conjugation conditions as those for ^{67}Ga-DFO-MESS-IgG, using a nonmetabolizable heterogeneous bifunctional reagent [*N*-[(6-maleimidocaproyl)oxy]succinimide, EMCS] instead of MESS (^{67}Ga-DFO-EMCS-IgG). HPLC size-exclusion chromatography of both preparations showed a single radioactivity and UV peak corresponding to the intact IgG. Generation of ^{67}Ga-SDF from the ^{67}Ga-DFO-MESS-IgG was demonstrated by reverse-phase HPLC analysis and cellulose acetate electrophoresis after the incubation of ^{67}Ga-DFO-MESS-IgG in a buffered solution containing carboxyesterase. After injection of ^{67}Ga-DFO-MESS-IgG into mice, faster radioactivity clearance from the blood and less radioactivity accumulation in the liver, kidney, and spleen was noted than when ^{67}Ga-DFO-EMCS-IgG was injected. These results indicate that MESS has the ability to conjugate antibodies with ^{67}Ga-SDF via ester bonding and to release ^{67}Ga-SDF by the action of carboxyesterase both in vitro and in vivo.

INTRODUCTION

Metallic radionuclides have numerous advantages over radioiodine for radioimmunoimaging and radioimmunotherapy due to their superior nuclear properties and simplicity of labeling. On the other hand, a heavy localization of radioactivity has been observed in nontarget organs such as the liver when metallic radionuclides are used as labels for antibodies (*1-7*). This results in a high background radioactivity in imaging diagnosis and also increases the radiation dose to the patients, thus limiting the therapeutic use of these compounds.

Recently, Carney et al. reported that they decreased the hepatic radioactive uptake of ^{111}In-labeled B72.3 antibody by using a new bifunctional chelating agent which afforded a higher stability against transchelation (*8*). In a clinical study, however, a high hepatic uptake of radioactivity was still observed after the injection of this labeled antibody (*9*). This seemed to suggest the need for further studies on the radiochemistry of antibodies with the aim of reducing the localization of radioactivity in nontarget organs.

One attractive solution to this problem appears to be the conjugation of antibodies with a radiochelate via a metabolizable linkage (*10-15*). Such a drug design necessitates the efficient cleavage of the bond between the antibody and the radiochelate in organs such as the liver and the subsequent transfer of the chelate in its intact form to the bloodstream, followed by its rapid excretion in the urine. The development of appropriate conjugation chemistry, therefore, is required to enable the release of a radiochelate of known chemical and biological characteristics from a radiolabeled antibody by well-understood mechanisms.

In the present study, a novel bifunctional metabolizable linker, *N*-[[4-(maleimidoethoxy)succinyl]oxy]succinimide (MESS) (Scheme I) was designed and synthesized. Conjugation of nonspecific human IgG with the ^{67}Ga chelate of succinyldeferoxamine (SDF) via an ester bond was then carried out with MESS. For comparison, IgG labeled with ^{67}Ga via a nonmetabolizable linker was prepared under the same conjugation conditions as those for ^{67}Ga-DFO-MESS-IgG, using *N*-[(6-maleimidocaproyl)oxy]succinimide (EMCS) instead of MESS (^{67}Ga-DFO-EMCS-IgG). Enzyme-catalyzed hydrolysis of the two preparations was investigated in vitro and the biodistribution of radioactivity after the intravenous injection of both preparations was also compared in non-tumor-bearing mice.

EXPERIMENTAL PROCEDURES

All the chemicals used were of reagent grade and they were utilized as received. Organic compounds were characterized by ^{1}H NMR and elemental analysis. ^{1}H NMR was performed with a Bruker AC-300 apparatus for MESS and a JNM PMX-60 for HEM and MEHS, using tetramethylsilane as the internal standard. HPLC was performed on a Shimadzu LA-5A instrument (Shimadzu, Japan) equipped with a UV detector and a radiodetector, using a reverse-phase column (Wakosil C_{18}, 4 × 250 mm, Wako Pure Chemical Industries, Japan) or a gel permeation column (TSK G3000SW, 7.5 × 600 mm, Toso, Japan). $^{67}GaCl_3$ and feroxamine-B hydrochloride were kindly supplied by Nihon Medi-Physics Co. Ltd. and Ciba-Geigy Ltd., respectively. *N*-Succinyldeferoxamine (SDF) was

*Author for correspondence.
† Faculty of Pharmaceutical Sciences.
‡ School of Medicine.

1043-1802/91/2902-0071$02.50/0 © 1991 American Chemical Society

synthesized with ferioxamine B as the starting material, according to the procedure of Herscheid et al. (*16*).

Synthesis of *N*-(2-Hydroxyethyl)maleimide (HEM). The precursor, *N*-(methoxycarbonyl)maleimide (NMCM) was prepared with maleimide as the starting material, according to the procedure of Keller et al. (*17*). Then, NMCM (1.6 g, 10.3 mmol) was added to a solution of ethanolamine (0.63 g, 10.3 mmol) in saturated $NaHCO_3$ (50 mL) at 0 °C with vigorous stirring. After 10 min, the solution was diluted with water (200 mL) and then stirred at room temperature for 30–40 min. It was then brought to pH 6–7 with concentrated H_2SO_4, evaporated to 30 mL, acidified to pH 1–2 with 1 M H_2SO_4, and extracted with EtOAc. After drying the EtOAc layer over anhydrous $CaSO_4$, the solvent was evaporated under reduced pressure. Treatment of the residue with a mixture of EtOAc and petroleum ether yielded 0.58 g of HEM (39.9% yield) with a melting point (mp) of 72 °C (uncorr) (lit. mp 70–71 °C) (*18*, *19*). ^1H NMR (CD_3CN): 2.77 (s, 1 H), 3.43 (m, 4 H), 6.51 (s, 2 H) ppm. Anal. Calcd for $C_6H_7NO_3$: C, 51.07; H, 5.00; N, 9.93. Found: C, 50.80; H, 4.88; N, 9.99.

Synthesis of 2-Maleimidoethyl Hydrogen Succinate (MEHS). A mixture of HEM (0.3 g, 2.1 mmol) and succinic anhydride (0.85 g, 8.5 mmol) in 4 mL of toluene was stirred at 100 °C for 4 h. After evaporation of the solvent, the residue was purified by flash column chromatography (40 × 600 mm) and eluted with a mixture of $CHCl_3$ and CH_3CN (4:1) to produce 0.383 g of MEHS (75.6% yield) with a mp of 96 °C (uncorr) (lit. mp 93–95 °C) (*20*). ^1H NMR (CD_3CN): 2.39 (m, 4 H), 3.54 (t, 2 H), 4.04 (t, 2 H), 6.49 (s, 2 H) ppm. Anal. Calcd for $C_{10}H_{11}NO_6$: C, 49.80; H, 4.60; N, 5.81. Found: C, 49.98; H, 4.61; N, 5.80.

Synthesis of *N*-[[4-(2-Maleimidoethoxy)succinyl]oxy]succinimide (MESS). To a cold (0 °C) solution of MEHS (1 g, 4.1 mmol) and *N*-hydroxysuccinimide (0.53 g, 4.6 mmol) in 20 mL of dry THF was added dropwise a solution of dicyclohexylcarbodiimide (0.93 g, 4.5 mmol) in dry THF (4 mL). After 2 h of stirring at 0 °C, acetic acid (27 μL) was added to quench the reaction, and the mixture was stirred for another 1 h. Then the solution was filtered and evaporated to dryness; the residue was dissolved in a mixture of AcOEt and hexane, and it was allowed to crystallize. MESS (0.96 g, 69.2% yield) was thus obtained as a white crystal with a melting point of 136–137 °C (uncorr). ^1H NMR ($CDCl_3$): 2.63 (dd, 2 H, J = 5.4, 6.1 Hz), 2.76 (bs, 4 H), 2.86 (dd, 2 H, J = 6.1, 5.4 Hz), 3.70 (dd, 2 H, J = 5.6, 5.4 Hz), 4.20 (dd, 2 H, J = 5.4, 5.6 Hz), 6.76 (s, 2 H). Anal. Calcd for $C_{14}H_{14}N_2O_8$: C, 49.71; H, 4.17; N, 8.28. Found: C, 50.01; H, 4.27; N, 8.68.

Preparation of an IgG–MESS–DFO Conjugate. Thiolation of nonspecific human IgG (Sigma) was carried out with *N*-succinimidyl 3-(2-pyridyldithio)propionate (SPDP), according to the procedure described previously (*12*). Briefly, IgG (5 mg/mL) in 0.05 M phosphate buffered-saline (PBS) (pH 7.5) was reacted with a 20 mM ethanolic solution of SPDP, followed by the reduction of pyridyl disulfide in the presence of 50 mM dithiothreitol (DTT) at pH 4.5. Under these conditions, one thiol group was introduced per molecule of IgG, as determined by measuring the absorption maximum at 343 nm (*21*), and the concentration was adjusted to 5 mg/mL in 0.1 M PBS (pH 7.0). A solution of MESS in DMF (40 mM, 100 μL) was added to the same volume of an 80 mM solution of deferoxamine (DFO) in borate buffer (0.05 M, pH 8.2), and the reaction mixture was then stirred for 30 min at room temperature. Then, 65 μL of this mixture was added dropwise to the freshly thiolated IgG solution (5 mL) in 0.1 M PBS (pH 7.0). After gentle stirring for 2 h at room temperature, the IgG–MESS–DFO conjugate was separated from unreacted small molecules with a Sephadex G-50 column (1.5 × 25 cm) equilibrated with 0.1 M PBS (pH 6.0). Finally, the collected conjugate was concentrated to 1 mg/mL by ultrafiltration (8MC, Amicon).

Freshly thiolated nonspecific human IgG was also conjugated with DFO through a nonmetabolizable spacer, EMCS (Dojindo, Japan), by using the same procedure as described above but incorporating EMCS instead of MESS.

To examine the possibility that the amino group of the antibody could react with the maleimido group of MESS, nonthiolated IgG (native IgG) was also reacted with MESS- or EMCS-coupled DFFO according to the same procedure as described above.

^{67}Ga Labeling of the Conjugates. Fifty microliters of $^{67}GaCl_3$ (2 mCi/mL) in 0.01 N HCl was added to a solution of each conjugate (1 mg/mL, 1 mL) and incubation was performed at room temperature for 30 min. The labeling efficiency was determined by HPLC using elution with 0.1 M PBS (pH 6.8) at a flow rate of 0.5 mL/min, or by paper chromatography (No. 50, Advantec Toyo Ltd., Tokyo, Japan) developed with saline.

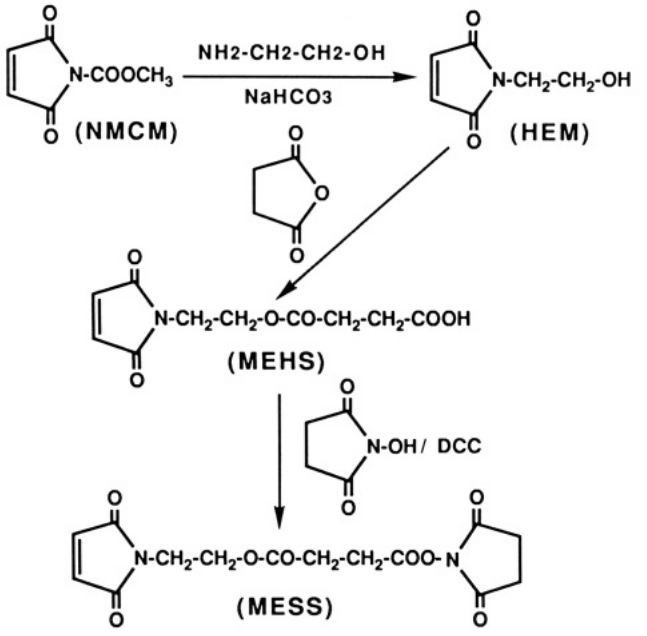
DFO and SDF were also labeled with ^{67}Ga by adding 50 μL of a solution of $^{67}GaCl_3$ to a solution of DFO and SDF (10^{-3} M, 1 mL) prepared in 0.1 M phosphate buffer (pH 6.0).

Hydrolysis of the ^{67}Ga–MESS–DFO Conjugate. Sixty microliters of the ^{67}Ga–MESS–DFO–IgG or ^{67}Ga–EMCS–DFO–IgG solution was added to a mixture of 200 μL of a suspension of pig liver esterase (EC 3.1.1.1, Boehringer Mannheim) and 350 μL of 0.1 M PBS (pH 6.0), and incubation was performed at 37 °C. Each of the labeled proteins (60 μL) was also added to 550 μL of 0.1 M PBS (pH 6.0) in the absence of the esterase, and the mixture was then incubated at the same temperature. After 6 h, small aliquots from the reaction mixture were analyzed by paper chromatography. In this system, protein-bound ^{67}Ga was detected at the origin, and ^{67}Ga released from the conjugate was found near the solvent front. The percent radioactivity released from the conjugate was determined by calculating the ratio of the radioactivity near the solvent front to the total radioactivity on the strip. To characterize the ^{67}Ga radioactivity released from the conjugate, the rest of the mixture was deproteinized by ultrafiltration (Centricon-10, Amicon), and the filtrate was analyzed by both cellulose acetate electrophoresis (EP) and reverse-phase HPLC. EP was performed in veronal buffer (I = 0.05, pH 8.6) using an electrostatic field of 0.8 mA/cm for 20 min. Under these conditions, ^{67}Ga–SDF remained at the origin and ^{67}Ga–DFO migrated 2 cm toward the cathode. Reverse-phase HPLC was eluted with a mixture of 10% (w/v) aqueous ammonium acetate and methanol (1:1, v/v) at a flow rate of 0.4 mL/min, with ^{67}Ga–SDF and ^{67}Ga–DFO being eluted at 8.6 and 10.8 min, respectively.

Twenty microliters of ^{67}Ga–DFO–MESS–IgG or ^{67}Ga–DFO–EMCS–IgG was also added to 230 μL of mouse plasma, and the mixture was incubated at 37 °C. For the control study, both labeled proteins were incubated in Tris buffer (20 mM, pH 7.4) instead of mouse plasma. After 6 and 24 h of incubation, samples were taken from the reaction mixture, and the percentage radioactivity released from the conjugates was determined by paper chromatography performed as described above.

Biodistribution of ^{67}Ga-Labeled Conjugates in Mice. Each labeled solution was diluted with 0.1 M PBS (pH

Scheme I



6.0) to adjust the antibody concentration to 0.4 mg/mL. The biodistribution of radioactivity after the intravenous injection of ^{67}Ga–DFO–MESS–IgG and ^{67}Ga–DFO–EMCS–IgG was then compared in 5-week-old ddY mice (22). Groups of five mice were injected with 50 μL (20 μg) of each ^{67}Ga-labeled antibody and then sacrificed at 1, 6, 24, or 48 h after the injection. The organs of interest were removed and weighed, and the radioactivity was counted in a well counter (Beckman Gamma 5500).

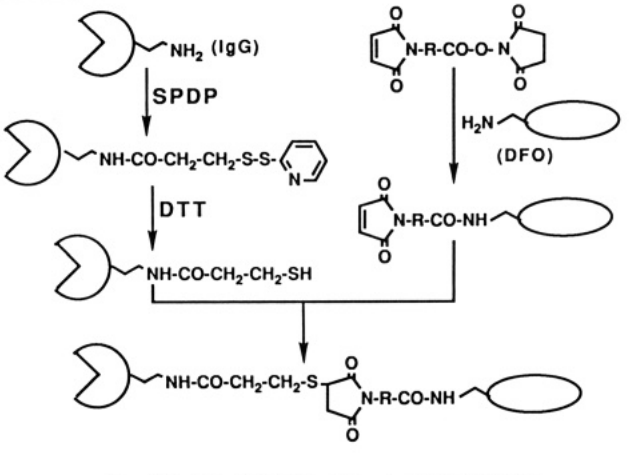
RESULTS

Synthesis of MESS. A novel heterogeneous bifunctional reagent containing an ester bond, MESS, was synthesized by a three-step procedure using (methoxycarbonyl)maleimide (NMCM) as the starting material. The reactions involved the displacement of the carbomethoxy group to a hydroxyethyl group in the presence of carbonate, followed by the formation of an ester bond of the hydroxy group with acid anhydride, and finally the activation of carboxylic acid to a succinimido ester (Scheme I). Each isolated product was characterized by ^{1}H NMR measurement and elemental analysis.

Preparation of the IgG–MESS–DFO Conjugate. Conjugation of nonspecific human IgG with SDF via ester bonding was carried out with MESS, as shown in Scheme II. A large excess of the reaction mixture of MESS and DFO (approximately a 7 molar excess of maleimide to thiol) was added to the freshly thiolated IgG solution, followed by purification using gel-permeation chromatography. DFO-conjugated IgG with a nonmetabolizable linkage, IgG–EMCS–DFO, was also prepared by using EMCS instead of MESS (Scheme II).

Radiolabeling of the Conjugates. Both ^{67}Ga–DFO–MESS–IgG and ^{67}Ga–DFO–EMCS–IgG formed chelates with ^{67}Ga, showing a good efficiency and reproducibility (more than 95% radiochemical yield and purity when analyzed by size-exclusion HPLC). Figure 1 shows the size-exclusion HPLC elution profile of ^{67}Ga–DFO–MESS–IgG. A single elution peak of radioactivity superimposed on the spectrophotometric elution curve was registered at 280 nm for the conjugate as well as for the parent protein. ^{67}Ga–DFO–EMCS–IgG showed an identical HPLC profile under the same analytical conditions. On the other hand, HPLC analysis of ^{67}Ga-labeled IgG prepared from un-

Scheme II



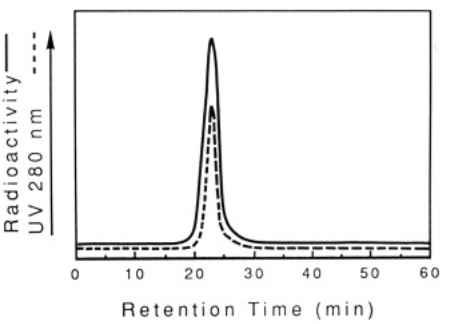


Figure 1. HPLC elution profiles of ^{67}Ga–DFO–MESS–IgG, as detected by radioactivity (—) and UV absorption at 280 nm (- -). Size-exclusion column chromatography (TSK G3000SW, 7.5 × 600 mm) was followed by elution with 0.1 M PBS (pH 6.8) at a flow rate of 0.5 mL/min.

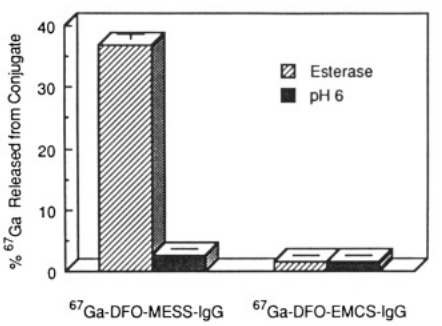


Figure 2. Release of radioactivity from ^{67}Ga–DFO–MESS–IgG and ^{67}Ga–DFO–EMCS–IgG in the presence or absence of carboxyesterase after 6 h of incubation at 37 °C (mean and 1 SD from triplicate experiments).

thiolated IgG and MESS–DFO or EMCS–DFO did not show any ^{67}Ga radioactivity in the IgG fraction. Both SDF and DFO instantly formed chelates with ^{67}Ga upon mixing, with quantitative yields being obtained.

Hydrolysis of ^{67}Ga–DFO–MESS–IgG. ^{67}Ga–DFO–MESS–IgG released a significant amount of radioactivity (37%) in the presence of esterase, while less than 5% of the radioactivity was released from the same conjugate in the absence of esterase, or from ^{67}Ga–DFO–EMCS–IgG in the presence or absence of esterase (Figure 2). Figure 3 shows the reverse-phase HPLC radioactivity profile of ^{67}Ga–DFO–MESS–IgG after esterase hydrolysis, followed by deproteinization (left). For comparison, the HPLC radioactivity profiles of ^{67}Ga–SDF (solid line) and ^{67}Ga–DFO (broken line) are also shown. The metabolic product

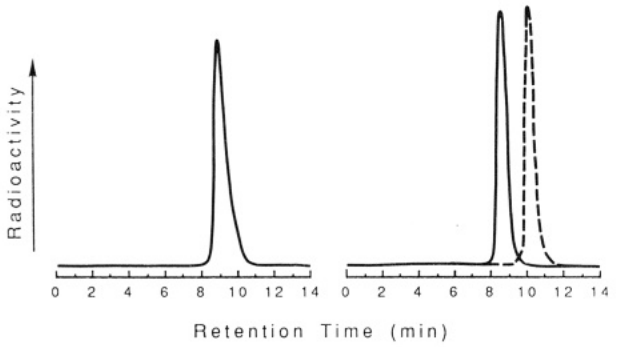


Figure 3. Reverse-phase HPLC elution profiles of the metabolic product of ^{67}Ga–DFO–MESS–IgG in the presence of carboxyesterase (left), as well as profiles for ^{67}Ga–SDF (—) and ^{67}Ga–DFO (- -) (right).

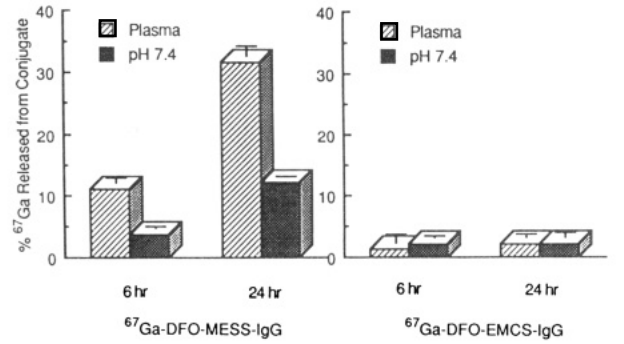


Figure 4. Release of radioactivity from ^{67}Ga–DFO–MESS–IgG and ^{67}Ga–DFO–EMCS–IgG in murine plasma or in Tris buffer (20 mM, pH 7.4) after 6 and 24 h of incubation at 37 °C (mean and 1 SD from triplicate experiments).

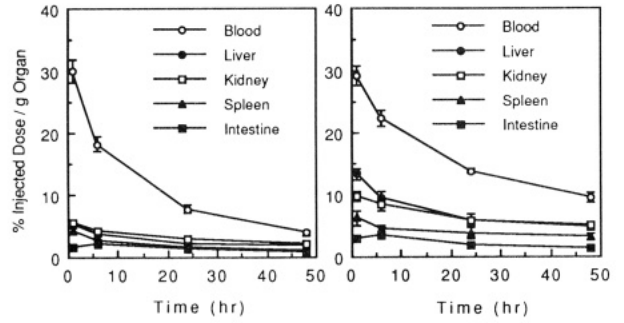


Figure 5. Biodistribution of radioactivity in mice after injection of ^{67}Ga–DFO–MESS–IgG (left) and ^{67}Ga–DFO–EMCS–IgG (right). The data were obtained from five mice per time point and are expressed as the percentage of the injected dose per gram organ (mean and 1 SD).

was a single component that had the same retention time as ^{67}Ga–SDF (8.6 min). EP analysis of the metabolite also showed a single zone of radioactivity corresponding to the ^{67}Ga–SDF fraction, with nondetectable radioactivity in the ^{67}Ga–DFO fraction. Release of radioactivity from ^{67}Ga–DFO–MESS–IgG was observed following incubation in murine plasma (Figure 4). In this experiment, ^{67}Ga–DFO–MESS–IgG generated three times higher radioactivity than ^{67}Ga–DFO–MESS–IgG at pH 7.4. Under the same conditions, the release of radioactivity from ^{67}Ga–DFO–EMCS–IgG was less than 3%.

Biodistribution of ^{67}Ga-Labeled Antibodies in Mice. The biodistribution of radioactivity after the intravenous injection of ^{67}Ga–DFO–MESS–IgG and ^{67}Ga–DFO–EMCS–IgG is shown in Figure 5. Faster clearance of radioactivity from the blood and less accumulation of radioactivity in the liver, kidney, and spleen was demonstrated by ^{67}Ga–DFO–MESS–IgG when compared with ^{67}Ga–DFO–EMCS–IgG. At 24 h after the injection of ^{67}Ga–DFO–MESS–IgG, 25.85% (±2.37, five mice) of the radioactivity was excreted in the urine.

DISCUSSION

In the conjugation of antibodies with metallic radiochelates via a metabolizable linkage, use of an ester bond as the link seems to be rational due to the high carboxyesterase activity levels in the liver and kidney, where the major nonspecific localization of radioactivity is observed (*23*). To conjugate antibodies with a radiochelate via ester bonding, a bifunctional reagent containing an ester bond is required due to the difficulty of directly esterifying antibodies. Ethylene glycol bis(succinimidylsuccinate) (EGS) is the only reagent currently available from a commercial source (*24*). This reagent, however, has homogeneous coupling sites along with two ester bonds per molecule, which might induce the formation of intermolecular and/or intramolecular cross-linking of antibodies as well as the formation of two metabolites upon hydrolysis. Cross-linking of antibodies has been reported to be responsible for enhanced nontarget radioactivity accumulation (*8*), and the production of two metabolites may cause problems in understanding and evaluating the resulting radioactivity distribution in vivo.

In the present study, we used ^{67}Ga–SDF as the radiochelate of choice and designed a way to release it from the antibody as a single metabolite by the action of carboxyesterase. ^{67}Ga–SDF consists of a neutral ^{67}Ga chelate along with a carboxylic acid, and this chelate has been reported to have the same urinary excretion mechanism as that of *o*-iodohippuran (OIH) (*16*). The high kinetic stability of ^{67}Ga-DFO has also been indicated by previous studies (*11*, *12*, *25*, *26*). In addition, DFO has been reported to be a useful reagent to remove ^{67}Ga and ^{59}Fe from the liver (*27–29*). These chemical and biological characteristics of ^{67}Ga–DFO and ^{67}Ga–SDF seem to favor their membrane transport from nontarget organs into the circulation and their subsequent urinary excretion.

Since SDF is synthesized by the succinylation of DFO, the production of MESS involved the succinylation of HEM and activation of the carboxylic acid of MEHS to a succinimido ester in order to generate a maleimide derivative of SDF through a ester bonding. Conjugation of this intermediate with freshly thiolated antibody was then carried out with maleimide thiol chemistry. The heterogeneous function of the two coupling sites in MESS afforded a ^{67}Ga–DFO–MESS–IgG conjugate without inducing intermolecular cross-linking of the protein (Figure 1), as was also seen in the preparation of the ^{67}Ga–DFO–EMCS–IgG conjugate (*11*, *12*). Under the conditions we used, only the thiol groups of IgG reacted with the MESS or EMCS derivatives; a control study using unthiolated IgG demonstrated that the alkylation of the lysine residues was negligible or nonexistent.

HPLC and EP analyses indicated that ^{67}Ga–DFO–MESS–IgG generated ^{67}Ga–SDF as its only metabolite via the action of carboxyesterase. Release of radioactivity from the conjugate was also observed in the plasma incubation study, suggesting the participation of plasma esterases (Figure 4). The relatively slow hydrolysis of the conjugate might have been due to the steric interference of the bulky IgG molecule and/or alkylation of another thiol group of the conjugate generated during the DTT reduction process, since rapid hydrolysis of ester bonds has previously been reported for some low molecular weight compounds (*30*, *31*). Although further studies of antibody thiolation chemistry are required, the high in vitro stability

of ^{67}Ga–DFO–EMCS–IgG in the presence of esterase and in plasma also indicated that selective hydrolysis of the ester bond of ^{67}Ga–DFO–MESS–IgG occurred by the action of esterase (Figures 2 and 4), since the only difference between the two preparations was the presence or absence of an ester bond.

In vivo studies were carried out with non-tumor-bearing mice to eliminate tumor-related variables such as changes in enzyme activity levels. Nonspecific human IgG was injected into mice in the reverse of the present clinical situation where murine antibodies are injected into humans. Study of the biodistribution of radioactivity from the two preparations indicated the faster clearance of ^{67}Ga–DFO–MESS–IgG from the blood with less localization of radioactivity in the liver, kidney, and spleen than was observed with ^{67}Ga–DFO–EMCS–IgG (Figure 5). These results were presumably due to the hydrolysis of the ester bond of ^{67}Ga–DFO–MESS–IgG in the plasma as well as in the liver, kidney, and spleen. These properties of ^{67}Ga–DFO–MESS–IgG appear to be advantageous for allowing a higher target to nontarget ratio in a short time postinjection. Studies are currently being performed in nude mice to assess this radioimmunoconjugate for diagnosis and therapy from the standpoint of target to nontarget ratios as well as the amount of radioactivity accumulated in the target.

In conclusion, the present study indicates that MESS can achieve the conjugation of ^{67}Ga–SDF with an antibody without inducing intramolecular cross-linking of the protein. It also showed the ability of MESS to release ^{67}Ga–SDF as the sole metabolite from the conjugate by hydrolysis of the ester bond. MESS may also be useful for the evaluation of chemical and biological properties of various chelating agents that are used for the preparation of radioimmunoconjugates.

ACKNOWLEDGMENT

We thank Ciba-Geigy Ltd., Takarazuka, Japan, and Nihon Medi-Physics Co. Ltd., Takarazuka, Japan, for providing ferrioxamine B hydrochloride and $^{67}GaCl_3$, respectively. This work was supported in part by a Grant-in-Aid for Developmental Scientific Research (No. 02771684) from the Ministry of Education, Science and Culture of Japan.

LITERATURE CITED

(1) Halpern, S. E., Hagan, P. L., Garver, P. R., Koziol, J. A., Chen, A. W. N., Frincke, J. M., Bartholomew, R. M., David, G. S., and Adams, T. H. (1983) Stability, characterization, and kinetic of ^{111}In-labeled monoclonal antitumor antibodies in normal animals and nude mouse-human tumor models. *Cancer Res. 43*, 5347–5355.

(2) Khaw, B. A., Strauss, H. W., Cahill, S. J., Soule, H. R., Edgington, T., and Cooney, J. (1984) Sequential imaging of indium-111-labeled monoclonal antibody in human mammary tumors hosted in nude mice. *J. Nucl. Med. 25*, 592–603.

(3) Khaw, B. A., Cooney, J., Edgington, T., and Strauss, H. W. (1986) Differences in experimental tumor localization of dual-labeled monoclonal antibody. *J. Nucl. Med. 27*, 1293–1299.

(4) Endo, K., Sakahara, H., Nakashima, T., Koizumi, M., Ohta, H., Kawamura, Y., Kunimatsu, M., Furukawa, T., Ohmomo, Y., Arano, Y., Nakamura, T., Tanaka, H., Kotoura, Y., Yamamuro, T., Hosoi, S., Toyama, S., Yokoyama, A., and Torizuka, K. (1987) Preparation and properties of antitumor monoclonal antibodies labeled with metallic radionuclides indium-111, gallium-67, and technetium-99m. *NCI Monogr. 3*, 135–140.

(5) Brown, B. A., Comeau, R. D., Jones, P. L., Liberatore, F. A., Neacy, W. P., Sands, H., and Gallagher, M. (1987) Pharmacokinetics of the monoclonal antibody B72.3 and its fragments labeled with either I-125 or In-111. *Cancer Res. 47*, 1149–1154.

(6) Larson, S. M., Carrasquillo, J. A. (1988) Advantageous of radioiodine over radioindium labeled monoclonal antibodies for imaging solid tumor. *Nucl. Med. Biol. 15*, 231–233.

(7) Koizumi, M., Endo, K., Watanabe, Y., Saga, T., Sakahara, H., Konishi, J., Yamamuro, T., and Toyama, S. (1989) Pharmacokinetics of internally labeled monoclonal antibodies as a gold standard: comparison of biodistribution of Se-75, In-111, and I-125-labeled monoclonal antibodies in osteogenic sarcoma xenografts in nude mice. *Cancer Res. 49*, 1752–1757.

(8) Carney, P. L., Rogers, P. E., and Johnson, D. K. (1989) Dual isotope study of iodine-125 and indium-111-labeled antibody in athymic mice. *J. Nucl. Med. 30*, 374–384.

(9) Yokoyama, K., Carrasquillo, J. A., Chang, A. E., Colcher, D., Roselli, M., Sugarbaker, P., Sindelar, W., Reynolds, J. C., Perentesis, P., Gansow, O. A., Francis, B., Adams, R., Finn, R., Schlom, J., and Larson, S. M. (1989) Differences in biodistribution of indium-111- and iodine-131-labeled B72.3 monoclonal antibodies in patients with colorectal cancer. *J. Nucl. Med. 30*, 320–327.

(10) Haseman, M. K., Goodwin, D. A., Meares, C. F., Kaminski, M. S., Wensel, T. G., McCall, M. J., and Levy, R. (1986) Metabolizable In-111 chelate conjugated anti-idiotype monoclonal antibody for radioimmunodetection of lymphoma in mice. *Eur. J. Nucl. Med. 12*, 455–460.

(11) Koizumi, M., Endo, K., Kunimatsu, M., Sakahara, H., Nakashima, T., Kawamura, Y., Watanabe, Y., Ohmomo, Y., Arano, Y., Yokoyama, A., and Torizuka, K. (1987) Preparation of Ga-67 labeled antibodies using deferoxamine as a bifunctional chelate: an improved method. *J. Immunol. Methods 104*, 93–102.

(12) Koizumi, M., Endo, K., Kunimatsu, M., Sakahara, H., Nakashima, T., Kawamura, Y., Watanabe, Y., Saga, T., Konishi, J., Yamamuro, T., Hosoi, S., Toyama, S., Arano, Y., and Yokoyama, A. (1988) 67-Ga-labeled antibodies for immunoscintigraphy and evaluation of tumor targeting of drug-antibody conjugate in mice. *Cancer Res. 48*, 1189–1194.

(13) Paik, C. H., Quadri, S. M., and Reba, R. (1989) Interposition of different chemical linkage between antibody and In-111–DTPA to accelerate clearance from non-target organs and blood. *Nucl. Med. Biol. 16*, 475–481.

(14) Deshpande, S. V., DeNardo, S. J., Meares, C. F., McCall, M. J., Adams, G. P., and DeNardo, G. L. (1989) Effect of different linkage between chelates and monoclonal antibodies on levels of radioactivity in the liver. *Nucl. Med. Biol. 16*, 587–597.

(15) Paik, C. H., Yokoyama, K., Reynolds, J. C., Quadri, S. M., Min, C. Y., Shin, S. Y., Maloney, P. J., Larson, S. M., and Reba, R. C. (1989) Reduction of background activities by introduction of a diester linkage between antibody and a chelate in radioimmunodetection of tumor. *J. Nucl. Med. 30*, 1693–1701.

(16) Herscheid, J. D., Hoekstra, A., and Vos, C. M. (1984) *N*-succinyldeferoxamine B: a potential radiopharmaceutical for assessing renal function. *Eur. J. Nucl. Med. 9*, 508–510.

(17) Keller, O., and Rudinger, J. (1975) Preparation and some properties of maleimido acids and maleoyl derivatives of peptides. *Helv. Chim. Acta 58*, 531–541.

(18) Miyadera, T., Kosower, E. M., and Kosower, N. S. (1971) Receptor site labeling through functional groups. Barbital and amphetamine derivatives. *J. Med. Chem. 14*, 873–878.

(19) Yamada, M., Takase, I., Hayashi, K., Hashimoto, Y., and Komiya, Y. (1964) Synthesis and polymerization of unsaturated dibasic acid derivatives. *Yuki Gosei Kagaku Kyokai Shi 23*, 166–170; *Chem. Abstr.* (1965) *63*, 489.

(20) Tawney, P. O. (1964) *Chem. Abstr. 33* 15742*f*.

(21) Carlsson, J., Drevin, H., and Axen, R. (1978) Protein thiolation and reversible protein–protein conjugate. *Biochem. J. 173*, 723–737.

(22) Imai, S., Morimoto, J., Tsubura, T., Esaki, K., Michalides, R., Holmes, R. S., Deimling, O., and Hilgers, J. (1986) Genetic maker patterns and endigenous mammary tumor virus genes in inbred mouse strains in Japan. *Exp. Anim. 35*, 263–273.

(23) Heymann, E. (1982) Hydrolysis of carboxylic ester and amides. In *Metabolic Basis of Detoxification: Metabolism of Functional Groups* (W. B. Jakoby, J. R. Bend, and J. Caldwell, Eds.) pp 229–241, Academic Press, New York.

(24) Abdella, P. M., Smith, P. K., and Royer, G. P. (1979) A new cleavable reagent for cross-linking and reversible immobilization of protein. *Biochem. Biophys. Res. Commun. 87*, 734–742.

(25) Weiner, R. E., Thakur, M. L., Goodman, M., and Hoffer, P. B. (1979) Relative stability of In-111 and Ga-67 desferrioxamine and human transferrin complexes. In *Radiopharmaceuticals II: Proceeding of the 2nd International Symposium on Radiopharmaceuticals* (D. R. Hoogland, D. R. Allen, and R. D. Ice, Eds.) pp 331–340, The Society of Nuclear Medicine, New York.

(26) Yokoyama, A., Ohmomo, Y., Horiuchi, K., Saji, H., Tanaka, H., Yamamoto, K., Ishii, Y., and Torizuka, K. (1982) Deferoxamine, a promising bifunctional chelating agent for labeling proteins with gallium: 67-Ga DF-HSA. *J. Nucl. Med. 23*, 909–914.

(27) Hershko, C., Cook, J. D., and Finch, C. A. (1973) Storage iron kinetics. III. Study of deferrioxamine action by selective radioiron labels of RE and parenchmal cells. *J. Lab. Clin. Med.* 876–886.

(28) Emergy, T., and Hoffer, P. B. (1980) Siderophore-mediated mechanism of gallium uptake demonstrated in the microorganism ustilgo sphaerogena. *J. Nucl. Med. 21*, 935–939.

(29) Ward, M. C., Roberts, K. R., Westwood, J. H., Coombes, R. C. C., and McCready, V. R. (1986) The effect of chelating agents on the distribution of monoclonal antibodies in mice. *J. Nucl. Med. 27*, 1746–1750.

(30) Dannals, R. F., Burns, H. D., Marzilli, L. G., Tragester, T. C., and Wagner, H. N., Jr. (1981) Radiolabeled benzoylcholine derivatives as possible myocardial-imaging agents. *J. Pharm. Sci. 70*, 439–442.

(31) Ohmomo, Y., Okuyama, S., Magata, Y., Ueno, Y., Tanaka, C., and Yokoyama, A. (1989) Radioiodinated phenoxyacetic acid derivatives as potential brain imaging agents. II. Structure–biodistribution relationship. *Chem. Pharm. Bull. 37*, 2282–2286.

Registry No. HEM, 1585-90-6; NMCM, 55750-48-6; MEHS, 13595-10-3; MESS, 132774-52-8; SPDP, 84891-69-0; succinic anhydride, 108-30-5; *N*-hydroxysuccinimide, 6066-82-6; dicyclohexylcarbodiimide, 538-75-0; carboxyesterase, 9016-18-6.

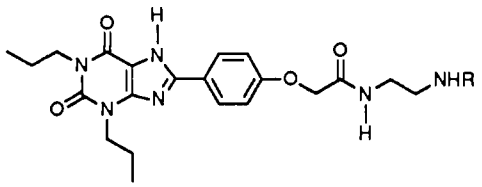
Trifunctional Agents as a Design Strategy for Tailoring Ligand Properties: Irreversible Inhibitors of A_1 Adenosine Receptors†

Daniel L. Boring,‡ Xiao-Duo Ji,‡ Jeff Zimmet,‡ Kirk E. Taylor,‡ Gary L. Stiles,§ and Kenneth A. Jacobson*,‡

Laboratory of Bioorganic Chemistry, National Institute of Diabetes, and Digestive and Kidney Diseases, National Institutes of Health, Bethesda, Maryland 20892, and Departments of Medicine and Biochemistry, Duke University Medical Center, Durham, North Carolina 27710. Received November 29, 1990

The 1,3-phenylene diisothiocyanate conjugate of XAC (8-[4-[[[[(2-aminoethyl)amino]carbonyl]methyl]-oxy]phenyl]-1,3-dipropylxanthine, a potent A_1 selective adenosine antagonist) has been characterized as an irreversible inhibitor of A_1 adenosine receptors. To further extend this work, a series of analogues were prepared containing a third substituent in the phenyl isothiocyanate ring, incorporated to modify the physiochemical or spectroscopic properties of the conjugate. Symmetrical trifunctional cross-linking reagents bearing two isothiocyanate groups were prepared as general intermediates for cross-linking functionalized congeners and receptors. Xanthine isothiocyanate derivatives containing hydrophilic, fluorescent, or reactive substituents, linked via an amide, thiourea, or methylene group in the 5-position, were synthesized and found to be irreversible inhibitors of A_1 adenosine receptors. The effects of the 5-substituent on water solubility and on the A_1/A_2 selectivity ratio derived from binding assays in rat brain membranes were examined. Inhibition of binding of [^{3}H]-N^6-(2-phenylisopropyl)-adenosine and [^{3}H]CGS21680 (2-[[2-[4-(2-carboxyethyl)phenyl]ethyl]amino]adenosine-5′-N-ethylcarboxamide) at central A_1 and A_2 adenosine receptors, respectively, was measured. A conjugate of XAC and 1,3,5-triisothiocyanatobenzene was 894-fold selective for A_1 receptors. Reporter groups, such as fluorescent dyes and a spin-label, were included as chain substituents in the irreversibly binding analogues, which were designed for spectroscopic assays, histochemical characterization, and biochemical characterization of the receptor protein.

Adenosine acts as a neuromodulator at two receptor subtypes, A_1 and A_2, which in general inhibit or stimulate adenylate cyclase, respectively (*1*, *2*). Selective agonists (*3*, *4*) and antagonists (*5*, *6*) of each receptor subtype have been reported. The high-affinity, A_1-selective antagonist XAC[1] (1), a 1,3-dipropylxanthine derivative that contains



1: R = H

2: R = CSNH– (NCS)

3: R = CSNH– (NCS)

an amine-functionalized chain, was developed by using a functionalized congener approach (*5*). XAC having a K_i value at rat brain A_1 receptors of 1.2 nM has been useful in characterizing the A_1 adenosine receptor both as a radioligand (*7*) and as a ligand immobilized via its alkyl amino group for affinity chromatography of the receptor protein (*8*, *9*). The *m*- and *p*-phenylene diisothiocyanate conjugates of XAC [*m*-DITC-XAC[2] (2) and *p*-DITC-XAC[3] (3)], were prepared as high-affinity, irreversible A_1 antagonists, with apparent K_i values at rat brain A_1 receptors of 2.4 and 6.6 nM, respectively (*10*, *11*). These chemically reactive ligands have been used for identifying the A_1 receptor on electrophoretic gels (*11*) and for blocking A_1 receptor mediated effects in physiological studies (*12*).

A general approach to systematically modifying the structure of irreversible ligand derivatives was desired to provide analogues with specific properties. In previous studies of reversible ligands bearing spectroscopic labels (*13*), only moderate receptor affinities were attained, and this limited the utility of the ligands for histochemical studies. A spectroscopic probe that binds irreversibly to the receptor would preclude the problems of rapid washout and long equilibration times associated with reversible ligands. Another difficulty encountered with 8-phenylxanthine derivatives in physiological studies (*12*) is their typically low water solubility (*14*). In this study, we explore a conceptually broad synthetic methodology that permits the incorporation of a reporter group (spin-label, radioligand, fluorescent, etc.) or of a group for altering physical properties, such as water solubility, into an irreversible inhibitor.

Figure 1 presents an overview of our trifunctional strategy. The essential feature of this plan is a cross-linking reagent (4), a 1,3,5-substituted benzene that includes three potentially reactive sites. These sites are (1) an acylating group for reaction with a functionalized

† Presented in part at the American Chemical Society, 200th National Meeting, August 26–31, 1990, Washington, DC, Abstract MEDI 43.

‡ NIH.

§ Duke University Medical Center.

[1] 8-[4-[[[[(2-Aminoethyl)amino]carbonyl]methyl]oxy]phenyl]-1,3-dipropylxanthine.

[2] 8-[4-[[[[[2-[[[(3-Isothiocyanatophenyl)amino](thiocarbonyl)]-amino]ethyl]amino]carbonyl]methyl]oxy]phenyl]-1,3-dipropylxanthine.

[3] 8-[4-[[[[[2-[[[(4-Isothiocyanatophenyl)amino](thiocarbonyl)]-amino]ethyl]amino]carbonyl]methyl]oxy]phenyl]-1,3-dipropylxanthine.

1043-1802/91/2902-0077$02.50/0 © 1991 American Chemical Society

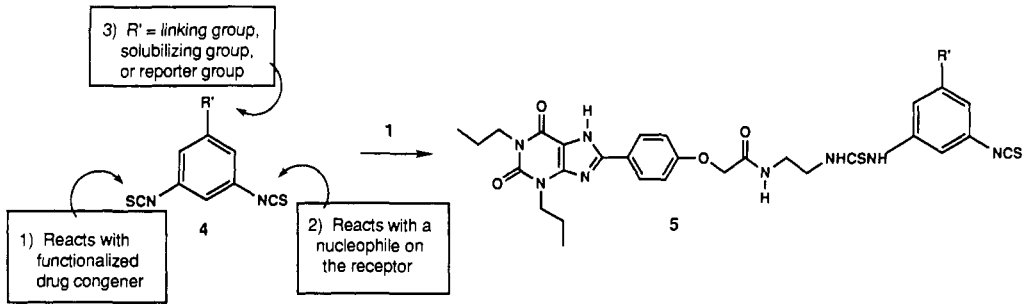


Figure 1. Synthesis of a class of irreversibly binding, high-affinity A_1 adenosine receptor antagonists (**5**) derived from trifunctional cross-linking reagents (**4**) present in molar excess.

congener, in this case the acylating group consisting of an isothiocyanate group to react with the primary amino group of xanthine **1** to afford general structure **5**; (2) another chemically reactive electrophilic group, such as an isothiocyanate, to combine irreversibly with the receptor protein; and (3) a site for incorporating a solubilizing or reporter moiety (group R′ in Figure 1).

EXPERIMENTAL PROCEDURES

General Procedures. New compounds were characterized (and resonances assigned) by 300-MHz proton nuclear magnetic resonance spectroscopy using a Varian XL-300 FT-NMR spectrometer. The assignments, for a typical xanthine derivative, are specified below for compound **5m**. Unless noted, chemical shifts are expressed as ppm downfield from tetramethylsilane. Synthetic intermediates were characterized by ^{1}H NMR and by chemical ionization mass spectroscopy (CIMS, NH_3) using a Finnigan 1015 mass spectrometer modified with EXTREL electronics or on a Finnigan 4500 MS. Accurate mass (using fast atom bombardment) was measured on a JEOL SX102 high-resolution mass spectrometer. Melting points were determined on a Thomas-Hoover melting point apparatus and are uncorrected. C, H, and N analysis was carried out by Atlantic Microlabs (±0.4% acceptable). The Chromatotron is a radially accelerated thin-layer chromatography device manufactured by Harrison Research, Palo Alto, CA. [^{3}H]-N^6-(Phenylisopropyl)adenosine and [^{3}H]-5′-(*N*-ethylcarbamoyl)adenosine were from Du Pont NEN Products, Boston, MA. N^6-Cyclopentyladenosine and XAC (**1**) were obtained from Research Biochemicals, Inc., Natick, MA. 3,5-Dinitroaniline and 2,6-diaminopyridine were obtained from Lancaster Synthesis (Windham, NH). 3,5-Dinitrobenzoyl chloride and 3,5-dinitrobenzamide were obtained from Aldrich Chemical Co. (Milwaukee, WI). 4-[[4-(Fluoromethyl)benzoyl]amino]-butylamine was synthesized as described (15). 5-[(2-Aminoethyl)thioureidyl]fluorescein was obtained from Molecular Probes, Inc. (Eugene, OR).

General Method for Coupling XAC with Diisothiocyanates. XAC (25 mg, 58.4 μM) was suspended in 0.5 mL of dimethylformamide, and a 3 molar excess of the requisite diisothiocyanate was added. This was sonicated for 3–5 min, during which time complete dissolution occurred. The reaction was monitored by HPLC (UV detection at 254 nm) for disappearance of XAC and was complete within 5 min. With a gradient mixture of 20–60% acetonitrile and water containing 0.1% TFA[4] over 20 min, the retention time for XAC was 4 min (Altex Ultrasphere ODS column, 4.6 mm × 25 cm). The conjugates were retained much longer than XAC (roughly 20 min). After XAC had disappeared from the reaction, either ethyl acetate or ether was added to precipitate the product. This precipitate was collected by centrifugation and was washed three times with fresh ether. The solid material was then dried overnight in vacuo at 50 °C.

8-[4-[[[[[2-[[[5-(Ethoxycarbonyl)-3-isothiocyanatophenyl](thiocarbonyl)]amino]ethyl]amino]carbonyl]methyl]oxy]phenyl]-1,3-dipropylxanthine (5a) was synthesized by the above method from compound **26**. The product was homogeneous by TLC (R_f = 0.73, silica, chloroform/methanol/acetic acid 85/10/5; NMR (DMSO[5]-d_6) δ 8.30 (s, 1 H), 8.05 (d, 2 H, J = 8.5 Hz), 7.92 (s, 2 H), 7.55 (s, 1 H), 7.08 (d, 2 H, J = 8.5 Hz), 4.57 (s, 2 H), 4.30 (q, 2 H), 4.00 and 3.86 (each m, 2 H), 1.75 and 1.57 (each m, 2 H), 1.30 (t, 3 H), 0.90 (m, 6 H) ppm.

8-[4-[[[[[2-[[[5-(Hydroxymethyl)-3-isothiocyanatophenyl](thiocarbonyl)]amino]ethyl]amino]carbonyl]methyl]oxy]phenyl]-1,3-dipropylxanthine (5b) was synthesized by the above method from compound **28**: NMR (DMSO-d_6) δ 8.31 (m, 1 H), 8.07 (d, 2 H, J = 8.7 Hz), 7.48 (s, 1 H), 7.24 (s, 1 H), 7.10 (d, 2 H, J = 8.7 Hz), 7.06 (s, 1 H), 4.58 (s, 2 H), 4.47 (s, 2 H), 4.01 and 3.86 (each m, 2 H), 1.74 and 1.58 (each m, 2 H), 0.90 (m, 6 H) ppm.

The following compounds were synthesized by the above method from structure **14** or **19**.

8-[4-[[[[[2-[[[5-(Aminocarbonyl)-3-isothiocyanatophenyl](thiocarbonyl)]amino]ethyl]amino]carbonyl]methyl]oxy]phenyl]-1,3-dipropylxanthine (5c): mp >250 °C; NMR (DMSO-d_6) δ 8.33 (m, 1 H), 8.06 (m, 3 H), 7.75, 7.61, and 7.55 (each s, 1 H), 7.10 (d, 2 H, J = 8.8 Hz), 4.58 (s, 2 H), 4.01 and 3.87 (each m, 2 H), 1.75 and 1.58 (each m, 2 H), 0.90 (m, 6 H) ppm. Accurate mass (FAB) consistent with assigned structure.

8-[4-[[[[[2-[[[5-[[[2-(Dimethylamino)ethyl]amino]carbonyl]-3-isothiocyanatophenyl](thiocarbonyl)]amino]ethyl]amino]carbonyl]methyl]oxy]phenyl]-1,3-dipropylxanthine (5d): mp >250 °C; NMR (DMSO-d_6) δ 8.35 (m, 1 H), 8.05 (d, 2 H, J = 8.6 Hz), 7.85–7.60 (m, 3 H), 7.10 (d, 2 H, J = 8.6 Hz), 4.60 (s, 2 H), 4.0 (m, 4 H), 3.85 (m, 4 H), 2.50 (s, 6 H), 1.74 and 1.58 (each m, 2 H), 0.90 (m, 6 H) ppm.

8-[4-[[[[[2-[[[5-[[[2-(Acetylamino)ethyl]amino]carbonyl]-3-isothiocyanatophenyl](thiocarbonyl)]amino]ethyl]amino]carbonyl]methyl]oxy]phenyl]-1,3-dipropylxanthine (5e): mp >250 °C; NMR (DMSO-d_6) δ 8.55 (m, 1 H), 8.05 (d, 2 H, J = 8.4 Hz), 7.90 (s, 2 H), 7.80 (s, 1 H), 7.08 (d, 2 H, J = 8.4 Hz), 4.50 (s, 2 H), 4.0 (m, 4 H), 3.80 (m, 4 H), 1.95 (s, 3 H), 0.90 (m, 6 H); IR 2100 (isothiocyanate), 1680 (C=O), and 1650 cm^{-1} (C=S).

8-[4-[[[[[2-[[[5-[[[2-(Dimethylamino)ethyl]amino](thiocarbonyl)]amino]-3-isothiocyanatophenyl](thiocarbonyl)]amino]ethyl]amino]carbonyl]methyl]oxy]phenyl]-1,3-dipropylxanthine (5f): mp >250 °C; NMR (DMSO-d_6) δ 8.35 (m, 1 H), 8.10 (d, 2 H, J = 8.7 Hz), 7.60–7.20 (m, 3 H), 7.10 (d, 2 H, J = 8.7 Hz), 4.55 (s, 2 H), 4.05 and 3.90 (each m, 2 H), 3.65 (m, 2 H), 2.60 (m, 2 H), 2.30 (s, 6 H), 1.75 and 1.60 (each m, 2 H), 0.9 (m, 6 H) ppm.

[4] Trifluoroacetic acid.

[5] Dimethyl sulfoxide.

8-[4-[[[[[2-[[[5-[[[[2-(Acetylamino)ethyl]amino]-(thiocarbonyl)]amino]-3-isothiocyanatophenyl]-(thiocarbonyl)]amino]ethyl]amino]carbonyl]methyl]oxy]phenyl]-1,3-dipropylxanthine (5g): mp >250 °C; NMR (DMSO-d_6) δ 8.35 (m, 1 H), 8.09 (d, 2 H, J = 8.7 Hz), 7.55–7.25 (m, 3 H), 7.10 (d, 2 H, J = 8.7 Hz), 4.60 (s, 2 H), 4.05 and 3.90 (each m, 2 H), 3.50 (m, 4 H), 1.80 and 1.62 (each m, 2 H), 0.9 (m, 6 H) ppm.

8-[4-[[[[[2-[[[5-[[[2-[[3-(4-Hydroxyphenyl)propionyl]amino]ethyl]amino]carbonyl]-3-isothiocyanatophenyl](thiocarbonyl)]amino]ethyl]amino]carbonyl]methyl]oxy]phenyl]-1,3-dipropylxanthine (5m). XAC (24 mg, 56 μmol) and 3-[2-[[[2-[(3,5-diisothiocyanatobenzoyl)amino]ethyl]amino]carbonyl]ethyl]phenol (35 mg, 82 μmol) were suspended in 1 mL of dimethylformamide and sonicated until a solution formed. After 1 h, ether was added, and a precipitate formed. The product (**5m**) was recrystallized from dimethylformamide/ether to give 39.9 mg (83% yield): NMR (DMSO-d_6) δ 9.93 (s, 1 H, CSN*H*Ar), 9.12 (s, 1 H, ArO*H*), 8.36 (t, 1 H, NH of oxymethylamide), 8.55 and 7.93 (each t, 1 H, NH), 8.07 (d, 2 H, J = 8.6 Hz, 8-phenyl ring, meta to ether), 7.75 (m, 1 H, NH), 7.95, 7.77, and 7.58 (each s, 1 H, 2,4,6-aryl protons), 7.10 (d, 2 H, J = 8.6 Hz, 8-phenyl ring, ortho to ether), 6.96 (d, 2 H, J = 8.3 Hz, meta to phenol), 6.63 (d, 2 H, J = 8.3 Hz, ortho to phenol), 4.58 (s, 2 H, CH_2OAr), 4.01 and 3.87 (each m, 2 H, C α of Pr), 3.62 (br m, 2 H, CH_2NHCS), 3.2–3.4 (m, 6 H, CH_2NH), 2.68 (t, 2 H, CH_2 α to phenol ring), 2.29 (t, 2 H, CH_2 β to phenol ring), 1.75 and 1.60 (each m, 2 H, C β of Pr), 0.9 (m, 6 H, C γ or Pr) ppm.

8-[4-[[[[[2-[[[5-[[[[4-[[4-(Fluoromethyl)benzoyl]-amino]butyl]amino](thiocarbonyl)]amino]-3-isothiocyanatophenyl](thiocarbonyl)]amino]ethyl]amino]-carbonyl]methyl]oxy]phenyl]-1,3-dipropylxanthine (5r). Compound **22** (100 mg, 0.15 mmol) and 4-[[4-(fluoromethyl)benzoyl]amino]butylamine trifluoroacetate (31.4 mg, 0.10 mmol) were added to 0.5 mL of dimethylformamide with stirring, followed by the addition of 14 μL of triethylamine. After stirring overnight at room temperature, the mixture was applied to a semipreparative thin-layer chromatography plate (silica, 1000 microns, Analtech, Newark, DE) and chromatographed with a mixture of chloroform/methanol/acetic acid (90/10/1, by volume). A major band was identified as homogeneous product by TLC, NMR, and IR: yield 20 mg (22%). A californium plasma desorption spectra (positive ions) showed peaks at m/z 956.8 (M + H + 2 Na), 924.8 (M + H + Na), 505.1, 447.2, and 389.2.

8-[4-[[[[[2-[[(3,5-Diisothiocyanatophenyl)(thiocarbonyl)]amino]ethyl]amino]carbonyl]methyl]oxy]-phenyl]-1,3-dipropylxanthine (22): was synthesized by the above method from compound **21**: mp >250 °C; NMR (DMSO-d_6) δ 8.30 (m, 1 H), 8.05 (d, 2 H, J = 8.5 Hz), 7.46 (s, 2 H), 7.24 (s, 1 H), 7.09 (d, 2 H, J = 8.5 Hz), 4.58 (s, 2 H), 4.01 (m, 2 H), 3.87 (m, 2 H), 1.74 (m, 2 H), 1.58 (m, 2 H), 0.90 (m, 6 H) ppm. Accurate mass (FAB) consistent with the assigned structure.

3,5-Bis[(*tert*-butyloxycarbonyl)amino]benzoic Acid (6). 3,5-Diaminobenzoic acid dihydrochloride (10 g, 44 mmol) was added to 120 mL of 1 M aqueous sodium hydroxide. Methanol (60 mL) was added. Di-*tert*-butyl dicarbonate (19 g, 87 mmol) dissolved in 15 mL of methanol was added to the diamine with stirring. After 12 h, the reaction was acidified with citric acid and extracted with ethyl acetate. The organic layer was dried (Na_2SO_4) and the solvent evaporated. Addition of ether to the residue resulted in the precipitation of salts, which were removed by filtration. The ether solution was extracted with cold 1 N HCl. After separation, the organic solvent was evaporated in vacuo, leaving a white solid: yield 9.65 g (62%); mp 113–116 °C.

Methyl 3,5-Bis[(*tert*-butyloxycarbonyl)amino]benzoate (7). 3,5-Bis[(*tert*-butyloxycarbonyl)amino]benzoic acid (5.00 g, 14.2 mmol) was esterified in methanol using EDAC[6] (14.2 mmol) and 4-(dimethylamino)pyridine (2.4 mmol). After 2 h the product precipitated as a solid and was collected, washed with a small amount of methanol, and dried in vacuo. A second crop was collected, yielding a total of 3.64 g (70%) of product.

2-[[3,5-Bis[(*tert*-butyloxycarbonyl)amino]benzoyl]-amino]ethylamine (8). Methyl 3,5-bis[(*tert*-butyloxycarbonyl)amino]benzoate (1.98 g, 5.4 mmol) was dissolved in a minimum of ethylenediamine and allowed to react at room temperature for 3 days. Water was added, and the product (1.84 g, 86% yield) precipitated as a white solid.

***N*-Succinimidyl 3,5-Bis[(*tert*-butyloxycarbonyl)-amino]benzoate (9).** 3,5-Bis[(*tert*-butyloxycarbonyl)-amino]benzoic acid (350 mg, 1 mmol) and 230 mg (1.2 equiv) of EDAC were placed in 30 mL of CH_3CN, and the solution was stirred at room temperature for 1 h. To this was added 130 mg (1.2 equiv) of *N*-hydroxysuccinimide, and the mixture was stirred overnight. The mixture was diluted with 150 mL of ethyl acetate and washed with 100 mL of pH 4 NaH_2PO_4 (0.5 M). The solvent was removed on a rotary evaporator, and the residual solid was placed on a Chromatotron and eluted with ether/petroleum ether (1/1). The fractions containing the first band eluted were combined and evaporated to dryness to provide 301 mg (67%) of product: NMR (DMSO-d_6) δ 9.75 (s, 2 H), 7.98 (s, 1 H), 7.90 (s, 2 H), 3.35 (s, 4 H), 1.45 (s, 18 H) ppm.

4-[2-[[[2-[[3,5-Bis[(*tert*-butyloxycarbonyl)amino]-benzoyl]amino]ethyl]amino]carbonyl]ethyl]phenol (10b). 2-[[3,5-Bis[(*tert*-butyloxycarbonyl)amino]benzoyl]-amino]ethylamine (**8**, 185 mg, 0.47 mmol) and *N*-succinimidyl 3-(4-hydroxyphenyl)propionate (Fluka, 105 mg, 0.40 mmol) were dissolved with sonication in 2 mL of MeOH/dimethylformamide (1/1). After 1 h, 3 mL of water was added, and an oil separated. The resulting residue was purified by precipitation from ethyl acetate/hexanes resulting in 136 mg of product [63% yield; homogeneous by TLC (R_f = 0.60, silica, chloroform/methanol/acetic acid 85/10/5)].

4-[[2-[[3,5-Bis[(*tert*-butyloxycarbonyl)amino]ben-zoyl]amino]ethyl]amino]-7-nitrobenzofurazane (10g). Compound **8** (462 mg, 1.0 mmol) and 4-chloro-7-nitrobenzofurazane (NBD-Cl, 0.25 g, 1.25 mmol) were added to 50 mL of acetonitrile and stirred overnight. The resulting dark solution was reduced in volume by evaporation and filtered through silica gel to remove polar impurities. The filtrate was purified using a Chromatotron, eluting with ether to yield 0.34 g of the product as an orange solid (60% yield).

5-[[[[2-[[3,5-Bis[(*tert*-butyloxycarbonyl)amino]-benzoyl]amino]ethyl]amino](thiocarbonyl)]-amino]fluorescein (10h). Compound **8** (0.23 g, 0.5 mmol) and fluorescein isothiocyanate isomer 1 (0.23 g, 0.6 mmol) were added to a small vial followed by 1 mL of DMF, and the mixture was sonicated for 5 min. The resulting viscous solution was applied directly to four 20 × 20 cm preparative silica TLC plates (1000 μm) and chromatographed with ethyl acetate containing 1% acetic acid. The major band ($R_f \approx 0.6$) was removed and eluted with methanol. The extract was evaporated and crystallized from a mixture of methanol/ether/petroleum ether, leaving 0.20 g (51% yield) of **10h** as an orange solid. Fast atom bombardment (positive) mass spectroscopy showed peaks at m/z 806 (M + 1 + Na), 784 (M + 1), 622, 390, 223, 154.

[6] 1-Ethyl-3-[3-(dimethylamino)propyl]carbodiimide.

[[[(2-Dimethylamino)ethyl]amino]carbonyl]-3,5-dinitrobenzene (12b). *N,N*-Dimethylethylenediamine (2.2 mL) and triethylamine (5 mL) were dissolved in 100 mL of DME.[7] A solution of dinitrobenzoyl chloride (4.6 g, 20 mmol) in DME (25 mL) was added, and the mixture was stirred overnight. Sodium hydroxide (10%, 150 mL) was added and the mixture was extracted with a 1/1 mixture of ether/ethyl acetate. The combined organic extracts were evaporated to dryness, leaving 2.5 g (44%) yield of the product, an oil. A final purification was carried out with a Chromatotron, eluting with ethyl acetate/methanol (1/10). The product was homogeneous by TLC (R_f = 0.69, silica, chloroform/methanol/NH_4OH 60/40/2); NMR ($CDCl_3$) δ 9.15 (s, 1 H), 9.04 (s, 2 H), 3.60 (m, 2 H), 2.31 (s, 6 H) ppm; IR 1650 cm^{-1} (amide).

[[[2-(Trimethylammonio)ethyl]amino]carbonyl]-3,5-dinitrobenzene Iodide (12c). Compound **12b** (0.50 g, 1.77 mmol), methyl iodide (1.0 mL), and diisopropylethylamine (0.5 mL) were added to methanol (50 mL) and stirred overnight at room temperature. The resulting precipitate was collected by filtration and washed with acetone. The product (725 mg) was dried in vacuo.

4-[2-[[[2-[(3,5-Diaminobenzoyl)amino]ethyl]amino]carbonyl]ethyl]phenol (13e). 4-[2-[[[2-[[3,5-Bis[(*tert*-butyloxycarbonyl)amino]benzoyl]amino]ethyl]amino]carbonyl]ethyl]phenol (**10b**) was deprotected in 95% yield upon dissolving in neat trifluoroacetic acid for 5 min, followed by evaporation and precipitation with ether. R_f = 0.10 (silica, chloroform/methanol/acetic acid 85/10/5).

General Methods for the Preparation of Diisothiocyanates (Compounds 14, 19, 26, 28, 33). Method A (Used for Ethyl 3,5-Diisothiocyanatobenzoate (26), 3,5-Diisothiocyanatobenzyl Alcohol (28), and 2,6-Diisothiocyanatopyridine (33)). The diisothiocyanates prepared in this section were derived from the commercially available aromatic diamines. To a solution of 10 mM of the diamine dissolved in 50 mL of a 1/1 mixture of $EtOH/CH_3CN$, containing 4 g (excess) of $NaHCO_3$, cooled to 0 °C in an ice/MeOH bath, was added 1.5 mL (excess) of thiophosgene all at once via syringe. This was allowed to warm to room temperature over a 1-h period, then quenched by the cautious addition of 100 mL of pH 4 NaH_2PO_4. The mixture was extracted three times with 100-mL portions of ethyl acetate. The extracts were combined, dried over anhydrous Na_2SO_4, and filtered, and solvent was removed by evaporation. Final purification was effected on a Chromatotron using ethyl acetate/petroleum ether (1/4) as eluent: NMR (**26**, $CDCl_3$) δ 7.76 (s, 2 H), 7.20 (s, 1 H), 4.40 (q, 2 H), 1.40 (t, 3 H) ppm; (**28**, $CDCl_3$) δ 7.14 (s, 2 H), 6.95 (s, 1 H), 4.69 (s, 1 H) ppm.

Method B (Used for 3,5-Diisothiocyanatobenzamide (14a)). The following procedure was employed in those cases where the necessary aromatic diamine was prepared from its dinitro precursor. The diamines were not isolated but were used in situ to prepare the desired diisothiocyanate. A solution of 10 mmol of the appropriate, commercially available, dinitro compound in 50 mL of MeOH was treated with 100 mg of 10% Pd on carbon catalyst. The mixture was hydrogenated in a Parr hydrogenator and shaken at room temperature under 25 psi of H_2 for 2 h. TLC was used to determine reaction completion. When finished, the solution was filtered through a plug of Celite to remove the catalyst, and the methanolic solution of diamine was treated directly to the conditions of method A (presuming complete reduction) to prepare the desired diisothiocyanate. Final purification was effected on a Chromatotron using ethyl acetate/petroleum ether (1/4) as eluent: NMR (DMSO-d_6) δ 8.15 (s, 1 H), 7.86 (s, 2 H), 3.35 (s, 2 H) ppm.

Method C (Used for *N*-[2-(Acetylamino)ethyl]-3,5-diisothiocyanatobenzamide (14b), *N*-[2-(Dimethylamino)ethyl]-3,5-diisothiocyanatobenzamide (14d)). To a stirring solution of 20 mM of either *N*-acetylethylenediamine (for **14b**) or *N,N*-dimethylethylenediamine (for **14d**) and excess triethylamine contained in 100 mL of DME at room temperature was slowly added 20 mM of 3,5-dinitrobenzoyl chloride in 20 mL of DME. A thick precipitate formed, and the mixture was allowed to stir overnight, whereupon 150 mL of 10% aqueous NaOH was added. The resulting mixture was extracted with 2 × 300 mL portions of ethyl acetate, and the combined extracts were washed sequentially with 0.5 N HCl and half-saturated NaCl solution. The organic fraction was separated and dried over anhydrous Na_2SO_4, then the solvent was removed by evaporation. The unpurified dinitro amide was then subjected to the conditions of method B to yield the corresponding diamine, then to method A to ultimately yield the listed diisothiocyanates. Final purification was either on a Chromatotron using ethyl acetate/petroleum ether (1/4) or by recrystallization from ethyl acetate: NMR (**14b**, DMSO-d_6) δ 7.85 (m, 2 H), 7.55 (m, 1 H), 4.2–4.0 (m, 4 H), 1.90 (s, 3 H) ppm; (**14d**, DMSO-d_6) δ 9.10 (m, 1 H), 7.92 (s, 2 H), 7.78 (s, 1 H), 3.65 and 3.28 (each m, 2 H), 2.80 (s, 6 H) ppm.

Method D (Used for *N*-[3,5-Diisothiocyanatophenyl]-*N'*-[2-(acetylamino)ethyl]thiourea (19a), *N*-[3,5-Diisothiocyanatophenyl]-*N'*-[2-(dimethylamino)ethyl]thiourea (19b)). To 500 mg (2 mmol) of triisothiocyanatobenzene (**21**) contained in 50 mL of DME, cooled to 0 °C in a bath of ice/MeOH, was added 0.66 mmol of either *N*-acetylethylenediamine (for **19a**) or *N,N*-dimethylethylenediamine (for **19b**). This was stirred in the cold for 1 h, and the solvent was removed by evaporation. The remaining residue was placed on a Chromatotron with the initial eluent being ethyl acetate/petroleum ether (1/4) until the first band (triisothiocyanatobenzene) was removed, then replaced with pure ethyl acetate until the second band (the desired homogeneous product) was collected: NMR (**19a**, $CDCl_3$) δ 7.35 (m, 2 H), 6.86 (s, 1 H), 6.75 (m, 1 H), 3.48 (m, 4 H), 2.05 (s, 3 H) ppm; (**19b**, $CDCl_3$) δ 7.20 (s, 2 H), 6.80 (s, 1 H), 3.65 (m, 2 H), 2.65 (m, 2 H), 2.35 (s, 3 H) ppm; CIMS (**19b**) m/z 338 (M + 1), 304, 293, 208; (**19b**) R_f = 0.42 (silica, ethyl acetate/methanol/triethylamine 75/25/1).

Method E (Used for Converting 13 to 14 or 18 to 19). 4-[2-[[[2-[[3,5-Diisothiocyanatobenzoyl]amino]ethyl]amino]carbonyl]ethyl]phenol (14e). 3-[2-[[[2-[(3,5-Diaminobenzoyl)amino]ethyl]amino]carbonyl]ethyl]-phenol (80 mg, 234 μmol) was dissolved in a mixture of chloroform (1 mL), dimethylformamide (0.5 mL), and saturated sodium bicarbonate (1 mL). With stirring, thiophosgene (60 μL, 0.8 mmol) was added. After 1 h, the organic layer was washed with water treated with ether. A white precipitate was collected: yield 56 mg (56% yield).

4-[[2-[[3,5-Diisothiocyanatobenzoyl]amino]ethyl]amino]-7-nitrobenzofurazane (14j). Compound **10g** (134 mg, 0.24 mmol) was treated with 0.5 mL of trifluoroacetic acid for 10 min at room temperature. The trifluoroacetic acid was removed under a stream of nitrogen, and the residue was dissolved in 5 mL of an equivolume mixture of methanol/acetonitrile. Sodium bicarbonate (0.2 g) was added to the stirred solution, followed by 100 μL of thiophosgene. After 10 min, 5 mL of aqueous 0.5 M monobasic sodium phosphate was added. The mixture was extracted twice with 15 mL of ethyl acetate. The combined organic extracts were dried in vacuo to yield the

[7] 1,2-Dimethoxyethane.

product, which was homogeneous by TLC (R_f = 0.57, silica, eluting with ether).

1,3,5-Triisothiocyanatobenzene (21). 3,5-Dinitroaniline, in methanol solution, was reduced to 1,3,5-triaminobenzene (**20**) in quantitative yield with hydrogen gas (20 psi) and 10% Pd/C at room temperature in a Parr shaker.

1,3,5-Triaminobenzene (**20**; 0.50 g, 4.06 mmol) and sodium bicarbonate (3 g) were added to 50 mL of a 1/1 (v/v) mixture of methanol and acetonitrile, and the mixture was cooled to −5 °C in an ice/methanol bath. Thiophosgene (2 mL) was added in one aliquot with vigorous stirring. The reaction was allowed to warm to room temperature slowly. A 0.5 M solution of sodium phosphate monobasic (100 mL) was added. The mixture was extracted three times with ether. The organic phase was evaporated to dryness, leaving a solid residue which was purified with a Chromatotron, eluting with 10% ethyl acetate in petroleum ether: 84% yield; NMR ($CDCl_3$) δ 7.01 (s) ppm; IR 2100 cm^{-1} (isothiocyanate); EIMS m/z (M^+) 249; mp 64–66 °C (lit. (*16*) mp 63–65 °C).

3-[(*tert*-Butyloxycarbonyl)amino]aniline (29). 1,3-Phenylenediamine (1.41 g, 13 mmol) and di-*tert*-butyl dicarbonate (2.73 g, 13 mmol) were dissolved in methanol (30 mL). After 1 h, ethyl acetate was added, and the mixture was extracted twice with water. The organic layer was dried by evaporation, and the product was purified on a Chromatotron to give 1.0 g (37%) of the product as a yellow oil, which crystallized slowly: mp 109–110 °C. Anal. ($C_{11}H_{16}N_2O_2$) C, H, N.

3-[(*tert*-Butyloxycarbonyl)amino]-1-isothiocyanatobenzene (30). Compound **29** (0.51 g, 2.45 mmol) was combined with a rapidly stirred mixture of chloroform (60 mL), water (20 mL), and sodium bicarbonate (0.50 g), and the mixture was treated with thiophosgene (0.25 mL) added rapidly. After 10 min the layers were separated, and the lower layer was dried in vacuo. The residue was redissolved in ethyl acetate and treated with petroleum ether, and a solid impurity was removed by filtration. The filtrate was dried in vacuo, leaving the pure product as a solid: 0.47 g; 77% yield; mp 82–83 °C. Anal. ($C_{12}H_{14}N_2O_2S_2$) C, H, N, S.

8-[4-[[[[[2-[[[(3-Aminophenyl)amino](thiocarbonyl)]amino]ethyl]amino]carbonyl]methyl]oxy]phenyl]-1,3-dipropylxanthine (34) was obtained in quantitative yield upon treatment of compound **35** with trifluoroacetic acid for 10 min. The product was homogeneous by TLC (R_f = 0.76, silica, chloroform/methanol/acetic acid 85/10/5).

8-[4-[[[[[2-[[[[3-[(*tert*-Butyloxycarbonyl)amino]-phenyl]amino](thiocarbonyl)]amino]ethyl]amino]-carbonyl]methyl]oxy]phenyl]-1,3-dipropylxanthine (35). Compound 1 (50 mg, 117 μmol) and compound **30** (40 mg, 0.16 mmol) were added to 1 mL of DMF[8] and stirred for 1 h. Ethyl acetate (30 mL) and ethylenediamine (0.1 mL, scavenger for unreacted isothiocyanate) were added, and the solution was extracted with water, sodium monophosphate, and saturated sodium chloride. The organic phase was dried (Na_2SO_4), the solvent evaporated, and the residue recrystallized from DMF/ethyl acetate/petroleum ether to provide 44 mg (56%) of pure product.

1,3-Dipropyl-8-[4-[[[[[2-[[[[3-[(*N*-succinimidyloxy)-carbonyl]phenyl]amino](thiocarbonyl)]amino]ethyl]-amino]carbonyl]methyl]oxy]phenyl]xanthine (37). Compound 1 reacted with 3-isothiocyanatobenzoic acid (mp 161–162 °C) in dimethylformamide to provide 8-[4-[[[[[2-[[[(3-carboxyphenyl)amino](thiocarbonyl)]amino]-ethyl]amino]carbonyl]methyl]oxy]phenyl]-1,3-dipropylxanthine (**36**).

Compound **36** (61 mg, 0.11 mmol), *N*-hydroxysuccinimide (40 mg), and EDAC (66 mg) were mixed in 2 mL of dimethylformamide. A solution formed and was allowed to react overnight. Two volumes of water were added, and the precipitate was filtered to yield the product (50 mg).

8-[4-[[[[[2-[[[(6-Isothiocyanatopyrid-2-yl)amino]-(thiocarbonyl)]amino]ethyl]amino]carbonyl]methyl]oxy]phenyl]-1,3-dipropylxanthine (40). 2,6-Diaminopyridine was converted in 41% yield to 2,6-diisothiocyanatopyridine **33** with thiophosgene and sodium bicarbonate (see procedure for **21**) in an equivolume mixture of acetonitrile/ethanol: mp 48–49 °C; (DMSO-d_6) δ 8.00 (t, 3 H), 7.30 (d, 1 H) ppm; IR 2100 cm^{-1}. Anal. ($C_7H_3N_3S_2$) C, H, N, S.

Compound 1 (25 mg, 58 μmol) and compound **33** (44 mg, 0.23 mmol) were added to 0.5 mL of DMF and sonicated for 5 min. Ether (3 mL) was added; the precipitate was collected by centrifugation, washed with ethyl acetate, and dried in vacuo to yield 26 mg (72%) of product **40**: mp >250 °C; NMR (DMSO-d_6) δ 8.38 (m, 1 H), 8.05 (d, 2 H, J = 8.8 Hz), 7.83 (t, 1 H, J = 8.0 Hz), 7.15 (d, 1 H, J = 8.0 Hz), 7.06 (d, 2 H, J = 8.8 Hz), 6.98 (d, 1 H, J = 8.0 Hz), 4.57 (s, 2 H), 4.02 and 3.87 (each m, 2 H), 1.74 and 1.58 (each m, 2 H), 0.9 (m, 6 H) ppm. Anal. ($C_{28}H_{31}N_9O_4S_2 \cdot 0.5H_2O$) C, H, N, S.

Solubility of Analogues. 25 μL of a DMSO solution containing ca. 10 mM of the xanthine to be assayed was mixed thoroughly with 675 μL of pH 7.2 phosphate buffer. This mixture was vortexed for 1 min and then left at room temperature for 2–3 h. In each case (except where noted) a fine precipitate resulted and was removed by centrifugation at the end of the waiting period. A 100-μL aliquot of the supernatant then was added to 1.0 mL of methanol, and the xanthine concentration was measured spectrophotometrically using an extinction coefficient of 28 180 at 310 nm for XAC and its N-acylated derivatives. Each xanthine was assayed three times, and the concentrations reported in Table IV represent the averages of three determinations.

Competitive Binding Assay in Rat Brain Using [^{3}H]-PIA and [^{3}H]CGS21680. Inhibition of binding of 1 nM *R*-PIA[9] (specific activity 42.5 Ci/mmol) to A_1 adenosine receptors in rat cerebral cortex membranes was assayed as described.[13] Stock solutions of the xanthine derivatives in DMSO (1–10 mM) were prepared. Inhibition of binding by a range of concentrations of a xanthine derivative was assessed in triplicate in at least three separate experiments. Separation of bound and free radioligand was accomplished by rapid filtration using a Brandel cell harvester (Brandel, Gaithersburg, MD) and a Whatman GF/B glass-fiber filter. Nonspecific binding was determined in the presence of 10 μM 2-chloroadenosine. At least seven different concentrations spanning 4 orders of magnitude, adjusted appropriately for the IC_{50} of each compound, were used. IC_{50} values, computer-generated with a non-

[8] Dimethylformamide.

[9] (*R*)-N^6-(2-Phenylisopropyl)adenosine.

[10] 2-[[2-[4-(2-Carboxyethyl)phenyl]ethyl]amino]adenosine-5′-*N*-ethylcarboxamide).

[11] 3-[(3-Cholamidopropyl)dimethylammonio]-1-propanesulfonate.

[12] 3-Isobutyl-1-methylxanthine.

[13] The long treatment with IBMX was found necessary to remove all of the nonincorporated ligands from membranes (*10*). Multiple washes (up to eight) with buffer alone were insufficient to remove all the reversibly bound ligands (*10*).

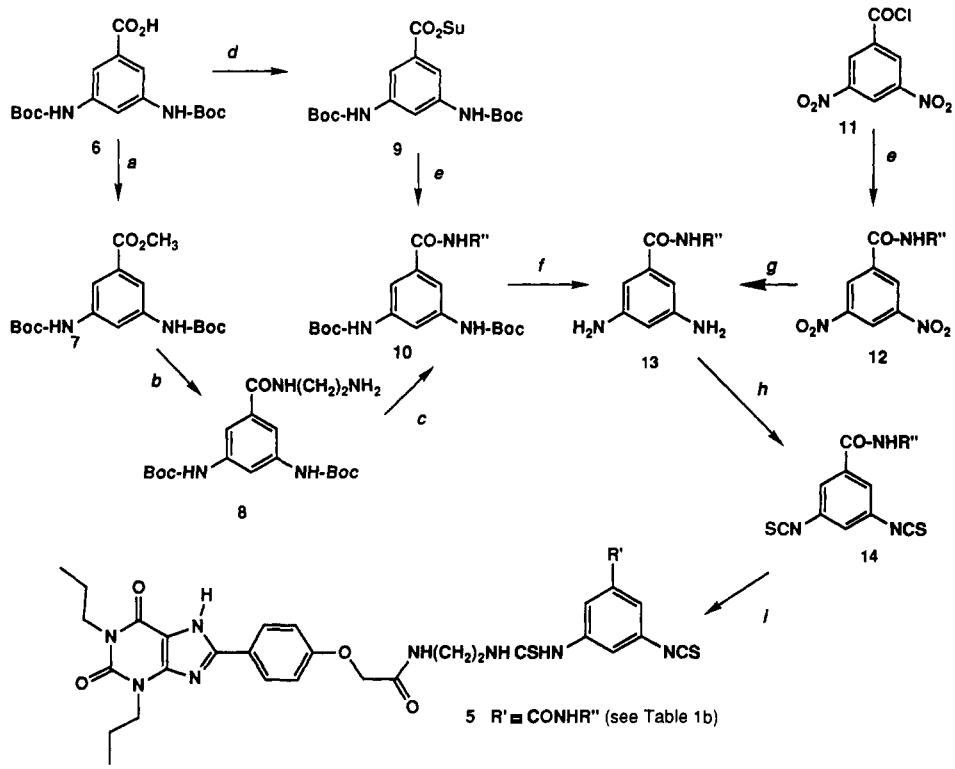


Figure 2. Routes of synthesis of trifunctional A_1 adenosine receptor inhibitors, in which the 5-position substituent (group R′ in Table I) is linked through a carboxamide. Reagents: (a) MeOH, EDAC, 4-(dimethylamino)pyridine; (b) $H_2N(CH_2)_2NH_2$; (c) acylation with a succinimido ester or an isothiocyanate; (d) *N*-hydroxysuccinimide, EDAC; (e) RNH_2; (f) TFA; (g) H_2/Pd; (h) $CSCl_2$, base; (i) compound 1, excess Ar–NCS.

linear regression formula of the GraphPAD program (Institute for Scientific Information), were converted to apparent K_i values with a K_D value for [^{3}H]PIA of 1.0 nM (*13*) and the Cheng–Prusoff equation (*17*). The use of K_i is justified for most of the compounds, since the degree of irreversible binding at A_1 receptors is relatively small in the range of the IC_{50} concentration (except for compounds **5c** and **22**). To account for the few compounds in which the K_i is expected to be shifted significantly due to partial irreversible inhibition of A_1 receptors in the pertinent concentration range, the expression "apparent K_i" value has been used.

Affinity at rat striatal A_2 receptors was measured similarly using [^{3}H]CGS21680[10] (*18*). IC_{50} and K_i values were determined as described above with a K_D value for [^{3}H]CGS21680 of 15 nM.

Irreversible Binding to Bovine Brain. For studies of irreversible incorporation, membranes from bovine brain were prepared as described (*10*) and then incubated with the indicated (Table IV) concentration of ligand for 45 min at 37 °C. Membranes were then washed three times by sequential resuspension and centrifugations with buffer A (50 mM Tris-HCl, 10 mM magnesium chloride, and 1 mM ethylenediamine tetraacetic acid, disodium salt) containing 0.02% Chaps.[11] Membranes were then suspended in buffer A containing 0.1 mM IBMX[12] and incubated at 25 °C for 18 h with shaking.[13] Membranes were then washed twice with buffer A, treated with adenosine deaminase (3 units/mL), and used in radioligand saturation studies as described (*10*) with a range of concentrations of [^{125}I]APNEA.[14] For xanthine derivatives that irreversibly inhibited receptor binding, such as m-DITC-XAC, initial experiments demonstrated that complete incorporation had occurred by 30 min (data not shown).

[14] [^{125}I]-N^6-[2-(4-Amino-3-iodophenyl)ethyl]adenosine.

RESULTS

Chemistry. The 1,3-diisothiocyanate structure was preserved in the synthetic design of cross-linking reagents **4** due to its proven merit both in reacting with an amine-containing xanthine pharmacophore (**1**) and in acylating receptor residues (*10*). The symmetry of compound **4** permits multiple synthetic pathways to a desired ligand, and several routes were investigated for feasibility during this study. The pathways may be conveniently broken into two schemes leading to cross-linker **4** and its subsequent transformation to xanthine conjugate **5**, depending on whether group R′ of Figure 1 is linked to the benzene ring in the 5-position through an amide (Figure 2) or a thiourea group (Figure 3). As shown in Figure 3, a central intermediate in the synthesis of 1,3,5-thiourea derivatives is symmetrical 1,3,5-triisothiocyanatobenzene (**21**). Alternately, hydroxymethyl, ester, and carboxylic anhydride groups at the 5-position (Figure 4) were explored. The synthesis and characterization of the intermediates are summarized in Table I.

The substituent R′ is intended for enhancing solubility, for introducing chemical or photochemical reactivity (*19*), or as a spectroscopic marker for characterization of the receptor (*13*). This reporter group may be introduced by two pathways: either (1) by incorporation in a symmetrical diisothiocyanate intermediate designed to react with **1** (e.g. **14** or **19**) or (2) by addition to a reactive center (an isothiocyanate) already linked to the pharmacophore (as in **22**). Monosubstituted conjugates of **14** or **19** (general structure **5**) were isolated following treatment of **1** with an excess of the necessary diisothiocyanate in dimethylformamide, using sonication to effect gradual solubilization of **1**. The product then precipitated upon addition of either diethyl ether or ethyl acetate. The second pathway required a roughly 2-fold molar excess of compound **21** to form **19**. Both approaches were explored in the development of the trifunctional methodology and are presented

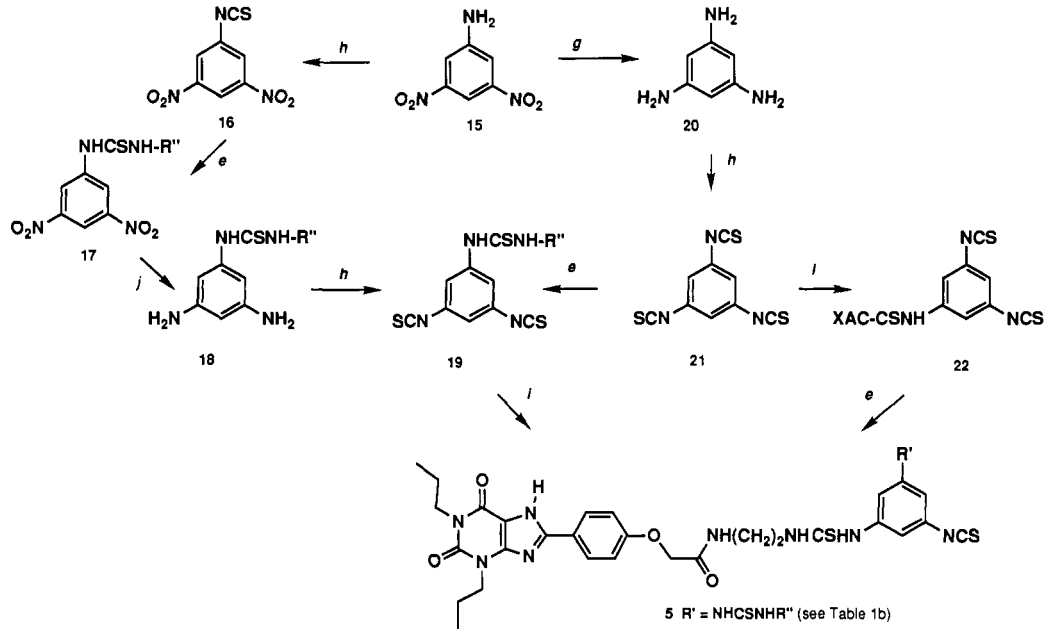


Figure 3. Routes of synthesis of trifunctional A_1 adenosine receptor inhibitors, in which the 5-position substituent (group R′ in Table I) is linked through a thiourea. Reagents: (a–i) as in Figure 2, (j) Zn/AcOH.

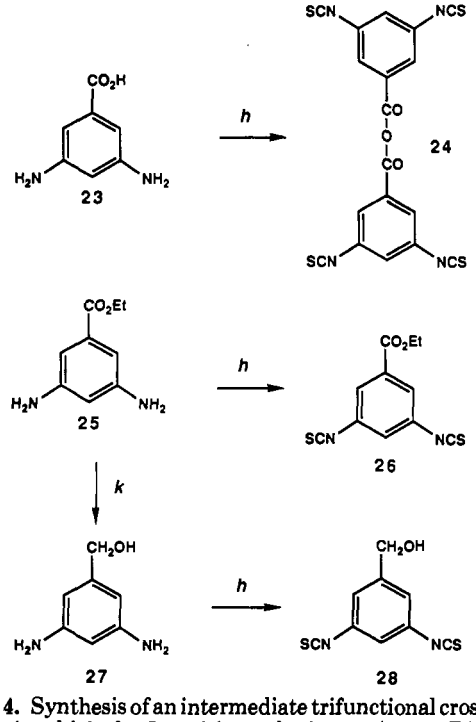


Figure 4. Synthesis of an intermediate trifunctional cross-linking reagent, in which the 5-position substituent (group R′ in Table I) consists of a hydroxymethyl, ester, or carboxylic anhydride group. Reagents: (a–j) as in Figures 2 and 3 (k) $LiAlH_4$.

in this paper. Table I lists representative xanthines synthesized (structures in Table II). Compounds **5k**, **5l**, **5o**, **5p**, and **5r** were prepared via compound **22**.

The first retrosynthetic operation on general structure **4** reveals a diamine (compounds **13** and **18**, in Figures 2 and 3, respectively). This generalized diamine was prepared by different routes, depending on the nature of the third substituent, R′. The aryl 1,3-diamines were obtained either from the corresponding 1,3-bis[*tert*-butyloxycarbonyl)amino] compound (**10**) by acid deprotection or through reduction of the 1,3-dinitro precursors (**12** or **17**), which were derived from 3,5-dinitrobenzoyl chloride (**11**) or were commercially available. Structure **12** was readily reduced by catalytic hydrogenation using 10% Pd/C; however, the same procedure failed to reduce the nitro groups of the analogous thiourea **17**. The reduction of the cationic 2-(trimethylamino)ethyl carboxamide dinitro intermediate **12c**, desired for purposes of water solubility, was sluggish. An alternative method, used successfully for compound **17** (R″ = $(CH_2)_2NHCOCH_3$), was reduction using zinc in acetic acid (*20*). Diamino carboxamides **13** were usually not isolated, but were subsequently converted to the corresponding diisothiocyanates **14**. The 1,3-diisothiocyanate intermediates included in this study (**14** and **19**) were prepared either by treatment of their penultimate 1,3-diamines with thiophosgene in the presence of base (*10*) or by addition of a primary amine to 1,3,5-triisothiocyanatobenzene (**21**, isothiocyanic acid, *s*-phenenyl triester) (*16*). The 5-thiourea-substituted cross-linkers (Figure 3) were prepared principally from **21**. Thiourea diisothiocyanates **19** were prepared by the reaction of excess **21** with amines such as *N*,*N*-dimethylethylenediamine or *N*-acetylethylenediamine in dimethoxyethane as presented in Figure 3.

As shown in Figure 2, a convenient means of introducing a variety of reporter groups was via an aliphatic amine-functionalized precursor, **8**. The two amino groups of 3,5-diaminobenzoic acid were protected as *tert*-butyl carbamates (Boc) (*10*), and resulting acid **6** was esterified in methanol with EDAC and 4-(dimethylamino)pyridine. The ester was aminolyzed in neat ethylenediamine to give **8**. This intermediate reacted either with an isothiocyanate (such as fluorescein isothiocyanate) (*13*) to afford an N-substituted thiourea or with an activated acyl group (such as *N*-succinimidyl 3-(4-hydroxyphenyl)propionate) (*21*) to give a carboxamide. This was followed by removal of the Boc protecting groups and treatment with thiophosgene. Alternatively, 3,5-bis[(*tert*-butyloxycarbonyl)-amino]benzoic acid (**6**) may be converted to its hydroxysuccinimide active ester (**9**), which may be conveniently coupled to an amine-bearing probe (such as 5-[(2-aminoethyl)thioureidyl]fluorescein) (*22*) then deprotected and transformed into the corresponding diisothiocyanate in the aforementioned manner (Figure 2).

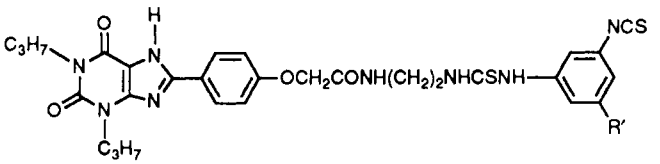
We attempted to prepare analogues in which group R′ was anionic, for increasing aqueous solubility. Treatment of 3,5-diaminobenzoic acid with the standard conditions ($CSCl_2$, base) failed to afford the expected 3,5-diisothiocyanatobenzoic acid. Instead, the isolated product (Figure 4) was the tetraisothiocyanato benzoic anhydride **24**,

Table I. Synthesis of Trifunctional Cross-Linking Reagents and Other Intermediates[j] and Xanthine Derivatives[j]

Cross-Linkers and Intermediates (for structures refer to Figures 2–4)

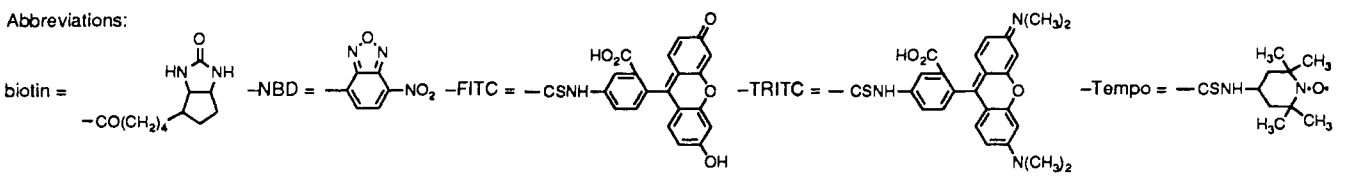
compd	R″	% yield	mp, °C	formula	anal.
6		51	183–185	$C_{17}H_{24}N_2O_6$	C, H, N
7		60	219–220 dec	$C_{18}H_{26}N_2O_6$	C, H, N
8		87	216–217	$C_{19}H_{30}N_4O_5$	C, H, N
9		67	217–218	$C_{21}H_{27}N_3O_8$	H, N; C[d]
10a	$(CH_2)_2NHCOCH_2Br$	99	160[a]	$C_{21}H_{31}N_4O_6Br$	C, H; N[f]
10b	$(CH_2)_2NHCO(CH_2)_2C_6H_4$-4-OH	63	154–156	$C_{28}H_{38}N_4O_7$	C, H, N
10c	$(CH_2)_2NH$-biotin	65	154–158	$C_{29}H_{44}N_6O_7S$·DMF	C, H, N
10d	$(CH_2)_2NHCO$-C_6H_4-4-CH_2Br	84	>250	$C_{27}H_{35}N_4O_6Br$·Et_2O	C, H, N
10e	$(CH_2)_2NHCO$-C_6H_3-2-NO_2-5-N_3	83	188–190 dec	$C_{26}H_{32}N_8O_8$·0.2DMF·0.4H_2O	C, H, N
10f	$(CH_2)_2NHCO$-C_6H_3-2-OH-4-N_3	85	196–198 dec	$C_{26}H_{33}N_7O_7$	C, H, N
10g	$(CH_2)_2NH$-NBD	60	213–215 dec	$C_{25}H_{31}N_7O_8$·0.5H_2O	C, H, N[e]
10h	$(CH_2)_2NH$-FITC	51	>300	$C_{40}H_{41}N_5O_{10}S$·2DMF·2H_2O	C, H, N
10i	$(CH_2)_2NH$-TRITC	71	>230	$C_{44}H_{51}N_7O_8$·0.5H_2O	C, H, N
10j	$(CH_2)_2NH$-Tempo	99	170–174 dec	$C_{29}H_{47}N_6O_6S$	C, H, N
12a	$(CH_2)_2NHCOCH_3$	62	204–205	$C_{11}H_{12}N_4O_6$	C, H, N
12b	$(CH_2)_2N(CH_3)_2$	44	oil	$C_{11}H_{14}N_4O_5$·0.33H_2O	C, H, N
12c	$(CH_2)_2N(CH_3)_3{}^+I^-$	96	233–235	$C_{12}H_{17}N_4O_5I$	C, H, N
13a	$(CH_2)_2NHCOCH_2Br$	83	*b*	$C_{11}H_{15}N_4O_2Br$·TFA·H_2O	C, H, N
13b	$(CH_2)_2NH$-biotin	99	*b*	$C_{19}H_{28}N_6O_3S$·2.5TFA·H_2O	C, H, N
13c	$(CH_2)_2NHCO$-C_6H_3-2-OH-4-N_3	80	122–124	$C_{16}H_{17}N_7O_3$·1.5TFA	C, H, N
13d	$(CH_2)_2NH$-Tempo	70	155–160 dec	$C_{19}H_{31}N_6O_2S$·3TFA	C, H, N
14a	H	87	152–153	$C_9H_5N_3OS_2$	C, H, N
14b	$(CH_2)_2NHCOCH_3$	67[c]	190–192	$C_{13}H_{12}N_4O_2S_2$·EtOAc·1.25H_2O	C, H, N
14c	$(CH_2)_2NHCOCH_2Br$	74	185–188	$C_{13}H_{11}N_4O_2BrS_2$	H, N; C[g,h]
14d	$(CH_2)_2N(CH_3)_2$·HCl	49[c]	170–172 dec	$C_{13}H_{15}N_4OClS_2$	C, H, N
14e	$(CH_2)_2NHCO(CH_2)_2$-C_6H_4-4-OH	56	>270	$C_{20}H_{18}N_4O_3S_2$·H_2O	C, H, N[h]
14f	$(CH_2)_2NH$-biotin	67	>270	$C_{21}H_{24}N_6O_3S_2$	*h*
14g	$(CH_2)_2NHCO$-C_6H_3-2-NO_2-5-N_3	40	146–150 dec	$C_{18}H_{12}N_8O_4S_2$	*h*
14h	$(CH_2)_2NHCO$-C_6H_3-2-OH-4-N_3	73	150–152	$C_{18}H_{13}N_7O_3S_2$	*h*
14i	$(CH_2)_2NH$-NBD	50	215–220	$C_{17}H_{11}N_7O_4S_2$	*h*
14j	$(CH_2)_2NH$-FITC	33	>240	$C_{32}H_{21}N_5O_6S_3$	*h*
16		89	176–178	$C_7H_3N_3O_4S$	C, H, N
17a	$(CH_2)_2NHCOCH_3$	92	212–214	$C_{11}H_{13}N_5O_5S$	C, H, N
17b	$(CH_2)_2N(CH_3)_2$	14	168–170	$C_{11}H_{15}N_5O_4S$	C, H, N
19a	$(CH_2)_2NHCOCH_3$	35	148–149	$C_{13}H_{13}N_5OS_3$	C, H, N
19b	$(CH_2)_2N(CH_3)_2$	41	>250	$C_{15}H_{15}N_5S_3$	*h*
19c	$CH_2CO_2C(CH_3)_3$	28	137–139	$C_{13}H_{16}N_4O_2S_3$	C, H, N
21		84	64–66	$C_9H_3N_3S_3$	C, H, N
22		81	171–175 dec	$C_{30}H_{31}N_9O_4S_3$·0.5H_2O	C, H, N
24		26	160–161	$C_{18}H_6N_2O_3S_4$	C, H, N
26		96	74–75	$C_{11}H_8N_2O_2S_2$	C, H, N
27		65	108–110	$C_7H_{10}N_2O$	C, H, N
28		63	79–80	$C_9H_6OS_2$	C, H, N

Xanthine Derivatives



compd	R′	% yield	formula	anal.
5a	$CO_2CH_2CH_3$	93	$C_{32}H_{36}N_8O_6S_2$·DMF·0.5H_2O	C, H, N
5b	CH_2OH	94	$C_{30}H_{33}N_8O_5S_2$·H_2O	C, H, N
5c	$CONH_2$	77	$C_{30}H_{33}N_9O_5S_2$·DMF·H_2O	C, H, N
5d	$CONH(CH_2)_2N(CH_3)_2$	79	$C_{34}H_{42}N_{10}O_5S_2$·HCl·2.5H_2O	C, H, N
5e	$CONH(CH_2)_2NHCOCH_3$	73	$C_{34}H_{40}N_{10}S_2$·DMF·3H_2O·HOAc	C, N; H[k]
5f	$NHCSNH(CH_2)_2N(CH_3)_2$	27	$C_{34}H_{43}N_{11}O_4S_3$	H, N; C[l]
5g	$NHCSNH(CH_2)_2NHCOCH_3$	33		
5h	$NHCSNHCH_2CO_2C(CH_3)_3$	64	$C_{32}H_{36}N_8O_6S_2$·5H_2O	C, N; H[m]
5i	$CONH(CH_2)_2NHCOCH_2Br$	74	$C_{34}H_{39}N_{10}O_6BrS_2$	C, H, N
5k	$NHCSNH(CH_2)_2NHCO$-C_6H_3-2-$NO_2$5-N_3	25	$C_{32}H_{36}N_8O_6S_2$·DMF·2H_2O·HOAc	C, H, N
5l	$NHCSNH(CH_2)_2NHCO$-C_6H_3-2-OH-4-N_3	30	$C_{32}H_{36}N_8O_6S_2$·DMF·2H_2O·4HOAc	C, H, N
40	*n*	72	$C_{28}H_{31}N_9O_4S_2$·0.5H_2O	C, H, N

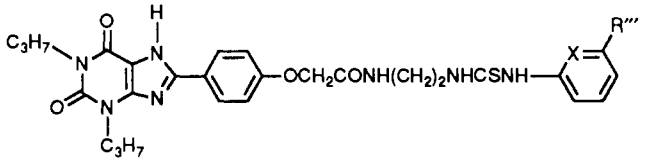
Abbreviations:



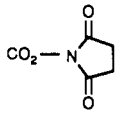
Footnotes for Table I

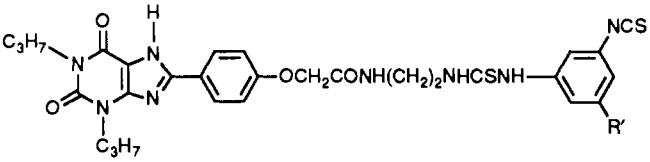
[a] Temperature raised rapidly, decomposes. [b] Amorphous solid. [c] Via compound 12, % yield from compound 13. [d] Calcd 56.12, found 56.62. [e] Calcd 17.31, found 16.36. [f] Calcd 10.87, found 11.61. [g] Calcd 39.11, found 40.58. [h] Accurate mass determined using fast atom bombardment mass spectroscopy (calculated mass for m + 1 in parentheses): **14c** + 0.2 ppm (399.9487) for ^{81}Br isotopic form; **14e** - 0.1 ppm (427.0899); **14f** + 0.8 ppm (505.1150); **14g** + 0.1 ppm (469.0501); **14h** + 0.0 ppm (440.0600); **14i** + 1.7 ppm (442.0392); **14j** - 0.6 ppm (668.0732); **19b** molecular ion + 0.5 ppm (338.0568) and fragment corresponding to loss of $(CH_3)_2NH$ + 0.7 ppm (292.9989). [i] For complete structures and methods of preparation refer to Figures 2–4. Compounds **14** were synthesized via **8** and **10**, unless noted. Compounds **19** were synthesized from **21**. Compound **12c** was synthesized from **12b** by methylation. [j] Compounds **5f**, **5g**, and **5h** were synthesized via structure **19**, and compounds **5k**, **5l**, **5o**, **5p**, and **5r** were synthesized via compound **22**. [k] Calcd H 6.14%, found 4.83. [l] Calcd. 53.32, found 48.15. [m] Calc. 6.05, found 5.42. [n] For structure refer to Table 2.

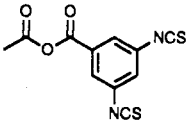
Table II. Receptor Affinities of Xanthine Derivatives, Expressed as the K_i Values in nM, for Inhibition of Binding of [^{3}H]PIA at A_1 Receptors in Rat Cerebral Cortical Membranes, or for Inhibition of Binding of [^{3}H]CGS21680 at A_2 Receptors in Rat Striatal Membranes



X = C, unless noted

compd	R''' [a]	apparent K_i at central rat adenosine receptors, nM		
		A_1	A_2	A_2/A_1 ratio
34	NH_2	10.0 ± 1.7	161 ± 38	16.1
35	$NH\text{-}CO_2C(CH_3)_3$	12.3 ± 3.1	142 ± 41	11.5
36	CO_2H	155 ± 11	*b*	*b*
37		6.43 ± 0.63	*b*	*b*
38	$NHCSNH(CH_2)_4\text{-}NHCO\text{-}C_6H_4\text{-}4\text{-}CH_2F$	13.5 ± 2.1	*b*	*b*
39	$CONH(CH_2)_4\text{-}NHCO\text{-}C_6H_4\text{-}4\text{-}CH_2F$	29.6 ± 4.9	*b*	*b*
40	NCS, X = N	16.2 ± 2.0	432 ± 20	26.7



compd	R'	apparent K_i at central rat adenosine receptors, nM		
		A_1	A_2	A_2/A_1 ratio
2	H (m-DITC-XAC)	2.39 ± 0.35	343 ± 74[c]	144
22	NCS	3.96 ± 0.59	3540 ± 940	894
5a	CO_2Et	41.6 ± 8.2	815 ± 145	19.6
5b	CH_2OH	13.4 ± 2.6	433 ± 45	32.3
5c	$CONH_2$	9.47 ± 2.99	365 ± 35	38.5
5d	$CONHCH_2CH_2N(CH_3)_2\cdot HCl$	7.62 ± 2.19	497 ± 74	65.2
5e	$CONHCH_2CH_2NHAc$	7.01 ± 0.52	247 ± 36	35.2
5f	$NHCSNHCH_2CH_2N(CH_3)_2$	77.2 ± 2.5	1910 ± 300	24.7
5g	$NHCSNHCH_2CH_2NHAc$	57.6 ± 15.7	2540 ± 280	44.1
5h	$NHCSNHCH_2CO_2\text{-}t\text{-}Bu$	8.30 ± 2.20	3980 ± 580	480
5i	$CONH(CH_2)_2NHCOCH_2Br$	18.9 ± 4.8	627 ± 53	33.2
5j		45.0 ± 3.5	493 ± 200	11.0
5k	$NHCSNH(CH_2)_2NHCO\text{-}C_6H_3\text{-}2\text{-}NO_2\text{-}5\text{-}N_3$	27.3 ± 7.2	851 ± 40	31.2
5l	$NHCSNH(CH_2)_2NHCO\text{-}C_6H_3\text{-}2\text{-}OH\text{-}4\text{-}N_3$	30.1 ± 7.6	353 ± 93	11.7
5m	$CONH(CH_2)_2NHCO(CH_2)_2\text{-}C_6H_4\text{-}4\text{-}OH$	7.08 ± 1.91	1400 ± 330	198
5n	$CONH(CH_2)_2NH\text{-}biotin$	20.1 ± 3.3	10700 ± 1300	532
5o	$NHCSNH(CH_2)_2NH\text{-}Tempo$	52.1 ± 16.4	593 ± 230	11
5p	$NHCSNH(CH_2)_2NH\text{-}FITC$	234 ± 33	2130 ± 480	9.13
5q	$CONH(CH_2)_2NH\text{-}NBD$	22.3 ± 7.2	1310 ± 220	58.7
5r	$NHCSNH(CH_2)_4NHCO\text{-}C_6H_4\text{-}4\text{-}CH_2F$	43.6 ± 12.3	593 ± 135	13.6

[a] TEMPO = 2,2,6,6-tetramethyl-1-piperidinyloxy, NBD = 4-nitrobenz-2-oxa-1,3-diazole, FITC = fluorescein isothiocyanate, for structures refer to Table I. [b] Not determined. [c] Versus [^{3}H]NECA.

resulting from dehydration of the acid. Changes in reaction conditions (solvent, base, or order of addition) had no effect on the reaction outcome. The anhydride was used, however, in preparing a conjugate with xanthine 1, and reaction occurred only at the isothiocyanate group. Another route to an acidic analogue involved the reaction of 2-aminoethanesulfonic acid with 3,5-dinitrobenzoyl chloride (11), followed by catalytic reduction of the nitro groups

to amines, then conversion to the diamine to the diisothiocyanate. The isolated diisothiocyanate sulfonic acid, however, failed to couple with 1. A third route involved reacting glycine *tert*-butyl ester with excess triisothiocyanatobenzene (21) to yield thiourea-linked diisothiocyanate 19. Reaction of this intermediate with 1 afforded desired product **5h**, but attempted cleavage of the *tert*-butyl ester group by brief treatment with CF_3CO_2H, under which conditions the aryl isothiocyanate is preserved, resulted in loss of the glycine side chain.

As shown in Figure 4, diamino ester **25** was also used to prepare ethyl 3,5-diisothiocyanatobenzoate (**26**) and 3,5-diaminobenzyl alcohol (**27**) by reduction of the ester. Compound **27** was converted to diisothiocyanate **28** by the usual thiophosgene procedure.

Table I lists the xanthine analogues synthesized, including monosubstituted model compounds (**34–40**) and derivatives containing both an isothiocyanate group and chemically reactive (**5i** and **5j**), photoreactive (**5k** and **5l**), spin-labeled (**5o**), fluorescent (**5p** and **5q**), fluorine-containing (**5r**, as a model for radiofluorination) (*15*), or iodinatable (**5l** and **5m**) (*21*) reporter groups or solubilizing (**5a–5h**) groups.

The types of groups chosen for enhancing solubility consisted of acidic, basic, ionic (quaternary amine), and hydrophilic (i.e. alcohol, amide and ester) moieties. The kinds of linking units explored in the derivatives were carboxamide, thiourea, and methylene. Pyridine isothiocyanate **40** was included in hopes that the annular heteroatom would afford some degree of solubilization or altered receptor subtype selectivity.

Biology. The apparent K_i values (nanomolar) for A_1 and A_2 binding in rat brain are presented in Table II. The inhibition of binding of [^{3}H]-N^6-(2-phenylisopropyl)adenosine at A_1 receptors in the cortex (*13*) and the inhibition of binding of [^{3}H]CGS21680 at A_2 receptors in the striatum (*18*) were measured. The relative selectivities are expressed as the ratio of K_i values. The most potent and selective of the potentially irreversibly binding xanthines were **5d**, **5e**, **5h**, **5m**, and **22**.

Several model compounds (**34–40**) having substitutions in the meta position of the thiourea-linked ring were prepared to probe the feasibility of chain extension from this site. The 3-amino (**34**) and 3-[(*tert*-butyloxycarbonyl)-amino] (**35**) derivatives were nearly equipotent in binding to A_1 receptors, indicating a tolerance for sterically large groups in this region. A carboxylic derivative (**36**) was 16-fold less potent than the corresponding aniline (**34**), indicating a detrimental effect of anionic groups in receptor binding, as has been previously noted for other 8-substituted xanthines (*5*). When blocked as a succinimido ester (**37**), which itself is potentially reactive toward amine nucleophiles on the receptor, the high potency was restored. Two long-chain derivatives (**38** and **39**) were of intermediate potency at A_1 receptors, suggesting that chain extension at the meta position is tolerated in receptor binding. A 2,6-disubstituted pyridine derivative (**40**) was 7-fold less potent than the benzene equivalent (**2**) at A_1 receptors, yet nearly equipotent at A_2 receptors.

Among trisubstituted isothiocyanate xanthine derivatives **5a–r** and **22** there was a large variation in potencies at both A_1 and A_2 receptors. Diisothiocyanate xanthine **22** was nearly as potent as **2** at A_1 receptors, yet 6-fold more selective. Among simple 5-substitutions, a carboxamide (**5c**) tended toward higher potency, suggesting that this linkage would be tolerated in extended structures, as was found for ethylenediamine derivatives **5d** and **5e**. The amide linkage was found to be preferred over the thiourea linkage in receptor binding, as in the corresponding compounds **5f** and **5g**. In comparison to ethylenediamine

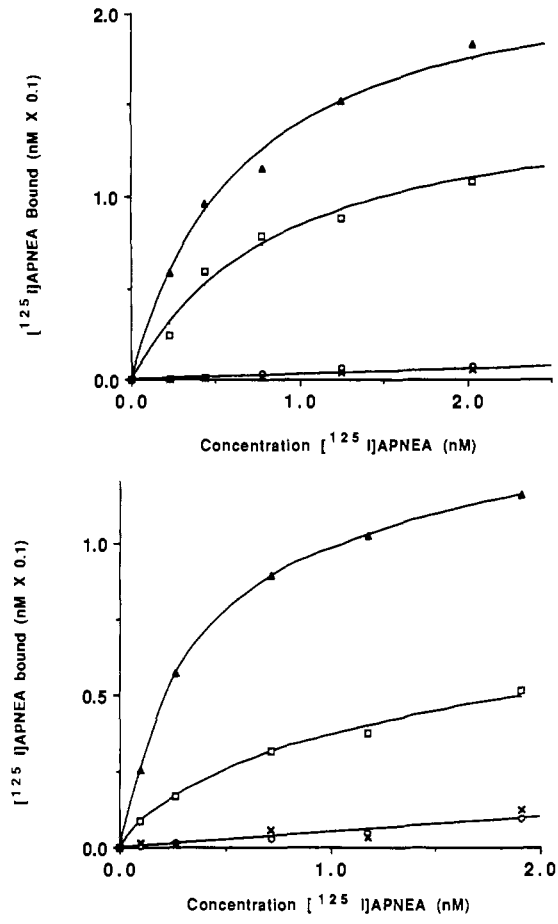


Figure 5. Concentration-dependent saturation of bovine cortical A_1 adenosine receptors with the radioligand [^{125}I]APNEA before and after treatment of the membranes with a xanthine isothiocyanate derivative (**22**): (top) incubation with 20 nM compound **22**, (bottom) incubation with 50 nM compound **22**. In each graph total binding before (△) and after (□) incubation is shown in comparison to nonspecific binding before (○) and after (×) incubation.

derivative **5f**, a glycine *tert*-butyl ester derivative (**5h**) displayed enhanced affinity for A_1 receptors and 480-fold selectivity.

The incorporation of chemically (**5i** and **5j**) and photochemically (**5k** and **5l**) reactive groups in the 5-position did not prevent receptor binding. (*p*-Hydroxyphenyl)-propionyl derivative **5m** and 4-azidosalicylic acid derivative **5l** are potentially iodinatable, for the covalent introduction of a radiotracer into the affinity-labeled receptor. Compound **5l** moreover could conceivably bridge two sites on the receptor molecule covalently, after photolysis of the azido group. Compound **5m** is of higher affinity for A_1 receptors and is 200-fold selective. A biotinylated probe (**5n**), potentially useful for receptor isolation and visualization (*23*), was 530-fold selective for A_1 receptors. Of the fluorescent-labeled ligands (**5p** and **5q**), an NBD (7-nitrobenz-2-oxa-1,3-diazol-4-yl) derivative (amide linked in the 5-position) displayed intermediate affinity for A_1 receptors and 60-fold selectivity.

The degree of irreversible binding was determined as previously described (*10*) in bovine brain. Saturation curves for [^{125}I]APNEA binding to A_1 adenosine receptors in bovine brain membranes, before and after 45-min incubation with the isothiocyanate-bearing xanthine, were measured (Figure 5). The percent inhibition (reduction in B_{max} relative to control) by selected compounds is presented in Table III. The most efficacious irreversible inhibitor in the series was carboxamide **5c**, which at a concentration of 20 nM irreversibly blocked >90% of the

Table III. Inhibition of [^{125}I]APNEA Binding to A_1 Adenosine Receptors in Bovine Brain Membranes by Xanthine Isothiocyanate Derivatives[a]

compd	IC_{50}[b]	concn, nM	% decrease[c]
2	nd	5	49[d]
		50	67[d]
		500	94[d]
5c	nd	5	68.0 ± 7.5 (3)
		20	90.3 ± 7.0 (3)
5d	nd	20	30.0 ± 8.7 (3)
		50	46.3 ± 21.8 (6)
5h	30.2	100	13 (1)
		250	23 (1)
5i	96.4	250	23 (2)
5k	116	50	0 (2)
		250	13 (2)
5k	22.9	250	34 (3)
5m	nd	250	18 (2)
5n	nd	500	50 (1)
5o	53.5	250	29 (1)
5p	85.7	250	15 (2)
5q	32.9	50	21 (2)
		100	41 (2)
5r	36.5	50	43 (2)
22	nd	20	30.3 ± 12.2 (3)
		50	66.0 ± 19.7 (3)

[a] Incubation (45 min) with compound followed by exhaustive washout and radioligand saturation experiment. [b] In competition binding assay. nd = not determined. [c] Percent decrease in density of A_1 adenosine receptors (ΔB_{max} relative to control) ± standard deviation for three or more experiments. The number of experiments is given in parentheses. [d] Data from ref 10.

Table IV. Maximum Solubilities of Selected Xanthine Isothiocyanate Derivatives in Aqueous Buffer (pH 7.2)

compd	solubility,[a] μM	compd	solubility,[a] μM
2	90.1±0.6	**5f**	5.07±0.73
5a	9.33±0.43	**5g**	>100
5b	10.8±0.0	**5p**	29.2±0.8
5c	31.4±0.4	**22**	112±2
5d	28.7±0.0	**40**	17.5±0.1
5e	>1000		

[a]Concentration measured by UV absorbance at 310 nm after transfer of an aqueous aliquot to methanolic solution.

receptors during a 45-min incubation. Other very potent irreversible inhibitors were compound **22** and, to a lesser extent, compounds **5r** and **5d**.

SOLUBILITY OF ANALOGUES

The aqueous solubility of selected xanthines was measured by a spectrophotometric method (see the Experimental Procedures). The method was not applicable to the fluorescent analogues which contain nonxanthine chromophores that absorb in the range of 310 nm. The solubilities (micromolar) of selected derivatives are presented in Table IV. The derivatives with the greatest aqueous solubility (all greater than compound **2**) were found to be **5e**, **5g**, and **22**. Several of the results were unexpected, i.e. xanthines bearing groups that were predicted to enhance solubility instead resulted in greater insolubility. For example, compound **5c**, which contains a carboxamido group, was only one-third as soluble as unsubstituted derivative **2**.

DISCUSSION

Previously, we demonstrated the feasibility of chemically cross-linking a functionalized congener, such as XAC or ADAC, to a receptor by prior monovalent reaction of the ligand with a bifunctional reagent (*10*, *11*). Given the proximity to a nucleophile on the receptor, the remaining chemically reactive group of the congener was available for irreversible cross-linking during receptor binding. This approach afforded optimized, irreversible ligands that proved useful in characterizing the A_1 receptor in membrane preparations (*11*) and in isolated guinea pig hearts (*12*).

It became apparent from this earlier work that it would be desirable to incorporate additional substituents on the irreversible ligand for the purposes of altering physicochemical and pharmacological properties. A number of possibilities can be envisioned involving prosthetic groups, reporter labels, additional reactive centers, and water-solubilizing moieties. The principal goals of this project were to develop symmetrical trifunctional linkers and a flexible synthetic methodology which could permit a diverse array of derivatives to be prepared.

In design considerations, it was important to maintain symmetry in the central linker in order to exercise a degree of regiochemical control. This control could be achieved by having three equivalent reactive centers (such as the triisothiocyanatobenzene **21**) and sequentially adding the necessary chemical components or by incorporating a desired modifying group at the outset then generating two equivalent reactive sites (as in compound **14**) at a later stage of functionalization. The isothiocyanate group had proven to be an effective reactive group both to couple to the xanthine amine pharmacophore and to bind covalently to the A_1 adenosine receptor, as was shown previously (*11*). Therefore, at least two of the three sites in the linker were chosen to be isothiocyanates. Some variability of the linking moiety in the third site R′ was needed to provide a logical means for attaching either a nucleophilic (in non-isothiocyanate intermediates) or electrophilic reagent for the desired chemical modification. For nucleophilic addition, the isothiocyanate group (leading to a thiourea) and succinimido active ester or acyl chloride (leading to a carboxamide) were chosen. To utilize the pool of commercially available amine reactive probes, a linker terminating in a free amine was developed (compound **8**). This range of reaction tuning permitted the permutability desired for different analogues.

Nonradioactive tracers, principally fluorescent-labeled ligands (*13*, *24*), are under development as an alternative to the use of radioisotopes in receptor-binding assays and in histochemical studies. We now present an approach to the design of fluorescent ligands using trifunctional reagents that contain a reactive group for covalent attachment of the ligand to the receptor protein. Previously, glucocorticoid receptors, which unlike adenosine receptors are located intracellularly, were affinity labeled with a fluorescent group (*25*).

The identification of a class of potentially bioavailable, irreversible inhibitors of adenosine receptors may enable the study of receptors in systems where this was previously not possible. For example, in the trachea (*26*) both A_1 and A_2 receptors are present, and these receptors are not readily characterized in competitive binding studies, but might be differentiated with a ligand such as compound **22**. Inhibitors with improved water solubility, such as **5e**, may be useful in tissue or in vivo studies.

The central effects of adenosine (evidenced in locomotor depression, analgesia, protection against convulsions) had not been ascribed clearly to either A_1 or A_2 receptor subtypes. Recently however, the locomotor depression has been characterized pharmacologically as having both A_1 and A_2 components (*27*). Addition of compound **22** as a specific inhibitor in isolated brain preparations or in vivo may prove useful in the study of regulatory effects of endogenous adenosine and delineation of the role of A_1 and A_2 receptor subtypes. It may be necessary to administer the drug intracerebroventricularly for studies of the central nervous system, due to low rates of passage

of complex purine derivatives across the blood–brain barrier and potential peripheral metabolism.

Irreversible inhibitors bearing fluorescent groups such as **5q** may be useful in histochemical studies. Radioisotopic labeled irreversible inhibitors, such as the radioactive equivalents of **5r**, may be useful in autoradiographic or imaging studies or in receptor assays. Due to possible nonspecific labeling in heterogeneous systems by the isothiocyanate group (*11*), these derivatives may be more useful with purified receptor preparations (*9*) than with tissue. Biotin conjugate **5n** would potentially be useful for all of the above applications and also for isolation of receptors on an avidin column (*14*). Several of the adenosine antagonists, such as **5k** and **5l**, bear chemically or photochemically reactive groups in addition to the *m*-isothiocyanate. These might be useful in studying peptide mapping or proximity of nucleophilic groups on the receptor protein, especially in combination with other protein-degradative techniques. Conceivably, this may be a means of cross-linking adjacent transmembrane regions of the receptor molecule. In the event that an additional chemically reactive group, such as the 5-isothiocyanate group of **22** or the bromoacetyl group of **5i**, would remain intact rather than react with the receptor protein, it conceivably could be utilized in a further reaction with a nucleophilic species added in high concentration externally. Such a "chemically functionalized" receptor would present versatile and unique possibilities for labeling or receptor isolation.

ACKNOWLEDGMENT

We thank Yoshiko Murata and Dr. Lewis Pannell of NIH for obtaining the mass spectral data.

LITERATURE CITED

(1) Ramkumar, V., Pierson, G., and Stiles, G. L. (1988) Adenosine receptors: clinical implications and biochemical mechanisms. *Prog. Drug Res. 32*, 196.

(2) Jacobson, K. A. (1990) Adenosine (P_1) and ATP (P_2) receptors. In *Comprehensive Medicinal Chemistry*, Vol. 3, pp 601–642, Pergamon Press, London.

(3) Hutchison, A. J., Williams, M., de Jesus, R., Oei, H. H., Ghai, G. R., Webb, R. L., Zoganas, H. C., Stone, G. A., and Jarvis, M. F. (1990) 2-Arylalkylamino-adenosine 5′-uronamides: a new class of highly selective adenosine A_2 receptor agonists. *J. Med. Chem. 33*, 1919–1924.

(4) Bridges, A. J., Bruns, R. F., Ortwine, D. F., Priebe, S. R., Szotek, D. L., and Trivedi, B. K. (1988) N^6-[2-(3,5-dimethoxyphenyl)-2-(2-methylphenyl)ethyl]adenosine and its uronamide derivatives. Novel adenosine agonists with both high affinity and high selectivity for the adenosine A_2 receptor. *J. Med. Chem. 31*, 1282.

(5) Jacobson, K. A., Kirk, K. L., Padgett, W. L., and Daly, J. W. (1985) Functionalized congeners of 1,3-dialkylxanthines: preparation of analogues with high affinity for adenosine receptors. *J. Med. Chem. 28*, 1334.

(6) Bruns, R. F., Lu, G. H., and Pugsley, T. A. (1986) Characterization of the A_2 adenosine receptor labeled by [^{3}H]NECA in rat striatal membranes. *Mol. Pharmacol. 29*, 331.

(7) Jacobson, K. A., Ukena, D., Kirk, K. L., and Daly, J. W. (1986) [^{3}H]Xanthine amine congener of 1,3-dipropyl-8-phenylxanthine: an antagonist radioligand for adenosine receptors. *Proc. Natl. Acad. Sci. U.S.A. 83*, 4089–4093.

(8) Nakata, H. (1989) Purification of A_1 adenosine receptor of rat brain membranes. *J. Biol. Chem. 264*, 16545–16551.

(9) Olah, M. E., Jacobson, K. A., and Stiles, G. L. (1990) Purification and characterization of bovine cerebral cortex A_1 adenosine receptor, *Arch. Biochem. Biophys. 283*, 440–446.

(10) Jacobson, K. A., Barone, S., Kammula, U., and Stiles, G. L. (1989) Electrophilic derivatives of purines as irreversible inhibitors of A_1 adenosine receptors. *J. Med. Chem. 32*, 1043–1051.

(11) Stiles, G. L., and Jacobson, K. A. (1988) High affinity acylating antagonists for the A_1 adenosine receptor: identification of binding subunit. *Mol. Pharmacol. 34*, 724–728.

(12) Dennis, D., Boykin, M., Jacobson, K. A., and Belardinelli, L. (1990) A novel irreversible adenosine antagonist attenuates the negative dromotropic effect of adenosine in guinea pig heart. *FASEB J. 4*, A1008, Abstract 4306.

(13) Jacobson, K. A., Ukena, D., Padgett, W., Kirk, K. L., and Daly, J. W. (1987) Molecular probes for extracellular adenosine receptors. *Biochem. Pharmacol. 10*, 1697–1707.

(14) Bruns, R. F., and Fergus, J. H. (1989) Solubilities of adenosine antagonists determined by radioreceptor assay. *J. Pharm. Pharmacol. 41*, 590.

(15) Shai, Y., Kirk, K. L., Channing, M. A., Dunn, B. B., Lesniak, M. A., Eastman, R. C., Finn, R. D., Roth, J., and Jacobson, K. A. (1989) ^{18}F-labeled insulin: a prosthetic group methodology for incorporation of a positron emitter into peptides and proteins. *Biochemistry 28*, 4801–4806.

(16) RTECS #NX9112000, NIOSH Registry of Toxic Effects of Chemical Substances (1988) (D. Sweet, Ed.) Government Printing Office, Washington, DC.

(17) Cheng, Y.-C., and Prusoff, W. H. (1973) Relationship between the inhibition constant (K_i) and the concentration of inhibitor which causes 50 percent inhibition (IC_{50}) of an enzyme reaction. *Biochem. Pharmacol. 22*, 3099–3108.

(18) Jarvis, M. F., Schutz, R., Hutchison, A. J., Do, E., Sills, M. A., and Williams, M. (1989) An A_2 selective adenosine receptor agonist directly labels A_2 receptors in rat brain tissue. *J. Pharmacol. Exp. Ther. 215*, 888.

(19) Bayley, H., and Knowles, J. (1977) Photoaffinity labeling. *Methods Enzymol. 46*, 69–114.

(20) Rodd, E. H., Ed. (1954) *Chemistry of Carbon Compounds*, Vol. 3, p 131, Elsevier Publishing Co., Amsterdam.

(21) Bolton, A. E., and Hunter, W. M. (1973) The labelling of proteins to high specific radioactivities by conjugation to a ^{125}I-containing acylating agent. *Biochem. J. 133*, 529–539.

(22) Gapski, G. R.; Whitely, J. M.; Rader, J. I.; Cramer, P. L.; Henderson, G. B.; Neef, V.; Huennekens, F. M. (1975) Synthesis of a fluorescent derivative of amethopterin. *J. Med. Chem. 18*, 526–528.

(23) Wilchek, M. and Bayer, E., Eds. (1990) Avidin–Biotin Technology. *Methods in Enzymology*, Vol. 184, Academic Press, New York.

(24) McCabe, R. T., de Costa, B. R., Miller, R. L., Havunjian, R. H., Rice, K. C., and Skolnick, P. (1990) Characterization of benzodiazepine receptors with fluorescent ligands. *FASEB J. 4*, 2934–2940.

(25) Simons, S. S., Jr., Thompson, E. B., and Johnson, D. F. (1979) Fluorescent chemoaffinity labeling. Potential application of a new affinity labeling technique to glucocorticoid receptors. *Biochemistry 18*, 4915–4922.

(26) Brackett, L. E., Shamim, M. T., and Daly, J. W. (199) Activities of caffeine, theophylline, and enprofylline analogs as tracheal relaxants. *Biochem. Pharmacol. 39*, 1897–1904.

(27) Nikodijevic, O., Daly, J. W., and Jacobson, K. A. Characterization of the locomotor depression produced by an A_2-selective adenosine agonist. (1990) *FEBS Lett. 261*, 67–70.

Preparation and Characterization of Spin-Labeled Oligonucleotides for DNA Hybridization

Oliver K. Strobel, David D. Kryak, Elizabeth V. Bobst, and Albert M. Bobst*

Department of Chemistry, University of Cincinnati, Cincinnati, Ohio 45221. Received December 14, 1990

Sequence-specific spin-labeled oligodeoxynucleotides with conformation-sensitive electron paramagnetic resonance (EPR) signals are synthesized and examined as solution-phase nucleic acid hybridization probes. Either a proxyl or tempo ring linked to the C(5) position of deoxyuridine (dU) by a nonrigid two-atom methylamino tether is incorporated within 15-mers by phosphotriester chemistry yielding stable spin-labeled probes with distinctive EPR specific activity (A_{EPR}) values. The A_{EPR} is greater for a proxyl-labeled than for a tempo-labeled probe and is consistant with EPR data of enzymatically labeled 26-mers [Bobst, A. M., Pauly, G. T., Keyes, R. S., and Bobst, E. V. (1988) *FEBS Lett. 228*, 33-36], after normalizing for percent labeling. The spectral characteristics of the free probes and the probe/target complexes are similar to those of enzymatically spin-labeled nucleic acids containing a different nonrigid two-atom-tethered spin label [Bobst, A. M., Kao, S.-C., Toppin, R. C., Ireland, J. C., and Thomas, I. E. (1984) *J. Mol. Biol. 173*, 63-70]. The presence of target DNA is detected in solution by EPR spectroscopy and the assay is based on the characteristic line-shape change associated with hybridization. The EPR spectra of free and bound probe reflect little interference from changes in global dynamics of the probe, and the line-shape change upon complexation results primarily from a change in local base dynamics. The presence or absence of hybridization can be detected in a loop-gap resonator with about 1 pmol of spin-labeled 15-mer within minutes.

The landmark experimental discovery that complementary nucleic acid sequences efficiently form highly specific double-stranded hybrids in the presence of noncomplementary nucleic acids was made by Hall and Spiegelman (1961). This discovery laid the experimental basis for all future nucleic acid probes and nucleic acid hybridization techniques. The past 2 decades of research have seen hybridization techniques proliferate and find widespread application in studies of gene structure and gene function, in the diagnosis of organismal pathogens, in the detection of human genetic abnormalities, and, most recently, as potential therapeutic agents for artificial regulation of gene expression (Symons, 1989; Hélène & Toulmé, 1990).

Since their inception, nucleic acid hybridization techniques relying on radioactively labeled probes predominated, mainly for reasons of sensitivity, over nonradioactive probes in research and diagnostics laboratories. However, increasing public concern for the environment has magnified the acuteness of some of the problems inherent to radioisotopes such as personnel exposure, storage, purchase and disposal cost, and record keeping and monitoring. User safety and economic factors, coupled with short shelf lives and long development times, have caused the waning utilization of radioisotopic probes, and in turn spawned the development of many nonradioactive nucleic acid probes. The reader is directed to a recent review (Matthews & Kricka, 1988) listing many of these new labeling strategies. An additional nonradioactive hybridization approach involves nitroxide-labeled nucleic acids. Its potential application is the subject of this work.

Nitroxide-labeled nucleic acids provide information on structure and local environment through the anisotropic motion of the spin label. The anisotropic motion, detected by EPR,[1] is recorded as a line shape which is characteristic for a particular nucleic acid conformation. Unique EPR

* Author to whom correspondence should be addressed.

[1] Abbreviations: EPR, electron paramagnetic resonance; A_{EPR}, EPR specific activity expressed as S/OD, where S is the digitized signal intensity (peak-to-peak height) of the center-field line measured at room temperature in a flat cell (outer dimensions 56 × 16 × 2 mm) with a TM_{110} cavity on a Bruker ESP 300 spectrometer at X-band (gain 10^5; modulation amplitude 1.0 G for monomers and 1.6 G for oligomers; microwave power 30 mW; field width 100 G; resolution 1024 addresses; conversion time 164 ms; time constant 164 ms) and OD (optical density) is the nucleic acid residue concentration at neutral pH (OD = Abs_{260}/mL); $(A)_n$, polymer of adenylic acid; complex, a labeled oligomer annealed to its target; CPG-dT, control pore glass long chain alkylamine-linked 5'-(dimethoxytrityl)-2'-deoxythymidine; DMSO-d_6, methyl-d_6 sulfoxide; $(dA)_n$, polymer of deoxyadenylic acid; $(dT)_{15}$, pentadecamer of thymidylic acid; $(dT)_7$-DUMPDA-$(dT)_7$, pentadecamer of thymidylic acid with DUMPDA as the central residue; $(dT)_7$-DUMPDA-$(dT)_7$-$(dA)_n$, pentadecamer of thymidylic acid with DUMPDA as the central residue annealed to a polymer of deoxyadenylic acid; $(dT)_7$-DUMTA-$(dT)_7$, pentadecamer of thymidylic acid with DUMTA as the central residue; $(dT)_7$-DUMTA-$(dT)_7$-$(dA)_n$, pentadecamer of thymidylic acid with DUMTA as the central residue annealed to a polymer of deoxyadenylic acid; dT[$(MeO)_2$Tr]-CPP, 5'-(dimethoxytrityl)-2'-deoxythymidine 3'-(*o*-chlorophenyl phosphate); dU, deoxyuridine; $(dUfl)_n$, polymer of 2'-fluorodeoxyuridine; DUMPDA, 5-[[(2,2,5,5-tetramethyl-1-oxy-3-pyrrolidinyl)amino]methyl]-2'-deoxyuridine; DUMTA, 5-[[(2,2,6,6-tetramethyl-1-oxy-4-piperidyl)amino]methyl]-2'-deoxyuridine; DUMPDA[$(MeO)_2$Tr], 5'-(dimethoxytrityl)-5-[[(2,2,5,5-tetramethyl-1-oxy-3-pyrrolidinyl)amino]methyl]-2'-deoxyuridine; DUMPDA[$(MeO)_2$Tr]-CPP, 5'-(dimethoxytrityl)-5-[[(2,2,5,5-tetramethyl-1-oxy-3-pyrrolidinyl)amino]methyl]-2'-deoxyuridine 3'-(*o*-chlorophenyl phosphate); DUMTA[$(MeO)_2$Tr], 5'-(dimethoxytrityl)-5-[[(2,2,6,6-tetramethyl-1-oxy-4-piperidyl)amino]methyl]-2'-deoxyuridine; DUMTA[$(MeO)_2$Tr]-CPP, 5'-(dimethoxytrityl)-5-[[(2,2,6,6-tetramethyl-1-oxy-4-piperidyl)amino]methyl]-2'-deoxyuridine 3'-(*o*-chlorophenyl phosphate); DUMMT, (1-oxy-2,2,6,6-tetramethyl-4-hydroxy-4-piperidinyl)methyl 1-β-D-2'-deoxyribofuranosyluracil-5-yl sulfide; FAB-MS, fast-atom bombardment mass spectrometry; h_+, height of low-field line; h_0, height of center-field line; h_-, height of high-field line; LGR, loop-gap resonator; [$(MeO)_2$Tr], 4,4'-dimethoxytrityl; [$(MeO)_2$Tr]-Cl, 4,4'-dimethoxytrityl chloride; MSNT, 1-(mesitylene-2-sulfonyl)-3-nitro-1,2,4-triazole; PCR, polymerase chain reaction; proxyl, 2,2,5,5-tetramethyl-1-pyrrolidine-*N*-oxyl; S/N, signal to noise ratio; tempo, 2,2,6,6-tetramethylpiperidine-*N*-oxyl; TMS, tetramethylsilane; $(U)_n$, polymer of uridylic acid.

1043-1802/91/2902-0089$02.50/0 © 1991 American Chemical Society

line shapes of several nucleic acid conformations, to include single strands, double stranded A, B (Kao and Bobst, 1985), and Z forms (Strobel et al., 1990a,b), and hairpin loops (Spaltenstein et al., 1989), are described in the literature. The signatures from these spin-labeled nucleic acids are quantifiable and thus make nonradioactive EPR-based nucleic acid hybridization assays possible. First to make use of this were Bobst et al. (1975) who employed randomly alkylated spin-labeled $(U)_n$ or $(dUfl)_n$ for detecting and quantitating $(A)_n$ tracts. To broaden the versatility of spin-labeled nucleic acids, the challenge remained to introduce spin-labels sequence specifically into nucleic acids. The possibility of attaining sequence-specific spin-labeled DNA by enzymatic means was recognized by Warwick-Koochaki et al. (1983). Through nick translation it was possible to incorporate spin-labels into viral DNA (Pauly et al., 1989). By carefully selecting template/primer sequences, the *Eco*R1 restriction fragment was spin-labeled sequence specifically (Bobst et al., 1988). Concomitant with enzymatic sequence-specific spin-labeling was the development of chemical oligonucleotide synthesis for spin-labeled nucleoside incorporation within a DNA sequence (Spaltenstein et al., 1988, 1989a; Makino et al., 1989).

Aside from spin-labeling DNA sequence specifically, advances in EPR resonators made an EPR-based DNA hybridization assay viable. The LGR technology (Froncisz & Hyde, 1982) is ideally suited for aqueous samples of limited quantity (Hyde & Froncisz, 1989) and has decreased the absolute amount of spin-labeled oligonucleotide required for EPR detection.

We outline here the synthesis and purification of sequence-specific spin-labeled oligonucleotides prepared by phosphotriester chemistry, which yields spin-labeled probes with distinctive A_{EPR} values that are consistant with EPR data of enzymatically labeled oligonucleotides. We show that these probes, which possess EPR signatures characteristic for single-strand and double-strand states, are readily detectable at the picomole level in an LGR.

EXPERIMENTAL PROCEDURES

Reagents. dT, dT[$(MeO)_2$Tr]-CPP, and CPG-dT (50 μmol/g) were obtained from Sigma Chemical Co. (St. Louis, MO). $(dA)_n$ was commercially procured from Pharmacia LKB Biotechnologies, Inc. (Piscataway, NJ) and was purified with Sephacryl S-200. The average molecular weight of $(dA)_n$ used for the annealing studies was 100 000–200 000. DUMPDA and DUMTA were synthesized according to a published procedure (Kryak & Bobst, 1990). All other chemicals and solvents not specifically mentioned were reagent grade or better and were purchased from either Sigma Chemical Co., Aldrich Chemical Co., Inc. (Milwaukee, WI), or Fisher Scientific (Pittsburg, PA).

Preparation and Removal of Solvents. Unless specifically described, all solvents for substrate and oligonucleotide synthesis were treated as outlined by Gait (Sproat & Gait, 1984). Solvents specified as dry were distilled at atmospheric pressure. Critical operations were performed in a glove box under dry N_2. N_2 referred to as dry was passed through a 19 × 5.5 cm column of Drierite (Xenia, OH). Solvent evaporation was achieved with either a Savant instruments SpeedVac (Farmingdale, NY), a Buchler rotary evaporator (Fort Lee, NJ), or a Virtis Model 10-010 freeze dryer (Gardiner, NY).

Chromatography. Size-exclusion chromatography was performed with BioGel P-2 (1.6 × 30 cm) from Bio-Rad (Richmond, CA) eluting with 10% (v/v) aqueous ethanol. Preparative adsorption chromatography employed Merck silica gel 60 (E. M. Science, Gibbstown, NJ) packed in a column (2.5 × 30 cm). Analytical TLC was performed with Analtech (Newark, DE) type GF Uniplates (250 μm, 2.5 × 5 cm). Analytical reverse-phase TLC was performed with C_{18} plates (2.5 × 5 cm) purchased from Whatman (England) and developed with 0.04 M ammonium bicarbonate (pH 7.0)/acetone (3/7, v/v). Oligonucleotide purification was accomplished with a Pharmacia LKB Biotechnologies FPLC system consisting of two P-500 pumps, a GP-250 gradient programmer, an ISCO variable-wavelength UV-absorbance detector (Lincoln, NE), and either a Pharmacia Mono Q HR 5/5 anion-exchange column or a ProRPC HR 5/10 reverse-phase column.

Spectrophotometric Detection and Analysis. UV spectra were obtained on a Perkin/Elmer Lambda 5 UV/VIS spectrophotometer (Norwalk, CT) with 1.0-mL quartz cells. All DNA oligomer and polymer concentrations, except where noted, are given as nucleotide residue concentrations. Nucleic acid monomer, oligomer, and polymer concentrations were calculated from solution absorbances (pH 7.0) with the following molar extinction coefficients (M^{-1} cm^{-1}): DUMTA and DUMPDA, ϵ_{265} = 9000; $(dT)_{15}$, ϵ_{260} = 8200; $(dT)_7$-DUMTA-$(dT)_7$ and $(dT)_7$-DUMPDA-$(dT)_7$ dT, ϵ_{260} = 8200 (estimated); $(dA)_n$, ϵ_{258} = 8600.

Trityl Assay. Trityl-containing monomers were detected on TLC and reverse-phase TLC by spraying with 60% (v/v) perchloric acid/ethanol and heating for 15 min at 120 °C; spots that turned orange were trityl-containing nucleos(t)ides.

NMR and Mass Spectrometry. NMR spectra of nucleoside analogues were obtained on a Bruker AC-250 instrument (Billerica, MA) in DMSO-d_6 with TMS as internal standard after reducing samples with 1.5–2.0 molar equiv of sodium dithionite (Ozinskas & Bobst, 1980). FAB-MS spectra were recorded on a VG ZAB2-SE mass spectrometer (Manchester, England). All samples were measured in a 2-nitrobenzyl alcohol matrix and were ionized with a Xe source. CsI served as the calibration standard.

EPR Spectroscopy. EPR spectra were obtained on a Bruker ESP300 EPR spectrometer (Billerica, MA). Samples were measured in a quartz flat cell (outer dimensions, 56 × 16 × 2 mm) with a Bruker TM_{110} cavity resonator or in Vitro Dynamics Inc. fused-quartz round (id × od, 0.6 × 0.84 mm) capillary tubes (Rockaway, NJ) with a Medical Advances X-0405 loop–gap (one-loop, two-gap) resonator (Wauwatosa, WI). The resonant frequencies and nonsaturating power settings for the TM cavity and LGR were 9.80 GHz/30 mW and 9.42 GHz/5 mW, respectively. All other parameters (see abbreviations) were independent of the resonator used. Routines for S/N calculations and Fourier transformations were performed with Bruker ESP Series 1600 software.

Sample Preparation for the LGR. As determined by UV, a 5.02×10^{-5} M solution of $(dT)_7$-DUMPDA-$(dT)_7$ in water was prepared. From this solution, duplicate 1–5-μL aliquots (50.3–251.3 pmol) were removed, placed into individual 400-μL polypropylene tubes, and evaporated to dryness with a SpeedVac. The first set of samples was dissolved in 2 μL of 0.1 M NaCl and 0.01 M sodium cacodylate (pH 7.0). The second set of samples was dissolved in 2 μL of 0.1 M NaCl, 0.01 M sodium cacodylate (pH 7.0), and 3.15×10^{-4} M $(dA)_n$. To mix thoroughly and minimize sample loss, all tubes were carefully and repeatedly vortexed and centrifuged prior to their contents being transferred with a Hamilton 7105 syringe (Reno, NV) to capillary tubes. The capillary tubes were gently centrifuged before being inserted into the LGR.

Synthesis of DUMPDA[$(MeO)_2$Tr] and DUMTA-

[(MeO)$_2$Tr]. To 23 mg (58 μmol) of DUMPDA or 23 mg (56 μmol) of DUMTA dried by coevaporation with 300 μL of dry pyridine (4×) were added 200 μL (64 μmol) of a [(MeO)$_2$Tr]-Cl/pyridine stock solution prepared by dissolving 49.3 mg of [(MeO)$_2$Tr]-Cl in 500 μL of dry pyridine. After stirring for 14 h at room temperature, an additional 100 μL (32 μmol) of [(MeO)$_2$Tr]-Cl/pyridine stock solution was added and stirring continued for an additional 3 h before stopping the reaction with 1 mL of methanol. The reaction mixture was rotary evaporated to dryness and the final compound purified over a silica gel column (40 g, 21 × 2.5 cm) with 5% (v/v) methanol/chloroform. Material resolving as one spot with R_f 0.15 on analytical TLC was combined and rotary evaporated to near dryness. After addition of 5 drops of dry pyridine, the solution was rotary evaporated to dryness to afford 8.8 mg of DUMPDA[(MeO)$_2$Tr] (22% yield) and 13 mg of DUMTA[(MeO)$_2$Tr] (34% yield). Characterization for DUMPDA[(MeO)$_2$Tr]: ^{1}H NMR (250 MHz) δ 7.7 (s, C6-H), 11.5 (br s, N3-H), 6.2 (t, C1′-H), 2.2 (br s, C2′-H), 6.8–7.5 (m, trityl phenyl), 1.4–1.7 (m, label CH_2), 0.9–1.4 (m, label CH_3); UV λ_{max} (pH 7.0) 266 nm; analytical reverse-phase TLC R_f 0.80; trityl assay positive. Characterization for DUMTA[(MeO)$_2$Tr]: ^{1}H NMR (250 MHz) δ 7.7 (s, C6-H), 11.5 (br s, N3-H), 6.2 (t, C1′-H), 2.2 (br s, C2′-H), 3.8 (s, trityl OCH_3), 6.8–7.5 (m, trityl phenyl), 1.5–1.8 (m, label CH_2), 1.3 (s, label CH_3); UV λ_{max} (pH 7.0) 266 nm; analytical reverse-phase TLC R_f 0.80; trityl assay positive.

Preparation of Phosphorylating Agent, Chlorophenyl Phosphoroditriazolide. Dry tetrahydrofuran (1.85 mL), freshly distilled triethylamine (90 μL, 0.65 mmol), 1,2,4-triazole (50 mg, 0.72 mmol), and 2-chlorophenyl phosphorodichloridate (46 μL, 0.28 mmol) were mixed in a 15-mL centrifuge tube fitted with a septum lid to give a white precipitate. After 2–3 h, the mixture was centrifuged and appropriate aliquots required for phosphorylation were removed with a gas-tight syringe.

Synthesis of DUMPDA[(MeO)$_2$Tr]-CPP and DUMTA[(MeO)$_2$Tr]-CPP. To 17.5 mg (26 μmol) of DUMPDA[(MeO)$_2$Tr] or 15 mg (22 μmol) of DUMTA-[(MeO)$_2$Tr] dried by coevaporation with 300-μL of dry pyridine (4×) was added 490 μL (70 μmol of phosphate) of the phosphorylating agent. The reaction progress was monitored by TLC. After 5 h the reaction mixture was transferred to a 15-mL centrifuge tube with an additional 250 μL of dry tetrahydrofuran. The reaction was stopped by adding 1.0 mL of 1.0 M triethylammonium bicarbonate (pH 8.0) and vortexing. The solution was extracted with 6.0 mL of chloroform, and the organic layer washed with 1.0 mL of 1.0 M triethylammonium bicarbonate (pH 8.0) and 1.0 mL of water (2×). After drying the organic phase with 0.5 g of sodium sulfate and adding a few drops of dry pyridine, the solution was rotary evaporated to dryness. Final purification was achieved by precipitation. The residue, dissolved in 10 drops of methylene chloride, was added dropwise to 30 mL of dry pentane in a 40-mL centrifuge tube. After centrifugation, the supernatant was removed and the pellet was washed with 10 mL of pentane and air-dried. The yellow powder was transferred to a 3-mL conical vial and capped with a septum lid and a needle was inserted. The sample was further dried by placing the vial in a desiccator containing KOH and P_2O_5. DUMPDA[(MeO)$_2$Tr]-CPP (24 mg, 96% yield) and DUMTA[(MeO)$_2$Tr]-CPP (21 mg, 95% yield) were obtained as triethylammonium salts. These derivatives were stored at −30 °C until used. Characterization for DUMPDA[(MeO)$_2$Tr]-CPP: UV λ_{max} (pH 7.0) 266 nm; FAB-MS$^+$ 890 $(M + H)^+$; analytical reverse-phase TLC R_f 0.65; trityl assay positive. Characterization for DUMTA-[(MeO)$_2$Tr]-CPP: UV λ_{max} (pH 7.0) 266 nm; FAB-MS$^+$ 904 $(M + H)^+$; analytical reverse-phase TLC R_f 0.65; trityl assay positive.

Synthesis of Spin-Labeled Oligonucleotides by Phosphotriester Chemistry. Pentadecathymidylic acids with DUMTA or DUMPDA incorporated in the middle position were synthesized according to standard solid-phase phosphotriester chemistry (Sproat & Gait, 1984) with a semimanual synthesizer from Cruachem Inc. (Herndon, VA) and an Omnifit reaction column (New York, NY). CPG-dT (25 mg, 1.3 μmol) was used for the synthesis with the following reaction cycles at a flow rate of 1 mL/min: wash (pyridine, 3 min), wash (dichloroethane, 2 min), detritylation (3% v/v, dichloroacetic acid/dichloroethane, 100 s), wash (dichloroethane, 1 min), wash (pyridine, 4 min), and coupling (20 mg of MSNT and 10 μL of 1-methylimidazole in pyridine, 15 min with 11 mg (13 μmol) of dT and 30 min with 11 mg (12 μmol) of DUMTA or DUMPDA). The intensity of the detritylation solutions was used as a measure of the efficiency of the individual coupling reactions.

Oligonucleotides were cleaved from the support and deblocked at the internucleotide phosphates with concentrated ammonia overnight at 55 °C. The final [(MeO)$_2$Tr] group was removed with 40% (v/v) aqueous acetic acid for 1.5 min. After neutralizing with concentrated ammonia, the crude oligonucleotide mixture was desalted on a BioGel P-2 column. Fully deprotected spin-labeled oligonucleotides were purified by Mono Q FPLC with a gradient of NaCl in NaOH (flow rate: 1.0 mL/min. Buffers: A = 0.5 M NaCl/0.01 N NaOH, pH 12, B = 0.67 M NaCl/0.01 N NaOH, pH 12. Program: buffer B at 30–100% for 50 min and 100% for 10 min. Retention times: $(dT)_7$-DUMPDA-$(dT)_7$, 38 min; $(dT)_7$-DUMTA-$(dT)_7$, 38 min; dT_{15}, 42 min). The last major eluting peak was collected and combined with corresponding fractions of other separations. After reducing the volume, the material was desalted over a BioGel P-2 column. Spin-labeled oligonucleotides showing only one peak by analytical Mono Q FPLC were further purified by ProRPC FPLC with a gradient of acetonitrile in triethylammonium acetate (Flow rate: 1.0 mL/min. Buffers: A = 0.1 M triethylammonium acetate, pH 7.0, B = 30% acetonitrile/0.1 M triethylammonium acetate, pH 7.0. Program: buffer B at 20–28% for 40 min, 28–100% for 15 min and 100–20% for 5 min. Retention times: $(dT)_7$-DUMPDA-$(dT)_7$, 42 min; $(dT)_7$-DUMTA-$(dT)_7$, 42 min; $(dT)_{15}$, 30 min). The DUMPDA and DUMTA labeled oligonucleotide containing fractions were evaporated to dryness, and the triethylammonium salt was further removed by coevaporation with water. A 1-μmol scale yielded 1–2 OD_{260} of $(dT)_7$-DUMTA-$(dT)_7$ and 2–4 OD_{260} of $(dT)_7$-DUMPDA-$(dT)_7$. Purified spin-labeled oligonucleotides characterized by a single peak on analytical ProRPC were dried and stored at −30 °C. For EPR characterization, 5.6–6.0 nmol of each spin-labeled oligonucleotide were added to 195 μL of buffer (0.1 M NaCl, 0.01 M sodium cacodylate, 0.01 M $MgCl_2$, pH 7.0) and spectra recorded in a TM_{110} cavity. To determine the presence of free-spin, a solution containing 2.0 equiv of poly(L-lysine) in 1–3 μL was added to the spin-labeled oligonucleotide solutions, and EPR spectra were recorded. Samples with h_0 peak heights that were 20% of the unbound h_0 peak heights were considered uncontaminated by free-spin.

RESULTS

The preparation of DUMPDA and DUMTA for incorporation into oligonucleotides by phosphotriester chemistry was achieved with procedures similar to those of

Scheme I. Structure of Spin-Labeled Nucleotides DUMTA and DUMPDA and Their Derivatization for Phosphotriester Synthesis

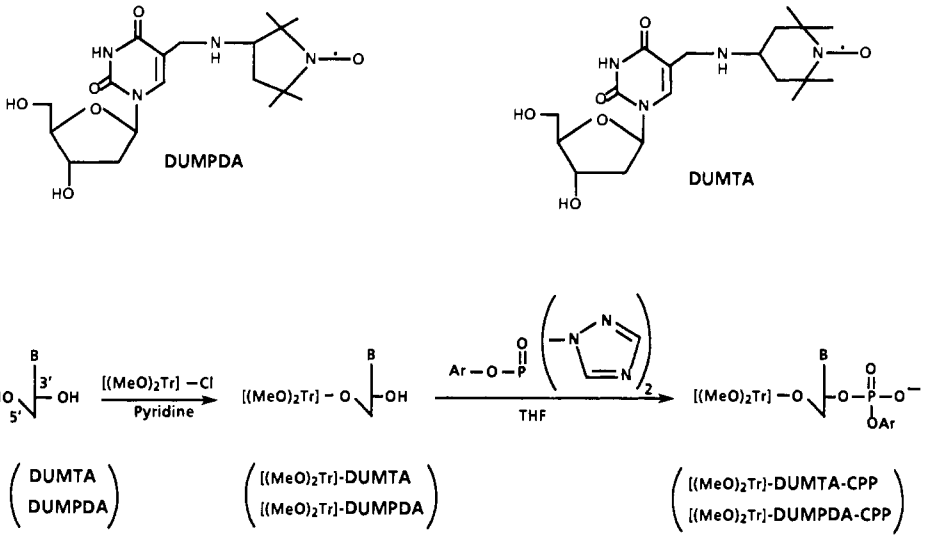


Table I. Experimental EPR Characteristics of the Spin-Labeled Precursors, Oligonucleotides, and Probe/Target DNA Complexes

compound	A_{EPR} × 10^{-3}	h_+/h_0 ± 0.05	h_-/h_0 ± 0.05
DUMPDA	4400	0.95	0.79
DUMPDA[$(MeO)_2$Tr]	2000	0.94	0.67
DUMPDA[$(MeO)_2$Tr]-CPP	2000	0.94	0.67
$(dT)_7$-DUMPDA-$(dT)_7$	250	0.93	0.43
$(dT)_7$-DUMPDA-$(dT)_7$-$(dA)_n$		0.47	0.14
DUMTA	2900	0.97	0.83
DUMTA[$(MeO)_2$Tr]	1300	0.98	0.75
DUMTA[$(MeO)_2$Tr]-CPP	1300	0.98	0.70
$(dT)_7$-DUMTA-$(dT)_7$	200	0.99	0.48
$(dT)_7$-DUMTA-$(dT)_7$-$(dA)_n$		0.67	0.14

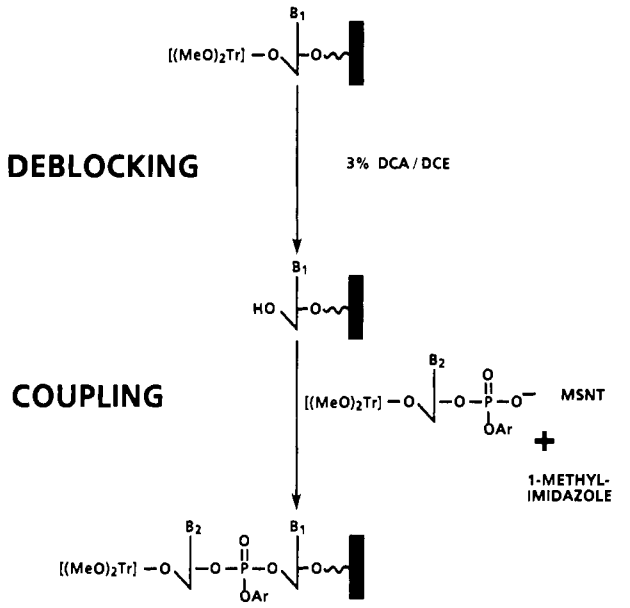
Narang et al. (1980) and is shown in Scheme I. The first step consisted of the tritylation of the 5′-OH, which was carried out under more stringent conditions for DUMPDA and DUMTA than for dT. Even so, the extent of tritylation of the labeled derivatives was less than that for dT. On the other hand, the chlorophenyl phosphate addition onto the 3′-OH in the second step succeeded equally well for modified and unmodified dT.

The EPR characteristics of the spin-labeled nucleosides and their derivatives are included in Table I. The A_{EPR} values of DUMPDA and DUMTA are different by about a factor of 1.5. The higher value of DUMPDA is attributed to the line-shape properties of the proxyl nitroxide. The decrease in A_{EPR} values upon tritylation is a direct result of the increased absorbance of the tritylated compound. The h_+/h_0 signal height ratio is similar for the labeled nucleosides with and without substituents on either 5′-OH or 5′-OH and 3′-OH, but additions to these sites cause a decrease in the h_-/h_0 ratio which is most sensitive to isotropic tumbling of the spin-labeled residues in that time domain.

DUMPDA and DUMTA triester derivatives were incorporated within oligonucleotides according to Scheme II. A lower coupling efficiency was noted with both the DUMPDA and DUMTA derivatives than with dT. This accounts for a purified labeled product yield which is no more than 30% of an unlabeled oligomer yield.

Well-characterized labeled oligomers with reproducible A_{EPR} values were obtained only after the synthesized materials were subjected to anion-exchange and reverse-phase FPLC (Kryak 1990). As shown in Table I, the DUMPDA-labeled oligomer still shows a higher A_{EPR} value, although the effect is no longer as pronounced as

Scheme II.[a] Reaction Cycle of Phosphotriester Syntheses



[a] B_1 signifies the tritylated dT which is covalently linked to the glass support bead. Additional derivatized thymidines or spin-labeled thymidine analogues, DUMPDA[$(MeO)_2$Tr]-CPP or DUMTA[$(MeO)_2$Tr]-CPP, are attached and numbered ($B_{2,3,4...n}$) in accordance with their position within the oligomer sequence.

with that of the monomer. The advantage of a proxyl label in terms of its large signal height is lessened at reduced label motion, which is expressed in a broadening of the spectrum and a reduction of the h_-/h_0 ratio (Table I). This phenomenon was already noted earlier with deuterated nitroxides when it was observed that the gain in signal height was rapidly lost with increasing tumbling time (Beth et al., 1980).

Characteristic EPR line shapes for single-stranded $(dT)_7$-DUMPDA-$(dT)_7$ and $(dT)_7$-DUMTA-$(dT)_7$ are shown in Figure 1, parts A and C, respectively. Although the hyperfine-splitting constant is distinctly different between DUMPDA and DUMTA (Kryak and Bobst, 1990), this difference is to a large extent masked upon incorporation of the labels into the oligomers. The three narrow lines h_+, h_0, and h_- are indicative of a label undergoing a relatively rapid molecular motion. Numerical values for the height ratios h_+/h_0 and h_-/h_0 are listed in Table I and are similar for proxyl- and tempo-labeled oligonucleotides.

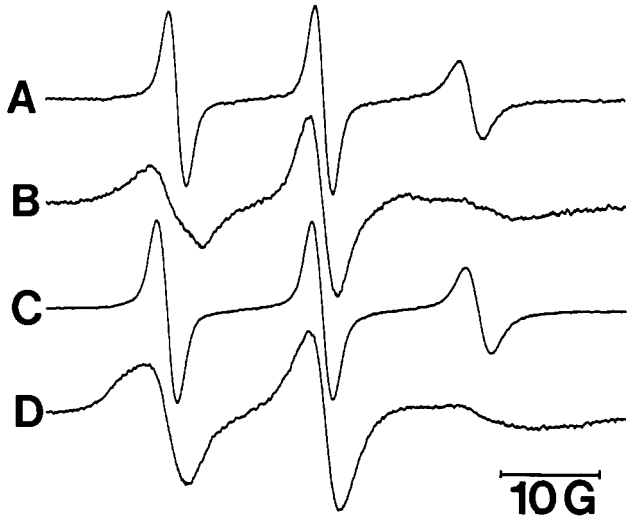


Figure 1. Typical EPR spectra for single-stranded and double-stranded DNA labeled with either DUMPDA (A and B) or DUMTA (C and D). The single-stranded spectra A and C represent 6.0 nmol of $(dT)_7$DUMPDA$(dT)_7$ and 4.9 nmol of $(dT)_7$DUMTA$(dT)_7$, respectively. Double-stranded spectra were obtained after annealing the oligomers at room temperature with a 1.2–1.4 molar excess of $(dA)_n$. The 175-μL solution volumes were measured in a quartz flat cell with a Bruker TM_{110} cavity. Each sample solution contained 0.1 M NaCl, 0.01 M sodium cacodylate (pH 7.0), and 0.01 M $MgCl_2$.

Regardless of annealing with a large or small excess of $(dA)_n$ (data for 50-fold $(dA)_n$ excess not shown), the anisotropic motion of the annealed DUMPDA- and DUMTA-labeled oligomers (Figure 1, parts B and D) is reduced to a similar extent. The extent of broadening upon annealing is similar for both probes, which results in a h_0 peak-to-peak reduction of about a factor of 2 (data not shown). Double integration of spectra A–D (Figure 1) showed that the observed h_0 reductions are not the result of decreased spin intensity. In addition, hybridization of the probes results in a significant decrease in all height ratio values with the largest reduction observed for h_-/h_0 (Table I). These ratio changes, which are independent of complex size, form the basis of the EPR-based nucleic acid hybridization assay. For practical reasons shown below, only the change in the h_+/h_0 ratio is used to monitor the presence of hybridization.

Since $(dT)_7$-DUMPDA-$(dT)_7$ has the highest A_{EPR}, this was the probe selected for determining the threshold of sensitivity of the EPR hybridization assay. Also, to maximize the sensitivity of the assay, a LGR was employed. Although a conventional EPR TM_{110} cavity can detect a slightly more dilute nitroxide solution, the LGR with its small active volume window (1–2 μL) (Altenbach et al., 1989) requires ca. 100 times less volume than what is required for a TM_{110} cavity resonator. In terms of absolute amounts, the LGR requires fewer nitroxides for the same S/N than the TM_{110} by at least a factor of 10. For that reason, the LGR is the optimal resonator for EPR hybridization assays. The requirement of a slightly more concentrated nitroxide solution for detection by the LGR is for the purpose of this assay advantageous since increased probe concentrations speed up rates of hybridization (Keller & Manak, 1989). A diagramatic representation of the hybridization assay components with corresponding EPR spectra is shown in Figure 2, which portrays a centrally labeled 15-mer, a complementary polymer, and a right-handed duplex with the reporter molecule positioned within the major groove. The experimental EPR spectra represent 3.3 pmol of oligomer probe as DUMPDA-labeled $(dT)_{15}$ before (top) and after (bottom) annealing to a large excess of $(dA)_n$. As with the more concentrated samples depicted in Figure 1, the same h_+/h_0 ratio differences between the single-stranded and double-stranded spectra are observed. Since h_-/h_0 for the double-stranded spectrum is difficult to calculate at low S/N, the h_+/h_0 is routinely determined to detect hybridization.

The S/N in the spectrum of Figure 2B is the result of a 14-min acquisition period. It would be difficult to extract meaningful numerical values from spectra that had S/N values much below that of Figure 2B. Without increasing acquisition time, one method of enhancing S/N, and thus lower the detection limit, is through signal conditioning via Fourier transformation. Since the broad EPR lines arising from nitroxides are low in frequency as compared to the noise, successful separation of high-frequency noise from the low-frequency nitroxide signal is readily accomplished. After the EPR spectrum is recorded, it is transformed, the high-frequency portion of the spectrum is deleted, and the spectrum is retransformed back into the familiar three-line nitroxide line shape with a substantially reduced noise level. An example of S/N increase realized with FT is illustrated with Figure 3. Figure 3A is the unaltered spectrum obtained with 3.3 pmol of $(dT)_7$-DUMPDA-$(dT)_7$ annealed to $(dA)_n$, and Figure 3B is the same spectrum digitally filtered, where most of the high-frequency noise was eliminated without distorting the low-frequency (nitroxide line shape) EPR signal of interest. In this case, an approximate factor of 4 increase in S/N is gained with the on-board Bruker FT software. This, in turn, further reduces the amount of spin-labeled probe required for detection.

In conclusion, the availability of probes with high A_{EPR} values, the use of an LGR, and spectral signal conditioning collectively form an EPR-based DNA hybridization assay requiring only picomole quantities of spin-labeled probe.

DISCUSSION

To maintain the speed and specificity of hybridization, it is essential that a balance of probe concentration and probe length exists. In addition, the reporter group should only minimally perturb the double-stranded conformation. The relatively high probe concentration requirement of the LGR is of considerable advantage in the case of the hybridization assay. A probe length of 15 residues affords rapid annealing while the fidelity of hybridization is still maintained. Finding a nonperturbing conjugation site for the reporter group is a major concern for a viable assay. For pyrimidines, C(5) is a logical choice as a modification site since this position of the heterocycle is not involved in Watson–Crick base pairing. Substituents, when properly tethered at C(5), project into the major groove of B-DNA without causing distortion to the helix. Therefore, selecting suitable tethers is very important, not only to preclude steric interference to hybridization but also to allow for proper reporter group function and/or detection (Brigati et al., 1983; Leary et al., 1983). EPR line-shape analyses and molecular modeling studies have also supported the importance of tether length and flexibility (Strobel et al., 1990b; Kryak & Bobst, 1990; Bobst et al., 1984; Pauly et al., 1987).

The EPR line-shape change upon hybridization is similar with proxyl- and tempo-labeled probes as shown with Figure 1. The spectra of the annealed probes show no slow motion component for the two nitroxide rings that are both attached to the nucleic acid base with a nonrigid two-atom tether. On the other hand, spectra of oligonucleotides labeled with either a rigid two-atom-tethered (Spaltenstein et al., 1988) or a one-atom-tethered (Duh, 1990) nitroxide display slow motion components reflecting global motion (Spaltenstein et al., 1989a). Therefore, the

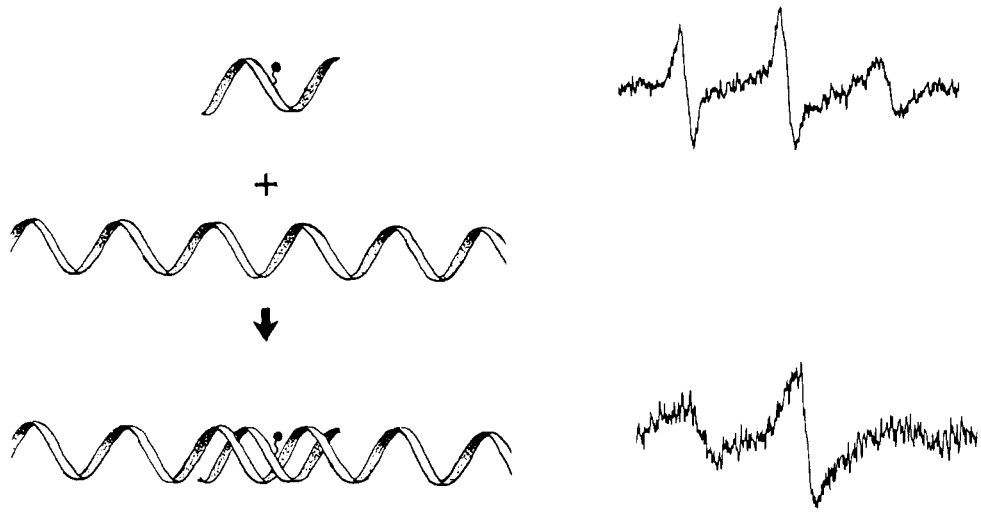


Figure 2. Pictorial description of hybridization and corresponding experimental EPR spectra of DUMPDA-labeled single- and double-stranded DNA obtained with a loop-gap resonator. Buffered in 2 μL of 0.1 M NaCl, 0.01 M sodium cacodylate (pH 7.0), and 0.01 M $MgCl_2$, the top spectrum represents 50 pmol of $(dT)_7$-DUMPDA-$(dT)_7$ (3.3 pmol probe), and the bottom spectrum represents 50 pmol of $(dT)_7$-DUMPDA-$(dT)_7$ annealed to an excess of $(dA)_n$ (630 pmol).

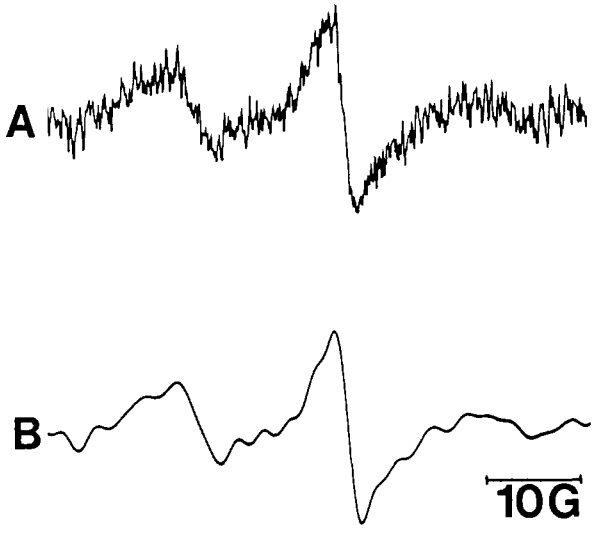


Figure 3. Signal to noise enhancement of EPR spectrum by Fourier transformation. A spectrum of 50 pmol of $(dT)_7$DUMPDA$(dT)_7$ annealed to an excess of $(dA)_n$ in 2 μL of 0.1 M NaCl, 0.01 M sodium cacodylate (pH 7.0), and 0.01 M $MgCl_2$ before (A) and after (B) signal conditioning by FT.

use of probes that monitor hybridization based solely on local dynamic change without interference from global dynamics will considerably simplify the interpretation of the experimental results. It is interesting to note that the line shape of the $(dT)_7$-DUMTA-$(dT)_7$·$(dA)_n$ complex is similar to that obtained earlier with the enzymatically prepared $(DUMMT,dT)_n$·$(dA)_n$ (Bobst et al., 1984). DUMMT, like DUMTA, contains a tempo ring attached via a nonrigid two-atom tether to the C(5) position of deoxyuridine.

While a correlation between the size of a spin-labeled system and its EPR line shape may usually not be desirable in EPR hybridization assays, the large difference in the EPR signature observed with rigidly coupled nitroxides should facilitate the detection of single base mismatches. Preliminary data with DUTA-labeled oligomers have shown that a DUTA-dG base pair mismatch causes a decoupling from the global motion as indicated by the loss of the slow motion component in the EPR spectrum. Therefore, such probes may be of importance for EPR assays designed specifically for direct detection of point mutations (Duh, 1990).

When preparing EPR hybridization probes by chemical synthesis to afford sequence-specific EPR-active oligonucleotides, it was important to synthesize probes with an EPR signal intensity equivalent to that obtained from previous work carried out on enzymatically prepared samples. The harsh chemistry encountered in oligonucleotide synthesis made it desirable to follow the integrity of the nitroxide moiety during the various reaction steps by EPR. By keeping the experimental conditions (solvent, temperature, etc.) and instrumental parameters constant (Dalal et al., 1981), and by normalizing for concentration, the A_{EPR} values (see footnote) can be determined for the spin-labeled material. Although the number of nitroxides is directly proportional to the area under the EPR absorption curve and is normally obtained by double integration of the EPR signal, it is convenient to quantify the EPR signal through the h_0 peak-to-peak height, provided the line shape remains the same.

The detection limit of this solution-phase assay is set by the minimum number of nitroxides that can be measured by the EPR spectrometer to give spectra with a S/N usable for analyses. The EPR spectra shown in Figure 3 represent this limit achieved with $(dT)_7$-DUMPDA-$(dT)_7$ and the LGR. With signal conditioning the limit is further reduced by a factor of 3–4 so that no more than 1 pmol of target DNA is required for detection. This makes the EPR assay only slightly less sensitive than a solution-phase fluorescence assay (Morrison et al., 1989) within similar time frames. In view of the possibility of 1 000 000-fold target amplification by PCR technology, the need for methods capable of ultrasensitive target detection no longer exists.

Based on this study, nitroxide-labeled probes now join a small number of nucleic acid probes which use spectroscopic labels to facilitate the direct detection of hybridization. Luminescent (Heller & Morrison, 1985; Arnold et al., 1989) and fluorescent (Morrison et al., 1989) probes have been among those described so far which are not subject to the tedious manipulations associated with collecting hybridized DNA on solid support. The ease of analysis as well as the potential for automation are considerable advantages of these solution-phase hybridization assays making them suitable for large-scale testing. The EPR approach, in addition, offers the potential of direct in vivo target detection.

ACKNOWLEDGMENT

We thank Marion Merrell Dow Inc. of Cincinnati, OH, for the use of their mass spectrometer and Dr. Bradley Ackermann for his technical assistance. This work was supported in part with NIH Grant GM27002, and the Bruker ESP300 was purchased with the NIH Shared Instrumentation Grant S10 RR04191.

LITERATURE CITED

Altenbach, C., Flitsch, S. L., Khorana, H. G., and Hubbell, W. L. (1989) Structural studies on transmembrane proteins. 2. Spin labeling of bacteriorhodopsin mutants at unique cysteines. *Biochemistry 28*, 7806–7812.

Arnold, L. J., Hammond, P. W., Wiese, W. A., and Nelson, N. C. (1989) Assay formats involving acridinium-ester-labeled DNA probes. *Clin. Chem. 35*, 1588–1594.

Beth, A. H., Perkins, R. C., Jr., Venkataramu, S. D., Pearson, D. E., Park, C. R., Park, J. H., and Dalton, L. R. (1980) Advantages of deuterium modification of nitroxide spin labels for biological EPR studies. *Chem. Phys. Lett. 69*, 24–28.

Bobst, A. M., Kao, S.-C., Toppin, R. C., Ireland, J. C., and Thomas, I. E. (1984) Dipsticking the major groove of DNA with enzymatically incorporated spin-labeled deoxyuridines by electron spin resonance spectroscopy. *J. Mol. Biol. 173*, 63–74.

Bobst, A. M., Pauly, G. T., Keyes, R. S., and Bobst, E. V. (1988) Enzymatic sequence-specific spin labeling of a DNA fragment containing the recognition sequence of *Eco*RI endonuclease. *FEBS Lett. 228*, 33–36.

Bobst, A. M., Sinha, T. K., and Pan, Y.-C. E. (1975) Electron spin resonance for detecting polyadenylate tracts in RNA's. *Science 188*, 153–155.

Brigati, D. J., Myerson, D., Leary, J. J., Spalholz, B., Travis, S. Z., Fong, C. K. Y., Hsiung, G. D., and Ward, D. C. (1983) Detection of viral genomes in cultured cells and paraffin-embedded tissue sections using biotin-labeled hybridization probes. *Virology 126*, 32–50.

Dalal, D. P., Eaton, S. S., and Eaton, G. R. (1981) The effects of lossy solvents on quantitative EPR studies. *J. Magn. Reson. 44*, 415–428.

Duh, J.-L. (1990) Incorporation of deoxyuridylic acid substituted in position 5 with one-atom-tethered nitroxides into oligonucleotides by the phosphotriester method. Ph.D. Thesis, University of Cincinnati, Cincinnati, OH.

Froncisz, W., and Hyde, J. S. (1982) The loop–gap resonator: A new microwave lumped circuit ESR sample structure. *J. Magn. Reson. 47*, 515–521.

Hall, B. D., and Spiegelman, S. (1961) Sequence complementarity of T2-DNA and T2-specific RNA. *Proc. Natl. Acad. Sci. U.S.A. 47*, 137–146.

Hélène, C., and Toulmé, J.-J. (1990) Specific regulation of gene expression by antisense, sense and antigene nucleic acids. *Biochim. Biophys. Acta 1049*, 99–125.

Heller, M. J., and Morrison, L. E. (1985) Chemiluminescent and fluorescent probes for DNA hybridization system. *Rapid Detection and Identification of Infectious Agents* (D. T. Kingsbury and S. Falkow, Eds.) pp 245–256, Academic Press, New York.

Hyde, J. S., and Froncisz, W. (1989) Loop gap resonators. *Advanced EPR: Applications in Biology and Biochemistry* (A. J. Hoff, Ed.) pp 277–305, Elsevier Science Publishing Comp., Inc., New York.

Kao, S.-C., and Bobst, A. M. (1985) Local base dynamics and local structural features in RNA and DNA duplexes. *Biochemistry 24*, 5465–5469.

Keller, G. H., and Manak, M. M. (1989) *DNA Probes*, Stockton Press, New York.

Kryak, D. D. (1990) Sequence specific incorporation of deoxyuridylic acid substituted in position 5 with two-atom-tethered nitroxides into oligothymidylic acids by phosphotriester chemistry. Ph.D. Thesis, University of Cincinnati, OH.

Kryak, D. D., and Bobst, A. M. (1990) Synthesis of two 2′-deoxyuridine analogs substituted in position 5 with 2-atom tethered nitroxide radicals. *Nucleosides Nucleotides*, in press.

Leary, J. J., Brigati, D. J., and Ward, D. C. (1983) Rapid and sensitive colorimetric method for visualizing biotin-labeled DNA probes hybridized to DNA or RNA immobilized on nitrocellulose: Bio-blots. *Proc. Natl. Acad. Sci. U.S.A. 80*, 4045–4049.

Makino, K., Murakami, A., Nagahara, S., Nakatsuji, Y., and Takeuchi, T. (1989) A study on spin-labelled oligonucleotide synthesis and its electron spin resonance behavior in solution. *Free Radical Res. Commun. 6*, 311–316.

Matthews, J. A., and Kricka, L. J. (1988). Analytical strategies for the use of DNA probes. *Anal. Biochem. 169*, 1–25.

McInnes, J. L., Symons, R. H., Hyypiä, T., Huovinen, P., Holmberg, M., Pettersson, U., Gowans, E. J., Jilbert, A. R., Burrell, C. J., Sutherland, G. R., and Mulley, J. C. (1989) *Nucleic Acid Probes* (R. H. Symons, Ed.) pp 1–211, CRC Press Inc., Boca Raton, FL.

Morrison, L. E., Halder, T. C., and Stols, L. M. (1989) Solution-phase detection of polynucleotides using interaction fluorescent labels and competitive hybridization. *Anal. Biochem. 183*, 231–244.

Narang, S. A., Brosseau, R., Hsiung, H. M., and Michniewicz, J. J. (1980) Chemical synthesis of deoxyoligonucleotides by the modified triester method. *Methods Enzymol. 65*, 610–620.

Ozinskas, A. J., and Bobst, A. M. (1980) Formation of *N*-hydroxyamines of spin labeled nucleosides for ^{1}H-NMR analysis. *Helv. Chim. Acta 63*, 1407–1411.

Pauly, G. T., Bobst, E. V., Bruckman, D., and Bobst, A. M. (1989) Template-dependent incorporation of spin-labeled thymidine analogs into viral DNA. *Helv. Chim. Acta 72*, 110–116.

Pauly, G. T., Thomas, I. E., and Bobst, A. M. (1987) Base dynamics of nitroxide-labeled thymidine analogues incorporated into $(dA\text{-}dT)_n$ by DNA polymerase I from *Escherichia coli*. *Biochemistry 26*, 7403–7310.

Spaltenstein, A., Robinson, B. H., and Hopkins, P. B. (1988) A rigid and nonperturbing probe for duplex DNA motion. *J. Am. Chem. Soc. 110*, 1299–1301.

Spaltenstein, A., Robinson, B. H., and Hopkins, P. B. (1989a) Sequence- and structure-dependent DNA base dynamics: Synthesis, structure, and dynamics of site and sequence specifically spin-labeled DNA. *Biochemistry 28*, 9484–9495.

Spaltenstein, A., Robinson, B. H., and Hopkins, P. B. (1989b) DNA structural data from a dynamics probe. The dynamic signatures of single-stranded, hairpin-looped, and duplex forms of DNA are distinguishable. *J. Am. Chem. Soc. 111*, 2303–2305.

Sproat, B. S., and Gait, M. J. (1984) Solid-phase synthesis of oligodeoxyribonucleotides by the phosphotriester method. *Oligonucleotide Synthesis: a practical approach* (M. J. Gait, Ed.) pp 83–114, IRL Press Limited, Oxford.

Strobel, O. K., Keyes, R. S., and Bobst, A. M. (1990a) An electron paramagnetic resonance probe to detect local Z-DNA conformations. *Biochem. Biophys. Res. Commun. 166*, 1435–1440.

Strobel, O. K., Keyes, R. S., and Bobst, A. M. (1990b) Base dynamics of local Z-DNA conformations as detected by electron paramagnetic resonance with spin-labeled deoxycytidine analogues. *Biochemistry 29*, 8522–8528.

Symons, R. H. (1989) Self-cleavage of RNA in the replication of small pathogens of plants and animals. *Trends Biochem. Sci. 14*, 445–450.

Warwick-Koochaki, P. E., Hakan, A., and Bobst, A. M. (1983) Interaction of polymerases with 2′-deoxyuridine-5′-triphosphate spin-labeled at the 5-position. *FEBS Lett. 152*, 157–162.

Registry No. DUMPDA, 132723-74-1; DUMPTA, 132723-75-2; DUMPDA[$(MeO)_2$Tr], 132723-76-3; DUMPTA[$(MeO)_2$Tr], 132723-77-4; DUMPDA[$(MeO)_2$Tr]-CPP, 132723-78-5; DUMPTA-[$(MeO)_2$Tr]-CPP, 132723-79-6; $(dT)_7$-DMPDA-$(dT)_7$, 132832-61-2; $(dT)_7$-DMPTA-$(dT)_7$, 132832-62-3; [$(MeO)_2$Tr]-Cl, 40615-36-9; poly(dA), 25191-20-2.

In Vitro Antitumor Activity of 2'-Deoxy-5-fluorouridine–Monoclonal Antibody Conjugates

Ada Goerlach, Kenia G. Krauer, Ian F. C. McKenzie, and Geoffrey A. Pietersz*

Research Centre for Cancer and Transplantation, Department of Pathology, The University of Melbourne, Parkville, Victoria 3052, Australia. Received February 27, 1990

5-Fluorouracil (5-FU) is an anticancer drug used in patients for the treatment of gastric and breast cancer and used either alone or in combination with methotrexate is one of the few drugs with some effect on colon cancer. 2'-Deoxy-5-fluorouridine (5-FUdr) (1) is an analogue based on 5-FU and can be covalently linked to a murine anti-Ly-2.1 monoclonal antibody (mAb) with the active ester derivative of 2'-deoxy-5-fluoro-3'-*O*-(carboxypropanoyl)uridine (5-FUdr-succ) (4). Such immunoconjugates can contain up to 42 residues of drug, although the most antibody activity was retained when substitution ratios were between 10 and 25 molecules of drug to mAb. In a cytotoxicity assay, 50% inhibition of [^{3}H]deoxyuridine incorporation (IC_{50}) with a murine Ly-2.1^{+ve} thymoma cell line was 6 nM for 5-FUdr-anti-Ly-2.1, which is 12-fold more than that for free 5-FUdr (IC_{50} = 0.51 nM) but similar to that of 5-FUdr-succ (IC_{50} = 5.2 nM). The 5-FUdr–monoclonal antibody conjugates (5-FUdr–mAb) were 100-fold more active on the Ly-2.1^{+ve} E3 cell line than on the Ly-2.1^{-ve} BW5147 OU$^-$ cell line. The high in vitro activity and specificity of 5-FUdr-MoAb conjugates indicates that potent in vivo activity of these conjugates should be expected.

INTRODUCTION

Most cytotoxic drugs used clinically have little selective toxic effect on tumors and although extensive structural modification has resulted in analogues with improved antitumor activity, dose-limited toxic side effects are still a major problem (*1*, *2*). However, the targeting of cytotoxic agents to tumors by covalently linking them to monoclonal antibodies confers a degree of specificity not found with the drugs alone (*3*). The specificity of the monoclonal antibody (mAb),[1] together with the internalization and subsequent release of the coupled drug, can lead to the selective killing of tumor cells expressing the antigen (*4*). There are, however, some limitations to this approach, as access of immunoconjugates to the tumor is inefficient and results in only a fraction of the dose entering the tumor (*5*). Immunoconjugates of highly toxic drugs or toxins may overcome the problem of inefficient delivery of a lethal dose to the tumor and one example of this was to use a more toxic folic acid antagonist, aminopterin, which was found to be more potent than the related but less toxic methotrexate when delivered as an immunoconjugate (*6–9*).

In this light it is appropriate to examine more cytotoxic compounds such as 5-fluorouracil. 5-Fluorouracil (5-FU) is used in the treatment of carcinoma of the breast and intestine, but its use is limited by toxicity to bone marrow and intestinal epithelium (*10*). This drug is metabolized by several enzymes and transformed into toxic species which interfere with several metabolic pathways (*11*). 5-FU enters the pyrimidine biosynthetic pathway at the orotic acid step, to form 5-fluorouridine diphosphate which can be incorporated into RNA; 5-fluorouridine diphosphate is transformed to 2'-deoxy-5-fluorouridine monophosphate, which inhibits thymidylate synthetase, resulting in the inhibition of DNA synthesis. In vitro 2'-deoxy-5-fluorouridine (5-FUdr, 1) (Figure 1) is more cytotoxic than 5-FU. We now report on the linkage of 5-FUDr to mAbs and the demonstration of the specific cytotoxic action of the compounds on tumor cells.

EXPERIMENTAL PROCEDURES

General Procedures. Melting points were determined in open capillary tubes on an Electrothermal digital melting point apparatus and are uncorrected. ^{1}H nuclear magnetic resonance (^{1}H NMR) spectra were recorded on a Bruker AM-300 wide-bore NMR spectrometer. Chemical shifts of compounds are reported in ppm downfield from internal standard tetramethylsilane. Mass spectra were obtained with a JOEL JMS-AX 505 H mass spectrometer. Thin-layer chromatography (TLC) was performed on silica gel coated plastic sheets (Kieselgel 60F_{254} plates) (E. Merck, Darmustadt, Germany), with products being visualized by exposure to UV light and/or 80% aqueous acetic acid.

2'-Deoxy-5'-*O*-[bis(4-methoxyphenyl)phenylmethyl]-5-fluorouridine (2). 2'-Deoxy-5-fluorouridine (1) (147.5 mg, 0.6 mmol) was evaporated three times with 2 mL of pyridine and then redissolved in 2 mL of pyridine. 4,4'-Dimethoxytriphenylmethyl chloride (304.5 mg, 0.9 mmol) in pyridine (2 mL) was added dropwise while being cooled and stirred, and the reaction mixture was stirred at room temperature for 16 h. The solution was poured into 10 mL of ice containing 5% $NaHCO_3$, extracted with dichloromethane, dried over anhydrous Na_2SO_4, and evaporated to give 340 mg of crude product. Column chromatography on silica gel (40 g) using CH_2Cl_2–MeOH (13:1) as eluant yielded 223.6 mg (68%) of **2**: TLC (CH_2Cl_2–MeOH, 13:1) R_f 0.25; ^{1}H NMR ($CDCl_3$) δ 2.26 and 2.48 (2 m, 2 H, 2'-H_2), 3.42 (m, 2 H, 5'-H_2), 3.79 (s, 6 H, OCH_3), 4.06 (dt, $J_{4,5} = J_{3,4}$ = 4 Hz, 1 H, 4'-H), 4.53–4.57 (m, 1 H, 3'-H), 6.29 (m, 1 H, 1'-H), 6.85 and 7.28 (2 m, 13 H, arom H), 7.83 (d, $J_{6\text{-H,F}}$ = 9 Hz, 1 H, 6-H).

2'-Deoxy-5'-*O*-[bis(4-methoxyphenyl)phenylmethyl]-5-fluoro-3'-*O*-(3-carboxypropanoyl)uridine (3). 2'-Deoxy-5'-*O*-[bis(4-methoxyphenyl)phenylmethyl]-

* To whom all correspondence should be addressed.

[1] Abbreviations used: 5-FU, 5-Fluorouracil; 5-FUdr, 2'-deoxy-5-fluorouridine; mAb(s), monoclonal antibody(ies); 5-FUdr-succ, 2'-deoxy-5-fluoro-3'-*O*-(3-carboxypropanoyl)uridine; IC_{50}, 50% inhibition of [^{3}H]deoxyuridine incorporation; E3, ITT(1)75NS E3; DMTr-Cl, 4,4'-dimethoxytriphenylmethyl chloride; DMAP, 4-(*N*,*N*-dimethylamino)pyridine; NHS, *N*-hydroxysuccinimide; DCC, dicyclohexylcarbodiimide; PBS, phosphate-buffered saline; TLC, thin-layer chromatography; BW, BW5147 OU$^-$.

1043-1802/91/2902-0096$02.50/0 © 1991 American Chemical Society

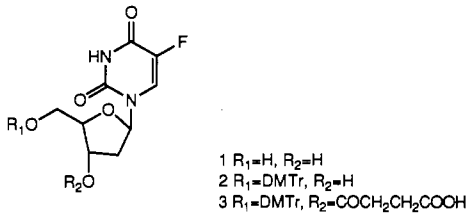


Figure 1. Structure of 5-FUdr (1) and other derivatives [(2) 2'-deoxy-5'-*O*-[bis(4-methoxyphenyl)phenylmethyl]-5-fluorouridine, (3) 2'-deoxy-5'-*O*-[bis(4-methoxyphenyl)phenylmethyl]-5-fluoro-3'-*O*-(3-carbonylpropanoyl)uridine, (4) 2'-deoxy-5-fluoro-3'-*O*-(3-carbonylpropanoyl)uridine].

5-fluorouridine (**2**) (191.8 mg, 0.35 mmol) was dissolved in dichloromethane (3 mL) and after the addition of 4-(*N*,*N*-dimethylamino)pyridine (64.1 mg, 0.525 mmol, 1.5 equiv) and succinic anhydride (140 mg, 1.4 mmol, 4 equiv) the mixture was kept at room temperature for 16 h and then poured into 10 mL of 5% $NaHCO_3$, acidified with 1 N HCl to pH 3, and extracted several times with dichloromethane. The extract was dried and evaporated to give 132.4 mg (77%) of **3**: TLC (90% aqueous CH_3CN) R_f 0.68.

2'-Deoxy-5-fluoro-3'-*O*-(3-carboxypropanoyl)uridine (4). 2'-Deoxy-5'-*O*-[bis(4-methoxyphenyl)phenylmethyl]-5-fluoro-3'-*O*-(3-carboxypropanoyl)uridine (**3**) (132.0 mg, 0.2 mmol) was dissolved in 80% aqueous acetic acid (2 mL) and left at room temperature for 2–3 h. The reaction mixture was diluted with water and extracted with chloroform. The aqueous solution was lyophilized and the residue passed through a column of 5 g of silica gel with 70% aqueous ethanol. Evaporation of the solvent gave 61 mg (86%) of **4** as a white hygroscopic powder: TLC (70% aqueous EtOH) R_f 0.80; ^{1}H NMR (D_2O) δ 1.8–2.5 (m, 6 H, succ-CH_2, 2'-H_2), 3.52–3.70, 3.95–4.05, (2 m, 5'-H_2, 4'-H), 5.09 (m, 1 H, 3'-H), 6.07 (m, 1 H, 1'-H), 7.84 (d, $J_{6\text{-H,F}}$ = 8 Hz, 1 H, 6-H).

Biological Testing. Tumor Cells. The cell lines used in this study were the E3 variant of the Ly-2.1^{+ve} murine thymoma ITT(1)75NS (E3) (*12*) and the Ly-2.1^{-ve} BW5147 OU$^-$ cells (BW) (*13*). The cells were maintained in vitro in Dulbecco's modified Eagle's medium supplemented with 10% heat-inactivated newborn calf serum (Flow Laboratories, Sydney, Australia), 2 mM glutamine (Commonwealth Serum Laboratories (CSL), Sydney, Australia), 100 μg/mL streptomycin (Glaxo, Melbourne, Australia), and 100 IU/mL penicillin (CSL).

Monoclonal Antibodies. Anti-Ly-2.1 (IgG_{2a}) (*14*) reactive with the murine Ly-2.1 antigen was isolated from ascites fluid. The ascites was diluted in phosphate-buffered saline (5 mM, 0.17 M NaCl, pH 7.2) (PBS) and adsorbed onto protein A-Sepharose (Pharmacia Inc., Piscataway, NY), washed extensively with PBS, and eluted with 0.2 M citrate buffer (pH = 4.0). Following neutralization the mAb was concentrated by precipitation with 45% aqueous $(NH_4)_2SO_4$ and dissolved in PBS, and aliquots (5 mg/mL) were stored at −70 °C. When tested with sodium dodecyl sulfate polyacrylamide gel electrophoresis (SDS-PAGE), this mAb preparation was 90–95% pure.

Preparation and Quantitation of Conjugates. The active ester derivative of 5-FUdr-succ (**4**) was prepared by dissolving 5-FUdr-succ (1.73 mg, 5 mmol) in 70 μL of dry DMF. *N*-Hydroxysuccinimide (0.59 mg, 5.1 mmol) in 17 μL of DMF and dicyclohexylcarbodiimide (6.18 mg, 30 mmol) in 50 μL of DMF were added, and the reaction mixture was kept at room temperature for 3 h and at 4 °C overnight. An aliquot of the active ester was mixed with the mAb (3–5 mg/mL) in PBS and maintained at room temperature for 3 h and then centrifuged (400*g* × 3 min) to remove any precipitate. The conjugate was purified by gel-filtration chromatography using a Sephadex G-25 column (PD-10, Pharmacia), with PBS as eluant. Antibody concentration was determined by using a standardized amount of ^{125}I-labeled antibody (*6*) and the amount of FUdr-succ bound was determined by absorbance spectrophotometry at 260 nm using the extinction coefficients ϵ_{260} = 7600 M^{-1} cm^{-1} (FUdr-succ) and ϵ_{260} = 12 9300 M^{-1} cm^{-1} (mAb). Analysis of these conjugates by SDS-PAGE and gel-permeation chromatography (TSK-SW2000, Pharmacia) showed less than 5% aggregated antibody (not shown).

Drug Activity. Cytotoxicity Assays. (a) Cells (100 μL, 2 × 10^5 cells) were added to a flat-bottom microtiter plate and incubated for 1 h at 37 °C. Free drug in PBS and conjugate solutions were filtered (0.22 μM) to sterilize them, various dilutions were made in PBS, and 100 μL was added to the cells. Control wells received 100 μL of PBS. The plates were then kept at 37 °C, 7% CO_2 for 24 h and harvested (see below).

(b) Cells (200 μL, 2 × 10^5 cells, E3 and BW) were added to sterile tubes, 100 μL of various dilutions of conjugate or free drug in PBS was added, and the mixtures were kept at room temperature for 30 min; 500 μL of growth medium was then added, and the cells were centrifuged (400*g* × 5 min). After resuspension in 200 μL of medium, 100-μL aliquots were added to a microtiter plate and incubated at 37 °C, 7% CO_2 for 16 h.

After incubation 50 μL of growth medium containing 1 μCi of [^{3}H]deoxyuridine (specific activity, 21 Ci/mmol; Amersham, Amersham, England) was added and the mixture incubated for 4 h, when the cells were harvested with a Dynatech automash cell harvestor (Dynatech, England) onto glass fiber-filters and dried and samples counted on a β-scintillation counter (Packard Instrument Co., Downers Grove, IL). The viability of the cells was expressed as a percentage inhibition of [^{3}H]deoxyuridine incorporation compared to that of the controls (we have previously shown that [^{3}H]deoxyuridine uptake is equivalent to cell viability using a dye exclusion assay (unpublished results). Duplicates did not show more than 10% variation.

Stability of Conjugate in Growth Medium. To determine the stability of 5-FUdr-anti-Ly-2.1 in growth medium, a conjugate prepared with radiolabeled anti-Ly-2.1 was mixed with an equal volume of fetal calf serum or PBS and incubated at 37 °C for 24 h. A similar incubation was performed with radiolabeled anti-Ly-2.1. After incubation, the samples were passed through a PD-10 column to remove any free drug and the peak fractions were pooled and counted for radioactivity. The concentration of antibody was determined from the known specific activity of ^{125}I-labeled anti-Ly-2.1 and the cytotoxicity of the peak fraction was measured by using the [^{3}H]deoxyuridine assay as described above.

Antibody Activity by Flow Cytometry. (a) Indirect Assay. E3 cells (2 × 10^5) in 500 μL of growth medium were incubated with 100 μL of various concentrations of unconjugated antibody or with the 5-FUdr-mAb conjugate for 1 h on ice. The cells were centrifuged, washed twice with 500 μL of PBS containing 0.025% sodium azide and 2% newborn calf serum, and resuspended in 500 μL of the same medium. PBS (100 μL) containing 10 μg of fluorescein isothiocyanate labeled rabbit anti-mouse immunoglobulin F(ab')$_2$ fragment (Silenus Laboratories Pty Ltd., Hawthorn, Australia) was then added and after an incubation period of 45 min on ice 500 μL of medium was added, and the cells were centrifuged, washed, and re-

suspended. Fluorescence was measured with a Becton and Dickinson FACScan. For calculations mean fluorescence values were used.

(b) Competition Assay. Various concentrations of unmodified anti-Ly-2.1 or conjugates with different substitution ratios were mixed with 5 μg of FITC-labeled anti-Ly-2.1, and 100 μL of the mixture was added to 2×10^5 E3 cells in 500 μL of growth medium. After a 1-h incubation on ice, the cells were centrifuged, washed twice with 500 μL of PBS containing 0.025% sodium azide and 2% new born calf serum, resuspended in 500 μL of the same medium, and analyzed with the FACScan.

RESULTS

Chemistry. According to procedures given by Thomas et al. (*15*) and Habener et al. (*16*) 5-FUdr (1) was reacted with 4,4′-dimethoxytriphenylmethyl chloride (DMTr-Cl) in pyridine to protect the 5′-hydroxyl group prior to succinylation.

Succinylation of hydroxyl compounds (mainly steroids and related substances) is usually performed with 1–1.5 equiv of succinic anhydride in the presence of 4-(*N*,*N*-dimethylamino)pyridine (DMAP). For example, Morvan et al. (*17*) performed the reaction in dichloromethane with 1.5 mmol of DMAP, 1.5 mmol of succinic anhydride, and 1.5 mmol of triethylamine per millimole of nucleoside. For compound **2** (Figure 1) the reaction was exceedingly slow, and these conditions were modified by increasing the amount of succinic anhydride to 4 mmol, and after 16 h at room temperature compound **3** was isolated with a 77% yield. Compound **3** was used for the deprotection step without further purification.

Removal of the dimethoxytrityl group of **3** was accomplished with 80% acetic acid without cleavage of the hemisuccinate ester bond. The crude product was purified by column chromatography on silica gel with 70% aqueous ethanol to yield 5-FUdr-succ (**4**) in 86% yield.

Coupling of 5-FUdr-succ to Monoclonal Antibody. Compound **4** was conjugated to mAb with the succinimido ester derivative. To obtain the active ester of **4** with NHS, various ratios of the reactants were tested (data not shown). The optimal reaction conditions were found to be 1.1 equiv of NHS and 6 equiv of dicyclohexylcarbodiimide (DCC). We were unable to crystallize the active ester and it was therefore used without further purification. To optimize coupling, different molar excesses of 5-FUdr-succ active ester were added to mAb to yield conjugates with different degrees of substitution. It was found that the addition of a 20-fold molar excess of the active ester of **4** led to an incorporation of nine molecules of 5-FUdr per antibody molecule with a protein recovery of 80%; a 60-fold excess yielded 21 incorporated 5-FUdr molecules (residues) with a 72% recovery of protein (Figure 2). The conjugates that were tested further in vitro had between 5 and 20 molecules of 5-FUdr incorporated per molecule of mAb.

To determine the stability of the 5-FUdr–mAb conjugate it was kept in phosphate-buffered saline at 4 °C and was passed through a Sephadex G-25 column to remove any dissociated 5-FUdr-succ and requantitated after 2 and 7 days; no loss of drug occurred (not shown).

Antibody Activity of 5-FUdr–mAb Conjugates. The antibody activity of the immunoconjugates was quantitated by flow cytometry. The binding of the conjugates to Ly-2.1^{+ve} ITT(1)75NS E3 (E3) cells was measured by fluorescence of the cells after incubating with immunoconjugate, washing, and exposing to fluorescein-labeled rabbit anti-mouse antibody. The concentration of the immunoconjugate giving 50% of maximum fluorescence was calculated and compared with that of unconjugated mAb to give a relative activity of conjugated to nonconjugated antibody. It was found that low numbers of 5-FUdr residues (1–10) slightly reduced the antibody activity (conjugates were 1.5–2-fold less active than the unconjugated antibody) while higher numbers of residues led to a further reduction (10–25 residues, 3–5-fold less active) (Figure 3A). A highly conjugated sample (42 residues) showed considerable loss of antibody activity and was 21-fold less active.

The antibody activity of conjugates were also measured by using a competition assay. The antibody activity of conjugate measured by using the competition assay was

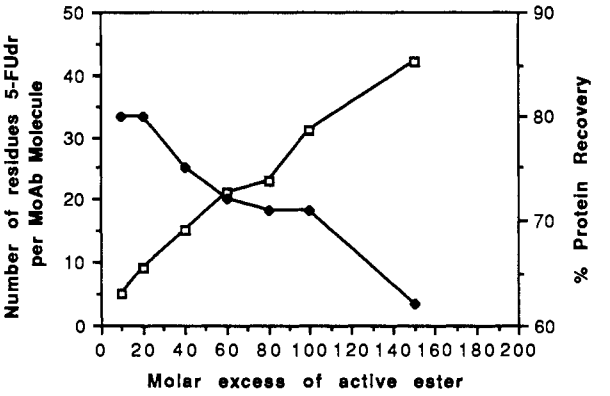


Figure 2. Coupling of 5-FUdr-succ active ester to anti-Ly-2.1 mAb. The number of residues of 5-FUdr incorporated per molecule of anti-Ly-2.1 (□) and protein recovery (◆) is shown as a function of the molar excess of 5-FUdr-succ active ester.

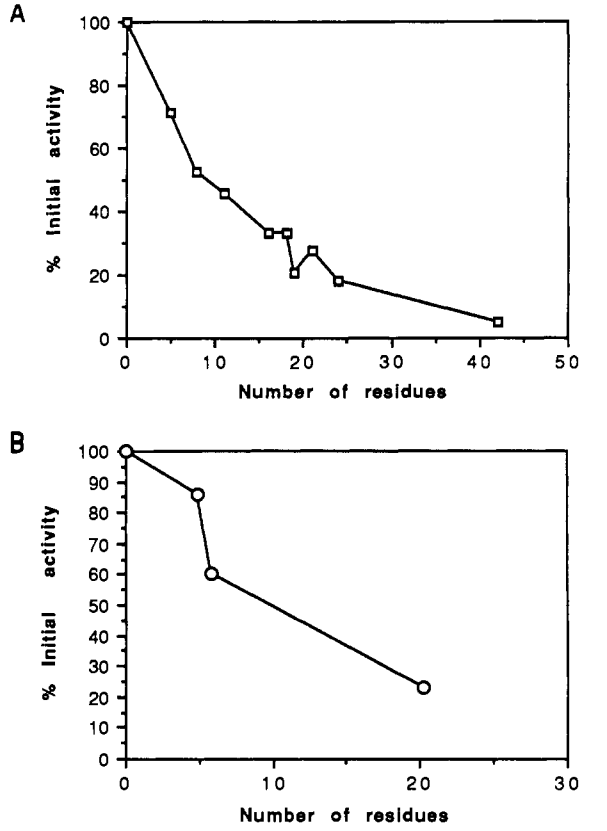


Figure 3. Antibody activity of 5-FUdr–anti-Ly-2.1 conjugates on E3 cells. The antibody activity is expressed as a percentage of the initial antibody activity determined by flow cytometry and is shown as a function of the number of 5-FUdr residues coupled to anti-Ly-2.1: (A) direct binding assay, (B) competition assay.

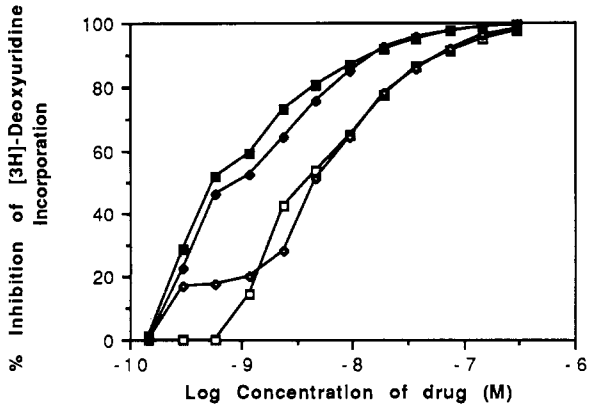


Figure 4. The inhibitory effect (as percent inhibition of [^{3}H]-deoxyuridine uptake) of 5-FUdr (◆) and 5-FUdr-succ (◇) on Ly-2^{-ve} BW5147 cells and of 5-FUdr (■) and 5-FUdr-succ (□) on Ly-2^{+ve} E3 cells.

Table I. Effect of 5-FUdr and 5-FUdr-succ on Tumor Cells[a]

	mean IC_{50}, M		
tumor cells	FUdr	FUdr-succ	5-FUdr-mAb
E3	5.1×10^{-10}(3)	5.2×10^{-9}(6)	6.0×10^{-9}(30)
BW5147	1.4×10^{-9} (2)	5.3×10^{-9}(2)	2.4×10^{-8} (6)

[a] The number of individual values is in parentheses.

similar to the activity measured by using the direct binding assay (Figure 3B).

Cytotoxicity of 5-FUdr–mAb Conjugates in Vitro. The in vitro cytotoxicity of 1 and 5-FUdr-succ (4) on the murine Ly-2.1^{+ve} E3 cell line and the Ly-2.1^{-ve} BW cell line was measured in an inhibition assay, and IC_{50} values were determined (Table I, Figure 4). With E3 the cytotoxicity of 5-FUdr-succ (4) (IC_{50} = 5.2 nM) was 10-fold less than that of 5-FUdr (1) (IC_{50} = 0.51 nM), suggesting that succinylation of the 3'-group of 5-FUdr (1) results in some loss of activity, possibly due to less efficient uptake into the cell by the nucleoside-transport system. With BW a 4-fold loss of activity was observed. It was also noted that E3 was 3-fold more sensitive to 5-FUdr than BW. However, the sensitivity of both cell lines to 5-FU-succ (4) was the same so that data using the immunoconjugates can be compared (Figure 4). The cytotoxicity of anti-Ly-2.1 conjugates with 2–20 molecules of 5-FUdr bound per molecule antibody was tested (Table I) on Ly-2.1^{+ve} E3 and Ly-2.1^{-ve} BW cell lines, where it was found that the IC_{50} values for E3 were in the range of $5.0–9.0 \times 10^{-9}$ M (average of 6.0×10^{-9} M from 30 individual values), while the IC_{50} for the BW cell line was $2–6 \times 10^{-8}$ M (average of 2.4×10^{-8} M), the results indicating that 5-FUdr–mAb is 4 times more active on the Ly-2^{+ve} cell line than on the Ly-2^{-ve} cell line. In both cases, no significant differences were found when using 5-FUdr–anti-Ly-2.1 conjugates with different degrees of 5-FUdr substitution (Figure 5). These data show that 5-FUdr–anti-Ly-2.1 conjugates are 12 times less toxic than 5-FUdr (1) on the E3 cell line but of similar toxicity to FUdr-succ (4).

Specificity in Vitro. To show that the cytotoxicity of the conjugates was due to specific targeting by the antibody, a cytotoxicity assay was carried out with both Ly-2.1^{+ve} E3 cells and Ly-2.1^{-ve} BW cells. In this assay conjugates were exposed to antibody reactive (E3) and antibody nonreactive (BW) cells for 30 min and washed and then incubated for 24 h and pulsed with [^{3}H]deoxyuridine. The IC_{50} of the anti-Ly-2.1 conjugate for E3 was 7.1×10^{-8} M while the IC_{50} for BW was $>5.01 \times 10^{-7}$ M (Figure 6) and indicates that the 5-FUdr–anti-Ly-2.1 conjugates are selectively toxic to Ly-2.1^{+ve} cells.

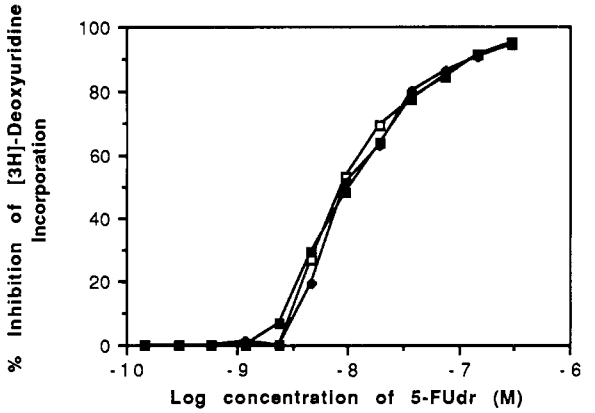


Figure 5. The inhibitory effect on Ly-2.1^{+ve} E3 cells of 5-FUdr–anti-Ly-2.1 conjugates containing different numbers of 5-FUdr residues: (□) 11 residues, (◆) 19 residues, (■) 26 residues.

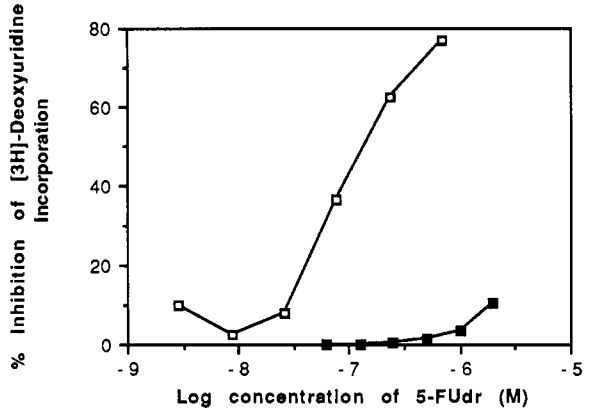


Figure 6. The inhibitory effect of 5-FUdr–anti-Ly-2.1 (11 residues) on Ly-2^{+ve} E3 (□) and Ly-2^{-ve} BW5147 (■) in a short-exposure cytotoxicity assay.

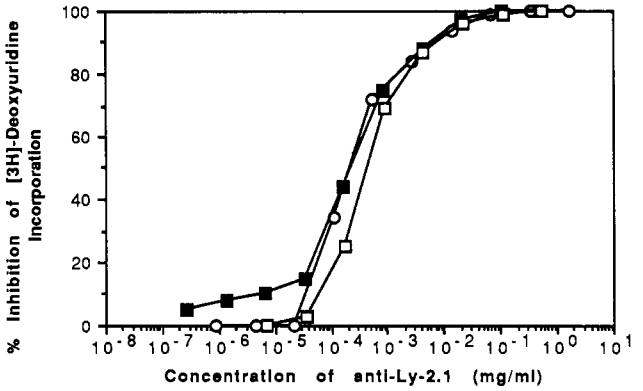


Figure 7. The inhibitory effect of 5-FUdr–anti-Ly-2.1 on E3 on day 1 (○), after a 24-h incubation without fetal calf serum (■) and with fetal calf serum (□).

Stability of 5-FUdr–anti-Ly-2.1 in Growth Medium. To ascertain the degree of dissociation of 5-FUdr–mAb in growth medium, conjugates prepared with radiolabeled anti-Ly-2.1 were incubated with fetal calf serum for 24 h as described in the Experimental Procedures. The cytotoxicity of the various samples are shown in Figure 7. The IC_{50} of the conjugate in terms of antibody concentration was 2.5×10^{-4} mg/mL on day 1. The IC_{50} of the conjugate after 24-h incubation without serum was identical with the initial IC_{50}. However, when the conjugate was incubated with serum the IC_{50} was increased to 4×10^{-4} mg/mL. Therefore, in the presence of fetal calf serum the cytotoxicity of the conjugate was reduced 1.6-fold,

indicating a loss of some 5-FUdr residues. Unconjugated radiolabeled anti-Ly-2.1 at the same specific activity as conjugate did not inhibit [^{3}H]deoxyuridine uptake in cells.

DISCUSSION

Monoclonal antibodies reactive with tumor antigens have been shown to be suitable carriers for drugs and toxins to target them to tumor cells (*3*). However, one major limitation to the use of drug–monoclonal antibody conjugates is the degree of drug and monoclonal antibody activity retained after conjugation. One approach in overcoming these problems is the use of more cytotoxic drugs such as 5-FUdr (**1**), which inhibit growth of cells at nanomolar concentrations (Figure 1) as reported herein.

5-FUdr (**1**) had to be chemically modified for conjugation and this was done by the introduction of a carboxyl group by succinylation of 5-FUdr. However to obtain a single product it was necessary to protect one of the two available hydroxyl groups of **1** prior to succinylation. By protecting of the 5′-position with a 4,4′-dimethoxytriphenylmethyl group, succinylation of the 3′-hydroxyl group occurred and deprotection gave the 3′-isomer as the only product, with a yield of 45% after the three steps. Subsequently, the carboxyl group was activated by forming an ester with *N*-hydroxysuccinimide for coupling with monoclonal antibody. Conjugates were obtained with protein recoveries in excess of 70%, even when up to 40 residues of 5-FUdr were coupled to mAb (Figure 2). This significant protein recovery may well be due to the high hydrophilicity of 5-FUdr-succ (**4**), which prevents precipitation of the antibody due to a loss of charged amino groups on the antibody. Thus, highly conjugated antibodies which could have good therapeutic effectiveness were obtained.

Coupling a large number of drug molecules to monoclonal antibodies often causes a loss in antibody activity, and FACS tests demonstrated this to be the case with 5-FUdr as 5-FUdr–anti-Ly-2.1 conjugates with up to 25 molecules of 5-FUdr bound demonstrated 20–80% of the antibody activity of unconjugated anti-Ly-2.1 (Figure 3A). It is possible that binding of FITC-bound sheep anti-mouse antibody maybe hindered by 5-FUdr groups linked to anti-Ly-2.1 and result in an inaccurate measure of antibody activity. With this in mind a competition assay was also performed with FITC-labeled anti-Ly-2.1. As shown in Figure 3B the results from the competition assay were comparable to those of the direct binding assay. It should be noted that the succinylation of 5-FUdr (**1**) in the 3′-position could have an influence on the mechanisms of action of the drug, and it was therefore important to test the in vitro activity of both 5-FUdr (**1**) and its derivative 5-FUdr-succ (**4**). 5-FUdr-succ was 10-fold less toxic than 5-FUdr on E3 cells and 4-fold less toxic than 5-FUdr for BW cells (Table I, Figure 4). The lower cytotoxicity of 5-FUdr-succ may possibly be due to some difficulty in its entry into cells via the nucleoside-transport system or due to the presence of a charged carboxylic acid group.

5-FUdr-succ–mAb containing 11, 19, or 26 drug residues showed no significant variation of their IC_{50} values in a cytotoxicity assay based on the concentration of 5-FUdr-succ (**4**) with an average 12 times lower toxicity than 5-FUdr (**1**) (Table I, Figure 5). This loss in drug activity is mainly due to the chemical modification, as the IC_{50} values for the 5-FUdr–anti-Ly-2.1 is similar to that of 5-FUdr-succ (**4**), indicating that coupling to mAb did not alter the cytotoxicity of the free drug. In a 30-min cytotoxicity assay the 5-FUdr–anti-Ly-2.1 conjugates were selectively toxic to only cells possessing the Ly-2.1 antigen (Figure 6). In a 24-h cytotoxicity assay 5-FUdr–anti-Ly-2.1 conjugates were 4-fold less active on Ly-2.1^{-ve} BW cells. The exact mechanisms for the observed cytotoxicity is not clear. However, it is possible that it may be due to internalization of conjugates by nonspecific pinocytosis or Fc receptor binding. This nonspecific cytotoxicity has been observed with a number of drug–mAb conjugates (*18*, *19*).

The cytotoxicity observed in the 24-h assays was demonstrated to be due to conjugate and not due to drug dissociated from the conjugate by investigating the stability in fetal calf serum. Following an incubation with fetal calf serum the cytotoxicity decreased 1.6-fold (Figure 7).

The exact mechanism of action of these 5-FUdr–mAb conjugates is not known. Several possible mechanism can be suggested. Two of which are the conjugates bind to the antigen and are internalized and digested in the lysosomes to release free drug, and esterases present in the lysosome could hydrolyze the ester bond between 5-FUdr (**1**) and the succinyl group to release 5-FUdr, which is likely to be metabolized to produce the active metabolites. However, the exact mechanism is unknown, and currently a ^{3}H-labeled 5-FUdr-succ is being prepared which will enable extensive stability studies and cellular processing studies to be carried out. Preliminary in vivo studies in mice demonstrate specific antitumor effects, and the results of these studies will be reported elsewhere.

LITERATURE CITED

(1) Chabner, B. A., Fine, R. L., Allegra, C. J., Yeh, G. W., and Curt, G. A. (1984) Cancer chemotherapy. Progress and expectations. *Cancer 54*, 2599–2608.

(2) Cassady, J. M., and Douros, J. D. (Eds.) (1980) Anticancer agents based on natural product models. *Medicinal Chemistry, Vol. 16*, Academic Press, New York.

(3) Pietersz, G. A., Kanellos, J., Smyth, M. J., Zalcberg, J., and McKenzie, I. F. C. (1987) The use of monoclonal antibody conjugates for the diagnosis and treatment of cancer. *Immunol. Cell Biol. 65*, 111–125.

(4) Smyth, M. J., Pietersz, G. A., and McKenzie, I. F. C. (1987) The mode of action of methotrexate monoclonal antibody conjugates. *Immunol. Cell Biol. 65*, 189–200.

(5) Epenetos, A. A., Snook, D., Durbin, H., Johnson, P. M., and Taylor-Papadimitriou, J. (1986) Limitations of radiolabeled monoclonal antibodies for localization of human neoplasms. *Cancer Res. 46*, 3188–3191.

(6) Smyth, M. J., Pietersz, G. A., and McKenzie, I. F. C. (1987) Use of vasoactive agents to increase tumor perfusion and the antitumor efficacy of drug–monoclonal antibody conjugates. *J. Natl. Cancer Inst. 79*, 1367–1373.

(7) Smyth, M. J., Pietersz, G. A., and McKenzie, I. F. C. (1988) Increased antitumor effect of immunoconjugates and tumor necrosis factor. *Cancer Res. 48*, 3607–3612.

(8) Kanellos, J., Pietersz, G. A., Cunningham, Z., and McKenzie, I. F. C. (1987) Anti-tumor activity of aminopterin monoclonal antibody conjugates; in vitro and in vivo comparison with methotrexate monoclonal antibody conjugates. *Immunol. Cell Biol. 65*, 483–493.

(9) Vitetta, E. S., and Uhr, J. W. (1985) Immunotoxins: Redirecting nature's poisons. *Annu. Rev. Immunol. 3*, 197–212.

(10) Meyers, C. E., Diasio, R. B., Eliott, H. M., and Chabner, B. A. (1976) *Cancer Treat. Rev. 3*, 175.

(11) Cheng, C. C., Ellis, G. P., and West, G. B. (Eds.) (1969) *Progress in Medicinal Chemistry, Vol. 6*, Butterworths, London.

(12) Smyth, M. J., Pietersz, G. A., Classon, B. J., and McKenzie, I. F. C. (1986) Specific targeting of chlorambucil to tumors with the use of monoclonal antibodies. *J. Natl. Cancer Inst. 76*, 503–510.

(13) Hyman, R., and Stallings, V. (1974) Complementation patterns of Thy-1 variants and evidence that antigen loss

variants "pre-exist" in the parental population. *J. Natl. Cancer Inst. 52*, 429–436.
(14) Hogarth, P. M., Edwards, J., McKenzie, I. F. C., Goding, J. W., and Liew, F. Y. (1982) Monoclonal antibodies to murine Ly-2.1 cell surface antigen. *Immunology 46*, 135–144.
(15) Thomas, H. J., and Montogomery, J. A. (1962) Complex esters of thioinosinic(5') acid. *J. Med. Pharm. Chem. 5*, 24–32.
(16) Habener, J. F., Vo, C. D., Le, D. B., Gryan, G. P., Ercolani, L., and Wang, A. H. (1988) 5-Fluorodeoxyuridine as an alternative to the synthesis of mixed hybridization probes for the detection of specific sequences. *Proc. Natl. Acad. Sci. U.S.A. 85*, 1735–1739.
(17) Morvan, F., Rayner, B., Leonetti, J.-P., and Imbach, J. L. (1988) α-DNA VII. Solid phase synthesis of α-anomeric oligodeoxyribonucleotides. *Nucl. Acid. Res. 16*, 833–847.
(18) Hermentin, P., Doenges. R., Gronski, P., Bosslet, K., Kraemer, H. P., Hoffmann, D., Zilg, H., Steinstraesser, A., Schwarz, A., Kuhlmann, L., Lüben, G., and Seiler, F. R. (1990) Attachment of Rhodosaminylanthracyclinone-type anthracyclines to the hinge region of monoclonal antibodies. *Bioconjugate Chem. 1*, 100–107.
(19) Pietersz, G. A., Smyth, M. J., and McKenzie, I. F. C. (1988) Immunochemotherapy of a murine thymoma with the use of idarubicin–monoclonal antibody conjugates. *Cancer Res. 48*, 926–931.

Conjugation of Phenyl Isothiocyanate Derivatives of Carborane to Antitumor Antibody and in Vivo Localization of Conjugates in Nude Mice

Aravamuthan Varadarajan,† Robert M. Sharkey,‡ David M. Goldenberg,‡ and M. Frederick Hawthorne*,†

Department of Chemistry and Biochemistry, University of California at Los Angeles, Los Angeles, California 90024, and Center for Molecular Medicine and Immunology, 1 Bruce Street, Newark, New Jersey 07103.
Received August 29, 1990

A systematic study of the conjugation of 1-(*p*-isothiocyanatophenyl)-1,2-dicarba-*closo*-[2-^{3}H]dodecaborane(12), ^{3}H-**1**, and 7-(*p*-isothiocyanatophenyl)dodecahydro-7,8-dicarba-*nido*-[8-^{3}H]undecaborate(1-) ion, ^{3}H-**2**, to the murine monoclonal anti-CSAp antibody, Mu-9, was carried out to compare charged and uncharged boron cages in their effect upon antibody loading. Approximately one neutral cage and four of the anionic cages were successfully linked to antibody in two separate conjugates which were subsequently radioiodinated and evaluated in vivo. No significant loss of the antibody or its immunoreactivity was observed in either case. In nude mice bearing GW-39 tumor xenografts the conjugate containing the anionic carborane derivative showed a reduced tumor uptake although the tumor:nontumor ratio was similar to that of the native antibody. The carborane cage in **2** was radiolabeled with ^{125}I followed by attempts to purify and conjugate product **4** to a model goat IgG protein. This exploratory conjugation study was undertaken as a prelude to linking new conjugation reagents, which contain multiple anionic boron cages, to antitumor antibodies. The latter conjugates are required to maximize boron loading for the purpose of neutron-capture therapy.

The application of the cytotoxic ^{10}B-neutron-capture reaction [^{10}B(n,α)^{7}Li] to selective neoplastic cell destruction has remained an attractive concept since it was first advanced by Locher (*1–3*). The employment of antitumor antibodies as the targeting vehicles for the selective delivery of therapeutic doses of boron-10 to tumor has evoked considerable interest following the original suggestion by Bale (*4*). Since then, selective tumor accretion of tumor-associated radiolabeled antibodies has been extensively reported (*5–8*). In addition, Mizusawa et al. have reported the conjugation of a cationic aryldiazonium carborane derivative, ^{3}H-**6**, to anticarcinoembryonic antigen and the biodistribution of the conjugate in hamsters bearing the human colon tumor GW-39 wherein the conjugate retained the immunological properties of the unmodified antibody (*9–11*). In attempts to increase the extent of boron loading on the antibody for viable therapeutic use, other carborane derivatives such as the *p*-phenylisothiocyanate derivatives were considered. The carborane cages each provide nine or 10 boron atoms for tumor delivery and the two carborane carbons provide ample means for functionalization and subsequent conjugation to the antibody protein. The isothiocyanate group was chosen for its hydrolytic stability and facile reaction with the amino groups of the protein. In fact, the isothiocyanate group has been the functional group of choice for the conjugation of metal chelates, boron compounds, and other reagents to antibody molecules. For example, Gansow and co-workers have reported the conjugation of (*p*-isothiocyanatobenzyl)diethylenetriaminepentaacetic acid to a monoclonal antibody for further labeling with ^{111}In (*12*). Soloway and co-workers have conjugated a polyhedral borane containing the isothiocyanate group to bovine serum albumin (*13*). Gabel and co-workers have synthesized a water-soluble deca-*B*-chloro-1,2-dicarba-*closo*-dodecaborane(12) isothiocyanate derivative which was then incorporated into poly(L-lysine) (*14*). To this end, Mizusawa and co-workers have synthesized a water-soluble isothiocyanate-containing carborane derivative, ^{3}H-**2**, and carried out initial studies of the conjugation of this species to an anti-CEA antibody (*15*). In this paper we report the conjugation of the isothiocyanate derivatives ^{3}H-**1** and ^{3}H-**2** with the murine monoclonal antibody Mu-9 and compare the results with those obtained with the previously reported cationic aryldiazonium carborane reagent ^{3}H-**6** (*9–11*). In the present case, biodistribution studies employed nude mice and GW-39 tumor xenografts. These studies serve to delineate the viability of small neutral (closo) and anionic (nido) carborane reagents in antibody conjugation and to provide guidelines for the design and synthesis of large assemblies of such structures collected in oligomeric conjugation reagents. These oligomeric reagents are under investigation and they may provide one method of linking large numbers of B atoms to each mAb. Also explored here is the possible use of the facile radioiodination of the anionic *nido*-carborane cage as a novel source of prosthetic labeling agents for proteins. The radioiodination of carborane derivatives **2** and **3** by the chloramine-T method to yield **4** and **5**, respectively, is represented in Scheme I. With sufficiently high specific activity it may prove possible to directly determine the biodistribution of radioiodinated *nido*-carborane cages, thus eliminating the need to iodinate antibody and the associated in vivo dehydrohalogenation reaction.

EXPERIMENTAL PROCEDURES

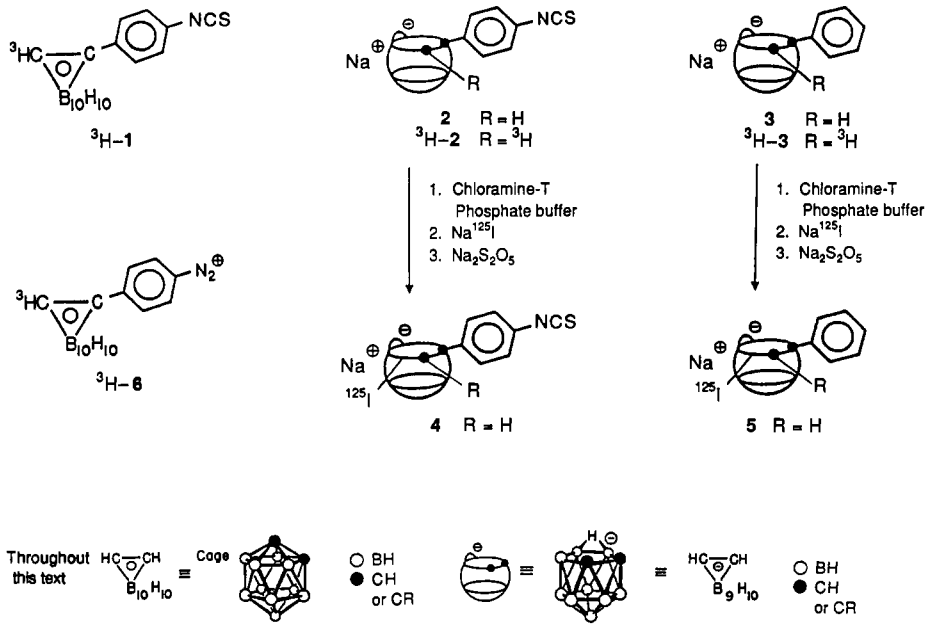
Preparation of 1-(*p*-Isothiocyanatophenyl)-1,2-dicarba-*closo*-[2-^{3}H]dodecaborane(12), ^{3}H-1. Compound ^{3}H-**1** was prepared from 1-(*p*-aminophenyl)carborane, ^{3}H-**7**, by reaction with thiophosgene as outlined in Scheme II. The method of preparation and isolation, yield, and spectral characterization were similar to those reported previously (*15*).

Preparation of 7-(*p*-Aminophenyl)dodecahydro-7,8-dicarba-*nido*-[8-^{3}H]undecaborate(1-) Ion, ^{3}H-8. The

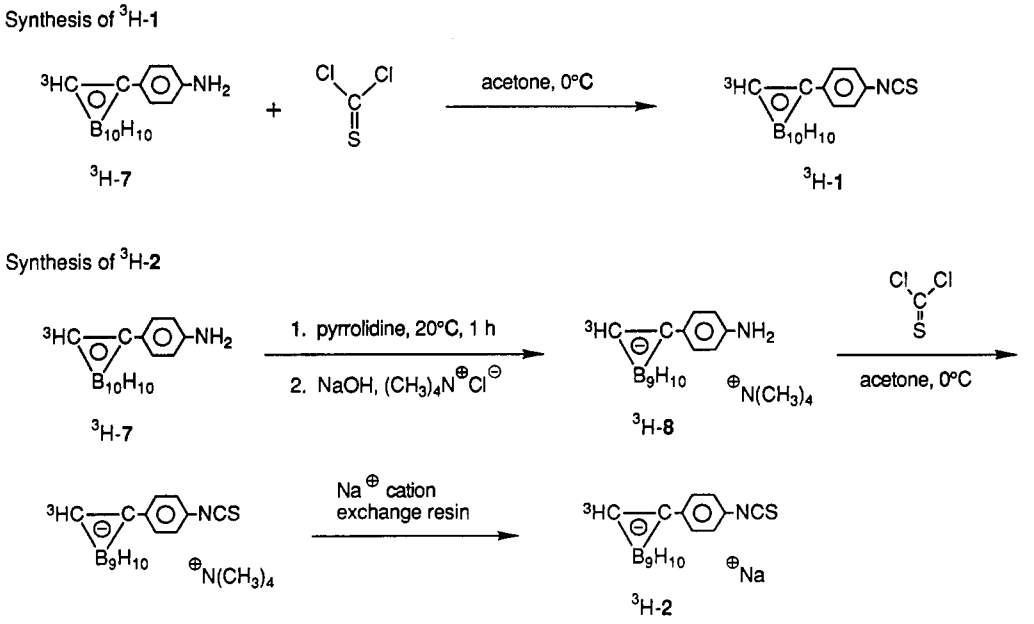
* To whom correspondence should be addressed.
† University of California at Los Angeles.
‡ Center for Molecular Medicine and Immunology.

1043-1802/91/2902-0102$02.50/0 © 1991 American Chemical Society

Scheme I



Scheme II



starting 1-(*p*-aminophenyl)carborane, ^{3}H-7 (0.10 g, 0.42 mmol, 2.1×10^8 cpm), was treated with pyrrolidine (1 mL) and the mixture was stirred under nitrogen at ambient temperature for 1 h. The excess pyrrolidine, which contained some of the tritium, was pumped off, with two traps cooled in liquid nitrogen and a potassium hydroxide trap. The residue was treated with dilute sodium hydroxide solution (1.0 M, 10 mL) and heated at 100 °C for 1 h. The mixture was cooled to ambient temperature and extracted with benzene. The aqueous layer was treated with tetramethylammonium chloride and the precipitated solid was collected. The benzene layer was concentrated; the residue was treated with a minimum amount of ethanol and diluted with water until the solution started to turn cloudy. Addition of tetramethylammonium chloride yielded a further crop of the product. The two solids were combined, washed with water, dried, and recrystallized from a mixture of acetonitrile and benzene. The cage degradation product was obtained as an off-white solid (0.06 g, 0.2 mmol, 1.9×10^8 cpm). The product was characterized by spectroscopic methods previously published (*15*). Conversion to the desired product, ^{3}H-2, was accomplished by the method of Mizusawa et al. (*15*).

Preparation of 7-(*p*-Isothiocyanatophenyl)dodecahydro-7,8-dicarba-*nido*-[8-^{3}H]undecaborate (1−) Ion, ^{3}H-2. Conversion of ^{3}H-8 to the desired product, ^{3}H-2, was carried out by the reaction of the tetramethylammonium salt of ^{3}H-8 with thiophosgene, followed by cation-exchange chromatography (Scheme II) as described by Mizusawa, et al. (*15*). The yield and the spectral characteristics of ^{3}H-2 were identical with those reported previously.

Antibody Purification, Radiolabeling, and Initial Characterization. The murine monoclonal antibody (mAb) Mu-9 was developed as described by Nocera, et al. (*16*). Mu-9 is an IgG_1 that was selected from hybridoma clones derived from the immunization of mice with GW-39, a human colonic tumor xenograft serially propagated in hamsters or nude mice (*17*). This mAb recognizes an epitope with characteristics that are similar to the antigen called colon-specific antigen-p (CSAp) (*18*, *19*). Additional characterization of the Mu-9 mAb, the epitope it recog-

Table I. Effect of the Protein Concentration on the Efficiency of Conjugation of ^{3}H-2 to Goat IgG[a]

compd	vol of IgG soln used, μL	IgG concn, mg/mL	conj time, h	molar ratio of carborane to IgG	carborane cage/IgG molecule[b]	% protein rec	% HMW[c]
^{3}H-2	50	2.0	3	12.7	8.7	38.0	18.3
			3	25.5	6.8	28.6	*d*
	50	10.0	*e*	33.9	*e*	*e*	
	68	12.6	*e*	22.4	*e*	*e*	
	50	6.3	*e*	26.8	*e*	*e*	
	50	3.16[f]	0.75	21.4	7.7	53.6	41.2
	50	3.16[g]	1	9.6	3.8	34.8	19.8
				19.2	3.2	33.1	28.7
	100	3.1[h]	1	10.0	2.0	96.1	26.4
	100	4.2		4.0	1.6	75.0	*d*
				8.1	3.3	77.0	*d*
				12.1	4.4	73.0	*d*
				16.1	4.5	53.0	*d*
^{3}H-3	50	3.0	1	17.5	0.3	24.0	5.6
				35.0	0.0	56.9	7.2

[a] In HCO_3/CO_3 buffer (0.5 M, pH 9.5) at ambient temperature. [b] Micromole carborane/micromole IgG in the conjugate. [c] High molecular weight species from HPLC analysis of the conjugates. [d] Not measured. [e] Not measured due to precipitation. [f,g,h] High molecular weight species present initially, prior to conjugation, 8.4, 7.0, and 9.3%, respectively.

nizes, and biodistribution studies comparing Mu-9 to anticarcinoembryonic antigen mAbs and other colon-associated antigens have been reported elsewhere (*20, 21*).

Mu-9 was purified from mouse ascites by passage through protein A with an additional purification by ion-exchange chromatography. The mAb was tested for purity by SDS-PAGE under reducing and nonreducing conditions, immunoelectrophoresis, and size-exclusion HPLC using a TSK-250 column (Bio-Rad, Richmond, CA) with an in-line UV detector (Gilson, Middleton, WI).

Mu-9 was labeled with ^{131}I (NEN, Boston, MA) by the chloramine-T method as described previously (*17*). The immunoreactivity of the radioiodinated Mu-9 was determined by passage over an immunoadsorbent prepared by coupling a partially purified extract of CSAp extracted from GW-39 tumors to Affi-Gel 10 (Bio-Rad, Richmond, CA).

Conjugation Experiments. *a. Optimization Experiments Involving Small-Scale Conjugations.* A given amount of the protein solution was transferred to the conjugation buffer with a centrifuge column made up with Sephadex G50M (Pharmacia, Inc., Piscataway, NJ) swollen in the conjugation buffer (*22*). The solution was further diluted with the same buffer to the required volume and a known amount of the reagent ^{3}H-1 in DMF or ^{3}H-2 in water was added to the protein solution. The mixture was stirred for the given length of time at ambient temperature and the conjugate was purified with a centrifuge column made up with Sephadex G50M. The volume of the centrifugate was measured and aliquots were taken for Bio-Rad protein assay (Bio-Rad Laboratories, Richmond, CA), ^{3}H counting and gel filtration HPLC analysis (Du Pont GF-250 column, 0.10 M Tris HCl eluent with 0.15 M NaCl and 0.005% NaN_3, pH 7.5, flow rate 1 mL/min, UV detector at 280 nm). The actual conditions for conjugation are given in Tables I and II. From the Bio-Rad assay for protein content and the tritium counts associated with the boron reagent in the conjugate, the average number of carborane cages per antibody protein molecule was calculated.

b. Larger Scale Preparation of Conjugate for Biodistribution Studies. Two 300-μL samples of the monoclonal antibody (Mu-9) in phosphate-buffered saline were diluted with carbonate/bicarbonate buffer (0.1 M, containing 0.15 M NaCl, pH 9.6) to 6.02 mL. Aliquots (20 μL) were withdrawn from each sample for protein concentration determination by Bio-Rad assay and gel-filtration HPLC analysis for the determination of the presence of high molecular weight (HMW) species. To each of the remaining solutions a known volume of ^{3}H-1 in DMF (33 μL, 13 mM) or ^{3}H-2 in H_2O (21 μL, 20 mM) was added separately. The addition was carried out very slowly to minimize the separation of precipitates. The solution containing ^{3}H-2 remained clear but that with ^{3}H-1 was cloudy due to the separation of the water-insoluble carborane species. The solutions were agitated in a vortex mixer for 1 min and stirred for 2.5 h. They were filtered through Millex GV (22 μm) filters (Millipore Corporation, Milford, MA) and concentrated with Centricon-30 concentrators (Amicon Division, W. R. Grace & Co., Danvers, MA). The concentrates were passed through Sephadex G50M columns swollen in 0.1 M carbonate/bicarbonate buffer. The eluted materials were centrifuged again at 6000 rpm for 1 h (using a Sorval RC5C centrifuge with a SS-34 rotor). This process was repeated with the centrifugates until no visible solid residue separated upon centrifugation and thin-layer chromatography of the conjugates revealed the absence of the free carborane derivatives. Aliquots were withdrawn for ^{3}H counting, Bio-Rad protein assay, and HPLC analysis. The remaining antibody conjugates were used for radioiodination and biodistribution studies.

Biodistribution of Boron-Conjugated Mu-9 in Tumor-Bearing Nude Mice. The unconjugated Mu-9 (control) and the two boron-conjugated Mu-9's were radioiodinated separately with ^{131}I, and 25 μCi (about 2 μg) of each of the labeled Mu-9's were injected iv in nude mice bearing 14-day-old subcutaneous GW-39 tumors. The average size of the tumor (range 0.1–0.3 g) was 0.25 g. Groups of five or six mice were sacrificed 1, 3, and 7 days after radioantibody injection, and the tumor and tissues were weighed and counted to determine the percent injected dose per gram tissue and tumor: nontumor ratios according to methods described previously (*23*). Samples of the radiolabeled Mu-9, Mu-9–^{3}H-1, and Mu-9–^{3}H-2 were tested within 1 day after labeling by size-exclusion HPLC with an in-line radiation detector (Beckman, Fullerton, CA) to determine the molecular sizing properties of the conjugated Mu-9 compared to those of the unconjugated Mu-9. The immunoreactivity of the labeled samples was determined by passage over the partially purified CSAp immunoadsorbent, and the binding to an anti-mouse IgG immunoadsorbent was also tested.

General Method for Radioiodination of 2 and Its Conjugation to IgG. To a solution of Na^{125}I (1 mCi, Amersham) in a vial were added phosphate buffer (40 μL, pH 7.45, 0.05 M), the aqueous solution of the sodium salt of 2 (25 μL, 3.96 mM), and chloramine-T (15 μL, 0.01 M in phosphate buffer) in succession. After 5 min a solution

Table II. Conjugation of ^{3}H-1 and ^{3}H-2 to Mu-9 Antibody[a]

compd	buffer (pH)	Mu-9 concn, mg/mL	volume of Mu-9 soln used	initial % HMW[b] species	conj time, h	molar ratio of carborane to Mu-9	carborane cage/Mu-9 molecule[c]	% protein rec	final % HMW[d]
			Effect of Buffer						
^{3}H-2	0.5 M CO_3 (10.0)	3.0	100 μL	1.7	2	16.7	5.5	63.8	42.0
^{3}H-2	0.1 M HEPES (8.2)	3.1	100 μL	0.0	2	16.4	0.8	72.2	0.0
^{3}H-2	0.1 M CO_3 (10.0)	3.0	100 μL	0.0	2	16.9	7.4	68.3	negl
^{3}H-2	0.1 M borate (9.2)	2.9	100 μL	1.3	5	17.5	4.6	46.2	46.9
^{3}H-2	0.1 M HCO_3 (8.1)	3.4	100 μL	1.5	5	15.0	4.1	64.5	33.8
^{3}H-2	0.1 M citrate (8.9)	3.1	100 μL	1.1	5	16.4	1.2	44.6	4.6
^{3}H-2	0.1 M CO_3/HCO_3 (10.0)	3.1	100 μL	0.8	5	16.5	6.3	29.9	100.0
			Effect of Added Reagents						
^{3}H-2	0.5 M CO_3/HCO_3 (9.6) + DMSO (10 μL)	4.8	100 μL	1.2	1	15.6	6.8	66.4	61.4
^{3}H-2	0.1 M CO_3 (10.0) + DMF (5 μL)	3.0	100 μL	0.0	2	16.9	6.3	76.2	negl
^{3}H-2	0.1 M CO_3 (10.0) + SDS (5 μL)	3.0	100 μL	0.0	2	16.9	6.2	78.8	br peak
^{3}H-2	0.1 M CO_3/HCO_3 (10.0) + CH_3CN (10 μL)	3.0	100 μL	0.8	5	16.5	8.7	70.0	59.0
			Control Conjugation						
^{3}H-3	0.1 M CO_3 (10.0)	3.0	100 μL	0.0	2	20.5	0.1	84.4	0.9
			Conjugation under High-Dilution Conditions						
^{3}H-1	0.1 M CO_3/HCO_3 (10.0)	0.6	100 μL	0.0	4	27.1	3.3	29.3	1.6
^{3}H-2	0.1 M CO_3/HCO_3 (10.0)	0.6	100 μL	0.0	2	26.9	7.3	76.2	100.0
^{3}H-2	0.1 M CO_3/HCO_3 (10.0)	0.6	100 μL	0.0	1	53.8	8.7	63.5	100.0
^{3}H-1	0.1 M CO_3/HCO_3 (10.0)	0.6	100 μL	0.0	1	108.2	24.6	79.2	17.6
			Large-Scale Conjugation under High-Dilution Conditions						
^{3}H-2[e]	0.1 M CO_3/HCO_3 (9.6)	0.6	6 mL	0.0	2.5	17.7	4.2	59.6	8.89
^{3}H-1[e]	0.1 M CO_3/HCO_3 (9.6)	0.6	6 mL	0.0	5	17.9	0.9	82.7	2.32

[a] All conjugations were carried out at ambient temperature. [b] High molecular weight species present in the antibody prior to conjugation (HPLC assay). [c] Micromole carborane/micromole Mu-9 in the conjugate. [d] High molecular weight species from the HPLC analysis of the conjugates. [e] Conjugates used for the biodistribution studies.

of NaI carrier (20 μL, 0.01 M in phosphate buffer) was added. The iodination was carried out for a further 5 min and the reaction mixture was quenched by the addition of sodium metabisulfite (10 μL, 0.2 M in phosphate buffer). The product mixture was analyzed for 4 by TLC on silica gel (9:1 EtOAc/CH_3CN solvent system; R_f values: IgG, 0.0; NaI, 0.0; carboranes 0.3–0.4) and the different TLC fractions were counted for ^{125}I activity. A carbonate/bicarbonate buffer (0.5 M, pH 10.05, 100 μL) was then added to the iodination mixture and followed by the slow addition of goat IgG (61 μL, 10.5 mg/mL in normal saline). After 30 min, the conjugation mixture was passed through a Pharmacia PD-10 column equilibrated with carbonate/bicarbonate buffer and eluted with the same buffer to collect 6 mL in the void volume and 4 mL in the included volume. These fractions were analyzed by thin-layer chromatography on silica gel (9:1 EtOAc/CH_3CN) and the different TLC fractions were counted for ^{125}I activity. HPLC purification of 4 was attempted with a C_{18} column and 1:1 acetonitrile/water solvent system (flow rate 1 mL/min, UV detector).

A control iodination experiment was carried out under identical conditions using the sodium salt of 7-phenyldodecahydro-7,8-dicarba-*nido*-undecaborate(1−) (**3**; 16 μL, 6.06 mM in H_2O) and iodinated product **5** incubated with IgG as a further check for nonspecific binding. Various modifications to the general method for radioiodination, conjugation, and purification are discussed in the Results section of the text.

RESULTS

Synthetic Aspects. The degradation of the *closo*-carborane cage with a secondary amine to produce the anionic *nido*-carborane derivative has been previously reported (*24*). This method of degradation of the neutral 1-(*p*-aminophenyl)carborane using pyrrolidine as represented in Scheme II led to high retention of the tritium label. Whereas the degradation product from the previously reported alcoholic KOH method (*15*) retained only 10% of the initial tritium activity, the pyrrolidine-degraded product retained 50% of this activity. Consequently, this led to a 5-fold increase in the specific activity of the final product, ^{3}H-**2**. The product of degradation, ^{3}H-**8**, was only partially converted to its sodium salt by direct treatment with NaOH. The remainder of the pyrrolidinium salt, due to its extreme hydrophobicity, dissolved in the solvent (benzene) used for extraction of the free pyrrolidine and required recovery by removal of benzene followed by dissolution in a minimum amount of ethanol and precipitation with tetramethylammonium chloride.

Conjugation Studies. The conjugation of ^{3}H-**2** to goat IgG was carried out under a variety of conditions to maximize the conjugation efficiency with high protein recovery and minimize antibody protein aggregation. While significant nonspecific binding was observed when ^{3}H-**2** was conjugated to IgG in phosphate buffer, conjugation in carbonate/bicarbonate buffer proceeded cleanly and efficiently with no detectable nonspecific binding of ^{3}H-**2** to IgG using TLC techniques. In addition, the tritiated *nido*-phenylcarborane ^{3}H-**3**, which does not have the isothiocyanate group, did not show significant binding to the protein in the carbonate/bicarbonate buffer. The conditions employed for conjugation and the results are summarized in Table I.

From the data presented in Table I, the following observations were made: At concentrations above 2 mg/mL extensive precipitation of the protein occurred leading to severe losses and at relatively higher ratios of ^{3}H-**2** to IgG greater protein loss and lower ^{3}H-**2** incorporation occurred. Upon conjugation of ^{3}H-**2** to IgG, the proportion of the high molecular weight (HMW) species increased considerably and peak broadening occurred in the HPLC of the conjugated protein. This effect was not observed when the nonconjugating ^{3}H-**3** was incubated with IgG prior to HPLC analysis. Tritium counting of the TLC fractions of the conjugates showed that no significant nonspecific binding occurred with ^{3}H-**2** or ^{3}H-**3** and IgG protein recovery improved significantly when the reaction

Table III. HPLC Analysis of Mu-9, Mu-9-^{3}H-2, and Mu-9-^{3}H-1

sample	HPLC[a] analysis (% recovered)				immunoreactivity[d]	
	HMW[b]	IgG	post-IgG	SMW[c]	CSAp	anti-mouse
Mu-9	none	95.9	3.7	0.4	93.3	93.1
Mu-9-^{3}H-2	22.9	72.9	1.6	1.0	86.0	94.1
Mu-9-^{3}H-1	none	89.7	10.4	none	89.5	98.6

[a] HPLC analysis done on TSK-250 using an in-line radiation detector and automatic peak analysis. [b] High molecular weight species. [c] Small molecular weight materials. [d] Nonspecific binding was less than 5% in all the cases.

volume was increased to 100 μL from 50 μL. Therefore, it appeared that an initial protein concentration of 2 mg/mL and a protein to ^{3}H-2 ratio of 1:10 would be optimum for conjugation.

Based on the above information, conjugation of ^{3}H-2 and ^{3}H-1 to the murine monoclonal antibody Mu-9 was carried out under a variety of conditions. An account of the results obtained in these experiments is given in Table II.

From Table II, it is clear that extensive formation of HMW species occurred upon conjugation of ^{3}H-2 to the antibody. The extent of this process was directly dependent upon the proportion of ^{3}H-2 to the antibody. At higher protein concentrations, precipitation occurred when ^{3}H-2 was added and this loss of protein was dependent on the amount of added ^{3}H-2. However, no precipitation was observed with Mu-9 in the presence of DMSO under the same conditions and the protein recovery was significantly higher. In addition, the proportion of the HMW species was higher relative to unmodified antibody, but was significantly lower when compared to the conjugates prepared in the absence of DMSO. Among the buffers used, the carbonate/bicarbonate buffer proved to be the medium of choice for conjugation since it gave consistently higher conjugation efficiency. The addition of small amounts of other organic solvents increased the formation of HMW species along with a marginal increase in conjugation efficiency. As expected, no significant incorporation of the *nido*-phenylcarborane ^{3}H-3 into the antibody was observed when ^{3}H-3 was substituted for ^{3}H-2 in carbonate buffer, thus proving that nonspecific binding does not occur at high pH. Antibody precipitation did not occur when conjugations were carried out at low protein concentrations. Poor recovery of the antibody was observed when the proportion of ^{3}H-2 relative to antibody was increased beyond 25 to 1. For the same reason, prolonged conjugation times proved to be unfavorable. Conjugation of the neutral isothiocyanate derivative, ^{3}H-1, led to erroneous results for the conjugation efficiency due to the precipitation of the unbound ^{3}H-1 as fine particles when it was transferred from DMF solution to the aqueous protein solution. This precipitate passed through centrifuge columns and membrane filters. In subsequent experiments, extensive centrifugation techniques were employed to remove the unbound particulate matter. Consistently better results were obtained by carrying out the conjugation under conditions of high dilution followed by concentration of the samples.

On the basis of the available data, preparative-scale conjugations of ^{3}H-1 and ^{3}H-2 to anti-CSAp Mu-9 were carried out and the samples were extensively purified by membrane filtration, concentration, gel filtration, and centrifugation. The last two entries listed in Table II were the conjugates employed in the biodistribution experiments. These samples were radioiodinated by the chloramine-T method prior to use. The labeling was 69% and 70% efficient for ^{3}H-2- and ^{3}H-1-conjugated Mu-9, respectively, and 76% for unconjugated Mu-9 (relative standard deviation ±5%). The molecular sizing properties and immunoreactivity of these radiolabeled preparations are given in Table III. The molecular sizing properties of the ^{131}I-labeled Mu-9, Mu-9-^{3}H-2, and Mu-9-^{3}H-1 indicated no significant difference in the size distribution of the unconjugated Mu-9 and Mu-9-^{3}H-1 after conjugation with about one closo-C_2B_{10} cage. However, after radioiodination, the Mu-9-^{3}H-2 that contained about four nido-$C_2B_9^-$ cages contained a small amount of HMW species that carried 23% of the total radioactivity. There was no difference in the immunoreactivity of the radiolabeled Mu-9 control and conjugates with all of the samples binding between 86 and 93% of the CSAp immunoadsorbent. The nonspecific binding was less than 5% in all the cases. Less than 5% of a radioiodinated irrelevant IgG (an anti-α-fetoprotein IgG_1 mAb) bound to the CSAp immunoadsorbent while less than 5% of the radiolabeled Mu-9 bound to an α-fetoprotein immunoadsorbent. In addition, the labeled Mu-9 control and conjugates bound equally to an anti-mouse IgG immunoadsorbent, as anticipated.

Biodistribution Studies. The biodistribution studies are summarized in Table IV and Figures 1 and 2. The percent injected dose per gram in the tumor for the unconjugated Mu-9 increased from 13.9 on day 1 to 28.9 on day 3, where it remained through day 7. Similar results were found for Mu-9-^{3}H-1, but there was 2–3-fold less tumor uptake for Mu-9-^{3}H-2. The percentage of radiolabeled Mu-9-^{3}H-2 in the blood was about 3-fold lower than unconjugated Mu-9 on day 1, and by day 7 there was 4-fold less Mu-9-^{3}H-2 in the blood than unconjugated Mu-9. Tumor:nontumor ratios for all of the tissues except the liver were similar for boron-conjugated and unconjugated Mu-9's on day 1. Tumor:liver ratios on day 1 for the Mu-9-^{3}H-2 was 1.3 ± 0.4, but 3.7 ± 0.6 and 4.3 ± 1.0 for the unconjugated Mu-9 and Mu-9-^{3}H-1, respectively. The lower tumor:liver ratio for the Mu-9-^{3}H-2 was due principally to the lower tumor uptake, but there was also slightly more liver uptake (5.4 ± 0.8%) in the Mu-9-^{3}H-2 in comparison to the unconjugated Mu-9 and Mu-9-^{3}H-1 (3.8 ± 0.6% and 3.3 ± 0.3%, respectively). The similarity of tumor:nontumor ratios exhibited by Mu-9-^{3}H-2, Mu-9-^{3}H-1, and unconjugated Mu-9 was the result of lower uptake of radiolabeled Mu-9-^{3}H-2 in the other normal tissues. Tumor:nontumor ratios improved for all groups over time, reflecting the increased tumor uptake with gradual clearance from the normal tissues. By day 7 tumor:nontumor ratios were slightly higher in the Mu-9-^{3}H-1 group with the Mu-9-^{3}H-2 tumor:nontumor ratios similar to those of unconjugated Mu-9. Tumor:blood ratios were higher for both of the boron-conjugated Mu-9's than unconjugated Mu-9.

Radiolabeling of 2 with ^{125}I and Conjugation to IgG. Larger scale carrier-added iodination with Na^{125}I was successful and the product, 4, could be isolated as the tetramethylammonium salt. Starting with 388 μCi Na^{125}I, the product isolated had an activity of 332 μCi as measured by a dose calibrator. TLC on silica gel followed by γ-counting of the TLC fractions showed that the spot corresponding to 4 accounted for 85–95% of the total counts spotted, thereby indicating the radioiodination of the carborane cage, while the spot on the baseline (Na^{125}I)

Table IV. Biodistribution of ^{131}I-Labeled Mu-9 and Mu-9-Boron Conjugates in GW-39 Tumor-Bearing Nude Mice[a,b]

sample	time, h	blood	GW-39	kidney	liver	lung	spleen
			% Injected Dose/Gram of Organ				
Mu-9	24	13.8 ± 1.5	13.9 ± 2.5	4.2 ± 0.5	3.8 ± 0.6	5.7 ± 0.2	3.4 ± 0.7
	72	11.5 ± 2.3	28.9 ± 1.4	3.1 ± 0.7	2.9 ± 1.0	5.1 ± 0.8	3.6 ± 1.3
	168	6.1 ± 1.3	32.0 ± 6.0	1.5 ± 0.4	1.9 ± 0.5	2.3 ± 0.5	1.5 ± 0.6
Mu-9-^{3}H-2	24	6.7 ± 0.8	7.0 ± 1.7	3.0 ± 0.4	5.4 ± 0.8	2.9 ± 0.5	2.0 ± 0.3
	72	3.1 ± 1.1	11.8 ± 1.0	1.6 ± 0.2	2.4 ± 0.2	1.2 ± 0.4	1.0 ± 0.2
	168	1.5 ± 0.2	14.1 ± 4.9	0.8 ± 0.1	1.1 ± 0.2	0.6 ± 0.1	0.5 ± 0.1
Mu-9-^{3}H-1	24	13.4 ± 0.9	13.9 ± 2.7	2.9 ± 0.7	3.3 ± 0.3	4.6 ± 0.8	2.9 ± 0.7
	72	8.5 ± 1.2	28.8 ± 6.6	2.7 ± 0.7	2.4 ± 0.3	3.7 ± 0.5	2.0 ± 0.2
	168	4.3 ± 0.9	46.8 ± 8.0	1.2 ± 0.1	1.2 ± 0.2	1.5 ± 0.2	0.9 ± 0.2
			Tumor:Nontumor Ratio				
Mu-9	24	1.0 ± 0.1		3.3 ± 0.5	3.7 ± 0.6	2.4 ± 0.4	4.1 ± 0.9
	72	2.6 ± 0.7		9.8 ± 2.6	10.8 ± 3.9	5.9 ± 1.2	9.1 ± 3.7
	168	5.5 ± 1.4		21.9 ± 5.0	17.9 ± 3.8	14.0 ± 2.8	23.9 ± 9.6
Mu-9-^{3}H-2	24	1.1 ± 0.3		2.4 ± 0.6	1.3 ± 0.4	2.5 ± 0.9	3.7 ± 1.3
	72	4.1 ± 2.3		6.7 ± 0.6	4.6 ± 0.9	9.7 ± 3.8	11.6 ± 3.2
	168	9.3 ± 2.6		17.1 ± 5.0	12.3 ± 2.2	22.7 ± 9.3	28.1 ± 4.1
Mu-9-^{3}H-1	24	1.0 ± 0.2		5.2 ± 2.0	4.3 ± 1.0	3.0 ± 0.6	5.0 ± 1.4
	72	3.4 ± 0.5		11.0 ± 1.7	11.9 ± 1.8	7.8 ± 1.6	14.7 ± 3.2
	168	11.2 ± 2.6		39.0 ± 11.2	38.9 ± 12.5	31.9 ± 10.9	55.9 ± 16.9

[a] Values quoted are mean ± standard deviation. [b] Average tumor weight was ca. 0.25 g in all the cases.

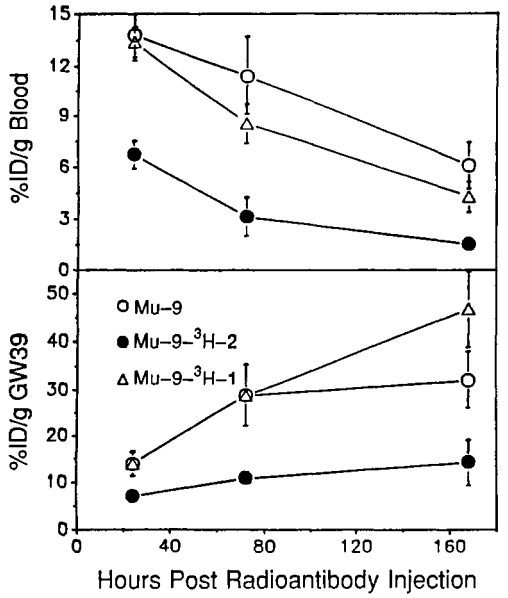


Figure 1. Blood clearance and tumor localization rates for Mu-9, Mu-9-^{3}H-2, and Mu-9-^{3}H-1.

accounted for the remainder of the counts. A control experiment (without any of the added **2**) had nearly all of the activity located on the baseline in the TLC analysis (the relative standard deviation being ±5% in all the cases).

Radiolabeling was carried out under several sets of conditions in order to develop the method for the production of the labeled material with very high specific activity needed for biological studies. With this in mind, conjugation of the labeled material to IgG and analysis of the conjugated product (after purification on a prepacked PD-10 column used for handling of the radioactive material in a closed system) was carried out in order to employ the method for in vitro and, if possible, in vivo studies using monoclonal antibodies.

The following results were obtained: Iodination with Na^{125}I (typically 1 mCi), which typically required Na^{127}I as an added carrier, was rapid (ca. 5 min) and prolonged reaction times gave rise to unidentified side products. Although in a typical experiment 15–30 μg of **2** could be radiolabeled, the use of smaller amounts of **2** (<1 μg) to obtain labeled material of very high specific activity was not successful. Furthermore, iodination occurred poorly in CO_3/HCO_3 buffer. In all cases, TLC analyses revealed the presence of a less polar material which moved along the solvent front and carried some of the activity. This material and/or the labeled *nido*-carborane was found to bind nonspecifically to IgG, even after passing the material through a PD-10 column. The TLC analysis of the conjugated IgG showed one spot moving close to the solvent front. HPLC analysis on a TSK column also showed the presence of labeled material eluting in the included volume when the same sample was incubated with 10–15% DMSO prior to injection.

Similar problems were noted when **3** was radiolabeled with ^{125}I and the resulting **5** incubated with IgG in control experiments. It should be noted that **5** cannot bind to IgG covalently. In order to minimize the nonspecific binding, following radiolabeling the iodination mixture was treated with CO_3/HCO_3 buffer to raise the pH prior to conjugation with IgG. Although this did not completely eliminate the problem of nonspecific binding, it was reduced.

In a typical experiment, outlined in the experimental section, TLC analysis of the iodination mixture indicated that ca. 80% of the label was associated with **2**. After conjugation and gel filtration, the IgG protein eluting in the void volume was analyzed by TLC and was found to contain 52% of the spotted activity with the solvent front accounting for 21% of the counts. The remainder of the activity was smeared along the plate.

In a similar experiment **3** was radioiodinated with 61% efficiency (by TLC) and incubation with IgG yielded the protein containing 14% of the spotted activity after gel filtration through PD-10 while the solvent front had 38% of the spotted activity. The remainder of the counts was distributed evenly along the plate.

These experiments demonstrated the presence of nonspecifically bound material arising from either the radioiodinated cage or some other radioactive impurity. Purification of the labeled cage by HPLC yielded less than satisfying results. For example, new reverse-phase C_{18} columns were initially effective in separating **2** and **4** when 1:1 acetonitrile/water solvent mixture was employed, but with repeated use, the column performance decreased drastically, owing to the degradation of the column support. Optimization of elution conditions with different solvent combinations, such as methanol/water, as well as the employment of buffers failed to alleviate this problem. Furthermore, both cation- and anion-exchange columns were also ineffective for the separation of **2** and **4**.

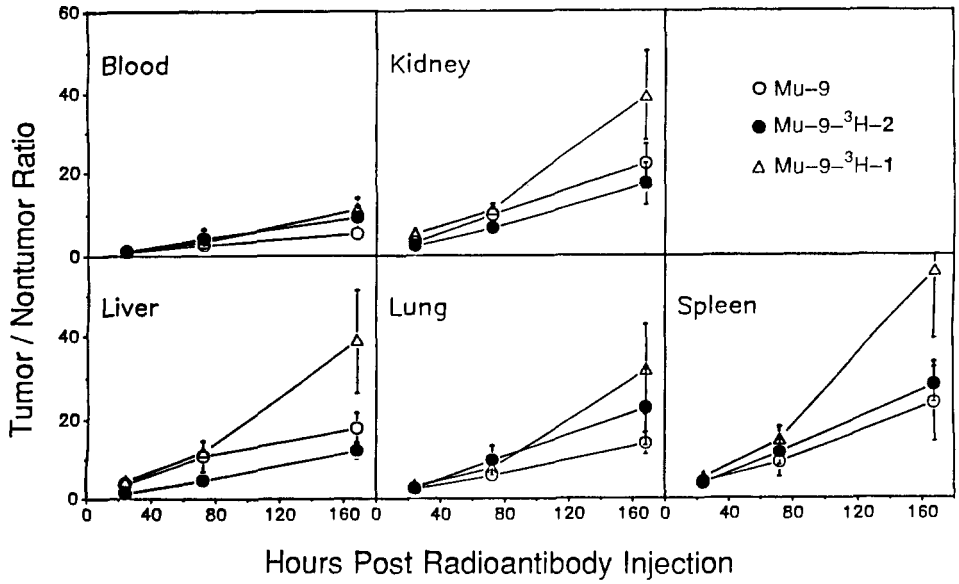
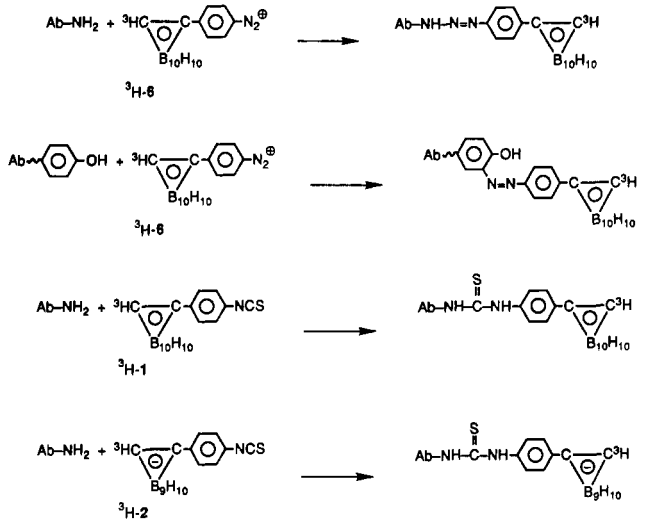


Figure 2. Tumor:nontumor ratios for Mu-9, Mu-9-^{3}H-2, and Mu-9-^{3}H-1.

Scheme III



DISCUSSION

The present study of the conjugation of the representative anionic and neutral carboranyl isothiocyanates, ^{3}H-2 and ^{3}H-1, complements our earlier work on the conjugation of the cationic aryldiazonium derivative of carborane to anti-CEA antibody (*9-11*). The cationic carborane derivative ^{3}H-6 employed previously was conjugated to anti-CEA antibody through the aryldiazonium cation function, which is expected to react with the free amino groups on the antibody protein to form triazenes as well as undergo electrophilic substitution reactions with the activated aromatic nucleus of tyrosine residues. It should be noted that following the conjugation reaction, the positive charge associated with the conjugation reagent is lost. However, in the case of the anionic *nido*-carboranyl isothiocyanate, the negative charge on the carborane is not dissipated after conjugation to form the isothiourea linkage. These charge effects are absent in the case of the neutral *closo*-carboranyl isothiocyanate ^{3}H-1. These reactions are summarized in Scheme III. The presence of ionic charge on the carborane reagent is essential for water solubility and hence for improved conjugation efficiency, as can be seen from the number of carborane cages of each of these species that can be successfully attached to the antibody molecule under a given set of conditions. The absence of charge in the conjugates of ^{3}H-1 and ^{3}H-6 is expected to lower their solubility.

The nonspecific binding observed in the present study with the isothiocyanate derivatives at lower pH could arise from the association of the anionic boron cages with any available positively charged sites (such as the protonated amine residues) in the protein. Another contributing factor would be the inherent hydrophobicity of both the *closo*- and *nido*-carborane cages, which would enable them to interact noncovalently with the hydrophobic regions within the protein. Presumably the use of carbonate/bicarbonate buffer at higher pH has reduced the extent of ionic association.

The loss of protein when conjugation of ^{3}H-2 was carried out at high protein concentration could arise from several factors such as the solubility of the conjugate, the salting-out effect of the added ions, and so on. However, conjugation at low concentration circumvented the problem, although it reduced the rate of reaction, as expected. The nature of the HMW species is unknown. It could be an aggregate of the immunoglobulin, such as a dimer, or a heavily conjugated protein derivative. Due to the early exploratory nature of the current study, the HMW species was only detected in HPLC assays and was not removed from the conjugates employed for biodistribution. We have subsequently separated and investigated the HMW material in greater detail in our later studies involving antibody conjugates containing boron-rich oligomers.

The conjugation of a single boron cage of ^{3}H-1 to the Mu-9 mAb did not appreciably change the tumor uptake or normal tissue clearance rates of the Mu-9 mAb. Quality assurance of the radiolabeled Mu-9-^{3}H-1 showed that the conjugation did not alter the physical or immunological properties of Mu-9. The coupling of about four ^{3}H-2 ions to the Mu-9 mAb resulted in ca. 20% aggregation in the radioiodinated Mu-9-^{3}H-2, but the immunoreactivity of the mAb was not impaired. Biodistribution studies suggested an early enhanced uptake of the Mu-9-^{3}H-2 in the liver, with a 2–3-fold decrease in the level of radioactivity in the blood and other organs. However, because the measured immunoreactivity of the mAb was unimpaired in vitro, tumor targeting was still possible, albeit at a lower level than that of unconjugated Mu-9. Since the reduction in tumor uptake of the Mu-9-^{3}H-2 was similar to the reduction in the amount of radioactivity uptake in the normal tissues other than liver, we infer that the reduced tumor association was directly related to

the increased rate of removal of Mu-9-^{3}H-2 from the blood. Thus, the coupling of four ^{3}H-2 boron cages to Mu-9 caused aggregation of Mu-9 that, in turn, increased the rate of blood clearance for Mu-9-^{3}H-2, with the liver acting as the principal organ for processing the removal of Mu-9-^{3}H-2 from the blood. Since we did not analyze the blood from the animals given Mu-9-^{3}H-2 on day 1, or at earlier times, for the relative proportions of the aggregated and native-sized antibody conjugates, we are uncertain whether more of the monomeric Mu-9-^{3}H-2 formed aggregated Mu-9-^{3}H-2 in vivo during the course of time. However, the 3–4-fold reduction in the percentage of radiolabeled Mu-9-^{3}H-2 as compared to its unconjugated counterpart in blood is greater than that expected if only the 20% of the aggregated Mu-9-^{3}H-2 initially present in the conjugate was cleared without additional increased clearance of the native-sized Mu-9-^{3}H-2. Indeed, the improved tumor:nontumor ratios with the Mu-9-^{3}H-1 on day 7 was related directly to a lower percentage of radioactivity remaining in the normal tissues than that seen with unconjugated Mu-9, suggesting that the coupling of even one boron cage may influence the clearance rate of the Mu-9 from normal tissues. In comparison, the anti-CEA conjugate of the diazonium ion derivative ^{3}H-6, containing three carborane cages per antibody molecule, was reported to exhibit biodistribution properties similar to those of the unmodified anti-CEA in hamsters (*11*).

With regard to the radioiodination of the *nido*-carborane cage itself, it is encouraging to note that the extent of radiolabeling is quite satisfactory, but the presence of radioactive impurities and their nonspecific binding to the protein limits the usefulness of the method in the present case. However, it is conceivable that other radioiodinated carborane derivatives that can be easily purified may be employed along with a variation in the conjugation buffer in such a manner as to deter nonspecific binding.

Besides serving as a tracer to follow the fate of the carborane and the antibody in vivo, the radiolabeled carborane would have several potential advantages. These reagents might provide alternatives to Bolton–Hunter reagents as prosthetic labeling agents for protein which would protect the proteins from exposure to harsh iodination conditions. Also, these iodinated carborane-containing antibodies could be useful in therapy (by means of an attached ^{131}I label) and in imaging (via an attached ^{123}I label).

Chemically, the B–I bond (bond dissociation energy = 91 ± 5 kcal/mol) is substantially stronger than the C–I bond (50 ± 5 kcal/mol). Consequently, it is not unreasonable to expect that this relative stability would be maintained in vivo and that the boron–iodinated derivative would be less prone to undergo the in vivo dehalogenation process encountered with the carbon–iodinated antibodies. This thermodynamic effect would be enhanced by the fact that the carborane iodine carrier is inorganic in nature and should not be recognized in vivo by the enzymes required for dehalogenation.

It is interesting to note that the native Mu-9 and the carborane-conjugated antibody Mu-9-^{3}H-2 underwent radioiodination with comparable labeling efficiency. The lack of enhanced radiolabeling in the case of the latter could arise from the unavailability of the carborane cages which are likely to be held within the hydrophobic regions of the protein. Furthermore, if the radioiodination of the boron cages did not occur in Mu-9-^{3}H-2, the metabolism of the iodine label in vivo would be the same for both the conjugates and the unmodified antibody, thereby rendering the biodistribution assay in the present study meaningful.

CONCLUSION

Although it is possible to conjugate four anionic *nido*-carborane cages to the mAb molecule without severely hampering its immunoreactivity, the number of boron atoms attached to each antibody molecule still falls short of the very large number of boron atoms required for effective use in boron-neutron-capture therapy. Theoretical calculations have set a minimum of 10^3 boron atoms per antibody molecule in order for this therapy to be viable (*25*). The aim of the present study has been to explore the conjugation and localization behavior of monomeric *nido*-carborane cage reagents which bear a negative charge as single prototypes of their oligomeric counterparts that, in principle, can deliver significantly larger numbers of boron atoms. Such conjugation reagents are currently under active development.

In conclusion, the coupling of multiple boron cages to an mAb without altering the apparent immunoreactivity of the mAb is possible, but the in vivo tumor uptake may be reduced and the rate of clearance from the blood and normal tissues increased if the conjugation with the carborane reagent alters the physical properties of the mAb. In the case of the Mu-9-^{3}H-2 conjugate, the immunoreactivity measured in vitro did not coincide with the observation of reduced tumor uptake. Thus, mAbs may be coupled with carborane reagents and still retain tumor-targeting abilities, but the reduced tumor uptake will further increase the need for a greater quantity of boron per mAb, or large doses of boron-conjugated mAbs will be required to deliver adequate amounts of boron to tumor for neutron-capture therapy. Clearly, the selective attachment of a few boron-rich oligomeric reagents to the antibody is expected to be superior to the attachment of a large number of small molecules containing boron at random points on the antibody and our current interests, as well as those of others, are focused on the former approach (*26–30*). Notable efforts in this direction are the attachment of boronated poly(DL-lysine) to monoclonal antibodies by Barth and co-workers (*31*), the conjugation of boronated polyornithine to melanoma monoclonal antibody by Tamat et al. (*32*) and the boronation of a dextranized antibody by Gabel and co-workers (*25*, *33*). Our most recent studies have been focused upon the precision synthesis of water-soluble anionic carboranyl peptide derivatives derived from a novel carboranyl α-amino acid, the conjugation of these peptides to antitumor antibodies, and the determination of the biodistribution of these conjugates in nude mice (*34*). These results will be reported elsewhere in full.

ACKNOWLEDGMENT

This research was supported in part by National Institutes of Health Grants CA 31753 and CA 39841. We also thank Ms. Susan Rasmussen for her assistance in the preparation of ^{3}H-2 and the referees for their helpful comments.

LITERATURE CITED

(1) Locher, G. L. (1936) Biological Effects and Therapeutic Possibilities of Neutrons. *Am J. Roentgenol. Radium Ther. 36*, 1–13.

(2) Kruger, P. G. (1940) Some Biological Effects of Nuclear Disintegration Products of Neoplastic Tissue. *Proc. Natl. Acad. Sci., U.S.A. 26*, 181–192.

(3) Zahl, P. A., Cooper, F. S., and Dunning, J. A. (1940) Some in Vivo Effects of Localized Nuclear Disintegration Products of a Transplantable Mouse Sarcoma. *Proc. Natl. Acad. Sci., U.S.A. 26*, 589–598.

(4) Bale, W. F. (1952) Relative Effects of Alpha, Beta, Gamma and Neutron Radiation. *Proc. Natl. Cancer Conf. 2*, 967–976.
(5) Goldenberg, D. M., De Land, F. H., Kim, E. E., Bennett, S., Primus, F. J., van Nagell, J. R., Jr., Estes, N., De Simone, P., and Rayburn, P. (1978) Use of Radiolabeled Antibodies to Carcinoembryonic Antigen for the Detection and Localization of Diverse Cancers by External Photoscanning. *N. Engl. J. Med. 298*, 1384–1388.
(6) Goldenberg, D. M., Kim, E. E., De Land, F. H., Bennett, S., and Primus, F. J. (1980) Radioimmunodetection of Cancer with Radioactive Antibodies to Carcinoembryonic Antigen. *Cancer Res. 40*, 2984–2992.
(7) Goldenberg, D. M., Kim, E. E., De Land, F. H., Spremulli, E., Nelson, M. O., Gockerman, J. P., Primus, F. J., Corgan, R. L., and Alpert, E. (1980) Clinical Studies on the Radioimmunodetection of Tumors Containing Alpha-Fetoprotein. *Cancer 45*, 2500–2505.
(8) Goldenberg, D. M., Kim, E. E., De Land, F. H., van Nagell, J. R., Jr., and Javadpour, N. (1980) Clinical and Radioimmunodetection of Cancer with Radioactive Antibodies to Human Chlorionic Gonadotropin. *Science 208*, 1284–1286.
(9) Hawthorne, M. F., Wiersema, R. J., and Takasugi, M. (1972) Preparation of Tumor-Specific Boron Compounds. 1. In Vitro Studies Using Boron–Labeled Antibodies and Elemental Boron as Neutron Targets. *J. Med. Chem. 15*, 449–452.
(10) Mizusawa, E., Dahlman, H. L., Bennett, S. J., Goldenberg, D. M., and Hawthorne, M. F. (1982) Neutron-Capture Therapy of Human Cancer: In Vitro Results on the Preparation of Boron-Labeled Antibodies to Carcinoembryonic Antigen. *Proc. Natl. Acad. Sci., U.S.A. 79*, 3011–3014.
(11) Goldenberg, D. M., Sharkey, R. M., Primus, F. J., Mizusawa, E., and Hawthorne, M. F. (1984) Neutron-Capture Therapy of Human Cancer: In Vivo Results on Tumor Localization of Boron-10-Labeled Antibodies to Carcinoembryonic Antigen in the GW-39 Tumor Model System. *Proc. Natl. Acad. Sci., U.S.A. 81*, 560–563.
(12) Brechbiel, M. W., Gansow, O. A., Atcher, R. W., Schlom, J., Esteban, J., Simpson, D. E., and Colcher, D. (1986) Synthesis of 1-(*p*-isothiocyanatobenzyl) Derivatives of DTPA and EDTA. Antibody Labeling and Tumor-Imaging Studies. *Inorg. Chem. 25*, 2772–2781.
(13) Sneath, R. L., Jr., Soloway, A. H., and Dey, A. S. (1974) Protein-Binding Polyhedral Boranes. 1. *J. Med. Chem. 17*, 796–799.
(14) Gabel, D., and Walczyna, R. (1982) Decachloro-*o*-Carborane Derivatives Suitable for the Preparation of Boron-Labeled Biological Macromolecules. *Z. Naturforsch., C. Biosci. 37C*, 1038–1039.
(15) Mizusawa, E. A., Thompson, M. R., and Hawthorne, M. F. (1985) Synthesis and Antibody-Labeling Studies with the *p*-Isothiocyanatobenzene Derivatives of 1,2-Dicarba-*closo*-dodecaborane(12) and the Dodecahydro-7,8-dicarba-*nido*-undecaborate(1–) Ion for Neutron Capture Therapy of Human Cancer. Crystal and Molecular Structure of $Cs^+[nido\text{-}7\text{-}(p\text{-}C_6H_4NCS)\text{-}9\text{-}I\text{-}7,8\text{-}C_2B_9H_{11}]^-$. *Inorg. Chem. 24*, 1911–1916.
(16) Nocera, M. A., Shochat, D., Primus, F. J., Krupey, J., Jesperson, D. L., and Goldenberg, D. M. (1987) Representation of Epitopes on Colon-Specific Antigen-p Defined by Monoclonal Antibodies. *J. Natl. Cancer Inst. 79*, 943–948.
(17) Goldenberg, D. M., Witte, S., and Elster, K. (1966) GW-39: A New Human Tumor Serially Transplantable in the Golden Hamster. *Transplantation 4*, 760–765.
(18) Pant, K. D., Dahlman, H. L., and Goldenberg, D. M. (1977) A Putatively New Antigen (CSAp) Associated with Gastrointestinal and Ovarian Plasma. *Immunal. Commen. 6*, 411–421.
(19) Shochat, D., Pant, K. D., and Goldenberg, D. M. (1982) Colon-Specific Antigen-p (CSAp): Further Characterization in Colorectal and Pancreatic Cancer. *Cancer 50*, 927–931.
(20) Gold, D. V., Nocera, M. A., Stephens, R., and Goldenberg, D. M. Murine Monoclonal Antibodies to Colon-Specific Antigen-p (CSAp). *Cancer Res.*, in press.
(21) Sharkey, R. M., Gold, D. V., Aninipot, R., Vagg, R., Ballance, C., Newan, E. S., Ostella, F., Hansen, H. J., and Goldenberg, D. M. (1990) Comparison of Tumor Targeting in Nude Mice by Murine Monoclonal Antibodies Directed Against Different Human Colorectal Cancer Antigens. *Cancer Res. (Suppl.) 50*, 828s–834s.
(22) Meares, C. F., McCall, M. J., Reardan, D. T., Goodwin, D. A., Diamanti, C. I., and McTigue, M. (1984) Conjugation of Antibodies with Bifunctional Chelating Agents: Isothiocyanate and Bromoacetamide Reagents, Methods of Analysis and Subsequent Addition of Metal Ions. *Anal. Biochem. 142*, 68–78.
(23) Sharkey, R. M., Primus, F. J., Shochat, D., and Goldenberg, D. M. (1988) Comparison of Tumor Targeting of Mouse Monoclonal and Goat Polyclonal Antibodies to Carcinoembryonic Antigen in the GW-39 Human Tumor-Hamster Host Model. *Cancer Res. 48*, 1823–1828.
(24) Hawthorne, M. F., Wegner, P. A., and Stafford, R. C. (1965) Comments on the Reaction of Amines with 1,2-Dicarbaclovododecaborane(12). *Inorg. Chem. 4*, 1675.
(25) Abraham, R., Müller, R., and Gabel, D. (1989) Boronated Antibodies for Neutron Capture Therapy. *Strahlenther. Onkol. 165*, 148–151.
(26) Elmore, J. J., Jr., Borg, D. C., Micca, P., and Gabel, D. (1983) Coupling of Dextrans Conjugated with Boron to Gamma Globulin: A Model for NCT. *Proceedings of the First International Symposium on Neutron Capture Therapy*, Oct. 12–14, 1985, Cambridge, MA; Brookhaven National Laboratory, Report No. 51730 (R. G. Fairchild and G. L. Brownell, Eds.) pp 237–244.
(27) Elmore, J. J., Jr., Borg, D. C., Gabel, D., Fairchild, R. G., Temponi, M., and Ferrone, S. (1985) Boronated Dextran–Monoclonal Antibody Conjugates for NCT. *Proceedings of the Second International Symposium on Neutron Capture Therapy*, Oct. 18–20, 1985, Tokyo, Japan, pp 367–381.
(28) Barth, R. F., Alam, F., Soloway, A. H., and Adams, D. M. (1985) Delivery of Boron-10 for Neutron Capture Therapy by Means of Polyclonal and Monoclonal Antibodies: Progress and Problems. *Proceedings of the Second International Symposium on Neutron Capture Therapy*, Oct. 18–20, 1985, Tokyo, Japan, pp 346–352.
(29) Barth, R. F., Alam, F., Soloway, A. H., Adams, D. M., and Steplewski, Z. (1986) Boronated Monoclonal Antibody 17-1A for Potential Neutron Capture Therapy of Colorectal Cancer. *Hybridoma 5, Suppl. 1*, s43–s50.
(30) Barth, R. F., Soloway, A. H., and Fairchild, R. A. (1990) Boron Neutron Capture Therapy of Cancer. *Cancer Res. 50*, 1061–1070.
(31) Barth, R. F., Mafune, N., Alam, F., Adams, D. M., Soloway, A. H., Makroglow, G. E., Oredipe, O. A., Blue, T. E., and Steplewski, Z. (1989) Conjugation, Purification and Characterization of Boronated Monoclonal Antibodies for Use in Neutron Capture Therapy. *Strahlenther. Onkol. 165*, 142–145.
(32) Tamat, S. R., Patwardhan, A., Moore, D. E., Kabral, A., Bradstock, K., Hersey, P., and Allen, B. J. (1989) Boronated Monoclonal Antibodies for Potential Neutron Capture Therapy of Malignant Melanoma and Leukaemia. *Strahlenther. Onkol. 165*, 145–147.
(33) Pattersson, M. L., Courel, M.-N., Girard, N., Gabel, D., and Delpech, B. (1989) In Vitro Immunological Activity of a Dextran-Boronated Monoclonal Antibody. *Strahlenther. Onkol. 165*, 151–152.
(34) Hawthorne, M. F. (1991) Biochemical Applications of Boron Cluster Chemistry. *Pure Appl. Chem. 63*, 327–334.

Radioiodinated Iodobenzoyl Conjugates of a Monoclonal Antibody Fab Fragment. In Vivo Comparisons with Chloramine-T-Labeled Fab

D. Scott Wilbur,*[1] Stephen W. Hadley, Leah M. Grant, and Mark D. Hylarides

NeoRx Corporation, 410 West Harrison Street, Seattle, Washington 98119. Received October 5, 1990

A comparative investigation of the biodistributions of radioiodinated *p*- and *m*-iodobenzoyl conjugates of a monoclonal antibody Fab fragment, NR-LU-10 Fab, and the same antibody Fab fragment radioiodinated by the chloramine-T (ChT) method has been carried out in mice. Coinjected, dual-isotope studies in athymic mice with tumor xenografts have demonstrated that there are only minor differences in the in vivo distributions of the iodobenzoyl-labeled Fabs, except in the excretory organs, kidneys, and intestines, where major differences were observed. Similarly, coinjection of either the *p*-iodobenzoyl or *m*-iodobenzoyl conjugate of NR-LU-10 Fab with the Fab radioiodinated with ChT/radioiodide into BALB/c mice provided additional data that indicated that the two iodobenzoyl conjugates distributed similar in a number of selected tissues. The tissue-distribution differences of the regioisomeric iodobenzoyl conjugates in relation to the ChT-radioiodinated Fab were large for the stomach and neck, consistent with previous studies. The most notable difference between the two iodobenzoyl conjugates was the kidney activity, where the *m*-iodobenzoyl conjugate was similar to the directly labeled Fab, but the *p*-iodobenzoyl-conjugated Fab was higher by nearly a factor of 2.

INTRODUCTION

Monoclonal antibody Fab fragments have a rapid blood clearance and have good tumor-to-surrounding-tissue ratios at 4–12 h postinjection, which makes their use favorable for radioimmunoscintigraphy of cancers (*1*). Indeed, clinical studies have shown that imaging of tumors can be achieved when monoclonal antibody Fab or Fab′ fragments are radiolabeled with technetium-99m ($t_{1/2}$ = 6.02 h, γ = 140 keV) as early as 2–6 hours postinjection (*2*, *3*). However, due to the Fab's propensity to localize in the kidneys and the hepatobiliary excretion observed for some technetium-99m-labeled antibodies (*4*), there can be questions concerning the masking of cancer sites by radioactivity localized in the region of the excretory tissues. By 30 h postinjection much of the radioactivity in the kidneys and colon has cleared, unfortunately the short half-life of technetium-99m makes imaging at that time difficult. Application of iodine-123 ($t_{1/2}$ = 13.1 h, γ = 159 keV) labeled monoclonal antibody Fab fragments, which can be imaged at 30 h postinjection, could provide additional information about cancer sites in the abdominal region.

While radioiodinated antibodies can be readily obtained by standard radioiodination procedures (*5*), the application of radioiodinated antibodies to the diagnosis and therapy of cancer has been limited by an apparent in vivo deiodination (*6*, *7*). Radioiodinated antibodies studied in vitro and in serum are generally quite stable, suggesting that deiodination occurs via an enzymatic process, presumably deiodinases involved in thyroid hormone biochemistry (*8–11*). The problem of in vivo instability of radioiodinated antibodies led us, and other investigators, to study alternative methods of antibody radioiodination (*12–18*). Thus, we have studied a number of radioiodinated conjugates of monoclonal antibodies which were designed to stabilize the radioiodine in vivo (*19–21*). In the reagents tested, stabilization of the radioiodine was accomplished by attachment of the radioiodine to a nonactivated aromatic ring in the position para to the functionality used in the antibody conjugation. Indeed, these *p*-iodophenyl (PIP) antibody conjugates have been found to be quite stable toward in vivo deiodination. Similar studies by Zalutsky et al. (*12–14*, *22*) have demonstrated that *m*-iodobenzoyl antibody conjugates are also stable toward in vivo dehalogenation. Further, Garg et al. (*24*) have reported that significant differences were observed between the in vivo distributions of dual-labeled *m*- and *p*-iodobenzoyl conjugates of an intact antibody, 81C6, and a $F(ab')_2$ fragment of another antibody, OC 125. However, there were no reports in the literature delineating the differences between *m*- and *p*-iodobenzoyl conjugates on antibody Fab fragments. Due to these factors, it was not evident a priori which radioiodinated conjugate should be used in imaging studies employing radioiodinated antibody Fab fragments.

Reported herein are the results of an investigation which was designed to help determine whether radiolabeling with the *m*- or *p*-iodobenzoyl conjugates of a pancarcinoma antibody fragment, NR-LU-10 Fab,[2] affected the distribution of radioactivity. To alleviate the animal-to-animal variation in the in vivo distribution studies, dual-labeled (^{125}I and ^{131}I), coinjected preparations of *m*-iodobenzoyl- and *p*-iodobenzoyl-conjugated NR-LU-10 Fab were employed. Additionally, comparative studies, where NR-LU-10 Fab was radioiodinated with either of the iodobenzoyl conjugates and (separately) radioiodinated directly by use of a modified radioiodide and chloramine-T (ChT) labeling method (*25*), were conducted to assess the relative amounts of deiodination.

EXPERIMENTAL PROCEDURES

Materials. All reagents used were analytical reagent grade or better and were used as obtained. HPLC solvents were obtained as HPLC grade and were filtered (0.2 μm) prior to use. Radioiodine was obtained from Du Pont/

[1] Address correspondence to D. Scott Wilbur, Dept. of Radiation Oncology, RC-08, University of Washington Medical Center, 1959 N.E. Pacific St., Seattle, WA 98195.

[2] The NR-LU-10 monoclonal antibody is a pancarcinoma antibody of the IgG_{2b} subclass which reacts with a glycoprotein antigen of ca. 40 kDa. The antigen is found on several carcinomas such as colon, breast, ovarian, prostate, and lung. Radiolabeled NR-LU-10 Fab is currently undergoing clinical investigation for application to imaging of several different carcinomas in patients.

1043-1802/91/2902-0111$02.50/0 © 1991 American Chemical Society

NEN (Billerica, MA) as high-concentration, high specific activity solutions in 0.1 N NaOH. Phosphate-buffered saline was purchased from Gibco Laboratories (Baltimore, MD) as Dulbecco's phosphate-buffered saline (#310-4190) or from Whittaker Bioproducts, Inc. (Walkersville, MD).

General Procedures. High-performance liquid chromatography (HPLC) was conducted on either a gradient system consisting of two Beckman Model 110B pumps, a Beckman Model 153 UV detector, a Rheodyne Model 7125 injector, and a Beckman Model 170 radioisotope detector or an isocratic system identical with the gradient except having only one solvent pump. All separations were run at a flow rate of 1 mL/min. Spectrophotometric analysis of the HPLC effluent was performed with UV detection at 254 nm and in-line γ-radiometric detection. Compounds 1–4 were analyzed by reverse-phase chromatography, and the Fab conjugates 5 and 6 were analyzed by size-exclusion chromatography.

Reverse-phase chromatography was conducted on a 4.6 mm × 12.5 cm, C-18 column (Whatman) using a binary gradient solvent system. Eluant A in the gradient was a mixture of 98% MeOH and 2% of a 1% HOAc/H_2O solution. Eluant B used in the gradient was a mixture of 20% MeOH and 80% of a 1% HOAc/H_2O solution. The gradient was begun by eluting for 2 min at 50% of each eluant. After 2 min the solvent mixture was increased in eluant A over the next 8 min to a final composition of 98% eluant A and 2% eluant B. The eluant mixture remained at that composition for the next 10 min to complete the gradient. Retention times under these conditions were as follows: free radioiodide eluted at 1.4 min (solvent front), compound 1 eluted at 14.6 min, compound 2 eluted at 15.1 min, compound 3 eluted at 3.4 min, and compound 4 eluted at 4.2 min.

Size-exclusion chromatography was conducted on a Zorbax Bio Series GF-250 9.4 mm × 24 cm column (Du Pont) with 0.2 M phosphate, pH 6.8, as the eluant. All radioiodinated Fab fragments eluted at 9.8 min. Less than 5% of the protein aggregates were detectable by HPLC analysis of the radioiodinated Fabs.

Thin-layer chromatography of protein conjugates was conducted on silica gel impregnated glass-fiber strips (ITLC, Gelman) eluting with 80% MeOH/H_2O. In this system, the protein is denatured at the origin and the free iodide or radioiodinated small molecules that are present move with the solvent front. Radiochemical purity of the radiolabeled Fab preparations was defined as the percent protein-bound activity, which was assessed by dividing the counts at the TLC origin by the total TLC counts.

Radioactive samples were counted in a Packard Autogamma 5650 instrument. Protein concentrations in solution were measured by UV spectrophotometry at 280 nm. The concentrations of the radioiodinated Fab fragments were obtained by using the Beer–Lambert equation with the molar absorptivity being equal to 1.53.

Athymic (nude) mice were obtained from Simonsen Laboratories, Inc. (Gilroy, CA) and were used at 10–12 weeks of age. Female nude mice (nu/nu), weighing 20–27 g (23.8 g ± 1.4 g average body weight, $N = 16$), were housed in microisolator caging with bonnet filter tops and maintained on sterilized chow and water in a controlled environment. Tumor xenografts were derived from subcutaneous flank implantation of 2.5×10^6 LS-180 cultured human colon tumor cells.[3] The tumors were allowed to grow for 7–10 days to produce tumors which had an average tumor weight of 201 ± 100 mg (a range of weights from 61 to 400 mg).

[3] The LS-180 tumor model is a human colon carcinoma xenograft derived from the LS-174T tumor line.

Table I. Tissue Distribution of Radioiodine (%ID/g) at 4 and 20 h Postcoinjection of the NR-LU-10 Fab Conjugates of *p*-Iodobenzoyl ([^{131}I]-5) and *m*-Iodobenzoyl ([^{125}I]-6) in Athymic Mice

	4 h		20 h	
tissues	[^{131}I]-5	[^{125}I]-6	[^{131}I]-5	[^{125}I]-6
blood	1.58 ± 0.18	1.46 ± 0.27	0.07 ± 0.02	0.10 ± 0.03
tumor	7.45 ± 1.39	7.24 ± 1.40	4.51 ± 1.65	4.46 ± 1.67
skin	1.14 ± 0.10	1.06 ± 0.10	0.05 ± 0.02	0.06 ± 0.02
muscle	0.44 ± 0.06	0.43 ± 0.07	0.03 ± 0.01	0.03 ± 0.01
lung	5.83 ± 2.87	5.59 ± 2.73	0.77 ± 0.77	0.66 ± 0.53
liver	0.73 ± 0.12	0.74 ± 0.12	0.07 ± 0.01	0.12 ± 0.04
spleen	0.53 ± 0.12	0.57 ± 0.12	0.04 ± 0.02	0.10 ± 0.03
stomach	0.80 ± 0.41	0.77 ± 0.41	0.04 ± 0.03	0.05 ± 0.04
neck (thyroid)	1.00 ± 0.13	0.99 ± 0.15	0.13 ± 0.05	0.17 ± 0.08
kidneys	14.11 ± 1.18	8.25 ± 0.84	0.27 ± 0.07	0.15 ± 0.05
intestines	1.18 ± 0.19	0.61 ± 0.08	0.03 ± 0.02	0.03 ± 0.01

BALB/c mice were obtained from Charles River Laboratories, Inc. (Wilmington, MA) and were used at 10–12 weeks of age. Female BALB/c mice weighed 19–24 g (22.6 g ± 3.1 g average body weight, $N = 16$, and 21.3 g ± 1.0 g average body weight, $N = 16$, for the two experiments, respectively).

Preparation of *N*-Succinimidyl *p*-Tri-(*n*-butylstannyl)benzoate (1) and Preparation of *N*-Succinimidyl *m*-(Tri-*n*-butylstannyl)benzoate (2). The synthesis of the para-substituted aryltin reagent 1 was accomplished in three synthetic steps involving the palladium-catalyzed metal–halogen exchange of methyl *p*-bromobenzoate, followed by methyl ester hydrolysis and subsequent formation of the succinimido ester as previously described (*16*). The synthesis of the meta-substituted aryltin reagent 2 was accomplished in a manner similar to that previously reported by Zalutsky and Narula (*13*).

Preparation of Radioiodinated *N*-Succinimidyl *p*-Iodobenzoate (3) and *N*-Succinimidyl *m*-Iodobenzoate (4). Radioiodination of the regioisomeric *N*-succinimidyl (tri-*n*-butylstannyl)benzoates was conducted in a manner similar to that previously described (*16*). To exemplify the labeling conditions, reaction of meta positional isomer is described below.

Into a reaction vial fitted with a septum was placed a 50 μL solution containing 12.5 μg (0.025 mmol) of *N*-succinimidyl *m*-(tri-*n*-butylstannyl)benzoate in 5% HOAc/MeOH, a 10 μL solution containing 10 μg (0.075 mmol) of *N*-chlorosuccinimide (NCS) in MeOH, and 10 μL of phosphate-buffered saline. To this mixture was added 2 μL (1.2 mCi) of Na^{125}I in 0.1 N NaOH. After 5 min at room temperature the reaction was quenched by the addition of a 10 μL solution containing 0.72 mg/mL (0.076 mmol) $Na_2S_2O_5$ in H_2O. The crude product was a mixture of three radioactive components: 48% of [^{125}I]-4, 34% of *m*-[^{125}]iodobenzoic acid, and 4% of [^{125}I]iodide, by radio-HPLC analysis.

In a like manner, radioiodination of 1 with NCS/^{131}I afforded a 77% radiochemical yield of [^{131}I]-3, 5% of *p*-[^{131}]-iodobenzoic acid, and 11% [^{131}I]iodide. Preparation of [^{125}I]-3, employed in the second biodistribution (Table II), afforded a radiochemical yield of 85%, with 5% of *p*-[^{125}I]iodobenzoic acid and 2% of [^{125}I]iodide being present.

The methanol was evaporated from the crude mixture by passing a stream of N_2 gas through the reaction vial. To contain any volatile radioiodine, the reaction vial was stoppered with a septum seal, N_2 was introduced by means of a needle inlet, and a needle outlet was attached to a syringe barrel containing granulated charcoal. The crude

Table II. Tissue Distribution of Radioiodine (%ID/g) at 4 and 16 h Postcoinjection of the NR-LU-10 Fab Conjugate of *p*-Iodobenzoyl ([^{125}I]-5) and [^{131}I]Iodide/ChT-Labeled NR-LU-10 Fab in BALB/c Mice

	4 h		16 h	
tissues	[^{125}I]-5	[^{131}I]ChT	[^{125}I]-5	[^{131}I]ChT
blood	2.73 ± 0.49	3.13 ± 1.10	0.34 ± 0.04	0.27 ± 0.07
lung	2.93 ± 0.77	3.34 ± 1.07	0.40 ± 0.12	0.36 ± 0.10
stomach	1.67 ± 2.70	10.26 ± 6.36	0.07 ± 0.02	0.41 ± 0.18
neck (thyroid)	0.95 ± 0.22	9.01 ± 4.54	0.46 ± 0.25	12.36 ± 10.59
kidney	24.52 ± 4.38	11.03 ± 2.23	1.56 ± 0.45	0.50 ± 0.17

Table III. Tissue Distribution of Radioiodine (%ID/g) at 4 and 16 h Postinjection of the NR-LU-10 Fab Conjugate of *m*-Iodobenzoyl ([^{125}I]-6) and [^{131}I]ChT-Labeled NR-LU-10 Fab in BALB/c Mice

	4 h		16 h	
tissues	[^{125}I]-6	[^{131}I]ChT	[^{125}I]-6	[^{131}I]ChT
blood	1.60 ± 0.34	2.24 ± 0.62	0.20 ± 0.07	0.25 ± 0.06
lung	1.28 ± 0.40	1.96 ± 0.39	0.19 ± 0.06	0.24 ± 0.05
stomach	0.64 ± 0.11	6.52 ± 1.46	0.04 ± 0.01	0.36 ± 0.16
neck (thyroid)	0.83 ± 0.13	5.30 ± 2.69	0.19 ± 0.12	5.11 ± 3.58
kidney	8.96 ± 1.05	7.72 ± 0.88	0.52 ± 0.16	0.39 ± 0.05

evaporated product was used in the subsequent conjugation reactions without further purification. (Previous studies[4] had indicated that purification of the crude radioiodinated benzoate **3** was not necessary prior to conjugation to the antibody, as immunoreactivities and tissue distributions were not altered from the purified examples.)

Conjugation of Radioiodinated 3 and 4 to Antibodies. To the vial containing evaporated crude radioiodinated **3** or **4** was added a solution containing 200 μL (1 mg) of NR-LU-10 Fab (50 μL of a 20 μg/μL PBS solution of Fab and 150 μL of a 1.0 M, pH 9.25, solution of Na_2CO_3). After 5 min at room temperature, the crude labeled protein was assessed by TLC to obtain the conjugation yield (percent bound to protein) and was purified via a Sephadex G-25 column (PD-10, Pharmacia) eluting with PBS. The early-eluting radioactive fractions were collected and pooled to yield purified conjugate **5** or **6**. Protein-bound activity (final purity) was assessed by TLC analysis. HPLC analyses were conducted to assess aggregate formation (i.e. higher molecular weight species) and to evaluate relative retention times.

The preparations of radioiodinated **5** and **6** employed in the initial biodistribution study (Table I) gave the following results. Conjugation of NR-LU-10 Fab with [^{131}I]-**3** afforded 1027 μCi (56% overall radiochemical yield), with a specific activity of 0.82 mCi/mg and a radiochemical purity of 98.3% by TLC analysis. Conjugation of NR-LU-10 Fab with [^{125}I]-**4** afforded 415 μCi (35% overall radiochemical yield) with a specific activity of 0.41 mCi/mg and a radiochemical purity of 97.3% by TLC analysis.

The preparation of [^{125}I]-**3**-conjugated NR-LU-10 Fab used for in vivo comparison with [^{131}I]iodide/ChT-labeled NR-LU-10 Fab (Table II) afforded an overall radiochemical yield of 46%, a specific activity of 1.76 mCi/mg, and a final purity of 99.4%.

The second preparation of [^{125}I]-4-conjugated NR-LU-10 Fab used for in vivo comparison with [^{131}I]iodide/ChT-labeled NR-LU-10 Fab (Table III) was carried out in the same manner as the first preparation and afforded a 31% overall radiochemical yield, a specific activity of 0.57 mCi/mg, and a 96.4% purity by TLC analysis.

[4] Unpublished results.

Radioiodination of NR-LU-10 Fab with Chloramine-T. To a reaction vial was added a 60-μL aliquot of Na^{131}I, 100 μL of PBS, and 25 μL (500 μg, 0.01 mmol) of NR-LU-10 Fab in PBS. Following mixing, a 10 μL solution containing 1 mg/mL chloramine-T (10 μg, 0.046 mmol) was added. After 10 min at room temperature, the reaction was quenched with 6 μL of a 0.72 mg/mL solution of $NaHSO_3$ (0.046 mmol) in H_2O. The crude product was purified by chromatography on a Sephadex G-25 (PD-10) column eluting with PBS. The preparation used in the second biodistribution was obtained in a radiochemical yield of 52%, a specific activity of 0.75 mCi/mg, and a final purity of 98.8%. The preparation used in the third biodistribution (Table III) had a radiochemical yield of 95%, a specific activity of 0.73 mCi/mg, and a radiochemical purity of 99.3%.

Injection Mixtures for Animal Biodistributions. Radioiodinated NR-LU-10 Fab mixtures were diluted to obtain ca. 100 μL of injectate per mouse. The injectate solution for the initial biodistribution study (Table I) contained 5 μg of NR-LU-10 Fab labeled with 1.0 μCi ^{125}I and 2.1 μCi ^{131}I in each 100-μL aliquot.

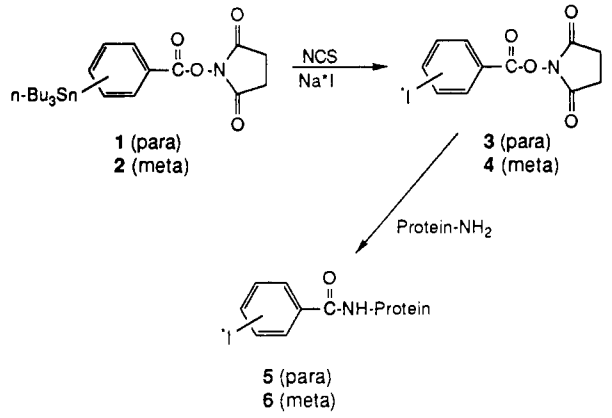
The injectate solution for the second biodistribution study (Table II) contained 10 μg of NR-LU-10 Fab labeled with 2.7 μCi ^{125}I and 3.7 μCi ^{131}I in each 100-μL aliquot.

The injectate in the third biodistribution study (Table III) contained 9.1 μg of NR-LU-10 Fab labeled with 2.9 μCi ^{125}I and 3.7 μCI ^{131}I in each 100-μL aliquot.

Animal Biodistribution Studies. Biodistribution studies were conducted by administering the above solutions of radiolabeled protein via the lateral tail vein in the mice. The tumored athymic mice and BALB/c mice were each marked for identification and were handled in the same manner. Replicate (4×) 5-mL aliquots of the injectate were prepared and counted to serve as standards for the calculation of the total injected dose. Mice were restrained, weighed, and injected; weighing the syringe before and after to determine the volume injected. At designated times postinjection, groups of mice (eight animals) were sacrificed by cervical dislocation and dissected. Blood samples were collected just prior to sacrificing the mouse by collecting a sample from retroorbital bleeding into a Pasteur pipet, transferring the blood into a preweighed tube, and weighing the tube. Tails were removed and counted as an indicator of the completion of injection (data not shown). Ten additional tissues were excised from the mice. These tissues were tumor, skin (from back), muscle, lung, liver, spleen, neck (soft tissue from the ventral portion of the neck), kidney and intestine. Bone (femur) was also excised, but the counts were too low, and the variability too high, to lead to any conclusive analyses. In the studies employing BALB/c mice fewer tissues were excised, evaluating those that were different in the first biodistribution. The tissues excised in BALB/c mice were lungs, liver, kidneys, stomach, and neck. The organs were removed and counted intact. Tissue samples were blotted, weighed using an analytical balance, placed in plastic test tubes, and counted in a γ-scintillation counter.

Dual-channel counting was carried out using a low-energy window (20–80 keV) for iodine-125 and a high-energy window (240–400 keV) for iodine-131. A 19% spillover of counts from ^{131}I was measured in the ^{125}I window. All ^{125}I counts were corrected (after background subtraction) for spillover. Data analysis included calculation of the percent injected dose per gram (%ID/g) for each isotope in each tissue, an average and standard deviation for the %ID/g in each set of eight animals, the

Scheme I. Scheme for Radioiodination of Monoclonal Antibodies Using Iodobenzoyl Conjugates



ratios of the % ID/g for the two isotopes ($^{125}I/^{131}I$) in the tissues of each animal, and the average ratio and standard deviation for each tissue. Statistical analysis of the data were conducted [with the computer program StatWorks (Cricket Software, Philadelphia, PA)] on % ID/g data for ^{125}I and ^{131}I from the eight animals in each group by using paired analyses. Criterion of significance was set at $p < 0.05$.

RESULTS

The synthetic scheme for radioiodination of antibodies (or other proteins) with iodobenzoyl conjugates is given in Scheme I. The synthesis of the aryltin reagent **1** by palladium-catalyzed metal–halogen interchange has been carried out many times in these laboratories and usually gives 25–35% overall yields. Contrary to this, several attempts to employ the palladium-catalyzed reaction of hexabutylditin and methyl *m*-bromobenzoate to synthesize meta isomer **2** failed. An alternative synthetic method used for preparation of **1** was aryl lithiation at −100 °C (*26*), followed by stannylation with tri-*n*-butylstannyl chloride to provide **2** in 36% overall yield.

Radioiodination of the two aryltin intermediates was comparable. The radioiodination yields were higher for para isomer **3** than for meta isomer **4**, but this was easily attributed to the fact that the starting aryltin compound **2** was not as pure (free of stannylbenzoic acid) as was aryltin intermediate **1**. Even trace quantities of free tri-*n*-butylstannylbenzoic acid will cause an appreciable loss of yield, because the stannylbenzoic acid reacts faster than the corresponding *N*-succinimidyl ester.

The in vivo comparison of the para and meta positional isomers of radioiodinated iodobenzoyl–antibody conjugates was conducted in three separate animal biodistribution studies. To distinguish the in vivo distribution of Fab conjugated with **3** from that conjugated with **4**, iodine-125 ($t_{1/2}$ = 60.14 d, X-ray = 27 keV) and iodine-131 ($t_{1/2}$ = 8.04 d, γ = 364 keV) were used in dual-labeled experiments. In the initial study, the Fab fragment of NR-LU-10, an anticarcinoma antibody,[2] was radioiodinated with *N*-succinimidyl *p*-iodobenzoate ([^{131}I]-**3**) and *N*-succinimidyl *m*-iodobenzoate ([^{125}I]-**4**) in two separate vessels. Following radioiodination, the radioiodinated compounds were conjugated to NR-LU-10 Fab. Once conjugated, the two preparations were purified by gel-permeation chromatography and combined prior to injection into the mice. The biodistributions of the coinjected Fab conjugates [^{131}I]-**5** and [^{125}]-**6** were assessed in athymic mice bearing LS-180 colon carcinoma xenografts.[3] Animal biodistributions were obtained at 4 and 20 h postinjection with eight animals being sacrificed at each time point. A compilation of the data obtained is shown in Table I.

A second biodistribution study compared the in vivo stability of *p*-iodobenzoyl Fab conjugate ([^{125}I]-**5**) with coinjected radioiodinated NR-LU-10 Fab labeled by using [^{131}I]iodide and chloramine-T. A limited biodistribution study was conducted in BALB/c mice, since information on the localization of radioiodine in a few specific tissues was sought. Thus, two groups of eight BALB/c mice were injected with a mixture of [^{125}I]-**5** and [^{131}I]iodide/ChT-labeled Fab and were sacrificed at 4 and 16 h postinjection. The stability of the radiolabels with regard to in vivo deiodination was of interest, so tissues where free radioiodide accumulates, neck tissue (containing thyroid) and stomach, were examined. The large differences in the kidney values obtained in the initial study prompted evaluation of that tissue as well. The lung was also included because the values obtained in the initial biodistribution study were higher than those normally obtained in similar studies. The biodistribution data obtained are shown in Table II.

A third biodistribution study compared the in vivo distribution of *m*-iodobenzoyl NR-LU-10 Fab conjugate ([^{125}I]-**6**) coinjected with NR-LU-10 Fab radioiodinated by using [^{131}I]iodide/ChT. The biodistributions were conducted in BALB/c mice, as described previously. The biodistribution data obtained are presented in Table III.

DISCUSSION

Our interest in development of radiolabeled antibodies for diagnostic imaging prompted an investigation of the *p*- and *m*-iodobenzoyl radiolabels on a pancarcinoma Fab fragment, NR-LU-10 Fab, currently in clinical trials for detection of a number of different carcinomas. In the investigation we sought to obtain data on the in vivo distributions of NR-LU-10 Fab when radiolabeled as *p*-iodobenzoyl and *m*-iodobenzoyl conjugates. The biodistribution data was sought to help determine if there were differences which would point to the choice of one of these reagents for use in clinical trials.

The data obtained from the initial biodistributions of coinjected *m*-[^{125}I]iodobenzoyl- and *p*-[^{131}I]iodobenzoyl-labeled Fab (Table I) show that the two radioiodine nuclides, and presumably the radiolabeled Fabs, have very minor differences in tissue distribution, except in the kidneys and intestines. In these two tissues isotopic ratios of 1.7 and 1.9 for [^{131}I]-**5**/[^{125}I]-**6** were obtained, respectively, at 4 h postinjection. At 20 h postinjection the ratio of [^{131}I]-**5**/[^{125}I]-**6** in the kidneys remained at 1.8, whereas no difference in isotopes was noted in the intestines at that time. It should be noted that at the later time point isotopic ratios in the tissues varied more than those at the 4-h time, presumably due to the fact that there were low number of counts in many tissues. The only tissue that retained much of its activity by 20 h was the tumor. The isotopic ratios in the tumor were found to be nearly identical at both time points studied, suggesting that NR-LU-10 Fab radioiodinated with either reagent would be equally effective at tumor localization. These results appear to be in contrast to those reported by Zalutsky et al. (*23*, *24*), but we believe that this may be due to the nature of the antibody and tumor type under study.

Interestingly, even though the differences in tissue distribution were small in this study, analyses of the data using a paired Student's *t* test (on paired data from each animal) pointed out that there were statistically significant differences in the % ID/g values for all of the tissues except

muscle, liver, and neck at 4 h and tumor, muscle, lung, stomach, and neck at 20 h. These very small, but significant, differences appeared to be due to the fact that animals injected with the *m*-[^{125}I]iodobenzoyl Fab conjugate had slightly lower concentrations in tissues than those injected with the *p*-[^{131}I]iodobenzoyl labeled Fab. However, it cannot be ruled out that the (consistent) small differences may have been brought about by radioisotope counting errors. Repeat of the biodistribution with a reversal of isotopes on the *m*- and *p*-iodobenzoyl conjugates would have answered this question, but the differences were so small as to not warrant such an undertaking. While the data suggests a significant difference in isotopic ratio within an individual animal, the isotopic ratio differences were smaller, in general, than the differences noted from animal-to-animal variation.

The high lung activity observed in the first animal biodistribution study (Table I) was not observed in the second or third biodistribution studies (Tables II and III). The reason for the higher than normal lung concentrations is not readily apparent. If one isotope had been observed to be high in the lung while the other normal, an explanation might have been that the antibody had been damaged in the radiolabeling process. However, both iodobenzoyl-conjugated Fab preparations gave similar localization in the individual animals. Further, analysis of the HPLC chromatograms did not indicate that there was anything unusual about the preparations.

As expected, the stomach and neck radioisotopic localization was appreciably different for the *m*- and *p*-iodobenzoyl conjugates from that of the directly labeled Fab, denoting the differences in the in vivo deiodination for the labeled preparations. The values obtained were consistent with those previously observed for radioiodine-labeled NR-ML-05 Fab, an antimelanoma antibody (*16*). Also, consistent with the initial comparative biodistribution, *p*-iodobenzoyl-labeled Fab ([^{125}I]-**5**) had considerably higher quantities of radioactivity in the kidney than the chloramine-T-labeled Fab ([^{131}I]ChT) with isotopic ratios of 2.2 at 4 h and 3.1 at 16 h (Table II). In contrast, only small differences were noted for the kidneys when *m*-iodobenzoyl-labeled Fab ([^{125}I]-**6**) was compared with chloramine-T-labeled Fab (Table III).

From our studies, and other reported results on labeled Fab fragments, it is evident that Fab conjugates are rapidly accumulated in the kidneys. A large difference in the kidney localization or retention of the *p*-iodobenzoyl conjugate of NR-LU-10 Fab was observed in this study. Similar differences in kidney radioactivity had been observed previously when an antimelanoma antibody, NR-ML-05 Fab, labeled as the *p*-iodobebenzoyl conjugate was compared with the same antibody labeled with radioiodide/ChT (*16*). This same observation was made when iodovinyl–Fab conjugates (*27*) and an *N*-(*p*-iodophenyl)-maleimide–Fab conjugate[4] were compared with *p*-iodobenzoyl-labeled Fab. Indeed, the coinjected, dual-labeled Fab biodistribution studies presented herein demonstrate a reproducible difference in mice for the *p*-iodobenzoyl conjugate's accumulation or retention in the kidney from that of the *m*-iodobenzoyl conjugate of the same Fab. Presumably antibodies are metabolized in the same manner as other circulating proteins in renal cells (*28*), most likely resulting in complete hydrolysis to amino acids leading to either the free acid or lysine adducts of the iodobenzoates. Data obtained in these laboratories from metabolites in urine samples of patients suggests that the degradation of the *p*-iodobenzoyl conjugate yields principally the lysine adduct, with a minor amount of glycine adduct (hippuric acid) being present (*29*). Contrary to this, Zalutsky has reported (*22*) that free *m*-iodobenzoic acid is obtained from degradation of the intact antibodies in his studies and has observed principally the glycine adduct being present in studies of the *m*-iodobenzoic acid (*30*). Such a difference in the metabolism could readily explain the differences in kidney activity noted. However, other factors such as alteration of metabolite binding in the renal transport system and/or the rate of transport (*31*) may be involved. Delineation of the mechanism of the observed kidney radioactivity differences is beyond the scope of this investigation.

Unlike the results obtained in the radioiodinated Fab, other investigations of *p*-iodobenzoyl antibody conjugates involving intact antibodies or F(ab')$_2$ fragments dual-labeled and coinjected with the same antibody radioiodinated by using chloramine-T have not shown the appreciable differences observed in kidney radioactivity concentrations (*16*, *32*, *33*). Additional information is needed as to whether the observed kidney differences for the *p*- and *m*-iodobenzoyl conjugated NR-LU-10 Fab are unique to mice or common in other species of animal. The fact that the differences in most tissues are minor, with the exception of the kidneys and intestines, has led us to the conclusion that no difference would be expected to be seen in a clinical application of antibodies radioiodinated as either the *m*-iodobenzoyl conjugate or the *p*-iodobenzoyl conjugate due to patient-to-patient variability. This statement is made with the caveat that determination of variance in the kidney activity between the two radiolabeling agents could be important as a substantial difference in the radiation dose to that organ may ultimately favor the use of the *m*-iodobenzoyl conjugate.

ACKNOWLEDGMENT

We thank Dr. Mary Ann Gray, Karen Poole, Denise DuPont, and Joanne Stevens for their efforts in obtaining the biodistribution data presented herein. We also thank Dr. Alan R. Fritzberg, Dr. A. Charles Morgan, and Dr. Paul L. Beaumier for their discussions on the experiments and manuscript.

LITERATURE CITED

(1) Larson, S. M. (1990) Clinical Radioimmunodetection, 1978–1988: Overview and Suggestions for Standardization of Clinical Trials. *Cancer Res. (Suppl.) 50*, 892s–898s.

(2) Lamki, L. M., Zukiwski, A. A., Shanklin, L. J.; Legha, S. S., Benjamin, R. S., Plager, C. E., Salk, D. F., Schroff, R. W., and Murray, J. L. (1990) Radioimaging of Melanoma Using ^{99m}Tc-Labeled Fab Fragment Reactive with a High Molecular Weight Melanoma Antigen. *Cancer Res. (Suppl.) 50*, 904s–908s.

(3) Goldenberg, D. M., Goldenberg, H., Sharkey, R. M., Higginbotham-Ford, E., Lee, R. E., Swayne, L. C., Burger, K. A., Tsai, D., Horowitz, J. A., Hall, T. C., Pinsky, C. M., and Hansen, H. J. (1990) Clinical Studies of Cancer Radioimmunodetection with Carcinoembryonic Antigen Monoclonal Antibody Fragments Labeled with ^{123}I or ^{99m}Tc. *Cancer Res. (Suppl.) 50*, 909s–921s.

(4) Salk, D., and Multicenter Study Group (1988) Technetium-Labeled Monoclonal Antibodies for Imaging of Metastatic Melanoma: Results of a Multicenter Clinical Study. *Semin. Oncol. 15*, 608–618.

(5) Regoeczi, E. (1984) Methods of Protein Iodination. In *Iodine-Labeled Plasma Proteins*, Vol. I, Chapter 3, pp 35–102, CRC Press Inc., Boca Raton, FL.

(6) Carrasquillo, J. A., Krohn, K. A., Beaumier, P., McGuffin, R. W., Brown, J. P., Hellstron, K. E., Hellstrom, I., and Larson, S. M. (1984) Diagnosis of and Therapy for Solid Tumors

with Radiolabeled Antibodies and Immune Fragments. *Cancer Treat. Rep. 68*, 317–328.
(7) Stern, P., Hagan, P., Halpern, S., Chen, A., David, G., Adams, T., Desmond, W., Brautigram, K., and Royston, I. (1982) The Effect of the Radiolabel on the Kinetics of Monoclonal Anti-CEA in a Nude Mouse–Human Colon Tumor Model. In *Hybridomas in Cancer Diagnosis and Treatment* (M. S. Mitchell, and H. F. Oettgen, Eds.) pp 245–253, Raven Press, New York.
(8) Eary, J. F., Krohn, K. A., Kishore, R., and Nelp, W. B. (1989) Radiochemistry of Halogenated Antibodies. In *Antibodies in Radiodiagnosis and Therapy*. (M. R. Zalutsky, Ed.) pp 97–98, CRC Press, Inc., Boca Raton, FL.
(9) Regoeczi, E. (1987) In Vivo Behavior of Catabolized Labels Derived from Iodo Proteins. In *Iodine Labeled Plasma Proteins*, Vol. II, Part B, pp 43–71. CRC Press, Boca Raton, FL.
(10) Engler, D., and Burger, A. G. (1984) The Deiodination of the Iodothryonines and of their Derivatives in Man. *Endocr. Rev. 5*, 151–184.
(11) Sinsheimer, J. E., Wang, T., Roder, S., and Shum, Y. Y. (1978) Mechanisms for the Biodehalogenation of Iodocompounds. *Biochem. Biophys. Res. Commun. 83*, 281–286.
(12) Zalutsky, M. R., and Narula, A. S. (1987) An Improved Method for the Radiohalogenation of Monoclonal Antibodies. In *Immunological Approaches to the Diagnosis and Therapy of Breast Cancer*, pp 187–203, Plenum Press, New York.
(13) Zalutsky, M. R., and Narula, A. S. (1987) A Method for the Radiohalogenation of Proteins Resulting in Decreased Thyroid Uptake of Radioiodine. *Int. J. Radiat. Appl. Inst. [A] 38*, 1051–1055.
(14) Zalutsky, M. R., and Narula, A. S. (1988) Radiohalogenation of a Monoclonal Antibody Using an *N*-Succinimidyl 3-(Tri-*n*-butylstannyl)benzoate Intermediate. *Cancer Res. 48*, 1446–1450.
(15) Srivastava, P. C., Buchsbaum, D. J., Allred, J. F., Brubaker, P. G., Hanna, D. E., and Spickler, J. K. (1990) A New Conjugating Agent for Radioiodination of Proteins: Low in Vivo Deiodination of a Radiolabeled Antibody in a Tumor Model. *BioTechniques 8*, 536–545.
(16) Wilbur, D. S., Hadley, S. W., Hylarides, M. D., Abrams, P. G., Beaumier, P. A., Morgan, A. C., Reno, J. M., and Fritzberg, A. R. (1989) Development of a Stable Radioiodination Reagent to Label Monoclonal Antibodies for Radiotherapy of Cancer. *J. Nucl. Med. 30*, 216–226.
(17) Khawli, L. A., and Kassis, A. (1989) Synthesis of 125I Labeled *N*-Succinimidyl *p*-Iodobenzoate for Use in Radiolabeling Antibodies. *Nucl. Med. Biol. 16*, 727–733.
(18) Rea, D. W., Ultee, M. E., Belinka, B. A., Coughlin, D. J., and Alvarez, V. L. (1990) Site Specifically Radioiodinated Antibody for Targeting Tumors. *Cancer Res. (Suppl.) 50*, 857s–861s.
(19) Wilbur, D. S., Jones, D. S., and Fritzberg, A. R. (1986) Synthesis and Radioiodinations of Some Aryltin Compounds for Radiolabeling of Monoclonal Antibodies. *J. Labeled Compds. Radiopharm. 23*, 1304–1306.
(20) Hylarides, M., Jones, D., Seubert, J., Hadley, S., and Wilbur, D. S. (1987) Synthesis and Radioiodinations of Iodophenyl Conjugates for Protein Labeling. *J. Nucl. Med. 28*, 560.
(21) Hadley, S. W., Grant, L. M., Hylarides, M. D., Fritzberg, A. R., and Wilbur, D. S. (1989) Synthesis, Radioiodination, and Evaluation of a Para-Iodobenzyl Alcohol Ester Antibody Conjugate. *J. Nucl. Med. 30*, 924.
(22) Zalutsky, M. R., Noska, M. A., Colapinto, E. V., Garg, P. K., and Bigner, D. D. (1989) Enhanced Tumor Localization and in Vivo Stability of a Monoclonal Antibody Radioiodinated Using N-Succinimidyl 3-(Tri-*n*-butylstannyl)benzoate. *Cancer Res. 49*, 5543–5549.
(23) Garg, P. K., Slade, S., and Zalutsky, M. R. (1988) Meta vs Para Substituted *N*-Succinimidyl Stannyl Benzoates: Relative Utility for Antibody Labeling. *J. Nucl. Med. 29*, 834–835.
(24) Garg, P. K., Slade, S. K., Harrison, C. L., and Zalutsky, M. R. (1989) Labeling Proteins Using Aryl Iodide Acylation Agents: Influence of Meta vs Para Substitution on in Vivo Stability. *Nucl. Med. Biol. 16*, 669–673.
(25) Osterman, L. A. (1984) Iodination with Chloramine-T. In *Methods of Protein and Nucleic Acid Research*, Chapter 3, pp 131–133. Springer-Verlag, New York.
(26) Parham, W. E., and Sayed, Y. A. (1974) Synthesis of Benzoylbenzoic Acids. *J. Org. Chem. 39*, 2051–2053.
(27) Hadley, S. W., and Wilbur, D. S. (1990) Evaluation of Iodovinyl Antibody Conjugates: Comparison with a *p*-Iodobenzoyl Conjugate and Direct Radioiodination. *Bioconjugate Chem. 1*, 154–161.
(28) Maack, T., Park, C. H., and Camargo, M. J. F. (1985) Renal Filtration, Transport, and Metabolism of Proteins. In *The Kidney: Physiology and Pathophysiology* (D. W. Sheldin, and G. Giebisch, Eds.) Chapter 76, pp 1773–1802, Raven Press, New York.
(29) Axworthy, D. B., Vanderheyden, J. L., Wilbur, D. S., Hadley, S. W., Hylarides, M. D., Wahl, R. L., Hanelin, L., and Fritzberg, A. R. (1989) Urinary Metabolites of I-131 and Re-186 Radiolabeled Conjugates of Monoclonal Antibodies and Fragments in Patients. *J. Nucl. Med. 30*, 793.
(30) Garg, P. K., Harrison, C. L., and Zalutsky, M. R. (1990) Comparative Tissue Distribution in Mice of the α-Emitter ^{211}At and ^{131}I as Labels of a Monoclonal Antibody and F(ab')$_2$ Fragment. *Cancer Res. 50*, 3514–3520.
(31) Moller, J. V., and Sheikh, M. I. (1983) Renal Organic Anion Transport System: Pharmacological, Physiological, and Biological Aspects. *Pharmacol. Rev. 34*, 315–358.
(32) Badger, C. C., Wilbur, D. S., Hadley, S. W., Fritzberg, A. R., and Bernstein, I. D. (1990) Biodistribution of *p*-Iodobenzoyl (PIP) Labeled Antibodies in a Murine Lymphoma Model. *Nucl. Med. Biol. 17*, 381–387.
(33) Murray, J. L., Mujoo, K., Wilmanns, C., Mansfield, P., Wilbur, D. S., and Rosenblum, M. G. (1991) Variables Influencing Tumor Uptake of Antimelanoma Monoclonal Antibodies Radioiodinated Using the Para-Iodophenyl (PIP) Technique. *J. Nucl. Med. 32*, 279–287.

Registry No. 1, 107759-58-0; **2**, 112725-22-1; [^{125}I]-**3**, 125215-72-7; [^{131}I]-**3**, 126296-26-2; [^{125}I]-**4**, 125215-73-8; [^{131}I]-**4**, 127733-21-5.

Hepatobiliary Delivery of Polyaminopolycarboxylate Chelates: Synthesis and Characterization of a Cholic Acid Conjugate of EDTA and Biodistribution and Imaging Studies with Its Indium-111 Chelate

David A. Betebenner,† Patrick L. Carney,† A. Michael Zimmer,‡ Joanne M. Kazikiewicz,‡ Erno Brücher,§,∥ A. Dean Sherry,§ and David K. Johnson*,†

Abbott Laboratories, Department 90M, Abbott Park, Illinois 60064, Department of Nuclear Medicine, Northwestern University Medical Center, Chicago, Illinois 60601, and Department of Chemistry, The University of Texas at Dallas, Richardson, Texas 75083. Received December 20, 1990

A conjugate in which the steroid nucleus of cholic acid was linked to EDTA via an 11-atom spacer was obtained by reacting the succinimidyl ester of cholic acid with the amine formed by reaction of a benzyl isothiocyanate derivative of EDTA with *N*-(*tert*-butoxycarbonyl)ethylenediamine and subsequent deprotection. Potentiometric titration studies with model complexes showed that the EDTA moiety retained the ability to form 1:1 chelates of high thermodynamic stability, although formation constants were some 3–4 log *K* units lower for complexes of the conjugate than for the analogous chelates with underivatized EDTA. A complex formed between the cholic acid–EDTA conjugate and $^{111}In^{III}$ was clearly rapidly into the liver when injected iv into mice, with subsequent excretion from the liver into the gastrointestinal tract being complete within 1 h of injection. Radioscintigraphic imaging studies conducted in a rabbit given the ^{111}In-labeled conjugate also showed early liver uptake followed by rapid clearance from the liver into the intestine, with good visualization of the gallbladder in images obtained at 20–25 min postinjection. It is concluded that conjugation to cholic acid provides a useful means for the hepatobiliary delivery of EDTA chelates that otherwise exhibit predominantly extracellular distribution and renal clearance.

INTRODUCTION

Metal complexes of polyaminopolycarboxylate chelators find use in diagnostic radiology both as radiopharmaceuticals and as MRI[1] contrast agents. Chelates of DTPA with the γ-emitting radiometals technetium-99m and indium-111 are used as radiopharmaceuticals in renal clearance studies and cisternography (*1–4*). The gadolinium(III) complex of DTPA has been widely studied as an MRI contrast agent (*5, 6*) and is finding clinical use, particularly in delineating brain lesions that result in altered capillary permeability (*7*). Characteristics that make these chelates useful for such applications include the thermodynamic stability of the complexes, the inertness of the polyaminopolycarboxylate framework to metabolic degradation, and the primarily extracellular distribution of these agents that results from their highly hydrophilic nature. Because of these properties, such chelates are largely restricted to the vascular compartment when given intravenously and are rapidly excreted, intact, into the urine.

While metal complexes that distribute extracellularly are useful in studying blood flow, perfusion, and disease states that cause changes in capillary transit, there are instances where an agent must be able to distribute intracellularly in order to provide useful physiological information. One such case is the study of liver disease and hepatobiliary function. Agents for detecting tissue abnormalities in the liver and for evaluating the status of the bile ducts and gallbladder must be able to cross the hepatocyte membrane and eventually be excreted via the bile. The design of chelates that fulfill this requirement has generally involved the use of hydrophobic ligands. For example, recent work on the development of liver MRI contrast agents (*5, 8, 9*) has concentrated on high-spin iron(III) complexes of EHPG, as these are substantially more hydrophobic than the analogous EDTA chelates by virtue of the two phenolic substituents that function as metal binding groups. We set out to examine an alternative approach to the hepatobiliary targeting of chelates, in which hydrophilic polyaminopolycarboxylates that do not normally cross the hepatocyte membrane to any great extent are conjugated to endogenous compounds that possess the intrinsic property of circulating through liver parenchyma. The first such endogenous compound chosen for study was cholic acid.

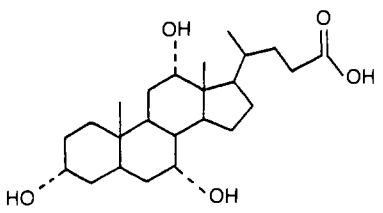
Cholic acid (**1**, Chart I) is one of a number of acidic steroid derivatives that are produced by cholesterol catabolism and are secreted by hepatocytes into the bile (*10*). A significant fraction of secreted bile acids is resorbed in the ileum and returned via the plasma compartment to the liver, in a process termed the enterohepatic circulation (*11*). Cholic acid radiolabeled with selenium-75 has previously been used for hepatobiliary radioimaging (*12*), and efforts to develop therapeutic chelators for the decorporation of toxic metals have included the synthesis of several metal-binding derivatives of cholic acid, among them a hydroxamate (**2**, Chart I) (*13*) and analogues containing thioether and carboxymethyl thioether substituents (**3**, **4**, Chart I) (*14*). However, the latter compounds contain only bidentate metal binding sites and the sulfur donors would be expected to bind only weakly to many metals of interest. We undertook the synthesis of conjugates in which polyaminopolycarboxylate chelators, which have a well-defined coordination

† Abbott Laboratories.
‡ Northwestern University Medical Center.
§ The University of Texas at Dallas.
∥ Present address: Lajos Kossuth University, H-4010 Debrecan, Hungary.

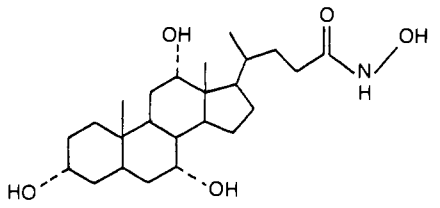
[1] Abbreviations used: DTPA, diethylenetriaminepentaacetic acid; EDTA, ethylenediaminetetraacetic acid; EHPG, *N*,*N*′-ethylenebis(2-hydroxyphenylglycine); MRI, magnetic resonance imaging; TMS, trimethylsilane; TSP, 3-(trimethylsilyl)-1-propanesulfonic acid.

1043-1802/91/2902-0117$02.50/0 © 1991 American Chemical Society

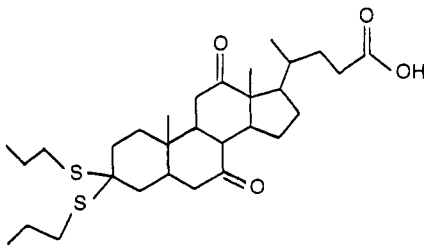
Chart I



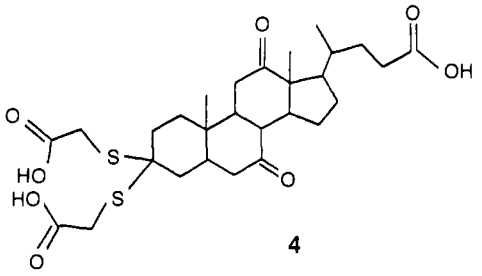
1



2



3



4

chemistry, are coupled to cholic acid via the C-24 carboxylic carbon atom. This report describes the preparation and characterization of an EDTA conjugate of this type (**9**, Scheme I) and its ability to deliver indium-111 to the hepatobiliary system in animals.

EXPERIMENTAL PROCEDURES

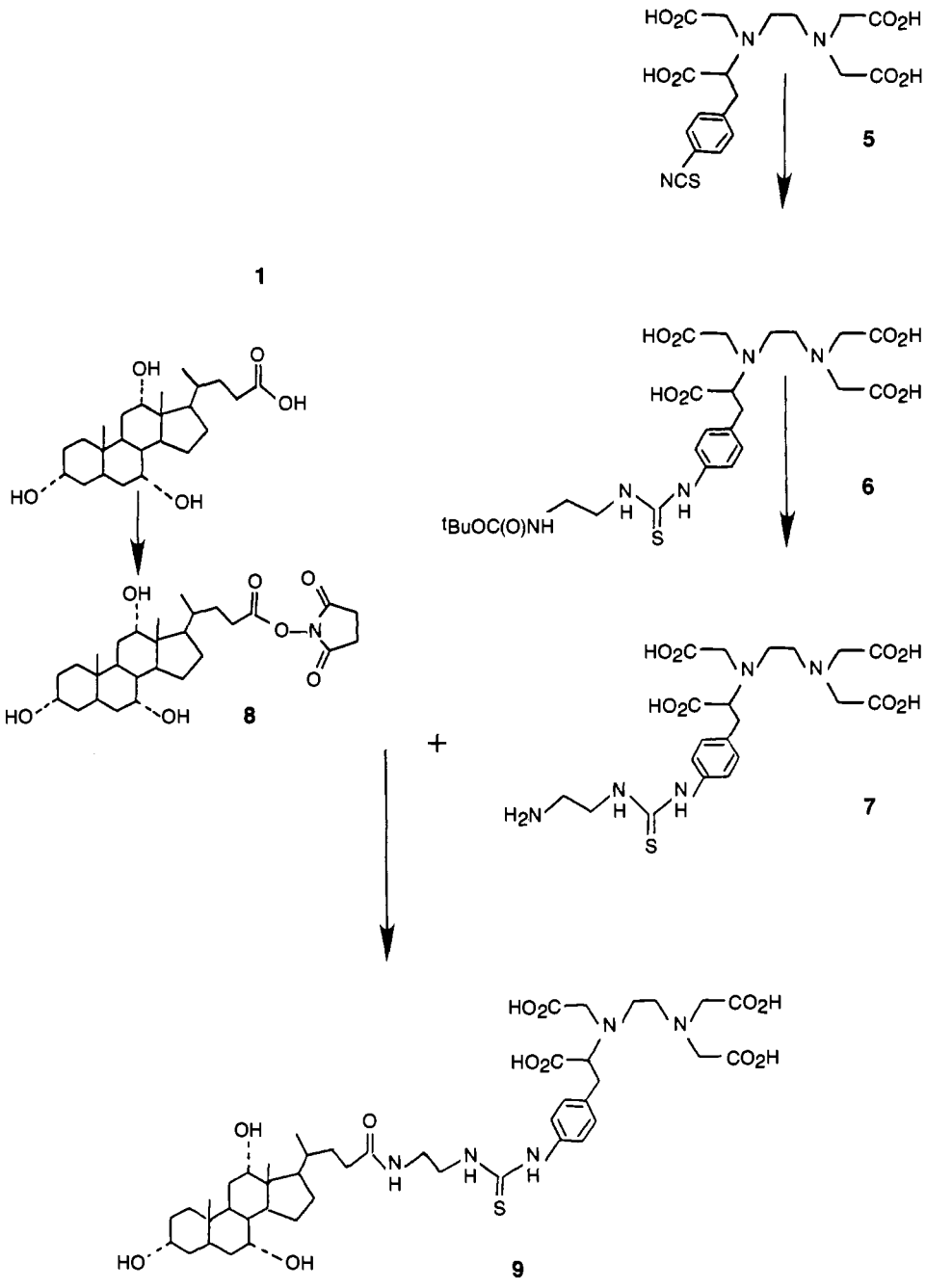
Materials and Methods. *N*-(Carboxymethyl)-*N*-[2-[bis(carboxymethyl)amino]ethyl]-3-(4-isothiocyanatophenyl)alanine (**5**) was synthesized as previously described (*15*). All other starting materials and reagents were obtained from Aldrich Chemical Co., Milwaukee, WI, unless otherwise specified, and were used without further purification. AG1-X4 anion-exchange resin (formate form, Bio-Rad Laboratories, Richmond, CA) was slurried with 5 M HCO_2H for 30 min then filtered and washed with deionized water until the pH of the washings reached 5. The resin was then swelled in deionized water for 90 min and poured into a glass chromatography column. Acid-washed glassware, reagent-grade buffer salts and deionized water from a MILLI-Q system (Millipore Corp., Bedford, MA) were employed in preparing all buffers for use with chelator derivatives. ^1H NMR and ^{13}C NMR spectra were recorded on a General Electric QE-300 spectrometer, operating at 300.23 and 75.5 MHz, respectively. Chemical shifts are reported in ppm relative to TMS or TSP and coupling constants (J) are given in hertz. Mass spectra were obtained by either the fast atom bombardment technique using a glycerol/thioglycerol matrix or by direct chemical ionization using ammonia. Elemental analyses were performed by Galbraith Laboratories, Knoxville, TN.

Metal chloride stock solutions used in formation constant determinations were prepared from the corresponding oxides (Aldrich, 99.9%) by dissolution in concentrated HCl and subsequent evaporation of the excess acid. Concentrations of these stock solutions were determined by complexometry using xylenol orange as indicator. Buffered solutions of indium-111 for labeling conjugates were obtained by diluting carrier-free research-grade indium-111 chloride (Nordion International, Inc, Kanata, Ontario, Canada) with 0.5 M HCl to a specific activity of of 13 mCi/mL then adding an equal volume of 1.0 M aqueous NaOAc, pH 6. Radioscintigraphic studies were performed with a Raytheon γ-camera equipped with a medium-energy parallel-hole collimator.

***N*-(Carboxymethyl)-*N*-[2-[bis(carboxymethyl)amino]-3-[4-[*N*-[2-[(*tert*-butoxycarbonyl)amino]ethyl](thioureido)]phenyl]alanine (6).** A solution of the dihydrochloride salt of **5** (0.52 g, 1.01 mmol) and triethylamine (0.39 g, 3.84 mmol) in DMF (10 mL) was stirred in an argon-purged flask at 0 °C as a solution of *N*-(*tert*-butoxycarbonyl)ethylenediamine (0.59 g, 3.69 mmol, prepared as described in ref 16) in DMF (8 mL) was added. The resulting solution was stirred at 0 °C for a further 15 min then at room temperature for 48 h. Water (3 mL) was added and stirring at room temperature continued for a further 6 h, after which time the solution was evaporated to dryness under vacuum to yield a brown oil. This was dissolved in H_2O (30 mL) and extracted with CH_2Cl_2 (3 × 35 mL) and the aqueous layer lyophilized to give a yellow powder which was dissolved in H_2O (10 mL), adjusted to pH 9, and applied to an AG1-X4 anion-exchange column (formate form, bed volume 65 mL). The column was eluted successively with H_2O (300 mL), 3.5 M HCO_2H (300 mL), and 7.0 M HCO_2H (300 mL), fractions being monitored for the presence of the desired product by TLC on silica gel plates developed in 40% concentrated aqueous NH_4OH/60% EtOH (95%) (R_f of **6** = 0.33). Fractions containing the desired product, which eluted in 7 M HCO_2H, were combined and evaporated to dryness under vacuum to afford 0.49 g (81%) of **6** in the form of a yellow solid: ^1H NMR (DMSO-d_6, TMS) δ 1.38 (s, 9 H), 2.68–3.15 (m, 8 H), 3.28–3.58 (m, 8 H), 3.63 (dd, 1 H, J = 8.5, 6.25), 6.90 (t, 1 H), 7.18 (d, 2 H, J = 8.5), 7.19 (s, 1 H), 7.25 (d, 2 H, J = 8.5), 7.72 (m, 1 H), 8.42 (s, 1 H), 9.55 (s, 2 H), 9.78 (s, 1 H); mass spectrum (FAB, EtOH/H_2O), m/e 600 $(M + H)^+$; high-resolution mass spectrum calcd for $C_{25}H_{38}N_5O_{10}S$ 600.2339, found 600.2346.

***N*-(Carboxymethyl)-*N*-[2-[bis(carboxymethyl)amino]ethyl]-3-[4-[*N*-(2-aminoethyl)(thioureido)]phenyl]alanine Trihydrochloride (7).** A solution of **6** (0.48 g, 0.80 mmol) in trifluoroacetic acid (15 mL) was stirred at room temperature for 6 h then evaporated to dryness under vacuum to give a yellow oil. This was dissolved in 2 M HCl (25 mL) and reevaporated to dryness and the residue redissolved in H_2O (5 mL). The pH of the resulting solution was adjusted to 9 then it was applied to an AG1-X4 anion-exchange column (formate form, bed volume 40 mL). The column was eluted first with H_2O (250 mL) then with 1 M HCO_2H (1 L) with collection of 15-mL fractions, which were monitored for the presence of the

Scheme I



desired product by TLC on silica gel plates developed in 40% concentrated aqueous NH_4OH/60% EtOH (95%) (R_f for **7** = 0.60, ninhydrin positive). Fractions containing the product were combined, evaporated to dryness, redissolved in 4 M HCl (150 mL), and reevaporated to dryness. Drying of the resulting residue under vacuum over P_2O_5 afforded 0.45 g (92%) of **7** in the form of an off-white solid: ^{1}H NMR (D_2O, TSP) δ 3.06 (dd, 1 H, J = 14.1, 8.2), 31.6–3.27 (m, 5 H), 3.40–3.52 (m, 2 H), 3.68 (d, 1 H, J = 18.7), 3.87–3.96 (m, 4 H), 7.27 (d, 2 H, J = 8.0), 7.37 (d, 2 H, J = 8.0); ^{13}C NMR (D_2O, TSP) δ 37.36, 42.09, 44.45, 52.23, 54.04, 56.78, 56.94, 68.94, 129.03, 133.25, 138.33, 139.43, 171.34, 177.59, 178.83, 183.72; mass spectrum (FAB, DMF), m/e 500 $(M + H)^+$; high-resolution mass spectrum calcd for $C_{20}H_{30}N_5O_8S$ 500.1815, found 500.1809. Anal. Calcd for $C_{20}H_{32}Cl_3N_5O_8S$: C, 37.24; H, 5.63; N, 10.86. Found: C, 37.16; H, 5.36; N, 11.06.

3α,7α,12α-Trihydroxy-5-cholan-24-oic Acid, *N*-Succinimidyl Ester (8). Cholic acid (Sigma Chemical Co., St. Louis, MO) was recrystallized from absolute EtOH prior to use. This material was then converted to the active ester following the procedure of Okahata et al. (*17*), employing 4.27 g (10 mmol) of the recrystallized cholic acid. Recrystallization of the resulting ester from $CHCl_3$/hexane afforded 3.17 g (60%) of **8** in the form of a white crystalline solid: mp 118–120 °C (lit. (*17*) 119–120 °C); ^{1}H NMR (DMSO-d_6 TMS) δ 0.60 (s, 3 H), 0.69–1.06 (m, 9 H), 1.13–1.50 (m, 10 H), 1.56–1.86 (m, 6 H), 1.92–2.30 (m, 3 H), 2.54–2.75 (m, 2 H), 2.81 (s, 4 H), 3.12–3.25 (br m, 1 H), 3.61 (br s, 1 H), 3.80 (br s, 1 H), 4.03 (d, 1 H), 4.15 (d, 1 H), 4.32 (d, 1 H); ^{13}C NMR ($CDCl_3$, TMS) δ 12.38, 17.18, 22.38, 22.58, 25.54, 26.23, 27.41, 28.09, 30.22, 30.50, 33.86, 34.62, 34.72, 35.01, 35.24, 39.41 (two atoms), 41.41, 41.53, 46.41, 46.70, 68.35, 71.79, 72.94, 169.16, 169.29; mass spectrum (DCI, NH_3) m/e 523 $(M + NH_4)^+$, 506 $(M + H)^+$; high-resolution mass spectrum calcd for $C_{28}H_{44}NO_7$ 506.3118, found 506.3124. Anal. Calcd for $C_{28}H_{43}NO_7$:

C, 66.51; H, 8.57; N, 2.77. Found: C, 66.77; H, 8.89; N, 3.29.

N-(Carboxymethyl)-N-[2-[bis(carboxymethyl)amino]ethyl]-3-[4-[N'-[2-[(3α,7α,12α-trihydroxy-5-cholan-24-oyl)amino]ethyl](thioureido)]phenyl]alanine Dihydrochloride (9). A solution of 8 (0.245 g, 0.48 mmol) in DMF (1.0 mL) was added dropwise to a stirred solution of 7 (0.268 g, 0.44 mmol) and triethylamine (0.313 g, 3.09 mmol) in DMF (4.0 mL). The resulting reaction mixture was stirred at room temperature, the contents being monitored periodically by TLC on silica gel plates developed in 25% concentrated aqueous NH_4OH/75% EtOH (95%) (R_f for 7 = 0.15, R_f for 9 = 0.35). After 3 days of stirring at room temperature, the reaction mixture was evaporated to dryness under vacuum to give a yellow oil which was dissolved in H_2O (5 mL). The pH of the resulting solution was adjusted to 9.5 by addition of 6 M NaOH then it was applied to an AG1-X4 anion-exchange column (formate form, bed volume 90 mL). The column was eluted sequentially with H_2O (200 mL), 1 M HCO_2H (200 mL), 4 M HCO_2H (200 mL), 5 M HCO_2H (800 mL), and 6 M HCO_2H (400 mL), collecting 10-mL fractions which were monitored by TLC. The desired product eluted in the 6 M HCO_2H fractions, and these were combined and evaporated to dryness under vacuum. The residue was dissolved in 4 M HCl (100 mL) and the resulting solution evaporated to dryness to give an oil. This was dissolved in H_2O (100 mL) and evaporated to dryness under vacuum. Further drying under vacuum over P_2O_5 afforded 0.22 g (52%) of 9 in the form of a pale beige solid: ^1H NMR (DMSO-d_6 TMS, 60 °C) δ 0.59 (s, 3 H), 0.78–1.05 (m, 9 H), 1.10–1.51 (m, 10 H), 1.53–1.91 (m, 6 H), 1.93–2.37 (m, 5 H), 2.87 (dd, 1 H, J = 13.7, 5.7), 2.94 (dd, 1 H, J = 13.7, 8.9), 3.03–3.15 (m, 2 H), 3.17–3.39 (m, 6 H), 3.43–3.56 (m, 4 H), 3.60–3.68 (m, 3 H), 3.73 (dd, 1 H, J = 8.9, 6.1), 3.77–3.83 (m, 1 H), 4.10 (s, 4 H), 7.18 (d, 2 H, J = 8.1), 7.39 (d, 2 H, J = 8.1), 7.78 (t, 1 H, J = 4.8), 7.91 (br s, 1 H), 9.69 (s, 1 H); mass spectrum (FAB, EtOH/DMF), m/e 890 $(M + H)^+$; high-resolution mass spectrum calcd for $C_{44}H_{68}N_5O_{12}S$ 890.4585, found 890.4584. Anal. Calcd for $C_{44}H_{69}Cl_2N_5O_{12}S$: C, 54.87; H, 7.22; N, 7.27. Found: C, 55.52; H, 7.49; N, 7.16.

Potentiometric Measurements. A 0.5 mM stock solution of 9 was prepared by suspending the dihydrochloride salt in deionized water and adding 6 equiv of KOH to completely dissolve the conjugate. Immediately prior to titration, 5 equiv of HCl were added to an aliquot of the stock solution to yield the pentaprotonated ligand. The concentration of the standard 0.1 M KOH solution used in the pH potentiometric titrations was determined by titration against a 0.01 M potassium hydrogen phthalate solution. The pH potentiometric titrations were performed with a Corning Ion Analyzer 250 pH meter, an Orion 8103 combination electrode, and a Metrohm 665 Dosimat automatic burette. Titrated solutions (5–10 mL) were covered by a cyclohexane layer to exclude CO_2 and the cell was thermostated at 25 ± 1 °C. All solutions were maintained at constant ionic strength with 0.1 M KCl. The hydrogen ion concentration was obtained from the measured pH values by the method of Irving et al. (*18*). Stability constants for the Zn^{2+} and Lu^{3+} chelates of 9 were determined by potentiometric titration of 1:1 mixtures of the metal ion and the conjugate.

Radiolabeling of 9 with Indium-111. A stock solution of 9 was prepared by dissolving 2 mg of the conjugate in 0.1 M aqueous NaOAc, pH 6 (2 mL). An aliquot of this solution (40 μL) was then mixed with a buffered solution of indium-111 (20 μL) and incubated at room temperature for 30 min. Uncomplexed indium-111 was then removed by centrifugation through a spin column containing Chelex resin (Sigma, bed volume 0.3 mL) equilibrated in 0.1 M aqueous NaOAc. The resulting eluate had a specific activity of ca. 85 μCi/mL and was used in subsequent animal studies without further purification.

Biodistribution Studies. BALB/c mice (n = 4 per group) were injected intravenously with indium-111-labeled 9 (100 μL per mouse) via a tail vein. At various time points postinjection, groups of animals were sacrificed by cervical dislocation and the internal organs were removed, weighed, and counted in a gamma-counter (Clinigamma 1272, Pharmacia LKB Biotechnology, Inc., Gaithersburg, MD). A weighed aliquot of blood was also counted and the tail was counted separately to check for extravasation at the injection site. The residual carcass was counted so as to obtain an estimate of the whole-body retention of radioactivity, by totaling the carcass counts and all individual organ counts. A 100-μL aliquot of the injectate was counted at the same time as the tissues, and the radioactivity in each tissue expressed as a percentage of this injected dose per gram of tissue.

Radioscintigraphy Studies. A female New Zealand rabbit was fasted for 24 h then anesthetized by intramuscular injection of nembutal and positioned on the head of the γ-camera so as to provide anterior views of the whole body. A commercially available hepatobiliary imaging agent (technetium-99m disofenin, NEN-Du Pont, N. Billerica, MA) was administered via a marginal ear vein and serial scintigraphic images were taken beginning at 5 min postinjection. Subsequently, the rabbit was revived, rested, and fed for 24 h then fasted for a further 24 h. An identical radioscintigraphic study was then performed, by administering indium-111-labeled 9 (1.0 mCi) via an ear vein and placing the animal on the γ-camera head in the same position as before.

RESULTS

Benzyl isothiocyanate derivatives of EDTA have been used in the past to covalently link the chelating moiety to proteins (*15*, *19*, *20*). The same reaction was used here to prepare an EDTA derivative containing a side chain that terminated in an aliphatic amino group (7), by reaction of 5 with a monoprotected ethylenediamine derivative and subsequent deprotection. Both steps proceeded in good yield, with anion-exchange chromatography being the preferred method for purification of both 6 and 7. Reaction of 7 with an active ester of cholic acid (8), prepared by standard methods, proceeded rather slowly at room temperature, but was complete after 3 days. Anion-exchange chromatography was again the method of choice for purification of the final product (9), which featured the EDTA moiety linked by an 11-atom spacer to the C-24 carbon atom of cholic acid.

As it was of interest to evaluate the effect of this derivatization of the EDTA framework on the thermodynamic stability of its chelates, potentiometric titration studies were undertaken (Figure 1). Protonation constants for 9, defined as

$$K_i = [H_iL]/[H_{i-1}L][H^+] \quad (i = 1, 2, \text{or } 3; L = 9)$$

and calculated from the titration data using a Simplex/Marquardt algorithm (*21*), were found to be $\log K_1 = 9.84$, $\log K_2 = 5.44$, and $\log K_3 = 3.44$. The corresponding values for EDTA are 10.23, 6.13, and 2.69, suggesting that conjugation to cholic acid affected the basicity of both nitrogen atoms (assuming that the two highest protonations occur at the nitrogens, as in EDTA). Complexes of

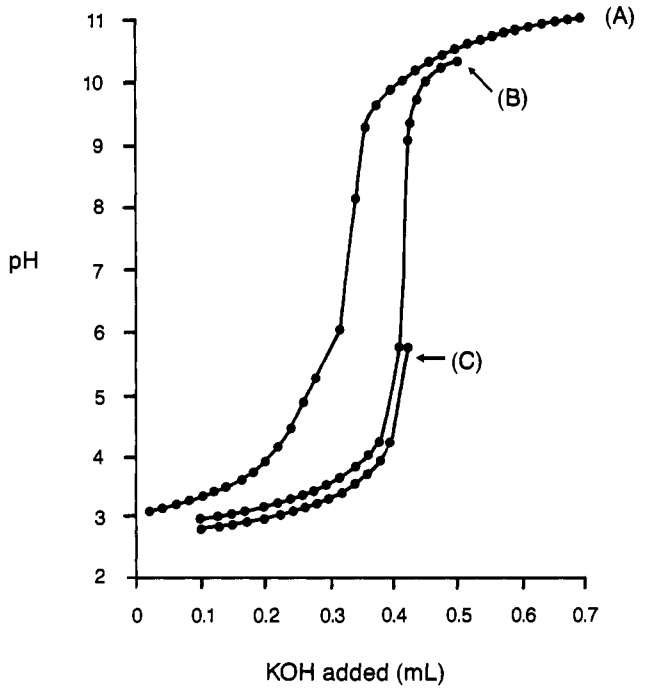


Figure 1. Potentiometric titration curves for (A) 0.42 mM **9**, (B) 0.42 mM **9** + 0.4 mM $ZnCl_2$, (C) 0.42 mM **9** + 0.4 mM $LuCl_3$. All measurements were made at 25 °C in the presence of 0.1 M KCl.

Table I. Biodistribution of Indium-111-Labeled 9 in BALB/c Mice

	mean % injected dose/g of tissue (±SD)		
tissue	15 min[a]	60 min[a]	120 min[a]
blood	5.5 (1.5)	1.0 (0.6)	0.2 (0.1)
liver	10.2 (2.6)	1.5 (0.9)	1.8 (1.0)
GI tract	14.9 (7.8)	14.5 (2.9)	17.6 (3.0)
gallbladder	164.6 (42.3)	69.3 (57.0)	10.3 (8.2)
kidney	4.0 (1.3)	1.0 (0.5)	0.3 (0.1)
lungs	3.1 (1.9)	0.9 (0.4)	0.5 (0.2)
spleen	2.6 (2.4)	0.8 (0.2)	4.6 (4.4)

[a] Time postinjection.

9 with lanthanum(III), gadolinium(III), and copper(II) were too insoluble to permit potentiometric measurements. It was however possible to obtain data for chelates of **9** with zinc(II) and lutetium(III) (Figure 1), the titration curves giving an excellent fit to a model that assumes the formation of 1:1 complexes. Stability constants (K = [ML]/[M][L]), derived from the potentiometric data using a Simplex algorithm, were determined to be log K = 15.9 for the $[Lu(\mathbf{9})]^-$ complex and log K = 13.9 for the $[Zn(\mathbf{9})]^{2-}$ chelate.

The $[In(\mathbf{9})]^-$ chelate used in biodistribution studies showed rapid clearance from the blood when injected iv into normal mice, with early localization in the liver, gallbladder, and gastrointestinal (GI) tract (Table I). Approximately 90% of the injected radiometal had left the circulation by 15 min postinjection, while all of the dose was still present in the animals at that time (108 ± 15%). Even at this early time point, significant excretion into the gut had occurred and this level remained virtually constant throughout the study. The intense early localization in the gallbladder decreased rapidly with time and liver activity had essentially cleared by 1 h postinjection. Whole-body retention of radioactivity after 2 h (55 ± 3%) was virtually unchanged from that at 1 h (57 ± 1%). It is doubtful that these whole-body losses of radioactivity represented fecal excretion, given the relatively short time span involved, loss of some 40% over the dose of the first 60 min being best explained by clearance through the urine of that fraction of injected activity not taken up by the liver. The relatively high initial kidney activity seen, and the order of magnitude decrease observed over the subsequent 2 h, are also indicative of early renal clearance of a proportion of the injected dose. Taken together, these data suggest rapid extraction by the liver of a substantial fraction of the injected dose of indium-111, with the radiometal subsequently leaving the liver and being excreted into the GI tract within 1 h of administration.

These findings were confirmed in radioscintigraphic imaging studies conducted in a rabbit (Figure 2). To facilitate anatomic identification and provide a basis for comparison with subsequent images obtained with **9**, a clinically used hepatobiliary radioimaging agent (technetium-99m–disofenin) was first administered (Figure 2A). Early images showed prominent uptake of ^{99m}Tc activity in the liver, with some excretion into the intestinal tract apparent even at 5 min postinjection. Clearance of activity from the liver into the gut proceeded continuously over the following 30 min and was essentially complete by 40 min postinjection. The gallbladder was most easily visualized in images obtained between 25 and 35 min after giving the radiopharmaceutical. Images obtained in the same animal after administration of indium-111-labeled **9** (Figure 2B) showed essentially the same pattern of uptake and clearance as had been seen with the Tc-99m agent. In the initial image, obtained at 5 min postinjection, only the liver was visualized. Clearance of In-111 activity from the liver into the GI tract had begun by 10 min postinjection and proceeded rapidly, such that most of the radioactivity was in the gut after 20 min. The gallbladder was clearly visualized in the 20- and 25-min images, with all subsequent views showing only intestinal activity. Although these data suggest that hepatic clearance of radioactivity may be faster for indium-111-labeled **9** than for technetium-99m–disofenin, this observation would have to be repeated several times before drawing any such conclusion, as the difference seen here may simply reflect metabolic variability in the particular animal studied.

DISCUSSION

Clinical experience over the past 5 decades with the systemic administration of exogenous chelators and chelates has been limited to a very small number of compounds. Except for radiologic applications, the only other area of clinical practice in which such agents have been given with any frequency is the treatment of metal intoxications and, here again, the polyaminopolycarboxylates have been prevalent among the handful of chelators used for such purposes (*22*). Efforts to improve upon the limited tissue penetration and, hence, efficacy of compounds such as EDTA and DTPA have for the most part focused on the design and synthesis of alternative, frequently biomimetic, chelators that in many cases employ aromatic metal-binding moieties (*8*, *9*, *23–27*). While such systems often display improved thermodynamic stability and greater tissue penetration, they have frequently proven to be more toxic and, despite much preclinical development, they have to date rarely been used clinically. In contrast, the polyaminopolycarboxylates have toxicities that are generally both low and well-understood, and there exists an extensive body of data on their use in man that dates back to the 1950s. An attractive alternative strategy for the development of high-affinity metal-binding entities with enhanced ability to target selected tissues and metabolic processes in vivo is to conjugate known polyaminopolycarboxylate structures to molecules that alter their biodistribution.

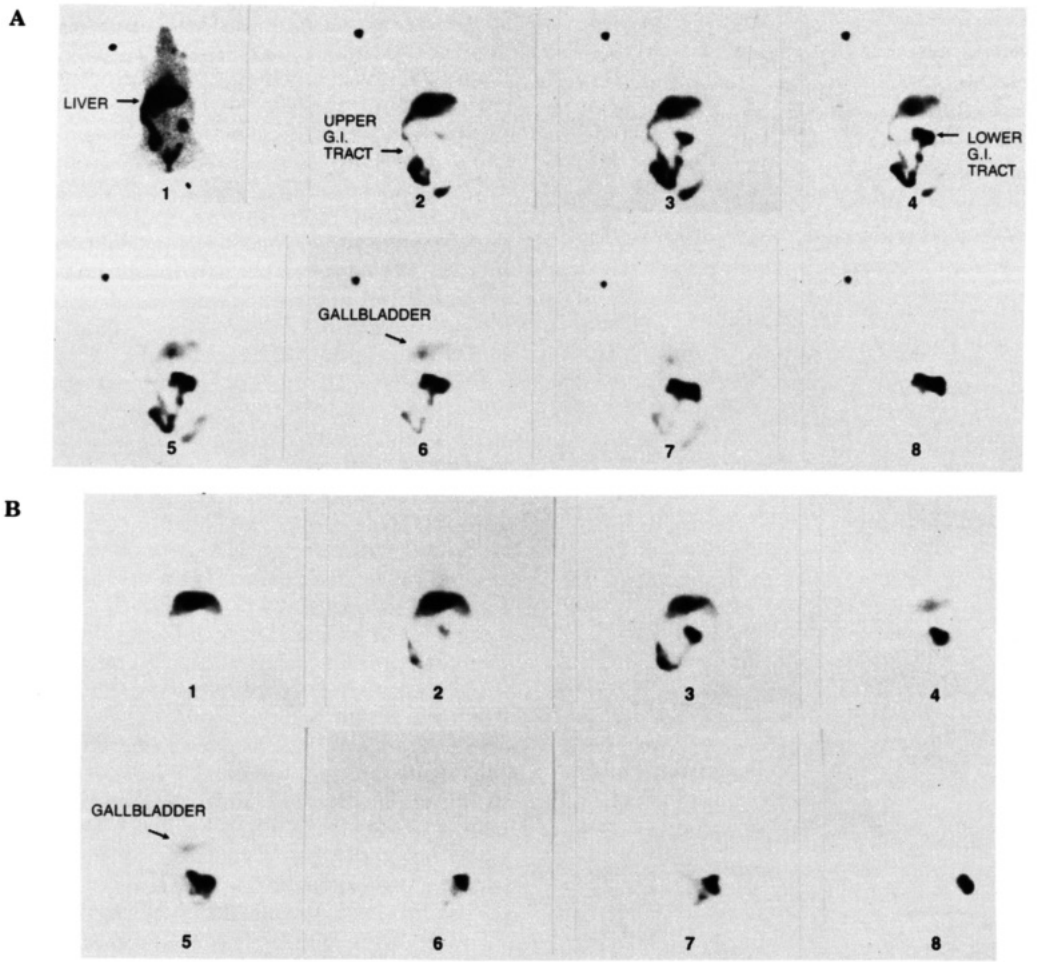


Figure 2. Anterior whole-body radioscintigraphic images of a rabbit given (A) ^{99m}Tc–disofenin, (B) ^{111}In-labeled **9**. Images were obtained at 5 (1), 10 (2), 15 (3), 20 (4), 25 (5), 30 (6), 35 (7), and 40 min (8) postinjection. To provide anatomic orientation, the 5-min image obtained with the ^{99m}Tc agent is shown at contrast settings that result in visualization of a whole-body contour. All other images show only the organs of interest (liver and GI tract).

Such a strategy was used in the past to prepare an EDTA derivative with tumor-targeting properties, by linking the chelator to the anti-tumor antibiotic bleomycin (*28*). Similarly, we employed a bifunctional chelator to link the EDTA moiety to a bile acid that targets hepatocytes. Examples of hybrid molecules that contain both a steroid nucleus and a high-affinity metal-binding site are rare, although a series of compounds in which high affinity Fe^{II} and Fe^{III} chelators were linked to various 21-amino steroids was recently described by Braughler et al. (*29*).

Linkage of a steroid moiety to EDTA through one of the carboxymethyl arms of the chelator proved to have a measurable impact on the thermodynamic stability of chelates formed by the resulting conjugate. The stability constants for 1:1 complexes of EDTA with Lu^{III} and Zn^{II}, measured under similar conditions to those employed in studies of **9**, are ca. 19.8 and 16.5, respectively. Thus, conjugation reduced these values by ca. 4 log K units for Lu^{III} and 3 log K units in the case of Zn^{II}. Although the stability constant for the $[In(\mathbf{9})]^-$ complex that was used in the biological studies has not been determined, it would seem reasonable to assume a log K value on the order of 20, as the stability constant for $[In(EDTA)]^-$ is variously reported to be 25.3 (*30*) or 25.8 (*31*).

Whatever the actual reduction in thermodynamic stability of the In^{III} chelate of **9** relative to free EDTA may be, it is apparently not sufficient to produce any evidence of chelate instability in vivo. The transient pulse of radioactivity through the liver that was documented in both the mouse biodistribution study and the rabbit imaging procedure is consistent with retention of the radiometal within the chelate throughout the course of these studies. If the complex had been unstable, liver levels of radioactivity would have been expected to remain elevated for many hours, and possibly days, as it is well-established that intracellular dissociation of indium(III) chelates results in prolonged retention of the radiometal within the cell (*32*).

When an indium-111 chelate of the aminobenzyl-DTPA analogue of **5** was injected intravenously into mice, virtually all of the radiolabel was cleared rapidly through the urine (unpublished data). This suggests that introduction of a hydrophobic benzyl group into a polyaminopolycarboxylate structure is not, in and of itself, sufficient to shift excretion to the hepatobiliary route. The cholic acid moiety is thus essential for efficient hepatic uptake, although it remains unclear whether this reflects entry into the hepatocyte via specific mechanisms of bile acid transport or whether the observed behavior of **9** in animals simply represents uptake by nonspecific anionic transport processes. Bile acid transport into liver cells is a poorly understood process that is known to require sodium ions and metabolic energy (*11*). Studies in isolated rat hepatocytes (*33*) have suggested that there may be separate carrier-mediated transport systems for cholic acid itself and for the amide formed from its reaction with taurine (2-aminoethanesulfonic acid), which is a prominent metabolite. Although the relatively bulky chelate formed between a trivalent metal and the benzyl-EDTA group in **9** does not sterically resemble the ethanesulfonic acid side

chain of taurocholic acid, the net uninegative charge and hydrophilic character that both moieties share may enable the chelate conjugate to enter hepatocytes through the taurocholate transport system. The preparation of analogues of **9** that contain chelates of differing net electronic charge and studies of the pathways and kinetics of intracellular processing of these species will be needed to fully define the extent to which chelate conjugates of cholic acid are able to mimic the underivatized molecule.

Although details of the mechanism of hepatic uptake remain to be elucidated, the data presented here indicate that conjugation to cholic acid provides a useful means for the controlled delivery of polyaminopolycarboxylate chelates to parenchymal liver cells.

LITERATURE CITED

(1) Klopper, J. F., Hauser, W., Atkins, H. L., Eckelman, W. C., and Richards, P. (1972) Evaluation of ^{99m}Tc-DTPA for the measurement of glomerular filtration rate. *J. Nucl. Med. 13*, 107–110.

(2) Gates, G. F. (1982) Glomerular filtration rate: estimation from fractional renal accumulation of ^{99m}Tc-DTPA (stannous). *Am. J. Roentgenol. 138*, 565–570.

(3) Som, P., Hosain, F., Wagner, H. N., Jr., and Scheffel, U. (1972) Cisternography with chelated complex of ^{99m}Tc. *J. Nucl. Med. 13*, 551–553.

(4) Hosain, F., and Som, P. (1972) Chelated ^{111}In: an ideal radiopharmaceutical for cisternography. *Br. J. Radiol. 45*, 677–679.

(5) Lauffer, R. B. (1987) Paramagnetic metal complexes as water proton relaxation agents for NMR imaging: theory and design. *Chem. Rev. 87*, 901–927.

(6) Runge, V. M., Clanton, J. A., Herzer, W. A., Gibbs, S. J., Price, A. C., Partain, C. L., and James, A. E. (1984) Intravascular contrast agents suitable for magnetic resonance imaging. *Radiology 153*, 171–176.

(7) Carr, D. H., Brown, J., Bydder, G. M., Weinmann, H.-J., Speck, U., Thomas, D. J., and Young, I. R. (1984) Intravenous chelated gadolinium as a contrast agent in NMR imaging of cerebral tumors. *Lancet 1*, 484–486.

(8) Lauffer, R. B., Greif, W. L., Stark, D. D., Vincent, A. C., Saini, S., Wedeen, V. J., and Brady, T. J. (1988) Iron-EHPG as an hepatobiliary MR contrast agent: initial imaging and biodistribution studies. *Nucl. Med. Biol. 15*, 47–49.

(9) Lauffer, R. B., Vincent, A. C., Padmanabhan, S., Villringer, A., Saini, S., Elmaleh, D. R., and Brady, T. J. (1987) Hepatobiliary MR contrast agents: 5-substituted iron-EHPG derivatives. *Magn. Reson. Med. 4*, 582–590.

(10) Björkhem, I. (1985) Mechanism of bile acid biosynthesis in mammalian liver. *Sterols and Bile Acids* (H. Danielsson, and J. Sjövall, Eds.) pp 231–278, Elsevier, New York.

(11) Elliott, W. H. (1985) Metabolism of bile acids in liver and extrahepatic tissues. *Sterols and Bile Acids* (H. Danielsson, and J. Sjövall, Eds.) pp 303–329, Elsevier, New York.

(12) Merrick, M. V., Eastwood, M. A., Anderson, J. R., and Ross, H. M. (1982) Enterohepatic circulation in man of a gamma-emitting bile-acid conjugate, 23-selena-25-homotaurocholic acid (SeHCAT). *J. Nucl. Med. 23*, 126–130.

(13) Hershko, C., Grady, R. W., and Cerami, A. (1978) Mechanism of iron chelation in the hypertransfused rat: definition of two alternative pathways of iron mobilization. *J. Lab. Clin. Med. 92*, 144–151.

(14) Jones, M. M., Pratt, T. H., Mitchell, W. G. (1976) Enterohepatic chelating agents—1. General principles and examples. *J. Inorg. Nucl. Chem. 38*, 613–616.

(15) Westerberg, D. A., Carney, P. L., Rogers, P. E., Kline, S. J., and Johnson, D. K. (1989) Synthesis of novel bifunctional chelators and their use in preparing monoclonal antibody conjugates for tumor targeting. *J. Med. Chem. 32*, 236–243.

(16) Essian, H., Lai, J. Y.; and Hwang, K. J. (1988) Synthesis of diethylenetriaminepentaacetic acid conjugated inulin and utility for cellular uptake of liposomes. *J. Med. Chem. 31*, 898–901.

(17) Okahata, Y., Ando, R., and Kunitake, T. (1979) Catalytic hydrolysis of *p*-nitrophenyl esters in the presence of representative ammonium aggregates. Specific activation of a cholesteryl nucleophile bound to a dialkylammonium bilayer membrane. *Bull. Chem. Soc. Jpn. 52*, 3647–3653.

(18) Irving, H. M., Miles, M. G., and Pettit, L. D. (1967) A study of some problems in determining the stoichiometric proton dissociation constants of complexes by potentiometric titrations using a glass electrode. *Anal. Chim. Acta 38*, 475–488.

(19) Meares, C. F., McCall, M. J., Reardon, D. T., Goodwin, D. A., Diamanti, C. I., and McTigue, M. (1984) Conjugation of antibodies with bifunctional chelating agents: isothiocyanate and bromoacetamide reagents, methods of analysis and subsequent addition of metal ions. *Anal. Biochem. 142*, 68–78.

(20) Brechbiel, M. W., Gansow, O. A., Atcher, R. W., Schlom, J., Esteban, J., Simpson, D. E., and Colcher, D. (1986) Synthesis of 1-(*p*-isothiocyanatobenzyl) derivatives of DTPA and EDTA. Antibody labeling and tumor-imaging studies. *Inorg. Chem. 25*, 2772-2781.

(21) Sherry, A. D., Cacheris, W. P., and Kuan, K.-T. (1988) Stability constants for Gd^{3+} binding to model DTPA-conjugates and DTPA-proteins: implications for their use as magnetic resonance contrast agents. *Magn. Reson. Med. 8*, 180–190.

(22) Williams, D. R., and Halstead, B. W. (1983) Chelating agents in medicine. *J. Toxicol.: Clin. Toxicol. 19*, 1081–1115.

(23) Martell, A. E., Anderson, W. F., and Badman, D. G., Eds. (1981) *Development of Iron Chelators for Clinical Use*, Elsevier North-Holland, New York.

(24) Raymond, K. N., and Tufano, T. P. (1982) Coordination chemistry of the siderophores and recent studies of synthetic analogues. *NATO Adv. Study Inst. Ser. C 89*, 85–105.

(25) Martell, A. E., Ed. (1980) *Inorganic Chemistry in Biology and Medicine*. ACS Symposium Series 140; American Chemical Society, Washington, DC.

(26) Mathias, C. J., Sun, Y., Welch, M. J., Green, M. A., Thomas, J. A., Wade, K. R., and Martell, A. E. (1988) Targeting radiopharmaceuticals: comparative biodistribution studies of gallium and indium complexes of multidentate ligands. *Nucl. Med. Biol. 15*, 69–81.

(27) Finnegan, M. M., Lutz, T. G., Nelson, W. O., Smith, A., and Orvig, C. (1987) Neutral water-soluble post-transition-metal chelate complexes of medical interest: aluminum and gallium tris(3-hydroxy-4-pyronates). *Inorg. Chem. 26*, 2171–2176.

(28) DeRiemer, L. H., Meares, C. F., Goodwin, D. A., and Diamanti, C. I. (1979) BLEDTA: tumor localization by a bleomycin analog containing a metal-chelating group. *J. Med. Chem. 22*, 1019–1023.

(29) Braughler, J. M., Burton, P. S., Chase, R. L., Pregenzer, J. F., Jacobsen, E. J., VanDoornik, F. J., Tustin, J. M., Ayer, D. E., and Bundy, G. L. (1988) Novel membrane localized iron chelators as inhibitors of iron-dependent lipid peroxidation. *Biochem. Pharmacol. 37*, 3853–3860.

(30) Martell, A. E., and Smith, R. M. (1977) *Critical Stability Constants*, Vol. 1–4, Plenum Press, New York.

(31) Subramanian, K. M., and Wolf, W. (1990) A new radiochemical method to determine the stability constants of metal chelates attached to a protein. *J. Nucl. Med. 31*, 480–488.

(32) Thakur, M. L., Segal, A. W., Louis, L., Welch, M. J., Hopkins, J., and Peters, T. J. (1977) Indium-111-labeled cellular blood components: mechanism of labeling and intracellular location in human neutrophils. *J. Nucl. Med. 18*, 1020–1024.

(33) Anwer, M. S., Kroker, R., and Hegner, D. (1976) Effect of albumin on bile acid uptake by isolated rat hepatocytes: is there a common bile acid carrier? *Biochem. Biophys. Res. Commun. 73*, 63–71.

Synthesis and Characterization of Protein and Polylysine Conjugates of Sulfamethoxazole and Sulfanilic Acid for Investigation of Sulfonamide Drug Allergy

Jayant G. Tatake, Michele M. Knapp, and Charlotte Ressler*

Department of Pharmacology, University of Connecticut Health Center, Farmington, Connecticut 06030.
Received November 21, 1990

Conjugates of sulfamethoxazole (SMX) with human serum albumin (HSA), transferrin (TR), and poly(L-lysine) (PL, degrees of polymerization 16 and 430) have been prepared. As a model, succinylSMX-glycine methyl ester was synthesized by carbodiimide and active ester routes. The proteins and PL were acylated with succinylSMX succinimido ester, affording conjugates $(succinylSMX)_{2-21}$-HSA, $(succinylSMX)_{17,27}$-TR, $(succinylSMX)_{11}$-Lys_{16}, and $(succinylSMX)_{71}$-Lys_{430} in which SMX was linked by a spacer chain of four carbons. This represents substitution of up to 35, 46, 65, and 17% of the amino groups of HSA, TR, PL_{16}, and PL_{430}, respectively. HSA was also acylated with the succinimido esters of succinylSMX-glycine and succinylSMX-ε-aminohexanoic acid, affording conjugates $(succinylSMX\text{-}Gly)_{53}$-HSA and $(succinylSMX\text{-}\epsilon\text{-}NH_2hex)_{51}$-HSA. In these conjugates SMX was linked by a spacer chain of 7 and 11 carbons, respectively, and almost all the amino groups of HSA were substituted. Factors apparently influencing the extent of conjugation to HSA were the stability of the active ester and the solubility of the conjugation reaction mixture. A sulfanilic acid (SA) conjugate, containing 12 mol of ligand/mol of HSA, was also prepared. The route of synthesis involved acylation of HSA with sulfanilyl fluoride. N-ε-Sulfanilyl-L-lysine dihydrochloride, required for quantitation of bound SA, was synthesized by a new route starting from α-Boc-L-lysine. Conjugates $(sulfanilyl)_{12}$-HSA and $(succinylSMX)_{13}$-HSA, differing in molecular weight from HSA by only 2.6 and 6.5%, were distinguishable from HSA by gel-filtration HPLC, as were the more highly substituted conjugates from their respective unsubstituted materials. Conjugates $(succinylSMX)_n$-HSA (n = 2, 3, 6, 9) were readily distinguishable from each other and from HSA on cellulose acetate electrophoresis. Mobilities were clearly dependent on epitope density.

INTRODUCTION

Sulfonamides continue to have an important place as antibacterial, antiprotozoal, and antirheumatic drugs. Trimethoprim-sulfamethoxazole (Bactrim, Septra, Co-trimoxazole) in particular is valuable for the treatment of shigellosis, bronchitis, urinary tract infections, and otitis media and for the treatment and prophylaxis of *Pneumocystis carinii* pneumonia in AIDS (*1*). However, its use is limited by the development of adverse drug reactions generally attributed to the sulfonamide. Evidence suggesting an immunological basis for such drug reactions has been limited. In the absence of other information, the synthesis was undertaken of determinants that might be suitable for detecting serum antibodies to sulfamethoxazole with the idea that elevated levels of Ab might be diagnostic of sulfa drug allergy.

In general analogy to the design of penicilloylpolylysine, the major determinant that can detect up to 75% of individuals sensitive to penicillin (*2*, *3*), it was desired to prepare conjugates of SMX[1] linked covalently to proteins and polylysine. To provide an additional determinant and to derive salient information on the structural features of the SMX molecule required for immunological recognition, sulfanilic acid representing half the molecule of SMX, was also to be linked covalently. To our knowledge, well-characterized protein and polypeptide conjugates with sulfonamide drugs have not been previously reported, although largely undefined sulfonamide–azo serum proteins, sulfonamide–azoalbumin and –azocasein have long been known (*4*, *5*). Likewise, conjugates with sulfanilyl groups in which the *p*-amino group is free have not been described, although N^4-acetylsulfanilyl residues have been substituted on gelatin and polylysine (*6*, *7*), as have (N^4-acetysulfanilyl)glycyl residues on polylysine (*7*).

Albumin and transferrin, the two chief components of human serum, were selected for conjugation as possible carrier proteins in vivo. They are similar in size (69 000 and 80 000 Da) and in lysine content (60 and 59 residues per mol, respectively) (*8*, *9*), but they differ otherwise in structure and function and could afford information on accessibility to conjugation and on the immunological recognition of their conjugates. The less immunogenic polylysines of 3000 and 90 000 Da were selected for conjugation also for projected studies in vivo.

The unprotected sulfanilyl residue was covalently coupled to HSA through linkage of the sulfonyl group without difficulty. However, before SMX could be linked to HSA, it was necessary to derivatize its weakly reactive aromatic amino group. This afforded a conjugate of SMX separated from the protein by a spacer chain of four carbons. Conjugates of SMX and HSA separated by spacer chains of 9 and 11 carbons were also synthesized to gain information on the optimum length of the spacer chain

* To whom reprint requests should be addressed.

[1] Abbreviations used: DMF, dimethylformamide; THF, tetrahydrofuran; DCC, dicyclohexylcarbodiimide; EDC, 1-ethyl-3-[3-(diethylamino)propyl]carbodiimide hydrochloride; SMX, sulfamethoxazole; SA, sulfanilic acid; SA-Lys, N-ε-sulfanilylysine; NH_2Hex, ε-aminohexanoic acid; HONSu, N-hydroxysuccinimide; sucSMX, N^4-(3-carboxypropanoyl)sulfamethoxazole; HSA, human serum albumin; OVA, ovalbumin; TR, human transferrin; PL, polylysine; $(sucSMX)_n$-HSA, human serum albumin conjugated with n N^4-(3-carboxypropanoyl)sulfamethoxazole groups; AAA, amino acid analysis; Ab, antibodies; ELISA, enzyme-linked immunosorbent assay.

1043-1802/91/2902-0124$02.50/0 © 1991 American Chemical Society

Table I. Synthesis of $(SucSMX)_n$–HSA (9f): Conjugation of Drug to HSA under Various Conditions of Temperature, Reaction Time and Mode of Addition and Molar Ratio of Reactants

				condition		conjugate[a]		
expt	HSA, mg	7, mg	7/HSA NH_2 molar ratio	pH[b]	other[c]	purifcn method[d]	mg	SMX/HSA molar ratio
1	100	77	2	6.8	A	D	93	6.4
2	50	50	2.6	9.5	B	E	16	2
3	50	54	2.8	9.5	A	F	20	2.9
4	50	79	4	6.8	A	F	25	9
5	50	157	8	6.8	A, C	G	32	13
6	49	253	13.3	6.8	A, C	E	28	13
7	50	160	8.1	*e*	A, C	E	39	21

[a] Dialyzed products established by HPLC gel filtration to be free of low molecular weight contaminants and analyzed for bound SMX as described under "General Chemical Procedures". [b] pH 6.8 adjusted by addition of 1 equiv of $NaHCO_3$; pH 9.5, by 2 mL of 0.2 M $NaHCO_3$–Na_2CO_3 buffer. [c] A, solution of 7 in 0.5 mL of DMF added and reaction allowed to proceed for 4 h at room temperature; B, 7 added as a solid over 2 h and reaction allowed to proceed for 16 h at 4 °C; C, solid separated out of the reaction mixture. [d] Low molecular weight reagents/byproducts were removed by the following methods: D, concentration dialysis; E, dialysis; F, gel filtration on Sephadex G-25 with water; G, gel filtration on Sephadex G-15 with 0.05 M sodium phosphate followed by dialysis as described under "General Chemical Procedures". [e] Sodium bicarbonate limited to 4.7 mg.

for immunological recognition. In both the sulfanilyl- and spacer-linked SMX conjugates, the linkage of the ligand to the protein, as to polylysine, was expected to involve the ε-amino group of lysyl residues.

As a model reaction for the introduction of SMX into proteins and polylysines, the new sucSMX-glycine methyl ester was synthesized. Conjugation of SA and SMX to HSA, transferrin, and polylysine was judged qualitatively by enhanced UV absorption at 254 nm relative to the 280-nm protein peak on gel-filtration HPLC. This technique was particularly informative since it also was capable of distinguishing by retention volume conjugates from parent proteins or PL differing with only small changes in molecular weight. Quantitative determination of the degree of conjugation to HSA or transferrin was accomplished by reverse-phase HPLC analysis of hydrolysates for SMX or *N*-ε-sulfanilyllysine. Conjugation to PL was determined quantitatively by the ratio SMX:Lys as given by HPLC and amino acid analysis, respectively, of hydrolysates.

When tested as a capture antigen in a new ELISA (*10*), the conjugate $(sucSMX)_{13}$–HSA was found capable of detecting serum IgM antibodies to sulfamethoxazole in an individual with an adverse cutaneous reaction to Bactrim (*11*). The ELISA activity was proportional to the degree of substitution for at least 13 residues of the ligand. By contrast, conjugate $(SA)_{12}$–HSA was inactive, suggesting the need in antibody recognition for a spacer in the conjugate or for additional structural features residing in the SMX molecule.[2] The development and validation of the ELISA and an evaluation of its clinical applicability to detect hypersensitivity and cross-reactivity (*12*) to SMX, as well as comparison of the various conjugates, are to be presented in detail separately.

EXPERIMENTAL PROCEDURES

Materials. Sulfamethoxazole, succinic anhydride, poly(L-lysine) hydrobromide ($n = 430$), human transferrin, and crystalline human albumin were obtained from Sigma Chemical Co., St. Louis, MO. The latter was confirmed to be free of γ-globulins and macroglobulins by HPLC on Waters Protein-Pak I-125 column. Poly(L-lysine) hydrobromide ($n = 16$) was from Miles-Yeda LTD, Miles Scientific, Naperville, IL. *N*-Hydroxysuccinimide, sulfanilyl fluoride, and acetylsulfanilyl chloride were from Aldrich Chemical Co., Milwaukee, WI; pyridine, dicyclohexylcarbodiimide, ethyl chloroformate, 40% dimethylamine, and sulfanilamide were from Matheson, Coleman, Bell, Norwood, OH; 3-amino-5-methylisoxazole was from Pfaltz and Bauer, Flushing, NY; methyl glycinate hydrochloride and ε-aminocaproic acid were from Mann Research Labs, New York, NY; α-Boc-L-lysine from Bachem, Marina Del Ray, CA. *N,N'*-Dimethylformamide was obtained from Eastman Kodak Co., Rochester, NY, and was freed of dimethylamine as described (*13*).

General Chemical Procedures. Melting points were determined in open glass capillary tubes with a Thomas-Hoover apparatus and are uncorrected. Evaporations were carried out under reduced pressure. Elemental analyses were performed by Micro-tech Laboratories, Oakton, IL, or Galbraith Laboratories, Knoxville, TN. Proton magnetic resonance spectra were recorded on a Varian EM-360 spectrometer at concentrations near 0.1 M. Chemical shifts are given as δ values in ppm downfield from sodium 3-(trimethylsilyl)propionate-*2,2,3,3-d*$_4$ as internal reference in aqueous solution and from tetramethylsilane in nonaqueous solvents. Multiplicities of resonances are described as broad (br), singlet (s), doublet (d), triplet (t), quartet (q), or multiplet (m).

HPLC was carried out in the apparatus described elsewhere (*14*). A C_{18} μBondapak column (Waters) was used in the reverse phase with system A (30% MeOH–1% AcOH), system B (5% MeOH–1% AcOH), and system C (25% MeOH–1% AcOH) at flow rates of 1–2 mL/min. A Protein-Pak I-125 gel-filtration column (Waters) was used with 0.05 M potassium phosphate buffer, pH 6.8. Protein absorption was determined at 280 nm, sulfonamide absorption at 254 nm.

Analytical TLC was carried out on Eastman Chromagram, polymer-backed, fluorescent indicator cellulose 13254 strips with system A ($CHCl_3$–MeOH, 5:1), B (benzene–EtOAc, 5:1), C (benzene–EtOAc, 10:1) or D (benzene–EtOAc, 5:2) or with silica gel 13181 strips and system E ($CHCl_3$–MeOH, 10:1). The Bratton–Marshall test (*15*) was carried out with a sensitivity in solution of 0.5 nmol and with a sensitivity on paper of 0.05 μmol.

Gel filtration was carried out on an equilibrated Sephadex G-15 column (2.5 × 63 cm, Pharmacia, Piscataway, NJ) in 0.05 M sodium phosphate buffer, pH 8. The $(sucSMX)_{13}$–HSA conjugate, equiv to 25 mg of starting HSA (Table I, expt 5), was applied in 3 mL of 0.2 M phosphate buffer, pH 8. Filtration was at a flow rate of 2.5 mL/min and was monitored by absorbance at 280 nm. Peak materials were identified by HPLC on Protein-Pak I-125, which showed protein at 120–138 mL, well-separated from low molecular weight material at 212–250 mL. Protein-containing fractions were pooled and dialyzed against

[2] These findings were presented at the 43rd Annual Meeting of the American Academy of Allergy and Immunology, February 19–25, 1987, Washington, DC. (*11*).

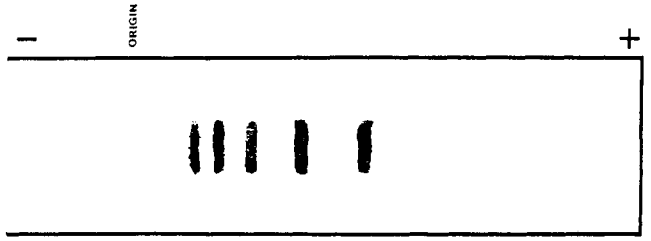


Figure 1. Effect of epitope density on the electrophoretic mobility of $(sucSMX)_n$–HSA conjugates. Composite electropherogram of HSA and conjugates of $n = 2, 3, 6$, and 9. Materials: 10 μg was applied to the center of 1 × 6 in. cellulose acetate strips and electrophoresed at pH 5.6 at 27 V/cm for 20 min, and then stained with Coomassie Blue. Mobilities were 10, 13, 18, 26, and 35 mm, respectively.

distilled water, then lyophilized to give the product as a white fluffy powder. Gel filtration on Sephadex G-25 (Pharmacia, Table I, expts 3 and 4) was carried out with water in a similar way.

Dialysis was carried out with membrane tubing (retention cutoff 12 000 Da, 1 in. flat, from A.H. Thomas, Philadelphia, PA) or Spectrapor tubing (cutoff 1000 Da, from Fisher Scientific, New York, NY) that was treated before use (*16*). Synthetic conjugates were dialyzed at 4 °C against three changes of 1.5 L of 0.05 M sodium phosphate buffer, pH 8, until the product was free of low molecular weight material as determined by HPLC on Protein-Pak I-125. Dialysis was then continued against 2 × 1.5 L of distilled water until the dialysate was free of phosphate ion (*17*).

Concentration dialysis was carried out in 8-mL collodion concentration bags (retention cutoff 25 000 Da, Schleicher & Scheull, Keene, NH), and was monitored by HPLC in a similar way.

Electrophoresis. $(SucSMX)_n$–HSA conjugates were electrophoresed on Sepraphore III cellulose acetate strips (Gilman Instrument Co., Ann Arbor, MI) in 0.06 M sodium acetate buffer, pH 5.6, at 27 V/cm for 20 min at room temperature. Paper electrophoresis was carried out on Whatman #1 strips in 2% sodium carbonate solution, pH 8.9, or pyridine–AcOH–H_2O (4.9:1.2:94), pH 5.6, at 13 V/cm for 1.5 h at room temperature.

Amino acid analysis of **9a** and **9b** for glycine was carried out semiquantitatively by hydrolysis in 6 N HCl at 110 °C for 18 h followed by paper electrophoresis and detection with 0.2% ninhydrin in acetone. Sulfamethoxazole–polylysine conjugates were hydrolyzed in 6 N HCl–2% phenol for 1 h at 150 °C and analyzed quantitatively on a Beckman 7300 amino acid analyzer.

Analysis of Conjugates for Covalently Bound Sulfonamide. Before hydrolysis, final conjugate products were established to be free of low molecular weight derivatives of SMX/sulfanilic acid by HPLC on Protein-Pak I-125. Typical elution volumes (in mL) were as follows: protein conjugate, 6.2; HSA, 6.4; **6**, 9.7; SA, 11. With $(sucSMX)_n$–HSA conjugates, the absence of HSA was confirmed by electrophoresis on cellulose acetate. Typical mobilities were as follows: HSA, 10 mm; $(sucSMX)_6$–HSA, 26 mm (Figure 1).

(a) Hydrolysis of Conjugates of Sulfamethoxazole and HSA (9f, 11b, c), TR (9g), and Polylysines (9d,e). The conjugate (1.3 mg) in 0.5 mL of N NaOH in a closed 5-mL borosilicate test tube was heated in a bath held at 65–70 °C for 16–18 h. The solution was cooled and adjusted to pH 7 with 1 N HCl and analyzed for SMX by absorbance at 254 nm on HPLC on the C_{18} column in system A in which SMX elutes at 6 mL. Treated under these conditions SMX and **6** yielded SMX with a recovery of 100 ± 7%.

(b) Hydrolysis of Sulfanilyl–HSA (2). Conjugate **2** (1.2 mg) in 1 mL of 6 N HCl was heated in a bath at 120 °C for 18 h. The solution was then taken to dryness, taken up in water, and analyzed for **3** by HPLC on the C_{18} column. The major peak, detected at 254 nm, eluted in the same position as a reference sample of SA-Lys·2HCl, and it gave a positive Bratton–Marshall reaction. On paper electrophoresis the hydrolysate showed ninhydrin- and Bratton–Marshall-positive material with the same mobility as authentic **3** at pH 9 and 5.6. When treated with acid under similar conditions, **3** was recovered as 80% **3** and 20% SA.

(c) Calculation of Degree of Substitution. For conjugates containing protein and SMX or SA, n was calculated from the HPLC analysis for SMX or **3** + SA, respectively, in a hydrolysate of the conjugate as follows:

$$n = M/[(1/A) - R]$$

where n = moles of substituent per mole of conjugate; **A** = micromoles of SMX or **3** + SA per milligram of conjugate as determined experimentally; $M = 10^{-3}$ MW of the unsubstituted protein, e.g., 69 for HSA; $R = 10^{-3} \times$ MW of the substituent, e.g., 0.335 for sucSMX. Such values of n are uncorrected for moisture in the conjugate and may be minimal.

For the conjugates of PL and SMX (**9d**), the fraction, f, of lysine amino groups substituted was given by the ratio SMX:Lys, the former determined by HPLC of a basic hydrolysate, the latter by AAA of an acid hydrolysate:

$$n = f(m + 1)$$

where m is the number of residues of Lys in PL.

Chemical Syntheses. *N*-ε-Sulfanilyl-L-lysine Dihydrochloride (3). To a solution of **4** (367 mg, 1.5 mmol) in 1.2 mL of water was added 0.4 mL of 30% NaOH (3 mmol) and 1 mL of acetone. Compound **5** (353 mg, 1.5 mmol) was added in portions with magnetic stirring over 2 h. Stirring was continued for an additional 2 h. The mixture was clarified by centrifugation, and acetone was evaporated. The mixture was then acidified with 2 N HCl. The sticky gum was extracted with several portions of EtOAc. The extract was washed with H_2O and taken to dryness. To the residue was added 3 mL of 6 N HCl, and the mixture was heated in a bath at 120 °C for 1 h. The hydrolysate was then taken to dryness over P_2O_5 and KOH: 248 mg (49%); mp 210–215 °C dec. HPLC analysis of the hydrolysate on the C_{18} column showed a single peak [elution volume 6.7 mL (solvent system B)]. Paper electrophoresis at pH 5.6 for 1.5 h at 13 V/cm showed a single spot (ninhydrin positive, Bratton–Marshall positive) located 1 cm toward the cathode and well-separated from reference sulfanilic acid and lysine. For analysis, the product was dissolved in a minimal volume of MeOH. The solution was diluted with an equal volume of *i*-PrOH and was allowed to evaporate in an open beaker to half its volume: 190 mg; mp 210–215 °C dec. Recrystallization furnished 111 mg of product of unchanged melting point [lit. mp 205 °C (*6*)]. Anal. Calcd for $C_{12}H_{19}N_3O_4S \cdot 2HCl$: C, 40.6; H, 5.82; S, 9.10; N, 14.1. Found: C, 40.5; H, 5.83; S, 9.10; N, 14.1.

***N*-ε-(Sulfanilyl)$_{12}$–HSA (2).** A solution of HSA (102 mg, 1.5 μmol) in 2 mL of H_2O in a two-necked conical 30-mL flask was adjusted to pH 9 with 50 μL of 1 N NaOH. To this a solution of **1** (91 mg, 0.52 mmol) in 1 mL of Et_2O was added with magnetic stirring over a period of 10 min. The mixture was maintained in a bath at 35 °C for 4 h

during which pH 9 was maintained by addition of 460 μL of NaOH in portions. The gelatinous mixture was transferred to a test tube and extracted three times with Et_2O during which the aqueous mixture gradually clarified. Residual ether in the aqueous solution was evaporated off. The solution was subjected to concentration dialysis, analyzed on the Protein-Pak I-125 column, and lyophilized (72 mg).

N^4-(3-Carboxypropanoyl)sulfamethoxazole (6). A solution of **12** (10.1 g, 40 mmol) in 140 mL of AcOH was prepared by heating to 60 °C with mechanical stirring. To it was added succinic anhydride (4.4 g, 44 mmol). The clear reaction mixture was stirred and maintained at 55–60 °C. The product separated out after 14 min. The thick mixture was then diluted with 30 mL of AcOH. After a total period of 40 min, the reaction mixture was cooled to room temperature, and the product was collected on a filter and washed with AcOH followed by warm water and then dried over KOH and P_2O_5: 13.1 g (92.8%); mp 211–215 °C dec; HPLC, elution volume 8.8 mL (solvent system A). A second peak indicated 2% starting SMX that was further confirmed by a quantitative Bratton–Marshall reaction. The product was considered suitable for further work. For analysis a sample was recrystallized from MeOH: mp 214–218 °C; TLC, R_f 0.93 (solvent system A); HPLC, elution volume 11.8 mL (solvent system C); ^1H NMR (NaOD) δ (ppm) 2.18 (s, 3, CH_3), 2.62 (m, 4, CH_2), 4.8 (HOD), 5.92 (s, 1, vinyl), 7.94 (m, 4, aromatic). Anal. Calcd for $C_{14}H_{15}N_3O_6S$: C, 47.6; H, 4.28; N, 11.9. Found: C, 47.5; H, 4.33; N, 11.8.

N^4-[3-[(Succinimidooxy)carbonyl]propanoyl]sulfamethoxazole (7). A mixture of **6** (354 mg, 1 mmol) and *N*-hydroxysuccinimide (117 mg, 1 mmol) in 7 mL of dry, peroxide-free THF was warmed slightly to effect solution. To the solution at room temperature was added DCC (209 mg, 1 mmol) with magnetic stirring. Stirring was continued for 3 h. The precipitate was filtered off and washed with 6 mL of THF. Combined filtrate and washings were evaporated to a glassy solid that was slurried with 10 mL of EtOAc and then collected by filtration: 436 mg (96%); mp 173–174 °C. Crystallization from THF–*i*-PrOH gave a white solid (mp 183–186 °C) that traveled as a single spot on TLC [R_f 0.5 (solvent system B)] and HPLC [12.7 mL (solvent system A)]; ^1H NMR (DMSO-d_6) δ 2.4 (s, 3, CH_3), 2.95 (m, 8, CH_2), 6.3 (s, 1, vinyl), 8.0 (s, 4, aromatic). Anal. Calcd for $C_{18}H_{18}N_4O_8S$: C, 48.0; H, 4.03; S, 7.12. Found: C, 48.2; H, 4.21; S, 7.18.

3-(4-Succinimidobenzenesulfonamido)-5-methylisoxazole (8). To a solution of **6** (353 mg, 1 mmol) in 1 mL of DMF was added with magnetic stirring DCC (103 mg, 0.5 mmol). Stirring was continued for 1 h. The precipitate was then filtered off and washed twice with 0.5 mL of DMF. The combined filtrate and washings were diluted with 5 mL of dry Et_2O and the mixture was allowed to stand in the cold overnight. The white solid was collected on a filter, washed well with Et_2O, and dried: 113 mg (66%); mp 238–242 °C dec. A run with 2 mmol of **6** and 2 mmol of DCC in 2.5 mL of DMF furnished **8** in 44% yield. The product was crystallized from CH_3CN–Et_2O: mp 240–242 °C; it was homogeneous on TLC [R_f 0.74 (solvent system C)] and HPLC [elution volume 7.0 mL (solvent system A)]; ^1H NMR (DMSO-d_6) δ 2.45 (s, 3, CH_3), 2.95 (s, 4, CH_2), 6.51 (s, H, vinyl), 8.17 (s, 4, aromatic). Anal. Calcd for $C_{14}H_{13}N_3O_5S$: C, 50.1; H, 3.91; S, 9.56. Found: C, 50.3; H, 3.98; S, 9.74.

N^4-[3-[(Methyl glycinate-*N*-yl)carbonyl]propanoyl]sulfamethoxazole (9a). (*a*) *Carbodiimide Procedure.* To a solution of methyl glycinate hydrochloride (723 mg, 5.8 mmol), NEt_3 (583 mg, 5.8 mmol), and **6** (1.77 g, 5 mmol) in 4 mL of DMF at 10 °C was added, with magnetic stirring, DCC (1.19 g, 5.8 mmol) in portions over 10 min. The mixture was allowed to warm to room temperature and maintained for 3 h. After addition of 0.4 mL of AcOH the insoluble byproduct was filtered off and washed with 1 mL of DMF. Dilution of the filtrates with an equal volume of water led to precipitation of the product. This was collected by filtration, washed successively with dilute HCl, water, sodium bicarbonate solution, and water, and dried: 1.78 g (84%); mp 200–202 °C dec. On HPLC the product eluted as a single substance [elution volume 10.6 mL (solvent system A)]. The product was recrystallized from CH_3CN: mp 206–208 °C dec; TLC, R_f 0.2 (solvent system E); ^1H NMR (DMSO-d_6) δ 2.41 (s, 3, CH_3), 2.68 (m, 4, CH_2), 3.78 (s, 3, OCH_3), 4.03 (t, 2, glycyl CH_2), 6.42 (s, 1, vinyl), 8.17 (4, aromatic), 8.77 (m, 1, glycyl amide), 10.89 (m, 1, amide), 11.88 (m, 1, amide). Anal. Calcd for $C_{17}H_{20}N_4O_7S$: C, 48.1; H, 4.76; N, 13.2. Found: C, 48.1; H, 4.76; N, 13.2.

(*b*) *Active Ester Procedure.* To a solution of methyl glycinate hydrochloride (76 mg, 0.6 mmol) and $NaHCO_3$ (51.8 mg, 0.6 mmol) in 0.4 mL of water was added, in portions, with magnetic stirring a solution of **7** (180.3 mg, 0.4 mmol) in 2 mL of DMF. The almost clear reaction mixture remained at pH 6.8–7. Additional $NaHCO_3$ (33.7 mg) was added, and stirring was continued for 3 h. TLC revealed no starting or cyclized **7**. The mixture was clarified by centrifugation, cooled, acidified with 5 N HCl to pH 1.5, and diluted (1.5×) with water. The solid that separated on cooling was collected by filtration, washed with 1 N HCl, then with water until neutral, and dried: 116 mg (68%); mp 200–202 °C dec. Recrystallization raised the melting point to 208 °C. On HPLC, the product had the same retention volume as that prepared under procedure a.

N^4-[3-(Glycinocarbonyl)propanoyl]sulfamethoxazole (9b). To a solution of glycine (43 mg, 0.58 mmol) and $NaHCO_3$ (82 mg, 0.98 mmol) in 0.5 mL of water at room temperature was added a solution of **7** (201 mg, 0.45 mmol) in 0.6 mL of DMF with magnetic stirring over 10 min. Stirring was continued for 3 h, after which the clear reaction mixture was diluted with an equal volume of water, cooled, and adjusted with 5 N HCl to pH 3. The solid product that gradually separated was collected on a filter, washed with dilute HCl, then with water until chloride-free, and then dried over P_2O_5 and KOH: 151 mg (82%); mp 223–225 °C dec. TLC showed along with the major component two minor components corresponding to **7** and **8**. Results of paper electrophoresis at pH 8.9 were in agreement. Hydrolysis followed by electrophoresis at pH 8.9 confirmed the presence of glycine (ninhydrin positive) and sulfanilic acid (Bratton–Marshall positive), when mobilities were compared with those of authentic samples. For analysis a solution of the product in boiling MeOH (16 mg/mL) was reduced in volume and cooled to room temperature. The colorless needles (mp 223–225 °C dec) were homogeneous on TLC [R_f 0.71 (solvent system A)] and HPLC [elution volume 9.6 mL (solvent system C)]. Anal. Calcd for $C_{16}H_{18}N_4O_7S$: C, 46.8; H, 4.42; S, 7.81. Found: C, 46.8; H, 4.35; S, 7.95.

N^4-[3-[(Succinimido glycinate-*N*-yl)carbonyl]propanoyl]sulfamethoxazole (10b). The reaction of **9b** (152 mg, 0.37 mmol) with HONSu (44 mg, 0.38 mmol) and DCC (80.6 mg, 0.39 mmol) was carried out as described for **7**, except that the solvent was 1.3 mL of DMF. The precipitate was washed twice with 0.3 mL of DMF, the combined filtrate and washings were diluted with 25 mL

Table II. Synthesis of Conjugates of Sulfamethoxazole and HSA, Transferrin, and Polylysines Linked via a Succinyl, Succinylglycyl, or Succinyl-ε-aminohexanoyl Spacer, and Conjugates of Sulfanilic Acid Linked Directly to HSA or Lysine[a]

						conjugate		
conjugate	nucleophile (N)	mg	reagent (R)	mg	R/N NH_2 molar ratio	purifcn method[b]	mg	% NH_2 of N substituted by R[c]
3	α-Boc-L-Lys	367	**5**	353	1	A	248	
2	HSA	102	**1**	91	6	B	72	20
9f n = 2–21[d]	HSA	50–100	**7**	–[d]	2–13	–[d]	–[d]	3–35
11b	HSA	49	**10b**	178	8.2	C	65	88
11c	HSA	50	**10c**	199	8.1	C	74	86
9g n = 27 ± 3	TR	50	**7**	139	8.4	C	47	46
n = 17 ± 1	TR	100	**7**	278	8.2	C	102	29
9d	Lys_{16}	50	**7**	119	1	D, E	51	65[e]
9e	Lys_{430}	47	**7**	109	1.1	D, E	56	17

[a] Reactions with activated esters were at pH 6.8 except where specified for **9f** in Table I. Reaction with **1** was at pH 9. [b] A, recrystallization; B, concentration dialysis; C, dialysis; D, insoluble product centrifuged off and washed; E, succinylation followed by dialysis and lyophilization. [c] Value uncorrected for moisture in the protein conjugate. [d] Data of Table I. [e] Determined by the ratio SMX:Lys in hydrolysates; in protein conjugates determined by SMX or **3** + SA in hydrolysates.

of dry Et_2O, and the mixture was kept at −20 °C overnight under anhydrous conditions. The oily material was separated by decantation, washed well with Et_2O, and then was crystallized from THF-Et_2O: 138 mg (74%); mp 179–181 °C dec. The product was recrystallized from THF–*i*-PrOH without change in melting point. It showed a single spot on TLC [R_f 0.14 (solvent system B)] and HPLC [elution volume 9.6 mL (solvent system A)]; ^1H NMR (DMSO-d_6) δ 2.4 (s, 3, CH_3), 2.7 (s, br, 4, succinoyl CH_2), 2.95 (s, br, 4, NSu CH_2), 4.47 (d, 2H, glycyl CH_2), 6.4 (s, 1, vinyl), 8.1 (s, 4, aromatic). The spectrum was unchanged after 8 days at room temperature. Anal. Calcd for $C_{20}H_{21}N_5O_9S$: C, 47.3; H, 4.17; S, 6.32. Found: C, 47.5; H, 4.18; S, 6.43.

N^4-[3-[[(5-Carboxypentyl)amino]carbonyl]propanoyl]sulfamethoxazole (9c). A solution of ε-aminohexanoic acid (2.2 g, 16.8 mmol) and $NaHCO_3$ (2.35 g, 28 mmol) in 16 mL of water was treated with a solution of **7** (4.95 g, 11 mmol) in 13 mL of DMF as described for the preparation of **9b**: 3.65 g (70%); mp 190 °C dec. It was 87% homogeneous on HPLC [elution volume 17.1 mL (solvent system A)] and contained 12% of **8**. A second crop of 300 mg (mp 195–197 °C) was also obtained. Impurity **8** was still present after two recrystallizations from 30–40 parts of MeOH. The recrystallized material was used for conversion to ester **10c**. For analysis a solution of 146 mg of the product in 1 mL of DMF was applied to a small column prepared from 4 g of silica (Fisher, grade 12, 28–200 mesh). Elution was performed with EtOAc in 5-mL fractions. The product was located by TLC: 40 mg; mp 193–197 °C. It was recrystallized from DMF–Et_2O without change in melting point and was homogeneous on HPLC and TLC [R_f 0.09 (solvent system D)]. Anal. Calcd for $C_{20}H_{26}N_4O_7S$: C, 51.5; H, 5.62; S, 6.87. Found: C, 51.3; H, 5.73; S, 6.76.

N^4-[3-[[[5-[(Succinimidooxy)carbonyl]pentyl]amino]carbonyl]propanoyl]sulfamethoxazole (10c). The reaction of **9c** (508 mg, 1.1 mmol) with HONSu (127 mg, 1.1 mmol) and DCC (232 mg, 1.1 mmol) in 3 mL of DMF was carried out as described for the preparation of **10b**. The precipitate was washed twice with 0.5 mL of DMF, then twice with 10 mL of Et_2O. An oil that settled after being washed four times with 5 mL of Et_2O furnished 170 mg (28%) of a solid, mp 155–210 °C. The product [TLC, R_f 0.24 (solvent system D)] was contaminated with **8** and was not improved by recrystallization from THF–*i*-PrOH. A second crop obtained from the filtrate and washings [341 mg (55%), mp 155–160 °C] on recrystallization furnished 283 mg, mp 173–178 °C. HPLC showed **10c** [elution volume, 26.9 mL (solvent system A)], **9c**, and **8** in the ratio 81:9:10. Anal. Calcd for $C_{24}H_{29}N_5O_9S$: C, 51.2; H, 5.19; S, 5.69. Found: C, 50.7; H, 5.05; S, 6.60.

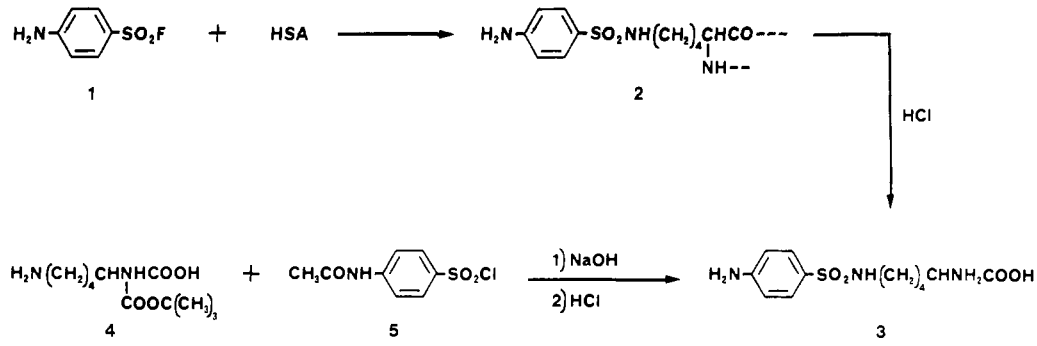
Conjugates of Sulfamethoxazole and Human Serum Albumin, Transferrin, and Polylysines. *N-ε-[N^4-(3-Carbonylpropanoyl)sulfamethoxazole]$_n$–HSA* (**9f**). To a solution of HSA (100 mg) and $NaHCO_3$ (23 mg) in 1 mL of water was added with magnetic stirring over 10 min a solution of **7** (77 mg) in 0.45 mL of DMF (Table I, expt 1). The somewhat turbid solution was stirred for 4 h and remained near pH 7. Highly substituted or other material that had precipitated out of the reaction mixture (Table I, expts 5 and 6) dissolved upon addition of 0.2 M sodium phosphate buffer, pH 8. Low molecular weight reagents and byproducts were removed by dialysis, concentration dialysis, or gel filtration as specified in Table I in the manner described under "General Chemical Procedures". The product was obtained on lyophilization.

N-ε-[N^4-[3-[[(Carbonylmethyl)amino]carbonyl]propanoyl]sulfamethoxazole]$_{53}$–HSA (11b) and N-ε-[N^4-[3-[[(5-Carbonylpentyl)amino]carbonyl]propanoyl]sulfamethoxazole]$_{51}$–HSA (11c). A solution of 50 mg of HSA and 38 mg of $NaHCO_3$ in 0.5 mL of water was treated with **10b** or **10c** in 0.55 mL of DMF essentially as described for **9f**. Within 30 min the reaction mixture became very thick. After 3 h the suspension was solubilized by addition of 0.2 M sodium phosphate buffer, pH 8, and clarified by centrifugation. It was then dialyzed and lyophilized (Table II).

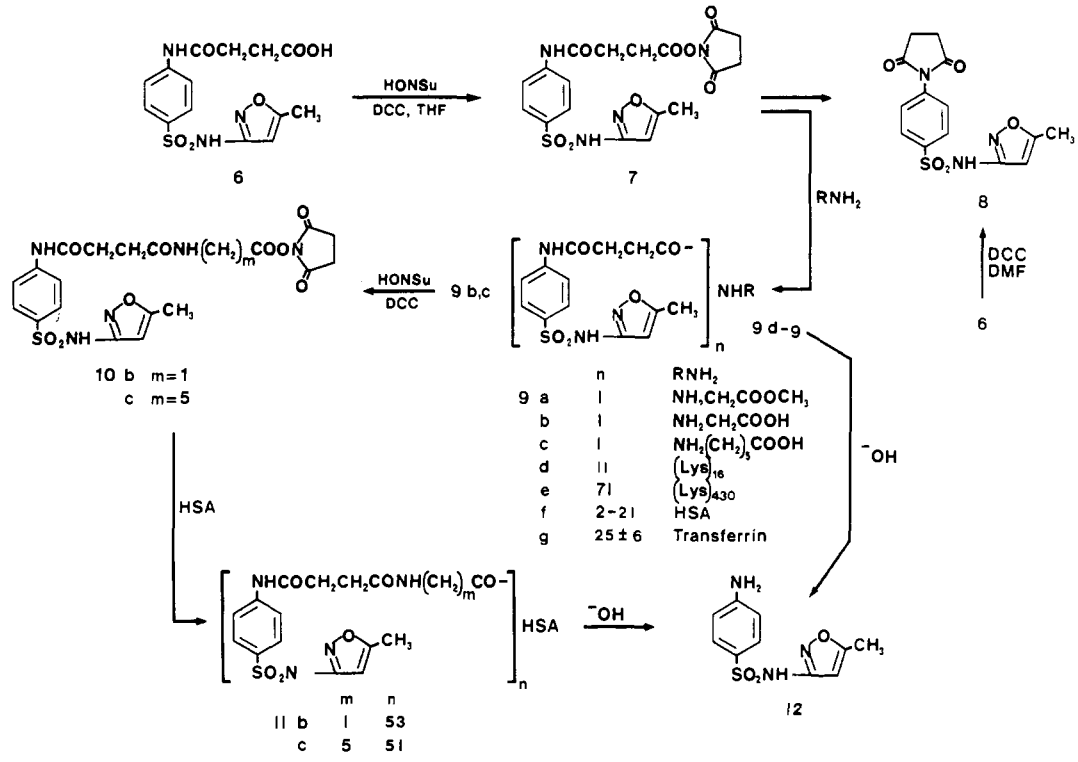
N-ε-[N^4-(3-Carbonylpropanoyl)sulfamethoxazole]$_n$–polylysines (9e and 9d). A solution of PL·HBr (n = 430, MW 90 000, 46.8 mg, 0.22 mmol of NH_2) in 0.6 mL of water was adjusted to pH 8 with 10 μL of 1 N NaOH. Sodium bicarbonate (24.5 mg, 0.29 mmol) was then added with magnetic stirring, followed by a solution of **7** (109 mg, 0.24 mmol) in 0.5 mL of DMF over 15 min. A few minutes later a white solid precipitated out. After a total period of 1.5 h, the solid was collected by centrifugation, washed successively (3×) with 2 mL of 0.1 N $NaHCO_3$, water, MeOH, 2 × 2 mL of DMF, and MeOH, and then was dried. The solid was suspended in 1.5 mL of water, and succinic anhydride (56.2 mg, 0.56 mmol) was added in 3 portions with stirring along with 1 N NaOH to maintain pH 8–8.5. The solid dissolved as the reaction progressed. Low molecular weight reagents and byproducts were removed from the clarified reaction mixture by dialysis, and product **9e** was obtained on lyophilization.

Essentially the same procedure was used to obtain **9d** from PL·HBr (n = 16, MW 3300, 49.5 mg, 0.26 mmol of NH_2). The insoluble product was collected and washed with sodium bicarbonate solution and water and dried,

Scheme I



Scheme II



then with DMF and MeOH and dried, then succinylated, dialyzed, and lyophilized (Table II).

RESULTS AND DISCUSSION

In the present study the use of sulfanilyl fluoride (**1**) as reagent in place of N^4-acetylsulfanilyl chloride (**5**) allowed sulfanilyl groups to be introduced directly into HSA, making subsequent deprotection of the conjugate unnecessary. The degree of substitution in the sulfanilyl–HSA conjugate **2** was determined by hydrolysis in acid followed by analysis by reverse-phase HPLC for N-ε-sulfanilyllysine (**3**) and sulfanilic acid. Quantitation of **3** was based upon comparison with an authentic sample of its crystalline dihydrochloride prepared by acylation of α-BOC-L-lysine (**4**) with N^4-acetylsulfanilyl chloride (**5**), followed by deprotection in acid. N-ε-Sulfanilyl-L- and DL-lysines had been prepared before through a less convenient acylation of the copper chelate of lysine reported without detail (*6*, *18*). The routes to compounds **2** and **3** are given in Scheme I.

Preliminary work showed that the introduction of a sulfonamide drug into HSA was not a routine procedure. Attempts to couple SMX and HSA with the carbodiimide DCC or EDC were unpromising, as was the use of disuccinimidyl suberate. The low reactivity was probably due to the weak basicity of the *p*-amino group of SMX: pK_a's of the protonated amine of sulfonamide drugs are near 2–2.5 (*19*). For construction of protein conjugates of sulfamethoxazole, a hemisuccinate route (*20*) was chosen, shown as Scheme II, in which the key intermediate was N^4-succinylsulfamethoxazole (**6**). This route served to convert the poorly reactive aromatic *p*-amino group of sulfamethoxazole to a fully reactive aliphatic carboxyl group in **6** that when activated by a conventional route proved to be capable of acylating protein nucleophiles effectively. Compound **6** was prepared in 92% yield by treatment of SMX with succinic anhydride in the manner used for succinylsulfathiazole (*21*). To react **6** with protein nucleophiles the active ester approach was considered more promising than carbodiimide with its risk of protein cross-linking side reactions. Compound **6** was converted to its succinimido ester (**7**) by a carbodiimide-catalyzed coupling with HONSu in THF. When the reaction of HONSu and **6** was attempted in DMF, in place of **7** its cyclized derivative, 3-(4-succinimidobenzenesulfonamido)-5-methylisoxazole (**8**), was isolated in 70% yield.

Active ester **7** was reasonably stable in the cold in the solid state. In solution in DMF, DMSO, or THF under anhydrous conditions, however, it tended to undergo ring closure with the elimination of HONSu to give **8**. Almost

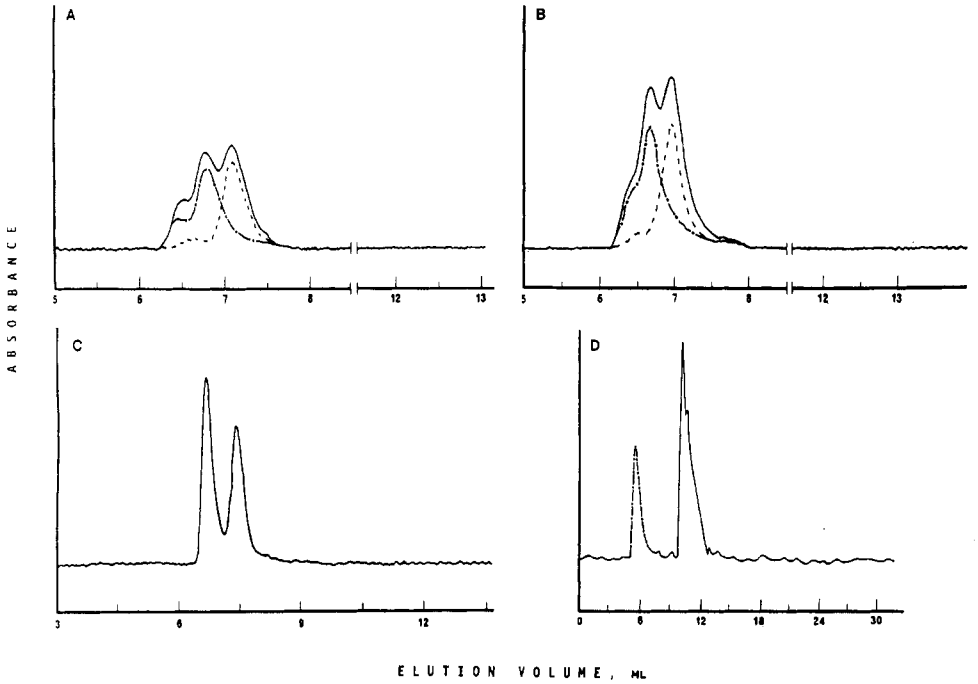


Figure 2. Characterization by HPLC of various dialyzed conjugates of HSA containing sulfamethoxazole or sulfanilyl groups, distinguishing them from HSA and confirming the absence of low molecular weight sulfonamides. Materials were filtered over a column of Protein-Pak I-125 in 0.05 M potassium phosphate buffer, pH 6.8, at a flow rate of 0.2 or 0.3 mL/min. Absorbance was determined at 254 nm. (A) HPLC of $(sulfanilyl)_{12}$–HSA: —·—, 0.5 μg of $(sulfanilyl)_{12}$–HSA; – –, 5 μg of HSA; —, mixture of 0.5 μg of $(sulfanilyl)_{12}$–HSA and 5 μg of HSA. (B) HPLC of $(sucSMX)_{13}$–HSA: —·—, 3 μg of $(sucSMX)_{13}$–HSA; – –, 10 μg of HSA; —, mixture of 3 μg of $(sucSMX)_{13}$–HSA and 10 of μg of HSA. SucSMX elutes at 9.7 mL. (C) HPLC of a mixture of 0.8 μg of $(sucSMX\text{-}NH_2\text{-}hex)_{51}$–HSA and 19.2 μg of HSA, respectively. (D) Composite chromatogram from HPLC of polylysine and a conjugate of it containing sulfamethoxazole groups, each chromatographed separately at a flow rate of 1.5 mL/min: —·—, 1.7 μg of succinylated $(sucSMX)_{71}$–Lys_{430} with absorbance determined at 254 nm; —, 5 μg of $(Lys\cdot HBr)_{430}$ with absorbance determined at 210 nm.

complete conversion of compound **7** to **8** was observed in a solution of **7** in DMSO-d_6 prepared for determination of ^1H NMR and reexamined after 8 days. In the coupling reactions between active ester **7** and proteins and polylysines in aqueous DMF the tendency of ester **7** to cyclize and to hydrolyze to acid **6**, also observed as a side reaction, were compensated by the use of an excess of the active ester.

As a model reaction to introduce SMX groups covalently into HSA, ester **7** was allowed to react with methyl glycinate in aqueous DMF at pH 6.8–7. The expected product sucSMX-glycine methyl ester (**9a**), obtained in satisfactory yield, agreed in melting point and chromatographic behavior with the product derived from a carbodiimide coupling of acid **6** and methyl glycinate. Treatment of methyl glycinate with **8** in aqueous DMF failed to furnish **9a** as indicated by TLC of the isolated product, making it unlikely that **8** was an intermediate in the reaction of **7** and methyl glycinate.

HSA was then treated with **7** under a variety of conditions of pH, temperature, time, and modes of addition and molar ratios of reactants. Reaction mixtures were subjected to gel filtration, concentration dialysis, or dialysis. The final conjugates were examined by gel-filtration HPLC. An increase above 0.88 in the 254:280 nm absorbancy ratio of the protein peak suggested successful conjugation. Low-voltage electrophoresis on cellulose acetate strips provided another rapid way to assess conjugation. As shown in Figure 1, $(sucSMX)_n$–HSA conjugates (n = 2, 3, 6, 9) were readily distinguishable from HSA, even when only a few residues of SMX, increasing the molecular weight by only 1%, had been incorporated. The products then were isolated by lyophilization.

For quantitative analysis of covalently bound SMX, conjugates were subjected to a novel mild alkaline hydrolysis. This cleaved the succinanilic linkage in the protein and polylysine conjugates smoothly to release SMX that was then readily determined by reverse-phase HPLC. The alkaline hydrolysis procedure applied to SMX and **6** afforded a quantitative recovery of SMX. It was more satisfactory than the usual acid hydrolysis that led to sulfanilic acid which was not as accurately determined, because of its highly polar nature, by reverse-phase HPLC under our conditions.

The degrees of substitution of HSA by **6** under the various coupling conditions are given in Table I. A reaction pH of 6.8 seemed superior to pH 9.5 (expts 1 and 2). Drug substitution into HSA increased as the mole ratio of active ester **7**:HSA amino groups increased from two to eight (expts 1, 4, 5). Conjugates were obtained containing 2, 6, 9, 13, and 21 mol of SMX/mol of HSA. The maximal introduction of SMX into HSA observed represents acylation of 22–35% of the available amino groups. This was attained by reaction of HSA at pH 6.8 in aqueous DMF for 4 h at room temperature with an 8-fold molar excess of **7**. These conditions were adopted for the synthesis of analogues.

Treatment of transferrin with ester **7** in a similar way yielded the corresponding conjugates of transferrin $(succinylSMX)_n$–TR (**9g**), some of which were more highly substituted than those of HSA. Two runs on a 50-mg scale led to about 46% substitution; two on a 100-mg scale led to 29% substitution. Treatment of polylysine (n = 16 and 430) with ester **7** at a lower mole ratio yielded conjugates **9d** and **9e** of polylysine covalently bound to sucSMX with 65 and 17% substitution, respectively. Both polylysine conjugates had limited solubility and were solubilized by succinylation.

Conjugates $(sucSMX)_n$–HSA (**9f**) have spacer chains of four carbons between SMX and the protein lysine ε-amino groups. Two additional activated esters, sucSMX-Gly-

NSu (**10b**) and sucSMX-NH_2Hex-NSu (**10c**), synthesized and allowed to react with HSA, furnished conjugates (sucSMX-Gly)$_{53}$–HSA (**11b**) and (sucSMX-NH_2Hex)$_{51}$–HSA (**11c**) with spacer chains of 7 and 11 units, respectively.

The route to **10b** involved the condensation of **7** with free glycine in aqueous DMF to give sucSMX-Gly (**9b**), followed by treatment of the latter with HONSu and DCC in the usual way. A similar route from **7** and ϵ-NH_2 hexanoic acid yielded sucSMX-NH_2Hex (**9c**) and from it, sucSMX-NH_2Hex-NSu (**10c**). In the synthesis of **9b** and **9c** from ester **7** the readily available glycine and ϵ-aminohexanoic acid were used in 30–50% excess.

All coupling and esterification reactions in the series leading to the activated ligands used for conjugation generally proceeded in good yield and afforded homogeneous compounds as judged by elemental analysis, TLC, and HPLC. The exceptions were in the ϵ-aminohexanoic acid series. Compound **9c** and **10c** prepared from it were both contaminated with about 10% of **8** that was not readily removed; **10c** also contained 9% **9c**. These products were used without further purification since the impurities were unreactive in the subsequent coupling with HSA and were readily removed during dialysis of the resulting conjugate.

Conjugates **11b** and **11c**, synthesized by treatment of HSA with **10b** and **10c** under conditions optimal for (sucSMX)$_{13}$–HSA, were ca. 87% substituted. Thus virtually all the amino groups of HSA are accessible to the mild active ester reagents. The higher acylation yields of **11b** and **11c**, as compared to the 22–35% in (sucSMX)$_n$–HSA, were probably determined by the greater stability of the active esters **10b** and **10c** as compared to **7** and the better solubility of their conjugation reaction mixtures. Table II summarizes the yields and degrees of substitution attained under various conditions in the synthesis of conjugates of sulfamethoxazole and HSA, transferrin, and two polylysines linked via a succinyl, succinylglycyl, or succinyl-ϵ-aminohexanoyl spacer and of conjugates of sulfanilic acid linked directly to HSA or lysine.

When the dialyzed conjugate (SA)$_{12}$–HSA was examined by HPLC gel filtration to confirm the absence of unbound ligand before estimating bound ligand, it became evident that the conjugate was distinguishable from HSA in the same system and that it was essentially free of unsubstituted HSA as well as of unbound ligand. The efficiency of an I-125 gel-filtration column is evaluated in practice partly by its ability to resolve a mixture of OVA and HSA that differ in molecular weight by 60%. In our hands these albumins separated partially with α = 1.67. It was therefore unexpected to find that HSA and its sulfanilyl conjugate **2**, differing in molecular weight by only 2.6%, could be distinguished chromatographically on this size-exclusion column. Figure 2A shows the elution patterns on a Protein Pak I-125 column of (SA)$_{12}$–HSA, HSA, and a synthetic mixture of the two substances. The conjugate eluted ca. 1 min earlier than HSA, and a synthetic 1:1 mixture clearly partially resolved, with α = 1.26. Chromatographic observations were similar with HSA and (sucSMX)$_{13}$–HSA (**9f**), differing in molecular weight by 6.5% (Figure 2B), and with HSA and (sucSMX-ϵ-NH_2Hex)$_{51}$–HSA (**11c**), which differ in molecular weight by 33% (Figure 2C). HSA and **9f** separated partially with α = 1.29, HSA and **11c** with α = 1.69. TR and (sucSMX)$_{25}$–TR likewise were distinguishable, with α = 2.0 (not shown). In the same gel-filtration system polylysine and its highly succinylated (sucSMX)$_{71}$–Lys$_{430}$ conjugate (**9e**) separated very effectively, with α = 46 (Figure 2D).

It is unlikely that such separations are based on size exclusion alone. Other factors that may have contributed to the observed separations include the anionic charges introduced by the SMX residues and in **9e** by the additional succinyl residues. Derivatization of PL, while increasing molecular weight by more than 2-fold, has converted the polyvalent cation into a polyvalent anion. Clear evidence for the anionic nature of the sulfonamide group is the electrophoretic migration at pH 5.6 of conjugates (sucSMX)$_n$–HSA (n = 2, 3, 6, 9) toward the anode with mobilities dependent on epitope density (Figure 1), behavior that corresponds to the relative charge density provided by the sulfonamide anion of the SMX residues whose pK_a is near 5.6 (*19*). Hydrophobicity of the sulfanilyl and spacer-linked SMX residues may also have contributed to the HPLC separations. Newer size-exclusion matrices designed to minimize ionic and hydrophobic interactions may lack the chromatographic advantage for examining protein– and polylysine–drug conjugates encountered with the SEC support used in this work.

ACKNOWLEDGMENT

This work was aided by the Burroughs Wellcome Co., the University of Connecticut Research Foundation (Grant 229), and the National Institutes of Health (Grant AI25341), for which we express thanks. Amino acid analysis was performed by Mr. George Korza of the Amino Acid Laboratory.

LITERATURE CITED

(1) Mandell, G. L., and Sande, M. A. (1990) Sulfonamides, Trimethoprim-Sulfamethoxazole, Quinolones, and Agents for Urinary Tract Infections. In *Goodman and Gilman's The Pharmacological Basis of Therapeutics* (A. G. Gilman, T. W. Rall, A. S. Nies, and P. Taylor, Eds.) Chapter 45, Pergamon Press, New York.

(2) Sogn, D. D. (1984) Penicillin Allergy. *J. Allergy Clin. Immunol. 74*, 589–593.

(3) Ressler, C., and Mendelson, L. M. (1987) Skin test for dignosis of penicillin allergy–current status. *Ann. Allergy 59*, 161–171.

(4) Wedum, A. G. (1942) Immunological Specificity of Sulfonamide Azoproteins. *J. Infect. Dis. 70*, 173–179.

(5) Tomarelli, R. M., Charney, J., and Harding, M. L. (1949) The Use of Azoalbumin as a Substrate in the Colorimetric Determination of Peptic and Tryptic Activity. *J. Lab. Clin. Med. 34*, 428–433.

(6) Drewes, S. E., von Klemperer, M., and Sutton, D. A. (1971) Separation of isomeric lysine derivatives by ion-exchange chromatography. *J. Chromatogr. 56*, 171–175.

(7) Berlinguet, L., and Gautier, J. (1969) *Can. J. Chem. 47*, 3641–3646.

(8) Fasman, G. D. (1976) Proteins. In *Handbook of Biochemistry and Molecular Biology*, 3rd ed., Vol. 3, p 498, CRC Press, Cleveland, OH.

(9) MacGillivray, R. T. A., Mendez, E., Sinha, S. K., Sutton, M. R., Lineback-Zins, J., and Brew, K. (1982) The complete amino acid sequence of human transferrin. *Proc. Natl. Acad. Sci. U.S.A. 79*, 2504–2508.

(10) Voller, A., and Bidwell, D. (1986) Enzyme-Linked Immunosorbent Assay. In *Manual of Clinical Laboratory Immunology*, 3rd ed. (N. R. Rose, H. Friedman, and J. L. Fahey, Eds.) American Society of Microbiology, Washington, DC.

(11) Ressler, C., Knapp, M. M., Tatake, J. G., Ballow, M., and Rapacz, P. (1987) Human IgM antibody to sulfamethoxazole in an adverse reaction to trimethoprim-sulfamethoxazole. *J. Allergy Clin. Immunol. 79*, 198.

(12) Ressler, C., Greaney, M. D., Tatake, J. G., Brettman, L. R., and Ballow, M. (1990) Immunological Cross-Reactivity in Vitro Between Sulfamethoxazole and Various Other Sulfur and Related Drugs. *J. Allergy Clin. Immunol. 85*, 156.

(13) Stewart, J. M., and Young, J. D., Eds. (1984) *Solid Phase Peptide Synthesis*, Pierce Chemical Co, Rockford, IL, pp 69–70.
(14) Ressler, C., and Knapp, M. M. (1985) Liquid Chromatography of Oxidized Sulfanilamide Derivatives. *J. Liq. Chromatogr. 8*, 1445–1453.
(15) Bratton, A. C., Marshall, E. K., Jr., Babbitt, D., and Hendrickson, A. R. (1939) A New Coupling Component for Sulfanilamide Determination. *J. Biol. Chem.* 537–550.
(16) Morris, G. J. O. R., and Morris P. (1976) Membrane separation methods. In *Separation Methods in Biochemistry*, 2nd ed., John Wiley, New York, p 950.
(17) Taussky, H. H., and Shorr, E. (1953) A Microcolorimetric Method for the Determination of Inorganic Phosphorus. *J. Biol. Chem. 202*, 675–685.
(18) Shchukina, M. N., and Yuan-Chen-e (1955) Synthesis of sulfanilamide derivatives in the lysine series. *Chem. Abstr. 49*, 6163e.
(19) Newton, D. W., and Kluza, R. B. (1989) pK_a Values of Drug Substances and pH Values of Tissue Fluids. In *Principles of Medicinal Chemistry* (W. A. Foye, Ed.) Appendix, Lea and Febiger, Philadelphia, PA.
(20) Erlanger, B. F. (1980) The Preparation of Antigenic and Hapten-Carrier Conjugates: A Survey. *Methods Enzymol. 70*, 85–104.
(21) Moore, M. L., and Miller, C. S. (1942) Dicarboxylic Acid Derivatives of Sulfonamides. *J. Am. Chem. Soc. 64*, 1572–1576.

Registry No. **1**, 98-62-4; **3**, 133071-56-4; **4**, 13734-28-6; **5**, 121-60-8; **6**, 133071-57-5; **7**, 133071-58-6; **8**, 133071-59-7; **9a**, 133071-60-0; **10b**, 133071-61-1; **10c**, 133071-64-4; **12**, 723-46-6; HONSU, 6066-82-6; PL·HBr, 25988-63-0; PL·HBr(SRU), 26588-20-5; NH_2-Hex, 60-32-2; succinic anhydride, 108-30-5; methyl glycinate hydrochloride, 5680-79-5; glycine, 56-40-6.

Bioconjugate Chemistry

MAY/JUNE 1991
Volume 2, Number 3

© Copyright 1991 by the American Chemical Society

ARTICLES

New Hydrazone Derivatives of Adriamycin and Their Immunoconjugates—a Correlation between Acid Stability and Cytotoxicity[1]

Takushi Kaneko,† David Willner,* Ivo Monkovíc, Jay O. Knipe, Gary R. Braslawsky, Robert S. Greenfield, and Dolatrai M. Vyas

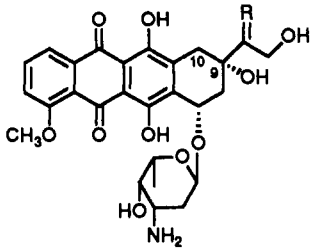
Bristol-Myers Squibb Company, 5 Research Parkway, P.O. Box 5100, Wallingford, Connecticut 06492-7660.
Received October 1, 1990

New N-substituted hydrazine linkers were synthesized and their hydrazone derivatives of adriamycin were prepared. These functionalized adriamycin derivatives were conjugated with a monoclonal antibody, 5E9. The release rate of adriamycin from the hydrazones and from some of the conjugates was studied, and their relationship to the IC_{50}'s of the conjugate against 5E9-positive Daudi cells was investigated.

Adriamycin (doxorubicin, 1; Chart I) is widely used as an antitumor agent in hematologic malignancies and solid tumors (*1–4*). Its use, however, is dose limited due to its cardiac toxicity and myelosuppression (*5*). In order to minimize this toxicity monoclonal antibody (mAb)[2] conjugates of adriamycin (and also other anthracyclines) have been prepared for selective delivery (*6*). Typically, adriamycin (or daunomycin) is modified at the C-3′ amino residue with a bifunctional linker in the form of an amide (*7*) or an aminoalkyl group (*8*). These linkers are not easily hydrolyzed and this may contribute to the generally reduced efficacy of these conjugates.

We reasoned that for a chemoimmunoconjugate to be effective it should have a conditional drug-release mechanism, i.e. the conjugate should be stable while being delivered and release drug selectively at the target site. Since it has been shown that an immunoconjugate is translocated to lysosomes (*9*), it appeared reasonable to take advantage of the lysosomal conditions in order to release

Chart I. Linkers and Their Adriamycin Derivatives



1: R = O

linkers (RH_2)	adriamycin derivatives
2: $NH_2NHCO(CH_2)_2SSPy$	2a
3: $NH_2NHCONH(CH_2)_2SSPy$	3a
4: $NH_2NHCONHNHCONH(CH_2)_2SSPY$	4a
5: $NH_2NHCSNHCH_2$(trans)$CH{=}CHCH_2SSPY$	5a
6: $NH_2NHCO_2(CH_2)_2SSPY$	6a
7: *p*-NH_2NH-Ar-$CONH(CH_2)_2SSPy$	7a,7b[a]
8: $NH_2NHCH_2CONH(CH_2)_2SSPY$	8b[a]

[a] 9,10-anhydro compounds, Py = 2-pyridinyl

† Present address: Pfizer Central Research, Groton, CT 06430.

[1] A brief abstract of this work was published in the Proceedings of the XIth International Symposium on Medicinal Chemistry, Jerusalem, Israel, September 1990.

[2] The abbreviations used are as follows: mAb, monoclonal antibody; HRMS, high-resolution mass spectra; PBS, phosphate-buffered saline; THF, tetrahydrofuran; TEA, triethylamine; TFA, trifluoroacetic acid; DMF, *N,N*-dimethylformamide; BOC, *tert*-butoxycarbonyl group; SPDP, *N*-succinimidyl 3-(2-pyridinyldithio)propionate; DTT, dithiothreitol; *i*-BuOCOCl, isobutyl chloroformate; CDI, carbonyldiimidazole; DCC, dicyclohexylcarbodiimide; NHS, *N*-hydroxysuccinimide; Su, succinimidyl; $(BOC)_2O$, di-*tert*-butyl dicarbonate.

1043-1802/91/2902-0133$02.50/0 © 1991 American Chemical Society

the conjugated drug. We were particularly interested in making use of the slightly acidic conditions (pH 5.0–5.5) existing in lysosomes (*10*) as our trigger mechanism. A similar rationale had been used for the development of the *cis*-aconityl linker to the C-3′ amino group of adriamycin (*11*) and acetal linkers to diphteria toxins (*12*). Imine derivatives of the C-13 carbonyl group of adriamycin—such as hydrazones and semicarbazones—appeared to be suitable compounds for release of drug in lysosome since the hydrolysis of these types of carbonyl derivatives were known to be acid catalyzed (*13*). Indeed, previous work from these laboratories (*14a–c*) has clearly shown that the C-13 hydrazone derivative of adriamycin, prepared from 3-(2-pyridinyldithio)propionohydrazide, released unmodified adriamycin under mild acidic conditions and it was further shown that the mAb conjugates derived from this hydrazone exhibited antigen-specific cytotoxicity both in vitro and in vivo. To explore further this approach we prepared several bifunctional linkers that can react with the C-13 carbonyl group of adriamycin and can be conjugated to mAb's. We chose to incorporate a nucleophilic amino group at one end of the linker and the pyridinyldithio group at the other. Attachment to the mAb was designed to be made through a disulfide bond as its formation via the pyridinyldithio group is one of the most facile reactions and can be effected under very mild conditions (*15*). Subsequent to our work acylhydrazide linkers appeared in the patent literature (*16*), and very recently similar derivatives of morpholinoadriamycin were reported (*17*).

In this paper we report synthesis of new linkers, adriamycin derivatives thereof, conjugation of these derivatives to mAb, and finally the relationship between their stability and cytotoxicity in vitro.

EXPERIMENTAL PROCEDURES

Melting points were determined on a Fisher-Johns melting point apparatus and are uncorrected. NMR spectra were obtained on a Bruker AM 300 instrument in various solvents (specified) and are reported as δ values downfield from tetramethylsilane. Multiplicities of resonances are described as broad (b), singlet (s), doublet (d), triplet (t), quartet (q), or multiplet (m). IR spectra were run as KBr pellets or $CHCl_3$ solutions on a Perkin-Elmer FTIR Model 1800 instrument. MS and HRMS were obtained with a Kratos MS25RFA and MS50TC instrument, respectively. Flash chromatography was performed with Woelm silica gel (silica 32-63). For reversed-phase flash chromatography Baker octadecyl (C_{18}) packing was used. TLC was carried out on Analtec silica gel GHLF plates or RPS-F reversed-phase plates, both 250 μm. For routine HPLC a Perkin-Elmer pump, series 4 LC, a Hewlett-Packard 1046A fluorescence detector, and a Phenomenex IB Sil-5C18 (150 × 4.6 mm) column were used. The mobile phase was a 70:30 methanol–phosphate buffer (50 mM ammonium phosphate, pH 4.4) at a flow rate of 1.5 mL/min. For release-rate measurements the HPLC system was comprised of two Waters pumps Model 510, an autosampler Model 712 and a gradient controller Model 680. Chromatography was performed on a Waters C_{18} column and the mobile phase was a 68:32 mixture of triethylammonium formate buffer solution (0.05 mM, pH 2.8) and acetonitrile, respectively. The fluorescence of the eluted adriamycin was detected by using an ABI fluorescence detector Model 980 (excitation, 254 nm; emission, 550 nm). Acetate buffer (50 mM) was used for pH 4.5 and 5.0; phosphate-buffered saline (PBS) was used for pH 7.4. Adriamycin hydrochloride was obtained from Sanraku Inc. (Japan). All other chemicals were obtained from commercial sources. Isolation of mAbs has been previously described (*14a*). Elemental analyses were performed in our analytical department and at Oneida Research Services.

3-(2-Pyridinyldithio)propanoic Acid Hydrazide (2). A solution of methoxycarbonylsulfenyl chloride (*18a*) (4.77 g, 38 mmol) in methylene chloride (100 mL) was treated with 3-mercaptopropionic acid (4.0 g, 38 mmol) in methylene chloride (50 mL). After stirring for 90 min the solvent was evaporated, the residue redissolved in methylene chloride (100 mL) and treated dropwise with a solution of 2-mercaptopyridine (4.19 g, 38 mmol) in the same solvent (50 mL). After stirring overnight, the solvent was evaporated to yield an oily residue the NMR of which was consistent with that of 3-(2-pyridinyldithio)propionic acid. The material was dissolved in anhydrous THF (100 mL), stirred and chilled in ice, and treated in succession with TEA (3.8 g, 38 mmol), isobutyl chloroformate (5.15 g, 38 mmol), and, 5 min later, *tert*-butyl carbazate (4.98 g, 38 mmol). The reaction was stirred at room temperature for 1 h and then partitioned between methylene chloride and water. The organic phase was washed and dried and the solvent evaporated. The residue was dissolved in ice-cold TFA (100 mL) and the solution stirred at 0 °C for 10 min and an additional 10 min at room temperature. Excess TFA was evaporated and the residue was chromatographed on silica gel using a methylene chloride–methanol–ammonium hydroxide (100:5:0.5) solvent system. The crystalline residue after evaporation of solvent (4.35 g, 50% overall yield) had mp 87–90 °C and was identical by TLC and NMR with the material reported previously (*14*).

Hydrazone Derivative of Adriamycin Hydrochloride and 3-(2-Pyridinyldithio)propanoic Acid Hydrazide (2a). Adriamycin hydrochloride (2.5 g, 4.3 mmol) was stirred in anhydrous methanol (375 mL) and treated with 3-(2-pyridinyldithio)propanoic acid hydrazide (1.34 g, 5.85 mmol) followed by 5 drops of TFA. After stirring overnight at room temperature a clear solution was obtained. The solvent was evaporated; the residue was redissolved in anhydrous methanol (50 mL). The methanolic solution was added dropwise to stirred acetonitrile (3 L) to precipitate the desired product. The solid obtained was collected by centrifugation and dried at high vacuum. The product (3.07 g, 90% yield) was identical (TLC, HPLC, NMR, MS, HRMS) with the one reported previously (*14*).

2-(2-Pyridinyldithio)ethanamine Hydrochloride (13). Although this compound was previously reported (*18b,c*) a new synthesis was developed. A solution of methoxycarbonylsulfenyl chloride (6.33 g, 50 mmol) in methanol (100 mL) was stirred under N_2 in an ice bath. To this a solution of 2-aminoethanethiol hydrochloride (5.7 g, 50 mmol) in methanol (50 mL) was added dropwise, and the solution was stirred at room temperature for 2 h. The solvent was then evaporated and the residual oil crystallized from acetone (100 mL) to yield a solid (6.9 g). This solid was dissolved in methanol (100 mL) and treated dropwise with a solution of 2-mercaptopyridine (3.82 g, 34 mmol) in methanol (50 mL) at 0 °C under N_2. The solution was stirred for 1 h at room temperature, concentrated to a small volume, and diluted slowly with acetone until crystallization occurred. The crystals were collected by filtration to yield the title compound: mp 123–5 °C (5.8 g, 52%); IR (KBr) 2952, 2913, 1610, 1575, 1559, 1451, 1115, 767 cm^{-1}; NMR (D_2O) δ 8.46, 7.83, 7.34 (d, m, m, 4 H) 3.37 (t, 2 H), 3.12 (t, 2 H); MS (*m/e*) 187 (corresponds to $[M + H]^+$) 170, 152, 142, 112, 104, 76. Anal. Calcd for C_7H_{11}-

$ClN_2S_2 \cdot {}^1/_4H_2O$: C, 37.00; H, 5.06; N, 12.33. Found: C, 36.82; H, 4.99; N, 12.37.

***N*-[2-(2-Pyridinyldithio)ethyl]-2-(*tert*-butoxycarbonyl)hydrazinecarboxamide (14).** 2-(2-Pyridinyldithio)ethanamine hydrochloride (2.22 g, 10 mmol) was suspended in dry methylene chloride (100 mL) and treated with TEA (5.8 mL). This solution was added dropwise to a solution of phosgene (10 mL of a 1.93 M toluene solution) in methylene chloride (200 mL) at 0 °C. After the reaction was over, nitrogen was passed through the mixture. *tert*-Butyl carbazate (1.32 g, 10 mmol) was then added and the mixture left to stir overnight. The solution was washed with water and the solvent evaporated. The residue was chromatographed over silica using a methylene chloride–methanol (100:2) solvent system. The appropriate fractions were combined to yield the title compound as a foam (1.74 g): IR (KBr) 3281, 2979, 2932, 1723, 1672, 1577, 1560, 1545, 1448, 1419, 1253, 1161, 762 cm^{-1}; NMR ($CDCl_3$) δ 8.50, 7.56, 7.51, 7.12 (d, m, m, m, 4 H), 3.51 (m, 2 H), 2.89 (t, 2 H), 6.84, 6.37, 6.17 (s, bs, 3 H), 1.44 (s, 9 H); MS (*m/e*) 345 (corresponds to $[M + H]^+$), 317, 289, 245, 213, 178, 134, 112.

***N*-[2-(2-Pyridinyldithio)ethyl]hydrazinecarboxamide (3).** *N*-[2-(2-Pyridinyldithio)ethyl]-2-(*tert*-butoxycarbonyl)hydrazinecarboxamide (0.57 g, 1.66 mmol) was dissolved in TFA (10 mL) at 0 °C. The solution was stirred at 0 °C for 10 min and an additional 10 min at room temperature. The excess of TFA was evaporated under reduced pressure and the residue chromatographed over silica using a methylene chloride–methanol–concentrated ammonium hydroxide (100:5:0.5) solvent system to give a crystalline residue (0.42 g, quantitative). An analytical sample was prepared by crystallizing from 2-propanol: mp 105–7 °C; IR (KBr) 3336, 3220, 3064, 2949, 2934, 1670, 1623, 1575, 1562, 1533, 1452, 1369, 1172, 1046, 770 cm^{-1}; NMR (CD_3OD) δ 8.41, 7.78, 7.21 (d, m, m, 4 H), 3.43 (m, 2 H), 2.91 (t, 2 H); MS (*m/e*) 245 (corresponds to $[M + H]^+$), 221, 213, 162, 134, 112. Anal. Calcd for $C_8H_{12}N_4OS_2$: C, 39.32; H, 4.95; N, 22.93; S, 26.24. Found: C, 39.19; H, 4.86; N, 22.48; S, 25.02.

Semicarbazone Derivative of Adriamycin Hydrochloride and *N*-[2-(2-Pyridinyldithio)ethyl]hydrazinecarboxamide (3a). Compound 3 (0.37 g, 1.5 mmol) in methanol (25 mL) was added to a stirred suspension of adriamycin hydrochloride (0.66 g, 1.14 mmol) in methanol (50 mL). TFA (5 drops) was added and the mixture left to stir overnight at room temperature. The clear solution was concentrated and chromatographed over a C_{18} reversed-phase column using methanol–water (60:40) containing 0.3% ammonium acetate, as solvent system. The appropriate fractions were combined, and the methanol was removed under reduced pressure. The aqueous phase was lyophilized and the residue dissolved in methanol and added to acetonitrile. The red precipitate was collected by centrifugation, dried to yield the title compound (0.65 g, 68%): IR (KBr) 3399, 2976, 2936, 1671, 1618, 1578, 1538, 1417, 1286, 1210, 1117, 1015, 989, 764 cm^{-1}; NMR (CD_3OD) δ 8.25, 7.76, 7.62, 7.48, 7.07 (d, m, m, d, m, 7 H), 5.4 (d, 1 H), 4.95 (m, 1 H), 4.63 (d, 2 H), 4.24 (m, 1 H), 3.97 (s, 3 H), 3.54–3.34 (m, 4 H), 3.32 (m, 4 H), 2.92 (m, 3 H), 2.36 (d, 2 H), 2.02–1.84 (s, m, 3 H), 1.29 (d, 3 H); MS (*m/e*) 770 (corresponds to $[M + H]^+$), 641, 437, 346; HRMS calcd $C_{35}H_{40}N_5O_{11}S_2$ 770.2166, found 770.2157.

2-[[[2-(2-Pyridinyldithio)ethyl]amino]carbonyl]-2,2′-bis(*tert*-butoxycarbonyl)carbonic Acid Dihydrazide (18). *tert*-Butyl carbazate (15) (0.396 g, 3 mmol) was dissolved in dry chloroform (10 mL). The solution was stirred under N_2 at room temperature and TEA was added (0.6 g, 6 mmol) followed by the addition of triphosgene (*19*) (0.296 g, 1 mmol) in one portion. When the initial reaction subsided, 2-(2-pyridinyldithio)ethanamine hydrochloride (0.667 g, 3 mmol) in chloroform containing TEA (0.3 g, 3 mmol) was added. The mixture was stirred at room temperature for 1.5 h, then washed with water and dried and the solvent evaporated under reduced pressure to leave a foam (0.91 g). This material was chromatographed over silica gel using a methylene chloride–methanol (100:2) solvent system to yield the title compound as a foam (0.54 g, 52%): IR (KBr) 3302, 2980, 2933, 1726, 1683, 1498, 1252, 1160, 1047, 1018, 763 cm^{-1}; NMR ($CDCl_3$) δ 8.50, 7.57, 7.49, 7.10 (d, q, d, t, 4 H), 3.52 (t, 2 H), 2.90 (t, 2 H), 1.46 (s, 9 H), 8.30, 6.50, 6.29 (bs, s, 4 H); MS (*m/e*) 503 (corresponds to $[M + H]^+$), 447, 431, 419, 403, 347, 303, 213, 179, 112.

2-[[[2-(2-Pyridinyldithio)ethyl]amino]carbonyl]-carbonic Acid Dihydrazide (4). Compound 18 (0.34 g, 0.68 mmol) was stirred for 10 min in TFA (5 mL) at 0 °C and an additional 10 min at room temperature. Excess TFA was evaporated and the residue was chromatographed over silica gel using a methylene chloride–methanol–concentrated ammonium hydroxide (100:5:0.5) solvent system. The appropriate fractions were combined, and the title compound was obtained as a hygroscopic foam (0.2 g, quantitative yield): IR (film) 3330, 2964, 2929, 1698, 1660, 1576, 1486, 1231, 1045, 759 cm^{-1}; NMR ($CDCl_3$) δ 8.50, 7.56, 7.10 (d, m, m, 4 H), 3.52 (q, 2 H), 2.91 (t, 2 H), 8.87, 8.85, 4.19, 3.78 (D_2O exchangeable protons, 5 H); MS (*m/e*) 303 (corresponds to $[M + H]^+$), 213, 112.

Semicarbazone Derivative of Adriamycin Hydrochloride and 2-[[[2-(2-Pyridinyldithio)ethyl]amino]-carbonyl]carbonic Acid Dihydrazide (4a). A solution of adriamycin hydrochloride (0.36 g, 0.6 mmol) and compound 4 (0.2 g, 0.68 mmol) in methanol (50 mL) containing 2–3 drops of TFA was stirred overnight at room temperature. The solvent was evaporated and the residue chromatographed over a C_{18} reversed-phase column using a solvent system of methanol–water (60:40) and containing 0.3% ammonium acetate. Most of the methanol was evaporated under reduced pressure and the aqueous solution was lyophilized and the red residue was dissolved in a small volume of methanol. The solution was filtered and added to stirred acetonitrile (1 L). The clear solution was concentrated to about one-third of its volume and the solid obtained was collected by centrifugation to give the title compound (0.16 g). A second crop (0.09 g) was obtained by concentrating the solution to 100 mL, diluting with ether, and collecting the solid by centrifugation (total yield 49%). IR (KBr) 3346, 2975, 2936, 1711, 1668, 1618, 1578, 1286, 1210, 1083, 1015, 765 cm^{-1}; NMR (CD_3OD) δ 8.43, 7.89, 7.77, 7.52, 7.21 (d, d, m, d, m, 7 H), 5.45 (s, H), 5.15 (s, H), 4.57 (q, 2 H), 4.25 (q, 1 H), 3.99 (s, 3 H), 3.53 (t, 2 H), 3.17 (q, 2 H), 3.05 (t, 2 H), 2.38 (m, 2 H), 1.90 (bs, 4 H), 1.29 (d, 3 H); MS (*m/e*) 828 (corresponds to $[M + H]^+$), 699, 572, 537, 377, 346, 289, 213; HRMS calcd for $C_{36}H_{42}N_7O_{12}S_2$ 828.2333, found 828.2361.

1-Bromo-4-*N*-phthalimido-2-butene (20). To a solution of 1,4-dibromo-2-butene (8.4 g, 40 mmol) in DMF (200 mL) was added at room temperature potassium phthalimide (4.62 g, 24 mmol) portionwise during 1 h. After stirring overnight, the solvent was evaporated and the residue partitioned between water and methylene chloride. The organic layer was washed with water and dried and the solvent evaporated. The residue was crystallized from 2-propanol, yielding the desired product (3.95 g, 59%): mp 101–2 °C; IR (KBr) 1775, 1711, 1466, 1436, 1393, 723 cm^{-1}; NMR ($CDCl_3$) δ 7.81, 7.73 (m, m, 4 H), 5.88, 5.81 (m,

m, 2 H), 4.30 (d, 2 H), 3.90 (d, 2 H); MS (*m/e*) 280 (corresponds to $[M + H]^+$) 200. Anal. Calcd for $C_{12}H_{10}BrNO_2$: C, 51.45; H, 3.60; N, 5.00. Found: C, 52.35; H, 3.47; N, 4.80.

1-(Acetylthio)-4-*N*-phthalimido-2-butene (21). A mixture of 1-bromo-4-*N*-phthalimido-2-butene (3.95 g, 14 mmol) and potassium thioacetate (1.77 g, 15.5 mmol) in absolute ethanol (50 mL) was heated to reflux for 0.5 h. The solvent was evaporated and the residue was extracted with methylene chloride. The solvent was evaporated to yield a crystalline residue (3.85 g, 99%) which was used as such for the next step. An analytical sample was prepared by crystallization from 2-propanol: mp 69–71 °C; IR (KBr) 1769, 1713, 1688, 1427, 1391, 1114, 958 cm^{-1}; NMR ($CDCl_3$) δ 7.80, 7.73 (m, m, 4 H), 5.70 (m, 2 H), 4.24 (d, 2 H), 3.48 (t, 2 H), 2.29 (s, 3 H); MS (*m/e*) 276 (corresponds to $[M + H]^+$), 234, 200. Anal. Calcd for $C_{14}H_{13}NO_3S$: C, 61.07; H, 4.76; N, 5.09. Found: C, 61.29; H, 4.82; N, 5.21.

1-Amino-4-(2-pyridinyldithio)-2-butene Hydrochloride (22). A solution of (acetylthio)-4-*N*-phthalimido-2-butene (6.5 g, 23.6 mmol) in absolute ethanol (150 mL) and hydrazine (1.74 g, 54 mmol) was heated to reflux. The solution then was chilled in ice and treated with 6 N HCl (10 mL). A precipitate formed and was filtered off. The filtrate was concentrated to 10 mL and diluted with water. The solid resulting was filtered off and the filtrate was washed with ether and methylene chloride, filtered through Celite, and lyophilized to give a waxy solid. This material was dissolved in methanol (75 mL) and treated with methoxycarbonylsulfenyl chloride (3.0 g, 23.7 mmol) at room temperature. After 0.5 h, the solvent was evaporated; the residue was redissolved in methanol (75 mL) and treated with 2-mercaptopyridine (2.7 g, 24 mmol). After 2 h the solvent was evaporated and the residue was dried under high vacuum. The residue was then dissolved in a mixture of 0.01 N HCl and methanol (90:10, 130 mL). The solution was washed with methylene chloride, filtered through Celite and lyophilized to yield the title compound as a hygroscopic material (4.0 g, 68%): IR (KBr) 3433, 2959, 2884, 1607, 1576, 1447, 1418, 1118, 767 cm^{-1}; NMR (D_2O) δ 8.51, 8.13, 8.02, 7.54 (m, 4 H), 5.87, 572 (m, m, 2 H), 3.54 (d, 2 H), 3.43 (d, 2 H); MS (*m/e*) 213 (corresponds to $[M + H]^+$), 196, 112.

***N*-[4-(2-Pyridinyldithio)-2-butenyl]hydrazinecarbothioamide (5).** 1-Amino-4-(2-pyridinyldithio)-2-butene hydrochloride (1.5 g, 6 mmol) was suspended in methylene chloride (30 mL). TEA was added (1.46 g, 14.6 mmol) followed by di-2-pyridyl thionocarbonate (*20*) (1.4 g, 6 mmol). *tert*-Butyl carbazate (0.8 g, 6 mmol) was then added and the solution stirred for 1 h. The solution was washed with water and the solvent evaporated. The residue was chromatographed over silica gel using a methylene chloride–methanol (100:2) solvent system and rechromatographed with hexane–ethyl acetate (75:25) solvent system to yield a foam which is the *t*-BOC derivative of **5** (1.4 g, 58%). The protected carbothioamide (0.86 g, 2.2 mmol) was treated with TFA at 0 °C for 10 min and at room temperature for 10 min. The excess acid was evaporated and the residue was chromatographed on silica using a methylene chloride–methanol–concentrated ammonium hydroxide (100:5:0.5) solvent system. The appropriate fractions were combined to yield a gum (0.39 g, 63%): IR (film) 3322, 3198, 2974, 1626, 1574, 1560, 1538, 1448, 1418, 1224, 760 cm^{-1}; NMR ($CDCl_3/D_2O$) δ 8.41, 7.63, 7.11 (m, m, m, 4 H), 5.64 (m, 2 H), 4.20 (d, 2 H), 3.41 (d, 2 H); MS (*m/e*) 287 (corresponds to $[M + H]^+$), 255, 221, 144, 112. The compound was used immediately for the preparation of **5a**.

Thiosemicarbazone Derivative of Adriamycin Hydrochloride and *N*-[4-(2-Pyridinyldithio)-2-butenyl]-hydrazinecarbothioamide (5a). To a stirred suspension of adriamycin hydrochloride (0.35 g, 0.6 mmol) in methanol (50 mL) was added a solution of compound **5** (0.35 g, 1.2 mmol) in methanol (25 mL). TFA (3–4 drops) was added and the mixture was stirred at room temperature overnight. The solution was concentrated to a small volume (5 mL) and added to acetonitrile (600 mL). The formed precipitate was collected by centrifugation and dried at high vacuum (0.28 g, 54%): IR (KBr) 3418, 2934, 1616, 1578, 1534, 1414, 1284, 1208, 1012, 986 cm^{-1}; NMR (CD_3OD) δ 8.30, 7.80, 7.74, 7.52, 7.16 (d, m, m, m, m, 7 H), 5.60 (m, 2 H) 5.40 (d, 1 H), 4.67 (d, 1 H), 4.22 (q, 1 H), 4.11 (d, 2 H), 4.02 (s, 3 H), 3.5–1.88 (14 H), 1.30 (d, 3 H); MS (*m/e*) 812 (corresponds to $[M + H]^+$), 701, 683, 669, 572, 554, 540, 536, 522, 504; HRMS calcd for $C_{37}H_{42}N_5O_{10}S_3$ 812.2094, found 812.2087.

2-(2-Pyridinyldithio)ethyl Hydrazinecarboxylate (6). To a solution of chlorocarbonylsulfenyl chloride (1.24 g, 9.45 mmol) in methylene chloride (10 mL) was added at 0 °C dropwise 2-mercaptoethanol (0.74 g, 9.45 mmol). The mixture was stirred at 0 °C for 30 min and then treated with a solution of 2-mercaptopyridine (1.05 g, 9.45 mmol) in methylene chloride (15 mL). The mixture was stirred at 0 °C for 1 h and then at room temperature for 16 h. After addition of an ammonium carbonate solution (1.0 g in 20 mL H_2O), the organic layer was washed with water, dried, and concentrated under reduced pressure to give crude 2-(2-pyridinyldithio)ethanol (**24**) (1.75 g) as a colorless oil. Carbonyldiimidazole (0.65 g, 4 mmol) was added to a solution of 2-(2-pyridinyldithio)ethanol (0.71 g, 3.8 mmol) in methylene chloride (10 mL). The mixture was stirred for 20 h and then cooled to −20 °C and treated with hydrazine (0.12 g, 3.8 mmol). The mixture was left standing at −5 °C for 16 h and then concentrated under reduced pressure. The residue was chromatographed on silica gel using a methylene chloride–methanol (100:3) solvent system to give 2-(2-pyridinyldithio)ethyl hydrazinecarboxylate (0.34 g, 37%) as a colorless oil: NMR ($CDCl_3$) δ 8.46 (1 H), 7.62 (2 H), 7.08 (1 H), 5.92 (1 H), 4.35 (t, 2 H), 3.70 (s, 2 H), 3.01 (t, 2 H); MS (*m/e*) 246 (corresponds to $[M + H]^+$), 142, 103.

Hydrazone Derivative of Adriamycin Hydrochloride and 2-(2-Pyridinyldithio)ethyl Hydrazinecarboxylate (6a). To a suspension of adriamycin hydrochloride (0.29 g, 0.5 mmol) in anhydrous methanol (4 mL) was added a solution of 2-(2-pyridinyldithio)ethyl hydrazinecarboxylate (0.17 g, 6.9 mmol) in methanol (4 mL) and 1 drop of TFA in methanol (1 mL). After stirring for 24 h the mixture was concentrated to about 4 mL and acetonitrile (50 mL) was added to this solution. The precipitate was isolated by centrifugation, redissolved in water–methanol, and then lyophilized to give the title compound (0.35 g, 88%) as dark red solid: NMR (CD_3OD) δ 8.34 (1 H), 7.93 (d, 1 H), 7.81 (m, 3 H), 7.54 (d, 1 H), 7.17 (m, 1 H), 5.49 (m, 1 H), 5.19 (s, 1 H), 4.59 (m, 2 H), 4.37 (m, 2 H), 4.25 (m, 1 H), 4.01 (s, 3 H), 3.63 (m, 1 H), 3.54 (m, 1 H), 3.10 (t, 3 H), 2.37 (m, 2 H), 2.03 (m, 1 H), 1.89 (m, 1 H), 1.29 (d, 3 H); MS (*m/e*) 771 (corresponds to $[M + H]^+$), 642; HRMS calcd for $C_{35}H_{39}N_4O_{12}S_2$ 771.2006, found 771.2008.

***N*-[2-(2-Pyridinyldithio)ethyl]-4-[2-(*tert*-butoxycarbonyl)hydrazino]benzamide (27).** *p*-Hydrazinobenzoic acid (0.76 g, 5 mmol) was dissolved in dioxane (10 mL), water (5 mL), and a 1 N NaOH solution (5 mL).

Di-*tert*-butyl pyrocarbonate (1.31 g, 6 mmol) was added at 0 °C and the reaction mixture was stirred at 0 °C for 1 h and at room temperature for 30 min. After this period the volume of the solution was reduced by one-half and the solution was acidified with 0.5% HCl solution and extracted with ethyl acetate. The combined ethyl acetate solution was washed with brine and dried over Na_2SO_4. Removal of the solvent gave a slightly brown solid which was recrystallized from ethyl acetate and hexane (0.95 mg, 75%): IR (KBr) 3316, 1688, 1607, 1298 cm^{-1}; NMR (CD_3OD) δ 7.84 (d, 2 H), 6.75 (d, 2 H), 1.48 (s, 9 H).

The compound above (0.25 g, 1 mmol), *N*-hydroxysuccinimide (0.2 g, 1 mmol), and dicyclohexylcarbodimide (0.25 g, 1.2 mmol) in DMF (5 mL) were stirred overnight at room temperature. Dicyclohexylurea was filtered off and the filtrate was concentrated. The residue was crystallized by addition of ether to give *N*-succinimidyl ester **26** (0.3 g). This material (0.25 g, 0.72 mmol) and 2-(2-pyridinyldithio)ethanamine hydrochloride (0.17 g, 0.75 mmol) were dissolved in DMF (4 mL). After addition of TEA (0.125 mL, 0.9 mmol), the mixture was stirred overnight at room temperature. DMF was removed and the residue was chromatographed on silica gel using a methylene chloride–methanol (100:2) solvent system to give a foam (0.22 g, 52%): IR (KBr) 3303, 1714, 1610, 1505 cm^{-1}; NMR ($CDCl_3$) δ 8.37 (d, 1 H), 8.01 (bt, 1 H), 7.78 (d, 2 H), 7.57 (m, 1 H), 7.46 (d, 1 H), 7.09 (m, 1 H), 6.84 (d, 2 H), 7.40 (bs, 1 H), 5.92 (bs, 1 H), 3.70 (m, 2 H), 2.98 (t, 2 H), 1.45 (s, 9 H); MS (*m/e*) 421 (corresponds $[M + H]^+$), 365, 321, 112; HRMS calcd for $C_{19}H_{25}N_4O_3S_2$ 421.1368, found 421.1358.

***N*-[2-(2-Pyridinyldithio)ethyl]-4-hydrazinobenzamide (7).** Compound **27** (0.2 g, 0.48 mmol) was treated with TFA (1.5 mL) at 0 °C for 1 h. After this period TFA was evaporated and the residue was triturated with ether to give ca. 0.2 g of an oil: IR (film) 3278, 1674, 1613 cm^{-1}; NMR (CD_3OD) δ 8.38 (d, 1 H), 7.81 (m, 4 H), 7.22 (t, 1 H), 6.97 (d, 2 H), 3.67 (t, 2 H), 3.06 (t, 2 H); MS (*m/e*) 321 (corresponds to $[M + H]^+$).

Hydrazone Derivative of Adriamycin and *N*-[2-(2-Pyridinyldithio)ethyl]-4-hydrazinobenzamide (7a). Compound **7** and adriamycin hydrochloride (0.25 g, 0.43 mmol) were dissolved in methanol (15 mL) and stirred in the dark for 2 days. The solvent was removed and the residue was chromatographed on C_{18} reversed-phase column. Elution with methanol–water containing 0.3% ammonium acetate (2:1) gave hydrazone **7a** as orange powder (0.03 g, 8%): IR (KBr) 3206, 1708, 1607, 1578 cm^{-1}; NMR (CD_3OD) δ 8.33 (d, 1 H), 7.85 (d, 1 H), 7.74 (t, 1 H), 7.66 (m, 4 H), 7.41 (d, 1 H), 7.14 (m, 1 H), 7.02 (d, 2 H), 5.46 (bs, 1 H), 5.16 (m, 1 H), 4.60 (s, 2 H), 4.23 (m, 1 H), 3.91 (s, 3 H), 3.62 (m, 4 H), 3.02 (m, 4 H), 2.61 (m, 1 H), 2.38 (m, 1 H), 1.97 (m, 2 H), 1.32 (d, 3 H); MS (*m/e*) 846 (corresponds to $[M + H]^+$), 737, 717; HRMS calcd for $C_{41}H_{44}N_5O_{11}S_2$ 846.2479, found 846.2380.

Elution with methanol–water containing 0.3% ammonium acetate (3:1) gave the C-9–C-10 anhydro derivative of hydrazone **7a** as a blue solid (0.12 g, 34%): NMR (CD_3OD) δ 8.40 (d, 1 H), 7.77 (m, 5 H), 7.42 (m, 1 H), 7.22 (m, 1 H), 7.16 (m, 2 H), 5.35 (bs, 1 H), 5.26 (m, 1 H), 4.65 (s, 2 H), 4.00 (m, 1 H), 3.93 (s, 3 H), 3.67 (t, 2 H) 3.44 (m, 1 H), 3.08 (t, 2 H), 2.49 (m, 1 H), 1.88 (m, 1 H), 1.63 (m, 1 H), 1.19 (d, 3 H); MS (*m/e*) 828 (corresponds to $[M + H]^+$) 699, 681, 495; HRMS calcd for $C_{41}H_{42}N_5O_{10}S_2$ 828.2373, found 828.2300.

[2-(*tert*-Butoxycarbonyl)hydrazino]acetic Acid (29). A solution of iodoacetic acid (0.95 g, 5 mmol) and *tert*-butyl carbazate (1.98 g, 15 mmol) in THF (30 mL) was refluxed for 6 h. The resulting solution was acidified with 0.1% aqueous HCl solution. The product was extracted with ethyl acetate and dried over Na_2SO_4. Removal of ethyl acetate and trituration of the residue with methylene chloride gave the title compound (0.74 g, 78%): NMR (CD_3COCD_3) δ 3.63 (s, 2 H), 1.54 (s, 9 H); MS (*m/e*) 191 (corresponds to $[M + H]^+$), 175, 163, 135.

***N*-Succinimidyl Ester of [2-(*tert*-Butoxycarbonyl)hydrazino]acetic Acid (30).** Acid **29**, obtained above (0.14 g, 0.745 mmol), and *N*-hydroxysuccinimide (0.09 g, 0.75 mmol) were dissolved in DMF (5 mL). Dicyclohexylcarbodiimide (0.18 g, 0.89 mmol) was added and the mixture was stirred at room temperature overnight. Dicyclohexylurea was filtered off and DMF was removed under reduced pressure to give a white solid (0.22 g quantitative yield): NMR ($CDCl_3$) δ 6.38 (bs, 1 H), 4.30 (m, 1 H), 3.99 (d, 2 H), 2.85 (s, 4 H), 1.45 (s, 9 H); MS (*m/e*) 288 (corresponds to $[M + H]^+$), 232, 188.

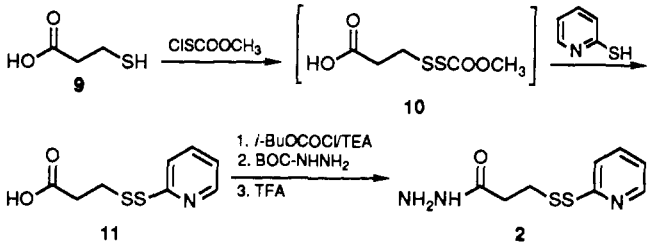
***N*-[2-(2-Pyridinyldithio)ethyl][2-(*tert*-butoxycarbonyl)hydrazino]acetamide (31).** Solid **30**, from the reaction above, and 2-(2-pyridinyldithio)ethanlamine hydrochloride (0.22 g, 1 mmol) were suspended in methylene chloride (15 mL). After addition of TEA (0.137 mL, 1 mmol), the mixture was stirred at room temperature for 30 min. The methylene chloride layer was washed with brine and dried over Na_2SO_4. The residue obtained after evaporation of the solvent was chromatographed on silica gel using a methylene chloride–methanol (100:5) solvent system to give the title compound (0.19 g, 53%): IR (KBr) 3362, 3317, 3244, 1710, 1647, 1528, 1421 cm^{-1}; NMR ($CDCl_3$) δ 8.55 (d, 1 H), 8.39 (bt, 1 H), 7.61 (t, 1 H), 7.52 (d, 1 H), 7.13 (dd, 1 H), 6.62 (bs, 1 H), 4.36 (bs, 1 H), 3.53 (m, 4 H), 2.94 (5, 1 H), 1.44 (s, 9 H); MS (*m/e*) 359 (corresponds to $[M + H]^+$), 303, 259.

***N*-[2-(2-Pyridinyldithio)ethyl]hydrazinoacetamide (8).** The previous compound, **31** (0.23 g, 0.65 mmol), was treated with a mixture TFA (1 mL) and methylene chloride (1 mL) at 0 °C for 2 h. After evaporation of the reagent the residue was chromatographed on silica using a methylene chloride–methanol (100:5) solvent system to give an oil (134 mg, 80%): NMR (CD_3OD) δ 8.42 (d, 1 H), 7.81 (m, 2 H), 7.23 (m, 1 H), 3.64 (s, 2 H), 3.55 (t, 2 H), 2.95 (t, 2 H); IR (film) 3268, 1673, 1576, 1562, 1420 cm^{-1}; MS (*m/e*) 259 (corresponds to $[M + H]^+$), 221, 112.

Condensation Product of Adriamycin Hydrochloride and *N*-[2-(2-Pyridinyldithio)ethyl]hydrazinoacetamide (8a). Adriamycin hydrochloride (0.19 g, 0.33 mmol) and compound **8** (0.12 g, 0.33 mmol) were dissolved in methanol (5 mL) containing solid $KHCO_3$ (0.03 g, 0.33 mmol). The solution was stirred in the dark at room temperature for 2.5 days. The residue obtained after evaporation of the solvent was chromatographed on C_{18} reversed-phase column using a methanol–water containing 0.3% ammonium acetate (2:1) solvent system. The fractions were combined and lyophilized. The dark blue residue was precipitated from methanol and acetonitrile to give 155 mg (62%) of solid: IR (KBr) 3323, 1732, 1616, 1581, 1286 cm^{-1}; NMR (CD_3OD) δ 8.38 (d, 1 H), 7.85 (d, 1 H), 7.76 (m, 3 H), 7.47 (d, 1 H), 7.18 (m, 1 H), 7.07 (s, 1 H), 5.27 (m, 1 H), 5.16 (d, 1 H), 4.57 (d, 1 H), 4.51 (d, 1 H), 3.96 (s, 3 H), 3.58 (m, 4 H), 3.19 (m, 1 H), 2.99 (t, 2 H), 2.38 (bd, 1 H); MS (*m/e*) 766 (corresponds to $[M + H]^+$), 619, 439. This corresponds to the C-9–C-10 anhydro derivative of hydrazone **8a**.

Preparation of Conjugates from Hydrazones and 5E9 mAb (14a). A solution (1 mL) of the mAb in PBS (5–10 mg/mL, concentration determined by UV absorption at 280 nm; 1 mg/mL = 1.4 absorbance units) was treated

Scheme I



with a freshly prepared 10 mM SPDP solution in absolute ethanol (0.05 mL). The protein solution was incubated at 30–1 °C for 30 min, then chilled in ice and treated with a 50 mM solution of DTT in PBS (0.05 mL). The reaction mixture was kept at 4 °C for 15 min and then the modified mAb was separated from excess reagent using a preequilibrated G-25 gel column (Pharmacia). The molar concentration of thiol groups was determined by the Ellman procedure (*21*) and the solution was treated with a thiol equivalent amount of hydrazone dissolved in DMF (5 mg/mL). The solution was incubated at 4 °C overnight then dialyzed three times in 1 L of PBS. The solution was centrifuged to remove any precipitate formed and the supernatant shaken gently several hours with Bio-beads (Bio-Rad Laboratories). Finally, the solution was filtered through a Millex-GV, 0.22-μm filter unit (Millipore Corp.) to provide the conjugate. The amount of conjugated adriamycin was determined by absorbance at 495 nm (ϵ_{495} = 8030 cm^{-1} M^{-1}). The amount of protein was determined by absorbance at 280 nm as above, however, with a correction for the absorbance at the same wavelength of adriamycin according to the general formula:

$$\text{mAb (mg/mL)} = \frac{A_{280} - (0.724 \times A_{495})}{1.4}$$

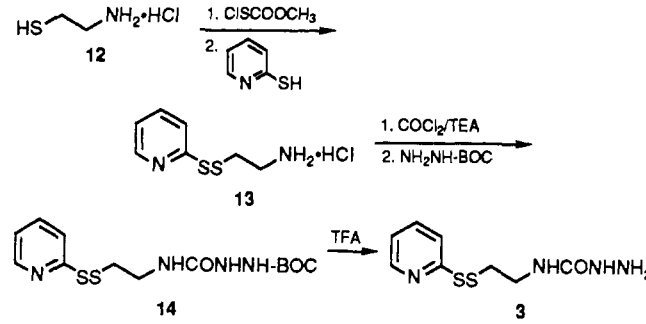
where A is the observed absorbance at noted wavelength.

RESULTS AND DISCUSSION

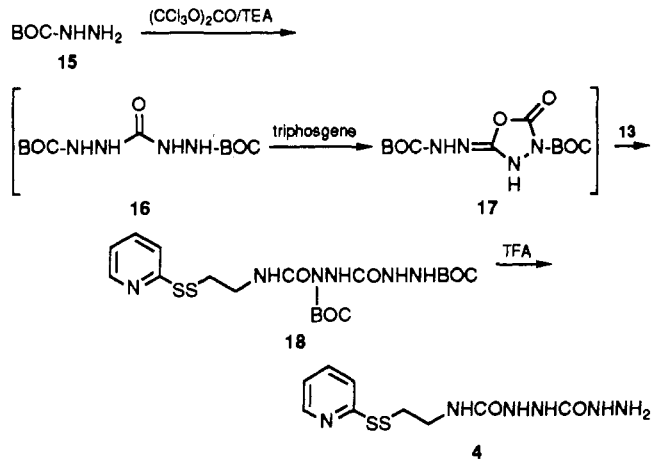
Chemistry. The linkers synthesized for the present purpose are listed in Chart I. They include acylhydrazide **2** (*14*), semicarbazide **3**, carbonic acid dihydrazide **4**, thiosemicarbazide **5**, hydrazide carboxylate **6**, arylhydrazide **7**, and alkylhydrazine **8**. The structurally diverse hydrazine linkers were proposed in order to provide various hydrolytic stability of the corresponding hydrazone derivatives of adriamycin. These linkers incorporated a pyridinyldithio moiety for conjugation with a mAb derivatived to contain thiol groups. Throughout our synthetic work it was found that the pyridinyldithio group was stable to acidic conditions; therefore most N-protection was effected with *tert*-butoxycarbonyl group.

The synthesis of linker **2** from SPDP was previously reported (*14a*). We subsequently found that it could be prepared by starting with mercaptopropionic acid and methoxycarbonylsulfenyl chloride. The reactive intermediate thus formed is then treated with 2-mercaptopyridine to provide 3-(2-pyridinyldithio)propionic acid (Scheme I). This method of incorporating the pyridinyldithio moiety was used in all subsequent syntheses. Thus, for semicarbazide **3** cysteamine hydrochloride was employed to give intermediate **13** (Scheme II), which was then treated with phosgene and *tert*-butyl carbazate. Even though it could potentially give the same product, when the reaction was started with *tert*-butyl carbazate and triphosgene as shown in Scheme III, the product was carbonic acid dihydrazide **4**, which indicated formation of cyclic intermediate **17**. Our attempt to prepare a thiosemicarbazide corresponding to **3** was not successful. An elimination of 2-mercaptopyridine was observed at the stage of *t*-BOC-protected thiosemicarbazide, which could be ascribed to the increased nucleophilicity of the thiosemicarbazide moiety compared to that of the semicarbazide. This problem was circumvented by employing a *trans*-2-butene group, as shown in Scheme IV, rather than an ethyl group as a spacer.

Scheme II



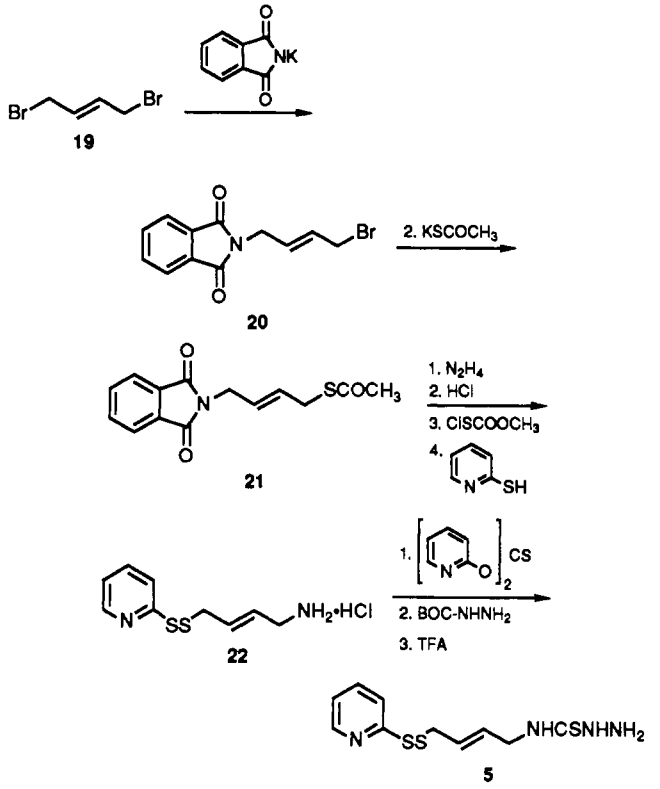
Scheme III



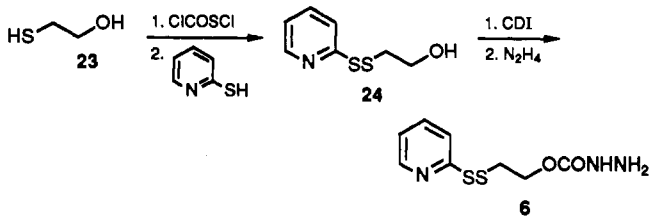
Another congener of semicarbazide is a hydrazinecarboxylate linker, **6**. This was prepared starting with mercaptoethanol, which was derivatized to (pyridinyldithio)ethanol as shown in Scheme V. This compound was then converted to an activated carbonyl derivative that was finally condensed with hydrazine. A bifunctional alkylhydrazine, **8**, was prepared from iodoacetic acid by first introducing a hydrazine moiety and then incorporating the 2-(2-pyridinyldithio)ethanamine group (Scheme VII). The corresponding arylhydrazine was synthesized in a similar manner from 4-*N*-Boc-hydrazinobenzoic acid (Scheme VI).

The imino derivatives of adriamycin were generally prepared by treating adriamycin hydrochloride with a linker in methanol at room temperature. It was found that addition of catalytic amounts of TFA accelerated the condensation so that the reaction was complete after an overnight stirring. If uncatalyzed, the reaction would take several days. Acid-catalyzed deglycosidation of adriamycin or formation of other byproducts was negligible. As a result, isolation of the product was simple and involved precipitation by addition of acetonitrile to the methanolic solution of the reaction. In the case of alkylhydrazine **8** the product obtained was the hydrazone of 9,10-anhydroadriamycin **8b**. It is likely that in this case the nonbonded electrons of the nitrogen atom α to the carbonyl group facilitates elimination of a molecule of water since they are not delocalized to the carbonyl group as in **2**.

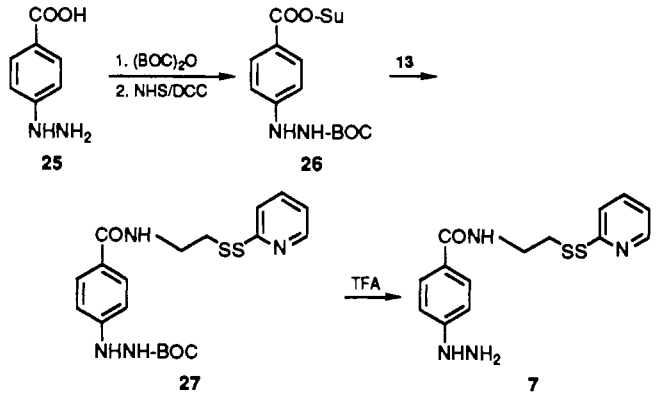
Scheme IV



Scheme V



Scheme VI



When linker **7** was condensed with adriamycin, the desired product **7a** as well as the 9,10-anhydro product **7b** was obtained.

These new N-substituted hydrazones of adriamycin were then conjugated with mAb 5E9 (22) in the manner reported previously for **2** (*14*), and the conjugates are listed in Table I. Since 9,10-anhydro derivatives of adriamycin were reported to be less cytotoxic than adriamycin (*23*), these hydrazones were not conjugated with mAb. However, linkers **7** and **8** may still be useful in a system where the product does not have increased instability. mAb 5E9, which is an anti-transferrin receptor mAb, and therefore expressed in rapidly proliferating cells (*24*), was used as an example. For therapy, tumor-selective mAb's rather than 5E9 can be conjugated with these adriamycin derivatives.

Scheme VII

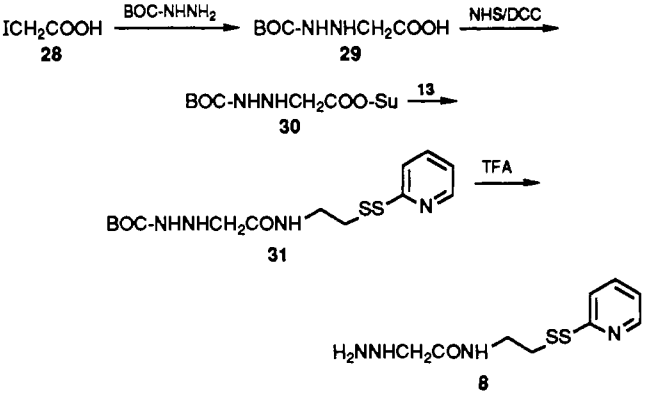


Table I

5E9 conjugate of compound	protein % yield	MR	% binding[a]
hydrazone **2**[b]	50–80	3–8	>80
semicarbazone **3**	83	3.42	97
carbonic acid dihydrazine **4**	74	4.37	92
thiosemicarbazone **5**	61	2.51	72
hydrazine carboxylate **6**	78	2.35	97
arylhydrazone **7**	86	2.52	91

[a] For binding assay method see ref 14. [b] Data taken from ref 14 and represent conjugates from multiple preparations.

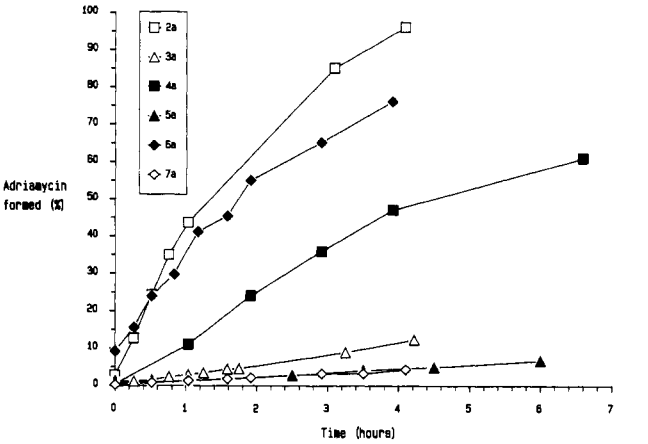


Figure 1. Formation of adriamycin from hydrazones as a function of time after their incubation in buffer at pH 4.5 (37 °C). Symbols refer to the number given to each compound in Chart I.

Release Rates and Cytotoxicity Data. The release of adriamycin by hydrolysis of each of its derivatives as a function of pH was monitored by HPLC. Stock solutions of derivatives were prepared in methanol and aliquots diluted into aqueous buffer solution at pH 4.5, 5.0, and 7.4 to achieve final concentrations of ca. 1.6 nmol/mL. Incubations in each buffer were carried out at 37 °C and aliquots analyzed. The released material was identified as adriamycin by retention time and by UV profile of the eluted material. It was the only compound detected. The release rates at pH 4.5, 5, and 7.4, expressed as a percentage of maximum amount of adriamycin calculated for each conjugate, are shown in Figures 1–3. The immunoconjugates of hydrazones **2a** and **4a** were also analyzed for their release of adriamycin. The results are essentially overlapping those of the linkers as shown specifically for the immunoconjugate of **4a**, (Figure 4). As apparent from these graphs, we were able to prepare derivatives of wide-

Table II

5E9 conjugate of compound	IC_{50},[a] M[b]	5E9 conjugate of compound	IC_{50},[a] M[b]
adriamycin hydrochloride	7.0×10^{-8}	thiosemicarbazone **5**	3.0×10^{-7}
hydrazone **2**	5.8×10^{-8}	hydrazine carboxylate **6**	5.9×10^{-7}
semicarbazone **3**	$>5.1 \times 10^{-7}$	arylhydrazone **7**	$>6.4 \times 10^{-7}$
carbonic acid dihydrazine **4**	4.0×10^{-7}		

[a] Measured after a 24-h exposure of cells to immunoconjugate. [b] Molar concentration of adriamycin.

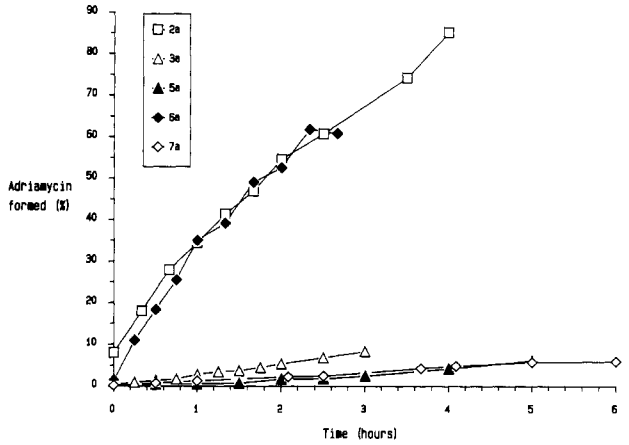


Figure 2. Formation of adriamycin from hydrazones as a function of time after their incubation in buffer at pH 5.0 (37 °C). Symbols refer to the number given to each compound in Chart I.

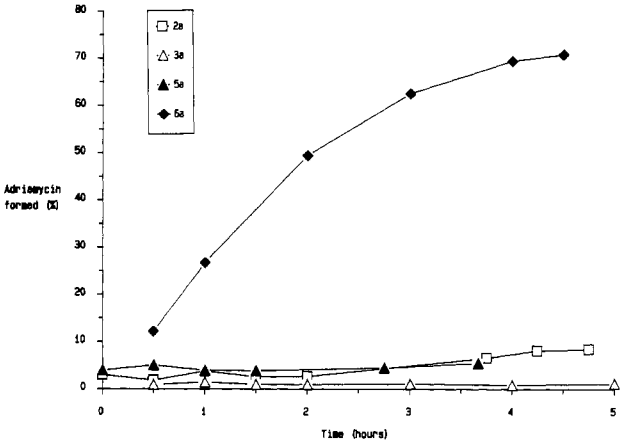


Figure 3. Formation of adriamycin from hydrazones as a function of time after their incubation in buffer at pH 7.4 (37 °C). Symbols refer to the number given to each compound in Chart I.

ranging release rates. In general, hydrolysis of semicarbazones and imines of various carbonyl compounds has been investigated extensively (*13*). The hydrolytic rate can be influenced by the pH, the ionic strength, and the counterion of the media (*13*, *25*)[3] as well as the added nucleophile (*26*), the temperature (*27*), and the stability of the carbinolamine intermediate (*28*). Indeed it may not be straightforward to reproduce the lysosomal environment for the presumed release of adriamycin from its mAb conjugates. In order to rank the adriamycin derivatives, release of adriamycin was studied in buffered solutions at pH 4.5, 5.0, and 7.4. As shown in Figure 1

[3] Recent investigations in our laboratories on the release rate of adriamycin from compounds **2a** and **4a** have shown dramatic effects of aqueous acetate buffer concentrations (pH 5, 37 °C) on the half-life of these compounds. These effects clearly indicate that in addition to simple H^+ catalysis, acetic acid is also an active participant in the release process (L. Padilla, unpublished results).

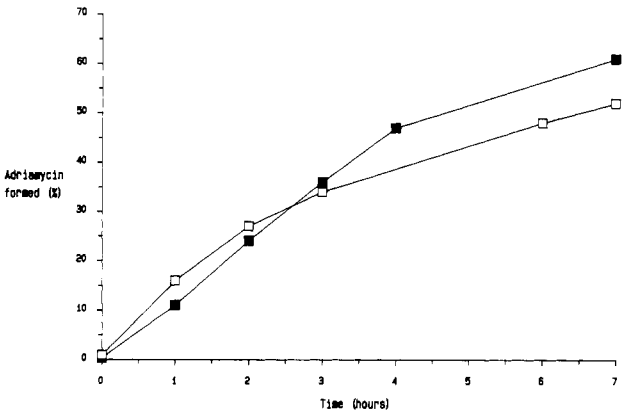


Figure 4. Formation of adriamycin from **4a** (filled symbols) and a 5E9 conjugate of **4a** (hollow symbols) as a function of time after their incubation in buffer at pH 4.5 (37 °C).

acylhydrazone **2a** has the highest release rate at pH 4.5, releasing within 3 h more than 85% of theoretical amount of adriamycin. It was followed by hydrazine carboxylate **6a** and carbonic dihydrazine **4a**, releasing 60% and 35% of theoretical amount, respectively. The semicarbazone, thiosemicarbazone, and arylhydrazone derivatives released very little adriamycin even after 6 h of incubation. In all cases the hydrolysis was clean and there was little decomposition products. At pH 7.4 little release of adriamycin was observed from derivatives **2a**, **3a**, and **7a** while hydrazine carboxylate **6a** released adriamycin relatively rapidly. For the selective delivery in an acidic environment as mentioned before, therefore, linkers 2 and 4 may fulfill the conditions whereas linker **6** will not be appropriate.

The cytotoxicity of the conjugates was determined by colony formation assay on soft agar using Daudi cells, a Burkitt's lymphoma cell line expressing 5E9 antigen and negative in 3A1 antigen (*14a*). The IC_{50} of adriamycin and the mAb conjugates having similar drug/mAb ratios are shown in Table II. The most active conjugate, as might be expected, turned out to be the one which releases the highest percentage of the total adriamycin incorporated in the conjugate at pH 4.5. 5E9, the mAb used in these conjugates, is an anti-transferrin receptor antibody which has been shown to internalize following binding to the target cell (*22a*) and conjugates prepared from this antibody have been shown to be internalized also (*22b*). Adriamycin is believed to be released from this mAb via hydrolysis in the acidic lysosomal environment to exert its cytotoxic effect. Releaseability of adriamycin may be a necessary condition but it may not be a sufficient one for the conjugate to be active. For example hydrazone carboxylate **6a** releases adriamycin at pH 4.5–5 at a similar rate as acylhydrazone **2a** (Figure 1, Chart I) however its conjugate is not particularly active ($IC_{50} > 5.9 \times 10^{-7}$). Indeed, the adriamycin hydrazone derived from this linker and conjugate also hydrolyze at pH 7.4. This fact may affect the specificity of the conjugate since the conjugate may be cytotoxic to both antigen-positive and antigen-negative cells.

In summary, several new linkers of adriamycin and their 5E9 immunoderivatives were synthesized and were shown

to have wide-ranging release rates under slightly acidic conditions that might mimic lysosomal environment. Acylhydrazone **2a** and its conjugate release the highest percentage of adriamycin at pH 4.5 and 5 but not at 7.4. This conjugate was the most active in the in vitro colony formation assay. The other linkers and conjugates show under the condition tested diminished release rates of adriamycin as well as lower cytotoxic activity.

ACKNOWLEDGMENT

We thank the Analytical Research group for providing analytical and spectroscopic data. The technical assistance of Kathleen Kadow, Ann Daues, and Kerry McGoff is also acknowledged. Finally, we thank Dr. Terrence W. Doyle for his encouragement and support.

LITERATURE CITED

(1) Weinstein, H. J., Mayer, R. J., and Rosenthal, D. S. (1980) Treatment of acute myelogenous leukemia in children and adults. *N. Engl. J. Med. 303*, 473–478.

(2) McCredie, K. B., Bodey, G. P., Freireich, E. J., Hester, J. P., Rodriguez, V., and Keating, M. J. (1981) Chemoimmunotherapy of adult acute leukemia. *Cancer 47*, 1256–1261.

(3) Smalley, R. V., and Bartalucci, A. A. (1980) Variation in responsiveness and survival of clinical subsets of patients with metastatic breast cancer to two chemotherapy combinations. *Eur. J. Cancer (suppl. 1)*, 145–146.

(4) Bruckner, H. W., Cohen, C. J., Goldberg, J. D., Kabakon, B., Wallach, R. C., Deppe, G., Greenspan, E. M., Grusberg, S. B., and Holland, J. F. (1981) Improved chemotherapy for ovarian carcinoma with *cis*-diamminedichloroplatinum and adriamycin. *Cancer 47*, 2288–2294.

(5) Carter, S. K. (1975) Adriamycin—a review. *J. Natl. Cancer Inst. 55*, 1265–1274.

(6) Hermentin, P., and Seiler, F. R. (1988) Investigations with monoclonal antibody drug (anthracycline) conjugates. *Behring Inst. Mitt. 82*, 197–215.

(7) Hurwitz, E., Levy, R., Maron, R., Wilchek, M., Arnon, R., and Sela, M. (1975) The covalent binding of daunomycin and adriamycin to antibodies with retention of both drug and antibody activities. *Cancer Res. 35*, 1175–1181.

(8) Hurwitz, E., Maron, R., Bernstein, A., Wilchek, M., Sela, M., and Arnon, R. (1978) The effect in-vivo of chemotherapeutic drug–antibody conjugates in two murine experimental tumor systems. *Int. J. Cancer 21*, 747–755.

(9) (a) deDuve, C. (1983) lysosomes revisited. *Eur. J. Biochem. 137*, 391–397. (b) Pastan, I. H., and Willingham, M. C. (1985) Pathways of endocytosis. In *Endocytosis* (I. H. Pastan, and M. C. Willingham, Eds.) p 1–44, Plenum Publishing Corp., New York.

(10) Poznansky, M. J., and Juliano, R. L. (1984) Biological approaches to the controlled delivery of drugs: a critical review. *Pharmacol. Rev. 36*, 277–336.

(11) (a) Shen, W. C., and Reiser, J. P. (1981) *cis*-Aconityl spacer between daunomycin and macromolecular carriers: A model of pH-sensitive linkage releasing drug from a lysosomotropic conjugate. *Biochem. Biophys. Res. Commun. 102*, 1048–1054. (b) Yang, H. M., and Reisfeld, R. A. (1988) Doxorubicin conjugates with a monoclonal antibody directed to a human melanoma-associated proteoglycan suppresses the growth of established tumor xenografts in nude mice. *Proc. Natl. Acad. Sci. 85*, 1189–1193.

(12) Srinivasachar, K., and Neville, D. M., Jr. (1989) New protein cross-linking reagents that are cleaved by mild acid. *Biochemistry 28*, 2501–2509.

(13) Reeves, R. L. (1966) Condensations leading to double bonds. *The Chemistry of the Carbonyl Group* (S. Patai, Ed.) pp 567–619. Interscience Publishers, New York.

(14) (a) Greenfield, R. S., Kaneko, T., Daues, A., Edson, M. A., Fitzgerald, K. A., Olech, L. J., Grattan, J. A., and Braslawsky, G. R. (1990) Evaluation in vitro of adriamycin–immunoconjugates synthesized using an acid sensitive hydrazone linker. *Cancer Res. 50*, 6600–6607. (b) Braslawsky, G. R., Edson, M. A., Pearce, W., Kaneko, T., and Greenfield, R. S. (1990) Antitumor activity of adriamycin (hydrazone linked) immunoconjugates compared to free adriamycin and specificity of tumor cell killing. *Cancer Res. 50*, 6608–6614. (c) Braslawsky, G. R., and Greenfield, R. S. (1989) Preclinical studies of adriamycin–antibody conjugates linked through the C-13 keto position. In *Proceedings of the 16th International Congress of Chemotherapy* (E. Rubenstein, D. Adam, Eds.) p 738.1–2, E. Lewin-Epstein Ltd., Tel Aviv, Israel.

(15) Carlsson, J., Drevin, H., and Axen, R. (1978) Protein thiolation and reversible protein–protein conjugation; *N*-succinimidyl 3-(2-pyridyldithio)propionate, a new heterobifunctional reagent. *Biochem. J. 173*, 723–737.

(16) Kato, Y., Endo, N., and Hara, K. (1988) Hydrazides and method for their preparation. J. P. Kokai No. 63-57569.

(17) Mueller, B. M., Wrasidlo, W. A., and Reisfeld, R. A. (1990) Antibody conjugates with morpholinodoxorubicin and acid-cleavable linkers. *Bioconjugate Chem. 1*, 325–330.

(18) (a) Zumach, G., and Kuhle, E. (1970) Chlorosulfenylated carbonic acid derivatives. *Angew. Chem. Int. Ed. Engl. 9*, 54–63. (b) Field, L., Harle, H., Owen, T. C., and Ferreti, A. (1964) Organic disulfides and related substances. VIII. Preparation and oxidation of some unsymmetrical dialkyl and alkyl pyridinium disulfides. *J. Org. Chem. 29*, 1632–1635. (c) Connor, J., and Schroit, A. J. (1988) Transbilayer movement of phosphatidylserine in erythrocytes: Inhibition of transport and preferential labeling of a 31000 dalton protein by sulfhyryl reactive reagent. *Biochemistry 27*, 848–851.

(19) Eckert, H., and Forster, B. (1987) Triphosgene: A crystalline phosgene equivalent. *Angew. Chem. 99*, 922–923.

(20) Kim, S., and Yi, K. Y. (1985) Di-2-pyridylthionocarbonate. A new reagent for the preparation of isothiocyanates and carbodiimides. *Tetrahedron Lett. 26*, 1661–1664.

(21) Riddles, P. W., Blakeley, R. L., and Zerner, B. (1979) Ellman's reagent: 5,5′-dithiobis(2-nitrobenzoic acid)—a reexamination. *Anal. Biochem. 94*, 75–81.

(22) (a) Haynes, B. F., Hemler, M., Cotner, T., Mann, D. L., Eisenbarth, G. S., Strominger, J. L., and Fauci, A. S. (1981) Characterization of a monoclonal antibody (5E9) that defines a human cell surface antigen of cell activation. *J. Immunol. 127*, 347–351. (b) Greenfield, R. S., Senter, P. D., Daues, A. T., Fitzgerald, K. A., Gawlak, S., Manger, W., and Braslawsky, G. R. (1989) In vitro evaluation of immunoconjugates prepared by linking mitomycin c to monoclonal antibodies via polyglutamic acid carriers. *Antibody Immunoconjugate Radiopharm. 2*, 201–216.

(23) Potti, G., and Israel, M. (1982) Adriamycin analogues. Preparation of 9,10-anhydrodaunorubicin, 9,10-anhydroadriamycin, and some related compounds. *J. Med. Chem. 25*, 478–481.

(24) Faulk, W. P., and McIntyre, J. A. (1983) Immunological studies of human trophoblast: markers, subsets and functions. *Immunol. Rev. 75*, 139–175.

(25) Cordes, E. H., and Jencks, W. P. (1963) The mechanism of hydrolysis of Schiff bases derived from aliphatic amines. *J. Am. Chem. Soc. 85*, 2843–2848.

(26) Kakemi, K., Sezaki, H., Takasugi, N., and Iwamoto, K. (1968) Studies on stability of drug in biological media (1). Stability of furylmethylketone isonicotinoylhydrazone in culture media. *Chem. Pharm. Bull. 16*, 1481–1486.

(27) Fiarman, I. D., and Gettler, J. D. (1962) Structure and reactivity in carbonyl reactions; Temperature coefficient of rate of formation of several thiosemicarbazones. *J. Am. Chem. Soc. 84*, 961–966.

(28) Reference 13, pp 611–614.

Identification of Peptides in the Adenine Ring Binding Domain of Glutamate and Lactate Dehydrogenase Using 2-Azido-NAD+ †,‡

Hyuntae Kim and Boyd Haley*

University of Kentucky, Department of Biochemistry, College of Medicine, Lexington, Kentucky 40536.
Received November 20, 1990

Previously, the synthesis and validation of [^{32}P]2N_3NAD+ as an active site directed photoaffinity probe for glutamate dehydrogenase (GDH) was reported (*8*). This report shows that 2N_3NAD+ is also an effective probe for the NAD+ binding site of lactate dehydrogenase (LDH). With the appropriate photolabeling procedures and immobilized boronate column chromatography the active site peptides of GDH and LDH involved in the adenine base binding domain have been isolated and sequenced. With both GDH and LDH a single photolabeled peptide, which contained the majority of the photoinserted radiolabel, was isolated. Additionally, these peptides had UV spectra that were markedly different from the nonphotolabeled peptides. The modified peptide from GDH corresponded to Cys^{270} through Lys^{289}. Both sequencing and compositional analysis identified Glu^{275} as the site of photoinsertion. Sequencing of this peptide aborted at Glu^{275} after five rounds of analysis, indicating that insertion was blocking further progress. Compositional analysis showed that the entire sequence from residues 270 to 289 was present except that the single Glu residue was missing. This is interpreted as indicating that the photoinsertion is into the polypeptide backbone at the Glu site. The peptide isolated from LDH corresponded to Asp^{82} through Arg^{90}. Sequencing of this peptide could be completed throughout with only the round at Tyr^{83} giving no identifiable residue. Compositional analysis of this peptide was in agreement with the peptide from Asp^{82} to Arg^{90} with the exception that the single Tyr residue was missing. This indicates that the photoinsertion is into the tyrosine side chain. This data was found to be in agreement with X-ray crystallographic results identifying the NAD+-binding domains.

INTRODUCTION

Conservation of a three-dimensional domain responsible for coenzyme binding has been demonstrated for a number of dehydrogenases by X-ray crystallography at a high resolution (*1–4*). A comparison of the structures of those dehydrogenases revealed that the coenzyme domain consists of several short stretches of parallel β-pleated sheets flanked by helices. The NAD+-binding domain of GDH has been proposed by combination of secondary structure predictions and sequence comparisons with other dehydrogenases of known structure (*5*, *6*). Crystallographic structure determination of GDH would be desirable to confirm the existence of a similar domain. To date the crystallization of mammalian GDHs in a form suitable for X-ray analysis has not been accomplished. However, the crystal structure of glutamate dehydrogenase from *Clostridium symbiosum* at 0.6-nm resolution has been reported (*7*). The similarity between the electron micrographs for the bovine enzyme and the X-ray structure of the bacterial enzyme support a similar three-dimensional structure of the two enzymes. This indicates that there may exist structural homology between NAD+-binding domains of these dehydrogenases, although a high-resolution structure analysis would be necessary to confirm the relationship.

In previous reports 2N_3NAD+ was shown to be a valid active-site probe for bovine liver GDH and IL-2 (*8*, *9*). By using enzyme photolabeled with this probe it should be possible to isolate and identify the active site peptides of dehydrogenases and other proteins that interact with the adenine ring of NAD+. This could be used to confirm the general binding site assignments obtained from X-ray crystallography and support the contention that the crystallized structure is very similar to the solubilized form. Also, it would verify the use of 2N_3NAD+ as a general probe for the active site peptides that interact with the adenine ring of NAD+.

A major problem encountered when trying to identify the peptides photolabeled with nucleotide photoaffinity probes is the lability of the photoinserted group (*10*). This is particularly true when photolabeled peptides are subjected to HPLC techniques where it is most often observed that the photoinserted radiolabel is lost on initial binding to the column and elutes in the void volume (*11*). Consequently, very few photolabeled peptides have been purified by HPLC that retain a convincing percentage of the initial photoinserted radiolabel to unequivocally allows their identification as the major photolabeled site in the protein from which they were derived. To resolve this problem our laboratory has concentrated on procedures that take advantage of the incorporated, highly negatively charged photoprobe by using such techniques as anion-exclusion chromatography (*11*). HPLC techniques are avoided except in the final step to verify the purity of the isolated peptide(s). In this study the availability of *cis*-hydroxyls on the two ribose moieties of the photoinserted NAD+ analogue indicated that the use of immobilized boronate column chromatography would aid in the isolation of the photolabeled peptides. This would be of considerable value since many of the photolabeled peptides our laboratory has worked with lose the photoinserted radiolabel when subjected to HPLC. The techniques described herein were very effective for isolating the photolabeled peptides in pure form using only one column procedure. Surprisingly, after purification on boronate columns, the

* To whom correspondence should be addressed.
† This work was supported by research grant GM-35766 from the National Institutes of Health.

‡ Abbreviations used: 2N_3NAD+, nicotinamide 2-azidoadenosine dinucleotide; SDS–PAGE, sodium dodecyl sulfate–polyacrylamide gel electrophoresis; GDH, glutamate dehydrogenase; LDH, lactate dehydrogenase; EDTA, ethylenediaminetetraacetic acid.

1043-1802/91/2902-0142$02.50/0 © 1991 American Chemical Society

majority of the photoinserted radiolabel remained attached during HPLC analysis. Also, since only the photolabeled peptide was isolated, the amino acid residue where photoinsertion occurred was easily identified. This technique should have good general application for investigating the NAD^+ binding sites of several enzymes.

EXPERIMENTAL PROCEDURES

Materials. Bovine liver glutamate dehydrogenase was obtained from Sigma as a solution in 50% glycerol and used without further purification. The protein concentration was determined by using $E_{280nm}^{1\%} = 8.9$ (*12*), and a molecular weight of 56 100 for the monomer was used in the calculations. Porcine muscle lactate dehydrogenase was purchased from Boehringer/Mannheim Corp. as a solution in 50% glycerol and stored at 4 °C. $E_{280nm}^{1\%} = 14.5$ was used for the protein concentration. TPCK-trypsin was purchased from Sigma. [(Dihydroxyboryl)-phenyl]succinamyl derivatives of aminoethyl polyacrylamide (Affi-gel 601) were obtained from Bio-Rad Laboratories. Phenyl boronate–agarose Matrex Gel PBA-30 was from Amicon. 2-Azido-NAD^+ and [^{32}P]-2-azido-NAD^+ were synthesized as previously described (*8*).

Methods. Analytical Photoaffinity Labeling of LDH. Five micrograms of enzyme were photolyzed in 30 μL of the buffer 50 mM Tris–acetate, pH 7.0, in the presence of 50 mM oxalate. Samples were incubated at room temperature for 5 min, then placed on ice and irradiated for 3 min with a Spectroline medium-wave ultraviolet lamp (302 nm, 6.4 mW/cm^2) at a distance of 5.5 cm. The reaction was stopped by addition of a half-volume of a protein-solubilizing mixture which consisted of 6% SDS, 30% glycerol, 0.2 M Tris–HCl, pH 6.8, 1.5% 2-mercaptoethanol, and 0.003% bromophenol blue. Aliquots of sample (2 μg of protein) were analyzed by 10% SDS–PAGE. The protein bands were cut from the gel and the radioactivity was measured by liquid scintillation counting as previously reported (*8*).

Photoaffinity Labeling of GDH and Isolation of Photolabeled Peptide. Bovine liver GDH (1 mg/mL, 17.8 μM subunit) was incubated with 50 μM [^{32}P]-2-azido-NAD^+ on ice in the presence of 12 mM glutarate and 1 mM GTP in 10 mM Tris–acetate buffer, pH 8.0, containing 10 μM EDTA. In each experiment, 10 mg of protein was photolabeled in a volume of 10 mL placed in a plastic weighing boat that gave a solution depth of less than 0.3 mm. After 5 min of incubation, the enzyme solution was irradiated for 3 min with the UV lamp as described above. Completion of photolysis of the photoprobe was determined by UV spectroscopy. The photoaffinity-labeling reaction was quenched by addition of dithiothreitol to a final concentration of 25 mM. The photolabeled protein was precipitated with ammonium sulfate (80% saturation) to remove excess unbound ligand. The resulting precipitate was desalted by gel filtration on Sephadex G-25 equilibrated with 0.1 M ammonium bicarbonate.

Urea was added to 2 M to the protein sample followed by digestion with 2% TPCK-trypsin (w/w) at room temperature overnight. The tryptic digest was applied to a 3-mL Affi-gel 601 column, equilibrated with 0.1 M ammonium acetate buffer, pH 8.8, and washed with the same buffer to elute the unmodified peptides. When the UV absorbance reached a minimum, a pH gradient (8.8–5.5) of 200 mL of 0.1 M ammonium acetate was started to elute the photolabeled peptide retained on the column. The location of the photolabeled peptide was followed by monitoring the UV absorbance and the radioactivity profile of the eluant.

Photoaffinity Labeling of LDH and Isolation of Photolabeled Peptide. LDH (1 mg/mL, 28.6 μM subunit) was incubated with 50 μM [^{32}P]-2-azido-NAD^+ in 100 mM Tris–acetate, pH 7.0, and 50 mM oxalate at room temperature for 5 min. The protein sample (10 mg) was placed on ice and photolyzed as above. After addition of dithiothreitol to 25 mM concentration, 100 μg of TPCK-trypsin was added to the protein solution and digestion was continued overnight at room temperature. The total digest was applied onto a 10-mL PBA-30 column, equilibrated in 0.1 M ammonium acetate, pH 8.8. After elution of photolabeled peptide with a pH gradient as described above, the radioactive pool was lyophilized and further analyzed by HPLC.

Separation of Photolabeled Peptides by HPLC. The pooled fractions which contained the radioactive photolabeled peptide were analyzed by reverse-phase HPLC (LKB, equipped with a diode-array spectral detector) with a Brownlee Lab Aquapore RP 300 C-8 column (4.6 mm × 25 cm) developed with a gradient of increasing acetonitrile concentration in 0.1% trifluoroacetic acid.

Analysis of Isolated Peptides. The photolabeled peptides were characterized by analysis of amino acid composition on a Beckman 6300 high performance amino acid analyzer. The amino acid sequence of the peptides was determined on an Applied Biosystem 477A pulse liquid protein sequencer with on-line identification of phenylthiohydantoin amino acids. Each experiment reported in this paper has been repeated a minimum of three times.

RESULTS

Purification of Photolabeled Peptides of GDH. To minimize the extent of nonspecific photoinsertion and at the same time to optimize the specific labeling of the enzyme, 50 μM [^{32}P]$2N_3$NAD$^+$ was used, which is the concentration at which photoincorporation approaches saturation. In addition, 1 mM GTP and 12 mM glutarate were included in the reaction mixture, since they were shown to increase the binding affinity of NAD^+ and $2N_3$-NAD^+ to GDH (*8*). Under these conditions, 40–60% of the enzyme incorporated photolabel as determined by both a decrease in enzyme activity and incorporation of radiolabel. In the previous report it was demonstrated that $2N_3NAD^+$ specifically photolabeled the coenzyme binding site of bovine liver glutamate dehydrogenase. To identify the site of photoinsertion, enzyme was digested with trypsin to produce peptides. Taking advantage of the existence of the two *cis*-hydroxyl groups on the ribose groups of the photoincorporated probe, the photolabeled peptide was isolated by using immobilized boronate column chromatography. The UV and radioactivity profiles of tryptic peptides from the boronate column are shown in Figure 1. All of the unlabeled peptides were eluted with ammonium acetate buffer, pH 8.8, in the void volume as determined by HPLC analysis (data not shown). However, photolabeled peptides were selectively retained on the column. These radioactive peptides were eluted with a pH gradient of 8.8–5.5 and subjected to reverse-phase HPLC (Figure 2). A major peak in both the UV and radioactivity profile at 33 min was obtained. The radioactive flow-through fraction contains unbound probe including any decomposition product of photoadduct produced as peptide binds to the HPLC column matrix. These flow-through fractions, covering 4–7 min, were subjected to analysis and no significant amounts of amino acids were detected. The major peak containing peptide and radiolabel also showed an unusual spectrum with an absorbance maximum at 264 nm, presumably due to the

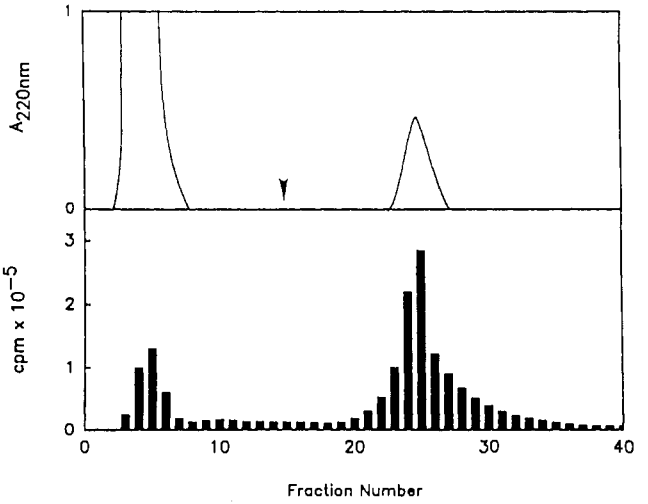


Figure 1. Purification of photolabeled peptide from GDH on a boronate column. Tryptic digests of 10 mg of 2-azido-NAD$^+$-labeled GDH were applied to a 3-mL boronate column, equilibrated in 0.1 M ammonium acetate buffer. Unmodified peptides were eluted with the same buffer and photolabeled peptide was eluted with a 200-mL gradient of pH 8.8–5.5 0.1 M ammonium acetate. Fractions (3 mL) were monitored for absorbance at 220 nm and for radioactivity.

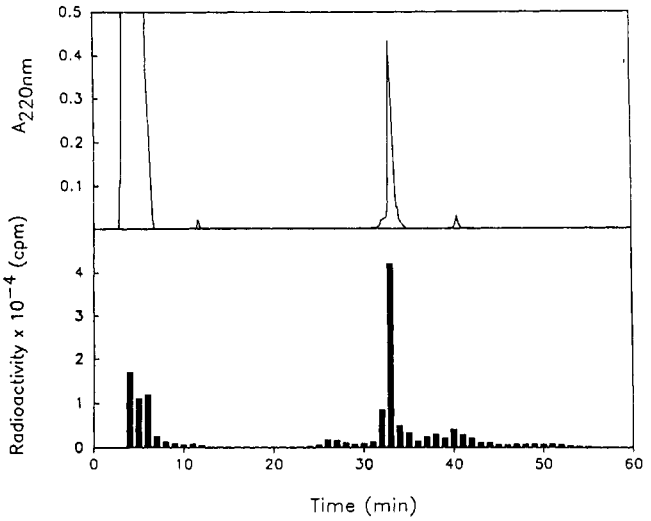


Figure 2. C-8 HPLC purification of the GDH peptide obtained after the boronate column chromatography step. The volume of pooled peak fractions was reduced to 1 mL by evaporation. Sample was injected into a C-8 HPLC column and the profile was developed with a linear gradient of solvent B (70% CH_3CN) into solvent A (0.1% trifluoroacetic acid) (10–50% B for 60 min). The flow rate was 1.0 mL/min, and fractions were collected every 1.0 min and levels of ^{32}P determined by liquid scintillation counting in aqueous phase.

covalently attached NAD$^+$ photoprobe. This is shown in Figure 3A, where it is compared to the spectrum of a typical unmodified GDH peptide with an absorbance maximum at 276 nm (Figure 3B). The shift from the expected 280 nm maximum may be due to some solvent interference.

Amino acid sequence analysis revealed that the peak fraction contained the amino acid sequence X-Val-Ala-Val-Gly, which was identified as residues 270–274 of the protein as judged by comparison with the known amino acid sequence of bovine liver GDH (*13*). The sequence data gave the following picamole amounts of the indicated residue at each cycle: 1; no detected residue (Cys expected), 2; 2612 of Val, 3; 1939 of Ala, 4; 2043 of Val, 5; 112 of Gly, 6; 102 of Gly 7; 100 of Gly. After cycle 5 only Gly was seen and it slowly bled down to where at cycle 20 the amount of Gly was 40 pmol. Since these are tryptic digests, it was

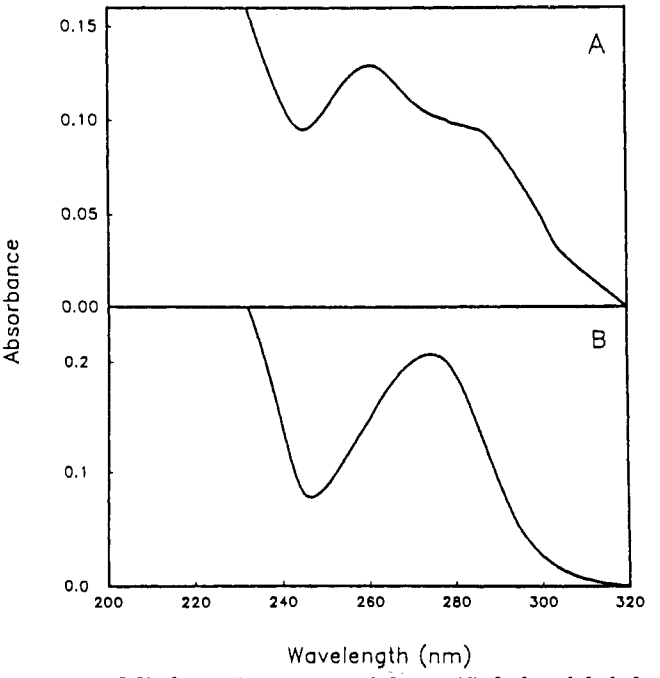


Figure 3. UV absorption spectra of the purified photolabeled peptide from GDH (A) and a typical unmodified GDH tryptic peptide (B).

Table I. Amino Acid Analysis of the Isolated GDH Peptides

amino acid	predicted	determined[a]	amino acid	predicted	determined[a]
Asx	4	4.34 (4)[b]	Met	0	0.03 (0)
Thr	0	0.07 (2)	Ile	2	1.83 (2)
Ser	2	1.78 (2)	Tyr	0	0.04 (0)
Glx	1	0.22 (0)	Phe	0	0.21 (0)
Pro	2	2.41 (2)	His	0	0.00 (0)
Gly	3	3.02 (3)	Lys	1	0.98 (1)
Ala	1	1.00 (1)	Arg	0	0.04 (0)
Val	2	1.85 (2)	Trp	1	N/D[c]

[a] Normalized values. [b] Nearest integer. [c] Not detected. Destroyed during hydrolysis.

expected to produce a sequence ending with Lys^{289}. However, the peptide could not be sequenced beyond Gly^{274}. The amino acid composition of the major peptide revealed that the peptide had a composition that was compatible with that of the tryptic peptide spanning residues 270–289 with the exception of Glu, where a significant reduction of recovery was seen (Table I). Trp and Cys could not be quantified because they are destroyed during acid hydrolysis. The amino acid composition data implied that the entire sequence from 270 to 289 was present but that sequencing aborts after Gly^{274}. This is supported by the rapid reduction of yields of phenylthiohydantoin amino acid residues observed from cycle 4 to 5 (2043 pmol to 112 pmol). Cycles 6–20 gave Gly at about 100–40 pmol per cycle. No other residues were released. Thus, sequencing of the peptide was prevented beyond Gly^{274} and this Gly residue bled off slowly presumably because modifications by $2N_3NAD^+$ occurred in the vicinity of Gly^{274}. The result from the amino acid analysis suggests Glu^{275} is the site of modification with the exact site of modification being in the peptide backbone between Gly^{274} and Glu^{275}. The side chain of Glu^{275} is an unlikely place of modification because modification at such a position should not abort sequencing of Gly^{274}. Since the picamole drop from cycle 4 to 5 was about 95% it is also

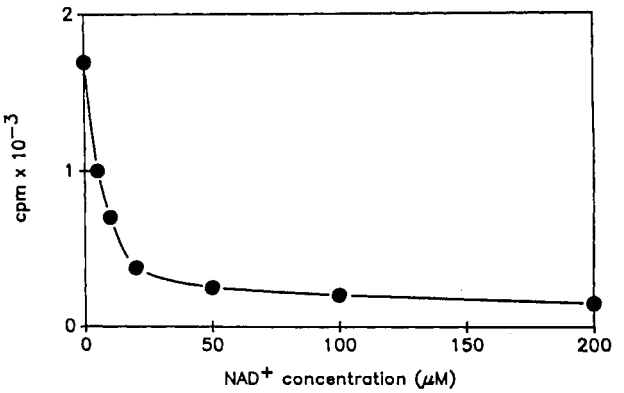


Figure 4. Protection against photolabeling of LDH by [^{32}P]-2-azido-NAD$^+$ in the presence of increasing concentrations of NAD$^+$. The concentration of [^{32}P]-2-azido-NAD$^+$ was 10 μM. Each photolabeling reaction was performed in 50 μL containing 50 mM HEPES, pH 7.0, buffer in the presence of 50 mM oxalate and 5 μg of enzyme. The photolabeling procedure and methods of analysis are described in Materials and Methods.

unlikely that Cys^{270} or Trp^{281} was also modified, and their absence is due to their known lability to the procedures used.

Specific Photolabeling of LDH. To demonstrate specific active site labeling of LDH, the enzyme was photolabeled with [^{32}P]2N$_3$NAD$^+$ in the presence of increasing NAD$^+$ concentrations. The presence of the natural ligand should prevent the photoincorporation of 2N$_3$NAD$^+$ into the active site at physiologically relevant concentrations. It was found that the inclusion of oxalate, which serves as a cosubstrate analogue, greatly increases the affinity of LDH for NAD$^+$ and 2N$_3$NAD$^+$ improves the efficiency of photolabeling of LDH. The results of the competition experiments are shown in Figure 4. The apparent K_d of NAD$^+$ for LDH is estimated to be about 5 μM in the presence of 50 mM oxalate. Without oxalate, NAD$^+$ binds to muscle LDH with a K_d of about 600 μM (*14*). The efficiency of 2N$_3$NAD$^+$ photoinsertion into LDH was determined to be over 50% by using previously reported procedures (*8*).

Purification of Photolabeled Peptides of LDH. Similar procedures were followed to obtain the photolabeled peptide from LDH, as was done for GDH. The exception was that the ammonium sulfate precipitation step used to remove unbound radiolabel was omitted. Reverse-phase HPLC analysis demonstrated the purity of photolabeled peptide obtained (Figure 5). The increase of the radioactivity in the flow-through fractions was due to the presence of the excess unbound photoprobe that was not removed prior to the trypsin digestion step by the ammonium sulfate precipitation step. Amino acid analysis confirmed the absence of any peptide in the flow-through fractions. Again, the photolabeled peptide exhibits a unique UV spectrum with an absorbance maximum at 264 nm similar to the one observed in Figure 3A (Figure 6).

From amino acid sequence determination and comparison with the known amino acid sequence of pig muscle LDH (*15*), the isolated peptide was identified as a fragment from Asp^{82} to Arg^{90}. However, at cycle 2, where the derivative of Tyr^{83} was expected, no standard PTH derivative was observed. Cycles 3 through 7 gave Asn, Val, Thr, Ala, and Asn at 491-, 241-, 90-, 37-, and 10-pmol levels, respectively. Accordingly, Tyr^{83} is presumed to be the residue which is covalently modified by 2N$_3$NAD$^+$. In this case the exact site of modification is probably the aromatic ring of the tyrosine rather than the peptide backbone since the sequencing did not stop at this residue

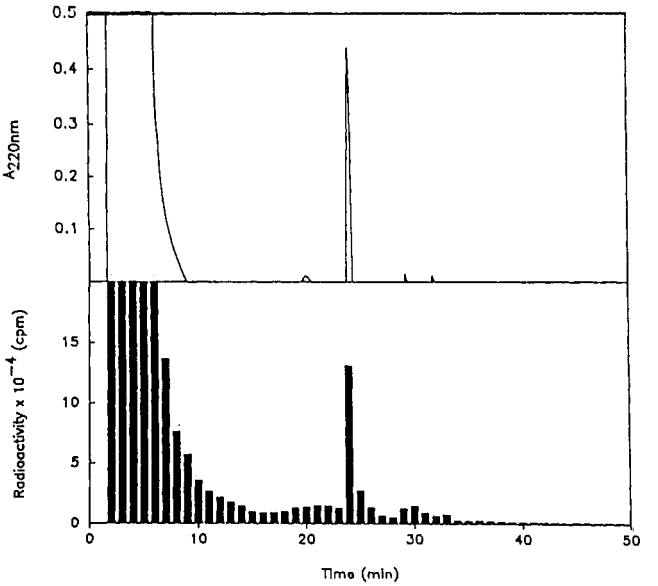


Figure 5. C-8 HPLC profile of LDH peptide obtained after a PBA-30 column chromatography. The peak fractions eluted from PBA-30 column were applied to a C-8 reverse-phase column at a flow rate of 1.0 mL/min. The profile was developed with a linear gradient of solvent B to solvent A (0–10 min, 0% B; 10–60 min, 0–60% B). Fractions were collected every 1.0 min and ^{32}P levels determined by liquid scintillation in the aqueous phase.

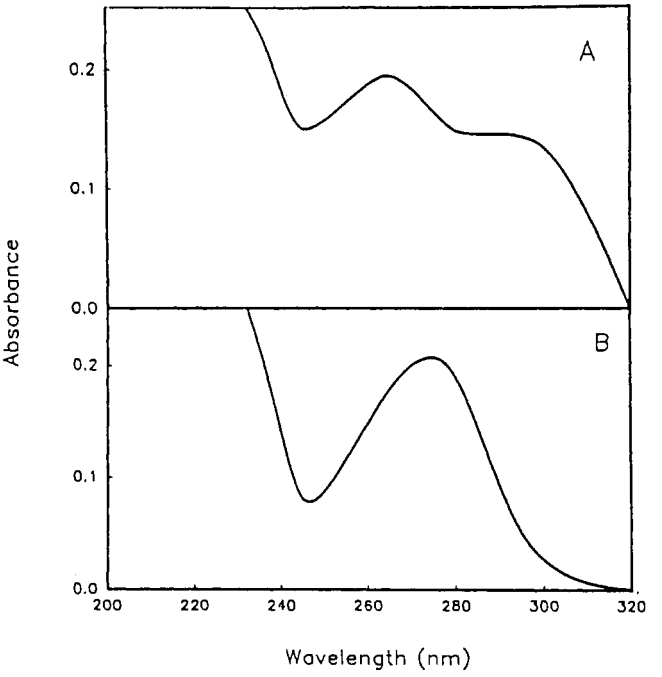


Figure 6. UV absorption spectra of the purified photolabeled peptide from LDH (A) and a typical unmodified tryptic peptide (B) also from LDH.

as occurred at the Glu residue in GDH. In order to further demonstrate that Tyr^{83} was the site of modification, the amino acid composition analysis was performed and the result is shown in Table II. The absence of a tyrosine residue was evident in the analysis data while other residues were recovered nearly quantitatively. Thus, both the amino acid sequencing and composition data are compatible with the interpretation that Tyr^{83} in porcine LDH is the site of covalent photoinsertion of 2N$_3$NAD$^+$.

None of the derivatives recovered after gas-phase sequencing were detectably radioactive in either GDH or LDH. Most of the loaded radioactivity remained bound to the sequencing filter. The high polarity of azido-NAD$^+$

Table II. Amino Acid Analysis of the Isolated LDH Peptide

amino acid	predicted	determined[a]	amino acid	predicted	determined[a]
Asx	3	3.14 (3)[b]	Val	1	1.12 (1)
Thr	1	0.91 (1)	Met	0	0.17 (0)
Ser	1	1.01 (1)	Ile	0	0.05 (0)
Glu	0	0.16 (0)	Leu	0	0.06 (0)
Pro	0	0.00 (0)	Tyr	1	0.00 (0)
Gly	0	0.34 (0)	Lys	0	0.04 (0)
Ala	1	1.08 (1)	Arg	1	1.00 (1)

[a] Normalized values. [b] Nearest integer.

may prevent extraction of the modified derivatives from the filter by organic solvents. It has been observed that the PTH derivative of amino acid residues modified by photo-cross-linking would not be detected during gas-phase sequencing (*16*).

DISCUSSION

NAD^+ is an important nucleotide that is utilized by a wide variety of enzymes to meet the synthetic, regulatory, and energetic needs of a cell. The fluctuation of levels of such enzymes, their structures, cellular location, membrane sidedness, etc. is therefore of importance in many areas of cell research. With two important NAD^+-utilizing enzymes the validation of $2N_3NAD^+$ as an active site directed probe has been established. This probe can be used to detect NAD^+-binding proteins in crude homogenates or to determine the peptide regions and amino acid residues located in the adenine-binding domain. The latter was accomplished by using the following procedures. After trypsin digestion of GDH and LDH photoaffinity labeled with $[^{32}P]2N_3NAD^+$, the modified peptides were isolated by using immobilized boronate column chromatography. The high specificity of the immobilized boronate ligand for *cis*-diol containing compounds has been utilized for chromatographic separations of a great number of biological substances. It has been shown that immobilized boronates can be used to fractionate adenine and pyridine nucleotides (*17, 18*). They also have been successfully used to isolate nucleosidyl peptides (*19–21*). By using a pH gradient elution, a single homogeneous radiolabeled peptide suitable for amino acid sequence determination was obtained from each enzyme. The purified photolabeled peptides exhibited a highly unusual UV spectrum with a maximum absorption of 260–264 nm and a shoulder near 280 nm, which verifies that an adduct of the NAD^+ photoprobe is still covalently attached to the peptide.

The active site peptide of GDH identified in this work is located within the proposed NAD^+-binding domain of bovine liver GDH spanning the residues 245–280 (*5, 22*). A sequence (Cys^{270}–Lys^{289}) is shown to be photolabeled by 2-azido-NAD^+. Therefore, this sequence is expected to interact with the adenine ring of the coenzyme. A part of this sequence spanning from Cys^{270} to Glu^{275} is predicted to form a β-pleated sheet (bB) which constitutes one of the six strands of parallel sheet found in the NAD^+-binding domain. On the basis of information obtained on the amino acid sequence determination and composition analysis of the isolated labeled peptide, we propose that the attachment site of 2-azido-NAD^+ is located at the peptide backbone between Gly^{274} and Glu^{275}.

Others have reported that the invariant, functional residue, Asp, is found in the bB region of four known dehydrogenases and is conservatively changed to Glu^{275} in GDH (*5*). This is based on the three-dimensional alignment of the common nucleotide-binding structure in dehydrogenases, on primary sequence homology. Crystallographic studies suggest that Asp in LDH and other dehydrogenases is involved in forming a hydrogen bond with the O-2′ hydroxyl of the adenine ribose and its potential to interact with the N-3 of adenine is also suggested (*23–25*). It is known that GDH utilizes either NAD^+ or $NADP^+$ as a substrate with almost equal efficiencies whereas LDH uses only NAD^+. It is therefore unlikely that Glu^{275} in GDH plays a role in forming a hydrogen bond with the O-2′ atom, as Asp does in LDH, because the carboxylate moiety of Glu^{275} moving close to the 2′-phosphate would lead to charge repulsion. Therefore, Glu^{275} is more likely to interact with the adenine N-3 position and it may do this through the amide linkage region. This may imply an important distinction between the two classes of dehydrogenases represented by GDH and LDH, respectively. It is also conceivable that the nitrene generated by the 2-azido group effectively inserts into this residue at the amide linkage when it is positioned close to the N-3 atom.

The presence of an additional NAD^+ binding site for GDH has been suggested by a number of investigators (*26–28*). This second site has a low affinity for NAD^+, is unaffected by cosubstrate addition, and is suspected to be a regulatory site. The possibility of photolabeling such a site was eliminated in this study because at the concentration of $2N_3NAD^+$ used, in the presence of cosubstrate, there is approximately one coenzyme molecule bound per subunit according to the equilibrium dialysis data and this is at the catalytic site (*29*).

The validity of the results obtained with GDH was further supported by identification of the NAD^+-binding site of porcine muscle LDH, whose X-ray structure has been determined at a high resolution. The site of photolabeling identified was located within the well-characterized coenzyme binding domain Asn^{22}–Cys^{165} of dogfish LDH (*23*). The sequence photolabeled in porcine LDH, Asp^{82}–Arg^{90}, is located at the connection between the two parallel strands of β-sheet structure, bC and bD. Furthermore, the determined site of attachment, Tyr^{83}, is thought to be one of the amino acid residues lining the domain involved in adenosine binding. In porcine LDH Tyr^{83} corresponds to Tyr^{85} of dogfish LDH. Tyr^{85} of dogfish LDH is proposed to interact with the N-1 of adenine through a hydrogen bond (*25*), which places it adjacent to the azide at the 2-position. Therefore, it is not contrary to expectation that Tyr^{83} of porcine LDH was photolabeled instead of Asp^{53}, which corresponds in three-dimensional orientation to Glu^{275} of GDH, considering the different roles in binding of Asp and Glu in these enzymes and the position of Tyr^{83}.

The results with porcine LDH show that Tyr^{83} is the site of modification by $2N_3NAD^+$ and this corresponding residue is proposed to be involved with hydrogen-bond formation with the N-1 position of adenine in dogfish LDH (*25*). It is therefore in very close proximity, being approximately only one carbon–nitrogen bond length away.

The situation with GDH is not quite as clear but does give some very interesting information. First, the Glu^{275} that is modified corresponds to an Asp residue that is highly conserved in several other dehydrogenases that will not utilize $NADP^+$ effectively, e.g. LDH, LADH, and GADPH. With these dehydrogenases Asp is proposed to be involved in hydrogen-bond formation with the O-2′ atom of the ribose group which could not be occurring, due to charge repulsion, with $NADP^+$. This probably accounts for the inability of $NADP^+$ to be a substrate for these dehydrogenases whereas it is a good substrate for GDH. This concept is supported by the observation that

the equivalent position of Glu^{275} in $NADP^+$ specific dihydrofolate reductase is replaced by a positively charged Arg residue. It is likely that the reason for the Glu replacement for Asp in GDH is to produce a different active site conformation that allows both NAD^+ and $NADP^+$ binding. The positioning of Glu^{275} near the N-3 position of the adenine ring (*7*, *25*) would place it approximately one carbon–nitrogen bond length away from the nitrene produced on $2N_3NAD^+$. Apparently, the orientation of the binding site in GDH is such that efficient photoinsertion occurs into Glu at the peptide backbone. It is very likely that the photoinsertion site is at the nitrogen of the amide linkage since (i) compositional analysis shows totally intact Gly but no Glu residues (ii) and sequential analysis shows Gly being slowly released with no Glu being released at all.

The data obtained from the sequence analysis of the $2N_3NAD^+$ photolabeled peptides support the selectivity of photoinsertion of this probe into GDH and LDH as validated by saturation and protection experiments (*8*). It also demonstrates that appropriately designed photoaffinity-labeling experiments combined with additional techniques, which take advantage of the properties of the photoinserted probe, will allow the isolation and sequencing of peptides in the binding domain and, at times, the determination of the exact amino acid residues involved. For NAD^+-binding proteins it is suggested that the technique used in this research will be of general utility. Additionally, we found that $8N_3GTP$ and $2N_3ADP$ mimic the allosteric properties of GTP and ADP in GDH with regard to NAD^+ binding. They also effectively photoinsert into GDH and are currently being used to determine the binding domains of GTP and ADP, respectively.

LITERATURE CITED

(1) Adams, M. J., Ford, G. C., Koekoek, R., Lentz, P. J., McPherson, A., Rossmann, M. G., Smiley, I. E., Schevitz, R. W., and Wonacott, A. J. (1970) *Nature (London) 227*, 1098–1103.

(2) Hill, E., Tsernoglou, O., Webb, L., and Banaszak, L. J. (1972) *J. Mol. Biol. 72*, 577–591.

(3) Eklund, H., Nordstrom, B., Zeppezauer, E., Soderlund, G., Ohlson, I., Boiwe, T., Soderberg, B. O., Tapia, O., Branden, C. I., and Akeson, A. (1976) *J. Mol. Biol. 102*, 27–591.

(4) Buehner, M., Ford, G. C., Moras, D., Olsen, K. W., and Rossmann, M. G. (1974) *J. Mol. Biol. 90*, 15–49.

(5) Rossmann, M. G., Moras, D., and Olsen, K. W. (1974) *Nature (London) 250*, 194–199.

(6) Wo otton, J. C. (1974) *Nature (London) 252*, 542–546.

(7) Rice, D. W., Baker, P. J., Farrants, G. W., and Hornby, D. P. (1987) *Biochem. J. 242*, 789–795.

(8) Kim, H., and Haley, B. E. (1990) *J. Biol. Chem. 265*, 3636–3641.

(9) Campbell, S., Kim, H., Doukas, M., and Haley, B. (1990) *Proc. Natl. Acad. Sci. U.S.A. 87*, 1243–1246.

(10) Lewis, C. T., Haley, B. E., and Carlson, G. M. (1989) *Biochemistry 28*, 9248–9255.

(11) King, S. M., Kim, H., and Haley, B. (1991) *Methods Enzymol. 196*, 449–466.

(12) Egan, R. R., and Dalziel, K. (1971) *Biochim. Biophys. Acta 250*, 47–50.

(13) Moon, K., Piszkiewicz, D., and Smith, E. L. (1972) *Proc. Natl. Acad. Sci. U.S.A. 69*, 1380.

(14) Stinson, R. A., and Holbrook, J. J. (1973) *Biochem. J. 131*, 719–728.

(15) Kiltz, H. H., Keil, W., Griesbach, M., Petry, K., and Meyer, H. (1977) *Hoppe-Seyer's Z. Physiol. Chem. 358*, 123–127.

(16) Knight, K. L., and McEntee, K. (1985) *J. Biol. Chem. 260*, 10185–10191.

(17) Gonzalez, R. A., Salinas, E. L., Jacobson, E. L., and Jacobson, M. K. (1983) *Anal. Biochem. 135*, 69–77.

(18) Moore, E. C., Peterson, D., Yang, L. Y., Yeung, C. Y., and Neff, N. F. (1974) *Biochemistry 13*, 2904–2908.

(19) Schmidt, J. A., and Coleman, R. F. (1984) *J. Biol. Chem. 259*, 14515.

(20) Bates, S. P., and Coleman, R. F. (1986) *Biochemistry 25*, 3508.

(21) Bailey, J. M., and Coleman, R. F. (1987) *J. Biol. Chem. 262*, 12620.

(22) Wooton, J. C. (1974) *Nature (London) 252*, 542–546.

(23) Rossmann, M. G., Liljas, A., Branden, C.-I., and Banaszak, L. J. (1975) *The Enzymes*, 3rd ed., Vol. XI, pp 61–102, Academic Press, New York.

(24) Grau, U. M. (1982) *The Pyridine Nucleotide Coenzymes*, pp 135–187, Academic Press, New York.

(25) Holbrook, J. J., Liljas, A., Steindel, S. J., and Rossmann, M. G. (1975) *The Enzymes, 3rd ed.*, Vol. XI, pp 191–292, Academic Press, New York.

(26) Bayley, P. M., and O'Neil, K. T. (1980) *Eur. J. Biochem. 112*, 521–531.

(27) Smith, T., and Bell, J. E. (1982) *Biochemistry 21*, 733–737.

(28) Banjeree, A., Levy, H. R., Levy, G. C., LiMuti, C., Golstein, B. M., and Bell, J. E. (1987) *Biochemistry 26*, 8443–8450.

(29) Dalziel, K., and Egan, R. R. (1972) *Biochem. J. 126*, 975–984.

Conjugation of *p*-Aminophenyl Glycosides with Squaric Acid Diester to a Carrier Protein and the Use of Neoglycoprotein in the Histochemical Detection of Lectins[1]

Lutz F. Tietze,*,† Claudia Schröter,† Sigrun Gabius,§ Ulrich Brinck,‖ Ada Goerlach-Graw,† and Hans-Joachim Gabius‡

Institut für Organische Chemie, Tammannstrasse 2, D-3400 Göttingen, FRG, Max-Planck-Institut für Experimentelle Medizin, Abteilung Chemie, Hermann-Rein-Strasse 3, D-3400 Göttingen, FRG, Medizinische Universitätsklinik, Abteilung Hämatologie-Onkologie, Robert-Koch-Strasse 40, D-3400-Göttingen, FRG, and Zentrum Pathologie der Universität, Robert-Koch-Strasse 40, D-3400 Göttingen, FRG. Received November 26, 1990

The coupling of *p*-aminophenyl 2-acetamido-2-deoxy-3-*O*-β-D-galactopyranosyl-β-D-galactopyranoside (gal-β 1,3-galNAc) to bovine serum albumin (BSA) was achieved by using 1,2-diethoxycyclobutene-3,4-dione (squaric acid diester) as a new coupling reagent. Two selective consequential steps afforded the desired neoglycoprotein: reaction of the *p*-aminophenyl group of gal-β 1,3-galNAc with squaric acid diester gave the corresponding squaric acid amide ester, which was transformed into the BSA conjugate by coupling with the lysyl ε-amino groups of BSA through formation of a squaric acid 1,2-bisamide. The experimental conditions for the reactions and the optimization of average were performed by using *p*-anisidine as model substance, the methyl group substituting for the carbohydrate part of a *p*-aminophenyl glycoside. Neoglycoproteins have proven to be valuable tools for lectin detection. To evaluate the properties of this type of probe, the obtained neoglycoprotein with the histochemically crucial T-antigen structure was used for glycocytological and glycohistochemical studies. Three cultured human tumor cell lines and tissue sections from human breast carcinomas were chosen. Its efficiency was similar in comparison to measurements with a probe, derived by diazotization with the *p*-aminophenyl glycosides of gal-β 1,3-galNAc and already shown to be a reliable marker for lectin localization in tissue sections and cultured cells.

INTRODUCTION

The coupling of carbohydrates onto proteins is of great interest, because the obtained synthetic sugar–protein conjugates, termed neoglycoproteins, can be used as tools with target specificity to cells. Especially the histochemical application of neoglycoproteins has underlined the value of this class of synthetic probes to localize endogenous sugar-binding proteins (*1,2*). In general, the specific interaction of the carbohydrate part of glycoconjugates with receptors like lectins is supposed to be important for cell–cell interactions, growth regulation, and cell differentiation (*3–5*). Since endogenous lectins, too, have been detected in tumors, their histochemical mapping is of potential value for histopathology (*6*). Notably, the detection of endogenous lectins in tumors may reveal functional aspects of the alterations in abundance and structure of cellular glycoconjugates.

It has already been emphasized that the structure of the linker between protein and carbohydrate can markedly influence the potency of the neoglycoprotein to serve as a detection device for tissue lectins (*7*). Thus, any expansion of the array of methods for the attachment of carbohydrates to proteins should concomitantly be tested for the efficiency of the formed neoglycoprotein in protein–carbohydrate interaction.

In our concept (*8*) for the construction of selective anticancer agents we use acetal glycosides which consist of carbohydrates, aldehydes, or ketones and alcohols and are in fact nontoxic prodrugs of the cytotoxic aldehydes or ketones. These compounds are acid labile and they are cleaved preferentially in an acidic environment with liberation of the cytotoxic principle. Since it has been proven that the tumor tissue is selectively acidified under hyperglycemic conditions due to an increase of "aerobic" glycolysis (*9*), these compounds may be advantageous in the treatment of cancer. Thus, recently we have shown that by applying acetal glycosides of aldophosphamide and ketophosphamide at pH 6.2 (pH of malignant tissue under hyperglycemia) the cloning efficiency of cells is decreased by the factor of $>10^4$ compared to that at pH 7.4 (pH of normal tissue) (*10, 11*). On the other hand, the carbohydrates employed in these compounds may enhance their concentration in the tumor tissue by binding to tumor-associated lectins on the cell surface. This would increase the pH-dependent selectivity and thus additionally diminish toxic effects of the used chemotherapeutica on the normal cell population. Trisaccharides or disaccharides such as gal-β 1,3-galNAc (2-acetamido-2-deoxy-3-*O*-β-D-galactopyranosyl-β-D-galactopyranoside) may therefore be used as the carbohydrate part in the acetal glycosides. When immobilized onto a carrier to give a neoglycoprotein, the carbohydrate moieties of the carrier will participate in directing these compounds to certain types of organ and also to the tumor, as indicated in a model for tumor-bearing mice with an array of neoglycoprotein (*12*). To underline the usefulness of this concept we synthesized a BSA conjugate with *p*-aminophenyl gal-β 1,3-galNAc using a newly developed technique.

Our current study was prompted by the observation that 1,2-diethoxycyclobutene-3,4-dione (**2**; squaric acid di-

[1] Anticancer Drugs, Part 16. This work was supported by the Bundesminister für Forschung und Technologie (Förderkennzeichen 03189-52A9) and the Fonds der Chemischen Industrie. C.S. thanks the Fonds der Chemischen Industrie for a scholarship. Part 15, ref 13.

* To whom correspondence should be addressed.
† Institut für Organische Chemie.
‡ Max-Planck-Institut für Experimentelle Medizin.
§ Medizinische Universitätsklinik.
‖ Zentrum Pathologie der Universität.

1043-1802/91/2902-0148$02.50/0 © 1991 American Chemical Society

ester) can be used as an coupling reagent for low molecular weight amines (*13*). First, a monoamide is formed between the ligand and the squaric diester. This derivative is then attached to an amino group of another low molecular weight amine or a polymer like poly(L-lysine) via controlled formation of an 1,2-bisamide of the squaric acid. Because of the different high-wavelength absorptions (λ_{max}) of mono- and bisamides of squaric acid, the progress of the coupling reaction to poly(L-lysine) could be monitored by UV spectroscopy. By employing this scheme, amenable preparation of neoglycoproteins can thus be performed in a highly efficient and simple way.

In this paper we describe the use of this new method for the formation of neoglycoproteins with an 1,2-bisamide moiety as linker. For immobilization we have chosen the oncologically interesting disaccharide gal-β 1,3-galNAc to address the issue whether binding sites can effectively be localized. The concentration of protein and carbohydrate was determined by UV spectroscopy. 1,2-Bisamide **10** could be formed in two selective steps: by the amidation of squaric diester **2** with the primary *p*-aminophenyl group of glycoside **8** and then by amidation of the resulting monoamide **9** with the lysyl ϵ-amino groups and perhaps the amino terminal group of bovine serum albumin (BSA) **6** to form 1,2-bisamide **10**. In order to obtain information about the suitability of this linkage group within protein–carbohydrate recognition, we carried out glycocytological and glycohistochemical studies in comparison to the probe **11**, derived by diazotization of the *p*-aminophenyl glycoside of gal-β 1,3-galNAc. The probe has already proven its capacity to serve as a potent lectin-localizing marker (*14*).

EXPERIMENTAL PROCEDURES

General Procedures. ^{1}H and ^{13}C NMR spectra of chemical compounds were recorded on a Varian FT-80A for monoamide **3** and Varian XL 200 for 1,2-bisamide **5** and carbohydrate **9** in either DMSO-d_6 or acetone-d_6/D_2O as solvents with TMS as internal standard. Melting points were measured on a Reichert Heiztischmikroskop Model Kofler, and the data are corrected. Infrared spectra were recorded on a Bruker infrared spectrometer Model IFS 25. UV spectra were recorded on a Perkin-Elmer spectrophotometer Model Lambda 2. Mass spectra of monoamide **3** and 1,2-bisamide **5** were obtained on Varian MAT 311 mass spectrometer by using an electronic ionization energy of 70 eV. Microanalyses were performed by the Mikroanalytisches Laboratorium, Göttingen, FRG. Chromatographic separation of product **5** and **9** was carried out by "flash chromatography" with Machery, Nagel & Co. 0.032–0.063 silica gel. Chemical reactions were monitored by thin-layer chromatography using Machery, Nagel & Co. 0.25-mm silica gel TLC plates SILG/UV_{254}, and spots were determined under ultraviolet light (λ = 254 nm). The neoglycoproteins were purified with Pharmacia Sephadex G-25M columns (PD-10 columns) (diameter 1 cm, high 5 cm, bed volume 9.1 mL). Before using a new PD-10 column, it was washed with a 0.5% BSA solution (1–2 mL), and after use it was regenerated by washing with phosphate buffer, pH 7.3 (50 mL). Bidistilled water was used to prepare the phosphate buffer with pH 7.3. The buffer with pH 9.0, which was used for the coupling reaction, was bought from Merck, Puffer-Titrisol, Art. 9889 (Darmstadt, FRG). The carrier protein bovine serum albumin (BSA) was of the highest commercially available purity from Biomol (Ilvesheim, FRG). ABC kit was from Camon (Wiesbaden, FRG). The cell lines were obtained from the American Type Culture Collection (Rockville, MD). Solvents and reagents were purified by standard methods.

Synthesis of 1-[(*p*-Methoxyphenyl)amino]-2-ethoxycyclobutene-3,4-dione (3). To a stirred solution of *p*-anisidine (0.23 g, 1.87 mmol) in dry ethanol (2 mL) was added 1,2-diethoxycyclobutene-3,4-dione (0.55 mL, 3.73 mmol) at room temperature. Stirring was continued for 2 h (TLC, silica, ethyl acetate/light petroleum, 1/2) and the mixture was afterward concentrated under reduced pressure. Crystallization of the residue from hot dry methanol produced light yellow needles (0.34 g, 74%): mp 159–160 °C; thin-layer chromatography (silica, ethyl acetate/light petroleum, 1/2). R_f = 0.1; ^{1}H NMR (DMSO-d_6) δ 1.42 (t, J = 6 Hz, CH_3), 3.75 (s, OCH_3), 4.75 (q, J = 6 Hz, CH_2O), 7.10 (2 d, AA′BB′ system, δ_A = 6.90, δ_B = 7.30, J_{AB} = 8.0 Hz, $H_{aromatic}$), 10.60 (s, br, NH); ^{13}C NMR (DMSO-d_6) δ 15.6 (CH_3), 55.2 (OCH_3), 69.3 (CH_2O), 114.2 (C-$3_{aromatic}$, C-$5_{aromatic}$), 121.3 (C-$2_{aromatic}$, C-$6_{aromatic}$), 131.0 (C-$1_{aromatic}$), 156.2 (C-$4_{aromatic}$), 169.2, 177.3, 177.5, 177.6, 177.7, 183.2, 188.0 (cyclobutene-C); IR (KBr) 3270 (OH, NH), 3086 (aromatic-H), 2996, 2938 (CH_2, CH_3), 1798, 1696, 1616, 1582 (C=O, C=C), 1068, 1026 (C—O), 828 (aromatic-H) cm^{-1}; UV λ_{max} (methanol) 296 (log ϵ 4.413) and 221 nm (log ϵ 4.114); MS m/z 247 (89) $[M]^+$, 191 (11) $[M - 2\ CO]^+$, 163 (17) $[M - 2\ CO - C_2H_4]^+$, 134 (100) $[M - 2\ CO - C_2H_4 - OCH_3]^+$, 122 (13), 107 (17), 92 (19), 77 (29), 64 (18). Anal. Calcd for $C_{13}H_{13}NO_4$: C, 63.15; H, 5.30. Found: C, 63.07; H, 5.38.

Synthesis of 1-[(*p*-Methoxyphenyl)amino]-2-[[5-acetamido-5-(methoxycarbonyl)pentyl]amino]cyclobutene-3,4-dione (5). To a stirred solution of **3** (0.15 g, 0.61 mmol) in dry ethanol (6 mL) at room temperature was added triethylamine (1.5 mL) and *N*-1-acetyl-L-lysine methyl ester (0.19 g, 0.92 mmol). Stirring was continued for 90 min and the solvent removed under reduced pressure. Chromatographic purification of the residue (50 g of silica, *tert*-butyl methyl ether/light petroleum, 2/1) afforded 0.22 g (89%) of bisamide **5** as a light yellow solid; mp 288–290 °C dec; thin-layer chromatography (silica, chloroform/methanol, 10/1) R_f = 0.3; ^{1}H NMR (DMSO-d_6) δ 1.22–1.80 (m, 2′-H_2, 3′-H_2, 4′-H_2), 1.84 (s, NAc), 3.51–3.68 (m, 1′-H_2), 3.62 (s, CO_2CH_3), 3.75 (s, phenyl-OCH_3), 4.18–4.32 (m, 5′-H), 7.15 (2 d, AA′BB′-system, δ_A = 6.94, δ_B = 7.36, J_{AB} = 8.0 Hz, $H_{aromatic}$), 7.55 (s, br, N^2H), 8.22 (d, J = 8.0 Hz, NHAc), 9.51 (s, N^1H); ^{13}C NMR (DMSO-d_6) δ 22.0 (CH_3), 22.2 (C-3′), 30.1, 30.5 (C-2′, C-4′), 43.3 (C-1′), 51.5 (CH_3O), 51.7 (C-5′), 55.2 (phenyl-OCH_3), 114.4 (C-$3_{aromatic}$, C-$5_{aromatic}$), 119.6 (C-$2_{aromatic}$, C-$6_{aromatic}$), 132.1 (C-$1_{aromatic}$), 155.2 (C-$4_{aromatic}$), 163.6, 168.7, 169.2, 172.5, 180.3, 183.4 (cyclobutene-C, C=O); IR (KBr) 3280 (NH), 3056 (aromatic-H), 2952 (CH_2, CH_3), 1794, 1740, 1660, 1612 (C=O), C=C), 1586, 1544, 1516 (aromatic-H, NH), 1374 (CH_3CO), 828 (aromatic-H) cm^{-1}; UV λ_{max} (methanol) 229 (log ϵ 4.384) and 303 nm (log ϵ 4.470); MS m/z 403 (6) $[M]^+$, 175 (32), 173 (26), 138 (15), 84 (62), 73 (29), 44 (63). Anal. Calcd for $C_{20}H_{25}N_3O_6$: C, 59.54; H, 6.25. Found: C, 59.68; H, 6.23.

Coupling of 3 to BSA. The reactions were performed in Eppendorf tubes. To a solution of BSA (0.25 mL of 3.3 mg/mL = 5×10^{-5} M in buffer pH 9.0) dissolved in dimethyl sulfoxide (DMSO) was added dropwise with vigorous stirring a 10-fold to 100-fold molar excess of **3**. According to Table I model substance **3** was diluted in a concentration of 1 mg/83 μL in DMSO, and to achieve the respective molar excess the following microliters of this solution were added to 0.25 mL of BSA solution: (fold molar excess/microliters of DMSO solution with 1 mg/83 μL) control,

Table I. Ligand Attachment of BSA and Yields of BSA Conjugates, Determined by UV Spectroscopy and in Different Experiments

no.	no. of exp	molar excess of 3	average no. of ligands attached to BSA	average % yield of BSA conjugates
1	4	0	0.2 ± 0.1	90.5 ± 7.4
2	4	10	7.3 ± 1.3	77.5 ± 6.9
3	4	20	12.8 ± 1.5	63.8 ± 9.9
4	4	40	20.0 ± 2.2	57.3 ± 9.0
5	3	60	20.7 ± 2.5	60.3 ± 2.9
6	3	80	22.0 ± 2.5	56.0 ± 9.3
7	3	100	24.7 ± 2.6	52.0 ± 5.7

0/20 μL of pure DMSO; 10/2.57; 20/5.15; 40/10.29; 60/15.36; 80/20.50; 100/25.65. The reaction mixtures were frequently shaken 3–4 h at room temperature. The mixtures were individually processed by chromatography on PD-10 columns. The samples were given onto the columns and these were eluated with buffer (pH 7.3) (5 × 0.5 mL each). The eluate was thrown away. Eluation was continued using 3–4 × 0.5 mL of buffer for each column to give an eluate containing the coupling product **7**. For UV measurement the eluate of **7** was diluted with buffer [1 mL of eluate/buffer (pH 7.3), 1/2] and the absorbance was determined for each sample at λ = 270 and 310 nm.

Standard Curves and Calculation of the Molar Extinction Coefficients. For BSA 6. The standard curve was established at a wavelength of λ = 270 nm with BSA concentrations of 1–10 × 10^{-6} M (in buffer pH 7.3). The calculated extinction coefficient was ϵ_{270nm} = 31 100 M^{-1}.

For 1,2-Bisamide 5. The standard curves were measured at wavelengths of λ = 270 and 310 nm in the initially chosen concentration range of 1–7 × 10^{-5} M, because the concentration of the bisamide is 10-fold higher in the coupling product. The following extinction coefficients were calculated: ϵ_{270nm} = 10 500 M^{-1} and ϵ_{310nm} = 25 300 M^{-1}. Because of 1,2-bisamide **5** was not easily soluble in buffer, it was first dissolved in methanol (1 mL) and the solution was then diluted with buffer (pH 7.3). This standard solution was used.

Synthesis of *p*-[(4-Ethoxy-2,3-dioxocyclobut-1-enyl)amino]phenyl 2-Acetamido-2-deoxy-3-*O*-β-D-galactopyranosyl-β-D-galactopyranoside (9). To a stirred solution of *p*-aminophenyl 2-acetamido-2-deoxy-3-*O*-β-D-galactopyranosyl-β-D-galactopyranoside (*14*) (27.4 mg, 58 mol) in dry ethanol (10 mL) at room temperature was added dropwise 1,2-diethoxycyclobutene-3,4-dione (17 μL, 115 μmol). Stirring was continued for 10 h (TLC, chloroform/methanol/water, 13/8/2) and the mixture then concentrated under reduced pressure. Purification by chromatography (20 g of silica, chloroform/methanol/water, 13/8/2) afforded 20.6 mg (60%) of **9** as a light yellow solid: 187–188 °C dec; thin-layer chromatography (silica, chloroform/methanol/water, 13/8/2) R_f = 0.5; ^{1}H NMR (acetone-d_6/D_2O) δ 1.33 (t, J = 7.0 Hz, OCH_2CH_3), 1.90 (s, NAc), 3.20–4.02, 4.12–4.78 (2 m, 2-H, 3-H, 4-H, 5-H, 6-H_2, 1′-H, 2′-H, 3′-H, 4′-H, 5′-H, 6′-H_2), 4.68 (q, J = 7.0 Hz, OCH_2CH_3), 5.04 (d, J = 8.5 Hz, 1-H), 1.70 (AB system, δ_A = 6.98, δ_B = 7.22, J_{AB} = 8.0 Hz, $H_{aromatic}$); IR (KBr) 3422 (OH, NH), 2930 (CH_2, CH_3), 1806, 1714, 1618, 1588 (C=O, C=C), 1512 (NH), 1382 (CH_3CO), 832 (aromatic-H) cm^{-1}; UV λ_{max} (methanol) 295 (log ε 4.338) and 219 nm (log ε 4.042).

Coupling of 9 to BSA. To a stirred solution of BSA (18.2 mg, 2.75 × 10^{-4} mmol) in buffer solution (pH 9.0, 5.5 mL) was added dropwise at room temperature a solution of **9** (14 mg, 2.34 × 10^{-2} mmol) in DMSO (1.12 mL). After stirring for 3.5 h the mixture was given in 11 × 0.6 mL aliquots onto 11 separate PD-10 columns and product **10** was obtained in eluate portion of 2 mL per column. The total volume of product solution was 22 mL. For the UV determination 1.2 mL of the product solution was diluted with pH 7.3 buffer (product solution/buffer, 1/2) and the absorbance was measured by λ = 270 and 310 nm.

The number of residues of squaric acid per BSA molecule was 15 ± 2 and the yield of the BSA conjugate was 93%.

Table II. Binding of Neoglycoproteins 10[a] and 11[b] to Tumor Cells in Sections of Malignant Breast Lesions

case[d]	cytoplasmic staining[c] gal-β 1,3-galNAc–BSA 10	gal-β 1,3-galNAc–BSA 11
1	−/0	−/0
2	+++/2	+++/2-3
2[e]	+++/1	+++/2
3	+++/1	+++/1
4	+++/1	+/1
4[e]	+/2	+/1-2
5	+++/1	+++/2
6	−/0	−/0
6[e]	+++/1-2	+++/2
7	−/0	−/0
7[e]	−/0	−/0
8	+++/2	+++/2-3
9	−/0	−/0
10	+++/1	+++/1
11	+++/1-2	+++/1-2
12	+++/1	+++/1
13	−/0	−/0
13[e]	−/0	−/0
14	+++/1	+++/1
14[e]	+++/2-3	+++/2

[a] Coupled by squaric acid. [b] Coupled by diazotization; synthesis and results described elsewhere (*14*). [c] Cytoplasmic staining is evaluated by the percentage of positive cells, grouped into the categories −, 0%; +, 0–5%; +, 5–20%; ++, 20–50%, and +++, 50–100%, and by the intensity of the individual staining reaction, grouped into the categories 0, no staining; 1, weak but significant staining; 2, medium staining; 3, strong staining; and 4, very strong staining. [d] The tumor cases were classified as invasive ductal carcinoma (1–11), noninvasive intraductal carcinoma (12), tubular carcinoma (13), and invasive lobular carcinoma (14). [e] Denotes lymph node metastasis of the same primary tumor were the metastasis in the same patient originated from an apocrine carcinoma.

The yield of product **10** was obtained in eluate portion of 2 mL per column. The total volume of product solution was 22 mL. For the UV determination 1.2 mL of the product solution was diluted with pH 7.3 buffer (product solution/buffer, 1/2) and the absorbance was measured by λ = 270 and 310 nm.

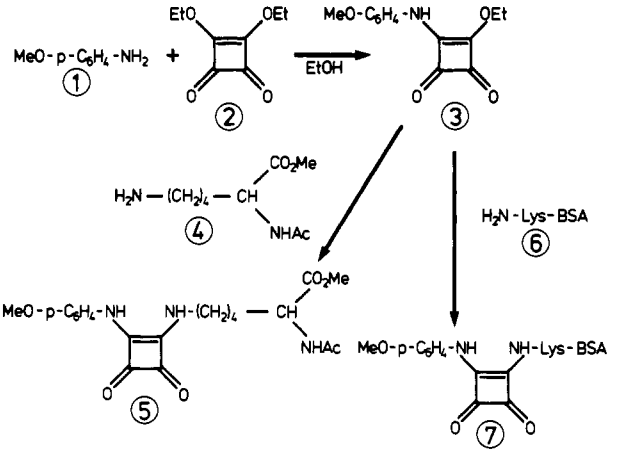
The number of residues of squaric acid per BSA molecule was 15 ± 2 and the yield of the BSA conjugate was 93%.

Analysis of Neoglycoprotein-Binding Sites in Tumor Cells and Tissue Sections. The glycocytological and glycohistochemical procedure for visualizing binding sites for the carbohydrate moiety of the biotinylated neoglycoprotein and the control reactions for specificity were described in detail elsewhere (*14*). Briefly, the cytospin preparations of the human colon adenocarcinoma cell line COLO205, the human breast carcinoma cell line DU4475, established from a metastatic cutaneous nodule, and the human erythroleukemia cell line HEL 92.1.7 as well as paraffin-embedded and formaldehyde-fixed sections of malignant breast lesions were processed by a series of steps including blocking endogenous peroxidase activity and nonspecific protein-binding sites, subsequent incubations with the labeled probe at a concentration of 100 μg/mL and with ABC reagents as well as enzyme substrates for development of the colored product to allow visualization of specific binding sites and with hemalum for counterstaining. Binding capacity for the carbohydrate part in the tumor cells in sections was semiquantified with respect to the cell percentage within the total cell compartment as well as with respect to the intensity, and these parameters were grouped into categories, as detailed in the footnote to Table II.

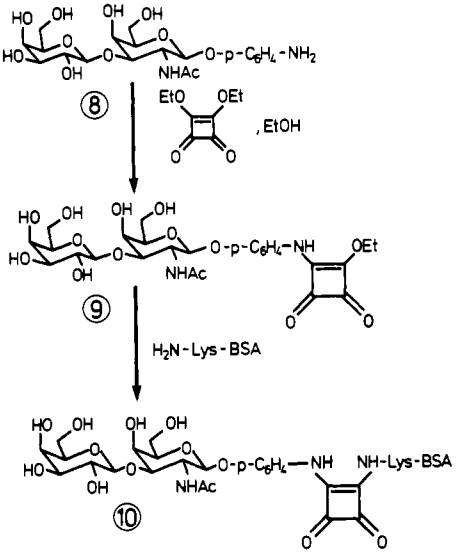
RESULTS AND DISCUSSION

Neoglycoprotein Synthesis. To develop a generally usable method for the coupling of *p*-aminophenyl glyco-

Scheme I. Synthesis of the Model Substances



Scheme II. Coupling of the Disaccharide Gal-β 1,3-GalNAc to BSA



sides to BSA we performed initial studies with model substance 1 (see Scheme I) in which the methyl group substitutes the carbohydrate moieties.

Formation of monoamide 3 was achieved by reaction of *p*-anisidine 1 with squaric acid diester 2. The 1,2-bisamide 5 that was needed as reference to determine the UV absorbance of one 1,2-bisamide was obtained via amidation of monoamide 3 with *N*-1-acetyl-L-lysine methyl ester 4. Each product was checked by ^{1}H NMR, ^{13}C NMR, MS, IR, UV, and microanalysis. Coupling monoamide 3 to BSA 6 afforded product 7.

Investigations to infer a possible structural rearrangement of 1,2-bisamide 5 to a corresponding 1,3-bisamide raised evidence that 5 is stable. In solution [methanol/buffer (pH 7.3), 1/9] no reaction was seen during 10 days despite heating to 50 °C twice for 4 h during this time, followed by routinely applied purification (PD-10 columns) and examination by UV spectroscopy. Scheme II summarizes the analogous synthetic route that has been used to prepare the T-antigen-bearing neoglycoprotein 10. Reaction of the *p*-aminophenyl group of disaccharide 8 (*14*) with squaric diester 2 afforded monoamide 9, which was checked by ^{1}H NMR, IR, and UV spectroscopy. Neoglycoprotein 10 was obtained via amidation of monoamide 9 with the lysyl ε-amino groups or terminal amino group of BSA. All reactions, except the coupling with BSA were followed, and the purity of the various compounds was determined by thin-layer chromatography on silica plates.

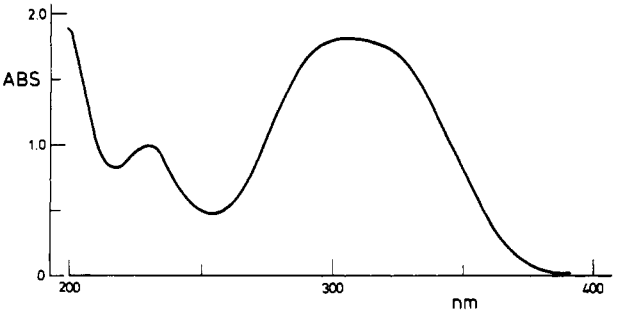


Figure 1. UV spectrum of 1,2-bisamide 5.

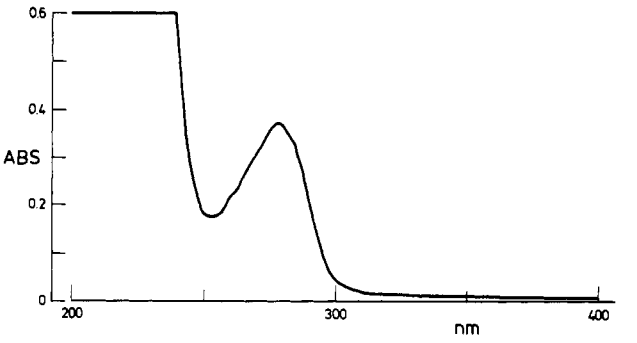
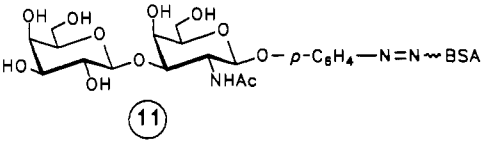


Figure 2. UV spectrum of BSA 6.

Scheme III. Neoglycoprotein 11 Derived by Diazotization (*14*)



UV Spectroscopic Determination. In order to measure the number of squaric acid residues per BSA molecule in BSA conjugates 7 and 10 we used UV-difference spectroscopy.

Figures 1 and 2 illustrate the UV spectra of 1,2-bisamide 5 and of BSA. 1,2-Bisamides of squaric acid usually have a broad absorption that clearly overlaps with the UV spectra of BSA. However, comparison of the two spectra (Figures 1 and 2) reveals that BSA has nearly no absorption at λ = 310 nm, whereas bisamide 5 shows a strong absorption at this wavelength, which is close to its λ_{max} (306.8 nm). Thus, in the coupled products 7 and 10 the absorption at λ = 310 nm can be attributed exclusively to the attached squaric acid bisamide moieties. Consequently, this wavelength was used for the assessment of the concentration of squaric acid bisamide moieties in the probe. The determination of the concentration of BSA was carried out at a wavelength of 270 nm, where BSA (λ_{max} = 280 nm) has a strong absorption, whereas bisamide 5 has a relative minimum. On the basis of the standard curves and calculation of the extinction coefficients the concentration of BSA and the molar ratios of ligand to carrier was accessible. In order to optimize the ligand attachment of BSA, the influence of the ratio protein/squaric acid of protein (BSA) and squaric acid amide ester 3 were respectively quantitated (Table I).

With a 30–40-fold molar excess of monoamide 3 a covalent attachment of almost 20 moieties was achieved. Increases of the molar excess of 3 to about 50-fold or even 100-fold did not result in a further increase of squaric acid bisamide moieties on BSA. When the number of squaric acid residues per BSA molecule increased, the yield of the BSA conjugate was concomitantly reduced. We suppose that the reason for this decrease can be the reduced

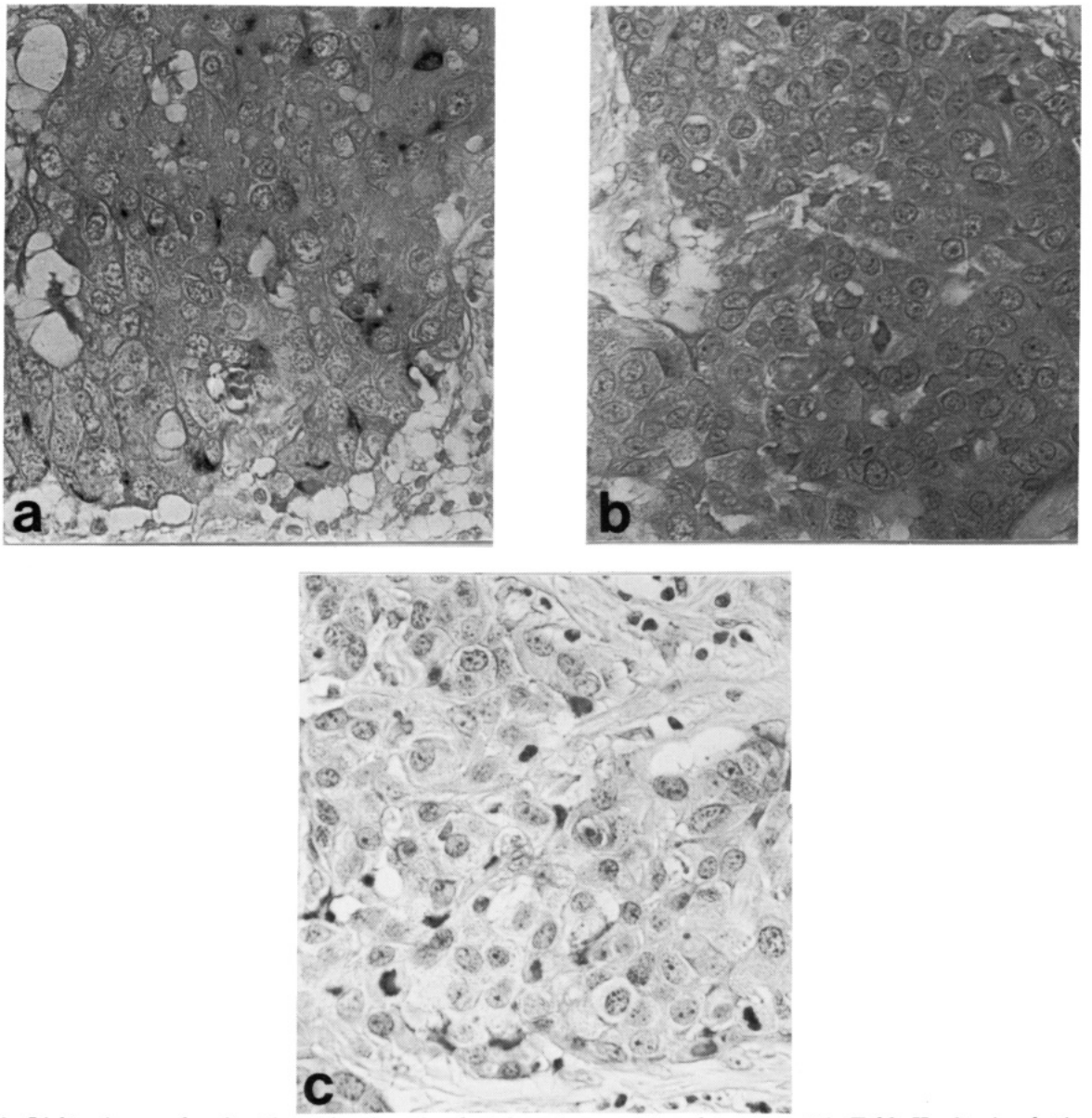


Figure 3. Light micrographs of sections of an invasive ductal carcinoma, referred to as case 2 in Table II, after incubation with 50 μg/mL biotinylated peanut lectin to localize presence of T-antigen in the tissue: (a) after incubation with 100 μg/mL neoglycoprotein **10** to localize carbohydrate-specific binding sites, (b) after coincubation with a 50-fold excess of label-free neoglycoprotein **10** in relation to the marker to show specificity of protein–carbohydrate interaction, and (c) after incubation with ABC reagents and enzyme substrates and hemalum counterstaining (*14*); Original magnification ×380 (figure reduced 90% for publication).

solubility of the protein conjugate due to the hydrophobic nature of the squaric acid bisamide moieties on the surface of the protein. Control experiments with pure BSA proved that the solubility of BSA was not affected by the organic solvent. Thus, there is no evidence for precipitation caused by the presence of dimethyl sulfoxide.

Investigation of the stability of coupled product **7** showed that it is stable for more than 2 days in buffer solution (pH 7.3) at room temperature. Time-course experiments revealed that the optimal time in terms of coupling and yield is about 3–4 h.

Determination of the Number of Gal-β 1,3-GalNAc Residues per BSA in 10. For the coupling of disaccharide **9** with BSA a 85-fold molar excess was used. The yield of BSA conjugate **10** was 93% and the ratio of carbohydrate (squaric acid bisamide) attachment was 15.3 ± <1 units per BSA molecule. Thus the ligand attachment of BSA in **10** is lower than that in **7** and the yield much better. Apparently, the free reactive amino functions in BSA will be blocked to a higher extent by the polar bulky carbohydrate moiety in **10** than by the small nonpolar methyl group in **7**. It can also be assumed that the conformation of the BSA conjugates **7** and **10** may be quite different due to hydrogen bonding of the hydroxy groups in the carbohydrate moiety to the peptide functionalities. The better yield in the formation of **10** is in accordance with our given explanation. Thus the solubility of **10** should be much better compared to that of **7** due to the hydrophilic character of the carbohydrate moieties.

Detection of T-Antigen-Specific Receptors by Labeled Neoglycoprotein 10 and Comparison to the Results with Neoglycoprotein 11 (See Scheme III). Most of the cells of the two carcinoma cell lines and the erythroleukemia line were found to react positively. A similar result was seen after processing paraffin-embedded tissue sections from malignant breast lesions. A representative result is illustrated in Figure 3. The detailed pattern of cytoplasmic staining with respect to percentage of positive tumor cells in the total cell population as well as staining intensity for each case is given in Table II.

No pronounced difference was seen in the extent of staining between this neoglycoprotein and the neoglyco-

protein obtained product of diazotization with the *p*-aminophenyl glycoside of gal-β1,3-galNAc. Semiquantitative analysis of these two markers in tumor cells of tissue sections from malignant breast lesions revealed no apparent correlation to metastasis formation. This application substantiated that this new type of linker will lead to an efficiently applicable probe for reliable lectin detection. Indeed, there are many advantages of this new linker compared to other methods; thus, (i) two amino groups can be coupled without interference by esters, hydroxy groups, and nearly all other functionalities in the substrates; (ii) the use of the linker is simple, requires no harsh conditions, and gives excellent yields; moreover, (iii) the coupling can be performed in slightly basic media; and (iv) finally the quantity of the coupled groups can be determined by UV spectroscopy.

LITERATURE CITED

(1) Stowell, C. P., and Lee, Y. C. (1980) Neoglycoproteins: the preparation and application of synthetic glycoproteins. *Adv. Carbohydr. Chem. Biochem. 37*, 225–281.

(2) Gabius, H.-J., and Bardosi, A. (1991) Neoglycoproteins as tools in glycohistochemistry. *Prog. Histochem. Cytochem. 22*, 1–75.

(3) Gabius, H.-J. (1991) Detection and functions of mammalian lectin with emphasis on membrane lectins. *Biochim. Biophys. Acta 1071*, 1–18.

(4) Sharon, N., and Lis, H. (1989) Lectins as cell recognition molecules. *Science 246*, 227–234.

(5) Barondes, S. H. (1981) Lectins: their multiple endogenous cellular functions. *Annu. Rev. Biochem. 50*, 207–231.

(6) Gabius, H.-J. (1988) Tumorlectinology: at the intersection of carbohydrate chemistry, biochemistry, cell biology and oncology. *Angew. Chem. Int. Ed. Engl. 27*, 1267–1276.

(7) Gabius, H.-J., Gabius, S., Brinck, U., and Schauer, A. (1990) Endogenous lectins with specificity to β-galactosides and α- or β-*N*-acetyl-galactosaminides in human breast cancer. *Pathol. Res. Pract. 186*, 597–607.

(8) Tietze, L. F. (1990) New concepts for the development of selective anticancer drugs. *Molecular Aspects of Chemotherapy* (E. Borowski, and D. Shugar, Eds.) pp 55–70, Pergamon Press, New York.

(9) Review: Tannock, I. F., and Rotin, D. (1989) *Cancer Res. 49*, 4373–4383.

(10) Tietze, L. F., Neumann, M., Fischer, R., Möllers, T., Glüsenkamp, K.-H., Rajewsky, M. F., and Jähde, E. (1989) Proton-mediated liberation of aldophosphamide from a non-toxic prodrug. A strategy for tumor-selective activation of cytocidal drugs. *Cancer Res. 49*, 4179–4184.

(11) Tietze, L. F., Beller, M., Fischer, Lögers, M., Jähde, E., Glüsenkamp, K.-H., Rajewsky, M. F. (1990) Development of tailor-made cytostatics activable by acid-catalyzed hydrolysis for selective tumor therapy. *Angew. Chem. Int. Ed. Engl. 29*, 782–783.

(12) Kojima, S., Gabius, H.-J. (1988) Biodistribution of neoglycoproteins in mice bearing solid Ehrlich tumor. *J. Cancer Res. Clin. Oncol. 114*, 468–472.

(13) Tietze, L. F., Arlt, M., Beller, M., Glüsenkamp, K.-H., Jähde, E., Rajewsky, M. F. (1991) Squaric acid diethyl ester: a new coupling reagent for the formation of drug biopolymer conjugates. Synthesis of squaric acid ester amides and squaric acid diamides. *Chem. Ber. 124*, 1215–1221.

(14) Gabius, H.-J., Schröter, C., Gabius, S., Brinck, U., and Tietze, L. F. (1990) Binding of T-antigen-bearing neoglycoprotein and peanut agglutinin to cultured tumor cells and breast carcinomas. *J. Histochem. Cytochem. 38*, 1625–1631.

Registry No. 1, 104-94-9; 2, 5231-87-8; 3, 132751-38-3; 4, 6072-02-2; 5, 132751-39-4; 9, 132751-40-7; *p*-aminophenyl 2-acetamido-2-deoxy-3-*O*-β-D-galactopyranosyl-β-D-galactopyranoside, 131339-22-5; 1,2-diethoxycyclobutene-3,4-dione, 5231-87-8.

Preparation of Well-Defined Protein Conjugates Using Enzyme-Assisted Reverse Proteolysis[1]

Keith Rose,* L. Antonio Vilaseca, Raymond Werlen, Anne Meunier, Igor Fisch, Robert M. L. Jones, and Robin E. Offord

Département de Biochimie Médicale, Centre Médical Universitaire, 1 rue Michel Servet, 1211 Geneva 4, Switzerland. Received February 15, 1991

A two-step approach to the production of well-defined protein conjugates is described. In the first step, a linker group, carbohydrazide, having unique reactivity (a hydrazide group) is attached specifically to the carboxyl terminus by using enzyme-catalyzed reverse proteolysis. Since the hydrazide group exists nowhere else on the protein, specificity is assured in a subsequent chemical reaction (formation of a hydrazone bond) of the modified protein with a molecule (chelator, drug, or polypeptide) carrying an aldehyde or keto group. The product is sufficiently stable at neutral pH, no reduction of the hydrazone bond being necessary for the hydrazones described. Protein modification is thus restricted to the carboxyl terminus and a homogeneous product results. With insulin as a model, conditions are described for producing such well-defined conjugates in good yields. The use of other linker groups besides carbohydrazide, and applications of these techniques to antibody fragments, are discussed.

INTRODUCTION

Artificial protein conjugates, consisting of a protein covalently linked to another group (reporter group, radiolabel, cytotoxic agent, polypeptide chain, etc.) are useful in many areas of research. However, most current methods for preparing protein conjugates suffer from two disadvantages.

The first disadvantage is that current methods of protein modification tend to produce inhomogeneous material. Even material substituted with only one modifying group is in general itself heterogeneous, being a mixture of species each having one group attached to one of several residues of the type involved in the modification reaction. The use of a heterogeneous preparation can lead to problems of interpretation of results, since different isomers may have different biological properties (e.g. the monoiodoinsulins). A homogeneous product is desirable, particularly for clinical applications.

The second disadvantage of current methods is that attempts to reach a high degree of substitution of the protein tend to lead rapidly to loss of protein function. This is illustrated by numerous attempts to increase the degree of labeling of antibodies: in general, a higher degree of labeling leads to a lower degree of antigen binding (*1*).

We believe that both these disadvantages of most current methodologies may be circumvented by attaching groups to proteins in a site-specific manner, ideally far from the functional region of the protein in question (active site, in the case of an enzyme, or antigen binding region, in the case of an antibody or fragment thereof). The advantages of "site-specific" modification, through oxidized carbohydrate, of antibodies of the IgG type have been reported (*2, 3*). The success of such an approach depends upon the existence of appropriate glycosylation, so it is not generally applicable to other classes of polypeptide (nor even to antibody fragments of the F(ab) and $F(ab)_2$ types, in general). Since some IgG molecules possess more than one site of glycosylation, the carbohydrate oxidation approach may not always be site-specific.

Several groups of workers have exploited the specificity of proteases working in reverse to fix, exclusively at the carboxyl terminus of polypeptides, groups which are not normally found in proteins. In a subsequent chemical reaction, the conjugation step, a bond is formed between this enzymatically introduced group and a molecule of interest carrying an appropriate functionality. (It is not usually possible or desirable to fix enzymically the molecule of interest directly to the polypeptide chain for reasons of enzyme specificity or the large excess of amino component generally required to drive the enzymic coupling to high yield.) Thus, Carpenter's group attached phenylhydrazine prior to oxidation to a diimide (*4*), and various workers (*5–7*) attached hydrazine or protected hydrazine as a prelude to azide coupling. Such approaches, used to join together two peptide fragments by means of a peptide bond, require a strategy involving protection and deprotection in order to obtain coupling to the desired amino group, a strategy which is inappropriate when dealing with proteins which are easily denatured. We (*8, 9*) have used reverse proteolysis to attach amino acid dichlorophenyl esters, which are aminolyzed in a subsequent step, but again protection and deprotection are required if aminolysis is to be attempted in cases where there is no conformational assistance. Wilchek's group (*10*) has used carboxypeptidase Y to attach biocytin amide and N^{ϵ}-(maleimidopropionyl)-L-lysinamide to the carboxyl terminus of a variety of proteins and reported yields of 40–75%. The conditions used were rather harsh (water/dimethylformamide/ethanol 2:1:1, with shaking), and "ragged ends" are to be expected since carboxypeptidase Y may remove more than one residue before the reaction is stopped.

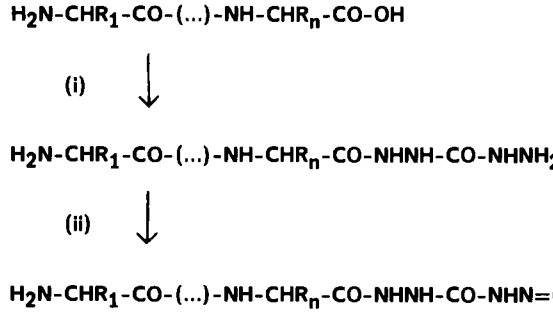
We are interested in conjugation techniques based on reverse proteolysis which do not require protection followed by deprotection and which yield homogeneous products under very mild conditions; such techniques should be applicable to polypeptides which are relatively easily denatured, such as antibodies and fragments of antibodies. Our initial approach involved reductive alkylation (*11, 12*), which gave good results with insulin but was less easy to apply to antibody fragments owing to the

* Author to whom correspondence should be addressed.

[1] Abbreviations used: DAI, des-Ala^{B30}-insulin; HPLC, high-pressure liquid chromatography; TPCK, L-1-chloro-4-phenyl-3-(tosylamino)butan-2-one; TFA, trifluoroacetic acid; FAB-MS, fast atom bombardment mass spectrometry; EDTA, ethylenediaminetetraacetic acid.

1043-1802/91/2902-0154$02.50/0 © 1991 American Chemical Society

Scheme I. Examples of the Formation of a Defined Protein Conjugate[a]



[a] Step i consists of a protease-catalyzed coupling step conducted under conditions where formation of a –CO–NH– bond is favored (reverse proteolysis). The nucleophile used in step i is carbohydrazide, and specificity in this step is assured by the choice of an appropriate protease. After isolation of the product of step i, step ii consists of a chemical conjugation reaction resulting in formation of a hydrazone. Specificity in step ii is assured by chemical complementarity.

substantial concentrations of organic solvents necessary to obtain high coupling yields. More recently, we have been able to combine the mild conjugation conditions offered by hydrazone bond formation (see e.g. ref *13*) with the specificity of reverse proteolysis (Scheme I). The fact that it is not necessary, nor sometimes even desirable, to form an amide bond between the protein and the group to be attached removes the difficulty of differential protection which would otherwise exist.

A preliminary presentation of our work has already appeared (*14*, *15*). Using insulin as a model, we present here a study of the range of conditions for attaching carbohydrazide to the carboxyl group of $LysB^{29}$ and conditions for producing well-defined protein conjugates from this modified species. The use of other linker groups besides hydrazide, and applications of these techniques, are also discussed.

EXPERIMENTAL PROCEDURES

Except where otherwise specified, solvents and reagents were of analytical grade or better, were obtained from commercial sources, and were used without further purification. Carbohydrazide was purchased from Fluka (Buchs, Switzerland). Pig insulin (Monocomponent grade) was obtained from Novo Industri (Bagsvaerd, Denmark). It was freed from zinc and then converted into des-Ala^{B30}-insulin (DAI), essentially according to the method of Morihara et al. (*16*), by incubating 100 mg of insulin with 0.5 mg of lysyl endopeptidase (from *Achromobacter lyticus*, Wako Pure Chemical Co.) in 20 mL of 0.1 M ammonium bicarbonate solution for 30 h at 37 °C followed by lyophilization. The dipeptide Trp-Phe and porcine trypsin were purchased from Sigma Chemical Co. (St. Louis, MO). For some experiments the trypsin was treated with L-1-chloro-4-phenyl-3-(tosylamino)butan-2-one (TPCK) (*17*). All reactions and chromatography were carried out at room temperature (ca. 23 °C) unless otherwise specified.

Reverse Proteolysis. All pH values are apparent values obtained with a glass electrode calibrated with aqueous standards, no corrections being applied. Solutions of carbohydrazide were prepared in water and in dimethyl sulfoxide/water (1:1 v/v) and were generally brought to the required indicated pH by addition of pure acetic acid. However, in order to obtain a pH below 5.5, the solutions were made 5 mg/mL in sodium acetate and then titrated to the desired pH value with 98% formic acid. DAI was dissolved in the carbohydrazide solutions at 1, 2, and 20 mg/mL. Enzyme was added as a freshly prepared solution in water (10 mg/mL for *Achromobacter* protease; 10 or 100 mg/mL for trypsin), and the samples were incubated at room temperature for various times.

Reversed-Phase High-Pressure Liquid Chromatography (HPLC). Samples were generally injected directly onto a Waters HPLC system, with monitoring at 214, 229, or 280 nm. In the case of incubations performed at a pH greater than 5.5, samples were acidified with 10 volumes of pure acetic acid then diluted with 100 volumes of 0.1% trifluoroacetic acid (TFA) prior to injection. For analytical work, a column 25 cm × 4 mm i.d. (Nucleosil 300-Å 5-μm C_8, Machery-Nagel, Oensingen, Switzerland) was used at a flow rate of 0.6 mL/min. Solvent A was prepared by adding 1 g of TFA (HPLC grade, ABI Inc.) to 1000 mL of HPLC-grade water (Milli-Q system), followed by vacuum filtration. Solvent B was prepared by adding 1 g of TFA to 100 mL of HPLC-grade water (previously degassed by vacuum filtration) then adding 900 mL acetonitrile (gradient grade, Merck, previously degassed by vacuum filtration). For preparative work, a column 25 cm × 1 cm i.d. of Nucleosil 300-Å 5-μm C_{18} (Machery-Nagel) was used at a flow rate of 4 mL/min. For this system, solvent A was prepared by mixing 100 mL of 3 M $(NH_4)_2SO_4$ with degassed HPLC-grade water to complete to 1000 mL. Solvent B was prepared by mixing 100 mL of 3 M $(NH_4)_2SO_4$ with 350 mL of degassed acetonitrile and completing to 1000 mL with degassed HPLC-grade water (thorough mixing is required). Before use, the pH of the 3 M $(NH_4)_2SO_4$ had been adjusted to 2.7 with concentrated sulfuric acid and the pH was not adjusted after dilution. Samples were recovered after preparative HPLC by dilution with an equal volume of 0.1% TFA followed by adsorption to a Sep-Pak C_{18} (Waters Associates) column, previously washed with methanol and equilibrated with 0.1% TFA. After washing thoroughly with 0.1% TFA, sample was eluted with 4 mL of 0.1% TFA containing 50% acetonitrile and dried in a vacuum centrifuge (SpeedVac, Savant Instruments).

HCO-*m*-C_6H_4CH=$NOCH_2CO$–Ferrioxamine and Similar Compounds. A solution of isophthalaldehyde was prepared by dissolving 6.7 mg (50 μmol) in 0.2 mL of CH_3CN and completing to 1 mL with a buffer made by bringing a 0.1 M solution of sodium acetate in water to pH 4.6 with glacial acetic acid. To the isophthalaldehyde solution was added dropwise, with mixing, a solution of NH_2-OCH_2CO–ferrioxamine (prepared according to ref *18*; 8 mg as isolated, ca. 10 μmol, dissolved in 1 mL of the acetate buffer). After 70 min, the reaction mixture was applied to a C_{18} Sep-Pak column, previously washed with methanol (10 mL) and equilibrated with 1% acetic acid (10 mL). The Sep-Pak was washed with 1% acetic acid/CH_3CN (9:1 v/v, 14 mL) to remove excess aldehyde and the product then eluted with 1% acetic acid/CH_3CN (8:2, v/v; 7 mL). Solvent was removed in the vacuum centrifuge and the product taken up in 0.1% TFA and purified by reversed-phase HPLC (4 mm i.d. column, TFA system, monitoring at 214 nm). Sample was injected at 15% B, and after 5 min a linear gradient of 0.5%/min was applied for 60 min. Product eluted as an orange solution with t_R = 41 min. Solvent was removed in the vacuum centrifuge. Product was characterized as the expected HCO-*m*-C_6H_4CH=$NOCH_2CO$–ferrioxamine by fast atom bombardment mass spectrometry (FAB-MS) in the positive ion mode using glycerol, thioglycerol, acetic acid as matrix. A strong signal was found at m/z 803 (protonated molecular ion) and a weaker signal at m/z 909 (adduct with thioglycerol,

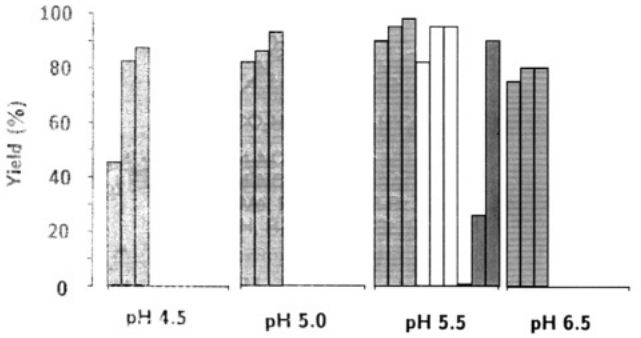


Figure 1. Yield of DAI–carbohydrazide as a function of time and pH. The conditions were DAI, 20 mg/mL; carbohydrazide, 0.5 M in DMSO/H_2O 1:1 v/v. Columns refer to time points 15 min, 4 h, and 16 h (left to right, respectively, in groups of three). Horizontally hatched columns refer to catalysis with TPCK-treated porcine trypsin (enzyme:substrate ratio 1:10 w/w). Open columns refer to catalysis with *Achromobacter* protease (enzyme:substrate ratio 1:10 w/w), and slanted hatched columns refer to catalysis with *Achromobacter* protease (enzyme:substrate ratio 1:50 w/w).

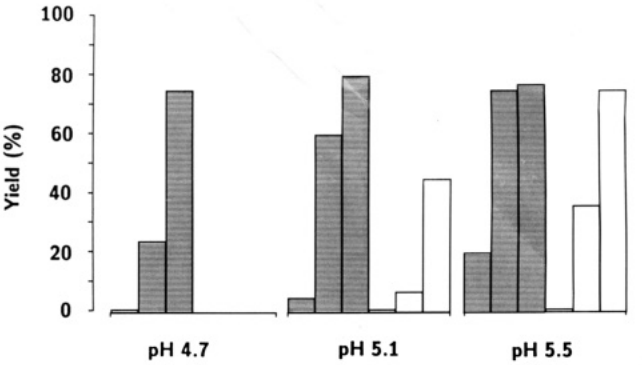


Figure 2. Yield of DAI–carbohydrazide as a function of time and pH. The conditions were DAI, 20 mg/mL; carbohydrazide, 2.5 M in water. Columns refer to time points 15 min, 4 h, and 16 h (left to right, respectively, in groups of three). Horizontally hatched columns refer to catalysis with TPCK-treated porcine trypsin (enzyme:substrate ratio 1:10 w/w). Open columns refer to catalysis with *Achromobacter* protease (enzyme:substrate ratio 1:50 w/w).

commonly found with aldehydes). Iron was removed from a portion of the material (1 mg in 0.1 mL of water) by incubating with Na_2EDTA (0.4 mL of a solution 50 mM made up in 1% acetic acid). All color was lost within 30 min and a white precipitate formed which was washed three times with 0.4-mL portions of 1% acetic acid. Drying under high vacuum afforded 0.74 mg of white powder, characterized by positive ion FAB-MS as the expected iron-free material (HCO-*m*-$C_6H_4CH{=}NOCH_2CO$–desferrioxamine, M + H, 750, three protons having replaced the trivalent iron). The metal-free material was loaded with gallium under conditions adapted later for radiolabeling with ^{67}Ga. A suspension of 0.36 mg (0.48 μmol) of metal-free compound in 1 mL of the acetate buffer, pH 4.6 (see above), was added to 0.7 μmol of $GaCl_3$ (in solution in 103 μL of 0.8 M HCl, brought to an indicated pH of 4.6 through the addition of 6.5 M ammonium acetate, ca. 40 μL, just prior to addition of the chelator). Within 2.5 h, the suspension had dissolved through capture of gallium. Analytical HPLC showed that the product eluted with approximately the same retention time as the iron-containing material. After isolation on a Sep-Pak column as described for the iron-containing material, the product was characterized as gallium-labeled HCO-*m*-C_6H_4-$CH{=}NOCH_2CO$–desferrioxamine by positive FAB-MS (protonated molecular ions at *m/z* 816 and 818 due to the natural isotopes ^{69}Ga and ^{71}Ga).

Hydrazone Formation. Des-Ala^{B30}-insulin–carbohydrazide (DAI–carbohydrazide) and zinc-free insulin control were dissolved separately (0.2 mM) in 0.1 M acetic acid, and the pH was adjusted to 4.6 with 5 M NaOH. To a given volume of sample solution (generally 100 μL) was added an equal volume of a solution of aldehyde dissolved in 0.1 M acetate (Na), pH 4.6. Various aldehydes at various concentrations were used (see Results and Discussion); for reasons of solubility, 2,4-dihydroxybenzaldehyde and 4-nitrobenzaldehyde were dissolved in acetonitrile and then diluted with 49 volumes of pH 4.6 buffer to obtain a final concentration of 1 mM. Analysis was by HPLC.

Mass Spectrometry. Equipment and operating conditions were as previously described (*19*).

RESULTS AND DISCUSSION

Coupling of Carbohydrazide in 50% DMSO. Figure 1 shows the yields of DAI–carbohydrazide (ratio of product to remaining DAI, as a percentage) obtained with 0.5 M carbohydrazide in 50% DMSO, expressed as a function of time at four pH values. At pH 3.85, no product was formed at all (not shown), most probably due to lack of sufficient enzymatic activity at this low pH value. At pH 4.5, porcine trypsin, which is remarkably active at low pH values (*6*), catalyzes the formation of DAI–carbohydrazide. Coupling is favored over cleavage, and less than 2% cleavage at Arg^{B22} occurs after 16 h as determined by HPLC. At pH 5, trypsin is still more active, and DAI–carbohydrazide is produced more rapidly (compare 15-min time points). Again, less than 2% cleavage at Arg^{B22} occurs after 16 h. At pH 5.5., DAI–carbohydrazide is produced very rapidly indeed and almost quantitative coupling yield (as defined above) is obtained under comparable conditions (horizontal hatching). Cleavage at Arg^{B22} was ca. 1% after 4 h but had risen to ca. 45% after 16 h. The yield of recoverable DAI–carbohydrazide is thus compromised at long reaction times under conditions of high enzymic activity, which is a function of pH, substrate concentration, and enzyme:substrate ratio. At pH 6.5, maximum coupling yield is attained after 4 h (Figure 1), but the yield is not as high as may be obtained at lower pH. Enzymic activity is high, and cleavage at Arg^{B22} reached 40% after 4 h and 70% after 16 h.

Also shown in Figure 1 are results obtained with *Achromobacter* protease at pH 5.5 at an enzyme:substrate ratio of 1:10 (w/w) (as for trypsin) and 1:50, open bars and slanted hatching, respectively. This protease, which is specific for the carboxyl side of Lys residues, permits the attainment of high yields without the danger of cleavage of Arg^{B22}.

Coupling of Carbohydrazide in Aqueous Solution. Similar results were obtained whether the porcine trypsin had been treated with TPCK or not. Figure 2 shows the yields of DAI–carbohydrazide (ratio of product to remaining DAI, as a percentage) obtained with 2.5 M carbohydrazide in aqueous solution, expressed as a function of time at three pH values and with two enzymes: porcine trypsin at an enzyme:substrate ratio of 1:10 (w/w) (hatched bars) and *Achromobacter* protease at an enzyme:substrate ratio of 1:50 (w/w) (open bars). *Achromobacter* protease was not studied at pH 4.7. Comparison with Figure 1 shows that coupling with trypsin is less rapid than in 50% DMSO, in spite of the higher nucleophile concentration. The 15-min and 4-h time points clearly show that coupling rate rises with increasing pH over the range studied. Cleavage at Arg^{B22} by trypsin was below 2% after 16 h at pH 5.1 but was ca. 25% after 16 h at pH 5.5. *Achromobacter* protease, used at an enzyme:substrate ratio of 1:50

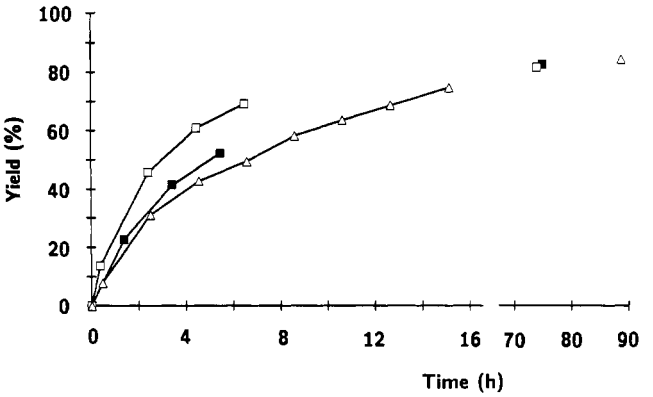


Figure 3. Yield of DAI–carbohydrazide as a function of time, substrate concentration, and *Achromobacter* protease concentration. Conditions were carbohydrazide, 2.5 M in water, pH 5.5 (adjusted with acetic acid): △, 1 mg/mL DAI (170 μM), 55 μg/mL enzyme (1.8 μM); ■, 2 mg/mL DAI (340 μM), 110 μg/mL enzyme (3.7 μM); □, 2 mg/mL DAI (340 μM), 210 μg/mL enzyme (7 μM).

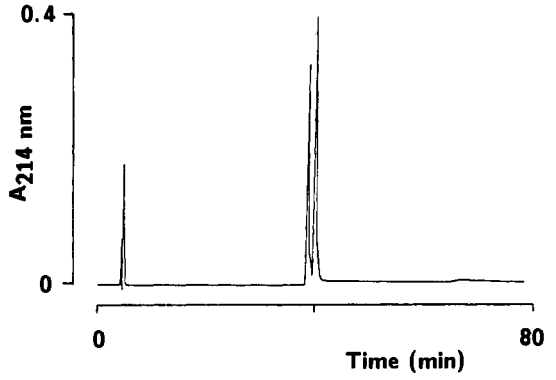


Figure 4. Separation of insulin and DAI–carbohydrazide. The above chromatogram was obtained by analytical reversed-phase HPLC (TFA system), with monitoring at 214 nm, AUFS 1.0. After 5 min at 30% solvent B, a linear gradient of 0.5%/min to 50% B was applied. DAI–carbohydrazide elutes as the earlier peak at t_R = 38.5 min, and insulin elutes at t_R = 40 min.

by weight (compared to 1:10 for trypsin), shows somewhat slower coupling rates but permits the attainment of high yield within 16 h at pH 5.5 without any hydrolysis at Arg^{B22}.

At pH 5.5, equilibrium is almost reached in 16 h and a yield of 75–77% obtained in fully aqueous medium (Figure 2). On a preparative scale, 10 mg of DAI in 5 mL of solution incubated with 0.2 mg of porcine trypsin gave a coupling yield of about 75% after 18 h. These yields are considerably lower than the nearly quantitative yield obtained at this pH in 50% DMSO. However, some protein substrates, such as antibodies and large fragments of antibodies, are denatured by and even precipitate from 50% DMSO, whereas these problems are not experienced in fully aqueous medium (data not shown). For this reason, we studied the aqueous coupling in more detail.

Figure 3 shows the yield of DAI–carbohydrazide as a function of time, substrate concentration, and enzyme concentration. At equilibrium, the yield is ca. 83%. Higher substrate concentration and higher enzyme concentration both lead to faster reaction (Figure 3).

Figure 4 shows an example of the separation between insulin (which elutes at the same retention time as DAI under the conditions used) and DAI–carbohydrazide on analytical reversed-phase HPLC. The hydrazide group is charged at the low pH of the HPLC system and this probably is responsible for the earlier elution of the modified form of DAI.

It is important to note that the reverse proteolysis reaction must be halted before separating excess carbohydrazide from the protein substrate; otherwise, particularly at neutral pH, the enzyme will rapidly remove the C-terminal carbohydrazide group. When working with DAI, we stop the reaction by injection onto an HPLC, which is operated at very low pH (2–3). When working with antibody fragments, however, it is preferable to add sufficient enzyme inhibitor prior to a separation by gel filtration at more moderate pH (4.6).

Characterization of DAI–Carbohydrazide and Hydrazone Formation. DAI–carbohydrazide, isolated by preparative HPLC, was found to react with a number of aldehydes (2,4-dihydroxybenzaldehyde, 4-nitrobenzaldehyde, and several derivatives of ferrioxamine—see below) under very mild conditions (pH 4.6, fully aqueous solution, room temperature, 1–5 equiv of aldehyde) to give a corresponding product eluting later than DAI–carbohydrazide on reversed-phase HPLC. Under similar conditions, native insulin (zinc free) did not react at all. This lack of reaction between aldehyde and the amino groups of insulin is as expected, since the corresponding Schiff bases are unstable at pH 4.6 and would require reduction to an alkylamine if a product is to be isolated. Figure 5 shows the results of incubation with 5 equiv of 2,4-dihydroxybenzaldehyde. A very clean and specific reaction occurs with DAI–carbohydrazide (panels c and d of Figure 5) while no reaction at all occurs with native insulin (panel a). Panel b shows that DAI–carbohydrazide is stable in the absence of aldehyde. In the case of 4-nitrobenzaldehyde, the later-eluting product was characterized as the expected hydrazone by isolation (HPLC), digestion with V8 enzyme, and analysis by FAB-MS (not shown). In addition to the known V8 fragments of insulin (*20*), the C-terminal fragment of the B-chain was shifted in mass from m/z 1015 (for DAI) to 1220, consistent with condensation with carbohydrazide followed by hydrazone formation with 4-nitrobenzaldehyde.

In accord with previous observations concerning hydrazone formation (*13*), we found that the yield of hydrazone at equilibrium depends on reagent concentrations and chemical structure. When using as aldehyde HCO-*m*-$C_6H_4CH{=}NOCH_2CO$–ferrioxamine at pH 4.6 and with a 0.1 mM final concentration of DAI–carbohydrazide, 1 equiv of aldehyde led to hydrazone yields of ca. 74% after 78 min and 91% after 13 h 17 min (Figure 6, panels b and c, respectively). Even with this reactive aldehyde, no trace of reaction occurred with native insulin (Figure 6, panel a), demonstrating the specificity of the proposed two-step process. Similar results were obtained with the gallium-containing derivative and with the paraisomers (HCO-*p*-$C_6H_4CH{=}NOCH_2CO$–ferrioxamine or the corresponding gallium derivative). It is thus possible to attach a chelator specifically to the C-terminal carboxy group of a protein. The known stability of unreduced hydrazones (*13*) at neutral pH was confirmed with polypeptides other than DAI (which is relatively insoluble at pH 7) and radiolabeled (^{55}Fe and ^{67}Ga) ferrioxamine derivatives (data not shown).

Since aldehydes are known to react with tryptophan residues under acid conditions (the Ehrlich reaction, occurring in strong HCl) and since insulin contains no tryptophan residues, it was important to establish whether, under mild conditions, any reaction occurred with Trp residues. Upon incubation at pH 4.6 of the peptide Trp-Phe (0.1 mM) with HCO-*m*-$C_6H_4CH{=}NOCH_2CO$–ferrioxamine (0.5 mM), analytical HPLC showed no trace of reaction even after 12 h (results not shown).

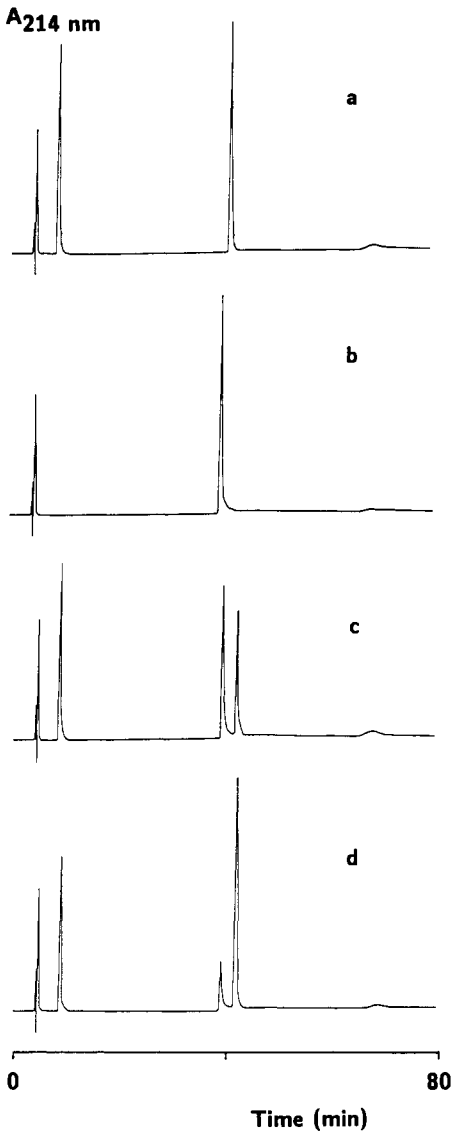


Figure 5. Analytical reversed-phase HPLC analysis of a conjugation reaction at pH 4.6 with 2,4-dihydroxybenzaldehyde. Chromatographic conditions were as for Figure 4. Panel a, control incubation of native insulin, 0.1 mM, with 2,4-dihydroxybenzaldehyde, 0.5 mM, after 8 h 54 min. The aldehyde elutes just after the front. Panel b, control incubation of DAI–carbohydrazide, 0.1 mM, after 14 h 28 min. Panel c, incubation of DAI–carbohydrazide, 0.1 mM, with 2,4-dihydroxybenzaldehyde, 0.5 mM, after 50 min. Panel d, as for c but after a 5 h 23 min reaction.

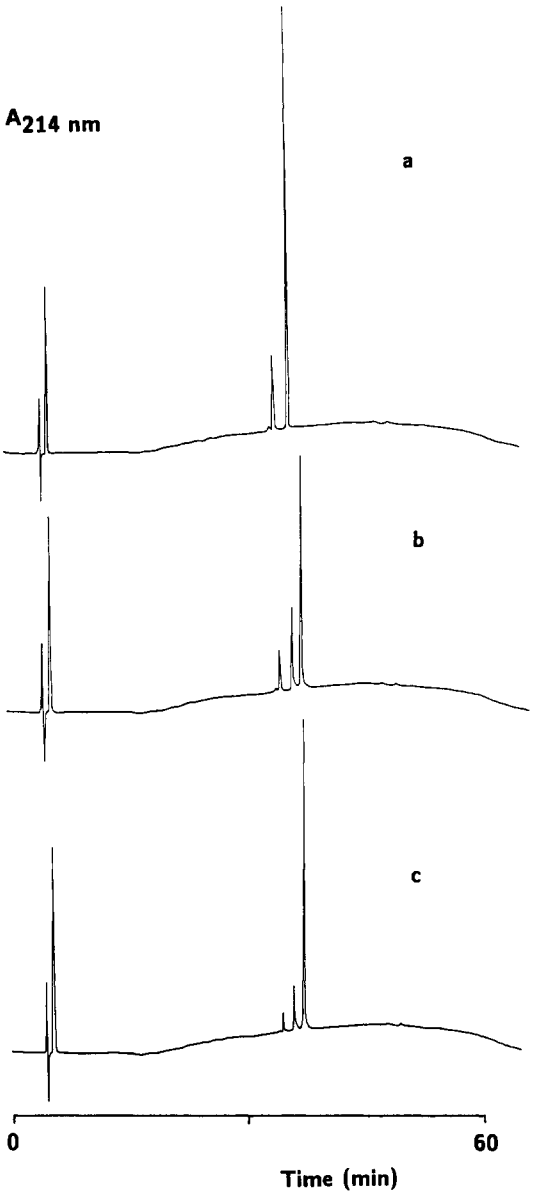


Figure 6. Analytical reversed-phase HPLC analysis of a conjugation reaction at pH 4.6 with HCO-*m*-$C_6H_4CH{=}NOCH_2$-CO–ferrioxamine. Chromatographic conditions: the TFA system was used; after 5 min isocratic at 0% B, a linear gradient of solvent B, 2%/min, was applied to 100% B, which was maintained for 5 min before descending to 0% B over 5 min. Reaction conditions: protein concentration and aldehyde concentration were both initially 0.1 mM. Panel a, control incubation of aldehyde with unmodified insulin after 14 h 30 min. The reagent and insulin elute at $t_R \approx 34.3$ and 36.3 min, respectively. Panel b, incubation of aldehyde with DAI–carbohydrazide after a reaction time of 78 min. DAI–carbohydrazide and the hydrazone reaction product elute at $t_R \approx 35.5$ and 36.8 min, respectively. Panel c, incubation of aldehyde with DAI–carbohydrazide after 13 h 17 min.

Reverse Proteolysis with Other Nucleophiles. Reverse proteolysis has been used to couple to oxygen nucleophiles (alcohols (*6*)) but high yields are normally obtained only by coupling to NH_2 groups. As referred to in the Introduction, reverse proteolysis may be used to couple nucleophiles other than hydrazides; for example, good results may be obtained with aldehyde precursors such as $NH_2C_6H_4CH(OR)_2$ or $NH_2CH[CH_2SCH_2CH(OH)CH_2OH]CONH_2$ (*11*, *12*). However, substantial proportions of organic solvent (at least 50%) are necessary in order to obtain high yields during reverse proteolysis with amines as nucleophiles, owing to their high pK (alkylamines) or low water solubility (aromatic amines). If reverse proteolysis is to be performed in fully aqueous medium, hydrazides permit high yields to be obtained (*6*). We have investigated the use of hydrazides other than carbohydrazide. Adipodihydrazide is not as soluble (0.5 M in water) and leads to yields of ca. 27% at equilibrium. Oxalodihydrazide is almost totally insoluble in water and so cannot be used. Succinodihydrazide is also insufficiently soluble in water (less than 0.125 M) to be useful.

CONCLUSION

Reverse proteolysis may be used to attach the linker molecule carbohydrazide specifically to the C-terminal carboxyl group of a protein substrate under mild, fully aqueous conditions. In a second step, not catalyzed by an enzyme, a molecule containing an aldehyde function may be conjugated to the protein through formation of a hydrazone bond, in high yield and under very mild conditions.

The two-step procedure described leads to the formation of well-defined, homogeneous protein conjugates with a minimum of side reactions. The results presented should permit the definition of parameters for applying the procedure to other protein substrates, such as antibodies and their fragments, to form conjugates with chelators, reporter groups, or cytotoxic agents.

ACKNOWLEDGMENT

We thank Ms. Irène Rossitto, Ms. Murielle Haldemann, and Mr. P.-O. Regamey for expert technical assistance. This work was supported by funding from the Fonds National de la Recherche Scientifique, Hoffmann-La Roche, Ligue Suisse Contre le Cancer. We thank the Schmidheiny Foundation for the purchase of some of the HPLC equipment.

LITERATURE CITED

(1) For example see: Ghose, T., and Blair, A. H. (1987) The design of cytotoxic-agent-antibody conjugates. *CRC Crit. Rev. Ther. Drug Carrier Syst. 3*, 263–359.

(2) For example, see: Murayama, A., Shimada, K., and Yamamoto, T. (1978) Modification of immunoglobulin G using specific reactivity of sugar moiety. *Immunochemistry 15*, 523–528.

(3) For example, see: Rodwell, J. D., Alvarez, V. L., Lee, C., Lopes, A. D., Goers, J. W. F., King, H. D., Powsner, H. J., and McKearn, T. J. (1986) Site-specific covalent modification of monoclonal antibodies: in vitro and in vivo evaluations. *Proc. Natl. Acad. Sci. U.S.A. 83*, 2632–2636.

(4) Canova-Davis, E., and Carpenter, F. (1981) Semisynthesis of insulin: specific activation of the arginine carboxyl group of the B chain of desoctapeptide-(B23–30)-insulin (bovine). *Biochemistry 20*, 7053–7058.

(5) Jones, R. M. L., and Offord, R. E. (1982) The proteinase-catalysed synthesis of peptide hydrazides. *Biochem. J. 203*, 125–129.

(6) Yagisawa, S. (1981) Studies on protein semisynthesis. I. Formation of esters, hydrazides and substituted hydrazides of peptides by the reverse reaction of trypsin. *J. Biochem. (Tokyo) 89*, 491–501.

(7) Zhang, Y. S., Cao, Q. P., Li, Z. G., and Cui, D. F. (1983) Preparation of [B23-D-alanine]des-(B25–B30)-hexapeptide-insulin by a combination of enzymic and nonenzymic synthesis. *Biochem. J. 215*, 697–699.

(8) Rose, K., Herrero, C., Proudfoot, A. E. I., Offord, R. E., and Wallace, C. J. A. (1988) Enzyme-assisted semisynthesis of polypeptide active esters and their use. *Biochem. J. 249*, 83–88.

(9) Proudfoot, A. E. I., Rose, K., and Wallace, C. J. A. (1989) Conformation-directed recombination of enzyme-activated peptide fragments: a simple and efficient means to protein engineering. *J. Biol. Chem. 264*, 8764–8770.

(10) Wilchek, M., Schwarz, A., Wandrey, C., and Bayer, E. A. (1990) Use of Carboxypeptidase Y for the introduction of probes into proteins via their carboxy terminus. *Peptides: Chemistry, Structure and Biology* (J. E. Rivier, and G. R. Marshall, Eds.) pp 1038–1040, Escom, Leiden.

(11) Offord, R. E., and Rose, K. (1986) Press-stud protein conjugates. *Protides of the Biological Fluids* (H. Peeters, Ed.) pp 35–38, Pergamon, Oxford.

(12) Offord, R. E., Pochon, S., and Rose, K. (1987) Press-stud protein conjugates. *Peptides 1986* (D. Theodoropoulos, Ed.) pp 279–281, W. de Gruyter, Berlin.

(13) King, T. P., Zhao, S. W., and Lam, T. (1986) Preparation of protein conjugates via intermolecular hydrazone linkage. *Biochemistry 25*, 5774–5779.

(14) Rose, K., Jones, R. M. L., Sundaram, G., and Offord, R. E. (1989) Attachment of linker groups of carboxyl termini using enzyme-assisted reverse proteolysis. *Peptides 1988* (G. Jung, and E. Bayer, Eds.) pp 274–276, W. de Gruyter, Berlin.

(15) Fisch, I., Pochon, S., Werlen, R., Jones, R. M. L., Rose, K., and Offord, R. E. (1991) Site specific modification of antibodies by enzyme-assisted reverse proteolysis. *Peptides 1990* (E. Giralt, and D. Andreu, Eds.) pp 819–821, ESCOM, Leiden, The Netherlands.

(16) Morihara, K., Oka, T., Tsazuki, H., Tochino, Y., and Kanaya, T. (1980) Achromobacter protease I-catalyzed conversion of porcine insulin into human insulin. *Biochem. Biophys. Res. Commun. 92*, 396–402.

(17) Carpenter, F. (1967) Treatment of trypsin with TPCK. *Methods Enzymol. 11*, 237.

(18) Pochon, S., Buchegger, F., Pélegrin, A., Mach, J.-P., Offord, R. E., Ryser, J. E., and Rose, K. (1989) A novel derivative of the chelon desferrioxamine for site-specific conjugation to antibodies. *Int. J. Cancer 43*, 1188–1194.

(19) Savoy, L.-A., Jones, R. M. L., Pochon, S., Davies, J. G., Muir, A. V., Offord, R. E., and Rose, K. (1988) Identification by fast atom bombardment mass spectrometry of insulin fragments produced by insulin proteinase. *Biochem. J. 249*, 215–222.

(20) Rose, K., Savoy, L.-A., Simona, M. G., Offord, R. E., and Wingfield, P. (1988) C-terminal peptide identification by fast atom bombardment mass spectrometry. *Biochem. J. 250*, 253–259.

Technetium Labeling of Monoclonal Antibodies with Functionalized BATOs. 1. $TcCl(DMG)_3PITC$

K. E. Linder, M. D. Wen, D. P. Nowotnik,* M. F. Malley, J. Z. Gougoutas, A. D. Nunn,* and W. C. Eckelman

The Bristol-Myers Squibb Pharmaceutical Research Institute, One Squibb Drive, New Brunswick, New Jersey 08903. Received March 6, 1991

BATO (boronic acid adduct of technetium dioximes) complexes, $TcCl(dioxime)_3BR$, were prepared in which the boron substituent (R) was the protein-reactive *m*-phenyl isothiocyanate (PITC). The $^{99}TcCl(dioxime)_3PITC$ complexes [dioxime = dimethylglyoxime (DMG) or cyclohexanedione dioxime (CDO)] were prepared from $^{99}Tc(dioxime)_3(\mu\text{-}OH)SnCl_3$ and characterized. The X-ray crystal structure of $^{99}TcCl(DMG)_3PITC$ was determined. The ^{99m}Tc complexes were prepared from $^{99m}TcO_4^-$ in a process using a freeze-dried kit, either in a one-step procedure or via $^{99m}TcCl(dioxime)_3$. Initial labeling studies with $^{99m}TcCl(dioxime)_3PITC$ were performed on glycine and polylysine and, subsequently, on mouse IgG and the B72.3 monoclonal antibody. Covalent attachment of $^{99m}TcCl(DMG)_3PITC$ to B72.3 was demonstrated by SDS-PAGE electrophoresis. B72.3 labeled with $^{99m}TcCl(DMG)_3PITC$ displayed high binding to a TAG 72 affinity column and had a distribution in normal mice similar to that reported for iodine-labeled B72.3.

INTRODUCTION

Due to the ideal properties of technetium-99m for medical imaging, there is wide spread interest in developing techniques for the rapid and specific labeling of monoclonal antibodies with this radionuclide. The attachment of ^{99m}Tc to monoclonal antibodies can be categorized as either direct attachment (where labeling is achieved by chelation of the reduced metal to unmodified or simply modified antibody) or indirect attachment (by way of a bifunctional chelating group). Examples of direct attachment have been reviewed (*1*). While direct labeling is simple to perform, without modification of the antibody, significant labeling of low-affinity sites does take place (*2*). When technetium is bound to these low-affinity sites, the metal-antibody link can be labile and subject to in vivo breakdown. This lowers target uptake and elevates background levels of radioactivity compared to that seen with a radiolabeled antibody with a stable metal-antibody link. As free thiols have a high affinity for reduced technetium (*3*), a modification of the direct attachment approach involves the production of free thiols on the monoclonal antibody (or a $F(ab')_2$ fragment) by reduction, followed by radiolabeling of the reduced antibody with technetium by transfer of the metal from a labile technetium chelate (*4-7*). This approach significantly reduces the binding to low-affinity sites, but does not entirely eliminate such binding (*2, 8*).

There are two ways in which bifunctional chelating agents (compounds which comprise of a multidentate ligand and a protein-reactive functional group) can be used in antibody labeling: (i) The ligand is first bound to the antibody, and the purified antibody-ligand conjugate is labeled with technetium. (ii) The technetium complex of the bifunctional chelate is formed initially and then reacted with the antibody.

For the first of these approaches, several tetradentate ligands have been utilized. These include derivatives of cyclam (*9, 10*), the dithiasemicarbazones (DTS) (*11, 12*), the diamide-disulfide ligand (DADS) (*13*), and the diamine-dithiol (DADT) ligand (*14-17*). Chelating macromolecules, such as metallothionein, have also been attached to antibodies for technetium labeling (*18-20*). Chelation of technetium to the antibody-ligand complex suffers from the same problems as the indirect labeling approach; the binding to low-affinity sites is not entirely avoided, and so, some in vivo loss of label may result (*2, 8*).

Previous studies involving the direct attachment of a preformed technetium chelate to the monoclonal antibody have concentrated on the use of three technetium cores: $^{99m}Tc(V)ON_2S_2$, diamido dithiol complexes; $^{99m}Tc(V)ON_3S$, triamido thiols (*21-23*), derivitized with an active ester group for linkage to primary amines on the protein; and ^{99m}Tc-cyclam complexes (*9, 24, 25*) derivatized with a maleimide or vinylpyridine, for conjugation to free thiols (obtained by derivatization of the protein with 2-iminothiolane). While indirect labeling generally involves greater manipulation (purification steps) of the radiolabeled protein than is the case for the direct labeling methods, it has the advantage that the radiolabel exists in a known chemical form, with no low-affinity binding of technetium. This report describes studies of indirect protein labeling utilizing a functionalized derivative of the seven-coordinate Tc(III) BATO (boronic acid adduct of technetium dioximes) class of technetium complexes (*26*).

The BATO complexes (general structure shown in Figure 1) are neutral, lipophilic complexes that are stable; i.e. the technetium atom cannot readily be removed by challange from other ligands. BATOs are formed by a template reaction involving a vicinal dioxime, a boronic acid, pertechnetate, and stannous ion (as reductant) at low pH (*27*). The versatility of this reaction has permitted the synthesis of a large number of BATOs (*28*). From this series, two compounds were selected for clinical evaluation, as myocardial and cerebral perfusion tracers (*29, 30*). By using a boronic acid derivatized with a protein-reactive functional group, we felt that we could extend the application of BATO complexes to protein labeling. A suitable protein-reactive functional group is isothiocyanate (R—N=C=S). Isothiocyanates react with free primary amine groups to form a stable thiourea link. Others have used isothiocyanates to link modified DTPA ligands to monoclonal antibodies (*31*). In this paper, we describe the synthesis and characterization of BATOs which contain an isothiocyanato functional group. The use of these bifunctional chelates in labeling amine-containing bio-

1043-1802/91/2902-0160$02.50/0 © 1991 American Chemical Society

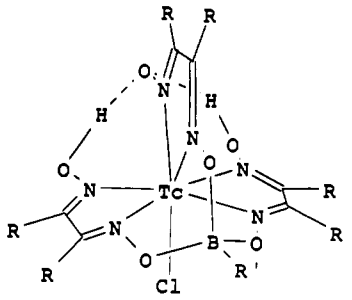


Figure 1. The general structure of BATOs. Technetium is bound to six nitrogen atoms, from three vicinal dioximes, and a monodentate anion (Cl^- in this example). One end of the BATO is capped by a boronic acid. In this paper, the protein-reactive isothiocyanate group is part of the R′ substitutent.

molecules and preliminary studies in animals of the monoclonal antibody B72.3 labeled with one of these reagents are also described.

EXPERIMENTAL PROCEDURES

Materials and Reagents. Dimethylglyoxime (DMG) (Eastern Chemicals), cyclohexanedione dioxime (CDO), and stannous chloride ($SnCl_2$) (MCB) were used as received. Polylysine (MW 102 000) bovine serum albumin fraction V (BSA), mouse IgG, and rat serum were purchased from Sigma. Sephadex G-25 (medium grade) was purchased from Pharmacia. B72.3 monoclonal antibody (2.81 mg/mL) was purchased from Damon Biotech. PRP-1 resin (12–20 μm) was purchased from Alltech Associates.

3-Isothiocyanatophenylboronic acid (PITC) was synthesized in our laboratories by reaction of 3-aminophenylboronic acid and thiophosgene; details are reported elsewhere (*32*). Ammonium pertechnetate (NH_4TcO_4) was purchased from Oak Ridge National Laboratories and recrystallized from dilute aqueous hydrogen peroxide. The complexes Tc(dioxime)$_3$(μ-OH)$SnCl_3$ (dioxime = DMG, CDO) were prepared as described previously (*27*). [^{99m}Tc]pertechnetate ($^{99m}TcO_4^-$) was obtained in a saline solution from a Squibb Minitec Generator. All other chemicals were of reagent grade and were used as received. All solvents were of either HPLC or reagent grade (except acetonitrile, which was pesticide grade) and were used as received. All water used in these studies was obtained from a Millipore Milli-Q water-purification unit.

Most reagents and standards used in the SDS–polyacrylamide gel electrophoresis were purchased from Bio-Rad. Phast gel blue, 10–15% gradient gel, and SDS buffer strips were purchased from Pharmacia.

The following buffers were prepared: 0.1 M ammonium acetate (pH 4.6), phosphate-buffered saline [PBS; 0.01 M sodium phosphate buffer (pH 6.0) and 0.15 M of NaCl], and 0.1 M sodium phosphate buffer (pH 9.5). The 6 M guanidine was prepared in water and filtered through a 0.2-μm membrane. Buffers and solutions used in Phast gel electrophoresis were prepared according to the directions in the Phast system manual.

A TAG-72-Reacti-Gel affinity column was prepared in-house (*33*).

Freeze-dried "kits" were prepared for the formation of $^{99m}TcCl(DMG)_3$ from $^{99m}TcO_4^-$. Each kit consisted of a sealed 5-mL siliconized serum vial containing DMG (12.9 μmol), NaCl (1.7 mmol), citric acid (52 μmol), diethylenetriaminepentaacetic acid (DTPA, 2.5 μmol), $SnCl_2$ (0.22 μmol), and γ-cyclodextrin (38.5 μmol). Immediately prior to freeze-drying, the solution pH was adjusted to 2.0 with HCl, and after freeze-drying, the vials were filled with nitrogen gas and sealed. Kits in which CDO (10.5 μmol) was substituted for DMG and pH was adjusted to 3.75 were also prepared as described above.

Analysis of the Labeling Reagents. Silica gel TLC plates (Bakerflex 1B) were developed with CH_2Cl_2 or CH_3CN.

HPLC separations were performed on a Spectra Physics Model SP8700XR HPLC system equipped with SP4270 integrator, spectrophotometer (Kratos, SF769Z), radiometric detector (Tennelec minibin), dual-pen recorder, and fraction collector. The outputs from the radiation detector and spectrophotometer (set at 280 nm) were integrated via the SP4270 integrator. The data were stored and reprocessed with LABNET software.

^{99}Tc- and ^{99m}Tc-labeling reagents were analyzed on a 30-cm Lichrosorb RP-18 column (E. Merck) using a mobile phase of acetonitrile/0.1 M ammonium acetate pH 4.6 (75/25, v/v) at a flow rate of 1 mL/min. The radiochemical purities (RCP) of the ^{99m}Tc complexes were determined as 100× the radioactivity associated with the complex peak, divided by the total radioactivity eluted from the column. ^{99}Tc complexes were monitored by UV detection at 250 nm. Proteins were monitored at 280 nm.

Infrared spectra were obtained on a Sirius 100 FT-IR spectrometer as KBr pellets. Proton NMR data were obtained on a JEOL GX 250 spectrometer. UV–visible spectra were measured on a Hewlett-Packard 8451A photodiode-array spectrophotometer. Fast-atom-bombardment mass spectra were obtained on a VG-ZAB-2F spectrometer, from a matrix of thioglycerol/CH_3CN. Elemental analyses were performed in-house by Squibb Microanalytical Department.

Synthesis and Characterization of ^{99}Tc Complexes. *Synthesis of ^{99}TcCl(CDO)$_3$PITC from Tc(CDO)$_3$(μ-OH)SnCl$_3$.* A solution containing Tc(CDO)$_3$(μ-OH)$SnCl_3$·3H_2O (77 mg, 0.095 mmol), 3-isothiocyanatophenylboronic acid (22 mg, 0.12 mmol), EtOH (10 mL), and 1 M HCl (2 mL) was boiled in a small beaker for 1 h. During this time, the color of the solution changed from yellow-orange to deep orange-red and the volume reduced to <2 mL. Orange crystals of the product precipitated on cooling to room temperature and were isolated by suction filtration, washed with 1 M HCl, and dried in vacuo. The crude product was purified by silica gel column chromatography on a column (1.5 × 10 cm) conditioned with CH_2Cl_2 and eluted with 5% CH_3CN/95% CH_2Cl_2. The product (39 mg, 60%), the first red-orange band eluted, was collected and the solvent removed. The residue was recrystallized from 5 mL of CH_2Cl_2/CH_3CN/EtOH (2:5:1). Anal. Calcd for $C_{25}H_{30}N_7BClO_6STc$: C, 42.78; H, 4.31; N, 13.97. Found: C, 42.65; H, 4.44; N, 14.26.

Synthesis of ^{99}TcCl(DMG)$_3$PITC from Tc(DMG)$_3$(μ-OH)SnCl$_3$. A solution containing Tc(DMG)$_3$(μ-OH)-$SnCl_3$·3H_2O (97 mg, 0.138 mmol), 3-isothiocyanatophenylboronic acid (32 mg, 0.18 mmol), EtOH (10 mL), and 1 M HCl (2 mL) was boiled in a small beaker for 1 h. During this time the volume of the solution reduced to 3 mL, and red-orange crystals of the product precipitated. After cooling of the reaction mixture to room temperature, the precipitate was isolated by suction filtration, washed with 1:1 EtOH/1 M HCl, and dried in vacuo to yield 52 mg of product. Recrystallization from 10 mL of a warm CH_2Cl_2/EtOH mixture (1:5) yielded crystals (47 mg, 54%) suitable for an X-ray crystal structure analysis. Material for analysis was washed with ethanol and dried in vacuo. Crystals for the X-ray structure determination were air-dried. Anal. Calcd for $C_{19}H_{24}N_7BClO_6STc$: C, 36.59; H, 3.89; N, 15.72. Found: C, 36.36; H, 3.80; N, 15.88.

Synthesis of $^{99}TcCl(DMG)_3PITC$ from NH_4TcO_4. Solid $SnCl_2$ (286 mg, 1.5 mmol) was dissolved in 1 mL of concentrated HCl and 4 mL of water. This solution was added dropwise, with stirring, to a solution containing NH_4TcO_4 (115 mg, 0.635 mmol), DMG (240 mg, 2.07 mmol), and 3-isothiocyanatophenylboronic acid (115 mg, 0.65 mmol) in EtOH (50 mL) and 1 M HCl (5 mL). The resultant deep red-orange solution was heated at a gentle boil in an open beaker for 1.5 h, then cooled to room temperature. Water (30 mL) was added, resulting in the precipitation of an orange solid, which was isolated by suction filtration and dried in vacuo (crude yield 99 mg). Additional product was extracted from the supernatant with 2 × 25 mL of CH_2Cl_2. These washings were combined, washed with 2 × 50 mL of 1 M HCl, dried over sodium sulfate, and evaporated to dryness to give an orange oil. Purification by silica gel chromatography (1 × 20 cm column conditioned with hexanes) yielded the product as an orange band on elution with CH_2Cl_2. On further elution with CH_2Cl_2/CH_3CN (95/5), a pink/orange compound was obtained. Individually, both bands were evaporated to dryness and recrystallized from CH_3CN/0.1 M HCl to yield $^{99}TcCl(DMG)_3PITC$ (85 mg, 21%) and 20 mg of an impure pink/orange product.

$^{99}TcCl(DMG)_3PITC$ prepared in this way was indistinguishable from that prepared from $Tc(DMG)_3(\mu\text{-}OH)\text{-}SnCl_3\cdot 3H_2O$, as determined by TLC ($R_f$ 0.85), HPLC, and UV–visible spectroscopy.

The impure pink/orange product was purified by silica gel chromatography (2.5 × 3 cm column conditioned with hexanes). The column was initially eluted with 50/50 CH_2Cl_2/hexanes and with CH_2Cl_2, and the product was eluted from the column with CH_2Cl_2 that contained 4% CH_3CN. Spectroscopic data on this compound are given in Table I.

Crystal Structure Analysis. Unit cell parameters (Table II) were obtained through a least-squares analysis of 15 high-angle reflections. The space group assignment was confirmed by means of Weissenberg and precession photographs. The crystal density was measured by flotation in carbon tetrachloride/bromoform/hexane mixtures. Intensities were measured on a SYNTEX P21 diffractometer at 23 °C using graphite-monochromated Mo Kα radiation (λ = 0.71069 Å) with the θ–2θ variable-scan technique and were corrected for Lorentz and polarization factors and for absorption (*34*). Background counts were collected at the extremes of each scan. No decrease of intensity was observed during data collection. The structure was solved by heavy-atom techniques and refined by full-matrix least-squares analyses (SDP program package (*35*)) based on "observed" reflections having $I \geq 3\sigma(I)$. Least-squares weights were assigned with the assumption that $\sigma^2 = \epsilon^2 + (pI)^2$, where ϵ is the statistical counting error and $p = 0.04$. The function minimized in the refinements was $\Sigma_w(|F_o| - |F_c|)^2$. R is defined as $\Sigma||F_o| - |F_c||/\Sigma|F_o|$ while $R_w = [\Sigma_w(|F_o| - |F_c|)^2/\Sigma_w|F_o|^2]^{1/2}$.

Synthesis of ^{99m}Tc Complexes. The radioactive concentration of $Na^{99m}TcO_4$, unless stated otherwise, was adjusted to approximately 10 mCi/mL prior to use.

Synthesis of $^{99m}TcCl(DMG)_3PITC$ from TcO_4^-. To a freeze-dried DMG kit was added 3.0 mg of 3-isothiocyanatophenylboronic acid in ethanol (50 μL). $Na^{99m}TcO_4$ in physiological saline (1.0 mL) was added to the vial, which was then heated at 100 °C for 5 min. The radiochemical purity (RCP) of $^{99m}TcCl(DMG)_3PITC$, as determined by Licrosorb RP-18 HPLC, was 35–40%, prior to purification.

Synthesis of $^{99m}TcCl(DMG)_3$ from TcO_4^-. Following the above procedure, but omitting the boronic acid entirely, and heating the kit for 2.5 min at 100 °C gave the uncapped complex $^{99m}TcCl(DMG)_3$. RCP of this product was 76%.

Synthesis of $^{99m}TcCl(CDO)_3PITC$ from TcO_4^-. To a freeze-dried CDO kit was added 2.4 mg of 3-isothiocyanatophenylboronic acid in ethanol (50 μL). $Na^{99m}TcO_4$

Table I. IR, UV, and ^{1}H NMR Spectroscopy and Mass Spectrometry Data of $^{99}TcCl(dioxime)_3PITC$ and $^{99}TcCl(DMG)_2(oxime\text{–}imine)PITC$

a. Main Bands in the IR Spectra

	cm^{-1}	assignment
$TcCl(CDO)_3PITC$	3430	OH
	2122, 2080, 2056	NCS
$TcCl(DMG)_3PITC$	3430	OH
	2111	NCS
$TcCl(DMG)_2(imine\text{–}oxime)PITC$	3450	OH
	2100, 2050	NCS

b. UV Spectra: λ_{max} Values (in ACN)

	nm
$TcCl(CDO)_3PITC$	216, 266, 320, 386, 468
$TcCl(DMG)_3PITC$	214, 266, 320, 382, 462
$TcCl(DMG)_2(oxime\text{–}imine)PITC$	216, 266, 322, 384, 480

c. ^{1}H NMR Spectroscopy Data

complex	chemical shift, δ	assignment	integration
$^{99}TcCl(CDO)_3PITC$	14.9 (s)	O- - -H- - -O	1.6
	7.2–7.6 (m)	phenyl	4
	2.9–3.9 (m)	CDO	12
	1.7–1.9 (m)	CDO	12
	1.2 (s)	H_2O	2
$^{99}TcCl(DMG)_3PITC$	15.1 (s)	O- - -H- - -O	1.5
	7.2–7.7 (m)	phenyl	3.9
	2.3–2.5 (m)	DMG	18
	1.5 (s)	H_2O	3
$TcCl(DMG)_2(imine\text{–}oxime)PITC$	11.8 (s)	O- - -H- - -O	~0.5
	7.2–7.8 (m)	phenyl	3.9
	2.3–2.5 (m)	DMG	12
	2.25, 2.65	CH_3s in oxime–imine	5.0

d. Mass Spectral Data

complex	FAB$^+$, m/z	FAB$^-$, m/z
$^{99}TcCl(CDO)_3PITC$	702 $(M + H)^+$	700 $(M - H)^-$
(MW = 701)	666 $(702 - HCl)^+$	666 $(M - HCl)^-$
$^{99}TcCl(DMG)_3PITC$	624 $(M + H)^+$	622 $(M - H)^-$
(MW = 623)	623 $(M)^+$	
	588 $(624 - HCl)^+$	587 $(622 - HCl)^-$
	571 $(588 - 17)^+$	570 $(587 - 17)^-$
	556 $(588 - 32)^+$	555 $(587 - 32)^-$
$^{99}TcCl(DMG)_2(oxime\text{–}imine)PITC$	608 $(M + H)^+$	
(MW = 607)	572 $(608 - HCl)^+$	
	557 $(572 - 15)^+$	
	540 $(572 - 32)^+$	

Table II. Crystal Data and Structure Refinement of $TcCl(DMG)_3PITC$

solvent	$EtOH/CH_2Cl_2$	D_{calc}, g cm^{-3}	1.606
color	red	formula	$TcClC_{19}H_{24}N_7O_6SB$
a, Å	12.725 (3)	fw	623.8
b, Å	13.126 (2)	$2\theta_{max}$, deg	50
c, Å	15.470 (2)	N_{ref}[a]	4806
β, deg	94.44 (2)	N_{uni}[b]	4372
V, Å^3	2576 (1)	N_{obs}[c]	2290
space group	$P2_1/n$	N_{var}[d]	325
Z	4	R	0.047
D_{obs}, g cm^{-3}	1.61	R_w	0.049

[a] Total number of measured reflections within $2\theta_{max}$. [b] Total number of symmetry independent measured reflections. [c] Total number of "observed" reflections with $I \geq 3\sigma(I)$ used for refinements. [d] Number of variables in least-squares refinements.

in physiological saline (1.0 mL) was added to the vial, which was then heated at 100 °C for 15 min. The RCP of ^{99m}TcCl(CDO)$_3$PITC was 33%, prior to purification.

Synthesis of ^{99m}TcCl(CDO)$_3$ from TcO_4^-. Following the above procedure, but omitting the boronic acid entirely, provided ^{99m}TcCl(CDO)$_3$, with an RCP of 92%.

Synthesis of ^{99m}TcCl(CDO)$_3$PITC from ^{99m}TcCl(CDO)$_3$. To ^{99m}TcCl(CDO)$_3$, prepared as described above, was added 2.4 mg of 3-isothiocyanatophenylboronic acid in ethanol (50 μL). The mixture was heated for 15 min at 100 °C. The RCP of ^{99m}TcCl(CDO)$_3$PITC prepared by this route was 48.5%.

Purification of ^{99m}TcCl(dioxime)$_3$PITC Prior to Labeling Studies. A small volume (ca. 0.1 mL) of a 40% v/v suspension of PRP-1 resin (10 μm diameter) in a 25% v/v ethanol/saline mixture was drawn into a 1-mL syringe. A Millex HV$_4$ 0.45 μm filter was attached to the end of the syringe and the suspension filtered, causing the PRP-1 resin to pack into a plug on the Millex filter.

The contents of the kit were drawn into a 1-mL syringe and loaded onto the top of the syringe containing the PRP-1 resin. The kit contents were passed through the PRP-1 resin, and the filtrate was discarded. The PRP-1 resin was washed twice with 0.5 mL of 50% v/v ethanol/water solution, to remove impurities and excess boronic acid.

The product radioactivity was eluted from the PRP-1 resin with 0.8 mL of absolute ethanol into a siliconized glass vial. The RCP of purified product was determined by Licrosorb RP-18 HPLC analysis.

Synthesis of ^{99m}TcCl(DMG)$_3$PA (PA = m-Aminophenyl) from TcO_4^-. To a freeze-dried DMG kit was added 4.0 mg of 3-aminophenylboronic acid in ethanol (50 μL). Na^{99m}TcO$_4$ in physiological saline (1.0 mL) was added to the vial, which was then heated at 100 °C for 5 min. The radiochemical purity (RCP) of ^{99m}TcCl(DMG)$_3$PA, as determined by Licrosorb RP-18 HPLC, was 81%.

Study of the Effect of pH and Heating Time on the RCP of ^{99m}TcCl(DMG)$_3$PITC. *Effect of pH.* To a freeze-dried DMG kit was added 3.0 mg of 3-isothiocyanatophenylboronic acid in ethanol (50 μL). The pH of the solution was adjusted to pH 2.0, 2.5, 3.0, and 4.0 by addition of (respectively) 50 μL of 1 M HCl, 50 μL of water, 50 μL of 1 M NaOH, and 100 μL of NaOH. Na^{99m}TcO$_4$ in physiological saline (1.0 mL) was added to each vial, which was then heated at 100 °C for 5 min. When the vials had cooled, the RCP of ^{99m}TcCl(DMG)$_3$PITC was determined by Licrosorb RP-18 HPLC.

Effect of Reaction Time. 3-Isothiocyanatophenylboronic acid (3 mg) in ethanol (50 μL) was added to each of four freeze-dried DMG kits. Na^{99m}TcO$_4$ in physiological saline (1.0 mL) was added to each vial, and vials were heated at 100 °C for 1, 5, 10, and 15 min. After cooling, the RCP of ^{99m}TcCl(DMG)$_3$PITC were determined by Licrosorb RP-18 HPLC.

Trial Labeling Reactions with ^{99m}TcCl(DMG)$_3$PITC. *Determination of a Suitable Solvent System for the Labeling Reaction.* Samples of ^{99m}TcCl(DMG)$_3$PITC in ethanol (purified on PRP-1 resin, as outlined above) were taken to dryness with a stream of nitrogen and redissolved in either DMSO (100 μL), 0.01 M pH 9 sodium phosphate buffer (100 μL), or ethanol (250 μL). Each sample was diluted with buffer, as outlined in Table V.

After storage at room temperature for 1 h, the total radioactivity in each vial was determined with a radioisotope calibrator (CAPINTEC, Model CRC-10R). The vial contents were transferred to a fresh vial, and the total radioactivity in solution was determined. The percentage recovery of labeling reagent was determined as

$$\% \text{ recovery of radioactivity} = \frac{\text{total radioactivity in solution} \times 100}{\text{total radioactivity in the vial}}$$

Labeling of Glycine. An aliquot of 200 μL of purified ^{99m}TcCl(DMG)$_3$PITC in ethanol was added to a solution of glycine (4 mg) in 0.1 M pH 8.5 sodium phosphate buffer (200 μL), and the mixture incubated at 37 °C for up to 2 h. The percent of the reaction mixture in the form of unreacted labeling reagent, glycine conjugate, and hydrolyzed labeling reagent was determined by HPLC (Licrosorb RP-18). The study was repeated with a buffer pH of 9.0.

Labeling of Polylysine. A 10 mg/mL aqueous solution of polylysine (average MW 102 000) was diluted with 0.1 M pH 9 sodium phosphate buffer to lower the polymer concentration to 5 mg/mL. ^{99m}TcCl(DMG)$_3$PITC was purified on PRP-1 resin, as outlined above; after removal of solvent (ethanol) in a stream of nitrogen, the reagent was dissolved in 50 μL DMSO. An aliquot (100 μL) of the polylysine solution was added to an aliquot (10 μL) of the ^{99m}TcCl(DMG)$_3$PITC solution, and the reaction mixture was incubated for 2 h at 37 °C. A control study was conducted by mixing 0.1 M pH 9 sodium phosphate buffer (100 μL) with an aliquot (10 μL) of the ^{99m}TcCl(DMG)$_3$PITC solution. Both reactions were monitored by HPLC, with a 1-cm ISRP precolumn (Alltech Associates), as described below.

Analysis of the Labeled Affinities. *Paper chromatography (PC)* was performed by placing a sample (2 μL) of the protein labeling reaction mixture on a 1.3 × 9 cm strip of Whatman 31 ET chromatography paper, at 2.0 cm from one end of the paper. The strip was developed by ascending chromatography using acetone/0.1 M pH 4.6 aqueous ammonium acetate (75/25, v/v) as eluent, until the solvent front had advanced 7 cm from the origin. The strip was dried, and separated into two portions by cutting the strip 1.0 cm above the origin. The radioactivity in both segments was assayed. The percentage of radiolabeled protein was determined as

$$\frac{\text{cpm in the origin section} \times 100}{\text{total cpm}}$$

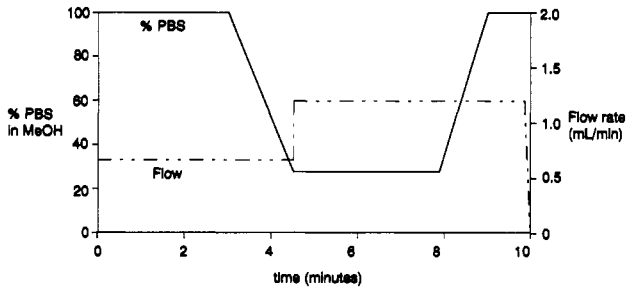
HPLC analysis of labeled proteins was performed by using the apparatus described earlier. Three different column/eluent systems were used for analysis of ^{99m}Tc-labeled proteins.

HPLC Analysis with a TSK-SWG3000 Column. The performance of a 7.5 mm × 30 cm TSK-SWG3000 (exclusion limit ca. 300 000 Da) column (Phenomenex) was evaluated by running a Bio-Rad gel-filtration standard through the column prior to the injection of the labeled protein sample.

The samples were eluted from the column with PBS buffer at a flow rate of 1 mL/min. for 20 min. Fractions of 1-mL volume were collected, and the radioactivity contained in each fraction was determined with a dose calibrator. The antibody concentration (mg/mL) was calculated by dividing the absorbance at 280 nm by 1.36 (*36*). Fractions containing labeled antibody were pooled into one tube and used for further analysis.

The percent recovery of radioactivity or protein was calculated by dividing the radioactivity or protein contained in the eluted protein peak tubes by the total radioactivity or protein loaded onto the column.

HPLC Analysis with an ISRP Column. Radiolabeled protein mixtures were analyzed on a 1-cm ISRP precolumn eluted with MeOH/PBS buffer, as follows:



Phast SDS-PAGE Electrophoresis. A Phast SDS-PAGE electrophoresis system (Pharmacia) was used for the characterization of ^{99m}Tc-labeled B72.3 antibody using 10–15% gradient gels and the reagents, buffers, separation protocols, and development methods recommended by the manufacturer.

Duplicate gels of each sample were prepared. At the end of the separation, one gel was stained, destained, and dried. Both gels were sliced transversely into 20 pieces, each 2 mm thick. The radioactivity of each slice was determined by counting in a γ counter, and these data were used to calculate the percent radioactivity associated with each antibody monomer/fragment fraction.

Labeling of Mouse IgG with ^{99m}TcCl(DMG)$_3$PITC. ^{99m}TcCl(DMG)$_3$PITC was purified as outlined above, and the ethanolic solution was dried in a stream of nitrogen. The reagent was dissolved in 50 μL of DMSO. This solution was used in the studies outlined below.

Effect of pH and Reaction Time on Labeling Yield. An aliquot (10 μL) of the ^{99m}TcCl(DMG)$_3$PITC solution was mixed with 100 μL of mouse IgG (5 mg/mL in 0.1 M pH 0.5 sodium phosphate buffer) and the mixture was incubated in a water bath at 37 °C. A control study containing TcCl(DMG)$_3$PITC and buffer, but no antibody, was also prepared. Both reaction mixtures were monitored by ISRP HPLC. The percent of radioactivity which eluted in the void volume in the control study was subtracted from the percent in the void volume in the study with IgG to correct the observed percent protein-bound figure for radioactivity in the void volume that was not associated with the protein.

Effect of Antibody Concentration on the Labeling Yield. An aliquot (10 μL) of the ^{99m}TcCl(DMG)$_3$PITC solution was mixed with 100 μL of mouse IgG (5 mg/mL, 10 mg/mL, and 15 mg/mL in 0.1 M pH 9.5 sodium phosphate buffer). The reaction mixture was incubated at ambient temperature or at 37 °C. The reaction mixtures were monitored by HPLC, with the ISRP precolumn. Control studies, with no IgG present, were performed, to correct for radioactivity in the void volume not associated with the protein, as described above.

Purification of Mouse IgG Labeled with ^{99m}TcCl(DMG)$_3$PITC. Three procedures were investigated for the purification of labeled IgG. For these studies, ^{99m}Tc-labeled mouse IgG was prepared by mixing 10 μL of ^{99m}TcCl(DMG)$_3$PITC in DMSO with 100 μL of mouse IgG (5 mg/mL in 0.1 M pH 9.5 sodium phosphate buffer) and the mixture was incubated at 37 °C for 2 h.

Method 1. Sephadex (G-25, medium grade, Pharmacia) was swollen overnight at pH 6.0 PBS buffer, and a G-25 column was prepared in a 10-mL disposable pipet. The column was pretreated with 1 mL of 10% bovine serum albumin (BSA), followed by washing with 20 mL of PBS. The labeled IgG was eluted with 10 mL of PBS buffer, with collection of 1-mL aliquots. Each fraction was assayed for radioactivity and protein; fractions containing protein were combined. The percentage recoveries of radioactivity (in the protein-containing fraction) and protein were determined by dividing the quantity found in the combined protein fraction by the total loaded onto the column.

Method 2. HPLC purification was performed on the TSK-SWG3000 column, as described in the analysis section above.

Method 3. Initial purification of the labeled IgG was achieved by Sephadex G25 gel chromatography, as outlined above. The pooled fractions containing protein were subjected to further purification by TSK-SWG3000 HPLC.

Labeling of B72.3 with ^{99m}TcCl(DMG)$_3$PITC. For the antibody coupling reactions, the B72.3 monoclonal antibody was first concentrated to 12–13 mg/mL with a Centricon-30 microconcentrator (Amicon) and buffer added such that the final concentration of antibody was about 10 mg/mL in 0.1 M sodium phosphate buffer, pH 9.5. An aliquot of 10 μL of the ^{99m}Tc complex in DMSO was mixed with 100 μL of antibody solution and the mixture was incubated at 37 °C for 2 h. The labeled antibody was purified by method 3 (above).

Immunoreactivity Assay. The immunoreactivity of ^{99m}Tc-labeled B72.3 antibody was evaluated by testing the binding of the labeled antibody to an affinity column prepared with TAG-72 antigen.

The column was equilibrated with 5.0 mL of 1% BSA in PBS at room temperature. ^{99m}Tc-labeled B72.3 antibody and 400 μL of 1% BSA in PBS were added to the column and allowed to stand for 30 min. The column was then eluted (in turn) with 15 mL of PBS buffer, 5.0 mL of 6 M guanidine hydrochloride, 5.0 mL of PBS buffer, and 5.0 mL of the 1% BSA in PBS, with collection of 1-mL fractions. The immunoreactivity of the antibody was determined as the percentage of radioactivity which was eluted from the column with the guanidine solution.

Serum Stability of ^{99m}Tc–B72.3. A 450-μL aliquot of the purified, labeled antibody was added to 50 μL of rat serum and incubated at 37 °C for 90 min. Aliquots of the sample were analyzed by the ISRP-TSK HPLC system, described earlier.

Biodistribution Studies. The biodistributions of ^{99m}TcCl(DMG)$_3$PITC and ^{99m}Tc-labeled B72.3 (purified by method 3) were studied in normal mice. Approximately 1 μCi of either ^{99m}TcCl(DMG)$_3$PITC or the ^{99m}Tc-labeled antibody were administered iv to normal mice. The animals were sacrificed at 1 or 21 h (n = 5 for each time point), and organs of interest removed and assayed for radioactivity.

RESULTS

The ^{99}Tc complexes TcCl(DMG)$_3$PITC and TcCl(CDO)$_3$PITC were prepared in >60% yield from the corresponding Tc(III) tin-capped complex Tc(dioxime)$_3$(μ-OH)SnCl$_3$. The yield of ^{99}TcCl(DMG)$_3$PITC is lower (21%) when the complex is prepared directly from ^{99}TcO$_4^-$ and SnCl$_2$. IR, UV, ^{1}H NMR spectroscopy, and mass spectrometry data (Table I) are in agreement with the assigned structures.

Single-crystal X-ray analysis demonstrates that the structure of TcCl(DMG)$_3$PITC is similar to that of other BATO complexes (*26*, *27*). The plane of the phenyl ring is rotated nearly parallel to the plane of one of the equatorial dioximes, while the approximately linear *m*-isothiocyanate group (angles CNC = 166°, NCS = 178°) extends well away from the bulk of the complex and accordingly represents a freely accessible point of attachment (a sphere of radius 6.1 Å centered on the technetium atom essentially contains the van der Waals surface of the Tc, Cl, B, and DMG atoms; the Tc–S distance is 10.3 Å).

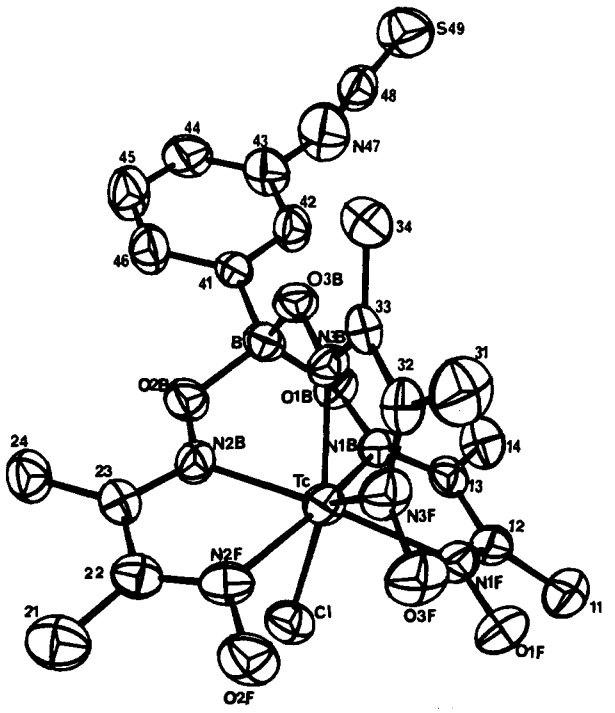


Figure 2. ORTEP diagram of ^{99}TcCl(DMG)$_3$PITC.

Table III. Selected Interatomic Distances and Angles in TcCl(DMG)$_3$PITC[a]

Distances, Å

atom 1	atom 2	distance	atom 1	atom 2	distance
Tc	Cl	2.423 (2)	B	C41	1.601 (11)
Tc	N1F	2.144 (6)	S49	C48	1.563 (9)
Tc	N2F	2.130 (6)	N47	C48	1.154 (11)
Tc	N3F	2.057 (6)	N47	C43	1.40 (1)
Tc	N1B	2.052 (6)	O1F	O2F	3.900 (8)
Tc	N2B	2.051 (6)	O1F	O3F	2.525 (8)
Tc	N3B	2.064 (6)	O2F	O3F	2.543 (8)
Tc	B	3.112 (9)	Tc	S49	10.288 (3)

Angles, deg

atom 1	atom 2	atom 3	angle	atom 1	atom 2	atom 3	angle
N1F	Tc	N2F	116.2 (2)	N3F	Tc	Cl	134.8 (2)
N1F	Tc	N3F	77.0 (2)	N1B	Tc	Cl	84.8 (2)
N2F	Tc	N3F	76.9 (2)	N2B	Tc	Cl	83.9 (2)
N1F	Tc	N1B	72.2 (2)	N3B	Tc	Cl	153.7 (2)
N2F	Tc	N2B	72.3 (2)	B	Tc	Cl	103.2 (2)
N3F	Tc	N3B	71.5 (2)	O1F	O2F	O3F	39.5 (2)
N1F	Tc	Cl	79.7 (2)	O2F	O3F	O1F	100.6 (3)
N2F	Tc	Cl	79.6 (2)	O3F	O1F	O2F	39.9 (2)

[a] Numbers in parentheses are estimated standard deviations in the least significant digits.

An ORTEP (*37*) diagram of the complex is given as Figure 2. Crystal data and some details of the structure refinement are given in Table II. Selected interatomic distances and angles are given in Table III. Tables of final atomic positional parameters, thermal parameters, structure factors, bond distances, and bond angles for TcCl(DMG)$_3$PITC are provided as supplemental material.

A pink/orange BATO-like side product was isolated from the TcCl(DMG)$_3$PITC reaction mixture. This product [TcCl(DMG)$_2$(butane-2,3-dione imine–oxime)PITC] was partially characterized; IR, NMR, and UV–visible spectral data for this compound also are given in Table I. On the basis of these data, we assign it an imine–oxime structure analogous to the byproduct previously encountered in studies (*38*, *39*) of the BATO derived from DMG and ethylboronic acid. The following retention times were observed for the ^{99}Tc complexes on the Licrosorb RP-18 HPLC system:

complex	solvent ratio (ACN/buffer)	t_R, min
TcCl(DMG)$_3$PITC	75/25	8.2
TcOH(DMG)$_3$PITC	75/25	10.5
TcCl(DMG)$_3$PA	75/25	3.2
TcCl(CDO)$_3$PITC	90/10	8.0
TcCl(DMG)$_2$(oxime–imine)PITC	75/25	6.3

Table IV. Effect of Reaction Temperature and pH on the Yield of ^{99m}TcCl(DMG)$_3$PITC

effect of reaction time[a]		effect of reaction pH[b]	
reaction time, min	% RCP	pH	% RCP
1	13	2.0	35
5	30	2.5	28
10	24	3.0	28
15	19	4.0	0

[a] Conditions: 100 °C, pH 2.5. [b] Conditions: 100 °C, heating for 5 min.

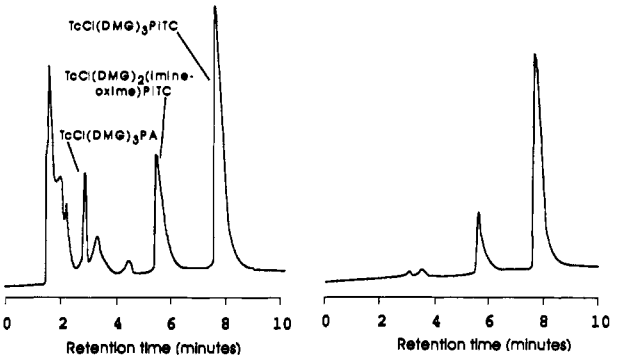


Figure 3. HPLC chromatograms of ^{99m}TcCl(DMG)$_3$PITC before (left) and after purification (right) on PRP-1 resin. HPLC conditions: 30-cm Lichrosorb RP-18 column eluted with acetonitrile/0.1 M ammonium acetate, pH 4.6 (75/25, v/v), at a flow rate of 1 mL/min.

Results of the study to investigate the influence of heating time and reaction pH on the formation of ^{99m}TcCl(DMG)$_3$PITC from ^{99}TcO$_4^-$ are shown in Table IV. An optimum RCP of the reagent of 35% RCP is obtained by heating at 100 °C for 5 min at pH 2. The RCP of the reagent was increased to 66% by purification through absorption onto PRP-1 resin, removal of hydrophilic impurities by washing the resin with buffer, and removal of the reagent with ethanol (Figure 3). ^{99m}TcCl(DMG)$_3$PITC proved to be poorly soluble in water, so a study was undertaken to find a solvent mixture which retained this reagent in solution, yet was compatible with proteins. Results are shown in Table V, which demonstrate that addition of 10% DMSO prevents significant deposition of the reagent onto the wall of the vial.

In trial labeling reactions with the amino acid glycine and synthetic peptide polylysine, BATO conjugates were formed in optimum yields of 88% (with glycine) and 33%, with polylysine, at pH 9, 37 °C. These data were used to determine conditions to be used in the labeling reactions of ^{99m}TcCl(DMG)$_3$PITC with mouse IgG. As shown in Figure 4, the optimum conditions for labeling of this antibody were pH 9.5, for 2 h at 37 °C, with a protein concentration of 15 mg/mL.

Several HPLC methods for the purification of the labeled IgG were studied. Using a G-25 column, an ISRP column, or a TSK-SWG3000 column alone was unsatisfactory. The TSK and G-25 columns did not give baseline resolution of the labeled protein and non-protein-

Table V. Solubility of the Labeling Reagent ^{99m}TcCl(DMG)$_3$PITC

reagent dissolved in	buffer added	% recovery after 1 h
100 μL of 0.01 M phosphate buffer, pH 9.0	100 μL of 0.01 M phosphate buffer, pH 9.0	10
25 μL of EtOH	500 μL of 0.01 M phosphate buffer, pH 9.0	20
10 μL of DMSO	100 μL of 0.01 M phosphate buffer, pH 9.0	59
10 μL of DMSO	100 μL of 0.025 M borate buffer, pH 9.0	67
10 μL of DMSO	100 μL of 0.01 M phosphate buffer, pH 9.0, and 10 mg of γ-cyclodextrin	74

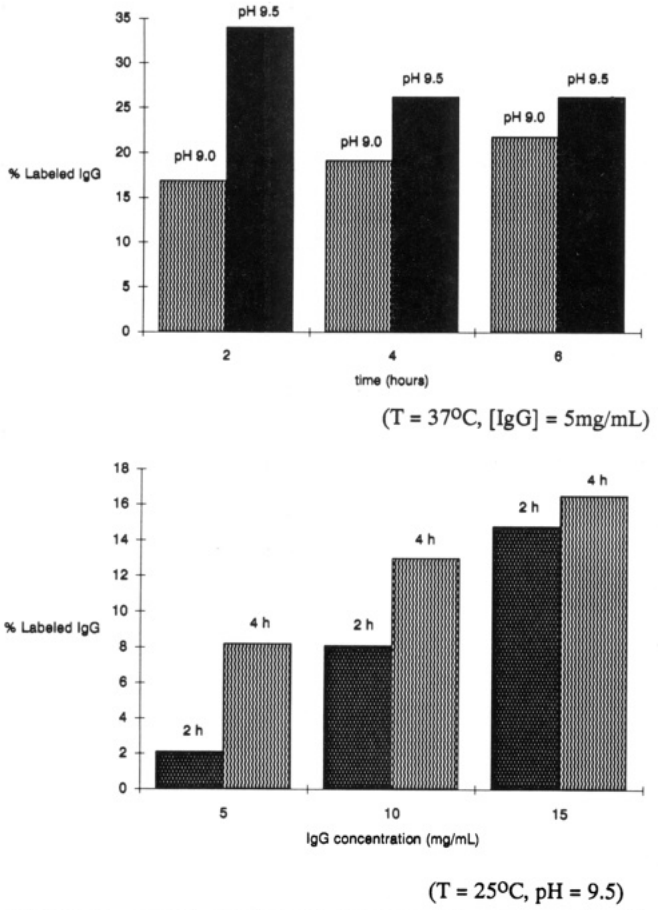


Figure 4. Effect of pH and reaction time (top) and IgG concentration (bottom) on the yield of labeling IgG with ^{99m}TcCl(DMG)$_3$PITC.

bound radioactive species. The ISRP column did not resolve labeled antibody monomer from antibody aggregates. Therefore, a two-step purification process, involving initial separation using G-25 gel chromatography, followed by TSK-SWG3000 HPLC, was used. After G-25 chromatography, protein and radioactivity recovery were 87 and 62%, respectively. After the subsequent purification using the TSK column, protein and radioactivity recovery were (over the two steps) 44 and 42%, respectively. HPLC chromatograms of labeled IgG, before and after purification, are shown in Figure 5. In the purified product, no radioactive peaks could be detected apart from labeled IgG monomer.

In contrast, purification of B72.3 labeled with ^{99m}TcCl-

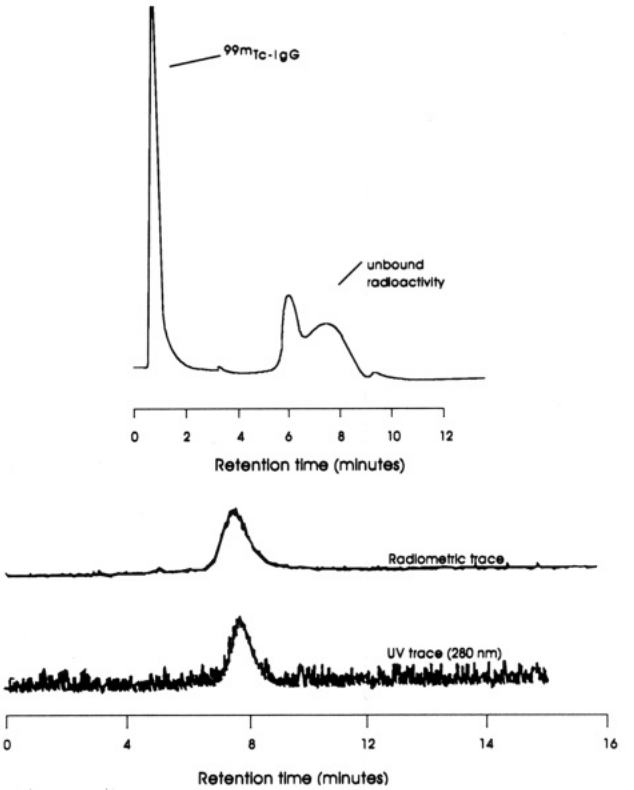


Figure 5. HPLC chromatograms of mouse IgG labeled with ^{99m}TcCl(DMG)$_3$PITC prior to purification (top) and after G25/TSK purification (middle and bottom). HPLC conditions: (top) ISRP-precolumn with gradient elution (see methods section), (middle, bottom), TSK-SWG3000 column. Mobile phase: PBS buffer at 1 mL/min.

(DMG)$_3$PITC by the G25/TSK method failed to separate labeled protein monomer from protein aggregate (Figure 6). To achieve separation of B72.3 monomer from all other components, other HPLC systems were evaluated; of these, a system in which ISRP and TSK-SWG3000 columns are placed in series was effective in the isolation of labeled B72.3 monomer. In five preparations involving ^{99m}TcCl-(DMG)$_3$PITC labeling of B72.3, the average protein labeling yield was 7.5%, with 67% protein recovery. ^{99m}Tc–B72.3 purified on the ISRP-TSK column was analyzed with the Phast system on a 10–15% acrylamide gel. The results are shown in Table VI.

Affinity chromatography of purified ^{99m}Tc–B72.3 indicated that 77% of this radiotracer bound to TAG-72 antigen. By comparison, on the same affinity column, ^{125}I–B72.3 (prepared in-house by the chloramine-T method) demonstrated 55–60% binding to TAG-72 antigen (*33*). Aliquots of ^{99m}Tc-labeled B72.3 incubated in rat serum were analyzed by HPLC on the ISRP-TSK column following incubation at 37 °C for 1 and 90 min. Both chromatograms indicated that all detected radioactivity was associated with the antibody peak, and no radioactivity was associated with serum components.

The results of the biodistribution studies of ^{99m}TcCl-(DMG)$_3$PITC and B72.3 labeled with ^{99m}TcCl(DMG)$_3$PITC in normal mice are given in Table VII.

DISCUSSION

Studies on the mechanism of BATO formation have shown that these technetium complexes form from pertechnetate, a vicinal dioxime, and stannous chloride via tin-capped Tc(III) complex, Tc(dioxime)$_3$(μ-OH)SnCl$_3$, which rearranges with loss of the tin cap to give an uncapped Tc(III) tris(dioxime) complex, TcCl(dioxime)$_3$ (Figure 7).

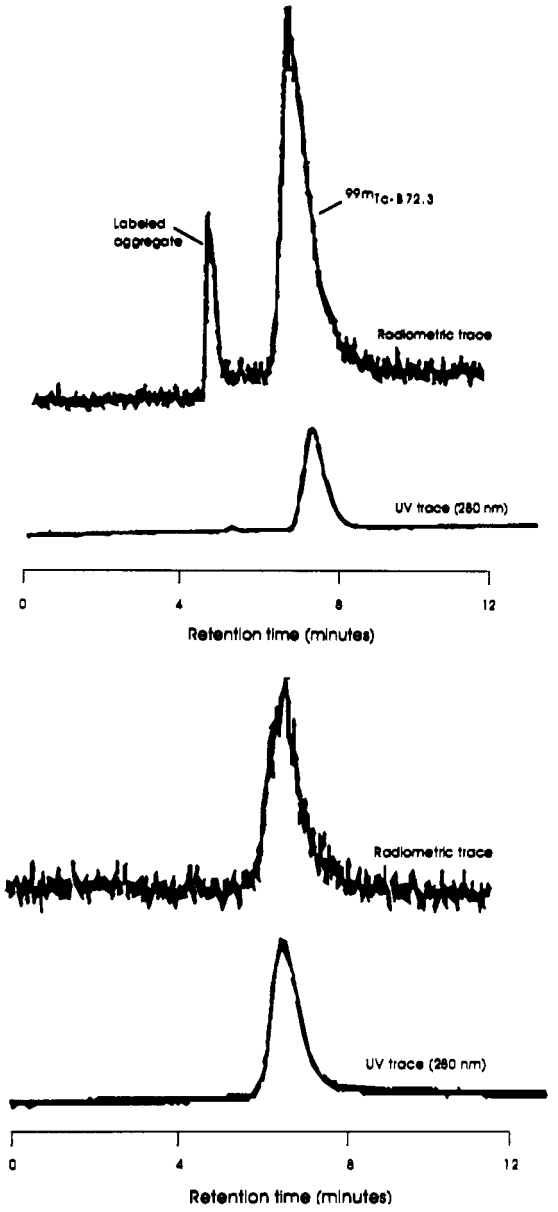


Figure 6. HPLC chromatograms of ^{99m}Tc-labeled B72.3 purified by the G25/TSK (top) and ISRP/TSK (bottom) methods. HPLC analysis method: TSK-SWG-3000 mobile phase: PBS buffer at 1 mL/min.

Table VI. SDS-PAGE of ^{99m}TcCl(DMG)$_3$PITC-B72.3 Conjugate

		reduced with 2-mercaptoethanol	
	unreduced: % bound to whole mAb	% bound to the heavy chain	% bound to the light chain
gel not stained	84	32	12
gel stained/destained	94	71	16

In the presence of a boronic acid, the TcCl(dioxime)$_3$ complex is capped at one end of the molecule to give the BATO, TcCl(dioxime)$_3$BR (*27*). All three steps require a low-pH environment and heating at ≤100 °C. BATOs can be prepared from either of the two precursor Tc(III) complexes or directly from TcO_4^- (*27*).

In this study, we prepared the potential protein-labeling reagents TcCl(dioxime)$_3$PITC, with ^{99}Tc, for characterization of the reagents, and with ^{99m}Tc, for labeling studies. The ^{99}Tc complexes were prepared either from the tin-capped complex or from pertechnetate. Yields of ^{99}TcCl(dioxime)$_3$PITC were ≥60% when prepared from ^{99}Tc(dioxime)$_3$(μ-OH)SnCl$_3$, whereas yields were ≤25% when prepared from $^{99}TcO_4^-$. Low yields from pertechnetate were unexpected as, generally, BATOs (with simple aryl or alkyl boronic acid caps) can be prepared in high yield by either route (*26*, *27*). All data obtained on the ^{99}TcCl(dioxime)$_3$PITC BATOs are consistent with the structure shown in Figure 7, and the structure was confirmed by an X-ray structure analysis. Of note are the strong bands at ~2100 cm^{-1} in the IR spectra of both ^{99}TcCl(DMG)$_3$PITC and ^{99}TcCl(CDO)$_3$PITC, which confirm the presence of the intact NCS group after BATO formation. The IR spectrum of the TcCl(DMG)$_2$(oxime–imine)PITC side product also confirms that this compound contains an intact NCS group.

Table VII. Biodistributions of ^{99m}TcCl(DMG)$_3$PITC and B72.3 Labeled with ^{99m}TcCl(DMG)$_3$PITC in Normal Mice[a]

	^{99m}TcCl(DMG)$_3$PITC % ID/g at times postinj		^{99m}Tc–B72.3 % ID/g at times postinj	
organ	1 h	21 h	1 h	21 h
whole blood	0.42 ± 0.24	2.29 ± 1.12	30.33 ± 5.12	13.09 ± 1.95
heart	4.33 ± 3.14	0.67 ± 0.21	6.90 ± 2.09	3.51 ± 1.35
lungs	3.52 ± 1.38	1.00 ± 0.34	8.57 ± 3.29	4.39 ± 1.48
brain	0.38 ± 0.10	0.11 ± 0.11	1.06 ± 1.06	0.51 ± 0.51
liver	1.03 ± 0.18	3.62 ± 0.23	8.18 ± 0.87	4.19 ± 0.34
spleen	n/d	1.18 ± 0.23	n/d	2.31 ± 0.29
GI tract	10.99 ± 1.16	1.80 ± 0.30	2.44 ± 0.16	2.91 ± 0.41
kidneys	42.49 ± 2.91	2.91 ± 0.67	5.61 ± 1.28	2.76 ± 0.56
muscle	2.22 ± 0.98	0.20 ± 0.15	0.98 ± 0.24	2.36 ± 0.77

[a] % ID/g = percent injected dose per gram. n/d = not determined. n = 5 for all experiments.

The ^{99m}Tc-labeling reagents were prepared from $^{99m}TcO_4^-$ and freeze-dried kits, and again, yields were poor (30–35% RCP), in contrast to the high RCP observed in the preparation of most other ^{99m}Tc–BATOs (*28*). There appear to be two primary reasons for the observed low yields of the TcCl(dioxime)$_3$PITC BATOs formed directly from TcO_4^-.

a. Under the reaction conditions used, the isothiocyanate functional group can be hydrolyzed to an amine. The hydrolysis product, TcCl(dioxime)$_3$PA, was observed in all reactions in which ^{99m}TcCl(dioxime)$_3$PITC was the desired product (Figure 7; **3** → **4**). The presence of TcCl(dioxime)$_3$PA was confirmed by use of ^{99m}TcCl(dioxime)$_3$PA as an HPLC reference standard; this BATO was prepared in high yield (81% RCP), by addition of 3-aminophenylboronic acid and $^{99m}TcO_4^-$ to a DMG freeze-dried kit and heating to 100 °C for 5 min.

b. In the reaction from pertechnetate, the formation of another lipophilic side product was noted. At the ^{99}Tc level, this side product has a distinctive pink/orange color. A sample of this product was isolated and partially characterized; those data suggest that the structure of this side product is similar to pink/orange BATO side products reported by us previously (*38*), which have one of the uncapped oxime groups reduced to an imine (TcCl(dioxime)$_2$(oxime–imine)BR). From HPLC analysis, it was concluded that TcCl(dioxime)$_2$(oxime–imine)PITC is also a significant side product in preparations at the ^{99m}Tc level.

From studies of the influence of pH, time, and temperature on product RCP, the best yields of ^{99m}TcCl(dioxime)$_3$PITC complexes were obtained by heating the kit at pH 2 for 5 min at 100 °C. The radiochemical purity of ^{99m}TcCl(dioxime)$_3$PITC was increased to ~65% by a purification process involving PRP-1 resin, with the major impurity at this stage being ^{99m}TcCl(dioxime)$_2$(oxime–imine)PITC (20–30%). These lipophilic complexes are retained by the resin when washed with saline and 50%

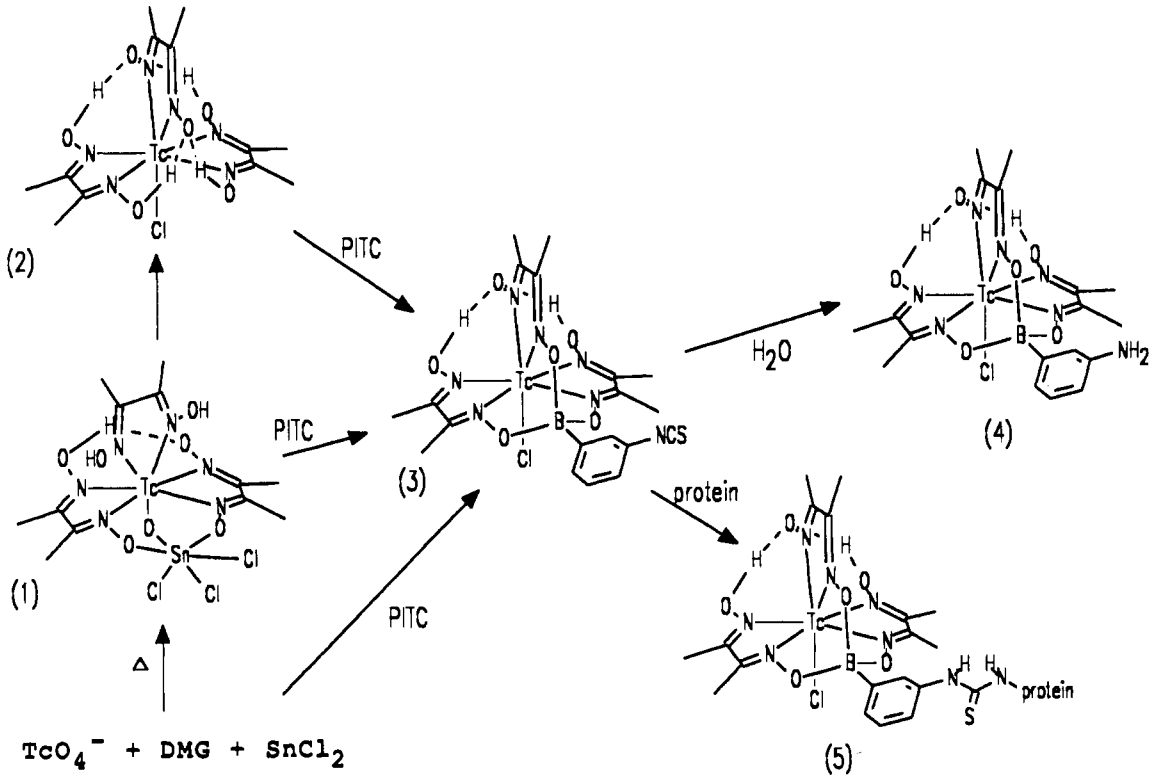


Figure 7. Schematic of the formation and reactions of ^{99m}TcCl(DMG)$_3$PITC. Key: 1 = Tc(DMG)$_3$(μ-OH)SnCl$_3$; 2 = TcCl(DMG)$_3$; 3 = TcCl(DMG)$_3$PITC; 4 = TcCl(DMG)$_3$PA; 5 = Tc-labeled protein.

ethanol/saline. Most hydrophilic impurities, including ^{99m}TcCl(DMG)$_3$PA, are removed by washing. The reagents ^{99m}TcCl(dioxime)$_3$PITC and ^{99m}TcCl(dioxime)$_2$(oxime–imine)PITC were removed from the resin by elution with 100% ethanol. HPLC chromatograms of the reaction mixture before and after purification are shown in Figure 3. As protein precipitation occurs if labeling is attempted with ethanol present, the solvent must be removed (in a stream of nitrogen gas) prior to protein labeling. As both ^{99m}TcCl(dioxime)$_3$PITC and ^{99m}TcCl(dioxime)$_2$(oxime–imine)PITC have an intact isothiocyanato functional group, ≥85% of the radioactivity in solution after purification has the potential to bind covalently to proteins.

The high lipophilicity of the BATO complexes is an essential requirement with respect to their application as perfusion tracers (*28*). However, for protein labeling, lipophilicity proved to be a problem. The reagents are poorly soluble in PBS, and are deposited on the walls of containers when in PBS alone. Similar problems have been reported for certain fluorochromes, particularly rhodamine derivatives, in protein solutions (*40*). In the latter case, the reagent was dissolved in dimethyl sulfoxide (DMSO) and diluted to 10% DMSO prior to protein labeling. It was reported previously that use of a 10% DMSO solution did not denature protein (*40*). We found that a 10% DMSO solution prevented much of the deposition of ^{99m}TcCl(DMG)$_3$PITC, without denaturing the protein. However, significant deposition of the more lipophilic ^{99m}TcCl(CDO)$_3$PITC (log *P* estimates of the DMG and CDO reagents, based on lipophilicity data for other BATOs (*28*) and MedChem software, are 5.61 and 8.04, respectively) to the inner surface of the vial could not be prevented by using a 10% solution of DMSO (data not reported). As a result, no labeling studies were conducted with the CDO reagent.

Protein labeling with NCS reagents results from the formation of a stable thiourea linkage between the reagent and a free primary amine group on a lysine residue. However, a competing reaction involves the hydrolysis of the NCS group leading to a nonreactive compound containing a primary amine. Trial labeling reactions were carried out to determine the conditions under which the highest possible yield of the coupled product was obtained, while hydrolysis is kept to a minimum.

In a trial labeling reaction with glycine, conjugation to ^{99m}TcCl(DMG)$_3$PITC was complete in 1 h, with 88% of the radioactivity associated with the presumed glycine conjugate peak. This reaction was conducted in ethanol, so little hydrolysis of the isothiocyanate group to amine was to be expected. In contrast, the yield of conjugate in the trial labeling reaction of polylysine with ^{99m}TcCl(DMG)$_3$PITC in aqueous DMSO was only 33% after 2 h at pH 9.0, 37 °C. The major side product was ^{99m}TcCl(DMG)$_3$PA, which resulted from hydrolysis of the isothiocyanate.

Labeling studies with mouse IgG examined the effects of solution pH, temperature, time, and IgG concentration on conjugation yield. From these studies, the labeling conditions of 2 h at 37 °C and pH 9.5 were selected as most suitable for routine use. These conclusions are similar to those found in other studies involving protein conjugation with the isothiocyanate group (*31*). As might be expected, the yield of labeled IgG did increase with increasing IgG concentration (Figure 4).

To eliminate the possibility that attachment of the BATO to antibody may occur by some mechanism other than reaction of the isothiocyanate group, ^{99m}TcCl(DMG)$_3$2MP (a BATO which does not contain a protein reactive group) was incubated with antibody at pH 9.5 (data not reported). On HPLC and SDS–PAGE analysis, there was no radioactivity associated with the protein fractions. Therefore, BATO attachment to proteins appears to result only by reaction of the isothiocyanate group.

Under the pH and temperature conditions used in

protein labeling, it is known that BATO complexes can undergo axial ligand exchange; the axial chloride ligand is displaced by hydroxide with a $t_{1/2}$ of between 10 and 30 min (*41*). HPLC analysis of protein-labeling reactions have demonstrated the formation of another lipophilic complex, presumed to be ^{99m}TcOH(DMG)$_3$PITC. This complex, like the ^{99m}TcCl(dioxime)$_2$(oxime–imine)PITC "impurity" (formed in 20–30% yield, as described earlier, during the preparation of ^{99m}TcCl(dioxime)$_3$PITC), retains its protein-reactive isothiocyanate functional group. Therefore, these "impurities" should react with proteins in an analogous manner to ^{99m}TcCl(DMG)$_3$PITC and contribute to the overall conjugate yield.

On completion of the labeling reaction, labeled IgG was obtained with >90% RCP by a two-step purification process involving initial purification on a G-25 column (which removed most of the low molecular weight byproducts) followed by TSK HPLC purification. In labeling B72.3, it was found that the G-25/TSK purification protocol failed to remove labeled high molecular weight protein aggregates. This problem was eliminated by substituting ISRP chromatography for G-25 as the initial purification step.

Covalent attachment of the labeling reagent to B72.3 monoclonal antibody was demonstrated by Phast SDS–PAGE. Under nonreducing conditions, 84% of the activity was associated with the antibody monomer. The stain/destain protocol (used to visualize proteins on the gel) removed most of the unbound activity, giving an apparent RCP of 94%. Protein reduction with 2-mercaptoethanol was used to fragment the antibody into heavy and light chains, SDS–PAGE following this treatment indicated that the label was randomly distributed on the whole antibody, as the distribution of radioactivity between heavy and light chains is similar to the molecular weight ratio of these fragments.[1] Protein reduction, by harsh treatment with 2-mercaptoethanol, did result in sigificant loss (45%) of the label from antibody, presumably due to transfer of technetium by a ligand-exchange process. However, under milder challenge conditions (incubation in serum), technetium remained bound to B72.3.

The preliminary examination of the biodistributions of ^{99m}TcCl(DMG)$_3$PITC and its B72.3 conjugate in normal mice also provide some demonstration that a stable link exists between the label and the antibody. The biodistribution of the labeling reagent was very different from that of the radiolabeled antibody. The labeling reagent showed relatively low blood values at 1 h, with rapid clearance to kidneys and to the GI tract. In contrast, the radiolabeled antibody showed, as expected, prolonged retention in blood. In addition, low levels of radioactivity in liver and spleen suggested that very few high molecular protein aggregates had formed in the ^{99m}Tc-labeled B72.3 preparation. Comparing our biodistribution data on ^{99m}Tc-labeled B72.3 to that of ^{125}I-labeled B72.3 and ^{111}In-labeled B72.3 reported by Sands et al (*42*), we observed that ^{99m}Tc–B72.3 demonstrated lower spleen and liver uptake than ^{125}I–B72.3. Liver uptake was distinctly lower with ^{99m}Tc–B72.3 than with ^{111}In–B72.3.

The immunoreactivity (77%) of B72.3 labeled with ^{99m}TcCl(DMG)$_3$PITC, measured with the TAG 72 column, is high, particularly when compared to ^{125}I-labeled B72.3 (55–60%). This indicates that the antibody retains most of its immunoreactivity after the labeling and purififcation processes.

These preliminary data suggest that the labeling reagent ^{99m}TcCl(DMG)$_3$PITC will form a stable conjugate with proteins, with little loss of immunoreactivity. However, the overall yield of the labeling process (starting from ^{99m}TcO$_4^-$) is low, and the process requires two purification steps. This, in part, can be attributed to the high lipophilicity, and some improvements in labeling efficiency and labeling convenience could be achieved by using analogues of lower lipophilicity. However, we have demonstrated that BATOs are suitable technetium chelates for the radiolabeling of monoclonal antibodies.

[1] A distribution of radioactivity in proportion to chain molecular weight is seen in unstained gels only. A greater proportion of radioactivity is associated with the heavy chain after the stain/destain process, suggesting preferential loss of label from the light chain during this process. The reason for the selective loss of radiolabel is unclear at this time.

ACKNOWLEDGMENT

We thank Lillian Belnavis, Maryann Homack, and Debbie Silva for technical assistance with the biodistribution studies.

Supplementary Material Available: Tables listing final atomic positional parameters, thermal parameters, bond distances, and bond angles for TcCl(DMG)$_3$PITC (7 pages); a table of structure factors (11 pages). Ordering information is given on any current masthead page.

LITERATURE CITED

(1) Eckelman, W. C., and Paik, C. H. (1986) Comparison of Tc-99m and In-111 labeling of conjugated antibodies. *Nucl. Med. Biol. 13*, 335–343.

(2) Paik, C. H., Eckelman, W. C., and Reba, R. C. (1986) Tranchelation of ^{99m}Tc from low affinity to high affinity sites of antibody. *Nucl. Med. Biol. 13*, 359–362.

(3) Deutsch, E., Libson, K., Jurisson, S., and Lindoy, L. F. (1983) Technetium Chemistry and Technetium Radiopharmaceuticals. *Prog. Inorg. Chem. 30*, 75–139.

(4) Reno, J. M., and Bottino, B. J. (1987) Improved radionuclide antibody coupling. Eur. Pat. Appl. 87300426.1.

(5) Bremer, K. H., Kuhlman, L., Schwartz, A., and Steinstrasser, A. (1987) Studies to discover an organ specific substance labeled with technetium-99m. Eur. Pat. Appl. 87118142.6.

(6) Jones, A. L., Kinz, A., Grebenau, R., et al. (1990) Radiolabeling of Monoclonal Antibody (MAb) Fragments with Technetium-99m (Tc-99m) Using a One Vial Kit. *J. Nucl. Med. 31*, 905.

(7) Pak, K. Y., Nedelman, N. A., Tam, S. H., et al. (1990) Stability and Immunoreactivity of Technetium-99m Antibody Fragments by a Direct Labeling Method. *J. Nucl. Med. 31*, 905.

(8) Fritzberg, A. R., Abrams, P. G., Beaumier, P. L., et al. (1988) Specific and stable labeling of antibodies with technetium-99m with a diamide dithiolate chelating agent. *Proc. Natl. Acad. Sci. 85*, 4025–4029.

(9) Franz, J., Volkert, W. A., Barefield, E. K., and Holmes, R. A. (1987) The production of Tc-99m labeled conjugated antibodies using a cyclam based bifunctional chelating agent. *Nucl. Med. Biol. 26*, 293–299.

(10) Morphy, J. R., Parker, D., Alexander, R., et al. (1988) Antibody Labelling with Functionalised Cyclam Macrocycles. *J. Chem. Soc. Chem. Commun.* 156–158.

(11) Arano, Y., Yokoyama, A., Magata, Y., et al. (1986) Synthesis and Evaluation of a New Bifunctional Chelating Agent for ^{99m}Tc Labeling Proteins: *p*-Carboxyethylphenylglyoxaldi(*N*-methylthiosemicarbazone). *Nucl. Med. Biol. 12*, 425–430.

(12) Arano, Y., Yokoyama, A., Furukawa, H., et al. (1987) Technetium-99m-Labeled Monoclonal Antibody with Preserved Immunoreactivity and High in Vivo Stability. *J. Nucl. Med. 28*, 1027–1033.

(13) Nicolotti, R. A., and Dean, R. T. (1987) Coupling agents for radiolabeling proteins. Eur. Pat. Appl. 87304716.1.

(14) Byrne, E. F., and Tolman, G. L. (1983) Technetium-99m bifunctional chelating agent—thiolactone coupling to biomolecules. N_2S_2 ligand for chelation to technetium. *J. Nucl. Med. 24*, P126.
(15) Lever, S. Z., Baidoo, K. E., Kramer, A. V., et al. (1988) Synthesis of a novel bifunctional chelate designed for labeling proteins with technetium-99m. *Tetrahedron Lett. 29*, 3219–3222.
(16) Misra, H. K., Virzi, F., Hnatowich, D. J., and Wright, G. (1989) Synthesis of a Novel Diaminodithiol Ligand for Labeling Proteins and Small Molecules with Technetium-99m. *Tetrahedron Lett. 30*, 1885–1888.
(17) Baidoo, K. E., and Lever, S. Z. (1990) Synthesis of a Diaminedithiol Bifunctional Chelating Agent for Incorporation of Technetium-99m into Biomolecules. *Bioconjugate Chem. 1*, 132–137.
(18) Morelock, M. M., and Tolman, G. L. (1987) Metallothionein: A Bifunctional Chelator for the Radiolabeling of Biologically Active Molecules. *Experientia 52 (Supplement: Metallothionein II)*, 247–253.
(19) Morelock, M. M., Cormier, T. A., and Tolman, G. L. (1988) Technetium Metallothioneins. *Inorg. Chem. 27*, 3137–3140.
(20) Brown, B. A., Drozynski, C. A., Dearborn, C.A., et al. (1988) Conjugation of Metallothionein to a Murine Monoclonal Antibody. *Anal. Biochem. 172*, 22–28.
(21) Fritzberg, A. R. (1987) Advances in ^{99m}Tc-labeling of antibodies. *Nuklearmedizin 26*, 7–12.
(22) Fritzberg, A. R., Kasina, S., Reno, J. M., et al. (1986) Radiolabeling of antibodies with ^{99m}Tc using N_2S_2 ligands. *J. Nucl. Med. 27*, 957–958.
(23) Wilkening, D., Srinivasan, A., Kasina, S., et al. (1988) Tc-99m Antibody Labeling with N_3S and N_2S_2 Amide Mercaptides: Active Ester Complex Yield and Side Chain Length. *J. Nucl. Med. 29*, 815.
(24) Parker, D., and Millican, T. (1987) Conjugate Compound. Int. Pat. Appl. PCT/GB87/00106.
(25) Morphy, J. R., Parker, D., et al. (1988) Antibody labeling with Functionalised Cyclam Molecules. *J. Chem. Soc. Chem. Commun.* 156–158.
(26) Treher, E. N., Francesconi, L. C., Gougoutas, J. Z., et al. (1989) Monocapped Tris(dioxime) Complexes of Technetium-(III): Synthesis and Structural Characterization of TcX-(dioxime)$_3$BR (X = Cl, Br; Dioxime = Dimethylglyoxime, Cyclohexanedione Dioxime; R = CH_3, C_4H_9). *Inorg. Chem. 28*, 3411–3416.
(27) Linder, K. E., Malley, M. F., Gougoutas, J. Z., et al. (1990) Neutral, Seven-Coordinate Dioxime Complexes of Technetium(III): Synthesis and Characterization. *Inorg. Chem. 29*, 2428–2435.
(28) Nunn, A. D., Feld, T., and Narra, R. K. (1990) Quantitative Structure Distribution Relationships (QSDRs) of BATOs. In *Technetium and Rhenium in Chemistry and Nuclear Medicine* (M. Nicholini, G. Bandoli, and U. Mazzi, Eds.) Vol. 3, pp 399–404, Cortina International, Verona, Italy.
(29) Zielonka, J. S., Cannon, P., Johnson, L., et al. (1990) Multicenter Trial of ^{99m}Tc-Teboroxime (Cardiotec): A New Myocardial Perfusion Agent. *Nuklear Medizine (Suppl. 26)* 211–212.
(30) Narra, R. K., Nunn, A. D., Kuczynski, B. L., et al. (1990) A Neutral Lipophilic Tc-99m Complex for Regional Cerebral Blood Flow Imaging. *J. Nucl. Med. 31*, 1370–1377.
(31) Mirzadeh, S., Brechbiel, M. W., Atcher, R. W., and Gansow, O. A. (1990) Radiometal Labeling of Immunoproteins: Covalent Linkage of 2-(4-Isothiocyanatobenzyl)diethylenetriaminepentaacetic Acid Ligands to Immunoglobulin. *Bioconjugate Chem. 1*, 59–65 (*and references therein*).
(32) Ramalingam, K., Nowotnik, D. P., and Nunn, A. D. The synthesis of some isothiocyanato phenylboronic acids. *Org. Prep. Proc.*, submitted for publication.
(33) Hagan, J., Croze, E., and Yost, F., unpublished data.
(34) Walker, N., and Stuart, D. (1983) An empirical method for correcting diffractometer data for absorption effects. *Acta Crystallogr., Sect. A 39*, 158–166.
(35) SDP. *Structure Determination Package*. A. Frenz and Associates, College Station, TX.
(36) Little, R. J., and Donahue, M. A. (1968) Spectral properties of proteins and small molecules of immunological interest. *Methods Immunol. Immunochem. 2*, 343–364.
(37) Johnson, C. K. (1965) ORTEP. Report ORNL-3794. Oak Ridge National Laboratory, Oak Ridge, TN.
(38) Linder, K. E., Jurisson, S., Francesconi, L., et al. (1990) Template Synthesis of Technetium and Rhenium Dioxime Complexes: The Mechanism of Formation of TcX(Dioxime)$_3$-BR from Pertechnetate. In *Technetium and Rhenium in Chemistry and Nuclear Medicine* (M. Nicholini, G. Bandoli, and U. Mazzi, Eds.) Vol. 3, pp 195–199.
(39) Linder, K. E., Malley, M. F., Nowotnik, D. P., et al. An unexpected by-product obtained during the preparation of technetium(III) boronic acid adducts of dioximes. The single crystal structure of TcCl(DMG)$_2$(BDI)BEt (DMG = dimethylglyoxime, BDI = butane-2,3-dione imine–oxime). *Inorg. Chim. Acta*, submitted for publication.
(40) Bergquist, N. R., and Nilsson, P. (1974) The conjugation of immunoglobulins with tetramethylrhodamine isothiocyanate by utilization of dimethylsulfoxide (DMSO) as solvent. *J. Immunol. Method 5*, 189–198.
(41) Jurisson, S. S., Hirth, W., Linder, K. E., et al. Chloro→Hydroxy Substitution on Technetium BATO (TcCl-(Dioxime)$_3$BR) Complexes. *Nucl. Med. Biol.*, in press.
(42) Sands, H., and Jones, P. L. (1987) Methods for the Study of the Metabolism of Radiolabeled Monoclonal Antibodies by Liver and Tumor. *J. Nucl. Med 28*, 390–398.

Astatine-211 Labeling of an Antimelanoma Antibody and Its Fab Fragment Using *N*-Succinimidyl *p*-Astatobenzoate: Comparisons in Vivo with the *p*-[^{125}I]Iodobenzoyl Conjugate

Stephen W. Hadley,[†] D. Scott Wilbur,[*,‡] Mary Ann Gray,[†,§] and Robert W. Atcher[∥]

University of Washington Medical Center, Seattle, Washington 98195, NeoRx Corporation, Seattle, Washington 98119, and Argonne National Laboratory, Argonne, Illinois 60439. Received January 7, 1991

Astatine-211 labeling of an antimelanoma antibody, NR-ML-05, and its Fab fragment with *N*-succinimidyl *p*-[^{211}At]astatobenzoate (**2a**) has been described. Preparation of the astatinated intermediate **2a** was accomplished by distilling astatine-211 from an irradiated bismuth target directly into a reaction mixture containing an organometallic compound, *N*-succinimidyl *p*-(tri-*n*-butylstannyl)benzoate (**1**), and an oxidant, *N*-chlorosuccinimide, in 5% HOAc/MeOH. Trapping of distilled astatine as **2a** was found to be efficient, resulting in 70–90% yields based on the amount of astatine-211 in the reaction mixture. The dry distillation technique employed gave recoveries of astatine-211 which ranged from 20% to 75%. Conjugation of **2a** to NR-ML-05 and its Fab fragment was accomplished in 40–60% yields. The [^{211}At]astatobenzoyl-conjugated antibodies were found to be stable in vitro when challenged by strong denaturants and nucleophilic reagents. Coinjected dual-labeled studies of the **2a** astatinated antibodies and the same antibodies labeled with *N*-succinimidyl *p*-[^{125}I]iodobenzoate (**2b**) in athymic mice bearing the human tumor xenograft A375 Met/Mix demonstrated that both radiolabeled antibodies had equivalent tumor localization. Data from the dual-labeled biodistribution of the intact antibody suggests that the astatine is stably attached. Data from the dual-labeled Fab fragment suggests that a portion of the astatine label is released as astatide, either from the astatinated Fab or from a catabolite.

INTRODUCTION

The application of α emitting radionuclides to radioimmunotherapy (RIT) of cancer is attractive due to the unique cytotoxic properties of the α particle (*1*, *2*). While there are concerns about general application to RIT, antibodies labeled with radionuclides that decay by α emission may have specific applications such as treatment of blood-borne cancers (e.g. leukemia), intracavitary administration for some types of cancers (e.g. peritoneal administration for ovarian carcinoma), or adjuvant treatment of disseminated micrometastatic disease (*3*). Of the many radionuclides that have α emissions, only bismuth-212 ($t_{1/2}$ = 60.1 min) and astatine-211 ($t_{1/2}$ = 7.2 h) are presently feasible for application to labeled antibodies (*4*, *5*).

Application of astatine-211-labeled antibodies for cancer therapy was suggested in 1954 (*6*). Since astatine is in the halogen group of elements it was reasoned that its chemistry would parallel radioiodine (*7*). Early attempts to radiolabel proteins (*8*, *9*) and tyrosine (*10*) with astatine provided evidence that its chemistry was different. Indeed, unlike radioiodine, labeling proteins directly with astatine produced a labile astatine–protein bond, which appeared to be formed from the reaction of astatine with the protein sulfhydryl groups (*11*). These studies indicated that another method of antibody labeling was needed.

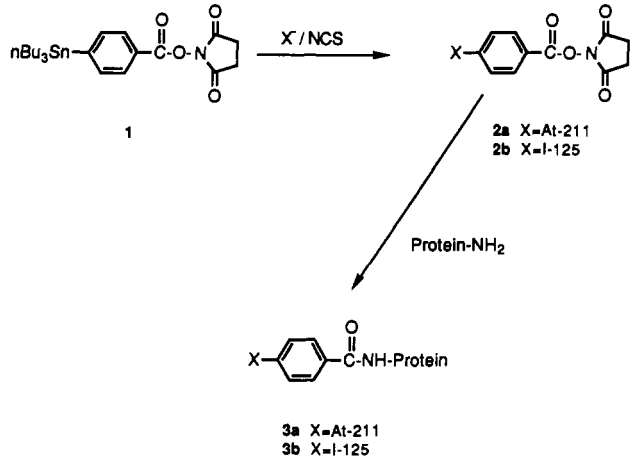
Friedman et al. (*12*) demonstrated that labeling of a protein with an astatinated benzoic acid resulted in a much less labile attachment of the astatine-211 label under the conditions encountered in vivo. In their study astatine-211 was incorporated into benzoic acid via a diazonium salt decomposition. Protein conjugation of the resultant *p*-[^{211}At]astatobenzoic acid was accomplished by preparing a mixed anhydride and subsequent reaction with the protein under basic conditions. Several other astatinated protein studies have been reported which used this method of labeling (*13–15*). A dramatic increase in the in vivo stability was obtained; however, there were several aspects of the labeling procedure which did not make it attractive for routine labeling. For example, diazonium salt reactions in aqueous solution have the potential to produce phenols (*16*, *17*) which could compete for the unreacted astatine-211, resulting in an astatinated product that would be expected to be less stable than *p*-astatobenzoyl conjugates. Further, the labeling procedure required a number of chemical manipulations, such as ether extraction, which were time consuming and potentially dangerous. Perhaps the most important limitation was the overall time for the labeling process, taking up to 3 h to complete, which resulted in a loss of nearly 25% of the astatine-211 by decay alone.

More recently, astatination of benzoic acid derivatives has been accomplished in high yield, without the concerns for phenolic byproducts, by using organometallic intermediates (*18–21*). For example, Zalutsky et al. (*20*, *21*) have labeled antibodies by using a protein-reactive organometallic intermediate (*N*-succinimidyl *m*-(trialkylstannyl)benzoate, termed ATE or MeATE), which could be astatinated readily and subsequently conjugated to the antibody. In this investigation, we have studied the use of the isomeric organometallic intermediate *N*-succinimidyl *p*-(tri-*n*-butylstannyl)benzoate (**1**) for astatine-211 labeling of antibodies as shown in Scheme I. The organometallic intermediate **1** used to obtain the protein-reactive astatinated product *N*-succinimidyl *p*-astatobenzoate (**2a**), like the *m*-(trialkylstannyl)benzoyl compound employed by Zalutsky (*22*), had been previously used in

* Address correspondence to D. Scott Wilbur, Department of Radiation Oncology, RC-08, University of Washington Medical Center, 1959 N.E. Pacific St., Seattle, WA 98195.
† NeoRx Corp.
‡ University of Washington.
§ Current address: Schering-Plough Research, Department of Tumor Biology, Bloomfield, NJ 07003.
∥ Argonne National Laboratory.

1043-1802/91/2902-0171$02.50/0 © 1991 American Chemical Society

Scheme I. Reaction Sequence for Astatine-211 (and Iodine-125) Labeling of Antibodies



radioiodinations of antibodies and had been shown to stabilize radioiodine from in vivo dehalogenation (*23*).

The primary objective of the investigation described herein was to develop a method of labeling antibodies with astatine-211 for subsequent investigation to their application to therapy of metastatic lesions or blood-borne cancers. The goal was to obtain an astatine-211-labeling method which was rapid, high yielding, and could be conducted in a safe manner. The organometallic intermediate 1 was used to provide a facile incorporation of astatine-211 into the protein-reactive benzoate **2a**. To simplify the chemical manipulations in the astatinations, we employed a method of distilling astatine (*24*) directly from the irradiated target into a reaction mixture containing 1. The astatine-labeling studies were carried out on an antimelanoma antibody, NR-ML-05, and its Fab fragment,[1] which had been previously studied employing the *p*-iodobenzoyl (PIB) conjugates (*23*). To determine if the labeling resulted in a method in which the desired antibody properties were retained, the in vitro stability and in vivo distribution of the astatinated antibodies were examined. To accomplish this, the astatinated antibodies were evaluated in vitro under a variety of challenge conditions and in vivo in athymic mice bearing a human tumor xenograft, A375 Met/Mix.[2] For comparative purposes, NR-ML-05, or its Fab fragment, was radioiodinated with ^{125}I-labeled *p*-iodobenzoate (**2b**) and was coinjected with the astatinated antibody.

EXPERIMENTAL PROCEDURES

General. All reagents used were analytical-reagent grade or better and were used as obtained. HPLC solvents were obtained as HPLC grade and were filtered (0.2 μm) prior to use. *N*-Succinimidyl *p*-(tri-*n*-butylstannyl)benzoate (1) was prepared as previously described (*23*). Disposable reverse-phase C-18 columns used for purification of radiolabeled intermediates were obtained from J.T. Baker, Inc. (6 mL, #7020-6).

Astatine-211 was produced at Argonne National Laboratory on the 60-in. cyclotron (*25*). The fixed-frequency 42 MeV beam was degraded with aluminum foils to ca. 28 MeV to avoid production of astatine-210 (*26*). Irradiation of aluminum-backed 0.5–0.8 mm thick bismuth targets was generally done at 10–12 μA and produced 13 mCi in 4 h. Once irradiated, the targets were shipped to Seattle for use in the experiments conducted the following day. Radioiodine was obtained from Du Pont/NEN (Billerica, MA) as high-concentration, high specific activity solutions in 0.1 N NaOH. Phosphate-buffered saline was purchased from Gibco Laboratories (Baltimore, MD) as Dulbecco's phosphate-buffered saline (#310-4190) or from Whittaker Bioproducts, Inc. (Walkersville, MD).

Protein Concentrations. Protein concentrations in solution were measured by UV spectrophotometry at 280 nm. The concentrations were obtained with the Beer–Lambert equation with the molar absorptivity being equal to 1.43 for whole antibody and 1.53 for Fab.

Astatine-211 Measurements. Radioactive materials were counted on a Packard Autogamma 5650 γ scintillation counter. Multiple standards were used in each counting to assess the quantity of astatine and radioiodine injected. Radioactivity counting was carried out with a low-energy window (20–80 keV) for both astatine-211 (^{211}Po X-rays) and iodine-125. Initial astatine-211 activity in the irradiated target was determined (at Argonne) using an EG&G Ortec Ace multichannel analyzer (MCA) with a modified version of the program Maestro. The amount of activity was determined with an Ortec Gamma-X Intrinsic Ge detector at a distance of 80–150 cm from the target. The integral of the 687 keV γ peak which is present in 0.245% abundance from the electron decay branch of ^{211}At was used as the basis for quantification. The measurement of astatine activity was calibrated with a standard traceable to NIST, standard set 2200 R2317. To help cross-calibrate the instruments at Argonne and in these laboratories, a sample was distilled at Argonne and quantified by MCA. The sample was then placed in a CRC-7 dose calibrator which was adjusted with the potentiometer until it read the correct value. That derived calibration factor, 25, was set on the CRC-7 dose calibrator in Seattle for readings of distilled astatine quantities. For quantification of the percent recovery of astatine from the irradiated target, the activity was measured by a Canberra Series 20 Model 2802 MCA using a Canberra Model 2007P (preamp) and Model 802-3 thin NaI crystal detector to obtain the integrated area under 687 keV peak at a set distance (ca. 60 cm) before and after distillation. These values were compared with the quantities of astatine in the reaction vial and in other parts of the distillation apparatus. Total astatine activity balances of 95–120% were obtained.

Analytical Chromatography. High-performance liquid chromatography (HPLC) was used to determine the purity of the radiolabeled species obtained from the reaction mixtures and to assist in the development/assessment of preparative purification methods (see Astatine Distillation and Labeling Procedure). HPLC was conducted on either a gradient system for separation of small molecules (1, **2a,b**) or an isocratic system for separations of labeled proteins (**3a,b**). The gradient system consisted of two Beckman Model 110B pumps, a Beckman Model 153 UV detector, a Rheodyne Model 7125 injector, and a Beckman Model 170 radioisotope detector. The isocratic system was identical with the gradient except it had only one solvent pump. All separations were run at a flow rate of 1 mL/min. Spectrophotometric analysis of the HPLC effluent was performed with UV detection at 254 nm.

Reverse-phase chromatography was conducted on a 4.6 mm × 12.5 cm C-18 column (Whatman) using a binary gradient solvent system which minimized outgassing. Eluant A in the gradient was a mixture of 98% MeOH and

[1] NR-ML-05 is an IgG_{2b} antibody that is reactive with a high molecular weight antigen on most melanoma cells (*50*). The $F(ab')_2$ fragment could not be prepared.

[2] The A375 Met/Mix xenograft is a metastatic variant of the A375 cell line isolated from nude mice. (*51*).

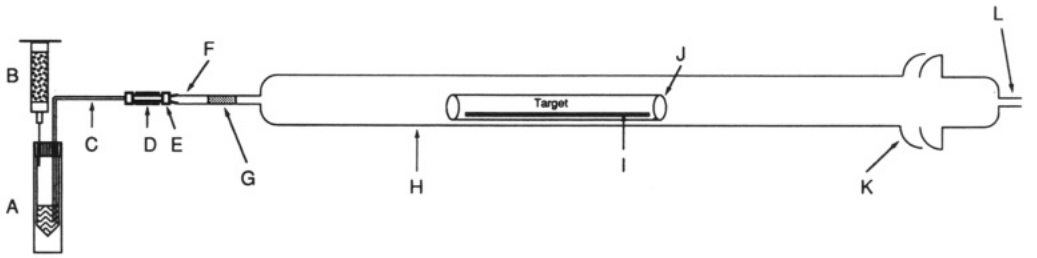


Figure 1. Schematic of astatine distillation setup. Components are (A) reaction vessel; (B) charcoal filter; (C) Teflon tubing, 15 cm × 0.8 mm i.d. × 1.5 mm o.d., fitted on one end with a $^1/_4$–28 threaded polypropylene bushing; (D) coupling, $^1/_4$–28 thread polypropylene; (E) Tefzel adapter, $^1/_4$–28 thread to a female Luer adapter; (F) Pyrex Luer tip; (G) graded seal; (H) quartz distillation tube; (I) irradiated bismuth target; (J) quartz tube boat; (K) standard ball/socket joint (50/30); (L) carrier gas inlet.

2% of a 1% HOAc/H_2O solution. Eluant B was a mixture of 20% MeOH and 80% of a 1% HOAc/H_2O solution. The gradient was begun by eluting for 2 min at 50% of each eluant. After 2 min the solvent mixture was increased in eluant A over the next 8 min to a final composition of 98% eluant A and 2% eluant B. The eluant mixture remained at that composition for the next 10 min to complete the gradient. Retention times for *N*-succinimidyl *p*-(tri-*n*-butylstannyl)benzoate (**1**) was 14.6 min and for astatine-211-labeled benzoate **2a** was 4.1 min with the gradient described. The retention time for *p*-astatobenzoic acid was 4.9 min and astatide ion came off at the solvent front, 1.2 min.

Size-exclusion chromatography was conducted on a Zorbax Bio Series GF-250 9.4 mm × 24 cm column (Du Pont) with 0.2 M phosphate buffer, pH 6.8, as the eluant. The retention times for NR-ML-05 labeled with **2a** or **2b** on the size-exclusion column were 8.5 min for intact IgG and 9.8 min for Fab.

Thin-layer chromatography of protein conjugates was conducted on silica gel impregnated glass-fiber strips (ITLC, Gelman) eluting with 80% MeOH/H_2O. In this system, the protein is denatured at the origin and the free halide or radiolabeled small molecules move with the solvent front. Radiochemical purity of the radiolabeled Fab preparations was defined as the percent protein-bound activity, which was estimated by dividing the counts at the TLC origin by the total counts on the TLC strip.

Astatine Distillation/Reaction Setup. The astatination reactions were conducted in a glovebox that was vented through a charcoal filter into an adjacent fume hood. The astatine distillation and labeling reactions employing **1** were conducted in the glassware setup depicted in Figure 1. The quartz distilling tube was prepared with dimensions to fit the commercially available tube oven (Thermolyne Model 21100). Prior to insertion into the distillation oven the 17 mm × 132 mm × 1.25 mm irradiated targets were placed in a single-use 22 mm o.d. × 180–200 mm quartz tube (boat). This was done to alleviate the problem of cracking caused by the cooling of dripped molten bismuth (mp 271 °C) in contact with the quartz distilling tube. As an additional precaution, a larger quartz tube, 25 mm i.d., was kept in the distilling tube as a liner. The quartz distilling tube was coupled to the glass tube by a Tefzel $^1/_4$–28 thread (Alltech, #20055) to a female Luer fitting. Distillation of astatine was accomplished at 600–700 °C with a stream of argon to carry the astatine into the reaction vessel. The distillation apparatus was vented to the inside of the glovebox through a charcoal filter prepared from a packed syringe barrel. Introduction of reagents into the reaction vessel was done by prefilled syringe. Distillation glassware, Teflon tubing, and fittings were soaked in concentrated HNO_3 and rinsed well with deionized H_2O prior to each distillation.

Astatine Distillation and Labeling Procedure. The distillation apparatus was placed in the glovebox and assembled. The reaction vial was removed from the quartz distillation tube by disconnecting the Tefzel adapter. In the experiments with the best recovery of astatine-211 from the irradiated target, the furnace was preheated to ca. 650 °C under a stream of argon and allowed to equilibrate for 30–60 min. During the equilibrium process the argon gas was allowed to pass through the heated still and exit into the glove box. While this was occurring, the reaction mixture was prepared in the following manner.

Into the reaction vial was placed 100 μL of a 1 mg/mL solution of **1** (0.20 mmol) in 1% glacial HOAc/MeOH, 80 μL of a 1 mg/mL solution of *N*-chlorosuccinimide (NCS) (0.60 mmol) in MeOH, 400 μL of a 5% glacial HOAc/MeOH mixture, and 50 μL of phosphate-buffered saline (PBS). After the oven temperature had equilibrated, the reaction vial was reconnected to the distillation apparatus. The flow rate of argon gas was metered to between 25 and 75 mL/min. An irradiated bismuth target was wiped and placed into a quartz boat. The preheated quartz distilling tube was opened by disconnecting the carrier gas inlet adapter at the ball joint end of the still. The quartz boat containing the irradiated target was carefully slid into the center of the heated quartz distillation tube with tongs. The ball joint was quickly reconnected and clamped to secure it.

The distillation was allowed to proceed for 1 h with the reaction vial at ambient temperature. During the distillation, the volume in the reaction vial was maintained by addition of two 25-μL aliquots of MeOH. The distillation was terminated by turning off the furnace and the argon flow. A 10-μL aliquot of a 5.8 mg/mL aqueous solution of $Na_2S_2O_5$ (0.61 mmol of $NaHSO_3$) was added to the reaction mixture to reduce any volatile astatine species. The reaction vial was then removed from the distilling apparatus by disconnecting the Tefzel adapter from the Luer tip. The labeled **2a** was separated from [^{211}At]-astatide and the aryltin compound **1** prior to its use in the conjugation reaction as follows.

Two reverse-phase C-18 disposable columns (J.T. Baker, SPE octadecyl C-18) were activated by elution with 5 mL of 95% EtOH, followed by 5 mL of PBS. The solution containing astatinated benzoate **2a** prepared above was then loaded onto one of the columns. The reaction vial was rinsed with less than 0.5 mL of EtOH/PBS (1:1) and six 1-mL fractions were eluted with EtOH/PBS (6:4). The activity in each of the eluted fractions was measured and those fractions with the highest levels of activity (typically 60–70% in fractions 3 and 4) were used in the following steps. To each of the 1-mL fractions with the highest activity was added 2 mL of PBS. The entire volume of the diluted fractions was loaded onto the second C-18 column and was eluted through the column. The astatinated benzoate **2a** remained on the column. The column

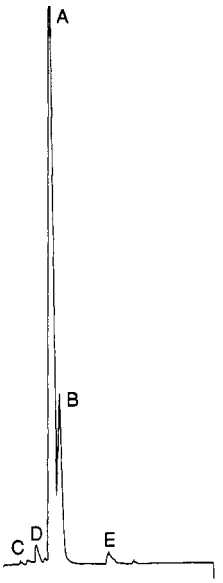


Figure 2. HPLC radiochromatogram of astatination reaction mixture after purification by two C-18 columns. Retention times indicate that peak A (4.14 min) is *N*-succinimidyl *p*-astatobenzoate (**2a**), peak B (4.94 min) is *p*-astatobenzoic acid, peak C (solvent front) is likely to be remaining astatide, and peaks D (2.88 min) and E (9.28 min) are unidetermined.

was then dried by passing a stream of nitrogen gas over it for ca. 5 min. The activity was eluted from the dried column with dry CH_3CN, collecting three 1-mL fractions. Typically >90% of the activity was in fractions 1 and 2. These fractions were combined and the CH_3CN was then removed under a gentle stream of dry nitrogen. A typical radio-HPLC chromatogram of the combined fractions is shown in Figure 2. The concentrated material, composed principally of **2a**, was used for antibody labeling by using the following procedure.

To the vial containing **2a** was added 500 μL of a solution containing 1 mg of NR-ML-05 antibody in 200 μL of PBS and 300 μL of 1.0 M, pH 9.2, $NaHCO_3/Na_2CO_3$ buffer. After 10 min at room temperature, the crude labeled antibody was purified by size-exclusion chromatography (Sephadex G-25, PD-10) eluting with PBS. Overall antibody astatine-211-labeling yields of 34–41% (decay corrected) have been achieved.

Radioiodine Labeling. Labeling of NR-ML-05 and its Fab fragment with iodobenzoate **2b** used in the in vitro and in vivo experiments was conducted as previously described (*23*), except that **2b** was separated from 1 and [^{125}I]iodide via the two C-18 columns prior to conjugation as described in the procedure above. Overall antibody radioiodine-labeling yields of 42–47% were obtained using this procedure.

In Vitro Stability Experiments. The stability of the astatine-211-labeled NR-ML-05 was examined by subjecting it to solutions of PBS and a variety of reagents at 37 °C for several hours. In the experiments test tubes were charged with 0.5 mL of (a) PBS, (b) 1 M glycine in PBS, (c) 1 M $Na_2CO_3/NaHCO_3$ buffer, pH 9.2, and (d) 1 M glycine + 1 M $Na_2CO_3/NaHCO_3$. To each test tube was added 65 μg of astatinated antibody. After this addition, the samples were lightly vortexed and an aliquot was removed and analyzed by TLC (80% MeOH) as the $t = 0$ time point. The tubes were then incubated at 37 °C for 20 h. Aliquots were removed periodically and examined by TLC.

Animals and Tumor Model. Athymic (nude) mice were obtained from Simonsen Laboratories, Inc. (Gilroy, CA) and were used at 10–12 weeks of age. Female athymic mice (nu/nu) were housed in microisolator caging with filter bonnet tops and maintained on sterilized chow and water in a controlled environment. The 18 mice used in the experiment with intact NR-ML-05 weighed 24.04 g ± 2.04 g and the 18 mice used in the experiment with the NR-ML-05 Fab weighed 24.61 g ± 1.55 g. Tumors were established by injection of 10^7 A375 Met/Mix[2] melanoma cells in the subscapular region of the back. The cells were allowed to grow for 7–10 days to produce tumors which had an average tumor weight of 18 mg ± 9 mg for the study involving intact NR-ML-05 and 34 mg ± 13 mg for the study involving NR-ML-05 Fab.

Biodistribution Studies. In each experiment athymic mice bearing human melanoma A375 Met/Mix tumor xenografts were injected intravenously (ca. 100 μL) via the lateral tail vein. The mice were each marked for identification and were handled in the same manner. Replicate (4×) 5-μL aliquots of the injectate were prepared and counted to serve as standards for the calculation of the total injected dose. Mice were weighed, restrained, and injected; weighing the syringe before and after injection to determine the volume injected. At designated times postinjection, groups of mice were sacrificed by cervical dislocation and dissected. Blood samples were collected just prior to sacrificing the mouse by obtaining a sample by retroorbital bleeding. Eleven additional tissues were excised from each mouse. These tissues were as follows: tumor, skin (from back), muscle, bone (femur), lung, liver, spleen, stomach (including contents), neck (soft tissue from the ventral portion of the neck, including thyroid), kidneys, and intestines (including contents). Organs were removed, blotted, weighed, and counted in a γ scintillation counter. Initial radioactivity counting was conducted shortly after sacrifice of the animals to obtain combined ^{125}I and ^{211}At counts. The tissues were recounted 6–7-days postsacrifice when only ^{125}I counts remained. Data analysis was conducted by subtracting the ^{125}I counts from the total initial counts to obtain the astatine-211 counts, subtracting the background counts from the ^{125}I counts, and finally decay correcting every sample counted. Further analyses of the data included calculation of the percent injected dose per gram (%ID/g) for each isotope in each tissue, an average and standard deviation for the %ID/g in each set of six animals, the ratios of the %ID/g for the two isotopes (^{211}At/^{125}I) in the tissues of each animal, and the average ratio and standard deviation for each tissue.

Three animal biodistributions were performed. In one study, NR-ML-05 IgG labeled with purified **2a** and (separately) with purified radioiodinated **2b** was coinjected into 18 athymic mice with A375 Met/Mix human tumor xenografts. The NR-ML-05 labeled with **2a** used in the experiment had a specific activity of 0.3 μCi/μg and a 99% radiochemical purity. The radioiodinated **2b** labeled NR-ML-05 coinjected had a specific activity of 0.5 μCi/μg and a radiochemical purity of 98%. The injectate contained 7 μCi of astatine-211 and 1.5 μCi of iodine-125 on a total of 24 μg of protein. Groups of six mice were sacrificed at 1, 4, and 22 h postinjection. The tissue distribution data are given in Table II.

A second biodistribution study was conducted by coinjection of NR-ML-05 Fab labeled with purified **2a** and (separately) with purified **2b** into 18 athymic mice with A375 Met/Mix human tumor xenografts. The astatinated Fab employed had a specific activity of 0.5 μCi/μg and a radiochemical purity of >98%. The radioiodinated NR-ML-05 Fab employed had a specific activity of 0.5 μCi/μg and a radiochemical purity of >98%. The injectate

Table I. Astatine-211 Distillation Yields[a]

oven temp, °C	estimated[b] astatine, μCi	μCi (% recovered) reaction vial	charcoal trap	fittings/glassware	total recovery[c]
650–700	1320	988 (75)	76 (6)		1064 (81)
650–700	1610	837 (52)	7 (1)	68 (7)	912 (69)
650–675	916	275 (30)	26 (3)	70 (8)	371 (41)
600–625	1390	448 (44)	16 (2)	276 (27)	740 (73)
600	1134	325 (29)	31 (3)	407 (36)	763 (68)
625–675	1021	194 (19)	11 (1)	310 (30)	515 (51)
600–650	1624	341 (21)	27 (1)	457 (29)	825 (51)
600–650	1193	692 (58)	61 (5)	112 (9)	865 (72)
650–700	682	307 (45)	12 (2)	350 (51)	669 (98)
650–700	1250	250 (20)	12 (1)	87 (7)	349 (28)
600–650	1644	296 (18)	16 (1)	219 (13)	531 (32)

[a] Values were obtained from Capintec CRC-7 dose calibrator and should be considered estimates. [b] Values are estimates based on decay correction from end-of-bombardment of target to time of beginning distillation. [c] The remainder of the activity was present on the distillation glassware which could not be fit into the dose calibrator.

Table II. Distribution of Radioactivity for Coinjected [^{211}At]2a- and [^{125}I]2b-Labeled NR-ML-05 in Athymic Mice with A375 Met/Mix Xenografts[a]

tissue	1 h ^{211}At	1 h ^{125}I	4 h ^{211}At	4 h ^{125}I	22 h ^{211}At	22 h ^{125}I
blood	36.07 ± 1.65	36.78 ± 1.75	27.90 ± 1.51	28.45 ± 1.69	18.48 ± 2.85	21.27 ± 3.66
tumor	3.82 ± 1.32	4.65 ± 0.93	8.63 ± 3.03	9.43 ± 3.72	19.64 ± 6.57	23.62 ± 8.36
skin	3.06 ± 0.70	3.03 ± 0.66	4.20 ± 1.18	4.05 ± 1.12	5.57 ± 1.42	5.62 ± 1.43
muscle	0.97 ± 0.10	1.01 ± 0.09	1.27 ± 0.26	1.30 ± 0.24	1.89 ± 0.35	1.72 ± 0.26
bone	2.86 ± 0.52	2.83 ± 3.23	2.56 ± 0.48	2.59 ± 0.40	2.81 ± 0.69	2.70 ± 1.01
lung	13.79 ± 3.12	13.54 ± 3.23	14.06 ± 2.92	13.70 ± 3.02	9.23 ± 2.36	8.23 ± 2.45
liver	8.54 ± 1.47	8.57 ± 1.54	6.67 ± 0.86	6.69 ± 0.92	4.66 ± 1.52	5.03 ± 1.60
spleen	7.64 ± 1.83	7.38 ± 1.83	6.62 ± 2.07	5.75 ± 1.77	6.88 ± 1.66	5.15 ± 1.98
stomach	1.69 ± 0.42	1.09 ± 0.29	3.09 ± 0.51	1.32 ± 0.34	4.81 ± 0.87	0.92 ± 0.17
neck	7.11 ± 2.57	7.13 ± 2.72	7.28 ± 1.45	6.99 ± 1.41	7.28 ± 2.00	6.67 ± 1.93
kidney	7.70 ± 0.60	7.95 ± 0.64	6.14 ± 0.92	6.62 ± 0.96	5.08 ± 1.05	5.49 ± 1.11
intestine	1.34 ± 0.14	1.39 ± 0.13	1.47 ± 0.32	1.38 ± 0.36	1.44 ± 0.21	1.32 ± 0.18

[a] Results were obtained for $n = 6$ mice and are given as mean ± standard deviation of the percent injected dose/g (%ID/g).

Table III. Distribution of Radioactivity for Coinjected [^{211}At]2a- and [^{125}I]2b-Labeled NR-ML-05 Fab in Athymic Mice with A375 Met/Mix Xenografts[a]

tissue	1 h ^{211}At	1 h ^{125}I	4 h ^{211}At	4 h ^{125}I	20 h ^{211}At	20 h ^{125}I
blood	6.50 ± 0.79	6.26 ± 0.72	1.74 ± 0.19	1.17 ± 0.09	0.44 ± 0.06	0.14 ± 0.01
tumor	5.53 ± 0.68	5.20 ± 0.92	7.56 ± 1.35	5.68 ± 1.05	4.16 ± 1.21	3.07 ± 0.95
skin	2.80 ± 0.53	2.34 ± 0.46	2.31 ± 0.40	0.96 ± 0.15	0.91 ± 0.12	0.06 ± 0.01
muscle	1.18 ± 0.19	1.05 ± 0.19	0.67 ± 0.13	0.36 ± 0.05	0.22 ± 0.04	0.02 ± 0.01
bone	1.30 ± 0.34	1.05 ± 0.27	0.98 ± 0.13	0.31 ± 0.06	0.42 ± 0.12	0.02 ± 0.02
lung	5.66 ± 0.98	4.12 ± 0.85	4.52 ± 0.57	1.06 ± 0.08	2.04 ± 0.40	0.18 ± 0.12
liver	1.90 ± 0.24	2.04 ± 0.24	0.96 ± 0.16	0.57 ± 0.09	0.34 ± 0.06	0.10 ± 0.02
spleen	2.63 ± 0.56	1.35 ± 0.26	3.65 ± 0.77	0.34 ± 0.03	2.06 ± 0.54	0.06 ± 0.02
stomach	2.92 ± 0.94	0.94 ± 0.31	12.14 ± 2.56	0.85 ± 0.16	5.44 ± 1.55	0.07 ± 0.02
neck	3.54 ± 0.53	2.86 ± 0.43	3.37 ± 0.92	0.85 ± 0.09	1.40 ± 0.59	0.14 ± 0.12
kidney	34.38 ± 6.35	38.56 ± 6.84	9.82 ± 2.59	13.92 ± 4.14	1.49 ± 0.74	0.89 ± 0.48
intestine	0.94 ± 0.18	0.82 ± 0.19	0.89 ± 0.13	0.37 ± 0.03	0.39 ± 0.11	0.04 ± 0.01

[a] Results were obtained for $n = 6$ mice and are given as mean ± standard deviation of the percent injected dose/g (%ID/g).

contained 9 μCi of astatine-211 and 4 μCi of iodine-125 on a total of 25 μg of protein. Groups of six mice were sacrificed at 1, 4, and 20 h postinjection. The tissue distribution data are given in Table III.

A third biodistribution study was carried out to evaluate the in vivo distribution of astatide ion in athymic mice. In that study, eight mice were each injected with 9.3 μCi of [^{211}At]astatide in 100 μL of PBS solution. Sets of four animals were sacrificed at 2 and 4 h postinjection. The tissue distribution data are given in Table IV.

Table IV. Distribution of Astatine-211 in Athymic Mice[a]

tissue	2 h	4 h
blood	1.06 ± 0.08	1.06 ± 0.16
skin	2.90 ± 0.35	2.76 ± 0.44
muscle	0.87 ± 0.05	0.50 ± 0.08
bone	1.14 ± 0.10	1.05 ± 0.16
lung	7.05 ± 0.40	5.49 ± 0.89
liver	1.10 ± 0.13	0.99 ± 0.13
spleen	8.95 ± 1.69	6.38 ± 0.62
stomach	23.42 ± 5.53	19.07 ± 3.98
neck	4.29 ± 0.83	3.22 ± 0.26
kidneys	2.65 ± 0.19	2.29 ± 0.23
intestines	1.45 ± 0.14	1.28 ± 0.17

[a] Results were obtained for $n = 4$ mice and are given as mean ± standard deviation of the percent injected dose/g (%ID/g).

RESULTS

Astatine-211 was distilled into the reaction mixture containing the organometallic intermediate 1, the oxidizing agent *N*-chlorosuccinimide (NCS), and acetic acid in methanol by using the distillation setup shown in Figure 1. It was observed that the best distillation yields were obtained when the oven was preheated to the distilling temperature (or slightly higher) prior to insertion of the irradiated target. A compilation of the recovery of astatine

from several distillations is given in Table I. While the overall efficiency of the dry distillations was not high in many of the distillations, the efficiency of trapping the astatine appeared to be very good, as typically only a few percent (1–6%) of the distilled astatine was found in the charcoal trap on the reaction vessel. The reason for the low recovery of astatine in some of the distillations is not fully understood. In the distillations with low recovery of activity, the astatine activity was associated with yellow and black deposits (presumably bismuth) on the glass surfaces of the distilling apparatus. Routinely, the glassware and associated fittings were cleaned prior to use to avoid potential problems with surface contaminants and to clean off the deposits. In addition, use of HF to etch and clear the quartz distilling tube of deposited materials was studied. These procedures did not alleviate the deposition of visible material and astatine activity. Another consideration investigated was the use of oxygen in the carrier gas to oxidize the bismuth and make it less volatile (*27*). Initial distillations had been conducted under Argon gas (flowing) atmosphere. A premixed quantity of argon/oxygen (11 ppm) was studied to try to improve the recovery yields of astatine-211; however, this also did not improve the overall recovery yields. Since there were some concerns about the oxidation of astatine in the presence of oxygen at the elevated temperatures, all further studies have been conducted under argon atmospheres without having oxygen present. Another factor that may have contributed to the drop in recovery yields was the fact that the initial targets had a bismuth thickness of 0.5 mm, but later ones had a thickness of 0.8 mm. Thickness of target had previously been cited as a possible reason for low recovery of astatine in a dry distillation (*24*). Rather than pursuing the cause for the low recoveries further, vacuum distillations are presently being conducted which give higher and more consistent yields (*28*).

A number of reactions were carried out to study astatination of the aryltin intermediate 1 to produce **2a**. The stoichiometry of reagents and solvent compositions used in the astatination reactions were based on optimization studies with the analogous radioiodination reactions (*19*, *23*). The astatination of 1 was found to be facile with radiochemical yields of **2a** ranging from 70% to 90%. The composition of reaction mixtures were analyzed routinely by reverse-phase HPLC. The gradient employed readily separated starting material 1 from the astatine-labeled materials. The amount of astatinated impurities such as free astatide and *p*-[^{211}At]astatobenzoic acid observed in the crude reaction mixtures varied, but combined were generally less than 20%. Recovery of injected astatine activity from the HPLC was nearly quantitative (e.g. 92%), indicating that there were no major portions of activity unaccounted for.

Concern about the larger quantity of reagents used in the astatination reactions as compared to those in the radioiodination reactions (*23*) and their potential impact on antibody conjugation led to development of a simple and rapid method of separating astatinated benzoate intermediate **2a** (and *p*-astatobenzoic acid) from impurities. The separation was accomplished with two disposable C-18 columns. The first-18 column was used to separate the nonpolar impurities, including unreacted 1, from the more polar components which included **2a**. Immediately following the elution from the first column, the eluant was diluted with PBS and loaded onto the second C-18 column. Under these conditions **2a** was quantitatively retained on the column while the most polar impurities, including [^{211}At]astatide, eluted. Removal of the water from the column and elution of **2a** with dry acetonitrile provided a method of isolation in which very little hydrolysis of the *N*-succinimidyl ester occured. Overall recovery of activity from the columns was 60–70%, but was not optimized. HPLC analysis of the purified product showed it to be the desired **2a** and a small amount of *p*-astatobenzoic acid, free of aryltin precursor 1 and most of the [^{211}At]astatide (see Figure 2).

Conjugation of **2a** to the intact antibody and its Fab fragment were conducted under identical conditions and resulted in conjugation yields ranging from 40% to 60%. The yields obtained in the conjugations were consistent with those obtained with the corresponding radioiodinated *N*-succinimidyl *p*-iodobenzoate (**2b**) under similar reaction conditions.

The nature of the astatinated benzoyl bonding or association with the antibody was of interest. Previous studies with radioiodinated iodobenzoyl conjugates had shown that they were very stable in serum and under a variety of harsh denaturing conditions in vitro (*23*). Although the denaturing conditions of the TLC (80% MeOH) indicated that the astatine was bonded to the protein in a stable manner, we were concerned that differences in lipophilicity or reactivity might lead to a portion of astatinated **2a** (or *p*-astatobenzoate) being associated with the protein or potentially reacting with functional groups other than lysine amines. To evaluate this, astatinated antibodies (intact IgG and Fab) were subjected to the highly nucleophilic and strongly basic solutions of 1 M glycine and 1 M $Na_2CO_3/NaHCO_3$ at 37 °C for up to 24 h. Upon evaluation, initial TLC purities (97–98%) did not change in PBS (control), under highly denaturing conditions, or with 1 M glycine over an 18–24-h period.[3] A small decrease (less than 3%) in purity was observed in the highly basic 1 M $Na_2CO_3/NaHCO_3$ mixtures over that time period.

Evaluation of the in vivo distribution of [^{211}At]**2a**-labeled NR-ML-05 and its Fab fragment was conducted in two biodistribution experiments. In the biodistribution studies coinjection of [^{125}I]**2b**-labeled NR-ML-05 or its Fab fragment, previously shown to be stable in vivo (*23*), was carried out for comparison purposes. The distribution of ^{211}At and ^{125}I activity when labeled to intact NR-ML-05 were found to be quite similar. The only appreciable difference in the concentrations of radionuclides was in the stomach at 4 and 22 h postinjection. A slight difference was noted in the tumor and blood concentrations at 22 h. The distribution of ^{211}At and ^{125}I activity when labeled to NR-ML-05 Fab was similar at 1 h postinjection, but large differences in tissue activity were seen at 4 and 20 h postinjection. Although the immunoreactivities of the astatinated antibodies were not measured due to difficulties with the assay, nearly equivalent localization of activity between the astatinated and radioiodinated antibodies was observed in the tumor, indicating that the preparations were likely to have been immunocompetent.

A third animal study was conducted to evaluate the biodistribution of [^{211}At]astatide in athymic mice. A limited study was conducted, with sacrifices at 2 and 4 h postinjection, for comparison with data from the literature. Concentrations of ^{211}At appreciably higher than for blood were seen in skin, lung, spleen, stomach, neck, and kidneys.

[3] Similar experiments with another IgG_{2b} antibody, NR-LU-10, and its Fab fragment demonstrated that when astatinated with **2a**, they were stable in PBS and serum at 37 °C over 18 h. Further, challenges with 95% EtOH, 12% TCA, 6 M urea, and 85 mM $NaHSO_3$ at 37 °C over 18 h did not release astatine from the labeled antibody or its Fab fragment.

The highest concentrations were seen in the stomach, spleen, lung, and neck.

DISCUSSION

The cytotoxic properties of α particle emission of astatine-211 have been known for many years (*29*, *30*), as has the potential for tumor-site-selective delivery of different radionuclides by monoclonal antibodies (*31–33*). However, coupling of astatine to antibodies for use in radioimmunotherapy has presented a formidable challenge as the chemistry of astatine is not fully understood (*34*, *35*). Studies of the chemistry of astatine have been difficult because there are no nuclides of astatine with a half-life greater than 8.3 h (*36*). Introduction of astatine into amino acid functional groups on native proteins has led to attachments which were labile in vivo (*7–9*). Thus, our group, and other investigators, have studied an alternative method of protein labeling whereby astatine is attached to a molecule which can subsequently be attached (conjugated) to an antibody.

The goal of this investigation was to evaluate a method for astatination of the antimelanoma antibody NR-ML-05 and its Fab fragment[1] for subsequent studies of its potential application in therapy of metastatic melanoma. On the basis of our previous studies with *p*-iodobenzoyl conjugates of antibodies in animals (*23*,*37*,*38*), clinical evaluations (*39*), and the reported stability of the *p*-astatobenzoyl conjugate of proteins (*12–15*), we chose to investigate a method of producing *p*-astatobenzoyl-labeled antibodies which could be accomplished safely in a minimum time (e.g. <1 h). While the results obtained in studies by Friedman et al. (*12*), Harrison and Royle (*15*), and Vaughan et al. (*14*) indicated that the *p*-astatobenzoyl conjugate formed a stable attachment of astatine to proteins, the method of astatination used required many manipulations of solutions containing astatine and took up to 3 h to complete the labeling steps. An alternative to the use of diazonium salt decomposition to incorporate radiohalogens into a small molecule such as a benzoic acid derivative was the use of organometallic intermediates (*40*). Visser had shown that astatine could be incorporated into a number of compounds by the use of organomercury intermediates (*41–44*) and Milius et al. had shown that organostannyl intermediates could be used to incorporate astatine into compounds (*18*). A comparative study was conducted to evaluate astatination of aromatic compounds with several organometallic intermediates (*19*), and it was found that any of the organometallics studied could be used to introduce astatine into benzoic acid derivatives. Our studies of radioiodinations using iodobenzoyl conjugates prepared from the arylstannane intermediates had shown these compounds to be easily prepared and stable for long periods of time under various conditions, and the tri-*n*-butylstannanes could be readily separated from the desired radioiodinated product via reverse-phase chromatography. Also, Zalutsky et al. had shown that the *m*-astatobenzoyl conjugate of antibodies could be prepared readily by astatination of aryl trialkylstannyl intermediates (*20*, *21*). Thus, astatination of the protein-reactive intermediate *N*-succinimidyl *p*-astatobenzoate (**2a**) was accomplished via the first step shown in Scheme I.

To simplify the astatination procedure, distillation of the astatine directly into an acetic acid/methanol mixture containing an organometallic compound, **1**, and the oxidant *N*-chlorosuccinimide was carried out. Dry distillation of astatine gave variable results under the conditions studied, with recoveries of 20–75% being obtained. This method of obtaining astatine for labeling of molecules appears to require less manipulation of the astatine than "wet" distillation methods (*46*, *47*). Further, by distilling the astatine directly into the reaction mixture there was no need to isolate the distilled astatine, as had been done by Lambrecht (*27*), Zalutsky (*20*), and Appelman (*25*). Those investigators isolated the astatine onto support mediums such as a silica gel columns or a platinum disc. However, when astatine is isolated on a secondary medium it is necessary to reextract it for labeling purposes. This reextraction process can be time consuming and may result in loss of considerable astatine activity due to its adsorption to the surfaces (*44*). More recently, Zalutsky et al. have distilled the astatine into cooled $CHCl_3$ and subsequently added the organometallic intermediate (ATE) and other reactants to the $CHCl_3$ (*21*). The length of time required to conduct the distillations is very important because of the half-life of astatine-211. In our experiments the distillation process was carried out over a 1-h period. However, the majority (>95%) of the activity which was recovered was distilled from the target within the first 30 min.

Reaction of the organometallic intermediate **1** was found to be facile as predicted by our preliminary studies (*19*). In the experiments, labeling using the method described herein resulted in good incorporation of astatine (70–90%) into the protein-reactive intermediate **2a**, with only small quantities of astatide remaining unreacted. To preclude the reaction of **1** with the antibody, the crude astatination (and iodination) product was rapidly separated from **1** via a disposable C-18 cartridge elution. Likewise, the remaining astatide was removed from the crude reaction mixture by a second C-18 cartridge separation. The two separation steps using C-18 cartridges were conducted in a manner that they could be used to separate out the undesired components with a minimal loss (<5%) of the desired radiolabeled **2a** or **2b**. Conjugation of **2a** to the antibodies was conducted in a manner that was previously optimized for conjugation reactions of **2b**, and yields of 40–60% were obtained. Thus, while the labeling with astatine-211 involved a number of steps, the overall labeling efficiency (17–35%) was only slightly lower than for radioiodinations with **2b** (*23*).

The in vitro stability of astatinated intact NR-ML-05 and its Fab fragment was found to be high. No decrease in protein-bound astatine was noted when astatinated antibodies were incubated with PBS or 1 M glycine, and only a decrease of 2–3% in the amount of protein-bound astatine was noted for the labeled antibody incubated in strongly basic 1 M $Na_2CO_3/NaHCO_3$ solution for 20 h.

The in vivo distributions of activity for the [^{211}At]astatobenzoyl conjugates of NR-ML-05 and its Fab fragment were investigated. Coinjection with [^{125}I]iodobenzoyl conjugates of NR-ML-05 or its Fab fragment was carried out to provide an indication of the stability of the astatine label in vivo. For the dual-labeled intact NR-ML-05, the relative distribution of astatine-211 and iodine-125 at the three time points studied was similar (Table II), giving an indication that the astatine was stably attached. However, the difference in the %ID/g for the two nuclides in the stomach most likely indicated that a small amount of astatide was released from the antibody or its catabolites. The labeled NR-ML-05 Fab had a much larger variation between the two nuclides in tissues (Table III). Based on the fact that most of the activity was retained on the intact antibody in circulation, an argument can be made that observed differences in release of astatine activity have come from processes associated with the degredation of the Fab. Garg et al. (*48*) have recently reported that the

$F(ab')_2$ fragment of C110, an antibody reactive against carcinoembryonic antigen, when labeled with the *m*-astatobenzoyl conjugate releases astatine at a much higher level than the intact antibody. This correlates well with the results presented herein. Since the astatine-labeled Fab was found to be quite stable to chemical challenges in vitro, it seems likely that the degradation is brought about by an enzymatic process. However, it is unclear whether the release of astatide occurs prior to, or after, degradation of the antibody.

It is assumed that the in vivo stability of astatine-211-labeled antibodies will be crucial in the development of a therapeutic agent, since it is of paramount importance that the astatine remain attached to the antibody to achieve a tumor-specific localization. To evaluate the amount of free astatine in the biodistributions it was necessary to have data on the distribution of astatine in athymic mice. The distribution of free astatine-211 (vs radioiodine) was reported in 1953 by Hamilton et al. (*49*). Their extensive study provided data on the distribution of astatide in rats which indicated that astatine localized in stomach and neck (thyroid) similar to radioiodine, but unlike radioiodine, astatine localized in lung and spleen as well. Visser et al. (*10*) have also provided data on the distribution of astatide in rats; however, only one animal was used to obtain the data except at the 4-hour time point. Friedman et al. (*12*) included data on distribution of astatide in mice, but no data was readily available for astatide distribution in athymic mice. Therefore, we conducted a limited investigation of the distribution of astatide in athymic mice. The data from the astatide biodistribution study are given in Table IV. The data were compared with data from the Hamilton et al. study (*49*), and although the absolute values were different in the tissues, the ratios of the activity localized in the spleen and stomach relative to the lung for the two studies were nearly identical at the 4-h time point. That is, ratios of the spleen:lung activity of 1.2 and stomach:lung activity of 3.5 were obtained in athymic mice, and ratios for the spleen:lung of 1.1 and stomach:lung of 3.4 were obtained in the rat. We felt that these ratios might provide an indicator of free astatide in mice and might be usable to determine the percent of activity in an organ that was present as astatide (versus other labeled species). Thus, we examined the ratios for the amounts of astatine-211 activity in excess of iodine-125 in spleen, stomach, and lung for the astatine-labeled Fab biodistribution. Examination of the data obtained in the biodistributions of NR-ML-05 Fab at 4 h for the excess astatine activity in spleen (3.31% ID/g), stomach (11.29% ID/g), and lung (3.46% ID/g) provided data that resulted in a spleen:lung ratio of 1.0 and stomach:lung ratio of 3.3. Similar ratios were obtained for the 20-h data, where excess astatine activity in spleen (2.00% ID/g), stomach (5.37% ID/g), and lung (1.86% ID/g) gave a spleen:lung ratio of 1.1 and a stomach:lung ratio of 2.9. For comparison, the data from Hamilton et al. at 24 h gave ratios of spleen:lung of 1.0 and stomach:lung of 2.6. We feel that the agreement found in these correlations provides a strong indicator that astatine was released in vivo from the astatobenzoyl conjugates. However, the application of the ratios to determine amount of free astatide in tissues is less certain as the ratios obtained from data provided by Visser et al. (*10*) and Friedman et al. (*12*) were not in agreement with those above.

In summary, the in vivo distributions of [^{211}At]astatobenzoyl conjugate of an intact antibody and its Fab fragment were investigated. The astatine appeared to have a stable attachment to the intact antibody, with only minor amounts of free astatide being detected at 22 h postinjection. Contrary to this, substantial quantities of free astatide were found in tissues when the astatinated Fab fragment was investigated. On the basis of the results presented herein, further development of astatinated conjugates is warranted.

ACKNOWLEDGMENT

We acknowledge the efforts of Alan Posewitz (Radiation Safety Assistant) for assistance in setting up and monitoring the astatine distillations. We also thank other NeoRx personnel involved in the astatine labeling studies, in particular the technical assistance of Karen Poole, Denise Dupont, and Joanne Stevens in animal biodistribution studies. Likewise, we thank Argonne personnel, John Hines and Ed Kemereit, for their assistance in target irradiation, quantification, and shipment. We are grateful to the National Cancer Institute for partial funding for this study under a Small Business Innovative Research Contract (N43-CM-67939).

LITERATURE CITED

(1) Hall, E. J. (1988) LET and RBE. *Radiobiology for the Radiologist*, 3rd ed., Chapter 8, pp 161–177, J.B. Lippincott Comp., Philadelphia, PA.

(2) Held, K. D. (1986) Radiobiology: Biological Effects of Ionizing Radiation. *Nuclear Medicine Therapy* (J. C. Harbert, Ed.) Chapter 17, pp 257–284, Maple-Vail Book Mfg Group, Binghampton, NY.

(3) Brown, I. (1986) Astatine Radiopharmaceuticals. Astatine-211: Its Possible Applications in Cancer Therapy. *Appl. Radiat. Isot. 37*, 789–798.

(4) Zalutsky, M. R. (1989) Antibody-Mediated Radiotherapy: Future Prospects. *Antibodies in Diagnosis and Therapy* (M. R. Zalutsky, Ed.) Chapter 11, pp 219–225, CRC Press, Inc., Boca Raton, FL.

(5) Wilbur, D. S. (1990) Potential Use of Alpha Emitting Radionuclides in the Treatment of Cancer. *Antibody, Immunoconjugate Radiopharm. 4*, 85–97.

(6) Hughes, W. L., and Gitlin, D. (1954) The Reaction of Astatine with Protein, USAECD-BNL-314.

(7) Hughes, W. L., and Gitlin, D. (1955) Astatinated (At^{211}) Organic Compounds for Production of Highly Localized Radiobiological Effects. *Am. Soc. Biol. Chem. 14*, 229.

(8) Aaij, C., Tschroots, W. R. J. M., Lindner, L., and Feltkamp, T. E. W. (1978) The Preparation of Astatine Labeled Proteins. *Int. J. Appl. Radiat. Isot. 26*, 25–30.

(9) Vaughan, A. T. M., and Fremlin, J. H. (1978) The Preparation of Astatine Labeled Proteins Using an Electrophilic Reaction. *Int. J. Nucl. Med. Biol. 5*, 229–230.

(10) Visser, G. W. M., Diemer, E. L., Vos, C. M., and Kaspersen, F. M. (1981) The Biological Behavior of Some Organic Astatine Compounds in Rats. *Int. J. Appl. Radiat. Isot. 32*, 913–917.

(11) Visser, G. W. M., Diemer, E. L., and Kaspersen, F. M. (1981) The Nature of the Astatine–Protein Bond. *Int. J. Appl. Radiat. Isot. 32*, 905–912.

(12) Friedman, A. M., Zalutsky, M. R., Wung, W., Buckingham, F., Harper, P. V., Jr., Scherr, G. H., Wainer, B., Hunger, R. L., Appelman, E. H., Rotherberg, R. M., Fitch, F. W., Stuart, F. P., and Simonian, S. J. (1977) Preparation of a Biological Stable and Immunogenically Competent Astatinated Protein. *Int. J. Nucl. Med. Biol. 4*, 219–224.

(13) Vaughan, A. T. M. (1979) The Labeling of Proteins with ^{211}At Using an Acylation Reaction. *Int. J. Appl. Radiat. Isot. 30*, 576–577.

(14) Vaughan, A. T. M., Bateman, W. J., and Fischer, D. R. (1982) The In Vivo Fate of a ^{211}At Labelled Monoclonal Antibody with Known Specificity in a Murine System. *Int. J. Radiat. Oncol. Biol. Phys. 8*, 1943–1946.

(15) Harrison, A., and Royle, L. (1984) Preparation of a ^{211}At–IgG Conjugate Which is Stable In Vivo. *Int. J. Appl. Radiat. Isot. 35*, 1005–1008.

(16) Meyer, G.-J., Rossler, K., and Stocklin, G. (1979) Reaction of Aromatic Diazonium Salts with Carrier-Free Radioiodine and Astatine. Evidence for Complex Formation. *J. Am. Chem. Soc. 101*, 3121–3123.

(17) Visser, G. W. M., and Diemer, E. L. (1982) The Reaction of Astatine with Aromatic Diazonium Compounds. *Radiochem. Radioanal. Lett. 51*, 135–141.

(18) Milius, R. A., McLaughlin, W. H., Lambrecht, R. M., Wolf, A. P., Carroll, J. J., Adelstein, S. J., and Bloomer, W. D. (1986) Organoastatine Chemistry. Astatination via Electrophilic Destannylation. *Appl. Radiat. Isot. 37*, 799–802.

(19) Wilbur, D. S., Hylarides, M. D., and Fritzberg, A. R. (1989) Reactions of Organometallic Compounds with Astatine-211. Application to Protein Labeling. *Radiochem. Acta 47*, 137–142.

(20) Zalutsky, M. R., and Narula, A. S. (1988) Astatination of Proteins Using an *N*-Succinimidyl Tri-*n*-butylstannylbenzoate Intermediate. *Appl. Radiat. Isot. 39*, 227–232.

(21) Zalutsky, M. R., Garg, P. K., Friedman, H. S., and Bigner, D. D. (1989) Labeling Monoclonal Antibodies and $F(ab')_2$ with the α-Particle-Emitting Nuclide Astatine-211: Preservation of Immunoreactivity and In Vivo Localizing Capacity. *Proc. Natl. Acad. Sci. U.S.A. 86*, 7149–7153.

(22) Zalutsky, M. R., and Narula, A. S. (1987) An Improved Method for the Radiohalogenation of Monoclonal Antibodies. *Immunological Approaches to the Diagnosis and Therapy of Breast Cancer* (R. L. Ceriani, Ed.) pp 187–203, Plenum Press.

(23) Wilbur, D. S., Hadley, S. W., Hylarides, M. D., Abrams, P. G., Beaumier, P. A., Morgan, A. C., Reno, J. M., and Fritzberg, A. R. (1989) Development of a Stable Radioiodinating Reagent to Label Monoclonal Antibodies for Radiotherapy of Cancer. *J. Nucl. Med. 30*, 216–226.

(24) Eberle, S. H. (1985) Isolation and Purification of Astatine from Irradiated Targets. *Gmelin Handbook of Inorganic Chemistry, Astatine*, 8th ed. (H. K. Kugler, and C. Keller, Eds.) Chapter 10, pp 199–209, Springer-Verlag, New York.

(25) Appelman, E. H., Sloth, E. N., and Studier, M. H. (1966) Observation of Astatine Compounds by Time-of-Flight Mass Spectrometry. *Inorg. Chem. 5*, 766–769.

(26) Rosch, F., Henniger, J., Beyer, G.-J., and Dreyer, R. (1985) Optimization of Bombardment Conditions of the $^{209}Bi/\alpha,2n/$ Cyclotron Production of ^{211}At. *J. Radioanal. Nucl. Chem. Lett. 96*, 319–332.

(27) Lambrecht, R. M., and Mirzadeh, S. (1985) Cyclotron Isotopes and Radiopharmaceuticals—XXXV. Astatine-211. *Int. J. Appl. Radiat. Isot. 36*, 443–450.

(28) Wilbur, D. S., Hadley, S. W., Hines, J. J., and Atcher, R. W. (1990) Assessment of Dry Distillation Methods for Improving Protein Labeling Yields with Astatine-211. Eighth International Symposium of Radiopharmaceutical Chemistry, Princeton, New Jersey. *J. Labelled Compds. Radiopharm. 30*, 214–215.

(29) Hamilton, J. G., Durbin, P. W., and Parrott, M. (1954) The Accumulation and Destructive Action of Astatine^{211} (Eka-Iodine) in the Thyroid Gland of Rats and Monkeys. *J. Clin. Endocrinol. Metab. 14*, 1161–1177.

(30) Basson, J. K., and Shellbarger, C. J. (1956) Determination of the RBE of Alpha-Particles from Astatine-211 as Compared to Beta-Particles from Iodine-132 in the Rat Thyroid. *Radiat. Res. 5*, 502–514.

(31) Seiler, F. R., Gronski, P., Kurrle, R., Luben, G., Harthus, H.-P., Ax, W., Bosslet, K., and Schwick, H.-G. (1985) Monoclonal Antibodies: Their Chemistry, Functions, and Possible Uses. *Angew. Chem. Int. Ed. Engl. 24*, 139–160.

(32) Adelstein, S. J., and Kassis, A. I. (1988) Criteria for Selection of Nuclides for Radioimmunotherapy. *Radiolabeled Monoclonal Antibodies for Imaging and Therapy* (S. C. Srivastava, Ed.) pp 165–176, Plenum Press, New York.

(33) Cobb, L. M., and Humm, J. L. (1984) Radioimmunotherapy of Malignancy Using Antibody Targeted Radionuclides. *Br. J. Cancer 54*, 863–870.

(34) Berei, K. and Vasaros, L. (1983) Organic chemistry of astatine. *The Chemistry of Functional Groups* (S. Patai, and Z. Rappoport, Eds.) Supplement D, Chapter 10, pp 405–440, John Wiley & Sons, Ltd., New York.

(35) Brown, I. (1987) Astatine: Its Organonuclear Chemistry and Biomedical Applications. *Adv. Inorg. Chem. 31*, 43–88.

(36) Munzel, H. (1985) Nuclear Properties of Astatine Isotopes. *Gmelin Handbook of Inorganic Chemistry, Astatine*, 8th ed. (H. K. Kugler, and C. Keller, Eds.) Chapter 3, pp 15–94, Springer-Verlag, New York.

(37) Badger, C. C., Wilbur, D. S., Hadley, S. W., Fritzberg, A. R., and Bernstein, I. D. (1990) Biodistribution of *p*-Iodobenzoyl (PIP) Labeled Antibodies in a Murine Lymphoma Model. *Nucl. Med. Biol. 17*, 381–387.

(38) Murray, J. L., Mujoo, K., Wilmanns, C., Mansfield, P., Wilbur, D. S., and Rosenblum, M. G. (1991) Variables Influencing Tumor Uptake of Antimelanoma Monoclonal Antibodies Radioiodinated Using the Para-Iodophenyl (PIP) Technique. *J. Nucl. Med. 32*, 279–287.

(39) Wahl, R., Roberts, J., Hopkins, M., Drescher, C., Fig, L., Mallette, S., Mudgett, E., Foisie, D., Schroff, R., Abrams, P., Fer, M., and Wilbur, S. (1990) Phase I Evaluation of I-131 PIP Labeled Anti-Ovarian Carcinoma Antibody. *J. Nucl. Med. 31*, 777.

(40) Coenen, H. H., Moerlein, S. M., and Stocklin, G. (1983) No-Carrier-Added Radiohalogenation Methods with Heavy Halogens. *Radiochim. Acta 34*, 47–68.

(41) Visser, G. W. M., Diemer, E. L., and Kaspersen, F. M. (1979) The Preparation and Stability of Astatotyrosine and Astatoiodotyrosine. *Int. J. Appl. Radiat. Isot. 30*, 749–752.

(42) Visser, G. W. M., Diemer, E. L., and Kaspersen, F. M. (1980) The Preparation of Aromatic Astatine Compounds Through Aromatic Mercury Compounds. *J. Labelled Compds. Radiopharm. 17*, 657–665.

(43) Visser, G. W. M., Diemer, E. L., and Kaspersen, F. M. (1981) The Preparation of Aromatic Astatine Compounds Through Aromatic Mercury Compounds Part II: Astatination of Pyrimidines and Steroids. *J. Labelled Compds. Radiopharm. 18*, 799–807.

(44) Visser, G. W. M., Diemer, E. L., and Kaspersen, F. M. (1980) The Preparation and Stability of ^{211}At-astato-imidazoles. *Int. J. Appl. Radiat. Isot. 31*, 275–278.

(45) Reference deleted in press.

(46) Neirinckx, R. D., and Smit, J. A. (1973) Separation of Astatine-211 from Bismuth Metal. *Anal. Chim. Acta 63*, 201–204.

(47) Ruth, T. J., Dombsky, M., D'Auria, J. M., and Ward, T. E. (1988) *Radiochemistry of Astatine*, Nuclear Science Series, NAS-NS-3064, Chapter V, pp 41–60, U.S. Department of Energy, Washington, DC.

(48) Garg, P. K., Harrison, C. L., and Zalutsky, M. R. (1990) Comparative Tissue Distribution in Mice of the α-Emitter ^{211}At and ^{131}I as Labels of a Monoclonal Antibody and F(ab')2 Fragment. *Cancer Res. 50*, 3514–3520.

(49) Hamilton, J. G., Ashling, C. W., Garrison, W. M., and Scott, K. G. (1953) The Accumulation, Metabolism and Biological Effects of Astatine in Rats and Monkeys. *University of California Publications in Pharmacology* (H. H. Anderson, D. B. Taylor, and E. L. Way, Eds.) pp 283–343, University of California, Los Angeles.

(50) Morgan, A. C., Galloway, D. R., and Reisfeld, R. A. (1981) Production and characterization of a monoclonal antibody to a melanoma specific glycoprotein. *Hybridoma 1*, 27–36.

(51) Giard, D. J., Aaronson, S. A., Todaro, G. J., Arnstein, P., Kersey, J. H., Dosik, H., and Parks, W. P. (1973) In Vitro Cultivation of Human Tumors: Establishment of Cell Lines Derived From a Series of Solid Tumors. *J. Natl. Cancer Inst. 51*, 1417–1423.

TECHNICAL NOTES

A Convenient Synthesis of Bifunctional Chelating Agents Based on Diethylenetriaminepentaacetic Acid and Their Coordination Chemistry with Yttrium(III)

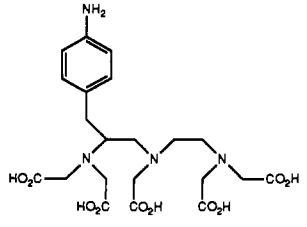
Clark H. Cummins,*,† Edward W. Rutter, Jr., and William A. Fordyce*,‡

The Dow Chemical Company, Midland, Michigan 48674. Received November 21, 1990

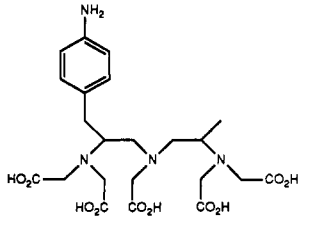
The bifunctional chelating agents *N,N,N′,N″,N″*-pentakis(carboxymethyl)-1-[(4-aminophenyl)methyl]-diethylenetriamine and *N,N,N′,N″,N″*-pentakis(carboxymethyl)-1-[(4-aminophenyl)methyl]-4-methyldiethylenetriamine were prepared in six-step syntheses in overall yields of 38% and 31%, respectively. The use of bromoacetate esters in the synthesis allowed large-scale flash chromatographic purification of reaction products. The synthesis of *N,N,N′,N″,N″*-pentakis(carboxymethyl)-1-[(4-aminophenyl)-methyl]-4-methyldiethylenetriamine resulted in a mixture of two diastereomers. Chelation of yttrium-(III) with these bifunctional chelating agents resulted in 1:1 chelates. In the case of *N,N,N′,N″,N″*-pentakis(carboxymethyl)-1-[(4-aminophenyl)methyl]diethylenetriamine, two diastereomers were observed upon chelation, as expected. In the case of *N,N,N′,N″,N″*-pentakis(carboxymethyl)-1-[(4-aminophenyl)-methyl]-4-methyldiethylenetriamine, only three of the four anticipated diastereomers were observed.

INTRODUCTION

Interest in the attachment of radioactive metal ions to monoclonal antibodies for the diagnosis and treatment of cancer has led to the development of "bifunctional" chelating agents (BFCA's).[1] These chelating agents possess functional groups capable of binding a metal ion and an additional group which allows covalent linkage to protein. In many of the studies reported to date, the backbone of the BFCA has been diethylenetriaminepentaacetic acid (DTPA). The most commonly used forms of DTPA, the cyclic anhydride (*1*) and the mixed anhydride (*2*), suffer from the sacrifice of a metal ion binding moiety for the covalent attachment to protein. The resulting loss of chelate stability relative to DTPA-based BFCA's with all eight metal binding moieties available has been demonstrated in vivo (*3–5*). Brechbiel et al. (*3*) have reported the synthesis of 1-(*p*-aminobenzyl)-DTPA (1B-DTPA, 1), a



1, 1B-H$_5$DTPA



2, 1B4M-H$_5$DTPA

DTPA-based BFCA with all eight metal ion binding moieties available and the protein-linking functional group located in the carbon backbone of the triamine. More recently, Westerberg et al. (*6*) and Keana et al. (*7*) reported the synthesis of an isomeric form of 1B-DTPA in which the protein-linking functional group is located on one of the terminal carboxylate arms. Despite the superiority of these BFCA's in terms of metal ion retention, their widespread use has been limited, likely due to the complex separations involved in their synthesis and the difficulties encountered in synthetic scale up. In this report we describe a convenient and high-yield synthesis of 1B-DTPA resulting in multigram quantities of the product. This procedure was extended to the synthesis of 1-(*p*-aminobenzyl)-4-methyl-DTPA (1B4M-DTPA, 2), a recently reported (*4, 8*) modified DTPA-based BFCA.[2] We have observed improved in vitro stability and in vivo biodistribution (*9*) of radiolanthanide-labeled conjugates with 1B4M-DTPA relative to those with 1B-DTPA. Finally, we report the preparation and characterization of the chelates of these BFCA's with yttrium(III).

EXPERIMENTAL PROCEDURES

General Methods. All solvents were Fisher HPLC grade and were used without purification. Flash chromatography was performed according to the method of Still (*10*), using 230–400 mesh silica gel (Merck Grade 60, 60 Å, Aldrich Chemical Co.). Chromatographic separations were generally performed with 100:1 silica:crude product by weight. Analytical thin-layer chromatography was performed with 250-μm silica gel plates (GHLF, Analtech, Inc.). TLC plates were visualized with either 5% phosphomolybdic acid in 2-propanol or Moffitt–Lyte reagent (200 mg of ninhydrin, 100 mg of $Cu(NO_3)_2 \cdot 2.5\ H_2O$, 200 mL of ethanol, 40 mL of glacial acetic acid, and 8 mL of collidine).

† Author to whom correspondence should be addressed concerning chelating agent synthesis.

‡ Author to whom correspondence should be addressed concerning chelation chemistry.

[1] Abbreviations used: BFCA = bifunctional chelating agent, DTPA = diethylenetriaminepentaacetic acid, 1B-DTPA = 1-(*p*-aminobenzyl)-DTPA, 1B4M = 1-(*p*-aminobenzyl)-4-methyl-DTPA.

[2] The authors of the original report of this compound used the abbreviation MX-DTPA, presumably to denote the mixture of positional isomers (the DTPA backbone methyl group in either the 3- or 4-position leading to 1B3M- and 1B4M-DTPA) they reported. We find that the synthesis provides a mixture of diastereomers of only one of the positional isomers, 1B4M-DTPA (vide infra).

1043-1802/91/2902-0180$02.50/0 © 1991 American Chemical Society

Proton and carbon-13 NMR spectra were obtained on a Varian VXR-300 spectrometer operating at 300 (^{1}H) and 75 MHz (^{13}C). Chemical shifts in all solvents except D_2O are reported in ppm relative to tetramethylsilane which was used as an internal standard. Chemical shifts in D_2O are reported in ppm relative to DSS using 0.3% dioxane as an internal standard (δ_H 3.743, δ_C 69.05). Infrared spectra were recorded on either a Nicolet SSX FT/IR or a Beckmann Acculab 4 spectrometer. Fast atom bombardment mass spectra were obtained on a Vacuum Generators ZAB HS high-resolution mass spectrometer at the Analytical Sciences Laboratory, Dow Chemical Co., Midland, MI. Samples for mass spectral analysis were prepared by dissolution in a 3:1 mixture of dithiothreitol/dithioerythritol ("magic bullet"). Elemental analyses were also performed at the above location. Melting points were determined in a Thomas-Hoover melting point apparatus and are uncorrected. HPLC chromatograms were obtained on a Hewlett-Packard 1090 liquid chromatograph with a 100-mm Alltech Econosphere C18 3-μm column with a flow rate of 1 mL min^{-1} and detection at 254 nm. Samples (10-μL injections of 1 mM solutions) were eluted with a gradient of 95:5 0.05 M pH = 6.0 sodium acetate/acetonitrile to 75:25 in 10 min.

Spectral data of compounds whose preparations are described here and also reported elsewhere were in agreement.

Methyl 4-Nitrophenylalaninate Hydrochloride (4). Thionyl chloride (3.113 g, 1.91 mL, 26.2 mmol) was added under nitrogen to 25 mL of stirred anhydrous methanol in an ice bath. To this stirred solution was added 5.00 g (23.8 mmol) of solid 4-nitrophenylalanine (**3**). The cooling bath was removed and stirring was continued for an additional 19 h. Removal of the solvent at reduced pressure on a rotary evaporator afforded 6.010 g (97%) of **4** as a white solid: mp 205–209 °C dec; R_f 0.81 (12:4:1 chloroform/methanol/concentrated aqueous ammonium hydroxide); ^{1}H NMR (D_2O, pH 2.5) δ 8.22 (d, J = 12 Hz, 2 H), 7.53 (d, J = 12 Hz, 2 H), 4.54 (t, J = 6.6 Hz, 1 H), 3.83 (s, 3 H), 3.43 (dd, J = 6, 6 Hz, 2 H); ^{13}C NMR ($CDCl_3$) δ 172.0, 149.7, 144.4, 133.0, 126.6, 56.1, 56.0, 37.8.

1-[(4-Nitrophenyl)methyl]-2-oxodiethylenetriamine (5). To a stirred suspension of 6.010 g (23.1 mmol) of **4** in 100 mL of anhydrous diethyl ether and 3 mL of methanol was added 3.54 mL (2.57 g, 25.4 mmol) of triethylamine. Vigorous stirring was continued for 1 min, at which time the reaction flask was stoppered and cooled for 1 h in a refrigerator. Filtration and evaporation of the solvent at reduced pressure on a rotary evaporator gave a yellow oil which was dissolved in 5 mL of methanol. This methanolic solution was added with stirring to 45 mL (41.6 g, 692 mmol) of ethylenediamine under nitrogen and the resulting solution was stirred for an additional 19 h. Distillation of methanol and residual ethylenediamine (first 42 °C, 8 mm, then 55 °C, 1 mm) provided 5.512 g (95%) of **5** as a red-brown oil which solidified upon standing: R_f 0.48 (12:4:1 chloroform/methanol/concentrated aqueous ammonium hydroxide); ^{1}H NMR ($CDCl_3$) δ 8.16 (d, J = 8.5 Hz, 2 H), 7.58 (br s, 1 H), 7.42 (d, J = 8.5 Hz, 2 H), 3.67 (dd, J = 4.4, 8.5 Hz, 1 H), 3.42 (s, 3 H), 2.93 (dd, J = 8.5, 13.7 Hz, 1 H), 2.81 (t, J = 5.9 Hz, 2 H), 1.86 (br s, 4 H); ^{13}C NMR ($CDCl_3$) δ 173.8, 146.8, 145.8, 130.1, 123.5, 56.1, 41.6, 41.2, 40.8; IR (neat) cm^{-1} 3363, 1652, 1518, 1347.

1-[(4-Nitrophenyl)methyl]diethylenetriamine (6). A solution of 5.512 g (21.9 mmol) of **5** in 85 mL of anhydrous tetrahydrofuran was stirred under nitrogen in an ice bath as 111.4 mL (111 mmol) of a 1.0 M solution of borane–tetrahydrofuran complex in tetrahydrofuran was added. Stirring was continued for an additional 1 h at 0 °C, at which point the cooling bath was removed and the solution was heated at reflux for 17 h. The solution was once again cooled in an ice bath, and 14 mL of methanol was added. Removal of the solvent at reduced pressure on a rotary evaporator, followed by the addition of a second 14 mL of methanol and concentration, afforded an oil which was dissolved in 55 mL of ethanol. The ethanolic solution was saturated with hydrogen chloride, heated at reflux for 2 h, and cooled in a refrigerator overnight. The white precipitate was filtered, washed with cold ethanol, and dried on a vacuum line. The crude tris-amine trihydrochloride was dissolved in 25 mL of water, and the pH was adjusted to 14 (pH paper) with 50% aqueous sodium hydroxide. The aqueous solution was extracted with six 25-mL portions of chloroform, and the chloroform extracts were combined and dried ($MgSO_4$). Filtration and evaporation of the solvent at reduced pressure on a rotary evaporator gave an amber oil, which was purified by flash chromatography on silica gel using 12:4:1 chloroform/methanol/concentrated aqueous ammonium hydroxide as the eluant to provide 3.545 g (68%) of **6**: R_f 0.50 (12:4:1 chloroform/methanol/concentrated aqueous ammonium hydroxide); ^{1}H NMR ($CDCl_3$) δ 8.16 (d, J = 8.5 Hz, 2 H), 7.39 (d, J = 8.5 Hz, 2 H), 3.15 (m, 1 H), 3.0–2.6 (m, 7 H), 2.50 (dd, J = 3.5, 11.8 Hz, 1 H), 1.68 (br s, 5 H); ^{13}C NMR ($CDCl_3$) δ 147.2, 146.5, 129.9, 123.5, 55.7, 52.3, 42.4, 41.6. IR (neat) cm^{-1} 3341, 1517, 1347.

***N,N,N',N'',N''*-Pentakis[(*tert*-butoxycarbonyl)methyl]-1-[(4-nitrophenyl)methyl]diethylenetriamine (7).** A suspension of 3.174 g (13.3 mmol) of **6**, 13.770 g (70.6 mmol) of *tert*-butyl bromoacetate, and 18.409 g (133 mmol) of anhydrous potassium carbonate in 125 mL of acetonitrile was stirred for 19 h. Removal of the solvent at reduced pressure on a rotary evaporator gave a residue, which was partitioned between 100 mL of water and 100 mL of chloroform. The aqueous layer was separated and was then extracted with two 100-mL portions of chloroform. The chloroform portions were combined and dried (Na_2SO_4). Filtration and evaporation of the solvent at reduced pressure on a rotary evaporator gave an amber oil, which was purified by flash chromatography on silica gel using 25% ethyl acetate in hexane as the eluant to provide 7.606 g (71%) of **7** as a yellow oil: R_f 0.41 (25% ethyl acetate in hexane); ^{1}H NMR ($CDCl_3$) δ 8.11 (d, J = 8.8 Hz, 2 H), 7.49 (d, J = 8.8 Hz, 2 H), 3.43 (s, 4 H), 3.42 (s, 2 H), 3.41 (s, 2 H), 3.31 (s, 2 H), 3.15–2.65 (m, 8 H), 2.47 (dd, J = 8.3, 13.1 Hz, 1 H), 1.45 (s, 18 H), 1.43 (s, 27 H); ^{13}C NMR ($CDCl_3$) δ 170.99, 170.88, 170.5, 149.2, 146, 130.2, 123.1, 80.8, 80.6, 63.0, 56.3, 56.0, 53.4, 53.2, 52.4, 37.4, 28.14, 28.06; IR (neat) cm^{-1} 1738, 1520, 1346; MS (FAB) m/e 809 ([M + H$^+$]$^+$).

***N,N,N',N'',N''*-Pentakis[(*tert*-butoxycarbonyl)methyl]-1-[(4-aminophenyl)methyl]diethylenetriamine (8).** To a stirred solution of 7.606 g (9.40 mmol) of **7** in 200 mL of ethyl acetate under nitrogen was added 4.001 g (3.76 mmol) of 10% palladium on carbon. Hydrogen was then bubbled through the solution for 15 h. The reaction mixture was filtered through a pad of prewashed (ethyl acetate) Celite, and the pad was washed well with ethyl acetate. Evaporation of the filtrate at reduced pressure on a rotary evaporator gave a yellow oil, which was purified by flash chromatography on silica gel using 15% methanol in chloroform as eluant to provide 6.596 g (90%) of **8** as a yellow oil: R_f 0.27 (10% methanol in chloroform); ^{1}H NMR ($CDCl_3$) δ 6.99 (d, J = 6.0 Hz, 2 H), 6.59 (d, J = 6.0 Hz, 2 H), 3.4 (m, 10 H), 3.0 (m, 1 H),

2.86–2.58 (m, 6 H), 2.5 (m, 2 H), 1.45 (s, 36 H), 1.41 (s, 9 H); ^{13}C NMR ($CDCl_3$) δ 171.4, 170.7, 144, 131, 129.9, 115.2, 80.7, 80.6, 80.34, 80.30, 63.3, 56.2, 56.0, 55.8, 55.7, 53.6, 52.9, 52.6, 36, 28.13, 28.08; IR (neat) cm^{-1} 3500, 3400, 1737; MS (FAB) *m/e* 779 ([M + H$^+$]$^+$).

***N,N,N′,N′,N″*-Pentakis(carboxymethyl)-1-[(4-aminophenyl)methyl]diethylenetriamine Tetrahydrochloride (1B-H_5DTPA·4HCl, 1).** A solution of 5.000 g (6.42 mmol) of 8 in 50 mL of concentrated aqueous hydrochloric acid (12 M) was stirred at room temperature for 2 h and then the solvent was removed at reduced pressure on a rotary evaporator. The residue was dried overnight at 40 °C in a vacuum oven to afford 3.928 g (95%) of the tetrahydrochloride salt of 1: R_f 0.19 (2:2:1 chloroform/methanol/concentrated aqueous ammonium hydroxide); ^{1}H NMR (D_2O, pH 0) δ 7.53 (d, *J* = 8.3 Hz, 2 H), 7.46 (d, *J* = 8.3 Hz, 2 H), 4.31 (s, 4 H), 4.10–3.73 (m, 9 H), 3.56 (m, 2 H), 3.44–3.18 (m, 3 H), 2.90 (dd, *J* = 9.0, 13.6 Hz, 1 H); ^{13}C NMR ($CDCl_3$) δ 175.3, 172.9, 170.8, 139.7, 133.4, 131.3, 126.2, 64.7, 58.2, 57.8, 56.4, 55.3, 54.0, 51.8, 34.7. MS (FAB) *m/e* 499 ([M + H$^+$]$^+$). Anal. Calcd for $C_{21}H_{34}N_4O_{10}Cl_4$: C, 39.15; H, 5.32; N, 8.70. Found: C, 38.89; H, 5.17; N, 8.34.

1-[(4-Nitrophenyl)methyl]-2-oxo-4-methyldiethylenetriamine (9). To a stirred suspension of 6.173 g (23.7 mmol) of 4 in 100 mL of anhydrous diethyl ether and 3 mL of methanol was added 3.63 mL (2.64 g, 26.1 mmol) of triethylamine. Vigorous stirring was continued for 1 min, at which point the reaction flask was stoppered and cooled for 1 h in a refrigerator. Filtration and evaporation of the solvent at reduced pressure on a rotary evaporator gave a yellow oil, which was dissolved in 5 mL of methanol. This methanolic solution was added with stirring to 60 mL (52.7 g, 710 mmol) of 1,2-diaminopropane under nitrogen, and the resulting solution was stirred for an additional 18 h. Distillation of methanol and residual 1,2-diaminopropane (first 55 °C, 8 mm, then 55 °C, 2 mm) provided 5.129 g (81%) of a red-brown oil, 9, as a mixture of isomers which solidified upon standing: R_f 0.45 (12:4:1 chloroform/methanol/concentrated aqueous ammonium hydroxide); ^{1}H NMR ($CDCl_3$) δ 8.15 (d, *J* = 8.7 Hz, 2 H), 7.62 (br s, 1 H), 7.43 (d, *J* = 8.7 Hz, 2 H), 3.69 (m, 1 H), 3.36–3.20 (m, 2 H), 3.09–2.81 (m, 3 H), 1.40 (br s, 4 H), 1.06 (m, 3 H); ^{13}C NMR ($CDCl_3$) δ 173.3, 146.6, 145.8, 130.0, 123.4, 55.9, 46.6, 46.3, 46.2, 40.7, 21.5, 21.4; IR (neat) cm^{-1} 3364, 1657, 1518, 1347.

Isomer content of 9 was determined by ^{1}H NMR: (DMSO-d_6) δ 7.84 (t, *J* = 6 Hz, 1 H, major positional isomer amide N*H*), 7.6 (d, *J* = 8.1 Hz, 1 H, minor positional isomer amide N*H*), 0.97 (d, *J* = 6.6 Hz, 3 H, minor positional isomer, diastereomer 1 CH_3), 0.93 (d, *J* = 6.6 Hz, 3 H, minor positional isomer, diastereomer 2 CH_3), 0.87 (d, *J* = 6 Hz, 3 H, major positional isomer, diastereomer 1 CH_3), 0.86 (d, *J* = 6 Hz, 3 H major positional isomer, diastereomer 2 CH_3).

1-[(4-Nitrophenyl)methyl]-4-methyldiethylenetriamine (10). A solution of 4.929 g (18.5 mmol) of 9 in 75 mL of anhydrous tetrahydrofuran was stirred under nitrogen in an ice bath as 94.4 mL (94.4 mmol) of a 1.0 M solution of borane–tetrahydrofuran complex in tetrahydrofuran was added. Stirring was continued for an additional 1 h at 0 °C, at which time the cooling bath was removed, and the solution was heated at reflux for 18 h. The solution was once again cooled in an ice bath, and 15 mL of methanol was added. Removal of the solvent at reduced pressure on a rotary evaporator, followed by the addition of a second 15 mL of methanol and concentration, afforded an oil which was dissolved in 50 mL of ethanol. The ethanolic solution was saturated with hydrogen chloride and heated at reflux for 2 h. After being cooled to room temperature, the reaction mixture was treated with 4 mL of concentrated aqueous hydrochloric acid, and the mixture was cooled in a refrigerator overnight. The white precipitate was filtered, washed with cold ethanol, and dried on a vacuum line. The crude tris-amine trihydrochloride was dissolved in 20 mL of water, and the pH was adjusted to 14 (pH paper) with 50% aqueous sodium hydroxide. The aqueous solution was extracted with six 25-mL portions of chloroform, and the chloroform extracts were combined and dried ($MgSO_4$). Filtration and evaporation of the solvent at reduced pressure on a rotary evaporator gave an amber oil, which was purified by flash chromatography on silica gel using 12:4:1 chloroform/methanol/concentrated aqueous ammonium hydroxide as the eluant to provide 3.192 g (68%) of 10 as a mixture of isomers: R_f 0.43 (12:4:1 chloroform/methanol/concentrated aqueous ammonium hydroxide). ^{1}H NMR ($CDCl_3$) δ 8.16 (d, *J* = 8.7 Hz, 2 H), 7.39 (d, *J* = 8.7 Hz, 2 H), 3.14 (m, 1 H), 3.03–2.86 (m, 2 H), 2.76–2.31 (m, 5 H), 1.82 (br s, 5 H), 1.06 (m, 3 H); ^{13}C NMR ($CDCl_3$) δ 147.2, 146.5, 129.9, 123.5, 58.2, 58.0, 55.9, 55.8, 52.4, 52.2, 46.6, 46.4, 42.33, 42.29, 21.84, 21.77; IR (neat) cm^{-1} 3355, 1516, 1345.

***N,N,N′,N′,N″*-Pentakis[(*tert*-butoxycarbonyl)methyl]-1-[(4-nitrophenyl)methyl]-4-methyldiethylenetriamine (11).** A suspension of 3.084 g (12.2 mmol) of 10, 12.636 g (64.8 mmol) of *tert*-butyl bromoacetate, and 16.893 g (122 mmol) of anhydrous potassium carbonate in 125 mL of acetonitrile was stirred for 24 h. Removal of the solvent at reduced pressure on a rotary evaporator gave a residue which was partitioned between 100 mL of water and 100 mL of chloroform. The aqueous layer was separated and was extracted with two 100-mL portions of chloroform. The chloroform portions were combined and dried (Na_2SO_4). Filtration and evaporation of the solvent at reduced pressure on a rotary evaporator gave an amber oil, which was purified by flash chromatography on silica gel using 25% ethyl acetate in hexane as the eluant to provide 6.813 g (68%) of a yellow oil, 11, as a mixture of isomers: R_f 0.43 (25% ethyl acetate in hexane); ^{1}H NMR ($CDCl_3$) δ 8.11 (d, *J* = 8.8 Hz, 2 H), 7.49 (d, *J* = 8.8 Hz, 2 H), 3.46–3.28 (m, 10 H), 3.22–2.74 (m, 6 H), 2.52–2.29 (m, 2 H), 1.43 (m, 45 H), 1.06 (m, 3 H); ^{13}C NMR ($CDCl_3$) δ 171.43, 171.38, 171.0, 170.9, 149.1, 146.3, 130.3, 130.2, 123.2, 80.7, 80.64, 80.55, 80.49, 62.9, 62.8, 60.3, 59.9, 59.5, 56.9, 56.7, 56.0, 55.8, 53.19, 53.16, 37.4, 37.2, 28.2, 28.10, 28.06, 27.9, 27.8, 15.8, 15.7, 14.2; IR (neat) cm^{-1} 1738, 1520, 1346; MS (FAB) *m/e* 823 ([M + H$^+$]$^+$).

***N,N,N′,N′,N″*-Pentakis[(*tert*-butoxycarbonyl)methyl]-1-[(4-aminophenyl)methyl]-4-methyldiethylenetriamine (12).** To a stirred solution of 6.702 g (8.14 mmol) of 11 in 125 mL of ethyl acetate under nitrogen was added 3.466 g (3.26 mmol) of 10% palladium on carbon. Hydrogen was then bubbled through the solution for 4 h. The reaction mixture was filtered through a pad of prewashed (ethyl acetate) Celite and the pad was washed well with ethyl acetate. Evaporation of the filtrate at reduced pressure on a rotary evaporator gave a green oil, which was purified by flash chromatography on silica gel using 15% methanol in chloroform as eluant to provide 5.729 g (89%) of a green oil, 12, as a mixture of isomers: R_f 0.23 (10% methanol in chloroform); ^{1}H NMR ($CDCl_3$) δ 6.98 (m, 2 H), 6.59 (d, *J* = 7.3 Hz, 2 H), 3.55–3.10 (m, 10 H), 3.10–2.20 (m, 8 H), 1.45 (m, 45 H), 1.04 (m, 3 H); ^{13}C NMR ($CDCl_3$) δ 171.4, 171.3, 171.2, 144.2, 130.2, 130.1, 129.9, 129.66, 129.62, 115.4, 115.1, 63.5, 63.4, 59.2, 56.7,

56.4, 56.3, 56.2, 56.1, 55.9, 55.8, 53.74, 53.65, 53.4, 53.1, 36.8, 36.7, 36.6, 36.5, 36.35, 36.28, 36.22, 36.18, 36.11, 36.08, 35.92, 35.86, 35.8, 35.7, 28.0, 16.05, 16.02, 15.97, 15.8, 15.7; IR (neat) cm^{-1} 3380, 1735; MS (FAB) m/e 794 ($[M + H^+]^+$).

***N,N,N',N'',N''*-Pentakis(carboxymethyl)-1-[(4-aminophenyl)methyl]-4-methyldiethylenetriamine Tetrahydrochloride (1B4M-H_5DTPA·4HCl, 2).** A solution of 5.650 g (7.12 mmol) of 12 in 75 mL of concentrated aqueous hydrochloric acid (12 M) was stirred at room temperature for 3 h and then the solvent was removed at reduced pressure on a rotary evaporator. The residue was dried overnight at 40 °C in a vacuum oven to afford 4.540 g (97%) of the tetrahydrochloride salt of 2 as a mixture of isomers: R_f 0.21 (2:2:1 chloroform/methanol/concentrated aqueous ammonium hydroxide); ^1H NMR (D_2O, pH 0) δ 7.49 (m, 4 H), 4.4–3.6 (m, 12 H), 3.48–2.88 (m, 6 H), 1.34 (m, 3 H); ^{13}C NMR ($CDCl_3$) δ 174.2, 174.0, 173.5, 172.3, 139.3, 139.1, 133.4, 133.3, 131.3, 131.2, 126.1, 66.2, 65.4, 61.6, 60.8, 58.5, 58.3, 57.0, 56.7, 56.0, 55.4, 55.2, 54.9, 54.7, 34.7, 34.6, 14.0, 13.8; MS (FAB) m/e 513 ($[M + H^+]^+$). Anal. Calcd for $C_{22}H_{36}N_4O_{10}Cl_4$: C, 40.14; H, 5.51; N, 8.51. Found: C, 39.62; H, 5.46; N, 8.19.

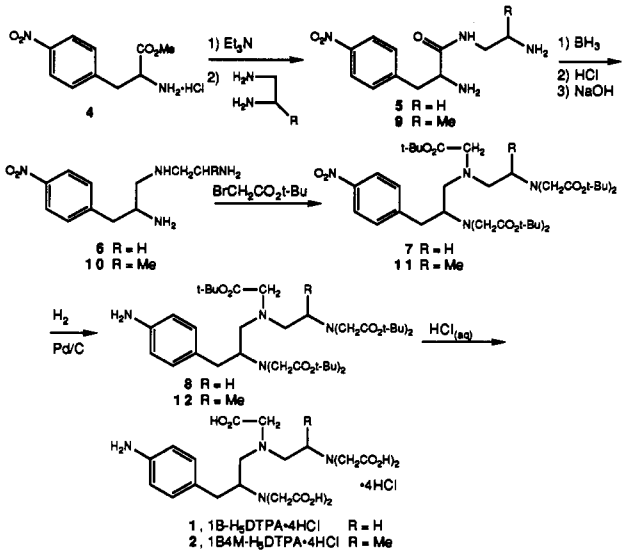
Na_2[Y(1B-DTPA)]·$2H_2O$. An aqueous (20 mL) solution of yttrium chloride hexahydrate (261.5 mg, 0.862 mmol) was added to an aqueous solution (45 mL) of 1B-H_5DTPA·4HCl (1, 504.3 mg, 0.782 mmol), producing a solution with a pH of 1.67. The pH of the solution was increased slowly (over a period of 0.5 h) by the dropwise addition of 0.1 M NaOH to the rapidly stirring mixture until the pH was 6.0. The solvent was removed from the crude reaction mixture by rotary evaporation.

Sodium chloride was removed from the crude product by gel-filtration chromatography. A glass column (25 × 550 mm) equipped with a coarse frit and Teflon stopcock at the bottom was packed with Pharmacia Sephadex G-10 resin (bead size 40–120 μm, 120 g of dry resin swelled in distilled water). The chelate was dissolved in 5 mL of distilled water and eluted from the column with distilled water. A constant flow rate was maintained through the column with a Gilson Minipuls peristaltic pump (flow rate ca. 3–4 mL min^{-1}). The eluent was monitored at 254 nm (Isco Model UA-5 ultraviolet detector) for the presence of chelate. The presence of NaCl (following the chelate) was detected by a positive AgCl test (several drops of eluent were added to a $AgNO_3$ solution). Sodium chloride free chelate solution was reduced to dryness on a rotary evaporator.

The product was dried overnight in a vacuum oven at 70 °C to produce 443 mg (90.1%) of the yellow glassy product as a mixture of isomers: R_f 0.78 (2:2:1 chloroform/methanol/concentrated aqueous ammonium hydroxide); ^1H NMR (D_2O) δ 7.15–6.83 (m, 4 H), 4.18–1.92 (m, 19 H); ^{13}C NMR (D_2O) δ 184.75, 184.60, 184.26, 183.98, 183.64, 183.44, 183.30, 183.23, 182.98, 145.55, 145.47, 133.15, 133.03, 132.83, 120.31, 120.18, 68.83, 68.33, 67.13, 66.41, 65.80, 65.66, 65.51, 64.80, 63.78, 63.48, 60.84, 60.50, 58.84, 58.08, 57.12, 56.65, 34.52, 32.78; MS (FAB) m/e 607 ($[M^{2-} + 2 H^+ + Na^+]^+$), 629 ($[M^{2-} + H^+ + 2 Na^+]^+$), 605 ($[M^{2-} + Na^+]^-$). Anal. Calcd for $C_{21}H_{25}N_4Na_2O_{10}Y·2H_2O$: C, 37.97; H, 4.40; N, 8.43. Found: C, 38.34; H, 4.00; N, 8.28.

Na_2[Y(1B4M-DTPA)]·H_2O. The procedure was the same as that described for Na_2[Y(1B-DTPA)] except that a solution of yttrium chloride hexahydrate (272.1 mg, 0.897 mmol) in water (15 mL) was added to a solution of 1B4M-H_5DTPA·4HCl (2, 504.4 mg, 0.766 mmol) in distilled water (30 mL), producing a solution with a pH of 1.3. The product obtained after gel-filtration chromatography was dried overnight in a vacuum oven at 70 °C to produce 423 mg (92.6%) of the yellow glassy product as a mixture of isomers: R_f 0.79 (2:2:1 chloroform/methanol/concentrated aqueous ammonium hydroxide); ^1H NMR (D_2O) δ 7.20–6.83 (m, 4 H), 4.11–1.83 (m, 18 H), 1.01–0.84 (3 overlapping doublets, 3 H, 0.97 [J = 6.1 Hz], 0.93 [J = 5.8 Hz], 0.87 [J = 6.1 Hz]); ^{13}C NMR (D_2O) δ 184.82, 184.54, 184.21, 184.18, 184.07, 183.65, 183.43, 183.35, 183.17, 182.90, 182.83, 144.82, 144.69, 144.62, 133.72, 133.62, 133.52, 132.90, 132.83, 120.65, 120.58, 120.48, 68.97, 68.67, 67.12, 66.78, 66.68, 66.50, 65.89, 65.73, 65.44, 65.30, 64.39, 64.18, 63.89, 63.72, 63.28, 62.50, 59.26, 59.13, 58.14, 57.16, 56.73, 56.23, 55.96, 55.78, 55.69, 34.51, 33.75, 32.83, 13.29, 12.40, 11.82; MS (FAB) m/e 621 ($[M^{2-} + 2 H^+ + Na^+]^+$), 643 ($[M^{2-} + H^+ + 2 Na^+]^+$), 665 ($[M^{2-} + 3 Na^+]^+$, 619 ($[M^{2-} + Na^+]^-$). Anal. Calcd for $C_{22}H_{27}N_4Na_2O_{10}Y·H_2O$: C, 40.01; H, 4.43; N, 8.48. Found: C, 39.82; H, 4.24; N, 8.20.

Scheme I



RESULTS AND DISCUSSION

BFCA Syntheses. The carboxymethylation step was the main concern with respect to scaling up the literature method for the synthesis of 1B-DTPA. In the published procedures (*3*, *8*), the only product purification was carried out after reaction of 6 or 10 with bromoacetic acid. The highly polar 1-(*p*-nitrobenzyl)pentaacid produced at this stage required anion-exchange chromatography, an HPLC separation, and finally a second ion-exchange chromatography for purification. This procedure limited the amount of the pentaacid which could be produced in a single synthesis. The use of bromoacetate esters as carboxymethyl synthons appeared quite applicable to this problem. The resulting pentaester was amenable to large-scale chromatography on normal-phase silica gel, allowing for purification of intermediates up to the final step. The synthesis (Scheme I), while one step longer than that previously reported, offered significant advantages in light of our desire for a reproducible multigram synthetic route.

Commercially available 4-nitrophenylalanine (3) was converted in 97% crude yield to the methyl ester hydrochloride 4 by the procedure of Brenner and Huber (*11*), using thionyl chloride in methanol. Elaboration of 4 to 7 was accomplished as previously described (*3*, *8*). Alkylation with *tert*-butyl bromoacetate provided a 71% yield of chromatographed 7. Catalytic hydrogenation with Pd/C in ethyl acetate provided 8 (*12*) in 90% yield after chromatography. Cleavage of the *tert*-butyl esters with aqueous hydrochloric acid provided a quantitative yield of the tetrahydrochloride salt of 1B-DTPA (1).

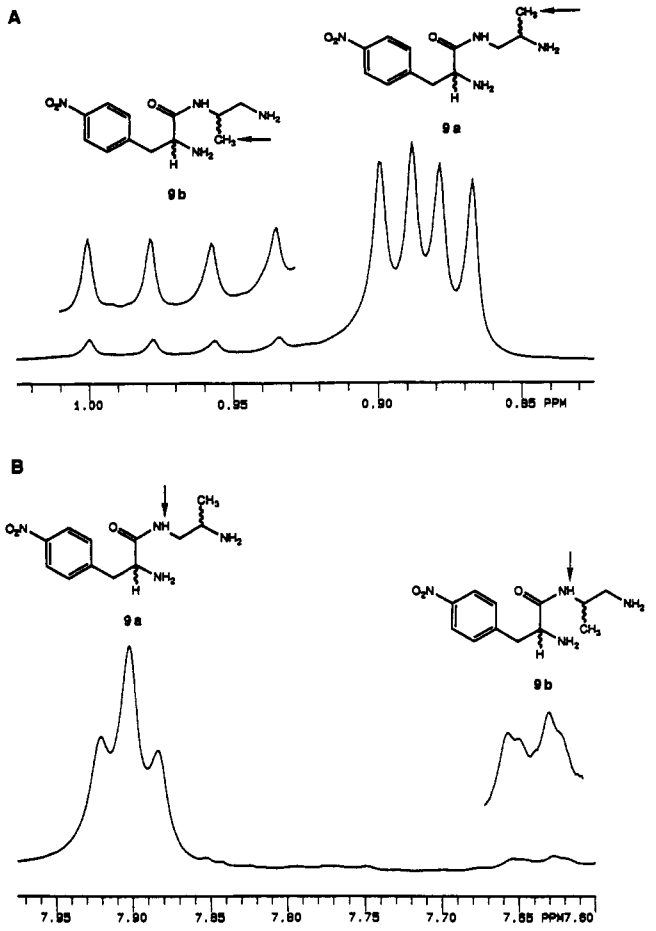


Figure 1. The (A) methyl and (B) amide portions of the ^1H NMR (DMSO-d_6) spectrum of the products of the reaction of methyl 4-nitrophenylalaninate with 1,2-diaminopropane.

As mentioned, a drawback to the use of bromoacetate esters as carboxymethylating agents is that an ester hydrolysis step was added to the synthesis. However, since hydrogenation of the nitro group to the aniline would also be required, an ester which would be cleaved under these reducing conditions would combine both transformations and eliminate the extra deprotection step. The obvious choice was the readily hydrogenolyzed benzyl ester. Unfortunately, a very low yield of the desired pentaester was obtained from the reaction of **6** with benzyl bromoacetate. Large amounts of benzyl alcohol were detected, suggesting amide or lactam formation. The attempt to combine the hydrogenation and deprotection steps was therefore abandoned.

The proposed synthesis of 1B4M-DTPA (Scheme I) was virtually identical with that of 1B-DTPA, with the exception that 1,2-diaminopropane was used instead of ethylenediamine in the condensation with 4-nitrophenylalanine. The questions to be addressed here were those of the stereochemistry of the new methyl group and the determination of isomer ratios.

The reaction of ester hydrochloride **4** (as its free base) with 1,2-diaminopropane provided an 81% yield of **9** as a mixture of isomers. Depending on which end of the diamine attacked the ester, two positional isomers could be formed. In addition, the two chiral centers present in **9** could result in a pair of diastereomers for each pair of positional isomers, leading to a possible total of four isomers (and their enantiomers). While one would not anticipate any significant kinetic selectivity in diastereomer formation for a given positional isomer, it does not seem unreasonable to expect a kinetic effect in the formation of the positional isomer mixture, in which the amine adjacent to the primary carbon would react preferentially to the amine adjacent to the secondary carbon. In the reported synthesis of 1B4M-DTPA (*8*), which at this stage is identical with ours, the isomeric composition of **9** was not determined. The issue of stereochemistry was instead addressed in a model study in which methyl glycine was condensed with 1,2-diaminopropane, and no preference for either end of the diamine was reported. This result led those workers to conclude that no selectivity should be expected for the more sterically hindered **4**. In our hands, close inspection of the 300-MHz ^1H NMR spectrum of **9** (Figure 1) showed four sets of doublets for the methyl group, two major and two minor, in a ratio of 84:16. The two major sets of doublets were in a 1:1 ratio, as were the two minor sets. On the basis of an assumed steric preference for reaction of the amine adjacent to the primary carbon, the major two sets of doublets were assigned to the two diastereomers of the positional isomer with the methyl next to the terminal amino group (**9a**), while the minor two sets of doublets were assigned to the other positional isomer (**9b**). This assignment is supported by examination of the two amide N*H* signals which were detected in the ^1H NMR spectrum obtained in DMSO-d_6 (Figure 1b). Again, there are two sets of peaks, a large triplet (amide connected to a methylene carbon) and a small doublet (amide connected to methine carbon).[3] These amide resonances were also in a ratio of 84:16. These data indicate that **9** is an 84:16 mixture of the methyl positional isomers **9a** and **9b**, with isomer **9a** predominating, and that each of these positional isomers is a 1:1 mixture of diastereomers.

With the isomeric composition established, the remainder of the synthesis was carried out. Borane reduction gave **10** in 68% yield after chromatography. Carboxymethylation with *tert*-butyl bromoacetate afforded a 68% yield of chromatographed **11**, which upon hydrogenation provided **12** in 89% purified yield. Acidic hydrolysis provided a 97% yield of the tetrahydrochloride salt of 1B4M-DTPA (**2**). For each of these compounds a mixture of isomers was observed, although the separation of the proton NMR resonances for the various isomers was never as clear as in the case of **9**. Also noteworthy is that there were small differences in chromatographic mobility of the various isomers so that minor losses of material on the column led to changes in the isomer ratio after each chromatography. Judging from the ^1H NMR spectrum of the final product, 1B4M-DTPA, the two diastereomers of the major positional isomer were in a 2:3 ratio (formerly 1:1 in **9**). The resonances for the minor positional isomer were not detected, indicating its removal during chromatographic purification.

Methods for the conversion of these BFCA's to the corresponding isothiocyanato compounds and subsequent conjugation to protein have been described in detail elsewhere (*3*, *13*).

Chelate Syntheses. Chelation of yttrium(III) was rapid at pH 6 and room temperature as determined by comparison of starting ligand to reaction mixtures by thin-layer chromatography and HPLC. Analytically pure samples of the chelates were obtained from the reaction

[3]The NMR spectrum presented in Figure 1 was obtained from the crude reaction product. The doublet assigned to compound **9b** was more readily apparent after chromatographic purification. However, we have chosen to present the NMR spectrum of the crude product to avoid any ambiguities in the isomer ratio resulting from purification.

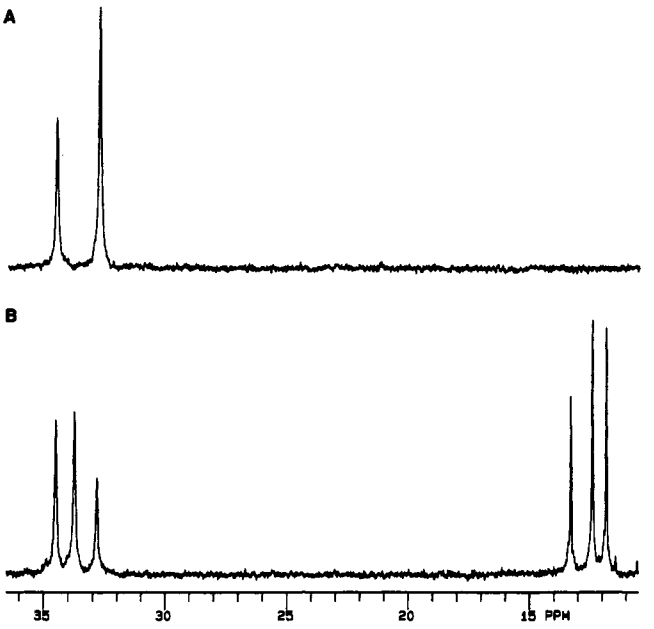


Figure 2. Portions of the ^{13}C NMR spectra of (A) Na_2[Y(1B-DTPA)] and (B) Na_2[Y(1B4M-DTPA)].

of the metal chlorides with the HCl salts of the ligands by raising the reaction solution pH to near neutral with NaOH. The chelates were easily separated from NaCl generated in the reaction mixtures by gel-filtration chromatography. The chelates were also prepared by the reaction of the metal acetates with the HCl salts of the ligands by raising the reaction solution pH with NH_4OH, followed by removal of ammonium acetate by sublimation. These materials were not further purified, but were characterized by comparison with authentic samples by HPLC and fast atom bombardment mass spectroscopy.

Recently, Maecke et al. (*14*) reported the X-ray structural characterization of Na_2[In(DTPA)] and ^{13}C NMR spectra of both the indium(III) and yttrium(III) chelates. They concluded that DTPA forms an octadentate 1:1 chelate with both metal ions (all the carboxylate groups bound to the metal ion). The formation of 1:1 chelates is substantiated here by our fast atom bombardment mass spectroscopy results.

The BFCA 1B-DTPA contains one chiral center at the carbon bound to the benzyl group. Coordination of a metal ion generates a second chiral center at the central nitrogen of the BFCA thereby producing two diastereomers. Due to the absence of a plane of symmetry in $[Y(1B\text{-}DTPA)]^{2-}$, all of the carbon atoms are nonequivalent in the ^{13}C NMR spectrum. The number of peaks observed was consistent with two diastereomers. In particular, two *p*-aminobenzylic CH_2 peaks were observed (Figure 2) at δ 32.76 and 34.50 ppm in a 63:37 ratio. The HPLC chromatogram (Figure 3) also contained two peaks in a ratio of 60:40. Similar HPLC results were obtained upon injection of buffered 1B-DTPA solutions containing an excess of yttrium(III) ion. The unequal ratio of diastereomers observed indicates a modest stereoselectivity in the chelation reaction. Chelation reactions with other lanthanide ions yielded comparable results.

On the basis of the presence of two diastereomers of 1B4M-DTPA (in a 60:40 ratio; vide supra) and the creation of a third chiral center (the central nitrogen) upon coordination of yttrium(III) we expected to observe four diastereomers of $[Y(1B4M\text{-}DTPA)]^{2-}$. Three diastereomers were observed by ^1H and ^{13}C NMR spectroscopy. In the ^1H NMR, three doublets due to the methyl groups on

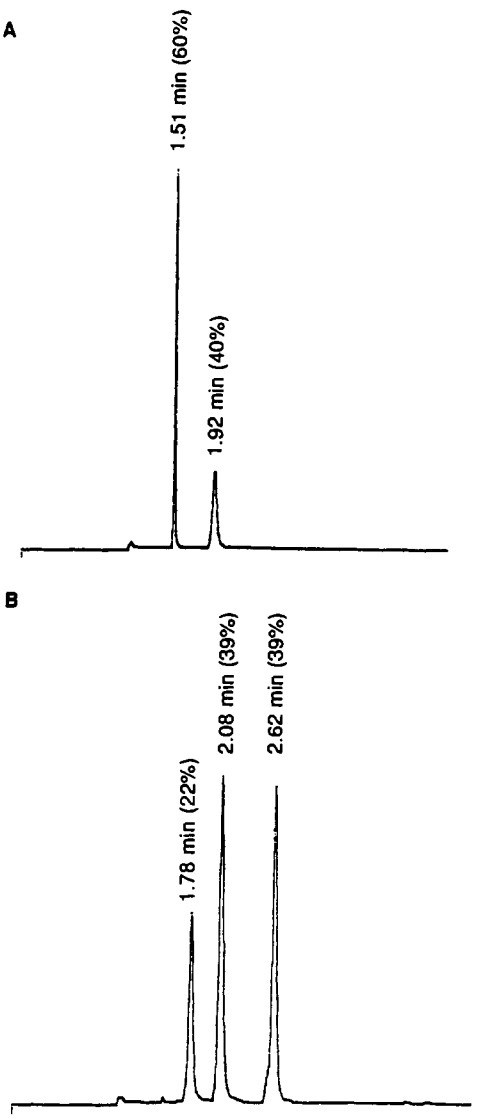


Figure 3. HPLC chromatograms of (A) Na_2[Y(1B-DTPA)] and (B) Na_2[Y(1B4M-DTPA)].

the DTPA backbone at δ 1.01–0.84 were observed. In the ^{13}C NMR (Figure 2), the three *p*-aminobenzylic CH_2 carbons were observed at δ 32.82, 33.73, and 34.49 ppm in a 22:40:38 ratio. Furthermore, the peaks due to the carbon atoms of the methyl groups substituted on the DTPA backbone were observed at δ 11.81, 12.39, and 13.28 ppm in a 35:40:25 ratio. The number of peaks in the remainder of the ^{13}C NMR spectrum were consistent with the presence of no more than three diastereomers. The HPLC chromatogram of $[Y(1B4M\text{-}DTPA)]^{2-}$ (Figure 3) contained three peaks in a ratio of 22:39:39. Changes in the gradient which increased the sample retention time failed to reveal a fourth peak. Similar HPLC results were obtained upon injection of buffered 1B4M-DTPA solutions containing an excess of yttrium(III) ion, thus discounting the possibility of the loss of a diastereomer upon purification and isolation of the chelate sample. Similar NMR and HPLC results were obtained with other lanthanide ions.

The failure to observe any evidence of a fourth chelate diastereomer can be explained by coincidental overlap of two diastereomers in the NMR spectroscopy and HPLC. Alternatively, stereospecific chelation of one of the ligand diastereomers with lanthanide metal ion may occur. We have no evidence to support either of these possibilities.

CONCLUSION

The BFCA's 1B-DTPA (1) and 1B4M-DTPA (2) were prepared in six-step syntheses in overall yields of 38% and 31%, respectively. A major advantage of the synthesis described here is the use of bromoacetate ester for alkylation, thereby allowing large-scale flash chromatographic purification of reaction products. In particular, chromatography of the final intermediate allows the preparation of the product chelating agent free of both organic and inorganic contaminants. The preparation of 1B4M-DTPA was stereoselective and in our hands did not result in a mixture of positional isomers, as reported previously (*4*, *8*), but did result in a mixture of diastereomers. Chelation of yttrium(III) with both 1B-DTPA and 1B4M-DTPA produced 1:1 chelates as mixtures of diastereomers.

LITERATURE CITED

(1) Hnatowich, D. J., Layne, W. W., Childs, R. L., Lanteigne, D., Davis, M. A., Griffin, T. W., and Doherty, P. W. (1983) Radioactive Labeling of Antibody: A Simple and Efficient Method. *Science 220*, 613–615.

(2) Krejcarek, G. E., and Tucker, K. L. (1977) Covalent Attachment of Chelating Groups to Macromolecules. *Biochem. Biophys. Res. Commun. 77*, 581–585.

(3) Brechbiel, M. W., Gansow, O. A., Atcher, R. W., Schlom, J., Esteban, J., Simpson, D. E., and Colcher, D. (1986) Synthesis of 1-(*p*-Isothiocyanatobenzyl) Derivatives of DTPA and EDTA. Antibody Labeling and Tumor-Imaging Studies. *Inorg. Chem. 25*, 2772–2781.

(4) Kozak, R. W., Raubitschek, A., Mirzadeh, S., Brechbiel, M. W., Junghaus, R., Gansow, O. A., and Waldmann, T. A. (1989) Nature of the Bifunctional Chelating Agent Used for Radioimmunotherapy with Yttrium-90 Monoclonal Antibodies: Critical Factors in Determining in Vivo Survival and Organ Toxicity. *Cancer Res. 49*, 2639–2644.

(5) Roselli, M., Schlom, J., Gansow, O. A., Raubitschek, A., Mirzadeh, S., Brechbiel, M. W., and Colcher, D. (1989) Comparative Biodistributions of Yttrium- and Indium-Labeled Monoclonal Antibody B72.3 in Athymic Mice Bearing Human Colon Carcinoma Xenografts. *J. Nucl. Med. 30*, 672–682.

(6) Westerberg, D. A., Carney, P. L., Rogers, P. E., Kline, S. J., and Johnson, D. K. (1989) Synthesis of Novel Bifunctional Chelators and Their Use in Preparing Monoclonal Antibody Conjugates for Tumor Targeting. *J. Med. Chem. 32*, 236–243.

(7) Keana, J. F. W., and Mann, J. S. (1990) Chelating Ligands Functionalized for Facile Attachment to Biomolecules. A Convenient Route to 4-Isothiocyanatobenzyl Derivatives of Diethylenetriaminepentaacetic Acid and Ethylenediaminetetraacetic Acid. *J. Org. Chem. 55*, 2868–2871.

(8) Brechbiel, M. W. (1988) New Bifunctional Chelates for Radioimmunoimaging and Therapy. Ph.D. Thesis, The American University, Washington, DC.

(9) Unpublished results.

(10) Still, W. C., Kahn, M., and Mitra, A. (1978) Rapid Chromatographic Technique for Preparative Separations with Moderate Resolution. *J. Org. Chem. 43*, 2923–2925.

(11) Brenner, M., and Huber, W. (1953) *Helv. Chim. Acta. 36*, 1109–1115.

(12) Liberatore, F. A., Comeau, R. D., McKearin, J. M., Pearson, D. A., Belonga, B. Q., III, Brocchini, S. J., Kath, J., Phillips, T., Oswell, K., and Lawton, R. G. (1990) Site-Directed Chemical Modification and Cross-Linking of a Monoclonal Antibody Using Equilibrium Transfer Alkylating Cross-Link Reagents. *Bioconjugate Chem. 1*, 36–50.

(13) Mirzadeh, S., Brechbiel, M. W., Atcher, R. W., and Gansow, O. A. (1990) Radiometal Labeling of Immunoproteins: Covalent Linkage of 2-(4-Isothiocyanatobenzyl)diethylenetriaminepentaacetic Acid Ligands to Immunoglobulin. *Bioconjugate Chem. 1*, 59–65.

(14) Maecke, H. R., Riesen, A., and Ritter, W. (1989) The Molecular Structure of Indium–DTPA. *J. Nucl. Med. 30*, 1235–1239.

Registry No. 1, 133097-22-0; (*R**,*R**)-2, 132979-68-1; (*R**,*S**)-2, 132979-67-0; 3, 2922-40-9; 4, 108450-75-5; 5, 133097-23-1; 6, 133097-24-2; 7, 132979-69-2; 8, 132979-70-5; (*R**,*R**)-9a, 132979-71-6; (*R**,*S**)-9a, 132979-72-7; (*R**,*R**)-9b, 132979-73-8; (*R**,*S**)-9b, 132979-74-9; (*R**,*R**)-10, 132979-75-0; (*R**,*S**)-10, 132979-76-1; (*R**,*R**)-11, 132979-77-2; (*R**,*S**)-11, 132979-78-3; (*R**,*R**)-12, 132979-79-4; (*R**,*S**)-12, 132979-80-7; $H_2NCH_2CH_2NH_2$, 107-15-3; $H_2NCH_2CH(CH_3)NH_2$, 78-90-0; $BrCH_2CO_2t$-Bu, 5292-43-3; Na_2[Y(1B-DTPA)] (isomer 1), 132979-81-8; Na_2[Y(1B-DTPA)] (isomer 2), 133070-97-0; Na_2[Y(1B4M-DTPA)], 132979-82-9.

Backbone-Substituted DTPA Ligands for ^{90}Y Radioimmunotherapy

Martin W. Brechbiel* and Otto A. Gansow*

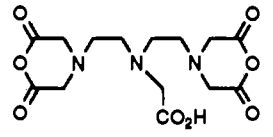
Chemistry Section, Radiation Oncology Branch, National Cancer Institute, National Institutes of Health, Bethesda, Maryland 20892. Received November 12, 1990

Four new bifunctional diethylenetriaminepentaacetic acid (DTPA) ligands were synthesized to provide an improved chelating agent for radioimmunotherapy with ^{90}Y. The new DTPA ligands contained a 4-isothiocyanatobenzyl group (pSCNBz) substituted onto the carbon backbone of DTPA for use in linkage to immunoprotein. Methyl groups were strategically incorporated onto the backbone of the ligands via a peptide route to provide 2-pSCNBz-5-Me-DTPA (2) and 3-Me-6-pSCNBz-DTPA (3). Addition of these functionalities was expected to sterically hinder the release of radiometal from the chelate. A new monosubstituted ligand, 3-pSCNBz-DTPA (4), was also prepared in order to determine whether a shift in position of the linking group had an effect on the in vivo stability of the yttrium complex. Additionally, by modification of known methods, a disubstituted DTPA ligand, 2-pSCNBz-6-Me-DTPA (1), was prepared.

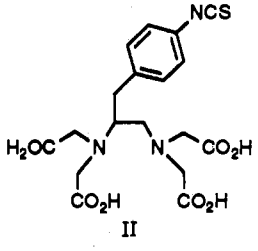
INTRODUCTION

The radiolabeling of monoclonal antibodies for radioimmunoimaging (RII)[1] and RIT is receiving increasing attention (*1–4*). Isotopes of iodine are currently being exploited primarily due to the convenience of protein halogenation (*5, 6*). However, their less than optimal physical characteristics and half-lives together with problems arising from in vivo dehalogenation (*7*) limit the usefulness of ^{131}I or ^{125}I in RIT applications (*8, 9*). ^{123}I possesses many favorable attributes for RII, but lack of availability continues as a limiting factor.

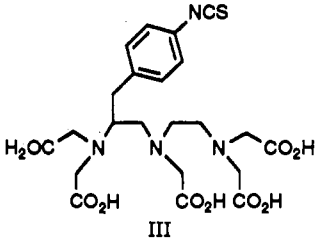
Metallic radionuclide complexes of ligands I–III have been used to expand the available choices of radionuclides



I



II



III

with both suitable emission characteristics and half-lives. We have previously reported (*10, 11*) that use of ligand III conjugated to mAb B72.3 and labeled with ^{111}In or ^{90}Y was superior both in tumor imaging and in biodistribution to the frequently used I, CA-DTPA, as well as EDTA analogue II. These results were attributed to the ability of an octadentate ligand III to maximize the in vivo stability of the indium complex. This view is strongly supported by the recent observation that the coordination number of indium in the [In(DTPA)$^{2-}$] complex is indeed eight (*12*). It has been a long-accepted tenet of coordination chemistry that the most stable complexes are formed when the coordination number of the metal is fully saturated by ligands (*13–15*).

A primary concern in the use of chelates linked to mAb for therapy is that undesirable localizations in vivo of free radiometal could occur from metal complex dissociation or transchelation. This would be an especially acute problem for ^{90}Y, which is often proposed for use in RIT (*16, 17*), since the principal biological site of yttrium deposition is the cortex of the bone (*18, 19*). Should ^{90}Y be released from the chelate and transported to the bone, radiosensitive marrow could be damaged.

Clinical reports have described the failure of CA-DTPA as a ligand for ^{90}Y RIT in that the isotope was released from the mAb conjugate and deposited on the bone (*20*). We did not initially attempt to employ II since very early studies had indicated that [Y(EDTA)]$^{1-}$ dissociated in vivo (*21*) and was in fact an excellent reagent for selective delivery of yttrium to bone surfaces (*22*).

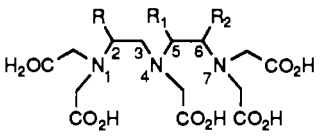
Herein we continue our studies of acyclic ligands to examine the importance of ligand structure features for retarding the release of yttrium in vivo. Eight is a common coordination number for Y(III) (*15*), so we initially employed the octadentate bifunctional DTPA ligand III. Recent biodistribution studies (*11, 23*) with ^{88}Y–III–B72.3 and ^{88}Y–III–α-TAC confirmed that its use markedly lowered bone dose compared to similar radioimmunoconjugates formed with I or II. However, even for protein conjugates of III, the ^{88}Y %ID/g in bone was measured to be higher than that seen when ^{111}In or ^{131}I were used in comparable experiments (*11*). Thus, our reported ^{111}In %ID/g bone result was set as a target to be reached for obtaining a DTPA ligand suitable for RIT with ^{90}Y.

We therefore have attempted to further improve the stability of the complex by addition of a methyl substituent on the ligand III carbon backbone along with the 4-nitrobenzyl group as pictured in 1–4. Such methyl substituents have been observed to increase EDTA complex stabilities (*24*). Since alkylation of diethylenetriamine (dien) to obtain a DTPA is facile, preparations of the desired ligands reduced to the synthesis of the appropriate dien intermediate. The only reasonable modification of our original synthesis of III to produce the target compounds is the substitution of 1,2-diaminopropane for 1,2-ethylenediamine in the aminolysis of methyl 4-nitrophe-

* Address for correspondence: National Institutes of Health, Building 10, Rm. B3B69, Bethesda, MD 20892.

[1] Abbreviations: BOC, *tert*-butyloxycarbonyl; CA-DTPA, DTPA dianhydride; DCC, 1,3-dicyclohexylcarbodiimide; DCU, 1,3-dicyclohexylurea; HOBT, *N*-hydroxybenzotriazole; mAb, monoclonal antibody; RIA, radioimmunoassay; RII, radioimmunoimaging; RIT, radioimmunotherapy; TFA, trifluoroacetic acid.

Not subject to U.S. Copyright. Published 1991 by American Chemical Society



1: R = 4-NCS-Bz, R_1 = H, R_2 = Me
2: R = 4-NCS-Bz, R_1 = Me, R_2 = H
3: R = Me, R_1 = 4-NCS-Bz, R_2 = H
4: R = H, R_1 = 4-NCS-Bz, R_2 = H

nylalaninate, followed by borane reduction of the resulting amino amide to give principally the dien precursor to 1 (Scheme I). We had previously reported the DTPA produced from this triamine to be "MX-DTPA", a mixture of geometric isomers (*23*, *25*), which is now recognized to be >95% 1 (vide infra) (*26*).

To obtain pure samples of methyl-substituted 4-isothiocyanatobenzyl-DTPA ligands **2** and **3**, a peptide synthesis route to the triamines was developed (Scheme II). The requisite blocked dipeptide amides **9** and **13** were prepared from commercially available precursors by diimide coupling reactions. Deprotection and amide reduction yielded the diens **10** and **14** from which **2** and **3** were obtained by well-described methods. This methodology also allowed us to investigate the importance of having the benzyl substituent in the C-2 vs the C-3 position by providing a synthesis of **4** from amino amide **17**. All ligands were synthesized both with natural carbon and with ^{14}C-labeled bromoacetate to allow precise quantitation of the number of ligands linked to proteins.

This report provides details of the syntheses of the target ligands. An earlier study reported on the in vivo stability of ^{88}Y–ligand–mAb conjugates of these ligands in normal mice in a set of dual label (^{131}I) experiments (*23*).

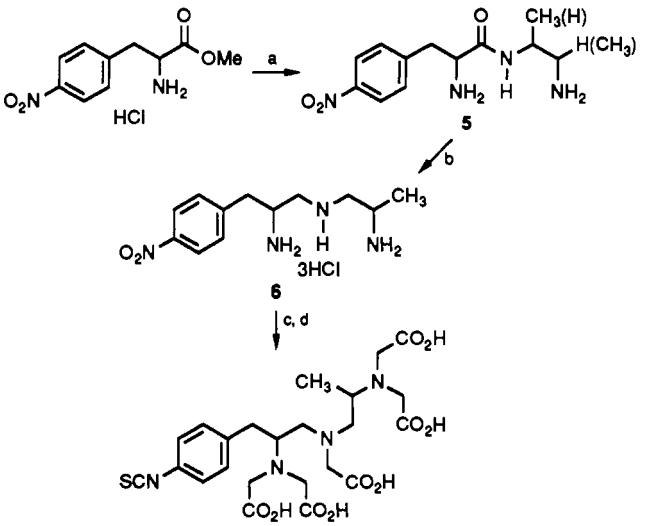
EXPERIMENTAL PROCEDURES

Materials and Methods. 4-Nitrophenylalanine (Aldrich/U.S. Biochemical) and diborane (1 M BH_3·THF) (Aldrich) were used as received. All other reagents were purchased from Aldrich, Fluka, or Sigma Chemical Comp. while amino acid derivatives were obtained from U.S. Biochemical Corp. or Research Organics Inc. All solvents were dried over either $LiAlH_4$ or CaH_2 at reflux and distilled as needed. Bromo-[$^{14}C_2$]-acetic acid (40 mCi/mmol) was obtained from Amersham Corp. and Chemsyn Science Laboratories.

Thin-layer chromatography (TLC) was performed on silica gel 60 F-254 plates from EM Reagents. TLC solvent systems used were (1) $CHCl_3$/MeOH (4:1); (2) 1-butanol/H_2O/HOAc (4:1:1); (3) EtOH/NH_4OH (4:1); (4) CH_3CN/H_2O (30:8); (5) MeOH/10% NH_4OAc(aq) (1:1). Column chromatography was performed by using Florisil (Sigma) or silica gel 60, 70–230 mesh ASTM (Fluka). Ion-exchange resin (AG50WX8, 200–400 mesh, H^+ form) was obtained from Bio-Rad.

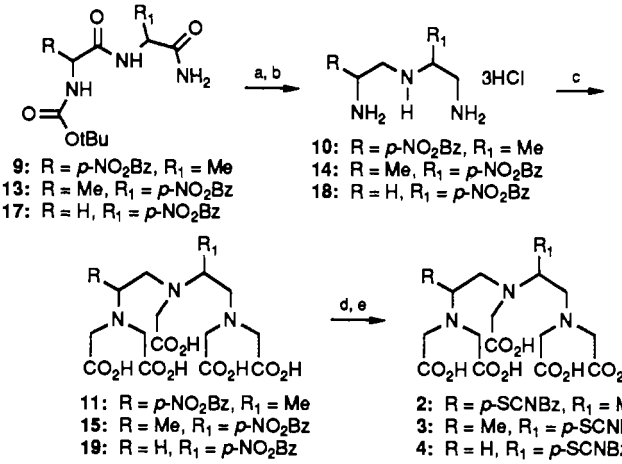
^1H NMR spectra were obtained by using either the Varian 220-MHz or Nicolet NTC500 spectrometers. Chemical shifts are reported in ppm on the δ scale relative to TSP (D_2O) or TMS (DMSO-d_6/$CDCl_3$). All coupling constants (J values) are reported in Hz. ^{13}C NMR spectra were recorded on a Varian XL300 instrument. Chemical shifts are reported in ppm on the δ scale relative to either methanol or dioxane. Infrared spectra were recorded on either a Beckman 4220 or 4240 infrared spectrophotometer. Chemical ionization mass spectra (CI-MS) were measured with a Finnegan 3000 spectrometer. Electron impact mass spectra (EI-MS) were recorded on a LKB 9000 instrument. Plasma desorption mass spectra (PDMS)

Scheme I[a]



[a] (a) Et_3N, 1,2-diaminopropane; (b) BH_3·THF, EtOH/HCl; (c) $BrCH_2CO_2H$, KOH; (d) H_2, Pd/C, Cl_2CS.

Scheme II[a]



[a] (a) TFA; (b) THF/EtOH, EtOH/HCl; (c) $BrCH_2CO_2H$, KOH; (d) H_2, Pd/C; (e) Cl_2CS.

(*27*) were obtained on the home-made instrument residing in the Laboratory of Chemistry in the National Heart, Lung, and Blood Institute at the National Institutes of Health.

A 1000-channel scintillation counter (LS5801, Beckman, Fullerton, CA) was used for quantitative determination of ^{14}C activity. Generally, a 50-μL aliquot of a sample containing ^{14}C was mixed with 10 mL of scintillation cocktail (Biofluor, NEN, Du Pont). Absolute disintegration rates for ^{14}C were determined by appropriate corrections for background and quench factors.

Elemental analyses were measured by Galbraith Laboratories. Analytical HPLC was done on a Beckman Model 746 system controlled by a Beckman 450 data system using a 4.56 mm × 15 cm Altex 5 μm ODS C_{18} column with a 25-min gradient of 100% aqueous 0.05 M triethylammonium acetate to 100% methanol at a flow rate of 1 mL/min. Preparative and semipreparative HPLC were performed to isolate the 4-nitrobenzyl-DTPA ligands. This purification step was initially begun with the Beckman system operating in a semipreparative mode using a 10 mm × 25 cm Altex 10 μm ODS C_{18} column at a flow rate of 3 mL/min employing the same gradient. Preparative HPLC performed with a Waters Delta Prep 3000 system using a PrepPak 500 cartridge at a 25 mL/min flow rate

replaced the semipreparative system midway through the syntheses. The gradients employed were Waters gradient curve 3 with 100% 0.05 M triethylammonium acetate to 50% methanol over 5 min followed by Waters gradient curve 4 from the 50:50 point to 100% methanol.

Syntheses of Ligands. Preparation of Geometric Isomer 1. *N*-(2-Aminopropyl)-*p*-nitrophenylalaninamide (5). Methyl 4-nitrophenylalanine hydrochloride (9.80 g, 37.63 mmol) in MeOH (25 mL) was treated with Et_3N (6.78 mL, 45.2 mmol) to liberate the amino ester. Ether (300 mL) was added and the precipitated hydrochloride salt was removed by filtration. After removal of the solvent, the residual oil in MeOH (5 mL) was added dropwise at room temperature to freshly distilled, vigorously stirred 1,2-diaminopropane (50 mL). After 18 h, the solvent was removed by rotary evaporation at 50 °C at 0.01 mm of vacuum until a constant weight was attained (10.01 g, 96%). TLC of the product in solvent system 1 on silica revealed an R_f = 0.10–0.12; ^{1}H NMR (220 MHz, D_2O, pH 10.0) δ 8.06 (d, 2 H, J = 7.5), 7.41 (d, 2 H, J = 7.5), 3.72 (t, 1 H, J = 8.0), 3.18–2.73 (m, 5 H), 0.918 (m, 3 H); ^{13}C NMR (300 MHz, $CDCl_3$) δ 173.79, 173.27, 146.96, 146.10, 130.25, 123.71, 56.29, 46.97, 46.81, 46.66, 41.07, 21.59 (The two amide carbonyl signals, 3:1 intensity, are indicative of a mixture of geometric isomers, see also ref 26); CI-MS 267 ((M + 1)/z). Anal. Calcd for $C_{12}H_{18}N_4O_3$: C, 54.53; H, 6.77; N, 21.05. Found: C, 54.33; H, 6.76; N, 20.92.

2-Methyl-6-(*p*-nitrobenzyl)diethylenetriamine Trihydrochloride (6). Amide 5 (9.90 g, 37.2 mmol) was dissolved in THF (200 mL) and transferred to a dried three-neck round-bottom flask fitted with condenser, stopper, and septum and under an argon atmosphere. The flask was cooled under argon in an ice bath and 1 M BH_3·THF (200 mL) was injected. The reaction was then refluxed for 6 h. After cooling to room temperature, MeOH (100 mL) was added slowly, and after hydrogen evolution ceased, the resulting solution was evaporated to dryness. The residue was taken up in 100% EtOH (175 mL) and the solution was saturated with HCl(g) while being cooled in a ice bath. The saturated solution was then refluxed for 6 h during which concentrated HCl (5 mL) was added if a finely divided powder was not observed. The product precipitated cleanly and after cooling to 0 °C for 6 h was collected and dried under vacuum (11.6 g, 86.3%). TLC of the product on silica gave a single spot, R_f = 0.48 using solvent system 3; ^{1}H NMR (500 MHz, D_2O, pH 11.5) δ 8.172 (d, 2 H, J = 8.0), 7.475 (d, 2 H, J = 8.0), 3.226 (m, 1 H), 3.0385 (q, 1 H, J = 6.0), 2.9435 (dd, 1 H, J = 13.5, 5.0), 2.699 (dd, 1 H, J = 13.5, 8.5), 2.6445 (dd, 1 H, J = 11.5, 5.0), 2.533 (m, 3 H), 1.0715 (d, 3 H, J = 6.5); (500 MHz, D_2O, pH 1.0) δ 8.2715 (d, 2 H, J = 8.5), 7.6105 (d, 2 H, J = 8.5), 4.138 (m, 1 H), 3.870 (m, 1 H), 3.607 (dd, 1 H, J = 13.5, 7.5), 3.56–3.34 (m, 4 H), 3.239 (m, 1 H), a pair of doublets for the two diastereomeric methyl groups which integrated to a total of 3 H at 1.494 (d, J = 4.0) and 1.485 (d, J = 3.5); ^{13}C NMR (300 MHz, $CDCl_3$) δ 147.50, 146.68, 130.17, 129.99, 123.69, 123.52, 58.33, 58.16, 56.14, 55.99, 52.57, 52.40, 46.82, 46.63, 42.49, 21.92, 21.85 (This spectrum is indicative of a single geometric isomer with the doubling of peaks due to the diastereomeric nature, other weak resonances of ≤5% intensity were seen near the reported peaks; see also ref 26); CI-MS 362 ((M + 1)/z). Anal. Calcd for $C_{12}H_{23}N_4O_2Cl_3$: C, 39.85; H, 6.65; N, 15.49. Found: C, 39.99; H, 6.64; N, 15.14.

2-Methyl-6-(*p*-nitrobenzyl)diethylene-*N,N,N′,N″,N‴*-pentaacetic Acid (7). Triamine 6 (1.00 g, 2.77 mmol) was added to bromoacetic acid (1.923 g, 13.8 mmol) in toluene at 0 °C with 7 N KOH (4.35 mL). The reaction was stirred at room temperature for 24 h, after which the solution was cooled in an ice bath prior to addition of more bromoacetic acid (3.846 g, 27.6 mmol) and 7 N KOH (8.69 mL). The reaction was then stirred for 7 days at room temperature. The solution was acidified to pH 2.0 with concentrated HBr and loaded onto a 2.6 × 25 cm AG50WX8, 200–400 mesh, H^+-form, ion-exchange column. The column was washed with water until the eluant was at neutral pH and then the crude product was eluted with 2 M NH_4OH. The product was then isolated by semipreparative HPLC with a t_R = 8.28 min. A second cation-exchange column (AG50WX8, 200–400 mesh, H^+ form) was used to remove the HPLC buffer, leaving the pure product (648 mg, 43.25%): ^{1}H NMR (500 MHz, D_2O, pH 1.0) δ 8.242 (t, 2 H, J = 6.5), 7.602 (d, 2 H, J = 8.0), 4.30–3.70 (complex series of signals integrating for 12 H), 3.50–3.00 (complex broad series of multiplets integrating for 6 H), a pair of doublets for the diastereomeric methyl group integrating for a total of 3 H at 1.4175 (d, J = 6.5) and 1.342 (d, J = 6.0); (500 MHz, D_2O, pH 13.0) δ 8.170 (d, 2 H, J = 8.0), 7.450 (d, 2 H, J = 8.0), 3.40–2.00 (complex series of overlapping multiplets integrating for 18 H), a pair of doublets for the diastereomeric methyl groups integrating for a total of 3 H at 0.9545 (d, J = 6.5) and 0.721 (d, J = 6.0); ^{252}Cf-PDMS m/z (M + K) 581, (M + Na) 565, (M + 1) 543. Anal. Calcd for $C_{22}H_{30}N_4O_{12}$: C, 48.70; H, 5.54; N, 10.33. Found: C, 48.61; H, 5.62; N, 10.57.

2-(*p*-Aminobenzyl)-6-methyldiethylenetriamine-*N,N,N′,N″,N‴*-pentaacetic Acid (8). Compound 7 (100 mg, 0.1845 mmol) was hydrogenated over 10% Pd/C (50 mg) at pH 8.5 (5 M KOH) in an atmospheric hydrogenation apparatus. The uptake of H_2 was monitored, and after the requisite amount had been consumed, the reaction was halted. The solution was filtered through a fine frit with Celite 535, then the solvent was removed and the residue dried under vacuum for 18 h (89.1 mg, 94.3%): ^{1}H NMR (500 MHz, D_2O, pH 1.0) δ 7.5035 (t, 2 H, J = 6.5), 7.437 (m, 2 H), 4.2–3.65 (complex series of multiplets integrating for 12 protons), 3.40–3.16 (m, 4 H), 3.10 (m, 1 H), 2.9385 (q, 1, J = 10.0), 1.36–1.25 [pair of doublets for the diastereomeric methyl groups integrating for 3 H total, 1.3415 (d, J = 6.5), 1.2675 (d, J = 6.5)]; (500 MHz, D_2O, pH 13.0) δ 7.11–7.04 (m, 2 H), 6.8055 (dd, 2 H, J = 8.5, 8.0), 3.40–2.05 (complex series of signals integrating for 18 H), 1.00–0.69 [series of doublets for the diastereomeric methyl groups integrating for 3 H total—0.9665 (d, J = 6.5), 0.9435 (d, J = 6.5), 0.846 (d, J = 6.0), 0.750 (d, 7.0), 0.7075 (d, J = 6.5)]; ^{252}Cf-PDMS m/z 511 (M − 1). Anal. Calcd for $C_{22}H_{27}N_4O_{10}K_5$: C, 37.61; H, 3.85; N, 7.98. Found: C, 37.36; H, 3.65; N, 7.72.

2-(*p*-Isothiocyanatobenzyl)-6-methyldiethylenetriamine-*N,N,N′,N″,N‴*-pentaacetic Acid (1). Aniline 8 (100 mg, 0.196 mmol) was taken up in H_2O (5 mL) and transferred into a small round-bottom flask. The pH was adjusted to between 8.5 and 9.0 with solid Na_2CO_3. Thiophosgene (15.0 μL, 0.196 mmol) in $CHCl_3$ (10 mL) was loaded into an addition funnel fitted to the flask. The thiophosgene solution was added in one rapid addition with maximum stirring and the reaction was left to stir for 2 h. After removal of the stir bar, the organic layer was removed by room-temperature rotary evaporation. The aqueous residue was then lyophilized, leaving an off-white powder. The crude product was then purified by use of a 1 × 30 cm silica column eluted with solvent system 4 with the product coming off of the column first. The solvent was removed with minimal warming on a rotary evaporator and the remaining aqueous solution was ly-

ophilized. TLC of the product on silica using solvent system 4 gave R_f = 0.20; IR (Nujol) 2100 cm^{-1}; ^1H NMR (220 MHz, D_2O/D_3CCO_2Na, pH 5.2) δ 7.28 (s, 4 H), 3.90–2.73 (broad complex multiplet integrating for 18 H), 1.39–1.28 (2 br d, 3 H). The reactivity of the compound precluded obtaining chemical analyses.

Preparation of Geometric Isomer 2. BOC-*dl*-(*p*-nitrophenylalaninyl)-*l*-alaninamide (9). BOC-*dl*-4-nitrophenylalanine (*10*) (13.0 g, 41.9 mmol) was dissolved in ethyl acetate (400 mL), and triethylamine (5.84 mL, 42.0 mmol), HOBT (4.55 g, 33.6 mmol), and *l*-alaninamide hydrochloride (7.098 g, 42.0 mmol) were added and dissolved. DCC (8.738 g, 42.4 mmol) in ethyl acetate (50 mL) was then added and the reaction solution was stirred for 24 h. Acetic acid (1 M, 1 mL) was added and after 0.5 hour the suspension was filtered. The filtrate was extracted with saturated salt solution (100 mL), 1 N HCl (3 × 100 mL), salt solution (100 mL), 5% $NaHCO_3$ solution (3 × 100 mL), and salt solution (100 mL). After drying over $MgSO_4$ and filtration, the solution was concentrated to 100 mL, petroleum ether was added, and the solution was held at 4 °C for 24 h. The product was collected and dried under vacuum (12.94 g, 81.3%): ^1H NMR (500 MHz, DMSO-d_6) δ 8.1075 (d, 2 H, J = 8.5), 7.777 (d, 1 H, J = 7.0), 7.4475 (d, 2 H, J = 8.5), 7.039 (s, 1 H), 6.407 (s, 1 H), 6.3675 (d, 1 H, J = 5.5), 4.414 (br s, 2 H), 3.252 (dd, 1 H, J = 13.0, 4.0), 3.024 (dd, 1 H, J = 12.5, 3.5), 1.420 (br s, 12 H); ^{13}C NMR (300 MHz, DMSO-d_6) δ 18.43, 27.95, 37.80, 47.94, 55.12, 78.23, 122.97, 130.51, 146.12, 146.66, 155.16, 170.50, 173.89; CI-MS 381 ((M + 1)/z). Anal. Calcd for $C_{17}H_{24}N_4O_6$: C, 53.68; H, 6.31; N, 14.73. Found: C, 53.55; H, 6.45; N, 14.23.

3-Methyl-6-(*p*-nitrobenzyl)diethylenetriamine Trihydrochloride (10). Dipeptide amide 9 (5.10 g, 13.42 mmol) was deprotected by treatment with trifluoroacetic acid (50 mL) for 1 h, after which the solution was rotary evaporated to near dryness. MeOH (50 mL) was added and the solution was again taken to dryness. The resulting solid was held at 0.01 mm and 50 °C for 8 h to ensure removal of residual acid. The resulting ammonium salt (5.10 g, 13.42 mmol) was taken up in THF (50 mL) and added to a flame-dried 250-mL three-neck flask fitted with a condenser and septum and held under an argon atmosphere. The flask was cooled to 0 °C and 1 M BH_3·THF (30.8 mL) was added by use of a syringe. The reaction solution was heated to vigorous reflux for 2 h and then stirred at room temperature for 2 h. The reaction flask was cooled to 0 °C and MeOH (25 mL) was slowly injected to decompose excess hydride. The solution was reduced to dryness, taken up in 100% EtOH (50 mL), and, after addition of concentrated HCl (50 mL), vigorously refluxed for 2 h and then stripped to dryness. The residue was dissolved in H_2O, loaded onto a 1.5 × 20 cm AG50WX8, 200–400 mesh, H^+-form, cation-exchange column, and washed with H_2O until the eluant was neutral. The product was eluted from the column with concentrated HCl (125 mL). The eluant was reduced to 10 mL and then lyophilized overnight (1.823 g, 66.2%). TLC of the solid on silica using solvent system 3 revealed one spot, R_f = 0.50; ^1H NMR (500 MHz, D_2O, pH 1.0) δ 8.268 (d, 2 H, J = 8.0), 7.614 (d, 2 H, J = 8.0), 4.106 (m, 1 H), 3.773 (m, 1 H), 3.635 (dd, 1 H, J = 13.0, 7.5), 3.574 (dd, 1 H, J = 13.5, 5.0), 3.54–3.15 (m, 4 H), 1.493 (br t, 3 H); (500 MHz, D_2O, pH 11.0) δ 8.091 (d, 2 H, J = 8.0), 7.438 (d, 2 H, J = 8.0), 3.167 (m, 1 H), 2.910 (m, 1 H), 2.75–2.45 (complicated m, 6 H), 1.031 (br s, 3 H); ^{13}C NMR (300 MHz, D_2O, pH 1.0) δ 24.78, 43.99, 44.06, 48.64, 49.03, 54.38, 54.60, 57.01, 57.62, 66.16, 66.50, 133.12, 139.31, 151.6, 155.97; (300 MHz, $CDCl_3$) δ 20.23, 20.40, 38.04, 38.17, 43.05, 43.24, 46.06, 46.29, 53.68, 53.85, 59.69, 59.80, 122.57, 129.10, 145.60, 146.48; CI-MS 253 ((M + 1)/z). Anal. Calcd for $C_{12}H_{23}N_4O_2Cl_3$: C, 39.85; H, 6.36; N, 15.49. Found: C, 39.88; H, 6.36; N, 15.28.

3-Methyl-6-(*p*-nitrobenzyl)diethylenetriamine-*N,N,N′,N″,N‴*-pentaacetic Acid (11). Triamine 10 (1.0 g, 3.97 mmol) was alkylated with bromoacetic acid (5.77 g, 41.51 mmol) and 7 N KOH (13.09 mL) as described above. Purification of the crude product by ion-exchange chromatography, preparative HPLC, and additional ion-exchange chromatography proceeded smoothly as described for 7 with a t_R for 11 by HPLC of 7.80 min (852 mg, 39.6%). TLC on silica using solvent system 3 revealed two spots of equal intensity, R_f = 0.092 and 0.182, while solvent system 5 revealed only one spot, R_f = 0.779; ^1H NMR (500 MHz, D_2O, pH 1.0) δ 8.246 (t, 2 H, J = 8.0), 7.583 (dd, 2 H, J = 13.5, 8.0), 4.223 (dd, 2 H, J = 39.0, 18.0), 4.121 (dd, 2 H, J = 39.0, 17.0), 3.95–2.98 [complex series of complex signals integrating for 15 H; decipherable signals within a complex area—3.828 (dd, 2 H, J = 37.5, 16.5) and 2.9335 (dd, 1 H, J = 13.0, 9.5)], two doublets for the diastereomeric methyl groups integrating for 3 H total at 1.308 (d, J = 6.0) and 1.0475 (d, J = 4.5); (500 MHz, D_2O, pH 13.0) δ 8.199 (br m, 2 H), 7.55–7.40 (m, 2 H), 3.40–1.90 (complex series of signals integrating for 18 H), 1.00–0.40 (complex series of apparent doublets with a broad singlet at 0.666 for the diastereomeric methyl groups integrating for 3 H total) (The spectra of 11 vs 7 were found to be incongruent, i.e., 7 contains <5% 11); ^{13}C NMR (300 MHz, D_2O, pH 5.0) δ 32.96, 49.00–64.00 (complex band of signals originating from the 20 possible diastereomeric carbon signals), 124.07, 130.16, 146.16, 146.37, 170.10, 179.05; ^{252}Cf-PDMS m/z 601 (M + $(NH_3)_3$), 579 (M + $(NH_3)_2$), 563 (M + Na), 541 (M − 1); EI-MS (The MS sample was silylated by reaction with excess bis(trimethylsilyl)trifluoroacetamide in dry acetonitrile) m/z 887 (M − 15), 612, 477, 425. Anal. Calcd for $C_{22}H_{30}N_4O_{12}$·$(NH_3)_3$·$4H_2O$: C, 39.69; H, 7.06; N, 14.74. Found: C, 39.39; H, 7.00; N, 14.68.

2-(*p*-Aminobenzyl)-5-methyldiethylenetriamine-*N,N,N′,N″,N‴*-pentaacetic Acid (12). Nitro compound 11 (50 mg, 0.0922 mmol) in H_2O (5 mL) at pH 8.5 was hydrogenated (10% Pd/C, 50 mg) as previously described above for 8 (45.7 mg, 96.8%): ^1H NMR (500 MHz, D_2O, pH 1.0) δ 7.5135 (dd, 2 H, J = 14.5, 8.0), 7.442 (t, 2 H, J = 8.5), 4.2545 (dd, 2 H, J = 38.0, 17.5), 4.156 (dd, 2 H, J = 37.5, 17.5), 4.00–3.65 (complex series of multiplets integrating for 4 H), 3.58 (m, 2 H), 3.496 (dd, 1 H, J = 14.0, 5.0), 3.45–3.15 (complex series of multiplets integrating for 3 H), 3.1035 (d, 1 H, J = 12.5), 2.975 (m, 2 H), 2.8785 (dd, 1 H, J = 13.5, 9.0), for the diastereomeric methyl group two doublets integrating for 3 H at 1.2875 (d, J = 6.5) and 1.0275 (d, J = 6.5); (500 MHz, D_2O, pH 13.0) δ 7.081 (dd, 2 H, J = 16.0, 8.0), 6.815 (dd, 2 H, J = 11.5, 9.0), 3.40–2.05 (complex series of multiplets integrating for 18 H), 1.00–0.45 [series of signals for the diastereomeric methyl groups integrating for 3 H—0.9675 (d, J = 6.5), 0.832 (d, J = 6.0), 0.7255 (d, J = 6.5), 0.702 (br s), 0.490 (d, J = 6.0)]; ^{252}Cf-PDMS m/z 511 (M − 1). Anal. Calcd for $C_{22}H_{28}N_4O_{10}K_5$: C, 37.61; H, 3.85; N, 7.98. Found: C, 37.35; H, 3.75; N, 7.98.

2-(*p*-Isothiocyanatobenzyl)-5-methyldiethylenetriamine-*N,N,N′,N″,N‴*-pentaacetic Acid (2). Aniline 12 (100 mg, 0.193 mmol) in H_2O (5 mL) at pH 8.5 was converted to the isothiocyanate by using thiophosgene (24.8 μL, 0.0193 mmol) in $CHCl_3$ (10 mL) as described for 1. The IR spectrum possessed a strong absorbance at 2100

cm^{-1} for the isothiocyanate; ^1H NMR (220 MHz, D_2O, pH 4.60) δ 7.32 (s, 4 H), 3.86–2.62 (broad series of multiplets integrating for 18 H), 1.13 (br d, 3 H).

Preparation of Geometric Isomer 3. BOC-*l*-alaninyl-*dl*-*p*-nitrophenylalaninamide (13). BOC-*l*-alanine (5.606 g, 29.66 mmol), 4-nitrophenylalaninamide (*10*) (6.2 g, 29.66 mmol), and HOBT (3.207 g, 23.7 mmol) were dissolved in ethyl acetate (400 mL). DCC (6.722 g, 32.6 mmol) in ethyl acetate (25 mL) was added. The reaction mixture was allowed to stir for 18 h, after which the workup proceeded as described for **9**. The product was crystallized from minimal ethyl acetate by addition of petroleum ether (100 mL) and cooling to 0 °C for 12 h. The product was collected on a Büchner funnel and dried under vacuum (9.84 g, 87.3%). TLC using solvent system 1 gave an R_f = 0.59; ^1H NMR (220 MHz, D_2O, $CDCl_3$/DMSO-d_6) δ 8.06 (d, 2 H, J = 8.0), 7.83 (d, 1 H, J = 7.0), 7.43 (d, 2 H, J = 8.0), 7.10 (d, 1 H, J = 7.0), 6.96 (m, 1 H), 5.46 (d, 2 H, J = 6.0), 4.63 (m, 1 H), 3.55 (m, 1 H), 3.24 (dd, 1 H, J = 13.0, 5.0), 2.99 (dd, 1 H, J = 13.0, 9.0), 1.43 (s, 9 H), 1.14 (dd, 3 H, J = 13.0, 8.0); ^{13}C (300 MHz, DMSO-d_6) δ 17.69, 17.75, 28.05, 37.12, 37.32, 49.72, 50.05, 52.67, 52.87, 78.01, 78.08, 122.91, 130.44, 146.11, 146.42, 155.03, 155.14, 172.26, 172.49; CI-MS 381 ((M + 1)/z). Anal. Calcd for $C_{17}H_{24}N_4O_6$: C, 53.54; H, 6.29; N, 14.69. Found: C, 53.44; H, 6.34; N, 14.65.

2-Methyl-5-(*p*-nitrobenzyl)diethylenetriamine Trihydrochloride (14). Dipeptide amide **13** (3.00 g, 7.89 mmol) was deprotected with trifluoroacetic acid (30 mL) as above [CI-MS 282 ((M + 1)/z)]. The ammonium salt (3.00 g, 7.59 mmol) in THF (50 mL) was reduced with 1 M BH_3·THF (30.8 mL) as described for **10** (1.87 g, 68.2%). TLC of the solid on silica using solvent system 3 revealed one spot, R_f = 0.68; ^1H NMR (500 MHz, D_2O, pH 1.6) δ 8.249 (d, 2 H, J = 8.0), 7.5985, 7.5945 (d, 2 H, J = 8.0, two doublets arising from diastereomers), 3.798 (m, 1 H), 3.687 (m, 1 H), 3.42–3.10 (m, 6 H), 1.402 (d, 3 H, J = 7.0); (500 MHz, D_2O, pH 10.0) δ 8.1485 (d, 2 H, J = 8.5), 7.4835 (d, 2 H, J = 8.5), 2.98–2.86 (m, 4 H), 2.660 (m, 2 H), 2.573 (dd, 1 H, J = 12.5, 5.5), 2.50 (m, 1 H), 1.011 (t, 3 H, J = 7.0); ^{13}C NMR (300 MHz, D_2O, pH 1.0) δ 24.74, 43.82, 48.4, 48.8, 54.19, 54.33, 56.9, 57.48, 66.19, 66.53, 133.1, 139.3, 151.5, 155.9; CI-MS 253 ((M + 1)/z). Anal. Calcd for $C_{12}H_{23}N_4O_2Cl_3$: C, 39.85; H, 6.36; N, 15.49. Found: C, 39.56; H, 6.49; N, 15.43.

2-Methyl-5-(*p*-nitrobenzyl)diethylenetriamine-*N,N,N′,N′,N″*-pentaacetic Acid (15). Diethylenetriamine **14** (1.00 g, 3.967 mmol) was alkylated with bromoacetic acid (5.769 g, 41.50 mmol) and 7 N KOH (13.04 mL) as described in the preparation of **11**. Purification proceeded smoothly as described earlier (compound **7**) with the HPLC t_R = 8.54 min (862 mg, 40.1%). TLC on silica using solvent system 3 revealed two spots of equal intensity, R_f = 0.09 and 0.17; while using solvent system 5 only one spot was observed, R_f = 0.774; ^1H NMR (500 MHz, D_2O, pH 1.0) δ 8.217 (d, 2 H, J = 8.0), 7.539 (t, 2 H, J = 8.5), 4.55–4.05 (complex series of diastereomeric multiplets integrating for 10 H), 3.97–2.95 (complex series of multiplets integrating for 7 H), 2.93–2.77 (m, 1 H), 1.384 (s, 3 H); (500 MHz, D_2O, pH 12.0) δ 8.187 (t, 2 H, J = 7.5), 7.435 (dd, 2 H, J = 14.0, 9.0), 3.70–2.10 (exceptionally complex series of signals integrating for 18 H), 1.10–0.90 (complex series of apparent doublets, 3 H, J = 6.0, 6.5, 6.5, 5.5); ^{13}C NMR (300 MHz, D_2O, pH 5.0) δ 33.77, 50.00–62.00 (complex band of signals originating from the possible diastereomeric carbon signals), 124.00, 130.18, 146.22, 146.48, 170.19, 179.43; ^{252}Cf-PDMS m/z 563 (M + Na), 541 (M − 1). Anal. Calcd for $C_{22}H_{30}N_4O_{12}(NH_3)_3$·$4H_2O$: C, 39.69; H, 7.06; N, 14.74. Found: C, 39.40; H, 6.83; N, 14.78.

3-(*p*-Aminobenzyl)-6-methyldiethylenetriamine-*N,N,N′,N″,N″*-pentaacetic Acid (16). Compound **15** (50 mg, 0.0922 mmol) was catalytically hydrogenated (10% Pd/C, 50 mg) to yield the aniline by using the procedure described for **12**. The product was carried on to the isothiocyanato compound by the methods described above (40.9 mg, 86.8%): ^1H NMR (500 MHz, D_2O, pH 1.0) δ 7.49–7.39 (m, 4 H), 4.40–4.05 (complex multiplet integrating for 10 H), 3.95–2.95 (complex series of diastereomeric multiplets integrating for 7 H), 2.82–2.67 (m, 1 H), 1.3665 (d, 3 H, J = 6.5); (500 MHz, D_2O, pH 13.0) δ 7.059 (d, 2 H, J = 7.0), 6.809 (d, 2 H, J = 7.0), 3.70–2.10 (complex series of overlapping diastereomeric multiplets integrating for 18 H), 1.04–0.89 [series of four asymmetric doublets for the diastereomeric methyl group integrating for 3 H total—1.0205 (d, J = 6.5), 0.9855 (d, J = 6.5), 0.9505 (d, J = 6.5), 0.910 (d, J = 6.0)]; ^{252}Cf-PDMS m/z 511 (M − 1). Anal. Calcd for $C_{22}H_{28}N_4O_{10}K_5$: C, 37.61; H, 3.85; N, 7.98. Found: C, 36.68; H, 3.95; N, 8.04.

3-(*p*-Isothiocyanatobenzyl)-5-methyldiethylenetriamine-*N,N,N′,N″,N″*-pentaacetic Acid (3). Aniline **16** (100 mg, 0.193 mmol) was treated with thiophosgene (222 mg, 1.93 mmol) as described in the preparation of **1** and the crude product was purified by employing the procedures therein. The IR spectra possessed a strong absorbance at 2100 cm^{-1} for the isothiocyanato group; ^1H NMR (220 MHz, D_2O, pH 4.90) δ 7.27 (s, 4 H), 3.84–2.92 (broad series of multiplets integrating for 18 H), 1.26 (br d, 3 H).

Preparation of Geometric Isomer 4. BOC-glycyl-*dl*-*p*-nitrophenylalaninamide (17). BOC-glycine (5.02 g, 28.70 mmol), 4-nitrophenylalaninamide (*10*) (6.00 g, 28.70 mmol), and HOBT (3.104 g, 22.9 mmol) were dissolved in ethyl acetate (400 mL). DCC (6.53 g, 31.67 mmol) in ethyl acetate (25 mL) was added and the reaction mixture was allowed to stir for 18 h. Three drops of glacial acetic acid were added and after 30 min the DCU was filtered from the solution. The filtrate was extracted as described for **9**. The product was crystallized from ethyl acetate (50 mL) by the addition of petroleum ether (100 mL) and cooling to 4 °C for 12 h (8.58 g, 81.7%): ^1H NMR (220 MHz, $CDCl_3$/DMSO-d_6) δ 8.06 (d, 2 H, J = 8.0), 7.43 (d, 3 H, J = 8.0, the third proton being one from the primary amide), 6.96 (br s, 1 H), 6.64 (t, 1 H, J = 5.0), 5.46 (d, 1 H, J = 8.0), 4.64 (m, 1 H), 3.29 (s, 2 H), 3.25 (dd, 1 H, J = 13.0, 5.0), 3.00 (dd, 1 H, J = 13.0, 9.0), 1.41 (s, 9 H); ^{13}C NMR (300 MHz, DMSO-d_6) δ 28.09, 37.36, 43.23, 52.98, 78.06, 123.04, 130.47, 146.14, 146.31, 155.73, 169.13, 172.24; CI-MS 367 ((M + 1)/z). Anal. Calcd for $C_{16}H_{22}N_4O_6$: C, 52.50; H, 6.01; N, 15.30. Found: C, 52.46; H, 5.96; N, 15.36.

3-(*p*-Nitrobenzyl)diethylenetriamine Trihydrochloride (18). Dipeptide amide **17** (3.00 g, 8.19 mmol) was deprotected as before by stirring for 1 h in trifluoroacetic acid (30 mL) (CI-MS 268 ((M + 1)/z)). The ammonium salt (3.00 g, 7.87 mmol) in THF (50 mL) was reduced with 1 M BH_3·THF (35 mL) by using the reaction conditions employed for **10** (1.17 g, 62.3%). TLC on silica of the residue using solvent system 3 gave one spot, R_f = 0.42; ^1H NMR (500 MHz, D_2O, pH 1.0) δ 8.2585 (d, 2 H, J = 8.5), 7.6515 (d, 2 H, J = 8.5), 4.116 (m, 1 H), 3.65–3.53 (m, 2 H), 3.50–3.45 (m, 4 H), 3.4125 (dd, 1 H, J = 14.5, 5.0), 3.3175 (dd, 1 H, J = 14.5, 8.0); (500 MHz, D_2O, pH 10.0) δ 8.1485 (d, 2 H, J = 8.5), 7.5095 (d, 2 H, J = 8.5), 3.150 (br m, 1 H), 3.14–2.98 (m, 4 H), 2.8975 (dd, 1 H, J = 13.5, 7.0), 2.855–2.78 (m, 2 H); ^{13}C NMR (300 MHz, D_2O, pH 1.0) δ 34.39, 35.75, 39.17, 42.44, 57.21, 124.34, 130.55, 141.79,

147.19; CI-MS 239 ((M + 1)/z). Anal. Calcd for $C_{11}H_{21}N_4O_2Cl_3$: C, 38.00; H, 6.04; N, 16.12. Found: C, 37.83; H, 6.01; N, 16.27.

3-(*p*-Nitrobenzyl)diethylenetriamine-*N,N,N',N'',N''*-pentaacetic Acid (19). Triamine **18** (1.00 g, 2.87 mmol) was alkylated with bromoacetic acid (6.00 g, 43.16 mmol) and 7 N KOH (12.49 mL) by using the procedure employed for generating **11** and the crude product was purified by using the process described in the synthesis of **7** with t_R = 8.14 min by HPLC (67.5 mg, 44.6%). TLC of the product on silica revealed one spot using solvent system 3, R_f = 0.13, and one spot using solvent system 5, R_f = 0.765; ^{1}H NMR (500 MHz, D_2O, pH 1.0) δ 8.231 (d, 2, J = 8.0), 7.556 (d, 2 H, J = 8.0), 4.225 (br s, 9 H), 3.70–3.40 (m, 6 H), 3.2325 (br d, 1 H, J = 14.5), 3.065 (br s, 2 H), 2.910 (br m, 1 H); (500 MHz, D_2O, pH 12.0) δ 8.1885 (d, 2 H, J = 7.5), 7.454 (t, 2 H, J = 8.0), 3.50–2.35 (complex series of multiplets within which was an apparent singlet at 3.225 the sum total of which integrated for 19 H); ^{13}C NMR (300 MHz, D_2O, pH 4.5) δ 34.22, 55.18, 55.26, 55.35, 55.54, 57.09, 57.39, 59.92, 60.67, 62.49, 123.96, 130.50, 141.56, 146.68, 169.79, 168.89, 179.22; ^{252}Cf-PDMS m/z 527 (M − 1). Anal. Calcd for $C_{21}H_{28}N_4O_{12}(NH_3)_3 \cdot 2H_2O$: C, 40.97; H, 6.66; N, 15.93. Found: C, 40.88; H, 6.63; N, 15.84.

3-(*p*-Aminobenzyl)diethylenetriamine-*N,N,N',N'',N''*-pentaacetic Acid (20). Compound **19** (50 mg, 0.0947 mmol) was hydrogenated (10% Pd/C, 50 mg) by using the same conditions as for generating **12** (43.5 mg, 92.3%): ^{1}H NMR (500 MHz, D_2O, pH 1.0) δ 7.473 (d, 2 H, J = 8.0), 7.413 (d, 2 H, J = 8.0), 4.20 (m, 8 H), 3.75 (m, 1 H), 3.50 (m, 5 H), 3.1495 (dd, 1 H, J = 14.0, 4.5), 3.054 (br m, 2 H), 2.795 (dd, 1 H, J = 14.0, 8.0); (500 MHz, D_2O, pH 13.0) δ 7.066 (d, 2 H, J = 8.0), 6.8075 (d, 2 H, J = 8.0), 3.40–2.10 (complex series of multiplets integrating for 19 H); ^{252}Cf-PDMS m/z 497 (M − 1). Anal. Calcd for $C_{21}H_{24}N_4O_{10}K_5$: C, 36.63; H, 3.49; N, 8.14. Found: C, 36.54; H, 3.57; N, 8.15.

3-(*p*-Isothiocyanato)diethylenetriamine-*N,N,N',N'',N''*-pentaacetic Acid (4). Aniline **20** (100 mg, 0.201 mmol) was treated with thiophosgene (15.4 μL, 0.201 mmol) and purified following the earlier described procedure for generating **1**. The IR spectrum possessed a strong absorption at 2100 cm^{-1} for the isothiocyanato group; ^{1}H NMR (220 MHz, D_2O, pH 5.10) δ 7.41 (s, 4 H), 3.92–2.34 (broad series of multiplets integrating for 19 H).

Preparation of ^{14}C-Labeled Ligands. The ^{14}C-labeled isothiocyanate ligands **1–4** were prepared by using the methods described above except for substitution of Br-$^{14}CH_2CO_2H$ (3 mCi/3 mmol of triamine) in the alkylation procedure, as previously reported (*10*). The specific activity of the isothiocyanate ligands was determined by correlating the ^{14}C counting rate (dpm) of a known volume of a ligand solution with ligand concentration as measured by UV absorption at 280 nm (ε = 7730 M^{-1} cm^{-1}). The specific activity of the ligands **1–4** was found to be 0.516, 0.69, 0.814, and 1.29 mCi/mM, respectively (*28*).

RESULTS AND DISCUSSION

The synthetic strategies employed were devised with the intent of providing a general synthesis for both mono- and disubstituted diethylenetriamines. Since carboxymethylation of this class of compounds had already been demonstrated to be facile by standard methods (*10*, *29*), the dipeptide route to the triamines allowed entry into an array of substituted DTPA ligands. The substituents were limited to methyl groups only for demonstrative purposes.

The synthesis of **1** (Scheme I) was carried out essentially as a modification of the literature procedure for preparation of **III** (*10*). Aminolysis of the methyl ester using 1,2-diaminopropane as solvent produced exclusively monoamide. Borane reduction (*30*) yielded mostly (*26*) triamine **6** after the usual acidic workup to cleave boron adducts. The triamine was alkylated with bromoacetic acid (*31*), and after the pentaacetic acid had been isolated, the nitro group was hydrogenated and the resultant aniline converted to an isothiocyanate (*32*).

Ligands **2–4** were prepared from carbamate-protected dipeptide amides which provided the triamine backbone of the DTPA ligand and introduced the desired substituents. In the syntheses, the aryl nitro group was derived from 4-nitrophenylalanine, either as a carbamate or as the primary amide. In preparing **2**, carbamate **9** was coupled to alaninamide with DCC to provide dipeptide **10** (*33*). The blocking group was removed with TFA (*34*) and the resulting salt was reduced to triamine **10** with diborane. A serious complication was encountered during this sequence in that ca. 20% of the aryl nitro group was reduced to an aniline. This problem was obviated by use of the stoichiometric amount of hydride equivalents required for the reduction of two amides, neutralization of the TFA, and reduction of the TFA itself. Use of any excess borane generated the undesired and inseparable aniline. Presumably a borane–TFA intermediate was responsible for the decrease in reduction selectivity as this effect was not evident in the reduction of the hydrochloride salt of a similar compound (*10*).

Purification of the triamine was found to be most convenient by first decomposing the boron aggregate via a relatively short but harsh reflux in a 1:1 mixture of ethanol and concentrated hydrochloric acid. Ion-exchange chromatography using an AG50 cation-exchange resin yielded an exceptionally clean product when eluted from the resin with concentrated hydrochloric acid.

The pentaacetic acid portion of the molecule was formed by alkylation with excess bromoacetic acid in aqueous hydroxide solution. Purification of the DTPA was achieved by AG50 cation-exchange chromatography, preparative HPLC, and use of a second AG50 cation-exchange column. Catalytic hydrogenation generated the aniline, which was in turn converted to the isothiocyanato ligand with thiophosgene. Column chromatography on silica produced the pure bifunctional ligand **2**.

Ligands **3** and **4** were prepared by diimide coupling of the required *N-t*-BOC amino acid with 4-nitrophenylalaninamide. The diamides generated were then carried through a reaction sequence like that used to synthesize **2**, in order to generate **3** and **4**.

All intermediates and final products were identified by NMR and mass spectroscopy. High-resolution proton NMR spectra at 500 MHz at the pH extremes were obtained to demonstrate primary evidence of structure. Mass spectra of the DTPA compound were measured either by electron impact of the persilylated derivative or by plasma desorption of the pentaacetic acid. Both methods provided molecular ions of the compounds and interpretable fragmentation ion patterns. Elemental analysis and chromatography further established purity of synthesized materials. TLC of the disubstituted ligands clearly demonstrated the presence of diastereomers. No attempt was made to obtain optically pure products. IR spectra of the final products were used to confirm the presence of the isothiocyanate group. TLC and NMR along with the IR data were used as a measure of the purity of the isothiocyanates due to the limited stability of the compounds.

The choice of the isothiocyanate as the group to react

with the protein was maintained in part as an experimental constant. Additionally, we had already established that this was a useful linking group in terms of rate and efficiency (*10*, *35*). Stability of the product thiourea was accepted as comparable to that of an amide linkage since cleavage of both functional groups requires use of hot mineral acid (*36*).

With that knowledge in hand, the synthesis of a family of bifunctional 4-isothiocyanatobenzyl DTPA ligands wherein a methyl group was added to the carbon framework was accomplished to provide an additional measure of steric hindrance to increase the stability of the complex. Measurable selectivity in the aminolysis reaction of Scheme I due to the steric contribution of the added methyl group was expected. Initially, however, we had thought that an equimolar quantity of the two possible positional isomers had been formed, but, in fact, examination of the ^{13}C NMR spectra of the amide so formed revealed two amide carbonyl signals in a 3:1 ratio, indicative of a mixture. In the course of the review of this paper, we were made aware of the work of Cummins et al. (*26*) which employed a modified synthesis of the reported compound "MX-DTPA" (*25*) to obtain only the pentakis(*tert*-butyl ester) of isomer **7**. Inspection of ^{13}C and 500-MHz ^{1}H NMR spectra of our resultant triamine **6** versus those of our compound **10** revealed >95% of the product of the borane reduction of **5** to be compound **6** (*and not a mixture of* ***6*** *and* ***10*** **as** *we had earlier thought*) (*23*, *25*). NMR spectra of **1** showed the material referred to earlier as the "MX-DTPA" equimolar mixture of **1** and **2** to be >95% **1**, in agreement with the work of Cummins et al. (*26*).

The general synthesis of Scheme II for either of the monosubstituted DTPA's, **2**- vs **3**-position, will allow investigation of the structural influence over complex stability of the benzyl substituent when transposed from the C-2 to the C-3 position without an added methyl group. Synthesis of the disubstituted DTPA's should then provide an entry point into a vast array of potential ligands. The ability to control the substituents and their location on the backbone of the ligand should facilitate evaluation of which positions introduction of an alkyl group might be effective in maximizing the in vivo stability of the ^{88}Y–mAb conjugate, and, ultimately as well, indicate which groups might provide optimal results in vivo. We note that **1** is currently being employed for diagnosis and treatment of adult T-cell leukemia and B-cell lymphoma with ^{111}In and ^{90}Y.

ACKNOWLEDGMENT

We would like to thank Mr. William Comstock of the NHLBI, Laboratory of Chemistry, for his time and efforts in obtaining the EI-MS spectra of the ligands and Drs. Greg Pippin and Tom McMurry for suggestions for improving this manuscript. We thank Drs. Herman Yeh and Gui Ying Li for their assistance with NMR spectroscopy.

LITERATURE CITED

(1) Strand, M., Scheinberg, D. A., Gansow, O. A., et al. (1983) Monoclonal Antibody Conjugates for Diagnostic Imaging and Therapy. In *Monoclonal Antibodies and Cancer* (B. D. Boss, R. Langman, I. Trowbridge, R. Dulbecco, Eds.) pp 125–131, Academic Press, Orlando.

(2) Burchiel, S. W., Rhodes, B. A., Eds. (1983) *Radioimmunoimaging and Radioimmunotherapy*, Elsevier Science Publishing, New York.

(3) Gansow, O. A., Brechbiel, M. W., Mirzadeh, S., Colcher, D., and Roselli, M. (1990) Chelates and antibodies: Current Methods and New Directions. In *Cancer Imaging with Radiolabeled Antibodies* (D. M. Goldenberg, Ed.) Chapter 7, Kluwer Academic Press, Boston.

(4) Goldenberg, D. M., Ed. (1990) Second Conference on Radioimmunodetection and Radioimmunotherapy of Cancer. *Cancer Res. 50*, 774s–1059s.

(5) Mach, J. P., Carrel, S., Formi, M., Ritschard, J., Donath, A., and Alberto, P. (1981) Tumor localization of radiolabeled antibodies against carcinoembryonic antigen in patients with carcinoma. *New Engl. J. Med. 303*, 5–10.

(6) Ballou, B., Levine, G., Hakala, T. K., and Solter, D. (1979) Tumor location detected with radioactively labeled monoclonal antibody and external scintigraphy. *Science 206*, 844–847.

(7) Scheinberg, D. A., and Strand, M. (1982) Leukemic cell targeting and therapy by monoclonal antibody in a mouse model system. *Cancer Res. 42*, 44–49.

(8) Spencer, R. P., Ed. (1978) Therapy in Nuclear Medicine, Chapters 1–3, Greene and Stratton, New York.

(9) Fritzberg, A. R., Berninger, R. W., Hadley, S. W., and Wester, D. W. (1988) Approaches to radiolabeling of antibodies for diagnosis and therapy of cancer. *Pharm. Res. 5*, 325–334.

(10) Brechbiel, M. W., Gansow, O. A., Atcher, R. W., Schlom, J., Esteban, J., Simpson, D. E., and Colcher, D. (1986) Synthesis of 1-(*p*-isothiocyanatobenzyl) derivatives of DTPA and EDTA. Antibody labeling and tumor-imaging studies. *Inorg. Chem. 25*, 2772–2781.

(11) Roselli, M., Schlom, J., Gansow, O. A., Raubitschek, A., Mirzadeh, S., Brechbiel, M. W., and Colcher, D. (1989) Comparative biodistributions of yttrium- and indium-labeled monoclonal antibody B72.3 in athymic mice bearing human colon carcinoma xenografts. *J. Nucl. Med. 30*, 672–682.

(12) Maecke, H. R., Riesen, A., and Ritter, W. (1989) The molecular structure of Indium–DTPA. *J. Nucl. Med. 30*, 1235–1239.

(13) Kauffman, G. B. (1966) *Alfred Werner, Founder of Coordination Theory*; Springer, Berlin.

(14) Basolo, F., and Johnson, R. (1964) *Coordination Chemistry*, Benjamin/Cummings, Menlo Park, CA.

(15) Greenwood, N. N., and Earnshaw, A. (1984) *Chemistry of the Elements*, Chapter 19, Pergamon, New York.

(16) Wessels, B. W., and Rogus, R. D. (1984) Radionuclide selection and model absorbed dose calculations for radiolabeled tumor associated antibodies *Med. Phys. 11*, 638–645.

(17) Order, S. E., Klein, J. L., Leichner, P. K., Frincke, J., Lollo, C., and Carlo, J. (1986) ^{90}Y antiferritin. A new therapeutic radiolabeled antibody. *Int. J. Rad. Oncol. Biol. Phys. 12*, 277–281.

(18) Durbin, P. W. (1960) Metabolic characteristics within a chemical family. *Health Phys. 2*, 225–238.

(19) Kyker, G. C. (1962) Rare Earths. In *Mineral Metabolism* (C. L. Comar, and F. Bronner, Eds.) Vol. IIB, Chapter 36, Academic Press, New York.

(20) Hnatowich, D. J., Chino, M., Siebecker, D. A., Gionet, M., Griffin, T., Doherty, P. W., Hunter, R., and Kase, K. R. (1988) Patient biodistribution of intraperitoneally administered yttrium-90-labeled antibody. *J. Nucl. Med. 29*, 1428–1434.

(21) Kroll, H., Korman, S., Siegel, E., Hart, H. E., Rosoff, B., Spencer, H., and Laszlo, D. (1957) Excretion of yttrium and lanthanum chelates of cyclohexane 1,2-trans diamine tetraacetic acid and diethylenetriamine pentaacetic acid in man. *Nature 180*, 919–920.

(22) Dudley, H. C. (1955) Influence of chelates on the metabolism of radioyttrium (Y-90). *J. Lab. Clin. Med. 45*, 792–799.

(23) Kozak, R. W., Raubitschek, A., Mirzadeh, S., Brechbiel, M. W., Junghauns, R., Gansow, O. A., and Waldmann, T. A. (1989) Nature of the bifunctional chelating agent used for radioimmunotherapy with yttrium-90 monoclonal antibodies: Critical factors in determining in vivo survival and organ toxicity. *Cancer Res. 49*, 2639–2644.

(24) Margerum, D. W., Cayley, G. R., Weatherburn, D. C., and Pagenkopf, G. K. (1978) Kinetics and mechanisms of complex formation and ligand exchange. In *Coordination Chemistry, Monograph 174* (A. E. Martell, Ed.) Vol. 2, Chapter 1, American Chemical Society, Washington, DC.

(25) Brechbiel, M. W. (1988) New bifunctional chelates for radioimmunoimaging and therapy. Ph.D. Thesis, The American University, Washington, DC.
(26) Cummins, C. H., Rutter, E. W., and Fordyce, W. A. (1991) A convenient synthesis of bifunctional chelating agents based on diethylenetriaminepentaacetic acid and their coordination chemistry with yttrium(III). *Bioconjugate Chemistry*, preceding paper in this issue. (We thank the authors for use of their work as a reference in advance of publication.)
(27) Sundqvist, B., and Macfarlane, R. D. (1985) ^{252}Cf-Plasma desorption mass spectrometry. *Mass Spectrom. Rev. 4*, 421–460.
(28) The specific activity increase as ligands were synthesized correlates well with a change in vendor and a change in packaging. The reagent was purchased initially as a solid (1 mCi/ampoule) and gradually replaced with a toluene solution (3 mCi/ampoule).
(29) Westerberg, D. A., Carney, P. L., Rogers, P. E., Kline, S. J., and Johnson, D. K., (1989) Synthesis of novel bifunctional chelators and their use in preparing monoclonal antibody conjugates for tumor imaging. *J. Med. Chem. 32*, 236–243.
(30) Brown, H. C., and Kiem, P. (1973) Selective reductions. XVIII. The fast reaction of primary, secondary, and tertiary amides with diborane. A simple, convenient procedure for the conversion of amides to the corresponding amines. *J. Org. Chem. 38*, 912–916.
(31) Meikle, R. W. (1963) An application of paper electrophoresis to the examination of completeness of reaction and purification in the synthesis of radioactive compounds. *Nature (London) 190*, 61–62.
(32) Floch, L., and Kovac, S. (1975) Synthesis and properties of alkyl isothiocyanatocarboxylates. *Collect. Czech. Chem. Commun. 40*, 2845–2854.
(33) Bara, Y. A., Friedrich, A., Hehlein, W., Kessler, H., Kandor, P., Molter, M., and Veith, H. J. (1978) Synthesis of the cyclic pentapeptides containing 1-phenylalanine and glycine. *Chem. Ber. 111*, 1029–1044.
(34) Lundt, B. F., Johansen, N. L., Vylund, A., and Markussen, J. (1978) Removal of *t*-butyl and *t*-butoxycarbonyl protecting groups with trifluoroacetic acid. *Int. J. Pept. Protein Res. 12*, 258–268.
(35) Mirzadeh, S., Brechbiel, M. W., Atcher, R. W., and Gansow, O. A. (1990) Radiometal labeling of immunoproteins: Covalent linkage of 2-(4-isothiocyanatobenzyl)diethylenetriaminepentaacetic acid ligands to immunoglobulin. *Bioconjugate Chem. 1*, 59–65.
(36) Bly, R. S., Perkins, G. A., and Lewis, W. L. (1922) The preparation of phenylimido-phosgene, and the chlorination of formanilide. *J. Am. Chem. Soc. 44*, 2896–2903.

Bioconjugate Chemistry

JULY/AUGUST 1991
Volume 2, Number 4

© Copyright 1991 by the American Chemical Society

Development of Sensitive Radioiodinated Anti-Sense Oligonucleotide Probes by Conjugation Technique

Mrinal K. Dewanjee,* Abdol K. Ghafouripour, Rudolf K. Werner, Aldo N. Serafini, and George N. Sfakianakis

University of Miami, School of Medicine, Department of Radiology, Division of Nuclear Medicine, Biochemistry and Molecular Biology, Miami, Florida 33101. Received January 4, 1991; Revised Manuscript Received May 6, 1991

Radioactive and nonradioactive oligonucleotide (ON) probes have been used in a variety of studies of in vitro hybridization for locations of specific genes and determination of the level of mRNA transcription in activated and proliferative cells. Nuclease-resistant phosphorothioate derivatives of oligonucleotides are also finding potential therapeutic applications in intact cells and animal models. In this study, we have developed new techniques of radioiodination by the conjugation of oligonucleotides with *p*-methoxyphenyl isothiocyanate (PMPITC) and optimized the conditions of the radioiodination, e.g. concentration of reactants, oxidants, pH, time, and temperature. We have used a 25-mer actin mRNA probe as a model substrate for radioiodination. The ON probe was modified by conjugation with the addition of aminohexyl (AH) group at the 5′-terminal. Both the techniques of preiodination of PMPITC followed by conjugation and radioiodination of PMPITC-conjugated AHON were evaluated; the latter was found to be more convenient. The optimum pH of radioiodination of PMPITC with ^{125}I was 6.5; on the other hand, the optimum pH for PMPITC-conjugated AHON was 8.5. The conditions of conjugation were optimized with ^{125}I-labeled PMPITC. The techniques of paper chromatography and HPLC with a Spherogel column were developed for the purification and characterization of these oligonucleotide probes. Without PMPITC conjugation, the yield of direct radioiodination of the same oligonucleotide was very low (4–6%); the yield in our optimized technique is 50–60%. Radioiodination of conjugated oligonucleotides is a simple and efficient route to radiolabeled probes for hybridization studies.

INTRODUCTION

The base-pairing of adenine with thymine, or cytosine with guanine essential for maintaining the stability of duplex DNA is the basis for specific hybridization of synthetic oligonucleotides to complementary DNA or RNA molecules. Oligonucleotide probes have the ability to distinguish RNA and DNA sequences that differ by a single base (*1–6*). This specificity has led to the synthesis of 15–50-mer oligonucleotides as a tool for molecular biologists to identify and isolate specific gene sequences in bacteria, insects, animal models, and human genetic diseases (*7–22*). Double- and single-stranded DNA, RNA, and synthetic oligonucleotides have been labeled with a variety of radionuclides. The majority of the radiolabeling procedures involve the enzymatic incorporation of ^{3}H-, ^{14}C-, and ^{35}S-labeled nucleotides into the DNA or RNA molecules (*21a,b*). The 5′-OH end of a oligonucleotide can be labeled to a very high specific activity with polynucleotide kinase and [γ-^{32}P]ATP or [^{35}S]ATP (substitution of O by S) and used in Southern, Northern, colony, and plaque hybridization assays (*23–26*). These probes

* Send reprint requests to Mrinal K. Dewanjee, Ph.D., University of Miami, School of Medicine, Division of Nuclear Medicine (D-57), JMH Central C266, P.O. Box 016960, Miami, FL 33101.

1043-1802/91/2902-0195$02.50/0 © 1991 American Chemical Society

can be divided into either uniformly labeled or end-labeled probes. The former are used in the in vitro hybridization assays and the latter also in DNA sequencing. Commerford (*18a*) used the oxidant thallic chloride for the radioiodination of nucleic acids. Due to the hazards of radioiodination procedures and the commercial availability of ^{125}I-labeled nucleoside triphosphates with high specific activity, most investigators prefer these ready-made precursors for the preparation of probes. Iodine-125-labeled oligonucleotides complementary to part of the mRNA coding sequence for rat arginine–vasopressin were prepared by Lewis et al. from ^{125}I-labeled deoxycytidine triphosphate by the primer extension and 3′-tailing methods (*18b*). Piatyszek et al. used the oxidant Iodogen for the direct iodination of nucleic acids (*20*). We prepared these probes to test the hypothesis that they could be used for in vitro and in vivo hybridization in future studies.

Aminolink-2 (phosphoramidite aminohexyl phosphate, Applied Biosystems Inc.) permits introduction at the 5′-end of the oligonucleotide of a primary amine (*16*) which can be coupled with biotin, fluorescent dyes, EDTA and DTPA for labeling with ^{111}In, (hydroxyphenyl)succinimide, or an activated benzene ring for radioiodination with ^{125}I and ^{123}I, and conjugation with the bifunctional chelate containing TcO–N_2S_2 core (*27–40*). We have recently prepared the ^{111}In–DTPA–isothiocyanate-coupled oligonucleotide and demonstrated the potential for noninvasive imaging of histone4 mRNA transcription in a mammary tumor model (*41*).

β-emitting oligonucleotide probes containing ^{32}P or ^{35}S and nonradioactive probes conjugated with biotin or digoxin are widely used in in vitro hybridization experiments. In this study, we describe the development of sensitive hybridization probes labeled with the γ-emitting radionuclide iodine-125 by direct radioiodination of *p*-methoxyphenyl isothiocyanate–aminohexyl(PMPITC–AH)–oligonucleotide conjugate as well as conjugation of radioiodinated PMPITC with the oligonucleotide. The latter radioiodination technique is similar to that of Bolton and Hunter's method for the incorporation of the iodohydroxyphenyl ring into proteins (*27*). We have developed the radioiodinated probes and the techniques of thin-layer and high-performance liquid chromatography for the separation, purification, and characterization of these labeled probes.

EXPERIMENTAL PROCEDURES

Sterile techniques with sterile solutions, plasticware, and glassware were carried out in a laminar-flow hood to prevent bacterial nuclease degradation of the precursors and radiolabeled products.

Synthesis of Aminohexyl-Conjugated Oligonucleotides and Radiolabeling. The base sequence (*8–10*) of the 25-mer anti-sense oligonucleotide probe, specific for the mRNA of β-actin was selected from the nucleic acid data base (GenBank, University of Wisconsin, Madison, WI). This oligonucleotide carrying an aminohexyl group at the 5′-end was synthesized on a DNA synthesizer with the dimethoxytrityl nucleoside phosphoramidite triester coupling method (*9*) on a 10-μmol solid support column (Applied Biosystems Automated Synthesizer, three-column Model 380 B), deprotected, and purified by ion-exchange HPLC (Zorbax Bioseries Oligo column, MacMod Analytical Inc., Chadds Ford, PA); the probe was stored frozen at −20 °C in a microfuge tube. The nucleotide sequence of the 25-mer β-actin probe was as follows:

$H_2N(CH_2)_6OPO_3$-
CC-GTT-GTC-GAC-GAC-GAG-CGC-GGC-GA-OH

Purity of the probes and their stability were further checked by paper and gel-filtration chromatography, HPLC, gel electrophoresis, and autoradiography.

Radioiodination of *p*-Methoxyphenyl Isothiocyanate by the Chloramine-T Technique. Since both the oxidant Iodogen and PMPITC are soluble in nonpolar solvents, we used the oxidant Chloramine-T to facilitate separation of radioiodinated PMPITC (RPMPITC) from the oxidant and free radioiodide. An aliquot of PMPITC (1 mg) from a stock solution of PMPITC (Aldrich Chemical Co. Milwaukee, WI) in chloroform was transferred to a glass tube and solvent was removed by a stream of nitrogen; 100 μg of Chloramine-T (Fisher Scientific Co.) in 100 μL of 0.1 M phosphate buffer (pH = 7.0) and 100 μCi of [^{125}I]-sodium iodide (5–10 μL) was added. The capped vial was ultrasonicated in a water bath for 2 h and the oily drop of PMPITC was converted into an emulsion. Without ultrasonication, the rate of radioiodination was very slow. The reaction was stopped by the addition of 200 μg of sodium metabisulfite in 200 μL of 0.1 M phosphate buffer. The radioiodinated PMPITC was extracted 3 times with a 1-mL aliquot of diethyl ether; 70–80% of RPMPITC was removed in the first extraction. The ether in the sample was allowed to evaporate at room temperature. The RPMPITC was very volatile and should not be heated above 45 °C. The conjugation reaction was carried out directly in the same glass container after dissolving of the sample in DMSO or other appropriate solvent.

Direct Radioiodination of Oligonucleotide with the Oxidants Iodogen and Chloramine-T. The oligonucleotide (50 μg in 5 μL) was transferred to an Iodogen (Pierce Chemcial Co., Rockford, IL) coated tube (100 μg) and the pH was adjusted to 8.5 with 20 μL of 0.1 M phosphate buffer; 100 μCi of ^{125}I (5–10 μL) was added. The mixture was vortexed and incubated for 120 min at 45 °C. The unbound radioiodide was separated by gel filtration with a Spherogel column. Radioiodination was also performed by the Chloramine-T method (100 μg in 100 μL) followed by quenching reaction with 150 μg of sodium metabisulfite (150 μL) under similar conditions of concentration, pH, time, and temperature.

Conjugation of Aminohexyl–Oligonucleotide with ^{125}I-Labeled *p*-Methoxyphenyl Isothiocyanate. Radioiodination was carried out by two techniques: conjugation of iodine-125-labeled 4-*p*-methoxyphenyl isothiocyanate (PMPITC) with aminohexyl–oligonucleotide (AHON) and direct radioiodination of PMPITC-coupled AHON. The primary amino group on this aminohexyl oligomer was conjugated with the isothiocyanate group of PMPITC. The free radioiodide was removed by the molecular sieving technique (TSK-3000 Spherogel column) with a HPLC system (LDC Milton Roy, Vero Beach, FL) and the separated AHON conjugate was stored at −20 °C before use. The radioiodination of conjugated PMPITC–AHON (Figure 2) was carried out with the oxidant Iodogen by the Iodogen-transfer technique (*34*). Iodogen was dissolved in methylene chloride at a concentration of 1 mg/mL and aliquots of 100 μg were transferred to the 1.5-mL polypropylene microfuge tube and vortex-mixed for a uniform coating. The solvent was allowed to evaporate by placing the tubes (overnight) in a chemical hood.

An aliquot of PMPITC in chloroform (1 mg in 0.1 mL) was transferred to a glass tube with a vent. The chloroform was removed under a gentle stream of filtered nitrogen gas; 100 μL of phosphate buffer (0.1 M, pH = 7.0) was added and vortex-mixed for 10 s. The AHON (5 μL, 50 μg from a stock solution of 10 μg/μL) was added and vortex-mixed for 1 min and the mixture was incubated at 45 °C for 24 h. The unreacted PMPITC was separated on a

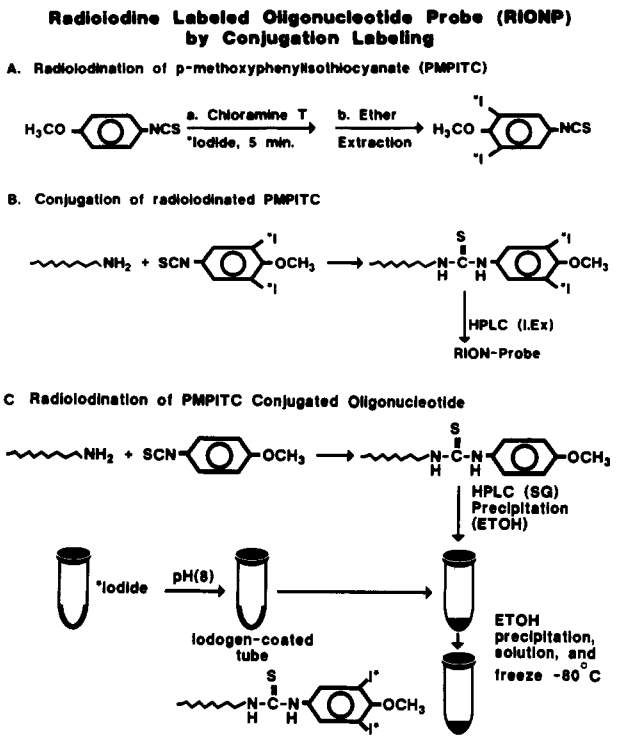


Figure 1. The scheme of radiodination of the oligonucleotide by two techniques: (A) radioiodination of PMPITC, (B) conjugation of ^{125}I-labeled RPMPITC with AH–oligonucleotide, and (C) radioiodination of PMPITC-conjugated aminohexyl–oligonucleotide.

Spherogel column. The PMPITC–AHON conjugate was lyophilized and stored frozen at −20 °C.

High-Pressure Liquid Chromatography of Radioiodinated PMPITC–Oligonucleotide. Radioiodinated PMPITC and PMPITC–AHON conjugates were purified by HPLC (LDC Milton Roy) using a TSK-3000 Spherogel molecular sieve column. The column was eluted with the 0.06 M phosphate-buffered saline (0.3 M NaCl, pH = 7.06) at a flow-rate of 1 mL/min and the absorbance of eluent was monitored at 254 nm (Spectromonitor III, LDC Milton Roy).

The conditions of conjugation of PMPITC with AHON were evaluated and the optimization of radioiodination of AHON was carried out with triplicate samples, at different stoichiometry of PMPITC/AHON, time, temperature, and pH values.

Effect of pH on the Radioiodination of PMPITC–Aminohexyl–Oligonucleotide Conjugate. The PMPITC conjugated to AHON at a stoichiometry of 1000/1, was radioiodinated (*19, 20*) with the Iodogen technique; 100 μCi of ^{125}I was added to the Iodogen-coated (100 μg, Pierce Co.) polypropylene tube and incubated for 60 min at room temperature in 100 μL of phosphate buffer (0.1 M) at a pH of 8.5. The labeling efficiency, estimation of the progress of the labeling reactions and optimizations of all labeling conditions were checked by the TLC (phosphated cellulose, Whatman P81) with 2 M sodium acetate in 95% 2-propanol. The R_f values of labeled PMPITC–oligonucleotide conjugate and radioiodide are 0.1 and 0.7, respectively.

Effect of Incubation Time on the Radioiodination of PMPITC–Aminohexyl–Oligonucleotide Conjugate. Aliquots of PMPITC–AH–oligonucleotide conjugate (50 μg) in triplicate were incubated with 100 μCi of ^{125}I in 0.1 M phosphate buffer (pH = 8.5) and 100 μg of Iodogen at room temperature for various time intervals, and the progression of radioiodination was checked by paper chromatography as described before.

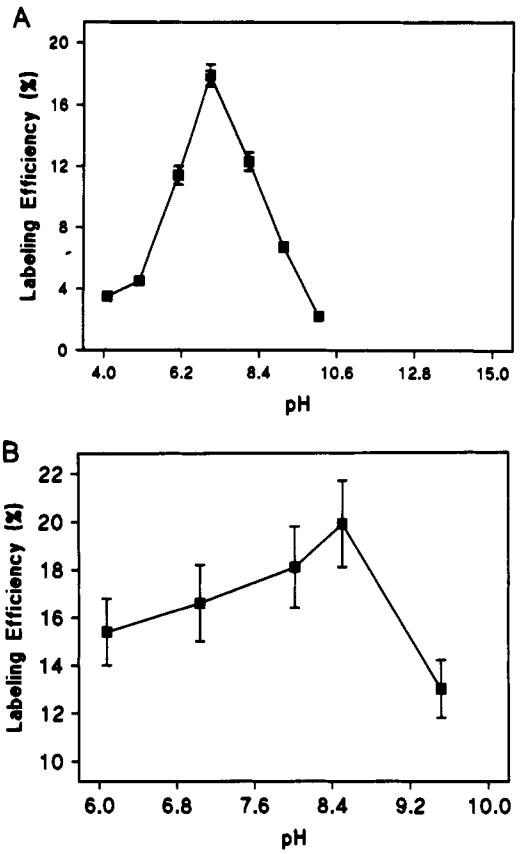


Figure 2. (A) Effect of pH on radioiodination of PMPITC with ^{125}I (100 μCi) and oxidant chloramine-T (100 μg in phosphate buffer); (B) effect of pH on the radioiodination of PMPITC-conjugated with 25-mer oligonucleotide actin mRNA probe. The oxidant Iodogen (100 μg) was used in this experiment. The radioiodination was carried out at room temperature with a PMPITC/AHON stoichiometry of 1000/1.

Effect of Stoichiometry on Conjugation of Radioiodinated PMPITC to Aminohexyl–Oligonucleotide. Different amounts of PMPITC were radioiodinated by the Chloramine-T (100 μg) method. The ether-extracted RPMPITC (100 μCi) was then conjugated with 50 μg of AH–oligonucleotide in 300 μL of 0.1 M phosphate-buffered saline at 45 °C for 60 min and at PMPITC/AHON ratios of 10, 50, 100, 200, and 500. Higher temperature (>45 °C) was avoided due to the higher volatility of PMPITC and the possibility of hydrolysis of the isothiocyanate group. The labeling efficiency was calculated for each experiment by measurement of radioactivity in the original and final sample with an ionization chamber (CRC-5RH3, Capintec Inc.).

Effect of Radioiodination on Stoichiometry of PMPITC–Aminohexyl–Oligonucleotide Conjugate. The PMPITC–AH–oligonucleotide conjugates were prepared from 50 μg of AH–oligonucleotide at 45 °C for 24 h using a 10-, 50-, 100-, 200-, 500-, 1000-, and 5000-fold excess of PMPITC; the radioiodinations were carried out with Iodogen (100 μg) at a pH of 8.5 (phosphate buffer) at room temperature for 60 min. The labeling efficiency was calculated from the initial and final radioactivity for each experiment as before.

RESULTS

The schemes of radiodination of the oligonucleotide by two techniques are described in Figure 1. The different parameters of the conjugation of PMPITC with AHON and the optimization of radioiodination of PMPITC and PMPITC–AHON are shown in Figures 2–6. Figure 2, parts a and b, indicate that the labeling efficiency of PMPITC

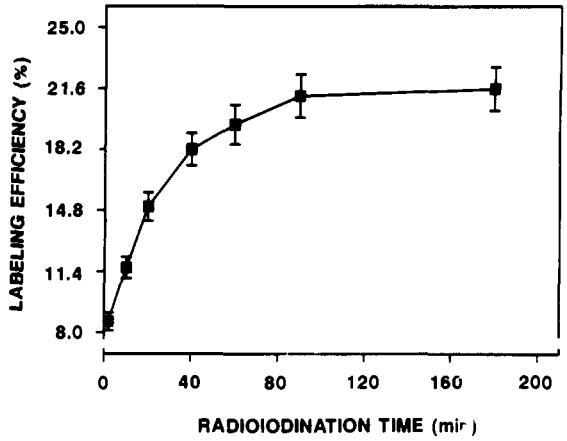


Figure 3. Effect of reaction time on radioiodination of RPMPITC-conjugated oligonucleotide probe (50 μg in phosphate buffer, pH = 8.5). The reaction was carried out with 100 μg of iodogen at room temperature.

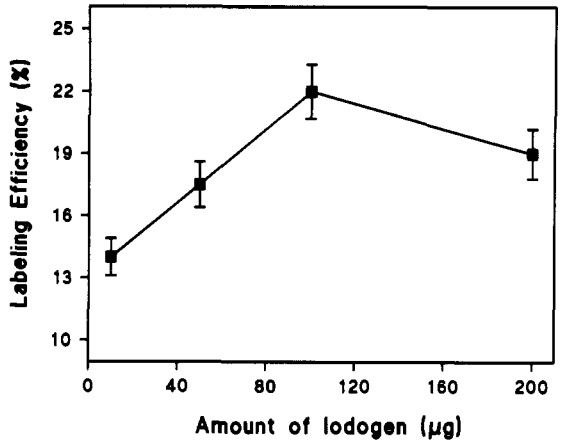


Figure 4. Effect of amount of iodogen (100 μg) on the radioiodination of conjugated PMPITC–aminohexyl–oligonucleotide (50 μg) at room temperature.

and the AHON conjugate is dependent on pH of the incubation media; the optimum pH of radioiodination of PMPITC–AHON conjugate is 8.5 (Figure 2b); on the other hand, it is lower (pH = 7.1) for PMPITC (Figure 2a). At lower and higher pH values, the labeling efficiency decreases. Hence, all the conjugation reactions were carried out at a pH of 8.5 in phosphate-buffered saline. The optimum time of incubation of radioiodide with PMPITC-conjugated oligonucleotide is about 60 min or more (Figure 3); the labeling efficiency almost reaches a saturation value at about 90 min. Figure 4 indicates that labeling of conjugate is optimum at 100 μg of Iodogen; higher amounts may result in oxidative degradation. Figure 5 indicates that a higher ratio of PMPITC/AHON gives greater labeling efficiency. The conjugation of radioiodinated PMPITC to AH–oligonucleotide is slower than radioiodination of conjugated AH–oligonucleotide. The labeling efficiency also increases with higher ratio of PMPITC conjugation to AH–oligonucleotide (Figures 5 and 6). At higher stoichiometry of PMPITC/AH–oligonucleotide, the labeling efficiency increases with time of incubation; at higher stoichiometry, the labeling efficiency is much higher. Without conjugation with PMPITC, the yields of radioiodination with both oxidants, Iodogen and Chloramine-T, were very low (4–6%). The PMPITC conjugation thus increases the specific activity of labeled oligonucleotide by a factor of 10.

Similar results were obtained for the thiourea-bond formation between DTPA–isothiocyanate and lysine groups of antibody (*36, 40*). The schematics of the two techniques

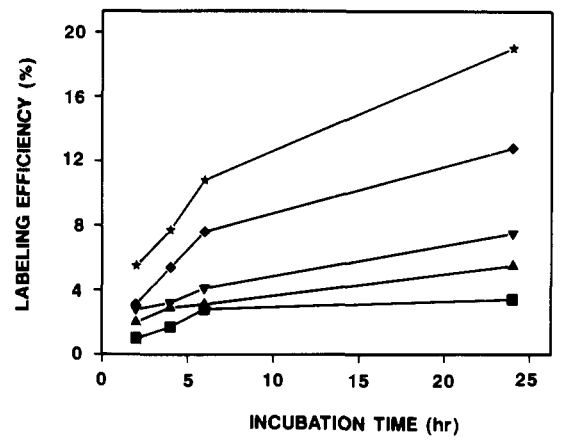


Figure 5. Effect of reaction time on the conjugation of radioiodinated PMPITC to AHON at different stoichiometry (■, 10/1; ▲, 50/1; ▼, 100/1; ◆, 200/1 and ★, 500/1) of RPMPITC/oligonucleotide at 45 °C. The free RPMPITC was separated after conjugation by gel filtration. The RPMPITC was radioiodinated with 100 μg of Chloramine-T at pH 7.0 and the radioiodination was quenched by addition of 200 μg of sodium metabisulfite.

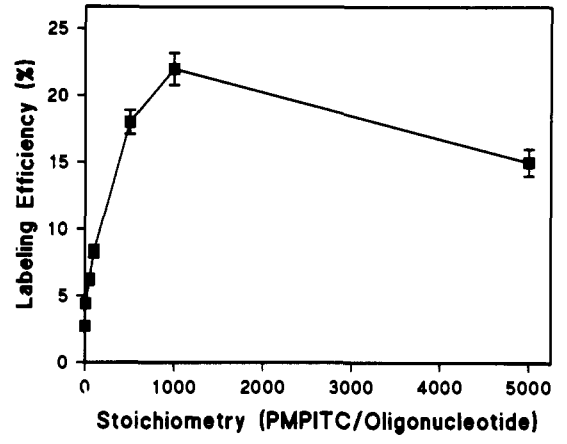


Figure 6. Effect of stoichiometry of PMPITC-conjugated oligonucleotide on radioiodination. The PMPITC was conjugated to AHON and radiodinated by Iodogen (100 μg) at 45 °C for 24 h in phosphate buffer.

of radioiodination are shown in Figure 1a–c. Method C was also convenient to label tyrosine-less protein (*42*), peptides, and nucleosides, as well as oligonucleotides (*41*). The PMPITC-conjugated AH–oligonucleotide could be separated by gel-filtration or precipitation from absolute ethanol and subsequently radioiodinated by the nucleophilic substitution. The conjugation of radioiodinated PMPITC to nucleoside was found to be more convenient; in this procedure the unconjugated radioiodinated PMPITC could be separated easily from the labeled nucleoside by ether extraction, and radioiodination could be carried out in one step. The labeling efficiency with the two-step Bolton–Hunter technique is always lower (15–30%) and time-consuming. The HPLC chromatogram of the radioiodinated PMPITC–AHON conjugate is shown in Figure 7. The incorporation of PMPITC into AH–oligonucleotide increases the lipophilicity as indicated by the higher retention time of the labeled PMPITC–AHON conjugate over the absorbance peak of the oligonucleotide alone. The full-width at half-maximum of the peak of radiolabeled PMPITC is also high, suggesting strong adsorption to the matrix of the Spherogel column.

DISCUSSION

Commerford used the toxic oxidant thallic chloride for iodination of nucleic acids (*18a*). The drawback of this

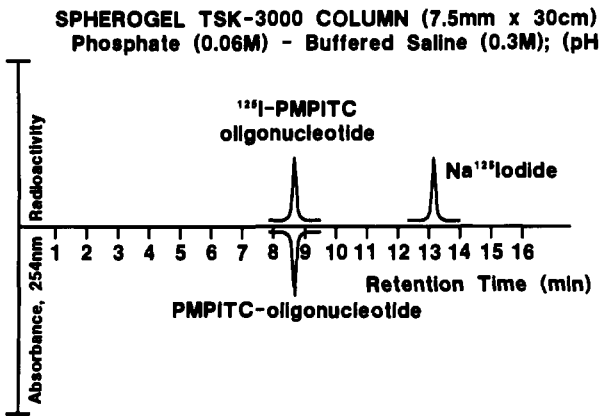


Figure 7. HPLC chromatogram of the ^{125}I-labeled oligonucleotide on a Spherogel column eluted with phosphate-buffered saline.

technique of heating at 60 °C with the heavy metal is the possible resulting degradation of nucleic acid. Piatyszek et al. (*19*) used the oxidant Iodogen (*20*) for the direct radioiodination of tRNA. Previous studies indicated the higher stability of a C–I bond in the benzene ring (*28, 35*) than in the heterocyclic rings (uridine, guanidine, and cytosine). In addition, the stability of the thiourea bond formed between the amino group of aminohexyl–oligonucleotide and isothiocyanate may be more stable in vivo than the peptide linkage formed by the acylating agent of radioiodinated (hydroxyphenyl)succinimide (*27, 35*) to amino group of lysine as used in the conventional Bolton–Hunter technique. The conjugation technique we developed increases the specific activity of radioiodinated AHON conjugate to higher than 10 mCi/mg of oligonucleotide. This could be raised to higher values by increasing the stoichiometry of PMPITC/AHON. The shelf life of the probes at high specific activity may be lower. We believe that due to the more reactive sites for two iodine substitutions at each PMPITC group, more radioiodine will be incorporated at the substituted benzene ring than at the heterocyclic rings of the purines and pyrimidines. Without PMPITC conjugation, only 4–6% of the ^{125}I may be incorporated in the bases of the AHON. The PMPITC conjugation labeled under optimum conditions thus increases the specific activity of labeled oligonucleotide by a factor of 10 over that obtained by direct iodination.

Higher PMPITC/AHON stoichiometry and a higher degree of radioiodine incorporation may also increase the steric hindrance, resulting in reduced helix stability (*21*) of the hybridized probe to the mRNA transcript. We also observed poorer coupling of PMPITC with single nucleoside (unpublished data) than with AHON conjugates, suggesting that terminal conjugation does occur preferentially to that of the side-chain amino groups of the bases. The radioiodinated PMPITC provided an ideal tracer for the optimization of the conditions of conjugation of isothiocyanate-containing moiety to peptide, proteins (*42*), and oligonucleotides (*41*). Further studies are in progress to evaluate the role of specific activity on the efficiency of hybridization and turnover rate of radiolabeled AHON probes containing phosphodiester, phosphoramidate, and phosphothioate bonds. The exact roles of these derivatives of oligonucleotides in the in vivo diagnosis and therapy are not yet defined; considering the toxicity of the relatively stable phosphoramidate and phosphothioate, they also may be more toxic (*26, 31*).

Although the β-emitting radionuclides of ^{32}P and ^{35}S had been used extensively for labeling the oligonucleotide probes for in vitro hybridization studies, the γ-emitting iodine-125 probes will be more sensitive and easier to use for in vitro measurements and ^{123}I-, ^{111}In-, and ^{99m}Tc-labeled ON probes will provide a new avenue of in vivo hybridization for the detection of DNA alteration, proliferation (*41*), and cell necrosis. Since the phosphodiester bond is unstable in vivo, due to nuclease sensitivity, we have been comparing the imaging potential of the phosphodiester and phosphorothioate derivatives as model probes (*41*). The techniques of labeling of these derivatives were found to be similar to that of the oligonucleotide probes we had described in this study. Preliminary results with the radioiodinated anti-sense oligonucleotides show high specific activity and comparable hybridization efficiency with the β-actin mRNA as the ^{32}P-labeled probes. The in vivo stability of the radioiodinated AHON probes was acceptable; this may be due to the steric hindrance of methoxy group of PMPITC to the dehalogenase enzyme. The ease of handling of these γ-emitting probes will expedite their use in mechanistic and diagnostic applications. Although the protein product of a gene can be detected by biochemical or immunochemical methods, the use of labeled antibodies had been criticized for the lack of specificity. The specificity of the AHON-probes far exceeds that of antibodies and the intensity of the specific mRNA is directly related to gene activity. In addition, during the replication phase, the mRNA level in proliferative cells is 20–100-fold higher than that of resting cells, indicating a high probability of detection due to high signal/noise ratios in malignant tissues.

Several syntheses of specific bifunctional chelating agents will permit the radiolabeling of oligonucleotide with the γ-emitting radionuclides of ^{111}In and ^{99m}Tc (*35–40*). Although cell permeability of labeled probe may be a limiting factor in the study of proliferation, the ease of accessibility in infarcted myocardium should facilitate the use in the detection of myocardial ischemia and infarction (*32, 33*). These new radiolabeled γ-emitting probes will provide new applications in the understanding of oligonucleotide transport, turnover, and localization in altered, proliferative, and damaged cells. These probes when labeled with α- and β-emitting radionuclides may also provide information about microdosimetry, radiation biology, and radiation therapy.

ACKNOWLEDGMENT

We highly appreciate the supports of DOE DE-FG05-88ER60728, Baxter Healthcare Corp., and Florida High Tech and Industry Council, encouragement of Dr. Catherine A. Poole, Chairperson, Radiology, during the writeup of this article, and photographic assistance of Mr. Bob and Bill Burke.

LITERATURE CITED

(1) Lum, J. B. (1986) Visualization of mRNA transcription of specific genes in human cells and tissues using in situ hybridization. *BioTechniques 4*, 32–39.

(2) Sambrook, J., Fritsch, E. F., and Maniatis, T. (1989) Synthetic oligonucleotide probes. In *Molecular Cloning, A Laboratory Manual*, Vol 2, Chapter 11, pp 11.3–11.58, Cold Spring Harbor Laboratory Press, New York.

(3) Davis, L. G., Dibner, M. D., and Battey, J. F. (1989) *Basic Methods in Molecular Biology*, New York Elsevier Press, pp 75–78, 147–156, 355–359.

(4) Southern, E. M. (1975) Detection of specific sequences among DNA fragments separated by electrophoresis. *J. Mol. Biol. 98*, 503–517.

(5) Doel, M. T., and Smith, M. (1973) The chemical synthesis of deoxyribo-oligonucleotides complementary to the lysozyme gene of phage T4 and their hybridization to phage specific RNA phage DNA. *FEBS Lett. 34*, 99–102.

(6) Khorana, H. G. (1979) Total synthesis of a gene. *Science 203*, 614–625.
(7) Grunstein, M., and Hogness, D. S. (1975) Colony hybridization: A method for the isolation of cloned DNAs that contain a specific gene. *Proc. Natl. Acad. Sci. U.S.A. 72*, 3961–3965.
(8) Connolly, B. A. (1987) The synthesis of oligonucleotides containing a primary amino group at the 5′-terminus. *Nucleic Acids Res. 15* (7), 3131–3139.
(9) Matteucci, M. D., and Caruthers, M. H. (1981) Synthesis of deoxyoligonucleotides on a polymer support. *J. Am. Chem. Soc. 103*, 3185–3191.
(10) Nakajima-Iijima, S., Hamada, H., Reddy, P., and Kakunaga, T. (1985) Molecular structure of the human cytoplasmic beta-actin gene: interspecies homology of sequences in the introns. *Proc. Natl. Acad. Sci. U.S.A. 82*, 6133–6137.
(11) Smith, L. M., Sanders, J. Z., Kaiser, R. J., Hughes, P., Dodd, C., Connell, C. R., Heiner, C., Kent, S. B. H., and Hood, L. E. (1986) Fluorescence detection in automated DNA sequence analysis. *Nature 321*, 674–678.
(12) Ross, J. (1989) The turnover of messenger RNA. *Sci. Am.* 48–55.
(13) Chirgwin, J. M., Przybyla, A. E., MacDonald, R. J., and Rutter, W. J. (1979) Isolation of biologically active ribonucleic acid from sources enriched in ribonuclease. *Biochemistry 18*, 5294–5299.
(14) White, B. A., and Bancroft, F. C. (1982) Cytoplasmic dot hybridization. Simple analysis of relative mRNA levels in multiple cell or tissue samples. *J. Biol. Chem. 257*, 8569–8573.
(15) Aviv, H., and Leder, P. (1972) Purification of biologically active globin messenger RNA on oligo–thymidylic acid–cellulose column. *Proc. Natl. Acad. Sci. U.S.A. 69*, 1048–1052.
(16) Salalila, B. Aminolink-2, User Bulletin No. 49, private communications, Applied Biosystems.
(17) Pulaski, S. P., and Hatzenbuhler, N. T. (1989) Investigations of columns and conditions for the large scale HPLC purification of oligodeoxyribonucleotides. *BioChromatography* 41–45.
(18) (a) Commerford, S. L. (1971) Iodination of nucleic acids in vitro. *Biochemistry 10*, 1993–1999. (b) Lewis, M. E., Arentzen, R., and Baldino, F. (1986) Rapid, high resolution in situ hybridization histochemistry with radioiodinated synthetic oligonucleotides. *J. Neurosci. Res. 16*, 117–124.
(19) Piatyszek, M. A., Jarmolowski, A., and Augustyniak, J. (1988) Iodo-Gen mediated radioiodination of nucleic acids. *Anal. Biochem. 172*, 356–359.
(20) Fraker, P. J., and Speck, J. C. (1978) Protein and cell membrane iodinations with a sparingly soluble chloramide, 1,3,4,6,3a,6a-diphenylglycoluril. *Biochem. Biophys. Res. Commun. 80*, 849–857.
(21) (a) Hames, B. D., and Higgins, S. J. (1985) Quantitative analysis of solution hybridization. In *Nucleic Acid Hybridization*, pp 47–71, IRL Press, Oxford. (b) Lewis, M. E., and Baldino, F. (1990) Probes for in situ hybridization histochemistry. Chapter 1, In *In Situ Hybridization Histochemistry* Ed. (M.-F. Chesselet, Ed.) pp 1–21, CRC Press, Boca Raton, FL.
(22) Hodges, R. R., Conway, N. E., and McLaughlin, L. W. (1989) "Postassay" covalent labeling of phosphorothioate-containing nucleic acids with multiple markers. *Biochemistry 28* (1), 261–267.
(23) Plagemann, P. G. W., and Woffendin, C. (1989) Permeation and salvage of dideoxyadenosine in mammalian cells. *Mol. Pharm. 36*, 185–192.
(24) Walder, J. (1988) Anti-sense DNA and RNA: progress and prospects. *Genes Dev. 2*, 502–504.
(25) Lawrence, J. B., and Singer, R. H. (1986) Intracellular localization of messenger RNAs for cytoskeletal proteins. *Cell 45*, 407–415.
(26) Miller, P. S. (1989) Nonionic Antisense Oligonucleotides. In *Oligonucleotides as Inhibitors of Gene Expression* (J. Cohen, Ed.) The Macmillan Press, Ltd., London.
(27) Bolton, A. E., and Hunter, W. M. (1973) The labeling of proteins to high specific radioactivities by conjugation to a I-125 containing acylating agent: application to the radioimmunoassay. *Biochem. J. 133*, 529–539.
(28) Dewanjee, M. K. (1991) Radioiodination: Theory, Practice, and Biomedical Applications. Kluwer Academic Publishers, Inc., Boston. Dewanjee, M. K. (1989) *Ind. J. Nucl. Med. 4* (3) 162–174.
(29) Assony, S. J. (1961) The Chemistry of Isothiocyanates. In *The Chemistry of Organic Sulfur Compounds* (N. Kharasch and C. Y. Meyers, Eds.) pp 326–338, Pergamon Press, New York.
(30) Ghosh, S. S., Kao, P. M., McCue, A. W., and Chappellee, H. L. (1990) Use of maleimide–thiol coupling chemistry for efficient syntheses of oligonucleotide–enzyme conjugate hybridization probes. *Bioconjugate Chem. 1*, 71.
(31) Goodchild, J. Conjugates of oligonucleotides and modified oligonucleotides: a review of their synthesis and properties. *Bioconjugate Chem. 1*, 165–187.
(32) Dewanjee, M. K., and Kahn, P. C. (1976) Mechanism of localization of Tc-99m tetracycline and Tc-99m pyrophosphate in myocardial infarct. *J. Nucl. Med. 17*, 639–646.
(33) Dewanjee, M. K. and Prince, E. (1974) Cellular necrosis model in tissue culture. Uptake of Tc-99m tetracyclines and pertechnetate ion. *J. Nucl. Med. 15*, 577–581.
(34) Dewanjee, M. K., Singh, S. K., Wooley, P. H., Mackey, S. T., Solis, E., and Kaye, M. P. (1986) Identification of new collagen formation with 125-iodine labeled antibody in bovine pericardial tissue valves implanted in calves. *Nucl. Med. Biol., Int. J. Radiat. Appl. Instrum., Part B 13* (4), 413–422.
(35) (a) Srivastava, P. C., Knapp, F. F., Karl, D. W., and Mills, D. C. B. (1986) *N*-(*p*-iodophenyl)maleimide, a new radioiodinated thiol reagent with selective effects on platelet membrane functions. *J. Nucl. Med. 27*, 1046. (b) Srivastava, P. C., Buchsbaum, D. J., Allred, J. F., Brubaker, P. J., Hanna, D. E., and Spicker, J. K. (1990) A new conjugating agent for radioiodination of proteins; low in vivo deiodination of a radiolabeled antibody in a tumor model. *BioTechnique 8*, 536–545.
(36) Meares, C. F., McCall, M. J., Reardan, D. T., Goodwin, D. A., Diamanti, C. I., and McTigue, M. (1984) Conjugation of antibodies with bifunctional chelating agents: Isothiocyanate and bromoacetamide reagents, methods of analysis and subsequent addition to metal ions. *Anal. Biochem. 142*, 68–78.
(37) Dewanjee, M. K. (1990) The chemistry of Tc-99m labeled radiopharmaceuticals. *Semin. Nucl. Med. XX* (1), 5–27.
(38) Hnatowich, D. J., and McGann, J. (1987) DTPA-coupled proteins—procedures and precautions. *Int. J. Appl. Instrum. Part B 14*, 563–568.
(39) Fritzberg, A. R., Abrams, P. G., Beaumier, P. L. (1988) Specific and stable labeling of antibodies with technetium-99m using a diamide dithiolate (N_2S_2) chelating agent. *Proc. Natl. Acad. Sci. U.S.A. 85*, 4025–4029.
(40) Mirzadeh, S., Brechbiel, M. W., Atcher, R. W., and Gansow, O. A. (1990) Radiometal labeling of immunoproteins: covalent linkage of 2-(4-isothiocyanatobenzyl)diethylenetriaminepentaacetic acid ligands to immunoglobulin. *Bioconjugate Chem. 1*, 59–65.
(41) Dewanjee, M. K., Ghafouripour, A. K., Kapadvanjwala, M., Werner, R. K., Ganz, W. I., Serafini, A. N., Sfakianakis, G. N., Lopez, D. M. (1990) Non-invasive imaging of histone4 mRNA transcription in mammary tumor with In-111 labeled aminohexyloligonucleotide in a mouse model. Miami Winter Symposium on BioTechnology; Advances in Gene Technology: The Molecular Biology of Human Genetic Diseases, Miami, FL (Abstract); Vol 1, 137.
(42) Dewanjee, M. K., Ghafouripour, A. K., Ganz, W. I., McCarthy, K., Serafini, A. N., Sfakianakis, G. N. (1990) Radioiodination of proteins by a new conjugation technique with activated methoxyphenylisothiocyanate. *J. Nucl. Med. 31*, 907.

Registry No. PMPITC, 2284-20-0; 2,5-[125-I]$_2$-PMPITC, 134360-29-5; $H_2N(CH_2)_6OP(O)(OH)OCCGTTGTCGACGACGAGCGCGGCGAOH$, 134528-72-6.

Oxidative Degradation of Cationic Metalloporphyrins in the Presence of Nucleic Acids: A Way to Binding Constants?[1]

Li Ding, Jean Bernadou,* and Bernard Meunier*

Laboratoire de Chimie de Coordination du CNRS, 205 Route de Narbonne, 31077 Toulouse Cedex, France.
Received February 23, 1991; Revised Manuscript Received May 6, 1991

Mn(III) and Fe(III) complexes of *meso*-tetrakis(*N*-methylpyridinium-4-yl)porphyrin (M-TMePyP) and related hybrid molecules ("metalloporphyrin-ellipticine") were activated by potassium monopersulfate in the presence of variable calf thymus (CT) DNA and NaCl concentrations. Monitored by visible spectroscopy (Soret band), fast degradation of the free metalloprophyrin was observed while the DNA-bound form appeared protected. This direct quantitation of free versus bound metalloporphyrin ratios allowed determination of binding constants: Mn- and Fe-TMePyP respectively bind to CT DNA (5 mM phosphate buffer, 0.1 M NaCl, pH 7) with $K = 3 \times 10^4$ and 1.2×10^4 M^{-1}. Mn-TMePyP showed a greater affinity for poly[d(A-T)] ($K = 1.2 \times 10^5$ M^{-1}) than for poly[d(G-C)] ($K = 0.2 \times 10^4$ M^{-1}). This method allowed us access to the intrinsic DNA affinity of the metalloporphyrin moiety of the hybrid molecules "metalloporphyrin-ellipticine".

Iron(III) and manganese(III) derivatives of *meso*-tetrakis(*N*-methylpyridinium-4-yl)porphyrin are efficient DNA cleavers after activation in the presence of O_2 and a reducing agent (Fiel et al., 1982; Aft & Mueller, 1983) or in the presence of an oxygen atom donor such as iodosylbenzene (Ward et al., 1986b), potassium monopersulfate (Fouquet et al., 1987; Bernadou et al., 1989a,b; Pratviel et al., 1989), or magnesium monoperphthalate (Pratviel et al., 1989). So they are of interest because of their potential as nucleic acids probes (Van Atta et al., 1990) or as tools in DNA- or RNA-footprinting experiments (Dabrowiak et al., 1989); moreover, after coupling of the metalloporphyrin with an intercalating agent (Ding et al., 1989, 1990a,b, 1991) or an oligonucleotide, they might have a future as antitumor or antiviral drugs.

Investigating the structure-activity relationships in this series of metalated water-soluble porphyrins, we examined their DNA-binding properties. For intercalating agents, the determinations of association constants by the ethidium displacement method and other classical methods (spectrophotometry, equilibrium dialysis) are in excellent agreement (Baguley et al., 1981). Recent studies (Marzilli, 1990; Pasternack et al., 1983; Sari et al., 1990; Strickland et al., 1988) on the interactions of Fe-TMePyP and Mn-TMePyP with nucleic acids have shown that they bind electrostatically in the minor groove specifically at AT regions. The paramagnetism of these two latter complexes does not allow NMR studies to ascribe precise binding sites as established for diamagnetic metalloprophyrins (Strickland et al., 1989). For metalloporphyrins covalently linked to an intercalating agent like ellipticine (in fact 9-methoxyellipticine), interaction with DNA probably associates intercalation (ellipticine) with outside binding to DNA (metalloporphyrin) (Ding et al., 1991). These considerations may explain difficulties in obtaining apparent equilibrium constants (K) spectroscopically due to the minimal change in the spectrum of these nonintercalating metalloporphyrins upon addition of DNA (Pasternack et al., 1983). Competitive binding with ethidium bromide (Sari et al., 1990) gives relative values as it reflects only the ability of the molecule to prevent intercalation of ethidium bromide into DNA. Data are also available by the equilibrium dialysis technique, but it is a time-consuming method requiring a very careful experimental approach.

In the present work, we report the easy and fast determination of binding constants of Mn(III) and Fe(III) complexes of various cationic porphyrins and related compounds by chemical activation in the presence of calf thymus DNA. A similar approach has been very recently proposed by Rodriguez et al. (1990) using an electrochemical activation. Inhibition of 1,10-phenanthroline-cupric ion reduction by DNA allows the determination of DNA binding constants and it constitutes another example of determination of DNA binding constants by chemical activation (Thederahn et al., 1989).

EXPERIMENTAL PROCEDURES

Materials. Potassium monopersulfate, available as the triple salt $2KHSO_5$, $KHSO_4$ and K_2SO_4, was purchased from Janssen or Alfa Ventron. Calf thymus DNA was purchased from Sigma; poly[d(A-T)] and poly[d(G-C)] were obtained from Pharmacia; concentrations, always calculated in base pairs (bp), were determined spectrophotometrically with $\epsilon_{260nm} = 1.31 \times 10^4$ M^{-1} cm^{-1} for CT DNA, $\epsilon_{262nm} = 1.32 \times 10^4$ M^{-1} cm^{-1} for poly[d(A-T)] and $\epsilon_{254nm} = 1.68 \times 10^4$ M^{-1} cm^{-1} for poly[d(G-C)] (Pasternack et al., 1983).

Spectrometry. Spectral measurements were carried out on a Varian-Cary 2300 spectrophotometer using a 10-mm quartz cuvette.

Porphyrins and Complexes (Figure 1). 5-(4-Nitrophenyl)-10,15,20-tris(4-pyridyl)porphyrin was prepared by condensation of mixtures of 4-nitrobenzaldehyde, 4-pyridinecarboxaldehyde, and pyrrole (all chemicals from Aldrich) by standard procedures (Ding et al., 1990b). 5-(4-Aminophenyl)-10,15,20-tris(4-pyridyl)porphyrin was obtained by reduction of the nitro group of 5-(4-nitrophenyl)-10,15,20-tris(4-pyridyl)porphyrin by stannous chloride in acid medium. The metalation was carried out in DMF with a large excess of manganese acetate at reflux

[1] Abbreviations used: H_2TMePyP, *meso*-tetrakis(*N*-methylpyridinium-4-yl)porphyrin; Mn-TMePyP and Fe-TMePyP, manganese(III) and iron(III) complexes of H_2TMePyP; Mn-Por(MePy)$_3$(PhNO$_2$), Mn-Por(MePy)$_3$(PhN$^+$Me$_3$), Mn-InC$_7$, Mn-InC$_{11}$, and Mn-InC$_{12}$; see structures of Figure 1; CT DNA, calf thymus DNA; poly[d(A-T)], polydeoxyadenylic acid-thymidylic acid; poly[d(G-C)], polydeoxyguanylic acid-deoxycytidylic acid; bp, base pair; DMF, dimethylformamide; EB, ethidium bromide.

* To whom correspondence should be addressed.

1043-1802/91/2902-0201$02.50/0 © 1991 American Chemical Society

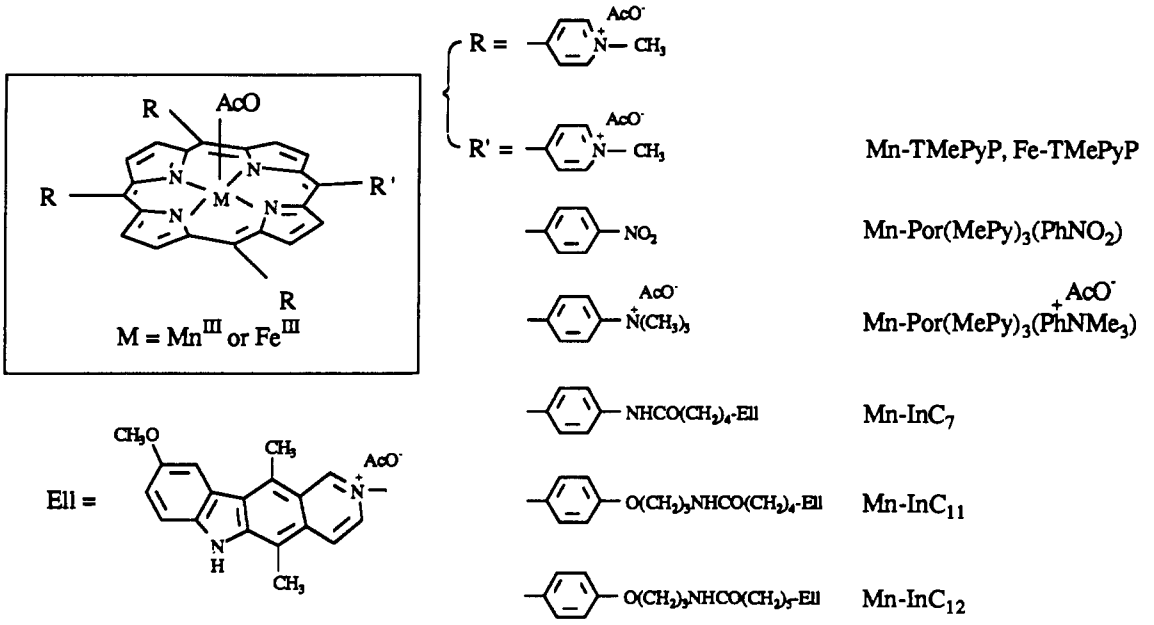


Figure 1. Structures of metalloporphyrin derivatives.

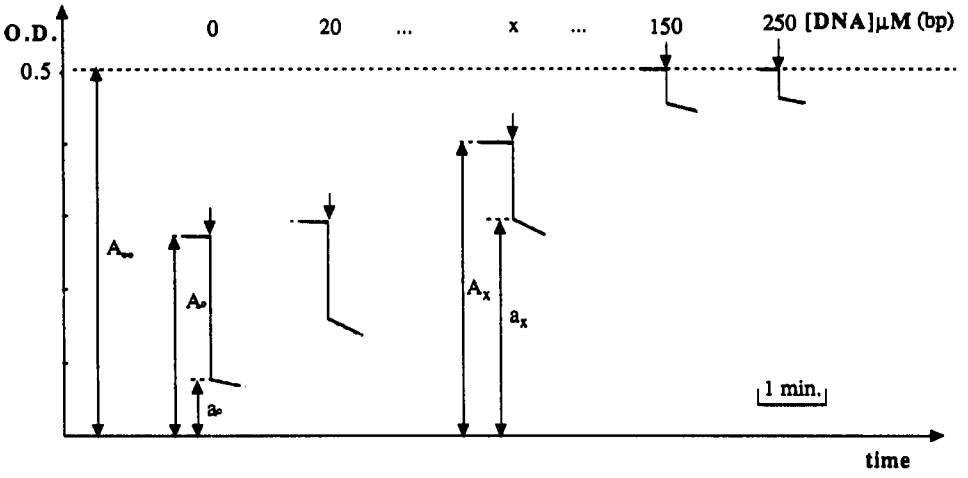


Figure 2. Influence of a range of CT DNA concentration on the Soret band of Mn-TMePyP and its degradation in the presence of $KHSO_5$. All OD decays occurred within 12 s. (↓): addition of $KHSO_5$ in the reaction medium.

for 2–3 h. The methylation reaction was performed in DMF solution in the presence of a large excess of methyl iodide overnight at room temperature. The iron and manganese tetrakis(*N*-methylpyridinium-4-yl)porphyrin, manganese 5-(4-nitrophenyl)-10,15,20-tris(*N*-methylpyridinium-4-yl)porphyrin and manganese 5-[4-(trimethylamino)phenyl]-10,15,20-tris(*N*-methylpyridinium-4-yl)-porphyrin were obtained according to methods previously described (Bernadou et al., 1989a; Ding et al. 1989).

Hybrid "Manganese–Porphyrin–Ellipticine" Molecules. They were prepared by the coupling between N_2-(4-carboxybutyl)-9-methoxyellipticinium chloride or N_2-(5-carboxypentyl)-9-methoxyellipticinium chloride and 5-(4-aminophenyl)-10,15,20-tris(4-pyridyl)porphyrin or 5-[4-[(3-aminopropyl)oxy]phenyl]-10,15,20-tris(4-pyridyl)-porphyrin followed by metalation and methylation reaction; their detailed preparations are published elsewhere (Ding et al., 1991).

Determination of Metalloporphyrin–DNA Association Constants (Table I). The degradation of manganese (or iron) porphyrins or hybrid "manganeseporphyrin–ellipticine" molecules was assayed with the mixture of 5 μM metalloporphyrin or hybrid "Mn–porphyrin–ellipticine" molecule, 0–500 μM calf thymus DNA or poly[d(A-T)] or poly[d(G-C)], and indicated concentrations of NaCl (0–200 mM) in 5 mM phosphate buffer (pH 7) with a preincubation period of 30 min at room temperature in 2-mL glass test tubes. Then, the reaction mixture (3 mL) was transferred to a 10-mm cuvette and the reaction was initiated by adding 200 μM $KHSO_5$ (50 μL, 12 mM). The absorption change at the Soret band of the manganese porphyrin was recorded every 12 s. The binding constants were determined as follows.

Considering the binding of a metalloporphyrin, P, to a binding site, S, located on the duplex DNA strand and resulting in a bound species P–S:

$$P + S \rightleftarrows P\text{–}S \quad (1)$$

The association constant of the metalloporphyrin can be represented by eqs 2 and 3

$$K = P_b/P_f S_f \quad (2)$$

$$P_t/P_f = KS_f + 1 \quad (3)$$

In these expressions P_t, P_f, and P_b are the concentrations of total metalloporphyrin, free metalloporphyrin, and bound metalloporphyrin (with $P_t = P_f + P_b$), respectively. S_f is the concentration of free potential DNA sites

Table I. Interactions of Various Mn- or Fe-Porphyrins with CT DNA or Polynucleotides

CT DNA, 0–250 μM (bp); NaCl, 100 mM			Mn-TMePyP			
M-Por or Mn-InC	%H[a]	$K^b \times 10^4$ M^{-1}	DNA, 0–250 μM (bp)	NaCl mM	%H[a]	$K^b \times 10^4$ M^{-1}
Mn-TMePyP	41	3.0	CT DNA	25	43	17
Fe-TMePyP	−15	1.2		50	41	11
Mn-Por(MePy)$_3$(PhNO$_2$)	23	0.8		75	41	7.0
Mn-Por(MePy)$_3$(PhN$^+$Me$_3$)AcO$^-$	23	3.6		100	41	3.0
Mn-InC$_7$	64	23				
Mn-InC$_{11}$	36	6	poly[d(G-C)]	100	14	0.2
Mn-InC$_{12}$	43	34	poly[d(A-T)]	100	57	12

[a] H% = percent hyperchromicity effect. [b] K = binding constant for CT DNA, poly[d(A-T)] or poly[d(G-C)] (see conditions in Experimental Procedures).

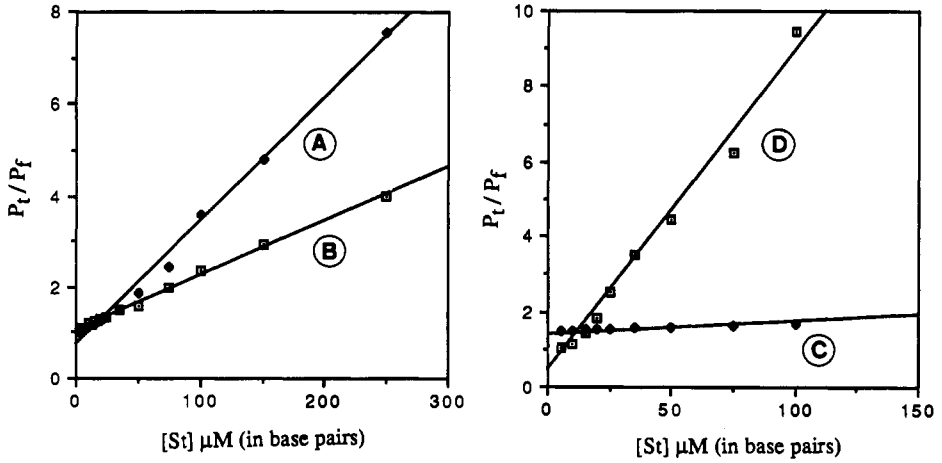


Figure 3. Plots of P_t/P_f vs S_t for Mn-TMePyP (A) and Fe-TMePyP (B) binding to CT DNA, and for Mn-TMePyP binding to poly[d(G-C)] (C) and to poly[d(A-T)] (D). The data are linear with the form $P_t/P_f = KS_t + 1$ and have correlation coefficients of 0.992 (A), 0.996 (B), 0.965 (C), and 0.982 (D).

expressed in base-pair units (with $S_f \approx S_t$ = total DNA site concentration if $S_t \gg P_t$).

If we assume (see below) that the low absorption A_0 observed in the absence of DNA (Figure 2) is related to the stacking of metalloporphyrin molecules in solution and/or to their partial adherence to the glass of the tube, then the destacking process and/or the inhibition of the porphyrin adsorption on the tube walls in the presence of DNA leads to the maximal optical density A_∞ for the highest DNA concentrations (nearly all the metalloporphyrin was bound as monomer on DNA); then we have

$$A_\infty = \epsilon_b P_t$$

with ϵ_b = absorption coefficient of metalloporphyrin when bound to DNA. a_0 is the residual absorption observed after the metalloporphyrin degradation in the absence of DNA.

In the presence of DNA, only the free metalloporphyrin was degraded while the bound form was protected from degradation. So a_x, the absorption observed after activation by $KHSO_5$, is the sum of the residual absorption of free porphyrin degradated ($=P_f a_0/P_t$) and the absorption of the bound porphyrin ($\epsilon_b P_b$) at the given concentration x of DNA

$$a_x = P_f a_0/P_t + \epsilon_b P_b \quad (4)$$

These different equations lead to

$$P_t/P_f = (A_\infty - a_0)/(A_\infty - a_x) = KS_t + 1 \quad (5)$$

A_∞, a_0, a_x, and S_t are experimental values and allowed determination of K (see Figure 3 for examples). S_t is expressed as micromolar in base pairs. The simple model outlined here adequately describes the binding data. More complex analyses of the binding equilibria taking in consideration the binding site size are possible (McGhee & von Hippel, 1974; Carter et al., 1989).

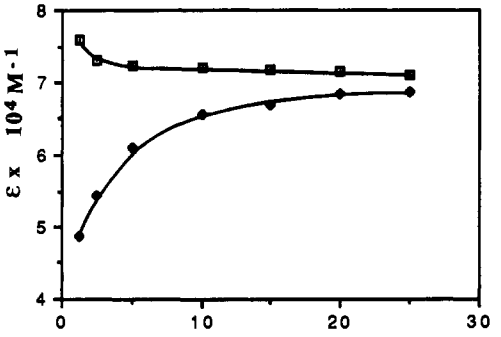
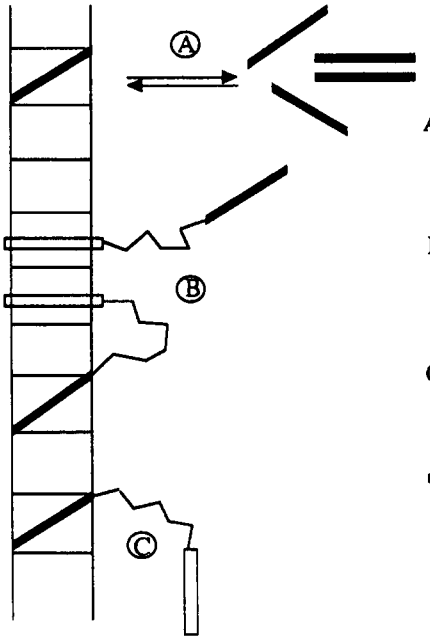


Figure 4. Plot of ε (λ = 463 nm) vs [Mn-TMePyP] (μM) determined after a 30-min preincubation in plastic (□) or in glass (●) tubes.

Evidence for Stacking of Mn-TMePyP in Solution and Its Adherence to Glass Tube Walls (Figure 4). Spectra were recorded for solutions of Mn-TMePyP in 5 mM phosphate buffer (pH 7) in the range 1.25–25 μM. Absorptions at the Soret band (463 nm) were determined in 10-mm quartz cuvettes after a 30-min incubation at 25 °C in either glass or plastic 2-mL test tubes. Variations of the absorption coefficient ε versus Mn-TMePyP concentrations are given in Figure 4.

Hyper- and Hypochromic Effects of DNA on the Soret Band of Metalloporphyrins (Table I). Absorptions at the respective Soret maxima of 5 μM solutions of the different porphyrin derivatives in 5 mM phosphate buffer, pH 7, containing 100 mM NaCl, at 25 °C, were determined before and after addition of 150 μM (bp) CT DNA (or synthetic nucleic acids). The percentage hy-

Scheme I. Schematic Mode of DNA Interactions of Metalloporphyrins [Iron(III) or Manganese(III) Derivatives] and Related Hybrid Molecules



A. Equilibrium between bound porphyrin and free porphyrin derivative (partially stacked depending on the concentration).

B. Intrinsic affinity of the metalloporphyrin moiety for DNA was enhanced as it is maintained close to DNA by intercalation of the ellipticine part.

C. Unlikely situation due to the higher affinity for DNA of the ellipticine *vs* the porphyrin moieties.

▬▬ : Cationic porphyrin (in the minor groove)

▭ : Ellipticine (intercalated).

perchromicity (%H) was determined from $(A_b-A_p)/A_p \times 100$, where A_p and A_b respectively represent the absorption of the metalloporphyrin in the absence and in the presence of DNA (or synthetic nucleic acids). A negative value for %H corresponds to an hypochromic effect.

RESULTS AND DISCUSSION

Hyper- or Hypochromicity of Metalloporphyrins in the Presence of DNA. Figure 4 shows variations of the absorption coefficient ϵ of Mn–TMePyP when solution concentrations ranged from 1.25 to 25 μM. The two different curves obtained with a 30-min incubation in plastic or glass test tubes do respectively refer to self-aggregation of the porphyrin when concentration increased and to adherence to the glass walls of the tube [adsorption of H_2TMePyP and metalated derivatives to different surfaces has previously been observed (Strickland et al., 1988)]. When the porphyrin complex was in the presence of increasing amounts of DNA, it progressively bound to DNA as monomer (Scheme I) and the optical density at the Soret band increased and reached a maximum (Figure 1) when all the porphyrin bound to DNA (generally for all the metalloporphyrins studied in this paper 150–250 μM (bp) DNA was sufficient to reach the maximum). This hyperchromic effect was described by %H in Table I (as defined in Experimental Procedures). All the manganese derivatives exhibited a high hyperchromicity in the presence of nucleic acids (23–57%), especially the hybrid derivatives (36–64%). In contrast, a low hypochromic effect was observed for the iron compound Fe–TMePyP (–14%). Hyperchromicity of Mn–TMePyP in the presence of DNA was intermediate (41%) between those observed in the presence of poly[d(G-C)] (14%) and poly[d(A-T)] (57%). These last results are in agreement with previous observations on hypochromicity of Fe–TMPyP (Pasternack et al., 1990) and on hyperchromicity of Mn–TMePyP (Pasternack et al., 1983) in the presence of nucleic acids.

Salt Effect on Hyperchromicity. As shown in Table I, an increase in salt concentrations (25–100 mM NaCl) decreased the binding constant of Mn–TMePyP (from 1.7×10^5 to 3.0×10^4 M^{-1}) but did not affect the percent hyperchromicity in the presence of CT DNA. This result suggests that increased ionic strength increases mainly the rate of the dissociation of Mn–TMePyP from CT DNA (see Strickland et al., 1988, for a discussion on this point concerning other metalated cationic porphyrins): so values of K are effectively lowered, but dissociation of stacked porphyrins or inhibition of adherence to the glass surface were not affected, giving hyperchromic effects unchanged whatever the ionic strength may be.

Salt Effect on Binding Constant. The association constant of Mn–TMePyP was markedly lowered when salt concentration increased (Table I); the slope of the straight line corresponding to log K versus log [Na^+] (figure not shown) is close to 1.2, indicating that 1.2 positive charge is involved in the binding of this metalloporphyrin to CT DNA (Record et al., 1976).

Binding Constants of Metalloporphyrins with DNA. To study interaction of these porphyrins with DNA, we analyzed their self-degradation in the presence of $KHSO_5$ as oxygen atom donor and with different amounts of DNA. In these conditions, the free metalloporphyrin (monomers or aggregates) underwent a fast degradation: in less than 10–12 s (Figure 2), the initial absorption (A_0) of the Soret band fell in the absence of DNA to a residual value (a_0) corresponding to absorption of degradation products of the metalloporphyrin. When DNA was present, initial absorption (A_x) at the Soret band was higher (see paragraph on hyperchromicity), the metalloporphyrin degradation was limited, and the residual absorption consisted of that of bound metalloporphyrin on DNA (which is therefore protected) added to that of porphyrin residues resulting from the oxidative degradation. The oxidative degradation ("bleaching") of M–porphyrins by $KHSO_5$ is probably due to both intermolecular and intramolecular oxygen atom transfer from the metal–oxo species generated by the oxygen atom donor, potassium monopersulfate in the present case. The optical density decay within 12 s corresponds quite exclusively to the degradation of free metalloporphyrin derivatives; after a 12-s reaction, the optical density slowly diminishes, cor-

Table II. DNA Affinity Constants (M^{-1}) of Iron and Manganese Derivatives of *meso*-Tetrakis(4-*N*-methylpyridiniumyl)porphyrin, Fe-TMePyP and Mn-TMePyP[d]

	EB competition	electrochemistry	chemical oxidation
Fe-TMePyP	6×10^5 [a]	1.9×10^4 [b,*]	1.2×10^4 [c]
Mn-TMePyP		3.6×10^6 [b,**]	3.0×10^4 [c]

[a] From Sari et al., 1990. [b] From Rodriguez et al., 1990. [c] Present work. [d] Conditions of ionic strength were 0.1 M NaCl (*a* and *c*), 0.05 M NaCl (*b*,**), 0.1 M NaCl and 0.1 M Tris (*b*,*). Metalloporphyrin concentrations were 0.5–5 (*a*), 100 (*b*), and 5 μM (*c*).

responding to a further release from DNA bound (and so protected) metalloporphyrin to the free form (which is degraded).

As indicated in the Experimental Procedures, analysis of this phenomenon for different concentrations of DNA allowed the determination of binding constants for various metalloporphyrins, all of them being activable by $KHSO_5$ to reactive species leading to self-destruction in the absence of substrate.

Figure 3 shows examples of experimental determinations of K: the value obtained with CT DNA for the manganese derivative of H_2TMePyP appeared somewhat larger than that of the iron complex, respectively 3.0 and 1.2×10^4 M^{-1}. The binding affinity of Mn-TMePyP with poly[d(G-C)], 0.2×10^4 M^{-1}, was clearly smaller than the one determined with poly[d(A-T)], 1.2×10^5 M^{-1}; result obtained with CT DNA, 3.0×10^4 M^{-1}, was intermediate between these two last values (all the binding constant values are listed in Table I). These results are in agreement with the literature data since Mn-TMePyP is a manganese–porphyrin complex with a strong axial ligand unable to intercalate at GC sites but which strongly interacts externally to DNA in the minor groove in AT regions (Strickland et al., 1988; Pasternack et al., 1983; Ward et al., 1986a).

Other functionalized porphyrins, Mn-Por$(MePy)_3(PhNO_2)$ and Mn-Por$(MePy)_3(PhN^+Me_3)$, presented DNA affinity constants in the same range: 0.8 and 3.6×10^4 M^{-1}, respectively. For the hybrid molecules Mn-InC_7, Mn-InC_{11}, Mn-InC_{12}, drug-DNA affinity constants of the metalloporphyrin moiety increased from 0.6 to 3.4×10^5 M^{-1}. These hybrid molecules combine a metalloporphyrin with an ellipticine, which is a good intercalating agent for DNA (Le Pecq et al., 1975). Their affinity for DNA results from contribution of the intercalation of the ellipticine moiety between DNA base pairs and the strong interaction of the positively charged manganese–porphyrin entity outside the nucleic acid both by hydrophobic contribution and electrostatic interaction (Ding et al., 1989, 1991) (see Scheme I).

GENERAL DISCUSSION

Few data were available in the literature on the DNA binding constants of iron or manganese cationic porphyrin complexes which are known for their high nuclease affinity. $K_{CT\ DNA}$ values reported for Fe-TMePyP are 6×10^5 M^{-1} and 1.9×10^4 M^{-1} (Sari et al., 1990; Rodriguez et al., 1990, respectively) and for Mn-TMePyP, 3.6×10^6 M^{-1} (Rodriguez et al., 1990) (Table II).

Both K values obtained for Fe-TMePyP by electrochemical oxidation (Rodriguez et al., 1990) or chemical oxidation (this work) are within the sameorder of magnitude, 10^4 M^{-1}, with very similar values, 1.9 and 1.2, respectively; for the manganese derivative Mn-TMePyP the reported values are 3.6×10^6 M^{-1} by electrochemistry and 1.2×10^4 M^{-1} by chemical oxidation (this work). Experimental conditions were not sufficiently close to allow a direct comparison: higher ionic strength (which lowers the experimental value of K) in the case of iron derivative or higher concentrations of both metalloporphyrins (which could increase the experimental value of K due to the metalloporphyrin stacking) required for the determination of association constants by electrochemistry (see Table II) may explain the observed variations between K values determined by electrochemistry and by chemical oxidation. Moreover these oxidation methods are only valid if the kinetic constant of the complex oxidation step is much higher than the kinetic constant of the release (k_{off}) of the bound complex from DNA. In the absence of data on the kinetic aspects of the DNA binding of metalloporphyrins, a fourth method (besides oxidations or ethidium bromide competition) will be useful to understand such discrepancies of the K values.

Presently, the DNA binding constants determinations by oxidation (electrochemical or chemical) are in fact the only available direct method to access to the K values for iron or manganese porphyrins. The other approach, by competition with an intercalating agent like ethidium bromide, is probably more controversial. The higher value, 6×10^5 M^{-1} for Fe-TMePyP (Table II), found by this method might be due to the fact that both molecules are not competing for the same DNA binding sites. In a detailed study, Baguley et al. (1981) have shown that the competition with EB is an accurate method for the determination of the binding constant of intercalating agents, but many data indicate that is less true when the EB competitor is not competiting for the same binding sites on DNA than EB (for a recent article on the EB competition method, see Carrier et al., 1990, and references therein). Manganese and iron derivatives are minor-groove binders. Such binding sites have been confirmed by the identification of the sugar degradation product, 5-methylene-2-furanone, formed during the oxidative cleavage of double-stranded DNA by Mn-TMePyP or hybrid molecules like Mn-InC_n (unpublished work). This sugar oxidation is the signature of an oxidizing complex located in the minor groove, since it results from the attack of the anomeric C–H bond which is only accessible from the minor groove (for a preliminary article on the identification of 5-methylene-2-furanone, see Bernadou et al., 1989, and references therein).

The EB method is probably more valid for hybrid molecules like Mn-InC_n. The K_{AT} values obtained by this method are 2.3×10^9 and 6.7×10^9 M^{-1} for Mn-InC_7 and Mn-InC_{11}, respectively (Ding et al., 1991). In this case, the high affinity constant reflects the global hindrance of the molecule to intercalation of EB; it results from the combination of the intercalation of the ellipticine moiety and the binding of the manganese porphyrin part in the minor groove, the exact position of the chelate being controlled by the length of the tether (Ding et al., 1989, 1990a). The main target of these DNA cleavers is also the C–H bond at $C_{1'}$ (unpublished data). The binding constant values of the tethered manganese porphyrins in Mn-InC_n complexes determined by chemical oxidation are 23×10^4, 6×10^4, and 34×10^4 M^{-1} for Mn-InC_7, Mn-InC_{11}, and Mn-InC_{12}, respectively. They are slightly above the value found for the parent complex Mn-TMePyP and can be attributed to the intrinsic DNA affinity of the porphyrin moiety. So, since the affinity constant for the ellipticine-linker moiety is 2.5×10^6 M^{-1} (EB method), higher than for Mn-TMePyP, interaction with DNA of hybrid molecules can probably be summarized by the two situations represented in Scheme I, process B: either the chelate

binds to DNA or it exists partially free (sufficiently far of the nucleic acid to be chemically destroyed in the presence of $KHSO_5$ but maintained close to DNA by its attachment to the intercalated ellipticine part; this last situation may explain the low increase of the affinity constants of hybrid molecules compared to parent metalloporphyrin). Consequently, the biological properties of these hybrid molecules which depend on the presence of the porphyrin (DNA cleavage, cytotoxicity, ...) have to be tentatively correlated to the intrinsic affinity of the metalloporphyrin part determined by chemical oxidation rather than the global affinity determined for example by the more classic EB method.

In conclusion, the chemical oxidation of the free metalloporphyrin at equilibrium is a simple way to access to the DNA affinity constants of DNA cleavers and minor-groove binders on the basis of manganese- or iron-porphyrin complexes. This approach is a suitable alternative to the well-known ethidium bromide competition method which is questionable for nonintercalating drugs.

ACKNOWLEDGMENT

One of us (L.D.) is indebted to the CNRS for a 6-month fellowship. We thank Dr. M. Bonnafous for preliminary experiments. Pierre Fabre Médicaments and the "Association pour la Recherche sur le Cancer" (Villejuif) are acknowledged for a financial support.

LITERATURE CITED

Aft, R. L., and Mueller, G. C. (1983) Hemin mediated DNA strand scission. *J. Biol. Chem. 258*, 12069–12072.

Baguley, B. C., Denny, W. A., Atwell, G. J., and Cain, B. F. (1981) Potential antitumor agents. 34. Quantiative relationships between DNA binding and molecular structure for 9-anilinoacridines substituted in the anilino ring. *J. Med. Chem. 24*, 170–177.

Bernadou, J., Pratviel, G., Bennis, F., Girardet, M., and Meunier, B. (1989a) Monopersulfate and water-soluble manganese porphyrin complexes as an efficient reagent for the oxidative cleavage of DNA. *Biochemistry 28*, 7268–7275.

Bernadou, J., Lauretta, B., Pratviel, G., and Meunier, B. (1989b) Hydroxylation at 1′-carbon of deoxyribose as key step in the cleavage of poly(dA) by a manganese porphyrin associated to potassium monopersulfate. *C.R. Acad. Paris 309 III*, 409–414.

Carrier, A., Le Ber, P., and Auclair, C. (1990) Spin-labeled oxazolopyridocarbazole as a probe for studying nonintercalating DNA groove binding ligands. *Biochemistry 29*, 6002–6009.

Carter, M. T., Rodriguez, M., and Bard, A. L. (1989) Voltammetric studies of the interaction of metal chelates with DNA. 2. Tris-chelated complexes of cobalt(III) and iron(II) with 1,10-phenanthroline and 2,2′-bipyridine. *J. Am. Chem. Soc. 111*, 8901–8911.

Dabrowiak, J. C., Ward, B., and Goodisman, J. (1989) Quantitative footprinting analysis using a DNA-cleaving metalloporphyrin complex. *Biochemistry 28*, 3314–3332.

Ding, L., Etemad-Moghadam, G., Cros, S., Auclair, C., and Meunier, B. (1989) Cytotoxic hybrid molecules "metalloporphyrin-ellipticine" having a high affinity for DNA. *J. Chem. Soc., Chem. Commun.* 1711–1713.

Ding, L., Etemad-Moghadam, G., and Meunier, B. (1990a) Oxidative cleavage of DNA mediated by hybrid metalloporphyrin–ellipticine molecules and functionalized metalloporphyrin precursors. *Biochemistry 29*, 7868–7875.

Ding, L., Casas, C., Etemad-Moghadam, G., and Meunier, B. (1990b) Synthesis of water soluble, cationic functionalized metalloporphyrins having a cytotoxic activity. *New J. Chem. 14*, 421–431.

Ding, L., Etemad-Moghadam, G., Cros, S., Auclair, C., and Meunier, B. (1991) Syntheses and in vitro evaluation of water-soluble "cationic metalloporphyrin–ellipticine" molecules having a high affinity for DNA. *J. Med. Chem.* 34, 900–906.

Fiel, R. J., Beerman, T. A., Mark, E. H., and Datta-Gupta, N. (1982) DNA strand scission activity of metalloporphyrins. *Biochem. Biophys. Res. Commun. 107*, 1067–1074.

Fouquet, E., Pratviel, G., Bernadou, J., and Meunier, B. (1987) Nuclease activity of a water-soluble manganese–porphyrin associated to potassium hydrogen persulfate: oxidative cleavage of DNA. *J. Chem. Soc., Chem. Commun.* 1169–1171.

Le Pecq, J. B., Le Bret, M., Barbet, J., and Roques, B. (1975) DNA polyintercalating drugs: DNA binding of diacridines derivatives. *Proc. Natl. Acad. Sci. U.S.A. 72*, 2915–2919.

Marzilli, L. G. (1990). Medical aspects of DNA–porphyrin interactions. *New J. Chem. 14*, 409–420.

McGhee, J. D., and von Hippel, P. H. (1974) Theoritical aspects of DNA–protein interactions: co-operative and non-co-operative binding of large ligands to a one-dimensional homogeneous lattice. *J. Mol. Biol. 86*, 469–489.

Pasternack, R. F., Gibbs, E. J., and Villafranca, J. J. (1983) Interactions of porphyrins with nucleic acids. *Biochemistry 22*, 2406–2414.

Pasternack, R. F., Brigandi, R. A., Abrams, M. J., Williams, A. P., and Gibbs, E. J. (1990) Interactions of porphyrins and metalloporphyrins with single-stranded poly(dA). *Inorg. Chem. 29*, 4483–4486.

Pratviel, G., Bernadou, J., Ricci, M., and Meunier, B. (1989) Magnesium monoperoxophthalate as efficient single oxygen atom donor in DNA cleavage catalyzed by metalloporphyrins. *Biochem. Biophys. Res. Commun. 160*, 1212–1218.

Record, M. T., Lohman, T. M., and de Haseth, P. (1976) Ion effects on ligand-nucleic acid interactions. *J. Mol. Biol. 107*, 145–158.

Rodriguez, M., Kodadek, T., Torres, M., and Bard, A. J. (1990) Cleavage of DNA by electrochemically activated Mn^{III} and Fe^{III} complexes of *meso*-tetra(*N*-methyl-4-pyridiniumyl)porphyrin. *Bioconjugate Chem. 1*, 123–131.

Sari, M. A., Battioni, J. P., Dupre, D., Mansuy, D., and Le Pecq, J. B. (1990) Interaction of cationic porphyrins with DNA: importance of the number and position of the charges and minimum structural requirements for intercalation. *Biochemistry 29*, 4205–4215.

Strickland, J. A., Marzilli, L. G., Gay, K. M., and Wilson, W. D. (1988) Porphyrin and metalloporphyrin binding to DNA polymers: rate and equilibrium studies. *Biochemistry 27*, 8870–8878.

Strickland, J. A., Marzilli, L. G., Wilson, W. D., and Zon, G. (1989) Metalloporphyrin DNA interactions: insights from NMR studies of oligonucleotides. *Inorg. Chem. 28*, 4191–4198.

Thederahn, T. B., Kuwabara, M. D., Larsen, T. A., and Sigman, D. S. (1989) Nuclease activity of 1,10-phenanthroline–copper: kinetic mechanism. *J. Am. Chem. Soc. 111*, 4941–4946.

Van Atta, R. B., Bernadou, J., Meunier, B., and Hecht, S. M. (1990) On the chemical nature of DNA and RNA modification by a hemin model system. *Biochemsitry 29*, 4783–4789.

Ward, B., Skorobogaty, A., and Dabrowiak, J. C. (1986a) DNA binding specificity of a series of cationic metalloporphyrin complexes. *Biochemistry 25*, 7827–7833.

Ward, B., Skorobogaty, A., and Dabrowiak, J. C. (1986b) DNA cleavage specificity of a group of cationic metalloporphyrins. *Biochemistry 25*, 6875–6883.

Registry No. Poly[d(G-C)], 36786-90-0; poly[d(A-T)], 24939-09-1; Mn-TMePyP, 110989-01-0; Fe-TMePyP, 133892-88-3; Mn-Por(MePy)$_3$(PhNO$_2$), 134418-68-1; Mn-Por(MePy)$_3$(PhNMe$_3$)$^+$AcO$^-$, 134391-43-8; Mn-InC$_7$, 125333-98-4; Mn-InC$_{11}$, 134391-45-0; Mn-InC$_{12}$, 134391-47-2; 5-(4-aminophenyl)-10,15,-20-tris(4-pyridyl)porphyrin, 127800-97-9; 5-(4-nitrophenyl)-10,-15,20-tris(4-pyridyl)porphyrin, 127800-96-8; N_2-(5-carboxypentyl)-9-methoxyellipticinium chloride, 124040-06-8; N_2-(4-carboxybutyl)-9-methoxyellipticinium chloride, 127801-09-6; 5-[4-[(3-aminopropyl)oxy]phenyl]-10,15,20-tris(4-pyridyl)porphyrin, 127801-04-1.

Influence of Endogenous Thy1.1 Cells upon the Efficacy of an Anti-Thy1.1 Antibody–Diphtheria Toxin Conjugate

Bai Yan,† Patricia D. Baker,‡ Charles H. Evans,‡ and Jon W. Marsh*

Laboratory of Molecular Biology, National Institute of Mental Health, Bethesda, Maryland 20892, and Laboratory of Biology, National Cancer Institute, Bethesda, Maryland 20892. Received February 19, 1991

The chemical conjugation of antibodies to protein toxins results in cell-specific cytotoxic agents that can be defined in terms of in vitro potency and efficacy; however, it is the in vivo utilities that are largely being pursued in clinical trials. The nature of in vivo target cell depletion by toxin conjugates is largely unknown. The anti-murine Thy1.1 antibody–diphtheria toxin conjugate possesses high in vitro efficacy, and because mice are remarkably resistant to the native toxin, the conjugate possesses in vivo efficacy. When administered intravenously, the conjugate is shown to deplete peripheral blood Thy1.1$^+$ target cells in a concentration-dependent fashion. When the log kill of Thy1.1$^+$ tumor cells was analyzed by the life span extension method, it was determined, however, that the log kill is inversely proportional to the number of target cells. That is, the presence of an endogenous cell population, which is expressing the same surface antigen targeted by the antibody conjugate as on the pathological cell, may drastically lower the clinical efficacy of the immunotoxin. Thus, the greatest potential for antibody–toxin conjugates will be for low target cell burdens and for pathogenic cell populations expressing unique surface antigens. These are important considerations in the design of bioconjugates to insure high in vivo efficacy in elimination of intended target cells.

INTRODUCTION

The covalent linkage of monoclonal antibodies to protein toxins has resulted in the development of numerous new cell-specific cytotoxic agents (*1*). The action of these conjugates against isolated target cells has been studied extensively, and the mechanisms of immunotoxin-mediated cytotoxicity are presently being elucidated. Although these conjugates have successfully been used in vitro to eliminate graft-versus-host disease (*2*), there is greater anticipation for successful in vivo applications in the clinic; however, there has been no attempt to define the in vivo mechanisms of cell depletion by antibody–toxin conjugates.

In this report we use the highly efficacious anti-Thy1.1 antibody–diphtheria toxin conjugate (*3*) to determine the mechanism of in vivo cell depletion by an immunotoxin. We and others have previously used the life span extension method of Skipper and co-workers (*4*) to determine the in vivo log kill of tumor cells by treatment with antibody–toxin conjugates (*5*,*6*). Previous work has used a relatively low tumor cell number, with immunotoxin treatment resulting in multilog kill. When we examined the log kill of Thy1.1 SL2 leukemia cells in a Thy1.2 mouse, we found that the log kill varied with the number of introduced leukemia cells. At identical immunotoxin concentrations, a tumor burden of 10^7 SL2 cells was depleted by 2 log units (99% depletion), whereas all tumorigenic cells were eliminated from mice previously injected with 10^6 cells, consistent with a greater than 3 log (99.9%) kill (*5*). Free antibody at the same concentration had no effect on leukemia cell elimination. There were two problems with this system. First, tumor-induced mortality required 10^3 cells (presumably due to allotypic differences in the Thy antigen), and secondly, injection of higher cell numbers was difficult.

We have now examined the syngeneic system of Thy1.1 SL2 leukemia cells in a Thy1.1 AKR mouse. We demonstrate here that the Thy1.1-specific immunotoxin depletes Thy1.1 T lymphocytes in vivo in a concentration-dependent fashion and further support the earlier finding that the resultant log kill is inversely proportional to the target cell number. This implies that the targeting of immunotoxins to a tumor antigen that also exists on an endogenous population of (nontumor) cells can bring about a remarkable decrease in efficacy of the immunotoxin.

EXPERIMENTAL PROCEDURES

Immunotoxin. Diphtheria toxin was obtained in nicked form from Connaught Laboratories (Toronto, Canada) and purified as previously described (*3*). The murine anti-Thy1.1 monoclonal antibody, Ox7, was purified from ascites and then conjugated to diphtheria toxin via a thioether linkage (*3*). The fractionated preparation yielded a monotoxin–antibody conjugate. The conjugate was administered intraperitoneally or intravenously via the tail vein in phosphate-buffered saline in volumes of 100 μL.

Mice. Thy1.1 AKR mice were purchased from the Jackson Laboratory, Bar Harbor, ME.

Life-Span Experiments. The methods of Skipper and co-workers were followed (*4*, *5*). Thy1.1 SL2 leukemia cells were maintained in RPMI 1640 media containing 10% fetal calf serum as previously described (*3*) and, immediately prior to injection, were centrifuged and resuspended in serum-free RPMI at appropriate cell densities and injected intraperitoneally in volumes of 200 μL. Five weight-matched (ca. 25 g) mice were used for each experimental group. Mice were examined daily, and mortality was recorded.

Flow Cytometry. Enumeration of Thy1.1-positive cells in peripheral blood was achieved by flow cytometry on a FACScan instrument (Becton Dickinson, Mountain View, CA) calibrated to detect fluorescein fluorescence. Peripheral blood was withdrawn from the tail vein. Viable lymphocytes were isolated on a Ficoll gradient (Lympholyte-M, Cedarlane Laboratories, Hornby, Ontario,

* Address for correspondence: Laboratory of Molecular Biology, NIMH, Bld 36/Rm 1B08, Bethesda, MD 20892.
† Present address: Institute of Basic Medical Sciences, P.O. Box 130 (3), Beijing 100850, People's Republic of China.
‡ National Cancer Institute.

Not subject to U.S. Copyright. Published 1991 by American Chemical Society

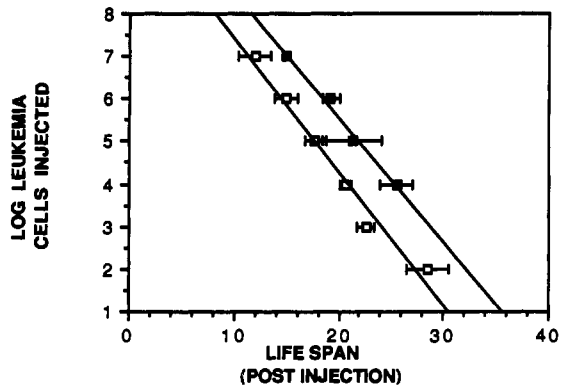


Figure 1. Life-span extension for Thy1.1 AKR mice receiving Thy1.1 SL2 leukemia cells. AKR mice were injected ip with defined levels of SL2 cells (10^2–10^7) in 200 μL of RPMI media (five mice for each group). Twenty-four hours later 10 μg of Ox7-DT conjugate was injected ip into certain groups of mice (■). Mortality was then recorded as days following cell injection. Each data point represents the mean value ± standard error. This data is plotted in the typical fashion; however, for statistical analysis: y = life span, x = log cells injected. Least-squares fit of the mice not receiving immunotoxin: $y = 33.3 - 3.09x$, $r^2 = 0.975$. For immunotoxin-treated mice: $y = 38.74 - 3.36x$, $r^2 = 0.984$.

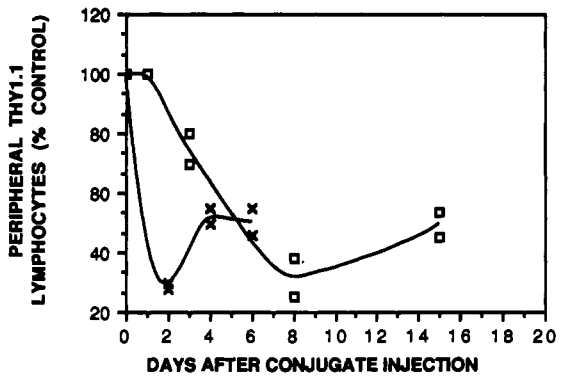


Figure 2. Kinetics of in vivo Thy$^+$ cell depletion. Thy1.1 AKR mice were injected with 10 μg of anti-Thy1.1 antibody–diphtheria toxin conjugate either intravenously (×) or intraperitoneally (□), and on the days designated on the x axis (posttreatment) mice were sacrificed and peripheral blood Thy$^+$ lymphocytes were enumerated by flow cytometry (see the Experimental Procedures). Each data point represents a FACS analysis of 10 000 cells from a different mouse. Individual mouse scores of the percent of peripheral blood mononuclear cells that are Thy$^+$ are normalized to a mean control value of Thy$^+$ cells in untreated mice.

Canada) and then stained with the purified anti-Thy1.1 antibody followed by an anti-IgG_1-FITC secondary antibody (Southern Biotechnology, Birmingham, AL). In the absence of the Thy1.1 antibody there was no fluorescence above background autofluorescence. The lower forward light scatter threshold was set during data collection to exclude contaminating red blood cells from the analysis. Postrun analysis of the list mode data was accomplished by placing gates at forward light scatter positions above and below the sample of Thy-positive cells isolated from untreated mice to capture Thy-positive cells. In normal mice ca. 50% of the gated cells are positive for Thy1.1. This control level of Thy1.1-positive lymphocytes was normalized to 100%. To describe cell depletion in experimental mice, the instrumentally determined percent of peripheral blood mononuclear cells positive for Thy1.1 for each mouse was then normalized to this control level (and expressed as percent control).

Data Analysis. Curve-fitting and statistics were performed with Cricket Graph software (Cricket Software, Philadelphia, PA), StatView, and SuperANOVA (Abacus Concepts, Berkeley, CA).

RESULTS

Thy1.1 AKR mice were injected with varied levels of Thy1.1 SL2 leukemia cells. In this syngeneic system less than 100 SL2 cells were required to kill 100% of recipient mice. These mice possess, however, an endogenous population of Thy1.1-positive T lymphocytes, and the influence of this large population of endogenous target cells (ca. 10^8) on the elimination of various levels of intraperitoneally injected Thy1.1 tumor cells was examined in the life span extension model (Figure 1). The immunotoxin-mediated increase in life span for mice receiving 10^7 cells was equivalent to a 1 log kill; however, unlike the results previously reported with Thy1.2 mice (*5*), decreases in tumor burden did not measurably increase the log kill in Figure 1. Results from analysis of covariance indicate that the slopes of the two regression lines for nontreated and immunotoxin-treated mice were not significantly different, $P = 0.693$. This finding indicates that the log kill of leukemia cells is dependent on the total Thy1.1-positive target cell number (leukemia cells and endogenous lymphocytes). In concert with our previous findings that the immunotoxin generates a 2 log kill with 10^7 and a greater than 3 log kill with 10^6 introduced Thy1.1 cells in a Thy1.2 mouse (*5*), we, therefore, conclude that the extent of cell depletion, as expressed by log kill or fraction of target cell population, is inversely related to the number of target cells.

The kinetics of target-cell depletion was then examined following intravenous or intraperitoneal injection of immunotoxin. Thy1.1 mice were injected with the anti-Thy1.1 antibody–diphtheria toxin conjugate, and levels (relative to untreated controls) of residual endogenous peripheral T lymphocytes were determined (Figure 2). Maximal cell depletion of peripheral Thy1.1 positive cells was similar for the two routes of immunotoxin administration; however, the rate of decline was considerably different, with maximal depletion being reached at 2 days for the intravenous route and at 1 week for intraperitoneal administration. Equivalent levels of unconjugated antibody or toxin had no effect (data not shown).

To examine the influence of immunotoxin concentration on in vivo depletion of target cells, varied concentrations of the antibody–toxin conjugate were injected into Thy1.1 mice and the level of residual peripheral Thy1.1 positive lymphocytes was determined by flow cytometry. In order to examine a meaningful range of conjugate concentrations, we chose to use intravenous administration of immunotoxin, as immunotoxin levels in excess of 10 μg per mouse resulted in death in ca. 1 week. Thus, cell depletion by lethal doses of conjugate could be examined by flow cytometry 2 days after injection. The relationship between administered dose and target-cell depletion appears to be an exponential function (Figure 3), with the slopes of this and a second experiment (not shown) equal to −0.034 ± 0.003 (SE) and −0.038 ± 0.01 log percent control cells/μg injected conjugate, respectively. It should be noted that an extrapolated value of 30 μg per mouse would be required to deplete peripheral blood Thy1.1 cells by 1 log.

DISCUSSION

Antibody–toxin conjugates are presently being used in clinical trials to bring about in vivo depletion of unwanted cells, such as those seen in cancer and autoimmunity (*7*). However, the quantitative nature of in vivo immunotoxin-

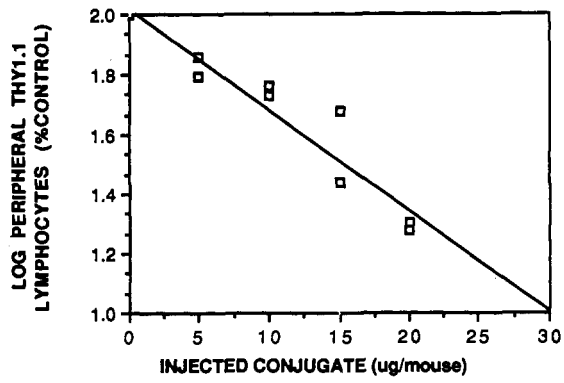


Figure 3. In vivo Thy$^+$ cell depletion. Thy1.1 AKR mice were injected iv with varying levels of antibody-DT conjugate. After 2 days peripheral blood was examined by flow cytometry to determine residual Thy$^+$ cells, as in Figure 2. Each data point represents a FACS analysis of 10 000 cells. Individual mouse scores are plotted as the log of residual Thy$^+$ cells relative to a mean control value of Thy$^+$ cells in untreated mice. Least-squares fit: $y = 2.0214 - 0.0337x$, $r^2 = 0.918$. A second similar experiment (not shown) generated a similar least-squares fitting: $y = 1.9688 - 0.0376x$, $r^2 = 0.813$.

mediated cell depletion has not been previously described. The log cell kill by the diphtheria toxin–anti-Thy1.1 antibody conjugate, and presumably by other toxin conjugates, is now shown to be dependent upon the size of the target-cell population; this differs from the mechanism of chemical agents, where a defined dosage results in a percent depletion (or log kill) independent of the total target cell number (*4*). This difference between chemical and antibody conjugate cytotoxic agents may reflect a nonequilibrium state of antibody binding to target cells; that is, high-affinity antibody binding is largely irreversible, and in the presence of excess target cells, the initial free concentration of conjugate is not maintained. Nevertheless, there is a conjugate concentration dependence on cell depletion (Figure 3), and the decline in Thy$^+$ cells follows a single hit exponential process.

Many of the factors affecting efficacy of toxin–antibody conjugates that have been described with in vitro systems, such as conjugate construction, undoubtedly play a role in in vivo cell kill (*8*). In vivo conjugate stability and circulation kinetics have also been examined (*9–15*). In practice, the maximal cell kill by a single injection of the anti-Thy–diphtheria toxin conjugate is limited by the maximal tolerated dose, and as such, upper limits to cell kill do not become apparent. In vitro examination of cytotoxicity by highly efficacious diphtheria and holo-ricin conjugates do display saturable phenomena, and in the case of a ricin conjugate, this saturable feature is not due to antigen–antibody binding. The limiting step is some yet undefined intracellular process (*16*). We have previously shown that injection of unconjugated anti-Thy antibody at the concentrations used for these immunotoxin studies does not result in measurable tumor-cell depletion (*5*), nor do similar levels of this antibody affect peripheral T cell populations in AKR mice. This may be in part due to the influence of antibody isotypes on in vivo efficacy with IgG_{2a} (and sometimes IgG_{2b}) being the most efficacious and IgG_1 having lesser efficacy (*17–20*). The anti-Thy Ox7 is a murine IgG_1 antibody. It is also of interest that the conjugate-treated mice did not possess viable lymphocytes with detectable surface-bound IgG_1 (from the conjugate), indicating a rapid death/clearance from the circulation (data not shown).

We have utilized the inoculum size (log of the number of tumor cells) versus survival time plot as originally described by Skipper and co-workers (see ref 21 for review). Figure 1 demonstrates a constant exponential growth rate of the SL2 cells over the cell number range of 10^2–10^7. After finding that increasing the number of tumor cells injected decreased the log kill for a set immunotoxin dose, it was not totally unexpected to find that the endogenous Thy1.1 positive cell population would decrease further the effective log kill on a defined Thy1.1 positive tumor burden. What was somewhat unexpected was the lack of contribution of compartmentalization. The Thy1.1 SL2 cells were injected intraperitoneally followed by the immunotoxin injection intraperitoneally 24 h later. Where such a tumor burden in Thy1.2 mice would be completely eliminated, reduction of a 10^6 Thy1.1 SL2 cell tumor burden in Thy1.1 mice approximated a 1 log kill (Figure 1). In fact, this log kill changed little over the examined 10^4–10^7 tumor cell burden range. This finding suggests that an endogenous, antigen-positive cell population found largely outside of a defined body cavity or compartment may have rather drastic effects on target cell kill.

The loss of cells appears to be due to immunotoxin-specific killing. The elimination of Thy1.1 cells from the blood is not due to modulation of Thy antigen off the cell surface. The flow cytometric studies of control mice display (with respect to fluorescence intensity) two populations of cells: background autofluorescent cells (Thy$^-$) and positively stained Thy$^+$ cells. The difference in fluorescence intensity mode values between these two populations is ca. 2 logs. The loss of Thy$^+$ cells in immunotoxin-treated mice is not accompanied by the appearance of a cell population with intermediate fluorescence intensity, as would be expected if Thy antigen modulation was occurring to a significant degree. Altered trafficking of T cells is also not expected to play a major role in T cell elimination from the blood. Yet unpublished work in this laboratory indicates that as opposed to an increase, as would be expected with trafficking, simultaneous, equivalent losses are seen in the spleen; other lymph organs have not yet been examined.

Indeed, the question now is not only whether an endogenous (nonpathogenic) antigen-positive cell population can tolerate cell depletion by immunotoxin administration but also whether its presence drastically reduces the log kill of the targeted pathogenic cell. This work suggests that the greatest clinical potential for toxin–antibody conjugates will be in the elimination of pathological cells expressing unique surface antigens.

ACKNOWLEDGMENT

We thank Dr. David Neville, Jr., for his encouragement and support, David Lang for assistance with the statistical analysis, and Monese Christensen and Jeralyn Thomson for their assistance in manuscript preparation.

LITERATURE CITED

(1) Frankel, A. E. (Ed.) (1988) Immunotoxins, Kluwer Academic Publishers, Dordrecht, the Netherlands.

(2) Filipovich, A. H., Vallera, D. A., Youle, R. J., Haake, R., Blazar, B. R., Arthur, D., Neville, D. M., Jr., Ramsay, N. K. C., McGlave, P., and Kersey, J. H. (1987) Graft-Versus-Host Disease Prevention in Allogeneic Bone Marrow Transplantation from Histocompatible Siblings. *Transplantation 44*, 62–69.

(3) Marsh, J. W. (1988) Antibody-mediated Routing of Diphtheria Toxin in Murine Cells Results in a Highly Efficacious Immunotoxin. *J. Biol. Chem. 263*, 15993–15999.

(4) Skipper, H. E., Schabel, F. M., Jr., and Wilcox, W. S. (1964) Experimental Evaluation of Potential Anticancer Agents.

XIII. On the Criteria and Kinetics Associated with "Curability" of Experimental Leukemia. *Cancer Chemother. Rep. 35*, 1–111.
(5) Marsh, J. W., and Neville, D. M., Jr. (1987) Development of an Immunotoxin with in Vivo Efficacy for Murine Systems. *Ann. N. Y. Acad. Sci. 507*, 165–171.
(6) Thorpe, P. E., Brown, A. N. F., Bremmer, J. A. G., Jr., Foxwell, B. M. J., and Stirpe, F. (1985) An Immunotoxin Composed of Monoclonal Anti-Thy 1.1 Antibody and a Ribosome-Inactivating Protein from *Saponaria officinalis*: Potent Antitumor Effects in Vitro and in Vivo. *J. Natl. Cancer Inst. 75*, 151–159.
(7) Program and Abstracts (1990) Second International Symposium on Immunotoxins, Lake Buena Vista, FL.
(8) Neville, D. M., Jr., and Marsh, J. W. (1988) Methods for quantifying immunotoxin efficacy. *Immunotoxins* (A. E. Frankel, ed) pp 393–404, Kluwer Academic Publishers, Dordrecht, the Netherlands.
(9) Bourrie, B. J. P., Casellas, P., Blythman, H. E., and Jansen, F. K. (1986) Study of the Plasma Clearance of Antibody–ricin-A-chain Immunotoxins. *Eur. J. Biochem. 155*, 1–10.
(10) Letvin, N. L., Goldmacher, V. S., Ritz, J., Yetz, J. M., Schlossman, S. F., and Lambert, J. M. (1986) In Vivo Administration of Lymphocyte-specific Monoclonal Antibodies in Nonhuman Primates. *J. Clin. Invest. 77*, 977–984.
(11) Letvin, N. L., Chalifoux, L. V., Reimann, K. A., Ritz, J., Schlossman, S. F., and Lambert, J. M. (1986) In Vivo Administration of Lymphocyte-specific Monoclonal Antibodies in Nonhuman Primates. *J. Clin. Invest. 78*, 666–673.
(12) Scott, C. F., Jr., Goldmacher, V. S., Lambert, J. M., Jackson, J. V., and McIntyre, G. D. (1987) An Immunotoxin Composed of a Monoclonal Antitransferrin Receptor Antibody Linked by a Disulfide Bond to the Ribosome-Inactivating Protein Gelonin: Potent in Vitro and in Vivo Effects Against Human Tumors. *J. Natl. Cancer Inst. 79*, 1163–1172.
(13) Thorpe, P. E., Wallace, P. M., Knowles, P. P., Relf, M. G., Brown, A. N. F., Watson, G. J., Knyba, R. E., Wawrzynczak, E. J., and Blakely, D. C. (1987) New Coupling Agents for the Synthesis of Immunotoxins Containing a Hindered Disulfide Bond with Improved Stability in Vivo. *Cancer Res. 47*, 5924–5931.
(14) Fulton, R. J., Tucker, T. F., Vitetta, E. S., and Uhr, J. W. (1988) Pharmacokinetics of Tumor-reactive Immunotoxins in Tumor-bearing Mice: Effect of Antibody Valency and Deglycosylation of the Ricin A Chain on Clearance and Tumor Localization. *Cancer Res. 48*, 2618–2625.
(15) Fulton, R. J., Uhr, J. W., and Vitetta, E. S. (1988) In Vivo Therapy of the BCL_1 Tumor: Effect of Immunotoxin Valency and Deglycosylation of the Ricin A Chain. *Cancer Res. 48*, 2626–2631.
(16) Marsh, J. W. (1989) Cellular Processing of a Ricin-Antibody Conjugate. *J. Biol. Chem. 264*, 10405–10410.
(17) Lanier, L. L., Babcock, G. F., Raybourne, R. B., Arnold, L. W., Warner, N. L., and Haughton, G. (1980) Mechanism of B Cell Lymphoma Immunotherapy with Passive Xenogeneic Anti-Idiotype Serum. *J. Immunol. 125*, 1730–1736.
(18) Seto, M., Takahashi, T., Nakamura, S., Matsudaira, Y., and Nishizuka, Y. (1983) In Vivo Antitumor Effects of Monoclonal Antibodies with Different Immunoglobulin Classes. *Cancer Res. 43*, 4768–4773.
(19) Hale, G., Clark, M., and Waldmann, H. (1985) Therapeutic Potential of Rat Monoclonal Antibodies: Isotype Specificity of Antibody-Dependent Cell-Mediated Cytotoxicity with Human Lymphocytes. *J. Immunol. 134*, 3056–3061.
(20) Denkers, E., Badger, C., Ledbetter, J., and Bernstein, I. (1985) Influence of Antibody Isotype on Passive Serotherapy of Lymphoma. *J. Immunol. 135*, 2183–2186.
(21) Griswold, D. P., Jr., (1986) Body Burden of Cancer in Relationship to Therapeutic Outcome: Consideration of Preclinical Evidence. *Cancer Treat. Rep. 70*, 81–86.

Introduction of Unnatural Amino Acids into Chalcone Isomerase

Rodney A. Bednar,* Catherine McCaffrey, and Kaiyu Shan

Departments of Pharmacological Sciences and Chemistry, State University of New York at Stony Brook, Stony Brook, New York 11794-8651. Received March 19, 1991; Revised Manuscript Received May 7, 1991

The active site cysteine residue of chalcone isomerase was rapidly and selectively modified under denaturing conditions with a variety of electrophilic reagents. These denaturated and modified enzyme were renatured to produce enzyme derivatives containing a series of unnatural amino acids in the active site. Addition of methyl, ethyl, butyl, heptyl, and benzyl groups to the cyteine sulfur does not abolish catalytic activity, although the activity decreases as the steric bulk of the amino acid side-chain increases. Modification of the cyteine to introduce a charged homoglutamate or a neutral homoglutamine analogue results in retention of 22% of the catalytic activity. Addition of a methylthio group (SMe) to the cysteine residue of native chalcone isomerase preserves 85% of the catalytic activity measured with 2',4',4-trihydroxychalcone, 2',4',6',4-tetrahydroxychalcone, or 2'-hydroxy-4-methoxychalcone as substrates. The competitive inhibition constant for 4',4-dihydroxychalcone, the substrate inhibition constant for 2',4',4-trihydroxychalcone, and other steady-state kinetic parameters for the methanethiolated enzyme are very similar to those of the native enzyme. The strong binding of 4',4-dihydroxychalcone to the methanethiolated enzyme shows that there is no steric repulsion between this modified amino acid residue and the substrate analogue. This structure–activity study clearly demonstrates that the active site cysteine residue does not function as an acid–base or nucleophilic group in producing the catalysis or substrate inhibition observed with chalcone isomerase. The method presented in this paper allows for the rapid introduction of a series of unnatural amino acids into the active site as a means of probing the structure–function relationship.

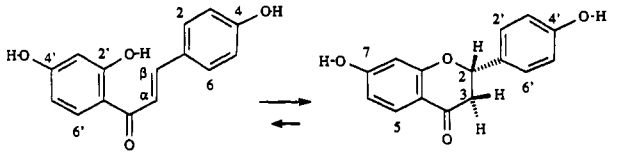
INTRODUCTION

A basic tenet of biochemistry is that structure determines function. To understand this structure–function relationship, we must have tools that allow us to produce enzyme molecules with defined altered structures. Using the enzyme chalcone isomerase (EC 5.5.1.6), we illustrate a method to rapidly introduce a series of unnatural amino acid residues in place of a cysteine residue and use this method to probe the role of hydrophobic and charge interaction in binding and catalysis.

Chalcone isomerase catalyzes the cyclization of 2',4',4-trihydroxychalcone (I) to 4',7-dihydroxyflavanone (II) (Dixon et al., 1982, 1988; Ebel & Hahlbrock, 1982) (see Chart I). Although several mechanisms have been suggested for how the enzyme catalyzes this simple addition–elimination reaction (Hahlbrock et al., 1970; Boland & Wong, 1979), little is known about the role of active-site residues. Chalcone isomerase loses activity upon treatment with iodoacetamide (Boland & Wong, 1975), *N*-ethylmaleimide (Bednar, 1990), and mercurials (Moustafa & Wong, 1967; Dixon et al., 1982; Bednar et al., 1989). The single cysteine residue in the chalcone isomerase from soybeans (Glycine max) is located at or near the active site, but its function has not yet been unequivocally defined (Bednar et al., 1989).

In order to probe the role of the active site cysteine residue of chalcone isomerase we have produced enzyme derivatives in which the cysteine residue has been converted to a series of unnatural amino acids. The results presented in this paper clearly demonstrate that the cysteine residue in chalcone isomerase does not function as an acid-base or nucleophilic group during catalysis nor does it play any role in the substrate inhibition observed for this enzyme. Further, the series of unnatural amino acids introduced into chalcone isomerase allow us to probe the effects of adding hydrophobic and charged groups into an active site.

Chart I



EXPERIMENTAL PROCEDURES

Materials. MMTS,[1] *p*-(hydroxymercuri)benzoate, BSA, 4-(iodoacetamido)salicylic acid, iodoacetamide, iodoacetate, and naringenin were purchased from Sigma. Methyl iodide, bromoethane, iodoheptane, and benzyl bromide were obtained from Aldrich. Bromobutane was obtained from Eastman.

2'-Hydroxy-4-methoxychalcone was obtained from the Alfred Bader Library of Rare Chemicals (Aldrich) and the purity was determined to be greater than 98% by HPLC analysis. 2',4',6',4-Tetrahydroxychalcone was prepared from naringenin by using the method of Moustafa & Wong (1967). The 4',4-DHC and 2',4',4-trihydroxychalcone were synthesized and purified as described previously (Bednar & Hadcock, 1988; Geissman & Clinton, 1946). Stock solutions of flavonoids were prepared in 95%

* To whom inquires and reprint requests should be addressed.

[1] Abbrevations used: BSA, bovine serum albumin; 4',4-DHC, 4',4-dihydroxychalcone; DTT, dithiothreitol; EDTA, ethylenediaminetetraacetic acid; NEM, *N*-ethylmaleimide; pMB, *p*-(hydroxymercuri)benzoate; MMTS, *S*-methyl methanethiosulfonate; CHES, 2-(cyclohexylamino)ethanesulfonic acid; HEPES, *N*-(2-hydroxyethyl)piperazine-*N*'-2-ethanesulfonic acid; MES, 2-*N*-morpholinoethanesulfonic acid; MOPSO, 3-*N*-morpholino-2-hydroxypropanesulfonic acid; Tris, tris(hydroxymethyl)-aminomethane.

1043-1802/91/2902-0211$02.50/0 © 1991 American Chemical Society

EtOH. Other materials and methods have been described previously (Bednar & Hadcock, 1988; Bednar et al., 1989).

Chalcone isomerase was isolated from Williams-82 cultivar of soybeans (Glycine max) and purified to homogeneity (Bednar & Hadcock, 1988). The standard assay for chalcone isomerase activity was performed by monitoring the loss of the chalcone absorbance at 390 nm at 25 °C using 40 μM 2′,4′,4-trihydroxychalcone in 50 mM Tris–chloride buffer (pH 7.6) containing 1% EtOH (Bednar & Hadcock, 1988). One international unit of enzyme activity is defined as the amount of enzyme that catalyzes the loss of 1 μmol of 2′,4′,4-trihydroxychalcone in 1 min at 25 °C in 50 mM Tris-chloride, pH 7.6. The concentration of active enzyme was calculated from the observed activity (IU/mL) using a molecular weight of 24 000 and a specific activity of 340 IU/mg (Bednar & Hadcock, 1988).

Treatment of Chalcone Isomerase with Alkylating Agents. Stock solutions of iodoacetamide (1 M), iodoacetate (1 M Na salt), 4-(iodoacetamide)salicylic acid (0.1 M titrated with KOH), sodium tetrathionate (0.1 M), NEM (0.1 M), and MMTS (0.1 M) were freshly prepared in Milli-Q water. The alkyl halides methyl iodide, bromoethane, bromobutane, iodoheptane, and benzyl bromide were used neat. Chalcone isomerase (0.18 μM) was incubated at pH 7.5 with a 100-fold dilution of the alkylating agent in 5 M urea, 50 mM HEPES containing 0.1 mg/mL BSA and 1 mM EDTA. After a 5–10-min incubation at 25 °C, the enzyme was renatured by a 20-fold dilution into 50 mM HEPES at pH 7.5 containing 0.1 mg/mL BSA and 1 mM EDTA. The activity of the modified enzyme was measured by the standard assay procedure (E) and also with assay solution supplemented with 1 mM pMB (E_{+pMB}). A control incubation lacking the alkylating reagent was run in parallel and its activity determined by the standard assay procedure (E_C). Native enzyme is instantaneously inactivated in the presence of 1 mM pMB, while the activity of cysteine-modified enzyme is insensitive to the presence of pMB. The activity observed in the presence of pMB depends on the catalytic activity of the modified enzyme (E_M) and the fraction of the enzyme modified (f_M) (eq 1). The activity observed

$$E_{+pMB} = E_M f_M \quad (1)$$

in the absence of pMB has an additional contribution from any unmodified enzyme (E_C) remaining (eq 2).

$$E = E_M f_M + E_C (1-f_M) \quad (2)$$

Rearrangement of eqs 1 and 2 allows us to calculate the fraction of the enzyme modified (f_M) and the relative catalytic activity of completely modified enzyme (E_M/E_C) according to eqs 3 and 4, respectively.

$$f_M = E_{+pMB}/E_C - E/E_C + 1 \quad (3)$$

$$E_M/E_C = (E_{+pMB}/E_C)/f_M \quad (4)$$

Kinetics of Modification of Chalcone Isomerase with MMTS. Chalcone isomerase (1.1 μM) was incubated with MMTS (1 mM) at 25 °C and pH 6.8 in 50 mM MOPSO buffer I = 0.1 M (KCl). Aliquots of enzyme were periodically removed and assayed as described above. For an irreversible reaction with a constant concentration of a modifying reagent, the fraction of the enzyme modified will follow a single exponential (eq 5). Substitution of eq

$$f_M = 1 - e^{(-k_{mod}[MMTS]t)} \quad (5)$$

5 into eqs 1 and 2 yields a description for the time-dependent change of the relative activity assayed in the presence and absence of pMB (eqs 6 and 7). The second-order rate constant for modification (k_{mod}) and the relative activity of completely modified enzyme (E_M/E_C) were determined by a nonlinear least-square fit of the time-dependent activity data according to eqs 6 and 7.

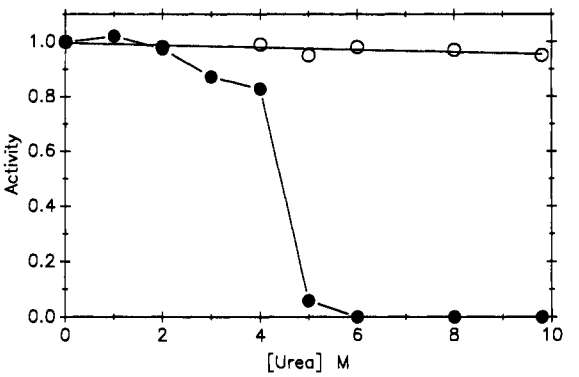


Figure 1. Reversible denaturation of chalcone isomerase in urea: (●) the activity of chalcone isomerase measured in the indicated concentration of urea at 25 °C at pH 7.6 (50 mM Tris containing 0.1 mg/mL BSA and 1 mM EDTA) using 2′,4′,4-trihydroxychalcone (100 μM) as substrate; (○) chalcone isomerase was incubated with the indicated concentration of urea (in 5 mM HEPES, pH 7.6, containing 0.1 mg/mL BSA, 100 μM EDTA, and 100 μM DTT) and the activity was determined after a 100-fold dilution into the assay solution.

$$\frac{E_{+pMB}}{E_C} = \frac{E_M}{E_C}(1 - e^{-k_{mod}[MMTS]t}) \quad (6)$$

$$\frac{E}{E_C} = \frac{E_M}{E_C}(1 - e^{-k_{mod}[MMTS]t}) + e^{-k_{mod}[MMTS]t} \quad (7)$$

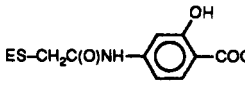
Protection against Modification by 4′,4-DHC. Chalcone isomerase (0.27 μM) was incubated with MMTS (1 mM) containing 4′,4-DHC (0–210 μM) in 50 mM MOPSO (50% base, I = 0.1 M KCl, pH 6.8). Aliquots were removed over time and assayed for enzymatic activity in the presence and absence of pMB. Control incubations lacking 4′,4-DHC were run in parallel. The observed rate constants for modification, k_{mod}, were obtained according to eqs 6 and 7. The binding constant for 4′,4-DHC at the site from which it protects, K_P, and the rate constant for modification in the absence of protectant, $(k_{mod})_{max}$, were determined by fitting a plot of log k_{mod} as a function of [4′,4-DHC] according to eq 8.

$$\log k_{mod} = \log\{(k_{mod})_{max}/(1 + [4',4\text{-DHC}]/K_P)\} \quad (8)$$

RESULTS

Effect of Urea on Enzyme Structure and Activity. Incubation of chalcone isomerase with greater than 5 M urea results in loss of the catalytic activity (Figure 1). However, essentially all the catalytic activity is rapidly regained by a 100-fold dilution of the mixture into assay solution (Figure 1). Incubation of chalcone isomerase with iodoacetamide (0.8 M) results in a slow time-dependent loss in enzymatic activity. The loss of activity is biphasic (k = 0.1 M^{-1} min^{-1} for the fast phase after correction for the slow phase) with little change in the time-dependence for inactivation between pH 6.5 and 9.2 (data not shown). When the incubation with iodoacetamide is performed at pH 7.5 in 5 M urea, the cysteine residue is rapidly modified (k_{mod} > 35 M^{-1} min^{-1}) to produce an analogue of homoglutamine with only partial loss in enzymatic activity (Table I). The denaturation of the enzyme in urea increases the rate constant for modification of the enzy-

Table I. Activity of Chalcone Isomerases containing an Altered Active Site Cysteine[a]

altered enzyme	relative activity (E_M/E_C)
ES–H	1.00
ES–SCH_3	0.86
ES–CH_3	0.66
ES–CH_2CH_3	0.31
ES–$CH_2C(O)NH_2$	0.22
ES–$CH_2C(O)O^-$	0.22
ES–$CH_2CH_2CH_2CH_3$	0.19
ES–$CH_2CH_2CH_2CH_2CH_2CH_2CH_3$	0.12
ES–$CH_2C_6H_5$	0.10[b]
	<0.01
ESH + $Na_2S_4O_6$	<0.03
ESH + NEM	<0.01
ESH + $HgCl_2$	≤0.004[c]
ESH + pMB	≤0.0004[c]

[a] The cysteine residue of chalcone isomerase (ESH) was modified to form the indicated altered enzyme species as described in Experimental Procedures. The relative activities of the altered enzyme molecules were determined with eq 4. The estimated uncertainty in these activities is ±20%. [b] Corrected for a 35% loss of activity when the methanethiolated enzyme was treated with benzyl bromide under the same conditions as the native enzyme. [c] Modified under native conditions (Bednar et al., 1989).

matic cysteine residue close to that expected for a free thiol; the rate constant for the reaction of iodoacetamide with glutathione at this pH is 55 M^{-1} min^{-1} (Dahl & McKinley-McKee, 1981). The reversible denaturation of chalcone isomerase by urea and the rapid reactivity of the cysteine residue in the denaturated enzyme provide the basis for the ready conversion of the single cysteine residue in chalcone isomerase to a series of unnatural amino acids.

Alkylation of the Cysteine Residue in Chalcone Isomerase. Chalcone isomerase was incubated with a variety of electrophilic reagents in 5 M urea. After renaturation, the activity of the modified enzymes were determined as described in Experimental Procedures. Table I lists the structures of the modified cysteine residues and the relative catalytic activities of the resulting altered enzymes. When the cysteine residue was modified with an SMe group, the modified enzyme retains 85% of the catalytic activity of the native enzyme. Treatment of this cysteine-blocked enzyme with each of the electrophilic reagents in urea resulted in no additional activity loss. This result indicates that the lower catalytic activities reported in Table I result from modification of the cysteine residue and not from any nonspecific modification of protein.

Modification of the Cysteine Residue in Chalcone Isomerase by MMTS under Native Conditions. The reaction of MMTS with a cysteine residue results in the addition of a methylthio group (SMe) onto the cysteine sulfur atom (Smith et al., 1975; Kenyon & Bruice, 1977). Incubation of chalcone isomerase with MMTS results in complete modification of the cysteine residue with loss of about 15% of the enzymatic activity (Figure 2). The extent of modification of the enzyme by MMTS can be conveniently monitored by following the loss in the ability of pMB to inactivate the enzyme. When native enzyme is assayed in the presence of 1 mM pMB, no enzymatic activity is detected. As shown in Figure 2, treatment of the enzyme with MMTS results in a time-dependent increase in the enzymatic activity observed when the assay is performed in the presence of pMB. MMTS-modified enzyme shows no difference in activity when measured in the presence or absence of pMB.

The substrate analogue 4′,4-DHC provides protection

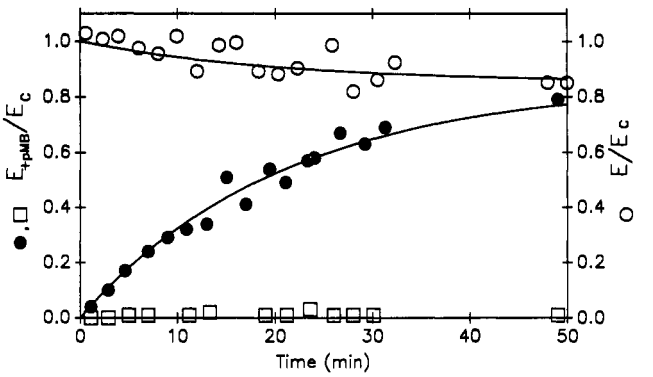


Figure 2. Kinetics for the methanethiolation of chalcone isomerase by MMTS. Chalcone isomerase (1.1 μM) was incubated with MMTS (1 mM) as described in Experimental Procedures. Aliquots were removed at the indicated times and assayed for activity. The activity was measured in the standard assay in the presence (●) or absence (○) of 1 mM pMB. A control incubation lacking MMTS was incubated under the same conditions and all activities are reported relative to the activity of the control incubation (E_C) assayed in the absence of pMB. The absence of catalytic activity for the control enzyme assayed in the presence of 1 mM pMB is shown by the open squares. The lines are drawn according to eqs 6 and 7 with a fractional activity for the modified enzyme, E_M/E_C, of 0.85 and a rate constant for modification, k_{mod}, of 48 M^{-1} min^{-1}.

against the modification of chalcone isomerase by MMTS. At high concentrations of 4′,4-DHC, the rate constant for modification is reduced by over 100-fold. A binding constant, K_P = 3.9 ± 1.0 μM, for 4′,4-DHC was obtained from the dependence of the rate constant for modification on the concentration of 4′,4-DHC (eq 8). This binding constant is numerically identical with the K_I obtained from inhibition of catalytic turnover by 4′,4-DHC (Table II). Complete kinetic protection against modification by MMTS is expected on blocking the active site with 4′,4-DHC, since the only cysteine residue in chalcone isomerase is at or near the active site (Bednar et al., 1989).

Characterization of the Methanethiolated Enzyme (ESSMe). Methanethiolated chalcone isomerase was prepared by a 1-h room temperature incubation of the chalcone isomerase (1–5 μM) with MMTS (1 mM). Complete modification of the cysteine residue was verified by the insensitivity of the enzymatic activity to the presence of 1 mM pMB in the assay. The methylthio group (SMe) attached to a cysteine residue is reported to be very easily removed by traces of free thiol (Smith et al., 1975; Kenyon & Bruice, 1977). However, treatment of methanethiolated chalcone isomerase for 24 h with up to 1 M DTT or β-mercaptoethanol failed to regenerate the free enzyme. When the enzyme was reversibly denaturated by adding urea or by raising the pH to 13, β-mercaptoethanol and DTT rapidly regenerated the free enzyme. The failure to regenerate free enzyme under nondenaturing conditions suggests that the methanethio group is buried in the enzyme and not accessible to DTT or β-mercaptoethanol (Nishimura et al., 1975).

Table II compares the steady-state kinetic parameters of the methanethiolated enzyme with native chalcone isomerase at pH 7.6. The initial velocities of the native ($v°_{ESH}$) and the methanethiolated enzyme ($v°_{ESSMe}$) were also compared in parallel experiments under identical conditions. Table III summaries these results as a function of pH and concentration of 2′,4′,4-trihydroxychalcone. Similar results were obtained with 2′,4′,6′,4-tetrahydroxychalcone and 2′-hydroxy-4-methoxychalcone as substrates.

DISCUSSION

Site-directed mutagenesis is a powerful technique for altering the structure of a protein in order to probe the

Table II. Steady-State Kinetic Parameters for Methanethiolated Enzyme (ESSMe) Compared to Native Enzyme (ESH) at pH 7.6[a]

parameter	ESSMe	ESH	ESSMe/ESH[b]
	2′,4′,6′,4-Tetrahydroxychalcone[c]		
k_{cat}, min^{-1}	42,000 ± 1,200	50,000 ± 1,700	0.84 ± 0.04
k_{cat}/K_m, μM^{-1} min^{-1}	9,800 ± 1,500	8,000 ± 1,000	1.2 ± 0.2
K_M, μM	4.3 ± 0.7	6.3 ± 0.9	0.7 ± 0.2
	2′,4′,4-Trihydroxychalcone[d]		
k_{cat}, min^{-1}	6,400 ± 1,000	10,000 ± 1,500	0.64 ± 0.14
k_{cat}/K_m, μM^{-1} min^{-1}	660 ± 120	700 ± 140	0.9 ± 0.3
K_M, μM	10 ± 3	14 ± 4	0.7 ± 0.3
K_i^s, μM	120 ± 40	180 ± 60	0.7 ± 0.4
K_i for 4′,4-DHC,[e] μM	2.9 ± 0.5	3.9 ± 0.6	0.7 ± 0.2
K_P for 4′,4-DHC,[f] μM		3.9 ± 1.0	

[a] Chalcone isomerase (5 μM) was methanethiolated by treatment with MMTS (1 mM) at pH 7.6 (50 mM HEPES, I = 0.1 M) and 25 °C for 1.5 h. The enzyme was then diluted and stored on ice. The initial velocities (v^o) for native and methanethiolated enzyme were measured at 25 °C (pH 7.6, 50 mM HEPES, I = 0.1 M) with the indicated substrate. [b] The absolute uncertainty (U) for the ratio (R) was calculated from the standard deviations (SD_i) of the fitted parameters (X_i) by using the equation $U = R[\sum_i(SD_i/X_i)^2]^{1/2}$. [c] The initial velocities were determined at 30 substrate concentrations ranging from 0 to 112 μM. The steady-state kinetic parameters were determined by a nonlinear-least-square fit of the data to the equation $v^o/[E] = (k_{cat}[S]k_{cat}/K_M)/(k_{cat} + [S]k_{cat}/K_M)$ (Northrop, 1983). No substrate inhibition was observed for either enzyme at up to 850 μM of substrate. [d] The initial velocities were determined at 46 concentrations of substrate ranging from 0 to 512 μM. The steady-state kinetic parameters were obtained by a nonlinear-least-square fit of initial velocity data using the equation $v^o = k_{cat}[E][S]/\{[S] + K_M + [S]^2/K_i^s\}$, where K_i^s is the substrate inhibition constant. [e] The competitive inhibition constant, K_i, was calculated from a Dixon plot of initial velocity data obtained with 10 μM of 2′,4′,4-trihydroxychalcone and five concentrations of 4′,4-DHC ranging from 0 to 36 μM. [f] The concentration dependence of the protection against MMTS modification afforded by 4′,4-DHC was determined as described in Experimental Procedures. The fitted value of $(k_{max})_{mod}$ is 100 ± 10 M^{-1} min^{-1}.

Table III. Initial Velocities of Methanethiolated Enzyme Compared to Native Enzyme as a Function of pH and Substrate Concentration[a]

pH	[S], μM	v^o_{ESSMe}/v^o_{ESH}	N^b
5.5	2	0.60 ± 0.03	2
5.5	38	0.66 ± 0.01	3
5.5	100	0.72 ± 0.01	2
5.5	*avg*	*0.66 ± 0.05*	*7*
7.6	2	0.87	1
7.6	39	0.86 ± 0.10	18
7.6	85	0.82 ± 0.02	3
7.6	620	0.63 ± 0.04	3
7.6	*avg*	*0.83 ± 0.12*	*25*
9.4	32	0.88 ± 0.10	3
9.4	1024	0.85 ± 0.05	3
9.4	*avg*	*0.87 ± 0.08*	*6*

[a] Chalcone isomerase (4.2 μM) was methanethiolated by incubation with MMTS (1 mM) at pH 7.6 (50 mM HEPES, I = 0.1 M) and 25 °C for 1 h. The enzyme was then diluted 25-fold with the HEPES buffer and stored on ice. The initial velocities for native enzyme (v^o_{ESH}) and methanethiolated enzyme (v^o_{ESSMe}) were measured with 2′,4′,4-trihydroxychalcone as substrate at 25 °C and pH 5.5 (50 mM MES, I = 0.1 M), pH 7.6 (50 mM HEPES, I = 0.1 M and 50 mM Tris-HCl), and pH 9.4 (50 mM CHES, I = 0.1 M). [b] N is the number of initial velocity measurements used in calculating the standard deviations.

function of specific residues. This method is generally limited to the substitution of one natural amino acid for another (Knowles, 1987). The procedures employed here with chalcone isomerase illustrate a rapid means of altering an active site residue to produce protein molecules containing a variety of unnatural amino acids. Both techniques have utility in probing the structure–function relationship in proteins and in the engineering of enzymes with altered activities and substrate specificities. Alternative methods for introducing unnatural amino acids may soon be applied more generally, but currently they are too cumbersome for routine use (Bain et al., 1989; Noren et al., 1989; Anthony-Cahill et al., 1989).

Cysteine is one of the most reactive amino acids as a result of its highly nucleophilic thiol side chain. Thiol groups can be readily alkylated by reaction with alkyl halides and other electrophilic reagents (Lundblad, 1984; Torchinsky, 1981; Kenyon & Bruice, 1977; Liu, 1977; Friedman, 1973; Jocelyn, 1972). The high reactivity of the freely accessible cysteine residue of papain has been exploited to link a flavin at the active site in order to produce an oxidoreductase (Kaiser & Lawrence, 1984; Kaiser, 1988). Similarly, a solvent-accessible cysteine residue introduced into staphylococcal nuclease by site-directed mutagenesis was used as a site of attachment of an oligonucleotide to produce a sequence-specific single-stranded deoxyribonuclease (Corey & Schultz, 1987). However, in many natural cases cysteine residues are not fully accessible to the solvent. Their rates of reactions can often be considerably reduced due to ionization state, hydrogen bonding, electrostatic effects, hydrophobic interactions, and steric effects (Webb 1966a; Torchinsky, 1981; Boyer, 1959; Friedman, 1973). By denaturing a protein, the full intrinsic reactivity of the thiol group is expressed. This allows for the selective and rapid modification of a thiol group that is otherwise slow to react. If the protein is unfolded to facilitate the modification reaction, then it would be necessary that the protein be able to refold into a nativelike conformation. Fortunately, the ability of proteins to be denatured reversibly is fairly common (Jaenicke, 1987). Our approach couples this ability to renature proteins (Figure 1) with the high intrinsic reactivity of cysteine in a denatured protein to produce highly selective modifications. The unnatural amino acid derivatives produced supplement the other 19 natural amino acids used for altering the structure of a protein. This added capability should prove useful for modulation of substrate specificity, for dissection of mechanisms, and for creation of steric probes of binding sites and will aid in our understanding of the role of hydrophobic and charge interaction in binding and catalysis.

Chalcone isomerase contains a single cysteine residue located at or near the active site (Bednar et al., 1989). The exact role of this cysteine residue has yet to be determined. There is precedent for the involvement of active-site cysteine residues as acid–base catalysts and covalent catalysts in proline racemase (Alberty & Knowles, 1986) and thymidylate synthase (Santi & Danenberg, 1984), respectively. Hahlbrock and co-workers (Hahlbrock et al., 1970) propose a mechanism for chalcone isomerase involving general acid–base catalysis through an intermediate flav-3-en-4-ol. In contrast, Boland & Wong (1979) have suggested nucleophilic catalysis by an active-site imidazole, followed by a S_N2 displacement by the 2′-phenolate of the substrate. Although all five of the histidine residues have recently been shown not to be essential for catalysis (Bednar & Adeniran, 1990), it is possible that another amino acid residue, such as cysteine, could function as a nucleophile. A rapid means of producing chalcone isomerase molecules which contain an altered active site amino acid has provided a means of assessing the functional role of this amino acid residue in binding and catalysis.

Altered chalcone isomerases were produced by modifying the cysteine residue to introduce a series of unnatural amino acid residues containing increasing alkyl chain lengths or new functional groups (Table I). Enzyme containing an analogue of homoglutamate or homoglutamine displays a similar reduction in catalytic activity

with surprisingly no differential effect between the negatively charged and neutral substitution (Table I). Interpretation of this observation is currently complicated by the possibility of additional structural changes in the protein. For example, attempts to alter substrate specificity by replacement of the aspartate in the specificity pocket of trypsin with a lysine residue resulted in the charged residue extending through the wall of the pocket to form hydrogen bonds to various acceptors outside of it (Graf et al., 1987).

The role of hydrophobic amino acid residues in protein structure and enzymatic catalysis is currently not well understood. Hydrophobic residues can have dramatic effects on binding and catalysis. For example, the hydrophobic side chain of leucine-54 of dihydrofolate reductase results in a 10^4-fold stabilization of the transition state for hydride transfer (Mayer et al., 1986). Table I shows the results of adding increasingly larger alkyl chains to the cysteine residue of chalcone isomerase. The activity of the altered enzyme decreases as the alkyl chain length or steric bulk is increased. Modification of the cysteine residue with 4-(iodoacetamido)salicylic acid, sodium tetrathionate, *N*-ethylmaleimide, $HgCl_2$, or *p*-mercuribenzoate results in loss of greater than 99% of the enzymatic activity (Table I). These results suggest that the essentially complete inactivation observed with the latter reagents is a consequence of the steric bulk of the modified residue. It may not be immediately apparent why $HgCl_2$ results in greater than 99.6% inactivation of the enzyme. However, the ion Hg^{2+} is multicoordinate and may likely coordinate to other amino acids in addition to the thiol group of this cysteine and thereby distort the structure of the enzyme (Webb, 1966b).

The activities reported in Table I should be considered to be lower limits for the activities of the altered enzymes since the modification could affect the refolding of the enzyme molecules. In order to remove any complication resulting from the necessity for refolding we wanted to be able to add a group with small steric bulk to the cysteine residue under native conditions. MMTS is a very potent and selective reagent for modification of sulfhydryl groups (Smith et al., 1975; Kenyon & Bruice, 1977; Kluger & Tsui, 1980). Its rate constant for reaction with the cysteine residue of glutathione is 4.9 orders of magnitude greater than that of iodoacetate and 6.4 orders of magnitude greater than that of an unactivated alkyl halide.[2] The high intrinsic reactivity of MMTS toward thiol groups makes it an excellent reagent for selective cysteine modification. As shown in Figure 2, MMTS rapidly modifies native enzyme to produce methanethiolated enzyme. The rate constant for the modification of the enzyme by MMTS, while quite large (48 M^{-1} min^{-1} at pH 6.8), is still 17 000-fold smaller than its rate constant for reaction with glutathione. The removal of the methylthio group (SMe) by β-mercaptoethanol and DTT was only possible under denaturing conditions. These results confirm the general inaccessibility of the cysteine residue noted previously with the use of NEM to modify the native protein (Bednar, 1990).

Chalcone isomerase increases the rate constant for cyclization of 2′,4′,4-trihydroxychalcone (I) by 36 million-fold over that of spontaneous reaction (Bednar & Hadcock, 1988). Alteration of the active site cysteine residue by attachment of a group to the sulfur atom removes the acidic, basic, and nucleophilic properties of this residue. However, methanethiolation of the chalcone isomerase only reduces the catalytic activity by 15% (Figure 2). The preservation of catalytic activity in these altered enzymes (Table I) clearly demonstrates that the cysteine residue does not function as nucleophile or general acid–base in the catalytic reaction.

In order to further probe the role of the cysteine residue in chalcone isomerase, we undertook a comparison of the steady-state kinetic parameters for the native and the methanethiolated enzyme (Table II). All the parameters for the methanethiolated enzyme are similar, within the experimental error of the measurements, to the native enzyme. Additionally, the substrate specificity of the enzyme was not changed. Preventing the ionization of the enzymatic cysteine residue (pK = 9.2 Bednar, 1990) by methanethiolation results in no differential effect on the enzyme activity at pH 9.4 as compared to pH 7.6 (Table III). The ionization of the cysteine appears not to modulate catalytic activity. The methanethiolated enzyme is slightly less active than native enzyme at pH 5.5 compared to pH 7.6 suggesting that methanethiolation might cause a 0.1 pH unit increase in the pK seen in the V and V/K pH–rate profiles. The formation of a reversible Michael adduct of the chalcone substrate with the enzymatic cysteine residue could result in substrate inhibition. Chalcones are known to be powerful electrophiles and react in aqueous solution with free thiols (Dhar, 1981). However, the absence of an effect of methanethiolation on the substrate inhibition constant (K_i^s, Table II) demonstrates that the observed substrate inhibition is not mediated by the enzymatic cysteine residue.

The binding constant for 4′,4-DHC to the methanethiolated enzyme is the same as for its binding to the native enzyme (Table II), suggesting there is no steric repulsion between 4′,4-DHC and the methylthio group (SMe). However, blocking the active site by binding of 4′,4-DHC offers complete kinetic protection against the modification caused by the MMTS molecule, which is considerably larger than the methylthio group. The observed protection supports an assignment that places the cysteine residue in the vicinity of the active site.

The method presented in this paper provides a rapid and selective means of altering the cysteine residue of chalcone isomerase to produce enzyme molecules containing a variety of unnatural amino acids. These chemical modification techniques complement site-directed mutagenesis for studying the structure–function relationship. Each method allows for the introduction of different types of amino acid substitutions. Spectroscopic techniques, such as CD, fluorescence, NMR and X-ray crystallography, will be necessary to fully understand the basis for the effects observed upon the addition of hydrophobic and charged unnatural amino acids into the active site. However, our results with chalcone isomerase, clearly demonstrate that the active site cysteine residue does not function as an acid–base or nucleophilic group in producing the catalysis or substrate inhibition observed with this enzyme.

ACKNOWLEDGMENT

This research was supported by Grant GM 34832 from the National Institutes of Health. The assistance of Jeff Harvey in performing initial experiments of the methanethiolation of the enzyme is gratefully acknowledged. We thank Drs. Steven E. Rokita, Adejare J. Adeniran,

[2] The rate constants for reaction of the thiolate of glutathione [pK = 9.0 (Rabenstein, 1973)] with the electrophilic reagents pMB, MMTS, NEM, iodoacetate, iodomethane are 4.5×10^{11} M^{-1} min^{-1} (for $HOCH_2CH_2S^-$, Hasinoff et al., 1971), 1.3×10^8 M^{-1} min^{-1} (Roberts et al., 1986), 5.9×10^6 M^{-1} min^{-1} (Bednar, 1990), 1.6×10^3 M^{-1} min^{-1} (Dahl & McKinley-McKee, 1981), and 55 M^{-1} min^{-1} (Halasz & Polgar, 1976), respectively.

and Ming Zeng for helpful discussions and their critical review of this manuscript.

LITERATURE CITED

Albery, W. J., and Knowles, J. R. (1986) Energetics and mechanism of proline racemase. *Biochemistry 25*, 2572–2577.

Anthony-Cahill, S. J., Griffith, M. C., Noren, C. J., Suich, D. J., and Schultz, P. G. (1989) Site-specific mutagenesis with unnatural amino acids. *Trends Biochem. Sci. 14*, 400–403.

Bain, J. D., Glabe, C. G., Dix, T. A., and Chamberlin, A. R. (1989) Biosynthetic site-specific incorporation of a non-natural amino acid into a polypeptide. *J. Am. Chem. Soc. 111*, 8013–8014.

Bednar, R. A., and Hadcock, J. R. (1988) Purification and characterization of chalcone isomerase from soybeans. *J. Biol. Chem. 263*, 9582–9588.

Bednar, R. A., Fried, W. B., Lock, Y. W., and Pramanik, B. (1989) Chemical modification of chalcone isomerase by mercurials and tetrathionate. Evidence for a single cysteine residue in the active site. *J. Biol. Chem. 264*, 14272–14276.

Bednar, R. A. (1990) Reactivity and pH dependence of thiol conjugation to *N*-ethylmaleimide: Detection of a conformational change in chalcone isomerase. *Biochemistry 29*, 3684–3690.

Bednar, R. A., and Adeniran, A. J. (1990) Chemical modification of chalcone isomerase by diethyl pyrocarbonate: Histidine residues are not essential for catalysis. *Arch. Biochem. Biophys. 282*, 393–398.

Boland, M. J., and Wong, E. (1975) Purification and kinetic properties of chalcone-flavanone isomerase from soya bean. *Eur. J. Biochem. 50*, 383–389.

Boland, M. J., and Wong, E. (1979) Mechanism of action of chalcone isomerase. *Bioorg. Chem. 8*, 1–8.

Boyer, P. D. (1959) Sulfhydryl and disulfide groups in enzymes. *The Enzymes*, 2nd ed. (P. D. Boyer, H. Lardy, and K. Myrback, Eds.) Vol. 1, pp 511–588, Academic Press, New York.

Corey, D. R., and Schultz, P. G. (1987) Generation of a hybrid sequence-specific single-stranded deoxyribonuclease. *Science 238*, 1401–1403.

Dahl, K. H., and McKinley-McKee, J. S. (1981) The reactivity of affinity labels: A kinetic study of the reaction of alkyl halides with thiolate anions—a model reaction for protein alkylation. *Bioorg. Chem. 10*, 329–341.

Dhar, D. N. (1981) *The Chemistry of Chalcones and Related Compounds*, p 119, John Wiley and Sons, New York.

Dixon, R. A., Dey, P. M., and Whitehead, I. M. (1982) Purification and properties of chalcone isomerase from cell suspension cultures of *Phaseolus vulgaris*. *Biochim. Biophys. Acta 715*, 25–33.

Dixon, R. A., Dey, P. M., and Lamb, C. J. (1983) Phytoalexins: enzymology and molecular biology. *Adv. Enzymol. Relat. Areas Mol. Biol. 55*, 1–121.

Dixon, R. A., Blyden, E. R., Robbins, M. P., van Tunen, A. J., and Mol, J. N. (1988) Comparative biochemistry of chalcone isomerases. *Phytochemistry 27*, 2801–2808.

Ebel, J., and Hahlbrock, K. (1982) Biosynthesis. *The Flavonoids: Advances in Research* (J. B. Harborne, and T. J. Marbry, Eds.) pp 641–670, Chapman and Hall, London.

Friedman, M. (1973) *The Chemistry and Biochemistry of the Sulfhydryl Group in Amino Acids, Peptides and Proteins*, Pergamon Press, New York.

Geissman, T. A., and Clinton, R. O. (1946) Flavonones and related compounds. I. The preparation of polyhydroxychalcones and -flavanones. *J. Am. Chem. Soc. 68*, 697–700.

Graf, L., Craik, C. S., Patthy, A., Roczniak, S., Fletterick, R. J., and Rutter, W. J. (1987) Selective alteration of substrate specificity by replacement of aspartic acid-189 with lysine in the binding pocket of trypsin. *Biochemistry 26*, 2616–2623.

Hahlbrock, K., Wong, E., Schill, L., and Grisebach, H. (1970) Comparison of chalcone-flavanone isomerase heteroenzymes and isoenzymes. *Phytochemistry 9*, 949–958.

Halasz, P., and Polgar, L. (1976) Use of methyl iodide for probing the polarity of the immediate environment of -SH groups in thiolenzymes. *Eur. J. Biochem. 71*, 563–569.

Hasinoff, B. B., Madsen, N. B., and Avramovic-Zikic, O. (1971) Kinetics of the reaction of *p*-chloromercuribenzoate with the sulfhydryl groups of glutathione, 2-mercaptoethanol, and phosphorylase b. *Can. J. Biochem. 49*, 742–751.

Jaenicke, R. (1987) Folding and association of proteins. *Prog. Biophys. Mol. Biol. 49*, 117–237.

Jocelyn, P. C. (1972) *Biochemistry of the SH Group*, Academic Press, London.

Kaiser, E. T. (1988) Catalytic activity of enzymes altered at their active sites. *Angew. Chem. Int. Ed. Engl. 27*, 913–922.

Kaiser, E. T., and Lawrence, D. S. (1984) Chemical mutation of enzyme active sites. *Science 226*, 505–511.

Kenyon, G. L., and Bruice, T. W. (1977) Novel sulfhydryl reagents. *Methods Enzymol. 47*, 407–430.

Kluger, R., and Tsui, W. C. (1980) Amino group reactions of the sulfhydryl reagent methyl methanesulfonothioate. Inactivation of D-3-hydroxybutyrate dehydrogenase and reaction with amines in water. *Can. J. Biochem. 58*, 629–632.

Knowles, J. R. (1987) Tinkering with enzymes: What are we learning? *Science 236*, 1252–1258.

Liu, T.-Y. (1977) The role of sulfur in proteins. *The Proteins*, 3rd ed. (H. Neurath, and R. L. Hill, Eds.) Vol. III, pp 239–402, Academic Press, New York.

Lundblad, R. L., and Noyes, C. M. (1984) *Chemical Reagents for Protein Modification*, Vol. I, pp 55–93, CRC Press, Boca Raton, FL.

Mayer, R. J., Chem, J.-T., Taira, K., Fierke, C. A., and Benkovic, S. J. (1986) Importance of a hydrophobic residue in binding and catalysis by dihydrofolate reductase. *Proc. Natl. Acad. Sci. U.S.A. 83*, 7718–7720.

Moustafa, E., and Wong, E. (1967) Purification and properties of chalcone-flavanone isomerase from soya bean seed. *Phytochemistry 6*, 625–632.

Nishimura, J. S., Kenyon, G. L., and Smith, D. J. (1975) Reversible modification of the sulfhydryl groups of *Escherichia coli* succinic thiokinase with methanethiolating reagents, 5,5′-dithiobis-(2-nitrobenzoic acid), *p*-hydroxymercuribenzoate, with ethylmercurithiosalicylate. *Arch. Biochem. Biophys. 170*, 461–467.

Noren, C. J., Anthony-Cahill, S. J., Griffith, M. C., and Schultz, P. G. (1989) A general method for site-specific incorporation of unnatural amino acids into proteins. *Science 244*, 182–188.

Northrop, D. B. (1983) Fitting enzyme-kinetic data to V/K. *Anal. Biochem. 132*, 457–461.

Rabenstein, D. L. (1973) Nuclear magnetic resonance studies of the acid–base chemistry of amino acids and peptides. I. Microscopic ionization constants of glutathione and methylmercury-complexed glutathione. *J. Am. Chem. Soc. 95*, 2797–2803.

Roberts, D. D., Lewis, S. D., Ballou, D. P., Olson, S. T. and Shafer, J. A. (1986) Reactivity of small thiolate anions and cysteine-25 in papain toward methyl methanethiosulfonate. *Biochemistry 25*, 5595–5601.

Santi, D. V., and Danenberg, P. V. (1984) in *Folates and Pterins* (R. L. Blakley, and S. J. Benkovic, Eds.) Vol. I, pp 345–398, John Wiley and Sons, New York.

Smith, D. J., Maggio, E. T., and Kenyon, G. L. (1975) Simple alkanethiol groups for temporary blocking of sulfhydryl groups of enzymes. *Biochemistry 14*, 766–771.

Torchinsky, Y. M. (1981) *Sulfur in Proteins* (D. Metzler, Ed.) Pergamon, New York.

Webb, J. L. (1966a) *Enzyme and Metabolic Inhibitors*, Vol. II, pp 635–654, Academic Press, New York.

Webb, J. L. (1966b) *Enzyme and Metabolic Inhibitors*, Vol. II, pp 729–986, Academic Press, New York.

Registry No. I, 13745-20-5; MMTS, 2949-92-0; 4′,4-DHC, 3600-61-1; 2′,4′,6′,4-tetrahydroxychalcone, 25515-46-2; cysteine, 52-90-4; chalcone isomerase, 9073-57-8.

Acridine- and Cholesterol-Derivatized Solid Supports for Improved Synthesis of 3'-Modified Oligonucleotides

Michael W. Reed,* A. David Adams, Jeffrey S. Nelson,† and Rich B. Meyer, Jr.

MicroProbe Corporation, 1725 220th Street SE #104, Bothell, Washington 98021. Received March 22, 1991

New solid supports are described which allow the direct synthesis of oligonucleotides bearing either cholesterol or acridine at the 3'-terminus. A stereochemically defined amino diol was prepared by reduction of *N*-Cbz-hydroxy-L-proline. This linker molecule was first acylated with the desired conjugate molecule, then protected as the dimethoxytrityl ether. The remaining secondary hydroxyl group was succinylated and immobilized on a controlled-pore glass support. 3'-Modified oligodeoxynucleotides (ODNs) were prepared from these supports by using standard phosphoramidite coupling and deprotection conditions. A cholesterol-modified support was prepared from cholesterol chloroformate and the amino diol linker. Two types of acridine-modified solid supports were prepared from acridine tetrafluorophenyl esters with linker arms of different length. In an alternative synthesis of 3'-derivatized ODNs, these active esters were also utilized for acylation of a 3'-amine-modified ODN. A thermal denaturation study was done to determine the effect of the different linker arms on hybridization to a complementary ODN target. Facile synthesis and purification of the 3'-modified ODNs makes these functionalized solid supports especially useful for preparation of oligonucleotides bearing these and other modifications.

INTRODUCTION

Attachment of small molecular weight groups to the 3'- or 5'-terminus of synthetic oligodeoxynucleotides has improved their diagnostic utility as DNA probes (*1*) and their potential therapeutic applications as "antisense" oligonucleotides (*2*, *3*). For example, ODNs[1] modified with intercalating groups such as acridine show enhanced binding to the target strand and improved inhibition of mRNA translation (*4*). The acridine-tailed ODNs also have shown improved uptake into mammalian cells, being sequestered in the nucleus after entry into the cytoplasm (*5*). The fluorescent properties of the acridine tail make it useful for biological probes and for studies of ODN biodistribution in the cell. ODNs modified at the 3'-end are less readily degraded by exonucleases, thus improving their serum stability (*3*). Addition of cholesterol to the 3'- or 5'-terminus of phosphorothioate ODNs has been shown to provide improved therapeutic effect in an HIV assay (*6*, *7*). It is unclear by what mechanism these compounds exert their effect due to their lack of sequence specificity, but the lipophilic tail has been shown to improve cellular uptake (*8*). In one cell line, cholesterol-modified ODNs localized in the nucleus, perhaps delivered by a cholesterol-binding protein (*9*).

Nonenzymatic methods for introducing 3'- and 5'-conjugated groups into ODNs have been reviewed (*3*, *10*). Modifications are most readily carried out at the 5'-terminus of the ODN, due to the accessibility of this site during solid-phase synthesis. Since the ODN is immobilized via the 3'-hydroxyl group, procedures for introduction of conjugate groups at the 3'-terminus generally involve cleavage from the support and postsynthetic modification of the ODN using solution-phase coupling. For example, 3'-tethered acridines were introduced by reaction of a hydroxyl group on a side chain of the acridine with the 3'-phosphate of the ODN using phosphotriester chemistry (*11*). In another method, a ribonucleoside residue can be attached to the 3'-terminus by chemical synthesis from an RNA solid support. Periodate oxidation of the ribose ring generates aldehyde residues which can be modified with amines by reductive amination (*12*). Solid supports that give rise to ODNs with 3'-phosphate groups have also been described (*13*, *14*). These can be activated and modified by addition of amines (*15*, *16*).

The most versatile methods for preparation of 3'-tailed ODNs involve synthesis of the ODN from a specially prepared solid support that incorporates a protected nucleophilic amino group (*17–19*) or thiol group (*20*). The conjugate group is introduced by postsynthetic treatment of the deprotected ODN with a suitable electrophile. There are several drawbacks to this approach. The aqueous environment can lead to side reactions such as hydrolysis of the electrophile. The required large excess of electrophilic reagent can give rise to undesired side reactions at other nucleophilic sites in the ODN. Isolation of the desired conjugate from the resulting mixture of products is tedious and can lead to low yields.

Described in this paper is a method for the preparation of 3'-tailed ODNs from modified solid supports which contain the desired tail molecule. We have prepared three CPG supports, Chol-CPG (**5**) and Acr-CPG (**9a,b**), that have been modified with cholesterol and acridine, respectively. These supports were prepared from a stereochemically defined and conformationally rigid amino diol linker **2** which provides attachment points for (a) the desired conjugate molecule, (b) the solid support, and (c) the initial 3'-nucleic acid residue. By using a CPG support that is functionalized with the desired conjugate group, the 3'-tailed ODN can be isolated directly after synthesis, thus saving time and improving yield. The synthesis of these novel solid supports and their use in the preparation of 3'-tailed ODNs are described. Synthesis and purification of 3'-acridine conjugates by acylation of an ODN bearing

† Present address: Department of Chemistry, Oregon State University, Corvallis, OR 97331-4003.

[1] Abbreviations: ODN, oligodeoxyribonucleotide; CPG, controlled-pore glass; LCAA-CPG, long chain alkylamine-CPG; EDC, 1-ethyl-3-[3-(dimethylamino)propyl]carbodiimide; DMAP, 4-(dimethylamino)pyridine; FMPT, 2-fluoro-*N*-methylpyridinium tosylate; TFP, 2,3,5,6-tetrafluorophenyl; PAGE, polyacrylamide gel electrophoresis; DMTr, 4,4'-dimethoxytrityl; M-pyrol, 1-methyl-2-pyrrolidinone; TEAA, triethylammonium acetate; Cbz, benzyloxycarbonyl.

1043-1802/91/2902-0217$02.50/0 © 1991 American Chemical Society

a 3′-amine using acridine TFP esters **6a** and **6b** are also described. The effect of the 3′-tails on the hybridization properties of the ODNs was examined.

EXPERIMENTAL PROCEDURES

General Chemical Procedures. All air- or water-sensitive reactions were carried out in oven-dried glassware under a slight positive pressure of argon. Anhydrous solvents were obtained from Aldrich (Milwaukee, WI). THF was distilled from sodium and benzophenone. Removal of solvents at 15–30 Torr was accomplished on a rotary evaporator. Melting points were determined in an open glass capillary tube using a Mel-Temp melting point apparatus and are uncorrected. Infrared spectra were obtained with a Perkin-Elmer 783 spectrophotometer using the 1601 cm^{-1} absorption of polystyrene as a standard reference. UV spectra were obtained with a Beckman DU-40 spectrophotometer using 0.1 mL quartz cuvettes. Proton magnetic resonance spectra were recorded using a Varian Gemini FT-200 (200 MHz) spectrometer. Appropriate solvent resonances were consistently used as internal references. All chemical shifts are reported in ppm downfield from tetramethylsilane. Elemental analyses were performed by Quantitative Technologies, Inc. (Bound Brook, NJ). Flash chromatography was performed with EM Science silica gel 60 (230–400 mesh). Analytical thin-layer chromatography was carried out on EM Science F_{254} aluminum-backed, fluorescence-indicator plates. Plates were visualized with UV light, unless otherwise indicated. Unless otherwise stated, yields refer to isolated compounds of greater than 95% purity, as determined by ^1H NMR spectroscopy.

1-(Benzyloxycarbonyl)-5-(hydroxymethyl)-(3*R-trans*)-3-pyrrolidinol (1). To an ice-cold solution of 4.76 g (18 mmol) of *N*-Cbz-hydroxy-L-proline (Sigma Chemical Co.) in 20 mL of dry THF was added 45 mL of a 1 M solution of BH_3·THF complex in THF (Aldrich). After stirring under argon for 15 min at 0–5 °C, and 4.5 h at room temperature, the mixture was cautiously quenched with 50 mL of methanol. After 30 min, the solution was concentrated. The residual colorless syrup was purified by flash chromatography (3.5 × 23 cm silica) using a gradient of methanol in methylene chloride. Product 1 eluted with 10% methanol. The fractions containing pure product were evaporated to dryness to give 2.18 g (46% yield) of 1 as a colorless syrup: TLC (95:5 methylene chloride–methanol) R_f = 0.16; IR (neat) 3600–3100 (br), 2940, 1680, 1420, 1355 cm^{-1}; ^1H NMR ($CDCl_3$) δ 7.36 (s, 5 H), 5.17 (s, 2 H), 4.50 (m, 2 H), 3.67 (m, 4 H), 2.09 (m, 3 H). Anal. Calcd for $C_{13}H_{17}NO_4$·0.3H_2O: C, 60.83; H, 6.91; N, 5.46. Found: C, 60.85; H, 6.88; N, 5.36.

5-(Hydroxymethyl)-(3*R-trans*)-3-pyrrolidinol (2). A solution of 1.92 g (7.6 mmol) of the Cbz-protected amino diol 1 in 50 mL of methanol was stirred with 320 mg of 10% Pd on carbon under a balloon of hydrogen. After 16 h no starting material remained as evidenced by TLC (9:1 methylene chloride–methanol). The mixture was filtered through Celite (washed with methanol), and the filtrate was concentrated to give product **2** as an amber syrup in quantitative yield. The syrup was dissolved in ethanol to give 15.2 mL of a 0.5 M stock solution. TLC (3:1:1:1 ethyl acetate–acetone–methanol–water) R_f = 0.06, pink spot with ninhydrin spray; IR (neat) 3600–3100 (br), 2920, 1530, 1410 cm^{-1}; ^1H NMR (D_2O) δ 4.40 (m, 1 H), 3.60 (m, 3 H), 3.02 (d of d, 1 H, J = 12.4, 4.8 Hz), 2.77 (d of t, 1 H, J = 12.4, 1.8 Hz), 1.84 (m, 1 H), 1.60 (m, 1 H).

1-[(Cholesteryloxy)carbonyl]-5-(hydroxymethyl)-(3*R-trans*)-3-pyrrolidinol (3). To 7.6 mL (3.8 mmol) of a 0.5 M stock solution of amino diol **2** in ethanol was added a solution of 1.48 g (3.3 mmol) of cholesterol chloroformate in 8 mL of methylene chloride. The solution was stirred at room temperature for 1.5 h. The cloudy solution was poured into 100 mL of ice water and the heterogeneous mixture was extracted with 3 × 150 mL of hot ethyl acetate. The combined organics were washed with brine, dried over magnesium sulfate, and concentrated. The solid residue was purified by flash chromatography (4 × 15 cm silica) using a gradient of methanol in 1:1 hexanes–ethyl acetate. Product **3** eluted with 10% methanol. The fractions containing pure product were evaporated to dryness to give 1.42 g (81% yield) of **3** as a white solid: TLC (45:45:10 hexanes–ethyl acetate–methanol) R_f = 0.11, stained black upon charring with 10% sulfuric acid in methanol; ^1H NMR ($CDCl_3$) δ 5.38 (d, 1 H), 4.85–4.00 (m, 3 H), 3.90–3.30 (m, 4 H), 2.50–2.15 (m, 2 H), 2.15–0.60 (m, 43 H). Anal. Calcd for $C_{33}H_{55}NO_4$: C, 74.81; H, 10.46; N, 2.64. Found: C, 74.74; H, 10.33; N, 2.50.

A mixture of 1 mg of **3** in 1 mL of 30% ammonium hydroxide was heated at 45 °C for 24 h in a sealed vial (ODN-deprotection conditions). The resulting heterogeneous mixture was analyzed by TLC. Neither the solution or the solid showed any signs of decomposition.

1-[(Cholesteryloxy)carbonyl]-5-[[bis(4-methoxyphenyl)phenylmethoxy]methyl]-(3*R-trans*)-3-pyrrolidinol (4). To a stirred solution of 1.42 g (2.68 mmol) of diol **3** in 27 mL of dry pyridine were added 0.524 mL of triethylamine, 16.5 mg of DMAP, and 1.10 g (3.23 mmol) of DMTrCl. After stirring under argon for 4.5 h, the mixture was stripped of solvent. Residual pyridine was removed by coevaporation with toluene. The residue was partitioned between 100 mL of ether and 40 mL of water. The aqueous layer was extracted with 80 mL of ether, and the combined organic layers were washed with brine, dried over sodium sulfate, and concentrated. The residue was purified by flash chromatography (4.5 × 20 cm silica) using a gradient of ethyl acetate in hexanes. The product eluted just after a yellow impurity using 2:1 hexanes–ethyl acetate. The fractions containing pure product were evaporated to dryness to give 1.33 g (60% yield) of **4** as a pale yellow solid foam: TLC (95:5 methylene chloride–methanol) R_f = 0.49, stained orange upon spraying with 10% sulfuric acid in methanol; ^1H NMR ($CDCl_3$) δ 7.26 (m, 9 H), 6.81 (d, 4 H, J = 8.8 Hz), 5.30 (m, 1 H), 4.50 (m, 2 H), 4.15 (m, 1 H), 3.78 (s, 6 H), 3.7–3.0 (m, 4 H), 2.4–0.6 (m, 46 H). Anal. Calcd for $C_{54}H_{73}NO_6$: C, 77.94; H, 8.84; N, 1.68. Found: C, 77.26; H, 8.82; N, 1.56.

Cholesterol–CPG Support (5). To a stirred solution of 1.22 g (1.47 mmol) of alcohol **4** in 12 mL of dry pyridine was added 443 mg (4.43 mmol) of succinic anhydride and 89 mg (0.73 mmol) of DMAP. The mixture was stirred under argon for 26 h and evaporated to dryness. Residual pyridine was removed by coevaporation with toluene. The residue was dissolved in 40 mL of chloroform, washed with brine, dried over sodium sulfate, and concentrated to give quantitative yield of the succinylated product as a beige solid foam: TLC (95:5 methylene chloride–methanol) R_f = 0.32, stained orange upon spraying with 10% sulfuric acid in methanol.

The crude succinylated cholesterol derivative was immobilized on 80–120 mesh, 500 Å, LCAA–CPG support (Sigma Chemical Co.) using standard conditions for immobilizing succinylated nucleosides (*21*). LCAA–CPG (5.0 g) was stirred for 3 h with 100 mL of 3% dichloroacetic acid in methylene chloride. The CPG was filtered on a 30-mL sintered-glass funnel (medium porosity) and washed with 150 mL of chloroform and 150 mL of ether.

The solid was dried under vacuum and combined in a 250-mL round-bottom flask with 50 mL of dry pyridine, 932 mg (1 mmol) of the succinylated cholesterol derivative, 0.4 mL of triethylamine, 1.92 g (10 mmol) of EDC, and 60 mg of DMAP. The mixture was swirled on an orbital mixer at 100 rpm for 38 h. The CPG was filtered on a 30-mL sintered-glass funnel and washed with 50 mL of pyridine, 100 mL of methanol, 50 mL of chloroform, and 50 mL of ether, then dried under vacuum. Residual amine groups on the CPG were capped by swirling the support in 15 mL of dry pyridine and 2 mL of acetic anhydride. After 2 h, the CPG was filtered and washed as described above and dried under vacuum to give 5.0 g of product **5**. A 4.5-mg sample of CPG support was analyzed for DMTr content according to the literature method (*22*) and was found to have a loading of 17.6 μmol/g.

2,3,5,6-Tetrafluorophenyl 3-(9-Acridinyl)propionate (6a). To a solution of 400 mg (1.59 mmol) of 3-(9-acridinyl)propionic acid (**23**) and 0.22 mL of triethylamine in 20 mL of methylene chloride was added 496 mg (1.75 mmol) of FMPT. The mixture was stirred at room temperature for 15 min. 2,3,5,6-Tetrafluorophenyl (317 mg, 1.91 mmol) and 0.22 mL of triethylamine were added, and the mixture was stirred for 15 min. The heterogeneous mixture was stripped of solvents, and the residue was purified by flash chromatography (2 × 29 cm silica) using 1:1 hexanes–ethyl acetate. The fractions containing pure product were combined and evaporated to dryness to give 250 mg (39% yield) of the desired product as a pale yellow solid: mp = 183–185 °C; TLC (1:1 hexanes–ethyl acetate) R_f = 0.70, blue fluorescence under long-wavelength UV; IR (KBr) 3075, 1790, 1520, 1095 cm^{-1}; ^{1}H NMR ($CDCl_3$) δ 8.29 (d, 4 H, J = 8.0 Hz), 7.82 (t, 2 H, J = 7.2 Hz), 7.64 (t, 2 H, J = 8.6 Hz), 7.04 (m, 1 H), 4.13 (t, 2 H, J = 8.7 Hz), 3.16 (t, 2 H, J = 8.7 Hz). Anal. Calcd for $C_{22}H_{13}NO_2F_4$: C, 66.17; H, 3.28; N, 3.51; F, 19.03. Found: C, 66.01; H, 3.11; N, 3.33; F, 19.13.

2,3,5,6-Tetrafluorophenyl 5-(9-Acridinyl)pentanoate (6b). A procedure similar to that described above was used for preparation of **6b**. 5-(9-Acridinyl)pentanoic acid (262 mg, 1 mmol) gave 180 mg (42% yield) of **6b** as a pale yellow solid: mp = 122–124 °C; TLC (1:1 hexanes–ethyl acetate) R_f = 0.63, blue fluorescence under long-wavelength UV; IR (KBr) 3075, 2960, 1790, 1515, 1105, 955, 750 cm^{-1}; ^{1}H NMR ($CDCl_3$) δ 8.26 (d, 4 H, J = 9.2 Hz), 7.92 (t, 2 H, J = 6.8 Hz), 7.58 (t, 2 H, J = 8.8 Hz), 7.00 (m, 1 H), 3.71 (t, 2 H, J = 7.8 Hz), 2.78 (t, 2 H, J = 6.4 Hz), 2.05 (m, 4 H). Anal. Calcd for $C_{24}H_{17}NO_2F_4$: C, 67.45; H, 4.01; N, 3.28; F, 17.78. Found: C, 67.18; H, 3.87; N, 3.02; F, 17.67.

1-[3-(9-Acridinyl)-1-oxopropyl]-5-(hydroxymethyl)-(3*R*-*trans*)-3-pyrrolidinol (7a). Method 1. A solution of 206 mg (0.52 mmol) of acridine TFP ester **6a** in 8 mL of methylene chloride was added dropwise to an ice-cold solution of 0.57 mmol of amino diol **2** and 86 μL of triethylamine in 1.14 mL of ethanol. The mixture was stirred at room temperature for 18 h and concentrated. The residue was purified by flash chromatography (1.5 × 25 cm silica) using 5% methanol in methylene chloride to give 181 mg (100% yield) of the desired product **7a** as a yellow solid foam: TLC (9:1 methylene chloride–methanol) R_f = 0.50, yellow spot with blue fluorescence under long-wavelength UV; IR (KBr) 3400 (br), 1620, 1440, 1070 cm^{-1}; ^{1}H NMR ($CDCl_3$) δ 8.30 (d, 4 H, J = 9.4 Hz), 7.82 (t, 2 H, J = 6.6 Hz), 7.62 (m, 2 H), 4.31 (m, 2 H), 4.05 (t, 2 H, J = 8.2 Hz), 3.70 (m, 1 H), 3.50 (m, 2 H), 3.22 (d, 2 H, J = 1.4 Hz), 2.78 (m, 2 H), 2.03 (m, 1 H), 1.64 (m, 1 H); UV (pH 7.2) λ_{max} = 252 (ε 101 000), 260 (ε 6400), 356 nm (ε 6200); fluorescence (pH 7.2) excitation at 355 nm, emission at 460 nm. Anal. Calcd for $C_{21}H_{22}N_2O_3 \cdot 0.5H_2O$: C, 70.18; H, 6.45; N, 7.79. Found: C, 70.41; H, 6.45; N, 7.68.

Method 2. To a stirred slurry of 125.5 mg (0.5 mmol) of 3-(9-acridinyl)propionic acid and 0.104 mL (0.6 mmol) of diisopropylethylamine in 1.5 mL of methylene chloride was added 0.6 mmol of FMPT. After 1.5 h at room temperature, the cloudy brown solution was added to a stirred solution of 0.5 mmol of amino diol **2** in 1.5 mL of ethanol in an ice–salt bath. After stirring for 1 h at room temperature, the mixture was quenched with 10 mL of methanol and concentrated. The residue was purified by flash chromatography (1.5 × 24 cm silica) using a gradient of methanol in methylene chloride. The fractions which contained pure product were evaporated to dryness to give 112 mg (64% yield) of **7a** as a yellow solid foam.

1-[5-(9-Acridinyl)-1-oxopentyl]-5-(hydroxymethyl)-(3*R*-*trans*)-3-pyrrolidinol (7b). A procedure similar to method 1 was used for the preparation of **7b**. Acridine TFP ester **6b** (1.28 g, 3.00 mmol) gave 1.04 g (92% yield) of **7b** as a pale yellow solid foam: TLC (45:45:10 hexanes–ethyl acetate–methanol) R_f = 0.14, yellow spot with blue fluorescence under long-wavelength UV; IR ($CHCl_3$) 3350 (br), 3010, 2930, 1610, 1435 cm^{-1}; ^{1}H NMR ($CDCl_3$) δ 8.22 (d, 4 H, J = 9.0 Hz), 7.77 (t, 2 H, J = 6.6 Hz), 7.56 (t, 2 H, J = 7.8 Hz), 4.27 (m, 2 H), 3.7–3.4 (m, 6 H), 2.3–1.6 (m, 10 H). Anal. Calcd for $C_{23}H_{26}N_2O_3 \cdot 0.75H_2O$: C, 70.48; H, 7.07; N, 7.15. Found: C, 70.33; H, 6.89; N, 7.15.

1-[3-(9-Acridinyl)-1-oxopropyl]-5-[[bis(4-methoxyphenyl)phenylmethoxy]methyl]-(3*R*-*trans*)-3-pyrrolidinol (8a). To a stirred solution of 100 mg (0.285 mmol) of diol **7a** in 2.5 mL of pyridine was added 6.4 mg of DMAP, 0.13 mL of triethylamine, and 154 mg of DMTrCl. After stirring for 16 h under argon, the mixture was evaporated to dryness. Residual pyridine was removed by coevaporation with methylene chloride. The residue was dissolved in 5 mL of methylene chloride, washed with 2 × 3 mL of water and 3 mL of brine, dried over sodium sulfate, and evaporated to dryness. The residue was purified by flash chromatography (1.5 × 20 cm silica) using a gradient of methanol in 1:1 hexanes–ethyl acetate. The fractions containing pure product were combined and evaporated to dryness to give 123 mg (66% yield) of **8a** as a yellow solid foam: TLC (45:45:10 hexanes–ethyl acetate–methanol) R_f = 0.26, yellow spot with blue fluorescence which stained orange upon spraying with 10% sulfuric acid in methanol; IR (KBr) 3400 (br), 2930, 1620, 1510, 1440, 1250, 1180, 1030, 830, 760 cm^{-1}; ^{1}H NMR ($CDCl_3$) δ 8.17 (m, 4 H), 7.75 (t, 2 H, J = 7.0 Hz), 7.57–7.09 (m, 11 H), 6.82 (d, 2 H, J = 8.8 Hz), 6.66 (m, 2 H), 4.56 (m, 2 H), 3.65–2.90 (m, 12 H), 2.69 (m, 2 H), 2.15 (m, 1 H), 1.95 (m, 1 H). Anal. Calcd for $C_{42}H_{40}N_2O_5 \cdot 0.5H_2O$: C, 76.23; H, 6.24; N, 4.23. Found: C, 76.53; H, 6.67; N, 3.80.

1-[5-(9-Acridinyl)-1-oxopentyl]-5-[[bis(4-methoxyphenyl)phenylmethoxy]methyl]-(3*R*-*trans*)-3-pyrrolidinol (8b). A procedure similar to that described above was used for preparation of **8b**. Diol **7b** (103 mg, 0.272 mmol) gave 78 mg (42% yield) of **8b** as a pale yellow solid foam: TLC (45:45:10 hexanes–ethyl acetate–methanol) R_f = 0.41, yellow spot with blue fluorescence which stained orange upon spraying with 10% sulfuric acid in methanol; IR (KBr) 3350 (br), 2930, 1610, 1510, 1250 cm^{-1}; ^{1}H NMR ($CDCl_3$) δ 8.24 (d, 4 H, J = 8.8 Hz), 7.76 (m, 2 H), 7.53 (m, 2 H), 7.35–7.10 (m, 9 H), 6.79 (m, 4 H), 4.7–4.3 (m, 2 H), 4.08 (m, 1 H), 3.9–3.3 (m, 11 H), 3.10 (m, 2 H), 2.32–1.71 (m, 6 H).

Acridine–CPG Support (9a). To a stirred solution of 120 mg (0.184 mmol) of alcohol **8a** in 1.5 mL of dry pyridine was added 55.5 mg (0.55 mmol) of succinic anhydride

and 11.2 mg of DMAP. The mixture was stirred under argon for 40 h and evaporated to dryness. Residual pyridine was removed by coevaporation with toluene. The residue was dissolved in 3 mL of chloroform, washed with brine, dried over sodium sulfate, and concentrated to give 128 mg (93% yield) of the succinate as a yellow solid foam. TLC (95:5 methylene chloride–methanol) R_f = 0.13. Product appeared as a yellow spot with blue fluorescence which stained orange upon spraying with 10% sulfuric acid in methanol.

To 128 mg (0.170 mmol) of the crude succinylated acridine derivative were added 0.85 g of acid-washed LCAA–CPG (0.85 g), 8.5 mL of dry pyridine, 0.068 mL of triethylamine, 325 mg (1.7 mmol) of EDC, and 10.2 mg of DMAP. The mixture was stirred under argon for 19 h. The CPG was filtered and washed with pyridine, methanol, chloroform, and ether, then dried under vacuum. Residual amine groups on the CPG were capped by stirring the support in 2.5 mL of dry pyridine and 0.34 mL of acetic anhydride. After 2 h, the CPG was filtered, washed with methanol, chloroform, and ether, then dried under vacuum to give 0.85 g of product **9a**. The CPG was analyzed for DMTr content and found to have a loading of 18.5 μmol/g.

Acridine–CPG Support (9b). A procedure similar to that described above was used for preparation of **9b**. Alcohol **8b** (58 mg, 80 μmol) and 0.39 g of LCAA–CPG gave **9b** with a DMTr loading of 20.6 μmol/g of CPG support.

General Synthesis of Oligodeoxynucleotides. ODNs were prepared on either a Milligen 7500 or an Applied Biosystems Model 380B by using the protocols supplied by the manufacturer. Protected β-cyanoethyl phosphoramidites, CPG supports, deblocking solutions, cap reagents, oxidizing solutions, and tetrazole solutions were purchased from either Milligen or Glen Research. Analytical and preparative HPLC were carried out with a Rainin pump system equipped with a Gilson 116 UV detector and a Milton Roy fluorescence detector. Pump control and data processing were performed with a Rainin Dynamax chromatographic software package on a Macintosh computer. After ammonia deprotection, the tritylated ODNs were HPLC purified by direct injection of the ammonia solution onto a Hamilton PRP-1 column (305 × 7.0 mm), and the product was eluted with a linear gradient of 20%–45% acetonitrile in 0.1 M TEAA (pH 7.5) over 20 min (flow rate = 4 mL/min). Appropriate fractions were combined and concentrated to dryness on a Savant Speed-Vac. The residue was detritylated in 80% acetic acid (500 μL, 28 °C, 70 min), precipitated with 100 μL of 3 M sodium acetate and 4 mL of 1-butanol, centrifuged, washed with 1 mL of ethanol, centrifuged, evaporated to dryness, and reconstituted with 1 mL of sterile distilled water. The concentration of ODNs was determined from the UV absorbance at 260 nm. All ODN concentrations were measured in pH 7.2 PBS (9.2 mM disodium phosphate, 0.8 mM monosodium phosphate, 0.131 M sodium chloride). An extinction coefficient for each ODN was determined with a nearest-neighbor model (*24*), and used to calculate a theoretical ratio of A_{260} to concentration in μg/mL (see Table I). The purified ODNs were analyzed by HPLC on a Dynamax C-18 column (0.75 × 25 cm) using a linear gradient of 5%–45% acetonitrile in TEAA over 20 min (flow rate = 1 mL/min). ODN purity was confirmed by denaturing PAGE analysis (see Figure 3).

Synthesis of a 3′-Cholesterol-Tailed ODN from Cholesterol–CPG (5). A quantity of Chol–CPG (**5**) corresponding to 1 μmol of DMTr content (57 mg) was packed into an empty ODN synthesis column (American Bionetics, Inc.). An ODN with the base sequence 5′-TCCATGTTCGT was prepared on an ABI 380B DNA synthesizer using standard phosphoramidite chemistry. The 5′-DMTr protecting group was not removed. The ODN was cleaved from the CPG and deprotected by treatment with 2 mL of 30% ammonium hydroxide at 45 °C for 19 h. The supernatant was injected directly on a PRP-1 reverse-phase HPLC column (305 × 7.0 mm) using a gradient of 35%–80% acetonitrile in 0.1 M TEAA (pH 7.5) over 25 min (flow rate = 2 mL/min). The product was collected in one fraction and concentrated on a Speed-Vac to give the 5′-DMTr protected product. The DMTr group was removed by treatment with 500 μL of 80% acetic acid (70 min at 28 °C), and the 3′-cholesterol-tailed ODN was isolated by precipitation from butanol, as described above. The white solid residue was reconstituted with 1 mL of sterile distilled water and analyzed by UV absorbance at 260 nm. The concentration of ODN was determined to be 1.87 mg/mL. Theoretical yield for 1 μmol is 3.89 mg. The purity of the ODN product was determined by HPLC and PAGE (see Figure 3).

Table I. Properties of Oligodeoxynucleotides

ODN[a] (3′-tail)	MW	A_{260} = 1,[b] μg/mL	% yield[c]	HPLC,[d] min	PAGE, R_m[f]	T_m,[h] °C
20-mer (none)	6199	29.6	21	8.7	0.60	
11-mer (none)	3298	33.6	53	8.0	0.79	45.4–45.9
11-mer (amine)	3451	35.2	42	9.0	0.80[g]	45.9
11-mer (chol)	3890	39.7	48	19.0[e]	0.74	52.4
11-mer (acr-10a)	3710	36.4	43	11.1	0.75	52.7
11-mer (acr-10b)	3738	36.7	64	12.8	0.74	52.7
11-mer (acr-11a)	3684	36.2	14	11.9	0.75	51.3
11-mer (acr-11b)	3712	36.4	27	13.0	0.74	52.8

[a] Sequence of 20-mer ODN (target strand) is 5′-GTGACGAA-CATGGAGAACAT. Sequence of 11-mer ODN (complementary to target) is 5′-TCCATGTTCGT. [b] Calculated concentration of ODN that gives 1.00 absorbance units at 260 nm. [c] Percent yield of isolated ODN from 1 μmol of CPG. Yields of **11a** and **11b** are based on μmol of starting amine tailed ODN. [d] Elution time; HPLC system described in Figure 1. [e] A gradient of 35–80% acetonitrile (30 min) was used. [f] R_m is the ratio of distance of migration relative to bromophenol blue. [g] R_m is given for the major component. [h] T_m is the temperature at the midpoint of the maximum slope of A_{260} vs temperature.

Method A. Synthesis of 3′-Acridine-Tailed ODN (10a). A quantity of Acr–CPG (**9a**) corresponding to 1 μmol of DMTr content (54 mg) was packed into an empty synthesis column. An ODN with the base sequence 5′-TCCATGTTCGT was prepared on an ABI 380B DNA synthesizer using standard phosphoramidite chemistry. The 5′-DMTr protecting group was not removed. The ODN was cleaved from the CPG and deprotected by treatment with 2 mL of 30% ammonium hydroxide at 45 °C for 24 h. The supernatant was injected directly on a PRP-1 reverse-phase HPLC column (305 × 7.0 mm) using 100% 0.1 M TEAA (3 min) and eluted with a linear gradient of 20%–45% acetonitrile in 0.1 M TEAA (pH 7.5) over 25 min (flow rate = 2 mL/min). The chromatogram corresponding to this preparation is shown in Figure 1 (panel A). The product was collected in one fraction and concentrated on a Speed-Vac to give the 5′-DMTr-protected product. The DMTr group was removed by treatment with 500 μL of 80% acetic acid (70 min at 28 °C) and the 3′-acridine-tailed ODN was isolated by

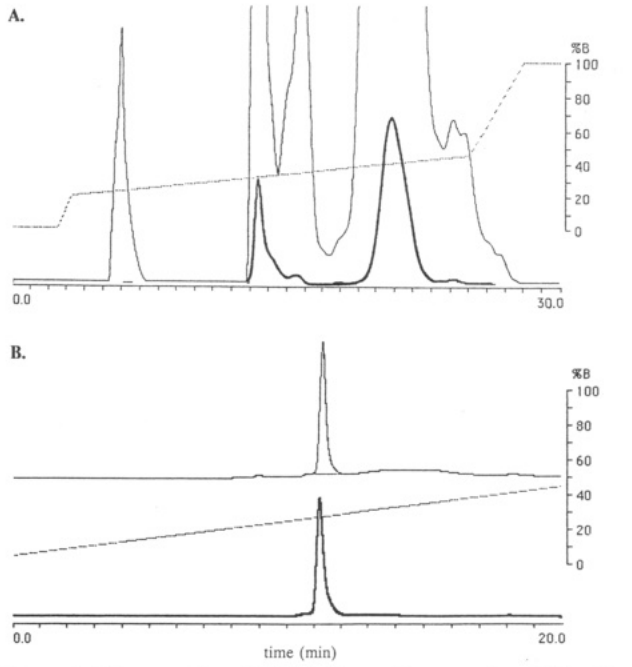


Figure 1. Reverse-phase HPLC chromatograms describing 3′-acridine tailing of method A. Panel A: preparative HPLC for the deblocked 5′-(dimethoxytrityl) derivative of acridine-tailed ODN **10a**. The HPLC system used a 305 × 7.0 mm PRP-1 column, flow rate = 2 mL/min. The fluorescent peak at 22 min was collected and the DMTr protecting group was removed to give **10a**. Panel B: analytical HPLC for the purified acridine-tailed ODN **10a**. The HPLC system used a 250 × 7.5 mm C-18 column, flow rate = 1 mL/min; for both HPLC systems, solvent A, 0.1 M triethylammonium acetate (pH 7.5); solvent B, acetonitrile; detection, UV absorbance at 260 nm; lower trace (bold) is fluorescence emission.

precipitation from butanol, as described above. The fluorescent, pale yellow solid residue was reconstituted with 1 mL of sterile distilled water and analyzed by UV at 260 nm. The ϵ_{260} for **7a** was used for calculation of the unit absorbance at 260 nm. The concentration of ODN was determined to be 1.59 mg/mL. Theoretical yield for 1 μmol is 3.71 mg. The purity of the ODN product **10a** was determined by HPLC (see Figure 1, panel B) and PAGE (see Figure 3).

Method B. Synthesis of 3′-Acridine-Tailed ODN (11a). A 1-μmol 3′-amine-ON CPG column (Clontech) was used for the preparation of an ODN with the base sequence 5′-TCCATGTTCGT. The general conditions described above were used for isolation of the 3′-amine-tailed ODN (see Table I). The isolated material appeared as one peak by HPLC (see Figure 2, panel A) but showed multiple bands by PAGE (see Figure 3). Isolated amine-tailed ODN (100 μg, 29 nmol) was dissolved in 100 μL water and 50 μL of 1.0 M borate buffer (pH 8.3). A freshly prepared 5.0 mg/mL solution (220 μL) of **6a** in 1:1 M-pyrol–acetonitrile (1.1 mg, 3.0 μmol) was added and the heterogeneous mixture was shaken for 22 h. The resulting homogeneous solution was transferred to a Centricon-3 microconcentrator (Amicon) with 1.5 mL of water, and the mixture was centrifuged to a final volume of ~100 μL. This solution was purified by HPLC on a Dynamax C-18 column (0.75 × 25 cm) using a linear gradient of 5%–45% acetonitrile in 0.1 M TEAA over 20 min (flow rate = 1 mL/min). The chromatogram corresponding to this preparation is shown in Figure 2 (panel B). The product was collected in one fraction and concentrated on a Speed-Vac. The residue was reconstituted with 100 μL of sterile distilled water and analyzed by UV at 260 nm. The concentration of ODN was determined to be 14.5 μg/100 μL. Theoretical yield for 29 nmol is 107 μg. The purity of the ODN product **11a** was determined by HPLC (see Figure 2, panel C) and PAGE (see Figure 3).

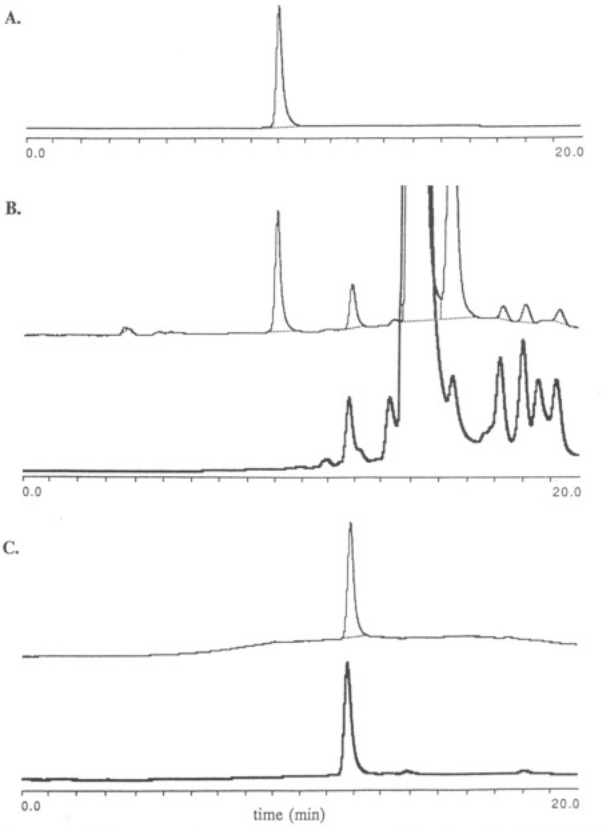


Figure 2. Reverse-phase HPLC chromatograms describing 3′-acridine tailing of method B. The HPLC system used a 250 × 7.5 mm C-18 column and a gradient of 5–45% solvent B over 20 min (flow rate = 1 mL/min) where solvent A = 0.1 M triethylammonium acetate (pH 7.5), solvent B = acetonitrile; detection was by UV absorbance at 260 nm; lower trace (bold) is fluorescence emission. Panel A: 3′-amine-tailed 11-mer ODN. Panel B: reaction with acridine TFP ester **6a** after 22 h shows unreacted 3′-amine ODN (9-min peak) and the desired 3′-acridine ODN **11a** (12-min peak). The peak at 14.5 min is acridine carboxylic acid. Panel C: C-18 HPLC purified 3′-acridine tailed ODN **11a**.

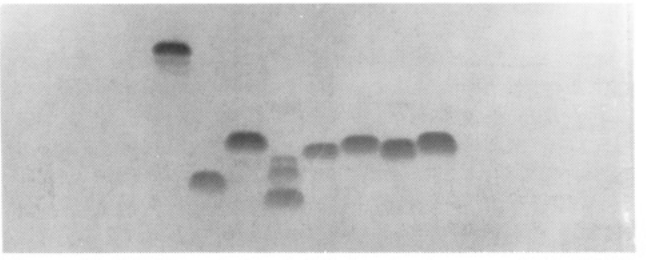
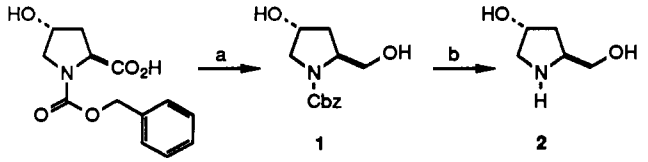


Figure 3. PAGE carried out with denaturing cross-linked 20% gels (bisacrylamide/acrylamide, 1:19, 0.4 × 170 × 390 mm) at 45 W for 40 min. Nucleotidic bands were visualized by UV shadowing and by staining with methylene blue (0.02%). Bromophenol blue was used as a marker. Lane 1 is the unmodified 20-mer target ODN. Lane 2 is the unmodified 11-mer ODN. Lanes 3–8 are 3′-modified 11-mer ODN: cholesterol tail (lane 3), amine tail (lane 4), acridine tail **10a** (lane 5), acridine tail **10b** (lane 6), acridine tail **11a** (lane 7), acridine tail **11b** (lane 8). Relative migration distances are reported in Table I.

Thermal Denaturation Studies. Thermal dissociation curves were obtained by following changes in A_{250} and A_{260} of aqueous solutions containing equimolar amounts of the 3′-tailed ODN described above and an unmodified 20-mer ODN complement with the base sequence 5′-GTGACGAACATGGAGAACAT. The unmodified 11-mer ODN was used as a control in each run.

Scheme I.[a] Synthesis of *trans*-4-Hydroxy-L-prolinol



[a] Reagents: (a) BH_3·THF, THF followed by MeOH; (b) H_2, Pd–C, MeOH.

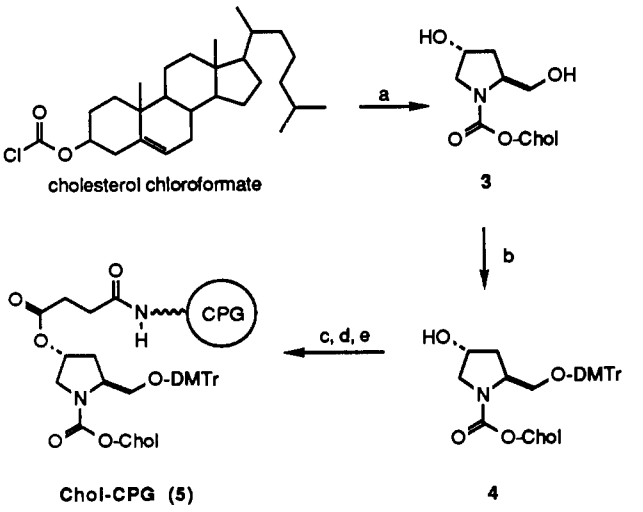
ODNs were prepared as 2 μM solutions in pH 7.2 PBS. A Gilford System 2600 UV–VIS spectrophotometer equipped with a Gilford 2527 Thermo-programmer was used. The samples were heated from 15 to 85 °C with a temperature increase of 0.5 °C/min. Absorbance vs time and the first derivative data were recorded automatically. The T_m was determined from the derivative maxima. Duplicate runs produced T_m within 0.5 °C. Data from one representative run is given.

RESULTS

trans-4-Hydroxy-L-prolinol (2) was prepared by reduction of commercially available *N*-Cbz-hydroxy-L-proline, as shown in Scheme I. The N-protected amino acid was chosen, since it provides a removable "chromatographic handle" which facilitates purification of diol product 1. The carboxylic acid residue was first reduced with BH_3·THF in 44% isolated yield. Although the stereochemical properties of 1 were not examined, it has been shown that reduction of *tert*-butylcarbamate (Boc) protected amino acids with BH_3·THF proceeds with retention of optical purity (25). The broadened peaks observed in the ^1H NMR of 1 suggest that the benzyl group in the carbamate linkage exists as an equilibrium mixture of the syn and anti conformations. This inversion about the nitrogen in the pyrrolidinol ring was apparent in the ^1H NMR of the starting carboxylic acid as evidenced by the presence of two benzyl peaks. Hydrogenolysis of the Cbz group in 1 gave the desired amino diol 2 in quantitative yield by simply filtering off the catalyst and removing the solvent. The product was stored as a stock solution in ethanol and was used without further purification for the following chemistry. ^1H NMR was consistent with the desired product and no longer showed the broadened peaks observed with the acylated compounds.

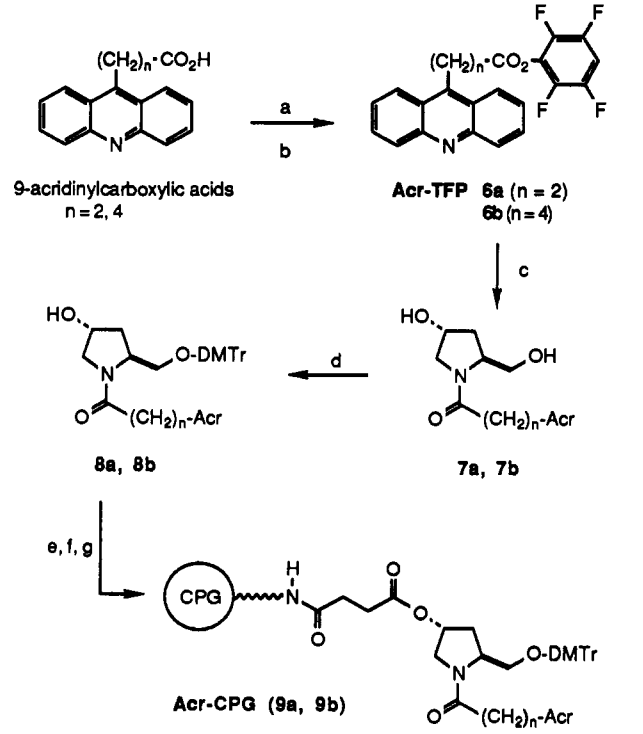
trans-4-Hydroxy-L-prolinol (2) was readily converted to Chol–CPG (5) as illustrated in Scheme II. Selective acylation of the amino group in the presence of the two hydroxyl groups was accomplished by treatment with cholesterol chloroformate in ethanolic solution. (Cholesteryloxy)carbonyl diol 3 was isolated in 81% yield after flash chromatography. The carbamate linkage in 3 was found to be stable to standard ODN-deprotection conditions. The primary hydroxyl group in 3 was selectively protected as the DMTr ether, under standard conditions to give 4 in 60% isolated yield. The remaining secondary hydroxyl group in 4 was esterified in quantitative yield by treatment with excess succinic anhydride in pyridine. The crude succinylated product was used directly for immobilization on LCAA–CPG using EDC as the coupling reagent (21). The residual unreacted amino groups on the CPG were capped with acetic anhydride in pyridine. The support was washed well with organic solvents and dried under vacuum to give 5.0 g of Chol–CPG (5). The loading of DMTr groups on the CPG was determined by treating an aliquot with perchloric acid in methanol and measuring the absorbance of trityl cation at 498 nm (22). The DMTr loading (17.6 μmol/g) was suitable for preparation of ODNs, since 1 μmol (57 mg) of Chol–CPG (5)

Scheme II.[a] Preparation of Cholesterol–CPG



[a] Reagents: (a) *trans*-4-hydroxy-L-prolinol (2), Et_3N, EtOH; (b) DMTrCl, DMAP, Et_3N, pyridine; (c) succinic anhydride, DMAP, pyridine; (d) LCAA–CPG, EDC, DMAP, pyridine; (e) acetic anhydride, pyridine.

Scheme III.[a] Preparation of Acridine–CPG

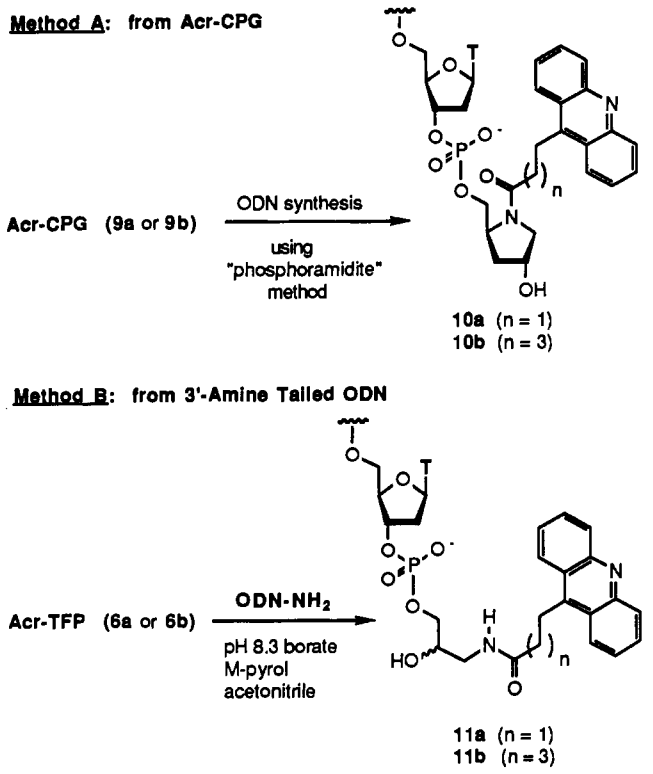


[a] Reagents: (a) FMPT, Et_3N, CH_2Cl_2; (b) TFP, Et_3N; (c) *trans*-4-hydroxy-L-prolinol (2), Et_3N; (d) DMTrCl, Et_3N, DMAP, pyridine; (e) succinic anhydride, DMAP, pyridine; (f) LCAA–CPG, Et_3N, DMAP, EDC, pyridine; (g) acetic anhydride, pyridine.

fits into the CPG cartridges which are commercially available for use on the automated DNA synthesizers. A reported procedure which utilized the *p*-nitrophenyl ester for immobilization of succinylated nucleosides on LCAA-CPG (22) gave almost identical loading with the described EDC procedure, but was more tedious.

The acridine–CPG supports (**9a** and **9b**) were prepared from *trans*-4-hydroxy-L-prolinol (2) and the appropriate acridinylpropionic or -pentanoic acid TFP ester (**6a** or **6b**), as shown in Scheme III. The 9-acridinylalkanoic acids can be prepared with a variety of alkyl chain lengths by heating the corresponding aliphatic diacid with diphenylamine and zinc chloride (23). For example, 45 g (16%

Scheme IV. Synthesis and Structure of 3'-Acridine-Tailed ODNs



yield) of 5-(9-acridinyl)pentanoic acid were obtained from the condensation reaction with adipic acid. TFP ester **6a** or **6b** was prepared by first activating the carboxylic acid with FMPT and then reacting with 2,3,5,6-tetrafluorophenol (*26*). Purified TFP ester **6a** was reacted with amino diol **2** to give quantitative yield of amide product **7a** (method 1). Diol amide **7a** was also prepared directly from the carboxylic acid via the intermediate *N*-methylpyridinium ester (method 2), but this approach was less reproducible. The primary hydroxyl group in **7a** or **7b** was selectively protected as the DMTr ether under standard conditions to give good yields of **8a** or **8b**. The remaining secondary hydroxyl group was succinylated and the resulting carboxylic acids were immobilized on LCAA–CPG, as described above, to give the desired Acr–CPG (**9a** or **9b**). The DMTr loading for these CPGs were 18.5 and 20.6 μmol/g, respectively.

Unmodified ODNs, 3'-amine-tailed ODN, 3'-cholesterol-tailed ODN, and 3'-acridine-tailed ODNs (**10a** and **10b**) were prepared from the appropriate CPG supports on a 1-μmol scale with standard β-cyanoethyl phosphoramidite coupling chemistry (*22*). The ODNs were deblocked and cleaved from the CPG by ammonia treatment. The trityl-ON ODNs were isolated in good yield by a single HPLC purification using a PRP-1 semipreparative column. After detritylation and butanol precipitation, all ODNs showed less than 5% impurity when checked by analytical C-18 HPLC. Cholesterol-tailed ODNs are retained well on reverse-phase chromatography packings, and elution required a high concentration of acetonitrile.

Scheme IV illustrates the two different methods used for preparation of ODNs with acridine conjugated to the 3'-terminus. The properties of the 3'-modified ODNs and related unmodified ODNs synthesized for this study are listed in Table I.

In method A, the ODNs were synthesized directly from acridine–CPG (**9a** or **9b**). Although the 5'-DMTr group can be removed prior to deblocking, HPLC purification of the acridine-tailed ODNs was easier with the additional hydrophobic DMTr group. Fluorescence detection facilitated identification of the desired ODN products (**10a** and **10b**). The chromatogram from preparative HPLC of the 5'-DMTr derivative of **10a** is shown in Figure 1 (panel A). Detritylation with 80% acetic acid and isolation by butanol precipitation gave 3'-acridine ODN **10a** as a single peak by C-18 HPLC (Figure 1, panel B).

In method B, the ODN bearing a 3'-phosphate (*R,S*)-1-amino-2-hydroxyprop-3-yl ester was first prepared from the commercially available "amine-ON" CPG. The purified 3'-amine-tailed ODN appeared as a single peak by C-18 HPLC (Figure 2, panel A), but several bands by PAGE. This material was treated with acridine TFP ester (**6a** or **6b**) in pH 8.3 borate buffer. Acetonitrile and 1-methyl-2-pyrrolidinone were used to help dissolve the TFP ester. After shaking for several hours, HPLC analysis showed unreacted 3'-amine-tailed ODN (Figure 2, panel B). Treatment with additional aliquots of borate buffer and **6a** did not increase the extent of reaction (data not shown). After 22 h, the mixture was concentrated and small molecular weight impurities were removed by centrifugation through a 3000 MW cutoff ultrafiltration membrane. The retentate was purified by C-18 HPLC and concentrated to gived ODN **11a** or **11b**. The chromatogram of the purified 3'-acridine ODN **11a** is shown in Figure 2 (panel C).

The purity of the 3'-tailed ODN products described above, as evidenced by PAGE, is shown in Figure 3. Aliquots each containing 2.5 μg of the indicated ODN were placed in each well, and the gel was run until the bromophenol blue marker reached the bottom of the gel. The bands, when visualized by UV shadowing on a fluorescent background, appeared of equal intensity. On a nonfluorescent background, the acridine-tailed ODNs could be visualized as fluorescent bands. The gel was then stained with methylene blue and washed with cold water. Differences in intensity of the bands are presumably due to differential staining of the various tails by methylene blue. Although C-18 HPLC of the 3'-amine-tailed ODN showed only one peak (Figure 2, panel A), PAGE indicated the presence of impurities. The ODN with the bulky 3'-cholesterol tail showed one band by PAGE which was less mobile than the unmodified ODN, presumably due to the sieving effect of the polyacrylamide gel. A similar effect is seen with the acridine-tailed ODNs, where an increase in linker arm length of two methylene groups gives a detectable decrease in mobility.

To assess the effect of the 3'-modifications on hybridization, the dissociation of complexes formed from equimolar concentrations of 3'-modified 11-mer ODN and an unmodified 20-mer ODN target was examined. Changes in absorbance at 250 and 260 nm were measured as a function of temperature. No significant differences were observed for melting temperature (T_m) at these two wavelengths and only the 260-nm values are reported (Table I). T_m curves typical for ODN duplexes were obtained.

DISCUSSION

Amino diols which contain both a primary and secondary hydroxyl group provide the necessary functionality for use as derivatizable linkers. For example, (*R,S*)-1-amino-2,3-propanediol is used for preparation of the commercially available "amine-ON" CPG (*17*). Although this amino diol could be used for the preparation of modified CPG supports, we were concerned about lack of defined stereochemistry and the possibility of side reactions involving

the *vic*-amino diol functionality. A similar protected amino diol has also been used for preparation of ODNs bearing reporter groups at the 5′-terminus (*27*).

Although (2*S*)-1-amino-2,3-propanediol can be prepared (*28*), we chose to use a rigid amino diol of defined stereochemistry, *trans*-4-hydroxy-L-prolinol (**2**). The fixed trans geometry of the hydroxyl groups in **2** reduces the possibility of intramolecular side reactions during deblocking and modification. It may also allow more control over the linker geometry for improved interaction of intercalating agents and other reactive groups with the target nucleic acid strand. The secondary amino group is easily acylated but does not generate an amide proton which can give rise to hydrogen-bonding effects that are important in delivery of reactive groups (*29*).

The cholesterol and acridine tails were chosen for initial studies since they contain no functional groups which react under the ODN synthesis and deprotection conditions. More sensitive 3′-tail molecules such as biotin would require appropriate protecting groups. We prepared Chol–CPG (**5**) because the existing methods for preparation of 3′-cholesterol-tailed ODNs were cumbersome, requiring the first two nucleotides to be preattached to the solid support, with a modified internucleotide phosphoramidate linkage (*6*). The 9-acridinyl carboxylic acids were chosen for preparation of Acr–CPG (**9a,b**) since they have been shown to interact strongly with DNA (*30*) and can be prepared with a variety of different chain lengths. The two chain lengths that were used in this study were chosen to approximate the length shown to be optimal for other 3′-acridine tailed ODN (*31*). A variety of activated esters of the acridinyl carboxylic acids were evaluated as potential precursors to Acr–CPG (**9a,b**). The TFP esters were found to be suitably reactive with the nucleophilic amino group in **2**, yet stable enough to allow purification by flash chromatography. In addition, they can be used for postsynthesis modification of amine-containing ODNs in aqueous solution (method B).

In comparison to the direct synthesis of 3′-acridine-tailed ODNs from Acr–CPG (method A), postsynthetic modification of 3′-amine-tailed ODN (method B) by acridine TFP esters **6a** and **6b** was problematic. Most of these difficulties were due to the nature of the synthetic 3′-amine-tailed ODN. Although the HPLC-purified 3′-amine-tailed ODN appeared as a single peak by HPLC (Figure 2), PAGE indicated the presence of more than one compound (Figure 3). This material would not react cleanly with acridine TFP esters **6a** or **6b**. In fact, PAGE analysis of the crude reaction mixture indicated that only the least mobile band reacted completely (data not shown). We have not identified these compounds, but mobility on PAGE also suggests that the major component does not possess a cationic tail. The relative migration of the 3′-amine-tailed ODN is anomalous, since the addition of a cationic tail should decrease mobility toward the positively charged anode. It is possible that the phosphoryl group in the 3′-amine-tailed ODN migrates from the primary hydroxyl group to the neighboring hydroxyl group. Such migrations are well known for *vic*-diols under both acidic and basic conditions (*32*). Further O→N phosphoryl migration could explain the mixture of components shown in Figure 3. If an *N*-phosphoryl derivative were formed, it would have no cationic tail. It should be noted that HPLC, PAGE, or yield data were not presented for 3′-amine-tailed ODNs prepared using "amine-ON" CPG (*17*).

The 3′-tailed 11-mer ODNs were prepared with a sequence complementary to the initiation codon region of the mRNA for the hepatitis B surface antigen protein (*33*). The 20-mer ODN target chosen for the T_m studies provides nucleotide overhangs that may influence interactions with the 3′-modification. Presumably these interactions will be important in the actual biological target. In this preliminary study, the target is DNA and not the likely biological target, RNA. It is interesting to note that there was a significant increase in the melting temperature of the 3′-cholesterol-tailed derivative as compared to the unmodified ODN. Other studies of cholesterol-modified ODNs and phosphorothioates showed no increase in T_m (*6*). However, those studies were performed with complements of the same length, so it may be that we are seeing effects with the overhang on the complementary target. This increase in T_m is not totally unexpected, as other workers have shown the attractive interaction of lipophilic tails with ODN targets (*34*). T_m studies of **10a** and **10b** showed comparable binding affinity to the target ODN. The increase in T_m of 7 °C is not as large as the 14 °C increase reported for a 3′-acridine-tailed $(dT)_{12}$ ODN (*31*), but this is probably due to sequence-dependent intercalation effects. Variation of T_m with intercalator position, especially with respect to the overhang regions of the target nucleic acid, may be important in the selection of suitable biological target sequences. There was no dramatic difference in the T_m of the various acridine tails, although **11a** gave a slightly smaller increase.

This study reports an improved method for synthesis of oligonucleotides having groups conjugated to the 3′-terminus. Better yield and simplified purification are achieved by building the ODN chain directly from the immobilized conjugate group (method A). Although postsynthetic modification of nucleophilic ODN (method B) resulted in poor recovery of the desired conjugate, this method has advantages for introduction of more sensitive 3′-tail molecules that cannot survive the synthesis conditions required for method A. An improved method for preparation of 3′-amine-tailed ODNs would undoubtedly give better yields of the desired conjugate. The large number of available electrophilic conjugate groups make method B attractive for preparation of small quantities of modified ODNs.

ACKNOWLEDGMENT

The competent technical assistance of Dina Furin and Tom Cox is greatly appreciated. We also thank John Tabone, Charles Petrie, Howard Gamper, and Debra Leith for helpful discussions. We thank NeoRx Corp. for use of the NMR spectrometer. This research was supported by grants from the National Institutes of Health (R01 CA40336, R44 AI25266, and R43 AI29277).

LITERATURE CITED

(1) Tenover, F. C. (1988) Diagnostic deoxyribonucleic acid probes for infectious diseases. *Clin. Microbiol. Rev. 1*, 82.
(2) Cohen, J. (1989) *Oligodeoxynucleotides, Antisense Inhibitors of Gene Expression*, Macmillan Press, London.
(3) Uhlmann, E., and Peyman, A. (1990) Antisense oligonucleotides: a new therapeutic principle. *Chem. Rev. 90*, 543.
(4) Toulmé, J.-J., Krisch, H. M., Loreau, N., Thuong, N. T., Hélène, C. (1986) Specific inhibition of mRNA translation by complementary oligonucleotides covalently linked to intercalating agents. *Proc. Natl. Acad. Sci. U.S.A. 83*, 1227.
(5) Leserman, L., Degols, G., Machy, P., Leonetti, J.-P., Mechti, N., and Lebleu, B. (1991) Targeting and intracellular delivery of antisense oligonucleotides interfering with oncogene expression. *Abstracts of Papers, International Conference on Nucleic Acid Therapeutics*, p 40.
(6) Letsinger, R. L., Zhang, G., Sun, S., Ikeuchi, T., and Sarin, P. S. (1989) Cholesterol-conjugated oligonucleotides: Syn-

thesis, properties, and activity as inhibitors of replication of human immunodeficiency virus in cell culture. *Proc. Natl. Acad. Sci. U.S.A. 86*, 6553.
(7) Stein, C. A., Pal, R., DeVico, A. L., Hoke, G., Mumbauer, S., Kinstler, O., Sangadharan, M. G., and Letsinger, R. L. (1991) Mode of action of 5'-linked cholesteryl phoshorothioate oligonucleotides in inhibiting syncytia formation and infection by HIV-1 and HIV-2 in vitro. *Biochemistry 30*, 2439.
(8) Boutorin, A. S., Gus'kova, E. M., Ivanova, E. M., Kobetz, N. D., Zarytova, V. F., Ryte, A. S., Yurchenko, L. V., and Vlassov, V. V. (1989) Synthesis of alkylating oligonucleotide derivatives containing cholesterol or phenazinium residues at their 3' terminus and their interaction with DNA within mammalian cells. *FEBS Lett. 254*, 129.
(9) Erickson, S. K., Meyer, D. J., and Gould, G. K. (1978) Purification and characterization of a new cholesterol-binding protein from rat liver cytosol. *J. Biol. Chem. 253*, 1817.
(10) Goodchild, J. (1990) Conjugates of oligonucleotides and modified oligonucleotides: A review of their synthesis and properties. *Bioconjugate Chem. 1*, 165.
(11) Asseline, U., Thuong, N. T., Sun, J.-S., and Hélène, C. (1986) Oligothymidylates substituted in the 3'-position with an acridine derivative. *Nucleosides Nucleotides 5*, 45.
(12) Lemaitre, M., Bayard, B., and Lebleu, B. (1987) Specific antiviral activity of a poly(L-lysine)-conjugated oligodeoxyribonucleotide sequence complementary to vesicular stomatitis virus N protein mRNA initiation site. *Proc. Natl. Acad. Sci. U.S.A. 84*, 648.
(13) Markiewicz, W. T., and Wyrzykiewicz, T. K. (1989) Universal solid supports for the synthesis of oligonucleotides with terminal 3'-phosphates. *Nucleic Acids Res. 17*, 7149.
(14) Kumar, P., Bose, N. K., and Gupta, K. C. (1991) A versatile solid phase method for the synthesis of oligonucleotide-3'-phosphates. *Tetrahedron Lett. 32*, 967.
(15) Godovikov, T. S., Zarytova, V. F., and Khalimskaya, L. M. (1986) Reactive phosphoramides of mono- and dinucleotides. *Biorg. Khim. 12*, 475.
(16) Boutorine, A. S., Le Doan, T., Battioni, J. P., Mansuy, D., Dupre, D., and Hélène, C. (1990) Rapid routes of synthesis of chemically reactive and highly radioactively labeled α- and β-oligonucleotide derivatives for in vivo studies. *Bioconjugate Chem. 1*, 350.
(17) Nelson, P. S., Frye, R. A., Liu, E. (1989) Bifunctional oligonucleotide probes synthesized using a novel CPG support are able to detect single base pair mutations. *Nucleic Acids Res. 17*, 7187.
(18) Haralambidis, J., Duncan, L., Angus, K., and Tregear, G. W. (1990) The synthesis of polyamide-oligonucleotide conjugate molecules. *Nucleic Acids Res. 18*, 493.
(19) Asseline, U., and Thuong, N. T. (1990) New solid-phase for automated synthesis of oligonucleotides containing an aminoalkyl linker at their 3'-end. *Tetrahedron Lett. 31*, 81.
(20) Zuckermann, R., Corey, D., and Schultz, P. (1987) Efficient methods for attachment of thiol specific probes to the 3' ends of synthetic oligodeoxyribonucleotides. *Nucleic Acids Res. 15*, 5305.
(21) Pon, R. T., Usman, N., and Ogilvie, K. K. (1988) Derivatization of controlled pore glass beads for solid phase oligonucleotide synthesis. *BioTechniques 6*, 768.
(22) Atkinson, T., and Smith, M. (1984) Solid-phase synthesis of oligodeoxyribonucleotides by the phosphite-triester method. In *Oligonucleotide Synthesis, A Practical Approach* (M. Gait, Ed.) pp 35–81, IRL Press, Washington, DC.
(23) Jensen, H., and Howland, L. (1926) The synthesis of acridine-9-ethylamine. *J. Am. Chem. Soc. 48*, 1989.
(24) Cantor, C. R., Warshaw, M. M., and Shapiro, H. (1970) Oligonucleotide interactions. III. circular dichroism studies of the conformation of deoxyoligonucleotides. *Biopolymers 9*, 1059.
(25) Stanfield, C. F., Parker, J. E., and Kanellis, P. (1981) Synthesis of protected amino alcohols. *J. Org. Chem. 46*, 4799.
(26) Mukaiyama, T. (1979) New synthetic reactions based on the onium salts of aza-arenes. *Angew. Chem. Int. Ed. Engl. 18*, 707.
(27) Misiura, K., Durrant, I., Evans, M. R., and Gait, M. J. (1990) Biotinyl and phosphotyrosinyl phosphoramidite derivatives useful in the incorporation of multiple reporter groups on synthetic oligonucleotides. *Nucleic Acids Res. 18*, 4345.
(28) Reed, M. W. (1986) Synthesis of a host specific toxin from *Alternaria alternata* f. sp. *lycopersici*. Dissertation, University of California, Davis.
(29) Meyer, R. B., Jr., Tabone, J. T., Hurst, G. D., Smith, T. M., and Gamper, H. (1989) Efficient, specific cross-linking and cleavage of DNA by stable, synthetic complementary oligodeoxynucleotides. *J. Am. Chem. Soc. 111*, 8517.
(30) Takenaka, S., Aoyagi, Y., Dohtsu, K., and Takagi, M. (1988) Simple characterization of DNA intercalators by retarded gel electrophoresis. *Anal. Sci. 4*, 481.
(31) Asseline, U., Delarue, M., Lancelot, G., Toulmé, F., Thuong, N. T., Montenay-Garestier, T., and Hélène, C. (1984) Nucleic acid-binding molecules with high affinity and base sequence specificity: intercalating agents covalently linked to oligonucleotides. *Proc. Natl. Acad. Sci. U.S.A. 81*, 3297.
(32) Bruice, T. C., Benkovic, S. (1966) *Bioorganic Mechanisms: Volume II*, pp 37–48, W. A. Benjamin, Inc., New York.
(33) Hemling, M. E., Carr, S. A., Capiau, C., and Petre, J. (1988) Structural characterization of recombinant hepatitis B surface antigen protein by mass spectrometry. *Biochemistry 27*, 699.
(34) Jager, A., Levy, M. J., and Hecht, S. M. (1988) Oligonucleotide *N*-alkylphosphoramidites: Synthesis and binding to polynucleotides. *Biochemistry 27*, 7237.

DNA-Binding Transferrin Conjugates as Functional Gene-Delivery Agents: Synthesis by Linkage of Polylysine or Ethidium Homodimer to the Transferrin Carbohydrate Moiety

Ernst Wagner,* Matt Cotten, Karl Mechtler, Helen Kirlappos, and Max L. Birnstiel

Research Institute of Molecular Pathology, Dr. Bohr-Gasse 7, A-1030 Vienna, Austria. Received March 26, 1991

We have previously demonstrated that transferrin–polycation conjugates are efficient carrier molecules for the introduction of genes into eucariotic cells. We describe here a more specific method for conjugation of transferrin with DNA-binding compounds involving attachment at the transferrin carbohydrate moiety. We used the polycation poly(L-lysine) or the DNA intercalator, ethidium homodimer as DNA-binding domains. Successful transferrin-receptor-mediated delivery and expression of the *Photinus pyralis* luciferase gene in K562 cells has been shown with these new transferrin conjugates. The activity of the transferrin–ethidium homodimer (TfEtD) conjugates is low relative to transferrin–polylysine conjugates; probably because of incomplete condensation of the DNA. However, DNA delivery with TfEtD is drastically improved when ternary complexes of the DNA with TfEtD and the DNA condensing agent polylysine are prepared. The gene delivery with the carbohydrate-linked transferrin–polylysine conjugates is equal or superior to described conjugates containing disulfide linkage. The new ligation method facilitates the synthesis of large quantities (>100 mg) of conjugates.

INTRODUCTION

Transferrin–polycation conjugates are efficient carriers for the uptake of DNA into eucariotic cells (*1*). This gene transfer technique, termed *transferrinfection*, is based on receptor-mediated endocytosis of DNA complexed with polycation–transferrin conjugates (*2, 3*). Our initial conjugate synthesis (*1*) involved the modification of one to two amino groups on the transferrin molecule with the bifunctional reagent succinimidyl 3-(2-pyridyldithio)propionate (SPDP), followed by ligation to similarly modified polycations (polylysine or protamine) through the formation of disulfide bonds. Because there are more than 50 lysines on the large (about 80 kDa) transferrin protein, the actual site (or sites) of ligation to the polycation is unknown with this method.

In this paper we describe the synthesis of new transferrin conjugates that are ligated with DNA-binding compounds in a specific manner through modification of the transferrin carbohydrate moiety. The conjugates thus obtained are free of any groups derived from chemical linking agents, since the connecting atoms are already present within the starting compounds. The carbohydrate group acts as a natural spacer that puts a 32-atom distance between the transferrin and the DNA binding moiety. This spacer effect may be important for appropriate presentation of the ligand to its receptor. As a DNA-binding compound, the polycation polylysine was used, similar to the use described in ref 1 or to the asialo–orosomucoid conjugates prepared by Wu and Wu (*4*). We have also prepared a novel type of transferrin conjugate that contains the DNA intercalator ethidium homodimer (*5*) as the DNA-binding group and demonstrate successful receptor-mediated gene delivery with these conjugates.

EXPERIMENTAL PROCEDURES

Human transferrin (iron-free), conalbumin (iron-free), and poly(L-lysine) were obtained from Sigma. Liquid chromatography was performed with a Merck-Hitachi L-6210 pump, a L-4200 UV–vis detector, and a Kontron SFM25 fluorescence detector.

Quantitative Assays. Polylysine content of fractions was estimated spectrophotometrically by ninhydrin assay and in the case of FITC-labeled polylysine by absorption at 495 nm. The amount of dithiopyridine linkers in modified transferrin was determined after reduction of an aliquot with dithiothreitol followed by absorption measurement of released pyridine-2-thione at 340 nm. The amount of free mercapto groups was determined with 5,5′-dithiobis(2-nitrobenzoic acid) (*6*) and measurement at 412 nm. The transferrin content of fractions was determined by UV measurement at 280 nm and correction of the value (where necessary) by substraction of the corresponding UV absorption of FITC, dithiopyridine, or buffer at 280 nm. The content of sialic acids in transferrin was determined by a thiobarbituric acid assay (*7*).

Transferrin–Polylysine Conjugate Synthesis. A solution of 102 mg (1.28 μmol) of transferrin (human, iron-free) in 3 mL of a 30 mM sodium acetate buffer (pH 5) was subjected to gel filtration on a Sephadex G-25 (Pharmacia) column. The resulting 3.8 mL of solution was cooled to 0 °C and 80 μL of a 30 mM sodium acetate buffer (pH 5) containing 4 mg (19 μmol) of sodium periodate was added. The mixture was kept in an ice bath and in the dark for 90 min. For removal of the low molecular weight products an additional gel filtration (Sephadex G-25, 30 mM sodium acetate buffer, pH 5) was performed; this yielded a solution containing about 82 mg (1.03 μmol) of oxidized transferrin (monitoring: UV absorption at 280 nm and ninhydrin assay). In order to detect the oxidized aldehyde-containing form that gives a color reaction upon staining with anisaldehyde reagent, samples were dropped on a silica gel thin-layer plate, dried, immersed into *p*-anisaldehyde/sulfuric acid/ethanol (1/1/18), dried, and heated. The modified transferrin solution was promptly added (within 10–15 min) to a solution containing 0.50 μmol of fluorescent labeled poly(L-lysine) with an average chain length of 300 lysine monomers in 4.5 mL of 100 mM sodium acetate (pH 5) with vigorously mixing at room temperature. [The labeled poly(L-lysine) was derived by

[1] Abbreviations used: FITC, fluorescein isothiocyanate; TfEtD, transferrin–ethidium homodimer conjugate; TfpL, transferrin–poly(L-lysine) conjugate; HEPES, 4-(2-hydroxyethyl)-1-piperazineethanesulfonic acid.

1043-1802/91/2902-0226$02.50/0 © 1991 American Chemical Society

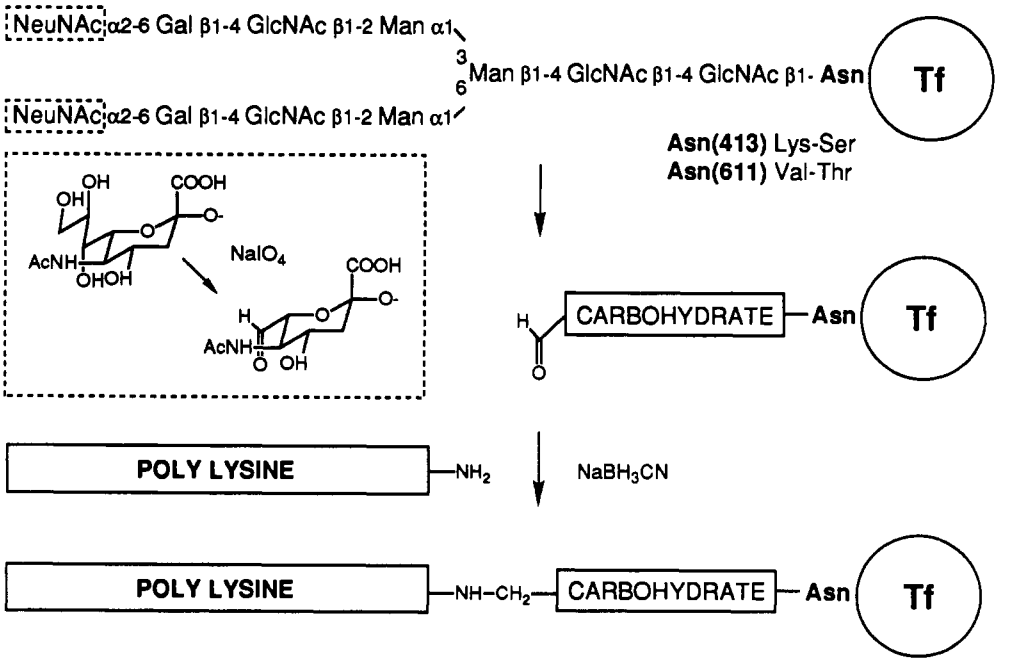


Figure 1. Conjugation via transferrin glycosylation sites. The molecular structure of sialic acid (*N*-acetylneuraminic acid, NeuNAc) and its oxidation with sodium periodate is shown within the dashed box. Tf, transferrin.

reacting 34 mg of hydrobromide salt with 130 μg of fluorescein isothiocyanate in sodium bicarbonate buffer (pH 9) for 3 h and subsequent gel filtration.] The pH of the mixed solution was brought to 7.5 by addition of 1 M sodium bicarbonate after 20 min; four portions of 9.5 mg (150 μmol) of sodium cyanoborohydride each were added at 1-h intervals. After 18 h, 1.9 mL of 5 M sodium chloride were added to bring the solution to an overall salt concentration of about 0.75 M. The reaction mixture was loaded on a cation-exchange column (Pharmacia Mono S HR 10/10) and was fractionated with a salt gradient from 0.75 to 2.5 M sodium chloride with a constant content of 25 mM HEPES (pH 7.3). The high salt concentration during the loading of the column and at the beginning of the gradient was essential for the efficient recovery of the polycation conjugates. Some transferrin protein (about 30%), together with a weak fluorescence activity, eluted in the flowthrough; the major amount of fluorescent conjugate eluted between 1.35 and 1.9 M salt (see Figure 2) and was pooled into three fractions. These, after dialysis against 2 × 2 L of 25 mM HEPES (pH 7.3), yielded (in order of elution) fraction TfpL300A containing 19 mg (0.24 μmol) of transferrin modified with 80 nmol of polylysine, fraction TfpL300B containing 27 mg (0.34 μmol) of transferrin modified with 150 nmol of polylysine, and fraction TfpL300C containing 5 mg (62 nmol) of transferrin modified with 80 nmol of polylysine. The overall yield of these conjugates based on transferrin was 50%, based on polylysine, 62%.

Transferrin conjugates, unless immediately used, were stored (after shock-freezing in liquid nitrogen) at −20 °C for up to several months in the iron-free form. Before iron incorporation, samples (ca. 0.5–1.5 mg) were brought to physiological salt concentration (150 mM) by addition of sodium chloride; the iron incorporation was performed by addition of 6 μL of 10 mM iron(III) citrate buffer (containing 200 mM citrate and adjusted to pH 7.8 by sodium bicarbonate addition)/mg of transferrin content. The iron-loaded conjugates were used for DNA-complex formation as described below. To limit the deterioration of the conjugates that often occurs upon several freeze–thaw cycles, the conjugates were divided into convenient

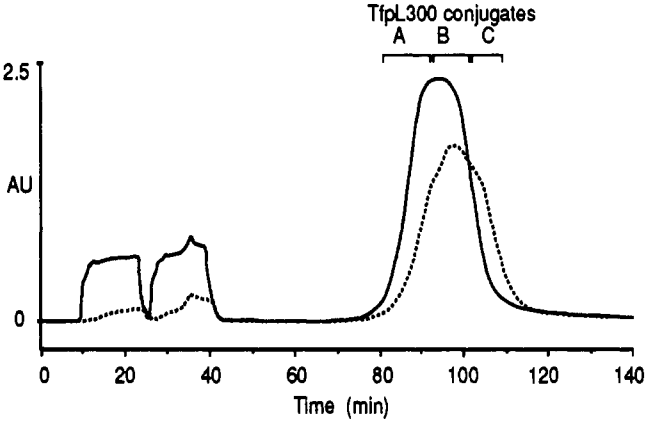


Figure 2. Isolation of transferrin–polylysine conjugates by cation-exchange chromatography. The crude reaction mixture was loaded in two portions (containing 0.75 M salt) onto a Pharmacia Mono S column, and conjugate fractions A, B, and C eluting between 1.35 and 1.9 M salt were collected: —, UV absorption at 280 nm; - -, fluorescence at 520 nm.

small aliquots, shock-frozen in liquid nitrogen (or dry ice/ethanol), and kept at −20 °C.

Transferrin–Ethidium Homodimer Conjugate (TfEtD) Synthesis. Oxidation of 32 mg (0.4 μmol) of transferrin (human, iron-free) with periodate was performed as described above; gel filtration (Sephadex G-25, 30 mM sodium acetate buffer pH 5) yielded a 1.9 mL solution containing about 20 mg (0.25 μmol) of oxidized transferrin. The transferrin was added to a solution containing 1 mg (1.17 μmol) of ethidium homodimer (5,5′-diazadecamethylenebis(3,8-diamino-6-phenylphenanthridium) dichloride dihydrochloride, E-1169, Molecular Probes) in 1.2 mL of water. The mixture was kept in the dark, the pH of the solution was brought to 7.3 by addition of HEPES buffer, and to the mixture were added two portions of 1 mg (16 μmol) of sodium cyanoborohydride in 50 μL of water with a 4-h interval between portions. The reaction mixture was left at room temperature in the dark for 2 days and then was subjected to gel filtration (Sephadex G-25, 50 mM HEPES buffer pH 7.3). In this step (according to UV absorption at 495 nm) about 200 μg of

unconjugated ethidium dimer together with other low molecular weight components were removed. The final volume of conjugate solution was 4.1 mL. One-third of the solution was used for preliminary purification experiments. The remainder (2.7 mL) was diluted with 0.6 M guanidinium hydrochloride (buffered with sodium acetate to pH 5) and loaded on a hydrophobic-interaction column (phenyl-Sepharose CL-4B, Pharmacia; 100 × 8 mm, ca. 4.5 mL). A slightly pink solution eluted in the flowthrough that also contained about 1.5 mg of transferrin. The violet conjugates remained on the column and, after a wash with 50 mL of 0.6 M guanidinium hydrochloride, were eluted with 0.6 M guanidinium hydrochloride containing first 2% and then 3% octyl glucopyranoside (Sigma). The conjugates were collected as two subsequent eluted fractions (7 and 27.5 mL), dialyzed against 2 L of 200 mM guanidinium hydrochloride for 3 days, then concentrated with a Speedvac (Savant) to a volume of about 3 mL each, and again dialyzed against 2 × 2 L of 25 mM HEPES buffer (pH 7.3) for 2 days. This procedure yielded (although there was some loss of material due to the extensive dialysis) two transferrin–ethidium dimer conjugate fractions containing 2 mg of transferrin each (according both to ninhydrin assay and Bio-Rad protein assay (Bio-Rad)); the two violet fractions had 0.42 AU (522 nm) and 0.68 AU (516 nm), respectively; as the transferrin conjugated ethidium dimer had changed UV absorbtion characteristics (ethidium homodimer: 1 mg corresponds to about 10 AU (495 nm) at pH 7.3), the exact content of conjugated ethidium dimer within the transferrin conjugates could not be determined. Iron incorporation was performed as described for the transferrin–polylysine conjugates.

DNA Complex Formation and Transfections. K562 cells were grown in suspension in RPMI medium plus 10% FCS, 100 units/mL penicillin, 100 μg/mL streptomycin, and 2 mM glutamine, reaching a density of 500 000 cells/mL. Cells were prepared for transfection as previously described (*3*). To increase the surface presentation of transferrin receptor, the cells were placed, 20 h before transfection, in fresh medium containing 50 μM desferrioxamine (Sigma) at about 200 000 cells/mL. The desferrioxamine pretreatment raises the transferrin receptor levels ca. 5-fold, resulting in an increase in DNA delivery (*3*). The morning of the transfection, the cells were collected, resuspended in fresh medium containing 10% fetal calf serum (plus 50 μM desferrioxamine) at 250 000 cells per mL, and placed in a 24-well dish, 2 mL per well.

Six micrograms of the DNA plasmid pRSVL [containing the *P. pyralis* luciferase gene under the control of the Rous sarcoma virus long terminal repeat enhancer/promoter (*8*)] in 330 μL of HBS (150 mM NaCl, 20 mM HEPES 7.3) were mixed with various amounts of TfpL conjugate in 170 μL of HBS as specified in Figure 3. After 30 min at room temperature the 500-μL mixture was added to K562 cells. Chloroquine was added to the 2-mL cell sample (100 μM final concentration) about 5–10 min before adding the 500-μL DNA/conjugate sample. After a 4-h incubation at 37 °C, the cells were washed into prewarmed, fresh medium (without chloroquine) and incubated at 37 °C. The cells were harvested 20 h after transfection and extracts were prepared. Aliquots of cell extracts, standardized for protein content, were assayed for luciferase activity as described (*3*); see Figure 3.

Complexes of DNA and transferrin–ethidium dimer conjugate were formed as described for the TfpL conjugates, by mixing a 330-μL solution of 6 μg of pRSVL in HBS with a 170-μL solution of various amounts of TfEtD

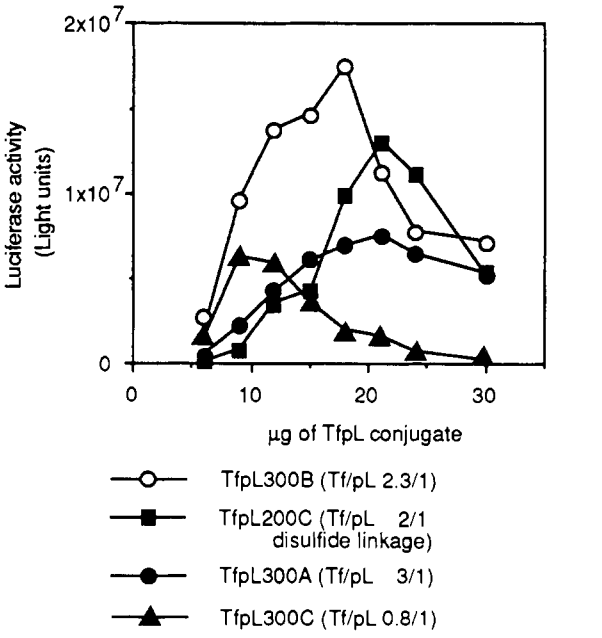


Figure 3. Luciferase gene expression mediated by transferrinfection in K562 cells. For complex formation with 6 μg of pRSVL plasmid DNA, 6–30 μg of the carbohydrate-linked transferrin–polylysine conjugate fractions TfpL300A, -B, or -C were used. DNA complexes with the most active conjugate fraction TfpL200C deriving from a ligation procedure via disulfide bonds (*16*) were prepared in parallel. The gene delivery resulting from the various complexes in K562 cells 20 h after the transfection was determined by assaying aliquots of cell extracts standardized for protein content. The values shown represent the activity of the entire cellular samples of about 500 000 cells.

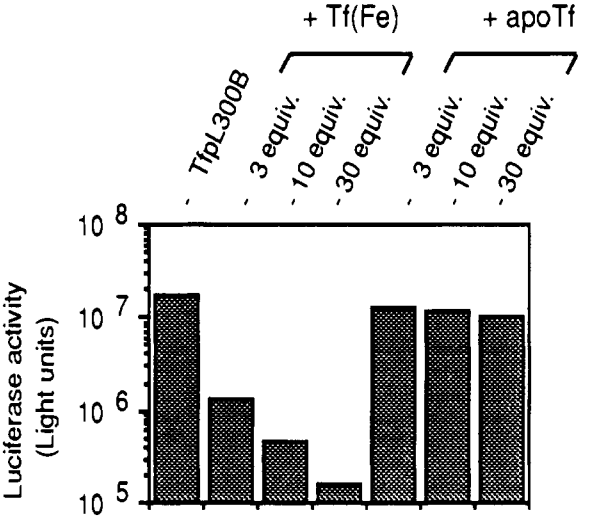


Figure 4. Transferrinfection is competitively inhibited by iron-loaded transferrin. Transferrinfection with complexes of 6 μg of pRSVL plasmid DNA and 18 μg of TfpL300B was performed in a similar fashion as described in Figure 3 and Experimental Procedures, with the difference that indicated amounts of either iron-loaded transferrin [Tf(Fe), equivalents given correspond to transferrin content within the DNA complexes] or iron-free apotransferrin (apoTf) were added to the tissue culture 30 min before the transfection. Serum-free medium was used during these experiments in order to eliminate possible iron sources. The resulting luciferase activity (corresponding to 500 000 cells) is shown.

conjugates in HBS as specified in Figure 5. Complexes were used for gene delivery to 500 000 K562 cells using standard conditions; aliquots of cell extracts standardized for protein content were assayed for resulting luciferase activity (see Figure 5).

Ternary complexes of DNA with transferrin–ethidium

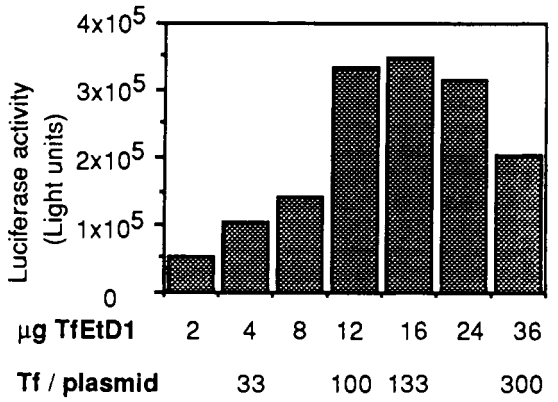


Figure 5. Transferrin–ethidium homodimer conjugates can mediate delivery and expression of the pRSVL luciferase gene. The transfections in K562 cells were performed with complexes of 6 μg of pRSVL plasmid DNA with indicated amounts of transferrin–ethidium homodimer conjugates (fraction 1; TfEtD1) and assayed as described in Figure 3.

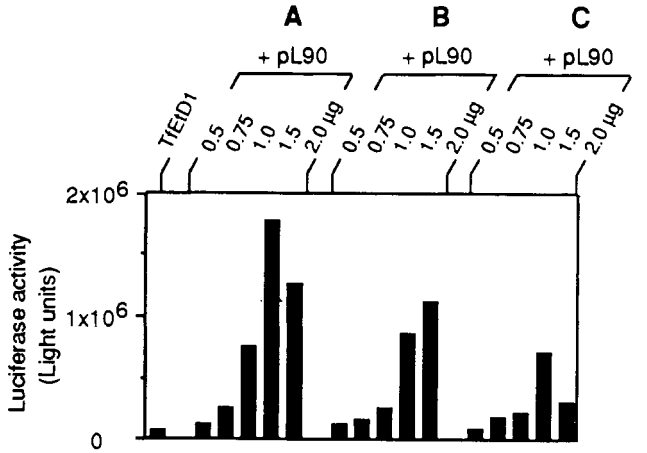


Figure 6. Transferrinfection with ternary complexes of pRSVL plasmid DNA, transferrin–ethidium homodimer conjugates (TfEtD), and various indicated amounts of polylysine (pL90). The improvement in gene delivery is dependent on the ordering of mixing the three components: (A) first complexation of 6 μg of DNA with 4 μg of TfEtD and then addition of pL90; (B) addition of a mixture of TfEtD and pL90 to the DNA; (C) first complex formation of DNA with pL90 followed by TfEtD addition.

dimer conjugates and poly(L-lysine) with an average chain length of 90 lysine monomers (pL90, hydrobromide salt, Sigma) were prepared in three different modes: (1) Complexes were formed by first mixing a 170-μL solution of 6 μg of pRSVL DNA in HBS with a 170-μL solution of 4 μg of TfEtD conjugates, and then mixing with a 170-μL solutions of various amounts of pL90 in HBS as specified in Figure 6. (2) Complexes were formed by first mixing 170-μL solutions of 4 μg of TfEtD conjugates with various amounts of pL90, followed by the addition to a 170-μL solution of 6 μg of pRSVL DNA. (3) Complexes were prepared by mixing a 170-μL solution of 6 μg of pRSVL in HBS with a 170-μL solution of various amounts of pL90 in HBS and subsequent addition of a 170-μL solution of 4 μg of TfEtD conjugates.

Gene delivery with the ternary complexes to K562 cells was performed as described above (see Figure 6).

RESULTS

Synthesis of Transferrin–Polylysine Conjugates with Linkage through the Transferrin Carbohydrate Moiety. The sequence of human serum transferrin (*9*), its glycosylation sites, and the structure of the carbohydrate parts (*10*) are known. The protein contains two identical carbohydrate chains that are attached by N-glycosylation to Asn-413 and Asn-611. The glycan chains have a bi-antennary structure, composed of a mannotriosidodi-*N*-acetylchitobiose core bearing two *N*-acetylneuraminyl-*N*-acetyllactosamine units. The glycosylation on the transferrin has no known influence on receptor binding or any other biological function (*11*) apart from the clearance of asialotransferrin from the plasma (*12*). Therefore we have chosen the transferrin carbohydrate moieties as the specific sites for attachment of polylysine and other nucleic acid binding domains, anticipating that this modification would not interfere with the binding of transferrin to its cellular receptor (see Figure 1).

Within the branched carbohydrate chains, sugars that contain a vicinal diol system can be oxidized by sodium periodate to yield aldehydes, with the concomitant cleavage of the HOC–COH bond. In our procedure the iron-free form of human transferrin was treated with 15 molar equiv of sodium periodate at 0 °C for 90 min. Under similar low temperature conditions, in glycoproteins (*13*) as well as in the special case of human transferrin (*14*) the two terminal exocyclic carbon atoms of the sialic acids within the carbohydrate chains are selectively removed by periodate oxidation; this has been confirmed by the subsequent selective tritium incorporation into the modified sialic acid residues (*14*).

We coupled the oxidized form of transferrin through its aldehyde group to the amino groups of polylysine (average chain length of about 300 lysine monomers per molecule). The junction that results from aldimine formation was stabilized by reduction to the secondary amine with sodium cyanoborohydride, which is no longer hydrolyzable (see Figure 1 for details). The transferrin–polylysine conjugates were obtained after purification (as described below and in Experimental Procedures) in a satisfactory overall yield (50% or 62% based on transferrin or polylysine). Compared to the published procedure (*1*) this new synthesis has the advantage of being less time-consuming, and the synthesis is useful for the preparation of large amounts (>100 mg) of conjugates with defined polycation–transferrin ligation sites.

Conalbumin Has No Sialic Acids and Does Not Form Polylysine Conjugates. Conalbumin (chicken egg transferrin) has been reported to lack sialic acids on the carbohydrate domain (*15*). We reinvestigated this in an assay with thiobarbituric acid (*7*). Accordingly conalbumin would not to be expected to function in ligation if the reaction is truly specific for the terminal sialic residues. Therefore, to test the specificity, we made several attempts with identical or slightly modified conditions. These did not yield significant amounts of conalbumin conjugates (less than 5%), although, as in the case of the human transferrin, the periodate oxidation at 0 °C or at room temperature produced some modified glycoprotein which showed staining with anisaldehyde that is characteristic for sugar aldehydes.

Although several sugars can be oxidized with periodate (at least at room temperature), the terminal sialic acid within the carbohydrate moiety of glycoproteins is especially suited for periodate oxidation and subsequent derivatization; the efficiency of the conjugation procedure as described in this paper seems to be strongly dependent on the presence of sialic acids.

Purification and Biological Properties of the New Conjugates. Isolation of the conjugates was performed by cation-exchange chromatography (Figure 2) with a salt gradient which allows fractionation into products with

increasing polylysine to transferrin ratios. In previous experiments (*1*) the recovery of the products from this chromatographic step was only moderate as a result of irreversible binding of some polylysine-rich conjugate fractions to the resin. This problem could be solved by the addition of salt to the conjugate reaction mixture and loading the column at a high salt concentration (0.75 M). With this modified procedure, not only was the yield of conjugates considerably increased but it could also be demonstrated that the recovered polylysine-rich conjugate fractions (with about one transferrin per 100 lysine moieties) are efficient in *transferrinfection* (*16*). Two main fractions, TfpL300A and TfpL300B, and a smaller fraction, TfpL300C, were obtained from the chromatographic purification of the new carbohydrate-linked conjugates (see Figure 2).

After loading of the transferrin ligands with iron (see Experimental Procedures), the new conjugates were tested for their ability to deliver pRSVL (*8*), a plasmid encoding *P. pyralis* luciferase as a reporter gene into the human K562 cell line in the same fashion as described in refs 3 and 16. A constant amount of 6 μg of pRSVL plasmid DNA was mixed with increasing amounts of conjugate TfpL300A, TfpL300B, or TfpL300C in a set of titration experiments; for comparison, the most efficient conjugate fraction TfpL200C, previously prepared by ligation through disulfide linkage (*16*) was also included in these titration experiments. The complexes thus obtained were added to the K562 tissue culture in the presence of chloroquine (see Experimental Procedures), protein extracts of the transfected cultures were prepared after 24 h and assayed for luciferase activity (Figure 3). The presence of luciferase activity indicates that DNA has been successfully internalized by the cell, transported to the nucleus, and expressed as a gene. The carbohydrate-linked conjugates have high gene-delivery efficiency, similar or slightly better than those prepared by the initial method of disulfide linkage (Figure 3). The molar ratio of transferrin to polylysine influences the transferrinfection efficacy as was seen with the TfpL200 conjugates (*16*); the TfpL300B conjugate fraction with a ratio of transferrin to polylysine of 2.3/1 was more active than either the polylysine-poor A fraction or the polylysine-rich C fraction.

In order to determine whether the internalization of the DNA complexes with the new conjugates proceeds via the transferrin receptor, complexes of 6 μg of pRSVL with 18 μg of TfpL300B were used for transferrinfection experiments in which K562 cells were treated with increasing amounts of either iron-loaded transferrin or iron-free apotransferrin (Figure 4). The presence of 3 or 30 equiv of iron-loaded transferrin results in a 10- or 100-fold decrease in the gene delivery, respectively. The strong competition by free transferrin suggests that the uptake of the complexes occurs via the transferrin-specific entry pathway. Iron-free apotransferrin, due to its low receptor affinity (*17*), has far less influence on the transferrinfection.

Transferrin–Ethidium Dimer Conjugates as Novel DNA-Intercalating Gene-Delivery Agents. Polylysine was chosen as a DNA-binding element in the initial transferrin conjugates. We already have shown that it can be replaced by small polycationic peptides like salmon sperm protamine (*1*, *16*). As an alternative to using charge interactions, as in polycation–DNA complexes, we are testing the utility of the strong intercalative binding interaction between a planar dye and DNA to attach transferrin to the nucleic acid. With the new procedure of coupling via the carbohydrate moiety, transferrin conjugates with ethidium homodimer (EtD), a known efficient DNA intercalator (*5*), have been synthesized. We considered the carbohydrate chain to act as a spacer that should prevent steric hindrance of the intercalator by the large transferrin protein. The transferrin–ethidium homodimer conjugates (TfEtD) were isolated by removal of the unbound ethidium dimer by gel filtration followed by fractionation through chromatography on an hydrophobic-interaction column (phenyl-Sepharose). A small fraction of unconjugated transferrin eluted in the flowthrough whereas the transferrin conjugates remained on the column bound by hydrophobic interactions between the attached ethidium homodimer and the matrix. The conjugates were then isolated in two fractions by elution with buffer containing 2 or 3% octyl glucopyranoside.

A transferrinfection using standard conditions with the transferrin–ethidium dimer conjugates showed a significant gene expression in K562 cells (Figure 5), however at a moderate level compared to the most effective transferrin–polylysine conjugates. The maximum delivery was obtained at a DNA/conjugate ratio at which about 130 transferrin were bound to a single DNA plasmid. From previous work (*16*) it is known that plasmid DNA coated with about 10–20 polylysine-conjugated transferrin molecules can be efficiently internalized by the transferrin receptor mediated pathway, if the DNA is packaged to compact structures of a size of about 80–100 nm by the addition of further polycations. Therefore we prepared ternary complexes of the plasmid DNA with amounts of transferrin–ethidium dimer conjugates that represent about 30 transferrin molecules per DNA plasmid and various amounts of additional polylysine. As the ethidium dimer is not expected to condense DNA to a similar extent as polylysine, the lower activity of the transferrin–ethidium homodimer DNA complex is not surprising. If the DNA condensation is incomplete in the transferrin–ethidium homodimer complexes, then the addition of free polylysine, which causes a strong condensation of the DNA structure (*18*), should result in an increase in DNA delivery. As shown in Figure 6, the inclusion of polylysine results in improved gene delivery and expression. We observed that the order of mixing the three components influences the quality of the ternary complexes. The most delivery-competent complexes were obtained if the attachment of the transferrin conjugates to the DNA preceded the binding of polylysine. Here, gene expression is more than 10-fold higher compared to that of complexes where polylysine is omitted from the complex formation (see Figure 6A). However, when the DNA was condensed with polylysine prior to the loading with the transferrin–ethidium homodimer conjugates gene expression is ca. 2-fold lower (see Figure 6C), probably the result of a less efficient binding of the transferrin–ethidium homodimer conjugates compared to the preparation used in Figure 6A.

DISCUSSION

We have described a simple and efficient procedure for the synthesis of transferrin–polylysine conjugates that is also suitable for the preparation of large quantities (100 mg or more) of conjugates. The two-step procedure is based on the selective oxidative modification and activation of the terminal sialic acids within the two well-defined carbohydrate moieties of human transferrin, followed by reductive coupling to the polylysine amino groups. Thus transferrin–polylysine conjugates are obtained with defined polycation–transferrin ligation sites with "nature-derived" carbohydrate spacers that are free of any modifications that might be derived from cross-

linking agents. Consistent with the fact that the transferrin carbohydrate moiety has no influence on transferrin receptor binding, we found that the new TfpL conjugates can mediate gene delivery to the human erythroid K562 cell line with similar or greater efficiency than TfpL conjugates prepared with a heterobifunctional linking agent (*1*). Furthermore we show that the uptake of the DNA complexes with the new transferrin conjugates occurs via the transferrin receptor, because native iron-loaded transferrin, if added to the medium, efficiently competes for the uptake into the cells.

Because the avian ovotransferrin (conalbumin) lacks sialic acids in the carbohydrate part, the method does not function for the preparation of conalbumin–polylysine conjugates. However, we have successfully applied the procedure for the synthesis of polylysine conjugates with mouse transferrin and with a recombinant HIV glycoprotein gp120 (our unpublished results). We are exploring a second mode of binding Tf to DNA involving an intercalative dye. We have synthesized conjugates of human transferrin with the intercalator ethidium–homodimer that function as novel gene-delivery agents. If polylysine, which is known to condense DNA efficiently, to yield small toroid structures (*18*), is included in the complex formation, the transfection efficiency is considerably increased (Figure 6). DNA polylysine complexes without the transferrin conjugate, on the other hand show only negligible activity (*16*). Our results demonstrate that transferrin which is attached to DNA via an intercalating agent is sufficient for receptor-mediated gene delivery which may be further improved by condensation of the DNA with free polylysine.

ACKNOWLEDGMENT

We are grateful to Dr. Martin Nicklin for critical reading of the manuscript. We appreciate the technical assistance of Karin Kos.

LITERATURE CITED

(1) Wagner, E., Zenke, M., Cotten, M., Beug, H., Birnstiel, M. L. (1990) *Proc. Natl. Acad. Sci. U.S.A. 87*, 3410–3414.
(2) Zenke, M., Steinlein, P., Wagner, E., Cotten, M., Beug, H., and Birnstiel, M. L. (1990) Receptor-mediated endocytosis of transferrin polycation conjugates: An efficient way to introduce DNA into hematopoietic cells. *Proc. Natl. Acad. Sci. U.S.A. 87*, 3655–3659.
(3) Cotten, M., Langle-Rouault, F., Kirlappos, H., Wagner, E., Mechtler, K., Zenke, M., Beug, H., and Birnstiel, M. L. (1990) Transferrin-polycation-mediated introduction of DNA into human leukemic cells: stimulation by agents that affect the survival of transfected DNA or modulate transferrin receptor levels. *Proc. Natl. Acad. Sci. U.S.A. 87*, 4033–4037.
(4) Wu, G. Y., and Wu, C. H. (1987) Receptor-mediated in vitro gene transformation by a soluble DNA carrier system. *J. Biol. Chem. 262*, 4429–4432.
(5) Gaugian, B., Barbet, J., Oberlin, R., Roques, B. P., and LePecq, J.-B. (1978) DNA bifunctional intercalators. 1. Synthesis and conformational properties of an ethidium homodimer and of an acridine ethidium heterodimer. *Biochemistry 17*, 5071–5078.
(6) Ellman, G. L. (1959) *Arch. Biochem. Biophys. 82*, 70.
(7) Uchida, Y., Tsukada, U., and Sugimori, T. (1977) Distribution of neuraminidase in *Arthrobacter* and its purification by affinity chromatography. *J. Biochem. 82*, 1425–1433.
(8) DeWet, J., Wood, K., DeLuca, M., Helinski, D., and Subramani, S. (1987) Firefly luciferase gene: structure and expression in mammalian cells. *Mol. Cell. Biol. 7*, 725–737.
(9) MacGillivray, R. T. A., Mendez, E., Shewale, J. G., Sinha, S. K., Lineback-Zins, J., and Brew, K. (1983) The primary structure of human serum transferrin. *J. Biol. Chem. 258*, 3543.
(10) Dorland, L., Haverkamp, J., Schut, B. L., Vliegenthart, J. F. G., Spik, G., Strecker, G., Fournet, B., and Montreuil, J. (1977) The structure of the asialo–carbohydrate units of human serotransferrin as proven by 360 MHz proton magnetic resonance spectroscopy. *FEBS Lett. 77*, 15–20.
(11) Huebers, H. A., and Finch, C. A. (1987) The physiology of transferrin and transferrin receptors. *Physiol. Rev. 67*, 520–582.
(12) Regoeczi, E., Chindemi, P. A., Debanne, M. T., and Hatton, M. W. C. (1982) Dual nature of the hepatic lectin pathway for human asialotransferrin type 3 in the rat. *J. Biol. Chem. 257*, 5431–5436.
(13) Lenten, L. V., and Ashwell, G. (1971) Studies on the chemical and enzymatic modification of glycoproteins. *J. Biol. Chem. 246*, 1889–1894.
(14) Kishimoto, T., and Tavassoli, M. (1986) Double labeling of transferrin: tritium labeling of sialic acid and ^{125}I or ^{59}Fe labeling of the protein moiety. *Anal. Biochem. 153*, 324–329.
(15) Williams, J. (1968) A comparison of glycopeptides from the ovotransferrin and serum transferrin of the hen. *Biochem. J. 108*, 57–67.
(16) Wagner, E., Cotten, M., Foisner, R., and Birnstiel, M. L. (1991) Transferrin–polycation DNA complexes: the effect of polycations on the structure of the complex and DNA delivery to cells. *Proc. Natl. Acad. Sci. U.S.A. 88*, 4255–4259.
(17) Dautry-Varsat, A. D., Ciechanover, A., and Lodish, H. F. (1983) pH and the recycling of transferrin during receptor-mediated endocytosis. *Proc. Natl. Acad. Sci. U.S.A. 80*, 2258–2262.
(18) Laemmli, U. K. (1975) Characterization of DNA condensates induced by poly(ethylene oxide) and polylysine. *Proc. Natl. Acad. Sci. U.S.A. 72*, 4288–4292.

Chemical Modification of Hyaluronic Acid by Carbodiimides

Jing-wen Kuo,[†,‡] David A. Swann,[‡] and Glenn D. Prestwich*[,†]

Department of Chemistry, State University of New York at Stony Brook, Stony Brook, New York 11794-3400, and MedChem Products, Inc., 232 West Cummings Park, Woburn, Massachusetts 01801. Received February 14, 1991

Hyaluronic acid (HA) is a linear polysaccharide with repeating disaccharide units of glucuronic acid and *N*-acetylglucosamine and is found in the extracellular matrix of connective tissues. Reaction of high molecular weight sodium hyaluronate (NaHA, MW $\sim 2 \times 10^6$) with EDC at pH 4.75, either in the presence or absence of a primary diamine, gave the *N*-acylurea and *O*-acylisourea as NaHA–carbodiimide adducts. None of the expected intermolecular coupling with the amine component was observed. On the basis of this new observation, this method for chemical modification of HA was used in conjunction with new synthetic carbodiimides to prepare HA derivatives bearing lipophilic, aromatic, cross-linked, and tethered functional groups. The degree of conversion to NaHA–acylurea products appears to depend upon both the characteristics of various carbodiimides and the conformational structure of NaHA.

INTRODUCTION

Hyaluronic acid (HA), a naturally occurring linear polysaccharide, is composed of repeating disaccharide units of glucuronic acid and *N*-acetylglucosamine (*1*, *2*). Both monosaccharides have the β-D-anomeric configuration at C-1. The linkage from glucuronic acid to *N*-acetylglucosamine is (1→3) and the linkage from *N*-acetylglucosamine to glucuronic acid is (1→4). The nomenclature for this repeating disaccharide unit is [→4)-*O*-(β-D-glucopyranuronosyl)-(1→3)-*O*-(2-acetamido-2-deoxy-β-D-glucopyranosyl)-(1→] (*2*) (Figure 1). HA is widely distributed in animal tissues, present in high concentrations in synovial fluid and the vitreous body of the eye, and in loose connective tissues of rooster comb, umbilical cord, and dermis (*3*). All HA molecules are thought to have the same primary structure, but differences occur in the degree of polymerization of the HA polysaccharide chains obtained from different tissues (*4*). Sodium hyaluronate (NaHA) is characterized by its large hydrodynamic volume (*5*). NaHA with a molecular weight of 1 million has an intrinsic viscosity of 3000 mL/g (*6*). It absorbs water, cushions cells, and lubricates the soft tissues of joints. The wide application of the purified, high molecular weight HA in eye surgery is an example of the utility of HA as a noninflammatory, viscoelastic biomaterial (*7*).

Studies on the chemical modification of hyaluronic acid have been mainly concerned with its *cross-linking* and *coupling*. Divinyl sulfone, bisepoxides, formaldehyde, and bishalides have been used to cross-link HA to produce highly swollen gels or virtually insoluble, plastic materials, depending upon the degrees of cross-linking (*8a,b*, *9*, *10*, *11a*). Coupling reactions, on the other hand, can also alter the properties of HA. For example, extensive esterification of HA with monofunctional organic halides can produce water-insoluble films (*11b*). These chemically modified HA are thought to have surgical and medical value as long-lasting biomaterials, and as potential drug-delivery vehicles.

The generation of a free amino group on HA for further coupling reaction has been a subject of much interest, both at the polymer and oligosaccharide level. Preparation of an alkylamine derivative of HA oligosaccharide modified at its reducing end was used for radioactive labeling (*12*). For high molecular weight HA, alkaline N-deacetylation of its glucosamine moiety produced a free amino group on HA polymer chain, but concomitant degradations of HA via β-elimination in the glucuronic acid moiety was observed (*13*). Hydrazinolysis of high molecular weight HA ($>2 \times 10^6$ Da) was performed at 100 °C, to give a partially N-deacetylated HA, but the molecular weight was decreased by 1 order of magnitude (*14*).

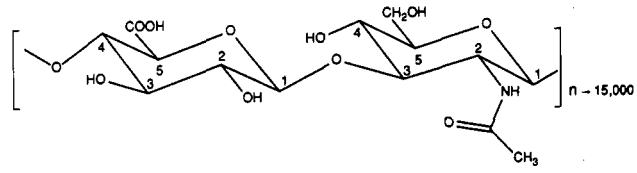


Figure 1. Hyaluronic acid is a linear polysaccharide, with repeating disaccharide units of glucuronosyl-β-1,3-*N*-acetylglucosamine linked by β-1,4-glycosidic bonds.

It was reported that the carbodiimide-catalyzed reaction of HA with monofunctional amines such as glycine methyl ester led to the formation of an amide linkage (*15*). Since carbodiimide–carboxylate reactions could be performed in aqueous solutions under mild conditions, we chose to explore carbodiimide-promoted coupling of HA carboxylic acid group with simple aliphatic diamines. When we began our studies using HA, difunctional amines, and carbodiimides, we expected to obtain an undegraded HA derivative with a free amino group. This was not realized, however, and only products from coupling of the carbodiimide to HA were observed. We now report the evidence for this reaction and the exploitation of this unexpected observation to prepare functionalized and cross-linked derivatives of HA.

EXPERIMENTAL PROCEDURES

General Experimental. Infrared spectra were taken on a Perkin-Elmer 1430 spectrophotometer. Only important, diagnostic peaks are reported. UV-vis spectra were taken on a Perkin-Elmer Lambda 4B spectrophotometer. Gas chromatography (GC) was performed on a Varian 3700 gas chromatograph (programmable temperature control) equipped with a flame ionization detector (FID), connected to helium carrier gas and interfaced to a HP 3380A integrator. The column used was DB-5 megabore (15 m × 0.5 mm) fused silica, at 30 psi He pressure. Thin-layer chromatography (TLC) was performed with

* Author to whom correspondence should be addressed.
† State University of New York.
‡ MedChem Products.

1043-1802/91/2902-0232$02.50/0 © 1991 American Chemical Society

Macherey-Nagel Polygram Sil G/UV$_{254}$ (40 × 80 mm, 0.25-mm silica gel) plastic TLC plates. Spots were visualized under UV light and/or under visible light by spraying the TLC plate with a ninhydrin spray solution (0.5% w/v of ninhydrin in water-saturated 1-butanol) or by dipping the TLC plate into a phosphomolybdic acid (10% w/w solution in EtOH) followed by heating with a heat gun. Flash column chromatography was performed under nitrogen pressure on Merck silica gel G (400–230 mesh). Low-resolution electron-impact mass spectra were obtained by using a Hewlett-Packard Model 5980A mass spectrometer interfaced to a HP 5710A GC. Only molecular ions (M^+) are listed. NMR spectra were obtained on a GE QE-300 spectrometer operating at 75 MHz for ^{13}C and 300 MHz for ^1H. Unless otherwise specified the chemical shifts for compounds dissolved in organic solvents are reported as ppm (δ) with $CDCl_3$ as standard. Chemical shifts of modified HA are reported as ppm (δ) with 3-(trimethylsilyl)-1-propanesulfonic acid sodium salt as the standard. The pH of the HA or modified HA samples was raised to about 14 by adding NaOD. The following abbreviations are used for peak multiplicities: s, singlet; d, doublet; t, triplet; q, quartet; m, multiplet. Concentration of HA was measured by the carbazole assay using glucuronolactone as standard (*16*). Intrinsic viscosity (IV) of HA and modified HA was measured with Cannon-Ubbelohde semimicro dilution type viscometer (size 75) at 37 °C. Hyaluronic acid was provided by MedChem Products, Inc., as its sodium salt, NaHA, which was purified from rooster comb by modifications of procedures described elsewhere (*17*). Unless otherwise stated, the molecular weight of HA used was from 1.5 to 2 million. Denatured ethanol containing 5% of methanol and 5% of 2-propanol was used in the purification of HA and its derivatives. The ninhydrin test was used to quantify the free primary amino groups of the amine-functionalized HA and D-glucosamine was used as the standard. The ratios of the reagents were the ratios of the molar equivalents based on the reacting functional groups. In the case of NaHA, it was the molar equivalents of its dissacharide units.

Procedures for Chemical Reactions *N*-(Benzyloxycarbonyl)-1,6-hexanediamine (8). To a solution of 1,6-hexamethanediamine (11.6 g, 100 mmol) in 50 mL of $CHCl_3$ was added dropwise at room temperature a solution of benzyl chloroformate (1.83 g, 10 mmol) in 50 mL of $CHCl_3$. The addition proceeded for 1 h, during which a white precipitate of the amine chloride was formed. The agitation was continued at room temperature for 5 h, the reaction mixture filtered, and the filtrate washed with water. The removal of the excess unreacted diamine was monitored by silica gel thin-layer chromatography ($CHCl_3$/MeOH/Et_3N = 90/10/5). The ninhydrin spray showed the disappearance of the purple spot at the bottom line on TLC plate, indicative of the complete removal of the unreacted 1,6-hexanediamine. The dried residue was weighed as 2.0 g. The crude product (1.2 g) was purified by column chromatography (silica gel, 0.8% MeOH, 5% Et_3N in $CHCl_3$) to provide 486 mg of the pure product (40.5%). ^1H NMR ($CDCl_3$): δ 1.26–1.43 (8 H), 2.60 (t, J = 6 Hz, 2 H, CH_2NH_2), 3.11 (m, 2 H, $-CH_2NHCOO-$), 5.08 (s, 2 H, CH_2Ph), 7.35 (m, 5 H, *Ph*). ^{13}C NMR ($CDCl_3$): δ 26.48 and 29.93 ($-CH_2-$) 33.60 (CH_2NH_2), 41.03 ($-CH_2NHCOO-$), 66.58 (CH_2Ph), 128.03, 128.47, and 136.70 (*Ph*), 156.38 (C=O).

***N*-[3-(Dimethylamino)propyl]-*N'*-[6-[(benzyloxycarbonyl)amino]hexyl]thiourea (9).** To a solution of *N*-(benzyloxycarbonyl)-1,6-hexamethylenediamine (8) (50 mg, 0.20 mmol) in 5 mL of $CHCl_3$ was added isothiocyanate 7 (40 mg, 0.28 mmol) predissolved in 5 mL of $CHCl_3$. After stirring for 6 h at room temperature, the solvent was evaporated to give 77 mg of the crude product (91%, GC). ^1H NMR ($CDCl_3$): δ 1.27–1.68 (10 H, $-CH_2-$), 2.19 (6 H, R-N*Me*$_2$), 2.30–2.39 (2 H, CH_2NMe_2), 3.11 (2 H, $-CH_2NHCOO-$), 3.13–3.52 (4 H, $-CH_2NH-$), 5.00 (s, 2 H, CH_2Ph), 7.27 (m, 5 H, *Ph*). ^{13}C NMR ($CDCl_3$): δ 26.02, 28.64, and 29.54 ($-CH_2-$), 40.59, 44.31 (N*Me*$_2$), 44.41, 44.47, 66.20 (CH_2Ph), 127.70, 127.75, 127.84, 128.22, and 136.45 (*Ph*), 156.24 (C=O), 181.80 (C=S).

***N*-Ethyl-*N'*-octylthiourea (5).** The experimental procedure of the synthesis of 9 was adopted. Thus octylamine (402 mg, 3 mmol) and ethyl isothiocyanate (270 mg, 3 mmol) gave 660 mg of thiourea 5, which was 97.5% homogenous (GC). ^1H NMR ($CDCl_3$): δ 0.86 (t, J = 6.2 Hz, 3 H, $(CH_2)_7Me$), 1.24 (t, 3 H, CH_2Me_2), 1.35–1.47 (10 H), 1.58 (m, 2 H, $-CH_2CH_2NH-$), 3.38–3.45 (4 H, $-CH_2CH_2NH-$), 5.77–5.80 (2 H, N*H*). ^{13}C NMR ($CDCl_3$): δ 13.97, 14.20, 22.51, 26.81, 28.91, 29.05, 29.11, 39.08, 44.34, 44.42, 181.12 (C=S).

***N*-Ethyl-*N'*-[6-[(benzyloxycarbonyl)amino]hexyl]thiourea (12).** The experimental procedure of the synthesis of 9 was adopted. Thus *N*-(benzyloxycarbonyl)-1,6-hexamethylenediamine (8) (100 mg, 0.4 mmol) and ethyl isothiocyanate (40 mg, 0.44 mmol) were combined in $CHCl_3$ to give 150 mg of the crude product with a purity of 86% (GC). ^1H NMR ($CDCl_3$) δ 1.18 (t, J = 7.2 Hz, 3 H, CH_3), 1.32 (4 H), 1.45–1.57 (4 H), 3.14 (t, J = 6.6 Hz, 2 H, $-CH_2NHCOO-$), 3.41 (4 H, $-CH_2NH-$), 4.96 (2 H, CH_2Ph), 7.26–7.33 (5 H, *Ph*). ^{13}C NMR ($CDCl_3$): δ 14.17, 25.81, 25.94, 28.64, 29.56, 38.94, 40.47, 43.91, 66.39 (CH_2Ph), 127.66, 127.90, 128.30, and 136.28 (*Ph*), 156.52 (C=O), 181.19 (C=S). MS: m/e 337.1 (M^+).

***N*-Ethyl-*N'*-(6-cyanohexyl)thiourea (15).** The experimental procedure of the synthesis of 9 was adopted. Thus 6-aminohexanenitrile (2.856 g, 22.8 mmol) and ethyl isothiocyanate (2.05 g) were combined in $CHCl_3$ to give 4.90 g of thiourea (15) (89.2% purity by GC). ^1H NMR ($CDCl_3$): δ 1.23 (t, J = 7.2 Hz, 3 H, CH_3), 1.52–1.73 (6 H), 2.37 (t, J = 7.0 Hz, 2 H, $CH_2C{\equiv}N$), 3.41–3.51 (4 H, $-CH_2NH-$), 5.77–5.80 (2 H, $-NH-$). ^{13}C NMR ($CDCl_3$): δ 13.68, 13.73, 16.39, 24.30, 25.19, 27.64, 38.45, 43.27, 119.32 (C≡N), 180.51 (C=S).

1,6-Hexamethylenebis(ethylthiourea) (23). To a solution of 1.351 g of ethyl isothiocyanate (15 mmol) in 10 mL of $CHCl_3$ was added dropwise 874 mg of 1,6-diaminohexane (7.5 mmol) predissolved in 10 mL of $CHCl_3$. The agitation continued for 2 h at room temperature as the reaction mixture gradually turned milky and viscous. The formed white solid was not soluble in hexane or Et_2O, poorly soluble in ethyl acetate and $CHCl_3$, and freely soluble in acetone and MeOH. Recrystallization of the crude product in MeOH improved its purity from 40% to over 75% (GC), and it was identified by ^1H NMR as bisthiourea 23. ^1H NMR ($CDCl_3$): δ 1.19 (6 H, CH_3), 1.22 (4 H), 1.56 (4 H), 3.46 (8 H, $-CH_2NH-$), 6.26–6.32 (4 H, N*H*). This material was used without further purification.

***p*-Phenylenebis(ethylthiourea) (26).** To a solution of 811 mg of *p*-phenylenediamine (7.5 mmol) in 15 mL of acetone was added 1.351 g of ethyl isothiocyanate (15 mmol). The reaction mixture was stirred 12 hr at room temperature and the formed precipitate was isolated by filtration, washed with cold methanol, and dried. The light brown precipitate was soluble in MeOH and DMSO, but not soluble in acetone, benzene, or $CHCl_3$. The solid product (510 mg) showed UV absorbance on silica gel TLC (R_f 0.6, CH_3Cl/MeOH/Et_3N = 90/10/5), and was homogeneous by GC. ^1H NMR (DMSO-d_6): δ 1.10 (t, J = 7.2

Hz, 6 H, CH_3), 3.45–3.49 (q, J = 6.1 Hz, 4 H, $-CH_2NH-$), 7.31 (s, 4 H, *Ph*).

Ethyl[6-[(benzyloxycarbonyl)amino]hexyl]carbodiimide (13). To a suspension of mercuric oxide (100 mg) in dry acetone (15 mL) was added thiourea **12** (77 mg) predissolved in 5 mL of dry acetone and refluxed for 3 h. Black mercuric sulfide was formed and was removed by filtration through Celite, dried ($MgSO_4$), and concentrated to give 60 mg of the product with a purity of 93% (GC). ^1H NMR ($CDCl_3$): δ 1.11–1.45 (8 H), 3.06–3.16 (6 H, $-CH_2N{=}C{=}N-$ and CH_2NHCOO), 4.98 (2 H, CH_2Ph), 7.24 (5 H, *Ph*). ^{13}C NMR ($CDCl_3$): δ 16.58, 26.13, 26.29, 29.73, 31.00, 40.79, 41.34, 46.44, 66.38 (CH_2Ph), 127.91, 128.34, and 136.50 (*Ph*), 156.30 ($C{=}O$) IR: 2120 (s, $-N{=}C{=}N-$) cm^{-1}. MS: m/e 303.2 (M^+).

[3-(Dimethylamino)propyl][6-[(benzoyloxycarbonyl)amino]hexyl]carbodiimide (10) was prepared as described for carbodiimide **13**, except that the crude product was chromatographed with a column packed with silica gel ($CHCl_3/Et_3N$ = 95/5). Thus, 77 mg of the thiourea **3** gave 15 mg of pure carbodiimide **6**. ^1H NMR ($CDCl_3$): δ 1.24–1.74 (10 H), 2.22 (s, 6 H, $N(CH_3)_2$, 2.34 (t, J = 7.5 Hz, 2 H), 3.16–3.26 (6 H, $-CH_2N{=}C{=}N-$ and CH_2NHCOO), 5.08 (s, 2 H, benzyl methylene), 7.34 (5 H, benzene). ^{13}C NMR ($CDCl_3$): δ 26.23, 26.42, 29.28, 29.89, 31.11, 44.80, 45.47, 46.51, 66.55 (CH_2Ph), 128.04 and 128.46 (*Ph*), 156.38 ($C{=}O$). IR: 2126 (s, $-N{=}C{=}N-$) cm^{-1}. MS: m/e 360 (M^+).

Ethyltridecylcarbodiimide (3) was prepared as described for carbodiimide **13**. Thus 320 mg of *N*-ethyl-*N'*-tridecylthiourea (**2**) gave 180 mg of carbodiimide **3**, which was 97.4% homogeneous by GC. ^1H NMR ($CDCl_3$): δ 0.87 (t, 3 H, $CH_3(CH_2)_{12}$), 1.21–1.33 (20 H, 1.57 (2 H, $-CH_2CH_2N{=}C{=}N-$), 3.17–3.24 (4 H, $-CH_2N{=}C{=}N-$). IR: 2120.1 cm^{-1} (s, $-N{=}C{=}N-$).

Ethyl-3-octylcarbodiimide (6) was prepared as described for carbodiimide **13**. Thus 600 mg of *N*-ethyl-*N'*-octylthiourea (**5**) gave 434 mg of carbodiimide **6**, which was 97.2% homogeneous. ^1H NMR ($CDCl_3$): δ 0.87 (t, 3 H, $CH_3(CH_2)_7$), 1.20–1.26 (12 H), 1.56 (2 H, $-CH_2CH_2N{=}C{=}N-$), 3.19–3.24 (4 H, $-CH_2N{=}C{=}N-$). IR: 2128.5 cm^{-1} (s, $-N{=}C{=}N-$).

Ethyl[6-(trifluoroacetamido)hexyl]carbodiimide (18) was prepared as described for carbodiimide **13**. Thus 108 mg of *N*-ethyl-*N'*-[6-(trifluoroacetamido)hexyl]thiourea (**17**) gave 90 mg of carbodiimide (**18**). GC showed the compound decomposed at elevated temperature. ^1H NMR ($CDCl_3$): δ 1.23 (t, J = 7.2 Hz, 3 H, CH_3), 1.25–1.58 (8 H), 3.19–3.26 (m, 4 H, $-CH_2N{=}C{=}N-$), 3.35–3.77 (2 H, $CH_2NHCOCF_3$). IR: 2128.5 cm^{-1} (s, $-N{=}C{=}N-$).

1,6-Hexamethylenebis(ethylcarbodiimide) (24). The dehydrosulfurization of bisthiourea **23** with mercuric oxide in acetone was performed for 2 h, with the oil bath at 72 °C. Higher temperature and longer reaction time may cause polymerization. Thus, the crude product after the reflux of 76.8 mg of bisthiourea **23** and 192 mg of HgO (in acetone) was purified by extracting with cold hexane to give 22.5 mg of **24**. ^1H NMR ($CDCl_3$): δ 0.87 (6 H), 1.21–1.41 (4 H), 1.54–1.61 (4 H), 3.19–3.27 (m, 8 H, $-CH_2N{=}C{=}N-$). IR: 2124 cm^{-1} (s, $-N{=}C{=}N-$).

***p*-Phenylenebis(ethylcarbodiimide) (27)** was prepared following the method above for biscarbodiimide **24**, using 108 mg of the aromatic bisthiourea **26**. The crude product was filtered through a silica gel column to give 45 mg of aromatic biscarbodiimide **27**, which was 97.3% homogeneous (GC). The compound was stored in a refrigerator and used within 3 days of preparation. ^1H NMR ($CDCl_3$): δ 1.33 (t, 6 H, methyls), 3.41–3.44 (4 H, $-CH_2N{=}C{=}N-$), 6.98 (s, 4 H, $-C_4H_4-$). IR: 2120.1 cm^{-1} (s, $-N{=}C{=}N-$). MS: m/z 214.1 (M^+), intensity 100.

General Procedure of Carbodiimide Reactions with NaHA. Sodium hyaluronate was dissolved in water to a concentration of ca. 4 mg/mL. For some reactions, as indicated below, amine was mixed with NaHA. The pH of the mixture was adjusted to 4.75 by 0.1 N HCl. The designed carbodiimide or commercially available carbodiimide was dissolved in water or 2-propanol, depending upon its solubility. After mixing HA and carbodiimide solutions, a pH increase was immediately observed. The reaction was monitored by pH meter and 0.1 N HCl was added dropwise to keep the pH at 4.75. The reaction was allowed to proceed for 2 h at room temperature. Then NaCl was added to make 5% w/v of the reaction mixture. Ethanol equal to 3 volumes of the reaction mixture was added and a stringy precipitate was obtained. The precipitate was redissolved for a second and third precipitation, thus removing all the unreacted or produced small organic compounds. The final precipitate was dissolved in deionized water to a concentration of no more than 6 mg/mL and was then lyophilized. The NMR sample solution of NaHA or modified NaHA was prepared by dissolving 5–10 mg of the lyophilized product into 1 mL of D_2O. The dissolution could be expedited by vortexing the sample and adding NaOD (sample pH ~14). The ratio of the reagents is defined as the molar equivalency ratio based upon the reaction of the carboxyl (HA) and carbodiimide functional groups.

***N*-Acylurea Products of HA and [3-(Dimethylamino)propyl]ethylcarbodiimide (EDC) (1a–e).** The above procedure was adopted in making these *N*-acylurea derivatives. The amount of reactants used and the analytical results are summarized as follows.

1a: The ratio of 1,6-diaminohexane/EDC was 3/1. The ratio of EDC/HA was 1/10. Thus NaHA (247.9 mg, 0.618 mequiv) and EDC (11.98 mg, 0.062 mmol) gave 221 mg of the lyophilized product (85% recovery). No amide linkage between HA and diaminohexane was formed. The purified product gave a negative ninhydrin test result. ^1H NMR (D_2O): δ 1.08 (t, J = 7.2 Hz, 3 H, CH_3CH_2N), 1.64 (m, 2 H), 2.18 (s, 6 H, $(CH)_3N$), 2.34 (t, J = 7.2 Hz, 2 H), 3.11 (m, 4 H, CH_2N).

1b: The ratio of 1,6-diaminohexane/EDC was 5/1. The ratio of EDC/HA was 1/10. Thus NaHA (246.4 mg, 0.615 mequiv) and EDC 11.78 mg, 0.062 mmol) gave 226 mg of the lyophilized product (88% recovery). The analytical results of ninhydrin and ^1H NMR are identical with those of **1a**.

1c: The ratio of 1,6-diaminohexane/EDC was 10/1. The ratio of EDC/HA was 1/10. Thus NaHA (247.7 mg, 0.618 mequiv) and EDC (11.84 mg, 0.062 mmol) gave 232 mg of the lyophilized product (89.5% recovery). The analytical results of ninhydrin and ^1H NMR are identical with use of **1a**.

1d: The ratio of 1,6-diaminohexane/EDC was 100/1. The ratio of EDC/HA was 1/10. Thus NaHA (122 mg, 0.304 mequiv) and EDC (11.78 mg, 0.062 mmol) gave 114 mg of the lyophilized product (85.4% recovery). The ninhydrin test result was negative.

1e: Thermally degraded NaHA with molecular weight of 60 000 was used in this reaction. The ratio of NaHA/1,6-diaminohexane/EDC was 1/1/1. Thus NaHA (264 mg, 0.66 mequiv) and EDC (126.5 mg, 0.66 mmol) gave 735 mg of the product which included **1e** and NaCl coprecipitate. No amide linkage between NaHA and diaminohexane was detected from NMR. The purified product showed less than 1% of the free amino group

during the ninhydrin test. ^{1}H NMR showed no amine α-methylene protons expected at δ 2.6. ^{1}H NMR (D_2O): δ 1.12 (t, J = 7.2 Hz, CH_3 of *N*-acylurea), 1.21 (t, CH_3 of *O*-acylisourea) (δ 1.12/δ 1.21 ≥ 4/1), 2.21 (s, $(CH_3)_2N$), 2.37, 3.15 (m, α-CH_2 of acylureas).

***O*-Acylurea Product of NaHA and EDC (1f).** The above procedure was also followed. The reaction condition was the same as for **1e**, except that NaHA was not thermally degraded. Thus NaHA (250.8 mg, 0.627 mequiv) and EDC (120.2 mg, 0.627 mmol, in 20 mL of water) gave 873 mg of the product which included **1f** and NaCl coprecipitate. No amide linkage between NaHA and diaminohexane was detected from NMR. The purified product showed less than 1% of the free amino group during the ninhydrin test. ^{1}H NMR (D_2O): δ 1.12 (t, CH_3 of *N*-acylurea), 1.21 (t, J = 7.2 Hz, CH_3, of *O*-acylisourea) (δ 1.21/δ 1.12 ≥ 5/1), 2.21 (s, $(CH_3)_2N$), 2.38 (t, J = 7.2 Hz), 3.15 (m, α-CH_2 of acylureas).

Acylurea Product of NaHA and Carbodiimide 6 (7a–c). The above procedure was followed. 2-Propanol (3 mL) was used to dissolve the carbodiimide.

7a: The ratio of carbodiimide/NaHA was 1/20. Thus NaHA (454 mg, 1.13 mequiv) and carbodiimide **6** (10.82 mg, 0.056 mmol) gave 440 mg of **7a** (94.6% recovery). The proton uptake was 0.02 mmol. Intrinsic viscosity (IV): 2866 mL/g (starting NaHA, 2354 mL/g).

7b: The ratio of carbodiimide/NaHA was 1/10. Thus NaHA (381 mg, 0.95 mequiv) and carbodiimide **6** (18.2 mg, 0.095 mmol) gave 388 mg of **7b** (95.6% recovery). The proton uptake was 0.04 mmol. IV: 2730 mL/g (starting NaHA, 2354 mL/g).

7c: The ratio of carbodiimide/NaHA was 1/5. Thus NaHA (477 mg, 1.19 mequiv) and carbodiimide **6** (45.6 mg, 0.238 mmol) gave 465 mg of **7c** (89.0% recovery). The proton uptake was 0.1 mmol. IV: 2534 mL/g (starting NaHA, 2354 mL/g).

Acylurea Product of HA and Carbodiimide 3 (4a–c). The above procedure was followed. 2-Propanol (3 mL) was used to dissolved the carbodiimide. In all three reactions, the proton uptake was less than 0.005 mmol.

4a: The ratio of carbodiimide/HA was 1/20. Thus NaHA (444 mg, 1.1 mequiv) and carbodiimide **3** (15.4 mg, 0.055 mmol) gave 397 mg of **4a** (89.5% recovery). IV: 2401 mL/g (starting NaHA, 2354 mL/g).

4b: The ratio of carbodiimide/HA was 1/10. Thus NaHA (400 mg, 1.0 mequiv) and carbodiimide **3** (25.8 mg, 0.1 mmol) gave 386 mg of **4b** (90.8% recovery). IV: 2591 mL/g (starting NaHA, 2354 mL/g). Additional proton resonance to HA from **4b** was not observed, but acid hydrolysis of **4b** (pH = 1, boiling water bath, 4 h) produced ^{1}H NMR signals as follows. ^{1}H NMR (D_2O): δ 1.34, 1.37, and 2.14 (br band, aliphatic protons), 3.12 (α-CH_2 of acylureas).

4c: The ratio of carbodiimide/HA was 1/5. Thus NaHA (529 mg, 1.32 mequiv) and carbodiimide **3** (66 mg, 0.264 mmol) gave 573 mg of **4c** (96.3% recovery). IV: 2651 mL/g (starting NaHA, 2354 mL/g).

Acylurea Products of NaHA and Carbodiimide 10 (11a,b). The above procedure was followed.

11a: The ratio of carbodiimide/NaHA was 1/10. Thus NaHA (252 mg, 0.63 mequiv) and carbodiimide **10** (25.2 mg, 0.063 mmol) gave 232 mg lyophilized product **11a** (92% recovery). IV: 2760 mL/g (starting NaHA, 2354 mL/g). ^{1}H NMR (D_2O): δ 1.25, 1.58, 2.12 ($N(CH_3)_2$), 3.07 (α-CH_2 of acylureas), 7.39 (*Ph*).

11b: The ratio of carbodiimide/NaHA was 1/5. Thus NaHA (126 mg, 0.315 mequiv) and carbodiimide **10** (25.2 mg, 0.063 mmol) gave 119.1 mg of the lyophilized product **11b** (94.5% recovery). The aqueous solution of **11b** was accidentally left stirring overnight without cooling. The temperature of the solution was measured as 42 °C. IV: 2323 mL/g (starting NaHA, 2354 mL/g). ^{1}H NMR (D_2O): δ 1.26, 1.42, 1.62, 2.21, 3.09 (α-CH_2 of acylureas), 7.41 (*Ph*).

Acylurea Product of NAHA and Carbodiimide 13 (14). The above procedure was followed. The ratio of carbodiimide/NaHA was 1/5. Thus NaHA (90.6 mg, 0.225 mequiv) and carbodiimide **13** (18 mg, 0.045 mmol) gave 105 mg of the lyophilized product **14**. The degree of coupling was measured as 16% by UV (240 nm). The proton uptake was 0.035 mmol. IV: 2734 mL/g (starting NaHA, 2354 mL/g). ^{1}H NMR (D_2O): δ 0.93 (CH_3 of *N*-acylurea), 1.33, 1.56, 3.15 (α-CH_2 of acylureas), 7.43 (*Ph*).

Acylurea Product of HA and Carbodiimide 18 (19). The above procedure was followed. The ratio of carbodiimide/NaHA was 1/5. Thus NaHA (400 mg, 1.0 mequiv) and carbodiimide **18** (60 mg, 0.2 mmol) gave 392 mg of **19** (85.2% recovery). The proton uptake was 0.06 mmol. IV: 3115 mL/g (starting NaHA, 2966 mL/g). ^{1}H NMR (D_2O): δ 1.11 (t, CH_3 of *N*-acylurea), 1.21 (CH_3 of *O*-acylisourea) (δ 1.11/δ 1.21 ≥ 5/1), 1.36, 1.49, 2.61 (CH_2NH_2 from decomposition of $CH_2NHCOCF_3$ in NaOD), 3.12 (α-CH_2 of acylureas).

NaHA Cross-Linked by Biscarbodiimide 24 (25a,b). The general procedure of the carbodiimide reaction with NaHA was adopted. The ratio of carbodiimide/NaHA was 1/10.

25a: The NaHA concentration was adjusted to 3.2 mg/mL and the carbodiimide concentration in 2-propanol was 2.75 mg/mL. Thus NaHA (423 mg, 1.05 mequiv) and biscarbodiimide **24** (11 mg, 0.05 mmol) gave 382 mg of **25a** (88% recovery). The proton uptake was 0.04 mmol. During the purification process, the precipitated NaHA derivative was only partially soluble in water. ^{1}H NMR (D_2O): δ 1.11 (t, CH_3 of *N*-acylurea), 1.36, 1.51, 3.12 (α-CH_2 of *N*-acylurea).

25b: The NaHA concentration was adjusted to 5.2 mg/mL and the carbodiimide concentration in 2-propanol was 0.92 mg/mL. Thus NaHA (416 mg, 1.04 mequiv) and biscarbodiimide **24** (11 mg, 0.05 mmol) gave 400 mg of **25b** (93.6% recovery). The proton uptake was 0.03 mmol. IV: 2554 mL/g (starting NaHA, 2354 mL/g).

NaHA Cross-Linked by Biscarbodiimide 27 (28a,b). The general procedure of the carbodiimide reaction with NaHA was adopted.

28a: The NaHA concentration was adjusted to 4.2 mg/mL and the carbodiimide concentration in 2-propanol was 1.5 mg/mL. The ratio of carbodiimide/HA was 0.18. Thus sodium hyaluronate (386 mg, 0.96 mequiv) and biscarbodiimide **27** (18 mg, 0.084 mmol) gave 389 mg of **28a** (96.4% recovery). The proton uptake was 0.12 mmol. The dried polymer from the first precipitation swelled in 200 volumes of water at 4 °C to form a cross-linked insoluble gel. The absorption of water appeared to reach an equilibrium after 5 days. Part of the gel was cut and stored in water at room temperature.

28b: The NaHA concentration was adjusted to 4.2 mg/mL and the carbodiimide concentration in 2-propanol was 0.89 mg/mL. The ratio of carbodiimide/HA was 0.10. Thus NaHA (404 mg, 1.01 mequiv) and biscarbodiimide **27** (10.7 mg, 0.05 mmol) gave 393 mg of **28b** (95% recovery). The proton uptake was 0.08 mmol. IV: 3073 mL/g (starting NaHA, 2354 mL/g). ^{1}H NMR (D_2O): δ 1.09 (t, CH_3CH_2 of *N*-acylurea), 1.19 (t, CH_3CH_2 of *O*-acylisourea) (δ 1.19/δ 1.09 ≥ 2/1), 1.62, 3.04 (α-CH_2 of acylureas).

***N*-Ethyl-*N'*-(6-aminohexyl)thiourea (16).** To a solution of 1.327 g of nitrile **15** (6.6 mmol) in 50 mL of dried

THF was added 600 mg of borane–dimethyl sulfide (7.92 mmol). The reactor was heated to reflux, and dimethyl sulfide was distilled off. After 3 h, the mixture was cooled to room temperature and quenched with 3 mL of 1 N HCl. Then pH was adjusted to 9 with 1 N NaOH and saturated with K_2CO_3. Et_2O was added to separate the layers. The aqueous layer was extracted twice with $CHCl_3$, and the combined organics were concentrated to give crude thiourea **16** (52%). The ^1H NMR spectrum showed the ratio of the amine α-methylene protons over nitrile α-methylene protons as over 10/1. ^1H NMR ($CDCl_3$): δ 1.21 (t, J = 7.2 Hz, 3 H, CH_3CH_2NH), 1.24–1.64 (8 H, 2.66 (t, J = 6.6 Hz, 2 H, CH_2NH_2), 3.44 (4 H, $-CH_2NH-$), 5.92 (2 H, NH). ^{13}C NMR ($CDCl_3$): δ 14.29 (CH_3CH_2), 26.37, 26.58, 28.95, 33.34, 39.02, 41.87 ($-CH_2NH-$), 44.20 (CH_2NH_2), 181.25 (C=S).

***N*-Ethyl-*N'*-[6-(trifluoroacetamido)hexyl]thiourea (17).** To an aqueous solution of 350 mg of thiourea **16** (1.5 mmol) mixed with 5 mL of 0.2 M $NaHCO_3$ was added 480 mg of ethyl thiotrifluoroacetate (3 mmol). The reaction was continued at room temperature overnight and a white precipitate was formed. The product was isolated by ether extraction to give 317 mg of a white solid, which was 84.4% homogeneous by GC. ^1H NMR ($CDCl_3$): δ 1.24 (t, J = 7.2 Hz, 3 H, CH_3CH_2), 1.37–1.40 (m, 4 H), 1.58–1.64 (m, 4 H), 3.38 (t, J = 6.6 Hz, 2 H, $CH_2NHCOCF_3$), 3.47 (4 H, $-CH_2NH-$). ^{13}C NMR ($CDCl_3$): δ 14.18 (CH_3CH_2) 25.99, 28.62, 28.77, 39.06, 39.65, 44.08, 65.79, 117.74 (CF_3), 157.22 (C=O), 181.22 (C=S).

Detrifluoroacetylation of HA Derivative 19 to Amine-Functionalized HA (20a). HA–trifluoroacetamide (**19**) (12.6 mg) was treated for 14 h at room temperature and pH 11. Then 0.1 N HCl was added to adjust the pH to 7.0–7.5. NaHA reaction products were precipitated with ethanol as described above. The precipitate was collected after centrifugation. The ethanol precipitation was repeated three times and the final aqueous solution was lyophilized to give 11.9 mg of a white, fibrous material. To test the amount of free amino group attached to the NaHA polymer chain, an aqueous solution of the NaHA–trifluoroacetamide (**19**) (1 mg/mL) was prepared and a quantitative ninhydrin test was performed. The percentage ratio of the detected free amine over NaHA was 3.1%. IV: 2865 mL/g (starting material (**19**), 3115 mL/g).

Detrifluoroacetylation of HA Derivative 19 to Amine 20b. The experimental procedure for **20a** was adopted except that the pH of the reaction mixture was adjusted to 11.5–12.0. Fourteen milligrams of the starting material (**19**) was used. The precipitate of **20b** was less stringy than that of **20a**. The lyophilized solid weighed 19.3 mg. Apparently, NaCl coprecipitated with and adhered to the NaHA derivative and was therefore also collected. The percentage ratio of the detected free amine over NaHA was 4.2%. IV: 2286 mL/g (starting material (**19**), 3115 mL/g).

RESULTS AND DISCUSSION

Commercially available carbodiimides have been widely used for carboxyl activation, such as in protein modification (*18*, *20*). EDC, [3-(dimethylamino)propyl]ethylcarbodiimide, for example, is a water-soluble carbodiimide. The following mechanism of the carbodiimide reaction in protein modifications is generally accepted: carbodiimide reacts with carboxyl groups to form an unstable, intermediate *O*-acylisourea, which, in the absence of nucleophiles, rearranges to a stable *N*-acylurea "by way of a cyclic electronic displacement" (*21*). In the presence of

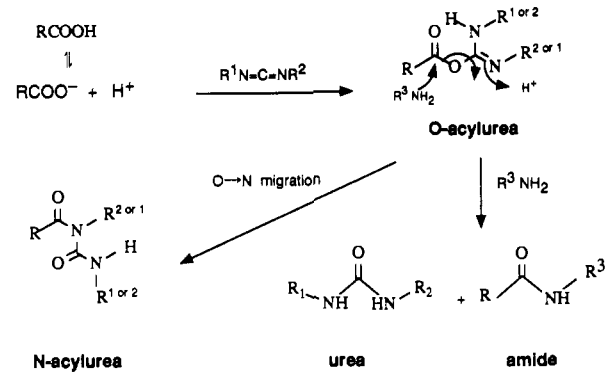


Figure 2. Mechanism of reaction between carboxylic acid and carbodiimide with and without primary amines.

a primary amine as nucleophile, the *O*-acylisourea formation is followed by a nucleophilic attack, forming an amide linkage between the amine and the acid (*18*) (Figure 2). An acidic environment is needed to catalyze the reaction, presumably through the protonation of the carbodiimide nitrogen. The reduced electron density at the carbodiimide central carbon is favorable to the nucleophilic attack of the carboxylate anion. At pH 4.75, carbodiimide nitrogens appear to be sufficiently protonated, while HA mainly exists as the carboxylate. The proton is not only a catalyst, but also a reagent. The stoichiometry of this process shows that one proton is consumed to form the urea compound. Thus the reaction can be monitored by the observed increase of pH and the consumption of hydrochloric acid during the reaction necessary to keep the reaction pH at 4.75.

Amidation reactions of glycosaminoglycans and primary amines catalyzed by carbodiimides have been reported. One example by Danishefsky and Siskovic is the reaction between glycine methyl ester (the amine component) and hyaluronic acid. The mechanism of the reaction was reported to be the same as mentioned above, i.e., the "condensation of the uronic acid moiety with EDC to form the *O*-acylurea followed by the displacement of the substituted urea by the amino group" (*15*). Similarly, we attempted to use diaminohexane and EDC to build an amide linkage between HA and the diamine.

The concentration of NaHA aqueous solution was adjusted to ca. 4 mg/mL, so that the solution would not be too viscous for thorough mixing with the added chemicals. A preliminary study without primary amine showed that carbodiimide was very reactive toward HA. The reaction started instantly at pH 4.75, as demonstrated by the immediate pH rise upon the addition of EDC. The attempted EDC-activated amidation using 1,6-diaminohexane was performed at the same pH. An initial pH surge was also observed. The equivalency ratios of the diamine to EDC in the reactions varied from 3/1 to 100/1, with the notion that the increased amine would favor the replacement reactions. The percentage equivalency ratio of EDC to NaHA was maintained at 10% as the base for comparison.

The reactions were allowed to proceed at room temperature for 2 h and in each case a pH increase was observed during the first hour at a progressively decreasing rate. This suggested that the formation of *O*-acylisourea had occurred, but it was not clear whether the replacement of amine or O → N migration of the *O*-acylisourea also proceeded during the reaction. Neither the displacement nor migration involve net proton gain or loss, according to the suggested mechanism (Figure 2). A ninhydrin test on the modified HA after the first precipitation was

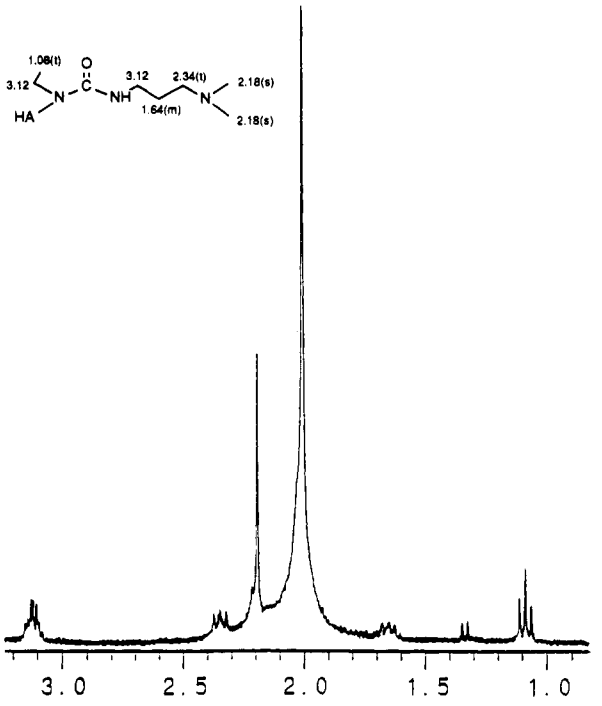


Figure 3. ^{1}H NMR spectrum and assignment for *N*-acylurea **1b** as the final product of NaHA and EDC in the presence of excess amine NaHA/EDC/1,6-diaminohexane = 1/0.1/0.5. δ 2 ppm is the *N*-acetyl group of NaHA.

positive, but became negative after the third precipitation. This indicated that the NaHA after the attempted modification did not contain coupled free amino groups.

An example of the ^{1}H NMR spectra of *N*-acylurea products of NaHA (**1b**) is shown in Figure 3. Samples were prepared in D_2O at pH 14 to reduce the viscosity of the modified NaHA. Assignments for the chemical shifts of the oligosaccharide of NaHA was reported (*42–44*). The *N*-acetyl protons have a sharp peak at around δ 2 and the rest of the protons fall in the range from δ 3.5 to 5. Therefore proton resonance in the other regions could be attributed to the modifying groups. For example, a proton resonance at δ 3.1 was observed, which could match the chemical shift of the methylene protons either adjacent to the urea linkage or the expected amide linkage. Three additional pieces of evidence, however, suggested that the linkage was not the expected amide. First, EDC protons were identified in the modified HA. Second, no methylene protons adjacent to the amino group (δ 2.6) were found. Finally, the ninhydrin test was negative.

Apparently, the *O*-acylisourea intermediate was relatively unreactive under the given conditions. Inoue and Nagasawa studied the reaction between *N*-acetylchondrosine and EDC and reported that the resulting *O*-acylisourea was relatively stable in the absence of amines; e.g., the *O*-acylisourea did not react further with glycine methyl ester. In addition, they found that the *O*-acylisourea was converted to *N*-acylurea under mild alkaline conditions (0.1 M Na_2CO_3). They noted that the chemical shift of the methyl triplet of the *N*-ethyl group of EDC in the *N*-acylurea was δ 1.09, while that of *O*-acylisourea was δ 1.19 (*22*). The ^{1}H NMR spectrum of the reaction product of HA and EDC from our work showed the *N*-ethyl methyl proton at δ 1.08, consistent with the structure of an *N*-acylurea. The assignments of the two carbon chains connected to the two nitrogen atoms of the urea could be interchanged, but in a separate study we provide evidence for a single isomer as the product (*46*). Only one of the isomers of an *N*-acylurea is shown in the ^{1}H NMR

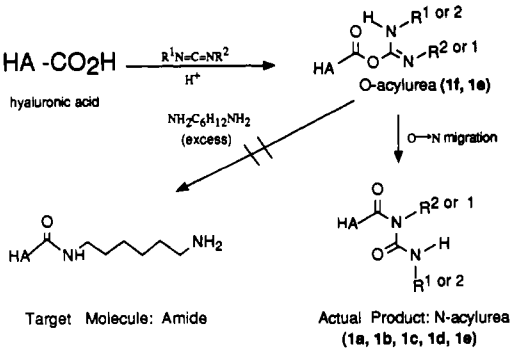


Figure 4. Reaction products of NaHA and EDC in the presence of excess 1,6-diaminohexane were *N*-acylurea, not amide.

assignments as in Figure 3. In spite of the excess diamine reagent added, no replacement reaction actually occurred. Instead, the *O*-acylisourea rearranged to a more stable *N*-acylurea, as shown in Figure 4.

The requirements for the rearrangement of *o*-acylisourea to *N*-acylurea were further investigated. The reaction products of EDC, 1,6-diaminohexane, and the thermally degraded NaHA (6×10^5 Da) and the high molecular weight NaHA (2×10^6 Da) were compared under the same condition (molar equivalent ratio of NaHA/EDC/HDA = 1/1/1). It was found that the major chemical shift of the methyl protons (triplet) from the reaction product of the high molecular weight NaHA was δ 1.21, while that from the thermally degraded NaHA was δ 1.12. This suggested that the end product from the lower MW NaHA was mainly *N*-acylurea and that from the high MW NaHA was largely *O*-acylisourea. It appears that *O*-acylisourea of NaHA with higher molecular weight and higher viscosity is less prone to rearrangement. In addition, it was reported that amines could catalyse the O → N migration (*23*). For the reactions using native NaHA (2×10^6 Da), the lower amine/EDC ratio (1/1) in the present experiments gave *O*-acylisourea, while the considerably higher amine/EDC ratio (5/1, 10/1 and 100/1) in the previous experiments produced *N*-acylurea as the final products. This appears to be consistent with the role of the added amine in the O → N migration of *O*-acylisourea.

Danishefsky and Siskovic (*15*) reported a 38.6% coupling of glycine methyl ester with NaHA from human umbilical cord, using approximately equal amount of EDC, glycine methyl ester, and NaHA. We performed a similar reaction using equal equivalent of EDC, 1,6-diaminohexane, and NaHA from rooster comb. However, no evidence of the free amino groups was found in the ^{1}H NMR spectrum and the ninhydrin tests only showed <1% coupling. Human umbilical cord HA and rooster comb HA have similar molecular weights (2–3 million). Therefore, molecular weight did not appear to be the factor for the different results obtained.

Tengblad (*24*) used partially degraded HA (52 000 Da) to react with the amino groups of AH-Sepharose 4B in the presence of EDC and reported a 1 mg of HA/1 mL of gel coupling. In the experiments conducted here using thermally degraded HA (60 000 Da), EDC, and 1,6-diaminohexane under similar conditions, there again was no evidence of the amidation reaction from the ^{1}H NMR spectrum. The free amine detected (≤1%) by ninhydrin test could only be considered as negligible.

The explanation for these discrepancies is not straightforward. Nevertheless, it is worth mentioning that (a) both HA and amine sources were different and (b) the claimed amide products in the above-mentioned literature were not characterized and their structures were not

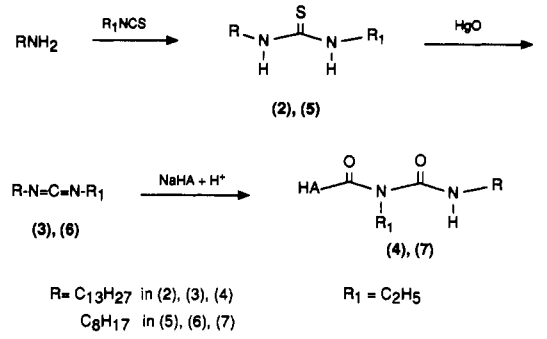


Figure 5. Synthesis of ethyltridecylcarbodiimide (3) and ethyloctylcarbodiimide (6) and their HA–acylureas 4 and 7. Only *N*-acylureas were shown, in which R and R_1 may be interchanged.

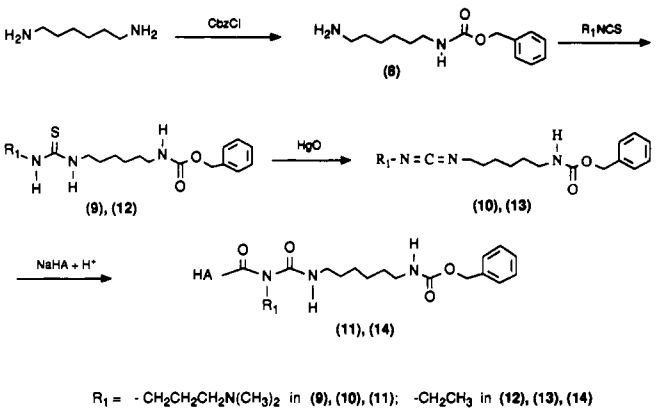


Figure 6. Synthesis of aromatic carbodiimides 10 and 13, and their HA–acylureas 11 and 14. Only *N*-acylureas were shown.

identified. In the experiments by Inoue and Nagasawa, it was also found that only when glycine methyl ester was added to HA before EDC did the HA and glycine ester form an unidentified linkage. This suggested that the reaction between HA and glycine ester might have occurred via a totally different, unknown mechanism (*22*). More recently, Nagasawa et al. (*25*) reported that the reaction of HA (rooster comb, 2×10^6 Da) and excess 5-aminofluorescein in the presence of EDC gave only 0.86% of the theoretical labeling of the fluorescent amine. That result of a very low degree of coupling is close to what has been observed here for the 1,6-diaminohexane/NaHA reaction in the presence of EDC.

Given the HA source, the reagents used, and the reaction conditions as mentioned above, the only significant products observed here were the acylureas. However, the facility of the reaction between carbodiimides and HA to form acylurea products and the mildness of carbodiimide reaction without degrading HA appears to provide a useful chemical method for HA modification.

Carbodiimide Synthesis and Coupling to NaHA. Synthetic methodologies of carbodiimides have been reviewed by, among others, Khorana (*26*), Kurzer (*21*), and Rasshofer (*27*). Dehydrosulfurization of the corresponding thiourea by yellow mercuric oxide is recommended as one of the best methods. In recent literature, examples of this method can be found in the application of the synthesis of some commercial carbodiimides, such as NCD-4 (*19*). The advantages of this synthetic route include (1) high yield (usually over 90%), (2) relatively mild reaction conditions of refluxing in low boiling point solvents such as acetone, (3) convenience in monitoring the reaction by the color change of HgO (yellow) to HgS (black), and (4) sharp contrast in terms of the polarity of the starting material thiourea (polar) and the product carbodiimide (nonpolar), which is favorable to the separation by column chromatography when necessary. In addition, the synthesis of the precursor thiourea from an amine and an isothiocyanate is simple and quantitative. The isothiocyanate can be made conveniently through reaction between amine and thiophosgene.

The synthesis of carbodiimides containing an aliphatic or an aromatic group was shown in (Figures 5 and 6). Thioureas 2 and 5 were synthesized through equimolar ethyl isothiocyanate and tridecylamine or octylamine (*33*). The thiourea function (C=S) was characterized by the δ 180 peak in the ^{13}C NMR spectrum. The carbodiimide products 3 and 6 were characterized by the IR (2120 cm^{-1}, N=C=N) and ^1H NMR (δ 3.2, the methylene protons adjacent to the carbodiimide nitrogens) spectra.

Reactions of the lipophilic carbodiimides with NaHA were carried out in the same way as the EDC–HA reactions described earlier, except that the carbodiimides were dissolved in 2-propanol instead of water. The pH was controlled at 4.75 and the proton consumption recorded. The proton uptake of the tridecyl carbodiimide was only ca. 10% of the theoretical value, while that of the less hydrophobic octyl carbodiimide was 35–42% of the theoretical value when the reaction was completed. Proton NMR spectra of 4 and 7 did not show any new peaks beside those of HA protons. After the carbodiimide-modified NaHA 4 was hydrolyzed in HCl solution (pH 1) to produce the oligosaccharides of 4, the methylene protons adjacent to the urea nitrogen (δ 3.1) and the aliphatic chain protons (a broad resonance at δ 1.2) from the carbodiimide were observed. The NMR spectra of NaHA and its derivatives usually show low intensity and line broadening due to their high viscosity and rigidity (*42*, *43*). Viscosity and rigidity factors contribute to spin–spin relaxation, which shortens T_2 and broadens the signal (*28–30*). The NMR resolution can be improved by treatment with base or acid. The addition of NaOD can break the hydrogen bondings of NaHA, thus reducing the viscosity and rigidity of the NaHA macromolecules (*42*, *43*). Acid hydrolysis has a similar effect on NaHA by decomposing it to fragments. The NMR resolution of 4 was improved after acid hydrolysis, but the methyl proton triplets of 4 could not be identified, so that the *N*-acylurea and *O*-acylurea could not be distinguished. This suggested that the lipophilic side chains on the modified NaHA may have contributed to the rigidity of the modified HA fragments. The hydrophobic interactions of the 4 oligosaccharides were not likely to be dissociated by alkali.

Aromatic carbodiimides 10 and 13 containing Cbz (carbobenzyloxy) groups were synthesized from their thiourea precursors 9 and 12, which were the reaction products of aromatic amine 8 and isothiocyanates, namely, ethyl isothiocyanate and 3-(dimethylamino)propyl isothiocyanate. The latter was synthesized from 3-(dimethylamino)propylamine and thiophosgene by a method described by Rice (*31*) and Hartman (*32*). The mono-Cbz-1,6-diaminohexane (8) was obtained with 10/1 equiv ratio of amine/Cbz-Cl.

Coupling reactions of NaHA and carbodiimides 10 and 13 gave modified aromatic NaHA's 11 and 14. The ^1H NMR spectra of purified 11 and 14 showed δ 7.4 band as aromatic protons and δ 3.1 band as methylene protons adjacent to the acylurea nitrogens. UV spectroscopy could be used in quantifying the aromatic NaHA derivatives as well as in monitoring their purification. The maximum absorbance wavelength of aromatic carbodiimide 13 was 240 nm and its was used as the standard. In the synthesis of aromatic NaHA 14, the equivalent ratio of carbodiimide 13 to NaHA was 0.21. The UV analysis and NaHA

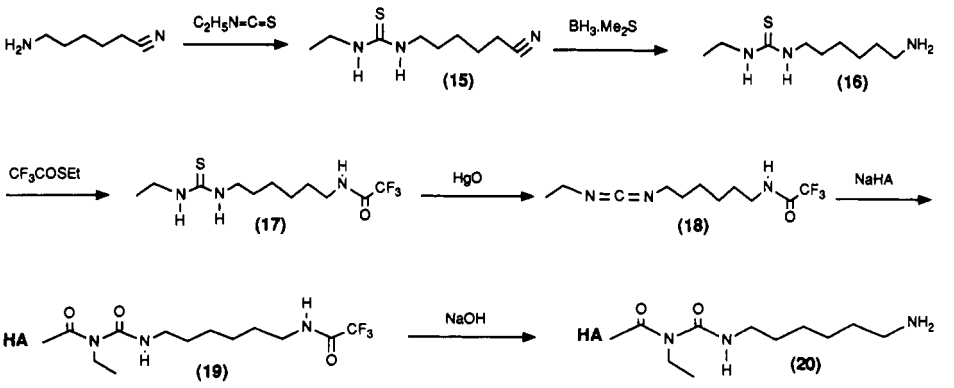


Figure 7. Synthesis of carbodiimide containing protected primary amine function (18), its reaction product (19) with NaHA, and amine-functionalized NaHA 20. Only *N*-acylureas were shown, in which ethyl and 6-aminohexamethylene may be interchanged.

concentration measurement showed that the ratio of the detected Cbz per disaccharide unit of 14 was 0.16, which was considered as the actual degree of coupling. On the other hand, the ratio of proton uptake per carboxyl group of NaHA was 0.15. The closeness of these two independent numbers suggested that proton uptake could also be used to estimate the degree of coupling. The degree of coupling of aromatic NaHA 14 was 25–30% lower than the theoretical value 0.21, indicating that the conversion of carbodiimide 13 to the NaHA side chains was in the range of 70–75%.

The removal of Cbz to deprotect the amino group is normally performed through hydrogenolysis under mild conditions (*34*). The adoption of this method to the aromatic HA was expected to yield free amine without degrading the HA macromolecules. Palladium over carbon (5%) was used as the catalyst for the hydrogenolysis of aromatic HA's 11 and 14. The purified product, however, gave a negative ninhydrin test result and the ^1H NMR spectra verified the aromatic HA's 11 and 14 as the recovered starting materials. It appears that the catalyst may have been trapped by the viscous NaHA solution and become inactive. As an alternative to Cbz, the amine functionalized NaHA was synthesized through trifluoroacetamide as shown in Figure 7. The trifluoroacetyl amine-protecting group is characterized by its convenient removal in slightly basic, aqueous solutions (*35, 36*).

The use of 6-aminohexanenitrile allowed us to avoid the basic reaction conditions necessary for the protecting reactions of 1,6-diaminohexane. The amino group at one end of the aminonitrile was first reacted with ethyl isothiocyanate to form thiourea 15. Then the cyano group was reduced to the corresponding primary amine at the other end of the molecule. Borane–dimethyl sulfide was used as reducing agent (*37*). The final product showed a δ 2.6 triplet in the ^1H NMR spectrum and a δ 180 peak in the ^{13}C NMR spectrum, which indicated that the reduction compound was the desired thiourea amine 16.

There are several advantages to the use of ethyl thiotrifluoroacetate as the acetylating agent for amine 16, as compared to the more commonly used trifluoroacetic anhydride (*36*). First, the intense electrophilic property of the trifluoroacyl group is combined with the unusual aminophilicity of the sulfur atom in the thioester. Second, the hydrolytic stability of the ester is much higher than the trifluoroacetic anhydride, so ethyl thiotrifluoroacetate can be conveniently used in aqueous solution. Finally, the volatile ethyl mercaptan as the byproduct obviates any tedious purification procedure. The most characteristic peak of trifluoroacetamide 17 was at δ 117 in the ^{13}C NMR spectrum, which confirmed the presence of the trifluoroacetyl group.

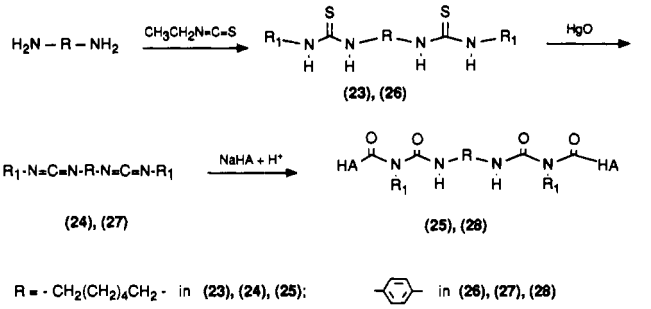


Figure 8. Synthesis of biscarbodiimides 24 and 27, and cross-linked NaHA 25 and 28. Only bis(*N*-acylureas) were shown.

The percentage coupling of NaHA–trifluoroacetamide 19 was ca. 6%. The ninhydrin test of 19 was negative. The treatment of 19 with NaOH in aqueous solution (pH 11–12) removed the trifluoroacetyl group to produce amine-functionalized NaHA 20, which then gave a positive ninhydrin test. The degree of coupling of the pendant primary amine, defined as the ratio of the free primary amine group to the disaccharide units of 20, was found to be between 3.1 and 4.2%.

Cross-Linking of NaHA with Biscarbodiimides. Hydrogels are defined by Peppas as "cross-linked macromolecular networks swollen in water or biological fluids" (*38*). Polymers with significant hydrophilicity have been examined as potential candidates for replacement of soft tissues or for other biomedical applications (*39*). NaHA hydrogel has the advantage of being bioerodible and catabolically removable as compared to the synthetic polymers. NaHA behaves like hydrogels by forming swollen networks, even without further cross-linking reactions. The networks of native HA, however, are not stable, because they are formed by noncovalent interactions such as hydrogen bonds and van der Waals forces. Upon the use of slight mechanical force, such as that produced by gentle swirling, an HA "gel" can be dispersed. Stable cross-links can only be formed by covalent bonding. To cross-link NaHA, we used biscarbodiimides, which were prepared from 1,6-diaminohexane and 1,4-phenylenediamine (Figure 8).

In the synthesis of bisthiourea 23 from 1,6-diaminohexane, cyclization appeared to have occurred as a side reaction. The ^1H NMR spectrum of the crude product showed that all the peaks belonged to the thioureas, but the integration of protons did not match that of bisthiourea 23, and the methyl protons were diminished. After recrystallization in methanol, the ^1H NMR spectrum showed the ratio of all the protons to be consistent with the structure of linear bisthiourea 23. In the synthesis of bisthiourea 26 from 1,4-phenylenediamine, the side re-

action was polymerization. A polymer insoluble in $CHCl_3$ was separated from **26**. The reflux of **23** and **26** to make biscarbodiimides **24** and **27** was controlled at 70 °C. The mass spectrum of the aromatic biscarbodiimide *p*-phenylenebis(ethylcarbodiimide) (**27**) showed the peak with the strongest intensity as the molecular ion (*m/e* 214). At higher temperature such as 90 °C, polymerization of the biscarbodiimides also occurred. Similar methods of making biscarbodiimides have been reported (*40*).

In NaHA cross-linking with the biscarbodiimides, the increase of the NaHA concentration in the reaction mixture and the decrease of the carbodiimide concentration as addition solution appeared to favor a homogeneous, intermolecular cross-linking. The cross-linked NaHA **25a** (NaHA, 3.2 mg/mL; biscarbodiimide, **24** 2.75 mg/mL) showed much less homogeneity in the reaction than **25b** (NaHA, 5.2 mg/mL; biscarbodiimide **24**, 0.92 mg/mL). When **25a** was precipitated with ethanol, the formed solid showed two distinct, separable physical forms: the cohesive, fibrous part and the loose, flaky part which deposited overnight. The sediment did not dissolve but swelled in water, characteristic of a gel. The fibrous part dissolved in water to form a clear viscous solution. The sediment was apparently the part of NaHA which had been cross-linked to a higher degree. Cross-linked **25b**, on the other hand, showed much better homogeneity. The solid formed during ethanol precipitation was all fibrous and the supernatant was quite clear and no sediment settled to the bottom of the container overnight. The collected cross-linked NaHA swelled in water at a slower rate than NaHA, but eventually became a homogeneous solution. It appeared that polymer **25b** was evenly, but not sufficiently, cross-linked to make a long-lasting, stable gel in aqueous solution.

NaHA cross-linking with aromatic biscarbodiimide **27** was performed at two molar equivalent ratios of the aromatic biscarbodiimides and HA, that is, 0.18 for **28a** and 0.1 for **28b**. The concentration of HA solutions were at 4.2 mg/mL and the concentration of biscarbodiimide **27** as addition solution was ca. 1 mg/mL. Similar to the cross-linked NaHA **25b**, the cross-linked HA **28b** showed some temporary, gel-like properties. The "gel" could be diluted to 0.5 mg/mL for intrinsic viscosity measurement. The cross-linked NaHA **28a** formed a true hydrogel in water. When 600 times the water was added to the lyophilized **28a**, the cross-linked HA slowly swelled to a gel in a refrigerator. Intermittent swirling did not break the gel. The size of the gel kept growing in the first 2 days. After 5 days there was no longer an obvious increase of the gel dimension, and the gel was thought to have reached its equilibrium with the water environment. The cross-linked NaHA **28a** absorbed a total of ca. 300 parts of water. The mixture was filtered and the collected filtrate was lyophilized. The amount of the un-cross-linked polymer separated from the gel is defined as the sol fraction and the stable crosslinked polymer is defined as the gel fraction (*38*). The gel/sol. ratio was found as 9/1 by weight. The gel was stable at room temperature. This suggests its potential application as surgical implant and drug-delivery system with a long in vivo half-life.

Another apparent difference was that aromatic biscarbodiimide **27** was more reactive than the aliphatic biscarbodiimide **24**. The molar ratio of proton/carbodiimide for aromatic biscarbodiimide **27** was found within the range of 0.71–0.80, as compared with that of aliphatic biscarbodiimide **24** at 0.30. Khorana pointed out that the reactivity of carbodiimides to nucleophilic reagents could be activated by aromatic residues (*41*). The adjacency of the aromatic ring to the carbodiimide functional groups in biscarbodiimide **27** might be considered as the main reason for the observed phenomena. Although the aromatic ring of **27** is less hydrophobic than the aliphatic chain of **24**, the difference between them may not be considered as significant. Therefore the rationale appears to be that the aromatic biscarbodiimide is functionally more reactive than the aliphatic biscarbodiimide.

CONCLUSIONS

The carbodiimide–NaHA reaction has been identified as a mild, efficient and specific chemical method for ligand immobilization to NaHA as well as for NaHA cross-linking. Dehydrosulfurization of the thiourea precursors is a convenient synthetic method for designed carbodiimides. The heterobifunctional 6-aminohexanenitrile has been shown to be a useful precursor for the synthesis of carbodiimides containing trifluoroacetyl-protected amine. The alkaline treatment of the acylurea obtained from the trifluoroacetyl-protected amine–carbodiimide, provides a free amine function linked to NaHA.

Rather than forming amides, NaHA–amine–carbodiimide reactions give *N*- and *O*-acylureas. The hydrophilic and cationic characteristics of the carbodiimides appears to favor their reactions with NaHA. The reactivity of the carbodiimides with NaHA is also dependent upon the intrinsic functionality of the carbodiimides. On the other hand, the chemical properties of NaHA are determined not merely by its functional groups per se but also by the accessibility of the carboxyl groups of NaHA to the carbodiimides in the aqueous media, which is related to the overall conformational structure (*44*, *45*) and rheological properties of sodium hyaluronate.

Finally, the significant increase of the intrinsic viscosity and the further line broadening of the NMR spectra of the carbodiimide-modified NaHA appears to suggest that such chemical modification has altered the conformational structure of NaHA to a more rigid and extended one, thus increasing the hydrodynamic volume of the macromolecules (*5*).

ACKNOWLEDGMENT

This work was supported by a grant from MedChem Products Inc. We thank Professor Eugene Davidson for his suggestions and Ms. Joy B. Scott for her technical assistance with the viscosity experiments.

LITERATURE CITED

(1) Meyer, K., and Palmer, J. W. (1934) *J. Biol. Chem. 107*, 629–634.

(2) Kenney, J. F., White, C. A. (1983) *Bioactive Carbohydrates in Chemistry, Biochemistry and Biology*, John Wiley & Sons, New York.

(3) Fransson, L-A. (1985) Mammalian Glycosaminoglycans. In *The Polysaccharides* (G. O. Aspinall, Ed.) Vol. 3, pp 338–415, Academic Press, New York.

(4) Laurent, T. C. (1970) Structure of Hyaluronic Acid. In *Chemistry and Molecular Biology of the Intercellular Matrix* (E. A. Balazs, Ed.) Vol. 2, pp 703–732, Academic Press, London.

(5) Morris, E. R., Rees, D. A., and Welsh, E. J. (1980) *J. Mol. Biol. 138*, 383–400.

(6) Leith, M. L., Kuo, J-W., Loftus, S. A., and DeVore, D. P. (1987) *J. Cataract Refractive Surg. 13*, 534–536.

(7) Miller, D., and Stegmann, R. (1980) *Am. Intra-Ocular Implant Soc. J. 66*, 13–15.

(8) (a) Balazs, E. A., and Leshchiner, A. (15 Apr 1986) *US Patent 4582865 A*. (b) Balazs, E. A.; Leshchiner, A. (15 Dec 1987) *US Patent 4,713,448*.

(9) De Belder, A. N., and Mälson, T. (13 Feb 1986) PCT Int. Appl. WO 8600,912.
(10) Mälson, T., and Lindqvist, B. L. (3 Jan 1986) PCT Int. Appl. WO 86/79 A1.
(11) (a) Della Valle, F., and Romeo, A. (27 Apr 1988) European Patent Application 87308863.7. (b) Della Valle, F., and Romeo, A. (1 Apr 1987) European Patent Application 86305233.8.
(12) Raja, R. H., LeBoeuf, R. D., Stone, G. W., and Weigel, P. H. (1984) *Anal. Biochem. 139*, 168–177.
(13) Curvall, M., Lindberg, B., and Lönngren, J. (1975) *Carbohyd. Res. 41*, 235–239.
(14) Dahl, L. B., Laurent, T. C., and Smedsrød, B. (1988) *Anal. Biochem. 175*, 397–407.
(15) Danishefsky, I., and Siskovic, E. (1971) *Carbohyd. Res. 16*, 199–201.
(16) Bitter, T., and Muir, H. M. (1962) *Anal. Biochem. 4*, 330.
(17) Swann, D. A. (1968) *Biochim. Biophys. Acta 156*, 17–30.
(18) Carraway, K. L., and Koshland, D. E., Jr. (1972) Carbodiimide Modification of Protein. *Methods Enzymol. 25*, 616–623.
(19) Chadwick, C, C., and Thomas, E. W. (1983) *Biochim. Biophys. Acta 730*, 201–206.
(20) Kunz, H. (1978) *Angew. Chem. Int. Ed. Engl. 17*, 67–68.
(21) Kurzer, F., and Douraghi-Zadeh, K. (1967) *Chem. Rev. 67*, 107–152.
(22) Inoue, Y., and Nagasawa, K. (1982) *Carbohyd. Res. 111*, 113–125.
(23) Mikolajczyk, M., and Kielbasinski, P. (1981) *Tetrahedron 37*, 233–284.
(24) Tengblad, A. (1978) *Biochim. Biophys. Acta 578*, 281–289.
(25) Ogamo, A., Matzuzaki, K., Uchiyama, H., and Nagasawa, K. (1982) *Carbohyd. Res. 105*, 69–85.
(26) Khorana, H. G. (1953) *Chem. Rev. 53*, 145–166.
(27) Rasshofer, W. (1983) *Methoden Org. Chem. (Houben-Weyl) E4*, 883–910.
(28) Ablett, S., Clark, A. H., and Rees, D. A. (1982) *Macromolecules 15*, 597–602.
(29) Jackman, L. M., and Sternhell, S. (1969) *Applications of Nuclear Magnetic Resonance Spectroscopy in Organic Chemistry*, Pergamon Press, Oxford.
(30) Bovey, F. A. (1969) *Nuclear Magnetic Resonance Spectroscopy*, Academic Press, New York.
(31) Rice, K. C., Brossi, A., Tallman, J., Paul, S. M., and Skolnick, P. (1979) *Nature 278*, 854–855.
(32) Hartmann, A. (1983) *Methoden Org. Chem. (Houben-Weyl) E4*, 835–845.
(33) Schroeder, D. C. (1955) *Chem. Rev. 55*, 181–228.
(34) Freifelder, M. (1978) *Catalytic Hydrogenation in Organic Synthesis Procedures and Commentary*, John Wiley & Sons, Inc., New York.
(35) Weygand, F., and Csendes, E. (1952) *Angew. Chem. 64*, 136.
(36) Schallenberg, E. E., and Calvin, M. (1955) *J. Am. Chem. Soc. 77*, 2779–2783.
(37) Brown, H. C., Choi, Y. M., and Narasimban, S. (1981) *Synthesis* 605–606.
(38) Peppas, N. A. (1986) *Hydrogels in Medicine and Pharmacy, Vol. I*, CRC Press, Inc. Boca Raton, FL.
(39) Wichterle, O., and Lim, D. (1960) *Nature 185*, 117.
(40) Iwakura, Y., and Noguchi, K. (1967) *Bull. Chem. Soc. Jpn. 40*, 2383–2388.
(41) Khorana, H. G. (1954) *Can. J. Chem. 32*, 227.
(42) Welti, D., Rees, D. A., and Weish, E. J. (1979) *Eur. J. Biochem. 94*, 505–514.
(43) Bociek, S. M., Darke, A. H., Welti, D., and Rees, D. A. (1980) *Eur. J. Biochem. 109*, 447–456.
(44) Scott, J. E., Heatley, F., and Hull, W. E. (1984) *Biochem. J. 220*, 197–205.
(45) Scott, J. E., and Tigwell, M. J. (1975) *Biochem. Soc. Trans. 3*, 662–664.
(46) Pouyani, T., Kuo, J-W., Harbison, G. S., and Prestwich, G. D., submitted.

Novel Carboranyl Amino Acids and Peptides: Reagents for Antibody Modification and Subsequent Neutron-Capture Studies

Aravamuthan Varadarajan and M. Frederick Hawthorne*

Department of Chemistry and Biochemistry, University of California at Los Angeles, Los Angeles, California 90024. Received March 8, 1991

A new α-amino acid derivative incorporating the 1,2-dicarba-*closo*-dodecarborane(12) cage, namely 5-(2-methyl-1,2-dicarba-*closo*-dodecarborane(12)-1-yl)-2-aminopentanoic acid (**2**), was synthesized by the alkylation of the benzophenone Schiff's base of glycine methyl ester with 3-(2-methyl-1,2-dicarba-*closo*-dodecaborane(12)-1-yl)propyl iodide (**8**). This amino acid was employed in the synthesis of peptide derivatives such as **19**–**21** using solid-phase Merrifield methods. Dipeptide **19** was converted to a water-soluble ionic derivative by the pyrrolidine-mediated carborane cage degradation reaction followed by cation exchange to afford sodium salt **22**. Dansylation of **22** with dansyl chloride yielded fluorescence-labeled dipeptide **23**. Undecapeptide **21** was dansylated while still anchored to the Merrifield resin. Following its cleavage from the resin with hydrogen fluoride, product **25** was acetylated to block the free amino group on the lysine residue and then converted to water-soluble derivative **27**. Trial conjugations of dipeptide **23** and undecapeptide **27** to T84.66, an anti-CEA antibody, were carried out by means of carboxyl activation with *N*-hydroxysulfosuccinimide and *N,N*-diisopropylcarbodiimide. Studies of the chemical syntheses of these and other peptide derivatives and the conjugation of **23** and **27** to the antibody are described.

INTRODUCTION

The possible utilization of boron-10 labeled antibodies for tumor cell destruction via the binary cytotoxic $^{10}B(n,\alpha)^7$-Li reaction has been extensively investigated (*1*). The problem associated with this form of therapy has been the lack of a viable method for the selective delivery of the required quantity of boron-10 to the neoplasm (10–30 μg/g tumor). Since a number of studies have previously revealed the limitations associated with attaching large numbers of small boron-containing molecules to the antibody (*2–4*), attention has recently focused upon the covalent linkage of boron-loaded polymers to the antibody. These methods include the use of boron-labeled poly-DL-lysine (*5–10*), a carborane-linked dextran moiety (oxidized for antibody coupling) (*11–13*), and boron-labeled poly-L-ornithine (*14*). While these studies demonstrated that it is possible to attach more that 10^3 boron atoms to each antibody molecule, such heavily boronated antibody conjugates suffered from either significantly reduced immunoreactivity or low tumor uptake. The inherent inhomogeneity of the attached boron-containing polymeric reagent in the conjugate is expected to aggravate the problem since no viable method for purification of the conjugated antibody is available. In order to mitigate these problems we have directed our attention toward Merrifield solid-phase peptide synthesis for the precision syntheses of designed oligomeric peptide molecules which contain a predetermined number of *closo*-$C_2B_{10}H_{11}$ carborane cages capable of delivering 100–500 boron atoms per oligomer. This methodology removes the problem of oligomeric boron reagent heterogeneity. The hydrophilicity of these peptide structures may be markedly increased by conversion of their hydrophobic neutral carborane cages to anionic [*nido*-7,8-$C_2B_9H_{11}$]$^-$ moieties.

EXPERIMENTAL PROCEDURES

General. The ^1H and ^{11}B NMR spectra were recorded on a Bruker AM500 Spectrometer operating at 500.137 and 160.463 MHz, respectively, and IR spectra were obtained with a Beckman FT 1100 spectrophotometer. Mass spectra were obtained from MS-9 and ZAB-SE mass spectrometers. Fluorescence measurements were performed on a Spex fluorimeter using 313 and 515 nm for the wavelengths of excitation and emission, respectively. Melting points were obtained with a Thomas-Hoover capillary melting point apparatus and are uncorrected. 3-(2-Methylcarboranyl)propanol (**10**) was synthesized from methylcarborane (**9**) by a previously reported method (*15*). Peptide syntheses were carried out with a Beckman-990C automated peptide synthesizer. Cleavage of the finished peptide from the resin with HF was accomplished by employing the hydrogen fluoride handling apparatus purchased from Peptide Institute Inc., Osaka, Japan. Dicyclohexylcarbodiimide, *N,N*-(dimethylamino)pyridine, dansyl chloride, trifluoroacetic acid, Merrifield chloromethyl resin (1% cross-linked, 200–400 mesh, 1 mequiv chloride/g) and di-*tert*-butyl dicarbonate were purchased from Aldrich Chemical Co. and were used without purification. Elemental analyses were performed by Galbraith Laboratories, Knoxville, TN. All solvents were dried and distilled by standard methods.

Synthesis of 3-(2-Methyl-1,2-dicarba-*closo*-dodecaboran(12)-1-yl)propyl Iodide (8). To a solution of 3-(2-methylcarboranyl)propanol (**10**; 12.0 g, 56 mmol) in anhydrous pyridine (50 mL) was added *p*-toluenesulfonyl chloride (21.3 g, 112 mmol) at 0 °C and the solution was stirred at this temperature for 10 h. The reaction mixture was quenched by the addition of ice-cold water (500 mL) and extracted with ether (4 × 60 mL). The combined ether extracts were washed repeatedly with ice-cold solutions of dilute HCl (1 M, 2 × 60 mL) and saturated $NaHCO_3$ (2 × 60 mL) and finally with ice-cold water. Drying over anhydrous $MgSO_4$, filtration, and concentration yielded the tosylate as a white solid. Due to its reactivity, tosylate **11**, which contained small amounts of tosyl chloride and the alcohol, was used without further purification. ^1H NMR ($CDCl_3$): δ 7.73 (d, 2 H, Ar-H), 7.32 (d, 2 H, Ar-H), 3.99 (t, 2 H, CH_2), 2.41 (s, 3 H, tosyl CH_3), 2.16 (m, 2 H, CH_2), 1.92 (s, 3 H, carboranyl CH_3), 1.88 (m, 2 H, CH_2). ^{11}B NMR (CH_2Cl_2): δ −4.78, −6.24, −9.46, −10.12, −11.03.

1043-1802/91/2902-0242$02.50/0 © 1991 American Chemical Society

To a solution of tosylate 11 (17.4 g, 47 mmol) in acetone (150 mL) was added sodium iodide (14.1 g, 94 mmol) and the solution refluxed under nitrogen for 20 h. After cooling to ambient temperature, the reaction mixture was filtered and the solid washed with acetone. The filtrate and washings were combined and concentrated. The residue was dissolved in ether and washed with sodium thiosulfate solution and water. Drying (anhydrous $MgSO_4$) and concentration produced the crude iodide which was purified by column chromatography on silica gel using petroleum ether as the solvent. Yield: 14.3 g (93%). Mp: 34–35 °C. ^{1}H NMR ($CDCl_3$): δ 3.19 (t, 2 H, CH_2), 2.33 (m, 2 H, CH_2), 2.06 (m, 2 H, CH_2), 2.05 (s, 3 H, CH_3). ^{13}C NMR ($CDCl_3$): δ 4.51, 22.18, 32.59, 35.87, 75.01, 76.67. ^{11}B NMR (Et_2O): δ −4.14, −5.61, −9.21, −9.72, −10.43, −10.75. IR (Nujol): 2587, 1239, 1172 and 729 cm^{-1}. FAB MS (*m/e*) calcd for $C_6{}^{11}B_{10}H_{19}I$: 328. Observed: cluster of peaks centered near 325. Anal. Calcd for $C_6B_{10}H_9I$: C, 22.09; B, 33.14; H, 5.87; I, 38.90. Found: C, 21.85; B, 32.80; H, 5.62; I, 38.42.

Akylation of Methyl *N*-(Diphenylmethylidene)-glycinate (6) with 3-(2-Methyl-1,2-dicarba-*closo*-dodecaboran(12)-1-yl)propyl Iodide (8). (*i*) *Homogeneous Alkylation in Solution.* To a solution of diisopropylamine (5.6 mL, 39.6 mmol) in a mixture of tetrahydrofuran (110 mL) and hexamethylphosphoramide (25 mL) at −78 °C was added *n*-butyllithium (2.4 M in hexane, 16.5 mL, 39.6 mmol). The solution was stirred at this temperature for 1 h, after which a solution of Schiff's base 6 (10.0 g, 39.6 mmol) in THF (30 mL) was added. The solution passed through a series of color changes from blood red to brownish yellow. After stirring for 1 h at −78 °C, a solution of iodide 8 (12.9 g, 39.6 mmol) in THF (20 mL) was added. The color of the solution changed from brownish yellow to orange yellow. After stirring at this temperature for 2 h, the reaction mixture was warmed to ambient temperature and stirred for a further 20 h and the solution then quenched with aqueous ammonium chloride. The organic layer was separated, washed with water, dried, and concentrated. Crude imine 12, containing some solvent (18.7 g, 41.3 mmol), was obtained as a viscous yellow material. (Due to its hydrolytic instability, it was not purified and was directly converted to amino ester 13). ^{1}H NMR ($CDCl_3$): δ 7.82–7.17 (m, 10 H, Ar-H), 4.07 (dd, 1 H, CH), 3.75 (m, 2 H, CH_2), 3.72, (s, 3 H, $COOCH_3$), 2.12 (t, 2 H, CH_2), 1.93 (s, 3 H, CH_3), 1.85 (m, 2 H, CH_2). ^{11}B NMR ($CH_2Cl_2 + Et_2O$): δ −4.89, −6.16, −9.66, −10.15, −11.08. ^{13}C NMR ($CDCl_3$): δ 172.33, 137.68, 132.40, 130.62, 130.06, 128.90, 128.83, 128.71, 128.43, 128.29, 128.19, 127.78, 67.98, 64.72, 52.22, 36.86, 35.11, 33.00, 25.19, 23.10.

(*ii*) *Alkylation by Phase-Transfer Catalysis.* To a solution of Schiff's base 6 (96 mg, 0.38 mmol) and iodide 8 (124 mg, 0.38 mmol) in acetonitrile (7 mL) were added K_2CO_3 (315 mg, 2.28 mmol) and tetra-*n*-butylammonium bromide (36.8 mg, 0.114 mmol), and the solution was refluxed under nitrogen for 3 days. The reaction mixture was cooled to ambient temperature and filtered to remove the solid which was washed with CH_2Cl_2. The filtrate and the washings were combined and concentrated. Crude imine 12 (126 mg, 0.28 mmol, 74%) was obtained as a yellow oil.

Partial Hydrolysis of Alkylated Schiff's Base 12. The crude alkylated Schiff's base (13.8 g, 30.5 mmol) was dissolved in ether (40 mL) and treated with dilute HCl (1 M, 40 mL). Upon stirring the mixture at ambient temperature, a white solid began to separate within a short time. The solution was stirred for 9 h and filtered to collect amino ester 13, which was purified by recrystallization from methanol (7.50 g, 23.2 mmol, 76%). Mp: 224–225 °C. ^{1}H NMR (CD_3OD): δ 4.10 (t, 1 H, α-CH), 3.85 (s, 3 H, $COOCH_3$), 2.36 (t, 2 H, δ-CH_2), 2.09 (s, 3 H, $COOCH_3$), 1.98 (m, 1 H, β-CH_2), 1.93 (m, 1 H, β-CH_2), 1.78 (m, 1 H, γ-CH_2), 1.67 (m, 1 H, γ-CH_2). ^{13}C NMR (CH_3OD): δ 170.33 (ester CO), 79.02 (carboranyl C), 76.64 (carboranyl C), 53.52 (ester CH_3), 53.23 (CH), 35.09 (γ-CH_2), 30.49, (α-CH_2), 26.08 (β-CH_2), 23.30 (CH_3). ^{11}B NMR (CH_3OH): δ −4.53, −5.93, −8.97, −9.70, −10.73. IR (Nujol): 3387 (br), 2604, 1757, 1529, 1516, 1268 cm^{-1}. FAB MS (*m/e*) calcd for $C_9{}^{11}B_{10}H_{26}NO_2$: 290. Observed: cluster of peaks centered around 288. Anal. Calcd for $C_9B_{10}H_{26}NO_2Cl$: C, 33.38; H, 8.09; N, 4.32; B, 33.38: Cl 10.95. Found: C, 33.08; H, 8.05; N, 4.15; B, 32.16; Cl, 10.49.

Hydrolysis of Amino Ester 13. Carboranyl amino ester derivative 13 (2.0 g, 6.2 mmol) was suspended in 6 M HCl (50 mL) and the mixture was refluxed for 24 h. Cooling and filtration of the mixture yielded amino acid derivative 14 as a colorless solid which was recrystallized from methanol (1.80 g, 5.8 mmol, 95%). Mp: 260–262 °C. ^{1}H NMR (CD_3OD): δ 3.98 (t, 1 H, α-CH), 2.36 (t, 2 H, CH_2), 2.08 (s, 3 H, CH_3), 1.96 (m, 1 H, β-CH), 1.89 (m, 1 H, γ-CH), 1.70 (m, 1 H, γ-CH). ^{11}B NMR (CH_3OH): δ −4.51, −5.92, −8.97, −9.70, −10.73. IR (Nujol): 3411 (br), 2597, 1740, 1602, 1514, 1209, 730 cm^{-1}. FAB MS (*m/e*) calcd for $C_8{}^{11}B_{10}H_{24}NO_2$: 276. Observed: cluster of peaks centered around 274. Anal. Calcd for $C_8B_{10}H_{24}NO_2Cl$: C, 31.01; H, 7.81; N, 4.52; B, 34.89; Cl, 11.44. Found: C, 30.80; H, 8.11; N, 4.29; B, 35.15; Cl, 10.82.

Synthesis of Free Base 2. Amino acid hydrochloride 14 (1.8 g, 5.8 mmol) was dissolved in methanol and treated with propylene oxide (11 mL). After stirring at ambient temperature overnight, crude product 2 was obtained by concentration and was purified by recrystallization from methanol (1.4 g, 5.1 mmol, 88%). Mp: 255–256 °C. ^{1}H NMR (CD_3OD): δ 3.54 (t, 1 H, α-CH), 2.32 (t, 2 H, δ-CH_2), 2.07 (s, 3 H, CH_3), 1.84 (m, 2 H, β-CH_2), 1.74 (m, 2 H, γ-CH_2). ^{11}B NMR (CH_3OH): δ −4.22, −5.59, −8.63, −9.38, −10.38; IR (Nujol): 3492–3216 (br), 2579, 1635, 1500, 1023, 730 cm^{-1}. FAB MS (*m/e*) calcd for $C_8{}^{11}B_{10}H_{23}NO_2$: 275. Observed: cluster of peaks centered around 275. Anal. Calcd for $C_6B_{10}H_{23}NO_2$: C, 35.15; H, 8.48; N, 5.12; B, 39.54. Found: C, 35.32; H, 8.47; N, 4.75; B, 37.20.

Preparation of 17, the *t*-BOC Derivative of Amino Acid 2. Amino acid 2 (1.6 g, 5.8 mmol) in absolute alcohol (30 mL) was treated with di-*tert*-butyl dicarbonate (2 mL, 9 mmol) and triethylamine (0.8 mL, 6 mmol). The mixture was heated to reflux under nitrogen for 12 h. The solvent was removed and the residue was cooled in ice prior to treatment with CH_2Cl_2 and HCl (1 M, 25 mL). After 30 min the aqueous layer was removed and the organic layer was washed with water. The solution was dried and concentrated. *t*-BOC-protected amino acid 17 was obtained as a fluffy white solid and was recrystallized from CH_2Cl_2/petroleum ether (2.0 g, 5.3 mmol, 90%). Mp: 84 °C (dec). ^{1}H NMR ($CDCl_3$): δ 5.02 (d, 1 H, NH), 4.33 (m, 1 H, CH), 2.27 (m, 1 H, CH_2), 2.18 (m, 1 H, CH_2), 2.01 (s, 3 H, CH_3), 1.90 (m, 1 H, CH_2), 1.68 (m, 3 H, CH_2), 1.46 (s, 9 H, *t*-BOC-CH_3). ^{11}B NMR ($CDCl_3$): δ −5.23, −6.60, −9.82, −10.48, −11.39. IR (KBr): 3432–2874 (br), 2596, 1723–1694 (br), 1509, 1477, 1455, 1405, 1396, 1369, 1284, 1250, 1156, 1060, 1025, 728 cm^{-1}. MS: no parent ion was observed, but a cluster of peaks centered around *m/e* 273.31 corresponding to $M^+ - (t\text{-BOC})$ was observed. Anal. Calcd for $C_{13}B_{10}H_{31}NO_4$: C, 41.81; H, 8.37; N, 3.75; B, 28.94. Found: C, 41.34; H, 8.83; N, 3.54; B, 28.67.

Conversion of Closo Amino Acid 2 to Its Anionic Nido Derivative 15. A mixture of amino acid 2 (0.81 g,

3.0 mmol) and sodium hydroxide (40 g, 8.9 mmol) in absolute alcohol (30 mL) was refluxed under nitrogen for 24 h. The excess base was neutralized by passing CO_2 through the reaction mixture and separation of Na_2CO_3 by filtration. The solvent was removed under vacuum and the sodium salt of *nido*-carboranyl amino acid **15** was obtained as a sticky yellow paste. The solid was dried under vacuum (0.82 g, 2.8 mmol). The material was dissolved in water, acidified with 1 M HCl, filtered, and treated with an excess of a solution of tetrabutylammonium bromide in water. The precipitation was not complete owing to the partial solubility of the tetrabutylammonium salt in water. The yield was 0.63 g (1.2 mmol, 40%). ^{1}H NMR disodium salt (CD_3OD): δ 3.82 (br, 1 H, α-CH); 1.64 (m, 3 H, CH_2), 1.56 (m, 3 H, CH_2), 1.38 (s, 3 H, CH_3). ^{11}B NMR (CH_3CN): δ −9.20, −10.61, −18.11, −34.63, −37.09. IR (Nujol): 3358 (br), 3287 (br), 2510, 1637, 1598, 1873, 736 cm^{-1}. IR (KBr): 3483–3103 (br), 3054, 3032, 2608, 1727, 1676, 1624, 1557, 1519, 1458, 1206, 1180, 1120, 1084–1034 (br), 730 cm^{-1}. FAB MS (negative ion) calcd for $C_8{}^{11}B_9H_{23}O_2N$: 264. Observed: cluster of peaks centered around m/e 263.

Preparation of 18, the *t*-BOC Derivative of *nido*-Carboranyl Amino Acid 15. Crude sodium salt **15** obtained (0.23 g, 0.78 mmol) from the cage degradation reaction was dissolved in absolute alcohol (7 mL) and treated with di-*tert*-butyl dicarbonate (0.35 mL, 1.6 mmol). After heating at 80 °C for 12 h, under nitrogen, the solvent was removed under vacuum. The residue was dissolved in water and the filtered solution cooled in ice and treated with dilute HCl (1 M, 2 mL). Addition of tetramethylammonium chloride yielded the tetramethylammonium salt of the nido *t*-BOC-amino acid **18** (140 mg, 0.32 mmol, 41%). ^{1}H NMR (CD_3OD): δ 4.02 (br, 1 H, α-CH), 3.2 (s, 12 H, $N(CH_3)_4$), 1.66 (br, H, CH_2), 1.53 (br, H, CH_2), 1.44 (s, 9 H, *t*-BOC CH_3), 1.38 (s, 3 H, CH_3). ^{11}B NMR (CH_3OH): δ −8.64, −10.16, −17.59, −34.10, −36.56. IR (Nujol): 3356 (br), 3217 (br), 2522, 1709, 1694, 1653, 1635, 1627, 1311, 1234, 1167, 725 cm^{-1}; FAB MS (negative ion, m/e) calcd for $C_{13}{}^{11}B_9H_{31}O_4N$: 364. Observed: cluster of peaks centered around 362. The triphenylmethylphosphonium salt was similarly prepared. Anal. Calcd for $C_{32}B_9H_{49}NO_4P$: C, 60.06; H, 7.72; N, 2.19; B, 15.20; P, 4.84. Found: C, 59.94; H, 7.75; N, 2.12; B, 13.23; P, 4.91.

Stepwise Synthesis of Carboranyl Peptides. The protected amino acids N_α-*t*-BOC-N_ϵ-2-chloro-CBZ-lysine, *t*-BOC-glycine, *t*-BOC-γ-aminobutyric acid, and *t*-BOC-carboranyl amino acid **17** were loaded as their cesium salts in DMF on the chloromethyl resin by following the reported procedure (*16*). The loading efficiency was monitored by the increase in weight of the resin, as well as by the amount of amino acid recovered after HF cleavage of an aliquot of the resin. The loading efficiency was 45–50% in the case of **17** and greater than 90% in the case of other amino acids. The coupling reactions were carried out in the Beckman solid-phase automated peptide synthesizer employing standard coupling programs provided by the manufacturer. The amino acids and DCC were used in 2.5-fold excess, and 0.5 equiv of DMAP was used as an acylation catalyst. The progress of coupling was monitored by the ninhydrin test applied to the resin. In the case of the carboranyl amino acids, coupling was allowed to proceed for 2 days and followed by recoupling for a further period of 2 days, when the initial coupling reaction did not proceed to completion. Except in the case of the ionic amino acid derivatives, dichloromethane was used as the solvent. The synthetic methods followed were taken from those reported for normal amino acids (*16*). The basic procedure involved the deprotection of the *t*-BOC group with TFA (25% in CH_2Cl_2, 0.5 h), washing with triethylamine (10% in CH_2Cl_2), coupling with the next *t*-BOC amino acid mediated by DCC and DMAP, washing with solvent (CH_2Cl_2), and recoupling, if necessary. ^{11}B NMR spectra of the resin-bound peptides were obtained by suspending the loaded resin (prior to HF cleavage) in a minimal amount of CH_2Cl_2 and employing the spectral acquisition parameters normally used for solution spectra.

The completed peptides were cleaved from the solid support by anhydrous HF using standard procedures (*16*). The resin was treated with anisole (1 mL/g of resin) and HF was condensed into the reaction vessel at −78 °C (*ca.* 5 mL/g of resin). The mixture was stirred at 0 °C for 30–60 min and HF was removed under vacuum at this temperature. Anisole was removed under high vacuum and the peptide was extracted with TFA (3 × 10 mL). The TFA extracts were concentrated and the peptide was precipitated by the addition of dry ether. The solid was separated by filtration, washed with ether, and dried under vacuum.

Synthesis of (*closo*-CB)$_2$ (19). Starting with 1.06 g of the Merrifield resin loaded with the *t*-BOC-protected *closo*-carboranyl amino acid (1.06 g, *ca.* 1 mequiv/g), the product dipeptide was obtained as an off-white solid (130 mg, 0.25 mmol) after purification by flash column chromatography through a reverse-phase C_{18} column employing an acetonitrile/water solvent gradient. ^{1}H NMR (CD_3OD): δ 7.57 (br, NH), 4.37 (m, CH), 3.92 (m, CH), 2.32 (m, CH_2), 2.06 (s, CH_3), 1.89 (m, CH_2), 1.67 (m, CH_2). ^{13}C NMR (CD_3OD): δ 79.67, 79.11, 76.97, 76.88, 55.58, 54.17, 53.87, 35.85, 35.74, 35.65, 35.57, 34.18, 32.61, 32.27, 32.06, 31.97, 30.10, 27.33, 27.25, 26.31, 25.67, 23.52, 23.47. ^{11}B NMR (CH_3OH): −4.24, −5.59, −8.65, −9.36, −10.38. IR (Nujol): 3360 (br), 2576, 1675 (br), 1065 (br), 728 cm^{-1}. FAB MS (m/e) calcd for $C_{16}{}^{11}B_{20}H_{44}N_2O_3$: 532. Observed: cluster of peaks centered around 530.

Synthesis of (*closo*-CB)$_5$-Lys (20). Chloromethyl resin (1.0 g) loaded with N_α-*t*-BOC-N_ϵ-2-chloro-CBZ-lysine (0.8 mequiv/g) was employed in the peptide synthesis which involved the successive coupling of five residues of the protected carboranyl amino acid **17**. After HF cleavage the crude peptide, which was obtained as an off-white solid (1.04 g), was subjected to flash chromatography on reverse-phase (C_{18}) silica gel using an acetonitrile/water solvent gradient (0.91 g). ^{1}H NMR (CD_3OD): δ 7.03 (br, COOH), 4.37 (br, CH), 2.30 (br, CH_2), 2.07 (s, CH_3), 2.06 (s, CH_3), 1.88 (br, CH_2), 1.69 (br m, CH_2). ^{11}B NMR (CH_3OH): δ −6.05 (br), −10.88 (br). IR (KBr): 3233 (br), 3057 (br), 2944, 2604, 1706, 1640, 1550, 1548, 1510, 1460, 1440, 1247, 1202, 1136, 1030, 802, 746, 725 cm^{-1}. FAB MS (m/e) calcd for $C_{46}{}^{11}B_{50}H_{119}O_7N_7$: 1432. Observed: cluster of peaks centered around 1424.

Synthesis of (*closo*-CB)$_{10}$-Lys (21). Chloromethyl resin (1.0 g) loaded with N_α-*t*-BOC-N_ϵ-2-chloro-CBZ-lysine as the first amino acid (0.8 mequiv/g) was employed in the peptide synthesis and the *t*-BOC protected carboranyl amino acid **17** was again employed as the repeating reagent. After coupling 10 monomer residues, the peptide loaded resin (2.66 g) was recovered. A portion of the resin (1.0 g) was subjected to treatment with HF and undecapeptide **21** was isolated as a colorless solid (0.72 g) after purification by flash chromatography through a reverse-phase (C_{18}) silica gel column (acetonitrile/water solvent gradient). ^{1}H NMR (DMSO-d_6): δ 8.11 (br, NH), 7.68 (br, NH), 4.36 (br, α-CH), 2.72 (br, Lys-CH_2), 2.06 (s, CH_3), 1.64 (br, CH_2), 1.52 (br, CH_2). ^{11}B NMR (CD_3OD

+ CD_3CN, $CDCl_3$): δ −6.21, −10.87. IR (Nujol): 3322, 3273, 2586, 1661, 1547, 1534, 1200, 1179, 1026, 726 cm^{-1}. FAB MS (*m/e*) calcd for $C_{86}{}^{11}B_{100}H_{224}O_{12}N_{12}$: 2719. Observed: cluster of peaks centered around *m/e* 2698.

Preparation of (*nido*-CB)$_2$ (22) by the Pyrrolidine-Mediated Cage Degradation of (*closo*-CB)$_2$ (19). Dipeptide **19** (130 mg, 0.24 mmol) was treated with pyrrolidine (1 mL, 12 mmol) under nitrogen. After stirring at ambient temperature for 1 h, the residue was treated with CH_2Cl_2 (1 mL) and stirred for a further period of 0.5 h. The reaction mixture was concentrated under vacuum and the residue was washed repeatedly with 1 M HCl (5 × 5 mL) and then with ether. The product was subjected to cation exchange on Bio-Rad AG-X2 (100–200 mesh) cation-exchange resin (Na^+ form) preequilibrated with water/acetonitrile/methanol (5:4:1) solvent mixture which was used as the eluent. After removal of the solvents, the product was dried under vacuum (127 mg, 0.23 mmol, 96%). ^1H NMR (CD_3OD): δ 4.12 (m, α-CH), 1.83 (m, CH_2), 1.73 (m, CH_2), 1.40 (s, CH_3), 1.39 (s, CH_3). ^{11}B NMR (H_2O + CH_3OH): δ −10.46, −11.83, −18.45, −20.07, −35.06, −38.03. IR (pyrrolidinium salt, thin film): 3411–3083 (br), 2955, 2524, 1673, 1622, 1456, 1200, 1077, 1025, 911, 843, 735 cm^{-1}. FAB MS (negative ion, *m/e*) calcd for $C_{16}{}^{11}B_{18}H_{44}N_2O_3$: 511. Observed: cluster of peaks centered around 511.

Dansylation of (*nido*-CB)$_2$ (22) with Dansyl Chloride. A mixture of (*nido*-CB)$_2$ (**22**; 127 mg, 0.23 mmol) and dansyl chloride (72 mg, 0.27 mmol) in a mixture of CH_3CN (3 mL) and THF (1 mL) was stirred at ambient temperature under nitrogen for 66 h. The solvent mixture was removed under vacuum and the solid was washed with CH_2Cl_2. The crude product (73 mg) was dried under vacuum. A portion of the crude product (41 mg) was purified by passage through a cation-exchange resin (Bio-Rad AG-X2 resin, 100–200 mesh, Na^+ form, 5:4:1, H_2O/CH_3CN/CH_3OH solvent system), decolorization with charcoal and by passage through a reverse-phase (C_{18}) flash chromatography column (1:1 CH_3CN/H_2O solvent system) twice. Product **23** was obtained as a yellow solid (31.3 mg). ^1H NMR (CD_3OD + CD_3CN + D_2O): δ 8.82 (t, Ar-H), 8.35 (d, Ar-H), 8.25 (d, Ar-H), 7.70 (m, Ar-H), 4.35 (br, α-CH), 3.23 (s, $N(CH_3)_2$), 1.68 (m, CH_2), 1.60 (m, CH_2), 1.37 (s, CH_3). ^{11}B NMR (CD_3CN + D_2O): δ −9.47, −12.01, −17.96, −34.74, −37.96. IR (Nujol): 3324–3181 (br), 2526, 1674, 1532, 1189 cm^{-1}. R_f (C_{18} silica gel, 1:1 CH_3CN/H_2O): 0.84.

Synthesis of Dansyl·GABA·(*closo*-CB)$_5$·GABA (24). Merrifield resin loaded with GABA as the initial amino acid residue (1.0 g, 1.0 mequiv/g) was employed for the coupling of five residues of **17** and a final *t*-BOC·GABA residue. The *t*-BOC-protecting group was cleaved in the synthesizer using the standard program. The resin (2.46 g) was treated with a solution of dansyl chloride (0.67 g, 2.5 mmol) in CH_2Cl_2 (10 mL) and triethylamine (0.35 mL, 2.5 mmol). After stirring for 48 h at ambient temperature, the solution was removed by filtration and the resin washed with dichloromethane. After testing for completion of dansylation with ninhydrin, peptide **24** was cleaved from the resin with HF. Crude product **24** (1.13 g) was purified by column chromatography on reverse-phase silica gel (acetonitrile/water solvent gradient) to yield 0.90 g (0.53 mmol) of dansyl·GABA·(*closo*-CB)$_5$·GABA. ^1H NMR ($CDCl_3$ + CD_3OD): δ 9.00 (d, Ar-H), 8.54 (br, Ar-H), 8.37 (d, Ar-H), 8.22 (d, Ar-H), 8.16 (br, Ar-H), 8.06 (d, Ar-H), 7.81 (d, Ar-H), 7.62 (d, Ar-H), 4.16 (br, α-CH), 3.20 (s, $N(CH_3)_2$), 2.84 (br, CH_2), 2.24 (br, CH_2), 2.14 (br, CH_2), 1.91 (s, CH_3), 1.70 (br, CH_2), 1.50 (br, CH_2). ^{11}B NMR (CH_2Cl_2 + CH_3OH): δ −6.31, −11.09. IR (KBr): 3413 (br), 3309 (br), 2445, 2577, 1629, 1529, 1457, 1321, 1206, 1179, 1076, 1024, 789, 744 cm^{-1}. FAB MS (*m/e*) calcd for $C_{60}{}^{11}B_{50}H_{132}O_{10}N_8S$: 1706. Observed: cluster of peaks centered around 1710.

Dansylation of Resin-Bound (*closo*-CB)$_{10}$·Lys, Cleavage from Solid Support, Acetylation, and Degradation. A sample of the resin with the undecapeptide (*closo*-CB)$_{10}$·Lys (0.48 g, 0.38 mequiv) was subjected to the deprotection of the terminal amino group in the synthesizer employing the standard program. The resin was treated with a solution of dansyl chloride (0.26 g, 0.96 mmol) in CH_2Cl_2 (12 mL) and triethylamine (53 μL, 0.38 mmol). After stirring for 46 h, the solution was removed by filtration and the resin was washed repeatedly with dichloromethane, methanol, acetonitrile, and dichloromethane. The resin was tested with ninhydrin for completion of dansylation and subjected to HF treatment as previously described. The cleaved, dansylated peptide was extracted with methanol and concentration of the solution yielded crude product **25** as a yellow solid (0.29 g, 0.10 mmol). ^1H NMR (CD_3OD + CD_2Cl_2): δ 8.48 (m, Ar-H), 8.27 (m, Ar-H), 8.08 (m, Ar-H), 7.44 (m, Ar-H), 4.11 (br, α-CH), 3.18 (s, $N(CH_3)_2$), 2.80 (br, CH_2), 2.16 (br, CH_2), 2.03 (s, CH_3), 1.78 (br, CH_2), 1.37 (br, CH_2). ^{11}B NMR (CD_3CN + CD_2Cl_2): δ −6.74, −11.37. IR (KBr): 3310 (br), 2944, 2607, 1661, 1548, 1458, 1202, 1181, 1141, 1023, 796, 728 cm^{-1}. FAB MS (*m/e*) calcd for $C_{98}{}^{11}B_{100}H_{235}O_{14}N_{13}S$: 2949. Observed: cluster of peaks centered around 2949.

The crude dansylated peptide obtained from the resin by HF cleavage (288 mg, 0.10 mmol) was treated with acetic anhydride (2 mL, 20 mmol) and triethylamine (40 μL, 0.29 mmol). The mixture was stirred at ambient temperature under nitrogen for 12 h, when the solution turned brown. The solution was concentrated *in vacuo* and was washed with petroleum ether. The brown solid material was dried under vacuum (0.29 g, 0.1 mmol). This crude product (**26**) was used in the subsequent reaction without purification. ^1H NMR (CD_2Cl_2): δ 8.50 (d, Ar-H), 8.38 (d, Ar-H), 8.12 (d, Ar-H), 8.05 (d, Ar-H), 7.48 (m, Ar-H), 7.37 (m, Ar-H), 7.18 (m, Ar-H), 7.15 (m, Ar-H), 6.38 (m, Ar-H), 3.78, (br, α-CH), 3.04 (q, $N(C_2H_5)_3H$), 2.87 (s, $N(CH_3)_2$), 2.28 (s, CH_3CO), 2.19 (br, CH_2), 2.01 (br, CH_3), 1.96 (s, CH_3), 1.95 (br, CH_2), 1.65 (br, CH_2), 1.27 (t, $N(C_2H_5)_3H$). ^{11}B NMR (CD_2Cl_2): δ −6.95, −11.14.

Crude acetylated peptide **26** obtained from above (0.29 g, 0.090 mmol) was treated with pyrrolidine (2 mL) and the mixture was stirred under nitrogen for 1 h at 25 °C. The solvent was removed under vacuum and the product was washed twice with 1 M HCl, once with water, and once with petroleum ether. The brownish solid was dried under vacuum (0.18 g). The pyrrolidinium cation was exchanged for sodium with Bio-Rad AG-X2 cation-exchange resin (mesh 100–200, Na^+ form) and acetonitrile/water mixture (1:1) as the solvent. Product **27** was further purified by flash chromatography on reverse-phase (C_{18}) silica gel column (1:1 acetonitrile/water) and decolorized with charcoal. The product was obtained as a pale yellow solid (95 mg, 0.030 mmol). ^1H NMR (CD_3OD + CD_3CN): δ 8.53 (d, Ar-H), 8.34 (d, Ar-H), 8.11 (d, Ar-H), 7.66 (d, Ar-H), 7.49 (m, Ar-H), 7.27 (d, Ar-H), 5.44 (br, Ar-H), 4.08 (br, α-CH), 2.85 (s, $N(CH_3)_2$), 1.68 (br, CH_2), 1.55 (br, CH_2), 1.38 (s, CH_3). ^{11}B NMR (H_2O): δ −8.82, −17.00, −33.23, −35.72. IR (Nujol): 3219 (br), 2512, 1658, 1192 cm^{-1}. R_f (C_{18} silica gel, 1:1 CH_3CN/H_2O): 0.63.

Activation of Dansyl·(*nido*-CB)$_2$ (23) and Conjugation to T84.66. A solution of **23** (6.36 mM, 80 μL) in phosphate buffer (0.1 M, pH 4.35) was treated with

Table I. Conjugation of Dansyl-(*nido*-CB)$_2$ (23) to T84.66 Antibody

	peptide activation		conjugation of 1 mg of T84.66 in 1.1 mL of buffer, 60 min, 25 °C				
expt no.	buffer (pH)	reaction time, min	buffer (pH)	[peptide]/[T84.66][a]	bound peptide/T84.66 molecule	% protein recovery	% HMW[c]
1	0.1 M PO_4 (4.4)	60	0.05 M PO_4 (7.4)	10.6	8.5 (6.1)[b]	77.6	7.3
				10.5 (control)	2.3	86.2	3.5
2	0.1 M PO_4 (4.4)	60	0.10 M CO_3/HCO_3 (9.3)	10.6	9.4 (7.1)[b]	78.9	6.1
				10.5 (control)	1.3	92.9	5.0

[a] High molecular weight material (HMW) comprised less than 4% of T84.66 protein. [b] Ratio observed after purification of conjugate by gel filtration HPLC. [c] High molecular weight species determined by HPLC analysis of the conjugate.

solutions of *N*-hydroxysuccinimide (55 mM, 18 μL) in water and *N,N*-diisopropylcarbodiimide (65 mM, 8 μL) in dimethylformamide. The mixture was incubated at ambient temperature for 1 h. An aliquot of the active ester solution (40 μL) was added to the T84.66 antibody solution (0.12 mM, 50 μL) diluted with phosphate buffer (0.05 M, 1 mL, pH 7.43). Another solution of the antibody (0.12 mM, 50 μL) diluted with carbonate/bicarbonate buffer (0.1 M, 1 mL, pH 9.30) was subjected to identical treatment. Two control experiments were run by treating the same amount of the antibody in the respective buffers with unactivated peptide **23** (6.3 mM, 10 μL) in phosphate buffer (0.1 M, pH 4.35). The molar ratio of the activated or unactivated peptide to the antibody was 10:5 in all cases. After incubating for 1 h at ambient temperature, the controls and the conjugates were subjected to ultrafiltration using Centricon-30 concentrators. The concentrates were treated with the respective conjugation buffers (2 × 2 mL) and water (1 × 2 mL) and concentrated after each dilution. The respective volumes of the final concentrates were measured and aliquots taken for Bio-Rad protein assay, fluorescence measurements, and gel filtration HPLC analysis.

The fluorescence intensities of a series of aqueous solutions of peptide **23** of different concentrations (in the range 1.27–12.7 mM) were measured and a linear plot of the fluorescence intensity vs concentration was obtained. A known volume (~5–10 μL) of the concentrate was diluted to 5 mL and the fluorescence intensity was measured. Neglecting the contribution of the antibody protein to the fluorescence and/or the quenching of fluorescence by the peptide, if any, the concentration of the peptide in the antibody concentrate was determined from the above data. The ratio of the peptide concentration measured from the fluorescence intensity and the protein concentration measured from the Bio-Rad protein assay revealed the average number of peptide units attached to each of the antibody molecules. HPLC analysis of the controls and the conjugates was carried out on a Du Pont Zorbax GF-250 column using 0.1 M Tris·HCl containing 0.15 M NaCl and 0.005% NaN_3) as solvent with a flow rate of 1 mL/min and monitored by UV detection at 280 nm. The results are reported in Table I.

Activation of Dansyl-(*nido*-CB)$_{10}$-Lys-Ac (27) and Conjugation to T84.66. To a solution of **27** (6.5 mM, 45 μL) in phosphate buffer (0.1 M, pH 4.35) were added solutions of *N*-hydroxysulfosuccinimide (46 mM, 13 μL) in water and *N,N*-diisopropylcarbodiimide (65 μM, 4.5 μL) in dimethylformamide, and the mixture was incubated at ambient temperature for 45 min. Different amounts of the active ester solution (6.5, 13, and 19.5 μL) were added to T84.66 antibody solutions (0.12 mM, 50 μL) diluted with phosphate buffer (0.05 M, 1 mL, pH 7.43). A control experiment was carried out by treating unactivated peptide **27** (6.46 mM, 5 μL) with the same amount of the antibody in phosphate buffer under identical conditions. The molar ratios of the activated peptide to the antibody in the conjugates were 5:1, 10:1, and 15:1, and in the case of the control it was 5.35:1. After 1 h, the conjugates and the control were subjected to ultrafiltration using Centricon-30 concentrators. The concentrates and the conjugates were treated with phosphate buffer used for conjugation (2 × 2 mL) and water (2 × 2 mL) and were concentrated after each dilution. Fluorescence measurements, Bio-Rad protein assay, and gel filtration HPLC analysis were carried out on the concentrates as described above. Table II lists the results obtained from the conjugation studies performed under a variety of experimental conditions.

RESULTS AND DISCUSSION

Synthesis of Amino Acids. The synthesis of the homogeneous macromolecular peptide derivatives described here required the availability of significant quantities of amino acids containing the carborane cage. Although such an amino acid, carboranylalanine (**1**), had been previously synthesized by Leuckart and co-workers (*17–20*) and employed in the preparation of short-chain peptides such as bradykinin, etc., it was desirable to prepare the carboranyl α-amino acid to be used here in higher yields than those available for **1**. Instead of attempting the unattractive carborane-forming reaction of acetylenic amino acid derivatives with decaborane, we initially chose to attach the carborane cage to a suitable α-amino acid derivative. The nucleophilic *closo* cage-opening reactions of *closo*-1,8-dicarbaundecaborane(11) (*21*, *22*) with derivatives such as N_α-*t*-BOC-lysine and anionic derivatives of *N*-*t*-BOC-tyrosine and *N*-*t*-BOC-serine did not proceed satisfactorily, and the products were found to be unstable. Our second approach, which attempted to attach the carborane cage to N_α-*t*-BOC-lysine and pentalysine employing *N*-succinimidyl esters of several carborane carboxylic acids, was also unsuccessful due to the instability of the active esters and solvent incompatibility problems (*23*). To this end, we chose to synthesize a different amino acid, namely, 5-(2-methyl-1,2-dicarbadodecaborane(12)-1-yl)-α-aminopentanoic acid (**2**; Scheme I).

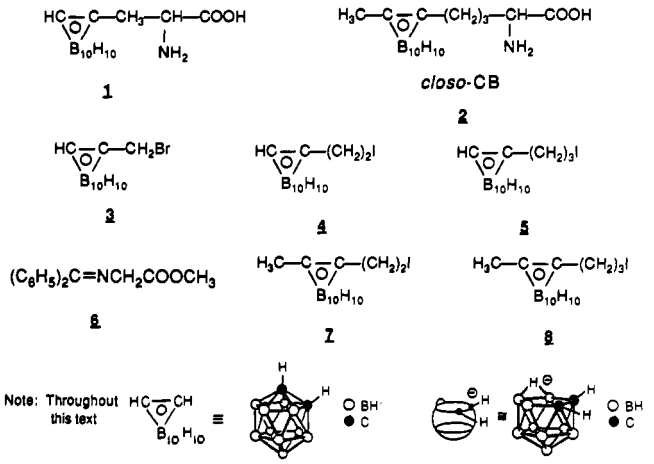
The alkylation of glycine ester Schiff's base is a widely used method for α-amino acid (*24*, *25*) synthesis. While it is conceivable to use an alkyl halide containing the carborane as a substituent, the simplest halide, namely (bromomethyl)carborane (**3**), is unreactive to nucleophilic substitution (*26*). The other halides such as the ethyl and propyl iodide derivatives **4** and **5** afforded only the starting materials upon attempted alkylation of the carbanion derived from methyl *N*-(diphenylmethylidene)glycinate (**6**). The outcome of the reaction did not change when leaving groups such as chlorides, bromides, and tosylates were employed and suggests that the hydrogen on the carboranyl carbon atom is sufficiently acidic to protonate the Schiff's base anion. While the incorporation of a me-

Table II. Conjugation of Dansyl-(*nido*-CB)$_{10}$-Lys-Ac (27) to T84.66 Antibody

	peptide activation		conjugation of 1 mg of T84.66 in 1.05 mL of buffer, 60 min, 25 °C				
expt no.	buffer (pH)	reaction time, min	buffer (pH)	[peptide]/[T84.66][a]	bound peptide/T84.66 molecule	% protein recovery	% HMW[b]
1	H_2O (7.0)	30	0.1 M CO_3/HCO_3 (9.3)	4.8	2.2	37.9	12.4
				9.7	2.7	30.8	17.3
				18.3	8.0	1.4	10.6
				17.6 (control)	6.8	15.3	22.0
2	0.1 M PO_4 (4.4)	60	0.1 M CO_3/HCO_3 (9.3)	5.2	5.5	56.8	17.0
				10.4	9.8	29.9	26.6
				15.6	15.3	4.1	0.0
				9.6 (control)	6.1	64.8	20.0
3	0.1 M PO_4 (4.4)	40	0.1 M HEPES (8.2)	5.0	2.9	59.9	14.6
				10.0	4.2	46.6	21.8
				15.0	6.9	38.4	21.0
				4.8 (control)	2.3	37.6	12.3
4	0.1 M PO_4 (4.4)	30	0.1 M HCO_3 (8.5)	5.3	2.8	66.3	16.2
				10.6	4.4	54.0	18.4
				15.9	9.1	30.0	20.9
				4.8 (control)	2.2	55.3	12.3
5	0.1 M PO_4 (4.4)	45	0.05 M PO_4 (7.4)	5.0	5.9	55.0	16.2
				10.0	8.5	35.8	23.8
				15.0	15.4	15.4	14.0
				5.4 (control)	4.1	78.9	14.9

[a] High molecular weight material (HMW) comprised less than 4% of T84.66 protein. [b] High molecular weight species determined by HPLC analysis of the conjugate.

Scheme I



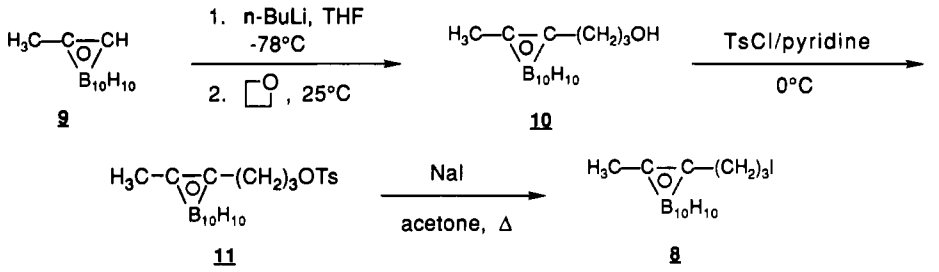
thyl substituent on the carborane carbon would be expected to alleviate this problem, the requirement remained that the leaving group be located on the γ-carbon of the alkyl chain for this substitution to occur. This is undoubtedly due to the unique stereoelectronic characteristics of the carborane cage. Thus, 2-(2-methyl-1,2-dicarbadodecaborane(12)-1-yl)ethyl iodide (7) seemingly yielded a product mixture which contained the abnormal N-alkylated product (27), but its homologue 3-(2-methyl-1,2-dicarbadodecaborane(12)-1-yl)propyl iodide (8), formed the desired alkylate. The starting propyl iodide derivative 8 was prepared from methyl carborane (9, Scheme II) and the Schiff's base alkylation proceeded smoothly to give monoalkylated product 12 (Scheme III). The alkylation could also be carried out under phase-transfer conditions (28), but it proceeded at a considerably slower rate in this medium. The alkylated Schiff's base was partially hydrolyzed to amino ester derivative 13 with dilute HCl. Complete hydrolysis of 13 yielded 14 from which free base 2 was obtained upon treatment with propylene oxide. No attempt was made to resolve the enantiomers of this chiral α-amino acid.

In order to prepare the water-soluble nido anion derived from this amino acid, we have subjected closo derivative 2 to base degradation in ethanolic medium. Sodium salt 15 was isolated as tetra-*n*-butylammonium salt 16a or triphenylmethylphosphonium salt 16b, since the tetramethylammonium salt proved to be water soluble. It is to be noted that amino ester 13 could be directly converted to the nido derivative 15 without the isolation of closo amino acid 2 (Scheme IV). (Note: Throughout this text, the neutral amino acid residue 2 and the anionic amino acid residue 15 are referred to as *closo*-CB and *nido*-CB, respectively, for convenience.)

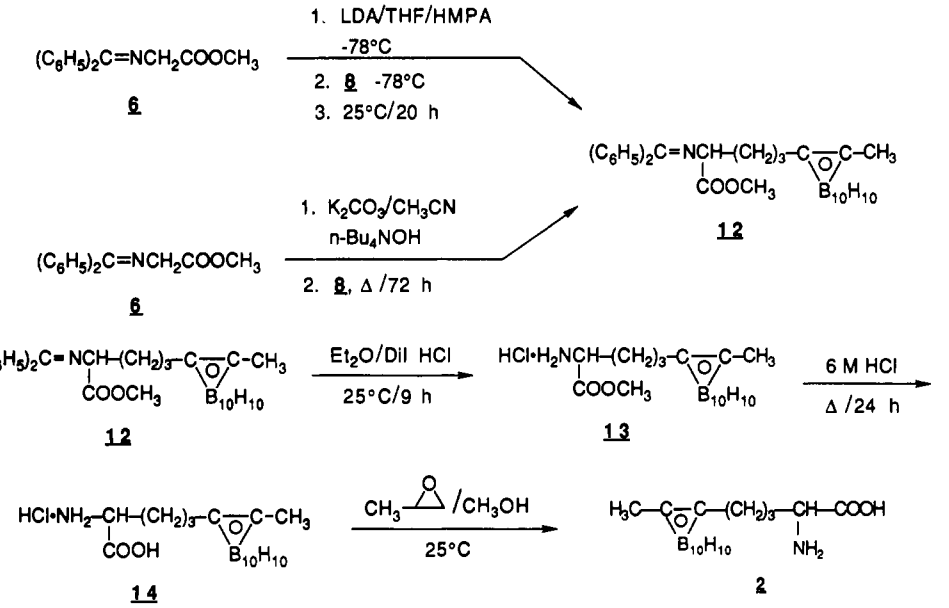
Preparation of *t*-BOC Derivatives. Amino acid 2 is exceptionally hydrophobic and it was for this reason that the preparation of *t*-BOC derivative 17 by the conventional method in aqueous medium, did not proceed in high yield. However, this problem was circumvented by carrying out the reaction in ethanol solution (Scheme V). A similar method which employs either DMF or methanol as the solvent has recently been reported in the literature (29). *t*-BOC derivative 18 of the nido amino acid derivative 15 was similarly prepared via its sodium salt (Scheme V). All of the simple amino acid derivatives mentioned here were characterized by both spectroscopic methods and elemental analyses. As is well-known in the case of boron compounds which contain nitrogen, boron analyses are frequently difficult and reveal less than the theoretical value for boron.

Reactions of *t*-BOC Amino Acids with Merrifield's Chloromethyl Resin. *t*-BOC derivatives 17 and 18 were converted to their cesium salts for loading on the Merrifield resin. Although closo derivative 17 was loaded with reasonable efficiency (40–50%), loading of the ionic derivative was poor. Initially, for the synthesis of simple dipeptide derivatives, 17 was directly loaded on the resin. However, for the synthesis of longer peptide sequences, common amino acids such as lysine, glycine, or γ-aminobutyric acid were employed as the initial amino acid of the series. These amino acids led to a considerably higher degree of loading (*ca.* 90–99%) and the lower loading efficiency for 17 and 18 could therefore be attributed to the presence of steric contraints imposed by the carborane cage. The ionic nature of 18 presumably further aggravated the resin-reactivity problem.

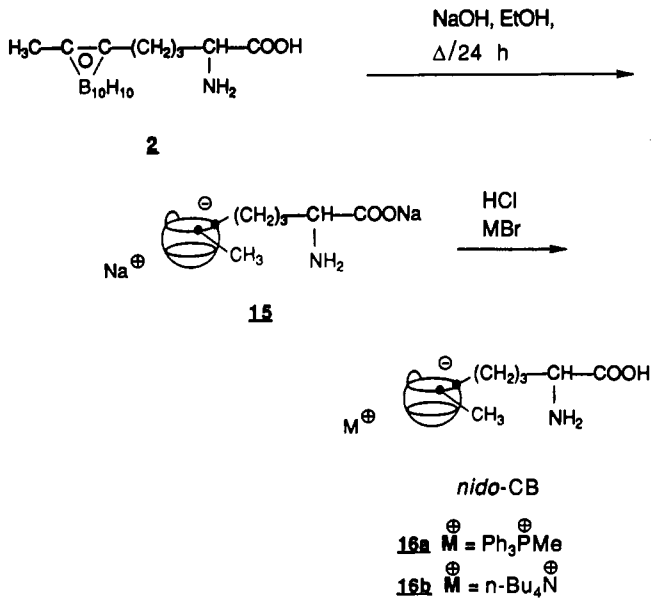
Scheme II



Scheme III



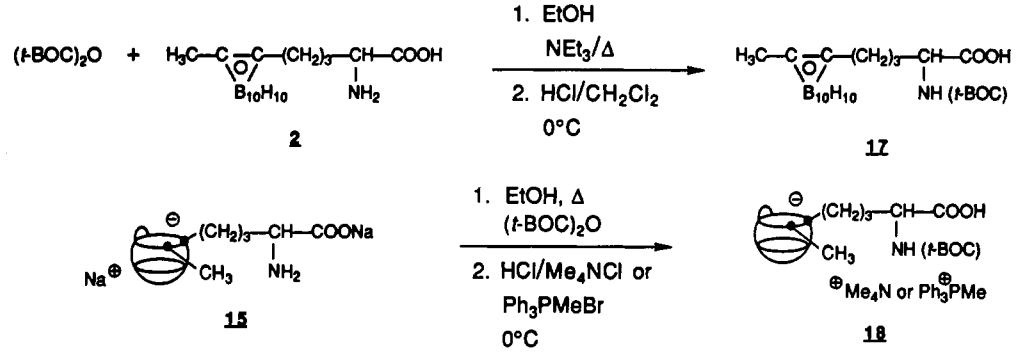
Scheme IV



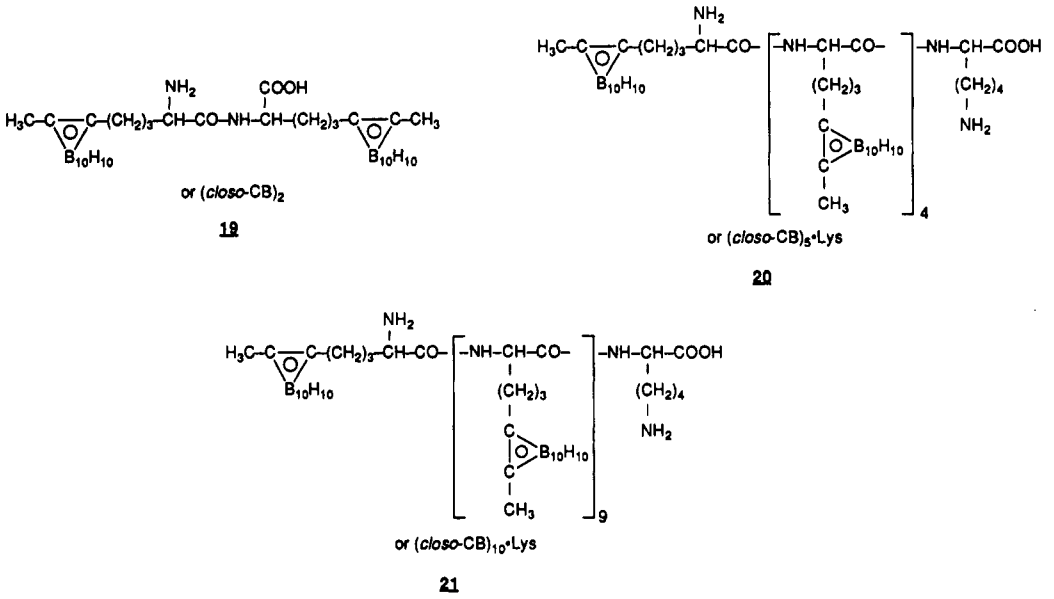
Stepwise Synthesis of Carboranyl Peptides. *A. Peptide Synthesis Involving the closo-Carboranyl Amino Acid.* The subsequent coupling of the *closo*-carboranyl amino acid residues to the resin-bound, first amino acid of the peptide sequence was carried out by using the dicyclohexylcarbodiimide-mediated coupling of **17** with *N,N*-(dimethylamino)pyridine as the acylation catalyst. Although various methods such as the use of the *N*-succinimide active ester and the *N*-hydroxybenzotriazole-mediated coupling were attempted, these methods did not lead to significant improvement in coupling efficiency. As observed in the case of carboranylalanine (*19*), coupling reactions using **2** were sluggish and frequently required a second coupling sequence to reach completion. Steric hindrance to coupling has been observed even in the case of such relatively less encumbered amino acids as leucine. Due to the slowness of the reaction, coupling was carried out over a period of 48 h with the same time period allotted for the recoupling process, as well. With this procedure each residue was coupled to the previous residue in a quantitative manner. Since the carboranyl amino acid employed was initially racemic, racemization due to longer coupling times gave no cause for concern. Using this standard procedure we have coupled 2, 5, and 10 residues of **2** in separate resin-supported peptide syntheses. In each case, cleavage of the peptide from the solid support was accomplished in the conventional manner employing hydrogen fluoride and anisole and with complete integrity of the *closo*-carborane cage. Subsequently, we found it convenient to carry out dansylation of the terminal amino group with the peptide still anchored to the resin. This procedure has recently been reported in the literature (*30*). We have synthesized the peptides (*closo*-CB)$_2$ (**19**), (*closo*-CB)$_5$-Lys (**20**), and (*closo*-CB)$_{10}$-Lys (**21**) by this procedure (Scheme VI). A typical example of the stepwise synthesis is presented in Scheme VII.

B. Peptide Synthesis Involving the nido-Carboranyl Amino Acid. In order to prepare water-soluble peptide derivatives, *nido*-carboranyl amino acid *t*-BOC derivative **18** was employed in coupling reactions with resin-bound glycine. As already mentioned, direct attachment of **18** to the resin was inefficient. It was found to be necessary to employ DMF as the reaction solvent to dissolve tet-

Scheme V

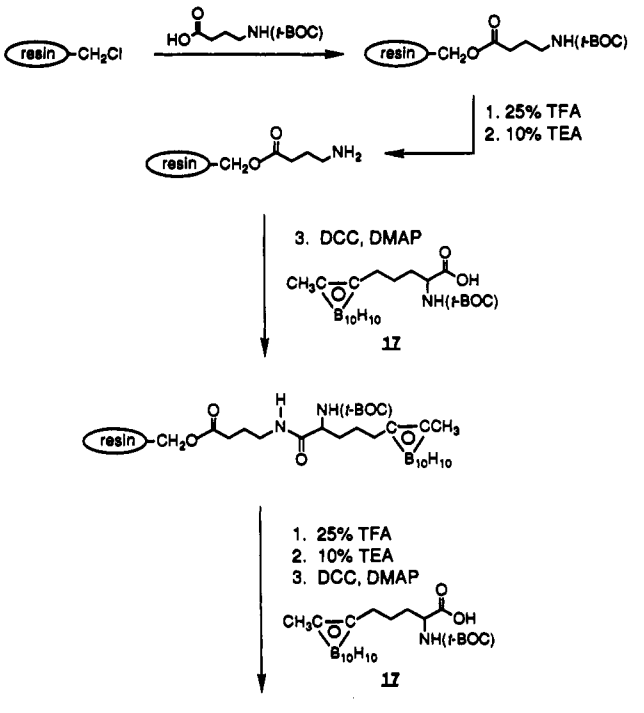


Scheme VI



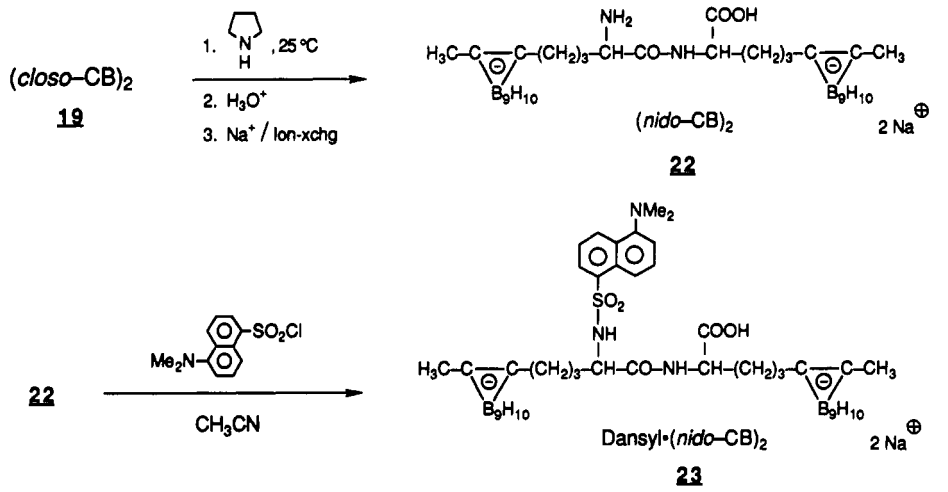
ramethylammonium salt 18 in the coupling reactions. The DCC-mediated coupling reactions of the nido species proceeded much more slowly than those of the closo derivative and did not reach completion, even after recoupling. The inefficiency of this reaction can be attributed to the polar medium (DMF) which has previously been reported to increase the rate of rearrangement of the active *O*-acylisourea intermediate to the inactive *N*-acylurea intermediate (*16*). It has also been reported that the presence of ionic materials accelerates this unwanted rearrangement. The reaction efficiency did not improve when an active ester such as *N*-succinimidyl (preformed) or HOBT (*in situ*) was utilized. Furthermore, the product peptides contained triethylammonium cation rather than the counterion (tetramethylammonium or triphenylmethylphosphonium) present in the starting materials. The cleavage of the peptide from the resin with HF did not present problems as indicated by the stability of model *nido*-carborane derivatives such as $[nido\text{-}7,8\text{-}C_2B_9H_{12}]^-$ with anhydrous HF. Due to the low yield of the coupling reactions, the anionic carboranyl amino acid was not employed in subsequent solid-phase syntheses. In order to obtain water-soluble peptides it was therefore necessary to convert the closo cages of the peptides derived from 2 to their anionic nido counterparts. This was accomplished without peptide bond disruption by the use of the pyrrolidine degradation (*21*) of the carborane cage. The resulting pyrrolidinium salts of the peptides were washed with dilute hydrochloric acid both to remove the excess pyrrolidine and to regenerate the free carboxyl function.

Scheme VII

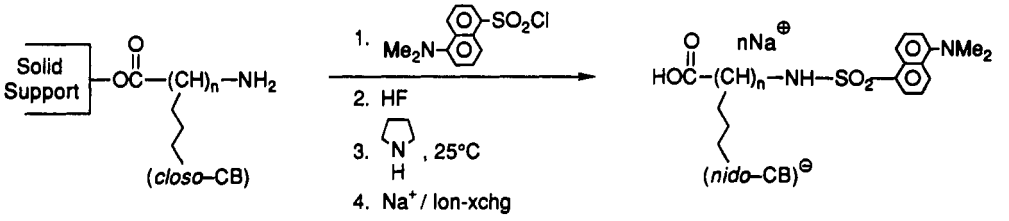


The pyrrolidinium counterion of the *nido*-carborane cages was exchanged for sodium with a cation-exchange resin.

Scheme VIII



Scheme IX



The synthesis of (*nido*-CB)$_2$ (**22**) from **19** is outlined in Scheme VIII.

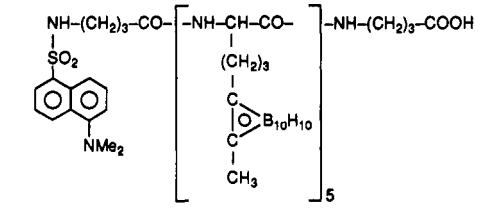
Fluorescent Labeling of the Peptides. The peptides with two functionally active end groups provide access to labeling for *in vitro* assays at one terminal group and activation for antibody conjugation at the other. Since we had previously demonstrated the carboxyl activation and subsequent conjugation of a radiometallacarborane sandwich to an anti-CEA antibody (*22*), we chose to label the terminal amino function with a fluorescent chromophore. Of all the fluorescent labels investigated, the dansyl group provided the most efficient method of introducing a sensitive fluorescent label and eliminated the alternative of a radiolabel for peptide assays prior to antibody conjugation. The dansylation process which leads to the synthesis of dansyl·(*nido*-CB)$_2$ (**23**) is depicted in Scheme VIII.

It was later observed that the dansylation procedure could be better carried out with the resin-bound peptide itself, as exemplified in Scheme IX. When labeling the peptides attached to the resin, the *t*-BOC protecting group was first removed by treatment with trifluoroacetic acid followed by triethylamine. Further exhaustive treatment of the resin with dansyl chloride and triethylamine completed the labeling process. Labeled peptides **24** and **25** were obtained by this method followed by cleavage from the resin (Scheme X).

Dansylated undecapeptide **25** was acetylated to block the free amino group on the lysine residue and the product, dansyl·(*closo*-CB)$_{10}$·Lys·Ac (**27**), was treated with pyrrolidine to accomplish quantitative carborane cage degradation. Following acidification and sodium cation-exchange, the desired product, dansyl·(*nido*-CB)$_{10}$·Lys·Ac (**27**), was obtained as its sodium salt (Scheme XI).

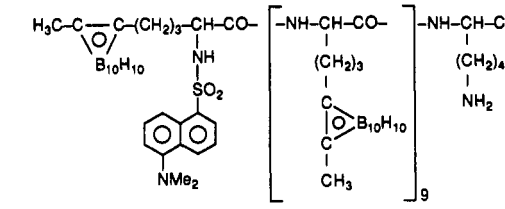
All the peptides were purified by flash chromatography on reverse-phase silica gel and characterized by spectroscopic means. Peptides which contained more than two *closo*-CB or *nido*-CB units often exhibited aliphatic proton resonances in the ^{1}H NMR spectra as broad multiplets,

Scheme X



Dansyl•GABA•(*closo*-CB)$_5$•GABA

24



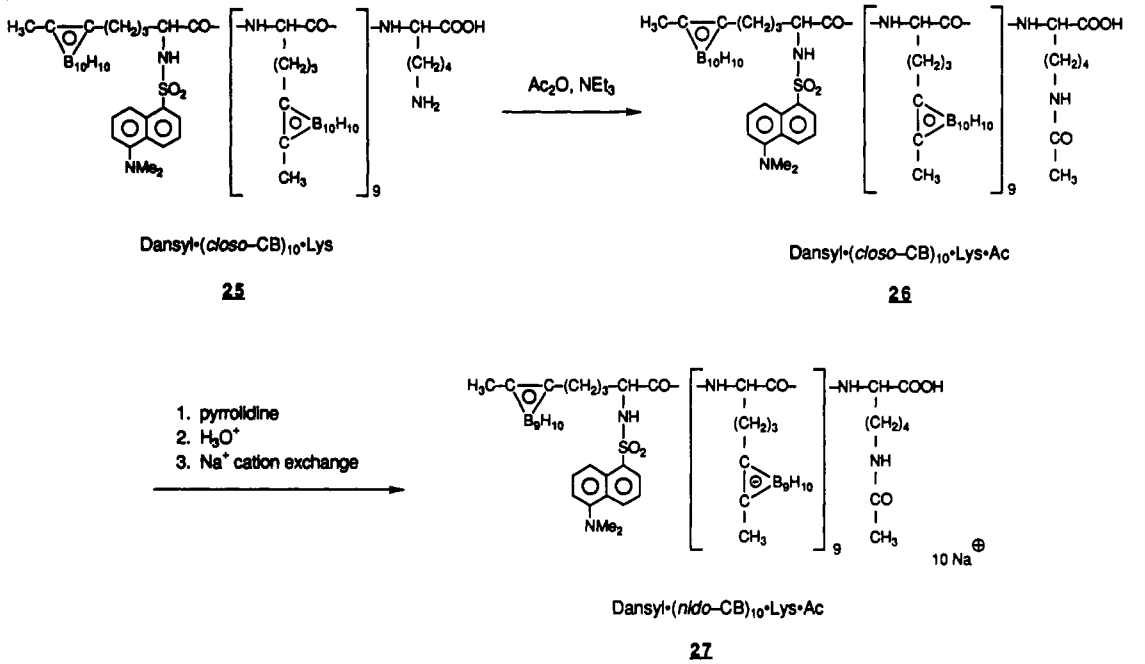
Dansyl•(*closo*-CB)$_{10}$•Lys

25

due to the reduction of their molecular tumbling motion in solution. The ^{11}B resonances of these same peptides were also broader than normal. Further, dansyl fluorescence intensity vs concentration curves were established for peptides **23** and **27** by measuring the fluorescence intensity at various concentrations using 313 and 515 nm as the excitation and emission wavelengths, respectively.

^{11}B NMR of Resin-Bound Peptides. A novel feature of the carborane cages attached to the resin is the fact that it was possible to obtain ^{11}B NMR spectra of the peptide-loaded resins in dichloromethane medium. The spectra so obtained strongly resembled those of the resin-free peptides. It is reasonable to assume that there is considerable

Scheme XI



Dansyl-(*closo*-CB)$_{10}$-Lys-Ac

25

Dansyl-(*closo*-CB)$_{10}$-Lys-Ac

26

Dansyl-(*nido*-CB)$_{10}$-Lys-Ac

27

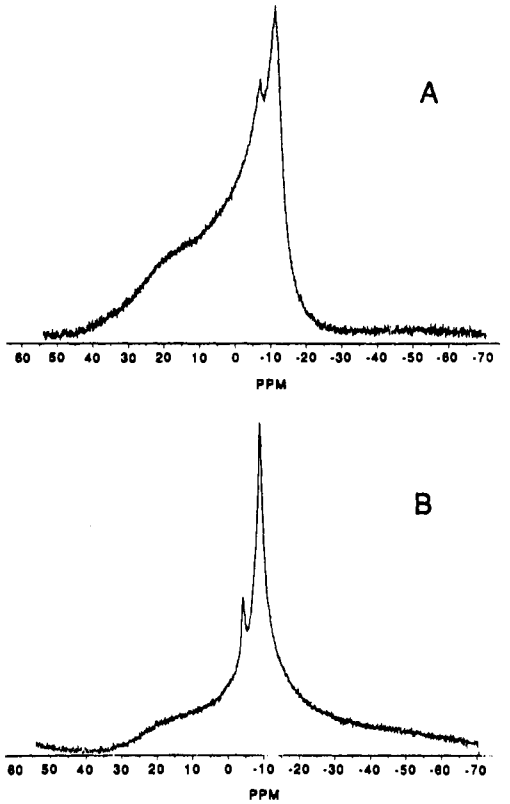


Figure 1. $^{11}B\{^1H\}$ FT NMR spectra of (**A**) dansyl-(*closo*-CB)$_{10}$-Lys-resin suspended in CH_2Cl_2 and (**B**) dansyl-(*closo*-CB)$_{10}$-Lys (**25**) as a solution CD_3OD.

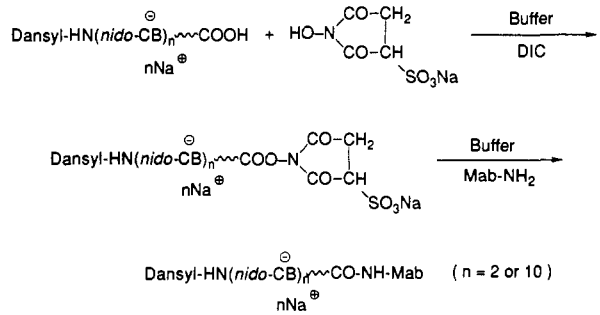
motion of the attached peptide moiety within the swollen resin and that this process, along with the inherent quadrupole-broadening of the boron resonances seen in homogeneous solutions, gave rise to the solutionlike spectra. Representative ^{11}B NMR spectra are illustrated in Figure 1.

Terminal Carboxyl Group Activation for Antibody Conjugation. As representative peptides prepared in this study which contain anionic *nido*-CB residues, **23** and **27** were chosen for antibody conjugation. A variety of attempts were made to prepare the N-succinimidyl ester derivatives by the *in situ* activation of the peptide terminal carboxyl group prior to antibody conjugation. In each case the carboxyl group was activated at pH 4.4 in order to ensure that this group was protonated. When water-soluble ionic carbodiimides such as EDC were employed, the anionic *nido*-carborane cages present in the peptide precipitated with the added ammonium counterion. Furthermore, DCC was found to be unsuitable due to its separation from the aqueous phase when added as a solution in DMF. However, a solution of diisopropylcarbodiimide proved to be the reagent of choice since no solid separation was observed in the aqueous peptide phase. Both *N*-hydroxysuccinimide and *N*-hydroxysulfosuccinimide in water were equally efficient in forming the active ester.

The conjugation of dipeptide **23** and undecapeptide **27** to T84.66 antibody was carried out by using the conditions described in Tables I and II. The conjugates were purified by ultrafiltration using Centricon-30 membrane microfilters. The concentrates were repeatedly washed with appropriate buffers and with water until the filtrates exhibited no detectable fluorescence. In the case of the conjugates of dipeptide **23**, further purification was performed by HPLC on a Dupont GF-250 gel filtration column. Control experiments were also carried out employing peptides **23** and **27** alone in the absence of the activating reagents. The activation and conjugation of the peptides to the antibody are depicted in Scheme XII. Measurement of the fluorescence intensities of standard solutions of the conjugates and comparison of these values with the standard calibration curves for the unconjugated peptides provided the concentration of the peptides in the solutions of the conjugates. These data, when taken in conjunction with the concentrations of the antibody protein in the corresponding solutions (measured by absorbance at 280 nm or by Bio-Rad protein assay) revealed the average number of peptide molecules attached to each antibody molecule of the conjugate samples. The results of the conjugation studies are reported in Tables I and II.

In the case of dipeptide **23**, control experiments (Table I) showed that the nonspecific binding of peptide to antibody, though present to a measurable extent, was not prohibitively large. Gel-filtration HPLC removed at least

Scheme XII



a detectable portion of the noncovalently bound peptide. Furthermore, there was only a slight increase in the proportion of the high molecular weight (HMW) species after conjugation and the conjugated protein was recovered in good yields.

As can be seen from Table II, the conjugation of the higher oligomer, undecapeptide **27**, revealed aspects of the peptide–antibody interaction that require attention. The control experiments clearly showed a significant increase in nonspecific binding of peptide **27** to T84.66 compared to that of dipeptide **23**. The proportion of this noncovalent binding increased with an increase in the proportion of starting peptide reagents to antibody and the recovery of the antibody protein decreased with an increase in the ratio of **27** to the antibody. For the undecapeptide, the proportion of the high molecular weight species (HMW) formed upon conjugation was considerably higher than that observed in the case of dipeptide **23**. Again, this proportion of the HMW species increased with an increase in the starting ratios of peptide **27** to the antibody.

It is clear from the foregoing study that with the increase in the average number of the anionic [*nido*-7,8-$C_2B_9H_{11}$]$^-$ cages attached to the antibody through increased conjugation of the *nido*-carboranyl amino acid residues, noncovalent bonding of peptide molecules to antibody also increases. This type of binding could conceivably result from the enhancement of the hydrophobic character of the peptide reagent which results from an increase in the number of such ambiphilic *nido*-carborane residues that constitute the peptide molecule. It is interesting to note, in this regard, that on the basis of partition coefficient values, carboranylalanine (**1**) has been empirically calculated to be the most lipophilic amino acid known (*32*). The strong hydrophobic interaction between the ambiphilic nido peptide and the hydrophobic regions of the antibody would be expected to lead to the entrapment of the peptide reagent inside the antibody structure in such a manner that traditional gel-filtration techniques would not be able to separate the nonspecifically bound peptide. This idea is further supported by the fact that the use of nonionic surfactants, such as Tween-20, in the gel-filtration buffer medium employed in our subsequent studies allowed the successful separation of the unbound peptide. Further observations also indicated that the HMW species, which were associated with disproportionately high fluorescence intensities, are likely to be heavily conjugated antibody molecules which result from a repetitive cascade conjugation process rather than an aggregate (dimer) of the antibody. Details of these conjugation studies will be reported elsewhere.

In conclusion, the foregoing study illustrates the feasibility of the precision synthesis of boron-rich oligomeric materials that circumvent the problems associated with oligomer heterogeneity in the antibody conjugates. However, with an increase in the monomer residues which constitute the oligomer, noncovalent hydrophobic binding of the oligomer to the antibody and the formation of HMW materials both undergo a significant increase. While the noncovalently bound materials can be removed by employing HPLC with nonionic detergents, it is also possible to incorporate amino acid residues which carry hydrophilic substituents, such as sugar residues (*15*, *33*), in the oligomeric peptide species. Such structural alteration should minimize or completely eliminate the hydrophobic interaction between the boron-rich oligomer and the antibody. In this regard, it is important to note that our method for the precision synthesis of oligomers also has the flexibility necessary for incorporating structural diversity in the product oligomer. Thus, in principle, it is possible to employ monomer residues which bear substituents that deter hydrophobic and other noncovalent interactions of the peptide with the antibody during conjugation. The problems associated with the formation of HMW materials during conjugation will be discussed elsewhere since further work in this direction is currently in progress.

ACKNOWLEDGMENT

This research was supported by National Institutes of Health Grant CA 31753 for which we express our gratitude.

LITERATURE CITED

(1) Barth, R. F., Soloway, A. H., and Fairchild, R. A. (1990) Boron Neutron Capture Therapy of Cancer. *Cancer Res. 50*, 1061–1070.

(2) Mizusawa, E., Dahlman, H. L., Bennett, S. J., Goldenberg, D. M., and Hawthorne, M. F. (1982) Neutron-Capture Therapy of Human Cancer: In Vitro Results on the Preparation of Boron-Labeled Antibodies to Carcinoembryonic Antigen. *Proc. Natl. Acad. Sci., U.S.A. 79*, 3011–3014.

(3) Goldenberg, D. M., Sharkey, R. M., Primus, F. J., Mizusawa, E., and Hawthorne, M. F. (1984) Neutron-Capture Therapy of Human Cancer: In Vivo Results on Tumor Localization of Boron-10-Labeled Antibodies to Carcinoembryonic Antigen in the GW-39 Tumor Model System. *Proc. Natl. Acad. Sci., U.S.A. 81*, 560–563.

(4) Mizusawa, E. A., Thompson, M. R., and Hawthorne, M. F. (1985) Synthesis and Antibody-Labeling Studies with the *p*-Isothiocyanatobenzene Derivatives of 1,2-Dicarba-*closo*-dodecaborane(12) and the Dodecahydro-7,8-dicarba-*nido*-undeacaborate(1−) Ion for Neutron Capture Therapy of Human Cancer. Crystal and Molecular Structure of Cs^+[*nido*-7-(*p*-C_6H_4NCS)-9-I-7,8-$C_2B_9H_{11}$]$^-$. *Inorg. Chem. 24*, 1911–1916.

(5) Alam, F., Soloway, A. H., Barth, R. F., Johnson, C. W., Carey, W. E., and Knoth, W. E. (1983) Boronation of Polylconal and Monoclonal Antibodies for Neutron Capture. *First International Symposium on Neutron Capture Therapy. Brookhaven National Laboratory Report No. BNl-51730* (R. G. Fairchild and G. L. Brownwell Eds.) pp 229–236; Cambridge, MA, Oct 12–14.

(6) Alam, F., Soloway, A. H., Barth, R. F., Mafune, N., Adams, D. M., and Knoth, W. H. (1989) Boron Neutron Capture Therapy: Linkage of a Boronated Macromolecule to Monoclonal Antibodies Directed against Tumor Associated Antigens. *J. Med. Chem. 32*, 2326–2330.

(7) Barth, R. F., Fazlul, A., Soloway, A. H., and Adams, D. M. (1985) Delivery of Boron-10 for Neutron Capture Therapy by Means of Polyclonal and Monoclonal Antibodies: Progress and Problems. *Proceedings of the Second International Symposium on Neutron Capture Therapy*, Oct 18-20, Tokyo, Japan, pp 346–352.

(8) Barth, R. F., Fazlul, A., Soloway, A. H., Adams, D. M., and Steplewski, Z. (1986) Boronated Monoclonal Antibody 17-1A for Potential Neutron Capture Therapy of Colorectal Cancer. *Hybridoma 5, Suppl. 1*, s43-s50.

(9) Alam, F., Soloway, A. H., McGillire, J. E., Barth, R. F., Carey, W. E., and Adams, D. (1985) Dicesium *N*-Succinimidyl 3-(Un-

decahydro-*closo*-dodecaboranyldithio)propionate, a Novel Heterobifunctional Boronating Agent. *J. Med. Chem. 28*, 522–525.
(10) Barth, R. F., Mafune, N., Adams, D. M., Soloway, A. H., Makroglou, G. E., Oredipe, O. A., Bule, T. E., and Steplewski, Z. (1989) Conjugation, Purification and Characterization of Boronated Monoclonal Antibodies for Use in Neutron Capture Therapy. *Strahlenther. Onkol. 165*, 142–145.
(11) Elmore, J. J., Jr., Borg, D. C., Gabel, D., Fairchild, R. G., Temponi, M., and Ferrone, S. (1985) Boronated Dextran–Monoclonal Antibody Conjugates for NCT. *Proceedings of the Second International Symposium on Neutron Capture Therapy*, Oct 18-20, Tokyo, Japan, pp 367–381.
(12) Abraham, R., Müller, R., and Gabel, D. (1989) Boronated Antibodies for Neutron Capture Therapy. *Strahlenther. Onkol. 165*, 148–151.
(13) Pettersson, M. L., Courel, M. N., Girard, N., Gabel, D., and Delpech, B. (1989) In Vitro Immunological Activity of a Dextran-Boronated Monoclonal Antibody. *Strahlenther. Onkol. 165*, 151–152.
(14) Tamat, S. R., Patwardhan, A., Moore, D. E., Kabral, A., Bradstock, K., Hersey, P., and Allen, B. J. (1989) Boronated Monoclonal Antibodies for Potential Neutron Capture Therapy of Malignant Melanoma and Leukaemia. *Strahlenther. Onkol. 165*, 145–147.
(15) Maurer, J. L., Serino, A. J., and Hawthorne, M. F. (1988) Hydrophilically Augmented Glycosyl Carborane Derivatives for Incorporation in Antibody Conjugation Reagents. *Organometallics 7*, 2519–2524.
(16) Stewart, J. M., and Young, J. D. (1984) *Solid Phase Peptide Synthesis*, Pierce Chemical Company, Rockford, IL.
(17) Leukart, O., Caviezel, M., Eberle, A., Escher, E., Tun-Kyi, A., and Schwyzer, R. (1986) L-*O*-Carboranylalanine, a Boron Analogue of Phenylalamine. *Helv. Chim. Acta 59*, 2184–2187.
(18) Fauchere, J. L., Leukart, O., Eberle, A., and Schwyzer, R. (1979) The Synthesis of [4-Carboranylalanine, 5-Leucine]-Enkephalin. *Helv. Chim. Acta 62*, 1385–1395.
(19) Leukart, O., Regoli, D., and Schwyzer, R. (1979) Synthesis of Angiotensins, Bradykinins and Substance P Octapeptides in which the Residues Phe and Tyr Have Been Replaced with Car and of [Car[1], Leu[5]]-Enkephalin. *Helv. Chim. Acta 62*, 526–552.
(20) Escher, E., Guillemette, G., Leukart, O., and Regoli, D. (1980) Pharmacological Properties of Two Analogues of Angiotensin II Containing Carboranylalamine (Car). *Eur. J. Pharmacol. 66*, 267–272.
(21) Owen, D. A., and Hawthorne, M. F. (1969) Preparation of 4-Substituted (3)-1,7-Dicarba-*nido*-dodecahydroundecaborate-(−1) Ions and 3-Substituted 1,8-Dicarba-*closo*-undecaborane-(11). *J. Am. Chem. Soc. 91*, 6002–6010.
(22) Hawthorne, M. F., Varadarajan, A., Knobler, C. B., Chakrabarti, S., Paxton, R. J., Beatty, B. G., and Curtis, F. L. (1990) Radiometallacarboranes as Tumor Imaging Reagents. *J. Am. Chem. Soc. 112*, 5365–5366.
(23) Varadarjan, A., and Hawthorne, M. F. Unpublished results.
(24) O'Donnell, M. J., and Polt, R. L. (1982) A Mild and Efficient Route to Schiff's Base Derivatives of Amino Acids. *J. Org. Chem. 47*, 2663–2666.
(25) Stork, A., Leong, A. Y. W., and Touzin, A. M. (1976) Alkylation and Michael Additions of Glycine Ethyl Ester. Use in α-Amino Acid Synthesis and as Acyl Carbanion Equivalent. *J. Org. Chem. 41*, 3491–3493.
(26) Zakharkin, L. I., Brarsev, V. A., Chapovskii, and Yu, A. (1965) Some Reactions of Alkyl Halides, Alcohols, and Acids of the Barene Series. *J. Gen. Chem. USSR. 35*, 2149–2155.
(27) Harris, C. J. (1981) Abnormal Alkylation of *N*-Benzylidene-α-Amino Ester Anions with α-Haloesters. *Tetrahedron Lett. 22*, 4863–4866.
(28) O'Donnell, M. J., and Wojciechowski, K. (1984) Alkylation of Protected α-Amino Acid Derivatives in the Presence of Potassium Carbonate. *Synthesis* 313–315.
(29) Ponnusamy, E. Fotador, U., Spisni, A., and Fiat, D. (1985) A Novel Method for the Rapid, Nonaqueous t-Butoxycarbonylation of Some ^{17}O-Labelled Amino Acids and ^{17}O-N.M.R. Parameters of the Products. *Synthesis* 48–49.
(30) Consalvo, A. P., Tamburini, P. P., Stern, W., and Young, S. D. (1989) Methods for the Carboxyl-Terminal Fluorescent Labeling of Peptides Using Solid Phase Peptide Synthesis. *Tetrahedron Lett. 30*, 39–42.
(31) Hawthorne, M. F., Wegner, P. A., and Stafford, R. C. (1965) Comments on the Reaction of Amines with 1,2-Dicarbaclovododecaborane(12). *Inorg. Chem. 4*, 1675.
(32) Fauchere, J. L., Do, K. Q., Jow, P. Y. C., and Hansch, C. (1980) Unusually Strong Lipophilicity of 'Fat' or 'Super' Amino-acids, Including, a New Reference Value for Glycine. *Experientia 36*, 1203–1204.
(33) Maurer, J. L., Berchier, F., Serino, A. J., Knobler, C. B., and Hawthorne, M. F. (1990) Glycosylcarborane Derivatives and the Determination of the Absolute Configuration of a Disastereomeric Triol from X-ray Diffraction. *J. Org. Chem. 55*, 838–842.

Synthesis and Evaluation of Radioiodinated Cholesteryl Ethers as Lipoprotein Probes

Laura E. DeForge,[†,‡] Mohamed K. Ruyan,[§] Susan W. Schwendner,[†] Roger S. Newton,[∥] and Raymond E. Counsell*[,†,§]

Department of Pharmacology and Interdepartmental Program in Medicinal Chemistry, University of Michigan, Ann Arbor, Michigan, and Parke-Davis Pharmaceutical Research Division, Warner-Lambert Co., Ann Arbor, Michigan. Received April 1, 1991

Two novel cholesteryl ether derivatives were synthesized and radioiodinated: (1) [^{125}I]cholesteryl *m*-iodobenzyl ether (^{125}I-CIBE) and (2) [^{125}I]cholesteryl 12-(*m*-iodophenyl)dodecyl ether (^{125}I-CIDE). These radioiodinated ethers were incorporated into low-density lipoprotein (LDL) by incubating the compounds (solubilized in saline with Tween-20) with isolated LDL or with whole plasma. Such LDL preparations were taken up by cultured fibroblasts in a receptor-dependent manner similar to that of radioiodinated LDL. Upon injection into guinea pigs, ^{125}I-CIBE-labeled guinea pig LDL cleared from the plasma similarly to radioiodinated guinea pig LDL. The primary sites of ^{125}I-CIBE uptake were the adrenal and the liver, and the compound was stable to both hydrolysis and deiodination over 24 h. In summary, ^{125}I-CIBE and ^{125}I-CIDE, like previously described tritiated cholesteryl ethers, appear to be potentially useful tracers of cholesteryl ester uptake. Moreover, these radioiodinated probes have the advantage of being more easily quantitated in tissue samples as well as being detectable by noninvasive scintigraphic imaging.

INTRODUCTION

The availability of lipid analogues that are both radiolabeled and nonmetabolizable has made an important contribution to understanding the tissue distribution and uptake of naturally occurring lipids. This has been particularly true for studies involving lipoproteins wherein the predominant components of the lipoprotein core are the readily hydrolyzable cholesteryl esters and triglycerides. The efforts of Halperin et al. (*1*) have been particularly noteworthy in this regard inasmuch as they have described the synthesis and biological properties of a variety of tritium-labeled lipid ethers such as [^{3}H]cholesteryl linoleyl ether and [^{3}H]trialkyl glycerol ethers.

Because of our interest in tracers for diagnostic imaging, our attention has focused on lipid analogues labeled with γ-emitting nuclides such as the various radioisotopes of iodine, namely ^{123}I, ^{125}I, and ^{131}I (*2*). Radioiodinated lipids, such as [^{131}I]19-iodocholesterol, have been found to be useful not only as diagnostic agents in nuclear medicine (*3, 4*) but also as radiolabeled probes in biochemical studies (*5*). Radioiodinated γ-emitting probes offer the advantage of being more readily counted than tritium or carbon-14-labeled compounds and frequently their synthesis is more readily accomplished.

One class of radioiodinated probes that we believe will be of interest to investigators involved in lipoprotein research evolved from our recent work with radioiodinated cholesteryl ethers. Earlier studies in our laboratories gave rise to several radioiodinated cholesteryl esters, such as [^{125}I]cholesteryl iopanoate, which were found to be relatively resistant to in vivo hydrolysis (*6, 7*). As a follow-up to these studies, we synthesized the ^{125}I-labeled cholesteryl ethers shown in Chart I. These two structures were selected to represent short (CIBE) and long-chain (CIDE) analogues of cholesteryl esters and depart from the cholesteryl ester structure by having (*1*) an ether rather than ester linkage at C-3 and (*2*) a radioiodinated benzene ring in place of part of the acyl chain. These chemical changes were introduced in order to prevent in vivo hydrolysis and to stabilize the tracer to in vivo deiodination.

This paper describes the synthesis of the iodinated cholesteryl ether analogues and their labeling with radioiodine. Also described in their preliminary evaluation as suitable probes for the lipophilic core of lipoproteins, with incorporation of these ^{125}I-labeled cholesteryl ethers into low-density lipoprotein (LDL) being of primary interest.

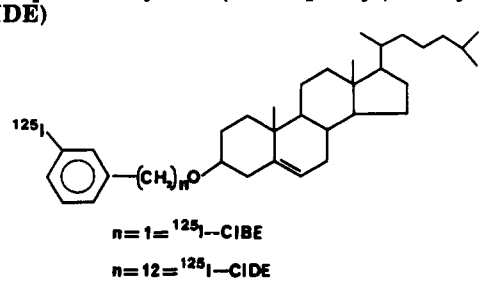
EXPERIMENTAL PROCEDURES

Materials. Melting points were determined on a Thomas-Hoover melting point apparatus and are uncorrected. Infrared spectra (IR) were obtained with KBr or NaCl pellets on a Nicolet 5DXT Fourier transform spectrophotometer. Proton nuclear magnetic resonance (^{1}H NMR) spectra were recorded on a Bruker WP270SY at 270 MHz. Chemical shifts were reported in parts per million relative to tetramethylsilane. Elemental analyses were performed by Midwest Microlab, Ltd., Indianapolis, IN. Thin-layer chromatography (TLC) was performed on either Merck silica gel-60 F_{254} polyethylene-backed plates or Analtech silica gel GHLF glass-backed plates. Visualization was achieved by UV, I_2, and charring after spraying with 50% H_2SO_4. TLC analyses of radioiodinated compounds were performed with Merck silica gel-60 plates which were then scanned with a Vanguard 930 autoscanner or Berthold radiochromatogram scanner Model LB2723. Column chromatography was carried out with Davisil 62 silica gel from Grace, Davison Chemical, Baltimore, MD. Radioiodinated compounds were purified by column chromatography with Merck silica gel-60 (230–400 mesh) or by HPLC. HPLC was performed with an ALTEX Model 110A pump, a Gibson Model 111 LC detector set at 254 nm, and a Whatman PXS 10/25 silica gel column. Radioiodination reactions were performed

* Address correspondence to R. E. Counsell, Ph.D., M6322 Medical Science Bldg. I, Department of Pharmacology, University of Michigan Medical School, Ann Arbor, MI 48109–0626.
† Department of Pharmacology, University of Michigan.
‡ Present address: Department of Pathology, University of Michigan Medical School, Ann Arbor, MI.
§ Interdepartmental Program in Medicinal Chemistry.
∥ Warner-Lambert Co.

1043-1802/91/2902-0254$02.50/0 © 1991 American Chemical Society

Chart I. Structures for Radioiodinated Cholesteryl Ethers [^{125}I]Cholesteryl *m*-Iodobenzyl Ether (^{125}I-CIBE) and [^{125}I]cholesteryl 12-(*m*-Iodophenyl)dodecyl Ether (^{125}I-CIDE)



inside a plexiglass glove box vented with a Model RIT-140 radioiodine trap (H_1Q Filter Products, La Jolla, CA). Tetrahydrofuran (THF) was distilled from $LiAlH_4$ under nitrogen. Benzene was distilled from sodium metal under nitrogen. The $CHCl_3$ was dried (K_2CO_3), distilled, and stored over molecular sieves. Chemical starting materials were purchased from Aldrich Chemical Co. (Milwaukee, WI), and Na^{125}I was obtained from Amersham (Arlington Hts., IL).

The University of Michigan Hospital apheresis clinic provided units of blood drawn from normal human volunteers. Guinea pigs were obtained from Charles River Laboratories (Portage, MI). LDL was isolated from human and guinea pig plasma with a Beckman L8-80 ultracentrifuge and a 60Ti rotor. Na^{125}I for radioiodination of LDL was obtained from ICN (Irvine, CA). Silica gel TLC plates backed with poly(ethylene terephthalate) were purchased from the Eastman Kodak Co. (Rochester, NY). Radioactive samples were counted in a Searle Model 1185 γ-counter (counting efficiency ca. 87%), and TLC strips were scanned with a Berthold radiochromatogram scanner. Sodium dodecyl sulfate–polyacrylamide gel electrophoresis was conducted with a Hoeffer SE-600 electrophoresis chamber (Hoeffer Scientific Instruments, San Francisco, CA) and a Bio-Rad 1420B power supply (Bio-Rad, Richmond, CA). Fibroblasts from a patient with familial hypercholesterolemia were obtained from the Human Genetic Mutant Cell Repository (Camden, NJ). Intramedic PE-50 polyethylene tubing (Clay Adams, Parsippany, NJ) was gas sterilized in Surgipeel packages (Suricot, Smithtown, NY) for use as cannulae in the guinea pig studies.

Synthesis of Cholesteryl m-Iodobenzyl Ether (CIBE). Cholesterol (568 mg, 1.98 mmol), anhydrous dimethoxyethane (8.0 mL), and NaH (140 mg, 15.8 mmol) were added to a flame-dried, nitrogen-flushed, round-bottom flask. The reaction mixture was stirred for 5 min at room temperature whereupon *m*-iodobenzyl chloride (500 mg, 1.98 mmol) was added slowly with continued stirring. The resulting mixture was heated to reflux for 6 h and allowed to cool, and water (20 mL) added. The contents were transferred to a separatory funnel and extracted with ether (3 × 20 mL). The ether extracts were combined and dried over anhydrous $MgSO_4$, and the solvent was removed under reduced pressure. The remaining solid residue was dissolved in a minimum amount of benzene–hexane (3:7) and chromatographed with a silica gel column (53 g silica) and benzene–hexane (3:7) as eluant. This afforded cholesteryl *m*-iodobenzyl ether (CIBE) as a white solid which was readily recrystallized from acetone to furnish an analytical sample (472 mg, 40%). Mp: 95–96 °C. NMR (270 MHz, $CDCl_3$): δ 7.71 (s, 1 H, arom H_2), 7.6 (d, 1 H, arom H_4), 7.32 (d, 1 H, arom H_6), 7.07 (t, 1 H, arom H_5), 5.35 (d, 1 H, 6 vinyl H), 4.49 (s, 2 H, $PhCH_2O$), 3.26 (m, 1 H, α-H), 1.02 (s, 3 H, 19-CH_3), 0.89 (d, 3 H, 21-CH_3, J = 6.46 Hz), 0.85 (d, 6 H, 26 and 27-CH_3, J = 6.54 Hz), 0.68 (s, 3 H, 18-CH_3). Anal. Calcd for $C_{35}H_{51}IO$: C, 67.76; H, 8.53; I, 21.06. Found: C, 67.56; H, 8.72; I, 21.25.

Synthesis of Cholesteryl 12-(m-Iodophenyl)dodecyl Ether (CIDE). NaH (40 mg, 1.33 mmol) was added in several portions under anhydrous conditions at room temperature to a solution of cholesterol (500 mg, 1.29 mmol) in ethyl ether (5 mL) and dimethyl sulfoxide (2 mL). The reaction mixture was allowed to stir for 5 min before a solution of 12-(*m*-iodophenyl)dodecylmethanesulfonate (400 mg, 0.86 mmol) (*8*) in ether (5 mL) was added dropwise over 5 min. The reaction mixture was heated at 40 °C for 10 h; TLC (silica; benzene–hexane 1:1) indicated the absence of starting methanesulfonate and the presence of the cholesterol ether (R_f = 0.6). The reaction mixture was added to a separatory funnel containing water (50 mL) and was extracted with ethyl ether (3 × 50 mL). The ether fractions were pooled and dried over $MgSO_4$ before removing the solvent under reduced pressure. The residue was dissolved in benzene–hexane (3:7, 5 mL) and applied to a column (silica; 10 g) which was subsequently eluted with benzene–hexane (3:7). The fractions containing the product were pooled and the solvent was removed under reduced pressure. The residual oil was dried overnight in vacuo to afford 216 mg (33.2%) of the desired ether (CIDE). NMR (270 MHz, $CDCl_3$): δ 7.54 (s, 1 H, arom H_2), 7.5 (d, 1 H, arom H_4), 7.13 (d, 1 H, arom H_6), 7.0 (t, 1 H, arom H_5), 5.35 (d, 1 H, 6 vinyl H), 3.45 (t, 2 H, CH_2O), 3.12 (m, 1 H, α-H), 2.53 (t, 2 H, $PhCH_2$), 1.0 (s, 3 H, 19-CH_3), 0.92 (d, 3 H, 21 CH_3, J = 6.46 Hz), 0.87 (d, 6 H, 26 and 27-CH_3, J = 6.54 Hz), 0.68 (s, 3 H, 18 CH_3). Anal. Calcd for $C_{45}H_{73}IO$: C, 71.40; H, 9.72. Found: C, 71.17; H, 9.64.

Radioiodination of Ethers—^{125}I-CIBE and ^{125}I-CIDE. [^{125}I]Sodium iodide (1.7 mCi) was added to a 1-mL vial containing CIBE (2.3 mg, 3.8 μM), L-ascorbic acid (4.5 mg, 25.6 μM), 0.4 M $CuSO_4$ solution (2 μL), and 1,3-dimethyl-3,4,5,6-tetrahydro-2(1*H*)-pyrimidinone (12 μL). The reaction vial was sealed with a Teflon septum and heated to 160 °C for 30 min. The reaction mixture was allowed to cool to room temperature and was then transferred to a silica gel column (4 g). Elution with 5% ethyl acetate–hexane provided a fraction that showed the radioiodinated products to comigrate with standard (R_f = 2.3) upon TLC (5% ethyl acetate–hexane). High-pressure liquid chromatography (HPLC) (2% ethyl acetate-hexane, flow rate = 1 mL/min) confirmed the purity of the CIBE product (t_R = 6.7 min). This procedure afforded radioiodinated CIBE (maximum yield, 1.54 mCi, 91%). Radioiodinated CIDE was prepared from CIDE in a similar manner. The product was purified by column chromatography (maximum yield, 200 μCi, 80%). Specific activities of the two compounds ranged between 60 and 400 mCi/mmol.

Incorporation of ^{125}I-CIBE and ^{125}I-CIDE into Human LDL. Tween-20 (100 μL/mg compound) was added to either ^{125}I-CIBE or ^{125}I-CIDE solubilized in hexane–ethyl acetate (19:1). The mixture was thoroughly agitated with a vortex mixer, the solvents were evaporated under a stream of nitrogen, and saline (0.9%) was added such that the Tween-20 constituted ≤3% of the final volume. The solution was vortexed again and placed briefly under nitrogen to remove any residual hexane. Aliquots of this final preparation were counted for radioactivity, and the radiochemical purity was evaluated by TLC in hexane–ethyl acetate (19:1). The TLC strips were analyzed either by radiochromatogram scanning or by

counting the strip as 1-cm segments in a γ-counter. The results demonstrated that the radioactivity migrated as a single peak of intact compound.

Blood was obtained from normal human volunteers. Preservatives and inhibitors of proteolysis were added as described by Edelstein and Scanu (*9*), and the plasma was obtained by low-speed centrifugation. The LDL (d = 1.020-1.063 g/mL) and lipoprotein deficient plasma (LDP, $d > 1.250$ g/mL) were then isolated by sequential ultracentrifugation (*10*) and dialyzed against at least 4 × 4 L of phosphate-buffered saline (PBS)–0.01% ethylenediaminetetraacetic acid (EDTA) prior to use. The LDL and LDP were then mixed with PBS such that their concentrations were roughly equivalent to those found in whole plasma (0.5 and 30–35 mg of protein/mL, respectively). An aliquot of formulated ^{125}I-CIBE or ^{125}I-CIDE equivalent to $^1/_{10}$ the volume of the LDL–LPD solution was then added. Typically, less than 0.5 mg of each compound (50–120 μCi) was added to a solution containing between 15 and 20 mg of LDL cholesterol. The mixture was then incubated at 37 °C with gentle agitation for 2 h. A preliminary time course study demonstrated that maximal incorporation of radioactivity was achieved at this time point. The radiolabeled LDL fraction (^{125}I-CIBE–LDL or ^{125}I-CIDE–LDL) was reisolated by a single ultracentrifugation step at a density of 1.063 g/mL (*10*) and dialyzed against PBS–0.01% EDTA. Aliquots of ^{125}I-CIBE-LDL and ^{125}I-CIDE–LDL were analyzed for protein (*11*) and radioactivity content. Additional analyses included lipid extraction (*12*), TLC analysis, 12% trichloroacetic acid (TCA) precipitation, and SDS–PAGE on 3-20% acrylamide gradient gels (*13*). Samples were extracted with ice-cold ether prior to SDS–PAGE analysis and were loaded onto the gels in a sample buffer containing 20 mM dithiothreitol. The gels were run overnight at 15 mA in a running buffer containing 25 mM Tris, 200 mM glycine, and 0.1% SDS (pH 8.4) and subsequently stained with Coomassie Blue G-250.

Incorporation of ^{125}I-CIBE into Guinea Pig LDL. Blood was obtained from male Hartley guinea pig (500–600 g) anesthetized with xylazine (10 mg) and ketamine (30 mg). Whole plasma, obtained by low-speed centrifugation and treated with preservatives and protease inhibitors (*9*), was incubated with formulated ^{125}I-CIBE as described above. The LDL fraction (^{125}I-CIBE–gpLDL) was then isolated by ultracentrifugation (*10*) between the densities of 1.020 and 1.100 g/mL (*14*).

Radioiodination of LDL. Human and guinea pig LDL were isolated from plasma as described above and radioiodinated on the surface protein (^{125}I-LDL or ^{125}I-gpLDL) by using the iodine monochloride method (*15*). Typically, the specific activities ranged between 100 and 300 dpm/ng, and the soluble and lipid-associated radioactivity constituted less than 3% and less than 8% of the total radioactivity, respectively.

Fibroblast Uptake Studies. Uptake of the ^{125}I-cholesteryl ether labeled LDL preparations was examined in both normal human fibroblasts and LDL receptor negative fibroblasts obtained from a patient with familial hypercholesterolemia (GM-1915). Radioiodinated LDL (either ^{125}I-LDL or ^{125}I-gpLDL) served as a control. Vials of both cell lines (10–13 passage) were removed from liquid nitrogen, quickly thawed, and diluted to a concentration of 3×10^5 cells/mL in Dulbecco's Modified Eagle Medium (DME) containing 100 units/mL penicillin, 100 μg/mL streptomycin, and 10% fetal bovine serum. Aliquots of the cell suspension (1 mL) were plated onto 35-mm cell culture dishes and incubated for 6 days at 37 °C in a humidified atmosphere containing 5% CO_2. The media was changed every other day. On day 6 (18 h prior to the experiment), the media was replaced with DME containing 5% human lipoprotein deficient serum (LDS). At the time of the experiment (day 7), the media was replaced with 1 mL of fresh DME + 5% LDS. The cells were then dosed with 10 μg/mL radiolabeled LDL, either in the absence or in the presence of a 20-fold excess of native human LDL, and incubated for 6 h at 37 °C.

At the end of the incubation period, the media was removed from the plates and stored for later analysis. The cells were placed on ice and washed during two 10-min incubations with PBS containing 2% BSA, followed by one 10-min incubation and two rinses with PBS without BSA. After drying overnight, the cells were digested in 1 N NaOH and aliquots were assayed for protein (*11*) and radioactivity content. Some samples were also subjected to lipid extraction (*12*) and TLC analysis as described above.

The radioactivity in the media corresponding to noniodide LDL degradation products was determined by precipitating the intact lipoproteins with 50% TCA followed by precipitation of free iodide with 5% silver nitrate (*16*). The total uptake of the LDL preparations over the 6-h incubation period (an expression which includes bound, internalized, and degraded LDL) was then calculated from the cell-associated radioactivity and the LDL degradation products in the media.

Determination of Plasma Clearance Rates. Male Hartley guinea pigs (500–600 g) were anesthetized as described above, and the cartoid artery was cannulated (*17*) with an 18-in. length of gas-sterilized PE-50 polyethylene tubing filled with sterile physiologic saline supplemented with 75 units/mL heparin. The cannula was externalized via a small incision centered at the back of the neck ca. 1 in. below the ears. The incisions were then closed with sutures or wound clips. After a short recovery period, either ^{125}I-CIBE–gpLDL or ^{125}I-gpLDL was injected via the cannula. The cannula was flushed with the saline–heparin solution, thereby delivering the dose to the animal with no retention of radioactivity in the tubing. Blood samples were drawn at several time points from conscious, restrained animals, flushing the cannula with saline–heparin and sealing the end of the tubing after each withdrawal. The plasma was immediately separated from the blood, and duplicate aliquots were counted for radioactivity. In addition, plasma samples from each time point were analyzed by 3% PAGE (*18*). The gels were cut according to the lipoprotein banding pattern (*18*) and counted to determine the percentage of radioactivity in association with the LDL fraction.

The percent injected dose remaining in the plasma at each time point was calculated, normalizing the 15 min time point to 100%. The fractional catabolic rates (FCR) of the LDL preparations were calculated by using a two-pool kinetic model (*19*) as originally described by Matthews (*20*).

Tissue Distribution of Radioactivity. The animals used in the plasma clearance studies were sacrificed at 24 h postinjection. Several tissues were removed, and duplicate samples of tissue minces were placed into gelatin capsules that were then weighed and counted for radioactivity. From this data, the dpm/mg of tissue was determined, thus allowing calculation of the percent injected dose/g of tissue. This value was then multiplied by the weight of the animal in kilograms, resulting in the final value in terms of percent (kg) dose/g, an expression

which corrects the results for any difference in the body weights of the animals.

Tissue Extraction. In additional studies, male Hartley guinea pigs were injected with formulated ^{125}I-CIBE and sacrificed at 24 h postinjection. Samples of adrenal, liver, and plasma were extracted according to the method of Folch et al. (*12*). The organic phase was analyzed by TLC in hexane–ethyl acetate (19:1) in order to determine the percentage of extractable tissue radioactivity comigrating with a ^{125}I-CIBE standard.

RESULTS

Synthesis. Of the various procedures discussed by Halperin et al. (*1*) for the preparation of cholesteryl ethers, the most satisfactory method was the classical Williamson-type reaction in which cholesteryl alcoholate is treated with the appropriate alkyl halide or alkyl methane sulfonate. The resulting iodinated long chain (CIDE) and short chain (CIBE) ethers (Chart I) were readily purified by column chromatography and subsequently characterized by NMR spectroscopy and elemental analysis. Labeling with radioiodine was accomplished by isotope exchange with [^{125}I]sodium iodide. Although this exchange reaction proceeded well in pivalic acid as previously described for cholesteryl iopanoate and other lipids (*21*), we found that superior results could be achieved by conducting the exchange in 1,3-dimethyl-3,4,5,6-tetrahydro-2(1*H*)-pyrimidinone in the presence of ascorbic acid and copper sulfate.

Analysis of ^{125}I-Cholesteryl Ether Labeled LDL. For preparations of human LDL labeled with the ^{125}I-labeled cholesteryl ethers, essentially all LDL protein and 63–71% of the added radioactivity were recovered. Specific activities ranged from 5 to 40 dpm/ng of protein. In addition, greater than 99% of the LDL-associated radioactivity was precipitable by 12% TCA, indicating that the compound was firmly associated with the lipoprotein. Furthermore, 95% of the radioactivity was extractable into chloroform–methanol (2:1), and 97% of the extracted radioactivity migrated as the parent compound upon TLC analysis in hexane–ethyl acetate (19:1), thus demonstrating that the compounds remained intact throughout the labeling and isolation procedures. Samples of ^{125}I-CIBE–LDL and ^{125}I-CIDE–LDL were also analyzed by SDS–PAGE on 3–20% gradient gels (*13*). The gels showed that as compared to a native LDL control, no degradation of the apoprotein B-100 (apo B-100) component appeared to have resulted from the labeling procedure. Preisolation of human LDL from whole plasma served both to increase the percentage of radioactivity recovered in the LDL fraction and to decrease the number of manipulations required with the radioactive preparations. The results of the labeling procedures were essentially identical with those for guinea pig LDL. In this instance, however, the formulated compound was added to whole guinea pig plasma, as the predominance of this lipoprotein fraction permitted adequate recovery of radioactivity within the LDL without its prior isolation.

Cell Uptake of ^{125}I-CIBE- and ^{125}I-CIDE-Labeled LDL. Fibroblast uptake studies were conducted to test the LDL receptor recognition capability of ^{125}I-CIBE–LDL and ^{125}I-CIDE–LDL, with ^{125}I-LDL as a control. The two cell lines used were a line of normal human fibroblasts and a line of mutant fibroblasts (obtained from a patient with familial hypercholesterolemia) which does not express the LDL receptor. The results showed that uptake of both ^{125}I-CIBE–LDL and ^{125}I-CIDE–LDL was quite similar to that of ^{125}I-LDL (Figure 1). The receptor-mediated

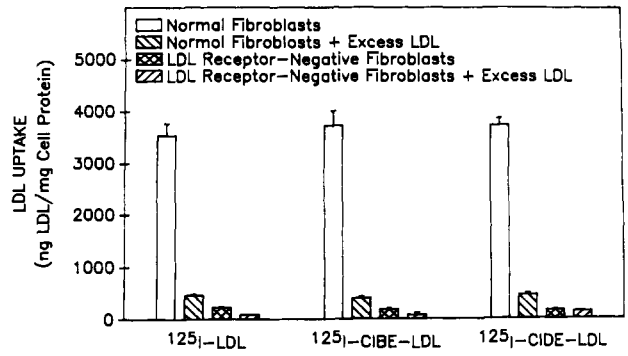


Figure 1. Fibroblast uptake of ^{125}I-LDL, ^{125}I-CIBE–LDL, and ^{125}I-CIDE–LDL. Plates of cells (n = 3) were incubated for 6 h with 10 μg/mL of each LDL preparation, either in the presence or the absence of a 20-fold excess of native human LDL. The cell lines used were normal human fibroblasts and mutant fibroblasts, obtained from a patient with familial hypercholesterolemia, which do not express the LDL receptor (GM-1915). The values shown are mean ± SEM.

nature of the uptake of all LDL preparations was validated by, first, the competitive reduction in uptake accompanying coincubation with a 20-fold excess of unlabeled native LDL, and, secondly, by the low levels of radioactivity taken up by the LDL receptor negative fibroblasts. Incubation of ^{125}I-CIBE and ^{125}I-CIDE solubilized in the Tween-20–saline vehicle with the cells resulted in extremely low levels of cell-associated radioactivity (data not shown). These results verified that nonspecific or detergent-mediated effects played a negligible role in the uptake of ^{125}I-CIBE–LDL and ^{125}I-CIDE–LDL. In addition, both compounds remained intact throughout the experiment. Lipid extraction and TLC analysis of the cell digests showed that the cell-associated radioactivity was still in the form of the parent compound. Moreover, radioactive LDL-degradation products recovered in the cell media accounted for less than 1% of ^{125}I-CIBE–LDL and ^{125}I-CIDE–LDL uptake, as compared to a value of 80% for ^{125}I-LDL.

Plasma Clearance of ^{125}I-CIBE-Labeled Guinea Pig LDL. While the above studies showed that both ^{125}I-CIBE and ^{125}I-CIDE were suitable for use as in vitro tracers of lipoprotein-associated cholesteryl esters, the question remained as to their suitability for in vivo experiments. To address this question, the more readily synthesized ^{125}I-CIBE was incorporated into guinea pig LDL. Guinea pigs were used in these in vivo studies since they are an excellent model of LDL metabolism, with the LDL fraction constituting between 70–80% of the plasma cholestrol (*22*, *23*).

The plasma clearance of ^{125}I-CIBE–gpLDL was compared to that of a ^{125}I-gpLDL control (Figure 2). Although the two curves are slightly different in shape, the calculated FCR values, which take into account the rate of clearance over the entire time course, were not significantly different. The FCR values were 0.098 ± 0.002 pools h^{-1} (mean ± SEM, n = 6) for ^{125}I-CIBE–gpLDL and 0.092 ± 0.003 pools h^{-1} (mean ± SEM, n = 3) for ^{125}I-gpLDL. These values were in the same range as those reported for guinea pig LDL by other investigators (*24*, *25*).

Each plasma sample was also analyzed in duplicate by 3% PAGE to assess the percent plasma radioactivity associated with the LDL fraction. The results showed that the LDL-associated radioactivity was consistently in the range of 72–77% for the animals injected with the ^{125}I-gpLDL control (Table I). For the ^{125}I-CIBE–gpLDL animals, the values were lower at the 15 and 30 min time points (62–65%), but paralleled the values observed for

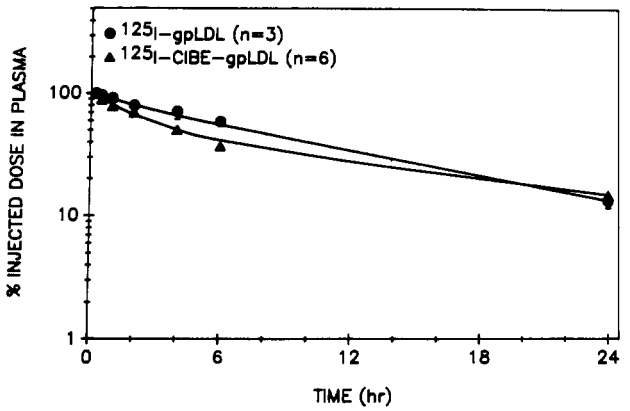


Figure 2. Clearance of radioactivity from the plasma of guinea pig injected with ^{125}I-CIBE–gpLDL or ^{125}I-gpLDL. Blood samples were drawn at several time points, and the percent injected dose remaining in the plasma was calculated, with the 15-min time point being normalized to 100%. The values represent mean ± SEM for the indicated number of animals.

Table I. Percent Plasma Radioactivity Associated with LDL in Guinea Pigs Injected with ^{125}I-CIBE–gpLDL or ^{125}I-gpLDL[a]

time, h	^{125}I-CIBE–gpLDL (n = 6)	^{125}I-gpLDL (n = 3)
0.25	63.9 ± 1.1[b]	71.8 ± 1.6
0.5	60.0 ± 1.5[b]	71.3 ± 1.4
1	72.0 ± 2.0	71.8 ± 1.4
2	72.2 ± 4.4	75.7 ± 1.8
4	77.7 ± 2.0	76.8 ± 2.3
6	77.1 ± 4.3	74.9 ± 3.2
24	95.7 ± 1.8[b,c]	73.8 ± 4.8

[a] Blood was obtained from the guinea pigs at the indicated time points, and the plasma was immediately separated and subjected to electrophoresis on 3% acrylamide gels. The gels were cut according to the lipoprotein banding pattern and counted for radioactivity. The results shown here represent the percentage of total gel radioactivity migrating within the LDL region (mean ± SEM for the indicated number of animals). [b] The values of the two groups are significantly different as assessed by unpaired Student's t tests: $p < 0.01$ at 0.25 h, $p < 0.005$ at 0.5 h, and $p < 0.01$ and 24 h. [c] n = 4 at this time point.

the ^{125}I-gpLDL group between 1 and 6 h. At 24 h, however, the percentage of plasma radioactivity associated with the LDL fraction was substantially higher for the ^{125}I-CIBE–gpLDL group as compared to the ^{125}I-gpLDL group. This difference can potentially be attributed to the stability of ^{125}I-CIBE to degradation (see below), which would result in lower plasma levels of radioactive degradation products as compared to ^{125}I-gpLDL.

Tissue Distribution of Radioactivity. The animals used in the clearance study were sacrificed at 24 h postinjection, and several tissues were analyzed for radioactivity. In both groups of animals, low levels of radioactivity (<1 % (kg) dose/g) were observed for most tissues (including bile, bone marrow, duodenum, fat, feces, kidney, lung, and spleen). The highest levels of radioactivity were observed for the adrenal and liver (Figure 3), tissues involved in lipoprotein metabolism and steroidogenesis which express the greatest numbers of LDL receptors (*26*). Radioactivity associated with the thyroid and urine was examined since it provides evidence of in vivo degradation of radioiodinated materials to such products as inorganic iodide and monoiodotyrosine (Figure 3). For the ^{125}I-gpLDL group, the lower levels of adrenal and liver radioactivity combined with the high levels of thyroid and urine radioactivity suggested that catabolism of the preparation resulted in the generation of radioactive degradation products. In contrast, the ^{125}I-CIBE–gpLDL animals showed higher

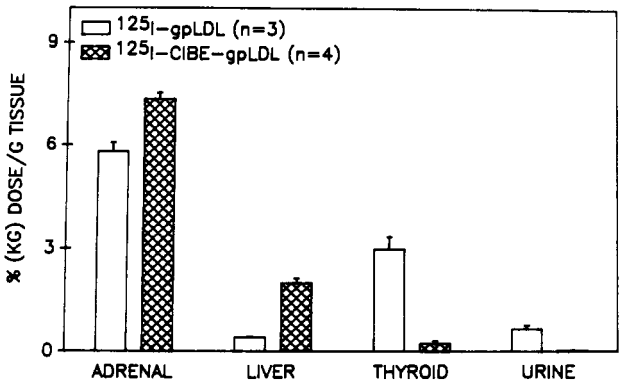


Figure 3. Tissue distribution of radioactivity in guinea pigs 24 h after injection of ^{125}I-CIBE–gpLDL or ^{125}I-gpLDL. The values represent the percent injected dose per gram of tissue multiplied by the weight of the animal in kilograms (mean ± SEM for the indicated number of animals).

Table II. Results of Lipid Extraction of Adrenal, Liver, and Plasma Samples Obtained from Male Guinea Pigs Sacrificed 24 h after Injection of ^{125}I-CIBE[a]

tissue	% $CHCl_3$–CH_3OH extractable (n = 5)	intact (n = 5)
adrenal	87.4 ± 1.7	96.2 ± 0.7
liver	89.9 ± 1.0	84.4 ± 3.1
plasma	90.0 ± 3.3	88.9 ± 2.0

[a] Lipid extractions were performed according to the method of Folch et al. (13) on adrenal, liver, and plasma samples obtained from guinea pigs 24 h after injection of ^{125}I-CIBE. Both the percent radioactivity extractable into the chloroform–methanol (2:1) phase and the percent of this radioactivity comigrating with the parent compound upon TLC analysis are shown. Values represent mean ± SEM for the indicated number of animals.

levels of adrenal and liver radioactivity and substantially lower thyroid and urine radioactivity. The low levels of thyroid and urine radioactivity indicate that ^{125}I-CIBE was quite stable to deiodination, a property which was likely conferred by placement of the radioiodine on the aromatic ring of the compound.

Stability of ^{125}I-CIBE in Vivo. The stability of ^{125}I-CIBE to hydrolysis in vivo was further evaluated by lipid extraction and TLC analysis of adrenal, liver, and plasma samples (Table II) obtained 24 h after injection of formulated ^{125}I-CIBE into guinea pigs. Greater than 87% of the tissue radioactivity present in the adrenal and liver was extractable into the chloroform–methanol (2:1) phase, with 84–96% of this radioactivity comigrating with the parent compound upon TLC analysis. These results were in close agreement with those derived from similar analysis of liver extracts from rats injected with [^{3}H]cholesteryl linoleyl ether (*27*) and with [^{125}I]cholesteryl iopanoate, a nonhydrolyzable cholesteryl ester analogue (*6*).

DISCUSSION

Evaluation of cholesteryl ester uptake both in vivo and in vitro is greatly simplified by the use of radiolabeled derivatives of cholesteryl ethers (*1*). Unlike naturally occurring cholesteryl esters, these compounds are not substrates for cholesteryl ester hydrolase and can thereby residualize at the site of uptake. The utility of compounds of this type has been amply illustrated by Stein and coworkers with [^{3}H]cholesteryl linoleyl ether (^{3}H-CLE) (*1*). Several additional advantages, however, could be gained by radiolabeling such agents with radioiodine. Not only is the synthesis often more readily accomplished, but γ-emitting radionuclides are more easily detected in tissue samples. In addition, radionuclides of this nature permit

noninvasive assessment of tissue distribution using nuclear medicine imaging techniques (*28*, *29*).

This report also describes a procedure for incorporating the radioiodinated cholesteryl ethers into LDL. This procedure is both comparatively simple and yields a specific activity compatible with scintigraphic imaging studies. The similarity of LDL labeled via this procedure to native LDL has been validated by studies that demonstrated that the preparations were taken up by cultured fibroblasts in a receptor-dependent manner indistinguishable from a radioiodinated LDL control. In addition, the fractional catabolic rate (an expression which takes into account the shape of the entire plasma clearance curve) of ^{125}I-CIBE–LDL was not significantly different from that of the ^{125}I-gpLDL control, verifying that the preparation was metabolized similarly to native LDL in vivo as well. Analyses such as TCA precipitation, chloroform–methanol extraction, and TLC have confirmed that ^{125}I-CIBE and ^{125}I-CIDE remain resistant to deiodination and hydrolysis both in vitro and in vivo and that they remain in firm association with the LDL particles.

The results obtained with Tween-20 in formulating the cholesteryl ethers prior to their incubation with LDL were equivalent or superior (in terms of recovery of radioactivity and LDL protein) to those obtained with other agents such as sodium deoxycholate, octyl glucoside, and Triton X-100 (unpublished observations). In addition, the labeling method described herein provided some advantages over other commonly used methods of incorporating lipids into the LDL core. For example, we have found the delipidation/reconstitution procedure described by Krieger et al. (*30*) to yield lower recoveries of protein and radioactivity and to result in an LDL preparation that is markedly heterogeneous in size. In addition, the labeling procedure described in this report allowed attainment of LDL specific activities which were ca. 1 order of magnitude greater than those reported for the lipid transfer protein mediated method described by Stein et al. (*31*). Lastly, it has been recently demonstrated that as compared to cholesteryl esters, cholesteryl ethers undergo a reduced rate of transfer via lipid transfer protein (*32*). We have observed this also to be true for ^{125}I-CIBE and ^{125}I-CIDE (paper in preparation). Although this may constitute a detriment to the use of cholesteryl ethers in certain types of studies, the lower rate of transfer of cholesteryl ethers may prove advantageous in studies wherein the retention of radiolabeled cholesterol derivatives within the core of a particular lipoprotein is desired, as in the case of tracing the in vivo tissue deposition of LDL labeled ex vivo with a radioactive tracer. Moreover, the impact of the reduced rate of cholesteryl ether transfer would be minimal in species, such as the guinea pig (*33*), with low levels of plasma lipid transfer activity.

In summary, these studies demonstrate that ^{125}I-CIBE and ^{125}I-CIDE are useful compounds for tracing the uptake of lipoprotein-associated cholesteryl esters both in vitro and in vivo. Although labeling LDL with these compounds was emphasized in this report, they appear similarly suitable for use in tracing the disposition of other lipoproteins in other animal species. In addition, both compounds can be alternatively labeled with ^{123}I or ^{131}I, isotopes better suited for noninvasive imaging.

ACKNOWLEDGMENT

We thank Ms. Edie Quenby and Ms. Lisa Flaherty for their expert assistance with the tissue distribution studies and Ms. Catherine Sekerke for radioiodination of the LDL. This research was supported in part by a grant from the National Institutes of Health (CA-08349).

LITERATURE CITED

(1) Halperin, G., Stein, O., and Stein, Y. (1986) Synthesis of ether analogs of lipoprotein lipids and their biological applications. *Methods Enzymol. 129B*, 816–848.

(2) Counsell, R. E., and Korn, N. (1979) Biochemical and pharmacological rationales in radiotracer design. In *Principles of Radiopharmacology* (L. G. Colombetti, Ed.) pp 53–77, CRC Press, Boca Raton, FL.

(3) Counsell, R. E., Ranade, V. V., Blair, R. J., Beierwaltes, W. H., and Weinhold, P. A. (1970) Tumor-localizing agents. IX. Radioiodinated cholesterol. *Steroids. 15*, 317–328.

(4) Britton, K. E. (1979) Radionuclide imaging in adrenal disease. In *The Adrenal Gland.* (V. H. T. James, Ed.) pp 309–322, Raven Press, New York.

(5) Counsell, R. E., and Korn, N. (1982) Radioiodinated cholesterol as a radiotracer in biochemical studies. In *Receptor-binding Radiotracers* (W. C. Eckelman, Ed.) pp 147–162, CRC Press, Boca Raton, FL.

(6) Seevers, R. H., Groziak, M. P., Weichert, J. P., Schwendner, S. W., Szabo, S. M., Longino, M. A., and Counsell, R. E. (1982) Potential tumor- or organ-imaging agents. 23. Sterol esters of iopanoic acid. *J. Med. Chem. 25*, 1500–1503.

(7) DeGalan, M. R., Schwendner, S. W., Weichert, J. P., and Counsell, R. E. (1986) Radioiodinated cholesteryl iopanoate as a potential probe for the in vivo visualization of atherosclerotic lesions in animals. *Pharm. Res. 3*, 52–55.

(8) Meyer, K. L., Schwendner, S. W., and Counsell, R. E. (1989) Potential tumor or organ-imaging agents. 30. Radioiodinated phospholipid ethers. *J. Med. Chem. 32*, 2142–2147.

(9) Edelstein, C., and Scanu, A. M. (1986) Precautionary measures for collecting blood destined for lipoprotein isolation. *Methods Enzymol. 128*, 151–155.

(10) Havel, R. J., Eder, H. A., and Bragdon, J. H. (1955) The distribution and chemical composition of ultracentrifugally separated lipoproteins in human serum. *J. Clin. Invest. 34*, 1345–1353.

(11) Lowry, O., Rosebrough, N., Farr, A., and Randall, R. (1951) Protein measurement with the Folin phenol reagent. *J. Biol. Chem. 193*, 265–275.

(12) Folch, J., Lees, M., and Sloane-Stanley, G. H. (1957) A simple method for the isolation and purification of total lipids from animal tissues. *J. Biol. Chem. 226*, 497–509.

(13) Cardin, A. D., Price, C. A., Hirose, N., Krivanek, M. A., Blankenship, D. T., Chao, J., and Mao, S. J. T. (1986) Structural organization of apolipoprotein B-100 of human low density lipoprotein. Comparison of B-48 of chylomicrons and very low density lipoproteins. *J. Biol. Chem. 261*, 16744–16748.

(14) Guo, L. S. S., Meng, M., Hamilton, R. L., and Ostwald, R. (1977) Changes in the plasma lipoprotein-apoproteins of guinea pigs in response to dietary cholesterol. *Biochemistry 16*, 5806–5812.

(15) Goldstein, J. L., Basu, S. K., and Brown, M. S. (1983) Receptor-mediated endocytosis of low-density lipoprotein in cultured cells. *Methods Enzymol. 98*, 241–260.

(16) Drevon, C. A., Attie, A. D., Pangburn, S. H., and Steinberg, D. 1981. Metabolism of homologous and heterologous lipoproteins by cultured rat and human skin fibroblasts. *J. Lipid Res. 22*, 37–46.

(17) Latham, A. N. (1977) A new chronically cannulated carotid artery preparation for determination of drug half-lives in guinea pig. *Can. J. Physiol. Pharmacol. 55*, 773–777.

(18) Narayan, K. A. (1975) Electrophoretic methods for the separation of serum lipoproteins. In *Analysis of Lipids and Lipoproteins* (E. G. Perkins, Ed.) pp 225–249, The American Oil Chemists Society, Champaign, IL.

(19) Langer, T., Strober, W., and Levy, R. I. (1972) The metabolism of low density lipoprotein in familial type II hyperlipoproteinemia. *J. Clin. Invest. 51*, 1528–1536.

(20) Matthews, C. M. E. (1957) The theory of tracer experiments with ^{131}I-labelled plasma proteins. *Phys. Med. Biol. 2*, 36–53.

(21) Weichert, J. P., Van Dort, M. E., Groziak, M. P., and Counsell, R. E. (1986) Radioiodination via isotope exchange in pivalic acid. *Appl. Radiat. Isot. 37*, 907–913.
(22) Spady, D. K., and Dietschy, J. M. (1983) Sterol synthesis in vivo in 18 tissues of the squirrel monkey, guinea pig, rabbit, hamster, and rat. *J. Lipid Res. 24*, 303–315.
(23) Sardet, C., Hansma, H., and Ostwald, R. (1972) Characterization of guinea pig plasma lipoproteins: the appearance of new lipoproteins in response to dietary cholesterol. *J. Lipid Res. 13*, 624–639.
(24) Witztum, J. L., Young, S. G., Elam, R. L., Carew, T. E., and Fisher, M. (1985) Cholestyramine-induced changes in low density lipoprotein composition and metabolism I. Studies in the guinea pig. *J. Lipid Res. 26*, 92–103.
(25) Luc, G., and Chapman, M. J. (1988) Guinea pig low density lipoproteins: structural and metabolic heterogeneity. *J. Lipid Res. 29*, 1251–1263.
(26) Spady, D. K., Bilheimer, D. W., and Dietschy, J. M. (1983) Rates of receptor-dependent and -independent low density lipoprotein uptake in the hamster. *Proc. Natl. Acad. Sci. U.S.A. 80*, 3499–3503.
(27) Higgs, D. W., van der Westhuyzen, D. R., Gevers, W., Coetzee, G. A., Stein, O., and Stein, Y. (1984) In vitro metabolism of LDL labeled with a nondegradable cholesteryl ester analogue. *Arteriosclerosis 4*, 208–213.
(28) Counsell, R. E., Schwendner, S. W., Gross, M. D., Longino, M. A., and McConnell, D. S. 1989. Lipoprotein incorporation enhances radioiodinated cholesteryl ester uptake into steroid hormone-secreting tissues. *J. Nucl. Med. 30*, 1088–1094.
(29) DeGalan, M. R., Schwendner, S. W., Skinner, R. W., Longino, M. A., Gross, M., and Counsell, R. E. (1988) Iodine-125 cholesteryl iopanoate for measuring extent of atherosclerosis in rabbits. *J. Nucl. Med. 29*, 503–508.
(30) Krieger, M., Brown, M. S., Faust, J. R., and Goldstein, J. L. (1978) Replacement of endogenous cholesteryl esters of low density lipoprotein with exogenous cholesteryl linoleate. Reconstitution of a biologically active particle. *J. Biol. Chem. 253*, 4093–4101.
(31) Stein, Y., Halperin, G., and Stein, O. (1981) The fate of cholesteryl linoleyl ether and cholesteryl linoleate in the intact rat after injection of biologically labeled human low density lipoprotein. *Biochem. Biophys. Acta 663*, 569–574.
(32) Green, S. R., Beltz, W. F., Goldberg, D. I., and Pittman, R. C. (1989) Cholesteryl oleyl and linoleyl ethers do not trace their counterparts in animals with plasma cholesteryl ester transfer activity. *J. Lipid Res. 30*, 1405–1410.
(33) Ha, Y. C., and Barter, P. J. (1982) Differences in plasma cholesteryl ester transfer activity in sixteen vertebrate species. *Comp. Biochem. Physiol. 71B*, 765–769.

Properties of Mitomycin C–Albumin Conjugates in Vitro and in Vivo

Tetsuro Tanaka, Yoshiharu Kaneo,* and Sadao Iguchi

Department of Pharmacy & Pharmaceutical Sciences, Fukuyama University, Sanzo, Higashimura-cho, Fukuyama 729-02, Japan. Received July 5, 1990

Mitomycin C, an antineoplastic agent, was covalently attached to bovine serum albumin through a spacer of the glutaryl group. Two different synthetic methods were adopted; one was by the prior glutarylation of albumin followed by binding to mitomycin C, and the other was by the synthesis of glutarylated mitomycin C followed by binding to albumin. Physicochemical properties of the conjugates, such as Stokes radius, molecular weight, and helical content, were comparatively examined. The glutarylation of albumin resulted in an increase in Stokes radius of the protein due to the conformational change. The conjugates significantly stabilized mitomycin C and liberated it gradually under the physiological condition ($t_{1/2}$ = 66–84 h). Both conjugates accumulated effectively in the tumor tissues. However, the distribution behavior of the conjugates depended on physicochemical properties such as molecular size. Treatment with the conjugates suppressed the tumor growth and increased the survival rate in the tumor-bearing mice.

INTRODUCTION

Macromolecular carrier systems have been developed in an attempt to optimize the delivery of antineoplastic agents. The idea behind use of drug–macromolecule conjugates is that they may show improvement in the distribution of the drug (*1*).

Mitomycin C (MMC) has the potential to act against a number of human neoplasms. However, it presents the problems of severe myelosuprression and gastrointestinal complications (*2*). A variety of macromolecular conjugates of MMC have been demonstrated in vitro and in vivo, e.g., antibodies (*3–6*), glycoprotein (*7*), albumin (*8, 9*), dextran (*10–14*), and synthetic macromolecules such as polylysine (*15*). Approaches that take advantage of antibodies show some potential for achieving active targeting; however, major obstacles remain in the application of these approaches (*16*). On the other hand, a process of passive targeting utilizes the natural distribution pattern of the macromolecular carrier to deliver the drug to the specific site of action.

Macromolecules such as albumin, globulins, and synthetic polymers accumulate in the tumor tissues because these tissues have a vascular network characterized by both enhanced permeability of the neovasculature and a lack of the lymphatic recovery system (*17, 18*). These findings led us to inquire whether MMC might accumulate in the tumor tissues by the use of albumin-conjugate system.

We have previously described the covalent attachment of MMC to serum albumin to give MMC–albumin conjugates which aided the tumor localization of MMC (*19*). Physicochemical properties of macromolecular carriers such as size and electric charge influence the biological properties of the macromolecular conjugate and hence require careful consideration (*12–15*). At the present stage of the investigation of MMC–albumin conjugates, little is known about these physicochemical and biological properties. In this study, we describe the methods to prepare MMC–albumin conjugates in which MMC is covalently attached to albumin through a glutaryl group spacer. The physicochemical properties of these conjugates, such as degree of chemical modification, molecular weight and size, α-helical content, and release of MMC, are reported, together with preliminary examinations of their biological behavior, such as antitumor activity, toxicity, pharmacokinetics, and tumor localization, in animals.

EXPERIMENTAL PROCEDURES

Reagents. Bovine serum albumin (BSA) (fraction V, Sigma Chemical Co., St. Louis, MO) was further purified by gel filtration on Sephadex G-150. Glutaric anhydride, MMC, 1-ethyl-3-[3-(dimethylamino)propyl]carbodiimide hydrochloride (EDC), *N*-hydroxysuccinimide, 2,4,6-trinitrobenzenesulfonic acid sodium salt (TNBS), and tetra-*n*-buthylammonium bromide (TBAB) were obtained from Nacalai Tesque, Inc. (Kyoto, Japan). Gel filtration calibration kits and molecular weight electrophoresis calibration kits were obtained from Pharmacia Fine Chemicals (Uppsala, Sweden). All other chemicals were of analytical grade or the best quality available.

Preparation of Albumin Conjugates of MMC. MMC was covalently attached to BSA through a glutaryl group spacer by the following methods.

Method 1. To a stirred solution of BSA (100 mg) in 1 M $NaHCO_3$ (10 mL) was added glutaric anhydride (400 mg) slowly in small portions. The pH of the reaction mixture was maintained within a range of 7.8–8.2 by the addition of 1 M NaOH for 1 h and gentle stirring at 4 °C for 16 h. The reaction mixture was washed repeatedly with a cold 0.9% NaCl solution by pressure dialysis using a Toyo UHP-43 ultrafiltration cell incorporating a UP-20 membrane (Toyo, Tokyo, Japan) and, finally, concentrated to a volume of 20 mL. Excess reagents and low molecular weight byproducts of the reaction were removed by this process. MMC (10 mg) and EDC (20 mg) were added to the solution of glutarylated BSA (G-BSA). The pH was maintained at 6.5, and the conjugating reaction was allowed to proceed for 1 h at room temperature. The reaction mixture was applied on a column of Sephadex G-25 (5 × 20 cm) developed with 0.9% NaCl. The conjugate of G-BSA and MMC (G-BSA–MMC) was eluted in the void volume, and free MMC was retarded by the gel. Fractions containing G-BSA–MMC were collected and lyophilized, producing a water-soluble powder. It was further purified by the use of a Sephadex G-150 column (2.5 × 47 cm).

Method 2. Glutaric anhydride (20.5 mg) was added to a solution of MMC (10 mg) in dry tetrahydrofuran (4 mL), and the mixture was heated under nitrogen atmosphere

* To whom communication should be directed.

1043-1802/91/2902-0261$02.50/0 © 1991 American Chemical Society

at 60 °C for 10 h. At the end of the reaction the solvent was evaporated. The residue was dissolved in distilled methanol (1 mL) and was chromatographed on a Sephadex LH-20 column (2.5 × 97 cm) developed with distilled methanol. The violet fractions were collected and evaporated to dryness to produce a glutarylated MMC (G-MMC). It was dissolved in dimethylformamide (1 mL), followed by the addition of EDC (11.6 mg) and *N*-hydroxysuccinimide (7.0 mg). The mixture was kept at room temperature for 17 h, then added dropwise to 15 mL of 0.1 M $NaHCO_3$ containing BSA (100 mg). The final mixture was allowed to react for 3 h, then applied on a column of Sephadex G-25 (5 × 20 cm) developed with 0.9% NaCl. Fractions containing the conjugate (BSA–G-MMC) were collected and lyophilized, producing a water-soluble powder. It was further purified by the use of a Sephadex G-150 column (2.5 × 47 cm).

MMC Content of the Conjugates. The MMC content of the conjugates was calculated from the UV absorbance at 363 nm in 0.9% NaCl with reference to the absorbance rate of the MMC standard. The protein content of the conjugate was determined by the method of Lowry et al. (*20*) with a BSA standard. The MMC content of the conjugate was calculated by dividing the content of MMC by that of protein.

Determination of Amino Groups. Free amino groups were determined according to the method of Fields (*21*). The sample solution (0.5 mL) was diluted with 0.5 mL of a borate buffer (0.1 M $Na_2B_4O_7$ in 0.1 M NaOH). Then, 0.2 mL of a solution of 0.11 M TNBS was added. After exactly 5 min, the reaction was stopped by addition of 2 mL of 0.1 M NaH_2PO_4 containing 1.5 mM Na_2SO_3. The absorption at 420 nm was correlated with the number of free amino groups.

Size-Exclusion Chromatography. The sample (3 mg in protein equivalents) dissolved in 0.3 mL of 0.2 M NaCl was applied on a column (1.0 × 47 cm) of Sephadex G-150. The mobile phase was 0.2 M NaCl, and the flow rate was 17.1 mL/h. The fractions (0.35 mL) were collected automatically. The absorbance of the eluted solution was monitored at 280 and 363 nm. The Stokes radius of the conjugate was determined by the calibration curve with four kinds of standard proteins. The data were analyzed according to the method of Laurent et al. (*22*).

Gel Electrophoresis. Sodium dodecyl sulfate polyacrylamide gel electrophoresis (SDS–PAGE) was performed according to the method of Laemmli (*23*). A separating gel (7 cm long) containing 10% acrylamide was used in combination with a stacking gel (1 cm long, 4.5% acrylamide). The samples (1.5 mg) were dissolved in 10 mL of Tris-HCl buffer (62.5 mM, pH 6.8) containing 2% of SDS, 10% of glycerol, 5% of $HSCH_2CH_2OH$, and 0.001% of bromophenol blue. After immersion into boiling water for 3 min, 10 μL of the loading buffer solution was applied on the stacking gel. Electrophoresis was carried out with a current of 20 mA per 8-cm width of the gel until the marker of bromophenol blue reached the bottom of the gel. After electrophoresis, the protein bands were visualized by staining with Coomassie Brilliant Blue. The molecular weight of the conjugate was estimated by the calibration curve.

Estimation of Helical Content. Circular dichroism (CD) spectra were recorded on a JASCO J-20C spectropolarimeter equipped with a J-DPZ data processor (Japan Spectroscopic Co. Ltd., Tokyo, Japan) using a 0.1 mm thick cuvette at room temperature (25 ± 3 °C) under constant nitrogen flush. The spectropolarimeter was calibrated by using androsterone, and each spectrum was the result of four or more accumulations. The sample concentration of the conjugate was 1.0 mg/mL. The helical content of the conjugate was estimated according to the method of Chang et al. (*24*).

Stability Experiments. The release of MMC and G-MMC from the conjugate was determined in a 0.1 M phosphate buffer system (pH 5.0, 6.0, 7.4, 8.0, and 9.0, $\mu = 0.3$) at 37 °C according to the method of Hashida et al. (*11*). The experiment was initiated by dissolving the conjugate in a preheated buffer solution to produce a concentration of 10 mg/mL. At a fixed time interval, the amounts of MMC and G-MMC released were determined simultaneously by using an HPLC method described later. The stability of MMC and the conjugates was also measured photometrically under the same conditions.

Animals and Tumor Cells. Male Wistar rates (190–210 g) and male ddY mice (20–30 g) were obtained from Japan SLC, Inc. (Shizuoka, Japan). Ehrlich ascites carcinoma (EAC) and Sarcoma 180 (S180) cells were kindly supplied by Dr. Sato (Sasaki Laboratory, Tokyo, Japan) and maintained in ddY mice by weekly intraperitoneal transplantation.

In Vitro Cytotoxicity. S180 cells were cultivated as a suspension in Eagle's minimum essential medium supplemented with 10% of heat-inactivated calf serum and incubated at 37 °C in a humidified 5% CO_2 atmosphere to prepare a cell stock solution. The number of viable cells was determined by the trypan blue exclusion method by using a Burker-Turk hematocytometer 3 days after incubation. The test compound was dissolved in the cultivation medium and 0.1 mL of this solution was added to test wells containing 0.1 mL of suspended S180 cells (2×10^5 cells/mL) such that 0.2 mL of the cell suspension had a test compound concentration of 0.1, 0.2, 0.3, 0.4, 0.6, and 0.8 mg/mL in MMC equivalents, respectively. Control wells were identical, except that the test compound was absent. The growth inhibition was calculated as growth inhibition (%) = $(C-T)/C \times 100$, where T and C represent the number of surviving cells in a treated group and that in an untreated group, respectively.

Animal Experiments. *1. Pharmacokinetics in Rats.* Rats fasted for 24 h were anesthetized with sodium pentobarbital (40 mg/kg, intraperitoneal injection). Depression of the body temperature was prevented with a heating plate and lamp. The femoral artery was cannulated with polyethylene tubing (PE-50, i.d. 0.58 mm, o.d. 0.965 mm, Clay Adams, Parsippany, NJ). The conjugate (0.5 mg/kg in MMC equivalents) or MMC (1 mg/kg) in 0.2 mL of 0.9% NaCl was injected through the jugular vein. Blood (0.5 mL) was collected periodically from the femoral artery after the injection. Plasma concentration of MMC was determined with a HPLC described later.

2. Tissue Distribution in Tumor-Bearing Mice. EAC cells (1×10^7 cells/mouse) were inoculated into the subcutaneous tissue of the axillary region of ddY mice. Fourteen days after the inoculation, the EAC-bearing mice were administered the conjugate (20 mg/kg in MMC equivalents) in 0.2 mL of 0.9% NaCl intravenously through the tail vein. After 24 h, the blood was collected from the vena cava under ether anesthesia and the tumor tissue, liver, spleen, kidney, lung, heart, intestine, and muscle were excised and weighed. Tissue levels of MMC were determined by using an HPLC method described later.

3. In Vivo Antitumor Activity. Inhibitory effect of the conjugate on the growth of S180 was studied according to the procedure of Takakura et al. (*14*). S180 cells (1×10^7 cells/mouse) were inoculated into the subcutaneous tissue of the axillary region of ddY mice. Four days after the

inoculation, a single intravenous dose of the conjugate (20 mg/kg in MMC equivalents) or MMC (5 mg/kg) dissolved in 0.2 mL of 0.9% NaCl was administered to the tumor-bearing mice. Tumor sizes were measured with calipers, and the tumor volumes (V) were calcualted as: $V = L \times W^2/2$, where L and W are length (mm) and width (mm), respectively. The tumor growth was monitored by the increasing rate of the tumor volume after the inoculation.

4. Acute Toxicity in Mice. Toxicities of the conjugates and MMC were evaluated with the survival on the 7th day after the intravenous single injection of the test compound to male ddY mice. LD_{50} values were determined according to Dixon (*25*). The mice were permitted access to food and water ad libitum. If a mouse died or appeared moribund the day after dosing, the dose for the next animal was decreased by a factor of 1/1.41; otherwise the dose for the next animal was increased by a factor of 1.41. By the up-and-down protocol, mice were observed for 7 days after dosing.

Analytical Method. The amounts of MMC and G-MMC released from the conjugate in vitro were determined simultaneously by HPLC. The chromatographic system (LC-6A, Shimadzu, Kyoto, Japan) with a variable-wavelength UV detector (SPD-6A) operated at 350 nm. A 4.6 × 250 mm, 5-μm particle size, C_{18} reversed-phase column (TSK gel 120T, Tosoh, Tokyo, Japan) was used at ambient temperature. The mobile phase was 20% acetonitrile in 40 mM phosphate buffer (pH 7.0), containing 2.5 mM TBAB as an ion-pairing agent. The injection volume was 80 μL, and the flow rate was 1.0 mL/min. It was confirmed that the determination of both MMC and G-MMC was not affected by the presence of the conjugate, and neither MMC nor G-MMC was liberated from the conjugate during the determination process. The concentration of MMC in plasma and tissue was determined as follows. Blood was centrifuged at 8000g for 30 s to obtain a plasma sample. The excised tissues were homogenized (25%) in 0.1 M phosphate buffer (pH 7.4). The plasma samples and the tissue homogenates were assayed according to the procedures of Hashida et al. (*11*). Briefly, the sample solution was added to four volumes of 1 M sodium carbonate buffer (pH 9.0). The mixture was ultrafiltered with a micropatition system (MPS-1, Amicon K.K., Tokyo, Japan), and the filtrate was injected into the HPLC. The mixture was heated at 90 °C for 5 min before ultrafiltration in order to determine the conjugated MMC. The amount of conjugated MMC was estimated by subtracting the amount of free MMC from that of total MMC obtained from the alkali hydrolysis. The recoveries of both free and conjugated MMC from each biological medium were highly reproducible. The HPLC conditions were identical with those described above except that the mobile phase of 20% acetonitrile in 50 mM phosphate buffer (pH 7.0) was used.

RESULTS

Preparation of Mitomycin C–Albumin Conjugates. Two types of MMC–albumin conjugates, namely, G-BSA–MMC and BSA–G-MMC, were synthesized. Figure 1 shows the UV absorption spectra of G-BSA–MMC, BSA–G-MMC, and the precursors G-BSA and BSA. Both MMC–albumin conjugates showed an absorbance which contains the pattern of free MMC between 300 and 400 nm, while the precursors themselves showed no UV absorption in this range. Since all free MMC and G-MMC had been previously removed by gel filtration, only MMC linked to the precursors would lead to the identical spectra.

Physicochemical properties of the conjugates are summarized in Table I. The MMC contents of G-BSA–MMC and BSA–G-MMC were 6.0 and 2.8 w/w %, respectively, corresponding to 12.1 and 5.6 mol of MMC/mol of BSA. The number of free amino groups of the conjugates was estimated by the method of Fields (*21*). One mole of BSA showed the color intensity of 28.5 mol of free amino groups with reference to the molar absorptivity of ϵ-amino groups of lysine (13 300 M^{-1} cm^{-1}). Table I shows that 22.9 mol of free amino groups was detected on the BSA–G-MMC molecule. The molar MMC content of BSA–G-MMC was equal to the decrease in the number of free amino groups. On the other hand, the acylation of BSA with glutaric anhydride caused a significant decrease in the number of free amino groups. One mole of G-BSA and G-BSA–MMC showed the color intensity of only 1.2 and 1.5 mol of free amino groups, respectively.

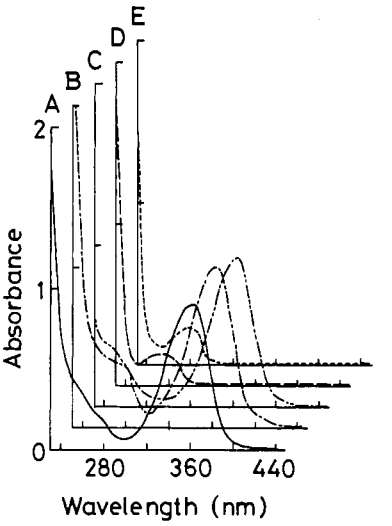


Figure 1. Representative UV absorption spectra of G-BSA–MMC (A), BSA–G-MMC (B), MMC (C), G-BSA (D), and BSA (E) in 0.9% NaCl.

Molecular Size. The effective molecular sizes of the conjugates were determined by size-exclusion chromatography (Figure 2). The elution volumes of G-BSA–MMC and G-BSA were smaller than that of BSA, indicating a significant increase in the Stokes radius (Table I). BSA–G-MMC showed, however, a small increase in the molecular size compared to that of BSA.

Molecular Weight. The molecular weights of the conjugates were determined by SDS–PAGE (Figure 3). The samples were treated with 2% SDS at 100 °C for 3 min prior to the gel electrophoresis. The molecular weights of both G-BSA–MMC and G-BSA were estimated to be somewhat larger than that of BSA by this method (Table I).

Helical Content. Figure 4 shows the CD spectra of the conjugates. Each spectrum consists of two negative dichroic bands located at 222 and 208 nm, respectively, and a crossover point at 200–201 nm, indicating the presence of a right-handed α-helical structure. Table I shows the estimated helical content of the conjugates. Both BSA–G-MMC and BSA contained ca. 50% of helical content. However, G-BSA–MMC and G-BSA had significant low values of helical content under the same conditions.

Stability of the Conjugates. The degradation of the conjugates was investigated in aqueous phosphate buffer solutions. The release of MMC was observed during the degradation of the conjugate at the pH range of 5.0–9.0 (Figure 5A,B). G-MMC was entirely undetected, however, in the experimental medium. The disappearance of both

Table I. Physicochemical Properties of G-BSA–MMC and BSA–G-MMC

	G-BSA–MMC	BSA–G-MMC	G-BSA	BSA
MMC content				
w/w %	6.03 ± 0.92	2.82 ± 0.51		
molar ratio	12.1 ± 1.8	5.59 ± 1.00		
free amino residue,[a] mol	1.5 ± 0.5	22.9 ± 1.4	1.2 ± 0.4	28.5 ± 0.8
effective molecular size,[b] Å	45.1	36.6	45.5	34.4
apparent molecular weight,[c] kDa	84	73	94	68
% helical content[d]	32.2 ± 3.3	50.4 ± 0.3	30.1 ± 4.4	51.6 ± 1.3

[a] Free amino groups were determined by the method of TNBS. [b] Effective molecular sizes were determined by a size-exclusion chromatography. [c] The apparent molecular weights were determined by SDS–PAGE. [d] Helical contents were estimated by the measurement of CD according to the method of Chang et al. (*24*).

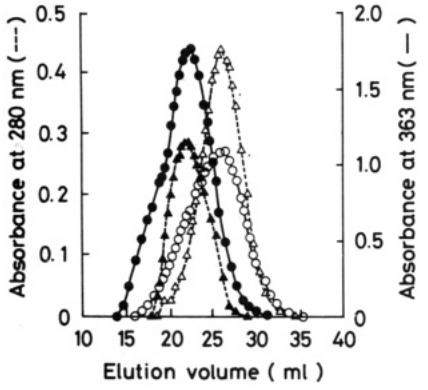


Figure 2. Elution profiles of G-BSA–MMC (—●—), G-BSA (--▲--), BSA–G-MMC (—○—), and BSA (--△--). Size-exclusion chromatography was carried out on a Sephadex G-150 column (1.0 × 47 cm) with 0.2 M NaCl at room temperature. G-BSA–MMC and BSA–G-MMC were spectrophotometrically detected at 363 nm, whereas G-BSA and BSA were detected at 280 nm.

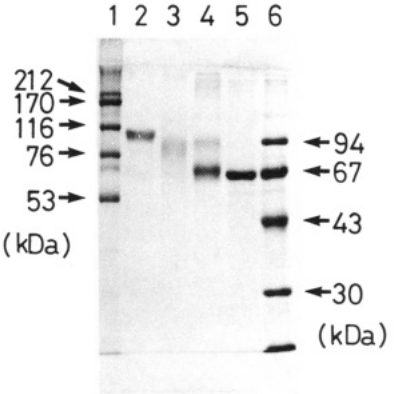


Figure 3. SDS–PAGE of G-BSA (lane 2), G-BSA–MMC (lane 3), BSA–G-MMC (lane 4), and BSA (lane 5). Aliquots of the sample were dissolved in the SDS–gel loading buffer containing 5% mercaptoethanol, heat-denatured, and loaded on the gel. After electrophoresis, the gel was stained with Coomassie Brilliant Blue. Lane 1 and lane 6 show the migration patterns for the standard proteins.

G-BSA–MMC and BSA–G-MMC in buffered solutions followed pseudo-first-order kinetics (Figure 5A,B). The degradation of MMC at each pH followed apparent first-order kinetics, as did that of the conjugates (Figure 5C).

On the basis of the present results, the overall reactions may be described by Scheme I, where k_1, k_2, and k_3 are apparent first-order rate constants for the depicted reactions. Thus, the concentration of the conjugate ([CONJUGATE]) and that of MMC released ([MMC]) in the buffered solution have a time dependence given by the following equations:

$$[\text{CONJUGATE}] = [\text{CONJUGATE}]_0 \times \exp(-(k_2 + k_3)t) \quad (1)$$

$$[\text{MMC}] = k_2 \times [\text{MMC}]^*/(k_1 - (k_2 + k_3)) \times \exp(-(k_2 + k_3)t) - \exp(-k_1 t) \quad (2)$$

where $[\text{CONJUGATE}]_0$ and $[\text{MMC}]^*$ represent the initial concentration of the conjugate and that of MMC covalently bound to the conjugate, respectively.

Based on these equations, curve fitting was done by using the nonlinear-least-squares program MULTI (*26*). The values of k_1 and k_2 showed good convergence. The degradation of MMC bound to the conjugate was regarded as negligible ($k_3 \doteq 0$) because a small negative value of k_3 with an extraordinarily large standard deviation was obtained.

The pH–rate profiles of k_1 and k_2 are shown in Figure 6. MMC was very stable above neutral pH, but decomposition increased markedly under acidic conditions (k_1, Figure 6). Both G-BSA–MMC and BSA–G-MMC were relatively stable at low pH contrary to the findings with MMC, but they predominantly release MMC at pH 9.0 (k_2, Figure 6). These results were similar to those obtained

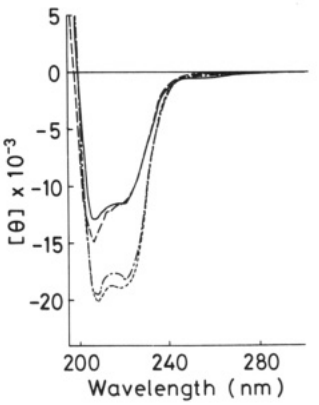


Figure 4. Circular dichroism spectra of G-BSA–MMC (—), BSA–G-MMC (— · —), G-BSA (– –), and BSA (--). Each spectrum was recorded in a 0.1 mm path length cell on a JASCO J-20C spectropolarimeter equipped with a J-DPZ data processor.

in the experiment of the MMC–asialofetuin conjugate (*7*). Half-lives of the release of MMC from G-BSA–MMC and BSA–G-MMC under specific physiological conditions (pH 7.4 and 37 °C) were 66.0 and 84.0 h, respectively.

In Vitro Cytotoxicity of the Conjugates. The cytotoxicity of G-BSA–MMC and BSA–G-MMC were evaluated in comparison with that of MMC by using a S180 cell line (Figure 7). As is evident, the cytotoxic effects of these compounds on S180 cells were concentration dependent. The concentrations required to produce 50% inhibition of growth (IC_{50}) are assembled in Table II. Both G-BSA–MMC and BSA–G-MMC had inhibitory effects on the cell growth slightly less than that of MMC.

Behavior of the Conjugates in the Circulation. The plasma concentration–time curve of MMC after a single intravenous injection of MMC is shown in Figure 8. The

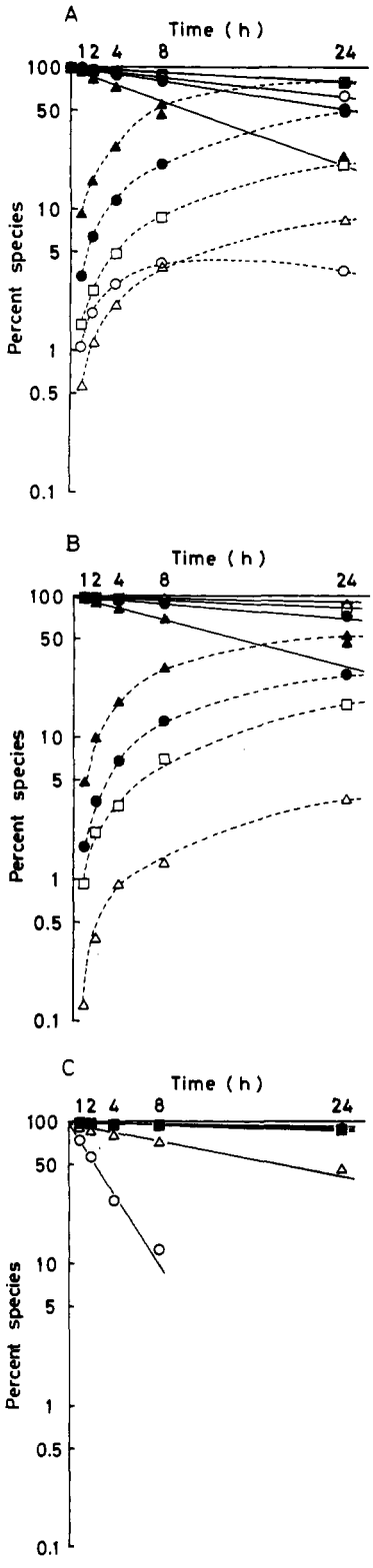


Figure 5. Stability of G-BSA–MMC (A), BSA–G-MMC (B), and MMC (C) in 0.1 M phosphate buffer solution (μ = 0.3) of pH 5.0 (○), 6.0 (△), 7.4 (□), 8.0 (●), and 9.0 (▲) at 37 °C. The dashed lines represent the time course of the regeneration of MMC from the conjugates.

pharmacokinetic evaluation of the data required a two-compartment open model with elimination occurring from the central compartment. Estimation of the pharmacokinetic parameters was done by using a nonlinear-least-squares program MULTI (*26*). A short half-life of 3.24 ± 1.08 min in the distribution phase (α-phase) suggested a rapid equilibration between plasma and tissues. The half-life of the elimination phase (β-phase) and the volume of

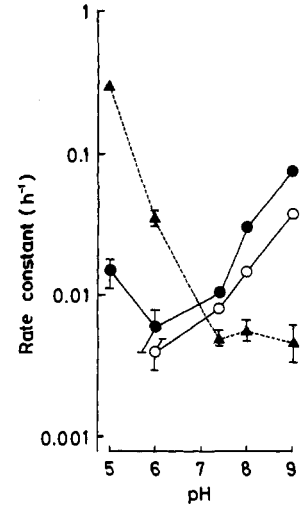


Figure 6. pH profile of the rate constants in the formation of MMC from the conjugates (k_2) and the degradation of MMC (k_1) in 0.1 M phosphate buffer solutions (μ = 0.3) at 37 °C: —●—, G-BSA–MMC; —○—, BSA-G-MMC; --▲--, MMC. Vertical bars represent SD calculated from 15–20 sets of experimental data by the least-squares method.

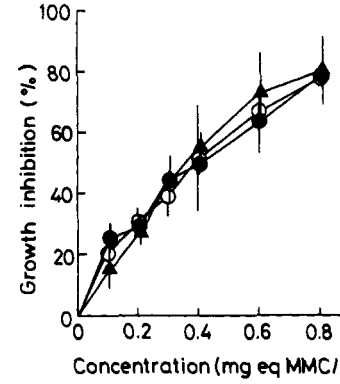
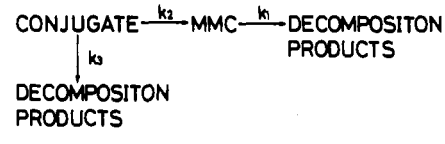


Figure 7. Cytotoxicity of G-BSA–MMC (●), BSA-G-MMC (○), and MMC (▲) against the S180 cell line. S180 cells were cultivated in the medium containing each test compound for 3 days, and the number of viable cells was determined by the trypan blue exclusion method. Growth inhibition (%) = $(C - T)/C \times 100$, where T and C represent the number of surviving cells in a treated group and that in an untreated group, respectively. Vertical bars represent SD of three experiments.

Scheme I



distribution of the central compartment were 22.8 ± 9.8 min and 435 ± 154 mL/kg, respectively.

Plasma concentration–time curves of G-BSA–MMC and BSA–G-MMC after a single injection of the conjugates are shown in Figure 9A and 9B, respectively. Since the MMC attached to the conjugate was determined, the concentrations of the conjugates were expressed as μg equivalents of MMC per mL. Both the conjugates showed the maximum levels immediately after injection and exhibited a monoexponential decline. Calculated elimination rate constants of G-BSA–MMC and BSA–G-MMC were 0.0179 ± 0.0032 and 0.0150 ± 0.0049 min^{-1}, corresponding to half-lives of 38.7 and 46.2 min, respectively. BSA–G-MMC was eliminated from the circulation a little slower than G-BSA–MMC. The values of the volume distribution of G-BSA–MMC and BSA–G-MMC were

Table II. Cytotoxicity, Antitumor Activity, and Acute Toxicity of G-BSA-MMC, BSA-G-MMC, and MMC

treatment	cytotoxicity:[a] IC_{50}, mg/mL in MMC equivalents	% survival after 40 days[b]	no. of mice	LD_{50},[c] mg/kg in MMC equivalents
G-BSA-MMC	0.4	75.0	8	51.1
BSA-G-MMC	0.4	100.0	6	67.3
MMC	0.3	71.4	14	11.1
control		39.3	27	

[a] S180 cells were cultivated in the medium containing each test compound for 3 days, and the number of viable cells was determined by the trypan blue exclusion method. Values express as the concentration required to produce 50% inhibition of growth. [b] Mice were inoculated subcutaneously with S180 cells (1×10^7 cells/mouse). Four days after the inoculation, mice were treated by single intravenous injection of G-BSA-MMC (20 mg/kg in MMC equivalents), BSA-G-MMC (20 mg/kg in MMC equivalents), or MMC (5 mg/kg). [c] Acute toxicity was evaluated with the survival on the 7th day after the intravenous single injection of the test compound to male ddY mice. LD_{50} values were determined according to the method of Dixon (25).

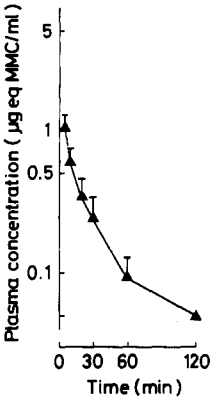


Figure 8. Plasma concentrations of MMC after a single intravenous injection of 1 mg/kg of MMC in rats. Each point represents the mean value and SD of three rats.

almost identical, being 33.5 ± 5.1 mL/kg and 33.1 ± 6.9 mL/kg, respectively.

Sustained concentrations of MMC after injection of the conjugates were observed in spite of the rapid elimination of MMC (Figure 9A,B). Higher and continuous levels of MMC were established especially by the administration of G-BSA-MMC. These conjugates appeared to release MMC continuously in the body.

Tissue Distribution of the Conjugates. Figure 10 shows the tissue distribution of MMC 24 h after a single intravenous injection of 20 mg/kg in MMC equivalents of the conjugates. Although free and conjugated forms of MMC were detected separately, most of MMC was detected as the conjugated form in the tissues. Both the conjugates mainly accumulated in the tumor tissues. G-BSA-MMC was distributed to the lung and the heart to some extent, and trace amounts of the conjugate were detected in the plasma (Figure 10A). BSA-G-MMC accumulated not only in the tumor tissue but also in tissues such as liver, spleen, and lung (Figure 10B). Significant amounts of BSA-G-MMC remained in the circulation even after 24 h. The concentration ratios of the tumor against the plasma were 62 and 2.8 for G-BSA-MMC and BSA-G-MMC, respectively.

In Vivo Antitumor Activity. Figure 11 shows the growth inhibition curves against S180 subcutaneously inoculated in mice. In the control, a remarkable tumor growth was observed, showing an 80 times increase in the ratio of the tumor volume after 30 days. A marked growth

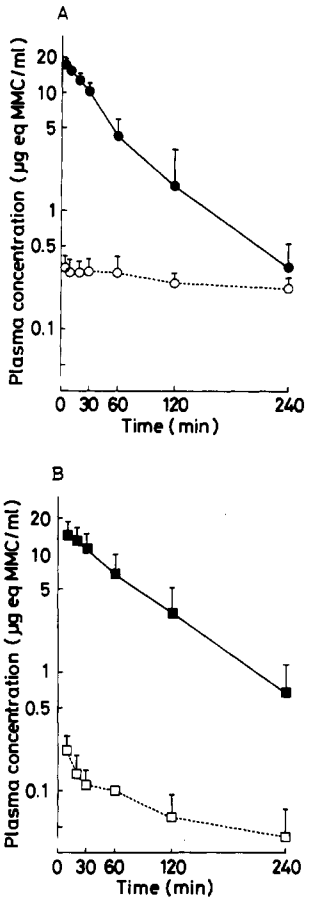


Figure 9. Plasma concentrations of the conjugated MMC (closed symbols) and the released MMC (open symbols) after a single intravenous injection of G-BSA-MMC (A) and BSA-G-MMC (B). Each dose was 0.5 mg/kg in MMC equivalents. Each point represents the mean value with SD of three rats.

inhibition was achieved by a single dose of each conjugate; the ratios of tumor volume were kept at low values even 30 days after inoculation. Table II shows the percentage of surviving mice in each treatment group. S180-bearing mice (control) exhibited a survival rate of 39% 40 days after inoculation. By the treatment with G-BSA-MMC and BSA-G-MMC (both 20 mg/kg in MMC equivalents), the 40-day survival rate increased to 75% and 100%, respectively. Similarly, an improvement of the 40-day survival rate was observed in the mice treated with MMC (5 mg/kg).

Acute Toxicity of the Conjugates. Acute intravenous LD_{50} values were determined by Dixon's up-and-down method. All animals were observed for 7 days after treatment. The LD_{50} values of G-BSA-MMC, BSA-G-MMC, and MMC were 51.1 mg/kg in MMC equivalents, 67.3 mg/kg in MMC equivalents, and 11.1 mg/kg, respectively (Table II). Severe weight loss and diarrhea were observed above the dose of LD_{50}.

DISCUSSION

A total of 60 mol of free amino groups (provided by the lysyl side chains and the single amino terminus)/mol of BSA has been determined by amino acid analysis and its primary sequence (28). In the case of BSA-G-MMC, 5.6 mol of free amino groups were modified by the binding of MMC. The number of the modified amino groups was identical with the MMC content of BSA-G-MMC (Table I). One mole of BSA showed the color development comparable to that of 28.5 mol of free amino groups according to the TNBS method. The extent of acylation

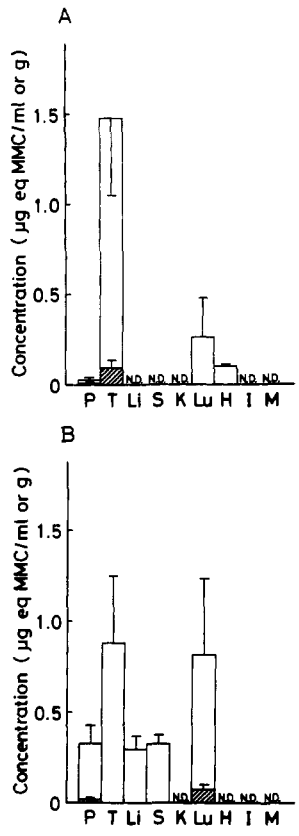


Figure 10. Tissue distribution of the conjugate (open column) and the released MMC (slant lines column) in mice bearing EAC 24 h after a single intravenous injection of G-BSA-MMC (A) and BSA-G-MMC (B). The EAC cells (1×10^7 cells/mouse) were inoculated subcutaneously, and 14 days later each conjugate (20 mg/kg in MMC equivalents) was administered. Results are expressed as the mean ± SD of three mice. Key: P, plasma; T, tumor; Li, liver; S, spleen; K, kidney; Lu, lung; H, heart; I, intestine; M, muscle; ND, not detectable.

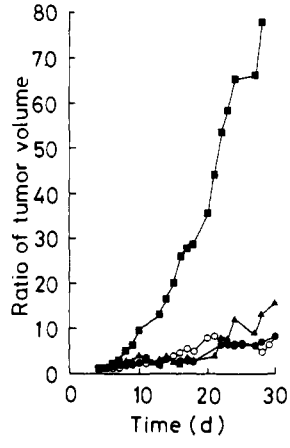


Figure 11. Growth inhibitory effects of G-BSA-MMC, BSA-G-MMC, and MMC on implanted S180 tumor. Mice were inoculated with S180 cells (1×10^7 cells/mouse) subcutaneously. Four days after the inoculation, a single intravenous dose of the test compound was administered as follows: ●, G-BSA-MMC (20 mg/kg in MMC equivalents); ○, BSA-G-MMC (20 mg/kg in MMC equivalents); ▲, MMC (5 mg/kg); ■, control (0.9% NaCl, 10 mL/kg). The ratio was calculated by dividing the tumor volume by the reference volume 4 days after the inoculation. Each point represents the mean value of the ratio (n = 6-27).

of BSA by glutaric anhydride could not be estimated adequately by the colorimetric method. It was found, however, that G-BSA and G-BSA-MMC had only 1-2 mol of reactive lysine residues on the molecular surface (Table I).

Kato and co-workers have prepared an albumin conjugate of MMC (BSA-MMC, 5.0% (w/w) MMC content) by binding MMC directly to BSA using large amount of carbodiimide (*8*). The effective molecular size of BSA-MMC they made (99 Å) was much larger than that of BSA (34.4 Å). BSA is readily polymerized during the carbodiimide reaction because it has both carboxyl and amino groups in its molecule. The prior acylation of BSA was found to prevent the protein polymerization in the presence of carbodiimide since the estimated molecular weight of G-BSA-MMC (84 kDa) was similar to that of BSA (68 kDa) (Table I). Thus, G-BSA-MMC prepared in this study showed a much smaller Stokes radius (45.1 Å) according to the size-exclusion chromatography on a Sephadex G-150 column (Table I). On the other hand, the synthetic method of preparing G-MMC followed by binding to BSA (Method 2) did not influence the effective molecular size nor the molecular weight of BSA (Table I).

Acylation, such as acetylation and succinylation, have been reported to cause conformational changes of the protein which are attributed to an electrostatic destabilization (*29*, *30*). Glutarylation also resulted in a 30% increase in the Stokes radius of BSA (Table I). Since a 40% decrease in the helical contents of G-BSA-MMC and G-BSA occurred, a partial unfolding and/or a conformational change of the BSA molecule were suggested (Table I).

HPLC analysis showed that the conjugates did not release G-MMC but MMC directly. The conjugates were very stable at pH 6.0, contrary to the findings for MMC, but it predominantly released MMC with the elevation of pH (Figure 5A,B and 6). MMC was relatively stable at basic pH, but the decomposition increased markedly below neutral pH (Figures 5C and 6). These results were similar to those obtained in the experiment with an MMC-dextran conjugate (*11*). Under the physiological conditions (pH 7.4 and 37 °C), BSA-G-MMC showed higher stability, with a half-life of 84.0 h, than G-BSA-MMC (66.0 h). The BSA-MMC conjugate synthesized by Kato et al. showed monoexponential release of MMC with a half-life of 20.2 h (*8*). The introduction of a glutaric spacer arm resulted in the slower release rate of MMC from the albumin conjugate. These findings indicate that covalent binding to BSA stabilizes MMC and that the macromolecular prodrugs G-BSA-MMC and BSA-G-MMC liberate MMC gradually under the physiological conditions.

The cytotoxic effects of MMC and its BSA conjugates on the S180 tumor cells were determined in the stationary cell culture. It was suggested that both G-BSA-MMC and BSA-G-MMC possess a cytotoxic activity against S180 in the in vitro cell culture system that was almost equivalent to that of MMC (Figure 7 and Table II).

In rats, the α- and β-half-lives of free MMC given as MMC were 3.2 and 22.8 min, respectively (Figure 8). The elimination of the conjugated MMC from the plasma after dosing G-BSA-MMC and BSA-G-MMC was slower than that of free MMC given as MMC, with $t_{1/2}$ of 38.7 and 46.2 min, respectively (Figure 9A,B). Since the plasma concentration-time profiles of free MMC after dosing the conjugates were not reconciled with the compartment model, the elimination parameters were calculated by the method of noncompartment model (*31*). The elimination half-lives of free MMC after administration of G-BSA-MMC and BSA-G-MMC were 8 and 2 h, respectively, and were much longer than that after dosing as MMC (Figure 9A,B). Sustained levels of free MMC in the plasma suggested that the conjugates release MMC continuously in the body.

Macromolecules such as albumin, globulins, and synthetic polymers accumulate in the tumor tissues because of the unique vascular characteristics and a lack of the lymphatic recovery system (*17, 18*). We found that both G-BSA–MMC and BSA–G-MMC markedly accumulate in the tumor tissues in mice (Figure 10A,B). Serum albumin is known to also distribute in the normal tissues including lung (*32*). These findings may account for the high concentration of BSA–G-MMC in the lung (Figure 10B). G-BSA–MMC, however, scarcely distributed to those normal tissues including lung, liver, and spleen (Figure 10A). The characteristic distribution patterns of the conjugates were partly explicable by the difference of the higher structure such as molecular size and helical content (Table I), because the pore radius of 40–58 Å was, for example, estimated for the pulmonary capillary membrane (*33*).

Effects of a single dose of 20 mg/kg in MMC equivalents of the conjugates on the growth inhibition of the tumor and on the survival rate in S180-bearing mice were almost equivalent to those of a 5 mg/kg single dose of MMC (Figure 11 and Table II). MMC has severe side effects such as myelosuppression, gastrointestinal complications, and so on. In practice, the treatment with the conjugates did not result in necrosis of the site of injection nor severe diarrhea, which were observed at all times by the treatment with MMC. These findings should account for the excellent efficiency of the conjugates compared to MMC.

The relative toxicities of the conjugates and MMC, as assessed by acute intravenous LD_{50} in the mice, were represented in order of decreasing potency by the following: MMC (11.1 mg/kg) ≫ G-BSA–MMC (51.1 mg/kg in MMC equivalents) > BSA–G-MMC (67.3 mg/kg in MMC equivalents). The slow release rates of MMC from G-BSA–MMC and BSA–G-MMC may account for their lower acute toxicities compared to that of MMC. Similarly, Kojima et al. suggested that the low acute toxicity of MMC–dextran conjugate compared to that of MMC was due to its slow hydrolytic liberation of MMC under physiological conditions (*10*).

The present investigation showed that the albumin conjugates of MMC effectively accumulate in the tumor tissues and that the distribution of the conjugates depends on physicochemical properties such as molecular size. Further experiments are in progress to evaluate the chemotherapeutic index of the macromolecular prodrug of MMC.

ACKNOWLEDGMENT

The authors are grateful to Dr. Sato of Sasaki Laboratory for gifts of EAC and S180 cells. The authors particularly acknowledge H. Kawashima and T. Sakaue for their technical assistance.

LITERATURE CITED

(1) Friend, D. R., and Pangburn, S. (1987) Site-specific drug delivery. *Med. Res. Rev. 7*, 53–106.

(2) Philips, F. S., Schwartz, H. S., and Sternberg, S. S. (1960) Pharmacology of mitomycin C. I. Toxicity and pathologic effects. *Cancer Res. 20*, 1354–1361.

(3) Suzuki, T., Sato, E., Goto, K., Katsurada, Y., Unno, K., and Takahashi, T. (1981) The preparation of mitomycin C, adriamycin and daunomycin covalently bound to antibodies as improved cancer chemotherapeutic agents. *Chem. Pharm. Bull. 29*, 844–848.

(4) Umemoto, N., Kato, Y., Takeda, Y., Saito, M., Hara, T., Seto, M., and Takahashi, T. (1984) Conjugates of mitomycin C with the immunoglobulin M monomer fragment of a monoclonal anti-MM46 immunoglobulin M antibody with or without serum albumin as intermediary. *J. Appl. Biochem. 6*, 297–307.

(5) Manabe, Y., Tsubota, T., Haruta, Y., Kataoka, K., Okazaki, M., Haisa, S., Nakamura, K., and Kimura, I. (1985) Production of a monoclonal antibody–mitomycin C conjugate, utilizing dextran T-40, and its biological activity. *Biochem. Pharmacol. 34*, 289–291.

(6) Iwasa, S., Konishi, E., Kondo, K., Suzuki, T., Akaza, H., and Niijima, T. (1987) Selective cytotoxicity of drug–monoclonal antibody conjugates against murine bladder tumor cells. *Chem. Pharm. Bull. 35*, 1128–1137.

(7) Kaneo, Y., Tanaka, T., and Iguchi, S. (1991) Targeting of mitomycin C to the liver by the use of asialofetuin as a carrier. *Chem. Pharm. Bull. 39*, 999–1003.

(8) Kato, A., Takakura, Y., Hashida, M., Kimura, T., and Sezaki, H. (1982) Physico-chemical and antitumor characteristics of high molecular weight prodrugs of mitomycin C. *Chem. Pharm. Bull. 30*, 2951–2957.

(9) Kato, Y., Tsukada, Y., Hara, T., and Hirai, H. (1983) Enhanced antitumor activity of mitomycin C conjugated with anti-α-fetoprotein antibody by a novel method of conjugation. *J. Appl. Biochem. 5*, 313–319.

(10) Kojima, T., Hashida, M., Muranishi, H., and Sezaki, H. (1980) Mitomycin C–dextran conjugate: a novel high molecular weight pro-drug of mitomycin C. *J. Pharm. Pharmacol. 32*, 30–34.

(11) Hashida, M., Takakura, Y., Matsumoto, S., Sasaki, H., Kato, A., Kojima, T., Muranishi, S., and Sezaki, H. (1983) Regeneration characteristics of mitomycin C–dextran conjugate in relation to its activity. *Chem. Pharm. Bull. 31*, 2055–2063.

(12) Hashida, M., Kato, A., Takakura, Y., and Sezaki, H. (1984) Disposition and pharmacokinetics of a polymeric prodrug of mitomycin C, mitomycin C–dextran conjugate, in the rat. *Drug. Metab. Dispos. 12*, 492–499.

(13) Matsumoto, S., Yamamoto, A., Takakura, Y., Hashida, M., Tanigawa, N., and Sezaki, H. (1986) Cellular interaction and in vitro antitumor activity of mitomycin C–dextran conjugate. *Cancer Res. 46*, 4463–4468.

(14) Takakura, Y., Takagi, A., Hashida, M., and Suzaki, H. (1987) Disposition and tumor localization of mitomycin C–dextran conjugates in mice. *Pharm. Res. 4*, 293–300.

(15) Roos, C. F., Matsumoto, S., Takakura, Y., Hashida, M., and Sezaki, H. (1984) Physicochemical and antitumor characteristics of some polyamino acid prodrugs of mitomycin C. *Int. J. Pharm. 22*, 75–87.

(16) Ram, B. P., and Tyle, P. (1987) Immunoconjugates: Applications in targeted drug delivery for cancer therapy. *Pharm. Res. 4*, 181–188.

(17) Potchen, E. J., Elliot, A. J., Siegal, B. A., Studer, R., and Evens, R. G. (1971) Phathophysiologic basis of soft tissue tumor scanning. *J. Surg. Oncol. 3*, 593–602.

(18) Matsumura, Y., and Maeda, H. (1986) A new concept for macromolecular therapeutics in cancer chemotherapy: mechanism of tumoritropic accumulation of proteins and the antitumor agent Smancs. *Cancer Res. 46*, 6387–6392.

(19) Kaneo, Y., Tanaka, T., and Iguchi, S. (1990) Preparation and properties of mitomycin C–albumin conjugate. *Chem. Pharm. Bull. 38*, 2614–2616.

(20) Lowry, O. H., Rosebrough, N. J., Farr, A. L., and Randall, R. J. (1951) Protein measurement with the folin phenol reagent. *J. Biol. Chem. 193*, 265–275.

(21) Fields, R. (1972) The rapid determination of amino groups with TNBS. *Methods Enzymol. 25*, 464–468.

(22) Laurent, T. C., and Killander, J. (1964) A theory of gel filtration and its experimental verification. *J. Chromatogr. 14*, 317–330.

(23) Laemmli, U. K. (1970) Cleavage of structural proteins during the assembly of the head of bacteriophage T4. *Nature 227*, 680–685.

(24) Chang, T.-S., and Sun, S. F. (1978) Structural studies on the succinylated bovine serum albumin. *Int. J. Pept. Protein Res. 11*, 65–72.

(25) Dixon, W. J. (1965) The up-and-down method for small samples. *J. Am. Statist. Assoc. 60*, 967–978.

(26) Yamaoka, K., Tanigawara, Y., Nakagawa, T., and Uno, T. (1981) A pharmacokinetic analysis program (MULTI) for microcomputer. *J. Pharmacobio*-Dyn. *4*, 879–885.

(27) Reference deleted in press.

(28) Reed, R. G., Putnam, F. W., and Peters, T., Jr. (1980) Sequence of residues 400–403 of bovine serum albumin. *Biochem. J. 191*, 867–868.

(29) Habeeb, A. F. S. A. (1966) Evaluation of conformational changes in chemically modified bovine serum albumins on a column of Sephadex. *Biochim. Biophys. Acta 121*, 21–25.

(30) Habeeb, A. F. S. A. (1967) Quantitation of conformational changes on chemical modification of proteins: Use of succinylated proteins as a model. *Arch. Biochem. Biophys. 121*, 652–664.

(31) Gibaldi, M. (1984) Noncompartmental Pharmacokinetics. In *Biopharmaceutics and Clinical Pharmacokinetics*, 3rd ed. (M. Gibaldi, Ed.) pp 17–28, Lea & Febiger, Philadelphia, PA.

(32) Ghitescu, L., Fixman, A., Simionescu, M., and Simionescu, N. (1986) Specific binding sites for albumin restricted to plasmalemmal vesicles of continuous capillary endothelium: Receptor-mediated transcytosis. *J. Cell. Biol. 102*, 1304–1311.

(33) Taylor, A. E., and Gaar, K. A., Jr (1970) Estimation of equivalent pore radii of pulmonary capilary and alveolar membrenes. *Am. J. Physiol. 218*, 1133–1140.

Ca^{2+}-Responsive Extensible Monolayer Membrane of Calmodulin-Albumin Conjugate

Tetsuya Miwa, Eiry Kobatake, Yoshihito Ikariyama, and Masuo Aizawa*

Department of Bioengineering, Faculty of Bioscience and Biotechnology, Tokyo Institute of Technology 4259 Nagatsuta, Midori-ku, Yokohama 227, Japan. Received January 14, 1991

A Ca^{2+}-responsive monolayer protein membrane was prepared by developing calmodulin and bovine serum albumin at the air-water interface and by conjugating them with a bifunctional agent. In the case of the BSA monolayer, complex formation with Mg^{2+} generated a larger change in surface pressure than that with Ca^{2+}. On the other hand, a drastic change in surface pressure was observed for the conjugated thin membrane associated with Ca^{2+} than that associated with Mg^{2+}. Due to a drastic change in the conformation of calmodulin, the conjugated protein film changes its morphology (STM image), depending on Ca^{2+} concentration: the extended structure in the presence of Ca^{2+} transforms to a shrinked structure in the absence of Ca^{2+}. The largest surface pressure change was detected when calmodulin was mixed with an equimolar amount of bovine serum albumin.

INTRODUCTION

Ca^{2+} plays a very important role in the regulation of some biochemical reactions, which are modulated by a group of Ca^{2+}-binding proteins. The modulating proteins, calmodulins (CaM), undergo a drastic conformational change when they bind to Ca^{2+} (*1*, *2*) and amphiphilic peptides such as mastoparan and endorphin (*3*), which results in the modulation of many important biochemical reactions (*4*, *5*). Babu et al. have reported that the N-terminal and C-terminal rigid-structured globular domains of CaM are connected by a long flexible peptide of α-helical structure (*6*). Two Ca^{2+} ions are bound to each domain of CaM, and upon complexation with Ca^{2+}, CaM has two hydrophobic sites at both end domains (*7*, *8*).

We have already observed that such proteins as CaM and bovine serum albumin (BSA) can be developed at the air-water interface to form monolayer protein films (*9*, *10*). In previous works, the developed BSA monolayer was stabilized by cross-linking with a bifunctional reagent immediately after the preparation of protein monolayer. The BSA thin film thus prepared can be employed as a passive material, e.g., an ultrathin protein film for a matrix of enzyme-linked immunosorbent assays (*10*).

Here we describe a method of manufacturing an active material by conjugating a modulating protein with a matrix protein by using a multicompartment Langmuir-Blodgett trough (*11*, *12*) of Fromherz type (*13*, *14*). The modulating protein is expected to play the role of a trigger in the regulation of the matrix protein (bovine serum albumin). This is confirmed by the direct observation of the conjugated thin membrane in the presence (or absence) of Ca^{2+}. The Ca^{2+}-responsive conformationally changeable membrane may be a good model of a new drug-delivery system, where calcitonin or parathyloid hormone can be released for the homeostasis of serum Ca^{2+} level.

EXPERIMENTAL PROCEDURES

Materials. Calmodulin (CaM) was purified from porcine brain by following the method of Ishioka (*15*). The purity was ascertained by SDS-PAGE. Bovine serum albumin (BSA) was obtained from Nacalai Tesque (Kyoto, Japan), and glutaraldehyde was purchased from Kanto Chemical (Tokyo, Japan). All chemicals were guaranteed to be reagent grade. Highly oriented pyrolytic graphite (HOPG) having a surface area of 5×5 mm^2 was obtained from Le Carbone-Lorraine (Lorraine, France). All solutions were prepared with ultrapure water ($\geq$15 MΩ/cm) supplied by a Barnsted (Boston, MA) Water-I system.

Protein Monolayer Preparation. The surface pressure (F) of every protein monolayer at the air-water interface was monitored by a Wilhelmy balance, as a function of the surface area (A). Protein solutions (10 μM) of 10-20 μL were spread onto ultrapure water or a 1 mM $CaCl_2$ containing subphase at 15 °C and compressed at a rate of 14 mm^2/s from a trough whose initial surface area was 200 cm^2. Limiting molecular areas were obtained by linear extrapolation of the experimental data ($5 \leq F \leq 20$ mN/m) to $F = 0$. The limiting surface area corresponds to the molecular size.

Cross-Linking of Protein Monolayer. A multicompartment LB trough of Fromherz type was employed (*13*), and the trough was composed of eight compartments, each having a 45 cm^2 surface area. The surface pressure of each protein monolayer was kept at 11 mN/m before conjugation. Protein monolayer enclosed by two barriers was transported to a 0.5% glutaraldehyde subphase at a rate of 43 mm^2/s in the manner illustrated in Figure 1. After incubation for 1 h, the resulting cross-linked protein monolayer was rinsed by moving it to a compartment filled with ultrapure water. The rinsing was consecutively repeated in the next compartment.

Changing of Ion Concentration. Protein monolayer was moved to a neighboring trough of $CaCl_2$ or $MgCl_2$ solution of different cation concentration from an ultrapure water subphase at a rate of 43 mm^2/s to examine the roles of divalent cations. After the experimentation the transferred membranes were rinsed twice by shifting them to another two compartments filled with ultrapure water in a similar manner to the above-mentioned.

Scanning Tunneling Microscopy (STM) Image of Conjugated Protein Monolayer. Transferring each conjugated monolayer onto HOPG was performed as follows: a freshly cleaved piece of HOPG was placed in one compartment of the trough. After each cross-linked protein monolayer was shifted to this compartment, the transferring of each monolayer to HOPG was made with the decrease of water level by aspiration. The protein monolayer was dried at room temperature for 1 h before every STM study.

* To whom correspondence should be addressed.

1043-1802/91/2902-0270$02.50/0 © 1991 American Chemical Society

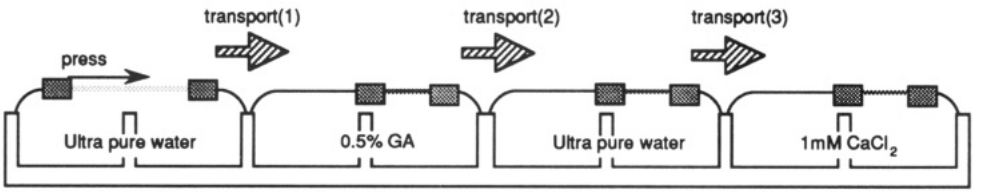


Figure 1. A schematic illustration of the multicompartment LB trough: transport 1 is the transfer of the monolayer developed on the subphase from ultrapure water to a 0.5% glutaraldehyde containing trough; transport 2 is from the 0.5% glutaraldehyde trough to an ultrapure water compartment; transport 3 is the movement from an ultrapure water to the 1 mM $CaCl_2$ containing compartment.

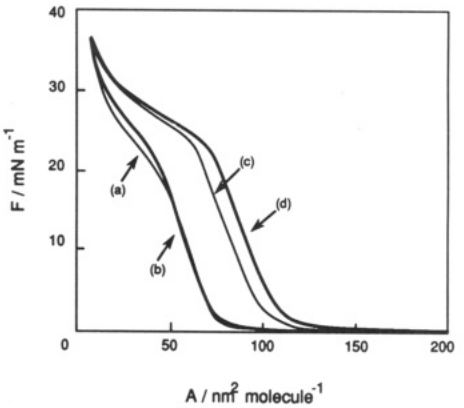


Figure 2. Surface pressure–area curves for BSA (a, c) and CaM–BSA mixture (b, d) at the air–water interface. Each protein (0.1 nmol) was spread onto ultrapure water (a, b) and onto a 1 mM $CaCl_2$ containing solution (c, d).

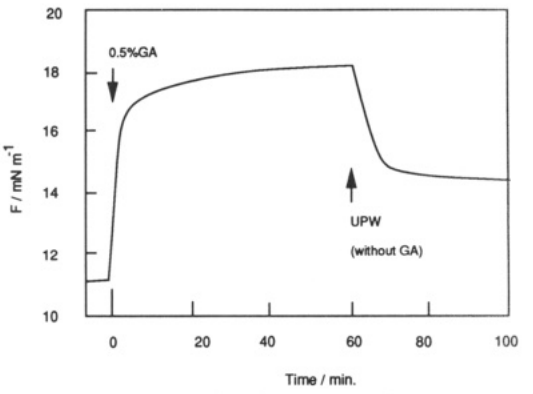


Figure 3. Time course of the change in surface pressure of the CaM–BSA monolayer upon transferring to 0.5% glutaraldehyde solution. The 0.5% GA arrow indicates the transferring to the subphase of 0.5% glutaraldehyde. The UPW arrow indicates the retransfer to ultrapure water for rinsing the monolayer.

STM was carried out with a SAM 3000 (Seiko Instruments Inc., Tokyo, Japan) in the room's atmosphere and temperature under a constant tunneling current of 0.8 nA. A mechanically polished Pt/Ir wire probe was employed. The distance between the probe tip and the targeted protein monolayer was set by a bias potential of less than 100 mV.

RESULTS AND DISCUSSION

Protein Monolayer from a Mixture of BSA and CaM. Figure 2 shows the force–area (F–A) curves obtained for BSA and CaM mixed with equimolar quantity of BSA (isomole mixture). The X axis corresponds to cross section in nm^2. In the compression of BSA and CaM mixed with BSA, typical F–A curves were obtained. In the case of ultrapure water, the F–A curve became a straight line in the range from 1 to 20 mN/m. The collapse of both the protein layer and the protein mixture layer was found to occur when the pressure was greater than 32 mN/m. Extrapolation of the linear portion of the F–A curve of the BSA monolayer to F = 0 yielded a limiting area of 76 nm^2/BSA molecule, whereas that obtained for the CaM–BSA mixture was slightly smaller. This is due to the molecular weight of CaM (16.7 kDa) being smaller than that of BSA (69.0 kDa). On the other hand, in the presence of 1 mM $CaCl_2$ and in the surface pressure range from 1 to 24 mN/m, more straight F–A curves were obtained for both BSA and the BSA–CaM mixture. These straight lines were slightly longer than those for the F–A curves obtained in the subphase of Ca^{2+}–free ultrapure water. Extrapolation of the linear portions of the F–A curves of the BSA monolayer and the CaM–BSA monolayer to F = 0 yielded limiting areas of 102 and 110 nm^2 for a BSA molecule and for a mixture of the proteins BSA and CaM, respectively. The difference in the limiting area (8 nm^2) between the BSA monolayer and the CaM–BSA conjugated monolayer is probably due to the conformational change of Ca^{2+}-bound CaM in the monolayer. Recent studies on the binding of CaM to other proteins have clarified that CaM binds to its target protein as long as the target protein contains an amphiphilic helix (*16*, *17*). Amphiphilic peptides such as mastoparan and melittin are believed to be sandwiched by hydrophobic clefts in the two halves of calmodulin (*8*). BSA seems likely to have four amphiphilic helices involving Ile-67 through Ala-86, Gly-131 through Lys-153, Ile-240 through Ser-260, Ile-465 through Ser-485, and Gln-580 through Thr-598 by hydropathy plot (*18*). The flexibility of the central connecting polypeptide between two end domains in CaM is indispensable for the binding of the two proteins and the following modulation (*1*, *19*). The conformational change seems large enough to induce stretching of the thin protein film, which is in good agreement with the direct STM observation described later. The reason for shifting of the F–A curves to the right side in the presence of Ca^{2+} will also be discussed later.

Conjugation of CaM with BSA in Monolayer. Figure 3 shows the change in surface pressure after transferring the BSA–CaM monolayer to a 0.5% glutaraldehyde containing trough. The arrow indicates transport step 1 as illustrated in Figure 1, whereas the UPW arrow indicates transport step 2. The surface pressure of the protein monolayer increased about 7 mN/m by transferring the monolayer from the ultrapure water compartment to a 0.5% glutaraldehyde containing trough under a constant area. The change (decrease) in the surface pressure of the protein monolayer from the 0.5% glutaraldehyde trough to another ultrapure water trough was approximately one-half of the change (increase) of the surface pressure observed during glutaraldehyde coupling. This result suggests that a less flexible conformational change was caused by the cross-linking of proteins by the bifunctional reagent. Besides intermolecular coupling, the bifunctional agent seems to produce intramolecular bridging, since 8 and 60 amino groups including N-terminal amino acid are in CaM and BSA, respectively. The amino residues of Lys-75 and Lys-94 at

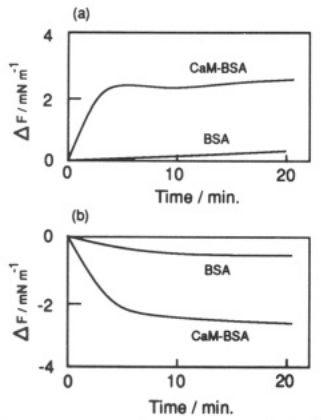


Figure 4. Surface pressure–time curves of the BSA monolayer and the CaM–BSA monolayer upon transferring from one compartment to another: (a) the monolayers were transferred to 1 mM $CaCl_2$ containing solution; (b) the monolayers were moved from Ca^{2+} solution to ultrapure water.

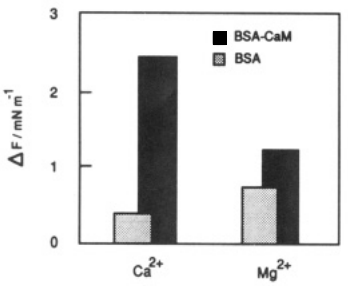


Figure 5. Histograms of the change in surface pressure of the BSA–CaM monolayer coexisted with either Ca^{2+} or Mg^{2+}. A conjugated BSA monolayer was also investigated for comparison.

the connecting polypeptide in CaM are likely to be most reactive in glutaraldehyde coupling (*3*).

Time Course of Surface Pressure Change of the Conjugated Monolayer. Figure 4 shows the time course of the changes in surface pressure of the BSA monolayer and BSA–CaM conjugated monolayer at a constant area when the protein monolayers were transferred from one trough to another. The measurement was done by moving the BSA monolayer and the BSA–CaM monolayer from an ultrapure water trough to a Ca^{2+}-containing one, by transport process 3 as illustrated in Figure 1. The surface pressure change of the monolayer protein film was stable for over 20 min. When the conjugated protein monolayer was transferred from an ultrapure water trough to a 1 mM $CaCl_2$ containing trough, the surface pressure of the isomolar mixture increased by over 2 mN/m, as shown in Figure 4a. In the case of the BSA monolayer manufactured in a similar way to the conjugated monolayer, the change in surface pressure was much smaller (about 0.4 mN/m) than that of the BSA–CaM monolayer. A larger increase in surface pressure of the conjugated monolayer of a unimolar mixture of CaM and BSA upon the transport to a 1 mM $CaCl_2$ containing trough seemed to be caused by the conformational change of Ca^{2+}-bound CaM in the BSA–CaM monolayer. On the other hand, the monolayer demonstrated the decrease in surface pressure, when it was moved to another trough of ultrapure water as shown in Figure 4b. The net change in surface pressure of the conjugated monolayer in the presence of Ca^{2+} was almost the same as that in the absence of Ca^{2+}. However, in case of the BSA monolayer, little change was observed.

Figure 5 shows the histograms of the net change of surface pressure of the BSA monolayer and the BSA–CaM monolayer to compare the effect of Ca^{2+}. Besides Ca^{2+}, we have taken Mg^{2+} as a typical divalent cation. The

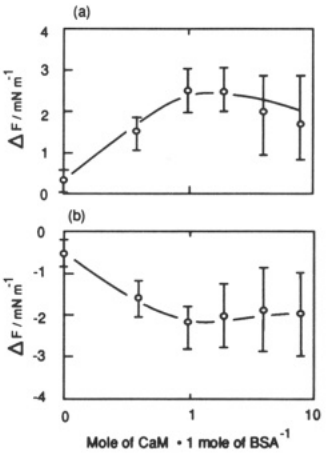


Figure 6. The change in surface pressure of the BSA–CaM conjugated monolayer in relation to the molar ratio of BSA to CaM: (a) the monolayer was moved from ultrapure water to 1 mM $CaCl_2$ solution; (b) the monolayer was transferred from Ca^{2+} solution to ultrapure water.

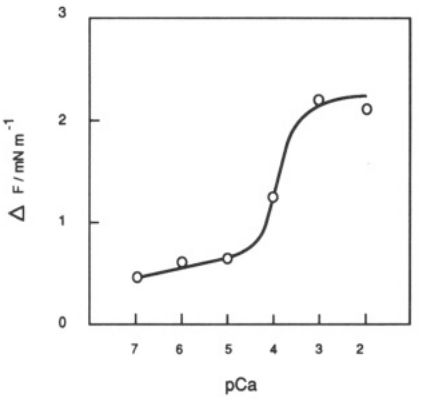


Figure 7. Dependence of the surface pressure change of the conjugated CaM–BSA monolayer on Ca^{2+} concentration.

net change was measured at 20 min after transferring from a subphase of ultrapure water to a trough of the respective divalent cation containing compartment. In the case of the glutaraldehyde-treated BSA monolayer, Mg^{2+} binding caused a greater change in surface pressure than Ca^{2+} binding; however, in the case of the conjugated CaM–BSA monolayer, Ca^{2+} binding produced a much greater change in surface pressure than Mg^{2+} binding. In Ca^{2+} binding the net change in surface pressure of BSA–CaM monolayer was 6 times larger than that of BSA monolayer. On the other hand, the change of BSA–CaM monolayer in the presence of Mg^{2+} was not more than 2 times the BSA monolayer. The results were repeatedly obtained as long as the concerned proteins were cross-linked.

The change in surface pressure as a function of a molar mixing ratio was investigated for the BSA–CaM conjugated monolayer (Figure 6). Also in this experiment, the surface pressure change was compared by transferring the conjugated monolayer from an ultrapure water trough to a 1 mM $CaCl_2$ containing trough and from the Ca^{2+}-containing compartment to another ultrapure water compartment. In both cases maximum changes of surface pressure were obtained when CaM was mixed with an equimolar amount of BSA. The net change (increase) of surface pressure in the presence of Ca^{2+} was slightly larger than that (decrease) in the absence of Ca^{2+} probably due to the stretching of CaM caused by Ca^{2+}-induced conformational change. When the mixing ratio of CaM to BSA was greater than 2 times the equimolar ratio, the change in surface pressure tended to fluctuate. The reason for this fluctuation may be ascribed to the instability of the resulting BSA–CaM

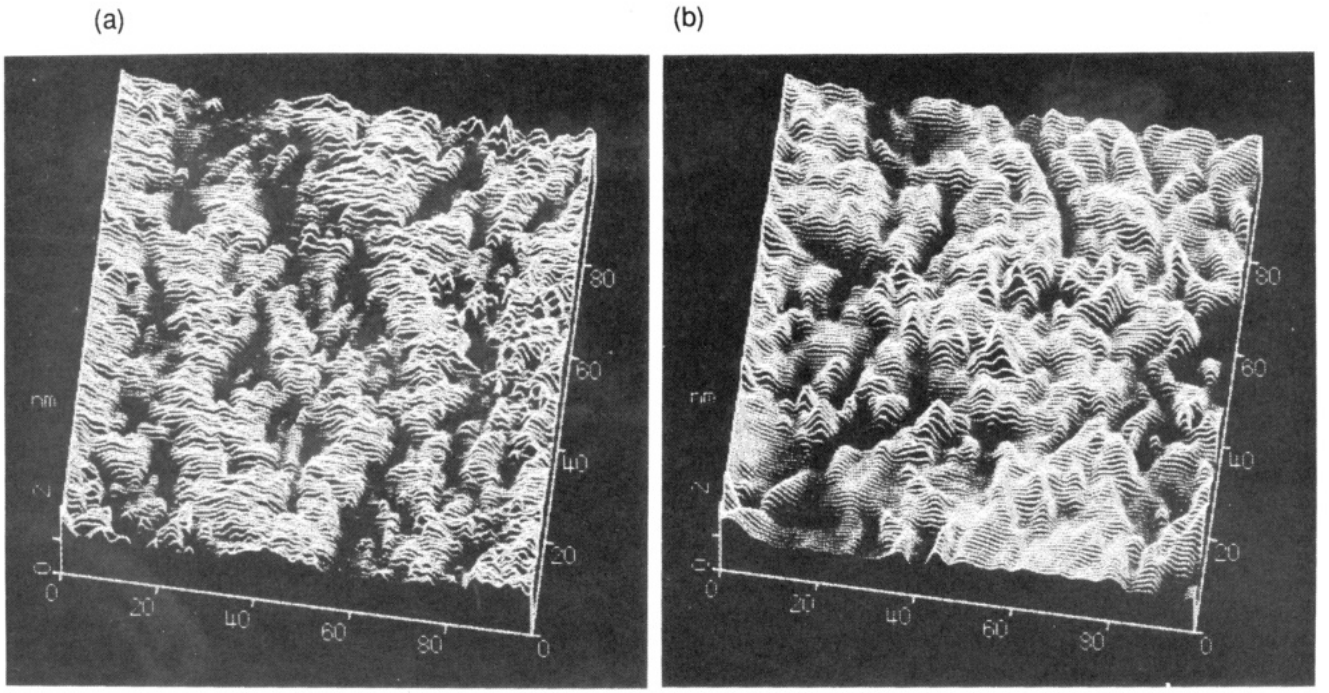


Figure 8. STM images of the conjugated CaM–BSA monolayer on the surface of highly oriented pyrolytic graphite after air-drying: (a) in the absence of Ca^{2+} and (b) in the presence of Ca^{2+}. The bias voltage and the average tunneling current were set at 100 mV and 0.6 nA, respectively.

conjugate where excess amount of CaM of lower molecular weight (16.7 kDa) was cross-linked with BSA of higher molecular weight (69.0 kDa).

A more detailed role of Ca^{2+} in the surface pressure change was further investigated from the viewpoint of Ca^{2+} concentration. Crouch et al. (*20*) have reported that a dynamic change in surface pressure of free CaM was observed in the Ca^{2+} concentration range from pCa 6 to 5. However, in the case of the conjugated BSA–CaM monolayer a big difference in surface pressure was obtained in the range from pCa 4 to 3, as shown in Figure 7. The ΔF value was determined at 20 min after the transport from one trough of a fixed Ca^{2+} concentration to another one. Another conjugated BSA–CaM monolayer, both protein components previously treated at 100 °C for 5 min and then developed at the air–water interface, had a dependency on Ca^{2+} concentration. Although BSA was denatured in the heating condition, CaM underwent no denaturation in this heating process. Also in the combination of CaM and denatured BSA, a conjugated protein monolayer was manufactured that retained the surface pressure dependency on Ca^{2+} concentration. Therefore, one can understand that the conjugated protein monolayer works as a Ca^{2+}-driven ultrathin protein film whose extensibility or permeability may be controlled by the divalent cation.

Direct Observation of the Conjugated BSA–CaM Monolayer by STM. Deposition of the conjugated BSA–CaM monolayer was performed by transferring the monolayer from a trough to the surface of highly oriented pyrolytic graphite. Two states of the monolayer were prepared in two subphases, i.e., a compartment with ultrapure water and another with 1 mM $CaCl_2$. STM is a near-field technique that can resolve structures at the nanometer level and thus can image individual molecules (*21–23*). Figure 8 represents a conjugated BSA–CaM monolayer without Ca^{2+} (a) and another monolayer with Ca^{2+} (b). The transferred protein film was speculated to be as thick as the molecular diameter of BSA. In both images, any ordered structure was not observed. Due to

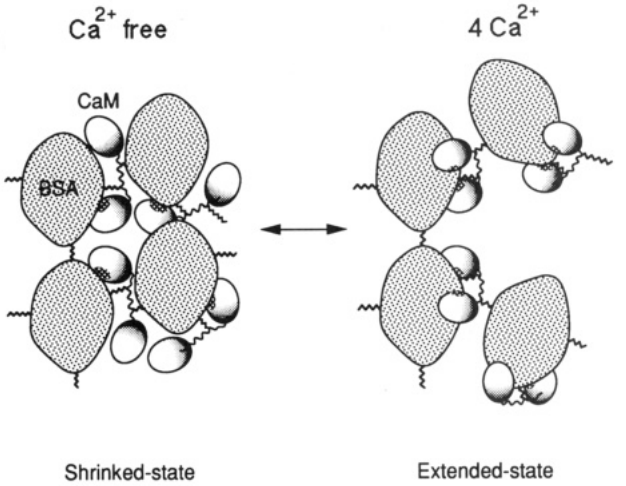


Figure 9. An postulated scheme for the extensibility of CaM–BSA monolayer film.

the large monolayer weight of BSA, STM did not effectively distinguish between BSA and CaM. Both films have uneven surface and have wrinkles; however, the Ca^{2+}-free conjugated monolayer was much more uneven than the Ca^{2+}-bound one. It is indicated that the shrinked thin protein film was extended when it associated with Ca^{2+} for complex formation. In other words, the shrinked Ca^{2+}-free protein monolayer was extended by the CaM moieties, and hence the Ca^{2+}-bound protein film was less susceptible to wrinkles.

The reason for the positive shifting of F–A curves in the presence of Ca^{2+} with respect to the conformational change induced by Ca^{2+} binding seems to be the following. By assuming a network of BSA molecules whose cross-points are occupied by calmodulins, the effect of Ca^{2+} binding may extend not only to the modulating protein but also the matrix protein. Dumbbell-shaped structure of Ca^{2+}-bound CaM turns to a spheroid-shaped one in the presence of an amphiphilic peptide such as mastoparan (*24*). Therefore, it is likely that the extent of the conformational change is large enough to twist the thin protein

film, provided that CaM binds to the amphiphilic domains of BSA. The connecting polypeptide of two domains of CaM seems to play an important role in causing a drastic change in membrane structure, as illustrated in Figure 9, because the connecting polypeptide assists in twisting of the two domains (*8*). The drastic surface change can be explained by assuming that CaM behaves as an indispensable hinge in the protein network: the twisted hinge protein may induce an outstretching of the network by a drastic change in its conformation. Giedroc et al. found that Lys-75 and -94 were the most reactive amino groups in Ca^{2+}-saturated CaM (*3*). Both amino acids are part of the long connecting helix between the two homologous halves of CaM. Since some of the amino residues in an N-terminal half-domain seem likely to be buried in the hydrophobic cleft, it is highly probable that one CaM molecule is conjugated to BSA molecules through its Lys-75 and -94 by glutaraldehyde coupling. It seems likely that the newly formed spacer arm by the glutaraldehyde coupling assists the flexible change in CaM conformation.

Although the permeability of the BSA–CaM thin film is currently under further investigation, the Ca^{2+}-responsive monolayer may be usable as a new intelligent material for the delivery of drugs such as calcitonin and porathyloid hormone, which are responsible for the regulation of Ca^{2+} concentration in serum.

ACKNOWLEDGMENT

We wish to thank T. Nakagawa and the other members of Komatsu Co. Ltd., for providing their facilities and for valuable discussions.

LITERATURE CITED

(1) Yazawa, M., Matsuzawa, F., and Yagi, K. (1990) Inter-Domain Interaction and Structural Flexibility of Calmodulin in the Connecting Region of the Terminal Two Domains. *J. Biochem. 107*, 287–291.

(2) Yoshino, H., Minari, O., Matsushima, N., Ueki, T., Miyake, Y., Matsuo, T., and Izumi, Y. (1989) Calcium-induced Shape Change of Calmodulin with Mastoparan Studies by Solution X-ray Scattering. *J. Biol. Chem. 264*, 19706–19709.

(3) Giedroc, D. P., Sinha, S. K., Brew, K., and Puett, D. (1985) Differential Trace Labeling of Calmodulin: Investigation of Biding Sites and Conformational States by Individual Lysine Reactivities. *J. Biol. Chem. 260*, 13406–13414.

(4) Kakiuchi, S., Hidaka, H., and Means, A. R. (1982) Calmodulin and Intracellular Ca^{2+} Receptors. Plenum. Press, New York.

(5) Kasai, H., Kato, Y., Isobe, T., Kawasaki, H., and Okuyama, T. (1980) Determination of the Complete Amino Acid Sequence of Calmodulin (Phenylalanin-rich Acidic Protein II) from Bovine Brain. *Biomed. Res. 1*, 248–264.

(6) Babu, Y. S., Sack, J. S., Greenhough, T. J., Bugg, C. E., Means, A. R., and Cook, W. J. (1985) Three-dimensional Structure of Calmodulin. *Nature 315*, 37–40.

(7) Kretsinger, R. H., Rundnick, S. E., and Weissman, L. J. (1986) Crystal Structure of Calmodulin. *J. Inorg. Biochem. 28*, 289–302.

(8) Babu, Y. S., Bugg, C. E., and Cook, W. J. (1988) Structure of Calmodulin Refined at 2.2 Å Resolution. *J. Mol. Biol. 204*, 191–204.

(9) Kondo, Y., Miwa, T., Ikegami, H., Naoi, M., Ogoma, Y., Fujii, T., Ohki, K., and Akaike, T. (1987) Preparation of Mono- and Multilayer Films of Calmodulin Using Langmuir–Blodgett Technique. *Chem. Lett.* 1117–1120.

(10) Owaku, K., Shinohara, H., Ikariyama, Y., and Aizawa, M. (1989) Preparation and Characterization of Protein Langmuir–Blodgett Films. *Thin Solid Films 180*, 61–64.

(11) Blodgett, K. B., and Langmuir, I. (1937) Built-up Films of Barium Stearte and Their Optical Properties. *Phys. Rev. 51*, 964–982.

(12) Roberts, G. G., and Pitt, C. W. (1983) Diacetylene Langmuir–Blodgett Layers for Integrated Optics. *Thin Solid Films 99*, 249–255.

(13) Fromherz, P. (1975) Instrumentation for Handling Monomolecular Films at an Air–water Interface. *Rev. Sci. Instrum. 46*, 1380–1385.

(14) Sriyudthsak, M., Yamagishi, H., and Moriizumi, T. (1988) Enzyme-immobilized Langmuir–Blodgett film for a biosensor. *Thin Solid Films 160*, 463–469.

(15) Ishioka, N., Isobe, T., Okuyama, T., Numata, Y., and Wada, H. (1980) A New Acidic Protein in Porcine Brain. *Biochem. Biophys. Acta 625*, 281–290.

(16) Persechini, A., Blumenthal, D. K., Jarrett, H. W., Klee, C. B., Hardy, D. O., and Kretsinger, R. H. (1989) The Effects of Deletions in the Central Helix of Calmodulin on Enzyme Activation and Peptide Binding. *J. Biol. Chem. 264*, 8052–8058.

(17) VanBerkum, M. A. F., George, S. E., and Means, A. R. (1990) Calmodulin Activation of Target Enzymes. Consequences of Deletions in the Central Helix. *J. Biol. Chem. 265*, 3750–3756.

(18) Kyte, J., and Doolittle, R. F. (1982) A Simple Method for Displaying the Hydropathic Character of a Protein. *J. Mol. Biol. 157*, 105–132.

(19) Persechini, A., and Kretsinger, R. H. (1988) The Central Helix of Calmodulin Functions as a Flexible Tether. *J. Biol. Chem. 263*, 12175–12178.

(20) Crouch, T. H., and Klee, C. B. (1980) Positive Cooperative Binding of Calcium to Bovine Brain Calmodulin. *Biochemistry 19*, 3692–3698.

(21) Feng, L., Andrade, J. D., and Hu, C. Z. (1989) Scanning Tunneling Microscopy of Proteins on Graphite Surfaces. *Scanning Microsc. 3*, 399–410.

(22) Edstrom, R. D., Meinke, M. H., Yang, X., Yang, R., and Evans, D. F. (1989) Direct Observation of Phosphorylase Kinase and Phosphorylase b by Scanning Tunneling Microscopy. *Biochemistry 28*, 4939–4942.

(23) Salmeron, M., Beebe, T., Odriozola, J., Wilson, T., Ogletree, D. F., and Siekhaus, W. (1990) Imaging of Biomolecules with the Scanning Tunneling Microscope: Problems and Prospects. *J. Vac. Sci. Technol. A 8*, 635–641.

(24) Malencik, D. A. and Anderson, S. R. (1983) High-affinity Binding of the Mastoparans to Calmodulin. *Biochem. Biophys. Res. Commun. 114*, 50–56.

Specific Interchain Cross-Linking of Antibodies Using Bismaleimides. Repression of Ligand Leakage in Immunoaffinity Chromatography†

Michel Goldberg,* Kaja L. Knudsen, David Platt, Fortune Kohen,‡ Edward A. Bayer, and Meir Wilchek

Department of Biophysics and Department of Hormone Research, The Weizmann Institute of Science, Rehovot, Israel. Received May 2, 1991

The extensive use of antibody-containing affinity columns in the purification of biologically active compounds (e.g., genetically engineered proteins) is severely hampered by the leaching of antibody (or portions thereof) from the immunoaffinity resin during elution of the target antigen. One of the major problems in this context is the combined use of reducing (i.e., thiols) and chaotropic (e.g., detergents and denaturants) agents in the elution step, which causes the disassociation of heavy and/or light chains from the immobilized antibody, thereby contaminating the resultant product. In order to overcome this problem, we have cross-linked the four antibody chains at their sites of disulfide interlinkage, thus producing a single antibody chain. To accomplish this, interchain disulfide bonds were reduced, and the resultant thiol groups were cross-linked by using bifunctional SH-specific reagents (particularly bismaleimides). Cross-linking of up to 95% of the available SH groups produced was achieved with concomitant retention of antigen-binding activity. The cross-linked antibody was immobilized onto CNBr-activated Sepharose, and the resultant column was found to be substantially more stable to harsh elution conditions than similar columns which contain the un-cross-linked antibody.

INTRODUCTION

In affinity chromatography, antibodies are commonly used as immobilized ligands to purify specifically, and in one step, many kinds of antigens (Wilchek et al., 1984; Mohr & Pommerening, 1985). The recovery of the purified compound occurs during the elution step, which is performed under conditions which cause a decrease in the affinity between the antibody and the antigen. The purification process thus reflects the biological recognition which takes place between the antibody and antigen and, when successfully applied, is much more efficient than conventional procedures for the purification of biologically active materials.

An important drawback of immunoaffinity chromatographic purification is the partial chemical or enzymatic hydrolysis of the antibody which can result in a leakage of the antibody or portion thereof (e.g., light and/or heavy chains) which then contaminates the affinity-purified product (Dean et al., 1985). One source of such leakage involves the chemistry of immobilization of an antibody to the resin and has been dealt with extensively in previous studies (Wilchek et al., 1975; Wilchek & Miron, 1987). Another source of leakage involves the presence of reducing agents commonly used in many of the purification steps (Linn, 1990; Deutscher, 1990). These may sever the interchain disulfide bonds which connect the four chains of the immunoglobulin molecule; those of which not directly coupled chemically to the resin may then be released.

Many methods have been suggested to avoid the problem of antibody leakage (Ernst-Cabrera & Wilchek, 1988), including the intramolecular cross-linking of the antibody and the selection of conjugation methods that yield a more stable chemical linkage between the antibody and the resin. For example, glutaraldehyde has been used both as a general reagent to cross-link between the chains of the immobilized antibody (Kowal & Parsons, 1980) and, in a more specific case, to cross-link (and thus stabilize chemically) antibody molecules which have been bound to protein A columns (Gyka et al., 1983). Cross-linking with glutaraldehyde usually involves lysine groups of the antibody, some of which may occupy or indirectly affect the combining site and thus the binding activity of the resultant cross-linked immunoaffinity column would have been reduced.

The antibody combining site is located in the Fv portion of the antibody molecule. The Fv, which includes the variable parts of both the heavy and light chains, contains lysine residues, but the interchain disulfides are located elsewhere in the antibody molecule (i.e., in the constant regions). The two chains of the Fv have recently been prepared by genetic engineering, either as a single chain linked together by a designed peptide (Bird et al., 1988) or separately as double chains which associated spontaneously after their production (Ward et al., 1989). The engineered bacterial proteins expressed high levels of biological (antigen-binding) activity. This shows clearly that disulfide groups are not important for recognition and that the chains can reassemble themselves in the correct orientation.

In this context, the purpose of this study was to prepare a stable single-chain equivalent of a native antibody by cross-linking the interchain thiol groups via noncleavable bonds. The results have demonstrated the feasibility of using bismaleimides (Figure 1) for this purpose. To this end, the disulfide bonds of antibiotin antibodies were reduced, cross-linked with the desired reagent, and immobilized onto CNBr-activated Sepharose, and the resultant immunoaffinity column was used to isolate biotin-linked proteins. This approach served as a model system to demonstrate enhanced stability which can be achieved for an immobilized, cross-linked antibody.

EXPERIMENTAL PROCEDURES

Materials. *N,N'*-Bismaleimidohexane (BMH) was a product of Pierce, Rockford, IL. *N,N'*-Bis(3-maleimidopropionyl)-2-hydroxy-1,3-propanediamine and *N,N'*-

† Abbreviations used: BMH, *N,N'*-bismaleimidohexane; MPH-PD, *N,N'*-bis(3-maleimidopropionyl)-2-hydroxy-1,3-propanediamine; PDM, *N,N'-o*-phenylenebismaleimide; ELISA, enzyme-linked immunosorbent assay; PBS, phosphate-buffered saline, pH 7.4; Fv, the variable region of the light and heavy antibody chains.

‡ Department of Hormone Research.

1043-1802/91/2902-0275$02.50/0 © 1991 American Chemical Society

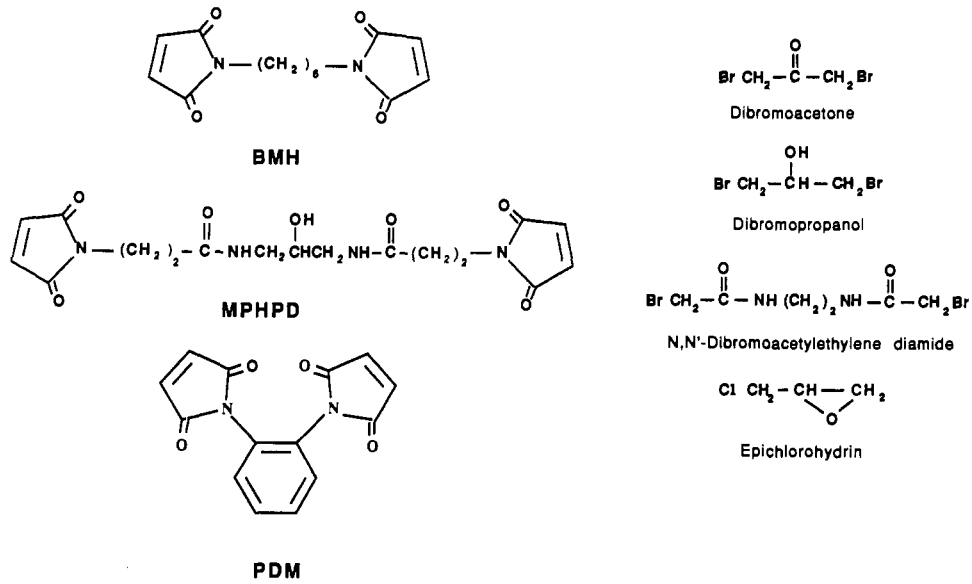


Figure 1. Chemical structures of bifunctional reagents used in this study.

o-phenylenebismaleimide (MPHPD and PDM, respectively) were obtained from Sigma Chemical Co. (St. Louis, MO). Dibromoacetone (DBA) was purchased from K & K Laboratories (Cleveland, OH). Ferritin (2× crystallized) was from Pentex Biochemicals (Kankakee, IL). 2,2′-Azinobis(3-ethylbenzthiazolinesulfonic acid) diammonium salt (ABTS), and all other reagents, proteins, chemicals, and biochemicals were obtained from Sigma. *N,N′*-Dibromoacetylethylenediamide was prepared by reacting diaminoethane with a 3-fold excess of bromoacetic anhydride in dioxane. The product was precipitated with water, filtered, and dried in vacuo.

Purification of Antibodies. Antibiotin antibodies were elicited in mice against biotinylated bovine serum albumin mainly according to Dakshinamurti and Spectro (1990) following a procedure described by Kohen et al. (1982). The antibodies were purified from ascites fluids on a protein A–Sepharose CL-4B column (Pharmacia, Uppsala, Sweden) according to the manufacturer's instructions. Briefly, the ascitic fluids were diluted with an equal volume of glycine buffer (1.45 M glycine, 3 M NaCl, pH 8.9) and passed through the protein A column (1 mL of ascites per 3 mL of gel) preequilibrated with the same buffer. After a 15-min incubation period, the column was washed with glycine buffer until the absorbance (280 nm) of the eluate approached a minimum value. The elution of the monoclonal antibiotin antibodies was performed with sodium citrate buffer (40 mM citric acid, 20 mM NaCl, pH 3.2). The antibody preparation was dialyzed overnight at 4 °C against phosphate-buffered saline, pH 7.4 (PBS), resuspended at a concentration of 1.5–2 mg/mL and stored at −20 °C.

Reduction of Antibodies. An antibody sample (1.5–2.0 mg/mL) was reduced for 1 h at 37 °C with 2 mM dithiothreitol (Cleland, 1964) according to Gunewardena (1966). The reduced antibody was dialyzed against 5 mM EDTA in PBS (presaturated with N_2) in a stirred ultrafiltration cell (Amicon, Danvers, MA) using an XM 50 membrane. The ultrafiltration step (three washings, 50 mL of buffer per wash) was performed until no trace of dithiothreitol could be detected in the ultrafiltrate solution as measured spectrophotometrically with 5,5′-dithiobis(2-nitrobenzoic acid) (Ellman, 1959).

Cross-Linking with Bismaleimides. Antibodies were cross-linked by mixing the reduced antibody solution with a preparation of the desired cross-linker, diluted (as indicated later in the text) in a dimethylformamide–water (1:1) solution. The volume of the antibody solution was 3–5-fold that of the reagent solution. For example, a solution (300 μL) of antibody (10.8 μM, 1.6 mg/mL of PBS containing 5 mM EDTA) was mixed with a solution (100 μL) of 20 mM MPHPD (8 mg/mL in PBS–DMF, 1:1). In this particular case, the ratio of reagent to interchain disulfide bond was 120. The reaction was carried out overnight at room temperature.

Measurement of Binding Activity. An ELISA test, based on the method described by Eshhar (1985), was used to compare the binding of the native and bismaleimide-cross-linked antibody. Briefly, 100-μL aliquots of biotinyl-*N*-(ε-aminocaproyl)–BSA (50 μg/mL in PBS) were incubated in a 96-well poly(vinyl chloride) microplate (Flow Laboratory, Irvine, Scotland). After washing (Wash Concentrate, Delfia, Turku, Finland), 100 μL of antibody preparation at the desired dilution (in PBS as indicated later in the text) was introduced to the wells and incubated for 1 h at room temperature. After washing, a sample (100 μL) of protein A conjugated horseradish peroxidase (3800 units/mL; BioMakor, Rehovot, Israel) was diluted 400 times in PBS (pH 8) and incubated at 37 °C for 30 min. Following another washing step, 100 μL of freshly prepared substrate solution was added [1 mg/mL ABTS and 0.003% H_2O_2 in citrate–phosphate buffer (28 mM citric acid, 44 mM disodium phosphate, pH 4.7)]. The results were read at 600 nm with a Microplate Autoreader (BioTek Instruments, Winooski, VT).

Miscellaneous Methods. The concentration of protein in solution was measured by the Bradford method (Bradford, 1976) using ovalbumin as a standard. Iodination with ^{125}I was performed according to the Chloramine T procedure (Bolton & Hunter, 1986). Amino acid analysis of native or cross-linked antibodies was performed by using a Dionex amino acid system (Dionex Corp., Sunnyvale, CA).

Proteins (e.g., antibodies or avidin) were immobilized on CNBr-activated Sepharose following the previously described method (Kohn & Wilchek, 1984).

Biotinylation was performed either with the *N*-succinimide ester of biotin or the long-chained *N*-ε-aminocaproyl derivative as previously described (Bayer & Wilchek, 1990). The extent of biotinylation was assessed on an avidin column by measuring spectrophotometrically the percentage of the biotinyl–protein preparation

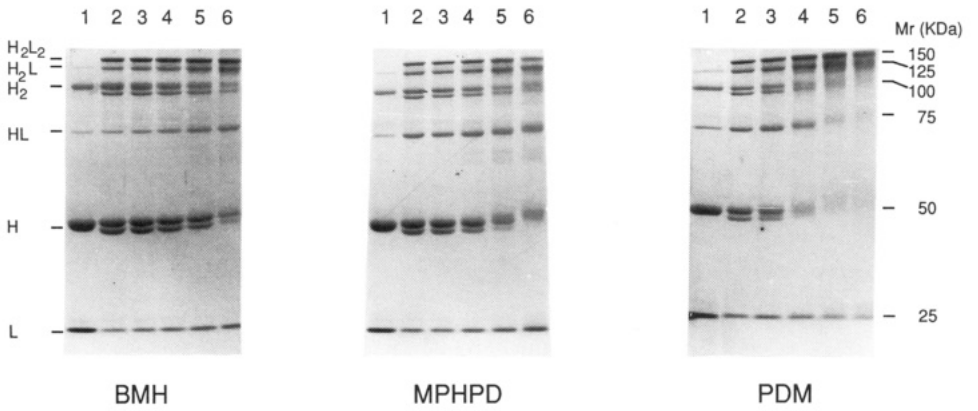


Figure 2. SDS-PAGE of bismaleimide-cross-linked antibodies. Anti-biotin antibody samples were reduced with dithiothreitol and cross-linked with various concentrations of the designated bismaleimide reagent. Samples 1–6 represent 0.2-, 1-, 5-, 24-, 120-, and 600-fold molar ratios, respectively, of the given reagent to the calculated amount of interchain disulfide bonds in the antibody. Following ultrafiltration, the samples were subjected to electrophoresis under reducing conditions on 10% polyacrylamide gels and stained with Coomassie Brilliant Blue. H_2L_2 marks the position of the cross-linked intact antibody (two heavy and two light chains); H_2L, two heavy chains coupled to one light chain; H_2, two crosslinked heavy chains; HL, a light chain coupled to a heavy chain; H, an uncoupled heavy chain; and L, an uncoupled light chain.

which bound to the column. For biotinyl–ferritin, a solution containing 1 mg/mL (2.1 nmol; A_{280} = 13.9) was added to a 0.4-mL avidin column (containing 2 mg of avidin/mL of resin; i.e., 12.5 nmol total). The extent of binding was determined by assessing the amount of protein which appeared in the effluent fractions.

Polyacrylamide gel electrophoresis in the presence of sodium dodecyl sulfate (SDS–PAGE) was performed on slab gels according to Laemmli (1970). Samples were electrophoresed on 10 or 12% gels under either reducing (in the presence of β-mercaptoethanol) or nonreducing conditions (as indicated later in the text). The proteins were stained with Coomassie Brilliant Blue R250.

Densitometry measurements were conducted on photographic transparencies of the desired lane of an SDS–PAGE gel. The measurements were performed on a computing densitometer apparatus (Model 300A, Molecular Dynamics, Sunnyvale, CA), using Image Quant Software, Program 3.0.

RESULTS AND DISCUSSION

Cross-Linking with Bifunctional Thiol-Specific Reagents. In order to cross-link antibodies via sulfhydryl groups, the interchain disulfides of the antibody have to be reduced. We found that a concentration of 2 mM dithiothreitol appears to reduce the interchain disulfides, whereas intrachain cystine linkages appeared to be unaffected by such treatment. Antibodies, reduced in this manner, were then subjected to ultrafiltration under reducing conditions (nitrogen gas in the presence of EDTA) and immediately cross-linked with the desired reagent (Figure 1). After the reaction (employing different concentrations of the respective reagent), the antibody preparation was examined by SDS–PAGE under reducing conditions, i.e., conditions under which un-cross-linked heavy and light chains would be completely dissociated and separated on the gel (Figure 2).

The gels showed six different bands which corresponded to the expected species of the cross-linked and un-cross-linked antibody chains, i.e. (from the top to the bottom of the gel), (a) the intact antibody which comprised the two heavy and two light chains (designated H_2L_2 in the figure), (b) two heavy chains coupled to one light chain (H_2L), (c) two cross-linked heavy chains (H_2), (d) one light chain coupled to a heavy chain (HL), (e) an uncoupled heavy chain (H), and (f) an uncoupled light chain (L). Intermolecular cross-linking (i.e., species larger than the intact cross-linked molecule) was not observed. At intermediate concentrations of the cross-linkers, two additional distinct bands were also apparent at M_rs slightly less than those of the H and H_2 bands. These new bands may be accounted for by interchain cross-linking between two light chains (i.e., the designated bands could represent L_2 and HL_2, respectively); alternatively, these bands may be attributed to "incorrect" cross-linking of two H chains, (i.e., the interchain or intrachain cross-linking between cysteine and lysine groups).

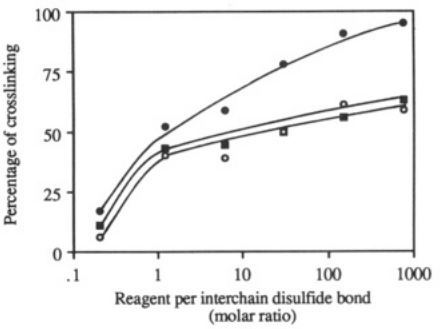


Figure 3. Extent of interchain antibody cross-linking as a function of reagent concentration. Samples of anti-biotin antibody were reduced and cross-linked with various concentrations of either BMH (■), MPHPD (○), or PDM (●) and treated further as described in the legend to Figure 2. The percentage of cross-linking was measured by densitometry tracings of the SDS–PAGE gel as described in the text.

The different cross-linked species could not be facilely separated by conventional means (such as gel filtration), since, in the absence of denaturing agents, all species migrated as a single antibody entity, irrespective of internal cross-linking. Therefore, the final yields of cross-linking (defined as the molar percent of the total cross-linked species) for the various reagents were determined densitometrically from the bands on the SDS–PAGE gels. Interestingly, the results (Figure 3) showed that, for the bismaleimide derivatives, a 2-fold molar excess of the respective cross-linking reagent was sufficient to provide a majority of the final cross-linking yield (i.e., between 35 and 55%); in order to achieve significantly higher yields, a great (several-hundred-fold) excess of reagent was required. The probable reason for the high levels of reagent necessary for extensive cross-linking is that the antibody molecule was subjected to reduction but not denaturation; therefore the molecule would be expected to retain its

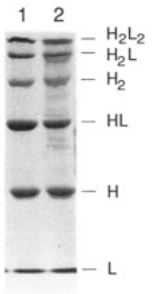


Figure 4. SDS–PAGE of antibodies cross-linked with dibromoacetyl reagents. Antibody samples were reduced with dithiothreitol and cross-linked by using a 40-fold molar ratio (reagent to interchain disulfide bonds) of either dibromoacetone (lane 1) or dibromoacetylethylenediamine (lane 2). The gel was electrophoresed under reducing conditions. See legend to Figure 2 for additional details and key to symbols.

Table I. Modification in Amino Acid Composition of Bismaleimide-Cross-Linked Antibodies

antibody preparation	Cys/Ala	Leu/Ala	Lys/Ala
native	0.286	1.707	1.612
dithiothreitol-reduced	0.285	1.800	1.623
after ultrafiltration	0.273	1.726	1.522
BMH-cross-linked	0.229	1.884	1.520
MPHPD-cross-linked	0.217	1.865	1.402
PDM-cross-linked	0.214	1.809	1.538

native structure, wherein certain cysteines are likely unexposed. Only in the presence of high concentrations of reagent would some of the bismaleimide molecules reach and react with the newly formed thiols. Since the disulfide-derived SH groups are in spatial juxtaposition, they would be expected to react simultaneously with the bismaleimide reagent. This would also explain why PDM, which is the shortest bismaleimide reagent, gave the highest yield (over 90% cross-linking). Unfortunately (perhaps due to its hydrophobicity), about 50% of the antibody precipitated.

Due to the fact that complete cross-linking could not be achieved with bismaleimide reagents, we decided to try another family of reagents which contain dibromoacetyl groups (see Figure 1). In this case, we took into account the possibility that the bromoacetyl moiety can also react with other nucleophiles on the protein and that the cross-linking could therefore occur at a later stage and at other positions (not only with cysteines). With these reagents, however, a similar specificity of cross-linking was obtained, but at lower overall yields (Figure 4). Attempts to cross-link the reduced cysteines by using dibromopropanol or epichlorohydrin were unsuccessful. An interesting observation was the appearance of a series of new bands, which resulted from the reaction of the longer (but not the shorter) dibromoacetyl reagent. This may reflect the type of "incorrect" cross-linking mentioned above. In view of these results, we decided to continue our studies with the bismaleimide reagents, since the goal of this work was to achieve stabilization of the antibody in the highest possible yield.

Properties of the Cross-Linked Antibody. To examine the specificity of the cross-linking reaction, amino acid analysis was performed which showed a reduction of about 25% of the content of cysteines in the cross-linked antibody (Table I). Since there are five interchain disulfides out of a total of 17, this result suggests that the major sites of bismaleimide-induced cross-linking indeed occur between the interchain disulfides. The data also indicate that other types of amino acids (lysines in particular) are not extensively involved in the cross-linking.

To examine the biological activity of the respective cross-linked antibody preparation, we employed an ELISA assay. For these studies, a monoclonal anti-biotin antibody was employed and its binding to a biotinylated target protein was assessed (Figure 5). It is emphasized here that since the various species were not separated, the antibody preparation consists of a mixture of un-cross-linked and partially and fully cross-linked molecules, the latter bearing between one and four bismaleimide adducts. Consequently, the binding measurements represent mean values which correspond to the nonhomogeneous cross-linked antibody preparations. Nevertheless, in all cases, high levels of binding activity were observed. Increasing the concentration of bismaleimide did not drastically affect the binding capacity of the resultant antibody. In the case of MPHPD, the pattern of the binding curves were quite similar to that of the native antibody, indicating once again that the cross-linked interchain disulfides are not essential for activity. In the case of PDM (and perhaps the highest concentration of BMH), the observed decrease in binding activity may be related to the insolubility of the cross-linked product.

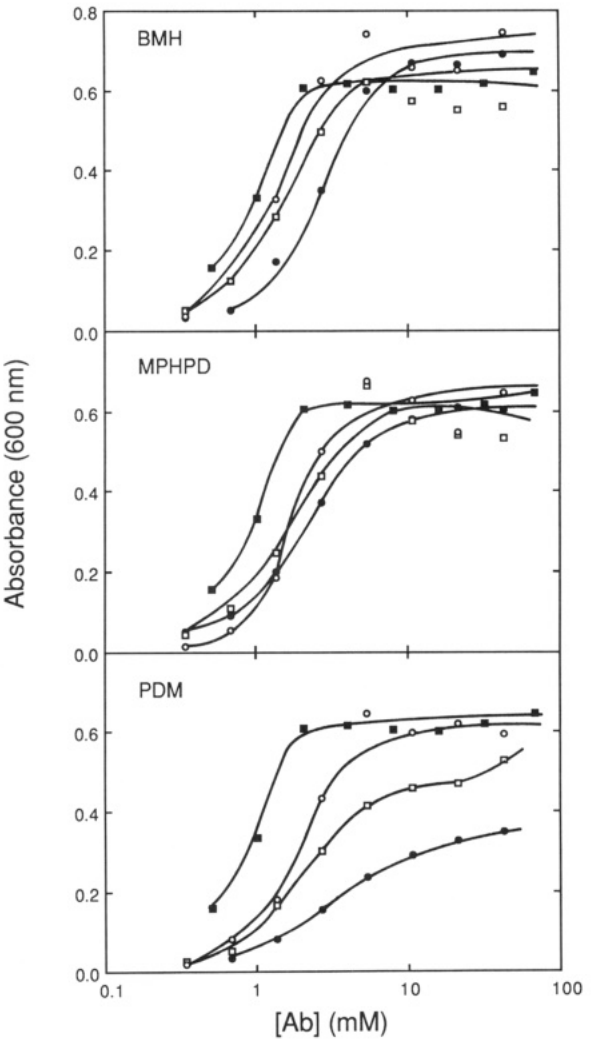


Figure 5. Binding activity of bismaleimide-cross-linked antibodies. Native or cross-linked preparations (using the designated reagent) of antibiotin antibody were examined by ELISA. The samples were incubated with a biotinylated target protein coupled to wells of a microtiter plate, washed, and treated further with protein A conjugated peroxidase, prior to incubation with substrate. The curves represent native antibody (■) and cross-linked antibody preparations using 5- (○), 120- (□), and 600-fold (●) molar concentrations of the given reagent over interchain disulfide groups, respectively.

In order to determine whether such cross-linked anti-

Table II. Release of Biotinyl-Ferritin from Native or Cross-Linked Anti-Biotin Antibody-Sepharose Column[a]

eluent	anti-biotin antibody column	
	native	cross-linked
distilled water	8	46
PBS (pH 7.1)	37	45
sodium phosphate buffer (0.1 M, pH 7.0, + 1 M NaCl)	23	22
acetic acid (0.1 M)	<1	<1
citrate buffer (0.1 M, pH 4.7)	35	42
ammonium hydroxide (0.1 M)	100	100

[a] A solution (100 μg) of biotinylated ferritin was applied at room temperature to a 0.4-mL column of native or cross-linked antibiotin antibody (2.65 mg of protein per mL of Sepharose). The molar ratio of MPHPD to interchain disulfide bond was 120. Values represent percent of applied protein which was released from the column as a result of the designated treatment.

bodies provide advantages over the native antibody as ligands in affinity chromatography, we decided to immobilize one of the highly cross-linked preparations which showed a high level of binding activity. For this purpose, we used the MPHPD-cross-linked antibody for the separation (binding and release) of biotinylated ferritin. The molar ratio of MPHPD and interchain disulfide bonds used in these experiments was 120. The very high ϵ_{280} and visible color renders the latter a very convenient target molecule for these studies. This column may eventually prove very useful for separation of biotinylated proteins from nonbiotinylated material for use in avidin–biotin technology (Wilchek & Bayer, 1988, 1990).

Initial experiments showed that over 90% of the biotinyl–ferritin preparation bound to avidin columns. Similar experiments using the MPHPD-cross-linked antibody column showed that less than 60% of the biotinyl–ferritin bound to the column if the protein was dissolved in PBS (Table II). It was determined that the performance of the column could be improved dramatically by carrying out the affinity chromatographic procedure at high ionic strength (1 M NaCl); under these conditions, 86% of the target protein bound to the column. The entire amount of bound biotinyl–ferritin could be eluted from the column with 0.1 M NH_4OH. Interestingly, by simply reducing the ionic strength of the solution, particularly by washing the loaded cross-linked immunoaffinity column with distilled water, almost half of the protein could be eluted. Water wash had only a very minor effect on columns containing the native antibody. This difference may reflect the hydrophobic nature of the bismaleimide cross-linking reagents. The biotinyl–ferritin could not be effectively eluted from the native or crosslinked immunoaffinity column by the use of acidic conditions (Table II).

It is common practice to employ relatively harsh chromatographic conditions (i.e., the presence of reducing reagents, chaotropic agents, and/or detergents) when using native antibody columns for the purification of antigens, particularly antigens prepared by recombinant DNA technology. Consequently, leakage of the ligand is a commonly observed feature in immunoaffinity chromatography. We were therefore interested in determining whether cross-linking with bismaleimides would significantly improve the stability of such columns. Thus, columns containing either native or MPHPD-cross-linked antibodies were compared for their stamina to harsh conditions, as measured by leakage. For this purpose, the respective ligands were radioiodinated and immobilized onto CNBr-activated Sepharose. We used this particular activation procedure and not the more recent developments (e.g., chloroformate or hydrazide activation methods), since most of the accumulated experience in studying

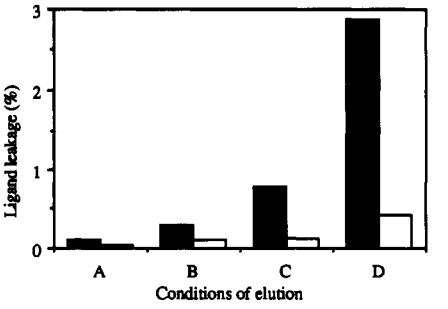


Figure 6. Ligand leakage from anti-biotin immunoaffinity column. Native (filled bars) or MPHPD-cross-linked (open bars) preparations of antibiotin antibody were attached to CNBr-activated Sepharose. The elution was performed in PBS with the following additives: (A) 2 mM dithiothreitol, (B) 2 mM dithiothreitol and 4 M urea, (C) 2 mM dithiothreitol and 6 M urea, and (D) 10 mM dithiothreitol and 6 M urea.

the leakage phenomenon has been accomplished with CNBr-activated columns. Moreover, about 95% of the affinity chromatographic works currently described in the literature still use this procedure. The columns were then treated with the indicated test solution, and the amount of radioactivity which appeared in the eluent was measured. The results showed that the leakage properties of the cross-linked immunoaffinity column were far superior to those of the column which contained the native antibody (Figure 6). The amount of leakage which was directly induced by the reducing agent (i.e., dithiothreitol) was relatively low; the structure of the antibody appeared to remain stable in its presence, presumably due to other (noncovalent) interchain interactions. The combined action of the reducing and chaotropic agents (dithiothreitol and urea) led to a marked increase in the levels of ligand leakage, since both the interchain disulfide and the noncovalent forces were disrupted. The observed leakage could be further increased by elevating the concentration of urea and/or dithiothreitol. Another important source of leakage which was observed for both column types occurred during treatment of the columns with NH_4OH; this phenomenon can be ascribed to the severing of the bond between the antibody and the CNBr-activated resin and has been described extensively in the literature (Kohn & Wilchek, 1982).

CONCLUDING REMARKS

In this article, we describe an approach to render an antibody more resistant to reducing and chaotropic agents by stabilizing the thiol-sensitive interchain disulfide bonds. This is accomplished by the controlled reduction and subsequent chemically selective interaction with bismaleimide reagents; the resultant covalent linkage is irreversible.

We have shown that the major sites of cross-linking appear to constitute almost exclusively the five interchain disulfide bonds; the number of bonds required to render the five polypeptide chains of the antibody resistant to dissociation are thus kept to a minimum. The cross-linking of these disulfide bonds does not markedly interfere with the antibody–antigen interaction, and upon immobilization, the behavior of the resultant immunoaffinity column is improved with respect to mild elution conditions and decreased leakage properties. It is therefore anticipated that such columns will in many cases help to overcome the problem of the immune response to murine immunoglobulins (Shawler, 1985; Ehrlich, 1987) which contaminate purified preparations of biologically active

compounds, prepared either from natural sources or by genetic engineering.

ACKNOWLEDGMENT

We thank R. Alon for valuable discussions. This work was supported by the Yeda Foundation, Rehovot, Israel.

LITERATURE CITED

Bayer, E. A., and Wilchek, M. (1990) Protein Biotinylation. *Methods Enzymol. 184*, 138–160.

Bird, R. E., Hardman, K. D., Jacobson, J. W., Johnson, S., Kaufman, B. M., Lee, S.-M., Lee, T., Pope, S. H., Riordan, G. S., and Whitlow, M. (1988) Single-Chain Antigen-Binding Proteins. *Science 242*, 423–426.

Bolton, A. E., and Hunter, W. M. (1986) Radioimmunoassay and Related Methods. In *Handbook of Experimental Immunology, Vol. I. Immunochemistry*. (M. Weir, Ed.) 4th Ed., pp 26.1–26.55. Blackwell Scientific Publications, Oxford, UK.

Bradford, M. M. (1976) A Rapid and Sensitive Method for the Quantitation of Microgram Quantities of Protein Utilizing the Principle of Protein-Dye Binding. *Anal. Biochem. 72*, 248–254.

Cleland, W. W. (1964) Dithiothreitol, a New Protective Reagent for SH Groups. *Biochemistry 3*, 480–482.

Dakshinamurti, K., and Rector, E. S. (1990) Monoclonal Antibody to Biotin. *Methods Enzymol. 184*, 111–119.

Dean, P. D. G., Johnson, W. S., and Middle, F. A. (1985) Operational Methodologies. In *Affinity Chromatography. A Practical Approach* (P. D. G. Dean, W. S. Johnson, F. A. Middle, Eds.) pp 75–98, IRL Press, Oxford, UK.

Deutscher, M. P. (1990) Maintaining Protein Stability. *Methods Enzymol. 182*, 83–89.

Ehrlich, P. H., Harfeldt, K. E., Justice, J. C., Moustafa, Z. A., and Ostberg, L. (1987) Rhesus Monkey Responses to Multiple Injections of Human Monoclonal Antibodies. *Hybridoma 6*, 151–160.

Ellman, G. L. (1959) Tissue Sulfhydryl Groups. *Arch. Biochem. Biophys. 82*, 70–77.

Ernst-Cabrera, K., and Wilchek, M. (1988) Immunoaffinity Chromatography and Its Application for the Purification of Pharmaceutically Active Proteins. *Med. Sci. Res. 16*, 305–310.

Eshhar, Z. (1985) Monoclonal Antibody Strategy and Techniques. In *Hybridoma Technology in the Biosciences and Medicine* (T. A. Springer, Ed.) pp 3–41, Plenum Press, New York.

Gunewardena, P., and Cooke, K. B. (1966) 1,4-Dithiothreitol as a Reagent for the Reductive Degradation of Human γ-G Globulin. *Biochem. J. 99*, 8P.

Gyka, G., Ghetie, V., and Sjosquist, J. (1983) Crosslinkage of Antibodies to Staphylococcal Protein A. Matrices. *J. Immunol. Methods 57*, 227–233.

Kohen, F., Lichter, S., Eshhar, Z., and Lindner, H. R. (1982) Preparation of Monoclonal Antibodies Able To Discriminate between Testosterone and 5α-Dihydrotestosterone. *Steroids 39*, 453–459.

Kohn, J., and Wilchek, M. (1982) Mechanism of Activation of Sepharose and Sephadex by Cyanogen Bromide. *Enzyme Microb. Technol. 4*, 161–163.

Kohn, J., and Wilchek, M. (1984) The Use of Cyanogen Bromide and Other Novel Cyanylating Agents for the Activation of Polysaccharide Resins. *Appl. Biochem. Biotechnol. 9*, 285–305.

Kowal, R., and Parsons, R. G. (1980) Stabilization of Proteins Immobilized on Sepharose from Leakage by Glutaraldehyde Crosslinking. *Anal. Biochem. 102*, 72–76.

Laemmli, U. K. (1970) Cleavage of Structural Proteins during the Assembly of the Head of Bacteriophage T4. *Nature (London) 227*, 680–685.

Linn, S. (1990) Strategies and Considerations for Protein Purifications. *Methods Enzymol. 182*, 9–15.

Mohr, P., and Pommerening, K. (1985) Immunoaffinity Chromatography and Immunoassays. In *Affinity Chromatography. Practical and Theoretical Aspects.* (P. Mohr, Ed.) pp 131–142, Marcel Dekker, Inc., New York.

Shawler, D. L., Bartholomew, R. M., Smith, L. M., and Dillman, R. O. (1985) Human Immune Response to Multiple Injections of Murine Monoclonal IgG. *J. Immunol. 135*, 1530–1535.

Ward, E. S., Gussow, D., Griffiths, A. D., Jones, P. T., and Winter, G. (1989) Binding Activities of a Repertoire of Single Immunoglobulin Variable Domains Secreted from *Escherichia coli*. *Nature (London) 341*, 544–546.

Wilchek, M., and Bayer, E. A. (1988) The Avidin–Biotin Complex in Bioanalytical Applications. *Anal. Biochem. 171*, 1–32.

Wilchek, M., and Bayer, E. A., Eds. (1990) Avidin–Biotin Technology. *Methods Enzymology, Vol. 184*, Academic Press, San Diego, CA.

Wilchek, M., and Miron, T. (1987) Limitations of *N*-Hydroxysuccinimide Esters in Affinity Chromatography and Protein Immobilization. *Biochemistry 26*, 2155–2161.

Wilchek, M., Oka, T., and Topper, Y. J. (1975) Structure of a Soluble Super-Active Insulin Is Revealed by the Nature of the Complex between Cyanogen-Bromide-Activated Sepharose and Amines. *Proc. Natl. Acad. Sci. U.S.A. 72*, 1055–1058.

Wilchek, M., Kohn, J., and Miron, T. (1984) Affinity Chromatography. *Methods Enzymol. 104*, 3–55.

Iron Transport Mediated Drug Delivery Systems: Synthesis and Antibacterial Activity of Spermidine- and Lysine-Based Siderophore–β-Lactam Conjugates

Julia A. McKee, Sushil K. Sharma, and Marvin J. Miller*

Department of Chemistry and Biochemistry, University of Notre Dame, Notre Dame, Indiana 46556.
Received February 4, 1991

Conceptually, the penetration of β-lactam antibiotics through the bacterial cell wall can be enhanced by utilizing various active transport systems such as the active iron-transport system that exists in bacteria. Several β-lactam–siderophore analogue (microbial iron chelators) conjugates were prepared to investigate this approach. Thus, monocyclic (oxamazin) and bicyclic (carbacephalosporin) β-lactams were separately linked to dihydroxybenzoyl derivatives of spermidine and lysine. The antibacterial activity of these conjugates has been investigated and the potential use of the iron-transport system as a drug-delivery system is discussed.

INTRODUCTION

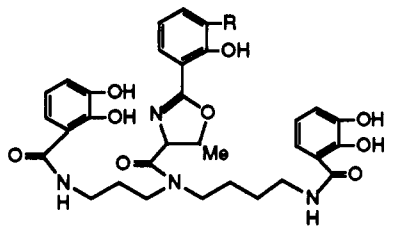
The construction of naturally occurring and synthetic β-lactams, with control of functional groups and stereochemistry, has been the goal of synthetic organic chemists for the past 50 years. The various ways of constructing the β-lactam ring system have been reviewed (*1*). However, bacteria have evolved defense mechanisms to protect themselves from the intruding antibiotics. These include (*2*): (1) mutations that decrease the affinity of essential penicillin-binding proteins (PBP) for β-lactams, (2) β-lactamase production, and (3) inhibition of β-lactam penetration to the PBP targets in the cytoplasmic membrane. The last mode of defense is a serious problem associated with Gram-negative bacteria in which the outer cell membrane presents a significant permeability barrier to many β-lactam antibiotics. This may be the primary cause of the high resistance of *Pseudomonas aeruginosa* to many β-lactam antibiotics (*3*).

The iron-binding proteins transferrin and lactoferrin, in combination with antibiotics, often show powerful bacteriostatic effects in vitro and are essential for protection against many infections (*4*). It has been established that iron-chelating compounds (siderophores) form complexes with Fe(III) and are readily accepted into the bacterial cell via specific iron-transport systems (*5*). Neilands and Valenta have published an excellent review of iron-containing antibiotics (*6*). The albomycins and ferrimycine A_1 are natural examples of siderophore-containing antibiotics that are incorporated into bacterial cells by the use of the iron-transport system (*7*). Sulfonamides have been attached to the natural siderophores ferricrocin and ferrioxamine B, and these conjugates have been shown to inhibit the growth of *Staphylococcus aureus* (*8*). Recently, our laboratory reported the synthesis and antimicrobial activity of several β-lactam–hydroxamate-based siderophore conjugates and have established that these β-lactam–siderophore conjugate systems may be incorporated into the microbial cell through the iron-transport mechanism (*9*). The syntheses of semisynthetic β-lactam derivatives having catechol moieties have been accomplished by several groups, and the biological activities of such derivatives against several Gram-positive and Gram-negative bacteria were reported (*10*). Several of these catechol-containing antibiotics have been shown to rely on the *ton*B iron-transport system for their activity (*10c,d, 11*). The successful incorporation of a new catechol-containing cephalosporin, E-0702, into *Escherichia coli* using an iron-transport system has been recently reported (*12*). The albomycins are the best known examples of natural hydroxamate siderophore containing antibiotics; however, there are no examples of natural catechol siderophore antibiotics. This paper describes our first attempts to link β-lactam antibiotics with catechol siderophore analogues and discusses the growth-promoting ability of the siderophore analogues and the preliminary studies of the antimicrobial activity of the siderophore–antibiotic conjugates.

Agrobactin (**1a**) and parabactin (**1b**) are catechol-containing, spermidine-based siderophores (Figure 1). These microbial iron chelators are being studied as potential drugs to treat iron overload resulting from treatment of Cooley's anemia (*13*), and are very effective in deferration of mammalian cell lines (*14*). Recently, an analogue of these spermidine-based siderophores **1a** and **1b** was synthesized in our laboratory (*15*). This synthetic siderophore, spermexatol [2] (**2**, Figure 1), was shown to stimulate the growth of *E. coli* mutants and required the enterobactin receptor (*16*) for activity. Spermexatol [2] also stimulated growth of *Vibrio cholerae* but did not require the vibriobactin receptor. Due to its growth-promoting abilities, spermexatol [2] was chosen as the siderophore component for our initial synthetic efforts. In addition, a lysine-based catechol siderophore was chosen. N^{α},N^{ϵ}-Bis(2,3-dihydroxybenzoyl)-L-lysine (**3**) was isolated from iron-deficient cultures of *Azotobacter vinelandii* and its structure was established by synthesis (*17*). Another synthesis was recently reported by Chimiak and Neilands (*18*).

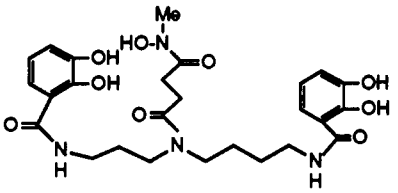
A new class of monocyclic β-lactam antibiotics, [[3(*S*)-(acylamino)-2-oxo-1-azetidinyl]oxy]acetic acid (oxamazins), has been recently synthesized in our laboratory (*19*). These compounds have shown potent activity against Gram-negative bacteria even though the ionizable carboxyl group is displaced one atom further from the β-lactam nitrogen than in the penicillins, cephalosporins, and norcardicins. Due to the bactericidal activity of the oxamazins, the oxamazin–siderophore conjugates **4** and **5** were chosen as synthetic target compounds (Figure 2). Since cephalosporin derivatives are generally broader spectrum antibiotics than monobactams, carbacephalosporin–siderophore conjugates **6** and **7** were also selected for study (Figure 3). In addition, neither the oxamazin

1043-1802/91/2902-0281$02.50/0 © 1991 American Chemical Society

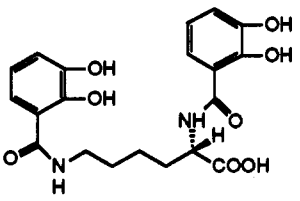


1a Agrobactin, R = OH

1b Parabactin, R = H

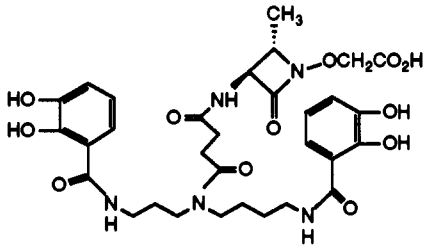


2 Spermexatol-[2]

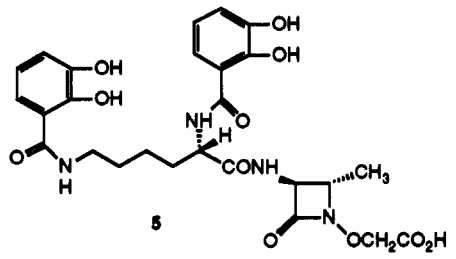


3 N^{α},N^{ω}-Bis(2,3-dihydroxybenzoyl) lysine

Figure 1. Catechol siderophores.



4



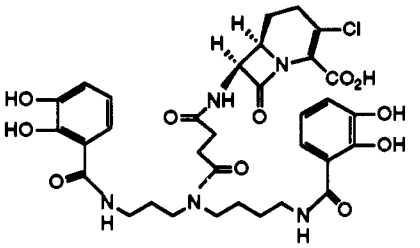
5

Figure 2. Siderophore–oxamazin conjugates.

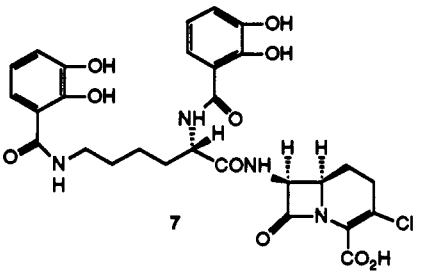
nor the carbacephalosporin contain sulfur, thereby allowing the use of hydrogenolysis as a convenient means of deprotection of the synthetic conjugates.

EXPERIMENTAL PROCEDURES

General Methods. Melting points were taken on a Thomas-Hoover capillary melting point apparatus and are uncorrected. Infrared spectra (IR) were recorded on a Perkin-Elmer 727B or Perkin-Elmer 1420 spectrophotometer. Proton NMR spectra were obtained on a Magnachem A-200 or General Electric GN-300 spectrometer. Chemical shifts are reported in ppm relative to tetramethylsilane (δ units). Carbon-13 NMR were obtained on a General Electric GN-300 spectrometer. Carbon NMR references were the center peak of deuterochloroform (77.0



6



7

Figure 3. Siderophore–carbacephalosporin conjugates.

ppm) or the center peak of deuteromethanol (49.0 ppm). Electron-impact mass spectra, chemical-ionization mass spectra, and fast atom bombardment were performed by Dr. Bruce Plashko on an AEI Scientific Apparatus MS 902 or Du Pont DP 102 spectrometer. Field-desorption mass spectra were obtained by Dr. John L. Occolowitz (Eli Lilly and Co.). Elemental analyses were performed by M-H-W Laboratories, Phoenix, AZ. Radial chromatography was performed with a Chromatotron Model 7924 purchased from Harrison Research Inc., Palo Alto, CA. Flash silica gel chromatography was performed with Merck silica gel 60. Opti-up C_{18} glass-backed plates, purchased from Fluka Chemical Corp., were used for reversed-phase TLC. Whatman #1 filter paper was used for paper chromatography. Solvents used were dried and purified by standard methods. The term "dried" refers to the drying of an organic solvent over anhydrous magnesium sulfate. Carbacephalosporin **24** was kindly provided by Eli Lilly and Co., Indianapolis, IN.

***N*-(*tert*-Butoxycarbonyl)-L-threonine (9).** To a solution of L-threonine (40.50 g, 0.34 mol) and $NaHCO_3$ (29.40 g, 0.35 mol) in water was added a solution of Boc_2O (74.80 g, 0.34 mol) in THF at room temperature. The solution was stirred overnight. The solution was made acidic with 10% citric acid and extracted with ethyl acetate. The organic layer was dried and filtered and the solvent was removed under reduced pressure to give compound **9** in 81% yield (59.66 g) as a white solid: mp 76–77 °C (lit. (*20*) mp 76–80 °C); IR (TF) 3600–2200 (br), 1770 (br), 1720 cm^{-1}, ^1H NMR (200 MHz, $CDCl_3$) δ 1.22 (d, J = 12 Hz, 3 H, CH_3), 1.42 (s, 9 H, $C(CH_3)_3$), 4.14–4.58 (m, 2 H, CH), 5.74 (br s, 1 H, NH), 7.58 (br s, 1 H, COOH).

***O*-Benzyl *N*-(*tert*-Butoxycarbonyl)-L-threoninehydroxamate (11).** *N*-Boc-(L)-threonine (**9**) (20.0 g, 91.24 mmol) and *N*-hydroxysuccinimide (11.51 g, 101 mmol) were dissolved in dry THF and cooled to 0 °C (ice bath). To this was added slowly a solution of DCC (20.63 g, 100 mmol) in dry THF. The reaction mixture was stirred for 14 h. Dicyclohexylurea was removed by filtration, and the solvent was removed under vacuum. The oily residue was taken up in dry THF and a solution of *O*-benzylhydroxylamine (**10**) (13.47 g, 110 mmol) in THF was added. The solution was stirred overnight at room temperature. The solvent was evaporated and the residue was taken up in ethyl acetate, washed with 10% citric acid, 5% $NaHCO_3$, and water, dried, and filtered. The solvent was removed under reduced pressure and the product was recrystal-

lized from ethyl acetate/hexanes to provide the product in 77% yield (22.83 g) as a white solid: mp 86–88 °C; $[\alpha]^{25}_D = -39.0°$ (c = 5.0, $CHCl_3$); IR (KBr) 3500–3180 (br), 2970, 1670, 1530 cm^{-1}; ^1H NMR (200 MHz, $CDCl_3$) δ 1.12 (d, J = 10 Hz, 3 H, CH_3), 1.44 (s, 9 H, $C(CH_3)_3$), 3.91–3.97 (m, 1 H, C*H*OH), 4.34–4.18 (m, 1 H, NHC*H*CO) 5.00 (s, 2 H, benzylic H), 6.02 (d, J = 10 Hz, 1 H, NH), 7.52 (m, 5 H, aromatic H), 10.3 (br s, 1 H, NH); TLC (ethyl acetate/hexanes, 1:1) R_f = 0.29, (ethyl acetate) R_f = 0.75. Anal. ($C_{16}H_{24}N_2O_5$) C, H, N.

***N*-(Benzyloxy)-4(*S*)-methyl-3(*S*)-[(*tert*-butoxycarbonyl)amino]-2-azetidinone (12).** Hydroxamate 11 (12.0 g, 37 mmol), triphenylphosphine (9.703 g, 37 mmol), and CCl_4 (5.7 mL, 37 mmol) were dissolved in 150 mL of dry acetonitrile under nitrogen and triethylamine (3.74 mL, 37 mmol) was added at room temperature. The reaction mixture was followed by normal-phase TLC on silica gel. The solution was stirred for 2 h, the solvent was removed under reduced pressure, and the oily residue was taken up in ethyl acetate. Some of the triphenylphosphine oxide was removed by filtration, and the solution was washed with water, brine, dried, and filtered. The solvent was evaporated and the product was purified by flash column chromatography from ethyl acetate/hexane (1:3) to provide the product in 75% yield (8.43 g) as needles and plates after crystallization from ethyl acetate/hexanes: mp 75–77 °C; $[\alpha]^{25}_D = -11.9°$ (c = 5.0, $CHCl_3$); IR (KBr) 3300, 3040, 2980, 1780, 1710 cm^{-1}; ^1H NMR (200 MHz, $CDCl_3$) δ 1.20 (d, J = 6 Hz, 3 H, CH_3), 1.42 (s, 9 H, $C(CH_3)_3$), 3.50–3.82 (m, 1 H, C*H*CH_3), 4.02–4.38 (m, 1 H, COC*H*), 5.08 (s, 2 H, benzylic H), 5.90 (br s, 1 H, NH), 7.58 (s, 5 H, aromatic H); TLC (ethyl acetate/hexanes, 1:3) R_f = 0.44, (ethyl acetate), R_f = 0.82. Anal. ($C_{16}H_{22}N_2O_4$) C, H, N.

***N*-Hydroxy-4(*S*)-methyl-3(*S*)-[(*tert*-butoxycarbonyl)amino]-2-azetidinone (13).** *O*-Benzyl β-lactam 12 (3.525 g, 11.52 mmol) was dissolved in 150 mL of methanol and 10% Pd/C (20% w/w) was added. Hydrogen gas was bubbled through the solution. After 1 h, Pd/C was removed by filtration and the methanol was evaporated under reduced pressure to provide the product in 94% yield (2.318 g) as a white solid. There was no need for further purification: mp 153–154 °C; IR (KBr) 3360, 2930, 1780, 1690 cm^{-1}; ^1H NMR (200 MHz, acetone-d_6) δ 1.20 (d, J = 6 Hz, 3 H, CH_3), 1.30 (s, 9 H, $C(CH_3)_3$), 3.00 (br s, 1 H, OH), 3.58–3.88 (m, 1 H, NC*H*(CH_3)), 3.90–4.18 (m, 1 H, NHC*H*CO), 6.64 (br s, 1 H, NH); TLC (ethyl acetate) R_f = 0.43. Anal. ($C_9H_{16}N_2O_4$) C, H, N.

Benzyl [[4(*S*)-Methyl-3(*S*)-[(*tert*-butoxycarbonyl)amino]-2-oxo-1-azetidinyl]oxy]acetate (14). *N*-Hydroxy β-lactam 13 (2.07 g, 9.57 mmol) and K_2CO_3 (1.323 g, 9.57 mmol) were dissolved in water and a solution of benzyl bromoacetate (1.52 mL, 9.57 mmol) in THF was added. The mixture was stirred overnight. The solution was concentrated and extracted with ethyl acetate. The organic layer was separated and washed with 0.5% NaOH and water, dried, and filtered. The solvent was removed *in vacuo* to provide the crude product in quantitative yield (3.596 g) as an oily residue. The product was purified by silica gel column chromatography using ethyl acetate/hexanes (1:4) as the elutant to give 79% yield (2.746 g) of 14 as a colorless oil: $[\alpha]^{25}_D = -41.3°$ (c = 5.2, $CHCl_3$); IR (TF) 3350, 3040, 2980, 1780, 1710 cm^{-1}; ^1H NMR (300 MHz, $CDCl_3$) δ 1.40–1.50 (m, 12 H, CH_3 and $C(CH_3)_3$), 3.84 (dq, J = 2 and 6 Hz, 1 H, NC*H*(CH_3)), 4.09 (m, 1 H, NHC*H*CO), 4.61 (AB q, J = 17 Hz, 2 H, OCH_2CO), 5.21 (AB q superimposed over a br s, 3 H, NH and benzylic H), 7.36 (s, 5 H, aromatic H); ^{13}C NMR (75 MHz, $CDCl_3$) δ 15.82, 27.93, 60.12, 63.71, 66.70, 72.38, 79.83, 128.19, 128.28, 134.63, 154.73, 162.59, 167.89; TLC (ethyl acetate/hexanes, 1:2) R_f = 0.24. Anal. ($C_{18}H_{24}N_2O_6$) C, H, N.

2,3-Bis(benzyloxy)benzoic acid *N*-succinimide ester (15) was prepared by the method of Chimiak and Neilands (*18*) in 88% yield after crystallization from ethyl acetate/hexanes: mp 105.5–107.5 °C (lit (*18*) mp 112–114 °C); IR (KBr) 1770, 1740 cm^{-1}; ^1H NMR (300 MHz, $CDCl_3$) δ 2.86 (s, 4 H, $COCH_2$), 5.14 (s, 4 H, benzylic H), 7.10–7.60 (m, 13 H, aromatic H); exact MS (EI) calcd for $C_{25}H_{21}NO_6$ m/z 431.1369, found m/z 431.1367.

N^{α},N^{ϵ}-Bis[2,3-bis(benzyloxy)benzoyl]-L-lysine (16). *N*-Succinimide active ester 15 (3.000 g, 6.95 mmol), L-lysine monohydrochloride (0.631 g, 3.45 mmol), and triethylamine (1.470 g, 14.54 mmol) were dissolved in a homogenous mixture of acetone/water and stirred for 24 h. The solution was concentrated and the residue was dissolved in ethyl acetate, washed with 1 N HCl, water, and brine, dried, filtered, and concentrated to provide 2.69 g (100%) as a colorless oil: $[\alpha]^{22}_D = +8.8°$ (c = 1.0, $CHCl_3$); IR (TF) 3380 (br), 1710, 1660 (br) cm^{-1}; ^1H NMR (300 MHz, $CDCl_3$) δ 1.00–1.95 (m, 6 H, CH_2), 3.02–3.24 (m, 2 H, CH_2), 4.65 (m, 1 H, CH_2CHNH), 4.97–5.22 (merging singlets, 8 H, benzylic H), 7.03–7.80 (m, 26 H, aromatic H), 7.93 (br s, 1 H, NH), 8.58 (br s, 1 H, NH); ^{13}C NMR (75 MHz, $CDCl_3$) δ 23.01, 28.70, 39.43, 71.01, 71.10, 75.82, 76.12, 77.20, 116.84, 124.06, 128.52 (m), 136.45 (m), 146.66, 146.78, 151.53; TLC (methanol/$CHCl_3$, 1:5) R_f = 0.56; MS (positive-ion FAB, glycerol) m/z 779 (M + 1), 817 (M + K^+).

N^{α},N^{ϵ}-Bis[2,3-bis(benzyloxy)benzoyl]-L-lysine *N*-Succinimide Ester (17). To a mixture of compound 16 (0.508 g, 0.651 mmol) and *N*-hydroxysuccinimide (0.075 g, 0.651 mmol) in anhydrous tetrahydrofuran at 0 °C under nitrogen was added a solution of dicyclohexylcarbodiimide (0.148 g, 0.717 mmol) in anhydrous tetrahydrofuran dropwise. The solution was warmed to room temperature and stirred overnight. The solvent was evaporated and the residue was dissolved in benzene and filtered to remove dicyclohexylurea. The filtrate was concentrated to provide 0.569 g (100%) of an oil which was used without further purification: IR (TF) 3480, 2940, 1740, 1650 cm^{-1}; ^1H NMR (300 MHz, $CDCl_3$) δ 1.10–2.00 (m, 6 H, CH_2), 2.75 (s, 2 H, $COCH_2$), 3.05–3.15 (m, 2 H, CH_2), 4.95 (m, 1 H, NHC*H*CO), 5.04–5.12 (merging s, 8 H, benzylic H), 7.00–7.90 (m, 27 H, aromatic H and NH), 8.50 (d, J = 11.6 Hz, 1 H, NH); TLC (ethyl acetate/hexanes, 3:1) R_f = 0.51; MS (positive-ion FAB, *m*-nitrobenzyl alcohol/glycerol) m/z 876 (M + 1).

N^{α},N^{ϵ}-Bis(2,3-dihydroxybenzoyl)-L-lysine (3). Compound 16 (0.223 g, 0.286 mmol) and 10% Pd/C (0.045 g, 20% w/w) were dissolved in 2.0 mL of methanol and exposed to hydrogen at atmospheric pressure for 4 h. The catalyst was removed by filtration and the filtrate was concentrated to provide 0.106 g (100%) of a glassy oil: $FeCl_3$ positive (red-purple); IR (TF) 3650–2300 (br), 1730 cm^{-1}; ^1H NMR (300 MHz, methanol-d_4) δ 1.51–2.10 (m, 6 H, CH_2), 3.30–3.42 (m, 2 H, CH_2), 4.63 (m, 1 H, CH), 6.66–6.75 (m, 2 H, aromatic H), 6.92–6.98 (m, 2 H, aromatic H), 7.20 (dd, J = 1.5 and 8.1 Hz, 1 H, aromatic H), 7.35 (dd, J = 1.5 and 8.1 Hz, 1 H, aromatic H); ^{13}C NMR (75 MHz, methanol-d_4) δ 24.31, 29.88, 40.15, 53.94, 116.71, 116.92, 118.61, 119.42, 119.52, 119.72, 147.05, 147.12, 149.63, 150.09, 170.86, 171.40; reverse-phase TLC (isopropyl alcohol/water, 1:1) R_f = 0.45; MS (positive-ion FAB, *m*-nitrobenzyl alcohol/glycerol) m/z 419 (M + 1), 441 (M + Na^+). With the procedure of Raymond (*21*), the formation constant for the 3:2 siderophore–iron (III) complex of compound 3 was measured. Spectrophotometric competition experiments were performed on the iron(III) complex

of 3 with a slight excess of EDTA at pH 7. The formation constant for compound 3 was calculated to be 10^{27}.

N^4-(3-Carboxypropanoyl)-N^1,N^8-bis[2,3-bis(benzyloxy)benzoyl]spermidine (18) was prepared by the method of Sharma and Miller (*15*).

N^4-[3-[(Succinimidooxy)carbonyl]propanoyl]-N^1,N^8-bis[2,3-bis(benzyloxy)benzoyl]spermidine (19) was prepared in the same manner as 17 in 88% yield as a colorless oil: IR (TF) 3380, 2920, 1810, 1770, 1730 cm^{-1}; ^1H NMR (300 MHz, $CDCl_3$) δ 1.10–1.80 (m, 6 H, CH_2), 2.50–2.60 (m, 2 H, CH_2), 2.72 (s, 4 H, $COCH_2$), 2.95 (m, 2 H, CH_2), 5.00–5.10 (m, 8 H, benzylic H), 7.00–8.00 (m, 28 H, aromatic H and NH); TLC (methanol/ethyl acetate, 1:30) R_f = 0.44; MS (positive-ion FAB, *m*-nitrobenzyl alcohol/glycerol) *m/z* 976 (M + 1).

N^4-(3-Carboxypropanoyl)-N^1,N^8-bis(dihydroxybenzoyl)spermidine (20). Compound 18 and 10% Pd/C (0.068 g, 20% w/w) were dissolved in methanol and exposed to hydrogen at atmospheric pressure for 4 h. The catalyst was removed by filtration and the filtrate was concentrated to provide 0.20 g (100%) of a colorless oil: $FeCl_3$ positive (red-purple); IR (TF) 3650–2300 (br), 1710 cm^{-1}; ^1H NMR (300 MHz, methanol-d_4) δ 1.15–2.00 (m, 6 H, CH_2), 2.65 (br s, 4 H, CH_2), 3.30–3.45 (m, 8 H, CH_2), 6.65–6.75 (m, 2 H, aromatic H), 6.94 (d, J = 7.8 Hz, 2 H, aromatic H), 7.22 (d, J = 8.1 Hz, 2 H, aromatic H); ^{13}C NMR (75 MHz, methanol-d_4) δ 25.94, 26.84, 27.55, 28.35, 28.87, 29.51, 30.21, 37.59, 37.99, 39.82, 40.00, 44.35, 46.68, 47.83, 48.54, 116.55, 116.68, 118.53, 118.62, 119.62, 147.17, 150.15 (m), 171.43, 171.56, 173.64, 174.22, 176.66; reverse-phase TLC (isopropyl alcohol/water, 1:1) R_f = 0.64); MS (positive-ion FAB, *m*-nitrobenzyl alcohol/glycerol) *m/z* 535 (M + H_2O), 517 (M+), 499 (M – H_2O); Spectrophotometric competition experiments were performed on the ferric iron complex of 20 at pH 7 with a slight excess of EDTA (*21*). The calculated formation constant for the ferric complex of 20 was 10^{27}.

Benzyl [[4(*S*)-Methyl-3(*S*)-[[[N^1,N^8-bis[2,3-bis(benzyloxy)benzoyl]spermidin-N^4-yl]succinyl]amino]-2-oxo-1-azetidinyl]oxy]acetate (22). In an oven-dried flask, *N*-Boc-oxamazin benzyl ester 14 (0.705 g, 1.93 mmol) was dissolved in dry methylene chloride under nitrogen. The solution was cooled to 0 °C (ice bath) and trifluoroacetic acid (TFA) (4–6 equiv) was added slowly. The reaction mixture was allowed to warm up to room temperature and further stirred for 30 min. The solvent and TFA were removed under a vacuum. Traces of TFA were removed by evaporating the oily residue with toluene and hexanes to provide the TFA salt 21 as a pale yellow solid.

The TFA salt 21 and $NaHCO_3$ (1.36 g, 1.93 mmol) were dissolved in water. To this a solution of *N*-succinimide ester 19 (1.72 g, 1.76 mmol) in ethyl acetate was added at room temperature. The reaction mixture was stirred overnight and the organic layer was separated. The ethyl acetate layer was washed with 1 N HCl, water, 5% $NaHCO_3$, water, and brine, dried, filtered, and evaporated. The crude product was purified by silica gel chromatography, eluting with ethyl acetate to provide 0.920 g (63%) of 22 as an oil: IR (TF) 3382 (br), 1760, 1690 (br) cm^{-1}; ^1H NMR (200 MHz, $CDCl_3$) δ 1.20–1.67 (m, 11 H, NCH(CH_3) and CH_2), 2.41–2.62 (m, 4 H, CH_2), 3.01–3.34 (m, 8 H, CH_2), 3.81–3.97 (m, 1 H, NC*H*(CH_3)), 4.11–4.25 (m, 1 H, NHC*H*CO), 4.52 (s, 2 H, OCH_2CO), 5.02–5.26 (merging singlets, 10 H, benzylic H), 7.06–8.01 (m, 38 H, aromatic H and two NH); TLC (ethyl acetate) R_f = 0.12. Anal. ($C_{66}H_{69}N_5O_{12}$) C, H, N.

Benzyl [[4(*S*)-Methyl-3(*S*)-[[N^α,N^ϵ-bis[2,3-bis(benzyloxy)benzoyl]-L-lysyl]amino]-2-oxo-1-azetidinyl]oxy]acetate (23) was obtained in the same manner as 22 as an oil in 61% yield: IR (TF) 3380 (br), 1770, 1710, 1680, 1610 (br) cm^{-1}; ^1H NMR (200 MHz, $CDCl_3$) δ 1.10–1.78 (m, 9 H, NCH(CH_3) and CH_2), 3.05–3.22 (m, 2 H, CH_2), 3.88–4.01 (dq, J = 2 and 6 Hz, 1 H, NC*H*(CH_3)), 4.24 (m, 1 H, NHC*H*CO), 4.47–4.61 (m, 3 H, CH_2CHNH and OCH_2CO), 5.00–5.24 (m, 10 H, benzylic H), 7.04–7.95 (m, 37 H, aromatic H and NH), 8.54 (d, 1 H, NH); TLC (ethyl acetate) R_f = 0.54. Anal. ($C_{61}H_{60}N_4O_{11}$) C, H, N.

[[4(*S*)-Methyl-3(*S*)-[[[N^1,N^8-bis(2,3-dihydroxybenzoyl)spermidin-N^4-yl]succinyl]amino]-2-oxo-1-azetidinyl]oxy]acetic acid (4) was prepared from its benzyl protected precursor 22 upon catalytic hydrogenation using 10% Pd/C (20% w/w) in methanol for 1 h. After filtration to remove the catalyst and concentration, compound 4 was obtained in 97% yield as a colorless oil which required no purification: $FeCl_3$ positive (red-purple); IR (TF) 3380 (br), 1750 (br), 1660 (br) cm^{-1}; ^1H NMR (200 MHz, methanol-d_4) δ 1.10–1.77 (m, 11 H, NCH(CH_3) and CH_2), 2.22–2.49 (m, 4 H, CH_2), 3.02–3.25 (m, 8 H, CH_2), 3.73 (m, 1 H, NC*H*(CH_3)), 3.98 (m, 1 H, NC*H*CO), 4.30 (s, 2 H, OCH_2CO), 6.47 (m, 2 H, aromatic H), 6.70 (m, 2 H, aromatic H), 6.98 (m, 2 H, aromatic H); reverse-phase TLC (2-propanol/H_2O, 1:1) R_f = 0.71; paper chromatography (2-propanol/H_2O, 3:1) R_f = 0.61; MS (FD) *m/z* 674 (M + 1).

[[4(*S*)-Methyl-3(*S*)-[[N^α,N^ϵ-bis(2,3-dihydroxybenzoyl)-L-lysyl]amino]-2-oxo-1-azetidinyl]oxy]acetic acid (5) was prepared from 23 in a manner similar to that for 4 and was obtained in quantitative yield as a colorless oil which required no further purification: $FeCl_3$ positive (red-purple); IR (TF) 3700–2300 (br), 1780–1720 (br), 1650 (br) cm^{-1}; ^1H NMR (200 MHz, methanol-d_4) δ 1.33–2.05 (m, 11 H, NCH(CH_3) and CH_2), 4.01–4.13 (q, J = 5 Hz, 1 H, NC*H*(CH_3)), 4.31 (m, 1 H, NHC*H*CO), 4.52–4.60 (m, 3 H, OCH_2CO and CH_2CHCO), 6.70–7.31 (m, 7 H, aromatic H and NH), 8.15 (br s, 1 H, COOH); reverse-phase TLC (2-propanol/H_2O, 1:1) R_f = 0.82; paper chromatography (2-propanol/H_2O, 3:1) R_f = 0.76; MS (FD) *m/z* 575 (M + 1), 597 (M + Na^+).

4-Nitrobenzyl 7β-[[[N^1,N^8-Bis[2,3-bis(benzyloxy)benzoyl]spermidin-N^4-yl]succinyl]amino]-1-carba-3-chloro-3-cephem-4-carboxylate (25). Compound 18 (0.173 g, 0.197 mmol) and carbacephalosporin 24 (0.077 g, 0.198 mmol) were suspended in 1.0 mL of anhydrous methylene chloride under nitrogen. Triethylamine (0.012 g, 0.197 mmol) and EEDQ (0.063 g, 0.255 mmol) were added, and the solution was stirred for 19 h. The solution was diluted with ethyl acetate and washed with 0.5 N HCl, water, and brine, dried, filtered, and concentrated to provide 0.273 g of a yellow oil. The oil was purified by radial chromatography eluting with 1:20 MeOH/ethyl acetate to give 0.198 g (84%) of 25 as a yellow oil: $[\alpha]^{25}_D$ = +10.1° (*c* = 0.7, $CHCl_3$); IR (TF) 3420–2860 (br), 1770, 1650, 1520, 1345 cm^{-1}; ^1H NMR (300 MHz, $CDCl_3$) δ 1.20–2.00 (m, 10 H, CH_2), 2.39–2.70 (m, 6 H, CH_2 including allylic CH_2), 3.00–3.34 (m, 8 H, CH_2), 3.75 (m, 1 H, C8 CH_2CH), 5.00–5.40 (m, 11 H, benzylic H and C7 NHC*H*), 7.11–7.70 (m, 27 H, aromatic H), 7.90–8.20 (m, 4 H, aromatic H and NH); ^{13}C NMR (75 MHz, $CDCl_3$, all signals at 25 °C reported) δ 21.80, 24.84, 25.75, 26.47, 26.60, 27.47, 28.34, 28.51, 30.98 and 31.60 (allylic), 36.90, 38.79, 42.96, 45.18, 45.25, 47.04, 52.36, 58.47, 65.93, 70.99, 71.08, 76.04 (m), 77.20, 116.54–116.94 (m) 122.72, 122.94, 123.51, 124.29, 126.78, 126.96, 127.31, 127.52, 128.07–128.61 (m), 130.91, 131.18, 136.23, 136.31, 136.47, 142.13, 146.41–146.66 (m), 147.53, 151.59, 159.88, 159.91, 164.95–165.33 (m), 171.09, 171.39, 172.91; TLC (ethyl acetate) R_f = 0.13, (methanol/ethyl acetate, 1:30) R_f = 0.20; MS (positive ion FAB, *m*-nitrobenzyl alcohol/glycerol) *m/z* 1212 (M + 1).

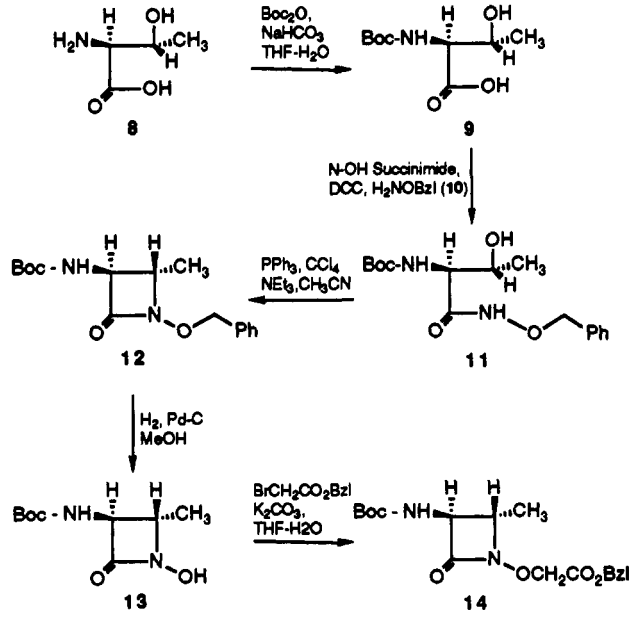
4-Nitrobenzyl 7β-[[N^α,N^ϵ-bis[2,3-bis(benzyloxy)benzoyl]-L-lysyl]amino]-1-carba-3-chloro-3-cephem-

4-carboxylate (26) was prepared by coupling **17** and **24** in the same manner as **22** to provide **26** in 84% yield as a colorless oil: $[\alpha]^{25}_D = -3.1°$ (c = 0.9, $CHCl_3$); IR (TF) 3380, 1775, 1740, 1650, 1525 cm^{-1}; ^1H NMR (300 MHz, $CDCl_3$) δ 1.00–1.40 (m, 6 H, CH_2), 1.60–1.90 (m, 2 H, C1 $CHCH_2$), 2.40–2.60 (m, 2 H, allylic CH_2), 3.01–3.30 (m, 2 H, CH_2), 3.82 (m, 1 H, C8 CH_2CH), 4.49 (m, 1 H, $NHCHCO$), 5.05–5.41 (m, 13 H, C7 NHCH and benzylic H), 7.09–7.68 (m, 26 H, aromatic H), 7.86 (d, J = 8.1 Hz, 1 H, NH), 7.95 (t, J = 5.4 Hz, 1 H, NH), 8.17 (m, 2 H, aromatic H), 8.46 (d, J = 7.2 Hz, 1 H, NH); ^{13}C NMR (75 MHz, $CDCl_3$) δ 21.78, 22.85, 28.53, 30.59, 31.71, 38.90, 52.38, 53.21, 58.57, 66.05, 75.99, 76.25, 77.20, 116.87, 117.46, 122.96, 123.03, 123.10, 123.61, 124.31, 124.53, 126.15, 127.21, 127.56, 127.67, 128.14, 128.23, 128.53, 128.64, 128.74, 130.86, 136.30 (m), 142.20, 146.67, 167.88, 147.67, 151.62, 151.70, 159.96, 165.08, 165.54, 172.26; TLC (ethyl acetate/hexanes, 4:1) R_f = 0.53; MS (positive ion FAB, m-nitrobenzyl alcohol/glycerol) m/z 1112 (M+).

7β-[[[N^1,N^8-Bis[2,3-bis(benzyloxy)benzoyl]spermidin-N^4-yl]succinyl]amino]-1-carba-3-chloro-3-cephem-4-carboxylic Acid (6). To a solution of **25** (0.104 g, 0.086 mmol) in 1.0 mL of 5% aqueous dimethylformamide (made from deionized distilled water and HPLC grade DMF) was added 22.0 μL (0.294 mmol, 300 mol %) of concentrated HCl and 0.022 g of 10% Pd/C. This mixture was exposed to hydrogen at atmospheric pressure for 24 h. The catalyst was removed by filtration. The dimethylformamide/water mixture was removed by evaporation under high vacuum. The residue was redissolved in methanol and was evaporated repeatedly in an attempt to remove the residual DMF. ^1H NMR showed traces of DMF despite this attempt to remove it. Evidence that these types of compounds have a relatively high affinity for DMF has been reported (22). Product **6** was obtained in 100% yield as a dark amber oil: $FeCl_3$ positive (red-purple); IR (TF) 3590–2600 (br), 1760, 1650 cm^{-1}; ^1H NMR (300 MHz, methanol-d_4) δ 1.40–2.00 (m, 10 H, CH_2), 2.40–3.00 (m, 6 H, CH_2), 3.25–3.50 (m, 8 H, CH_2), 4.80 (m, 1 H, C8 $CHCH_2$), 5.25 (m, 1 H, C7 $CHNH$), 6.72 (m, 2 H, aromatic H), 7.20–7.40 (m, 3 H, aromatic H and NH); ^{13}C NMR (75 MHz, methanol-d_4, all signals at 25 °C reported) δ 23.22, 26.08, 26.98, 27.63, 28.50, 29.10, 29.61, 31.55 (m, allylic CH_2), 32.04, 37.64, 38.00, 39.82, 40.07, 44.44, 46.72, 53.80, 116.82, 118.59, 118.75, 119.68, 123.02, 126.64, 127.78, 130.28, 131.45, 147.22, 150.20 (m), 166.81, 171.45 (m), 173.61, 174.17, 175.26; Reverse-phase TLC (2-propanol/H_2O, 15:1) R_f = 0.70; paper chromatography (2-propanol/H_2O, 3:1) R_f = 0.67; MS (positive-ion FAB, glycerol) m/z 716 (M + 1); exact FAB (M + 1) calcd for $C_{28}H_{29}N_4O_{10}Cl$ 617.1650, found 617.1641.

7β-[[$N^α$,$N^ε$-Bis(2,3-dihydroxybenzoyl)-L-lysyl]amino]-1-carba-3-chloro-3-cephem-4-carboxylic acid (7) was prepared in the same manner as **6** from **26** in 100% yield as an amber oil: $FeCl_3$ positive (red-purple); IR (TF) 3680–2350 (br), 1770, 1650, 1540 cm^{-1}; ^1H NMR (300 MHz, methanol-d_4) δ 1.00–2.00 (m, 8 H, C1 $CHCH_2$ and CH_2), 2.02–3.30 (m, 4 H, CH_2 and allylic CH_2 obscured by residual DMF), 3.85–3.95 (m, 1 H, C8 CH_2CH), 4.60 (m, 1 H, $NHCHCO$), 5.30 (m, 1 H, C7 NHCH), 6.71 (m, 2 H, aromatic H), 6.98 (t, J = 6.9 Hz, 2 H, aromatic H), 7.28–7.42 (m, 4 H, aromatic and NH), 8.00 (s, 1 H, COOH); ^{13}C NMR (75 MHz, methanol-d_4, all signals at 25 °C reported) δ 23.04, 24.26, 25.84, 26.53, 29.78, 32.27, 32.47 (allylic), 34.45, 40.02, 53.80, 53.09, 59.50, 116.69, 118.72, 119.54, 119.76, 119.92, 122.90, 123.87, 125.28, 129.92, 131.45 (m), 146.96, 149.61, 150.08, 163.44, 166.38, 170.95 (m), 171.37, 174.87; Reverse-phase TLC (2-propanol/water, 1:1) R_f = 0.66; MS (positive ion FAB, m-nitrobenzyl alcohol/glycerol) m/z 618 (M + 1), 640 (M + Na^+); exact FAB (M + 1) for $C_{33}H_{38}N_5O_{11}Cl$ calcd 716.2334, found 716.2328.

Scheme I



Bioassay Testing Procedures. *Plate Bioassay to Measure Siderophore Activity by Zones of Growth Stimulation. E. coli* X580 was grown overnight in Luria broth at 300 rpm at 37 °C. The culture was diluted 1:200 000 into Luria agar containing the deferrated iron chelator ethylenediaminebis(*o*-hydroxyphenylacetic acid) (EDDA) (100 μg/mL) and the agar poured into sterile Petri dishes and allowed to solidify. Siderophores **3** and **20** were prepared as 10 mM stock solutions in 10% aqueous ammonium hydroxide and were diluted to the test concentrations with water and filtered through an Acro-Disc 0.2-μm assembly. Sterile 6.5-mm filter-paper disks containing 5 μL of the compounds were placed on the surface of the agar and the Petri dishes were incubated for 24 h at 37 °C. Diameters of zones of stimulation were measured.

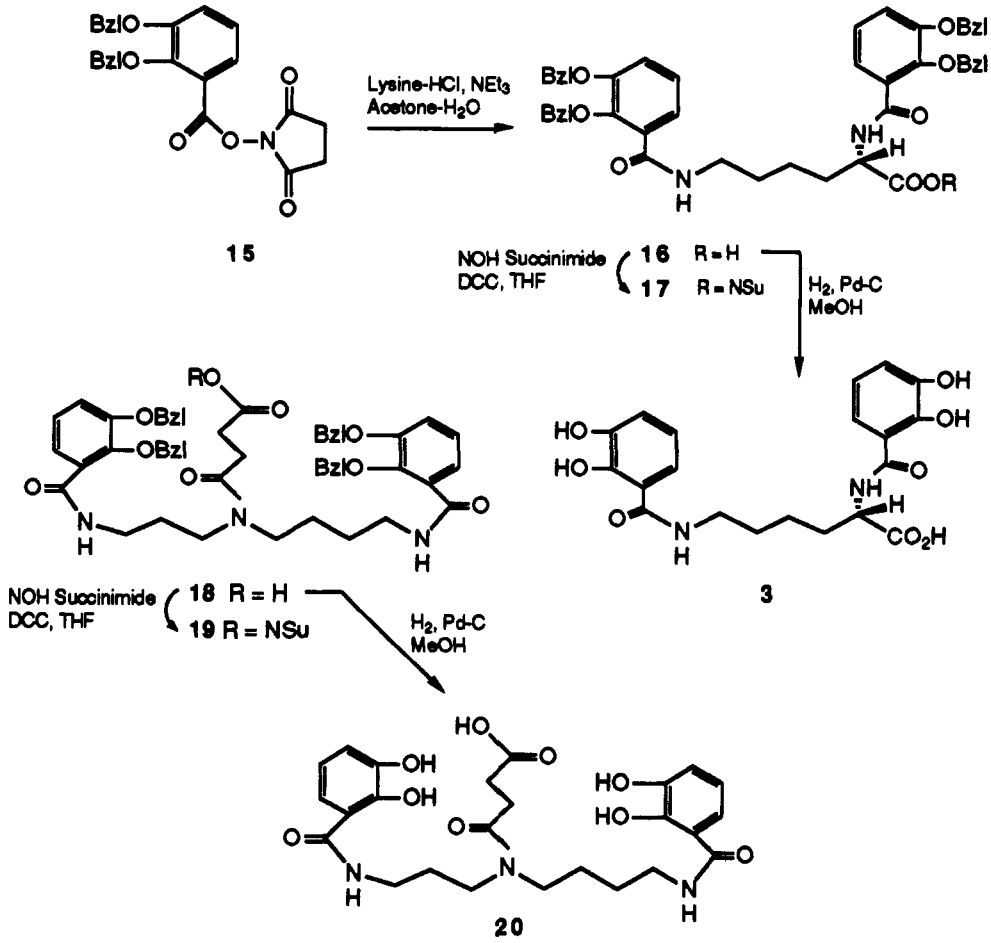
Liquid Growth Bioassay for Antimicrobial Activity. The test compounds were prepared as 5 mM stock solutions in dimethylformamide and were added to sterile Luria broth or sterile Luria broth containing deferrated EDDA (100 μg/mL) to give 1.0 or 10 μM final concentration of the conjugates. Ten microliters of a 24-h-old culture of *E. coli* X580 in Luria broth was added per 50 mL of Luria broth. The bacteria were added immediately after addition of the conjugates or after preincubation of the test compound in the Luria broth for 12 h at 37 °C. The culture flasks were then shaken at 37 °C at 300 rpm. Aliquots were removed every 2 h and the culture turbidity was measured at 600 nm. All the assays were performed in duplicate.

Minimum inhibitory concentration (MIC) values were determined by Eli Lilly and Co. using their standard cephalosporin broad-screen assay.

RESULTS AND DISCUSSION

Synthetic Aspects. As in all multistep syntheses, an important consideration in the synthesis of these conjugates was the careful choice of protecting groups. The most important factors in the choice of protecting groups were selective manipulation in high yields under mild conditions and, in the deprotection sequence, the formation of volatile byproducts so that extensive purification of the final products could be avoided. Since the stability of the target compounds was unknown, the use of protecting

Scheme II



groups that could be removed cleanly was important. Therefore, the *tert*-butoxycarbonyl and benzyl groups were chosen.

The ease of removal of a *tert*-butoxycarbonyl (*t*-Boc) group with trifluoroacetic acid (TFA) led to the use of *t*-Boc protection of the amino group of L-threonine enroute to a required modified synthesis of oxamazins (Scheme I). L-Threonine (**8**) was converted to its *N*-Boc-protected derivative **9** with di-*tert*-butyl dicarbonate (Boc_2O) in quantitative yield. *N*-Boc-threonine (**9**) was converted to hydroxamate **11** in 77% yield upon treatment with *O*-benzylhydroxylamine (**10**) (*23*), *N*-hydroxysuccinimide, and DCC. β-Lactam **12** was obtained from hydroxamate **11** in 75% yield with $Ph_3P/CCl_4/Et_3N$ (*24*). The benzyl group of β-lactam **12** was removed upon catalytic hydrogenation in methanol to provide *N*-hydroxy β-lactam **13** in 96% yield. The *N*-hydroxy group of β-lactam **13** was then alkylated with benzyl bromoacetate to afford the desired *N*-Boc-oxamazin as its benzyl ester **14** in 79% yield (35% overall yield from **8**).

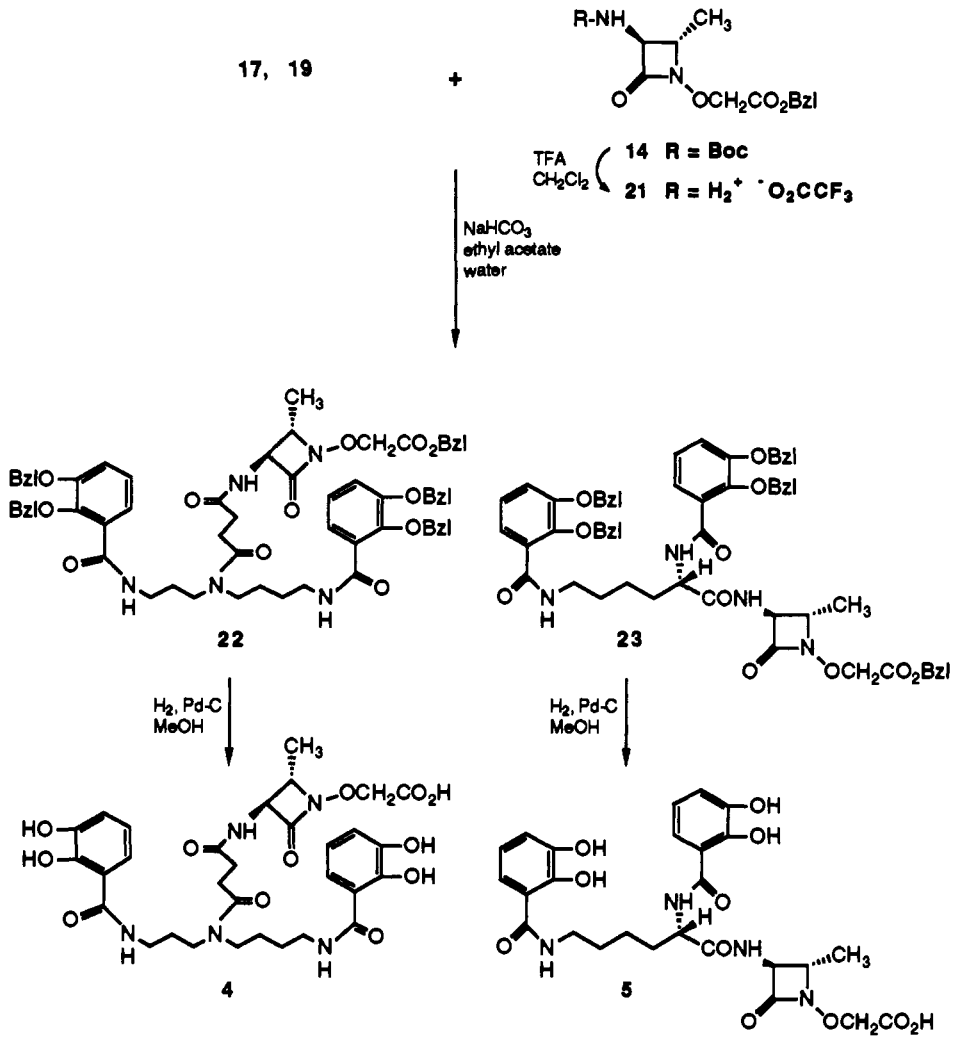
N^{α},N^{ϵ}-Bis[2,3-bis(benzyloxy)benzoyl]lysine (**16**) was prepared as described by Chimiak and Neilands (*18*). Thus, 2,3-dibenzoxybenzoic acid was converted to its *N*-succinimide ester **15** with *N*-hydroxysuccinimide and DCC in 92% yield (Scheme II). The active ester was then treated with L-lysine monohydrochloride and triethylamine to produce **16** in quantitative yield without further purification. Simple hydrogenolysis of **16** afforded the lysine siderophore **3** in quantitative yield. Synthesis of siderophore **18** from spermidine, 2,3-bis(benzyloxy)benzoic acid, and succinic anhydride was previously reported (*15*). Again, hydrogenolysis of **18** gave deprotected **20** in 100% yield. The formation constants for the 3:2 siderophore–iron(III) complexes of compounds **3** and **20** were measured by using the procedure of Raymond (*21*). Spectrophotometric competition experiments were separately performed on the ferric iron complexes with a slight excess of EDTA at pH 7. The formation constants for both compounds **3** and **20** were calculated to be 10^{27}.

Siderophores **16** and **18** were converted to their *N*-succinimide active esters **17** and **19** by using the standard *N*-hydroxysuccinimide and DCC method in 100% and 88% yields, respectively. These active esters were not purified but directly used after filtration to remove dicyclohexylurea. With the two siderophore active esters in hand, efforts were directed at the synthesis of the siderophore–β-lactam conjugates.

Coupling of *N*-succinimide esters **17** and **19** with oxamazin **14** was relatively straightforward (Scheme III). The procedure involved the removal of the *t*-Boc protecting group from **14** using anhydrous trifluoroacetic acid in anhydrous methylene chloride to produce amine salt **21** as an oil. Treatment of **21** with esters **17** and **19** in a two phase ethyl acetate/water solvent system provided the protected oxamazin/siderophore conjugates **22** and **23** in 63% and 61% yields, respectively. The desired oxamazins **4** and **5** were obtained as highly viscous oils upon simple catalytic hydrogenation of rigorously purified **22** and **23** using 10% Pd/C in methanol in 97% and 100% yields, respectively. Compounds **4** and **5** were determined to be homogeneous by reverse-thin-layer and paper chromatographic analysis.

The syntheses of the carbacephem conjugates **6** and **7** are shown in Scheme IV. The hydrochloride salt of carbacephalosporin **24** (*25*) was suspended in anhydrous methylene chloride and treated with triethylamine to liberate the free amine. The free amine was not isolated but was treated with siderophore **18** and 2-ethoxy-*N*-(ethoxycar-

Scheme III



bonyl)-1,2-dihydroquinoline (*26*) (EEDQ) in anhydrous methylene chloride to provide protected conjugate **25** in 83% yield. Lysine siderophore **16** was also converted to its carbacephalosporin conjugate **26** in this manner, but although the desired product was obtained, the yield was unacceptable (20%). Compound **26** was obtained in satisfactory yield (84%) by coupling **24** and active ester **17** in the same manner as the oxamazin conjugates **22** and **23**.

Deprotection of compound **25** proved to be a problem due to the presence of the double bond in the carbacephem. Initial deprotection using hydrogen and 10% palladium on carbon (20% w/w) in methanol reduced the double bond and reductively removed the chlorine atom. While it has been shown that carbacephalosporins without the vinylic chlorine demonstrate antibacterial activity, compounds without the double bond are devoid of activity (*27*). Successful deprotection was achieved with hydrogen, 10% palladium on carbon, concentrated hydrogen chloride, and 5% aqueous dimethylformamide (*28*) to produce compound **6** in 73% overall yield from **18** and **24**. Proof that the double bond was intact was facilitated by ^{13}C NMR analysis, which showed the allylic carbon signal at 31.55 ppm. Compound **26** was also deprotected in the same manner, providing **7** as an amber oil in quantitative yield (84% overall yield from **16** and **24**). The ^{13}C NMR spectrum indicated the presence of the allylic carbon signal at 32.47 ppm, confirming the presence of the double bond.

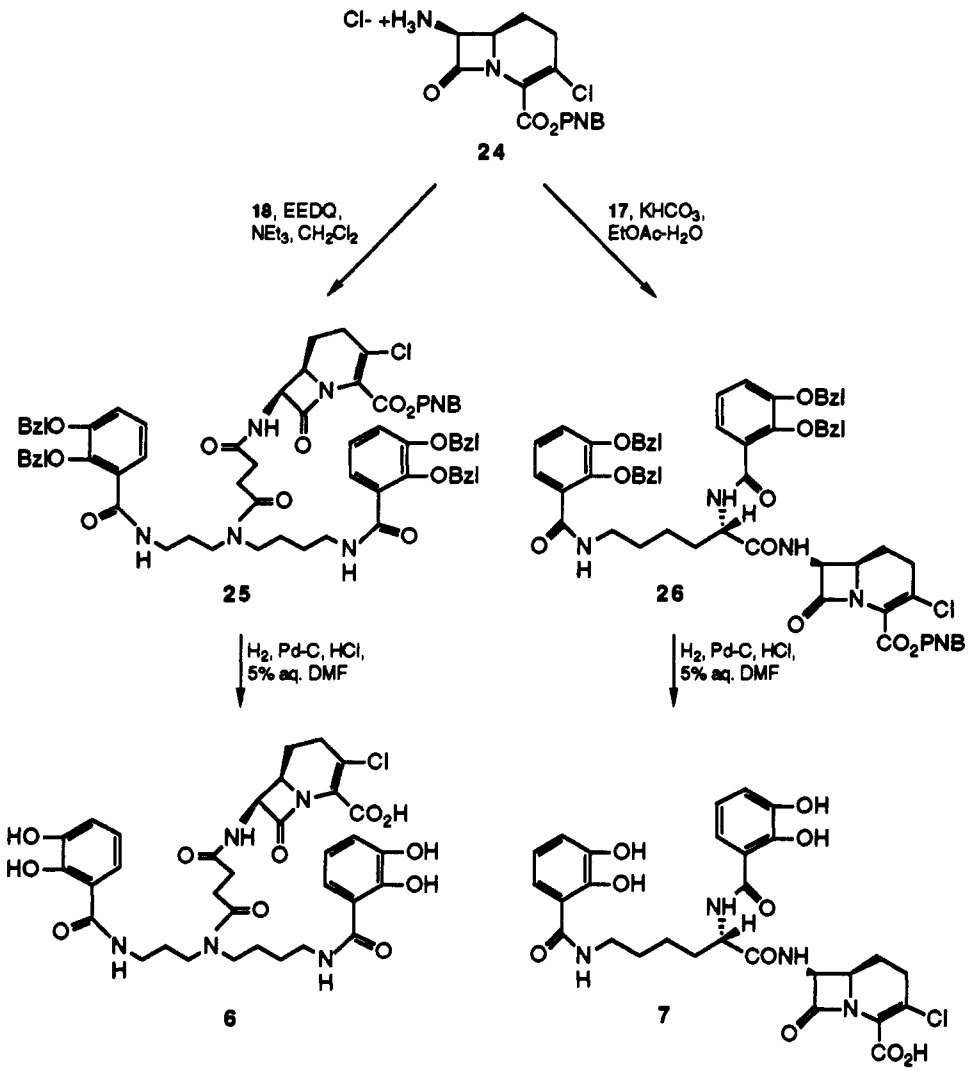
It is important to note that β-lactam–siderophore conjugates **4–7** appear to have quadradentate ligands instead of the required hexadentate ligands for typical 1:1 metal–siderophore chelation to Fe(III) and its subsequent transportation. However, the exact mode of coordination of these conjugates to ferric iron is not known. The quadradentate type siderophores have two binding sites for Fe(III) ion. Therefore, quadradentate siderophore–iron complexes must have a minimum 3:2 stoichiometry. Nature has utilized quadradentate siderophores such as rhodotorulic acid and N^{α},N^{ϵ}-bis(2,3-dihydroxybenzoyl)-lysine (**3**) to transport Fe(III) efficiently. It has been shown that rhodotorulic acid forms a 3:2 complex with ferric ions (*29*). Thus, it was anticipated that siderophore–β-lactam conjugates **4–7** would also chelate and transport ferric iron.

Another important concept to consider is the effect (on siderophore activity) of the stereochemistry at the metal center. Studies have shown that one of the factors which may help regulate recognition of the iron complex by a receptor protein is the chirality about the metal center (*30*). The asymmetric character of the antibiotic component of the siderophore/β-lactam conjugates may influence the chirality about the metal center, which in turn may influence the recognition of the conjugates at the receptor site.

Biological Aspects. An objective of this work was to determine if effective antimicrobial agents could be formed from catechol siderophores and β-lactam antibiotics. It was hoped that these conjugates would bypass the normal β-lactam-transport system (*3, 31*), and, instead, be transported through the iron-transport system.

Several assays were used to study the ability of compounds **4–7** to act as siderophores and antimicrobial agents for several strains of *E. coli* and other bacteria. The details

Scheme IV



of these assays are given in the Experimental Procedures. The *E. coli* strains which were used include *E. coli* RW193, *E. coli* RWB18, and *E. coli* X580. The RW193 strain is an *E. coli* K12 *ent*A, *fhu*A positive organism which cannot synthesize enterobactin, but is able to use both hydroxamate and catecholate type siderophores. *E. coli* RWB18 is a mutant from *E. coli* RW193 which is unable to bind colicin B (*32*). The inability to bind colicin B has been attributed to the absence of an outer-membrane protein which also has been implicated in the transport of ferric enterobactin (*32b*). *E. coli* X580 (*33*) is a β-lactam-hypersensitive organism which is commonly used to screen for antimicrobial activity. In addition, the organism and strain-selective antimicrobial activity was determined by the disk diffusion method (*34*).

Before the antimicrobial activity of conjugates 4–7 could be studied, it was necessary to establish that the siderophore portions of the conjugates were effective iron-transport agents by promoting the growth of *E. coli* under EDDA-induced iron-deficient conditions. Table I shows the growth-promoting ability of siderophores **3** and **20** in *E. coli* X580 with the agar plate method. Both of the compounds were growth promoters as seen by a zone of growth stimulation. Neither one of these compounds was tested as the preformed iron complex. This implies that these siderophores are able to scavenge the iron from the EDDA in the agar. A liquid growth assay showed that these siderophores **3** and **20** themselves are devoid of antimicrobial activity against *E. coli* X580.

The β-lactam–siderophore conjugates 4–7 were initially tested by using the disk diffusion method. Of the four conjugates, only compound **6** exhibited any antimicrobial activity. Compound **6** showed moderate activity against *Staphylococcus aureus* X1.1 (64) and V41 (64) and *Streptococcus* A C283 (16) and *Streptococcus pneumonae* PARK (64) (MIC values in μg/mL in parentheses).

Table I. Plate Bioassay for Siderophore Activity for the Siderophores 3 and 20

concn, mM	zone of stimulation,[a] mm		concn, mM	zone of stimulation,[a] mm	
	3	20		3	20
1	13	NS[b]	10	31	
5	26	28			

[a] *E. coli* X580 overnight culture, 1:200 000 dilution into Luria–EDDA (100 μg/mL) agar. Filter-paper disks containing 5 μL of the siderophores at the concentrations indicated were placed in the surface of the Luria agar. Plates were incubated at 37 °C for 24 h and examined for zones of stimulation of growth around the compounds. All plates were performed in duplicate. [b] No zone of stimulation was observed.

Figure 4 shows the results of incubation of the siderophore–carbacephalosporin conjugates **6** and **7** with the β-lactam-hypersensitive *E. coli* X580. Both of these conjugates show *significant* antimicrobial activity as shown by the delay in observed microbial growth compared to the control. The bacteria that eventually did grow were separately incubated again in the presence of each of test compounds **6** and **7**. This time, there was no observed delay in growth. These results may suggest that during

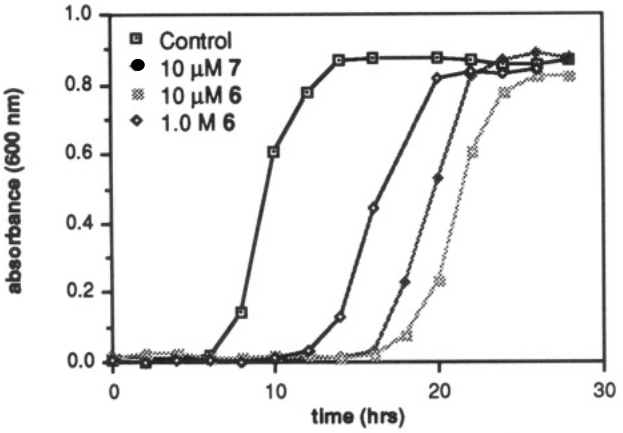


Figure 4. Effects of conjugates **6** and **7** in Luria broth on the growth rate of *E. coli* X580.

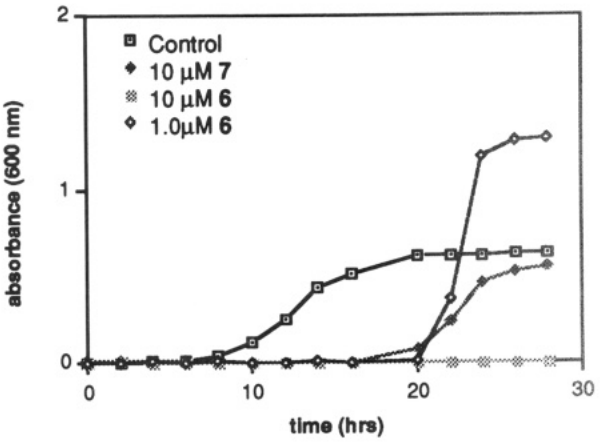


Figure 5. Effect of conjugates **6** and **7** in Luria broth containing 100 μg/mL of EDDA on the growth rate of *E. coli* X580.

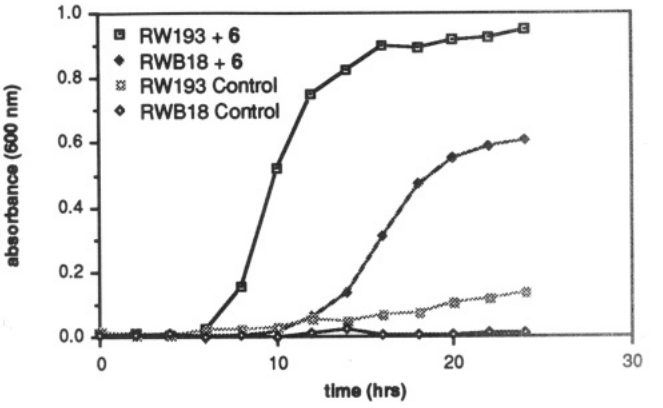


Figure 6. Effect of conjugate **6** (10 μM) in Luria broth with 100 μg/mL EDDA on the growth rate of *E. coli* RW193 and RWB18.

the first incubation, the microbial growth that was observed after the delay was due to selection of mutants from the parent *E. coli* strain. These mutants may be deficient in some form of iron transport since growth was observed in the presence of the conjugates. *E. coli* X580 survivors which were subsequently shown to be resistant to conjugate **6** have been isolated and a preliminary investigation to determine the mechanism of resistance has been performed (*36*). This type of overnight resistance to iron-transported antibiotics has been reported for the natural antibiotic albomycin, as well as the catechol-containing compound E-0702 (*7c*, *12*, *37*). The analogue of **6** that did not contain the double bond in the carbacephalosporin was also included in the assay. As expected (*38*), reduced **6** did display siderophore (growth promoting) activity, but exhibited no antimicrobial activity against *E. coli* X580.

In order to determine if these conjugates were stable under these test conditions, compound **6** was preincubated in Luria both at 37 °C for 12 h prior to addition of the organisms. Results from the incubation produced a growth curve identical with that of the test flask which was not preincubated. Apparently, the result of the preincubation test reveals that the test compound is stable under the assay conditions, indicating that the observed results are not due to spontaneous decomposition of the compound in the culture broth. In addition, a sample of the carbacephaolsporin nucleus (deprotected **24**) was incubated at 10 μM concentration against *E. coli* X580. The β-lactam, itself, did not inhibit the growth of the microorganisms, which provides further evidence of the conjugate's stability to the assay conditions.

The liquid growth assay using an iron chelator, EDDA is shown in Figure 5. In these low-iron conditions, incubation with a 10 μM final concentration of compound **6** resulted in no observed growth of the *E. coli* even after 30 h. Reinoculation of a loopful from this flask into fresh Luria broth resulted in normal growth of the organisms. It appears that **6** inhibited microbial proliferation but did not result in complete culture death (bacteriostatic activity). Incubation with 1.0 μM final concentration of **6** did result in observed growth after an initial delay. However, the organisms that did grow grew better than the control. These bacteria apparently were not as affected by the low-iron conditions as were the parent strain. Further work with these selected mutants under the low-iron conditions is currently in progress in an attempt to elucidate this interesting result observed at the different concentrations.

Figure 6 shows the results of incubation of conjugate **6** with the *E. coli* K12 strains RW193 and RWB18. After 12 h of incubation, the conjugation appears to *promote* growth of the RW193 strain compared to the control. It may be argued that a β-lactamase might be responsible for the lack of antimicrobial activity. However, this strain of *E. coli* was shown to be sensitive to both ampicillin and Loracarbef (a 7-(phenylglycyl)carbacephalosporin) (*22*). The observed growth-promoting activity is not easily explained, but may be attributed to the siderophore portion of conjugate **6**, which could be using a catechol iron-transport system to deliver iron to the organism. This result is supported by the results from the liquid growth assay with **6** under similar conditions using the RWB18 strain which lacks the catechol/colicin B receptor. After 12 h of incubation, there was little observed growth, similar to the RWB18 control. However, if one continued to measure the turbidity for an additional 12 h, some observed growth was eventually seen. Compound **7** revealed a similar growth curve. The growth promoting ability of **6** and **7** with the RWB18 strain is not without precedent. Other synthetic catechol-containing compounds such as MECAM were able to promote growth in *E. coli* mutants lacking an enterobactin receptor protein (*39*). Recall also, that spermexatol [2] could promote the growth in *Vibrio* mutants which lacked the vibriobactin receptor (*15*). The observed growth with the RWB18 strain may have arisen for several reasons which are under active study.

In addition to studying the potential antimicrobial activity of siderophore–carbacephalosporin conjugates **4**–**7**, the results described above also illustrate the importance of using a variety of assays and microbes to determine the biological activity of these types of compounds. Although, by the disk diffusion assay, compounds **6** and **7** showed only marginal or no activity, both appear to exhibit interesting activity as determined by a continuous liquid growth assay. The result of the liquid growth assay reveals

that possibly many potential antimicrobial agents have been erroneously undetected in broad-screening techniques such as the "disk diffusion zone of inhibition method" due to mutant formation. Compounds 4 and 5 did not appear to have any biological activity. While mutant organisms or lack of peptidase activity may be responsible, this result was not surprising since other siderophore–oxamazin conjugates synthesized in our laboratory also showed no antimicrobial activity (*9b*), and oxamazin β-lactam antibiotics are known to be very sensitive to the type of side chain contained in the molecule (*19*, *40*).

CONCLUSION

The synthesis and preliminary studies of the biological activity of several catechol siderophore–β-lactam conjugates have been discussed. Two of the conjugates (6 and 7) exhibited significant antimicrobial activity against *E. coli* X580. In order to study the transport mechanism of the conjugates and their fate once inside the microbe in more detail, a photoaffinity probe approach (*41*) is being developed in our laboratory. Drug delivery using the siderophore iron-transport system to deliver a toxic substance to the microorganism shows promise and may be extended to other antibiotics, siderophores, and microorganisms. Work along these lines is in progress and will be reported in due course.

ACKNOWLEDGMENT

We gratefully acknowledge support from the National Institutes of Health (Grant GM 25845). We thank Dr. Albert A. Minnick for help with the biological testing. Mass spectra were kindly obtained by Dr. Bruce Plashko. We thank Prof. Graham Lappin and Mr. Robert Warren for assistance with the measurement of the formation constants. The gift of carbacephalosporin from Eli Lilly and Co. and the performance of the broad-screen bacterial assays at Lilly were sincerely appreciated.

LITERATURE CITED

(1) (a) Miller, M. J. (1986) Hydroxamate approach to the synthesis of β-lactam antibiotics. *Acc. Chem. Res. 19*, 49. (b) Koppel G. A. (1983) The synthesis of β-lactam functions. In *Small Ring Heterocycles* A. Hassner, Ed. Part 2, pp 219–441, Interscience, New York.

(2) (a) Waxman, D. J., and Strominger, J. L. (1982) β-Lactam antibiotics: Biochemical mode of action. In *Chemistry and Biology of β-Lactam Antibiotics* (R. B. Morin, et al., Eds.) Vol. 3, pp 209–285, Academic Press, New York. (b) Lambert, P. A. (1983) The bacterial surface and drug resistance. In *Medical Microbiology 3* (C. S. F., Easmon, J. Jeljaszewicz, M. R. W. Brown, and P. A. Lambert, Eds.) Chapter 1, Academic Press, Inc., New York.

(3) (a) Bycroft, B. W., and Shute, R. E. (1985) The molecular basis for the mode of action of β-lactam antibiotics and mechanism of resistance. *Pharm. Res. 3.* (b) Nikaido, H. (1979) Nonspecific transport through the outer membrane. In *Bacterial Outer Membranes: Biosynthesis and Functions* (M. Inouye, Ed.) Chapter 11, John Wiley and Sons, New York. (c) Jaffe, A., Chabbert, Y. A., and Derlot, E. (1983) Selection and characterization of β-lactam resistant *Escherichia coli* K-12 mutants. *Antimicrob. Agents Chemother. 23*, 622. (d) Yoshimura, F., and Nikaido, H. (1985) Diffusion of β-lactam antibiotics through the porin channels of *Escherichia coli* K-12. *Antimicrob. Agents Chemother. 27*, 84.

(4) (a) Griffiths, E., and Bullen, J. J. (1987) Iron binding proteins and host defense. In *Iron and Infection* (J. J. Bullen, and E. Griffiths, Eds.) Chapter 5, John Wiley and Sons, New York. (b) Bullen, J. J. (1981) The significance of iron in infection. *Rev. Infect. Dis. 3*, 1127. (c) Bullen, J. J., Wilson, A. B., Cushnie, G. H., and Rogers, H. J. (1968) The abolition of the protective effect of *Pasteurella septica* antiserum by iron compounds. *Immunology, 4*, 889.

(5) (a) Neilands, J. B., Krystyna, K., Schwyn, B., Coy, M., Francis, R. T., Paw, B. H., and Bagg, A. (1987) Comparative biochemistry of microbial iron assimilation. In *Iron Transport in Microbes, Plants and Animals* (G. Winkelmann, D. van der Helm, and J. B. Neilands, Eds.) VCH Chapter 1, Weinheim, FRG. (b) Payne, S. M. (1988) Iron and virulence in the family Enterobactericeae. *CRC Crit. Rev. Microbiol. 16*, 81.

(6) Neilands, J. B., and Valenta, J. R. (1985) Iron containing antibiotics. In *Metal Ions in Biological Systems* (H. Sigel, Ed.) Vol 19, Chapter 11, Marcel Dekker, New York.

(7) (a) Benz, G., Schroder, T., Kurz, J., Wunsche, C., Karl, W., Steffens, G., Pfitzner, J., and Schmidt, D. (1982) *Angew. Chem. Suppl.* 1322. (b) Bickel, H., Mertenn, P., Prelog, V., Seibel, J., and Walser, A. (1966) *Tetrahedron Suppl. 8*, 171. (c) Braun, V., Guenthner, K., Hantke, K., and Zimmermann, L. (1983) Intracellular activation of albomycin in *Escherichia coli* and *Salmonella typhimurium. J. Bacteriol. 156*, 308.

(8) Zahner, H., Diddens, H., Keller-Schierlein, W., and Naegeli, H.-U. (1977) Some experiments with semi-synthetic sideromycins. *Jpn. J. Antibiot. 30*, S-201.

(9) (a) Dolence, E. K., Minnick, A. A., and Miller, M. J. (1990) N^5-Acetyl-N^5-hydroxy-L-ornithine derived siderophore–carbacephalosporin β-lactam conjugates: Iron transport mediated drug delivery. *J. Med. Chem. 33*, 464. (b) Dolence, E. K., Minnick, A. A., Lin, C.-E., Miller, M. J., and Payne, S. M. (1991) Synthesis, siderophore and antibacterial activity of N^5-acetyl-N^5-hydroxy-L-ornithine derived siderophore β-lactam conjugates: Iron transport mediated drug delivery. *J. Med. Chem. 34*, 956. (c) Minnick, A. A., Dolence, E. K., and Miller, M. J. Iron transport mediated delivery and antibacterial activity of hydroxamate siderophore/carbacephalosporin conjugates. Submitted. (d) Miller, M. J. (1989) Synthesis and therapeutic potential of hydroxyamic acid based siderophores and analogs. *Chem. Rev. 89*, 1563.

(10) (a) Ohi, N., Aoki, B., Shinozaka, T., Moro, K., Noto, T., Nehashi, T., Okazaki, H., and Matsunaga, I. (1986) Semisynthetic β-lactam antibiotics. I. Synthesis and antibacterial activity of new ureidopenicillin derivatives having catechol moieties. *J. Antibiot. 39*, 230. (b) Nikaido, H., and Rosenberg, E. Y. (1990) Cir and Fiu proteins in the outer membranes of *Escherichia coli* catalyze transport of monomeric catechols: Study with β-lactam antibiotics containing catechol and analogous groups. *J. Bacteriol. 172*, 1361. (c) Mochizuki, H., Yamada, H., Oikawa, Y., Murakami, K., Ishiguro, J., Kosuzume, H., Aizawa, N., and Mochida, E. (1988) Bactericidal activity of M14659 enhanced in low-iron environments. *Antimicrob. Agents Chemother. 32*, 1648. (d) Curtis, N. A. C., Eisenstadt, R. L., East, S. J., Cornford, R. J., Walker, L. A., and White, A. J. (1988) Iron-regulated outer membrane proteins of *Escherichia coli* K-12 and mechanism of action of catechol-substituted cephalosporins. *Antimicrob. Agents Chemother. 32*, 1879. (e) Nakagawa, S., Sanada, M., Matsuda, K., Hazumi, N., and Tanaka, N. (1987) Biological activity of BO-1236, a new antipseudomonal cephalosporin. *Antimicrob. Agents Chemother. 31*, 1100. (f) Nakagawa, S., Sanada, M., Matsuda, K., Hashizume, T., Asahi, Y., Ushijima, R., Ohtake, N., and Tanaka, N. (1989) In vitro and in vivo antibacterial activities of BO-1431, A new antipseudomonal cephalosporin. *Antimicrob. Agents Chemother. 33*, 1423.

(11) Silley, P., Griffiths, J. W., Monsey, D., and Harris, A. M. (1990) Mode of action of GR69153, a novel catechol-substituted cephalosporin and its interaction with the *ton*B-dependent iron transport system. *Antimicrob. Agents Chemother. 34*, 1806.

(12) (a) Watanabe, N.-A., Nagasu, T., Katsu, K., and Kitoh, K. (1987) E-0702, A new cephalosporin, is incorporated into *E. coli* cells via the *ton*B dependent iron transport system. *Antimicrob. Agents Chemother. 31*, 497. (b) Katsu, K., Kitoh, K., Inoue, M., and Mitsuhashi, S. (1982) In vitro antibacterial activity of E-0702, a new semisynthetic cephalosporin. *Antimicrob. Agents Chemother. 22*, 181.

(13) Anderson, W. F. (1973) Iron chelation in the treatment of Cooley's anemia. In *Inorganic Chemistry in Biology and Medicine* (A. E. Martel, Ed.) Chapter 15, American Chemical Society: Washington, DC.

(14) Jacobs, A., White, G. P., and Tait, G. H. (1977) Iron chelation in cell cultures by two conjugates of 2,3-dihydroxybenzoic acid (2,3-DHB). *Biochem. Biophys. Res. Commun. 74*, 1626.
(15) Sharma, S. K., Miller, M. J., and Payne, S. M. (1989) Spermexatin and spermexatol: New synthetic spermidine-based siderophore analogues. *J. Med. Chem. 32*, 357.
(16) Hider, R. C. (1984) Siderophore mediated absorption of iron. In *Structure and Bonding* (M. J. Clarke, Ed.) No. 58, pp 25–87, Springer-Verlag, Berlin.
(17) Corbin, J. L., and Bulen, W. A. (1969) The isolation and identification of 2,3-dihydroxybenzoic acid and 2-*N*,6-*N*-(2,3-dihydroxybenzoyl)-L-lysine formed by iron-deficient *Azotobacter vinelandii*. *Biochemistry 8*, 757.
(18) Chimiak, A., and Neilands, J. B. (1984) Lysine analogues of siderophores. In *Structure and Bonding* (M. J. Clark et al., Eds.) No. 58, pp 89–96, Springer-Verlag, Berlin.
(19) Woulfe, S. R., and Miller, M. J. (1985) Synthesis and biological activity of substituted [[3(*S*)-(Acylamino)-2-oxoacetidinyl]oxy]acetic acid. A new class of heteroatom-activated β-lactams. *J. Med. Chemd. 28*, 1447.
(20) Hofmann, K., Schmiechen, R., Wells, R. D., Wolman, Y., and Yanaihara, N. (1965) Studies on polypeptides. XXIX. Synthetic peptides related to the *N*-terminus of bovine pancreatic ribonuclease A (positions 1-7). *J. Am. Chem. Soc. 87*, 611.
(21) (a) Harris, W. R., Carrano, C. J., Cooper, S. R., Sofen, S. R., Avdeef, A. E., McArdle, J. V., and Raymond, K. N. (1979) Coordination chemistry of microbial iron transport compounds. 19. Stability constants and electrochemical behavior of ferric enterobactin and model complexes. *J. Am. Chem. Soc. 101*, 6097. (b) Harris, W. R., Carrano, C. J., and Raymond, K. N. (1979) Spectrophotometric determination of the proton-dependent stability constant of ferric enterobactin. *J. Am. Chem. Soc. 101*, 2213. (c) Garrett, T. M., McMurry, T. J., Hosseini, M. W., Reynes, Z. E., Hahn, F. E., and Raymond, K. N. (1991) Synthesis and characterization of macrobicyclic iron(III) sequestering agents. *J. Am. Chem. Soc. 113*, 2965.
(22) Bodurow, C. C., Boyer, B. D., Brennan, J., Bunnell, C. A., Burks, J. E., Carr, M. A., Doecke, C. W., Eckrich, T. M., Fisher, J. W., Gardner, J. P., Graves, B. J., Hines, P., Hoying, R. C., Jackson, B. G., Kinnick, M. D., Kochert, C. D., Lewis, J. S., Luke, W. D., Moore, L. L., Morin, J. M., Jr., Nist, R. L., Prather, D. E., Sparks, D. L., and Vladuchick, W. C. (1989) An enantioselective synthesis of Loracarbef (LY163892/KT3777). Tetrahedron Lett. *30*, 2321.
(23) Miller, M. J., Mattingly, P. G., Morrison, M. A., Kerwin, J. F., Jr. (1980) Synthesis of β-lactams from substituted hydroxamic acids. *J. Am. Chem. Soc. 102*, 7026.
(24) Mattingly, P. G., and Miller, M. J. (1981) Synthesis of 2-azetidinones from serine hydroxamates: approaches to the synthesis of 3-aminocardicinic acid. *J. Org. Chem. 46*, 1557.
(25) We thank Eli Lilly and Co., for the gift of the carbacephalosporin.
(26) (a) Belleau, B., and Malek, G. (1968) A new convenient reagent for peptide synthesis. *J. Am. Chem. Soc. 90*, 1651. (b) Bodanszky, M. (1984) *Principles of Peptide Synthesis*, Springer-Verlag, Berlin.
(27) Private communication from Eli Lilly and Co.
(28) We thank Eli Lilly and Co. for suggesting these unusual reaction conditions.
(29) Carrano, C. J., and Raymond, K. N. (1978) Coordination chemistry of microbial iron transport compounds. 10. Characterization of the complexes of rhodotoluric acid, a dihydroxamate siderophore. *J. Am. Chem. Soc. 100*, 5371.
(30) (a) Neilands, J. B., Erickson, T. J., and Rastetter, W. H. (1981) Stereospecificity of the ferric Enterobactin receptor of *Escherichia coli* K-12. *J. Biol. Chem. 256*, 3831. (b) Neilands, J. B., Peterson, T., and Leong, S. A. (1980) High affinity iron transport in microorganisms. Iron(III) coordination compounds of the siderophores agrobactin and parabactin. In *Inorganic Chemistry in Biology and Medicine* (E. A. Martell, Ed.) Chapter 16, American Chemical Society, Washington, DC.
(31) (a) Nikaido, H., Rosenberg, E. Y., and Foulds, J. (1983) Porin channels in *Escherichia coli*: Studies with β-lactams in intact cells. *J. Bacteriol. 153*, 232. (b) Sawai, T., Hiruma, R., Kawana, M., Taniyasu, F., and Inami, A. (1982) Outer membrane permeation of β-lactam antibiotics in *Escherichia coli*, *Proteus mirabilis*, and *Enterobacter cloaeae*. *Antimicrob. Agents Chemother. 22*, 585. (c) Nikado, H., and Rosenberg, E. Y. (1983) Porin channels in *Eschericia coli*: Studies with liposomes reconstituted from purified proteins. *J. Bacteriol. 153*, 241. (d) Jaffe, A., Chabbert, Y. A., and Semonin, O. (1982) Role of porin proteins OmpF and OmpC in the permeation of β-lactams. *Antimicrob. Agents Chemother. 22*, 942.
(32) (a) Wayne, R., Frick, K., and Neilands, J. B. (1976) Siderophore protection against colicins, M, B, V, and Ia in *Escherichia coli*. *J. Bacteriol. 126*, 7. (b) Hollifield, W. C., Jr., and Neilands, J. B. (1978) Ferric enterobactin transport system in *Escherichia coli* K-12. Extraction, assay, and specificity of the outer membrane receptor. *Biochemistry 17*, 1922. (c) Lee, B. H., Miller, M. J., Prody, C. A., and Neilands, J. B. (1985) Artificial siderophores. 1. Synthesis and microbial iron transport capabilities. *J. Med. Chem. 28*, 317.
(33) We thank Eli Lilly and Co. for the gift of this microorganism.
(34) Kirst, H. A., Wild, G. M., Baltz, R. H., Hammil, R. L., Ott, J. L., Counter, F. T., and Ose, E. E. (1982), Structure–activity studies among 16-membered macrolide antibiotics related to tylosin. *J. Antibiot. 35*, 1675.
(35) Performed at Eli Lilly and Co. by standard methods.
(36) Minnick, A. A., McKee, J. A., Dolence, E. K., and Miller, M. J. Iron transport mediated antibacterial activity of a catechol siderophore/carbacephalosporin conjugate alone and in the presence of a hydroxamate siderophore/carbacephalosporin conjugate. Submitted.
(37) (a) Braun, V., Gunthner, K., Hantke, K., and Zimmermann, L. (1983) Intercellular activation of albomycin in *Escherichia coli* and *Salmonella typhimurium*. *J. Bacteriol. 156*, 308. (b) Hartmann, A., Fiedler, H.-P., and Braun, V. (1979) Uptake and conversion of the antibiotic albomycin by *Escherichia coli* K-12. *Eur. J. Biochem. 99*, 517.
(38) (a) Ogasa, T., Saito, H., Hashimoto, Y., Sato, K., and Hirata, T. (1989) Synthesis and biological evaluation of optically active 3-*H*-1-carbacephem compounds. *Chem. Pharm. Bull. 37*, 315. (b) Saito, H., Matsushima, H., Shiraki, C., and Hirata, T. (1989) Synthetic studies on 1,2-dehydro-1-carbacephem compounds. *Chem. Pharm. Bull. 37*, 275.
(39) Heidinger, S., Braun, V., Pecoraro, V. L., and Raymond, K. N. (1983) Iron supply to *Escherichia coli* by synthetic analogs of enterochelin. *J. Bacteriol. 153*, 109.
(40) Boyd, D. B., Eigenbrot, C., Indelicato, J. M., Miller, M. J., Pasini, C. E., and Woulfe, S. R. (1987) Heteroatom-activated β-lactam antibiotics: Considerations of differences in the biological activities of [[3(*S*)-(acylamino)-2-oxo-1-acetidinyl]-oxy]acetic acids (oxamazins) and the corresponding sulfur analogues (Thiamazins). *J. Med. Chem. 30*, 528.
(41) (a) Bayley, H., and Knowles, J. R. (1977) [8] Photoaffinity labeling. *Methods Enzymol. 46*, 69. (b) Chowdhry, V., and Westheimer, F. H. (1979) Photoaffinity labeling of biological systems. *Annu. Rev. Biochem. 48*, 293. (c) Bergeron, R. J., Dionis, J. B., and Ingeno, M. J. (1987) Synthesis of a parabactin photoaffinity label. *J. Org. Chem. 52*, 144.

Bioconjugate Chemistry

SEPTEMBER/OCTOBER 1991
Volume 2, Number 5

© Copyright 1991 by the American Chemical Society

REVIEWS

Enhancement of the Thrombolytic Potency of Plasminogen Activators by Conjugation with Clot-Specific Monoclonal Antibodies

M. Dewerchin and D. Collen*

Center for Thrombosis and Vascular Research, University of Leuven, B-3000 Leuven, Belgium.
Received April 11, 1991

Thrombolytic therapy has become a routine treatment of acute myocardial infarction in man. Thrombolytic agents are plasminogen activators which activate the fibrinolytic system in blood (Figure 1) by converting the inactive proenzyme plasminogen to the active enzyme plasmin, a serine protease that degrades the fibrin in the blood clot and thereby causes dissolution of the thrombus. Plasmin, however, also degrades fibrinogen, the circulating precursor of fibrin. Extensive fibrinogen degradation may predispose one to bleeding although such correlation has not been unequivocally observed in clinical trials. Streptokinase and urokinase (two-chain urokinase-type plasminogen activator, tcu-PA, UK) are plasminogen activators belonging to the group of the "classic" thrombolytic agents. These indiscriminately activate fibrin-bound as well as circulating plasminogen and consequently induce a systemic fibrinolytic state, characterized by extensive depletion of α_2-antiplasmin, the physiologic plasmin inhibitor in blood, and degradation of fibrinogen and other circulating coagulation factors. With the "new generation" thrombolytic agents tissue-type plasminogen activator (t-PA) on one hand and single-chain urokinase-type plasminogen activator (scu-PA) on the other hand, plasminogen activation is assumed to occur preferentially at the fibrin surface. This fibrin-specific plasminogen activation, resulting in localized generation of active plasmin in the vicinity of the clot, would render these fibrin-specific thrombolytic agents superior to the classic agents. However, clinical experience has revealed that at the high doses of t-PA or scu-PA required for efficient coronary thrombolysis, the fibrin specificity is only relative and systemic activation of the fibrinolytic system with the risk of bleeding complications may still occur (*1*).

* Address for correspondence: D. Collen, M.D., Center for Thrombosis and Vascular Research, K.U. Leuven, Campus Gasthuisberg, O & N, Herestraat 49, B-3000 Leuven, Belgium.

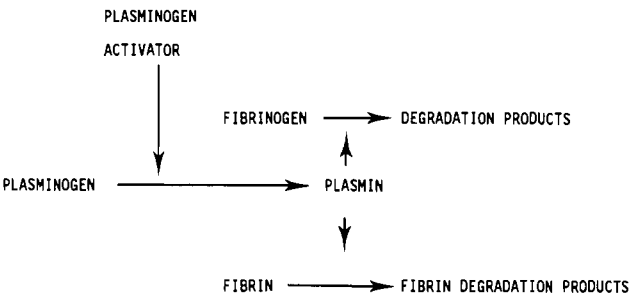


Figure 1. Schematic representation of the fibrinolytic system.

Several approaches to develop more potent and more clot-selective thrombolytic agents are being explored. These include the construction of mutants and variants of the physiologic plasminogen activators t-PA or scu-PA and of recombinant chimeric molecules containing the protease part of urokinase and fibrin-binding structures of t-PA or of plasminogen (for review, see refs 2 and 3).

In this review, we will focus on an alternative approach toward the development of improved thrombolytic agents, consisting of antibody-mediated targeting of plasminogen activators to the thrombus. The concept of using monoclonal antibodies as carrier molecules for therapeutic agents has proven its value in the area of tumor therapy (*4*). The same strategy was first applied to cardiovascular disease by Bode et al. (*5*), who showed successful targeting of a plasminogen activator to fibrin, one of the components of a thrombus, using a conjugate of urokinase with a monoclonal antibody directed against fibrin but not cross-reacting with fibrinogen. Apart from fibrin-like material, a thrombus also contains platelet-rich material, representing an alternative target site in the blood clot. Thus, targeting of plasminogen activators might also be achieved by monoclonal antibodies that discriminate between activated platelets in the thrombus and circulating resting platelets.

1043-1802/91/2902-0293$02.50/0 © 1991 American Chemical Society

Table I. In Vitro Fibrinolytic Properties of Antifibrin Antibody/Plasminogen Activator Conjugates

plasminogen activator moiety	antibody moiety	designation	conjugation	epitope	In vitro fibrinolytic potency: fibrin monomer assay[a] enhancement factor[c]	plasma clot lysis[b]: enhancement factor[c]	plasma clot lysis[b]: fibrinogen breakdown[d]	refs
rt-PA	IgG_1	t-PA-59D8	chemical	β-chain	10	3.2	reduced	12
B-chain t-PA	$F(ab')_2$	t-PA-59D8	recombinant	β-chain	–	ineffective	–	17, 18
B-chain UK	IgG_1	64C8-UK	chemical	β-chain	100	–	–	5
LMW-UK	Fab'	64C5Fab'-UK	chemical	β-chain	95	2–4	–	14
	IgG_1	64C5-UK	chemical	β-chain	250	–	–	15
	IgG_1	59D8-UK	chemical	β-chain	100–250	4.5	reduced	12, 15
	Fab'	59D8-UK	chemical	β-chain	250	–	–	15
scu-PA[e]	Fab'	scu-PA-59D8Fab'	chemical	β-chain	230	1.6–1.8	reduced	16
LMW-scu-PA	CH_2-truncated IgG	scu-PA-59D8	recombinant	β-chain	10–50	–	–	19
rscu-PA[f]	IgG_1	rscu-PA/MA-15C5	chemical	D-dimer	–	6.4	increased	6
rtcu-PA[g]	IgG_1	rtcu-PA/MA-15C5	chemical	D-dimer	–	2.2	reduced	6
rtcu-PA/T[h]	IgG_1	rtcu-PA/MA-15C5/T	chemical	D-dimer	–	>50	?	22
rscu-PA-32k[i]	$F(ab')_2$	rscu-PA-32k/MA-15C5-$F(ab')_2$	chemical	D-dimer	–	5	increased	24
rtcu-PA-32k	$F(ab')_2$	rtcu-PA-32k/MA-15C5-$F(ab')_2$	chemical	D-dimer	–	0.6	increased	25
rtcu-PA-32k/T	$F(ab')_2$	rtcu-PA-32k/MA-15C5-$F(ab')_2$/T	chemical	D-dimer	–	>2	?	25
rtcu-PA-33k[j]	scFv[l]	$K_{12}G_0S_{32}$	recombinant	D-dimer	–	13	reduced	26
rtcu-PA-33K[k]	scFv	$K_{12}G_0S_{32}$	recombinant	D-dimer	–	2.5	increased	26

[a] The fibrin monomer assay is a solid phase assay in which radiolabeled fibrin monomer, covalently linked to Sepharose, is pretreated with the different plasminogen activators after which it is incubated with plasminogen in buffer. The release of radiolabeled degradation fragments into the supernatant reflects lysis of bound fibrin. [b] The plasma clot lysis assay is an in vitro system composed of a [^{125}I]fibrin-labeled normal human plasma clot immersed in normal human plasma. The release of radiolabeled degradation products into the supernatant following incubation with the different plasminogen activators reflects the fibrinolytic potency of the agents. [c] Ratio of the activity obtained with conjugated plasminogen activator over the activity obtained with the corresponding unconjugated plasminogen activator. [d] Fibrinogen breakdown observed with conjugated plasminogen activator as compared to that observed with the corresponding unconjugated plasminogen activator at equieffective dose. [e] scu-PA: single-chain urokinase-type plasminogen activator produced by the human kidney cell line TCL-598. [f] rscu-PA: recombinant scu-PA, obtained by expression of cDNA in *Escherichia coli*. [g] rtcu-PA and rtcu-PA conjugates: two-chain derivatives obtained by treatment of rscu-PA or rscu-PA conjugates with plasmin. [h] rtcu-PA/T and rtcu-PA/T conjugates: two-chain derivatives obtained by treatment of rscu-PA or rscu-PA conjugates with thrombin. [i] rscu-PA-32k: a low molecular weight form of rscu-PA with M_r 32 000 and NH_2 terminal amino acid Leu^{144}. [j] rscu-PA-33k: a low molecular weight form of rscu-PA with M_r 33 000 and NH_2 terminal amino acid Ala^{132}. [k] rtcu-PA-33k in $K_{12}G_0S_{32}$: two-chain derivative obtained by treatment of the single-chain u-PA form of $K_{12}G_0S_{32}$ with plasmin. [l] scFv: single-chain variable domain fragment of an antibody.

ANTIBODY-MEDIATED TARGETING TO FIBRIN

Up to now, two different types of anti-human fibrin antibodies have been used for the construction of antifibrin antibody/plasminogen activator conjugates: the murine monoclonal antibodies 59D8 and 64C5, specifically recognizing the amino terminal residues of the β-chain of human fibrin which become exposed after release of fibrinopeptide B brought about by thrombin (*5*), and the murine monoclonal antibody MA-15C5, directed against fragment D dimer of cross-linked human fibrin (*6*). Both types of antibodies specifically bind to fibrin but not to fibrinogen (*7–9*) and have been used successfully for thrombus imaging in animal models (*10, 11*). Functional properties of conjugates of these antibodies with different types of plasminogen activators are summarized in Tables I and II.

Covalent Conjugates Targeted to the Fibrin β-Chain. Chemical coupling of recombinant t-PA (rt-PA) with the antifibrin β-chain antibody 59D8 (*12*) was found to result in a 10-fold enhancement of its potency toward fibrin monomer in a purified system and a 3.2-fold increase of its potency toward a human plasma clot in a plasma milieu in vitro (Table I). In vivo, the t-PA/59D8 conjugate was shown to possess a 2.8-fold higher thrombolytic potency toward a human plasma clot than rt-PA, by using a jugular vein thrombosis model in the rabbit (*13*) (Table II). The enhanced in vitro and in vivo thrombolytic potency of conjugated rt-PA was accompanied by a decrease in the consumption of α_2-antiplasmin, plasminogen, and fibrinogen, indicating an increased fibrin selectivity (*12, 13*).

Similar results were obtained with chemical conjugates of single-chain or two-chain urokinase-type plasminogen activator with the antibodies 59D8 or 64C5 or with fragments of the antibodies (*5, 14–16*). The purified conjugates had 100–250-fold higher fibrinolytic potencies than their respective unconjugated counterparts toward fibrin monomer and 1.6–4.5-fold enhanced potencies toward human plasma clots in vitro (Table I). In the rabbit jugular vein thrombosis model, a conjugate of scu-PA with 59D8-Fab' had a 29-fold enhanced in vivo thrombolytic potency as compared to unconjugated scu-PA (Table II).

Schnee et al. have constructed a recombinant version of the t-PA/59D8 conjugate (*17*). Therefore, the cDNA encoding the variable domain region of the 59D8 heavy-chain gene was cloned and recombined in an expression vector with the CH1 and hinge sequence of mouse immunoglobulin γ2b and with the cDNA coding for the catalytic B-chain of t-PA. This construct was transfected into a heavy-chain loss-variant cell line derived from hybridoma 59D8. The resulting fusion protein produced by these cells retained antifibrin antibody activity as well as plasminogen activating potential (*17*). However, the recombinant t-PA/59D8 conjugate was ineffective in plasma clot lysis (*18*). In contrast, a recombinant conjugate comprising the 59D8 variable region combined with the mouse immunoglobulin γ2b CH1, hinge, and CH2 domains and with a low molecular weight form of scu-PA (LMW-scu-PA) was 10–50-fold more efficient than urokinase in the fibrin monomer assay (*19*) (Table I).

Covalent Conjugates Targeted to Fibrin Fragment D Dimer. Targeting of recombinant scu-PA (rscu-PA)

Table II. Thrombolytic and Pharmacokinetic Properties of Antifibrin Antibody/Plasminogen Activator Conjugates in Animal Models in Vivo

plasminogen activator moiety	antibody moiety	designation	conjugation	epitope	species	enhancement factor[c]: thrombolytic potency[a]	enhancement factor[c]: specific thrombolytic activity[b]	fibrinogen breakdown[d]	α_2-antiplasmin depletion[d]	clearance prolongation factor	refs
rt-PA	IgG_1	t-PA-59D8	chemical	β-chain	rabbit[e]	2.8	-	reduced	reduced	-	13
scu-PA	Fab	scu-PA-59D8Fab'	chemical	β-chain	rabbit	29	-	equal	-	-	16
rscu-PA	IgG_1	rscu-PA/MA-15C5	chemical	D-dimer	rabbit	8	3	equal	equal	4-8	20
					baboon[f]	3	0.1	equal	equal	15	23
	IgG_1	rscu-PA/MA-1C8	chemical	-	rabbit	0.4	0.1	equal	equal	1.7-3	20
					baboon	0.9	0.03	equal	equal	15	23
rtcu-PA[g]	IgG_1	rtcu-PA/MA-15C5	chemical	D-dimer	rabbit	4	0.5	reduced	reduced	6	20
rtcu-PA/T[h]	IgG_1	rtcu-PA/MA-15C5/T	chemical	D-dimer	rabbit	1.4	0.3	equal	equal	4	20

[a] Thrombolytic potency, derived from the dose–response data based on percent lysis obtained versus the dose (in mg of compound per kg of body weight) administered, representing potency at comparable dose. [b] Specific thrombolytic activity, derived from the dose–response data based on percent lysis obtained versus steady-state plasma antigen level (in μg u-PA or t-PA antigen per mL plasma) representing potency at comparable steady-state plasma antigen levels. [c] Ratio of the activity obtained with conjugated plasminogen activator over the activity obtained with the corresponding unconjugated plasminogen activator. [d] Fibrinogen breakdown or α_2-antiplasmin depletion observed with conjugated plasminogen activator as compared to that observed with the corresponding unconjugated plasminogen activator at equieffective dose. [e] In the rabbit jugular vein model a [^{125}I]fibrin-labeled human plasma clot was produced in a segment of the jugular vein. Thrombolysis was quantitated 30 or 60 min after the end of a 4-h intravenous infusion of the different plasminogen activators, by determination of the residual radioactivity in the jugular vein segment. [f] In the baboon femoral vein model, a thrombus was produced in a segment of a femoral vein using fresh baboon blood mixed with a trace amount of ^{125}I-labeled human fibrinogen. Thrombolysis was quantitated 30 min after the end of a 2-h intravenous infusion of the different plasminogen activators by determination of the residual radioactivity in the femoral vein segment. [g] rtcu-PA and rtcu-PA conjugates: two-chain derivatives obtained by treatment of rscu-PA or rscu-PA conjugates with plasmin. [h] rtcu-PA/T and rtcu-PA/T conjugates: two-chain derivatives obtained by treatment of rscu-PA or rscu-PA conjugates with thrombin.

to fibrin fragment D dimer similarly resulted in an enhancement of the fibrinolytic and thrombolytic potency of the plasminogen activator (Tables I and II). Chemical conjugation of rscu-PA with MA-15C5 yielded a functionally intact conjugate, both with respect to the in vitro enzymatic properties of the rscu-PA moiety and the antigen-binding capacity of the antibody moiety (*6*). The conjugate, rscu-PA/MA-15C5, had a 6.4-fold higher fibrinolytic potency than rscu-PA in a human plasma clot lysis assay in vitro (*6*) and an 8-fold enhanced thrombolytic efficiency toward a human plasma clot in the rabbit jugular vein thrombosis model (*20*). The enhanced in vitro and in vivo thrombolytic potency of the conjugate as compared to unconjugated rscu-PA was not observed when the fibrin clots were produced with rabbit plasma or when rscu-PA was conjugated with a control antibody, MA-1C8 (*6*, *20*) (Table II).

Treatment of scu-PA with plasmin results in conversion of the single-chain molecule to tcu-PA (urokinase), a two-chain derivative in which the constituting A- and B-chains are still linked by a disulfide bond. In contrast to scu-PA, plasmin-derived tcu-PA indiscriminately activates circulating as well as fibrin-bound plasminogen. The plasmin-derived two-chain form of the conjugate rtcu-PA/MA-15C5 had a 2.2-fold higher fibrinolytic potency in the in vitro plasma clot lysis assay than unconjugated rtcu-PA (*6*) and a 4-fold enhanced thrombolytic potency in the rabbit jugular vein model (*20*). Fibrinogen breakdown or α_2-antiplasmin depletion during in vitro and in vivo thrombolysis was less pronounced with rtcu-PA/MA-15C5 than with rtcu-PA (Tables I and II), suggesting that the conjugate has an increased fibrin specificity. In contrast, fibrinogen breakdown during in vitro clot lysis was somewhat more pronounced with the single-chain form of the conjugate than with unconjugated rscu-PA (Table I). No increased fibrinogen breakdown or α_2-antiplasmin depletion was however observed with rscu-PA/MA-15C5 during in vivo thrombolysis (Table II).

Treatment of scu-PA with thrombin converts this single-chain molecule to tcu-PA/T, a two-chain derivative in which the A- and B-chains are still disulfide linked, but which is cleaved at a site different from the one cleaved by plasmin. Thrombin-derived tcu-PA/T is virtually inactive in in vitro assays but can be converted to active tcu-PA with plasmin. This conversion by plasmin occurs however with a 500-fold lower catalytic efficiency as compared to that of scu-PA (*21*). In contrast to rtcu-PA/T, the thrombin-derived two-chain form of rscu-PA/MA-15C5, rtcu-PA/MA-15C5/T, was found to have a significant fibrinolytic activity in in vitro or in vivo plasma clot lysis and this activity occurred in the absence of fibrinogen degradation or α_2-antiplasmin depletion (*20*, *22*) (Tables I and II). These results may be explained by targeting of the conjugate to the fibrin clot and reactivation by plasmin at the fibrin surface (*22*).

In the rabbit jugular vein thrombosis model, interference of endogenous rabbit fibrin or fibrinogen with clot lysis by rscu-PA/MA-15C5 is avoided since MA-15C5 does not cross-react with rabbit fibrin (*8*, *11*). Although fibrin fragments do not trigger activation of the fibrinolytic system by rscu-PA/MA-15C5 in plasma in vitro (*6*), they might well reduce its thrombolytic efficacy by blocking the antigen binding site of the antibody moiety. Therefore, the thrombolytic properties of rscu-PA/MA-15C5 were investigated in baboons with an autologous femoral vein clot, after demonstration of cross-reactivity of MA-15C5 with cross-linked baboon fibrin (*23*). In this system, the thrombolytic potency of rscu-PA/MA-15C5 was still 3-fold higher than that of rscu-PA (Table II).

Conjugation of rscu-PA or its two-chain derivatives with MA-15C5 significantly decreased their plasma clearance rate (Table II), resulting in considerably higher steady-state plasma u-PA antigen levels than observed with unconjugated u-PA (*20*, *23*). Therefore, specific thrombolytic activities (reflecting potency at comparable steady-state plasma antigen levels) were determined for the different conjugates in both the rabbit and baboon model. Unlike the thrombolytic potencies (potency at comparable dose), the specific thrombolytic activities of the conjugates in most cases were decreased as compared to those of the corresponding unconjugated moieties (Table II). However, the targeting effect of MA-15C5 in combination with the

prolonged half-life appears to compensate for the reduced specific thrombolytic activity, resulting in significantly enhanced thrombolytic potencies. Indeed, with a control conjugate (rscu-PA/MA-1C8) with similarly decreased plasma clearance rates, both the thrombolytic potency and specific thrombolytic activities were markedly reduced (*20*, *23*).

In order to reduce the molecular size of the conjugates, a low molecular weight form of rscu-PA, rscu-PA-32k (comprising amino acids Leu^{144}–Leu^{411}), was chemically coupled to $F(ab')_2$ fragments of MA-15C5 (*24*). This yielded a conjugate, rscu-PA-32k/MA-15C5-$F(ab')_2$, with M_r 130 000 and with similar in vitro biochemical properties for its single-chain form and its plasmin- or thrombin-derived two-chain derivatives as compared to intact rscu-PA/MA-15C5 and its two-chain derivatives (*24*, *25*). The in vitro fibrinolytic potency of rscu-PA-32k/MA-15C5-$F(ab')_2$ or of the thrombin-derived rtcu-PA-32k/MA-15C5-$F(ab')_2$/T was respectively increased 5- and 2-fold over that of the corresponding unconjugated counterpart (Table I). With the plasmin-derived two-chain form rtcu-PA-32k/MA-15C5-$F(ab')_2$, however, no enhancement of the in vitro fibrinolytic potency over plasmin-derived rtcu-PA-32k was observed (Table I).

Alternatively, a recombinant 57 kDa single-chain chimeric plasminogen activator, $K_{12}G_0S_{32}$, has been constructed (*26*), consisting of the variable region fragment (Fv) of MA-15C5 and of a 33 kDa low molecular weight form of rscu-PA (rscu-PA-33k, comprising amino acids Ala^{132}–Leu^{411}). The synthetic single-chain Fv fragment was obtained by linking the carboxy terminal end of the variable domain of the κ-chain of MA-15C5 to the amino terminal end of the variable domain of the MA-15C5 γ-chain by means of a seven amino acid residue synthetic linker (*27*). Purified $K_{12}G_0S_{32}$, produced in an insect cell expression system, retained the in vitro enzymatic properties of low molecular weight rscu-PA (rscu-PA-32k) and the fragment D dimer binding capacity of MA-15C5 (*26*). In the in vitro plasma clot lysis assay, the single-chain u-PA form of $K_{12}G_0S_{32}$ was found to have a 13-fold higher fibrinolytic potency than rscu-PA-32k. The plasmin-derived two-chain form of the chimera had a 2.5-fold higher in vitro fibrinolytic potency than plasmin-derived rtcu-PA-32k (*26*) (Table I).

Bispecific Antibodies. In another attempt to concentrate plasminogen activators to the surface of a fibrin clot, bifunctional antibodies have been prepared that are capable of binding both fibrin and t-PA (*28–31*) or both fibrin and u-PA (*31*, *32*). Such bispecific antibodies have been obtained by chemical coupling (*29*, *32*) or by somatic cell fusion (*28*, *30*, *31*). In the presence of bispecific antibody, u-PA or t-PA indeed were found to have 5–50-fold enhanced potencies for lysing fibrin monomer (*28*, *29*, *32*) and 2–5-fold higher fibrinolytic potencies toward human plasma clots in vitro (*29*, *32*). In the rabbit jugular vein thrombosis model, clot lysis with plasminogen activator administered in combination with bispecific antibody was 1.6–4-fold higher than lysis with plasminogen activator alone (*28*, *30*). In addition, after pretreatment of fibrin with bispecific antibody, subsequently administered plasminogen activator was concentrated at the fibrin surface, both in the in vitro fibrin monomer lysis assay (*29*, *32*) and in the rabbit model in vivo (*29*). The use of bispecific antibodies thus offers the possibility of avoiding administration of exogenous plasminogen activator, by inducing thrombolysis via concentration of endogenous plasminogen activator at the site of the thrombus.

In summary, antibody-mediated targeting of plasminogen activators to fibrin appears to have the potential to increase the concentration of plasminogen activator in the vicinity of a thrombus, resulting in localized generation of active plasmin and enhanced clot lysis. Urokinase-type plasminogen activator displays fibrin specificity only in its single-chain form (*33*) and its fibrin specificity is not dependent on the presence of the NH_2-terminal 143 amino acids (*34*). With t-PA, the functional domains responsible for its fibrin affinity reside within the NH_2-terminal region (A-chain) of the molecule (*35*). Thus, conjugation of single-chain u-PA molecules (scu-PA or low molecular weight forms of scu-PA comprising amino acids Ala^{132}–Leu^{411} or Leu^{144}–Leu^{411}) or of the intact t-PA molecule with anti-fibrin antibodies yields plasminogen activators possessing fibrin specificity by two mechanisms. The results obtained with Fab' or scFv conjugates (Tables I and II) and with bispecific antibodies indicate that univalent antibody binding is sufficient for effective targeting. The specificity of the targeting effect is demonstrated (a) by the finding that the enhancement of the fibrinolytic potency in vitro is inhibited by addition of purified antigen (*5*, *6*, *15*, *26*), (b) by the lack of targeting to fibrin clots that do not cross-react with the targeting antibody (*6*, *20*), and (c) by the absence of targeting when using conjugates with a control monoclonal antibody (*5*, *6*, *12*, *13*, *20*, *23*).

ANTIBODY-MEDIATED TARGETING TO PLATELETS

Recently, evidence has accumulated that platelet-rich zones of a thrombus, particularly arterial thrombi, are very resistant to thrombolysis (*36*). In addition, platelet deposition may contribute to coronary artery reocclusion following successful thrombolytic therapy (*1*). Thus, monoclonal antibodies specific for activated platelets might represent an alternative means to target plasminogen activators to a thrombus.

Bode et al. (*37*) chemically coupled two-chain urokinase to 7E3, a monoclonal antibody selectively binding to platelet membrane glycoprotein IIb/IIIa, which is the platelet receptor for fibrinogen and other adhesive proteins (*38*). The resulting conjugate had a markedly enhanced potency toward platelet-rich human plasma clots in vitro (Table III).

We have chemically coupled rscu-PA to different monoclonal antibodies specifically recognizing surface proteins on activated platelets (*39*) (Tables III and IV): MA-TSPI-1, directed against human thrombospondin, a platelet α-granule glycoprotein expressed on the surface of stimulated platelets but minimally on the surface of resting platelets; and MA-PMI-2, MA-PMI-1, and MA-LIBS-1, recognizing different epitopes on the platelet surface glycoprotein IIb/IIIa that become exposed only when, upon platelet activation, fibrinogen has bound to the receptor. The purified conjugates retained rscu-PA activity, and binding to ADP-stimulated human platelets in a plasma milieu in vitro was significantly higher than binding to resting platelets (*39*). However, none of the conjugates appeared to have a higher fibrinolytic potency than rscu-PA toward platelet-rich human plasma clots in a plasma milieu in vitro, and lysis was associated with extensive fibrinogenolysis (Table III). Nevertheless, the conjugates rscu-PA/MA-PMI-1 and rscu-PA/MA-LIBS-1 were found to have a 2.3–3-fold increase in vivo thrombolytic potency as compared to rscu-PA and a 5–7-fold higher potency than a control conjugate rscu-PA/MA-1C8, when tested in hamsters with pulmonary embolism consisting of a platelet-rich human plasma clot (Table IV). The enhanced thrombolytic potency of these rscu-PA/antiplatelet an-

Table III. In Vitro Fibrinolytic Properties of Antiplatelet Antibody/Plasminogen Activator Conjugates

plasminogen activator moiety	antibody moiety	designation	conjugation	epitope	in vitro fibrinolytic potency[a] toward platelet-rich clots: enhancement factor[b]	in vitro fibrinolytic potency[a] toward platelet-rich clots: fibrinogen breakdown	refs
urokinase	Fab'	UK-7E3Fab'	chemical	GPIIb/IIIa	1.3–10	–	37
rscu-PA	IgG2a	rscu-PA/MA-TSPI-1	chemical	thrombospondin	<1	increased	39
	IgG2a	rscu-PA/MA-PMI-2	chemical	GPIIIa	<1	increased	39
	IgG2b	rscu-PA/MA-PMI-1	chemical	GPIIb	<1	increased	39
	IgG1	rscu-PA/MA-LIBS-1	chemical	GPIIIa	<1	increased	39

[a] The fibrinolytic potency toward platelet-rich human plasma clots was determined by using an in vitro system composed of a [^{125}I]fibrin-labeled plasma clot prepared from platelet-rich human plasma (platelet count > $10^5/\mu$L) and immersed in buffer containing plasminogen or in normal human plasma. The release of radiolabeled fibrin degradation products into the supernatant following incubation with the different plasminogen activators reflects the fibrinolytic potency of the agents. [b] Ratio of the activity obtained with conjugated plasminogen activator over the activity obtained with the corresponding unconjugated plasminogen activator.

Table IV. Thrombolytic and Pharmacokinetic Properties of Chemical Antiplatelet Antibody/rscu-PA Conjugates in a Hamster Pulmonary Embolism Model[a]

conjugate	epitope	enhancement factor[d]: thrombolytic potency[b]	enhancement factor[d]: specific thrombolytic activity[c]	fibrinogen breakdown[e]	α_2-antiplasmin depletion[e]	clearance prolongation factor	refs
rscu-PA/MA-PMI-1	GPIIb	3.1	0.39	increased	increased	8	39
rscu-PA/MA-LIBS-1	GPIIIa	2.3	0.16	increased	increased	10	39
rscu-PA/MA-1C8		0.4	0.03	increased	increased	9	39

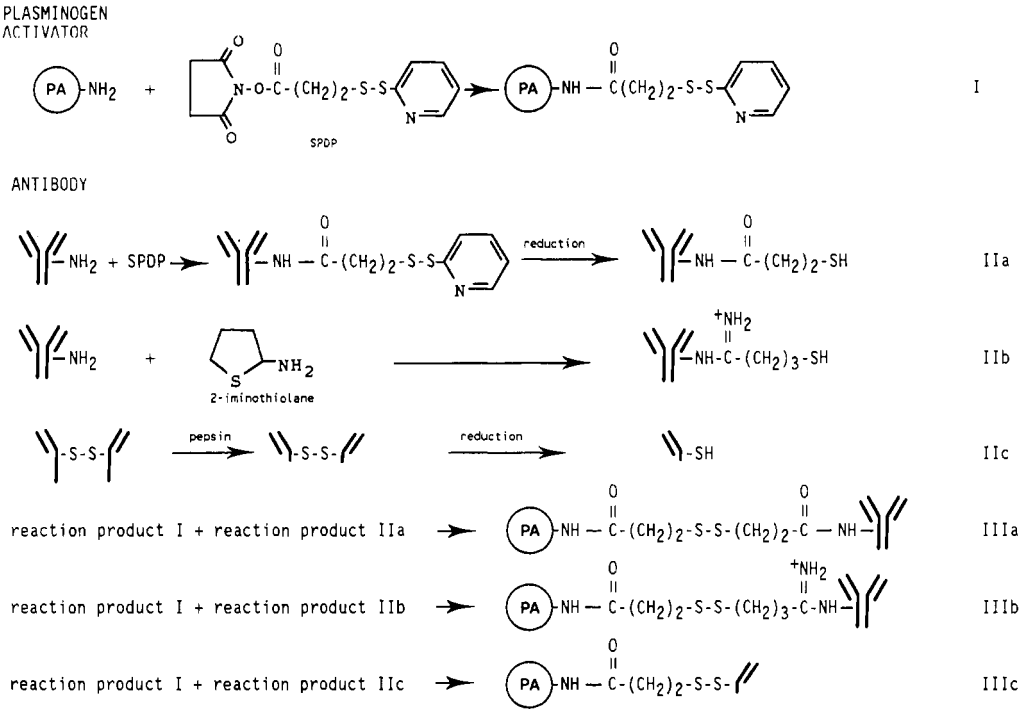
[a] In the hamster pulmonary embolism model, a [^{125}I]fibrin-labeled platelet-rich human plasma clot, produced in vitro from freshly prepared platelet-rich human plasma (platelet count $3 \times 10^5/\mu$L) was injected into the jugular vein, after which it usually embolized into the lungs and occasionally into the heart. Thrombolysis was determined 30 min after the end of a 60-min intravenous infusion of the different plasminogen activators, as the difference between the radioactivity initially incorporated in the clot and the residual radioactivity in the lungs and heart. [b] Thrombolytic potency, derived from the dose–response data of percent lysis obtained versus the dose (in mg of μ-PA per kg of body weight) administered, reflecting potency at comparable dose. [c] Specific thrombolytic activity, derived from the dose-response data of percent lysis obtained versus plasma antigen level (in μg of u-PA antigen per mL), reflecting potency at comparable steady state plasma u-PA antigen levels. [d] Ratio of the activity obtained with the conjugates over the activity obtained with unconjugated rscu-PA. [e] Fibrinogen breakdown or α_2-antiplasmin depletion observed with the conjugates as compared to that observed with unconjugated rscu-PA at equieffective doses.

tibody conjugates was not observed in hamsters with pulmonary embolism consisting of a platelet-poor human plasma clot (*39*). Thrombolysis with the conjugates was associated with fibrinogen degradation and with extensive α_2-antiplasmin depletion (Table IV). The reason for the extensive fibrinogenolysis during in vivo or in vitro clot lysis is not known. Increased systemic activation of the fibrinolytic system was also observed with the control conjugate rscu-PA/MA-1C8 (*6*, *39*) (Table IV) as well as with the conjugate of rscu-PA with the fragment D dimer specific antibody MA-15C5, rscu-PA/MA-15C5, described above (*6*) (Table I). Conversion of these conjugates to two-chain u-PA derivatives by plasmin occurred with initial activation rates (*39*) or catalytic efficiencies (*22*) comparable to the values found with rscu-PA (*21*, *39*). Thus, the difference in systemic activation between conjugated and unconjugated rscu-PA appeared not to be related to differences in the rate of activation to two-chain moieties by plasmin. Conjugation of rscu-PA to the antiplatelet antibodies or to the control antibody MA-1C8 decreased its plasma clearance rate about 10-fold (Table IV), resulting in increased plasma u-PA antigen levels with the conjugates as compared to unconjugated rscu-PA at comparable doses (*39*). Again, specific thrombolytic activities (potency at comparable plasma u-PA antigen level) for rscu-PA/MA-PMI-1, rscu-PA/MA-LIBS-1, and rscu-PA/MA-1C8 were respectively reduced 2.6-, 6-, and 33-fold as compared to that of rscu-PA (Table IV), suggesting interference of the chemical conjugation procedure with the thrombolytic activity of rscu-PA (*39*). Impairment of the functional properties of rscu-PA conjugation was however only observed when specific thrombolytic activities in vivo were compared. In all experiments assaying in vitro biochemical properties (specific activities toward chromogenic substrate or on fibrin plates, catalytic efficiency for plasminogen activation, kinetics of the conversion to two-chain u-PA moieties by plasmin), results obtained with conjugated or unconjugated rscu-PA were comparable (*6*, *22*, *24*, *39*). With rscu-PA/MA-PMI-1 or rscu-PA/MA-LIBS-1, the targeting effect of the antiplatelet antibody moiety in combination with the prolonged half-life apparently compensated for the partial loss of thrombolytic activity of conjugated rscu-PA, resulting in a relatively marginal but statistically significant improvement of their in vivo thrombolytic potency as compared to rscu-PA (Table IV). With rscu-PA/MA-1C8, with similarly prolonged half-life, the 33-fold decrease in specific thrombolytic activity was associated with a reduction of its thrombolytic potency of only 2.5-fold (Table IV). Similar differences between the extent of reduction of specific thrombolytic activity and the extent of reduction of the thrombolytic potency were observed with rscu-PA/MA-1C8 in the rabbit and the baboon model (Table II) and might reflect the effect of the prolonged half-life of conjugated rscu-PA. Prolongation of the half-life might also explain the results obtained with rscu-PA/MA-1C8, rscu-PA/MA-PMI-1, or rscu-PA/MA-LIBS-1 in hamsters with pulmonary embolism consisting of a platelet-poor human plasma clot: the specific thrombolytic activity of the control conjugate as well as of the two antiplatelet antibody conjugates was 6–10-fold reduced as compared to that of rscu-PA, whereas no reduction of the thrombolytic potency was found (*39*). Thus, the increased thrombolytic potency toward platelet-rich human plasma clots in vivo of rscu-PA conjugated with antiplatelet antibodies resulted from the combination of a prolonged half-life and a targeting effect by the antibody moiety of the conjugate.

CHEMICAL CONJUGATION PROCEDURES

Chemical conjugates of plasminogen activators with antifibrin or antiplatelet antibodies were prepared with the

Scheme I.[a] Schematic Representation of the Steps Involved in the Preparation of Chemical Conjugates between Plasminogen Activators and Antibodies



[a] Reactive disulfide groups are introduced into the plasminogen activator (PA) molecule by treatment with the heterobifunctional cross-linking reagent *N*-succinimidyl 3-(2-pyridyldithio)propionate (SPDP) (reaction I). Thiol groups are introduced into intact antibody (or its $F(ab')_2$ fragment) either by treatment with SPDP, followed by mild reduction (reaction IIa), or by treatment with 2-iminothiolane (reaction IIb). Alternatively, the antibody is digested by pepsin and the inter-heavy-chain disulfide bond is reduced under mild conditions to yield Fab' fragments containing a free thiol group (reaction IIc). Finally, the SPDP-treated plasminogen activator is coupled with the thiol-containing antibody following a disulfide-exchange reaction as shown in reaction IIIa (*6, 24, 39*), reaction IIIb (*12, 15*), and reaction IIIc (*14–16*).

heterobifunctional cross-linking reagent *N*-succinimidyl 3-(2-pyridyldithio)propionate (SPDP) (*40*) and/or the thiolating reagent 2-iminothiolane (*41*) by using a three-step procedure as outlined in Scheme I. Briefly, reactive disulfide bonds were introduced into the plasminogen activator molecule by treatment with SPDP (reaction I) (*6, 12, 14–16, 24, 39*). In a second step, thiol groups were introduced into the antibody either by treatment with SPDP followed by reduction of the introduced disulfide bonds (reaction IIa) (*6, 24, 39*) or by treatment with 2-iminothiolane (reaction IIb) (*12, 15*). Alternatively, $F(ab')_2$ fragments were prepared by digestion of the antibody with pepsin and the inter-heavy-chain disulfide bond was reduced under mild conditions, yielding Fab' fragments containing a free thiol group (reaction IIc) (*14–16*). In the third step, the SPDP-treated plasminogen activator reacts with the thiol-containing antibody via a thiol–disulfide exchange to form a disulfide-linked protein–protein conjugate (Scheme I, reactions IIIa–c). Chemically coupled bispecific antibodies (*29, 32*) were prepared by using a procedure analogous to steps I, IIb, and IIIb of Scheme I.

CONCLUSION

Conjugation of plasminogen activators with antifibrin antibodies as well as with antiplatelet antibodies has resulted in significantly enhanced thrombolysis, both in vitro and in vivo. Antibody-mediated targeting thus appears to hold promise for the development of plasminogen activators with enhanced potency and clot-selectivity. The use of such agents may allow a significant reduction of the total dose of plasminogen activator which in turn might reduce systemic side effects. On the other hand, the use of bispecific antibodies with high affinities for both fibrin and plasminogen activator might allow concentration of endogenous plasminogen activator at the site of a thrombus and might eliminate the need for the administration of high doses of exogenous thrombolytic agent.

Chemical conjugation methods, involving the introduction of reactive groups by treatment with cross-linking agents such as *N*-succinimidyl 3-(2-pyridyldithio)propionate and 2-iminothiolane, have the disadvantage of low yields and random coupling. In addition, chemical conjugation may affect the enzymatic properties of the plasminogen activator moiety of covalent plasminogen activator/antibody conjugates. Chemically prepared conjugates are therefore unsuitable for large-scale production for in vivo application. The construction of plasminogen activator/antibody conjugates by recombinant DNA technology may avoid most of these problems, and results obtained with such recombinant conjugates are encouraging. In addition, this approach permits humanization of the murine monoclonal antibody by substituting the murine constant regions with those of a human antibody (*42, 43*) or by engrafting the complementarity-determining regions of the targeting monoclonal antibody into the corresponding positions of a human antibody (*44, 45*). In this way, one might circumvent immunogenicity problems associated with the use of nonhuman antibodies in man. Alternatively, recombinant DNA techniques allow the use of small-size binding units of an antibody such as single-chain Fv fragments containing the variable domains of the antibody only (*46, 47*). Results obtained with the chimera $K_{12}G_0S_{32}$ indicate that a plasminogen activator can indeed be targeted to a fibrin clot with a single-chain Fv fragment derived from fibrin-specific monoclonal antibody (*26*). Changing the size of the conjugate molecule

by using fragments of the antibody may affect the clearance rate of the molecule. The optimal size giving the desired pharmacokinetic properties will have to be determined. Thus, with the use of recombinant DNA technology, the potential exists to develop improved thrombolytic agents with an optimal circulatory half-life and minimal immunogenicity.

LITERATURE CITED

(1) Collen, D., and Gold, H. K. (1989) Fibrin-specific thrombolytic agents and new approaches to coronary arterial thrombolysis. *Thrombolysis in Cardiovascular Diseases* (D. Julian, W. Kübler, R. M. Norris, H. J. C. Swan, D. Collen, and M. Verstraete, Eds.) pp 45–67, Marcel Dekker Inc., New York.

(2) Lijnen, H. R., and Collen, D. (1988) New strategies in the development of thrombolytic agents. *Blut 57*, 147–162.

(3) Lijnen, H. R., and Collen, D. (1990) Tissue-type plasminogen activator: mutants, variants and adjunctive treatment. *Biotechnol. Ther. 1*, 273–304.

(4) Koppel, G. A. (1990) Recent advances with monoclonal antibody drug targeting for the treatment of human cancer. *Bioconjugte Chem. 1*, 13–23.

(5) Bode, C., Matsueda, G. R., Hui, K. Y., and Haber, E. (1985) Antibody-directed urokinase: a specific fibrinolytic agent. *Science 229*, 765–767.

(6) Dewerchin, M., Lijnen, H. R., Van Hoef, B., De Cock, F., and Collen, D. (1989) Biochemical properties of conjugates of urokinase-type plasminogen activator with a monoclonal antibody specific for cross-linked fibrin. *Eur. J. Biochem. 185*, 141–149.

(7) Hui, K. Y., Haber, E., and Matsueda, G. R. (1983) Monoclonal antibodies to a synthetic fibrin-like peptide bind to human fibrin but not fibrinogen. *Science 222*, 1129–1132.

(8) Declerck, P. J., Mombaerts, P., Holvoet, P., De Mol, M., and Collen, D. (1987) Fibrinolytic response and fibrin fragment D-dimer levels in patients with deep vein thrombosis. *Thromb. Haemostasis 58*, 1024–1029.

(9) Holvoet, P., Stassen, J. M., Hashimoto, Y., Spriggs, D., Devos, P., and Collen, D. (1989) Binding properties of monoclonal antibodies against human fragment D-dimer of cross-linked fibrin to human plasma clots in an in vivo model in rabbits. *Thromb. Haemostasis 61*, 307–313.

(10) Liau, C. S., Haber, E., and Matsueda, G. R. (1987) Evaluation of monoclonal antifibrin antibodies by their binding to human blood clots. *Thromb. Haemostasis 54*, 49–54.

(11) Hashimoto, Y., Stassen, J. M., Leclef, B., De Roo, M., Vandecruys, A., Melin, J., Verhoeven-Mester, D., Trouet, A., and Collen, D. (1989) Thrombus imaging with an I-123-labeled F(ab')$_2$ fragment of an anti-human fibrin monoclonal antibody in a rabbit model. *Radiology 171*, 223–226.

(12) Runge, M. S., Bode, C., Matsueda, G. R., and Haber, E. (1988) Conjugation to an antifibrin monoclonal antibody enhances the fibrinolytic potency of tissue plasminogen activator in vitro. *Biochemistry 27*, 1153–1157.

(13) Runge, M. S., Bode, C., Matsueda, G. R., and Haber, E. (1987) Antibody-enhanced thrombolysis: targeting of tissue plasminogen activator in vivo. *Proc. Natl. Acad. Sci. U.S.A. 84*, 7659–7662.

(14) Bode, C., Runge, M. S., Newell, J. B., Matsueda, G. R., and Haber, E. (1987) Thrombolysis by a fibrin-specific antibody Fab'-urokinase conjugate. *J. Mol. Cell Cardiol. 19*, 335–341.

(15) Bode, C., Runge, M. S., Newell, J. B., Matsueda, G. R., and Haber, E. (1987) Characterization of an antibody-urokinase conjugate. A plasminogen activator targeted to fibrin. *J. Biol. Chem. 262*, 10819–10823.

(16) Bode, C., Runge, M. S., Schönermark, S., Eberle, T., Newell, J. B., Kübler, W., and Haber, E. (1990) Conjugation to antifibrin Fab' enhances fibrinolytic potency of single-chain urokinase plasminogen activator. *Circulation 81*, 1974–1980.

(17) Schnee, J. M., Runge, M. S., Matsueda, G. R., Hudson, N. W., Seidman, J. G., Haber, E., and Quertermous, T. (1987) Construction and expression of a recombinant antibody-targeted plasminogen activator. *Proc. Natl. Acad. Sci. U.S.A. 84*, 6904–6908.

(18) Haber, E., Quertermous, T., Matsueda, G. R., and Runge, M. S. (1989) Innovative approaches to plasminogen activator therapy. *Science 243*, 51–56.

(19) Runge, M. S., Huang, P., Savard, C. E., Schnee, J. M., Love, T. W., Bode, C., Matsueda, G. R., Haber, E., and Quertermous, T. (1989) A recombinant molecule with antifibrin antibody and single-chain urokinase activities has increased fibrinolytic potency. *Circulation 78 (Suppl. II)*, II-509.

(20) Collen, D., Dewerchin, M., Stassen, J. M., Kieckens, L., and Lijnen, H. R. (1989) Thrombolytic and pharmacokinetic properties of conjugates of urokinase-type plasminogen activator with a monoclonal antibody specific for cross-linked fibrin. *Fibrinolysis 3*, 197–202.

(21) Lijnen, H. R., Van Hoef, B., and Collen, D. (1987) Activation with plasmin of two-chain urokinase-type plasminogen activator derived from single-chain urokinase-type plasminogen activator by treatment with thrombin. *Eur. J. Biochem. 169*, 359–364.

(22) Dewerchin, M., Lijnen, H. R., Van Hoef, B., De Cock, F., and Collen, D. (1990) Characterization of conjugates of a thrombin-treated single chain urokinase-type plasminogen activator with a monoclonal antibody specific for cross-linked fibrin. *Fibrinolysis 4*, 19–26.

(23) Collen, D., Dewerchin, M., Rapold, H. J., Lijnen, H. R., and Stassen, J. M. (1990) Thrombolytic and pharmacokinetic properties of a conjugate of recombinant single-chain urokinase-type plasminogen activator with a monoclonal antibody specific for cross-linked fibrin in a baboon venous thrombosis model. *Circulation 82*, 1744–1753.

(24) Dewerchin, M., Lijnen, H. R., and Collen, D. (1990) Characterization of a chemical conjugate between a low molecular weight form of recombinant single chain urokinase-type plasminogen activator (comprising Leu^{144} through Leu^{411}) and F(ab')$_2$-fragments of a fibrin D-dimer-specific monoclonal antibody. *Fibrinolysis 4*, 11–18.

(25) Lijnen, H. R., Dewerchin, M., De Cock, F., and Collen, D. (1990) Effect of fibrin-targeting on clot lysis with urokinase-type plasminogen activator. *Thromb. Res. 57*, 333–342.

(26) Holvoet, P., Laroche, Y., Lijnen, H. R., Van Cauwenberge, R., Demarsin, E., Brouwers, E., Matthyssens, G., and Collen, D. Characterization of a chimeric plasminogen activator consisting of a single-chain Fv fragment derived from a fragment D-dimer specific antibody and a truncated single-chain urokinase. *J. Biol. Chem.*, in press.

(27) Laroche, Y.; De Meyer, M., Stassen, J. M., Ganseman, Y., Demarsin, E., Matthyssens, G., Collen, D., and Holvoet, P. Characterization of a recombinant single-chain molecule comprising the variable domains of a monoclonal antibody specific for human fibrin fragment D-dimer. *J. Biol. Chem.*, in press.

(28) Branscomb, E. E., Runge, M. S., Savard, C. E., Adams, K. M., Matsueda, G. R., and Haber, E. (1990) Bispecific monoclonal antibodies produced by somatic cell fusion increase the potency of tissue plasminogen activator. *Thromb. Haemostasis 64*, 260–266.

(29) Bode, C., Runge, M. S., Branscomb, E. E., Newell, J. B., Matsueda, G. R., and Haber, E. (1989) Antibody-directed fibrinolysis. An antibody specific for both fibrin and tissue plasminogen activator. *J. Biol. Chem. 264*, 944–948.

(30) Kurokawa, T., Iwasa, S., and Kakinuma, A. (1989) Enhanced fibrinolysis by a bispecific monoclonal antibody reactive to fibrin and tissue plasminogen activator. *Biotechnology 7*, 1163–1167.

(31) Kurokawa, T., Iwasa, S., and Kakinuma, A. (1990) Enhancement of fibrinolysis by bispecific monoclonal antibodies reactive to fibrin and plasminogen activators. *Thromb. Res. Suppl. X*, 83–89.

(32) Charpie, J. R., Runge, M. S., Matsueda, G. R., and Haber, E. (1990) A bispecific antibody enhances the fibrinolytic potency of single-chain urokinase. *Biochemistry 29*, 6374–6378.

(33) Collen, D. (1986) Tissue-type plasminogen activator (t-PA) and single chain urokinase-type plasminogen activator (scu-PA): potential for fibrin-specific thrombolytic therapy. *Prog. Hemostasis Thromb. 8*, 1–18.

(34) Stump, D. C., Lijnen, H. R., and Collen, D. (1986) Purification and characterization of a novel low molecular weight form of single-chain urokinase-type plasminogen activator. *J. Biol. Chem. 261*, 17120–17126.
(35) Rijken, D. C., and Groeneveld, E. (1986) Isolation and functional characterization of the heavy and light chains of human tissue-type plasminogen activator. *J. Biol. Chem. 261*, 3098–3102.
(36) Yasuda, T., Gold, H. K., Leinbach, R. C., Saito, T., Guerrero, J. L., Jang, I.-K., Holt, R., Fallon, J. T., and Collen, D. (1990) Lysis of plasminogen activator-resistant platelet-rich coronary artery thrombus with combined bolus injection of recombinant tissue-type plasminogen activator and antiplatelet GPIIb/IIIa antibody. *J. Am. Coll. Cardiol. 16*, 1728–1735.
(37) Bode, C., Meinhardt, G., Runge, M. S., Eberle, T., Schuler, G., Kübler, W., and Haber, E. (1989) Conjugation of urokinase to an antiplatelet antibody results in a more potent fibrinolytic agent. *Thromb. Haemostasis 62*, 483.
(38) Pytela, R. P., Pierschbacher, M. D., Ginsberg, M. H., Plow, E. F., and Ruoslahti, E. (1986) Platelet membrane glycoprotein IIb/IIIa: member of a family of Arg-Gly-Asp-specific adhesion receptors. *Science 231*, 1559–1562.
(39) Dewerchin, M., Lijnen, H. R., Stassen, J. M., De Cock, F., Quertermous, T., Ginsberg, M. H., Plow, E. F., and Collen, D. Effect of chemical conjugation of recombinant single-chain urokinase-type plasminogen activator with monoclonal antiplatelet antibodies, on platelet aggregation and on plasma clot lysis in vitro and in vivo. *Blood*, in press.
(40) Carlsson, J., Drevin, H., and Axén, R. (1978) Protein thiolation and reversible protein–protein conjugation. *N*-succinimidyl 3-(2-pyridyldithio)propionate, a new heterobifunctional reagent. *Biochem. J. 173*, 723–737.
(41) King, T. P., Li, Y., and Kouchoumian, L. (1978) Preparation of protein conjugates via intermolecular disulfide bond formation. *Biochemistry 17*, 1499–1506.
(42) Vandamme, A.-M., Bulens, F., Bernar, H., Nelles, L., Lijnen, H. R., and Collen, D. (1990) Construction and characterization of a recombinant murine monoclonal antibody directed against human fibrin fragment D-dimer. *Eur. J. Biochem. 192*, 767–775.
(43) Bulens, F., Vandamme, A.-M., Bernar, H., Nelles, L., Lijnen, H. R., and Collen, D. (1991) Construction and characterization of a functional chimeric murine-human antibody directed against human fibrin fragment D-dimer. *Eur. J. Biochem. 195*, 235–242.
(44) Jones, P. T., Dear, H., Foote, J., Neuberger, M. S., and Winter, G. (1986) Replacing the complementarity-determining regions in a human antibody with those from a mouse. *Nature 321*, 522–525.
(45) Hale, G., Dyer, M. J. S., Clark, M. R., Phillips, J. M., Marcus, R., Riechmann, L., Winter, G., and Waldmann, H. (1988) Remission induction in non-Hodgkin lymphoma with reshaped human monoclonal antibody CAMPATH-1H. *Lancet 11*, 1394–1399.
(46) Bird, R. E., Hardman, K. D., Jacobson, J. W., Johnson, S., Kaufman, B. M., Lee, S.-M., Lee, T., Pope, S. H., Riordan, G. S., and Whitlow, M. (1988) Single-chain antigen-binding proteins. *Science 243*, 423–426.
(47) Chaudhary, V. K., Queen, C., Junghans, R. P., Waldmann, T. A., FitzGerald, D. J., and Pastan, I. (1989) A recombinant immunotoxin consisting of two antibody variable domains fused to *Pseudomonas exotoxin*. *Nature 339*, 394–397.

Conjugation of Plasminogen Activators and Fibrin-Specific Antibodies To Improve Thrombolytic Therapeutic Agents

David J. Hayzer, Ira M. Lubin, and Marschall S. Runge*

Division of Cardiology, Drawer LL, Emory University School of Medicine, Atlanta, Georgia 30322.
Received April 30, 1991

The specific delivery of a therapeutic agent to sites in the circulation where intervention is required, and the concomitant presence of low levels elsewhere in the circulation, increases therapeutic efficacy and reduces toxic side effects. The strategies explored to achieve this benefit have included (1) physical delivery of an agent to its site of action (either by implantation, use of an intravascular catheter delivery system, or related methods); (2) development of agents with activity dependent on the presence of a "cofactor" that is an integral part of the target; (3) development of agents that interact only with a certain type of cell (for example, all rapidly dividing cells, or cells that have a specific receptor present on the cell membrane); and (4) use of hybrid molecules that contain both an "effector" domain and a "targeting" domain. In this last case, the ideal agent combines high affinity and specificity for its site of action with an efficient "effector" domain. The ability of antibodies to recognize and bind an immense diversity of epitopes, in a specific manner, has made them ideal candidates as carriers for attached effector molecules which may or may not themselves have affinity for the target. Indeed, the use of antibodies to target a therapeutic agent has now reached the clinical arena (for a review, see ref 1). Antibody–effector molecule hybrids are also unique experimental tools that have been useful in defining the potential for targeted drug delivery in vitro and in animal models. These hybrids have also offered insights into basic pathophysiological mechanisms. The linking of small molecular weight adjuncts to monoclonal antibodies has recently been reviewed (2). In this article we will discuss procedures currently available for the joining of antibodies to protein effectors for therapeutic uses.

A native antibody molecule comprises four polypeptide chains, a pair of identical light chains, and a pair of identical heavy chains (Figure 1). Both types of polypeptide have two defined regions, a constant region, the sequence of which is specific for a particular class of chain (κ or λ, light; α, γ, μ, etc, heavy), and a variable region, which actually bears the antigen-binding site. Each light chain is linked to a heavy chain by a disulfide bond between a highly conserved cysteine residue on each. The combination of the two variable regions is usually, but not always, required to give the conformation of the active antigen-binding site (3). Since the mature IgG class of antibody consists of two pairs of heavy and light chains, joined by disulfide bridges, it will have two antigen-binding sites and is thus bivalent. Only a portion of the intact bivalent antibody is actually involved in antigen binding, while other portions of the antibody have other functions. For example, the Fc domain is responsible for the induction of phagocytosis, the acceleration of the immune response by activation of complement, and directing the transport of immunoglobulins to their sites of action. Thus, from the standpoint of protein engineering, much of the basic antibody structure can be considered redundant and can be deleted or replaced without destroying the essential antigen-binding site.

There are three strategies that have been used to couple a target-specific antibody to an effector protein molecule:

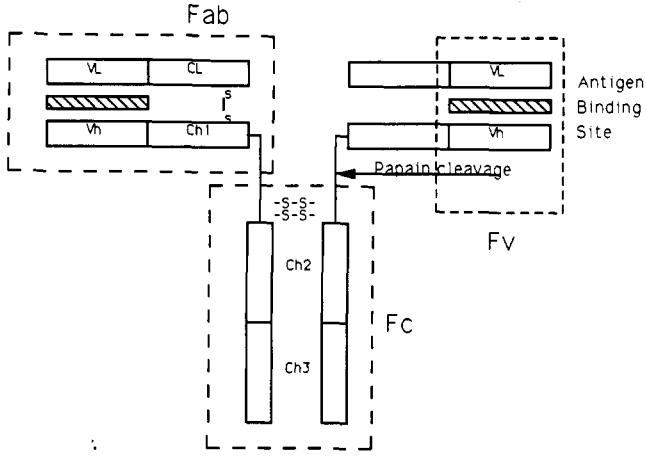


Figure 1. Schematic structure of an immunoglobulin. Papain cleavage above the double disulfide bridges releases the Fab' units, each comprising an entire light chain and that portion of a heavy chain containing the variable (Vh) domain and the constant domain CH1, cross-linked to the light chain constant domain by a disulfide bridge. Also released are the remaining, linked, heavy-chain constant domains, as the Fc fragment. The two variable domains give the antigen-binding site (cross-hatched). Isolated V_L and V_H domains retain the antigen-binding activity, as the Fv fragment.

(a) The antibody carrier can be covalently cross-linked to the protein agent, typically by chemically creating disulfide bridges between the two moieties.

(b) Antibodies possess two identical sites which, independently of each other, can bind an antigenic epitope. One might envision an antibody in which the two antigen binding sites recognize two different epitopes. In the case of targeted chemotherapy, one arm of the hybrid antibody would bind to the target, while the other arm would be specific for (but not inhibiting) the therapeutic agent. When the bifunctional agent is administered simultaneously with the therapeutic agent, the therapeutic agent is concentrated at the desired site by the bifunctional antibody. Alternatively, the arm specific for the therapeutic agent may recognize a protein normally present in the circulation in low concentrations, and the bifunctional antibody could be used to "concentrate" the endogenous effector to the desired site. It is possible to construct bifunctional antibodies chemically, by coupling the Fab' fragments of two different antibodies, and it is also possible to generate "hybrid hybridomas" that produce a recombined bifunctional antibody. Both of these approaches are discussed in this review.

(c) Recombinant DNA technology allows the replacement of selected domains of the antibody that are nonessential for binding to the epitope with the necessary domains of an effector protein. An additional benefit of this approach is that the antibody domain usually replaced is the Fc domain. This domain is the most antigenic region of an antibody, and the most likely domain to produce an immune response or complement activation in the host receiving the antibody-targeted therapeutic agent (this is particularly important in considering the use of murine antibodies in man).

The concept of antibody targeting of therapeutic agents

* Author to whom all correspondence should be addressed.

1043-1802/91/2902-0301$02.50/0 © 1991 American Chemical Society

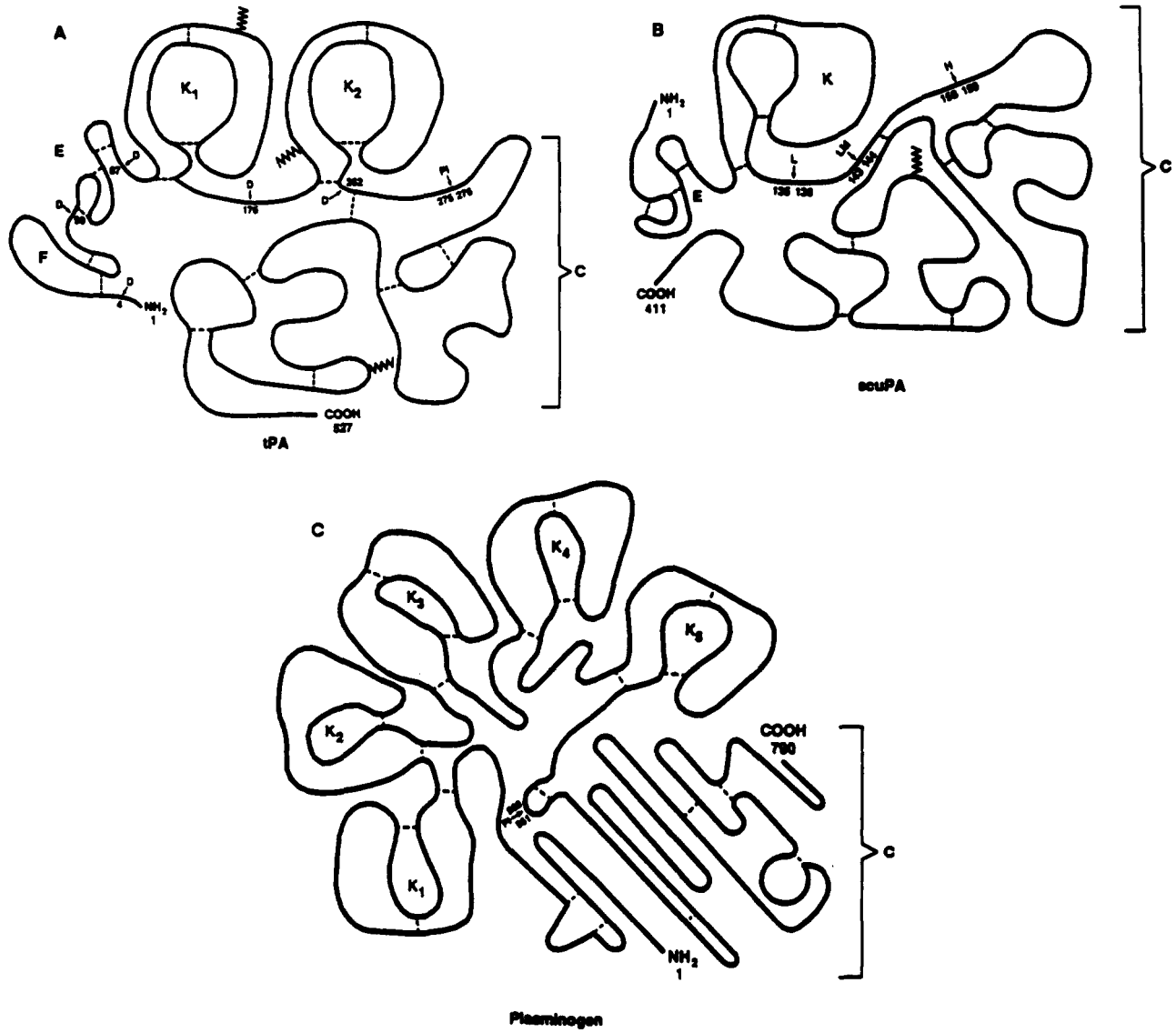


Figure 2. Schematic representations of the secondary structures of A, tissue plasminogen activator (tPA); B, single-chain urokinase (scuPA); C, plasminogen (taken from ref 2). Functional domains are F, finger; E, epidermal growth factor like; K, kringle; C, catalytic. The extremities of the domains, for tPA, are indicated by D. Dashed lines are intrachain disulfide bridges, zigzags are N-linked glycosylation sites. For tPA (A) and plasminogen (C), P1 indicates the site of plasmin cleavage. For scuPA (B), the plasmin cleavage site H gives high molecular weight two-chain urokinase, and the site L gives low molecular weight two-chain urokinase.

has been proposed for a number of different pathological conditions, notably in the treatment of certain cancers (for a review, see ref 1). Another potentially useful example of this approach is that of anti-fibrin antibodies used to target plasminogen activator molecules to a thrombus in patients who develop thrombotic obstruction of a coronary artery (*4*). Without therapy, myocardial infarction results from coronary artery occlusion. Administration of a plasminogen activator (such as tissue plasminogen activator (tPA), urokinase (UK), single-chain urokinase-type plasminogen activator (scuPA), or streptokinase—see Figure 2 for structural details) within 4–6 h of thrombotic occlusion reduces the amount of ischemic damage to the myocardial tissue distal to the occlusion and results in decreased mortality. The significance of this therapy is emphasized by the fact that myocardial infarction is still the most common cause of death in industrialized nations, and plasminogen activator therapy produces approximately a 30–50% reduction in mortality (*5*, *6*).

Plasminogen activator (or thrombolytic) therapy is effective because the plasminogen activators effect the conversion of zymogen plasminogen into plasmin (Figure 2C; *4*, *7*, *8*). Plasmin is an active enzyme that digests fibrin. The occlusive thrombi found in arteries or veins contain platelets, covalently linked to each other by fibrin and fibrinogen. In addition, cross-linked fibrin forms the underlying structural backbone of both arterial and venous thrombi (for a review, see ref 9). The principle limitation of plasminogen activator therapy is bleeding elsewhere in the circulation. In man, this results from the necessity to infuse massive doses of a plasminogen activator in order to effect thrombolysis (*10*). At such doses, plasminogen is converted to plasmin throughout the circulation, and the resulting plasminemia correlates with bleeding at sites of prior arterial or venous injury. Bleeding complications are most marked when either streptokinase (isolated from Lancefield group C strains of β-hemolytic streptococci) or urokinase (UK, a human protein isolated from human urine) are infused. This disruption of hemostasis frequently necessitates blood transfusion and is fatal in ca. 1% of patients treated with these agents (*5*, *6*).

The systemic disruption of the clotting process would be greatly reduced if plasminogen activators could convert plasminogen into plasmin only at the site of an obstructive thrombus. To a limited degree, this is the case with tPA, which binds directly to fibrin, and scuPA, which does not

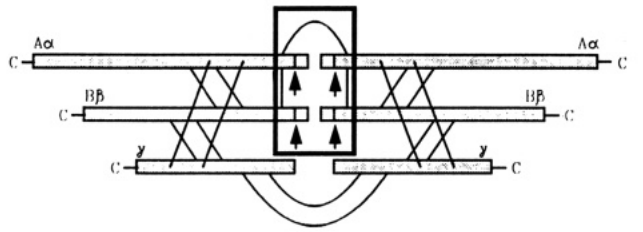


Figure 3. Schematic structure of fibrinogen. Heavy lines indicate disulfide bridges. Arrow heads indicate points of cleavage by thrombin, to convert fibrinogen to fibrin. Boxed region is the fragment D dimer, a plasmin cleavage product. Figure modified from *Biochemistry* [D. Voet, and J. A. Voet, Eds. (1990) J. Wiley and Sons, New York].

bind directly to fibrin but activates plasminogen only in the presence of fibrin (*11*, *12*). That tPA and scuPA are relatively fibrin-specific is demonstrated by the finding that patients treated with either of these agents experience much less consumption of serum fibrinogen, α-2-antiplasmin, or plasminogen than do patients treated with either streptokinase or UK (*13*).

The risk of generalized hemorrhage has led to interest in the engineering of plasminogen activators to improve their affinity for thrombus-bound fibrin (*4*, *8*). The principal approach initially used was to couple UK chemically to a fibrin-specific monoclonal antibody. This first required development of antibodies that bound to fibrin with high specificity. The antibodies that have been used bind to either of two unique sites present on fibrin that distinguish fibrin from fibrinogen. During the process of clot formation the protease thrombin cleaves NH_2-terminal peptides from the Aα- and Bβ-chains of fibrinogen. The exposed NH_2 terminus of the β-chain becomes, therefore, a novel epitope specific for fibrin (Figure 3). A number of monoclonal antibodies have been raised against a synthetic peptide consisting of this sequence, Gly-His-Arg-Pro-Leu-Asp-Lys-Cys. One such monoclonal antibody, designated 59D8, has a much greater affinity for fibrin than does tPA itself, does not cross-react with fibrinogen (*14*), and has been used to make plasminogen activator–antibody hybrid molecules.

CHEMICAL CROSS-LINKING

Fibrin-specific antibodies have been chemically cross-linked to plasminogen activators, among them urokinase (*15–17*), tPA (*18*), and scuPA (*19*, *20*). Following the coupling of urokinase to polyclonal rabbit anti-human fibrinogen antibodies, thereby demonstrating the practical feasibility of this approach (*15*), urokinase and the monoclonal antifibrin antibodies 64C5 and 59D8 were cross-linked (*16*). In the latter case, intramolecular bridges were provided by the agent *N*-succinimidyl 3-(2-pyridyldithio)-propionate (SPDP) (Figure 4a). The synthesis, chemical characterization, and potential uses of this compound to cross-link proteins have been described in depth by Carlsson et al. (*21*). SPDP is termed a heterobifunctional agent, because the attachment and the cross-linking steps are separate and involve different functional groups on each of the proteins participating in the conjugation. In the first step (attachment), a lysine amino group on one protein is modified by SPDP. In a second reaction, a sulfhydryl bond is formed between the SPDP-modified protein and an available cysteine residue on the recipient protein. This two step process significantly reduces the amounts of undesired homoconjugates of the two proteins.

When SPDP was coupled to the antibody 64C5 (*16*), analysis for the 2-pyridyl disulfide content showed 10.8 residues per antibody molecule. Urokinase was reduced

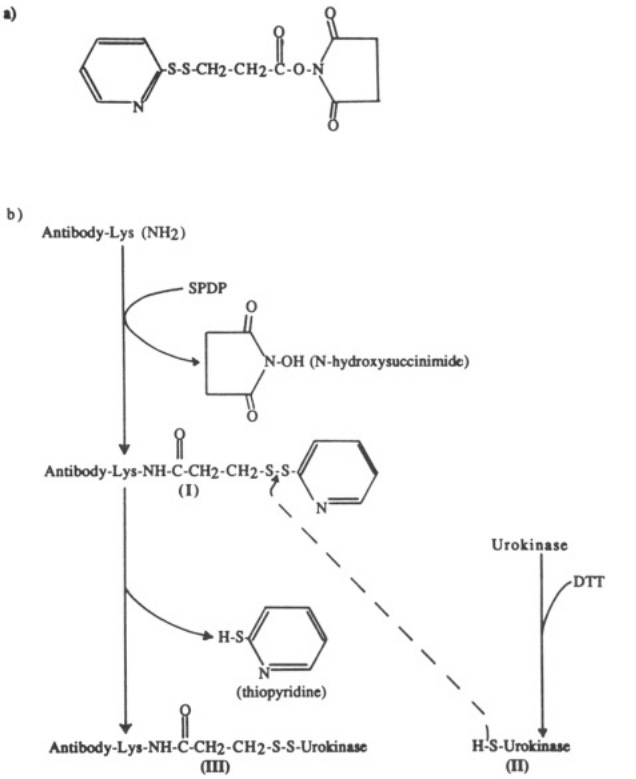


Figure 4. (a) Structure of *N*-succinimidyl 3-(2-pyridyldithio)-propionate. (b) Scheme for the coupling of anti-fibrin monoclonal antibody 59D8 and urokinase (ref 16).

by dithiothreitol and combined with the (2-pyridyl)dithiopropionyl-derivitized antibody (I, Figure 4b). The sulfydryl groups of the urokinase (II) displace the thiopyridine (thio–disulfide exchange), forming disulfide bridges between the two proteins (III, Figure 4b). Unlinked urokinase was removed by gel chromatography, leaving 1 mol of urokinase coupled per 3 mol of antibody, as shown by SDS–polyacrylamide gel electrophoresis. The conjugated protein retained the antibody's ability to bind to the NH_2 terminus of the β-chain of fibrin, and the urokinase plasminogen activation activity was also retained. The efficiency of fibrinolysis of the conjugate was a significant 100-fold over that of the urokinase alone.

A conjugate has also been constructed between the monoclonal anti-fibrin antibody 59D8 and tPA (*18*). For this coupling a somewhat different strategy was employed. SPDP was attached to amino groups of the plasminogen activator, and the amino groups of the antibody were reacted with 2-iminothiolane. A subsequent thiopyridine displacement reaction led to the formation of the cross-linking disulfide bridge (Figure 5a). The reaction products were purified by two affinity-column steps, the first a peptide (fibrin β-chain-specific)–Sepharose column to remove inactivated antibody and uncoupled tPA, followed by a benzamidine–Sepharose column (to which tPA binds) to remove uncoupled antibody. The purified tPA–59D8 conjugate showed a 10-fold improvement in the fibrinolytic potency, when compared to unconjugated tPA (in an in vitro chromogenic assay). In vivo studies also showed an increase in the fibrinolytic activity of the conjugate, compared to the tPA alone. The effect of tPA–59D8 on plasma fibrinogen was negligible, while doses of tPA required to produce the same amount of thrombolysis produced significant fibrinogen degradation. More recently, scuPA has been linked to the Fab′ portion of the antibody 59D8, again with SPDP as the linking agent (*22*). Conjugated and unconjugated 59D8 Fab′ were purified by a β-peptide–Sepharose affinity column to remove un-

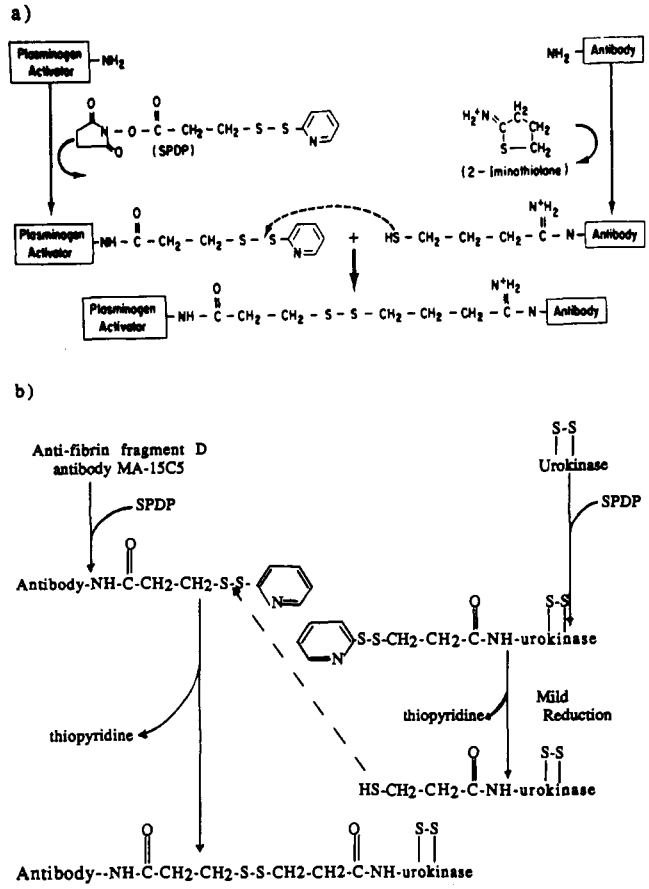


Figure 5. (a) Scheme for the coupling of anti-fibrin monoclonal antibody 59D8 and tissue plasminogen activator (tPA). Figure reproduced from ref 13. (b) Scheme for the coupling of anti-fibrin fragment D monoclonal antibody MA15C5 and urokinase (refs 17, 19, 20).

conjugated scuPA and inactive antibody, and a column of benzamidine–Sepharose to remove conjugates containing two-chain urokinase (tcuPA) arising from the proteolytic cleavage of scuPA during the course of the coupling reaction. (scuPA does not bind to benzamidine, thus the desired conjugate was found in the fall through from this column.) The final preparation contained scuPA–59D8, in a 1:2 molar ratio, and one free Fab′ per molecule of scuPA–59D8 conjugate. In vitro, fibrinolytic activity was 230-fold greater than unconjugated scuPA. In vivo, with a rabbit jugular vein thrombus model, potency was 29-fold greater than with scuPA alone.

Dewerchin and colleagues (*17*, *19*, *20*) have cross-linked scuPA with a monoclonal antibody directed to the fragment D dimer of fibrin (Figure 3), rather than against the NH_2 terminus of the β-chain of fibrin. Their rationale for using the anti-D-dimer antibody was based on data suggesting that the β-chain epitope is lost earlier in thrombolysis than is the D dimer epitope (*23*, *24*). By choosing this antibody, it was anticipated that the conjugate would be retained for a much longer period of time in the vicinity of the clot. Again, SPDP was used to introduce disulfide groups, but this time onto both the antibody and the plasminogen activator (Figure 5b). Mild reduction by dithiothreitol released the thiopyridine moieties, to give free sulfydryl groups, while leaving intact the disulfide bonds of the intact native proteins. The two preparations of proteins were mixed and allowed to react at room temperature, and excess thiol groups were blocked by alkylation. The desired products were purified by affinity chromatography. Fibrinolytic potency of these conjugates, both in vitro and in vivo, was comparable to that of the scuPA–59D8 conjugates previously described (*22*). These studies demonstrate that chemical cross-linking using bifunctional cross-linking reagents is practical and offers numerous advantages. Chemical cross-linking can be used to join two disparate molecules while retaining their native functions. The approaches described here require optimization, but once attained, conjugation can be completed rapidly and with good yield. The procedures and the resulting conjugates do, however, have certain disadvantages. There can be no effective control over the sites of attachment of the SPDP, i.e., which of the available lysine amino groups is modified. The result is a heterogeneous mix of active and inactive conjugates. Although affinity purification removes the latter contaminants, the overall yield of the desired product may be quite low (*3*). An important practical limitation is that the conjugated proteins display variable stability, severely restricting their use under clinical conditions. The ill-defined nature of the reaction products would also limit the ability to assess accurately the results of in vivo and clinical trials of such engineered agents.

BIFUNCTIONAL ANTIBODIES

Polyclonal and monoclonal antibodies contain two antigen-binding sites per molecule, each of which is functionally independent of the other. By substituting one heavy–light chain pair of an antibody for that derived from a second antibody recognizing a different epitope, however, a recombinant molecule can be formed, able to recognize and bind to two quite distinct epitopes. It is not our intention to detail this aspect of protein conjugation, which has recently been covered in depth by Nolan and O'Kennedy (*25*), except as it applies to the development of thrombolytic therapy.

One bispecific antibody has been constructed with dual affinity for fibrin and tPA. The monoclonal antibodies 59D8 and TCL8, the latter directed against tPA, were modified and joined by SPDP and 2-iminothiolane, by using the methodology described in the previous section (Figure 5a) (*26*). Significant increases in in vitro fibrinolysis were observed in the presence of the bifunctional conjugate and free tPA; in vivo, tPA was concentrated to improve the rate of thrombolysis with a concomitant reduction in fibrinogenolysis. The clinical use of a bifunctional antibody would potentially obviate the necessity to introduce high levels of tPA into the circulatory system of the patient. Instead, use could be made of circulating tPA concentrated at the thrombus target. Serum fibrinogen levels should be unaffected, with little, if any, generalized bleeding. An additional potential use for this approach is in concentrating endogenous tPA. Even though the amounts of tPA present in the circulation under normal conditions are not sufficient to effect thrombolysis, in theory localization of these small quantities to a site where a thrombus is present may facilitate lysis of that thrombus. This concept, however, has yet to be tested in vivo.

It has also been possible to generate a "hybrid hybridoma" cell that produces a chimeric antibody containing the binding site of both 59D8 and of TCL8 (*27*). 59D8 cells, secreting the fibrin β-chain-specific monoclonal antibody 59D8, were rendered thymidine kinase deficient by prolonged incubation in a medium containing 5-bromo-2′-deoxyuridine. In addition, the cell line TCL8, secreting the tPA-specific monoclonal antibody, was rendered hypoxanthine guanine phosphoribosyl transferase deficient by incubation in medium containing 6-thioguanine. The two mutated cell lines were fused in the presence of

polyethylene glycol, and successful fusions were selected by growth in HAT medium. Fusions secreting a bifunctional antibody, capable of binding to both fibrin and tPA, were detected by radioimmunoassays, and one such antibody, F36.23, was studied in detail. It was shown to contain one antibody heavy–light chain pair from 59D8 and one from TCL8. *Simultaneous* binding of fibrin and tPA was demonstrated by reacting F36.23 with tPA coating 96-well plates, and then incubating with the ^{125}I-labeled peptide, derived from the fibrin β-chain (against which 59D8 had been raised). The reverse experiment, by first reacting F36.23 with immobilized fibrin-specific peptide, was also performed. In vitro assays showed that F36.23 increased the potency of tPA as a fibrinolytic agent as much as 15-fold. In vivo, thrombolytic potency of tPA was augmented only 2-fold, consistent with the observation that the anti-tPA activity of the TCL8 moiety of F36.23 may inhibit bound tPA. However, the feasibility of creating bifunctional antibodies by cellular fusion methods, and attaining improvements in the specificity and activity of therapeutic agents, has been demonstrated.

RECOMBINANT DNA APPROACH

Chemical conjugation of plasminogen activators to carrier antibodies, to give products which can direct the functional agent to target fibrin molecules, has been successfully accomplished. The intrinsic disadvantages of the protocols used, however, are now directing the attention of researchers to genetic engineering methods, which promise products of a much more defined nature and permit the modification, at will, of regions of the proteins being linked (*28*). Unlike the chemical procedures, the recombinant DNA approach extends the range of proteins or protein fragments which may be linked, beyond those resulting from the proteolytic cleavage (for example, the Fab′ fragments of immunoglobulins), and thus greatly expands the likelihood of obtaining useful fusion products. The simplest molecule would be one containing the minimum antibody structure required for antigen binding, the 25 kDa Fv domain (see Figure 1), linked to the minimum sequence necessary for the therapeutically effective plasminogen activator to retain full activity. One may also readily modify any joining peptide inserted between the antibody and the effector, to favor the proteins attaining the optimum conformations for their respective activities and to prevent steric interactions that might limit the activity of either the antibody or plasminogen activator domains.

Each chain of an antibody molecule is encoded by several genetic elements that are widely dispersed on the genome and which rearrange during the maturation of the immunoglobulin-secreting B-lymphocyte. In the case of the light chain, genetic elements encoding the variable (V) region and a joining (J) region are juxtaposed. The V–J sequence encodes the antigen-binding region of the mature immunoglobulin and combines with a 3′ downstream C gene, encoding the constant region of the immunoglobulin. With respect to the heavy chains, an additional D genetic element links the V and J elements (Figure 6b). In mature B-cells, following somatic rearrangement, the V–J exon is separated, often by several kilobases, from the C gene, a situation which facilitates the cloning of the variable region elements to the exclusion of the C gene (*28*). The advent of polymerase chain reaction methods have now, however, greatly eased the task of cloning only this region of a monoclonal antibody chain. It is not necessary, with this technique, to clone and manipulate the genomic region containing the V gene, but rather to isolate the abundant mRNAs encoding the immunoglobulin chains, synthesize the first-strand cDNA, and PCR amplify the desired region (*29*, *30*). This provides a ready mechanism for the exchange of constant regions. For example, the mouse constant regions of monoclonal antibodies can be replaced by human constant regions (humanization). These "humanized" mouse immunoglobulins retain their binding specificity, but are considerably less antigenic when infused into man. Even so, the variable region is antigenic and although the framework regions may be replaced by the human equivalents, mouse antigen-binding regions must be retained, resulting in the potential for antiidiotypic immune responses (*31*). Overall immunogenicity can, therefore, be reduced but never entirely eliminated. It should also be remembered that since the constant region is not required for the antigen-binding activity, it may be totally replaced by a suitably cloned protein of chemical or therapeutic relevance.

The construction by genetic manipulation, of a chimeric protein consisting of a target-specific antibody moiety and a therapeutically functional agent, is a multistep procedure. Initially the individual genetic regions encoding each protein are cloned, then these regions are united in a suitable expression vector. The final step is the expression of this chimeric clone to give the desired protein. All of the protocols for such a project can again be illustrated by the construction of an antibody 59D8/tPA chimera.

The first construct to be made contained the genomic DNA encoding the variable region of the heavy chain of monoclonal antibody 59D8, joined to the cDNA encoding the β-chain of tPA, via the CH1 and hinge exons of the mouse γ2b heavy chain (*28*, *32*). Genomic DNA from the hybridoma secreting the antibody 59D8 was digested with the restriction endonuclease *Eco*RI and analyzed by Southern transfer with a probe designed to detect a rearranged V region, regardless of which of the J elements associated with the Vh gene (Figure 6). A 2.6 kbp *Eco*RI fragment was shown to include the V gene, the J element, a sufficient region 5′ of the V gene to include the immunoglobulin promoter, and a region extending far enough downstream of the J element to include the heavy-chain enhancer sequence. This 2.6 kbp fragment was first cloned into the vector λgt10 (Figure 7). To permit the expression of the clone in a suitable eukaryotic cell system the *Eco*RI insert was transferred to the vector pSV2^{gpt}. An XbaI DNA fragment containing the mouse γ2b constant region gene was also inserted 3′ of, and in frame with, the variable region-encoding construct. Upon expression, an entire immunoglobulin heavy chain was synthesized. The tPA molecule can functionally be divided into A (fibrin binding) and B (catalytic) chains (see ref 3 for review). Plasmin cleavage separates the A- and B-chains. In the first construction of a recombinant 59D8–tPA hybrid it was decided to use only the catalytic (B) chain of the tPA. cDNA encoding the B peptide of tPA replaced the γ2b CH2 and CH3 regions of the first construct, except for a small portion of the hinge region.

Hybridoma cells of the original 59D8 line were screened for the loss of ability to synthesize the immunoglobulin heavy chain by growing the cells in soft agar medium. Antimouse heavy-chain antiserum was allowed to diffuse into the agar, and cells which failed to show a precipitin halo were selected and further screened for the retention of the ability to synthesize the light chain. The pSV^{gpt} construct was transfected into this "heavy chain loss variant" cell line. Cells containing stably transfected pSV^{gpt} were cloned, on the basis of their ability to grow in selective media. These stable transfectants synthesized

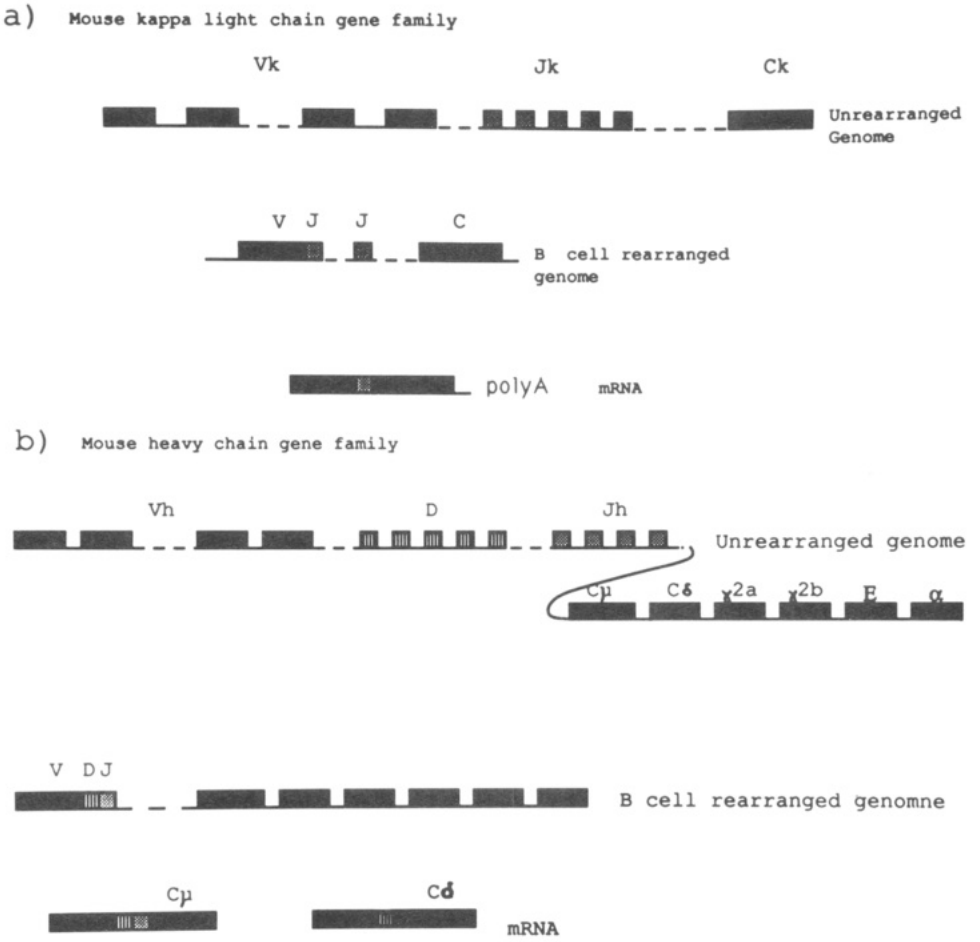


Figure 6. Arrangements and rearrangements of the genetic elements encoding mouse light and heavy immunoglobulin chains. The juxtoposition of the V, D, and J elements occurs during the maturation of the antibody-secreting B lymphocytes. The intervening region of the genome which remains between the V(D)J element and the gene encoding the constant domain is deleted as an intron during processing of the mRNA.

a protein of 170–180 kDa capable of recognizing fibrin in a radioimmunoassay and was recognizable by anti-tPA antibodies. (Indeed, the fusion protein expression product was purified by a two-step protocol, of an affinity column of the Gly-His-Arg-Pro-Leu-Asp-Lys-Cys peptide, against which the antibody 59D8 was raised, linked to Sepharose, followed by an anti-human tPA/Sepharose column.) The actual yield of the fusion protein was less than 1% of that obtained for the original 59D8 cell line, with the intact 59D8 heavy chain. The readiest explanation for this low yield is the replacement of the region 3′ of the γ2b immunoglobulin by the corresponding region of the tPA gene. In fact, subsequent evaluation has shown that the tPA 3′ untranslated domain contains sequences that result in decreased mRNA stability, and lower protein-expression levels.

The purified protein contained two light chains of the original 59D8 antibody and two modified heavy chains (residues 1–236 of the immunoglobulin heavy chain and residues 275–527 of tPA). In vitro the construct could bind to fibrin with the same affinity as did 59D8, and its activity as a plasminogen activator was undiminished when compared with that of native tPA. In vivo, however, unlike the case with the chemically cross-linked 59D8 and tPA, there was no plasminogen activator activity. Subsequent analysis of this construct has revealed that a plasmin cleavage site present on the B chain of tPA (intentionally engineered out of tPA so that plasmin would not separate the 59D8 domain from the tPA domain of this recombinant hybrid) is necessary for its activity. This problem has likely been overcome with the construction of a similar chimeric molecule, incorporating the Fv region of 59D8, the mouse CH1, hinge, and CH2 regions, and the exons encoding for the low molecular weight form of scuPA (*33*). Again, transfection into hybridoma cells expressing only the 59D8 light chain gave chimeric molecules bearing the epitopes of 59D8 and scuPA. This recombinant 59D8–scuPA is an effective fibrinolytic agent in vitro and in vivo.

The chimeric proteins possessing fibrin-binding activity and the ability to activate plasminogen, produced by recombinant DNA procedures, have obvious potential as effective therapeutic agents. A serious limitation to their clinical use is that the monoclonal antibodies which furnished the fibrin-binding activity were raised in mice. They will, therefore, contain epitopes specific to the mouse and have the potential to trigger an immune response in humans. While, for most individuals, this will likely not effect the short-term application of these agents, it might evoke an anaphylactic response in some individuals and would prevent reuse of the same agent at a later time. One approach to rectifying this potential problem is to "humanize" the antibody domain (tPA and scuPA are human proteins and have been used previously without an immune response in large numbers of patients). Several reports (*34–37*) describe the replacement of immunoglobulin light and heavy chain constant domains of one species (usually from mouse monoclonal antibodies) with the equivalent domains from human antibodies, thus reducing their immunogenic potential.

Much of the native antibody, most particularly the constant region domains, is nonessential for the correct

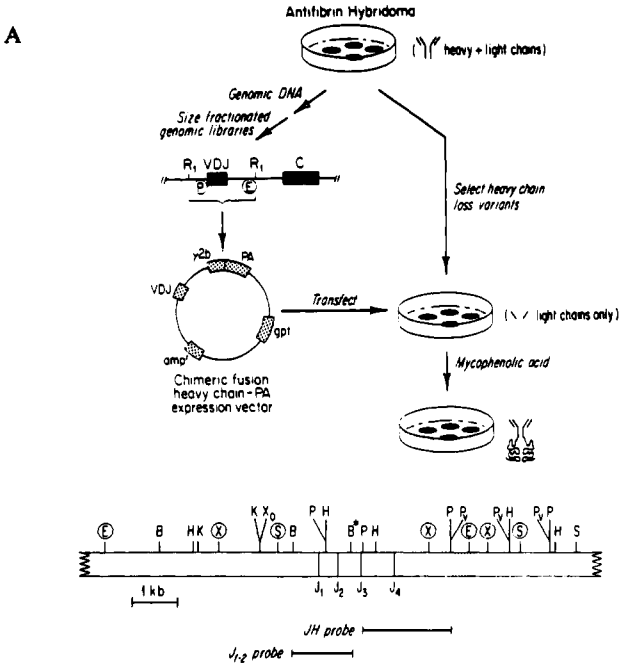


Figure 7. (a) Scheme for the engineering of recombinant antibody-targeted chimeric proteins (taken from ref 28). Left, genomic DNA coding for the heavy chain antigen combining site (VDJ) is cloned and placed in an expression vector with the sequence coding for the constant region–plasminogen activator fusion peptide. Right, heavy chain loss variants are selected and receive, via transfection, the expression vector. Abbreviations: R_1, *Eco*RI restriction enzyme site; C, constant region; VDJ, variable-diversity joining region; P, promoter; E, enhancer; γ2b, 2b mouse heavy chain constant region domain; PA, plasminogen activator; amp^r, pBR322 ampicillin-resistance gene; gpt, hypoxanthine-guanine phosphoribosyltransferase gene of *Escherichia coli*. (b) Mouse heavy chain joining region locus (taken from ref 16). The enhancer region is indicated by stippling; vertical bars indicate joining regions J_1 through J_4; circled restriction sites represent enzymes most convenient for the cloning of rearranged genes; B* represents a *Bam*HI restriction site not present in A/J mice; probes used in the Southern blots are indicated by solid bars. Abbreviations: E, *Eco*RI; B, *Bam*HI; H, *Hin*dIII; K, *Kpn*I; X, *Xba*I; Xo, *Xho*I; S, *Sac*I; P, *Pst*I; P$_v$, *Pvu*II.

conformation of the antigen-binding site. The expression of cloned V_L and V_H regions within the same bacterial host will result in active Fv proteins (*38*, *39*) but can have the unfortunate tendency to dissociate at low protein concentrations (*40*). One answer to this problem is to cross-link the two chains with glutaraldehyde. Alternatively, the DNA regions encoding the two chains may be placed in such a way that they are expressed as a single peptide chain. It has been demonstrated that such an expression product (with a single-chain Fv, sFv) will fold to give an active Fv region (*41–45*). Recombinant clones can be constructed which include tandem V_L and V_H regions, with an additional, effector molecule inserted contiguously to one chain or the other, in the position normally occupied by a constant region domain. The relevancy of such constructs to the production of more efficacious thrombolytic agents, however, remains to be seen.

SUMMARY

Here we have reviewed chemical and recombinant approaches to the construction of hybrid molecules that combine a "targeting" antibody and an "effector" enzyme activity. There are advantages and disadvantages to both chemical and recombinant methods, and one goal of this review has been to elucidate these so that the appropriate method can be used by those interested in using hybrid molecules to study questions of basic or therapeutic importance. The system studied in greatest detail has as its goal the targeting of a plasminogen activator to an occlusive intravascular thrombus. We have, therefore, used this system as an example of currently available approaches. Now that these methodologies have been studied and put into use, it is anticipated that this principle will be generalized both to other therapeutic applications, as well as to the design and construction of molecules that will allow more basic questions to be addressed.

LITERATURE CITED

(1) Mellstedt, H. (1989) Monoclonal antibodies in cancer therapy. *Curr Opinion Immunol. 2*, 708–713.
(2) Pietersz, G. A. (1990) The linkage of cytotoxic drugs to monoclonal antibodies for the treatment of cancer. *Bioconjugate Chem. 1*, 89–95.
(3) Ward, E. S., Gussow, D., Griffiths, A. D., Jones, P. T., and Winter, G. (1989) Binding activities of a repertoire of single immunoglobulin variable domains secreted from *Escherichia coli*. *Nature 341*, 544–546.
(4) Haber, E., Quertermous, T., Matsueda, G. R., and Runge, M. S. (1989) Innovative approaches to plasminogen activator therapy. *Science 243*, 51–56.
(5) ISIS Steering Committee (ISIS-2) (1987) Intravenous streptokinase given within 0-4 hours of onset of myocardial infarction reduced mortality in ISIS-2 (Letter). *Lancet i*, 502.
(6) Gruppo Italiano per Io Studio della Streptochinasi nell'infarto Miocardio (GISSI) (1986) Effectiveness of intravenous thrombolytic treatment in acute myocardial infarction. *Lancet i*, 397.
(7) Verstraete, M., and Collen, D. (1986) Thrombolytic therapy in the eighties. *Blood 67*, 1529–1541.
(8) Harris, T. J. R. (1987) Second-generation plasminogen activators. *Protein Eng. 1*, 449–458.
(9) Harker, L. A. (1987) Role of platelets and thrombosis in mechanisms of acute occlusion and restenosis after angioplasty. *Am. J. Cardiol. 60*, 20B–28B.
(10) Marder, V. J., and Sherry, S. (1988) Thrombolytic therapy: I and II. Current status. *N. Engl. J. Med. 318*, 1512–1520, 1585–1595.
(11) Lijnen, H. R., Zamarron, C., Blaber, M., Winkler, M. E., and Collen, D. (1986) Activation of plasminogen by pro-urokinase: I. Mechanism. *J. Biol. Chem. 261*, 1253–1258.
(12) Pannell, R., and Gurewich, V. (1986) Pro-urokinase: A study of its stability in plasma and of a mechanism for its selective fibrinolytic effect. *Blood 67*, 1215–1223.
(13) TIMI Study Group (1985) The thrombolysis in myocardial infarction (TIMI) trial. Phase 1 findings. *N. Engl. J. Med. 312*, 932–936.
(14) Hui, K. Y., Haber, E., and Matsueda, G. R. (1983) Monoclonal antibodies to a synthetic fibrin-like peptide bind to human fibrin but not fibrinogen. *Science 222*, 1129–1132.
(15) Sevilla, C. L., Mahle, N. H., Boylan, C. M., and Callewaert, D. M. (1985) Plasminogen activator-anti-human fibrinogen conjugate. *Biochem. Biophys. Res. Commun. 130*, 91–96.
(16) Bode, C., Matsueda, G. R., Hui, K. Y., and Haber, E. (1985) Antibody-directed urokinase: a specific fibrinolytic agent. *Science 229*, 765–767.
(17) Lijnen, H. R., Dewerchin, M., De Cock, F., and Collen, D. (1990) Effect of fibrin-targeting on clot lysis with urokinase-type plasminogen activator. *Thromb. Res. 57*, 333–342.
(18) Schnee, J. M., Runge, M. S., Matsueda, G. R., Hudson, N. W., Seidman, J. G., Haber, E., and Quertermous, T. (1987) Construction and expression of a recombinant antibody-targeted plasminogen activator. *Proc. Natl. Acad. Sci. U.S.A. 84*, 6904–6908.
(19) Dewerchin, M., Lijnen, H. R., van Hoef, B., De Cock, F., and Collen, D. (1989) Biochemical properties of conjugates of urokinase-type plasminogen activator with a monoclonal antibody specific for cross-linked fibrin. *Eur. J. Biochem. 185*, 141–149.
(20) Collen, D., Dewerchin, M., Rapold, H. J., Lijnen, H. R., and Stassen, J. M. (1990) Thrombolytic and pharmacokinetic

properties of a conjugate of recombinant single-chain urokinase-type plasminogen activator with a monoclonal antibody specific for cross-linked fibrin in a baboon venous thrombosis model. *Circulation 82*, 1744–1753.
(21) Carlsson, J., Drevin, H., and Axen, R. (1978) Protein thiolation and reversible protein-protein conjugation. *Biochem. J. 173*, 723–737.
(22) Bode, C., Runge, M. S., Schonermark, S., Eberle, T., Newell, J. B., Kubler, W., and Haber, E. (1990) Conjugation to antifibrin Fab' enhances fibrinolytic potency of single-chain urokinase plasminogen activator. *Circulation 81*, 1974–1980.
(23) Declerck, P. J., Mombaerts, P. P., Holvoet, P., De Mol, M., and Collen, D. (1987) Fibrinolytic response and fibrin fragment D-dimer levels in patients with deep vein thrombosis. *Thromb. Haemostasis 58*, 1024–1029.
(24) Holvoet, P., Stassen, J. M., and Collen, D. (1987) Thrombosis imaging with murine monoclonal antibodies against fibrin D-dimer in a rabbit jugular vein thrombosis model. *Thromb. Haemostasis 58*, 23 (abstr. 92).
(25) Nolan, O., and O'Kennedy, R. (1990) Bifunctional antibodies: concept, production and applications. *Biochem. Biophys. Acta 1040*, 1–11.
(26) Runge, M. S., Bode, C., Matsueda, G. R., and Haber, E. (1987) Antibody-enhanced thrombolysis: capture of tissue plasminogen activator by a bispecific antibody and direct targeting by an antifibrin-tissue plasminogen activator conjugate in vivo. *Trans. Assoc. Am. Physiol. 100*, 250–255.
(27) Branscomb, E. E., Runge, M. S., Savard, C. E., Adams, K. M., Matsueda, G. R., and Haber, E. (1990) Bispecific monoclonal antibodies produced by somatic cell fusion increase the potency of tissue plasminogen activator. *Thromb. Haemostasis 64*, 260–266.
(28) Love, T. W., Runge, M. S., Haber, E., and Quertermous, T. (1989) Recombinant antibodies possessing novel effector functions. *Methods Enzymol. 178*, 515–527.
(29) Orlandi, R., Gussow, D. H., Jones, P. T., and Winter, G. (1989) Cloning immunoglobulin variable domains for expression by the polymerase chain reaction. *Proc. Natl. Acad. Sci. U.S.A. 86*, 3833–3837.
(30) Sastry, L., Alting-Mees, M., Huse, W. D., Short, J. M., Sorge, J. A., Hay, B. N., Janda, K. D., Benkovic, S. J., and Lerner, R. A. (1989) Cloning of the immunological repertoire in Escherichia coli for generation of monoclonal catalytic antibodies: construction of a heavy chain variable region-specific cDNA library. *Proc. Natl. Acad. Sci. U.S.A. 86*, 5728–5732.
(31) Co, M. S., Deschamps, M., Whitely, R. J., and Queen, C. (1991) Humanized antibodies for antiviral therapy. *Proc. Natl. Acad. Sci. U.S.A. 88*, 2869–2873.
(32) Runge, M. S., Bode, C., Matsueda, G. R., and Haber, E. (1988) Conjugation to an antifibrin monoclonal antibody enhances the fibrinolytic potency of tissue plasminogen activator in vitro. *Biochemistry 27*, 1153–1157.
(33) Runge, M. S., Huang, P., Savard, C. E., Schnee, J. M., Love, T. W., Bode, C., Matsueda, G. R., Haber, E., and Quertermous, T. (1988) A recombinant molecule with antifibrin antibody and single-chain urokinase activities has increased fibrinolytic potency. *Circulation Suppl. II Abstr. 78*, II-509.
(34) Morrison, S. L., Johnson, M. J., Herzenberg, L. A., and Oi, V. T. (1984) Chimeric human antibody molecules: mouse antigen-binding domains with human constant region domains. *Proc. Natl. Acad. Sci. U.S.A. 81*, 6851–6855.
(35) Boulianne, G. L., Hozumi, N., and Shulman, M. J. (1984) Production of functional chimaeric mouse/human antibody. *Nature 312*, 643–646.
(36) Jones, P. T., Dear, P. H., Foote, J., Neuberger, M. S., and Winter, G. (1986) Replacing the complementarity-determining regions in a human antibody with those from a mouse. *Nature 321*, 522–525.
(37) Riechmann, L., Clark, M., Waldmann, H., and Winter, G. (1988) Reshaping human antibodies for therapy. *Nature 332*, 323–327.
(38) Field, H., Yarranton, G. T., and Rees, A. R. (1990) Expression of mouse immunoglobulin light and heavy chain variable regions in *Escherichia coli* and reconstitution of antigen-binding activity. *Protein Eng. 3*, 641–647.
(39) Skerra, A., and Pluckthun, A. (1988) Assembly of a functional immunoglobulin Fv fragment in *Escherichia coli*. *Science 240*, 1038–1041.
(40) Glockshuber, R., Malia, M., Pfitzinger, I., and Pluckthun, A. (1990) A comparison of strategies to stabilize immunoglobulin Fv-fragments. *Biochemistry 29*, 1362–1367.
(41) Bird, R. E., and Walker, B. W. (1991) Single chain antibody variable regions. *Trends Biotechnol. 9*, 132–137.
(42) Bird, R. E., Hardman, K. D., Jacobson, J. W., Johnson, S., Kaufman, B. M., Lee, S-M., Lee, T., Pope, S. H., Riordan, G. S., and Whitlow, M. (1988) Single-chain antigen-binding proteins. *Science 242*, 423–426.
(43) Tai, M-S., Mudgett-Hunter, M., Levinson, D., Wu, G-M., Haber, E., Oppermann, H., and Huston, J. S. (1990) A bifunctional fusion protein containing Fc-binding fragment B of staphylococcal protein A amino terminal to antidigoxin single-chain Fv. *Biochemistry 29*, 8024–8030.
(44) Huston, J. S., Levinson, D., Mudgett-Hunter, M., Tai, M-S., Novotny, J., Margolies, M. N., Ridge, R. J., Bruccoleri, R. E., Haber, E., Crea, R., and Oppermann, H. (1988) Protein engineering of antibody binding sites: recovery of specific activity in an anti-digoxin single-chain Fv analogue produced in *Escherichia coli*. *Proc. Natl. Acad. Sci. U.S.A. 85*, 5879–5883.
(45) Chaudhary, V. K., Queen, C., Junghans, R. P., Waldmann, T. A., FitzGerald, D. J., and Pastan, I. (1989) A recombinant immunotoxin consisting of two antibody variable domains fused to *Pseudomonas exotoxin*. *Nature 339*, 394–397.

Registry No. tPA, 105913-11-9.

ARTICLES

Catalytic Activity and Thermostability of Dehydrogenase Conjugates with Cortisol and Progesterone[1]

Dmitriy I. Metelitza,* Alexandr N. Eryomin, Elena I. Karasyova, and Vera L. Markina
Institute of Bioorganic Chemistry, BSSR Academy of Sciences, 220045, Minsk, U.S.S.R.
Received September 17, 1990

The conjugates of glucose-6-phosphate dehydrogenase, lactate dehydrogenase, and malate dehydrogenase with progesterone and cortisol, containing 1–40 steroid molecules per enzyme molecule, were obtained by the reactions of *N*-succinimide esters of the 3-[*O*-(carboxymethyl)oximes)] of cortisol and progesterone with a protein in a water–DMFA (10%) medium. The catalytic activity and thermostability of dehydrogenases and their steroid conjugates were kinetically studied. The effects of the modification degree on the activity and thermostability of dehydrogenases caused by their hydrophobization were studied and discussed. Practical recommendations for using the dehydrogenase–steroid conjugates in enzyme immunoassay are given.

INTRODUCTION

Modern applied enzymology solves problems via two main directions: the first is biocatalyst engineering, which involves modification of a biocatalyst itself by using genetic, physical, and/or chemical methods; the second is medium engineering which involves modification of the microenvironment of a biocatalyst, either by introducing additives or solid matrices into an elaborated medium or by varying the composition of the liquid medium itself (*1*, *2*).

The practical requirements of biotechnology and basic research often join both foregoing approaches into one to solve any task, for instance, in enzyme immunoassay for a number of antigens (*3*, *4*). In this case it is necessary to obtain the enzyme conjugates with water-insoluble antigens in the water–organic media in order to retain the enzyme catalytic activity and the immunochemical reactivity of the bound antigens in a maximum degree (*3–5*).

The high hydrophobicity of some antigens, e.g. steroids, aromatic carcinogens, toxicants of environmental media, etc., causes the necessity of finding methods for enzyme immunoassay in organic media. We believe that enzyme immunoassay in reversed micelles of surfactants in organic solvents may be especially hopeful (*6–8*). Recently we have shown the principal possibility of the interaction of an antigen (peroxidase) with antibodies (anti-peroxidase) in the reversed AOT (sodium bis(2-ethylhexyl) sulfosuccinate) micelles in heptane (*9*). In 1989, we developed the homogeneous enzyme immunoassay of progesterone in the mixed reversed micelles of AOT and Triton X-45 in heptane using horseradish peroxidase as antigen label (*10*).

During the past 5 years, we have carried out a systematic kinetic study of the changes in the enzyme catalytic activity and thermostability that resulted from their modification with cortisol, progesterone, and strophantin.

In the present paper we summarize and discuss the effects of the chemical modification with cortisol and progesterone in water–organic solvents on catalytic activities and thermostabilities of three dehydrogenases having quaternary structure. Table I lists the characteristics of the dehydrogenases used and degrees of their modification, "*n*". We would like to especially note that all the enzyme–steroid conjugates were successfully applied by us in enzyme immunoassay.

EXPERIMENTAL PROCEDURES

Reagents. We used glucose-6-phosphate dehydrogenase from *Leuconostoc* sp 5_s (NPO Ferment, Vilnius, U.S.S.R.) with a specific activity of 350–400 IU/mg and L-lactate and L-malate dehydrogenase from pig heart mitochondria (Reanal, Hungary) with specific activities of 150 and 180 IU/mg, respectively. As emzyme substrates, we used glucose 6-phosphate and $NADP^+$ (Reanal), sodium oxalate and pyruvate (Sigma, St. Louis, MO), and NADH (Reanal). Cortisol and progesterone were purchased from Germed (FRG), and Sephadex G-25 was from Pharmacia (Uppsala, Sweden). *N*-Succinimide esters of the 3-[*O*-(carboxymethyl)oxime] of cortisol and progesterone were obtained according to ref 11a with some modifications and kindly provided by Dr. V. D. Matveentzev (Institute of Bioorganic Chemistry, Minsk, U.S.S.R.).

DMFA, ethanol, 1,4-dioxane, propanol, heptane, and octane were distilled before use. All other reagents were from Reachim (U.S.S.R.).

Preparation of Dehydrogenase Conjugates with Cortisol and Progesterone. The dehydrogenase conjugates with steroids were obtained in water–DMFA solutions of various compositions by a known method (*11*) with some modifications (*12*). We performed the reaction of 3-PROG or 3-COR with dehydrogenases at a modifier/enzyme molar ratio ranging from 10 to 100. The reaction was usually carried out at 25 °C in a $NaHCO_3$ buffer (pH 8.35) containing 10% of DMFA for 2 h. The modifier (3-COR, 3-PROG) stability is determined by pH value and strongly decreases at pH 9 and higher. At pH 8.35 the modifiers reacted with proteins much faster than their hydrolysis occurred, since the hydrolysis rate of modifiers at pH 8.35 was very slow.

[1] Abbreviations used: DMFA, dimethylformamide; GP, glucose 6-phosphate; G6PDH, glucose-6-phosphate dehydrogenase; LDH, L-lactate dehydrogenase; MDH, L-malate dehydrogenase; COR, cortisol; 3-COR, cortisol 3-[*O*-(carboxymethyl)oxime] *N*-succinimide ester; PROG, progesterone; 3-PROG, progesterone 3-[*O*-(carboxymethyl)oxime] *N*-succinimide ester; TNBS, trinitrobenzenesulfonic acid; EIA, enzyme immunoassay.

* To whom correspondence should be addressed: Professor Dr. D. I. Metelitza, Institute of Bioorganic Chemistry, BSSR Academy of Sciences, 5/2 Zhodinskaya, 220045, Minsk-45, U.S.S.R.

1043-1802/91/2902-0309$02.50/0 © 1991 American Chemical Society

Table I. Dehydrogenases Modified by Progesterone and Cortisol

enzymes	EC	MW, kDa	subunit number	modification degree
L-lactate dehydrogenase (LDH)	1.1.1.27	140	4	2–40
L-malate dehydrogenase (MDH)	1.1.1.37	70	2	3–28
glucose-6-phosphate dehydrogenase (G6PDH)	1.1.1.49	104	2	1–35

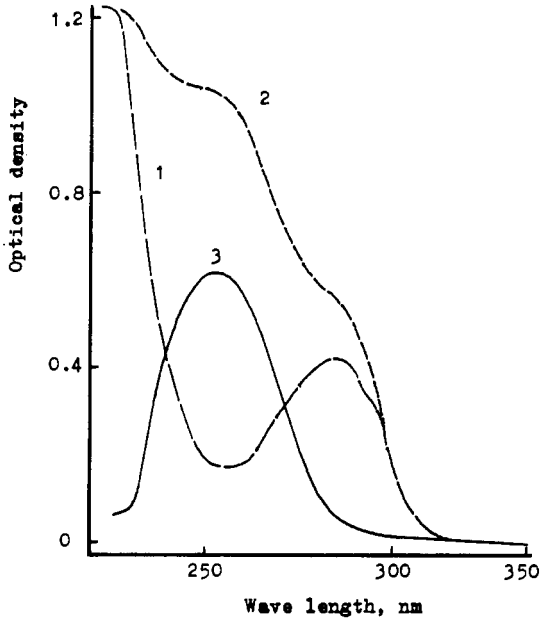


Figure 1. The absorption spectra of initial LDH (1) and its conjugate with cortisol (2) and the difference spectrum of conjugate LDH-3-COR-16 (3) at the concentration of 3.0 mg/mL.

Unreacted modifiers were removed by dialysis. The full absence of free modifiers and their hydrolization products in the conjugate samples was spectrophotometrically proved after the dialysis procedure.

For characterization of the conjugates, their difference absorption spectra were monitored versus the same concentrations of nonmodified proteins (see Figure 1). The numbers of the enzyme-bound modifier molecules "n" (or modification degree) were calculated from the intensity of the difference spectra of the conjugates at 250 nm using the molar extinction coefficient 16 000 M^{-1} cm^{-1} for COR (PROG) (*13*). The modification degree for the three dehydrogenases varied from 1 to 40 (see Table I). The conjugates of G6PDH with 3-PROG, containing 3, 5, 7, 15, 20, and 35 molecules of 3-PROG and abbreviated as G6PDH-3-PROG-3...G6PDH-3-PROG-35, were studied in detail as well as the conjugates of LDH with 2, 20, and 40 3-PROG and conjugates of MDH with 3, 15, 20, and 28 3-PROG, referred to as LDH-3-PROG-2...LDH-3-PROG-40 or MDH-3-PROG-3...MDH-3-PROG-28. The conjugates G6PDH-3-COR-25, MDH-3-COR-8, and some others were prepared and studied in detail. All the obtained conjugates were stored in 0.1 M phosphate buffer, pH 7.4, at 4 °C.

Determination of the Catalytic Activity of Dehydrogenases and Their Conjugates. The catalytic activity of the G6PDH and its conjugates was characterized by the GP dehydrogenation in 0.1 M NaOH–glycine buffer (pH 9.1) containing 0.4 mM $NADP^+$, 1.0 mM GP, and, as a rule, 500 ng/mL of a biocatalyst at 20 °C (*14*). The enzymatic activities of LDH, MDH, and their conjugates were characterized by the initial rates of pyruvate or oxaloacetate reduction in 0.1 M phosphate buffer, pH 7.5, containing 0.1 mM NADH and 0.5 mM pyruvate or oxaloacetate, respectively, at 20 °C (*15*). Both the reactions were spectrophotometrically monitored by using the absorption decrease of NADH at a wavelength of 340 nm (ϵ = 6220 M^{-1} cm^{-1}).

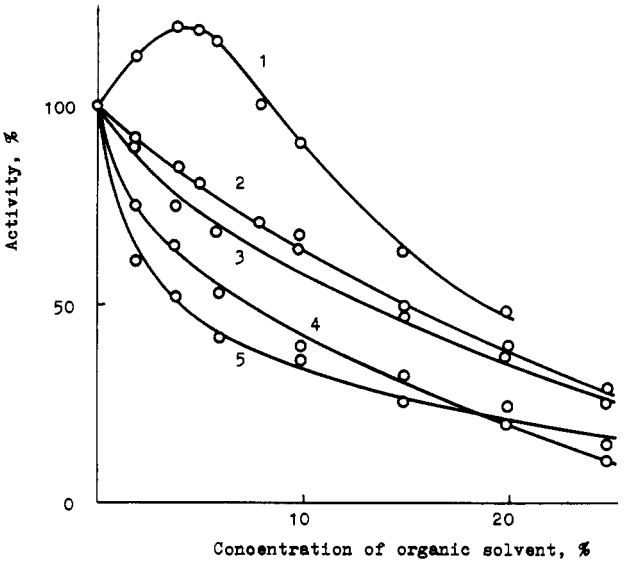


Figure 2. Effects of organic solvents on the initial catalytic activity of G6PDH: 1, DMFA; 2, propanol; 3, glycerol; 4, ethanol; 5, 1,4-dioxane.

In all the cases, the linear dependence of the optical density alteration on the reaction time was observed which permitted the correct calculation of the initial reaction rate in M s^{-1}.

Thermoinactivation of Dehydrogenases and Their Conjugates with Steroids. In a temperature range of 35–47 °C for G6PDH and 38–47 °C for its conjugates with progesterone, the biocatalyst thermoinactivation was studied in the twice-distilled water at various initial protein concentrations.

Thermoinactivation of two other dehydrogenases and their conjugates was studied at 20–45 °C in the twice-distilled water (LDH, LDH-3-PROG-19, MDH, MDH-3-PROG-16) or 0.1 M phosphate buffer, pH 7.5 (LDH, MDH, and MDH-3-PROG-24). The enzyme or its conjugate solutions with varying protein concentrations were kept at different temperatures and aliquots were taken for determination of the enzymatic activity under the standardizated conditions at 20 °C as described above.

The thermoinactivation of the dehydrogenases was characterized by the effective first-order rate constants, k_{in}, which were calculated from the semilogarithmic anamorphoses of kinetic curves of the enzymatic activity decrease, $\log (A/A_0) - t$, where A_0 and A are the catalytic activities of the native and partially inactivated biocatalyst, respectively, and t is the reaction time.

All the spectral measurements were carried out in the thermostated cuvettes of Specord UV VIS or Specol 21 instruments (Karl Zeiss, Germany).

RESULTS AND DISCUSSION

The Environment's Effects on the G6PDH Catalytic Activity. At the preparation of the dehydrogenase conjugates with steroids, it is necessary to add the organic solutions of the water-insoluble modifiers 3-COR and 3-PROG into the buffered enzyme solutions. Therefore, it is very important to know how the organic cosolvent acts on the enzyme itself.

As shown in Figure 2, the increasing concentrations of propanol, ethanol, or 1,4-dioxane decrease the G6PDH catalytic activity while DMFA concentrations below 8% increase it (dependence 1). In the futher experiments we

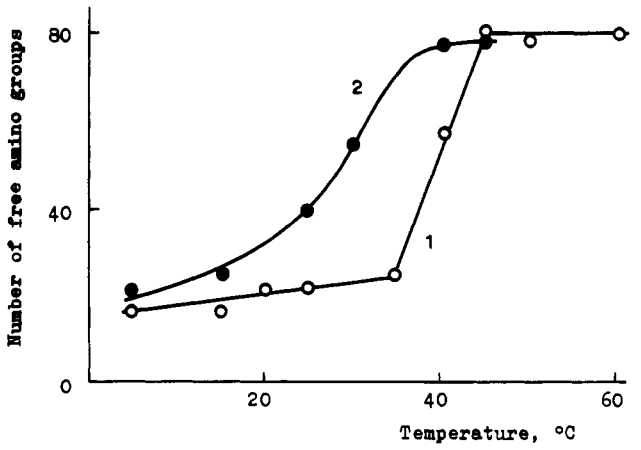


Figure 3. The number of free amino groups of the lysine residues of G6PDH determined by protein titration with TNBS at various temperatures: 1, initial enzyme; 2, G6PDH treated with a water–DMFA mixture for 1 h.

used the mixtures of the buffered solutions with DMFA (10%) as a solvent that permits retention of a high enzymatic activity of the prepared conjugates. The stimulating action on the G6PDH catalytic activity of another bipolar solvent, dimethyl sulfoxide, was shown earlier (*16*).

Optimization of the Synthesis of Dehydrogenase Conjugates with Steroids. The modification degree of dehydrogenases by the 3-COR and 3-PROG agents is determined by the enzyme structure (a number of free amino groups), the medium composition (the DMFA content), the modifier/enzyme ratio, the temperature, and the reaction time.

It is well-known that 3-COR and 3-PROG effectively react with free lysine amino groups (*5*, *11*). Each LDH subunit contains 24 lysines (*17*), i.e. the maximum modification degree of this enzyme (n = 96) may be achieved. When G6DPH was kept in a solution containing 10% DMFA, the total number of amino groups accessible for such an agent as TNBS significantly increased (see Figure 3). At 25 °C the number of such groups equaled 40, while only 22 such groups were available in the initial enzyme in a buffered solution. Noteworthy is that at 45 °C the difference between the initial enzyme and that kept in a water–DMFA (10%) mixture disappeared. The maximum modification degree that the G6PDH may achieve is n = 80.

Thus, the temperature increase causes a growth of the number of the free amino groups number which are accessible for the modifier but simultaneously the enzyme inactivation rate increases. Therefore, all the conjugates were prepared at 20–25 °C.

A growth of the modifier/enzyme ratio increases the modification degree of three dehydrogenases (Figure 4). For the G6PDH and LDH modification by progesterone, the linear dependences of "n" on the [3-PROG]/[enzyme] ratio were obtained. The modification degree and activity are determined by the reaction time, while an inactivation of enzymes and their conjugates is dependent on their contact with organic cosolvent.

The optimum combination of the modifier/enzyme ratio, the medium composition, and the reaction time permit us to obtain highly active conjugates of the dehydrogenases with cortisol and progesterone. Figure 5 shows the dependence of the conjugate catalytic activity on the modification degree of dehydrogenases. At a high modification degree the conjugates LDH-3-PROG were found to retain the catalytic activity of the initial enzyme. The conjugates MDH-3-COR and MDH-3-PROG with n = 16 had an activity that was 1.2–1.5-fold higher than that of nonmodified protein. The G6PDH modification resulted in a considerable loss of its catalytic activity. This loss increases with the growth of modification degree of LDH (Figure 5) or G6PDH (Table II). As seen from Table II, growth of the modification degree leads to an increase of the Michaelis constants for the substrate (GP) and cofactor (NADP) which is also unfavorable for the enzymatic catalysis.

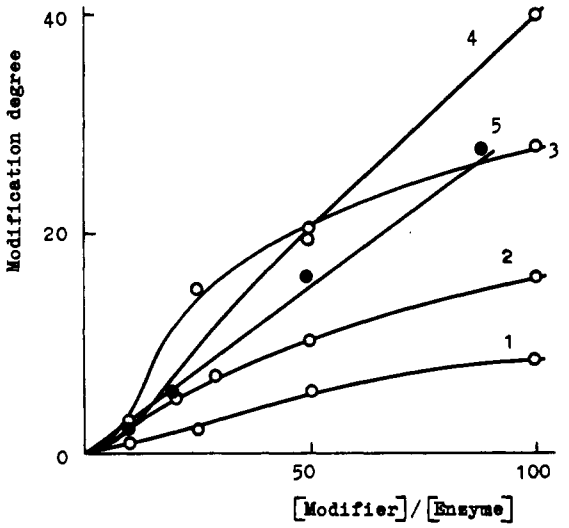


Figure 4. The dependence of the modification degree (n) on the initial [modifier]/[enzyme] ratio for MDH with cortisol (1) and progesterone (2), LDH with cortisol (3) and progesterone (4), and G6PDH with progesterone (5).

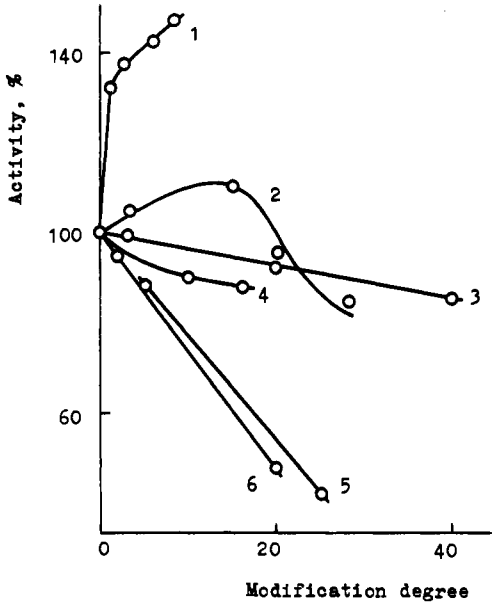


Figure 5. The dependences of catalytic activity of the conjugates of dehydrogenases on modification degree by cortisol and progesterone: 1, MDH-3-COR; 2, MDH-3-PROG; 3, LDH-3-PROG; 4, LDH-3-COR; 5, G6PDH-3-COR; 6, G6PDH-3-PROG.

The optimum conditions for the conjugate preparation allow achievement of a very high degree of protein modification: in LDH 42% of free amino groups and in G6PDH 44% of such groups were modified (see Figure 5 and Table II). It is clear that at such high modification degree of the enzyme, complete retention of its catalytic activity could hardly be expected. We believe its level equal to 50–70% of the initial enzyme activity is sufficiently high.

Interesting results were obtained at the MDH modification by 3-COR and 3-PROG (Figure 5, curves 1 and 2): the catalytic activity of conjugates MDH-3-COR-8 and

Table II. The Catalytic Activity of Glucose-6-phosphate Dehydrogenase and Its Conjugates with Progesterone

G6PDH and its conjugates	$10^4 K_m$, M for GP	$10^6 K_m$, M for $NADP^+$	activity vs that of initial G6PDH	activity vs that of G6PDH treated with DMFA (10%)
G6PDH in buffer solution	4.2–4.7	2.3–2.5	100	
G6PDH in buffer–DMFA mixture	3.9–4.7	2.4–3.5	76–85	100
G6PDH-3-PROG-3	4.2	3.4	83	98
G6PDH-3-PROG-10	4.3	3.0	82	97
G6PDH-3-PROG-15	7.7	3.3	61	75
G6PDH-3-PROG-20	10.5	4.7	55	68
G6PDH-3-PROG-25	10.5	4.2	47	58

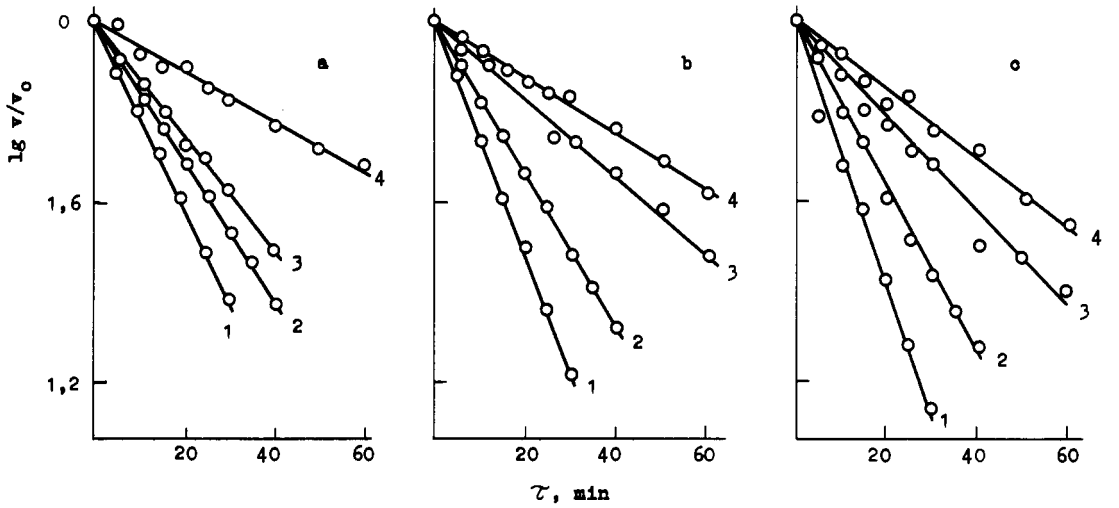


Figure 6. The semilogarithmic anamorphoses of the kinetic curves of the catalytic activity loss for MDH (a), control MDH (b), and conjugate MDH-3-PROG-16 (c) in buffered solution at 40 °C: 1, 0.005; 2, 0.010; 3, 0.050; 4, 0.10 mg/mL of protein.

MDH-3-PROG-15 equals to 149 and 111%, respectively, relative to that of the initial enzyme.

Thermoinactivation of the Dehydrogenases and Their Conjugates with Steroids. Figure 6 shows the semilogarithmic anamorphoses of kinetic curves of the catalytic activity loss at 40 °C for the initial MDH (a), the control enzyme incubated in the water–DMFA (10%) mixture (b), and conjugate MDH-3-PROG-16 (c). As seen, the biocatalyst inactivation at its various initial concentrations ranged from 0.005 to 0.1 mg/mL and is described by the first-order equation below, which gives a fair approximation for inactivation of two other dehydrogenases (G6PDH, LDH) and their numerous conjugates at various concentrations and different temperatures (*18–22*). In all the cases, the rate constants of the biocatalyst inactivation, k_{in}, were strongly dependent on the initial protein concentration. These dependences for G6PDH, LDH, MDH, and numerous conjugates of LDH and MDH are described by equation 1, connecting k_{in} with the initial

$$k_{in} = k_0/(1 + Ak_0[E]_0) \quad (1)$$

enzyme concentration, $[E]_0$ (*18–22*), where k_0 is the rate constant of the protein inactivation at its infinite dilution, A is the reverse rate in M^{-1} s and dependent on temperature, and $[E]_0$ is the initial concentration of subunit enzyme or its conjugate.

Transforming eq 1 as shown in Figure 7, one can calculate the value of the constants k_0 and A for the inactivation of dehydrogenases and their conjugates. Table III lists the k_0 values at 40 °C for various forms of LDH and MDH and their conjugates with progesterone. As seen from this table, the inactivation rate of LDH and MDH in buffered solution are significantly less than in water, i.e. the buffer salts stabilize both dehydrogenases. The MDH modification by 3-PROG results in some enzyme stabilization, while the LDH modification under the same conditions decreases the enzyme stability by 1.6-fold.

The experimental data obtained by us (*18–22*) support the assumption that the dissociative inactivation of dimeric (or tetrameric) dehydrogenases may be described by the following simplest scheme:

$$E_2 \underset{k_2}{\overset{k_1}{\rightleftharpoons}} 2E \xrightarrow{k_d} 2E_d \quad (2)$$

where E_2 is a dimer, E is a monomer (subunit), k_1 is the rate constant of the dimer dissociation, k_2 is the rate constant of the monomer association, and k_d is the rate constant of the monomer denaturation.

As it was shown by us earlier (*18–22*) the rate constants k_0 calculated with eq 1 were close to the rate constants of the dimeric dehydrogenases dissociation, k_1 (see eq 2); i.e. the biocatalyst dissociation may be the limiting stage of the enzyme thermoinactivation.

The temperature dependence of the rate constants, k_0, for the G6PDH inactivation is described by the Arrhenius plot (Figure 8), from which the activation energy for the thermal dissociative inactivation of this enzyme was calculated to be equal to 109.7 kcal/mol. For a comparison, from the temperature dependence of k_{in}, the effective E_{act}'s were calculated for the thermoinactivation of G6PDH at various initial concentrations:

G6PDH concn, mg/mL	E_{act}, kcal/mol
infinite dilution	109.7
0.001	135.5
0.002	142.0
0.004	143.0
0.005	143

As seen from these data, increase of the G6PDH solution concentration results in the rise of E_{act} values.

Modification of free amino groups of G6PDH gives the conjugates, the hydrophobicity of which increases with the growth of the modification degree. The G6PDH modification by steroids is always accompanied by an increase in the effective rate constant of the modified

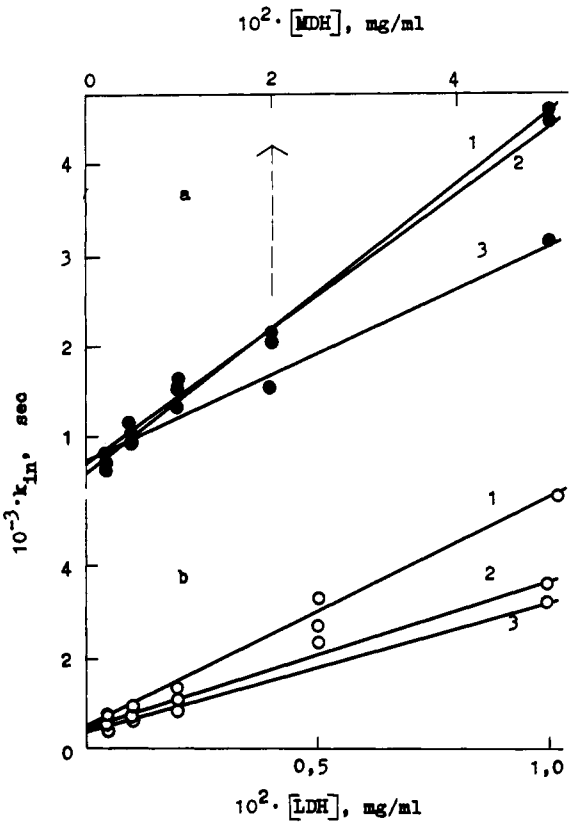


Figure 7. The dependences of the reverse effective inactivation rate constants for the different forms of MDH (a) and LDH (b) at 40 °C on the initial concentration of the biocatalysts: 1, initial enzyme; 2, control enzyme; 3, conjugates MDH-3-PROG-16 (a) and LDH-3-PROG-19 (b).

Table III. The Inactivation Rate Constants for Various Forms of MDH, LDH, and Their Conjugates at 40 °C Calculated from Experimental Data by Using Equation 1

biocatalyst, medium	$10^3 k_0$, s^{-1}
LDH, 0.1 M phosphate buffer, pH 7.5	0.13
LDH, water	2.00
$LDH_{control}$, water	3.33
LDH-3-PROG-19, water	3.33
MDH, 0.1 M phosphate buffer, pH 7.5	0.76
MDH, water	1.67
$MDH_{control}$, water	1.54
MDH-3-PROG-16, water	1.43

enzyme inactivation k_{in} as compared with its value for the initial enzyme (see Table IV).

It should be mentioned that for conjugates G6PDH-3-PROG, unlike the enzyme itself and LDH, MDH, and their conjugates with progesterone, a simple dependence of k_{in} on the initial protein concentration was not obtained; i.e. eq 1 was not fulfilled in this case. The dependences of k_{in} on the protein concentration for conjugate G6PDH-3-PROG-35 at 38, 45, and 47 °C are compared in Figure 9. These dependences are complex and have maximums, the positions of which are determined by temperature. The complicated dependence of k_{in} on the G6PDH concentration does not allow the calculation the k_0 values for this conjugate inactivation at various temperatures.

The temperature dependences of the effective rate constants k_{in} for G6PDH at various concentrations (0.001, 0.005, 0.010, and 0.020 mg/mL) are described by the Arrhenius equation and characterized by the same value of E_{act} equal to 109.7 kcal/mol. Table V lists the thermodinamic activation parameters calculated for the process of catalytic activity loss by G6PDH and its conjugate G6PDH-3-PROG-35 at 45 °C. Modification of this

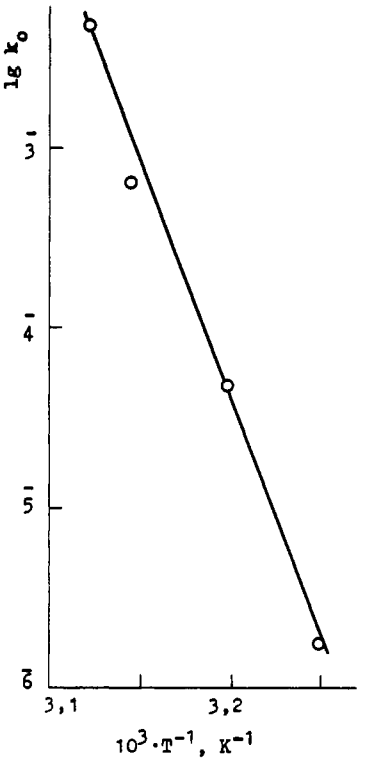


Figure 8. The temperature dependence of G6PDH inactivation rate constant in very diluted solution k_0 calculated by using eq 1.

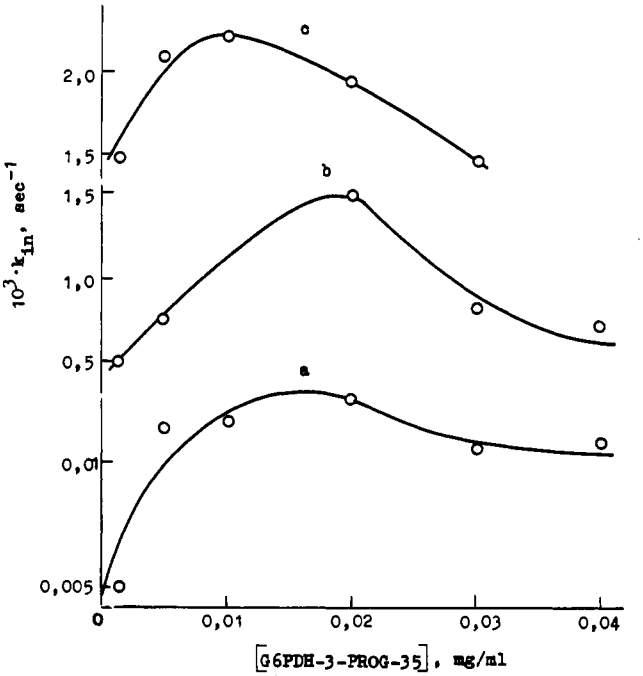


Figure 9. Effect of the initial concentration of conjugate G6PDH-3-PROG-35 on the effective values if the inactivation rate constants at 38 (a), 45 (b) and 47 °C (c).

enzyme does not change the activation parameters of its inactivation for such a process in strongly diluted solutions.

Increase of the modification degree of G6PDH is accompanied by gradual alterations of the character of dependence "k_{in} – protein concentration". Figure 10 shows such dependences at 45 °C for initial G6PDH, the control enzyme, and G6PDH conjugates with increasing progesterone content. As seen from Figure 10, k_{in} of G6PDH decreases with increasing enzyme concentration. The protein modification results in the reversed dependences that have been clearly shown for the conjugates of G6PDH

Table IV. Thermoinactivation Rate Constants for G6PDH and Its Conjugate G6PDH-3-PROG-35 (k_{in} 10^5, s^{-1}) at Various Temperatures and Protein Concentrations

	G6PDH, mg/mL				
temp, °C	0.001	0.002	0.003	0.004	infinite dilution
35	0.08	0.06	0.04	0.03	0.20
40	1.60	0.79	0.36	0.28	5.00
45	81.5	30.5	19.7	19.0	52.0
47	88.3	66.2	43.7	37.0	141.0

	G6PDH-3-PROG-35, mg/mL					
temp, °C	0.001	0.005	0.010	0.020	0.030	0.040
38	0.50	1.30	1.30	1.60	1.10	1.20
40	6.30	5.10	3.30			
45	53.0	79.0	50.6	16.0	77.0	73.0
47	150.0	220.0	240.0	190.0	140.0	290.0

with 7 and 35 molecules of 3-PROG. The k_{in} for these conjugates increases with the growth of the protein concentration up to 0.020 mg/mL. There are two possible explanations: first, the subunit protein is inactivated due to its dissociation into monomers; second, the same protein may be inactivated because of its "excessive" association. The increasing hydrophobicity of G6PDH conjugates results in the formation of the large aggregates which causes a loss of the protein activity with the increase of its concentration up to 0.02 mg/mL (see Figure 10b,c).

As seen from Table III, the LDH modification with progesterone slightly decreases the enzyme stability, while the MDH modification increases the enzyme stability below 30 °C (see Table VI), but above this temperature the thermostabilities of the initial and modified MDH are similar. Commenting on the data listed in Table VI, it should be emphasized that only the comparison of k_0 values is correct since the biocatalyst concentration can influence the k_{in} values of the enzyme and its conjugates in absolutely different ways.

It is very noteworthy that the changes in the catalytic activity and thermostability of these dehydrogenases after their modification by steroids are parallel. Owing to modification of LDH by 3–40 molecules of 3-PROG, its activity decreases up to 86% of the initial level, while at the moderate modification of MDH (3–15 molecules of 3-PROG) the biocatalyst activity increases up to 111%, which corresponds with an increase of thermostability of the modified enzyme (see the k_{in} values in Table III).

Increase of MDH modification (n = 20–28) results in decrease of the catalytic activity of this enzyme (Figure 5). The parallel change of catalytic activity and thermostability was found for G6PDH and its conjugates. The modification results in decrease of the catalytic activity (Figure 5, Table II) and a loss of thermostability (Figure 10, Table IV). The parallel changes of the enzyme activity and stability are often observed in applied enzymology (*23*).

In our opinion, change of the catalytic activity and thermostability of the dehydrogenase due to the modification appears to be connected with two main reasons: firstly, the DMFA action on the enzyme and, secondly, the enzyme hydrophobization owing to the insertion of modifiers, 3-COR or PROG, in its molecule. The contribution of the former factor is absolutely obvious from Figure 11: a loss of the G6PDH activity results from the enzyme incubation in DMFA-containing solutions. For instance, at 25 °C in the water–DMFA (30%) mixture G6PDH completely losses its activity after a 1-h incubation.

A comparison of the activities of the native and modified G6PDH (see Table II) indicates that they are significantly different. The enzyme activity decreases for 15–24% due to the DMFA action on enzyme. Increase of the degree of the protein modification decreases its activity in such a manner that the modifier itself decreases the activity value by 11–15% as compared with that of the control enzyme treated with the mixture of water with DMFA; i.e. the enzyme activity is supressed not only by an organic cosolvent but also by modifier itself. Modification results in decrease of the thermostability of the G6PDH conjugates as well (Table IV). As seen from Table III, the overall LDH stability after its modification decreases by 67% as compared with that of the control and initial protein; i.e. this dehydrogenase undergoes all the significant structural changes as a result of the DMFA action and then does not alter its stability owing to an insertion in its molecule of 19 modifiers.

The direction of the stability changes of modified LDH and MDH (as well as their catalytic activity) are quite opposite. Increase of the MDH activity and stability as a result of its modification by progesterone may be accounted for a hydrophobization of some free amino groups of the lysine residues responsible for the interaction between the MDH subunits. Presence of such lysine residues in MDH is well-known (*24*). Neutralization of the positive charge of the MDH as well as LDH groups by their acetylation reduces the enzyme stability (*17*, *24*). Hydrophobization of such residues stabilizes, probably, the quaternary structure of MDH. The known data show that the hydrophobization of the internal sites of a protein stabilizes it, while the hydrophobization of the enzyme surface destabilizes it in the buffered solutions (*25–27*).

What are the mechanisms of the action of DMFA and the modifiers, 3-COR and 3-PROG, on the dehydrogenases? Before giving an answer to this question, it should be mentioned that LDH and MDH easy dissociate into their subunits, which are inactive for LDH, while the immobilized MDH monomers have the same catalytic activity (*28–30*). The G6PDH subunits have much lower activity than that of the enzyme with undisturbed quaternary structure (*31*, *32*). It was assumed that the quaternary structure of G6PDH is supported by two molecules of $NADP^+$ (*32*, *33*). However, Yoshida (*34*) proposed a hexameric structure for G6PDH containing at least six structural $NADP^+$ molecules. The DMFA action on the dehydrogenases and their conjugates causes a solubilization of the enzyme subunits; i.e. a protein losses the structural water which is substituted by the dipolar aprotic solvent (*2*). The moderate substitution of water for DMFA may enhance the enzyme activity as in the case of G6PDH (Figure 2), but increase of the organic cosolvent content causes a sharp decrease of the enzyme activity (Figure 11). Also, the initial action of DMFA on the dehydrogenase dissociation cannot be excluded. However, in our laboratory the data obtained which prove that the inactivating action of DMFA is realized by means of a solubilization of the enzyme subunits but not its dissociation into monomers, since the bifunctional agents (glutaraldehyde, dimethyl suberimidate, and dimethyladipimidate) did not preserve G6PDH from the inactivating action of DMFA (*35*).

The effect of modification on the dehydrogenases involves a hydrophobization of internal and external sites of the enzyme (*21*, *25–27*). Modification of the external amino groups causes, as a rule, the destabilization of the enzyme, but its activity may be retained. At the modification of the internal amino groups, the enzyme, for instance MDH, may be stabilized and activated. At high modification degree the external amino groups react with a modifier which may inactivate a biocatalyst.

Analysis of the temperature dependences of the effective rate constants for the dehydrogenase inactivation, k_{in}, could not be overestimated, since the temperature course

Table V. Thermodynamic Activation Parameters for the G6PDH Inactivation at Various Concentrations and for Conjugate G6PDH-3-PROG-35 (45 °C)

protein, mg/mL	E_{act}, kcal/mol	ΔH^*, kcal/mol	ΔS^*, kcal/mol °C	ΔG^*, kcal/mol
G6PDH (infinite dilution)	109.7	109.0	269.1	23.4
G6PDH, 0.001 mg/mL	135.7	135.0	353.0	23.2
G6PDH, 0.005 mg/mL	143.6	143.0	374.0	24.0
G6PDH-3-PROG-35, 0.005 mg/mL	109.7	109.0	270.1	23.1

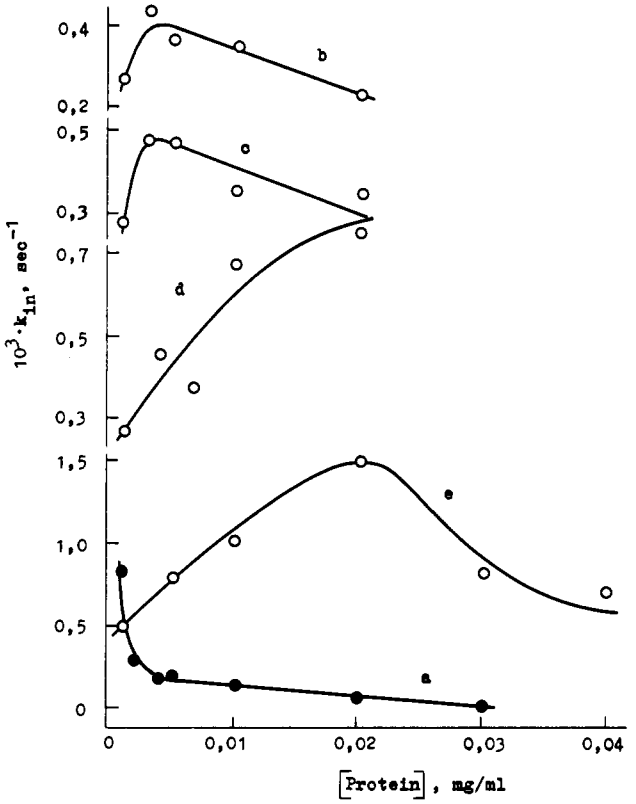


Figure 10. The dependences of the effective inactivation rate constants at 45 °C for the initial G6PDH (a), enzyme treated by water–DMFA (10%) mixture (b), and the G6PDH conjugates containing 3 (c), 7 (d), and 35 (e) molecules of modifier 3-PROG.

Table VI. The Effective Inactivation Rate Constants (10^4 k_{in}, s^{-1}) for the MDH Forms and Its Conjugates (5.0 10^{-4} mg/mL) at Various Temperatures

	enzyme, medium			
temp, °C	MDH, buffer, pH 7.5	$MDH_{control}$, buffer, pH 7.6	MDH-3-PROG-24, buffer, pH 7.5	MDH-3-PROG-16, water[a]
20	3.64	2.04	1.05	0.45
25	3.83	2.30	2.30	1.24
30	5.75	3.07	2.56	1.31
35	11.10	3.96	2.68	3.83
40	17.60	8.82	9.58	10.70
45	49.10	33.70	29.50	32.60
	E_{act}, kcal/mol above 30 °C			
	33.2	38.20	38.20	38.20

[a] Protein concentration equaled 5×10^{-3} mg/mL.

of these constants, as a rule, is complicated owing to the effect of the initial protein concentration on their values (*18–22, 36*). Only an analysis of the temperature dependences of k_0 constants, obtained by an extrapolation of k_{in} to "zero" concentration of a biocatalyst (see Figure 7), can have a definite physical meaning. As shown in Figure 8, the Arrhenius dependence of k_0 has no breaks. It should be mentioned that the thermodynamic activation parameters (ΔH^*, ΔS^*, and ΔG^*), obtained from the temperature dependences of k_0, cannot be related to a definite step of the protein thermoinactivation, since these parameters characterize the complex cooperative process of the conformational transformation of a protein. E_{act} for the G6PDH thermoinactivation, equal to 109.7 kcal/mol, may be related to the entire stage of the dissociation of oligomeric protein into its monomers but not to a cleavage of some definite bonds which can initiate this cooperative process.

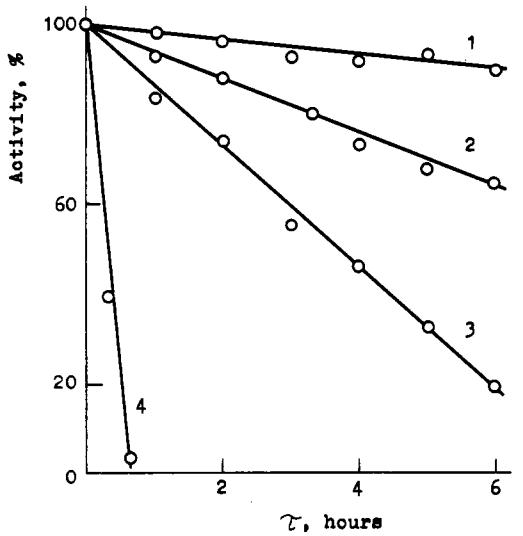


Figure 11. The dependences of the G6PDH activity on the DMFA content in a $NaHCO_3$ (2%) solution, pH 8.3 at 25 °C, and the enzyme concentration 1.5 mg/mL: 1, 5; 2, 10; 3, 20; 4, 30% DMFA.

The cooperative character of biopolymer thermoinactivation is a main difference between this process and thermolysis of low molecular weight compounds. The temperature dependence of the rate constants k_{in} reflect a nonelementary character of the thermoinactivation and a complexity of the characterized macrostage, i.e. the presence of intermediate nondisplayed microstages, the influence of the protein concentration, the solvent nature, and the enzyme microenvironment (*20*). Therefore, for a complete analysis of the thermodinamic and kinetic parameters of the enzyme inactivation, additional methods based on chemical kinetic theory and experimental data on much simpler systems as well as the results of the inactivation study by the methods of PMR, CD, densitometry, and sedimentational analysis should be used.

CONCLUSION

The catalytic activities of synthesized conjugates and their thermostabilities are determined by the DMFA content in a medium, the reaction time, and the modification degree of the dehydrogenases used.

Decrease of the thermostability of dehydrogenases and their conjugates is connected with the oligomeric enzyme dissociation into subunits, which may be limiting stage of the entire process of the biocatalyst inactivation. DMFA solubilizes the dehydrogenase subunits by substituting for the structural water and, probably, initiates the enzyme dissociation into monomers. As concerns the thermostability of dehydrogenases and their conjugates, only the constants k_0, obtained by an extrapolation of the effective rate constants, k_{in}, to "zero" concentration of a biocata-

lyst, are valid. The temperature dependences of the constant k_0 are always described by the Arrhenius equation, while those for k_{in} of the dehydrogenases and their conjugates are complicated by the breaks that are caused by the k_{in} dependence on the protein concentration.

Unfortunately, k_0 may not be calculated for all enzyme conjugates. For instance, the k_{in} dependences on the G6PDH-3-PROG concentrations are very complex; that is accounted for the protein association owing to its hydrophobization by steroids. At small modification degrees of dehydrogenases, only the external lysine residues of a protein react with a modifier, which does not change the biocatalyst activity but decreases its stability in aqueous medium. At higher modification degrees of dehydrogenases, not only external but internal lysine residues as well react with a modifier, which, in one case, activates and stabilizes an enzyme (MDH) and, in another case, inactivates and destabilizes it (G6PDH) owing to aggregation of the hydrophobizated molecules of an enzyme.

LITERATURE CITED

(1) Laane, C. (1987) Medium engineering for bioorganic synthesis. *Biocatalysis 1*, 17–22.

(2) Khmelnitski, Yu. L., Levashov, A. V., Klyachko, N. L., and Martinek, K. (1988) Engineering Biocatalytic Systems in Organic Media with Low Water Content. *Enzyme Microb. Technol. 10*, 710–724.

(3) Maggio, E. D., Ed. (1983) Enzyme-Immunoassay, CRC Press, Boca Raton, FL.

(4) Ngo, T. T., and Lenhoff, H. M., Eds. (1985) Enzyme-mediated Immunoassay, Plenum Press, New York and London.

(5) Means, G. E., and Feeney, R. E. (1990) Chemical Modifications of Proteins: History and Applications. *Bioconjugate Chem. 1*, 2–12.

(6) Luisi, P. L., and Magid, L. J. (1986) Solubilization of Enzymes and Nucleic Acids in Hydrocarbon Micellar Solutions. *CRC Crit. Rev. Biochem. 20*, 409–474.

(7) Martinek, K., Levashov, A. V., Klyachko, N. L., Khmelnitski, Yu. L., and Berezin, I. V. (1986) Micellar Enzymology *Eur. J. Biochem. 155*, 453–468.

(8) Metelitza, D. I., and Eryomin, A. N. (1988) Reversed micelles of surfactants in organic solvents as models of biomembranes (in Russian). *Rev. Biol. Chem. 28*, 145–173.

(9) Eryomin, A. N., Savenkova, M. I., and Metelitza, D. I. (1986) The peculiarities of "antigen–antibody" interaction in the reversed micelles of surfactants in heptane (in Russian). *Bioorg. Khimiya 12*, 606–612.

(10) Eryomin, A. N., and Metelitza, D. I. (1989) The homogeneous enzyme-immunoassay of progesterone in the reversed micelles of surfactants (in Russian). *Dokl. AN BSSR 33*, 932–935.

(11) Anderson, G. W., Zimmerman, J. E., and Callahan, F. M. (1964) The use of N-hydroxysuccinimide in peptide synthesis. *J. Am. Chem. Soc. 86*, 1839–1842. Janovski, A. H. (1974) Selective 3-*O*-carboxymethyloxime formation in steroidal 3,-20-diones for haptene immunospecificity. *Steroides 23*, 49–59.

(12) Karasyova, E. I., Eryomin, A. N., and Metelitza, D. I. (1987) Production and Characterization of the Glucose-6-phosphate Dehydrogenase Conjugates with Cortisol and Progesterone (in Russian). *Biotechnology 3*, 198–203.

(13) Blanford, A. T., Wittman, W., Stroup, S. D., and Westphal, U. (1978) *J. Steroid Biochem. 9*, 187–189.

(14) Karasyova, E. I., Eryomin, A. N., and Metelitza, D. I. (1986) Optimization of the glucose-6-phosphate dehydrogenase use in the conditions of cofactor chemical regeneration (in Russian). *Izv. AN BSSR 4*, 76–80.

(15) Markina, V. L., Eryomin, A. N., and Metelitza, D. I. (1986) Optimum conditions of the malate and lactate dehydrogenase use at the chemical regeneration of cofactor (in Russian). *Appl. Biochem. Microbiol. 22*, 635–641.

(16) Viola, R. E. (1984) Kinetic study of the reactions catalyzed by glucose-6-phosphate dehydrogenase from *Leuconostoc mesenteroides*: pH variation of kinetic parameters. *Arch. Biochem. Biophys. 228*, 415–424.

(17) Tungler, P., and Pfleiderer, G. (1977) Enhanced heat, alkaline and tryptic stability of acetamidinated pig heart lactate dehydrogenase. *Biochim. Biophys. Acta 484*, 1–8.

(18) Markina, V. L., Eryomin, A. N., and Metelitza, D. I. (1985) Peculiarities of the malate dehydrogenase thermoinactivation (in Russian). *Biophysika 30*, 971–976.

(19) Markina, V. L., Eryomin, A. N., and Metelitza, D. I. (1986) Thermoinactivation and stabilization of lactate- and malate-dehydrogenases (in Russian). *Izv. AN BSSR 6*, 61–67.

(20) Metelitza, D. I., and Eryomin, A. N. (1987) Kinetic aspects of irreversible thermoinactivation of enzymes (in Russian). *Usp. Khim. 56*, 1921–1948.

(21) Karasyova, E. I., Eryomin, A. N., and Metelitza, D. I. (1990) Effects of the glucose-6-phosphate dehydrogenase hydrophobization by progesterone on the enzyme thermoinactivation (in Russian). *Appl. Biochem. Microbiol. 26*, 342–348.

(22) Markina, V. L., Eryomin, A. N., and Metelitza, D. I. (1990) Influence of lactate and malate dehydrogenase modification on their stability and activity (in Russian). *Biophysika 35*, 30–35.

(23) Sadana, A., and Henley, J. P. (1986) Effects of chemical modification on enzymatic activities and stabilities. *Biotech. Bioeng. 88*, 256–268.

(24) Muller, J., and Klein, C. (1982) Stability of dehydrogenases III. Malate dehydrogenase. *Biochim. Biophys. Acta 707*, 133–141.

(25) Mozhaev, V. V., Martinek, K., and Berezin, I. V. (1987) Chemical, physical and biological approaches to development of stabilized enzymatic biocatalysts for biotechnology (in Russian). *Usp. Khim. 56*, 1659–1692.

(26) Kutuzova, G. D., Ugarova, N. N., and Berizin, I. V. (1984) Total regularities of changes of the proteins and enzymes thermostability owing to chemical modification of their functional groups (in Russian). *Usp. Khim. 53*, 1852–1890.

(27) Kutuzova, G. D., and Ugarova, N. N. (1986) Chemical modification as the production method for stabilized forms of the biocatalysts. In *Itogi nauki i tekhniki. Biotechnologia V.5* (in Russian), pp 5–49, Viniti, Moscow.

(28) Shore, J. D., and Chakraboti, S. K. (1978) Subunit dissociation of mitochondrial malate dehydrogenase. *Biochemistry 15*, 875–879.

(29) Wood, D. C., Hodges, C. T., and Harrison, J. H. (1978) Relation of the pH and concentration-dependent dissociation of porcine heart mitochondrial malate dehydrogenase. *Biochem. Biophys. Res. Commun. 82*, 943–950.

(30) Bleibe, D. M., Schulz, R. A., and Harrison, J. H. (1977) Investigation of the subunit interaction of malate dehydrogenase. *J. Biol. Chem. 252*, 755–758.

(31) Carson, P. E., Schrier, S. L., and Kellermeyer, R. W. (1959) Mechanism of inactivation of glucose-6-phosphate dehydrogenase in human erythrocytes. *Nature 184*, 1293–1295.

(32) Kirkman, H. N. (1962) Glucose-6-phosphate dehydrogenase from human erythrocytes. Further purification and characterization. *J. Biol. Chem. 237*, 2364–2370.

(33) Chang, A. E., and Langdo, E. G. (1963) *J. Biol. Chem.* 2309–2312.

(34) Yoshida, A., and Hoagland, V. D. (1970) Active molecular unit and NADP content of human glucose-6-phosphate dehydrogenase. *Biochem. Biophys. Res. Commun. 40*, 1167–1172.

(35) Puchkaev, A. V., and Metelitza, D. I. Catalytic activity of glucose-6-phosphate dehydrogenase in water–organic media (in Russian). *Appl. Biochem. Microbiol.*, in press.

(36) Poltorak, O. M., and Chukhray, E. S. (1986) Dissociative thermoinactivation of biocatalysts. In *Itogi nauki i tekhniki. Biotekhnologia. V.5* (in Russian), pp 50–86, Viniti, Moscow.

(37) Eryomin, A. N.; Karasyova, E. I., and Metelitza, D. I. (1989) Catalytic activity of glucose-6-phosphate dehydrogenase conjugates with progesterone in aqueous and micellar media in the presence of specific and nonspecific antibodies (in Russian). *Appl. Biochem. Microbiol. 25*, 524–531.

(38) Shultz, G. E., and Schirmer, R. H. (1979) *Principles of Protein Structure*, Springer-Verlag, New York.

(39) Jenks, W. P. (1969) *Catalysis in Chemistry and Enzymology* (pp 303–331 in Russian translation, 1972, Mir, Moscow) McGraw-Hill, New York.

o-Acetamidophenylboronate Esters Stabilized toward Hydrolysis by an Intramolecular O–B Interaction: Potential Linkers for Selective Bioconjugation via Vicinal Diol Moieties of Carbohydrates

Sui Xiong Cai and John F. W. Keana*

Department of Chemistry, University of Oregon, Eugene, Oregon 97403. Received January 28, 1991

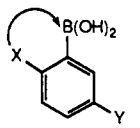
The synthesis and properties of o-acetamidophenylboronic acid 8 and the corresponding 1,2-diol cyclic boronates 13 and 16 are reported. The presence of an O–B interaction in 8 and 13 has been established by ^{11}B and ^{1}H NMR spectroscopy. The O–B interaction stabilizes boronate 13 toward hydrolysis and accelerates esterification of acid 8 in contrast to the non-ortho-substituted boronate 10 and acid 3. The enhanced stability of o-acetamidophenylboronate esters toward hydrolysis suggests their application as vicinal diol protecting groups in carbohydrate synthesis. Through the incorporation of an amino group as a second site for a coupling reaction (e.g. via isothiocyanate 22), o-acetamidophenylboronic acids may serve as novel agents for bioconjugation reactions involving carbohydrate moieties.

Carbohydrate residues are present in a wide variety of proteins including antibodies. Most of the reagents developed for the covalent modification or cross-linking of proteins are designed mainly for nucleophilic thiol and amino groups of cysteine and lysine residues, respectively (*1*). For example, active esters are commonly used for the attachment of reporter molecules such as fluorochromes or drugs (*2*) to antibodies. Owing to the limited specificity of the lysine modification reactions, the result is usually a heterologous labeling (*3*) and the targeting ability of the antibodies may be altered or eliminated (*4*).

While relatively few methods have been developed for the modification of carbohydrate residues (*5*), the advantages of modification of antibodies via the carbohydrate moieties have been well-demonstrated (*6*). In this approach, the carbohydrate is oxidized by periodate to generate aldehydes, which are then condensed with a hydrazino- or amino-containing molecule to produce the conjugates (*7*). Since the carbohydrate moiety is located remote to the antigen-binding region of antibodies (*8*), this method often leads to conjugates with improved immunoreactivity (*9*). However, potential problems include oxidation of certain amino acid residues, especially cysteine, cystine, methionine, tryptophan, tyrosine, and histidine, by periodate (*10*), as well as formation of intermolecular or intramolecular Schiff base linkages (*7*).

It occurred to use that the high specificity of the reaction between phenylboronic acid and vicinal diols to form cyclic boronic diesters (*11*) might serve as a basis for a general biconjugation approach. A reversible boronic esterification reaction plays a key role, for example, in affinity chromatography for the separation and purification of biological and pharmaceutical samples containing the *cis*-diol structure (*12*). Boronic esters are also widely used as protecting groups in the synthesis of nucleosides (*13*) and carbohydrates (*14*).

While boronates can be readily prepared in organic solvents, the esters generally undergo ready hydrolysis in aqueous media. Fortunately, lability toward hydrolysis (*15*) or transesterification (*16*) is significantly reduced when a functional group is present that can act as a fourth ligand for the electron-deficit boron atom. We have therefore incorporated this important structural feature into a new series of substituted phenylboronic acids 1 herein described. An amino group (Y = NH_2) is included as the site (e.g. via an isothiocyanate) for eventual conjugation to another target molecule. We also describe relevant esterification and comparative hydrolysis properties of derivatives of 1.



1

EXPERIMENTAL PROCEDURES

General Chemical Procedures. Solvents and chemicals were reagent grade and used as received unless otherwise specified. ^{1}H NMR spectra were measured on a QE-300 NMR spectrometer (*J* values are in hertz). ^{11}B NMR spectra ($F_3B{\cdot}OEt_2$, δ 0.0 as external standard) were measured on a NT-360 spectrometer (115.5 MHz). Melting points were obtained on a Thomas-Hoover apparatus (mp < 250 °C) or a Mel-Temp (Laboratory Devices) apparatus (mp > 250 °C) and are uncorrected. Equilibrium constant measurements were done with a QE-300 NMR spectrometer.

3-Acetamidophenylboronic Acid (3). Amide 3 was prepared from 3-aminophenylboronic acid monohydrate (2; Aldrich) and acetic anhydride (*17*). From 10.3 g of 2 (monohydrate) there was obtained 12.6 g (99%) of 3 as a white solid: mp 275–276 °C [lit. (*18*) mp 250 °C]; ^{1}H NMR (DMSO-d_6) δ 2.010 (s, 3), 7.228 (t, 1, J = 7.66), 7.439 (d, 1, J = 7.47), 7.687 (d, 1, J = 7.70), 7.781 (s, 1), 7.992 (s, 2), 9.839 (s, 1); ^{11}B NMR (D_2O) δ 29.2 (s), 19.6 (s); ^{11}B NMR (D_2O–NaOH) δ 2.5 (s).

Nitration of 3. (*a*). To 10 mL of fuming nitric acid kept at −50 °C was added 2.08 g of powdered 3. The solution was stirred at −45 °C for 40 min, then it was poured into 80 mL of ice–water. The yellow precipitate was filtered and washed by water (10 mL) and dried to leave a yellow solid (2.49 g, 98%). The mixture was extracted with xylene in a Soxhlet extractor for 1.5 h and the solid left in the thimble was dried to leave 1.78 g (70%) of 3-acetamido-6-nitrophenylboronic acid (4) as a yellow solid: mp 194–195 °C [lit. (*18*) 69%, 193–196 °C]; ^{1}H NMR (DMSO-d_6) δ 2.098 (s, 3), 7.614 (d, 1, J = 2.1), 7.791 (dd, 1, J = 2.1, 9.2), 8.119 (d, 1, J = 9.2), 8.145 (s, 2), 10.440 (s, 1); ^{11}B NMR (D_2O) δ 28.6 (s), 19.8 (s); ^{11}B NMR (D_2O–NaOH) δ 1.9 (s).

1043-1802/91/2902-0317$02.50/0 © 1991 American Chemical Society

(*b*). Nitration of 13.8 g of **3** by 6 mL of fuming nitric acid in 105 mL of acetic anhydride (*17*) gave 13.3 g (78.2%) of yellow solid. It was extracted with xylene in a Soxhlet extractor to give 6.9 g (41%) of **4**, mp 196–197 °C. The extract was cooled to 25 °C and the yellow precipitate was filtered and dried to leave 2.6 g of yellow solid. The mixture was subjected to fractional crystallization (*17*) in boiling ethyl acetate to give 0.68 g (4.0%) of 3-acetamido-2-nitrophenylboronic acid (**5**) as a yellow solid, mp 161–162 °C, and 1.43 g (8.4%) of 3-acetamido-4-nitrophenylboronic acid (**6**) as a yellow solid, mp 200–201 °C. **5**: ^{1}H NMR (DMSO-d_6) δ 2.022 (s, 3), 7.281 (d, 1, J = 6.3), 7.5 (m, 2), 8.303 (s, 2), 10.046 (s, 1). **6**: ^{1}H NMR (DMSO-d_6) δ 2.026 (s, 3), 7.701 (d, 1, J = 7.8), 7.833 (s, 1), 7.844 (d, 1, J = 6.6), 8.447 (s, 2), 10.249 (s, 1).

3-Acetamido-6-aminophenylboronic Acid (7). A mixture of 1.50 g of **4** and 0.136 g of 30% Pd/C in absolute ethanol (80 mL) was shaken under H_2 at 45 psi for 13 h. Methanol (100 mL) was added to the mixture to dissolve the white precipitate and the mixture was filtered. The filtrate was evaporated to leave a solid, to which water (1 mL) was added. The mixture was evaporated and dried to leave 1.29 g (100%) of **7** as a pale red solid: ^{1}H NMR (D_2O) δ 2.119 (s, 3), 6.850 (d, 1, J = 8.1), 7.242 (d, 1, J = 8.1), 7.437 (s, 1). To a solution of 92 mg of amine **7** in 5 mL of MeOH was added 0.3 mL of 7 N HCl–MeOH solution. The solvent was removed by evaporation to give solid. It was crystallized (MeOH–ether) to give 89 mg of the HCl salt of **7** as almost colorless solid: mp 204–205 °C; ^{1}H NMR (D_2O) δ 2.162 (s, 3), 7.340 (d, 1, J = 8.4), 7.630 (d, 1, J = 8.4), 7.806 (s, 1). Anal. Calcd for $C_8H_{11}BN_2O_2$·HCl: C, 41.69; H, 5.24; N, 12.15. Found: C, 41.51; H, 5.36; N, 12.29.

3,6-Diacetamidophenylboronic Acid (8). A mixture of 500 mg of **7** and 2 mL of acetic anhydride was heated in dioxane (20 mL) at 60 °C for 6 h. The solvent was evaporated and the solid was treated with water twice (5 mL) and evaporated to leave 598 mg (100%) of **8** as pale yellow solid: ^{1}H NMR (D_2O) δ 2.141 (s, 3), 2.349 (s, 3), 7.034 (d, 1, J = 8.1), 7.369 (s, 1), 7.395 (d, 1, J = 8.1); ^{1}H NMR (D_2O–NaOH) δ 2.128 (s, 6), 7.246–7.341 (m, 3); ^{11}B NMR (D_2O) δ 4.1 (s); ^{11}B NMR (D_2O–NaOH) δ 2.3 (s). The analytical sample of **8** (monohydrate) was obtained as a pale yellow solid, mp 295–296 °C, by crystallization from water. Anal. Calcd for $C_{10}H_{13}BN_2O_4$·H_2O: C, 47.28; H, 5.95; N, 11.02. Found: C, 47.10; H, 5.97; N, 10.86.

Ethylene 1,2-(3-Acetamidophenylboronate) (10). A solution of 141 mg (0.715 mmol) of **3** and 54 mg (0.871 mmol) of ethylene glycol (**9**) in benzene (10 mL) was heated at 60 °C for 30 min. The solvent was removed by distillation under vacuum to leave a solid which was triturated with dry ether (4 mL). The mixture was filtered and the solid was dried to give 141 mg (96%) of **10** as a white solid: mp 157–158 °C; ^{1}H NMR ($CDCl_3$) δ 2.178 (s, 3), 4.376 (s, 4), 7.10 (bm, 1), 7.364 (t, 1, J = 7.60), 7.55 (d, 1, J = 7.23), 7.645 (s, 1), 7.880 (d, 1, J = 7.81); ^{11}B NMR (DMSO-d_6) δ 31.7 (s). Anal. Calcd for $C_{10}H_{12}BNO_3$: C, 58.58; H, 5.90; N, 6.83. Found: C, 58.71; H, 5.93; N, 6.85.

Ethylene 1,2-(3-acetamido-6-nitrophenylboronate) (11) was prepared from **4** in a manner similar to that of **10**. From 138 mg (0.570 mmol) of **4** and 55 mg (0.870 mmol) of ethylene glycol there was obtained 135 mg (95%) of **11** as an orange solid: mp 150–151 °C; ^{1}H NMR ($CDCl_3$) δ 2.232 (s, 3), 4.451 (s, 4), 7.393 (bs, 1), 7.662 (s, 1), 7.780 (d, 1, J = 9.02), 8.165 (d, 1, J = 9.02); ^{11}B NMR (DMSO-d_6) δ 31.7 (s). Anal. Calcd for $C_{10}H_{11}BN_2O_5$: C, 48.04; H, 4.43; N, 11.20. Found: C, 47.80; H, 4.41; N, 11.13.

Ethylene 1,2-(3-acetamido-4-nitrophenylboronate) (12) was prepared from **6** in a manner similar to that of **10**. From 101 mg (0.413 mmol) of **6** and 30 mg (0.483 mmol) of ethylene glycol there was obtained 92 mg of **12** as a yellow solid (88%): mp 167–168 °C; ^{1}H NMR ($CDCl_3$) δ 2.289 (s, 3), 4.421 (s, 4), 7.570 (d, 1, J = 8.23), 8.172 (d, 1, J = 8.23), 9.081 (s, 1), 10.2 (s, 1). Anal. Calcd for $C_{10}H_{11}BN_2O_5$: C, 48.04; H, 4.43; N, 11.20. Found: C, 48.31; H, 4.28; N, 11.26.

Ethylene 1,2-(3,6-diacetamidophenylboronate) (13) was prepared from **8** in a manner similar to that of **10**. From 120 mg (0.472 mmol) of **8** and 40.0 mg (0.645 mmol) of ethylene glycol in dioxane (15 mL) there was obtained 115 mg (93%) of **13** as a white solid: mp 300 °C dec; ^{1}H NMR (DMSO-d_6) δ 1.988 (s, 3), 2.270 (s, 3), 3.806 (s, 4), 6.908 (d, 1, J = 8.6), 7.357 (d, 1, J = 1.83), 7.620 (dd, 1, J = 1.83, 8.60); ^{11}B NMR (DMSO-d_6) δ 8.6 (s). Anal. Calcd for $C_{12}H_{15}BN_2O_4$: C, 54.99; H, 5.77; N, 10.69. Found: C, 54.62; H, 5.79; N, 10.78.

Adenosine 2′,3′-(3-Acetamidophenylboronate) (15). A suspension of 63.5 mg (0.322 mmol) of **3** and 86.7 mg (0.324 mmol) of adenosine **14** in dioxane (25 mL) was refluxed for 2 h, and then the solvent was removed by distillation. The solid residue was dried by aspirator to give a solid which was triturated by ether. The mixture was filtered and the solid was dried to give 121 mg (90%) of **15** as a white solid: mp 233–234 °C; ^{1}H NMR (DMSO-d_6) δ 2.029 (s, 3), 3.615 (m, 2), 4.251 (m, 1), 5.175 (t, 1, J = 5.62), 5.226 (dd, 1, J = 3.47, 7.30), 5.731 (dd, 1, J = 2.98, 7.29), 6.255 (d, 1, J = 2.91), 7.30 (m, 4), 7.745 (d, 1, J = 7.80), 7.996 (s, 1), 8.167 (s, 1), 8.378 (s, 1), 9.985 (s, 1). Irradiation at δ 6.255 transformed the δ 5.731 doublet of doublets to a simple doublet. Irradiation at δ 5.731 transformed the δ 6.255 doublet to a singlet and the δ 5.226 doublet of doublets to a simple doublet. Irradiation at δ 4.251 transformed the δ 5.226 doublet of doublets to a simple doublet. Anal. Calcd for $C_{18}H_{19}BN_6O_5$·0.3H_2O: C, 52.02; H, 4.71; N, 20.22. Found: C, 52.33; H, 4.71; N, 19.87.

Adenosine 2′,3′-(3,6-diacetamidophenylboronate) (16) was prepared from **8** and adenosine in a manner similar to that of **15**. From 50.6 mg (0.199 mmol) of **8** and 53.9 mg (0.201 mmol) of adenosine there was obtained 91 mg (98%) of **16** as a white solid: mp 255–256 °C; ^{1}H NMR (DMSO-d_6) δ 2.018 (s, 3), 2.334 (s, 3), 3.612 (m, 2), 4.131 (m, 1), 4.692 (t, 1, J = 5.14), 5.026 (m, 1), 5.074 (t, 1, J = 7.40), 6.061 (d, 1, J = 2.72), 6.965 (d, 1, J = 8.43), 7.316 (bs, 2), 7.460 (s, 1), 7.737 (d, 1, J = 8.43), 8.137 (s, 1), 8.374 (s, 1), 9.946 (s, 1), 12.325 (s, 1). Anal. Calcd for $C_{20}H_{22}BN_7O_6$·1.3H_2O: C, 48.96; H, 5.05; N, 19.98. Found: C, 49.06; H, 4.77; N, 19.60.

3-Amino-6-nitrophenylboronic Acid (17). A mixture of 1.56 g of boronic acid **4** in 2 N HCl (20 mL) was heated at 85 °C for 1 h, giving a red solution which was partially neutralized by addition of 30% aqueous NaOH to pH = 4. The yellow precipitate was filtered and washed with water (4 mL) and then dried to give 1.10 g (85%) of **17** as a yellow solid: mp 270–271 °C [lit. (*18*) 250–255 °C]; ^{1}H NMR ($CDCl_3$ + DMSO-d_6), 5.030 (bs, 2), 6.378 (dd, 1, J = 2.17, 8.95), 6.460 (d, 1, J = 2.17), 7.144 (s, 2), 7.769 (d, 1, J = 8.95).

6-Nitro-3-(trifluoroacetamido)phenylboronic Acid (18). To a solution of 746 mg of **17** in dioxane (20 mL) cooled in an ice bath was added 2.5 mL of trifluoroacetic anhydride. The solution was stirred at 0 °C for 30 min and 25 °C for 3 h. Then the solvent was removed and the residue was treated with water (3 mL) and evaporated again to leave 1.09 g (99%) of **18** as a yellow solid: ^{1}H

NMR ($CDCl_3$ + DMSO-d_6) δ 7.50 (bm, 2), 7.693 (d, 1, J = 1.57), 7.785 (dd, 1, J = 1.57, 8.98), 7.951 (d, 1, J = 8.98), 10.962 (1, s). The analytical sample of **18** was obtained as a monohydrate by crystallization from water as yellow needles, mp 125–126 °C. Anal. Calcd for $C_8H_6BF_3N_2O_5 \cdot H_2O$: C, 32.47; H, 2.72; N, 9.46. Found: C, 32.38; H, 2.65; N, 9.10.

6-Amino-3-(trifluoroacetamido)phenylboronic Acid (19). A mixture of 1.58 g of **18** and 120 mg of 30% Pd/C in THF (40 mL) was shaken under H_2 at 40 psi for 2 h. DMSO (3 mL) and ethanol (180 mL) was added to dissolve the precipitate and the mixture was filtered. The filtrate was evaporated and the residue was dried under vacuum (0.05 mm) overnight. Water (10 mL) was added and the mixture was centrifuged. The precipitate was washed with water (2 × 10 mL) and dried to leave 1.18 g (84%) of **19** as a pale yellow solid: mp >360 °C; ^{1}H NMR (D_2O) δ 6.844 (d, 1, J = 8.4), 7.344 (d, 1, J = 8.4), 7.540 (s, 1). The HCl salt of **19** was obtained in a manner similar to that of **7** as a solid: mp >370 °C; ^{1}H NMR (D_2O) δ 7.416 (d, 1, J = 8.4), 7.756 (d, 1, J = 8.4), 7.756 (s, 1). Anal. Calcd for $C_8H_8BF_3N_2O_3HCl \cdot H_2O$: C, 31.77; H, 3.33; N, 9.26. Found: C, 31.85; H, 3.39; N, 9.00.

6-Acetamido-3-(trifluoroacetamido)phenylboronic Acid (20). A mixture of 1.05 g of **19** and 3 mL of acetic anhydride in dioxane (20 mL) was heated at 60 °C for 1 h. The solvent was removed by evaporation and the residue was treated with water (2 × 3 mL) and evaporated to leave a solid, which was triturated with ether (3 mL). The mixture was filtered and the solid was dried to give 1.11 g (85%) of **20** as a pale yellow solid: mp 325–326 °C; ^{1}H NMR (D_2O) δ 2.376 (s, 3), 7.516 (s, 2), 7.117 (s, 1). Anal. Calcd for $C_{10}H_{10}BF_3N_2O_4$: C, 41.42; H, 3.48; N, 9.66. Found: C, 41.13; H, 3.09; N, 9.52.

6-Acetamido-3-aminophenylboronic Acid (21). To 611 mg of **20** was added 10 mL of 7% K_2CO_3 aqueous methanol solution (water–methanol 2:5) and the solution was stirred at 25 °C for 4 h. Then ethanol (15 mL) was added and the mixture was filtered. The filtrate was evaporated to leave a solid which was redissolved in ethanol and filtered. The filtrate was evaporated and the residue was dissolved in water (2 mL), acidified by 2 N HCl in an ice bath to pH = 4, then diluted with ethanol (10 mL) and evaporated to leave a solid. The solid was dissolved in ethanol (6 mL) and centrifuged and the clear solution was added dropwise to ether (60 mL). The precipitate was centrifuged and dried to leave 374 mg (92%) of **21** as an almost colorless solid: ^{1}H NMR (D_2O) δ 2.383 (s, 3), 7.151 (d, 1, J = 8.7), 7.306 (dd, 1, J = 1.8, J = 8.7), 7.451 (d, 1, J = 1.8). Anal. Calcd for $C_8H_{11}BN_2O_3HCl$: C, 41.67; H, 5.25; N, 12.17. Found: C, 41.23; H, 4.74; N, 11.61.

6-Acetamido-3-isothiocyanatophenylboronic Acid (22). To a solution of 46.1 mg (0.200 mmol) of **21** in methanol (2 mL) was added 64.2 mg (0.764 mmol) of $NaHCO_3$ followed by 1.5 mL (0.315 mmol) of 0.21 N thiophosgene in $CHCl_3$. The mixture was stirred at 25 °C for 2 h and evaporated to dryness. The red solid was dissolved in methanol (3 mL) and the solution was added dropwise into ether (16 mL). After centrifugation, the clear pale red supernatant was removed and evaporated to leave a pale red solid which was partially dissolved in methanol (1 mL), and the mixture was diluted with ether (4 mL) and centrifuged. The pale red precipitate was washed twice with ether (4 mL) to remove colored material. The resulting colorless solid was air-dried, amounting to 32 mg (68%) of **22**: IR (KBr) 3000–3600, 2119 (s), 2078 (s), 1638, 1400, 1110 cm^{-1}; ^{1}H NMR (MeOH-d_4), 2.408 (s, 3), 7.047 (d, 1, J = 8.3), 7.201 (dd, 1, J = 2.2, J = 8.3), 7.300 (d, 1, J = 2.2), and 3.335 (s, 4, MeOH imp.). When the sample in the NMR tube was evaporated to dryness and redissolved in MeOH-d_4, the ^{1}H NMR spectrum then showed no peak at δ 3.335. A sample of **22** showed no weight loss nor NMR spectral changes after being dried under vacuum (0.05 mm) at 25 °C for 6 days and 58 °C for 1 day. Anal. Calcd for $C_9H_9BN_2O_3S$–1.4MeOH–1.0H_2O: C, 47.51; H, 4.83; N, 10.65. Found: C, 47.61; H, 4.37; N, 10.27. Another sample of **22** was dissolved in methanol (2 mL) and the solution was diluted with water (2 mL). The resulting solution was evaporated to dryness and the solid was dried under vacuum (0.05 mm) for 2 days. Anal. Calcd for $C_9H_9BN_2O_3S$+0.2MeOH–0.45H_2O: C, 47.15; H, 3.82; N, 11.95. Found: C, 47.48; H, 3.39; N, 11.55. These analytical results are consistent with ready partial formation of the methyl ester of **22** and associated water loss.

Measurement of Equilibrium Constant of Boronate 13 with Boronic Acid 8 and Ethylene Glycol (9). A solution of 1.5 mg of boronate **13** in 0.5 mL of DMSO-d_6 (newly opened bottle) was prepared and its ^{1}H NMR spectrum was measured. To the sample was added about 10 μL of water and ^{1}H NMR measurement was carried out several times (every 10–20 min) until no more change was observed (after 2.5 h). The equilibrium constant was calculated according to eq 3 based on the integrals of **8**, **9**, **13**, and H_2O of the equilibrium composition. A value of K_{eq} = 55 M was obtained. The time taken to reach equilibrium in hydrolysis was noted as t_h. In another experiment, a solution of 7.9 mg of boronic acid **8** with about 30 μL of water and 2.6 mg of ethylene glycol (**9**) in 0.5 mL of DMSO-d_6 was prepared. Its ^{1}H NMR spectrum was measured every 1–2 min until no more change was observed (after 10 min) and the equilibrium constant was calculated in a similar manner as above. A value of K_{eq} = 56 M was obtained. The time taken to reach equilibrium in esterification was recorded as t_e.

Equilibrium constants for other boronates were measured and calculated in a similar manner as above and the results are collected in Table I.

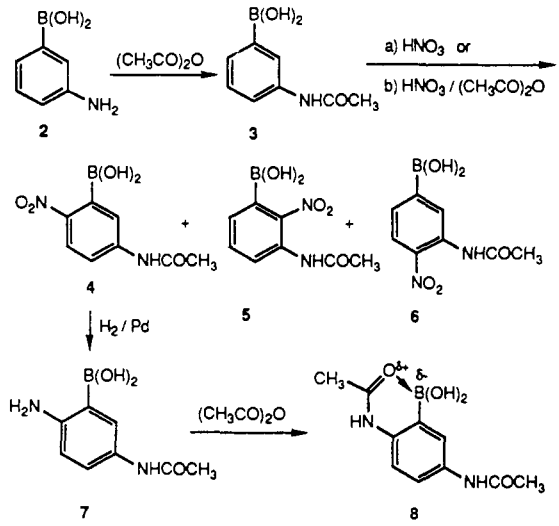
Comparative Hydrolysis of Boronates. A solution with 3.5 mg of boronate **16** and 2.9 mg of boronate **15** in 0.5 mL of DMSO-d_6 was prepared and its ^{1}H NMR spectrum was measured. Water (about 20 μL) was added and ^{1}H NMR was measured every 15–20 min until no more change was observed (in 1.5 h). The final composition, calculated from the integrals of the reactants and the products, showed that >98% of **15** was hydrolyzed while no hydrolysis of **16** was observed. Comparative hydrolysis of other pairs of boronates was measured in a similar manner and the results are collected in Table II.

RESULTS AND DISCUSSION

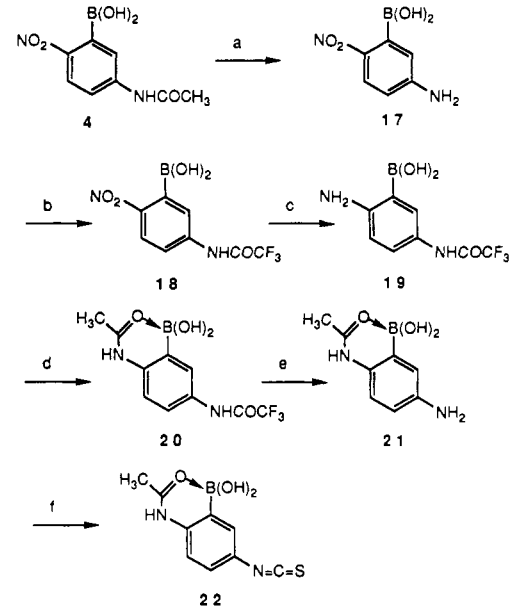
o-Acetamidophenylboronic acid (**8**) (Scheme I) was selected as our first target molecule with the expectation that the carbonyl group should act as a fourth ligand for the boron. *o*-Nitrophenylboronic acid **4** is known (*18*) and can be prepared easily. The *m*-acetamido group constitutes a masked active site which may be used for subsequent attachment to a reporter molecule. Apparently, only two substituted *o*-acetamidophenylboronic acids have been reported and those were described without detailed structural characterization (*19*).

Acetylation of 3-aminophenylboronic acid (**2**) monohydrate gave **3**, which was nitrated with fuming nitric acid (method a) to produce a mixture of 6-nitro (**4**) and 2-nitro (**5**) isomers in a ratio of 4:1 with little 4-nitro isomer as determined by ^{1}H NMR spectroscopy. Torssell (*18*)

Scheme I



Scheme II[a]



[a] (a) (1) $HCl/H_2O/85$ °C, (2) NaOH; (b) $(CF_3CO)_2O$; (c) H_2/Pd; (d) $(CH_3CO)_2O$; (e) $K_2CO_3/H_2O/MeOH$; (f) $SCCl_2/NaHCO_3$/MeOH.

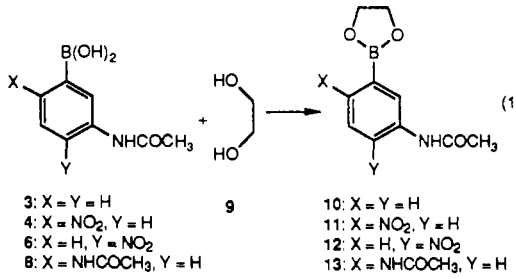
reported that extraction of the nitration mixture with boiling xylene (three times) left the 6-nitro isomer. We found that extraction of the mixture in a Soxhlet extractor with xylene left the desirable 6-nitro isomer **4** (70%) in the extraction thimble. The 2- and 4-nitro isomers were recovered from the xylene extract and separated by fractional crystallization from ethyl acetate. The 2-nitro isomer **5** was obtained as a yellow solid in 4% yield, while the 4-nitro isomer **6** was obtained as a yellow solid in 8% yield.

Catalytic hydrogenation of **4** produced amino boronic acid **7**, which was acetylated with acetic anhydride to give *o*-acetamidophenylboronic acid **8**. The ^1H NMR (D_2O) spectrum of **8** showed two three-proton singlets at δ 2.141 and 2.349, corresponding to the two CH_3CO groups. The singlet at δ 2.349 is ascribed to the *o*-acetamido group. The lower field position is consistent with the presence of an O–B interaction, which results in a partial positive charge on the carbonyl group. After excess NaOH was added to the D_2O solution, only one peak (δ 2.128) was observed for the two CH_3CO groups. This is probably because in basic solution the coordination of the carbonyl to the boron was replaced by hydroxide ion coordination. Arylboronic acids are generally known to behave as Lewis acids toward hydroxide ion and not as protic acids (*20*).

The presence of an O–B coordination in **8** was confirmed by ^{11}B NMR spectroscopy. ^{11}B NMR signals of tetracoordinate species are known generally to be found several tens of ppm (δ) to higher field (low δ value) compared to the nearest equivalent tricoordinate species (*21*). The ^{11}B NMR spectrum of **8** (D_2O) showed a peak at δ 4.1, which is in the region for tetracoordinate boron (*22*). By way of comparison, **3** and **4** (D_2O) showed a peak at δ 29.2 and 28.6, respectively, which is in the region for tricoordinated boron (*22*). Small sharp peaks at δ 19.5 and 19.8 were also observed for **3** and **4**, respectively. These are probably the weakly water coordinated complexes or, in the case of **4**, a nitro-coordinated complex.

When excess NaOH was added to the D_2O solution of boronic acids **3**, **4**, and **8**, the ^{11}B resonance peak shifted to δ 2.5, 1.9, and 2.3, respectively, consistent with tetracoordinated boron species. The relatively small chemical shift change for **8** (−1.8 ppm) and the large change for **3** (−26.7 ppm) and **4** (−26.7 ppm) demonstrates that there is likely a change of coordinate number with **3** and **4** (from tricoordinate to tetracoordinate) while no change occurs with **8**. These ^{11}B NMR chemical shift changes by addition of base parallel the observations made by Dewar and Jones (*20*) for phenylboronic acid (δ 28.4 in EtOH and δ 3.15 in H_2O–NaOH). We observed that the signals with lower δ values (tetracoordinated species) are relatively sharp while the signals with higher δ values (tricoordinated species) are broad, which is in agreement with other reported ^{11}B NMR spectra (*20*).

Having established the O–B interaction in boronic acid **8**, we next turned to the preparation of boronate esters derived from **8** in order to determine their stability toward hydrolysis. Condensation of boronic acids **3**, **4**, **6**, and **8** with ethylene glycol produced boronates **10**, **11**, **12**, and **13**, respectively (eq 1). Two features in the ^1H NMR



(1)

3: X = Y = H
4: X = NO_2, Y = H
6: X = H, Y = NO_2
8: X = $NHCOCH_3$, Y = H

9

10: X = Y = H
11: X = NO_2, Y = H
12: X = H, Y = NO_2
13: X = $NHCOCH_3$, Y = H

spectrum of boronate **13** (DMSO-d_6) suggested the presence of an O–B interaction. The acetyl methyl groups had quite different chemical shifts (δ 1.988 and 2.270, cf. **8**) and the protons of the ethylene group had a chemical shift of δ 3.806. By way of comparison, the protons of the ethylene group of boronates **10**–**12** all had chemical shifts around δ 4.4 (both in $CDCl_3$ and DMSO-d_6). The presence of a partial negative charge on the tetracoordinated boron of boronate **13** was likely responsible for the upfield shift of the ethylene group. Interestingly, boronates **10**–**12** were all easily soluble in $CDCl_3$, whereas **13** was insoluble in $CDCl_3$. This observation may be attributed to the zwitterionic nature of boronate **13**. The ^{11}B NMR spectrum was also consistent with the presence of an O–B interaction in boronate **13**. A peak for **13** was observed at δ 8.6, while boronates **10** and **11** both had a peak at δ 31.7.

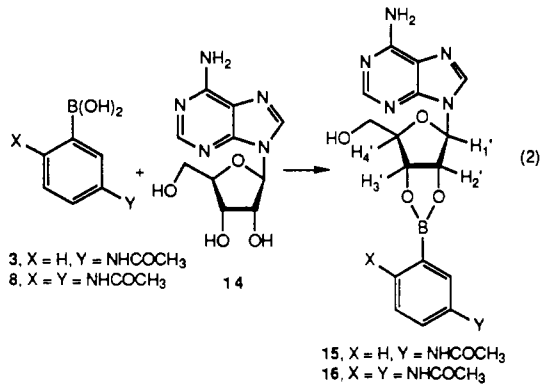
Phenylboronic acid has been used as a protecting group for the ribose 2′,3′-*cis*-diol group in the phosphorylation

Table I. Equilibrium Constants of Boronic Acids and Ethylene Glycol with Boronates in DMSO-d_6 Containing Limited Amounts of Water

acid	boronate	K_{eq},[a] M	t_e,[b] min	t_h,[b] min
3	10	0.48	120	11
4	11	0.20		
6	12	0.10		
8	13	55	10	150

[a] K_{eq} = [boronate][H_2O]^2/[boronic Acid][9]. [b] t_e is the time taken to reach equilibrium in esterification; t_h is the time taken to reach equilibrium in hydrolysis.

of adenosine. Deprotection during phosphorylation was observed which resulted in the production of monophosphates and diphosphates (*13*). We chose to study the protection–deprotection reaction using boronic acids 3 and 8 and adenosine as a model substrate for the vicinal *cis*-diol moiety of carbohydrates. Condensation of boronic acids 3 and 8 with adenosine (14) produced the 2′,3′-boronates 15 and 16, respectively (eq 2). The ^{1}H NMR



(2)

(DMSO-d_6) chemical shifts of the ribose protons of ester 16 are shifted upfield ($H_{1'}$, δ 6.061; $H_{2'}$, 5.026; $H_{3'}$, 4.692; $H_{4'}$, 4.131) compared to those of ester 15 ($H_{1'}$, δ 6.255; $H_{2'}$, 5.731; $H_{3'}$, 5.226; $H_{4'}$, 4.251), reflecting the presence of an O–B interaction in boronate 16. The peak assignments were supported by a series of proton-decoupling experiments applied to 15 (see Experimental Procedures).

There are few reports concerning the position of equilibrium of esterification and hydrolysis reactions of boronates in organic solvent (*23*). Since boronate 13 is soluble in DMSO, the hydrolysis of 13 was monitored by ^{1}H NMR spectroscopy in DMSO-d_6 containing limited amounts of water and compared to other boronates in the same solvent system. Identical values for the equilibrium constant were found for the forward reaction starting from boronic acid 8 and ethylene glycol (9), and the reverse reaction starting from boronate 13 (eq 3). Equilibrium constants for boronates 10–12 were measured under the same conditions and are shown in Table I.

$$8 + 9 \underset{k_{-1}}{\overset{k_1}{\rightleftharpoons}} 13 + 2H_2O \qquad (3)$$

Table I shows that the equilibrium constants of boronates 10–12 are close to each other. Therefore substitution of a nitro group at the ortho or para position had little effect on the boronate–boronic acid equilibrium. On the other hand, the equilibrium constant of boronate 13 is more than 100 times that of boronate 10. Thus the presence of an *o*-acetamido group in phenylboronic acid 8 shifted the equilibrium toward the boronate direction, possibly due to the O–B interaction.

Table II. Comparative Hydrolysis of Boronates in DMSO-d_6 Containing Limited Amounts of Water (Eq 4)

a	b	c	d
10	12	3 (18%)	6 (38%)
11	12	4 (70%)	6 (40%)
13	10	8 (<1%)	3 (92%)
16	15	8 (<1%)	3 (>98%)

It was noted from the difference in t_e (time taken to reach equilibrium in esterification) between 8 and 3 that, qualitatively, the rate of formation of boronate 13 from boronic acid 8 and ethylene glycol was faster than that of boronate 10 from boronic acid 3. The difference in t_h (time taken to reach equilibrium in hydrolysis) between 13 and 10 showed that hydrolysis of 13 was slower than that of 10. These values show that the O–B interaction in 8 both accelerates the rate of esterification and reduces the rate of hydrolysis of the corresponding boronate 13.

The differences in stability of the boronates toward hydrolysis were also measured by direct comparisons of pairs of boronates in the same solution. By measuring the equilibrium composition of a solution of pairs of boronates (a and b) in DMSO-d_6 in the presence of limited amounts of water using ^{1}H NMR spectroscopy, the percentages of hydrolysis of boronates a and b were obtained, respectively (eq 4). The results, reported as the percentage of the cor-

$$a + b + 2H_2O \overset{\text{DMSO-}d_6}{\rightleftharpoons} c + d + \text{diol} \qquad (4)$$

responding boronic acids c and d present in solution at equilibrium, are collected in Table II.

Table II shows that the differences in the extent of hydrolysis between two pairs of trigonal boronates 10 (18%) and 12 (38%) and 11 (40%) and 12 (70%) are quite small. These values are in accordance with the similar values of the equilibrium constants of the individual boronates (Table I). As expected from the values given in Table I for boronic acids 3 and 8, the difference in extent of hydrolysis between tetracoordinate boronate 13 (<1%) and trigonal boronate 10 (92%) is large. A similar observation was made for adenosine 2′,3′-boronates 16 and 15. With limited amounts of water, no hydrolysis of 16 could be detected by ^{1}H NMR while almost all of 15 had been hydrolyzed. The stability of boronates 13 and 16 toward hydrolysis demonstrates that boronic acid 8, or a more strongly coordinated version, is to be preferred for modification of carbohydrates.

Having demonstrated that the O–B interaction in boronic acid 8 stabilized its corresponding boronates 13 and 16 toward hydrolysis, we then turned to the synthesis of an *o*-acetamidophenylboronic acid containing a free amino group in the 3-position which may serve as a site for a bioconjugation reaction. Since a trifluoroacetamido group can be hydrolyzed under mild basic conditions such as potassium carbonate (25 °C) (*24*), we sought to replace the *m*-acetamido group in 8 by a trifluoroacetamido group (Scheme II). Thus the acetamido group in 4 was hydrolyzed to give amine 17. Reaction of 17 with trifluoroacetic anhydride gave amide 18. Hydrogenation of 18 gave amine 19, which was allowed to react with acetic anhydride to produce amide 20. Hydrolysis of 20 under mild conditions (K_2CO_3/MeOH/H_2O) selectively removed the trifluoroacetyl protecting group to give amine 21. Reaction of 21 with thiophosgene under basic conditions led to isothiocyanate 22, a derivative suitable for attachment to an amine-containing target molecule by way of a thiourea linkage.

In conclusion, the presence of an O–B interaction in boronic acid 8 has been established by ^{11}B and ^{1}H NMR

spectroscopy. The O–B interaction was found to stabilize boronates **13** and **16** toward hydrolysis and to accelerate esterification of boronic acid **8** in comparison with those without the O–B interaction. With these desirable properties, *o*-acetamido-substituted phenylboronic acids should find application as a linker for bioconjugation, as well as protecting groups in the synthesis of nucleosides and carbohydrates, and as ligands for affinity chromatography.

ACKNOWLEDGMENT

This work was supported by NIH Grant GM-27137. We thank Dr. Sandip K. Sur for his help in obtaining ^{11}B NMR spectra.

LITERATURE CITED

(1) Han, K.-K., Claude, R., and Delacourte, A. (1984) Chemical cross-links of proteins by using bifunctional reagents. *Int. J. Biochem. 16*, 129.

(2) Blair, A. H., and Ghose, T. I. (1983) Linkage of cytotoxic agents to immunoglobulins. *J. Immunol. Methods 59*, 129.

(3) Upeslacis, J., and Hinman, L. (1988) Chemical modification of antibodies for cancer chemotherapy. *Annu. Rep. Med. Chem. 23*, 151.

(4) Ghose, T. I., Blair, A. H., and Kulkarni, P. N. (1983) Preparation of antibody-liked cytotoxic agents. *Methods Enzymol. 93*, 280.

(5) Schweizer, E., Angst, W. and Lutz, H. U. (1982) *Biochemistry 21*, 6807.

(6) Rodwell, J. D., Alvares, V. L., Lee, C.; Lopes, A. D., Goers, J. W. F., King, H. D., Powsner, H. J., and Mckearn, T. J. (1986) Site-specific covalent modification of monoclonal antibodies: In vitro and in vivo evaluations. *Proc. Natl. Acad. Sci. U.S.A. 83*, 2632.

(7) O'Shannessy, D. J., and Quarles, R. H. (1987) Labeling of the oligosaccharide moieties of immunoglobulins. *J. Immunol. Methods 99*, 153.

(8) Koppel, G. A. (1990) Recent advances with monoclonal antibody drug targeting for the treatment of human cancer. *Bioconjugate Chem. 1*, 13.

(9) Pietersz, G. A. (1990) The linkage of cytotoxic drugs to monoclonal antibodies for the treatment of cancer. *Bioconjugate Chem. 1*, 89.

(10) Clamp, J. R., and Hough, L. (1965) The periodate oxidation of amino acids with reference to studies on glycoproteins. *Biochem. J. 94*, 17.

(11) Fulton, S. (1981) *Boronate Ligands in Biochemical Separations*, Amicon Corp., Danvers, MA.

(12) Mazzeo, J. R., and Krull, I. S. (1989) Immobilized boronates for the isolation and separation of bioanalytes. *BioChromatography 4*, 124.

(13) Yurkevich, A. M., Kolodkina, I. I., Varshavskaya, L. S., Borodulina-Shvetz, V. I., Rudakova, I. P., and Preobrazhenski, N. A. (1969) The reaction of phenylboronic acid with nucleosides and mononucleotides. *Tetrahedron, 25*, 477.

(14) Ferrier, R. J. (1978) Carbohydrate boronates. *Adv. Carbohydr. Chem. Biochem. 35*, 31.

(15) Bowie, R. A., and Musgrave, O. C. (1963) Organoboron compounds. Part V. The hydrolysis of cyclic phenylboronates. *J. Chem. Soc.* 3945.

(16) Wulff, G., Lauer, M., and Bohnke, H. (1985) Rapid proton transfer as cause of an unusually large neighboring group effect. *Angew. Chem. Int. Ed. Engl. 23*, 741.

(17) Johnson, B. J. B. (1981) Synthesis of a nitrobenzeneboronic acid substituted polyacrylamide and its use in purifying isoaccepting transfer ribonucleic acids. *Biochemistry, 20*, 6103.

(18) Torssell, V. K. (1957) Arylboronic acids IV. Nitration of several arylboronic acids and characteristics of the boron–carbon bond. *Ark. Kemi. 10*, 513 [*Chem. Abstr.* (1958) *51*, 14555].

(19) (a) Soloway, A. H. (1960) Synthesis of aromatic diboronic acids. *J. Am. Chem. Soc. 82*, 2442. (b) Bartlett, R. K., Turner, H. S., Warne, R. J., Young, M. A., and Lawrenson, I. J. (1966) The reaction of primary amines with boron halides. Part II. Arylamines. The effect of ortho-substitution: formation of di-*B*-halogenoborazoles. *J. Chem. Soc. A* 479.

(20) Dewar, M. J. S., and Jones, R. (1967) New heteroaromatic compounds. XXV. Studies of salt formation in boron oxyacids by B nuclear magnetic resonance. *J. Am. Chem. Soc. 89*, 2408.

(21) Kennedy, J. D. (1987) *Multinuclear NMR* (J. Mason, Ed.) Chapter 8, Plenum Press, New York.

(22) Noth, H., and Wrackmeyer, B. (1978) *Nuclear Magnetic Resonance Spectroscopy of Boron Compounds*, Springer-Verlag, Berlin.

(23) Wulff, G., Dederichs, W., Grotstollen, R., and Jupe, C. (1982) Specific binding of substances to polymers by fast and reversible covalent interactions. *Affinity Chromatography and Related Techniques* (T. C. J., Gribnau, J. Visser, and R. J. F., Nivard, Eds.) p 207, Elsevier, Amsterdam.

(24) Quick, J., Meltz, C. (1979) The pelletierine condensation. Mechanistic studies. *J. Org. Chem. 44*, 573.

Rapid Synthesis and Introduction of a Protected EDTA-like Group during the Solid-Phase Assembly of Peptides

Rajiv Arya and Jean Gariépy*

Department of Medical Biophysics, University of Toronto, 500 Sherbourne Street, Toronto, Ontario, Canada M4X 1K9. Received March 11, 1991

A simple two-step procedure is reported for the synthesis of a *tert*-butyl ester protected form of an EDTA-like bifunctional chelating agent. This reagent can be easily introduced on any available amino group during the assembly of peptides on solid-phase supports. Using the model tetradecapeptide OVA(323–336), we have introduced an EDTA group at the N-terminus of this T-cell epitope and confirmed that the EDTA group is present on the molecule, can chelate metals, and does not affect the biological activity of the peptide.

INTRODUCTION

Advances in the field of conjugate chemistry have allowed the introduction of metal-binding sites on macromolecules through the use of bifunctional chelators. Iron–EDTA[1]-labeled DNA-binding peptides and oligonucleotides are now being designed for the selective cleavage of DNA molecules (*1–4*). Furthermore, small molecules derivatized with this chelating group can act as sequence-specific cleaving agents for proteins such as streptavidin (*5*), calmodulin (*6*), and bovine serum albumin (*7*). More importantly, the labeling of proteins with metal chelators has allowed the use of more appropriate radionuclides (^{111}In, ^{99m}Tc, and ^{90}Y) for in vivo tumor localization and radioimmunotherapy (*8–10*). The widespread utility of bifunctional EDTA-like chelators for labeling proteins has been compromised by long and tedious synthetic routes required to make reactive or protected derivatives (*11–14*) or by the reduced metal-binding affinity of the chelating moiety for cations resulting from the use of one of the carboxylic arms of EDTA to anchor the chelating site to the macromolecule (*15*). This latter property can be particularly limiting if the metal-labeled bioconjugate is to be administered in vivo, where transchelation effects by serum proteins have been responsible for the observed loss of the radiolabel from radioimmunoconjugates labeled with bifunctional chelating agents (*16*).

In this report, we describe a simple two-step synthesis of an EDTA-like bifunctional chelating agent that carries, in addition to a protected form of the chelating function, a free carboxylic group that permits it to be covalently linked to macromolecules. The chelator has been synthesized with an acid-labile protecting group (*tert*-butyl group) at all four carboxylic arms of the EDTA site. The nature of this protected chelating agent allows it to be easily adapted to solid-phase peptide-synthesis techniques so as to introduce metal-binding sites at defined positions in peptides. In order to assess the usefulness of the compound, we introduced an EDTA-site at the N-terminus of a peptide comprising residues 323–336 of chicken ovalbumin using the protected bifunctional chelator **3** (Figure 1). This synthetic peptide represents a determinant recognized by the ovalbumin-specific, I-A^d restricted, T-cell hybridoma 3DO-54.8 (*17–19*).

EXPERIMENTAL PROCEDURES

Materials. Trifluoroacetic acid (sequencing grade), diisopropylethylamine (sequencing grade), and α,β-diaminopropionic acid were purchased from Schweizerhall Inc. (South Plainfield, NJ). *tert*-Butyl bromoacetate was obtained from Aldrich Chemical Co. (Milwaukee, WI). Sodium thiophenoxide was prepared by the addition of thiophenol to a molar equivalent of sodium metal in diethyl ether. The suspension was vigorously shaken for 72 h at room temperature and the resulting sodium thiophenoxide was recovered by filtration (*21*). All reagent grade solvents were purchased from BDH (Toronto, Ontario, Canada). $^{153}GdCl_3$ (specific activity < 84 μCi/μg) and $^{111}InCl_3$ (specific activity > 10 mCi/μg) were obtained from Amersham (Oakville, Ontario, Canada). Protected amino acids were purchased from Aminotech (Nepean, Ontario, Canada), and PAM-resin was from Applied Biosystems (Mississauga, Ontario, Canada). Peptide synthesis was performed on an Applied Biosystems Model 430 peptide synthesizer. ^{1}H NMR spectra were recorded at 500 MHz on a Bruker AM-500 spectrometer. Fast atom bombardment mass spectra were recorded on a VG mass spectrometer (VG Instruments; Danvers, MA). DEAE-Sephacel was purchased from Pharmacia (Montréal, Québec, Canada), while the HPLC C_{18} μBondapak analytical column and the C_{18} SEP-PAK cartridges were obtained from Waters (Millipore; Milford, MA). Thin-layer chromatography (TLC) was performed on Whatman (1 mm × 3 mm) silica gel coated glass plates. Silica gel (200–450 mesh) for column chromatography was obtained from Fisher Scientific (Toronto, Ontario, Canada). Elemental analysis was performed by Galbraith Laboratories (Knoxville, TN). The maintenance of cell lines 3DO.54.8 (*17*) and CTLL (*20*) was described elsewhere (*18, 19*).

Chemical Syntheses. Figure 1 illustrates the simple two-step procedure for the preparation of the *tert*-butyl-protected form of the chelate. In the first step, α,β-diaminopropionic acid (1; 4.75 g, 0.034 mol), was refluxed for 20 h in 100 mL of redistilled acetonitrile in the presence of diisopropylethylamine (DIEA; 30 mL, 0.33 mol) and $BrCH_2COO$-*t*-Bu (30 mL, 0.22 mol) to give the carboxy-

* Author to whom correspondence should be addressed.

[1] Abbreviations used: *t*-BOC, *tert*-butyloxycarbonyl; EDTA, ethylenediaminetetraacetic acid; EDTA–OVA(323–336), peptide comprising residues 323–336 of chicken ovalbumin and derivatized at its N-terminus with an EDTA group; OVA(323–336), peptide comprising residues 323–336 of chicken ovalbumin; PAM, (phenylacetamido)methyl; DIEA, diisopropylethylamine; TFA, trifluoroacetic acid; Asx, asparagine/aspartic Acid; Glx, glutamine/glutamic acid; Ser, serine; His, histidine; Ala, alanine; Val, valine; Ile, isoleucine; IL-2, interleukin-2.

1043-1802/91/2902-0323$02.50/0 © 1991 American Chemical Society

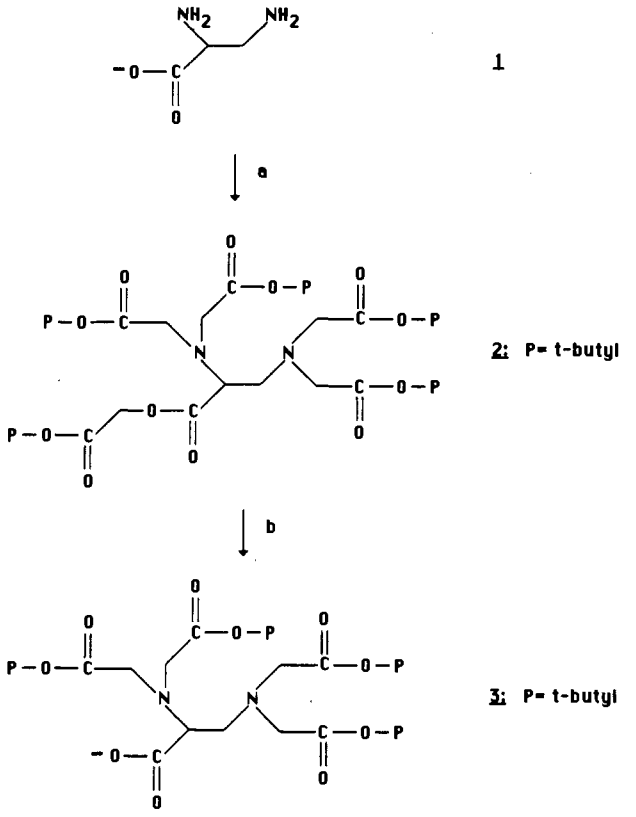


Figure 1. Two-step synthesis scheme for the preparation of a protected EDTA-like chelator starting with α,β-diaminopropionic acid. (a) *tert*-Butyl bromoacetate, DIEA, acetonitrile, reflux. 20 h; (b) thiophenoxide, DMF, 100 °C, 2 h.

methylated intermediate **2** in Figure 1. *tert*-Butyl-protected intermediate **2** was isolated from the reaction mixture by the following procedure: upon cooling, the reaction mixture was precipitated with toluene to remove DIEA·HBr, filtered through a Whatman #4 cellulose filter, and evaporated to dryness under reduced pressure on a rotary evaporator. The resulting oily cake was redissolved in 200 mL of toluene, refiltered, and extracted with 0.1 M phosphate buffer, pH 2, to remove excess DIEA. The extracted organic phase was dried over $MgSO_4$, filtered, and evaporated to dryness under reduced pressure. The resulting brown oil was diluted with a small volume of chloroform (2–5 mL) and loaded on a silica gel chromatography column (3 cm × 40 cm) equilibrated with 5% (v/v) acetone in chloroform. Eluting with 5% (v/v) acetone in chloroform provided *tert*-butyl-protected intermediate **2** in 60–80% yield as a golden-yellow oil. Homogeneity of the purified intermediate **2** was analyzed by TLC on silica plates using two solvent systems (system 1, acetone/chloroform, 5:95; system 2, glacial acetic acid/acetone, 2:98). R_f values for **2** were 0.50 (system 1) and 0.45 (system 2). ^1H NMR ($CDCl_3$): 1.5 (s, 45 H), 3.1 (2 d, J = 8.3 Hz, 1 H), 3.2 (2 d, J = 5.8 Hz, 1 H), 3.5 (m, 8 H), 3.8 (2 d, J = 6.0 Hz, 1 H), 4.5 ppm (2 d, J = 15.7 Hz, 2 H). IR: 1730 cm^{-1} (C=O, s). MS (FAB): m/e 675$^+$ (MH^+).

tert-Butyl-protected intermediate **2** (9.1 g, 13.5 mmol) was readily converted to the protected form of the bifunctional chelating agent (**3**) upon incubation at 100 °C for 2 h in 15 mL of redistilled dimethylformamide in the presence of 1 molar equiv of sodium thiophenoxide (1.75 g, 13.5 mmol) (*23*). Compound **3** was isolated from the reaction mixture by first precipitating the reaction mixture with ethyl acetate to remove excess thiophenoxide and polar reaction byproducts, followed by filtration through Whatman #5 cellulose filters, and finally by extracting the organic filtrate with 0.1 M phosphate buffer, pH 2. The resulting organic phase was evaporated under reduced pressure. The remaining oil was dissolved in a small volume of toluene (maximum of 5 mL) and loaded on a silica gel chromatography column (2.2 cm × 40 cm) equilibrated with toluene. The column was then washed with 5 column volumes of toluene to remove residual thiophenol and unreacted compound **2**. The desired product was eluted with 2% (v/v) glacial acetic acid in acetone. The silica gel chromatography purification step was repeated once to afford the final pure product (**3**) as a tertiary amine acetate salt in 70% yield upon evaporation. Homogeneity of the purified **3** was analyzed by TLC on silica plates using two solvent systems (system 1, acetone/chloroform, 5:95; system 2, glacial acetic acid/acetone, 2:98). R_f values for **3** were 0.0 (system 1) and 0.40 (system 2). ^1H NMR ($CDCl_3$): 1.5 (s, 36 H), 3.1 (d, J = 7.4 Hz, 2 H), 3.5 (m, 8 H), 3.7 ppm (t, J = 7.4 Hz, 1 H). IR: 3200 (COO–H, br), 1730 cm^{-1} (C=O, s). MS (FAB): m/e 561$^+$ (MH^+). Anal. Calcd (acetate salt of compound **3**) $C_{27}H_{48}N_2O_{10}\cdot C_2H_3O_2$: C, 56.21; H, 8.29; N, 4.52. Found: C, 56.09; H, 8.09; N, 4.61.

Introduction of an EDTA Site on a Model Peptide. A peptide comprising the residues 323–336 of chicken ovalbumin [OVA(323–336)] was assembled on a PAM-resin support using conventional solid-phase peptide-synthesis protocols and t-BOC-protected amino acids (*22*). Before the final cleavage of the peptide from the solid support, compound **3** (0.84 g, 1.5 mmol) dissolved in DMF was coupled to the N-terminal amino group (0.5 mmol of amino groups present on the resin sample) of the peptide in the presence of dicyclohexylcarbodiimide (0.32 g, 1.55 mmol). The reaction was left to proceed overnight at room temperature. The coupling procedure was repeated in dichloromethane to insure complete derivatization of all free amino groups as monitored by using a quantitative ninhydrin test (*22*). Cleavage of the peptide from the resin using anhydrous hydrogen fluoride gave the fully deprotected peptide carrying a free EDTA group [abbreviated EDTA–OVA(323–336)] (see Figure 2A).

Purification and Characterization of EDTA–OVA(323–336). The peptide EDTA–OVA(323–336) was purified by ion-exchange chromatography on DEAE-Sephacel (25 mm × 150 mm column) using a 0–0.5 M NaCl gradient, followed by reverse-phase HPLC on a μBondapak C_{18} column (1 cm × 25 cm column). The reverse-phase column was initially equilibrated in 0.1% (v/v) TFA/water and the peptide was eluted with a linear gradient of 0.08% (v/v) TFA/acetonitrile going from 0 to 40% in 30 min. Peaks isolated with HPLC were characterized by amino acid analysis, mass spectroscopy, and ^1H NMR (D_2O) in order to identify EDTA–OVA(323–336).

Radiolabeling of EDTA–OVA(323–336). To confirm that the EDTA group present could chelate metals, EDTA–OVA(323–336) was radiolabeled with $^{153}GdCl_3$ and $^{111}InCl_3$. The specific activities achieved were 3.7 μCi/μg and 1.0 mCi/μg, respectively. Radiolabeling of the peptide was performed as described below; deionized water used in preparing all buffers was initially depleted of any metal contaminants by passage through a Chelex-100 resin bed (200–400 mesh, sodium form; Bio-Rad Laboratories, Richmond, CA). Upon HPLC purification, EDTA–OVA(323–336) was lyophilized and redissolved in 0.1 M HCl. Ten microliters of $^{153}GdCl_3$ (20 μCi; > 1.3 × 10^{-9} mol) in 0.1 M HCl was added to a solution containing 1 μg of the peptide (5.5 × 10^{-10} mol) in 40 μL of 0.1 M HCl and

incubated for 30 min at room temperature. Four hundred and fifty microliters of 10 mM PIPES buffer, pH 6.5, was added to the radiolabeling mixture, and the resulting solution loaded on a C_{18} SEP-PAK cartridge equilibrated with 10 mM PEPES buffer, pH 6.5. The cartridge was washed with 10 mL of 10 mM PIPES, pH 6.5. The labeled peptide was eluted from the cartridge with a 1:1 solution of acetonitrile and 10 mM PIPES, pH 6.5. No counts above background were eluted from the cartridge with the 1:1 solution of AcN/10 mM PIPES, pH 6.5, when the same procedure was repeated in the absence of peptide. The radiolabeling procedure was also performed with 250 μL of $^{153}GdCl_3$ (500 μCi) in 0.1 M HCl to label either 1 μg or 10 μg of EDTA–OVA(323–336). In all cases, the specific activity achieved was 3.7 μCi/μg.

A similar protocol was used to label EDTA–OVA(323–336) with $^{111}InCl_3$. Briefly, 1 μg of EDTA–OVA(323–336) (5.5×10^{-10} mol) was incubated for 30 min in the presence of 100 μL of $^{111}InCl_3$ (1 mCi, $<9 \times 10^{-10}$ mol) in 0.1 M HCl, and the labeled peptide purified on a C_{18} SEP-PAK cartridge as described above. The specific activity achieved was 1.0 mCi/μg.

T-Cell Activation Assay. In order to evaluate the effect of modifying the peptide through the addition of an EDTA group, we measured the ability of EDTA–OVA(323–336) to activate the I-A^d restricted T-cell hydridoma 3DO-54.8 to secrete interleukin-2 (IL-2) (*18*, *19*). Concentration of IL-2 secreted into the cell supernatant was measured in a cell-proliferation assay using the IL-2 dependent cell line CTLL (*18*, *19*). The extent of cell proliferation was determined by the uptake of tritiated thymidine by CTLL cells in the presence of varying dilutions of IL-2-containing supernatants. Both EDTA–OVA(323–336) and the peptide lacking the chelating group gave identical response at a concentration of peptide previously shown to be limiting in the T-cell assay (Figure 2B) (*19*).

RESULTS AND DISCUSSION

In light of the growing interest in the design of novel protein conjugates containing metal chelators, we have developed a simple strategy for the synthesis of an EDTA-like chelator protected with an acid-labile *tert*-butyl ester group. The usefulness of this reagent stems from the fact that it can be easily produced in gram quantities and that it can be coupled readily to peptides by using standard solid-phase-synthesis protocols to produce an oligomer molecule carrying an intact EDTA-like chelating group.

Synthesis of Protected Bifunctional Chelators. The protocol outlined in Figure 1 (see Experimental Procedures) describes the two-step synthesis of a protected form of the EDTA-like bifunctional chelate. The first step consists of the carboxymethylation of α,β-diaminopropionic acid (1) to an intermediate containing five protected carboxylic groups (intermediate 2); the second step involves the selective conversion of the intermediate to the final product 3. We had hypothesized that such a selective cleavage of the *tert*-butyl ester group attached to the original carboxylic arm of the diaminopropionic molecule could be achieved in the presence of nucleophilic agents. Under such conditions, the ester groups (*t*-butyl esters) protecting the carboxylic arms of the EDTA site would remain unaffected while the selective cleavage of the *tert*-butyl acetate linkage would be enhanced as a consequence of the withdrawing effect of the acetate ester moiety and the resulting increased positive polarity associated with the carbon atom of the carbonyl group (see Figure 1). Experimentally, the selective cleavage was

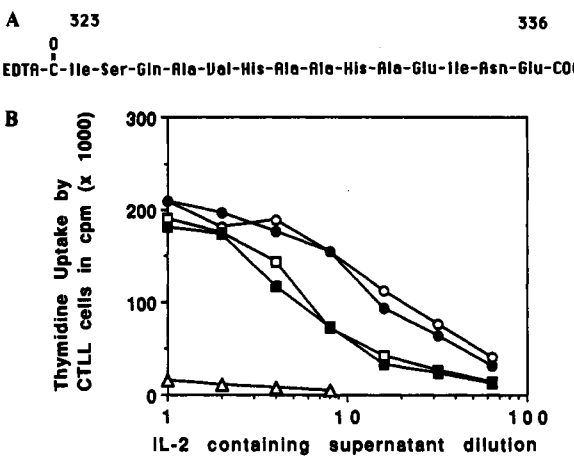


Figure 2. (A) Amino acid sequence of EDTA–OVA(323–336), a peptide comprising residues 323–336 of chicken ovalbumin representing a T-cell epitope recognized by the I-A^d restricted T-cell hybridoma 3DO-54.8. The N-terminus of this peptide was derivatized with an EDTA group. (B) Thymidine uptake by IL-2-dependent CTLL cells as a function of supernatant dilution from activated 3DO-54.8 T cells (*19*). The T-cells were activated to produce IL-2 by incubating them in the presence of peptides [either EDTA–OVA(323–336) (●, ■) or OVA(323–339) (○, □)] and antigen-presenting-cells expressing I-A^d. Titration curves for two peptide concentrations are presented [32 ng/mL (□, ■) and 160 ng/mL (○, ●)]. As a negative control (△), levels of thymidine incorporation by CTLL cells were recorded in the presence of supernatant dilutions from unstimulated 3DO-54.8 T cells (i.e. in the absence of peptide).

confirmed by characterization of the intermediate and final products. In particular, the selective removal of the *tert*-butyl acetate groups from 2, as opposed to the cleavage of the *tert*-butyl groups protecting the chelating moiety of the bifunctional chelate, results in a unique loss of 115 (*tert*-butyl acetate group) mass units. Indeed, the mass spectrum (FAB) of carboxymethylated intermediate 2 and of the purified final product 3 featured the expected molecular ion peaks of 675^+ (2) and 561^+ (3). The conversion of 2 to 3 was also confirmed by IR through the presence of a wide absorption band (O–H stretch at 3200 cm^{-1}), characteristic of a free carboxylic acid group, in the spectrum of the final product as opposed to the absence of the bond stretch in the spectrum of the intermediate. The structures of 2 and 3 were confirmed by ^1H NMR (see Experimental Procedures).

Synthesis, Purification, and Characterization of an EDTA-Containing Peptide. In order to assess the usefulness of the protected bifunctional chelators in labeling peptides on the solid phase, the *tert*-butyl protected chelator 3 was introduced at the N-terminus of a peptide comprising residues 323–336 of chicken ovalbumin to generate the peptide EDTA–OVA(323–336) (Figure 2A). The amino acid composition of the purified peptide was experimentally confirmed by amino acid analysis. The ratio of each amino acid detected in the sample was as follows: Asx, 0.91; Glx, 2.69; Ser, 1.08; His, 1.98; Ala, 3.89; Val, 0.95; Ile, 2.48. Mass spectroscopy (FAB) gave the expected molecular ion for EDTA–OVA(323–336) at 1808^+. ^1H NMR was used to confirm the presence of the EDTA group on the peptide: the characteristic sharp singlet of the NCH_2CO protons of EDTA appeared at 3.9 ppm (8 H); another singlet corresponding to the three *H*CN protons appeared at 3.7 ppm.

The EDTA-Containing Peptide Is Indistinguishable from the Native Peptide as a T-Cell Antigen. Dose–response curves in Figure 2B are reported for two concentrations of peptides (32 and 160 ng/mL). The pep-

tide concentration corresponding to 32 ng/mL of the T-cell epitope having or lacking the EDTA group gave an identical IL-2 response curve at a subsaturation dose of peptide, confirming that the incorporation of the chelating group did not reduce the potency of the peptide in stimulating the production of IL-2 by the ovalbumin specific T-cells.

In conclusion, our goal was to design an EDTA-like bifunctional chelator that could be used directly in solid-phase peptide synthesis. We have shown that (i) we can readily produce gram quantities of a *tert*-butyl-protected form of an EDTA-like metal-chelating agent using a simple two-step procedure, (ii) we can easily introduce this reagent on any available amino group during the assembly of the peptide on the solid phase; (iii) using the model peptide OVA(323–336), we have introduced an EDTA group at the N-terminus of this T-cell epitope; and, finally, (iv) we have confirmed that the EDTA group is present on the molecule, can chelate metals, and does not affect the biological activity of the peptide.

ACKNOWLEDGMENT

This work was supported by a grant from the National Cancer Institute of Canada (J.G.). J.G. is a scholar of the Medical Research Council of Canada. R.A. is a recipient of a University of Toronto Open studentship. We thank Dr. Henrianna Pang and Richard Crombie of the Carbohydrate Research Laboratory, University of Toronto, for performing mass spectroscopy and Dr. Tania Watts for the T-cell assays.

LITERATURE CITED

(1) Hertzberg, R. P., and Dervan, P. B. (1984) Cleavage of DNA with Methidiumpropyl-EDTA-Iron(II): Reaction Conditions and Product Analyses. *Biochemistry 23*, 3934–3945.

(2) Dervan, P. B. (1986) Design of Sequence Specific DNA-Binding Molecules. *Science 232*, 464–471.

(3) Moser, H. E., and Dervan, P. B. (1987) Sequence-Specific Cleavage of Double Helical DNA by Triple Helix Formation. *Science 238*, 645–650.

(4) Sluka, J. P., Horvath, S. J., Bruist, M. F., Simon, M. I., and Dervan, P. B. (1987) Synthesis of a Sequence-Specific DNA-Cleaving Peptide. *Science 238*, 1129–1132.

(5) Hoyer, D., Cho, H., and Schultz, P. G. (1990) A New Strategy for Selective Protein Cleavage. *J. Am. Chem. Soc. 112*, 3249–3251.

(6) Schepartz, A., and Cuenoud, B. (1990) Site Specific Cleavage of the Protein Calmodulin Using a Trifluoperazine-Based Affinity Reagent. *J. Am. Chem. Soc. 112*, 3247–3249.

(7) Rana, T. M., and Meares, C. F. (1990) Specific Cleavage of a Protein by an Attached Iron Chelate. *J. Am. Chem. Soc. 112*, 2457–2458.

(8) Hnatowich, D. J., Layne, W. W., Childs, R. L., Lanteigne, D., Davis, M. A., Griffin, T. W., and Doherty, P. W. (1983) Radioactive Labeling of Antibody: A Simple and Efficient Method. *Science 220*, 613.

(9) Meares, C. F., and Goodwin, D. A. (1984) Linking Radiometals to Proteins with Bifunctional Chelating Agents. *J. Protein Chem. 3*, 215.

(10) Fritzberg, A. R., Abrams, P. G.; Beaumier, P. L.; Kasina, S., Morgan, A. C., Rao, T. N., Reno, J. M., Sanderson, J. A., Srinivasan, A., Wilbur, D. S., and Vanderheyden, J.-L. (1988) Specific and Stable Labeling of Antibodies with Technetium-99m with a Diamide Dithiolate Chelating Agent. *Proc. Natl. Acad. Sci. U.S.A. 85*, 4025.

(11) Moi, M. K., DeNardo, S. J., and Meares, C. F. (1990) Stable Bifunctional Chelates of Metals Used in Radiotherapy. *Cancer Res. 50*, 789s–793s.

(12) Sundberg, M. W., Meares, C. F., Goodwin, D. A., and Diamanti, C. I. (1974) Selective Binding of Metal Ions to Macromolecules Using Bifunctional Analogues of EDTA. *J. Med. Chem. 17*, 1304–1307.

(13) Meares, C. F., McCall, M. J., Reardan, D. T., Goodwin, D. A., Diamanti, C. I., and McTigue, M. (1984) Conjugation of Antibodies with Bifunctional Chelating Agents: Isothiocyanate and Bromoacetamide Reagents, Methods of Analysis, and Subsequent Addition of Metal Ions. *Anal. Biochem. 142*, 68–78.

(14) Sergheraert, C., Mães, P., and Tartar, A. (1986) Specific Covalent Fixation of Chelating Agents on Peptides. *J. Chem. Soc. Perkin Trans. 1*, 1061–1064.

(15) Sluka, J. P., Griffin, J. H., Mack, D. P., and Dervan, P. B. (1990) Reagents and Methods for the Solid-Phase Synthesis of Protein–EDTA for Use in Affinity Cleaving. *J. Am. Chem. Soc. 112*, 6369–6374.

(16) Hnatowich, D. J., Griffin, T. W., Kosciuczyk, M., Ruscko-wski, R. L., Childs, R. L., Mattis, J. A., Shealy, D., and Doherty, P. W. (1985) Pharmacokinetics of an ^{111}In-Labeled Monoclonal Antibody in Cancer Patients. *J. Nucl. Med. 26*, 849–858.

(17) Shimonkevitz, R., Colon, S., Kappler, J. W., Marrack, P., and Grey, H. (1984) Antigen Recognition by H-2-Restricted T-Cells. *J. Immunol. 133*, 2067–2074.

(18) Watts, T. H., Brian, A. A., Kappler, J. W., Marrack, P., and McConnell, H. M. (1984) Antigen Presentation by Supported Planar Membranes Containing Affinity-Purified I-A^d. *Proc. Natl. Acad. Sci. U.S.A. 81*, 7564–7568.

(19) Watts, T. H., Gariépy, J., Schoolnik, G. K., and McConnell, H. M. (1985) T-Cell Activation by Peptide Antigen: Effect of Peptide Sequence and Method of Antigen Presentation. *Proc. Natl. Acad. Sci. U.S.A. 82*, 5480–5484.

(20) Baker, P. E., Gillis, S., and Smith, K. A. (1979) Monoclonal Cytolytic T-Cell Lines. *J. Exp. Med. 149*, 273–278.

(21) Sheehan, J. C., and Daves, G. D. (1964) Facile Alkyl-Oxygen Ester Cleavage. *J. Org. Chem. 29*, 2006–2008.

(22) Stewart, J. M., and Young, J. D. (1984) *Solid Phase Peptide Synthesis.*, p 58, Pierce Chemical Company, Rockford, IL.

(23) Stelakatos, G. C., Paganou, A., and Zervas, L. (1966) New Methods in Peptide Synthesis III. *J. Chem. Soc. C* 1191–1199.

(24) Hendrickson, J. B., and Kandall, C. (1970) The Phenacyl Protecting Group for Acids and Phenols. *Tetrahedron Lett. 5*, 343–344.

Comparison of ELISA with Activity and Ligand-Binding Methods for the Determination of Thymidylate Synthase Concentration[1]

William H. Tolleson,† Murtaza Alibhai,‡ Ralph J. Cisneros, and R. Bruce Dunlap*

Department of Chemistry, University of South Carolina, Columbia, South Carolina 29208. Received March 20, 1991

The determination of enzyme levels in cellular extracts by active site titrations or by catalytic activity measurements is relevant in both science and medicine. However, these techniques assume that enzymes exhibit the same response in crude sample matrices as they do in the purified state. We report here an example of how an enzyme-linked immunosorbent assay (ELISA) was used to determine the true enzyme concentration which was compared to the effective enzyme concentration obtained by ligand binding and catalytic assay methods in a crude bacterial cell extract. Rabbit antibodies specific for *Lactobacillus casei* thymidylate synthase (TS) were used to develop a highly specific and sensitive heterogeneous noncompetitive ELISA assay with a typical detection limit of 1.4 fmol of TS (100 pg) and a dynamic working range of 3 orders of magnitude. The antibodies showed identical responses for TS, its inhibitory binary complex with 5-fluoro-2′-deoxyuridylate, and its inhibitory ternary complex with 5-fluoro-2′-deoxyuridylate and 5,10-methylenetetrahydrofolate in the immunoassay. *L. casei* cell-free extracts were subjected to extraction with CM-Sephadex and the various fractions were analyzed by ELISA, active-site titrations, and catalytic assays which demonstrated that assays which assumed full catalytic or ligand-binding competence underestimated the true enzyme level.

INTRODUCTION

Thymidylate synthase (TS) constitutes the principal mechanism for the biosynthesis of thymidylate (dTMP) in most living cells. Because the supply of dTMP is critical for continued DNA synthesis and cell division, the enzymes of the thymidylate synthesis cycle have often been exploited as targets for chemotherapeutic strategies aimed at growth limitation. Two examples of this approach include the use of fluoropyrimidine-based inhibitors of thymidylate synthase (TS) in cancer chemotherapy (*1*) and the use of pyrimethamine as a specific inhibitor of dihydrofolate reductase in antimalarial treatments (*2*).

Although several effective assay strategies are available for estimating the levels of these enzymes in crude cell extracts, each assay technique is bound by certain limitations. In order to obtain an estimate of enzyme concentration, it must be assumed that all enzyme molecules in the sample exhibit full catalytic or ligand-binding competence. This assumption could prove to be faulty in several cases, such as (*1*) occasions in which specific inhibitors of the enzyme might interfere with ligand binding or catalytic activity; (*2*) circumstances in which an allosteric effector might be up- or down-regulating catalytic or ligand-binding activity; (*3*) cases where the enzyme has unknown catalytic or ligand-binding activity, such as with either naturally occurring mutant enzymes or with site-directed mutants of cloned enzymes; or (*4*) when the enzyme has suffered proteolytic, oxidative, or thermal degradation.

A cogent example of the need to develop a corollary enzyme assay technique is the measurement of thymidylate synthase concentrations in cell-free extracts obtained from cells exposed to fluoropyrimidines, such as 5-fluorouracil and 5-fluorodeoxyuridine. The latter compounds are precursors of 5-fluorodeoxyuridine 5′-monophosphate (FdUMP), a mechanism-based inhibitor, which forms binary and ternary complexes at the active sites of thymidylate synthase. In fact, fluoropyrimidine-treated, drug-resistant cancer cells often exhibit expanded TS pools after prolonged treatment (*1*, *3*). Obviously, since these agents perturb ligand binding and catalysis by interacting with the active site of the enzyme, then activity or ligand-based methods for estimating the concentration of thymidylate synthase in the presence of such antimetabolites will yield underestimates of the enzyme concentration.

In general, the problems associated with conventional ligand-binding or catalytic assays, which actually measure the effective concentration of an enzyme, can be overcome by an assay based on immunological recognition wherein the quantity of enzyme (the true enzyme concentration) is determined with little or no dependence on the status of the active site(s) of the enzyme. We report here the development and characterization of an ELISA for use in determining the true enzyme concentration of *L. casei* thymidylate synthase in purified samples and crude cell extracts.

Thymidylate synthase is present in most cells at very low levels, although it is expressed to a greater extent in rapidly dividing cells such as fetal and embryonic tissue, fibroblasts, and certain drug-resistant tumor cell lines (*4*). The extremely low levels of TS present in most cells

* Author to whom correspondence should be addressed.

† Current address: Department of Pathology, University of South Carolina School of Medicine, Columbia, SC 29208.

‡ Current address: Department of Chemistry, Pennsylvania State University, University Park, PA 16802.

[1] Abbreviations used: TS, thymidylate synthase; dTMP, thymidylate: dUMP, 2′-deoxyuridylate; FdUMP, 5-fluoro-2′-deoxyuridylate; $CH_2H_4PteGlu$, (±)-5,10-methylenetetrahydropteroylglutamic acid; ELISA, enzyme-linked immunosorbent assay; TSAb, rabbit IgG specific for *L. casei* thymidylate synthase; TSAb–HRP, horseradish peroxidase labeled rabbit IgG specific for *L. casei* thymidylate synthase; HRP, horseradish peroxidase; IgG–HRP, horseradish peroxidase labeled goat antibodies specific for rabbit IgG; CFE, cell-free extract; 5-AS, 5-aminosalicylic acid; 2-ME, 2-mercaptoethanol; Tris, tris(hydroxymethyl)aminomethane; Bis-Tris, [bis(2-hydroxyethyl)amino]tris(hydroxymethyl)methane; PBS, phosphate-buffered saline consisting of 10 mM KH_2PO_4, and 150 mM NaCl, pH 7.4; PBS-T, PBS containing 0.05% Tween 20; TBS, Tris-buffered saline consisting of 50 mM Tris and 500 mM NaCl, pH 7.4; TBS-T, TBS containing 0.05% Tween 20; TCA, trichloroacetic acid; PAGE, polyacrylamide gel electrophoresis; SDS, sodium dodecyl sulfate; BSA, bovine serum albumin.

1043-1802/91/2902-0327$02.50/0 © 1991 American Chemical Society

(estimated to be as low as a few molecules per cell) make sensitivity the critical requirement in designing any assay for this enzyme. The unique features of the heterogeneous noncompetitive enzyme-linked immunosorbent assay (ELISA) yield maximum sensitivity while the highly discriminatory nature of immunorecognition provides an optimal level of selectivity. In the strategy we report here, polyclonal antibodies were isolated from the serum of rabbits immunized with purified thymidylate synthase obtained from methotrexate-resistant *L. casei* and used in the development of an ELISA technique for thymidylate synthase. We chose to employ polyclonal rather than monoclonal antibodies in order to allow the application of this technique to the broadest possible range of analytes, including mutant forms and ligand-bound forms of *L. casei* thymidylate synthase.

EXPERIMENTAL PROCEDURES

Chemicals and Biochemicals. Goat anti-rabbit IgG antibodies conjugated to horseradish peroxidase (IgG–HRP) were obtained from Bio-Rad and used at a 2000-fold dilution in PBS-T. Horseradish peroxidase (HRP), nonspecific rabbit IgG, FdUMP, and 4-chloro-1-napthol were obtained from Sigma Chemical Co. 5-AS was obtained from Sigma and was recrystallized by the method of Ellens and Gielkens (*5*) as described by Tijssen (*6*). Carboxymethyl Sephadex C-50 (CM-Sephadex) and Sephacryl S-300 were obtained from Pharmacia. DEAE–cellulose resin was obtained from Pierce. [6-^{3}H]FdUMP was obtained from Moravek Biochemicals. Racemic tetrahydrofolate was prepared from folic acid by catalytic hydrogenation as described by Hatefi et al. (*7*) and was converted to (±)-5,10-methylene-5,6,7,8-tetrahydrofolate (CH_2H_4PteGlu) by adding a 25-fold molar excess of formaldehyde.

Cell-free extracts (CFE) of methotrexate-resistant *L. casei* (*8*) were prepared from 20 g of cells by sonication at 0–10 °C in 80 mL of CM-20 buffer (50 mM Bis-Tris, 20 mM KCl, 20 mM 2-ME, 1 mM EDTA, pH 6.5) followed by centrifugation for 30 min at 15000*g* at 4 °C to remove cellular debris and insoluble material. *L. casei* MTX^r provides a 200–400-fold increase in TS level over the sensitive organism. Crude TS was prepared from *L. casei* CFE by batch extraction with CM-Sephadex as described by Zapf and Dunlap (*9*). Briefly, 80 mL of CFE was incubated with 20 g of damp CM-Sephadex preequilibrated with CM-20 buffer for 60 min, followed by washing with 500 mL of CM-165 buffer (50 mM Bis-Tris, 165 mM KCl, 20 mM 2-ME, 1 mM EDTA, pH 6.5). Partially purified TS was eluted with 20 mL of CM-500 buffer (50 mM Bis-Tris, 500 mM KCl, 20 mM, 2-ME, pH 6.5).

Preparation of Immunoreagents. Homogenous thymidylate synthase (TS) was obtained from amethopterin resistant *L. casei* according to the method of Lyon et al. (*8*). The purity and quality of the enzyme was verified by a single protein band under native gel electrophoresis which exhibited a specific activity of 2.5–3.0 units/mg (*8*) and a ternary complex binding ratio of 1.7 (*9*). TS was prepared for immunization by centrifugal column chromatography (*10*) to exchange the buffer from thiol-free activation buffer (50 mM Tris, 50 mM KCl, pH 6.8). The latter enzyme solution was then passed through a 0.45-μm sterile filter and mixed 1:1 with Freund's Complete Adjuvant, and three New Zealand white rabbits were immunized subcutaneously with the resulting emulsion (100 μg of TS/rabbit). Rabbits were boosted twice at 3-week intervals with 190 μg of TS in Freund's Incomplete Adjuvant, and whole blood samples were collected by arterial puncture of the dorsal ear artery. Anti-TS IgG was isolated from rabbit serum by caprylic acid precipitation and DEAE–cellulose chromatography (*11*). The purity of the pooled rabbit IgG fractions was determined by native and denaturing PAGE, and the immunochemical specificity was demonstrated by using the IgG pool as a probe of cell lysates of *L. casei* MTX^r.

TSAb–HRP was prepared as described by Tijssen (*5*) by activating 2.5 mg of HRP (Sigma) in 0.25 mL of 0.1 M Na_2CO_3, pH 9.2, and 0.25 mL of 10 mM $NaIO_4$ at room temperature for 2 h. TSAb (6 mg) in 1.0 mL of 0.1 M Na_2CO_3, pH 9.2, was then added to the activated HRP solution. Dry Sephadex G-25 resin (Pharmacia, 85 mg) was then added to increase the effective protein concentration (by absorbing water) and to consume excess periodate. The mixture was incubated for 3 h at room temperature and the Schiff's base adduct was reduced by incubating for 60 min at 4 °C with 0.25 mg of $NaBH_4$. The TSAb–HRP conjugate was purified by chromatography on a 1 × 100 cm Sephacryl S-300 column equilibrated in PBS (10 mM KH_2PO_4, 150 mM NaCl, pH 7.4).

Enzyme Assays. TS catalytic activity was determined spectrophotometrically by the method described by Lyon et al. (*8*). Various amounts of purified *L. casei* TS (23, 46, or 92 pmol of TS, specific activity 2.0 units/mg) were added to 100-μL aliquots of freshly prepared *L. casei* CFE and incubated for 30 min at room temperature. These samples were then added to quartz cuvettes and diluted with a substrate-containing mixture, the reaction was monitored spectrophotometrically for 30 s at 25 °C, and the increase in absorbance at 340 nm due to the production of dihydrofolate was recorded. The final assay mixture contained 0.1 mM CH_2H_4PteGlu, 0.1 mM dUMP, and 0.1 M Tris, pH 7.3, in a total volume of 1.01 mL. These samples were compared to similar 100-μL aliquots of CFE to which only activation buffer was added and to samples of purified TS to which only cell-break buffer and no CFE were added.

Ligand-binding competence was measured by the trichloroacetic acid precipitation assay (TCA) described by Cisneros (*12*) and Moore et al. (*13*). In the TCA assay, purified or crude samples containing 0.08–0.25 nmol of TS were incubated with 0.5 μmol of CH_2H_4PteGlu and 1 nmol of [6-^{3}H]FdUMP at 0.76 Ci/mmol in 0.5 mL of buffer containing 0.2 M sodium acetate, 0.1 M 2-ME, and 0.1 mg of BSA/mL, pH 5.8, for 60 min at 37 °C. The reactions were quenched by adding TCA to a final concentration of 10% and the protein precipitates were collected by centrifugation for 3 min at 16000*g*. The pellets were washed three times with 1.5-mL portions of 10% TCA, solubilized in three 125-μL aliquots of 0.2 M NaOH in 50% ethanol, and the radioactivity of the covalently attached ligand was quantitated in 10 mL of Beckman HP scintillation cocktail with 75 μL of glacial acetic acid with a Beckman LS 7500 liquid scintillation counter.

Protein Concentration. Protein concentrations in crude extracts were determined by the Bio-Rad protein assay kit and confirmed by the BCA protein assay kit (Pierce). Concentrations of purified TS were calculated from absorbance values at 278 nm and a molar absorptivity of 1.10×10^5 M^{-1} cm^{-1} (*14*).

Western Blotting. Proteins from native and denaturing (SDS) polyacrylamide gels were electrophoretically transferred to nitrocellulose membranes in a Bio-Rad Trans Blot apparatus. Membranes were then soaked for 60 min in TBS-T (50 mM Tris, 500 mM NaCl, 0.05% Tween-20, pH 7.4) with 3% gelatin added to block excess protein binding sites on the membranes. The membranes were then incubated for 3 h in 100 mL of TBS-T with 4.0

μg of TSAb/mL on a tilting table. The membranes were then washed three times with 250 mL of TBS-T, incubated for 3 h in a 2000-fold dilution of Bio-Rad goat anti-rabbit IgG-HRP stock in TBS-T, then washed three times with TBS-T as before and once with TBS. Immunoreactive bands were revealed by adding 50 mL of TBS with 0.008% H_2O_2 and 10 mL of 6 mg of 4-chloro-1-napthol in 100% methanol.

Optimization of ELISA. To ensure that both the primary and secondary antibody preparations would always be in excess over the amount of TS in the sample and in order to drive the reaction forming the immune complexes as far toward completion as possible (to enhance sensitivity), we first endeavored to determine the maximal TSAb loading capacity of the microtiter plates. This was accomplished by adding various amounts of TSAb in PBS (0.02–20.0 μg of TSAb/mL) to the wells of a fresh Immulon II 96-well microtiter plate (Dynatech), incubating for 4 h at room temperature, and washing away the unbound TSAb with a Bio-Rad Model 1550 microplate washer adjusted to deliver three wash cycles of 300 μL of PBS-T (10 mM, KH_2PO_4, 150 mM NaCl, 0.05% Tween-20, pH 7.4) with 8-s soaks before aspiration of the spent wash liquid. The amount of TSAb necessary to saturate protein binding sites in the wells was then determined by adding 200-μL aliquots of Bio-Rad HRP-labeled goat anti-rabbit IgG antibodies (IgG–HRP) diluted 2000-fold with PBS-T and allowing the immune complexes to form for 4 h at room temperature. The excess IgG–HRP was then washed away with the plate washer as described above and the immune complexes were detected colorimetrically at 490 nm with a Dynatech MR 650 microtiter plate reader by adding HRP substrate cocktail (10 mM potassium phosphate, 150 mM NaCl, 1.0 mg of 5-AS/mL, 0.005% H_2O_2, pH 6.0) and incubating for 10 min at room temperature.

Optimization of the second antibody concentration was performed similarly by first adding 200 μL of TSAb in PBS per well of a fresh microtiter plate at twice the concentration of TSAb found to yield a maximal response in the previously mentioned experiment. The plate was maintained at room temperature for 4 h, then stored overnight at 4 °C, and the excess TSAb was washed away with the microplate washer as described above. The TS binding sites were saturated by adding 200 μL of 0.1 mg of purified *L. casei* TS/mL of PBS-T per well and incubating for 4 h at room temperature. The excess TS was washed away as described above, various amounts of TSAb–HRP in PBS-T was added to each well (0.01–10 μg/mL) and allowed to react for 4 h at room temperature. The excess TSAb–HRP second antibody was washed away as described above and the extent of immune complex formation was determined by adding 200 μL of HRP substrate cocktail per well and recording the absorbances at 490 nm with the microtiter plate reader.

ELISA. New Dynatech Immulon II 96-well microtiter plates were coated with TSAb solutions (typically 4.0 μg of TSAb/mL) in PBS for 4 h at room temperature and stored at 4 °C until use within 1 week. The coated plates were then washed with PBS-T with the Bio-Rad microplate washer as described above and either purified *L. casei* TS standards (0.05 ng–100 μg TS/well), TS-containing crude cytoplasmic extracts, or PBS-T blanks were then added and incubated for 4 h at room temperature before washing with PBS-T as described above. TSAb–HRP was then added (200 μL of 2.0 μg/mL solution) in PBS-T and incubated for 4 h at room temperature. The TSAb::: TS:::TSAb–HRP sandwiches were then revealed after washing of the plate as described above by adding 200 μL of HRP substrate cocktail and measuring the absorbance values at 490 nm with the microplate reader.

RESULTS AND DISCUSSION

Characterization of Immunoreactants. TS levels in cell-free extracts from *L. casei* MTX^r were determined by the TCA assay. Aliquots from these samples containing ca. 2.0 μg of TS were incubated either with activation buffer (50 mM Tris, 50 mM KCl, 20 mM 2-ME, pH 7.3) or with activation buffer containing a 10-fold molar excess of FdUMP and a 500-fold molar excess of CH_2H_4PteGlu for 60 min at 37 °C. These samples and purified *L. casei* TS standards were separated by native 8.0% PAGE and subjected to Western blotting. Similar samples and purified TS standards were denatured and separated by denaturing 9.0% PAGE and also subjected to Western blotting. The results of Western blot analyses conducted on both pure TS and cell-free extracts, in the presence or absence of ligands, and in the presence or absence of denaturants failed to show any bands other than those that could be attributed to TS or its complexes. Under native conditions, *L. casei* TS is a dimer of identical subunits, yielding a single band on native PAGE (with an apparent MW of 73 kDa), which is converted into two additional faster moving bands upon incubation with FdUMP and CH_2H_5folate (formation of covalent inhibitory ternary complexes). SDS denaturation of native enzyme or its inhibitory ternary complexes yields a single band (with an apparent MW of 35 kDa). In no case was evidence obtained that indicated the existence of any "structurally similar impurity in addition to TS" in the samples which we studied. These blots demonstrated that TSAb exclusively recognized bands which could be attributed to TS or TS–ligand complexes with no noticeable cross reactivity with other bands in the gel (data not shown).

Characterization of ELISA. The maximum capacity for loading TSAb on Immulon II plates was found to be ca. 1 μg of TSAb/mL of PBS (Figure 1), so all subsequent plates were coated with 4.0 μg of TSAb/mL of PBS. Similarly, the maximum ELISA response was observed at TSAb–HRP working concentrations of 2.0 μg of TSAb–HRP/mL of PBS-T. Subsequent plates were processed with a TSAb–HRP working concentration of 4.0 μg/mL.

Various amounts (0.01–100 ng) of purified *L. casei* TS were diluted with PBS-T to 200 μL/well in a microplate that had been coated with TSAb and washed with PBS-T. After incubation for 4 h at room temperature, the plates were washed with PBS-T, TSAb–HRP was added, and the plates were incubated as described above. The plates were washed again, and HRP substrate cocktail was added. The ELISA response was judged to be linear over 3 orders of magnitude when expressed as A_{490} vs log (ng of TS/well) (Figure 2) with typical detection limits around 100–200 pg of TS (1.4–2.8 fmol).

Recognition of Denatured TS and Native TS-Ligand Complexes. Denatured *L. casei* TS samples were prepared by incubating purified TS samples in a boiling-water bath for 10 min in the presence of 1% SDS. The buffer was exchanged by five cycles of concentration and dilution with PBS-T in a Centricon-10 device, and the concentration of the denatured protein was quantitated by UV absorbance at 278 nm and by the BCA protein assay kit (Pierce). The denatured TS sample was then compared to native *L. casei* TS standards by using the ELISA protocol described above (Figure 3). As shown in Figure 3, the ELISA assay was nearly 100-fold less sensitive

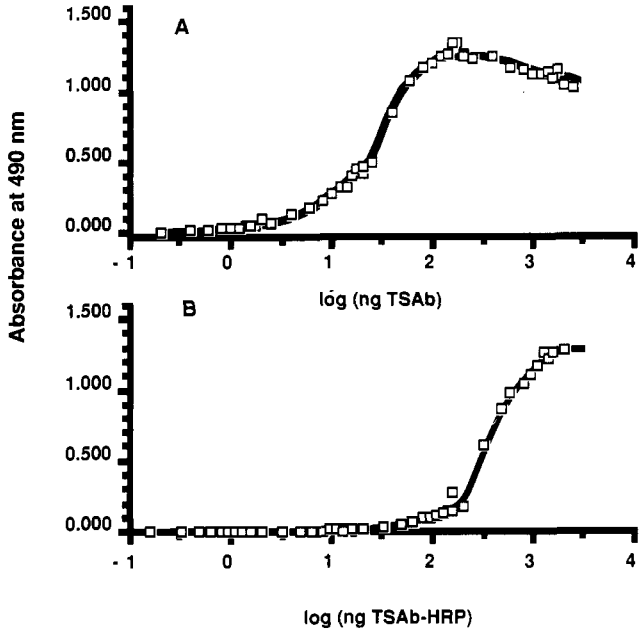


Figure 1. Optimization of conditions for ELISA. The optimum antibody concentrations for ELISA were established by determining the concentration thresholds necessary for maximal response. (A) 200-μL aliquots containing various amounts of TSAb (0.02–20.0 μg/mL TSAb) in PBS were added to individual wells of a 96-well microtiter plate, incubated for 4 h, and washed with PBS-T. Saturating amounts of IgG–HRP specific for rabbit IgG were added, incubated for 4 h, washed with PBS-T, and incubated for 10 min at room temperature with HRP substrate cocktail, and the absorbance at 490 nm was recorded. (B) 200-μL aliquots of 4.0 TSAb/mL PBS were added to the wells of a microtiter plate, allowed to incubate for 4 h, and washed with PBS-T, 200 μL of 0.1 mg of TS/mL of PBS-T was added, and the mixture was incubated for 4 h and washed with PBS-T. TSAb–HRP (0.01–10.0 μg/mL, 200-μL aliquots in PBS-T) was added, incubated for 4 h, and washed with PBS-T, HRP substrate cocktail was added, and the absorbance at 490 nm was recorded.

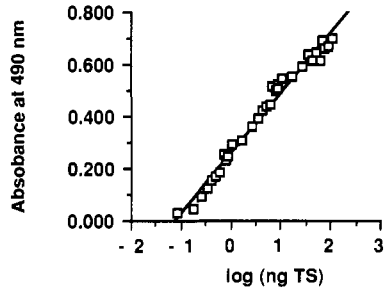


Figure 2. Sensitivity and dynamic working range of ELISA. The dynamic working range of ELISA was determined by adding various amounts of purified TS (0.10–100 ng TS/mL) in PBS-T to a microtiter plate previously coated with TSAb and washed with PBS-T, incubating for 4 h, washing with PBS-T, and developing with TSAb–HRP.

to denatured enzyme than to native TS, even though the concentration of the antibody used in both trials was the same. These results might be attributed to either the destruction or alteration of certain epitopes present in the tertiary structure of the native protein because of unfolding of the polypeptide chains or the blocking or shielding of the epitopes from the antibody by the denaturant.

Binary and ternary complexes of TS were formed by incubating purified TS (1.4–55 pmol) with 10 μM FdUMP alone or with 10 μM FdUMP and 27 μM (±)-CH_2H_4PteGlu, respectively, in the wells of a 96-well microplate. Ligand-free controls were prepared similarly to purified TS standards in 200 μL of PBS-T. The plate was incubated

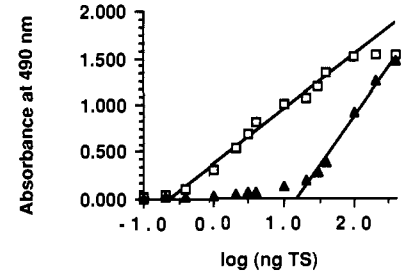


Figure 3. Recognition of denatured thymidylate synthase by ELISA. Purified TS was denatured with 1.0% SDS, the buffer was exchanged for PBS-T, and the ELISA response of the denatured sample (closed triangles) was compared to native TS (open squares).

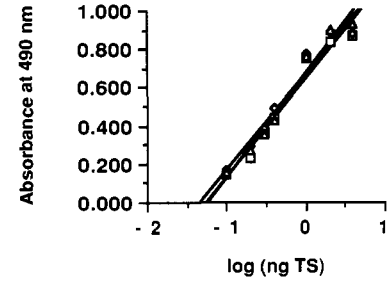


Figure 4. Recognition of thymidylate synthase ligand complexes by ELISA. Purified TS was incubated with excess FdUMP (open triangles) or FdUMP plus CH_2H_4PteGlu (open diamonds) in a microtiter plate and the ELISA response was compared to ligand-free TS (open squares).

Table I. Thymidylate Synthase from Cell-Free Extract

sample	quantitation of thymidylate synthase: by TCA,[a,d] μM	by ELISA,[d] μM	ELISA result/TCA result
CFE	1.2	2.0	1.7
CM-Sephadex[b] (unretained)	0.020	0.068	3.4
CM-Sephadex[c] (retained)	0.74	0.87	1.2

[a] Quantitation of TS by TCA assay of the inhibitory ternary complex assumed an FdUMP:TS binding stoichiometry of 1.7, found to be the typical binding ratio by Moore et al. (*13*). [b] CFE fraction which passed directly through CM-Sephadex. [c] CFE fraction which was retained by CM-Sephadex and eluted with CM-500 buffer. [d] These concentration values were derived from primary data for binding ratio determination accurate to within 5%.

for 4 h at room temperature and processed as described above. The ELISA responses from all three data sets were almost indistinguishable, indicating that TSAb would detect either ligand-bound or uncomplexed forms of TS with nearly identical responses (Figure 4), thus validating the utility of an assay based on the polyclonal antibodies.

Quantitation of TS Levels in *L. casei* Cytoplasmic Extracts. Samples of freshly prepared CFE were subjected to ELISA and the TCA ligand-binding assay. The ligand-binding assay measured the presence of only 1.2 μM TS in *L. casei* CFE while ELISA predicted 2.0 μM TS in that fraction (Table I). Among the possible explanations for the difference in the ligand binding and ELISA results are the following: (1) inactivation of TS by proteolysis, (2) protein denaturation or oxidation of the active-site sulfhydryl groups resulting in inactivation, and (3) the presence of an endogenous inhibitor of TS. First, the fact that Western blots (see above) exhibited only those bands known to be native TS or TS–ligand complexes effectively dismisses the possibility that TS in the CFE has undergone proteolytic degradation. Second, if partial denaturation or sulfhydryl group oxidation of TS had occurred during

Table II. Thymidylate Synthase Catalytic Activity in Cell-Free Extract

sample	TS added, pmol	volume CFE, μL	thymidylate synthase activity × 10^{-3}, units observed[a]	expected	difference
purified TS	23.1	0	3.7		
	46.2	0	6.6		
	92.4	0	13.0		
cell-free extract	0	100	7.9		
cell-free extract	23.1	100	9.4	11.7	2.3
with TS spike	46.2	100	12.3	14.5	2.7
	92.4	100	18.9	20.6	1.7

[a] Averages of two catalytic activity measurements with a spectrophotometric method (*8*). Pooled standard deviation was ±0.0005 units. A unit was defined as the amount of enzyme capable of catalyzing the production of 1 μmol of dihydrofolate per min at 25 °C.

cell storage, sonication, or centrifugation, then spiking the CFE with known amounts of purified TS should result in observed activities of the mixtures which are the simple sums of the activities of the individual components. When such an experiment was performed employing the spectrophotometric assay to measure TS activities, the results (Table II) indicated that the observed activities of the mixtures were uniformly lower (an average of 0.022 units/mL of CFE) than the expected sum of the activities of the two components.

Besides discounting the second possibility, these results are consistent with the third possibility, namely, that an endogenous inhibitor is present in the CFE. Should this be the case, then the subsequent separation of the enzyme from the putative inhibitor should lead to an increase in the total number of enzyme units as measured by the spectrophotometric assay. Interestingly, Zapf and Dunlap (*9*) found that batchwise extraction of the CFE with CM-Sephadex, which is a facile step in the purification of TS, resulted in the recovery of 114% of the TS activity originally present in the CFE. Accordingly, if CM-Sephadex separates an endogenous inhibitor from TS, then the quantitation of the TS in the fraction retained by CM-Sephadex using the ligand-binding assay should give a result which is similar to that from ELISA. In fact, as shown in Table I, the ratio of the ELISA result to the ligand binding result is 1.2, which suggests that the true concentration of thymidylate synthase protein (ELISA) is now quite similar to the effective enzyme concentration as reflected by a measure of the concentration of enzyme active sites (TCA assay). In our experience, both assay methods can routinely be performed, yielding results with less than 5% error.

Since these results suggest that the CM-Sephadex step resulted in the separation of the endogenous inhibitor from the bulk of the TS present in CFE, then it is reasonable to expect that the inhibitor might be present in another fraction from the CM-Sephadex extraction. When TS levels were examined in the fraction which was not retained by CM-Sephadex extraction (CM-20 wash), ELISA predicted 3.4 times as much TS as the TCA assay. These results suggest that the small but easily measurable level of TS present in the fraction which passed directly through CM-Sephadex must be inhibited to a greater extent than the TS molecules present in the fraction which was retained by CM-Sephadex. These results are especially interesting in light of the fact that Friedkin et al. (*15*) described a naturally occurring TS inhibitor in *E. coli* which they identified as N^5-formyltetrahydropteroyl oligoglutamate with a K_i value of 1.3 μM and speculated that it may play some role in the regulation of TS activity.

The foregoing results aptly demonstrate a fundamental problem in the determination of enzyme concentrations in biological samples. In this regard, a distinction must be made between the true enzyme concentration and its effective concentration. The true enzyme concentration is defined as the total number of protein molecules representing the particular enzyme per unit volume and can be readily measured by ELISA, while the effective concentration of enzyme is the number obtained by the use of methods which measure the extent of catalysis or ligand binding by the enzyme per unit volume under the prevailing conditions. Ideally, the true enzyme concentration should equal the effective enzyme concentration. However, as discussed in the Introduction, many situations are encountered in which the true enzyme concentration is not the same as the effective enzyme concentration. In this report, we described a situation where the effective concentration of TS in the bacterial cell extract is substantially lower than its true concentration, probably because of the presence of an endogenous inhibitor. Unfortunately, many investigators simply assume that enzyme concentrations measured by methods such as catalysis and ligand binding, which depend on the competence of the active site of an enzyme, are the true concentrations. Such an assumption can result in misleading conclusions. For example, consider the folllowing problem which is relevant to cancer chemotherapy. Treatment of colorectal tumor cells with 5-fluorouracil is often accompanied by at least some of the following events (for review, see ref 16): (1) the conversion of 5-fluorouracil to FdUMP, (2) its interaction with TS and CH_2H_4PteGlu to form a reversible inhibitory ternary complex, (3) an increase in the intracellular dUMP concentration, and (4) an increase in mRNA coding for the biosynthesis of TS. If one or more of the latter conditions pertain, the use of a ligand-binding or catalytic method will yield an effective TS concentration which is substantially different from the true concentration of the enzyme and could result in the administration of an inappropriate dose of the drug. The solution to this problem is to employ a combination of methods to estimate enzyme levels, at least one of which should be an ELISA to measure the true enzyme concentration. We are now in the process of extending the methodology described in these studies to measure true and effective TS concentrations in a variety of mammalian cell lines.

ACKNOWLEDGMENT

Support for this work was provided by the National Institutes of Health Grant CA 15645 from the National Cancer Institute. The purchase of the equipment necessary to perform ELISA was supported in part by NIH BRSG S07RR07160 awarded by the Biomedical Research Support Grant Program, Division of Research Resources, National Institutes of Health.

LITERATURE CITED

(1) Heidelberger, C. (1975) Fluorinated pyrimidines and their nucleosides. In *Handbook of Experimental Pharmacology*, Vol. 38, Part 2, pp 193–231, Springer-Verlag, Berlin.

(2) Rollo, I. M. (1980) Chemotherapy of Parasitic Diseases. In *The Pharmacological Basis of Therapeutics*, 6th ed. (Gilman, A. G., Goodman, L. S., and Gilman, A., Eds.) pp 1038–1069, MacMillan, New York.

(3) Berger, S. H., Jenh, C. H., Johnson, L. F., and Berger, F. G. (1985) Thymidylate Synthase Overproduction and Gene Amplification in Fluorodeoxyridine-Resistant Human Cells. *Mol. Pharmacol. 28*, 461–467.

(4) Santi, D. V., and Danenberg, P. V. (1984) Folates in Pyrimidine Nucleotide Biosynthesis. In *Folates and Pterins*

(Blakely, R. L., and Benkovic, S. J., Eds.) Vol. 1, pp 345–398, John Wiley and Sons, New York.

(5) Ellens, D. J., and Gielkens, A. L. J. (1980) A Simple Method for the Purification of 5-Aminosalicylic Acid—Application of the Product as Substrate in Enzyme-Linked Immunosorbent-Assay (ELISA). *J. Immunol. Methods* 37, 325–332.

(6) Tijssen, P. (1985) Practice and Theory of Enzyme Immunoassays. In *Laboratory Techniques in Biochemistry and Molecular Biology* (Burdon, R. H., and van Knippenberg, P. H., Eds.) Vol. 15, pp 230–241, Elsevier, New York.

(7) Hatefi, Y., Talbert, P. T., Osborn, M. J., and Huennekens, F. M. (1960) Tetrahydrofolic Acid. *Biochem. Prep. 7*, 89–92.

(8) Lyon, J. A., Pollard, A. L., Loeble, R. B., and Dunlap, R. B. (1975) Thymidylate Synthetase: An Improved Purification Procedure and Description of Some Spectral Properties. *Cancer Biochem. Biophys.* 121–128.

(9) Zapf, J. W., and Dunlap, R. B. (1989) A Rapid, Reliable, and Convenient Method for the Purification of Thymidylate Synthase from Amethopterin-Resistant *Lactobacillus casei*. *Adv. Enzyme Regul. 29*, 189–207.

(10) Bradshaw, T. P., Ahmed, F., and Dunlap, R. B. (1988) The Removal of Exogenous Thiols from Proteins by Centrifugal Column Chromatography. *Biochem. Biophys. Methods 17*, 159–170.

(11) Steinbuch, M., and Audran, R. (1969) The Isolation of IgG from Mammalian Sera with the Aid of Caprylic Acid. *Arch. Biochem. Biophys. 134*, 279–284.

(12) Cisneros, R. J., and Dunlap, R. B. (1990) Development of a Trichloroacetic Acid Precipitation Assay for Covalent Adducts of Thymidylate Synthase. *Anal. Biochem. 186*, 202–208.

(13) Moore, M. A., Ahmed, F., and Dunlap, R. B. (1986) Evidence for the Existence of Covalent Nucleotide-Thymidylate Synthase Complexes, Identification of Site of Attachment, and Enhancement by Folates. *J. Biol. Chem. 261*, 12745–12749.

(14) Maley, G. F., Bellisario, R. L., Guarino, D. U., and Maley, F. M. (1979) The Primary Structure of *Lactobacillus casei* Thymidylate Synthetase. I. The Isolation of Cyanogen Bromide Peptides 1 Through 5 and the Complete Amino Acid Sequence of CNBr 1, 2, 3, and 5. *J. Biol. Chem. 254*, 1288–1295.

(15) Friedkin, M., Plante, L. T., Crawford, E. J., and Crum, M. (1975) Inhibition of Thymidylate Synthetase and Dihydrofolate Reductase by Naturally Occurring Oligoglutamate Derivatives of Folic Acid. *J. Biol. Chem. 250*, 5614–5621.

(16) Cisneros, R. J., Silks, L. A., and Dunlap, R. B. (1988) Mechanistic Aspects of Thymidylate Synthase: Molecular Basis for Drug Design. *Drugs Future* 13, 859–881.

Registry No. TS, 9031-61-2.

Preparation of Hydrazino-Modified Proteins and Their Use for the Synthesis of ^{99m}Tc–Protein Conjugates

David A. Schwartz,*,† Michael J. Abrams,† Marguerite M. Hauser,† Forrest E. Gaul,† Scott K. Larsen,† Donald Rauh,‡ and Jon A. Zubieta§

Johnson Matthey Pharmaceutical Research, 1401 King Road, West Chester, Pennsylvania 19380-1497, McNeil Pharmaceutical Research, Spring House, Pennsylvania 19477-0776, and Department of Chemistry, Syracuse University, Syracuse, New York 132444-4100. Received April 15, 1991

The syntheses and protein linking properties of succinimidyl 4-hydrazinobenzoate hydrochloride (SHBH) and succinimidyl 6-hydrazinonicotinate hydrochloride (SHNH), two new heterobifunctional linkers which lead to hydrazino-modified proteins, are described. SHBH-modified proteins are unstable due to the presence of the phenylhydrazine moiety. This problem was overcome by synthesizing the hydrazinopyridine analogue SHNH, and the conjugates derived from this linker are stable. Tc(V) oxo precursors readily add to hydrazinopyridine-modified proteins to yield the desired ^{99m}Tc-radiolabeled protein. ^{99m}Tc–hydrazinopyridine–polyclonal IgG conjugates are useful agents for the imaging of focal sites of infection.

The use of radioisotopes conjugated to proteins for the diagnosis and therapy of diseases is of great current interest (*1*, *2*). A majority of the work has been directed toward conjugation to tumor-associated monoclonal antibodies of α- and β-emitting isotopes (e.g. ^{131}I, ^{90}Y, ^{67}Cu, ^{211}At, ^{212}Bi, and $^{186/188}$Re) for therapy of cancer and γ-emitting isotopes (^{131}I, ^{123}I, ^{111}In, and ^{99m}Tc) for its diagnosis. Other proteins hae been radiolabeled for the imaging of myocardial infarction (*3*) and also focal sites of infection (*4*).

Various linkers exist for conjugation of these radioisotopes to proteins. All of these are heterobifunctional molecules containing a moiety for chelation of the metal and a moiety for covalent attachment of the ligand backbone to the protein (e.g. an active ester or an isothiocyanate) (*5*, *6*). ^{99m}Tc is the preferred isotope for scintigraphic imaging applications (*7*) due to its favorable physical properties, cost, and availability. Rubin et al. (*8*) have reported the use of ^{111}In–DTPA–polyclonal IgG conjugates for the imaging of focal sites of infection. We were especially interested in the synthesis of ^{99m}Tc–polyclonal IgG conjugates for the imaging of focal sites of infection. The development of a readily preparable ^{99m}Tc conjugate would lead to a more widely available agent with better radiochemical properties.

Previous efforts directed toward the conjugation of ^{99m}Tc to proteins include the use of diethylenetriaminepentaacetic acid (DTPA) (*9*), N_2S_2 (*10*), and N_3S (*11*) functionalized ligands and direct reduction (*12*) of the protein disulfide bonds to form free sulfhydryl groups. We initiated a program to develop a novel technology for the conjugation of ^{99m}Tc to proteins and herein report our results.

Nicholson and Zubieta have reported on the reactivity of rhenium(V) oxo complexes and aromatic hydrazides and hydrazines to form rhenium diazenido species which have been characterized by X-ray crystallography (*13*). The known rapid reactivity of aromatic hydrazines and the proper rhenium precursor, the Re=N double bond character of the products identified in these crystal structures, which may confer in vivo stability, and the known reactivity similarities of rhenium and technetium (*14*) were characteristics which led us to examine the possibility of producing a ^{99m}Tc–aromatic hydrazine–protein conjugate linked via a Tc–diazenido bond.

The successful exploitation of the above outlined chemistry to produce a ^{99m}Tc–protein conjugate requires several components: (1) synthesis of an aromatic hydrazine linker, (2) efficient conjugation of this linker to a protein and a method for quantification of the modification, (3) stability of the hydrazine-modified protein, (4) choice of the proper technetium-99m precursor, (5) rapid and efficient radiolabeling, and (6) in vivo stability of the conjugate.

EXPERIMENTAL PROCEDURES

^{1}H NMR were recorded in DMSO-d_6 on a 300-MHz Bruker AF-300 spectrometer. Elemental analyses were performed at Atlantic Microlabs, Norcross, GA.

The synthesis of SHNH (*8*) is described in ref 20.

4-[2-(*tert*-Butoxycarbonyl)hydrazino]benzoic Acid (3). To a stirred solution of 4-hydrazinobenzoic acid (5 g, 32.8 mmol) and triethylamine (9.5 mL, 68.2 mmol) in dimethylformamide (100 mL) was added dropwise a solution of BOC-ON (8.09 g, 32.8 mmol) in dimethylformamide. The reaction mixture was stirred at room temperature for 3 h. Aqueous hydrochloric acid (10%) was added and subsequently the solution became cloudy. The solution was extracted with ethyl acetate, and the combined organic extracts were washed with water, dried over magnesium sulfate, filtered, and concentrated under reduced pressure to give a brown solid. The solid was recrystallized from chloroform to give the desired product as a pale brown solid: yield 69%; ^{1}H NMR δ 1.47 (s, 9 H), 6.77 (d, 2 H, J_{ab} = 8.6 Hz), 7.85 (d, 2 H, J_{ab} = 8.6 Hz). Anal. Calcd for $C_{12}H_{16}N_2O_4$: C, 57.13; H, 6.39; N, 11.10. Found: C, 57.02; H, 6.13; N, 11.61.

Succinimidyl 4-[2-(*tert*-Butoxycarbonyl)hydrazino]benzoate (5). To a solution of 4-[2-(*tert*-butoxycarbonyl)hydrazino]benzoic acid (7.0 g, 27.8 mmol) and *N*-hydroxysuccinimide (3.19 g, 27.8 mmol) in dioxane (100 mL) was added dropwise a solution of dicyclohexylcarbodiimide (5.72 g, 27.8 mmol) in dioxane (35 mL). The reaction mixture was stirred at room temperature for 16 h. After ca. 30 min a white precipitate formed (dicyclohexylurea). Acetic acid (0.5 mL) was added and stirring

* To whom correspondence should be addressed.
† Johnson Matthey Pharmaceutical Research.
‡ McNeil Pharmaceutical Research.
§ Syracuse University.

1043-1802/91/2902-0333$02.50/0 © 1991 American Chemical Society

was continued for 1 h. The reaction mixture was filtered to remove the urea byproduct. The filtrate was concentrated under reduced pressure to give a brown solid which was treated with ether, and the solids were isolated by filtration to give a pale brown solid: yield 86%; mp 185–186.5 °C; ^{1}H NMR δ 1.47 (s, 9 H), 2.88 (s, 4 H), 6.85 (d, 2 H, J_{ab} = 8.9 Hz), 8.04 (d, 2 H, J_{ab} = 8.9 Hz). Anal. Calcd for $C_{16}H_{19}N_3O_6$: C, 55.01; H, 5.48; N, 12.03. Found: C, 55.17; H, 5.84; N, 11.86.

Succinimidyl 4-Hydrazinobenzoate Hydrochloride (7, SHBH). To a solution of hydrogen chloride in dioxane (prepared by bubbling hydrogen chloride into dioxane for ca. 5 min) was added succinimidyl 4-[2-(*tert*-butoxycarbonyl)hydrazino]benzoate (1.5 g, 4.3 mmol). The reaction mixture was stirred at room temperature for 5 h. The reaction mixture was never homogeneous; however the color was initially pale brown and over 2 h became orange. The reaction mixture was filtered to give a pale yellow solid: yield 72%; mp 203.5–205 °C; ^{1}H NMR δ 2.87 (s, 4 H), 7.05 (d, 2 H, J_{ab} = 8.9 Hz), 7.97 (d, 2 H, 8.9 Hz). Anal. Calcd for $C_{11}H_{12}ClN_3O_4$: C, 46.25; H, 4.23; Cl, 12.40; N, 14.71. Found: C, 46.74; H, 4.38; Cl, 12.24; N, 14.26.

Protein Modification. A 4 molar excess of freshly dissolved SHNH (30 mM in DMF) was added dropwise to a stirred solution of IgG (1.0 g in 20 mL of 0.1 M phosphate buffer, pH 7.8). The solution was stirred gently for 5 h at room temperature protected from light. This was followed by dialysis against 10 mM citrate, pH 5.2, at 4 °C (five buffer changes over 24 h). The mixture was then filtered through a 0.2-μm filter and the protein concentration was determined by the Bradford method. The solution was diluted to 5 mg/mL with buffer (100 mM NaCl, 20 mM citrate, 1% mannitol, pH 5.2), divided into 200-μL aliquots and stored at −20 °C. The number of hydrazino groups was determined by converting the hydrazino groups to the corresponding hydrazone by reaction with *p*-nitrobenzaldehyde (*15*) and measuring the optical density at 385 nm (extinction coefficient: 2.53 × 10^4 L mol^{-1} cm^{-1}). Typically, approximately three hydrazino groups were present per IgG.

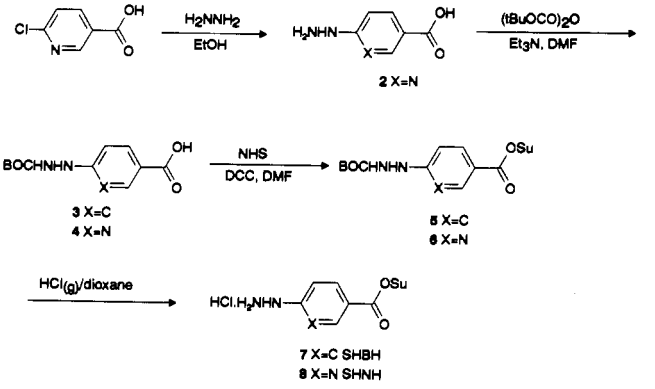
Radiolabeling. Twenty millicuries of freshly prepared ^{99m}Tc-glucoheptonate (Du Pont Glucoscan kit) was added to 0.5 mL of a solution hydrazino-modified IgG (5.0 mg/mL in citrate buffer, pH 5.2) and the mixture was incubated for 60 min at room temperature. Radiochemical purity was determined by using ITLC-sg chromatographic strips (Gelman Laboratories, Ann Arbor, MI) with 0.1 M sodium citrate (pH 5.5) as solvent. All preparations had at least 90% radioactivity bound to the antibody.

RESULTS AND DISCUSSION

The synthesis of alkyl hydrazide–protein conjugates has been reported by King et al. (*15*). They used a novel two-step method for the addition of hydrazide groups to proteins in which the protein is initially modified with an α-bromoacetamide followed by addition of a thiol hydrazide to produce the desired conjugate. Modification of this method for the addition of an aromatic hydrazine is not suitable for radiolabeling of disulfide-containing proteins with technetium-99m, as it has been demonstrated (*12*) that initial incubation of IgG with thiols (e.g. mercaptoethanol or dithiothreitol) causes nonspecific reduction of some disulfide bonds in the protein. In reactions of these proteins with labile technetium-99m precursors (e.g. ^{99m}Tc-glucoheptonate), nonspecific ^{99m}Tc binding occurs due to the thiophilic nature of technetium.

To test our hypothesis that an aromatic hydrazine-modified protein would react with a ^{99m}Tc(V) oxo species

Scheme I. Synthesis of 4-Hydrazinobenzoic Acid (SHBH) and 6-Hydrazinonicotinic Acid (SHNH)



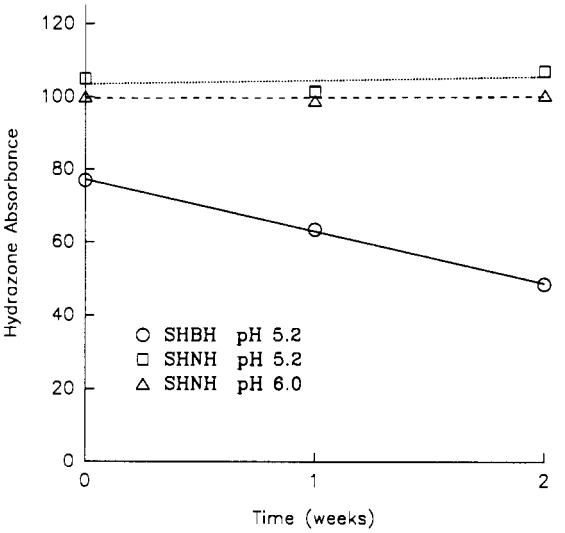


Figure 1. Stability (4 °C) of 4-hydrazinobenzoic acid modified (SHBH) and 6-hydrazinonicotinic acid modified (SHNH) proteins.

we required a heterobifunctional linker containing cross-reactive moieties, i.e. a hydrazine and an active ester. This was accomplished following the example of Keller and Rudinger (*16*). They synthesized a maleimido–hydrazide linker by the anhydrous acid (HCl(g)/dioxane) deprotection of a [2-(*tert*-butoxycarbonyl)hydrazido]maleimide leading to the desired stable hydrazinium salt. In our case we examined whether a [2-(*tert*-butoxycarbonyl)-hydrazino] succinimido ester would react similarly under these conditions. Thus 4-[2-(*tert*-butoxycarbonyl)hydrazino]benzoic acid (**3**) was converted to its succinimidyl ester **5** by using standard DCC coupling conditions (Scheme I). The ester was subsequently treated with anhydrous HCl/dioxane, which led to the precipitation and subsequent isolation of the desired hydrazinium salt, succinimidyl 4-hydrazinobenzoate hydrochloride (**7**, SHBH).

The conjugation of SHBH to polyclonal IgG proceeded smoothly. Addition of a 0.03 M solution of SHBH in DMF (4–24 equiv/mol IgG) to a buffered solution (phosphate, pH 7.8) of polyclongal IgG and subsequent incubation yielded the desired conjugate. Hydrazine substitution was quantified by using the colorimetric assay method of King et al. (*15*). Stability of the conjugate at both 4 and −20 °C was poor. This was determined by repeated hydrazine and protein (Bradford assay) analyses. Figure 1 shows the decrease in hydrazine residue substitution over time. This instability is believed to be due to the presence of the phenylhydrazine moieties. Phenylhydrazine itself readily oxidizes in solution and its stability has been studied (*17*).

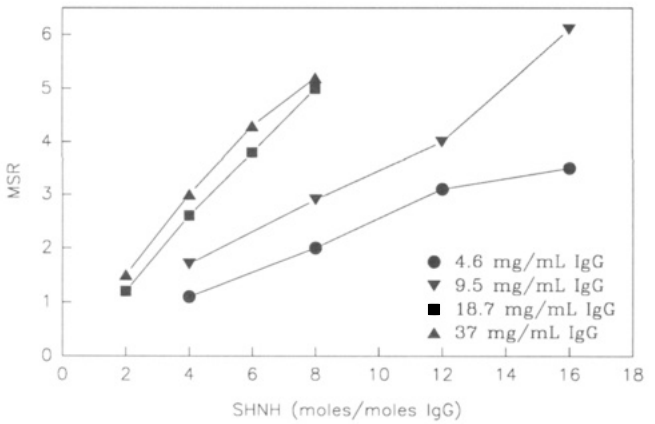


Figure 2. Protein modification efficiency of succinimidyl 6-hydrazinonicotinate hydrochloride (SHNH) at various linker and protein concentrations.

Jeon and Sawyer have recently reported on the hydroxide-induced synthesis of superoxide from dioxygen and phenylhydrazine, which may explain the loss of hydrazino moieties from the modified protein (*18*).

To circumvent this problem the pyridine analogue was synthesized, as hydrazinopyridine moieties are stable entities, and also the reaction of $Re^{V}OCl_3(PPh_3)_2$ and 2-hydrazinophthalazine (a similar heterocycle) yielded stable Re–diazenido structures (*13*). The synthesis of succinimidyl 6-hydrazinonicotinate hydrochloride (**8**; SHNH) is outlined in Scheme I. 6-Hydrazinonicotinic acid (**2**) was synthesized by treating 6-chloronicotinic acid with 85% hydrazine hydrate for 4 h at 80 °C, removal of excess hydrazine, acidification to pH 5.5, and isolation of the precipitated product. The hydrazine moiety was protected as its BOC derivative **4** (di-*tert*-butyl dicarbonate/Et_3N/DMF), and the succinimidyl ester **6** was synthesized under standard DCC coupling conditions (*N*-hydroxysuccinimide/DCC/DMF). Conversion of the BOC active ester to its hydrazinium salt under anhydrous acid conditions smoothly led to the desired product, **8** (SHNH).

Conjugation of SHNH to polyclonal human IgG as described above gave the desired hydrazinopyridine-modified protein. Figure 2 describes the conjugation efficiency at different linker and protein concentrations. As expected conjugation efficiency increased with increasing protein concentration. Over modification led to precipitation of the protein (molar substitution ratio (MSR) > 10). At 35 mg/mL protein concentration and a 4-fold excess of linker the conjugation yield was >70% (MSR 2.8–3.0 hydrazine groups/IgG) with excellent protein recovery (>90%). Treatment of the protein with 6-hydrazinonicotinic acid, the nonlinkable equivalent, gave negligible modification as determined by the hydrazone assay. Hydrazinopyridine-modified protein stored at 4 °C showed no loss of hydrazine residues over several months and storage at −20 °C gave no loss of hydrazine residues or protein precipitation over 13 months. The modified protein could be lyophilized and reconstituted without event.

The choice of the proper technetium species for conjugation was critical. As predicted, a technetium(V) oxo species was required. ^{99m}Tc–glucoheptanoate which is produced by the stannous chloride reduction of pertechnetate in the presence of sodium glucoheptonate was examined initially. Characterization of this species has not been established unambiguously, but it is known to possess a Tc=O bond (IR ν 950 cm^{-1}) (*19*). Incubation of the modified protein (10 mM; 2–3 hydrazines/IgG) with ^{99m}Tc–glucoheptonate for 45–60 min at room temperature gave >95% technetium incorporation at pH 5.2–6.2. In a control experiment polyclonal IgG was treated with 6-hydrazinonicotinic acid for 6 h and subsequently dialyzed (acetate buffer, pH 5.2). On addition of ^{99m}Tc–glucoheptonate there was <3% nonspecific binding of the isotope.

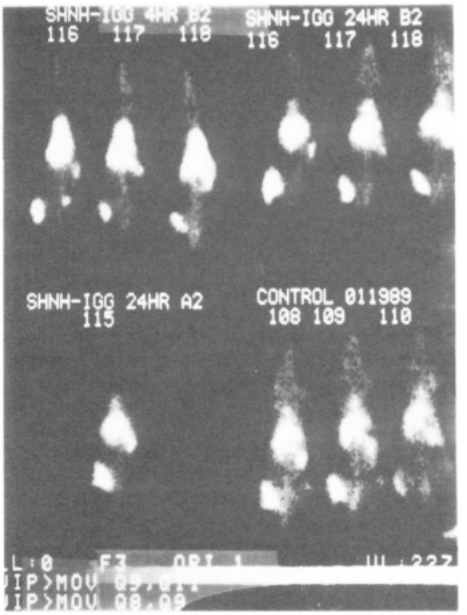


Figure 3. γ-camera images of a group of rats with *Escherichia coli* deep thigh infections: upper left quadrant, ^{99m}Tc-labeled human polyclonal human IgG at 4 h; upper right and lower left quadrants, at 24 h; lower right quadrant, ^{111}In-labelled human polyclonal IgG.

Further studies with other technetium precursors demonstrated that compounds with a putative TcO_4 structure, e.g. ^{99m}Tc–saccharate (*20*) and ^{99m}Tc–2-hydroxymethylbutyric acid (*21*) reacted with hydrazino-modified polyclonal IgG in >90% radiochemical yield in 1 h at room temperature. ^{99m}Tc-MAG-3 (*22*) which is a Tc(V) oxo complex with an N_2S_2 donor set did not react with the hydrazino-modified protein.

Incubation of hydrazino-modified polyclonal IgG with other ^{99m}Tc precursors yielded little or no radioincorporation, e.g. Tc–pyrophosphate (28% radioincorporation), Tc–methylenediphosphonate (*23*) (14%), pertechnetate (0%), and Tc(III)DMSA (0%).

The stability of the Tc–hydrazino–protein conjugate was studied by incubation of the conjugate with various chelators and human serum at 37 °C for 24 h. The radiolabeled protein conjugate retained its radiolabel in the presence of DTPA (98% retention of label as determined by HPLC and ITLC analyses), sodium diethyldithiocarbamate (98%) or L-cysteine (92%) (all 10 mM in PBS, pH 7.4), and human serum (95%). Imaging of focal sites of infection with the ^{99m}Tc–hydrazinopyridine–polyclonal IgG conjugate gave images of equal quality to ^{111}In–DTPA–polyclonal IgG conjugates, demonstrating the *in vivo* stability of the radiolabeled conjugate (see Figure 3). Biodistributions of the two conjugates were also similar (*24*).

The exact nature of the bonding between the Tc moiety and the hydrazinopyridine modified protein has not been unequivocally established. Abrams et al. (*25*) have recently isolated, characterized, and determined the crystal structure of $[TcCl_2(C_8N_5N_4)(PPh_3)_2]\cdot 0.75C_7H_8$ and demonstrated that it is a technetium–hydralazine complex. This structure shows the presence of a Tc=N bond (1.767 Å), demonstrating the multiple bond character of this bond.

A ^{99m}Tc–hydrazinopyridine-modified conjugate of fragment E1, a protein isolated from digests of blood clots

which has been shown to localize in blood clots in vivo, was prepared. This conjugate successfully imaged thrombi in rabbits and dogs (*26*).

In summary, we have developed a novel linker for the ready modification of proteins with hydrazino groups and demonstrated the ability of these hydrazino-modified proteins to react with ^{99m}Tc–glucopheptonate. These radiolabeled proteins have demonstrated in vivo stability and localization in two in vivo models. The characterization of the protein–Tc bonding and the further utility of this linker and other hydrazinopyridine analogues are areas of active interest in our laboratories.

ACKNOWLEDGMENT

We thank Drs. G. Henson and R. Brooks for helpful discussions. We also thank Drs. H. Solomon, P. Kramer, A. J. Fischman, R. Callahan, A. Fuccello, L. Knight, and Mr. D. Reixinger for their collaborations.

LITERATURE CITED

(1) Schlom, J. (1986) Basic Principles and Applications of Monoclonal Antibodies in the Management of Carcinomas. *Cancer Res. 46*, 3225. Cobb, L. M., and Humm, J. L. (1986) Radioimmunotherapy of malignancy using antibody targeted radionuclides. *Br. J. Cancer 54*, 863.

(2) Rosenblum, M. G., Murray, J. L., Lamki, L., David, G., and Carlo, D. (1987) Comparative clinical pharmacology of ^{111}In-labeled murine monoclonal antibodies. *Cancer Chemother. Pharmacol. 20*, 41.

(3) Goethals, P., Coene, M., Slegers, G., Vogelaers, D., Everaert, J., Lemahieu, I., Colardyn, F., and Heyndrickx, G. R. (1990) Production of carrier-free gallium-66 and labeling of antimyosin antibody for positron imaging of acute myocardial. *Eur. J. Nucl. Med. 16*, 237.

(4) Rubin, R. H., Young, L. S., Hansen, W. P., Nedelman, M., Wilkinson, R., Nelles, M. J., Callahan, R., Khaw, B.-A., and Strauss, H. W. (1988) Specific and Nonspecific Imaging of lacaliszed Fisher Immunotype 1 *Pseudomonas aeurginosa* Infection with Radiolabeled Monoclonal Antibody. *J. Nucl. Med. 29*, 651.

(5) Meares, C. F. (1986) Chelating Agents for the Binding of Metal Ions to Antibodies. *Nucl. Med. Biol. 13*, 311.

(6) Hnatowich, D. J., Layne, W. W., Childs, R. L., Lanteinge, D., Davis, M. A., Griffin, T. W., and Doherty, P. W. (1983) Radioactive Labeling of Antibody: A Simple and Efficient Method. *Science 220*, 613.

(7) Pinkerton, T. C., Desilets, C. P., Hoch, D. J., Mikelsons, M. V., and Wilson, G. M. (1985) Bioinorganic Activity of Technetium Radiopharmaceuticals. *J. Chem. Educ. 62*, 965.

(8) Rubin, R. H., Fischman, A. J., Needleman, M., Wilkinson, R., Callahan, R. J., Khaw, B.-A., Hansen, W. P., Kramer, P. B., and Stauss, H. W. (1989) Radiolabeled, Nonspecific, Polyclonal Human Immunoglobulin in the Detection of Focal Inflammation by Scintigraphy: Comparison with Gallium-67 Citrate and Technetium-99m-Labeled Albumin. *J. Nucl. Med. 30*, 385.

(9) Lanteingne, D., and Hnatowich, D. (1984) The Labeling of DTPA-coupled Proteins with ^{99m}Tc. *Int. J. Radiat. Isot. 35*, 617.

(10) Rao, T. N., Adhikesavalu, D., Camerman, A., and Fritzberg, A. R. (1990) Technetium(V) and Rhenium(V) Complexes of 2,3-Bis(mercaptoacetamide)propionate. Chelate Ring Stereochemistry and Influence on Chemical and Biological Properties. *J. Am. Chem. Soc. 112*, 5798.

(11) Fritzberg, A. R., Kasina, S., Vanderheyden, J. L., and Srinivasan, A. (1988) Metal-radionuclide-labeled proteins and glycoproteins and their preparation for diagnosis and therapy. Eur. Pat. Appl. EP 284071.

(12) Mather, S. J., and Ellison, D. (1990) Reduction-Mediated Technetium-99m Labeling of Monoclonal Antibodies. *J. Nucl. Med. 31*, 692.

(13) Nicholson, T., and Zubieta, J. (1988) Complexes of Rhenium with Benzoylazo and Related Ligands. *Polyhedron 7*, 171.

(14) Cotton, F. A., and Wilkinson, G. (1988) Advanced Inorganic Chemistry, 5th ed., p 847, John Wiley and Sons, Inc., New York.

(15) King, T. P., Zhao, S. W., and Lam, T. (1986) Preparation of Protein Conjugates via Intermolecular Hydrazone Linkage. *Biochemistry 25*, 5774.

(16) Keller, O., and Rudinger, J. (1975) Preparation and Some Properties of Maleimido Acids and Maleoyl Derivatives of Peptides. *Helv. Chim. Acta 58*, 531.

(17) Vulterin, J., and Zyka, J. (1963) Investigation of Some Hydrazine Derivatives as Reductiometric Titrants. *Talanta 10*, 891.

(18) Jeon, S., and Sawyer, D. T. (1990) Hydroxide-Induced Synthesis of the Superoxide Ion from Dioxygen and Aniline, Hydroxylamine or Hydrazine. *Inorg. Chem. 29*, 4612.

(19) Kieviet, W. (1981) Technetium radiopharmaceuticals: chemical characterization and tissue distribution of Tc–glucoheptonate using Tc-99m and carrier Tc-99. *J. Nucl. Med. 22*, 703.

(20) Pak, K. Y., Dean, R. T., Mattis, J. A., Buttram, S., and Lister-James, J. (1988) Method for Labelling Antibodies with a Metal Ion. International Patent Appl. PCT/US88/01048.

(21) Colombo, F., Matarrese, M., Bugaj, J., Gerundini, P., Fazio, F., and Deutsch, E. (1988) Tc-99m Complexes of α,α-Disubstituted Hydroxy α-Carboxylic Acids. *J. Nucl. Med. 29*, (*Supplement*) 934.

(22) Nosco, D., and Verbruggen, A. (1990) Technetium-99m complex for examining renal function. US4925650.

(23) Martin, J. L., Yuan, J., Lunte, C. E., Elder, R. C., Heineman, W. R., and Deutch, E. (1989) Technetium–Diphosphonate Skeletal Imaging Agents: EXAFS Structural Studies in Aqueous Solution. *Inorg. Chem. 28*, 2901.

(24) Abrams, M. J., Juweid, M., tenKate, C. I., Schwartz, D. A., Hauser, M. M., Gaul, F. E., Fuccello, A. J., Rubin, R. H., Strauss, H. W., and Fischman, A. J. (1990) Technetium-99m–Human Polyclonal IgG Radiolabeled via the Hydrazino Nicotinamide Derivative for Imaging Focal Sites of Infection in Rats. *J. Nucl. Med. 31*, 2022.

(25) Abrams, M. J., Larsen, S. K., and Zubieta, J. (1990) Synthesis and Crystal and Molecular Structure of a Technetium–Hydralazino Complex, $[TcCl_2(C_8H_5N_4)(PPh_3)_2]\cdot 0.75C_7H_8$. *Inorg. Chim. Acta 173*, 133.

(26) Knight, L. C., Abrams, M. J., Schwartz, D. A., Hauser, M. M., Kollman, M., Zaydenberg, I., Gaul, F. E., and Maurer, A. H. (1990) Tc-99m Labeling of Fragment E1 for Thrombus Imaging. *J. Nucl. Med. 31* (Suppl.), 776.

Photolysis of 3-Aryl-3-(trifluoromethyl)diazirines: A Caveat Regarding Their Use in Photoaffinity Probes

Matthew Platz,*,† Atnaf S. Admasu,† Stefan Kwiatkowski,‡ Peter J. Crocker,‡ Nobuyuki Imai,‡ and David S. Watt*,‡

Department of Chemistry, The Ohio State University, Columbus, Ohio 43210, and Department of Chemistry, University of Kentucky, Lexington, Kentucky 40506. Received May 6, 1991

The photolysis of 3-(4-tolyl)-3-(trifluoromethyl)diazirine in the presence of benzene, methanol, carbon tetrachloride, cyclohexane, triethylsilane, or diethylamine led to photoproducts consistent with the intermediacy of a singlet carbene. In the case of diethylamine, the photoinsertion into the N–H bond of diethylamine produced the expected adduct, 1-(diethylamino)-2,2,2-trifluoro-1-(4-tolyl)ethane. However, the base-catalyzed elimination of hydrogen fluoride from this adduct afforded an enamine, α-(diethylamino)-β,β-difluoro-4-methylstyrene, and the subsequent hydrolysis of this enamine furnished diethylamine and 2,2-difluoro-1-(4-tolyl)ethanone. This elimination and hydrolysis sequence effectively reversed the photoinsertion process. A similar photoinsertion and hydrolysis process using 3-(4-*n*-octylphenyl)-3-(trifluoromethyl)diazirine also produced 2,2-difluoro-1-(4-*n*-octylphenyl)ethanone in modest yield. These results suggest that the photoinsertion products from 3-aryl-3-(trifluoromethyl)-diazirines in biological systems may suffer similar fates limiting, in part, their utility in obtaining primary sequence data.

INTRODUCTION

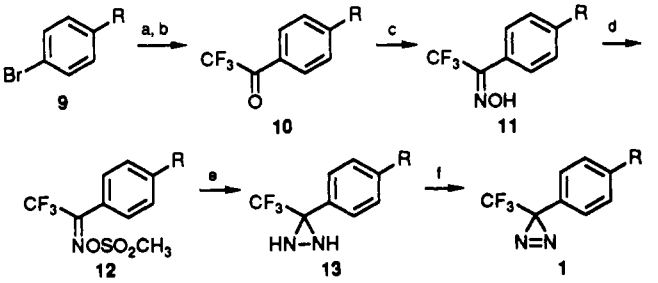
Interest in photoaffinity cross-linking reagents for elucidating the structure of receptors led to various probes that incorporate photoactive aryl azides (*1–4*), perfluorinated azides (*5–10*), and 3-aryl-3-(trifluoromethyl)diazirines (*11–27*). The diazirine category of photoactive probes has enjoyed considerable popularity as a result of a general impression that the photolysis of a 3-aryl-3-(trifluoromethyl)diazirine affords a reactive carbene intermediate and that the insertion of the carbene establishes an irreversible, covalent cross-link to a variety of amino acid residues within the target protein. In contrast, recent evidence suggested that the photolysis of the phenyl azide category of probes generated a less reactive, electrophilic dehydroazepine that selectively scavenged for nucleophilic Lys or Cys residues. It was expected, therefore, that 3-aryl-3-(trifluoromethyl)diazirines would result in more efficient cross-linking than their phenyl azide counterparts and would afford covalent adducts that would tolerate the subsequent digestion, purification, and sequencing process. Despite these advantages, relatively few studies using 3-aryl-3-(trifluoromethyl)diazirines have led to primary sequence data. Difficulties encountered in the biochemical application of photoaffinity probes bearing the 3-aryl-3-(trifluoromethyl)diazirine group to the acquisition of primary sequence data prompted this study of the distribution and stability of the photoproducts of two model systems, 3-(4-tolyl)-3-(trifluoromethyl)diazirine (**1a**) and 3-(4-*n*-octyl)-3-(trifluoromethyl)diazirine (**1b**).

EXPERIMENTAL PROCEDURES

3-(4-Tolyl)-3-(trifluoromethyl)diazirine (1a) and 3-(4-*n*-Octyl)-3-(trifluoromethyl)diazirine (1b). Literature procedures (*28–30*) were repeated with some modifications as shown in Scheme I and are described below.

2,2,2-Trifluoro-1-(4-tolyl)ethanone (10a). To 1.4 g (200 mmol) of lithium in 100 mL of anhydrous Et_2O at 25 °C was added 13.0 mL (105 mmol) of 4-bromotoluene (**9a**). After a 15-min induction period, the solution refluxed as a result of the slightly exothermic reaction. After stirring for 2 h, a N_2 flow was started, and the reaction was cooled to −78 °C. To this 4-tolyllithium solution was added 13.0 mL (113 mmol) of ethyl trifluoroacetate via syringe over a 10-min period. The solution was allowed to warm to 25 °C and was stirred for a total of 12 h. The reaction was quenched by adding 10 mL of saturated NH_4Cl solution and 5 mL of water. The Et_2O solution was separated, washed successively with half-saturated NH_4Cl and water, and dried over anhydrous $MgSO_4$. The solution was concentrated to afford 19 g of crude **10a** as a dark orange liquid. ^1H NMR indicated that this product was a 57:43 mixture of unreacted **9a** and the desired product **10a**: IR (TF) 1710 (C=O) cm^{-1}; ^1H NMR ($CDCl_3$) δ 2.45 (s, 3, CH_3), 7.34 and 7.96 (2 d, J = 8.6 Hz, 4, ArH). This crude mixture was used in the next reaction without further purification.

Scheme I.[a] Synthesis of 3-Aryl-3-(trifluoromethyl)-diazirines



[a] Series **a**, R = CH_3; series **b**, R = n-C_8H_{17}. Reagent legend: a, Li, Et_2O in the case of **10a** and n-BuLi, Et_2O, −78 °C in the case of **10b**; b, CF_3CO_2Et; c, H_2NOH; d, MsCl, Et_3N; e, NH_3, −78 °C; f, Ag_2O.

2,2,2-Trifluoro-1-(4-tolyl)ethanone Oxime (11a). To the crude mixture from the previous reaction, which was calculated to contain ca. 10 g (53 mmol) of **10a**, was added 11.1 g (159 mmol) of hydroxylamine hydrochloride and 6.39 g (160 mmol) of sodium hydroxide in 200 mL of absolute EtOH. The mixture was refluxed for 21 h and cooled. Most of the ethanol was removed under reduced

* Authors to whom correspondence should be addressed.
† The Ohio State University.
‡ University of Kentucky.

1043-1802/91/2902-0337$02.50/0 © 1991 American Chemical Society

pressure, and the residue was diluted with water. The aqueous solution was acidified to pH 1 with 3 M HCl solution and extracted with Et_2O. The Et_2O solution was washed with brine and dried over anhydrous $MgSO_4$. The solution was concentrated and the product was purified by flash chromatography on silica gel using 1:19 EtOAc–hexane to afford 11.1 g (53% for two steps) of **11a** as an *E,Z* mixture that was a pale orange liquid: IR (TF) 3340 (br, OH), 1705 (C=N) cm^{-1}; ^1H NMR ($CDCl_3$) δ 2.38 (s, 3, CH_3), 7.18–7.50 (m, 4, ArH), 9.52 (br s, 1, OH).

2,2,2-Trifluoro-1-(4-tolyl)ethanone *O*-(Methylsulfonyl)oxime (12a). To 11.1 g (54.5 mmol) of **11a** in 200 mL of anhydrous THF[1] at 0 °C was added 6.3 mL (81 mmol) of MsCl. To this solution was added dropwise a solution of 12 mL (88 mmol) of Et_3N in 40 mL of anhydrous THF over a 15-min period. The solution was stirred for an additional 15 min, and the ice–water bath was removed. The solution was stirred for an additional 1 h at 25 °C. The THF was removed under reduced pressure. The residue was dissolved in water and extracted with Et_2O. The Et_2O solution was washed with brine and dried over anhydrous $MgSO_4$. The solution was concentrated to afford 14.3 g (93%) of crude product that was used directly in the next reaction. A small portion was purified by column chromatography on silica gel using 1:9 EtOAc–hexane and by recrystallization from EtOAc–hexane to give **12a** as white needles: mp 80.5–82.0 °C; IR (KBr) 3035, 1610, 1373, 1200, 1187 cm^{-1}; ^1H NMR ($CDCl_3$) δ 2.42 (s, 3, $ArCH_3$), 3.25 (s, 3, OSO_2CH_3), 7.31 and 7.42 (2 d, J = 8 Hz, 4, ArH). Anal. Calcd for $C_{10}H_{10}F_3NO_3S$: C, 42.71; H, 3.58. Found: C, 42.73; H, 3.58.

3-(4-Tolyl)-3-(trifluoromethyl)diaziridine (13a). To 14.1 g (50 mmol) of **12a** in a flask cooled to −78 °C and equipped with a dry ice–acetone condenser was introduced ca. 150 mL of liquid ammonia. The solution was stirred for 6 h, the dry ice–acetone bath was removed, and the liquid ammonia was allowed to evaporate. The residue was dissolved in water and extracted with Et_2O. The aqueous layer was extracted with additional Et_2O. The Et_2O solutions were combined, washed with brine, and dried over anhydrous Na_2SO_4. The crude product (**13a**) was used in the next reaction without further purification: mp 44–46 °C (from hexane at −20 °C) [lit. (*30*) mp 45–46 °C]; IR (KBr) 3200 (NH), 1395 cm^{-1}; ^1H NMR ($CDCl_3$) δ 2.20 and 2.77 (2 d, J = 8 Hz, 2, HNNH), 2.38 (s, 3, $ArCH_3$), 7.23 and 7.50 (2 d, J = 8 Hz, 4, ArH).

3-(4-Tolyl)-3-(trifluoromethyl)diazirine (1a). To 7.7 g (38 mmol) of **13a** in 100 mL of Et_2O was added 15.6 g (67 mmol) of freshly prepared Ag_2O in portions over 1 h. The mixture was stirred for an additional 2 h and filtered through a bed of Celite. The filtrate was concentrated, and the crude product was chromatographed on silica gel using 1:19 EtOAc–hexane to afford 4.3 g (56%) of **1a** as a *volatile*, light yellow liquid: IR (TF) 3050, 2935, 1611, 1518, 1347, 1242, 1229, 1214, 1185, 1155, 1054, 939, 808, 730 cm^{-1}; UV (cyclohexane) λ_{max} 361 nm (ϵ = 346); ^1H NMR ($CDCl_3$) δ 2.36 (s, 3, $ArCH_3$), 7.09 and 7.21 (2 d, J = 8 and 1 Hz, 4, ArH).

2,2-Difluoro-1-(4-tolyl)ethanone (6a). A solution of 56 mg (0.28 mmol) of **1a** in 2.5 mL of diethylamine in a 5-mm Pyrex NMR tube was degassed with nitrogen and irradiated for 16 h in a Rayonet photochemical reactor (RPR-2537A tubes). The solution was transferred to a round-bottomed flask and was diluted with 25 mL of 1 M HCl. The solution was stirred for 30 min. The product was extracted with ether and the ether solution was washed with brine and dried over anhydrous $MgSO_4$. The solution was *partially* concentrated on a rotary evaporator. The ^1H NMR spectrum of this product displayed a signal at δ 6.28 (t, J_{HF} = 53.6 Hz, 1, CHF_2) consistent with the presence of **6a**. Isolation of **6a** in a pure state was hampered by its volatility, and a semicarbazone derivative failed to produce a satisfactory combustion analysis.

2,2,2-Trifluoro-1-(4-*n*-octylphenyl)ethanone (10b). To 9.0 mL (23 mmol, 2.1 equiv) of 2.5 M *n*-BuLi in hexane was added over a 10-min period 2.5 mL (11 mmol, 1.0 equiv) of 1-bromo-4-*n*-octylbenzene (**9b**) in 55 mL of anhydrous Et_2O at −78 °C under a N_2 atmosphere. The temperature was allowed to rise to 0 °C over a 5-h period. The solution was cooled to −78 °C, and 4.0 mL (34 mmol, 3.1 equiv) of ethyl trifluoroacetate was added. The solution was allowed to stir for 13 h, during which time the temperature was allowed to rise to 25 °C. The reaction was quenched with water, and the product was extracted with Et_2O. The ethereal solutions were combined, washed with brine, and dried over anhydrous $MgSO_4$. The solution was concentrated, and the crude product was chromatographed on silica gel using hexane to afford 1.88 g (61%) of **10b** (*38–41*) as a clear, colorless liquid: IR (TF) 2965, 2940, 2865, 1711 (CO), 1605, 1206, 1176, 1148, 942 cm^{-1}; ^1H NMR ($CDCl_3$) δ 0.88 (t, J = 6.2 Hz, 3, CH_3), 1.27 (br s, 10 $(CH_2)_5$), 1.64 (t, J = 7.3 Hz, 2, $ArCH_2CH_2$), 2.70 (t, J = 7.7 Hz, 2, $ArCH_2$), 7.35 and 8.00 (2 d, J = 8.3 Hz, 4, ArH). Anal. Calcd for $C_{16}H_{21}F_3O$: C, 67.12; H, 7.39. Found: C, 67.21; H, 7.43.

2,2,2-Trifluoro-1-(4-*n*-octylphenyl)ethanone Oxime (11b). The procedure described in the preparation of **11a** was repeated with 1.88 g (6.57 mmol, 1.0 equiv) of **10b**, 1.37 g (19.7 mmol, 3.00 equiv) of hydroxylamine hydrochloride, and 0.828 g (20.7 mmol, 3.15 equiv) of NaOH to afford, after chromatography on silica gel using $CHCl_3$, 1.17 g (59%) of **11b** as an *E,Z* mixture that was a clear, pale yellow oil. A sample for analysis was obtained by recrystallization at −20 °C from hexane: mp 32–34 °C; IR (KBr) 3320 (OH), 2960, 2930, 2860, 1178, 1138, 1010, 963 cm^{-1}; ^1H NMR ($CDCl_3$) δ 0.88 (t, J = 6.3 Hz, 3, CH_3), 1.27 (br s, 10, $(CH_2)_5$), 1.52–1.73 (m, 2, $ArCH_2CH_2$), 2.65 (t, J = 7.8 Hz, 2, $ArCH_2$), 7.30 and 7.49 (2 d, J = 8.2 Hz, 4, ArH), 9.24 (s, 1, OH). Anal. Calcd for $C_{16}H_{22}F_3NO$: C, 63.77; H, 7.36. Found: C, 63.82; H, 7.39.

2,2,2-Trifluoro-1-(4-*n*-octylphenyl)ethanone *O*-(Methylsulfonyl)oxime (12b). The procedure described for the preparation of **12a** was repeated with 1.12 g (3.72 mmol, 1.0 equiv) of **11b**, 0.45 mL (5.8 mmol, 1.6 equiv) of MsCl, and 0.80 mL (5.7 mmol, 1.5 equiv) of Et_3N to afford, after chromatography on silica gel using 2:3 hexane–$CHCl_3$, 943 mg (67%) of **12b** as an off-white, waxlike solid: mp 39–41 °C; IR (KBr) 2955, 2925, 2855, 1372, 1184, 1140 cm^{-1}; ^1H NMR ($CDCl_3$) δ 0.88 (t, J = 6.2 Hz, 3, CH_3), 1.27 (br s, 10, $(CH_2)_5$), 1.53–1.74 (m, 2, $ArCH_2CH_2$), 2.66 (t, J = 7.7 Hz, 2, $ArCH_2$), 3.26 (s, 3, CH_3SO_2), 7.31 and 7.44 (2 d, J = 8.3 Hz, 4, ArH). Anal. Calcd for $C_{17}H_{24}F_3NO_3S$: C, 53.81; H, 6.38. Found: C, 53.92; H, 6.39.

3-(Trifluoromethyl)-3-(4-*n*-octylphenyl)diaziridine (13b). The procedure described for the preparation of **13a** was repeated with 0.90 g (2.4 mmol) of **12b** to afford, after chromatography on silica gel using 1:19 acetone–$CHCl_3$, 610 mg (84%) of **13b** as a light yellow oil. A sample for analysis was obtained by recrystallization at −20 °C from hexane to afford a cottonlike, white solid: mp 41–43 °C; IR (KBr) 3210 (NH), 2930, 2855, 1180, 1142 cm^{-1}; ^1H NMR ($CDCl_3$) δ 0.88 (t, J = 6.5 Hz, 3, CH_3), 1.27 (br s, 10,

[1] Abbreviations used: *n*-BuLi, *n*-butyllithium; EPR, electron paramagnetic resonance; MsCl, methanesulfonyl chloride; PC, phenylcarbene; THF, tetrahydrofuran; TTC, 4-tolyl(trifluoromethyl)carbene.

$(CH_2)_5$), 1.51–1.72 (m, 2, $ArCH_2CH_2$), 2.21 and 2.77 (2 d, J = 8.6 Hz, 2, HNNH), 2.63 (t, J = 7.7 Hz, 2, $ArCH_2$), 7.23 and 7.52 (2 d, J = 8.1 Hz, 4, ArH). Anal. Calcd for $C_{16}H_{23}F_3N_2$: C, 63.98; H, 7.72. Found: C, 63.83; H, 7.78.

3-(Trifluoromethyl)-3-(4-*n*-octylphenyl)diazirine (1b). The procedure described for the preparation of **1a** was repeated with 571 mg (1.90 mmol, 1.0 equiv) of **13b** and 1.3 g (5.6 mmol, 2.9 equiv) of freshly prepared Ag_2O to afford, after chromatography on silica gel using $CHCl_3$, 460 mg (81%) of **1b** as a yellow liquid: IR (TF) 2965, 2935, 2860, 1343, 1237, 1182, 1155, 939 cm^{-1}; UV (95% EtOH) λ_{max} 363 nm (ϵ = 378); ^1H NMR ($CDCl_3$) δ 0.88 (t, J = 6.3 Hz, 3, CH_3), 1.27 (br s, 10, $(CH_2)_5$), 1.50–1.67 (m, 2, $ArCH_2CH_2$), 2.61 (t, J = 7.7 Hz, 2, $ArCH_2$), 7.10 and 7.21 (2 d, J = 8.3 Hz, 4, ArH). Anal. Calcd for $C_{16}H_{21}F_3N_2$: C, 64.41; H, 7.09. Found: C, 64.36; H, 7.14.

2,2-Difluoro-1-(4-*n*-octylphenyl)ethanone (6b). A solution of 58 mg (0.19 mmol) of **1a** in 1.7 mL of diethylamine in a 5-mm Pyrex NMR tube was degassed with argon and irradiated for 4 h in a Rayonet photochemical reactor (RPR-3500 tubes). The solution was allowed to stand for 20 h, transferred to a round-bottomed flask, and diluted with 20 mL of 1 M HCl. The solution was stirred for 3.5 h. The product was extracted with ether and the ether solution was washed with brine and dried over anhydrous $MgSO_4$. The solution was concentrated on a rotary evaporator and chromatographed on silver nitrate impregnated silica gel preparative layer plate using 1:9 EtOAc–hexane to afford 9 mg (18%) of **6b**: IR ($CHCl_3$) 2960, 2935, 2855, 1692, 1601 cm^{-1}; ^1H NMR ($CDCl_3$) δ 0.88 (t, J = 6.4 Hz, 3, $(CH_2)_5CH_3$), 1.20–1.30 (m, 10, $(CH_2)_5CH_3$), 1.52–1.76 (m, 2, $ArCH_2CH_2CH_2CH_2$), 2.69 (t, J = 7.7 Hz, 2, $ArCH_2CH_2CH_2CH_2$), 6.29 (t, J_{HF} = 53.6 Hz, 1, CHF_2), 7.34 and 8.00 (2 d, J = 8.3 Hz, 4, ArH). Anal. Calcd for $C_{16}H_{22}F_2O$: C, 71.62; H, 8.26. Found: C, 71.44; H, 8.31.

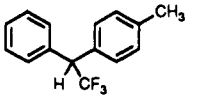
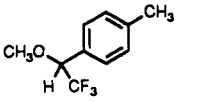
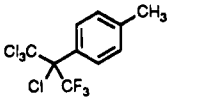
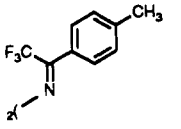
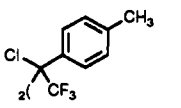
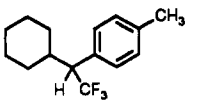
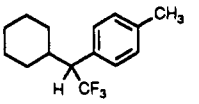
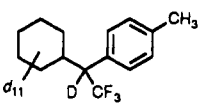
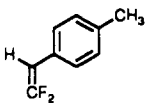
EPR Spectroscopy. A solution of **1a** (0.015 M initial concentration) in perfluoro-2-*n*-butyltetrahydrofuran (Fluorochem Limited, Glossop, U.K.) was placed in a 4-mm quartz tube. It was degassed by three freeze–pump–thaw cycles and sealed under vacuum. The tube was immersed in liquid nitrogen in a Wilmad (Buena Vista, NJ) EPR dewar and irradiated with four RPR 3500 bulbs (Southern New England Ultraviolet, Hamden, CT). The dewar was transferred to the cavity of a Varian (Palo Alto, CA) EPR 112 spectrometer, and the spectrum was recorded.

GC–MS Studies. Samples of **1a** (0.015 M initial concentration) in various solvents were placed in 5-mm Pyrex cells and degassed by three freeze–pump–thaw cycles and sealed under vacuum. The tubes were photolyzed at 350 nm with four Rayonet RPR 3500 bulbs for 4 h. The samples were analyzed by GC-MS immediately after the tubes were opened with a Hewlett-Packard 4021 gas chromatograph–mass spectrometer.

RESULTS

The photolysis of 3-(4-tolyl)-3-(trifluoromethyl)diazirine (**1a**) in benzene, methanol, carbon tetrachloride, cyclohexane, triethylsilane, and diethylamine led to the expected insertion or addition products as summarized in Table I. The principal photoproducts were identified by gas chromatography–mass spectrometry. The photolysis of **1a** in diethylamine solution (0.2 M initial concentration) for 4 h at 25 °C using a Rayonet RPR 3500 reactor led to the following product distribution: 4-(2,2,2-trifluoroethyl)-toluene (**7a**), 1-(diethylamino)-2,2,2-trifluoro-1-(4-tolyl)-ethane (**4a**), α-(diethylamino)-β,β-difluoro-4-methylstyrene (**5a**), 2,2-difluoro-1-(4-tolyl)ethanone (**6a**) in a 3.1:1.7:6.5:1.2 ratio (uncorrected), according to GC analysis.

Table I. The Products Formed on Photolysis of 1a in Various Solvents at Ambient Temperature As Determined by GC–MS

solvent	major products	trace products
		
CH_3OH		
CCl_4		 
		
1:1  + 		
Et_3SiH	 	

A related photolysis of 3-(4-*n*-octyl)-3-(trifluoromethyl)-diazirine (**1b**) produced a similar product distribution, but only ketone **6b** was fully characterized in this case.

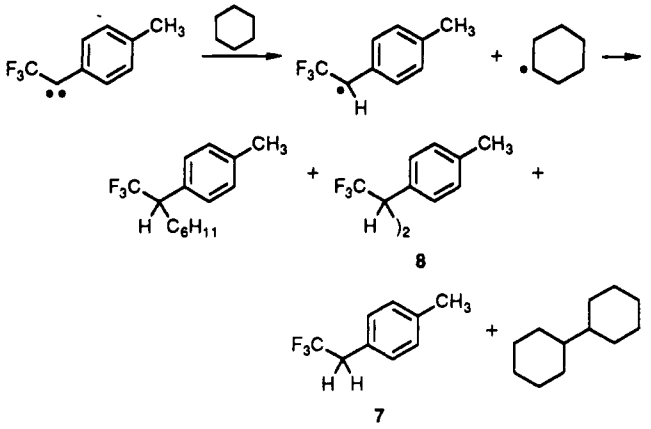
DISCUSSION

Current interest in the development of photoaffinity probes possessing 3-aryl-3-(trifluoromethyl)diazirines (*11–27*) stems in part from the expectation that the reactive carbene intermediate, generated on photolysis of these reagents, will establish an irreversible cross-link to amino acid residues within the protein receptor. Various reports outline the synthesis of novel probes of this type (*28–30*) and the successful cross-linking of radiolabeled diazirine probes. However, the characterization of the photophysical states, detailed photoproduct distributions, and photoproduct stabilities have not been reported.

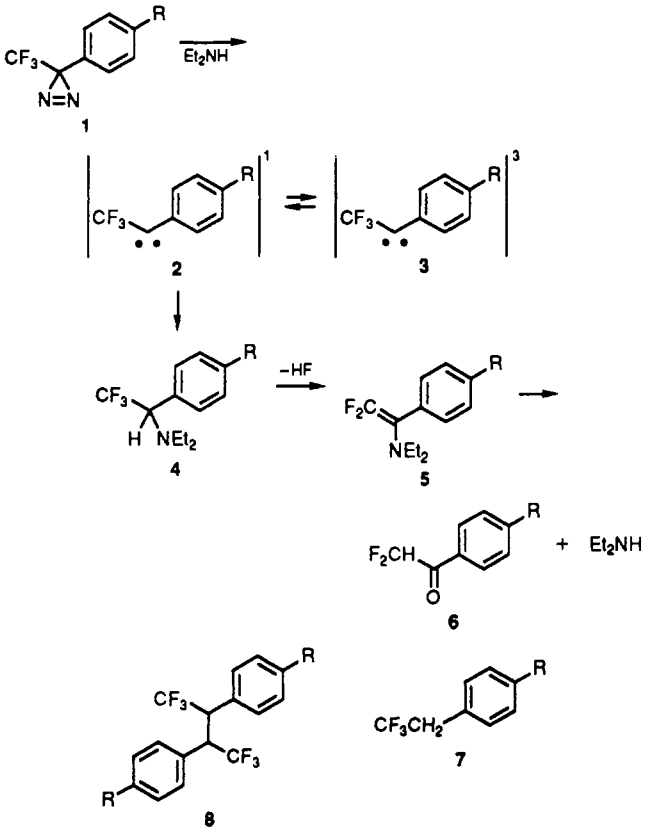
Phenylcarbene (PC)[1] is a rather well-characterized species having a triplet ground state as indicated by low-temperature EPR spectroscopy (*31*). Nevertheless, most of the solution-phase chemistry of this species derives from a low-lying, readily accessible, highly reactive singlet state (*32*). The evidence suggests that singlet and triplet PC equilibrate more rapidly than either state can trap a neighboring hydrocarbon (*33, 34*). The lifetime of the spin-equilibrated triplet PC in acetonitrile is ca. 1–10 ns (*35*).

The photolysis of **1a** at ca. 350 nm in glassy perfluoro-2-*n*-butyltetrahydrofuran at 77 K produced an easily discerned EPR spectrum characteristic of a triplet carbene with $|D/hc|$ = 0.5215 cm^{-1} and $|E/hc|$ = 0.0305 cm^{-1}

Scheme II. Expected Triplet-State Reactions



Scheme III.[a] Photolysis of 3-Aryl-3-(trifluoromethyl)-diazirines



[a] Series a, R = CH_3; series b, R = n-C_8H_{17}.

(*36*). The zero-field parameters are very similar to those of triplet PC, and consequently, the carrier of the EPR spectrum was attributed to 4-toly(trifluoromethyl)carbene (TTC). Thus, the triplet state was identified as the ground state of this species.

Diazirine **1a** was photolyzed in a variety of representative solvents, and the products were analyzed by GC–MS. The results (Table I) indicated that in most solvents, it was the low-lying singlet state of the carbene which was intercepted to give the predominant products. It was of particular interest that TTC inserted cleanly into a C–H bond of cyclohexane. There was no evidence for triplet carbene involvement because the characteristic products of hydrogen atom abstraction, shown in Scheme II, were not observed even in trace quantities. The CH/CD isotope effect for the singlet carbene CH insertion for TTC into cyclohexane and cyclohexane-d_{12} was 1.93, a value which matched that reported for singlet PC and 1-naphthylcarbene (*33*, *37*). TTC also inserted cleanly into the OH bond of methanol (a characteristic singlet carbene process), a C–Cl bond of CCl_4, the N–H bond of diethylamine, and the Si–H bond of triethylsilane. However, in the latter case, the adduct was not stable with respect to the loss of Et_3SiF. A similar observation involving the adduct of diethylamine undergoing the loss of HF and the presence of amine functionality in a number of biological targets for which these probes might be used prompted a more detailed investigation of this instability.

As shown in Scheme III, a myriad of products emerged from a detailed study of the photolysis of **1a** in diethylamine, in which insertion of the singlet carbene into the N–H bond of diethylamine produced the adduct 1-(diethylamino)-2,2,2-trifluoro-1-(4-tolyl)ethane (**4a**). Of particular interest was the rapid elimination of hydrogen fluoride from **4a** that produced enamine **5a** and a subsequent hydrolysis that furnished diethylamine and 2,2-difluoro-1-(4-tolyl)ethanone (**6a**). A similar elimination was noted in the case of a product formed from the insertion of a 3-aryl-3-(trifluoromethyl)diazirine into *tert*-butyl alcohol (*29*). This elimination and hydrolysis sequence effectively reversed the photoinsertion process and suggested that the use of photoaffinity probes bearing 3-aryl-3-(trifluoromethyl)diazirines may lead, in some cases, to chemically unstable photoadducts that are unlikely to survive peptide-sequencing conditions.

ACKNOWLEDGMENT

We thank the National Institutes of Health (HD 25961) and the National Science Foundation (CHE-8814950) for their generous financial support.

LITERATURE CITED

(1) Torres, M. J., Zayas, J., and Platz, M. S. (1986) A formal CH insertion reaction of an aryl nitrene into an alkyl CH bond. Implications for photoaffinity labeling. *Tetrahedron Lett. 27*, 791–794.

(2) Leyva, E., Platz, M. S., Persy, G., and Wirz, J. (1986) Photochemistry of phenyl azide: the role of singlet and triplet phenylnitrene as transient intermediates. *J. Am. Chem. Soc. 108*, 3783–3790.

(3) Shields, C. J., Chrisope, D. R., Schuster, G. B., Dixon, A. J., Poliakoff, M., and Turner, J. J. (1987) Photochemistry of aryl azides: Detection and characterization of a dehydroazepine by time-resolved infrared spectroscopy and flash photolysis at room temperature. *J. Am. Chem. Soc. 109*, 4723–4726.

(4) Schuster, G. B., and Liang, T.-Y. (1987) Photochemistry of 3- and 4-nitrophenyl azides: Detection and characterization of reactive intermediates. *J. Am. Chem. Soc. 109*, 7803–7810.

(5) Levya, E., Munoz, D., and Platz, M. S. (1989) Photochemistry of fluorinated aryl azides in toluene solution and in frozen polycrystals. *J. Org. Chem. 54*, 5938–5945.

(6) Young, M. J. T., and Platz, M. S. (1989) Polyfluorinated aryl azides as photoaffinity labelling reagents: The room temperature CH insertion reactions of singlet pentafluorophenyl nitrene with alkanes. *Tetrahedron Lett. 30*, 2199–2202.

(7) Soundararajan, N., and Platz, M. (1990) Descriptive photochemistry of polyfluorinated azide derivatives of methyl benzoate. *J. Org. Chem. 55*, 2034–2039.

(8) Keana, J. F. W., and Cai, S. X. (1990) New reagents for photoaffinity labeling: Synthesis and photolysis of functionalized perfluorophenyl azides. *J. Org. Chem. 55*, 3640–3647.

(9) Keana, J. F. W., and Cai, S. X. (1989) Functionalized perfluorophenyl azides: New reagents for photoaffinity labeling. *J. Fluorine Chem. 43*, 151–154.

(10) Cai, S. X., and Keana, J. F. W. (1989) 4-Azido-2-iodo-3,5,6-trifluorophenylcarbonyl derivatives. A new class of functionalized and iodinated perfluorophenyl azide photolabels. *Tetrahedron Lett. 30*, 5409–5412.

(11) Smith, R. A. G., and Knowles, J. R. (1973) Aryldiazirines. Potential reagents for photolabeling of biological receptor sites. *J. Am. Chem. Soc. 95*, 5072–5073.
(12) Bayley, H., and Knowles, J. (1978) Photogenerated reagents for membrane labeling. 2. Phenylcarbene and adamantylidene formed within the lipid bilayer. *Biochemistry 17*, 2420–2423.
(13) Erni, B., and Khorana, H. G. (1980) Fatty acids containing photoactivable carbene precursors. Synthesis and photochemical properties of 3,3-bis(1,1-difluorohexyl)diazirine and 3-(1,1-difluorooctyl)-3*H*-diazirine. *J. Am. Chem. Soc. 102*, 3888–3896.
(14) Standring, D. N., and Knowles, J. R. (1980) Photoaffinity labeling of lactate dehydrogenase by the carbene derived from 3-diazirino analogue of nicotinamide adenine dinucleotide. *Biochemistry 19*, 2811–2816.
(15) Brunner, J., and Semenza, G. (1981) Selective labeling of the hydrophobic core of membranes with 3-(trifluoromethyl)-3-(*m*-[^{125}I]-iodopheyl)diazirine, a carbene-generating reagent. *Biochemistry 20*, 7174–7182.
(16) Curatolo, W., Radhakrishnan, R., Gupta, C. M., and Khorana, H. B. (1981) Photoactivable carbene-generating phospholipids: physical properties and use in detection of phase separations in lipid mixtures. *Biochemistry 20*, 1374–1378.
(17) Radhakrishnan, R., Costello, C. E., and Khorana, H. B. (1982) Sites of photolytic intermolecular cross-linking between fatty acyl chains in phospholipids carrying a photoactivable carbene precursor. *J. Am. Chem. Soc. 104*, 3990–3997.
(18) Brunner, J., Spiess, M., Aggeler, R., Huber, P., and Semenza, G. (1983) Hydrophobic labeling of a single leaflet of the human erythrocyte membrane. *Biochemistry 22*, 3812–3820.
(19) Krebs, J., Buerkler, J., Guerini, D., Brunner, J., and Carafoli, E. (1984) 3-(Trifluoromethyl)-3-(*m*-[^{125}I]-iodophenyl)-diazirine, a hydrophobic, photoreactive probe, labels calmodulin and calmodulin fragments in a Ca^{+2}-dependent way. *Biochemistry 23*, 400–403.
(20) Hoppe, J., Brunner, J., and Jorgensen, B. B. (1984) Structure of the membrane-embedded F_o part of F_1F_o ATP synthase from *Escherichia coli* as inferred from labeling with 3-(trifluoromethyl)-3-(*m*-[^{125}I]-iodophenyl)diazirine. *Biochemistry 23*, 5610–5616.
(21) Brunner, J., Franzusoff, A. J., Luscher, B., Zugliani, C., and Semenza, G. (1985) Membrane protein topology: amino acid residues in a putative transmembrane α-helix of bacteriorhodopsin labeled with the hydrophobic carbene-generating reagent 3-(trifluoromethyl)-3-(*m*-[^{125}I]-iodophenyl)diazirine. *Biochemistry 24*, 5422–5430.
(22) Amiguet, P., Brunner, J., and Tschopp, J. (1985) The membrane attack complex of complement: lipid insertion of tubular and nontubular polymerized C9. *Biochemistry 24*, 7328–7334.
(23) Frey, A. B., Kreibich, G., Wadhera, A., Clarke, L., and Waxman, D. J. (1986) 3-(Trifluoromethyl)-3-(*m*-[^{125}I]-iodophenyl)-diazirine photolabels a substrate-binding site of rat hepatic cytochrome P-450 form PB-4. *Biochemistry 25*, 4797–4803.
(24) Montecucco, C., Schiavo, G., Brunner, J., Duflot, E., Boquot, P., and Roa, M. (1986) Tetanus toxin is labeled with photoactivatable phospholipids at low pH. *Biochemistry 25*, 919–924.
(25) Kreig, U. C., Isaacs, B. S., Yemul, S. S., Esmon, C. T., Bayley, H., and Johnson, A. E. (1987) Interaction of blood coagulation factor Va with phospholipid vesicles examined by using lipophilic photoreagents. *Biochemistry 26*, 103–109.
(26) Harter, C., Bachi, T., Semenza, G., and Brunner, J. (1988) Hydrophobic photolabeling identifies BHA2 as the subunit mediating the interaction of bromelain-solubilized influenza virus hemagglutinin with liposomes at low pH. *Biochemistry 27*, 1856–1864.
(27) Baldini, G., Martoglio, B., Schachenmann, A., Zugliani, C., and Brunner, J. (1988) Mischarging *Escherichia coli* $tRNA^{Phe}$ with L-4′-[3-(trifluoromethyl)-3*H*-diazirin-3-yl]-phenylalanine, a photoactivatable analogue of phenylalanine. *Biochemistry 27*, 7951–7959.
(28) Brunner, J., Senn, H., and Richards, F. M. (1980) 3-Trifluoromethyl-3-phenyldiazirine. *J. Biol. Chem. 255*, 3313–3318.
(29) Nassal, M. (1984) 4′-(1-Azi-2,2,2-trifluoroethyl)phenylalanine, a photolabile carbene-generating analogue of phenylalanine. *J. Am. Chem. Soc. 106*, 7540–7545.
(30) Nassal, M. (1983) 4′-(1-Azi-2,2,2-trifluoroethyl)benzoic acid, a highly photolabile carbene generating label readily fixable to biochemical agents. *Liebigs Ann. Chem.* 1510–1523.
(31) Trozzola, A. M., Murray, R. W., and Wasserman, E. (1962) The electron paramagnetic resonance of phenylmethylene and biphenylenemethylene; a luminescent reaction associated with a ground state triplet molecule. *J. Am. Chem. Soc. 84*, 4990–4991.
(32) Baron, W. J., DeCamp. M. R., Hendrick, M. E., Jones, M., Jr., Levin, R. H., and Sohn, M. B. (1973) Carbenes from diazo compounds. *Carbenes* (M. Jones, Jr., and R. A. Moss, Eds.) Vol. 1, p 1, Wiley, New York.
(33) Baer, T. A., and Gutsche, C. D. (1971) Chemistry of bivalent carbon intermediates. VI. The photolysis of 2-*n*-butylphenyldiazomethane. *J. Am. Chem. Soc. 93*, 5180–5186.
(34) Moss, R. A., and Dolling, U.-H. (1971) Photolysis of phenyl diazomethane in olefinic matrices. Chemistry of triplet phenylcarbene. *J. Am. Chem. Soc. 93*, 954–960.
(35) Admasu, A., and Platz, M. S., unpublished results.
(36) Trozzolo, A. M., and Wasserman, E. (1975) Structure of arylcarbenes. *Carbenes* (R. A. Moss, and M. Jones, Jr., Eds.) Vol. 2, p 185, Wiley, New York.
(37) Barcus, R. L., Hadel, L. M., Johnston, L. J., Platz, M. S., Savino, T. G., and Scaiano, J. C. (1986) 1-Naphthylcarbene: spectroscopy, kinetics, and mechanism. *J. Am. Chem. Soc. 108*, 3928–3937.
(38) Battaglia, C. J., Chang, J. C.-M., Daniel, D. S., Hamblen, D. P., Glover, C. P., and Kim, S. H. (1977) Ger. Offen. 2,-722,617 [*Chem. Abstr.* (1979) *90*, 199867*z*].
(39) Battaglia, C. J., Chang, J. C.-M., and Daniel, D. S. (1980) U. S. Pat. 4,214,968 [*Chem. Abstr.* (1980) *93*, 212413*g*].
(40) Seshimoto, O., Kubodera, K., and Kondo, A. (1983) Ger. Offen. DE 3,226,045 [*Chem. Abstr.* (1983) *98*, 103919*j*].
(41) Kitajima, M., Seshimoto, O., and Mizutani, S. (1983) Ger. Offen. DE 3,309,251 [*Chem. Abstr.* (1983) *99*, 191084*g*].

Registry No. **1a**, 87736-85-4; **1b**, 135481-93-5; **4a**, 135481-94-6; **5a**, 135481-95-7; **6a**, 704-36-9; **6b**, 135481-96-8; **7a**, 50562-01-1; **9a**, 106-38-7; **9b**, 51554-93-9; **10a**, 394-59-2; **10b**, 65440-56-4; **11a**, 75703-25-2; **11b**, 135481-97-9; **12a**, 135481-98-0; **12b**, 135481-99-1; **13a**, 87736-82-1; **13b**, 135482-00-7; PhH, 71-43-2; MeOH, 67-56-1; CCl_4, 56-23-5; Et_3SiH, 617-86-7; Et_2NH, 109-89-7; Li, 7439-93-2; *p*-MeC_6H_4Li, 2417-95-0; F_3CCO_2Et, 383-63-1; MsCl, 124-63-0; cyclohexane, 110-82-7; hydroxylamine hydrochloride, 5470-11-1.

Terminal-Modified Polylysine-Based Chelating Polymers: Highly Efficient Coupling to Antibody with Minimal Loss in Immunoreactivity

M. A. Slinkin,† A. L. Klibanov,‡ and V. P. Torchilin*

Laboratory of Enzyme Engineering, USSR Cardiology Research Center, Moscow 121552, USSR.
Received June 3, 1991

A method is suggested for the preparation of chelating polymers containing a single terminal reactive group capable of interaction with proteins. These polymers were synthesized from *N*-CBZ-polylysine and DTPA and contain a terminal SH or pyridyldisulfide group. A polymer molecule with MW 13 500 is able to carry up to 40 DTPA residues. Polymers easily and quantitatively bind with antibodies (Fab fragments of antimyosin antibodies R11D10) with minimal effect on antibody immunoreactivity as revealed in ELISA assay and in direct immunoanalysis. Conjugates prepared can chelate radioactive metal ions reaching very high specific radioactivity (>1 mCi ^{111}In/10 μg of protein). Perspectives for their application are discussed.

INTRODUCTION

Monoclonal antibodies of different specificity find multiple applications as vectors for the delivery of appropriate labels into affected regions in the body. There exist already a whole set of labels possessing variable properties which permit the use of labeled monoclonals for radioimmunoscintigraphy (*1*), NMR tomography (*2*), immunofluorescent analysis (*3*), etc. The ions of transition metals are often used as the labels, which can be bound with an antibody molecule via so called bifunctional chelating agents combining two different functions: (1) they are able to form a chemical bond with the functional groups of the antibody molecule, and (2) they are capable of high-affinity chelating of heavy-metal ions (*4*).

Among the problems arising with use of labeled antibodies, one of the most important ones is how to achieve high specific capacity of antibody molecule toward the metal ion. The reason is that currently used methods of antibody modification with chelating agents permit introduction into the antibody molecule of only few metal atoms prior to the complete loss of antigen-binding activity. This is explained by the possible modification with the chelating agent of the amino acid residue participating in the spatial organization of the antigen-binding region. At the same time it is known that in some cases it is desireable to achieve the binding of 50–100 metal atoms per single antibody molecule in order to get sufficient label accumulation. Thus, for example, only high concentration of target-accumulated metal makes it possible to obtain acceptable NMR tomographic tumor image using Gd-labeled specific antibodies (*5*, *6*).

Several years ago we (*7*, *8*) and other authors (*9*, *10*) described a general approach to solving the problem. It was suggested to use, for antibody modification, synthetic polymers containing multiple chelating groups and some groups able to bind chemically to antibody molecules, instead of low-molecular-weight chelates. The approach could permit the binding of dozens of metal ions to a single antibody via a chelating polymer chain, while modifying only one or few amino acid residues in protein molecule. Several different strategies to synthesize these chelating polymers were developed (*9*, *11–13*). Unfortunately, all of them resulted in random distribution of protein-binding groups along the polymeric chain. This type of distribution made it very difficult to achieve real one-point modification of the antibody molecule with the chelating polymer or to escape completely intra- or intermolecular cross-linking of antibody with polymer. Antibody overmodification or cross-linking were especially noticeable when one attempted to increase polymer and protein concentration in the reaction mixture in order to increase the reaction yield.

In the present paper we suggest a new strategy for the synthesis of protein-reactive chelating polymers. This strategy makes it possible to introduce into a polymer molecule a single antibody-reactive group strictly via a terminus of the polymeric chain. The advantages of the approach suggested, in comparison with the case of random distribution of reactive groups along the polymer molecule, are the following:

(1) The possibility of the inter- or intramolecular cross-linking of the antibody upon its conjugation with the chelating polymer is completely excluded. Since this cross-linking is often the reason for protein inactivation and the loss of antigen-binding ability, one can hope that the use of new "terminal-modified" polymers should cause minimal antibody inactivation.

(2) If the terminal reactive group of chelating polymer is not shielded with the polymer chain and can easily enter the conjugation reaction, one can also hope that the terminal-modified polymer will possess high binding efficacy toward proteins.

The new strategy, schematically represented in Figure 1, can be applied for the synthesis of different chelating polymers based on polylysine. We will discuss the preparation and the use of polymer IV (see Figure 1), which contains a PDP residue as the protein-reactive group and DTPA residues as chelating units.

EXPERIMENTAL PROCEDURES

Monoclonal anticardiac myosin antibody R11D10 was prepared according to the method of ref 14 by Dr. B. A. Khaw (Department of Nuclear Medicine, Massachusetts General Hospital, Boston, MA) and kindly provided to us as a gift. The purified antibody was then treated with

* To whom reprint requests should be addressed. Present address: Center for Imaging and Pharmaceutical Research, MGH, Charlestown, MA 02129.

† Present address: INSERM Unite 211, Plateau Technique du C.H.R., Quai Moncousu, 44035 Nantes CEDEX, France.

‡ Present address: Department of Biochemistry, University of Tennessee, Knoxville, TN 37996.

1043-1802/91/2902-0342$02.50/0 © 1991 American Chemical Society

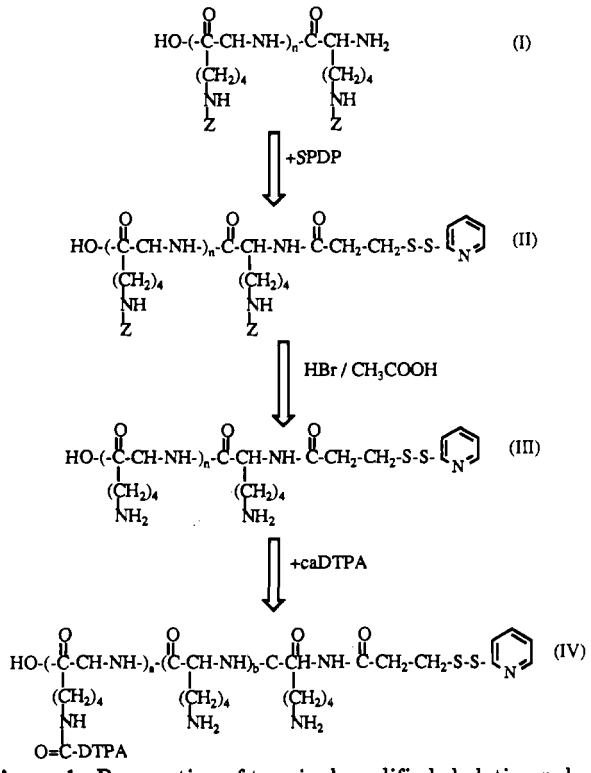


Figure 1. Preparation of terminal-modified chelating polymer based on polylysine.

papain (*15*) to obtain Fab fragments. Myoscint is a product of Centocor Co.

As a starting polymer *N*-(carbobenzoxy)poly(D,L-lysine) [*N*-benzyloxycarbonyl)poly(D,L-lysine), Z-protected poly-(D,L-lysine)] with MW 9000 was used (PL-Z, polymer I). PL-Z, *N*-succinimidyl 3-(pyridyldithio)propionate (SPDP), diethylenetriaminepentaacetic acid cyclic anhydride (caDTPA), trinitrobenzenesulfonic acid (TNBS), and dithiothrietol (DTT) are products of Sigma Co. Buffer solution components and organic solvents are products of Fluka. Carriers for gel chromatography (Sephadexes G-25, G-50, and G-100) were obtained from Pharmacia-LKB.

1. Polymer Synthesis. (*A*) *The Incorporation of PDP Residue into PL-Z* (*Synthesis of Polymer II*). SPDP (1.1 mg, 3.5 μmol) in 100 μL of DMFA and 0.14 μL of triethylamine (TEA, 1 μmol) were added to the solution of 7.6 mg of PL-Z (0.8 μmol) in 250 μL of DMFA. The mixture was incubated overnight at 4 °C and polymer II was precipitated with 2 mL of water. The precipitate was centrifugated and washed with water twice. The yield upon the lyophilization was 7.1 mg.

(*B*) *Z Deprotection* (*Synthesis of Polymer III*). A 250-μL portion of 36% HBr in acetic acid was added to dry fine-powdered polymer II and the mixture was vortexed for 20 min at room temperature. Then 2 mL of diethyl ether was added and the suspension formed was centrifugated. The precipitate was twice washed with diethyl ether and lyophilized. The yield was 6.5 mg.

To determine the quantity of PDP residues the product was dissolved in distilled water up to the concentration of 6.5 mg/mL, and 16 μL of the solution obtained was added to 434 μL of PBS, pH 7.0. The mixture obtained was supplemented with 50 μL of fresh 0.25 M DTT; the changes in the solution's optical density were registered on the Yanaco UO 2000 spectrophotometer, and PDP content in the polymer was calculated according to ref 17.

(*C*) *The Incorporation of DTPA Residues into Polymer III* (*Synthesis of Polymer IV*). The modification of polymer III with caDTPA was performed as described in ref 11. Briefly, the solution of 2 mg of polymer III (9.1 μmol as units) in 0.1 M carbonate, pH 8.0 (6 mg/mL), was supplemented under continuous stirring with eight aliquots from the solution of 3 mg of caDTPA (8.4 μmol as reactive groups) in DMSO (90 mg/mL). The product obtained was stored at 4 °C as reaction solution until needed.

The degree of modification of amino groups in polymer III with DTPA residues was estimated by the labeling of aliquots from the solution obtained with a trace amount of indium-113 citrate (*11*) and subsequent chromatography on a Sephadex G-100 column. The γ-counting of fractions obtained was performed by using a Compugamma (LKB) counter.

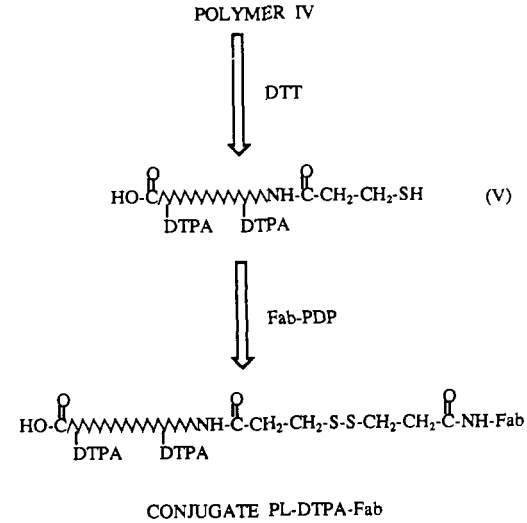


Figure 2. Conjugation of R11D10 Fab to chelating polymer V.

2. Conjugate Preparation. The conjugate between polymer IV and R11D10 Fab was obtained according to the scheme in Figure 2 with the formation of reducible S–S bond between both components.

(*A*) *Preparation of N-[3-(2-Pyridyldithio)propionylated] R11D10 Fab.* A 5-μL portion of DMSO, containing 94 μg (300 nmol) of SPDP, was added to the solution of 1.5 mg of R11D10 Fab in 0.05 M phosphate, pH 7.5 (3 mg/mL). The mixture was incubated for 2 h at room temperature and then dialyzed against 50 mM phosphate, pH 8.0, overnight at 4 °C. The content of PDP residues in the product obtained was estimated via the reduction of R11D10 Fab with DTT as described in ref 17.

(*B*) *Reduction of Polymer IV and Conjugation of SH Polymer with R11D10 Fab.* To generate SH groups on the terminus of the polymeric chain, polymer IV was reduced with DTT. For this purpose DTT was added to final concentration of 25 mM to the solution of polymer IV in water (6 mg/mL) and the mixture obtained was incubated for 20 min. The reduced polymer was separated from low molecular weight impurities (including DTPA) by centrifugation on the column with 2 mL of Sephadex G-25 equilibrated with 0.05 M phosphate, pH 8.0. Immediately after separation, the solution of polymer V (30–300 μg) was added to the solution of PDP–R11D10 Fab (100 μg, 3 mg/mL) and the mixture was incubated overnight at 4 °C.

3. Analysis of Immunoconjugates. The efficacy of the incorporation of PDP–R11D10 Fab and polymer V into conjugates was estimated by using chromatography of reaction mixtures upon conjugation on Sephadex G-100 and the labeling of conjugates with ^{111}In (see Figure 3 for details). The labeling was performed as follows: the

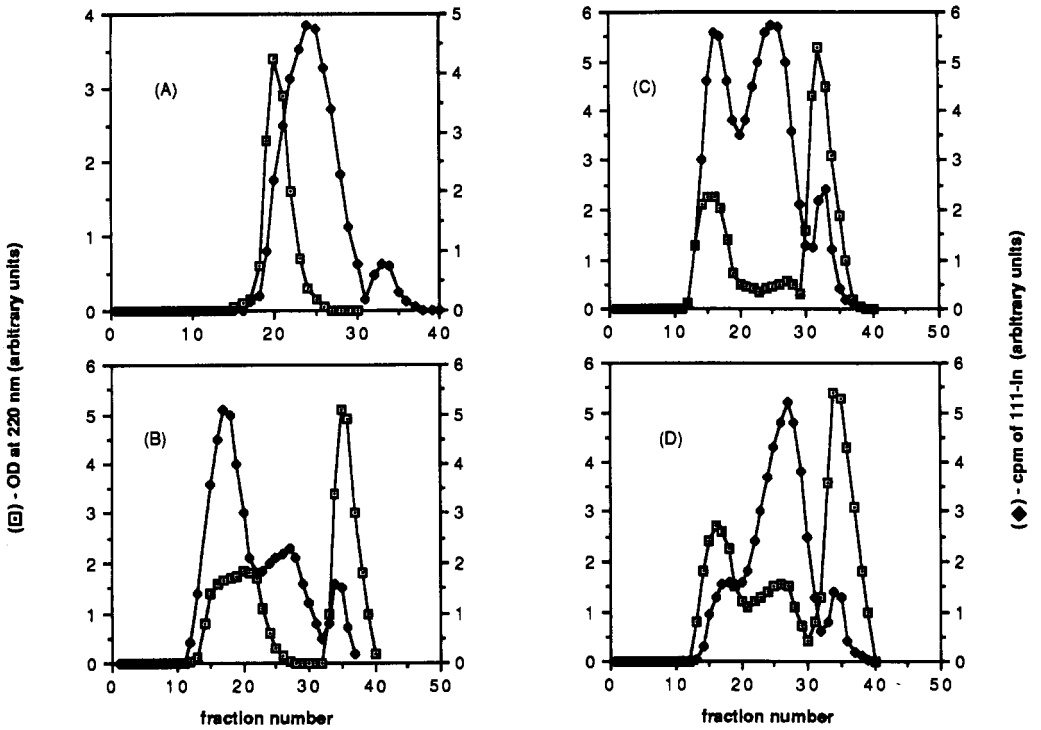


Figure 3. Gel chromatography of free R11D10 Fab and ^{111}In-labeled PL–DTPA (a) and of the mixtures resulting from conjugation of polymer V to R11D10 Fab at weight ratios 0.3:1 (b) 1:1 (c), and 3:1 (d). The chromatograms were generated by passage of the samples through a Sephadex G-100 column (1.0 × 20 cm) equilibrated with 0.05 M acetate + 0.15 M NaCl, pH 6.5. Fractions (0.6 mL) were collected, and γ-radioactivity and optical density at 220 or 280 nm were measured in each fraction. From b to d one can notice the increase in free PL–DTPA and free ^{111}In peaks.

appropriate reaction mixture was supplemented with sodium citrate (up to 20 mM), the pH value was adjusted to 6.0, trace amounts of indium-111 citrate were added, and the whole system was incubated for 30–60 min. The fractions after gel chromatography were analyzed by measuring their optical density at 280 (Fab content) and 220 nm and/or γ-radioactivity (the content of ^{111}In-labeled polymer).

The additional information about conjugate structure and composition was obtained by performing SDS–PAGE of reaction mixtures upon the conjugation in the absence or in the presence of mercaptoethanol with subsequent Coomassie staining for protein visualization. To perform SDS–PAGE the apparatus for minielectrophoresis (MINI Protean II, Bio-Rad Laboratories) was used.

Antigen-binding activity of R11D10 Fab in the native state and after its modification with SPDP and polymer V was determined by the ELISA method using peroxidase conjugate of anti-mouse antibodies (Pierce). In the case of polymer-containing-conjugate analysis, the absence of free R11D10 Fab was preliminary verified by SDS–PAGE.

Additional control of conjugate immunoreactivity was performed by direct immunoanalysis after conjugate labeling with ^{111}In. The efficacy of ^{111}In delivery to plate-adsorbed antigen was compared with that of the commercially available Myoscint preparation, which contains R11D10 Fab modified with DTPA mixed anhydride. For the labeling, 10 μg of polymer V–Fab conjugate or 10 μg of Myoscint were incubated in 20 mM citrate, pH 6.0, with equal quantities of fresh indium-111 citrate (1 mCi) for 30–40 min, and labeled preparations were separated on a PD-10 column with Sephadex G-50 in the presence of 1 mg of BSA.

RESULTS

Synthesis of PL–DTPA–PDP (Polymer IV). To introduce into PL-Z polymeric chain pyridyl disulfide residues, SPDP was taken in 5-fold molar excess. It is known that in organic media and in the presence of TEA, the reaction between a primary amino group and *N*-succinimide ester usually proceeds quantitatively (*12*). After the precipitation of the reaction product with water and its lyophilization, the absence of the residual free amino groups in the product was verified by using nonaqueous titration with perchloric acid (*18*). It was found that equal amounts of perchloric acid are required to change the color of the indicator (Thymol Blue), both in the solution of the modified polymer in DMSO and in pure DMSO.

It is known that the removal of the *N*-(benzyloxycarbonyl) group from Z-protected PL in 36% HBr solution in acetic acid proceeds smoothly and quantitatively during 15–60 min if the polymer is used as a fine powder (*16*). In our case fine-powdered polymer II upon the addition of 36% HBr in acetic acid was slowly dissolved with the formation of a transparent yellow solution. The solution gradually turned into a turbid one as the reaction proceeded, carbon dioxide was released, and benzyl bromide formed. The resulting polymer precipitated upon the addition of diethyl ether, and after double washing (to remove benzyl bromide) and lyophilization, it easily dissolved in the water, forming transparent colorless solution.

It was shown spectrophotometrically that 0.2 g of polymer III obtained contains 14.8 μmol of PDP residues. Supposing that (1) each polymeric chain of starting PL-Z contains a terminal amino group, (2) all terminal amino groups are modified with SPDP, and (3) all PDP residues in polymer II remain untouched in the process of Z deprotection, one can use the data obtained for the direct estimation of the average value of M_n for polymer III. Really, under the conditions mentioned 0.2 g of polymer III corresponds to 14.8 μmol, i.e. 1 mol of polymer III is equal to 13 500. Since the molecular weight of a single unit of PL bromide is 210, the polymerization degree of polymer III is 13500:210 = 64.

DTPA residues were introduced into polymer III in the manner similar to that usually used for PL (*11*). No changes in the PDP content were discovered upon polymer modification with caDTPA. Sephadex G-100 gel chromatography of the reaction mixture (containing polymer IV and free DTPA) upon its labeling with the trace amount of ^{111}In has shown that 70% of In radioactivity is associated with the peak of polymer IV, i.e. the efficacy of caDTPA binding with the polymer is 70%. From these data it is easy to calculate that the percent of polymer units capable of chelating is as high as 63% (see molar ratio of caDTPA used and polymer chain units). It means that each PL–DTPA–PDP chain with M_n 13 500 contains 0.63 × (13500:210) = 40 DTPA residues.

Preparation of Polymer IV–R11D10 Fab Conjugate. The average quantity of PDP residues introduced into each R11D10 Fab molecule was 3.4. These modified Fab fragments were allowed to react with SH-containing PL–DTPA, which was obtained by reducing polymer IV with DTT.

Gel chromatography of the reaction mixtures obtained at different polymer:Fab ratios (see Figure 3) shows that (1) polymer is incorporated into the conjugate with high efficacy; thus, at the weight ratio polymer:Fab = 0.3:1 (which corresponds to the molar ratio 1.2:1, when polymer M_n = 13 500) the efficacy of polymer incorporation is ca. 95%. It means, in addition, that all three assumptions made during the estimation of polymer IV molecular weight (all chains of starting PL-Z have a terminal amino group, all primary amino groups are modified with SPDP, and all PDP residues remain untouched during Z deprotection) are fulfilled, i.e. we made the proper estimation of polymer molecular weight; and (2) at the weight ratio polymer:Fab > 1, all R11D10 Fab molecules are incorporated into the conjugate.

Because complete absence of free R11D10 Fab in the conjugate is the necessary requirement for the proper estimation of antigen-binding ability of the conjugates, the reaction mixtures of the conjugation reaction were additionally analyzed by SDS–PAGE. DTT-free mixture with the weight ratio polymer:Fab = 0.3:1 gave both a wide band at 50 000–70 000 and a narrow band at 50 000, corresponding to conjugated and nonbound Fab, respectively. In two other mixtures (see Figure 3) the narrow band was absent, demonstrating the absence of nonbound Fab fragments. When the electrophoresis was done in the presence of DTT, only two narrow bands were discovered at 25 000 and 27 000, corresponding to light chains and fragments of heavy chains of immunoglobulins; PL–DTPA initially bound with R11D10 Fab via S–S bonds under the conditions used was split off and moved with the front.

To estimate the labeling efficacy of the polymeric derivative of R11D10 Fab with ^{111}In, the conjugate obtained at weight ratio polymer:Fab = 1:1 was separated from free polymer by Sephadex G-100 chromatography—fractions 13–20 were collected (see Figure 3). The data presented in Figure 4 clearly illustrate the effect of the modification of R11D10 Fab with chelating polymer: the specific radioactivity of Fab fragments in the conjugate is 35-fold higher than that of R11D10 Fab directly modified with DTPA mixed anhydride. Since under the experimental conditions used 100% of the added label was incorporated into the PL–DTPA–Fab conjugate, one can suppose that the specific radioactivity achieved for the conjugate obtained may be even further increased.

Immunoanalysis of the Conjugate. To perform immunoanalysis the same conjugate of Fab with polymer V

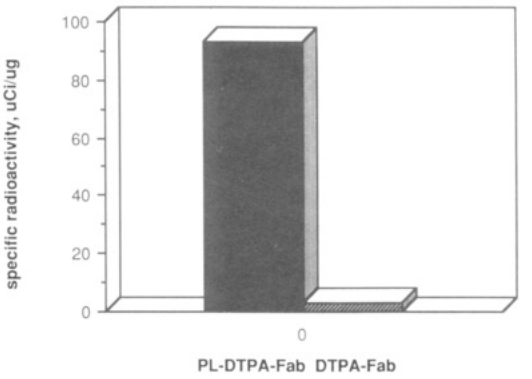


Figure 4. Specific radioactivity of ^{111}In-labeled R11D10 Fab modified with PL–DTPA or with mixed anhydride of DTPA (Myoscint). The same amounts of both preparations were labeled with the same amount of indium-111 citrate.

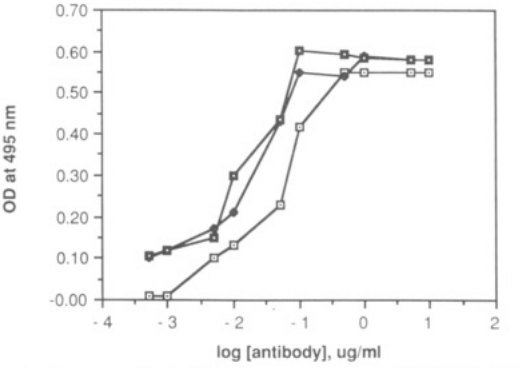


Figure 5. Enzyme-linked immunoassay of R11D10 Fab (□), PDP–R11D10 Fab (◆), and PL–DTPA–R11D10 Fab (⊡). Heavy chains of myosin from the human heart were used as antigen. Peroxidase-anti-mouse antibody was used to develop the antibodies bound with the plate.

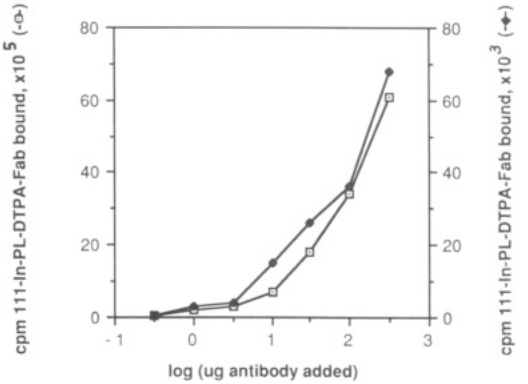


Figure 6. Comparative binding to myosin-coated microtiter wells of serial dilutions of ^{111}In-labeled PL–DTPA–R11D10 Fab (⊡) and ^{111}In-labeled Myoscint (◆). Two different figures are presented simultaneously (see ordinates) for easier comparison of the curves obtained for both preparations.

was used as for the estimation of the specific radioactivity. The results of nondirect immunoassay are shown in Figure 5. One can see that the apparent affinity of PL–DTPA–Fab toward the antigen is somewhat lower than that for nonmodified Fab and Fab–PDP: the half-binding point for the polymer-containing conjugate corresponds to ca. 3-fold higher concentration of antibodies per well. Still, the affinity of the conjugate remains high enough.

High affinity of the conjugate is confirmed by results of direct immunoanalysis, performed with ^{111}In-labeled PL–DTPA–Fab and Fab–DTPA at the conditions already described. It can be seen from Figure 6 that titration curves for both preparations coincide, i.e. antigen-binding

activity of R11D10 Fab upon its modification with DTPA mixed anhydride or with polymer V is the same. At the same time, polymer-containing conjugate is able to deliver to adsorbed antigen 40–60-fold more label than Fab–DTPA.

Thus, an immunoreactive polymer-containing conjugate of R11D10 Fab is obtained, containing a significantly higher quantity of chelating groups than commercial Fab–DTPA preparation.

DISCUSSION

In the present work we describe the method for covalent binding of proteins (antibody Fab fragments, in particular) with a polylysine-derived chelating polymer containing a single chain-terminal group for the attachment to the protein molecule. The approach suggested permits us to completely exclude intermolecular aggregation or intramolecular cross-linking of a protein upon its modification with chelating polymer. As a result the possibility of protein (especially antibody) inactivation during the conjugation can be noticeably diminished.

From the chemical point of view the approach described is rather obvious. ϵ-*N*-Carbobenzoxy-protected polylysine (PL-Z) used by us as the starting material (see the scheme in Figure 1) is obtained as a byproduct during polylysine synthesis (*19*). As a majority of other homopolypeptides, PL-Z can be prepared by polycondensation of the *N*-carboxy anhydride of ϵ-*N*-lysine. As a result, a polymeric chain is synthesized containing free terminal α-amino group. In some cases, because of so-called termination reactions, not all the synthesized polymeric chains contain terminal amino groups (*18*). For us it just means that in the resulting chelating polymer some polymer molecules can lack an activated terminal group capable of protein binding, which can decrease the yield of the conjugation reaction.

To activate the terminal amino group in PL-Z this group was modified with SPDP in organic medium. The pyridyl disulfide group appearing in PL-Z as the result of the modification is hydrophilic, stable toward hydrolysis, and practically does not react with primary amino groups, but very efficiently interacts with SH groups (*17*). In addition, upon the reduction with DTT, PDP–polymer obtained can be easily transformed into a SH-containing polymer. The latter can be bound both with another PDP-containing substance with the formation of a reducible S–S bond and with variable heterobifunctional reagents, containing maleimide or haloacetamide groups, with the formation of a stable thioester bond (*20*). And, finally, in our case the PDP residue serves as the orthogonal protection for the terminal amino group in PL-Z, since it is insensitive toward the relatively severe conditions of the removal of Z-protection from the side chains of polylysine.

It is interesting to compare the method suggested in the present study with another method, suggested recently for site-specific incorporation into an antibody molecule of a large number of photosensitizer tin(IV) chlorin e_6 ($SnCe_6$) residues (*21*). For this purpose Rakestraw et al. (*21*) also used a polymer containing the single active group at the terminus of a polymeric chain. Such a polymer was obtained (*21*) with dextran containing a single reducing terminus (an aldehyde group) to which the antibody was linked. The simplest and the most convenient way to modify the aldehyde group was chosen: dextran in the aqueous medium was modified with a large excess of adipic acid dihydrazide, which gave an hydrazide-containing polymer capable of the binding with oxidized oligosaccharide moieties of the antibody molecule.

The subsequent incorporation of active agents into dextran polymer with the preservation of an active hydrazide group required a number of additional labor-consuming steps: (1) first of all, the terminal group of hydrazinodextran was blocked by its modification with the hydroxyphtalimide ester of *N*-trityl-substituted adipic acid monohydrazide; (2) after that dextran units were transformed into cyclic *trans*-carbonate, which was then converted to carbazate by hydrazinolysis; (3) chlorin active ester was then allowed to react with dextran carbazate, and the remaining side chain hydrazide groups were capped by reaction with excess acetaldehyde under reduction trapping conditions; and (4) finally, the chain-terminal trityl blocking group was removed to expose the hydrazide group.

The synthetic scheme for the preparation of terminal-modified carrier polymer described in the present paper is obviously much more simple and convenient. Moreover, the interaction of the SH group with the pyridyl disulfide residue (maleimide residue being still better) proceeds in an aqueous medium with a much higher rate and efficiency than the interaction between hydrazide and aldehyde groups. It is clearly seen from the results obtained by the authors of ref 21 that while conjugating $SnCe_6$–dextran with antibodies the polymer was taken in 20-fold molar excess, but even under this condition not all of the antibody was observed to form conjugate. In our case to obtain the conjugate between PL–SPDP–SH and PDP–Fab we used only 3–4-fold molar excess of polymer, which was sufficient to transform into the conjugate all antibodies added and permitted us to avoid the unbound protein separation step.

The average number of polymeric chains per one protein molecule in the conjugate in our case and in ref 21 was ca. 2 polymer molecules per protein. The maximal quantity of $SnCe_6$ (which is limited by $SnCe_6$ solubility in water) incorporated into whole antibody molecule via two molecules of dextran with MW 40 000 was equal to 20 residues in ref 21. We succeeded to incorporate into R11D10 Fab 80 DTPA residues utilizing two molecules of PL–DTPA–SH with molecular weight 13 500. This estimation is confirmed by the comparison of the labeling efficiency of our R11D10 Fab–polymer V conjugate and that of Myoscint (Fab–DTPA). Under the assumption that the average number of DTPA residues in Fab–DTPA is ca. 2, and the minimal effect of polymer modification being in our system close to 35, we can roughly count that the average number of DTPA residues per one Fab fragment in polymeric conjugate is more than 70.

At the same time the conjugate obtained demonstrates only a slight decrease in immunoreactivity as compared with routinely modified antibody (not exceeding 3-fold, see Figures 5 and 6, whereas at least a 10-fold decrease was found for chelating polymer–antibody conjugates described in refs 9–13, 24).

Thus, we have shown that the approach suggested makes it possible to solve simultaneously two problems: (1) to reach extremely high reaction yield in the coupling of polymer V with Fab fragments—up to 100% of protein incorporation and (2) to achieve a high degree of preservation of antigen-binding ability of R11D10 Fab fragments during their modification with chelating polymer.

We believe that the latter effect is determined by the fact that the method described completely excludes the possibility of intramolecular protein cross-linking in the process of conjugation. Usually this cross-linking results in the decrease of Fab immunoreactivity due to both multipoint protein modification and conformational changes in protein globule. In our recent work (*12*) we have studied

the modification of R11D10 Fab with the chelating polymer PL–deferoxamine with the random distribution of reactive hydroxysuccinimide groups along the polymer chain. Under the conditions described in ref 12 we succeeded to achieve much lower protein conjugation efficacy than in the present study—25–50%. In addition, Fab immunoreactivity upon the conjugation decreased by at least 1 order of magnitude.

Very high specific activity (>1 mCi/10 μg of protein) of polymer-modified radiolabeled-antibody preparations could allow the use of substantially less antibody than is now being administered in clinical studies (*22*, *23*). For example, a clinical dose of 1.8 mCi ^{111}In (*22*) would require less than 20 μg of polymer-modified antimyosin Fab. A smaller amount of xeno-antibody protein will surely reduce the incidence of anti-murine antibody response that frequently occurs with diagnostic and therapeutic application of murine monoclonal antibodies in cancer patients (*24*, *25*). At the same time the authors realize that such extensive modification of antibody with charged polymers can cause some unpredictable changes in conjugate biodistribution as compared with that for routinely modified antibodies. This definitely should be taken into account for further supposed clinical applications. The problem is currently under our investigation.

As for some decrease in the antigen-binding activity of Fab fragments upon their modification with polymer, this effect, already being quite reasonable, can be still further reduced by performing site-specific modification of proteins. This modification is possible, for example, in case of Fab fragments in which one SH group can be specially generated far away from the antigen-binding site (*26*). On the other hand, while working with whole antibodies, one can introduce several SH groups into oxidized oligosaccharide units in the Fc portion of antibody (*27*). Still, in ref 28, where the modification of IgG with polymer was performed via an oxidized oligosaccharide moiety, the authors observed a 3-fold decrease in antibody affinity upon the conjugation.

In our opinion the data presented definitely prove that the chelating polymer described in the present study is more suitable and perspective for antibody modification than other polymers suggested for the same purpose earlier by us (*11–13*) and other authors (*9*, *10*, *24*). Moreover, the extension of the method reported in this work to other biologically active agents and chain-terminal groups could be easily performed.

The chelating residue of DTPA was used in this work as the active agent for the subsequent labeling of antibody-based conjugates with a number of heavy-metal ions. However, any other active agent (drug, photosensitizer, toxin) which can be derivatized with a group suitable for the attachment to polylysine side chains could be employed.

On the other hand, polymers can be synthesized with terminal reactive groups different from the SH or pyridyl disulfide group described by us (for example, aldehyde, hydrazide, isothiocyanate, and some others), but still be capable of binding with different residues in the protein globule. One can suppose that varying polymer terminal groups will provide additional possibilities for the optimization of conditions for the preparation of polymer–antibody conjugates with more complete preservation of antigen-binding activity. These approaches are currently under investigation.

LITERATURE CITED

(1) Larson, S. M., Carrasquillo, J. A., and Reynolds, J. C. (1984) Radioimmunodetection and radioimmunotherapy. *Cancer Invest. 2*, 363–381.

(2) Laufer, R. B. (1987) Paramagnetic metal complexes as water proton relaxation agents for NMR imaging: theory and design. *Chem. Rev. 87*, 901–927.

(3) Hemmila, I. (1985) Fluoroimmunoassays and immunofluorometric assays. *Clin. Chem. 318*, 359–370.

(4) Meares, C. F., and Goodwin, D. A. (1984) Linking radiometals to proteins with bifunctional chelating agents. *J. Protein Chem. 3*, 215–228.

(5) Anderson-Berg, W. T., Strand, M., Lempert, T. E., Rosenbaum, A. E., and Joseph, P. M. (1986) Nuclear magnetic resonance and gamma camera tumor imaging using Gd-labeled monclonal antibodies. *J. Nucl. Med. 27*, 829–833.

(6) Curtet, C., Tellier, C., Bohy, J., Conti, M. L., Saccavini, J. C., Thredrez, P., Douilard, J. Y., Chatal, J. F., and Koprowski, H. (1986) Selective modification of NMR relaxation time in human colorectal carcinoma by using Gd(DTPA) conjugated with monoclonal antibody 19-9. *Proc. Natl. Acad. Sci. U.S.A. 83*, 4277.

(7) Torchilin, V. P., Khaw, G. A., Klibanov, A. L., Slinkin, M. A., Haber, E., and Smirnov, V. N. (1986) Modification of monclonal antibodies with polymers possessing chelating properties. *Bull. Exp. Biol. Med. (USSR) 102*, 63–65.

(8) Torchilin, V. P., Klibanov, A. L., Nossiff, N. D., Slinkin, M. A., Strauss, H. W., Haber, E., Smirnov, V. N., and Khaw, B. A. (1987) Monoclonal antibody modification with chelate-linked high-molecular-weight polymers: major increases in polyvalent cation binding without loss of antigen binding. *Hybridoma. 6*, 229–240.

(9) Manabe, Y., Longley, C., and Furmanski, P. (1986) High-level conjugation of chelating agents onto immunoglobulins: use of an intermediary poly(L-lysine)–diethylenetriaminepentacetic acid carrier. *Biophys. Biochym. Acta 883*, 460–467.

(10) Shreve, P., and Aisen, A. E. (1986) Monclonal antibodies labeled with polmeric paramagnetic ion chelates. *Magn. Res. Med. 3*, 336–340.

(11) Klibanov, A. L., Slinkin, M. A., and Torchilin, V. P. (1989) Conjugation of proteins with chelating polymers via water-soluble carbodiimide and *N*-hydroxysulfosuccinimide. *Appl. Biochem. Biotech. 22*, 45–58.

(12) Slinking, M. A., Klibanov, A. L., Khaw, B. A., and Torchilin, V. P. (1990) Succinylated polylysine as a possible link between the antibody molecule and deferoxamine. *Bioconjugate Chem. 1*, 291–295.

(13) Torchilin, V. P., Klibanov, A. L., Slinkin, M. A., Danilov, S. M., Levitsky, D. O., and Khaw, B. A. (1989) Antibody-linked chelating polymers for radioimmunoimaging in vivo. *J. Controlled Release 11*, 297–303.

(14) Khaw, B. A., Mattis, J. A., Melincoff, G., Strauss, H. W., Gold, H. K., and Haber, E. (1984) Monoclonal antibody to cardiac myosin: imaging of experimental myocardial infarction. *Hybridoma. 3*, 11–23.

(15) Porter, R. R. (1959) The hydrolysis of rabbit gamma-globulin and antibodies with crystalline papain. *Biochem. J. 73*, 110–120.

(16) Ben-Ishai, D., and Berger, A. (1952) Cleavage of *N*-carbobenzoxy groups by dry hydrogen bromide and hydrogen chloride. *J. Org. Chem. 17*, 1564–1567.

(17) Carlsson, J., Drevin, H., and Axen, R. (1978) Protein thiolation and reversible protein–protein conjugation: *N*-succinimidyl-3-(2-pyridyldithio)propionate, a new heterobifunctional reagent. *Biochem. J. 173*, 723–727.

(18) Sela, M., and Berger, A. (1955) The terminal groups of poly-α-amino acids. *J. Am. Chem. Soc. 77*, 1893–1898.

(19) Katchalski, E., Grossfeld, I., and Frenkel, M. (1948) Polycondensation of ε-amino acid derivatives. III. Poly-lysine. *J. Am. Chem. Soc. 70*, 2094–2104.

(20) Partis, M. D., Griffiths, D. G., Roberts, G. C., and Beechy, R. B. (1983) Cross-linking of protein by ω-maleimido alkanoyl

N-hydroxysuccinimido ester. *J. Protein Chem. 2*, 263–277.
(21) Rakestraw, S. L., Tompkins, R. G., and Yarmush, M. L. (1990) Preparation and characterization of immunoconjugates for antibody targeted photolysis. *Bioconjugate Chem. 1*, 212–221.
(22) Khaw, B. A., Yasuda, T., Gold, H. K., Leinbach, R. C., Johns, J. A., Kanke, M., Barlai-Kovach, M., Strauss, H. W., and Haber, E. (1987) Acute myocardial infarct imaging with indium-111-labeled monclonal antimyosin Fab. *J. Nucl. Med. 28*, 1671–1678.
(23) Yauda, T., Palacios, I. F., Dec, G. W., Fallon, J. T., Gold, H. K., Leinback, H. W., Strauss, H. W., Khaw, B. A., and Haber, E. (1987) Indium-111–monoclonal antimyosin antibody imaging in the diagnosis of acute myocarditis. *Circulation 76*, 306–311.
(24) Schroff, R. W., Foon, K. A., Beatty, S. M., Oldham, R. K., and Morgan, A. C. (1985) Human anti-murine immunoglobulin responses in patients receiving monoclonal antibody therapy. *Cancer Res. 45*, 879–885.
(25) Pimm, M. V., Perkins, A. C., Armitage, N. C., and Baldwin, R. W. (1985) The characteristics of blood-borne radiolabels and the effect of anti-mouse IgG antibodies on localization of radiolabeled monoclonal antibody in cancer patients. *J. Nucl. Med. 26*, 1011–1023.
(26) Brennan, M. (1986) A chemical technique for the preparation of bispecific antibodies from Fab fragments of mouse monoclonal IgG1. *BioTechniques 4*, 424–427.
(27) O'Shannessy, D. J., and Quarless, R. H. (1987) Labeling of the oligosaccharide moieties of immunoglobulins. *J. Immunol. Methods 99*, 153–161.
(28) Sieving, P. F., Watson, A. D., and Rocklage, S. M. (1990) Preparation and characterization of paramagnetic polychelates and their protein conjugates. *Bioconjugate Chem. 1*, 65–71.

In Vitro and in Vivo Activities of Monoclonal Antibody-Alkaline Phosphatase Conjugates in Combination with Phenol Mustard Phosphate

Philip M. Wallace and Peter D. Senter*

Oncogen Division of the Bristol-Myers Squibb Pharmaceutical Research Institute, 3005 First Avenue, Seattle, Washington 98121. Received June 24, 1991

The prodrug *p*-[*N*,*N*-bis(2-chloroethyl)amino]phenyl phosphate (phenol mustard phosphate, POMP) was prepared from *p*-[*N*,*N*-bis(2-chloroethyl)amino]phenol (phenol mustard, POM) by phosphorylation with phosphoryl chloride, followed by aqueous hydrolysis. It was found that POMP was much less cytotoxic than POM when tested against H2981 human lung and H3396 human breast carcinoma cells in vitro. Pretreatment of the H2981 cells with L6-alkaline phosphatase (L6-AP), a monoclonal antibody conjugate that could bind to cell surface antigens, greatly enhanced the cytotoxic effects of POMP in an immunologically specific manner. Owing to its reduced toxicity in nude mice, larger amounts of POMP compared to POM could be administered. Neither agent exhibited significant in vivo antitumor activity when tested against subcutaneous H2981 tumors in nude mice. However, antitumor activity was observed in animals receiving L6-AP 48 h prior to POMP administration. This level of activity was greater than with the drugs alone, or a combination of 1F5-AP (nonbinding control) with POMP.

INTRODUCTION

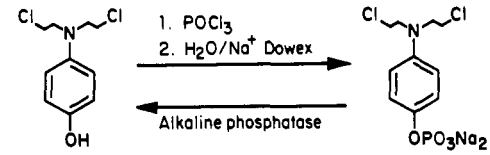
Monoclonal antibody-alkaline phosphatase (mAb-AP)[1] conjugates have been utilized in a two-stage approach to cancer chemotherapy for the activation of the phosphorylated prodrugs etoposide phosphate (EP) (*1-3*), mitomycin phosphate (MOP) (*3*), and doxorubicin phosphate (*1*). A potential drawback to the use of targeted AP for prodrug activation is that endogenous phosphatases which are present in many biological tissues (*4*) can effect prodrug hydrolysis, thus resulting in the nonspecific release of the parent drug. That this takes place is suggested by the small differences in maximum tolerated doses (MTDs) between etoposide and EP (*2, 3, 5*), and mitomycin alcohol and MOP (*3*). Greater differentials in MTDs would allow more prodrug to be administered and might lead to increased levels of active drug generated within the tumor mass.

In an effort toward developing less toxic phosphorylated prodrugs, we considered the work of Bukhari and co-workers (*6*), who demonstrated that phenol mustard phosphate (POMP) was 16 times less toxic (w/w) to mice than the product upon hydrolysis, phenol mustard (POM) (Figure 1). At high doses, POMP displayed activity against a mouse plasma cell tumor, probably as a result of being hydrolyzed by phosphatases present in the body.

On the basis of this work, we chose to investigate the possibility of using mAb-AP conjugates for site-specific activation of POMP. This paper describes the in vitro and in vivo antitumor activities of POM and POMP and the results of experiments in which POMP was used in combination with mAb-AP conjugates.

EXPERIMENTAL PROCEDURES

Materials. The mAbs used were L6 (IgG2a), which binds to an antigen on human carcinomas (*7*), and 1F5 (IgG2a), which binds to the CD20 antigen on normal and neoplastic B-cells (*8*). The cell lines used were H2981 (human lung adenocarcinoma) (*2*) and H3396 (human breast carcinoma) (*9*). Fluorescence-activated cell-sorter analysis indicated that L6 bound strongly to H2981 cells, while 1F5 showed very weak binding. Neither of the mAbs bound to H3396 cells. AP (calf intestinal) was purchased from Boehringer Mannheim. POM [*p*-[*N*,*N*-bis(2-chloroethyl)amino]phenol hydrochloride] (*10*) and POMP [*p*-[*N*,*N*-bis(2-chloroethyl)amino]phenyl phosphate disodium salt] (*6*) were prepared according to literature methods.



POM POMP

Figure 1. Structures and reactivities of POM and POMP.

HPLC Analyses. To a solution of POMP (0.1 mg/mL) in 20 mM Tris, 300 mM NaCl, 1 mM MgCl, and 0.1 mM $ZnCl_2$ at pH 7.5 was added AP to a final concentration of 20 μg/mL. Samples (20 μL) were analyzed by HPLC using a 7 μm C-8 column (4.6 × 250 mm) and the following conditions: elution buffer, 1:1 acetonitrile/10 mM sodium phosphate, pH 7.5, at 1 mL/min; monitored at 254 nm. POM (in H_2O) was analyzed under the same HPLC conditions. Plasma stability studies of POM (0.5 mM) were performed at 37 °C. Aliquots (30 μL) were quenched with acetonitrile (30 μL) and centrifuged at 4 °C for 2 min. HPLC analyses on 10-μL portions were performed as described above.

Preparation and Characterization of mAb-AP Conjugates. Conjugates in which the mAbs and AP were linked through a thioether bond were prepared as previously described (*2*). A two-step purification procedure was used to obtain monomeric conjugates that were apparently free (by sodium dodecyl sulfate-polyacrylamide gel electrophoresis, SDS-PAGE) of unconjugated proteins and high molecular weight aggregates. The crude

* Author to whom correspondence should be addressed.

[1] Abbreviations used: AP, alkaline phosphatase; EP, etoposide phosphate; mAb-AP, monoclonal antibody-alkaline phosphatase conjugate; MOP, mitomycin phosphate; MTD, maximum tolerated dose; PBS, phosphate-buffered saline, pH 7.2; POM, phenol mustard; POMP, phenol mustard phosphate; SDS-PAGE, sodium dodecyl sulfate-polyacrylamide gel electrophoresis; Tris, tris(hydroxymethyl)aminomethane.

1043-1802/91/2902-0349$02.50/0 © 1991 American Chemical Society

conjugate was applied to an S-300 Sephacryl (Pharmacia) column and eluted with phosphate-buffered saline (PBS) at pH 7.2. This separated aggregates and unbound AP from the conjugate. The small amount of unbound mAb present in the conjugate-containing fractions was removed by DEAE-Sephadex (Pharmacia) anion-exchange chromatography. The conjugate in tris(hydroxymethyl)aminomethane (Tris) (20 mM) containing NaCl (60 mM) at pH 7.5 was applied to the column and the unbound mAb was eluted with the above Tris buffer. After no more detectable protein eluted off the column, the conjugate was eluted with 200 mM sodium phosphate containing 1.5 M NaCl at pH 7.2. The purified conjugates thus obtained were dialyzed against PBS and characterized by SDS-PAGE, AP activity, and binding of the mAbs to cell-surface antigens.

In Vitro Cytotoxicity. H2981 and H3396 cells in medium (Iscove's modified Dulbeco's medium) with 10% v/v fetal calf serum, 200 units/mL penicillin, 100 μg/mL streptomycin, and 2 mM glutamine) were plated into 96-well microtiter plates at 8000 cells/well and allowed to adhere overnight at 37 °C. The cells were washed, and conjugate (10–50 μg mAb/mL) was added in 100 μL of medium. After 30 min at 4 °C, the cells were washed, and 0.2 mL of the above medium containing dilutions of POMP was added to each of the wells. POM and POMP were also added to cells untreated with conjugates. After 1–1.5 h at 37 °C, the plates were washed, 150 μL of medium was added, and incubation was continued at 37 °C for ca. 18 h. The cells were pulsed with [^{3}H]thymidine (1 μCi in 50 μL of medium) for 6 h, frozen, thawed, and harvested onto glass-fiber disks. The filters were counted on an LKB β-plate cell harvester.

In Vivo Therapy Experiments. Female athymic nude mice (8 weeks old from Harlan-Sprague Dawley, Indianapolis, IN) were implanted subcutaneously (sc) in the right flank with H2981 tumors (ca. 32 mm^3 sections from in vivo passaging). Therapy was initiated 13–15 days later, once the tumors were established. Conjugates (0.15 mL at 1 mg mAb/mL) in PBS were injected intravenously (iv) followed 48 h later by POMP (5 mg/mL in PBS), which was administered intraperitoneally (ip). This was repeated at weekly intervals for a total of three rounds of treatment. POM (2.25 mg/mL in PBS) was administered, according to the same schedule, to mice that received no conjugate. Tumor volumes were estimated by the formula: longest length × (perpendicular width)^2/2. Each treatment group consisted of seven or eight mice/group.

RESULTS

Preparation and Characteristics of POM, POMP, and mAb–AP Conjugates. POM (Figure 1) was prepared in a four-step synthesis from 4-aminophenol by using procedures described by Benn and co-workers (*10*). Phosphorylation of POM was achieved with phosphoryl chloride. After hydrolysis, neutralization, and cation-exchange chromatography, POMP (*6*) was obtained as the disodium salt in good overall yield. The structures of POM and POMP were confirmed by 300 MHz ^{1}H NMR.

POMP was susceptible to hydrolysis by AP. HPLC analysis indicated that the enzyme (at 20 μg/mL) effected nearly quantitative conversion of POMP (at 0.1 mg/mL) to POM within 10 min. In contrast to POMP, aqueous solutions of POM proved to be unstable. The half-lives for decomposition in H_2O at 23 °C or in mouse plasma at 37 °C were ca. 30 min.

The mAbs L6 (*7*) and 1F5 (*8*) were conjugated to AP as previously described (*2*). A two-step purification procedure involving gel filtration, followed by anion-exchange chromatography, was used to obtain monomeric conjugates that were apparently uncontaminated with aggregates or unconjugated proteins. FACS analysis indicated that L6 and L6–AP bound strongly to H2981 lung adenocarcinoma cells but did not bind to the H3396 breast carcinoma cell line. 1F5 showed no detectable binding to either of these lines.

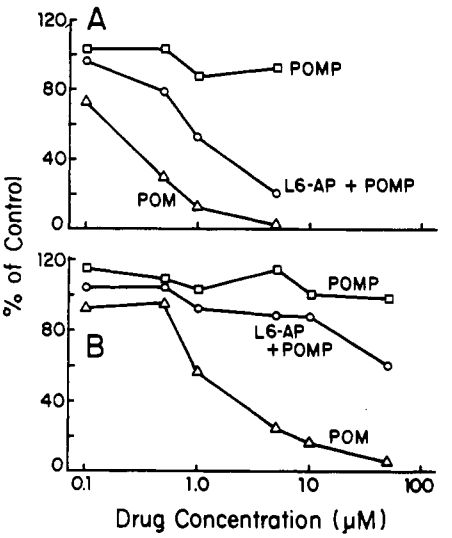


Figure 2. Cytotoxic effects of POM, POMP, and mAb–AP conjugates with POMP as measured by inhibition of [^{3}H]thymidine incorporation into DNA. (A) H2981 (binds L6–AP) and (B) H3396 (no detectable binding of L6–AP) cells were exposed to L6–AP (10 μg/mL) and washed prior to treatment with POMP.

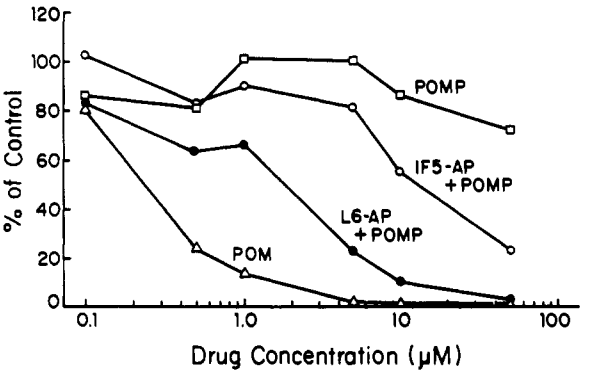


Figure 3. Immunologically specific activation of POMP by mAb–AP conjugates. H2981 cells (L6–AP positive, 1F5–AP negative) were exposed to the mAb–AP conjugates (50 μg/mL), washed, and then treated with POMP at the concentrations shown.

In Vitro Cytotoxicity. POM exerted a significant cytotoxic effect on both the H2981 and H3396 cell lines (Figure 2). In contrast, POMP was noncytotoxic under the conditions tested. Treatment of the H2981 cells (antigen positive) with L6–AP prior to exposure to POMP led to a level of cytotoxic activity that was slightly less than that observed for POM (Figure 2A), but much greater than that of similarly treated H3396 cells (antigen negative) (Figure 2B).

The activities of the binding (L6–AP) and nonbinding (1F5–AP) conjugates in combination with POMP on H2981 cells are shown in Figure 3. As before, POM was much more cytotoxic than POMP. Activation of POMP occurred in an antigen-specific manner, as evidenced by the fact that the L6–AP/POMP combination was much more cytotoxic (IC_{50} = 1.8 μM) than the combination of 1F5–AP and POMP (IC_{50} = 15 μM). The slight enhancement in cytotoxic activity observed for the nonbinding conjugates

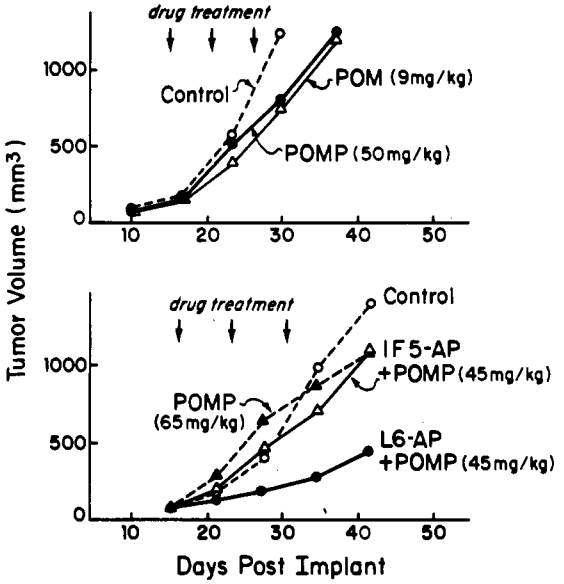


Figure 4. Effects of POM, POMP, and conjugates plus POMP on H2981 tumors in nude mice. Arrows indicate drug treatment schedule. Conjugates were administered 48 h earlier. The drug dosages indicated are for each injection.

in Figures 2B and 3 was probably due to residual amounts remaining after the cells were washed.

In Vivo Studies. POM was significantly more toxic to mice than POMP or POMP in combination with the mAb–AP conjugates. Administration of POM at 9 mg/kg ip weekly for three administrations gave no lethalities and resulted in ca. 12% weight loss. At 18 mg/kg ip weekly for three administrations, POM caused severe weight loss and was not tolerated. With this same schedule, it was possible to safely administer POMP (ip) at 45 mg/kg per injection in mice that received no prior treatment or treatment with mAb–AP conjugates (0.15 mg, iv) 48 h earlier. At this dose, there was no weight loss or apparent drug-associated toxicities. As much as 65 mg/kg per injection of POMP have been administered safely without apparent toxicity.

In vivo therapy experiments were performed on mice that had sc H2981 tumors that were approximately 75 mm^3 in volume. The conjugates were administered iv 48 h prior to treatment with POMP (ip). The antitumor effects of these combinations were compared to the prodrug without conjugate and to POM that was administered ip at the MTD.

Both POM and POMP had little effect on tumor growth (Figure 4). The antitumor activity of POMP was increased significantly in animals that received L6–AP 48 h before prodrug administration. This increase in activity was immunologically specific ($P < 0.1$ on day 42), since the nonbinding control conjugate 1F5–AP did not alter the activity of POMP. The activity of the combination of L6–AP with POMP was much greater than treatment with POM alone ($P < 0.01$).

DISCUSSION

One of the major limitations in the chemotherapeutic treatment of cancer is that the drugs employed have an inherent lack of specificity for the target site and have dose-limiting toxicities on normal tissues. An approach to overcome this problem has been to target enzymes to tumor cell surfaces that can activate prodrugs which are administered in a second step (*1*). There have been several indications, with both enzymes of nonmammalian (*1*, *11–14*) and mammalian (*1–3*) origin, that this approach to cancer chemotherapy has considerable potential.

AP may present some advantages over other enzymes being considered for this approach. Due to its lack of substrate specificity, a variety of prodrugs can be hydrolyzed by AP (*1–3*). In addition, conjugates of endogenous enzymes such as AP might tend to be less immunogenic than nonmammalian enzymes, thus permitting continuation of therapy over a longer period of time.

The prodrugs that have been reported for mAb–AP conjugates, EP (*2*, *3*) and MOP (*3*), have similar MTDs to the drugs they release upon hydrolysis (*2*, *3*, *5*). In this paper, we have demonstrated that POMP is much less toxic to mice than POM. The differential in MTDs between POMP and POM (w/w) is at least 5-fold even in mice that received mAb–AP conjugates 48 h prior to prodrug administration. This might be due to pharmacokinetic factors as well as to the prodrug's inability to permeate through cell membranes.

The enhanced in vivo antitumor activity of L6–AP combined with POMP (Figure 4) is analogous to what has been previously observed with EP (*2*, *3*) and MOP (*3*). Thus, a single mAb-enzyme conjugate has been shown to generate therapeutically useful amounts of drugs that differ widely in their mechanisms of activities (*15–17*). This presents the possibility of using mAb–AP conjugates and several prodrugs for combination chemotherapy.

ACKNOWLEDGMENT

We thank John MacMaster and Stephanie Ashe for technical assistance, Karl Erik and Ingegerd Hellström for their encouragement, and Ana Wieman for preparing the manuscript.

LITERATURE CITED

(1) Senter, P. D. (1990) Activation of prodrugs by antibody–enzyme conjugates: a new approach to cancer therapy. *FASEB 4*, 188–193.

(2) Senter, P. D., Saulnier, M. G., Schreiber, G. J., Hirschberg, D. L., Brown, J. P., Hellström, I., and Hellström, K. E. (1988) Anti-tumor effects of antibody–alkaline phosphatase conjugates in combination with etoposide phosphate. *Proc. Natl. Acad. Sci. U.S.A. 85*, 4842–4846.

(3) Senter, P. D., Schreiber, G. J., Hirschberg, D. L., Ashe, S. A., Hellström, K. E., and Hellström, I. (1989) Enhancement of the in vitro and in vivo antitumor activities of phosphorylated mitomycin C and etoposide derivatives by monoclonal antibody–alkaline phosphatase conjugates. *Cancer Res. 49*, 5789–5792.

(4) McComb, R. B., Bowers, G. N., and Posen, S. (1979) *Alkaline Phosphatase*, Plenum Press, New York.

(5) Doyle, T. W., and Vyas, D. M. (1990) Second generation analogs of etoposide and mitomycin C. *Cancer Treat. Rev. 17*, 127–131.

(6) Bukhari, M. A., Everett, J. L., and Ross, W. C. J. (1972) Aryl-2-halogenoalkylamines—XXVI. *Biochem. Pharmacol. 21*, 963–967.

(7) Hellström, I., Horn, D., Linsley, P. S., Brown, J. P., Brankovan, V., and Hellström, K. E. (1986) Monoclonal antibodies raised against human lung carcinoma. *Cancer Res. 46*, 3917–3923.

(8) Clark, E. A., Shu, G., and Ledbetter, J. A. (1985) Role of the Bp35 cell surface polypeptide in human B cell activation. *Proc. Natl. Acad. Sci. U.S.A. 82*, 1766–1770.

(9) Hellström, I., Garrigues, H. J., Garrigues, U., and Hellström, K. E. (1990) Highly tumor-reactive, internalizing, mouse monoclonal antibodies to Le^y-related cell surface antigens. *Cancer Res. 50*, 2183–2190.

(10) Benn, M. H., Creighton, A. M., Owen, L. N., and White, G. R. (1961) Cytotoxic compounds. Part II. Some amides of the nitrogen mustard type. *J. Chem. Soc.* 2365–2375.

(11) Bagshawe, K. D., Springer, C. J., Searle, F., Antoniw, P., Sharma, S. K., Melton, R. G., and Sherwood, R. F. (1988) A cytotoxic agent can be generated selectively at cancer sites. *Br. J. Cancer 58*, 700–703.

(12) Kerr, D. E., Senter, P. D., Burnett, W. V., Hirschberg, D. L., Hellström, I., and Hellström, K. E. (1990) Antibody-penicillin-V-amidase conjugates kill antigen-positive tumor cells when combined with doxorubicin phenoxyacetamide. *Cancer Immunol. Immunother. 31*, 202–206.

(13) Senter, P. D., Su, P. C. D., Katsuragi, T., Sakai, T., Cosand, W. L., Hellström, I., and Hellström, K. E. The generation of 5-fluorouracil from 5-fluorocytosine by monoclonal antibody–cytosine deaminase conjugates. *Bioconjugate Chem.*, submitted for publication.

(14) Shepherd, T. A., Jungheim, L. N., Meyer, D. L., and Starling, J. J. (1991) A novel targeted delivery system utilizing a cephalosporin-oncolytic prodrug activated by an antibody β-lactamase conjugate for the treatment of cancer. *Bioorg. Med. Chem. Lett. 1*, 21–26.

(15) Stahelin, H. F., and von Wartburg, A. (1991) The chemical and biological route from podophyllotoxin glucoside to etoposide: Ninth Cain memorial award lecture. *Cancer Res. 51*, 5–15.

(16) Wheeler, G. P. (1982) Alkylating agents. *Cancer Medicine* J. F. Holland, and E. Frei, Eds., pp 824–843, Lea and Febiger, Philadelphia, PA.

(17) Thomasz, M., Lipman, R., Chowdary, D., Pawlak, J., Verdine, G. L., and Nakanishi, K. (1987) Isolation and structure of a covalent cross-link adduct between mitomycin C and DNA. *Science 235*, 1204–1208.

Progestin–Rhenium Complexes: Metal-Labeled Steroids with High Receptor Binding Affinity, Potential Receptor-Directed Agents for Diagnostic Imaging or Therapy

James P. DiZio,† Rita Fiaschi,† Alan Davison,‡ Alun G. Jones,§ and John A. Katzenellenbogen*,†

Department of Chemistry, University of Illinois, 1209 West California Street, Urbana, Illinois 61801, Department of Chemistry, Room 6-435, Massachusetts Institute of Technology, Cambridge, Massachusetts 02139, and Department of Radiology, Harvard Medical School, 50 Binney Street, Boston, Massachusetts 02115.
Received July 1, 1991

In order to investigate the possibility of developing diagnostic imaging agents for steroid-positive tumors that are labeled with the readily available radionuclide technetium-99m, we prepared four conjugate systems in which a progestin is linked to a metal chelate system. Three of these are bis-amino bis-thiol (BAT or N_2S_2) systems and are linked through carbon-21 of progesterone or the 17α- or 11β-position of a nortestosterone type progestin. The fourth, an amino–amido–thiol–alcohol chelate (N_2OS) system, is linked at the 16α,17α-positions of a dihydroprogesterone. As a model for technetium-labeled complexes, all four chelate systems were converted to their oxo–rhenium complexes. Of the four possible diastereomers in the 16α,17α-system, only one was isolated, while of the four possible diastereomers in the other systems, a syn pair and an anti pair (linker methylene vs rhenium–oxo, relative to the N_2S_2 plane) were separated in the 17α-substituted series, a syn pair was isolated in the 21-substituted series, and a syn pair and the two individual anti diastereomers were separated in the 11β-substituted series. In competitive radiometric receptor binding assays, the 21-, 17α-, and 16α,17α-linked systems had low affinity for the progesterone receptor (less than 0.3% that of promegestone (R5020) or 2% that of progesterone). By contrast, the two anti diastereomers of the 11β-linked system had affinities that were 10% and 44% that of R5020 (or 64% and 283% that of progesterone) and the syn pair had an affinity 25% that of R5020 (or 161% that of progesterone). The latter finding indicates that it is possible to prepare metal-labeled steroids that retain high affinity for steroid receptors. These and related systems, when complexed with radioactive metals, may be useful in vivo as receptor-directed agents for diagnostic imaging or therapy of steroid receptor-positive tumors.

INTRODUCTION

In the development of in vivo diagnostic imaging agents for receptor systems such as steroid receptors, a major consideration is that the radiolabeled hormone analogue maintains high binding affinity for the receptor (*1*). Thus, the logical choices for labeling have been radionuclides such as carbon-11, fluorine-18, and isotopes of bromine and iodine, as these single-atom systems present a minimum of increased steric bulk when substituted on the ligand (*1*). While many receptor ligands labeled with the aforementioned radionuclides have been prepared, their use on a routine basis is constrained by the relative difficulty in producing or obtaining these radionuclides.

By contrast, diagnostic imaging agents based on technetium-99m have the advantage of radionuclide availability through the molybdenum-99/technetium-99m generator system (*2*). So, it is no surprise that almost all routine in vivo radioimaging is based on technetium-99m. The availability advantage of this radiotracer, however, is compromised by the nature of the labeling system, for attachment of a metal ion to an organic molecule requires the construction of a chelating system. Various neutral chelating systems have been used, the most common being the bis-amino bis-thiol (BAT or N_2S_2) systems (*3*) and amide analogues (*4*) thereof, the propylene amine oximes (HMPAO) (*5*), and the boronate-capped tris-dioximes (BATO) (*6*). These three and other technetium chelate systems are large, having molecular weights of 350 or greater, comparable to those of receptor ligands themselves, and they are bulky. Thus, they appear unsuitable for labeling receptor ligands where steric complementarity is a prime consideration.

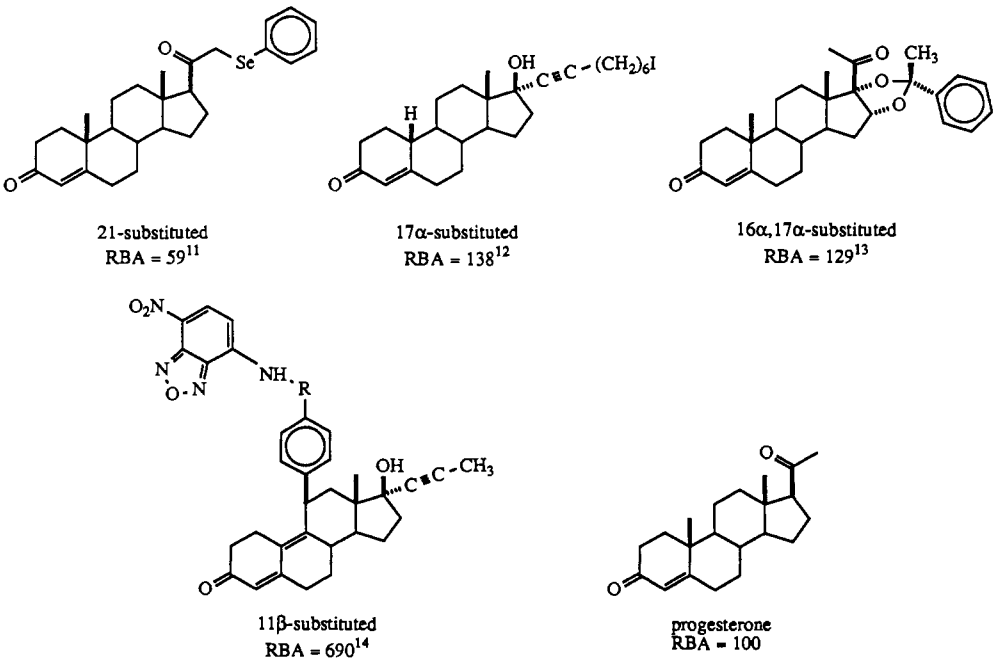
In our development of diagnostic imaging agents for steroid-receptor-positive tumors of the breast, we and others have prepared estrogens labeled with radionuclides of fluorine (*7*), bromine (*8*), and iodine (*9*) and measured their binding affinity toward the estrogen receptor. We have found that there are sites on the hormone analogue where even a minimal increase in steric bulk reduces binding affinity markedly, whereas other sites are quite tolerant of groups as bulky as bromine and iodine and may even show increased binding affinity (*1*, *10*). In more recent work on radiolabeled progestins for breast tumor imaging, we were struck by the fact that some synthetic progestins bearing very large substituents retain either good affinity for the progesterone receptor or have high biological activity. A number of these are shown in Chart I. The 21-(phenylseleno)progestin (*11*) has an affinity for progesterone receptor that is only somewhat lower than that of progesterone, and 17α- (*12*) and 16α,17α-substituted (*13*) systems are known to be potent progestins. Finally, certain derivatives of the antiprogestin RU 38486 (RU486, mefipristone) have high affinities for receptor (*14*).

Emboldened by these observations, we set out to prepare a series of progestins in which a metal-chelating system of the N_2S_2 type (and in one case a N_2SO system in which

* Address correspondence to John A. Katzenellenbogen, Department of Chemistry, Box 37 Roger Adams Laboratory, University of Illinois, 1209 W. California St., Urbana, Illinois 61801.
† University of Illinois.
‡ Massachusetts Institute of Technology.
§ Harvard Medical School.

1043-1802/91/2902-0353$02.50/0 © 1991 American Chemical Society

Chart I



one thiol is replaced by alcohol) is attached to the steroidal skeleton through the 21-, 17α-, 16α,17α-, or 11β-site. In order to avoid the use of radioactive metals at this preliminary stage, we prepared the oxo–rhenium rather than the oxo–technetium complexes of these systems, and determined their binding affinities toward the progesterone receptor. In all cases, introduction of the oxo–rhenium chelate system lowers the receptor binding affinity of these systems, except the 11β-substituted one; one diastereomer in this system has an affinity much greater than that of progesterone. These findings demonstrate that it is possible to prepare metal-chelate conjugates of receptor-binding hormone analogues that retain high binding affinity for their receptor. Such agents may have potential use in vivo as receptor-directed agents for diagnosis or therapy.

EXPERIMENTAL PROCEDURES

General. Solvents and reagents were purchased from the following commercial sources: Aldrich, Mallinckrodt, Sigma, Fisher, Baker, Eastman, or Alfa. Tetrahydrofuran (THF) was distilled from sodium/benzophenone ketyl immediately prior to use. Other solvents were used as received, unless otherwise noted.

Analytical thin layer chromatography (TLC) was performed with Merck silica gel F-254 glass-backed plates. Visualization was achieved by phosphomolybdic acid (PMA) or anisaldehyde spray reagents, iodine, or UV illumination. Flash chromatography was performed according to Still (*15*), using Woelm silica gel (0.032–0.064 mm) and Merck silica gel (0.040–0.063 mm). High-performance liquid chromatography (HPLC) was performed isocratically on a Spectra-Physics Model 8700 or a Varian 5060 liquid chromatograph with an analytical 5-μm SiO_2 column (4.6 mm × 30 cm, Varian Si-5 Micro Pak) or a preparative SiO_2 column (Whatman Partisil M-9, 0.9 cm × 50 cm). The UV absorbance of the eluent was monitored at 254 nm. Melting points were determined on either a Thomas Hoover, Fisher Johns, or Hacker melting point apparatus and are uncorrected. Infrared (IR) spectra were recorded on Perkin-Elmer 1320 spectrophotometer. The data are given in inverse centimeters with only diagnostic bands reported. Proton magnetic resonance (^{1}H NMR) spectra were obtained on a Varian XL-200 (200 MHz), a General Electric QE-300 (300 MHz), or a Nicolet NT-360 (360 MHz) spectrometer; chemical shifts are reported downfield of a tetramethylsilane internal standard (δ scale). Low-resolution electron-impact mass spectra were obtained on a Finnigan MAT CH-5 spectrometer. High-resolution, electron-impact, exact mass determinations were obtained on a Varian MAT 731 spectrometer. Both low- and high-resolution fast atom bombardment (FAB) mass spectra were obtained on a VG instrument (ZAB HF), employing a dithiothreitol matrix. Elemental analyses were performed by the Microanalytical Service of the University of Illinois.

A standard procedure for product isolation was utilized that involved quenching of the reaction mixture in an aqueous solution, followed by a thorough extraction with an organic solvent, washing of the extracts, drying of the organic extract over an anhydrous salt, filtration, and evaporation of solvent under reduced pressure. This is indicated by the phrase "product isolation" followed by a list of the components in parentheses. The chemical nomenclature for norgestrel is 13β-ethyl-17α-ethynyl-17β-hydroxy-4-gonen-3-one. Compounds **1** (*16*), **2** (*17*), BAT I (*17*), **C2** (*18*), **C3** (*18*), **C4** (*19*), and **D3** (*20*) were prepared according to literature procedures.

BAT II Chelator. *N,N'*-Bis[2-methyl-2-[(triphenylmethyl)thio]propyl]ethylenediamine (BAT II). BAT I (7.06 g, 29.9 mmol) was dissolved in 70 mL of trifluoroacetic acid. Triphenylmethanol (15.8 g, 60.6 mmol) was added and the solution was allowed to stir for 30 min. The solvent was evaporated over 18 h under a stream of nitrogen. The thick brown oil was diluted with 200 mL of Et_2O and the resulting white precipitate was collected and washed with 50 mL of Et_2O. The white solid was partitioned between 100 mL of EtOAc and 50 mL of 1 N NaOH. Product isolation (EtOAc, $MgSO_4$) and purification (flash chromatography, 10/1 Et_2O/MeOH) gave 7.1 g (33%) of BAT II as a white foam. The product runs as a streak with a median R_f = 0.30 on silica TLC: ^{1}H NMR ($CDCl_3$) δ 7.62 (d, J = 7.7, 12 H, *o*-ArH), 7.13–7.26 (m, 18 H, *m,p*-ArH), 2.38 (s, 4 H, NCH_2CH_2N), 1.75 (s, 4 H, $NCH_2C(CH_3)_2$), 1.03 (s, 12 H, CH_3); MS (LRFAB) m/z (relative intensity) 721 (M^+ + H, 18), 479 (5), 243 (100);

HRFAB calcd for $C_{48}H_{52}N_2S_2$ (+H) 721.3650, found 721.3641. Anal. Calcd for $C_{48}H_{52}N_2S_2$: C, 79.95; H, 7.27, N, 3.89. Found: C, 79.80; H, 7.45, N, 3.73.

Progesterone C-21 Series (A). 21-[[(Trifluoromethyl)sulfonyl]oxy]progesterone (A1). Trifluoromethanesulfonic anhydride (0.30 mL, 1.8 mmol) was added dropwise to a stirring 5 mL, −78 °C CH_2Cl_2 solution containing 0.5 g (1.5 mmol) of deoxycorticosterone and 0.23 mL (2.0 mmol) of 2,6-lutidine. After 30 min, the orange reaction mixture was allowed to warm to room temperature whereupon the solvent was evaporated under reduced pressure. The residue was purified by flash chromatography (1/1 EtOAc/hexane) to give 0.55 g (79%) of **A1** as a white foam. The product is unstable and cannot be stored, therefore it was carried on to the next step immediately: ^{1}H NMR ($CDCl_3$, 200 MHz) δ 5.84 (s, 1 H, 4-CH), 4.97 (AB q, 2 H, $\Delta\delta = 0.046$, $J = 16.71$ Hz, CH_2OTf), 4.20 (s, br, 1 H, 17-CH), 1.20 (s, 3 H, 18-CH_3), 0.73 (s, 3 H, 19-CH_3); MS (LRFAB) m/z (relative intensity) 463 (M^+ + H, 20); HRFAB calcd for $C_{22}H_{29}O_5SF_3$ (+H) 463.1758, fc ınd 463.1766.

21-[*N*-[2-[*N*-[2′-Methyl-2′-[(triphenylmethyl)thio]propyl]amino]ethyl]-*N*-[2′-methyl-2′-[(triphenylmethyl)thio]propyl]amino]progesterone (21-BAT II progesterone, A2). Steroid **A1** (150 mg, 0.32 mmol) dissolved in 1 mL of CH_2Cl_2 was added dropwise to a 3 mL, −78 °C solution of BAT II (500 mg, 0.69 mmol) in CH_2Cl_2. After the addition, the reaction mixture was allowed to warm to room temperature and was stirred for 2 h. Product isolation (H_2O and 1.5 equiv of 1 N NaOH, CH_2Cl_2, $MgSO_4$) resulted in a crude yellow oil that was purified through the use of two separate silica gel flash columns. The first column was eluted with 1/20 MeOH/EtOAc; this separated the desired product from BAT II and most of the side products. The second column was eluted with 1/20 MeOH/CH_2Cl_2; this separated the desired product from the deoxycorticosterone side product. The product runs as a streak with a median $R_f = 0.30$ on silica TLC (1/20 MeOH/CH_2Cl_2). The isolated yield after purification was 0.24 g (72%) of **A2** as a white foam: ^{1}H NMR ($CDCl_3$, 300 MHz) δ 7.57–7.62 (m, 12 H, *o*-ArH), 7.13–7.26 (m, 18 H, *m,p*-ArH), 5.74 (s, 1 H, 4-CH), 3.47 (AB q, 2 H, $\Delta\delta = 0.057$, $J = 18.79$ Hz, CH_2N), 1.17 (s, 3 H, 18-CH_3), 0.92 (s, 6 H, $C(CH_3)_2$), 0.89 (s, 6 H, $C(CH_3)_2$), 0.62 (s, 3 H, 19-CH_3); MS (LRFAB) m/z (relative intensity) 1033 (M^+ + H, 23), 859 (3), 791 (7), 547 (13), 244 (100); HRFAB calcd for $C_{69}H_{80}O_2N_2S_2$ (+H) 1033.5739, found 1033.5746.

Norgestrel 17α Series (B). $\Delta^{5(6)}$- and $\Delta^{5(10)}$-3,3-(Ethylenedioxy)-13β-ethyl-17α-ethynylgonen-17β-ol (B1). A catalytic amount of *p*-TsOH (6 mg, 0.03 mmol) was added to a solution containing ethylene glycol (0.054 mL, 0.97 mmol), benzene (25 mL), and norgestrel (100 mg, 0.32 mmol). The mixture was heated to reflux with azeotropic distillation for 4 h and then allowed to cool to room temperature. Product isolation (aqueous saturated $NaHCO_3$, EtOAc, $MgSO_4$) and purification (flash chromatography, 1/4 EtOAc/hexane) gave 99 mg (87%) of **B1** as a 1/2 mixture of $\Delta^{5(6)}/\Delta^{5(10)}$ double bond isomers (glass): ^{1}H NMR ($CDCl_3$) δ 2.59 (s, 1 H, C≡CH), 3.92–4.02 (m, 4 H, OCH_2CH_2O), 5.44–5.49 (m, 0.33 H, 6-CH); MS (LREI, 70 eV) m/z (relative intensity) 356 (M^+, 3), 294 (1), 273 (1), 99 (100), 86 (9), 55 (8). Anal. Calcd for $C_{23}H_{32}O_3$: C, 77.49; H, 9.05. Found: C, 77.23; H, 9.30.

$\Delta^{5(6)}$- and $\Delta^{5(10)}$-3,3-(Ethylenedioxy)-13β-ethyl-17α-(3′-hydroxypropynyl)gonen-17β-ol (B2). *n*-BuLi in hexane (1.6 M, 0.058 mL, 0.093 mmol) was added to a solution of steroid **B1** (15 mg, 0.042 mmol) in 0.5 mL of THF at −78 °C. After stirring for 10 min, the dianion mixture was then added to a heterogeneous slurry of 2.5 mg of paraformaldehyde in 0.5 mL of THF at −78 °C. The reaction was warmed to room temperature and stirred for 30 min. Product isolation (cold aqueous saturated NH_4Cl, CH_2Cl_2, $MgSO_4$) and purification (flash chromatography, 3/4 EtOAc/hexane) gave 12 mg (74%) of **B2** as a 1/2 mixture of $\Delta^{5(6)}/\Delta^{5(10)}$ double bond isomers (glass): ^{1}H NMR ($CDCl_3$) δ 3.95–4.01 (m, 4 H, OCH_2CH_2O), 4.33 (s, 2 H, CH_2OH), 5.46 (d, $J = 5.13$ Hz, 0.33 H, 6-CH); MS (LREI, 70 eV) m/z (relative intensity) 386 (M^+, 3), 368 (1), 330 (2), 99 (100), 86 (19), 55 (4). Anal. Calcd for $C_{24}H_{34}O_4$: C, 74.57; H, 8.87. Found: C, 74.34; H, 9.10.

$\Delta^{5(6)}$- and $\Delta^{5(10)}$-3,3-(Ethylenedioxy)-13β-ethyl-17α-[3′-[(methylsulfonyl)oxy]propynyl]gonen-17β-ol (B3). A solution of containing 5 mL of THF (at room temperature), steroid **B2** (12 mg, 0.031 mmol), and Et_3N (0.022 mL, 0.16 mmol) was treated with 4.8 μL (0.061 mmol) mesyl chloride and allowed to stir for 1 h. Product isolation (H_2O, EtOAc, $MgSO_4$) and purification (flash chromatography, 3/4 EtOAc/hexane) gave 12.2 mg (85%) of **B3** as a 1/2 mixture of $\Delta^{5(6)}/\Delta^{5(10)}$ double bond isomers (glass). The product is slightly unstable on silica gel: ^{1}H NMR ($CDCl_3$) δ 3.12 (s, 3 H, OSO_2CH_3), 3.94–4.00 (m, 4 H, OCH_2CH_2O), 4.93 (s, 2 H, CH_2OMs), 5.45–5.47 (m, 0.33 H, 6-CH); MS (LREI, 70 eV) m/z (relative intensity) 464 (M^+, 2), 446 (2), 373 (4), 99 (100), 79 (25), 43 (27). Anal. Calcd for $C_{25}H_{36}O_6S$: C, 64.63; H, 7.81; S, 6.90. Found: C, 64.78; H, 7.90; S, 6.78.

$\Delta^{5(6)}$- and $\Delta^{5(10)}$-3,3-(Ethylenedioxy)-13β-ethyl-17α-[3-[*N*-[2′-[*N*-[2″-methyl-2″-[(triphenylmethyl)thio]propyl]amino]ethyl]-*N*-[2″-methyl-2″-[(triphenylmethyl)thio]propyl]amino]propynyl]gonen-17β-ol (17α-BAT II norgestrel, B4). Steroid **B3** (1.7 g, 3.66 mmol) and BAT II (5.27 g, 7.31 mmol) were dissolved in 50 mL of *o*-dichlorobenzene and the mixture was then heated to 90 °C and stirred for 2 h. While still at 90 °C, the solvent was partially evaporated (blown off) under a stream of nitrogen for 0.5 h. The reaction mixture was then stirred for 15 h at room temperature while the rest of the solvent was evaporated under a nitrogen stream, resulting in a thick brown oil. Product isolation (0.5 N NaOH, CH_2Cl_2, $MgSO_4$) and purification (flash chromatography, 3/4 EtOAc/hexane, fully purified after two separate columns) gave product **B4** as a 1/2 mixture of $\Delta^{5(6)}/\Delta^{5(10)}$ double bond isomers (2 g, 51%, glass). The product runs as a streak with a median $R_f = 0.35$ on silica TLC: ^{1}H NMR ($CDCl_3$) δ 7.58–7.65 (m, 12 H, *o*-ArH), 7.14–7.26 (m, 18 H, *m,p*-ArH), 5.43–5.48 (m, 0.33 H, 6-CH), 3.90–4.00 (m, 4 H, OCH_2CH_2O), 3.31–3.29 (s, 2 H, C≡CCH_2N, 2/1 ratio), 2.47–2.54 (m, 2 H, NCH_2CH_2N), 2.32–2.37 (m, 2 H, NCH_2CH_2N), 0.97 (s, 6 H, $C(CH_3)_2$), 0.91 (s, 6 H, $C(CH_3)_2$); MS (LRFAB) m/z (relative intensity) 1089 (M^+ + H, 28), 847 (6), 603 (22), 529 (10), 244 (100); HRFAB calcd for $C_{72}H_{83}O_3N_2S_2$ (+H) 1089.6002, found 1089.5980. Anal. Calcd for $C_{72}H_{83}O_3N_2S_2$: C, 79.45; H, 7.69; N, 2.57. Found: C, 79.43; H, 7.95; N, 2.37.

Estradiene 11β Series (C). 3,3-(Ethylenedioxy)-5(10),9(11)-estradien-17β-ol (C5). Ethylene glycol (6 mL, 96.7 mmol) and concentrated H_2SO_4 (6 drops) were added to a suspension of estradienone **C4** (2.05 g, 7.53 mmol) in 60 mL of benzene. The mixture was slowly distilled over 1.5 h so that about 20 mL of benzene was lost. The reaction was then cooled to room temperature. Product isolation (solid $NaHCO_3$ and H_2O, Et_2O, $MgSO_4$) and purification (flash chromatography, 1/1 EtOAc/hexane) gave 2.3 g (96%) of **C5** as a glass: ^{1}H NMR ($CDCl_3$) δ 5.55–5.57 (m, 1 H, 11-CH), 3.98 (s, 4 H, OCH_2CH_2O), 3.76 (t, 1 H, J =

8.62 Hz, 17-CH), 0.73 (s, 3 H, 18-CH_3); MS (LREI, 70 eV) m/z (relative intensity) 316 (M^+, 100), 288 (62), 243 (84), 197 (31), 86 (69), 43 (92). Anal. Calcd for $C_{20}H_{28}O_3$: C, 75.91; H, 8.92. Found: C, 76.05; H, 9.01.

3,3-(Ethylenedioxy)-(5α,10α)- and -(5β,10β)-epoxy-9(11)-estren-17β-ol (C6 and C7). Steroid **C5** (0.60 g, 0.190 mmol) was dissolved in 2 mL of CH_2Cl_2 and cooled to 10 °C. Pyridine (1 μL, 0.012 mmol), CF_3COCF_3 (3 μL, 0.017 mmol), and a 30% solution of H_2O_2 (29 μL, 0.284 mmol) were added, respectively. The reaction was allowed to warm to room temperature and was vigorously stirred for 8 h. Product isolation (10% sodium thiosulfate, CH_2Cl_2, $CuSO_4$, H_2O, $MgSO_4$) gave a clear foam. The crude ratio of α/β-epoxide formation was 4.15/1 (by NMR). The α-isomer was partially purified (flash chromatography, 1/1 EtOAc/hexane), giving 0.45 g of a 6/1 α/β-epoxide mixture as a glass. The α-epoxide has an R_f = 0.23 whereas the β-epoxide has an R_f = 0.26 on silica TLC (1/1 EtOAc/hexane). The 6/1 mixture of isomers was used in the next reaction sequence. Analytically pure α-epoxide **C6** and β-epoxide **C7** were obtained by taking select fractions from the flash column: ^{1}H NMR of **C6** ($CDCl_3$) δ 6.02–6.04 (m, 1 H, 11-CH), 3.87–3.97 (m, 4 H, OCH_2CH_2O), 3.75 (t, br, 1 H, J = 8.44 Hz, 17-CH), 2.48 (ddd, 1 H, J = 2.54, 4.58, 14.58 Hz, 8-CH), 0.75 (s, 3 H, 18-CH_3); ^{1}H NMR of **C7** ($CDCl_3$) δ 5.84–5.86 (m, 1 H, 11-CH), 3.87–3.96 (m, 4 H, OCH_2CH_2O), 3.74 (dt, 1 H, J = 8.15, 4.56 Hz, 17-CH), 0.73 (s, 3 H, 18-CH_3). Anal. Calcd for (6/1 α/β-epoxide mixture) $C_{20}H_{28}O_4$: C, 72.26; H, 8.49. Found: C, 72.15; H, 8.75.

α-[(2-Tetrahydropyranyl)oxy]-p-bromotoluene (T1). Dihydropyran (1.22 mL, 13.4 mmol) was added to a 5 °C solution of 4-bromobenzyl alcohol (0.5 g, 2.7 mmol) dissolved in 7 mL of THF. A catalytic amount (20 mg) of p-toluenesulfonic acid was added and the reaction mixture was allowed to warm to room temperature and stirred for 3 h. Product isolation (solid $NaHCO_3$ and H_2O, Et_2O, $MgSO_4$) and purification (flash chromatography, 1/6 EtOAc/hexane) gave 0.7 g (97%) of **T1** as a liquid: ^{1}H NMR ($CDCl_3$, 300 MHz) δ 7.36 (AB q, 4 H, Δδ = 0.22, J = 8.43 Hz, Ar-H), 4.69 (t, br, 1 H, J = 3.38, OCHO), 4.60 (AB q, 2 H, Δδ = 0.28, J = 12.28 Hz, $ArCH_2O$), 3.90 (ddd, 1 H, J = 3.21, 8.24, 11.31 Hz, $OCHHCH_2$), 3.51–3.58 (m, 1 H, $OCHHCH_2$), 1.5–1.9 (m, 6 H, $OCH_2CH_2CH_2CH_2$). Anal. Calcd for $C_{12}H_{15}O_2Br$: C, 53.15; H, 5.58; Br, 29.47. Found: C, 53.16; H, 5.59; Br, 29.50.

3,3-(Ethylenedioxy)-5α-hydroxy-11β-[α-[(2′-tetrahydropyranyl)oxy]-p-tolyl]-9(10)-estren-17β-ol (C8). Aryl bromide **T1** (0.647 g, 2.39 mmol), diluted with 3 mL of THF, was added dropwise to a heterogeneous solution of magnesium turnings (61 mg, 2.5 mmol) in 3 mL of THF. The solution was then heated to reflux for 3 h and then cooled to 5 °C whereupon CuI (10 mg, 0.0525 mmol) was added. After stirring for 15 min, a 6/1 mixture of **C6/C7** (0.1 g, 0.301 mmol), dissolved in 3 mL of THF, was slowly added dropwise to the reaction mixture and the solution was stirred for 1 h at 5 °C. Product isolation (cold aqueous saturated NH_4Cl, CH_2Cl_2, $MgSO_4$) and purification (flash chromatography, 4/1 EtOAc/hexane) gave 0.139 g (88%) of **C8** as a mixture of THP diastereomers (glass): ^{1}H NMR ($CDCl_3$, 300 MHz) δ 7.22 (AB q, 4 H, Δδ = 0.05, J = 8.24 Hz, Ar-H), 4.71 (t, br, 1 H, J = 3.40, OCHO), 4.60 (AB q, 2 H, Δδ = 0.30, J = 11.93 Hz, $ArCH_2O$, doubling of some signals due to diastereomeric mixture), 4.36 (s, 1 H, 5-COH), 4.25 (d, br, 1 H, J = 7.01 Hz, 11-CH), 3.93–4.04 (m, 4 H, OCH_2CH_2O), 3.87–3.93 (m, 1 H, $OCH_2CH_2CH_2$), 3.61 (t, br, 1 H, J = 7.93 Hz, 17-CH), 3.50–3.57 (m, 1 H, $OCH_2CH_2CH_2$), 0.35 (s, 3 H, 18-CH_3). Anal. Calcd for $C_{32}H_{44}O_6$: C, 73.25; H, 8.45. Found: C, 73.30; H, 8.46.

3,3-(Ethylenedioxy)-5α-hydroxy-11β-[α-[(2′-tetrahydropyranyl)oxy]-p-tolyl]-9(10)-estren-17-one (C9). $(n\text{Pr})_4NRuO_4$ (65 mg, 0.19 mmol) was added to a solution containing steroid **C8** (1.08 g, 2.06 mmol), N-methylmorpholine N-oxide (362 mg, 3.09 mmol), and 15 mL of CH_2Cl_2. The reaction mixture slowly turned black as it was stirred for 10 min. After quenching with 7 mL of a 10% sodium thiosulfate solution and the further addition of 10 mL of CH_2Cl_2, the entire mixture was filtered through Celite. The organic layer of the filtrate was separated, washed with water, dried over $MgSO_4$, and evaporated under reduced pressure. Product purification (flash chromatography, 3/1 EtOAc/hexane) gave 1.04 g (98%) of **C9** as a mixture of THP diastereomers (glass): ^{1}H NMR ($CDCl_3$, 300 MHz) δ 7.23 (AB q, 4 H, Δδ = 0.048, J = 7.68 Hz, Ar-H), 4.71 (t, br, 1 H, J = 3.42 Hz, OCHO), 4.60 (AB q, 2 H, Δδ = 0.31, J = 12.00 Hz, $ArCH_2O$, doubling of some signals due to diastereomeric mixture), 4.40 (s, 1 H, 5-COH), 4.32 (d, br, 1 H, J = 7.14 Hz, 11-CH), 3.95–4.05 (m, 4 H, OCH_2CH_2O), 3.88–3.94 (m, 1 H, $OCH_2CH_2CH_2$), 3.50–3.59 (m, 1 H, $OCH_2CH_2CH_2$), 0.49 (s, 3 H, 18-CH_3). Anal. Calcd for $C_{32}H_{42}O_6$: C, 73.53; H, 8.10. Found: C, 73.34; H, 8.19.

3,3-(Ethylenedioxy)-5α-hydroxy-11β-[α-[(2′-tetrahydropyranyl)oxy]-p-tolyl]-17α-propynyl-9(10)-estren-17β-ol (C10). Steroid **C9** (1.2 g, 2.30 mmol), dissolved in 10 mL of THF, was added dropwise over 10 min to a room temperature heterogeneous solution of propynyllithium (0.54 g, 11.84 mmol) in 50 mL of THF. The reaction mixture was stirred for 1 h and concentrated to half its volume. Product isolation (H_2O, Et_2O, $MgSO_4$) and purification (flash chromatography, 2/1 EtOAc/hexane) gave 1.1 g (85%) of **C10** as a glass: ^{1}H NMR ($CDCl_3$, 300 MHz) δ 7.21 (AB q, 4 H, Δδ = 0.049, J = 8.14 Hz, Ar-H), 4.71 (t, br, 1 H, J = 3.20 Hz, OCHO), 4.60 (AB q, 2 H, Δδ = 0.30, J = 11.98 Hz, $ArCH_2O$, doubling of some signals due to diastereomeric mixture), 4.32 (d, br, 1 H, J = 7.30 Hz, 11-CH), 3.95–4.02 (m, 4 H, OCH_2CH_2O), 3.88–3.94 (m, 1 H, $OCH_2CH_2CH_2$), 3.52–3.56 (m, 1 H, $OCH_2CH_2CH_2$), 1.89 (s, 3 H, $C{\equiv}CCH_3$), 0.44 (s, 3 H, 18-CH_3). Anal. Calcd for $C_{35}H_{46}O_6$: C, 74.70; H, 8.25. Found: C, 74.51; H, 8.46.

11β-(α-Hydroxy-p-tolyl)-17α-propynyl-17β-hydroxy-4,9-estradien-3-one (C11). Steroid **C10** (195 mg) was dissolved in 4 mL of 7/3 acetic acid/water and the solution was heated at 50 °C for 1.5 h and then cooled to room temperature. Product isolation (aqueous saturated $NaHCO_3$, CH_2Cl_2, $MgSO_4$) and purification (flash chromatography, 2/1 EtOAc/hexane) gave 100 mg (70%) of **C11** as a glass: ^{1}H NMR ($CDCl_3$, 300 MHz) δ 7.22 (AB q, 4 H, Δδ = 0.070, J = 8.26 Hz, Ar-H), 5.78 (s, 1 H, 4-CH), 4.66 (d, 2 H, J = 5.71 Hz, $ArCH_2OH$), 4.43 (d, br, 1 H, J = 6.20 Hz, 11-CH), 1.90 (s, 3 H, $C{\equiv}CCH_3$), 0.50 (s, 3 H, 18-CH_3); MS (LREI, 70 eV) m/z (relative intensity) 416 (M^+, 54), 398 (30), 334 (45), 235 (70), 225 (54), 91 (100); HREI calcd for $C_{28}H_{32}O_3$ 416.2352, found 416.2356.

11β-[α-[(Methylsulfonyl)oxy]-p-tolyl]-17α-propynyl-17β-hydroxy-4,9-estradien-3-one (C12). Methanesulfonyl chloride (7.44 μL, 0.096 mmol) was slowly added to a stirring mixture containing steroid **C11** (20 mg, 0.048 mmol), 13.4 μL of Et_3N (0.096 mmol), and 1 mL of THF at room temperature. The reaction mixture was stirred for 0.5 h. Product isolation (H_2O, Et_2O, $MgSO_4$) and purification (flash chromatography, 2/1 EtOAc/hexane) gave 21 mg (88%) of **C12** as a glass. The product has a half-life of 1 day when subjected to ambient conditions

but is moderately stable if stored at −20 °C: ^{1}H NMR ($CDCl_3$, 300 MHz) δ 7.29 (AB q, 4 H, $\Delta\delta$ = 0.106, J = 8.10 Hz, Ar-H), 5.79 (s, 1 H, 4-CH), 5.21 (d, 2 H, J = 5.71 Hz, $ArCH_2OMs$), 4.45 (d, br, 1 H, J = 7.07 Hz, 11-CH), 2.88 (s, 3 H, OSO_2CH_3), 1.90 (s, 3 H, $C{\equiv}CH_3$), 0.47 (s, 3 H, 18-CH_3); MS (LRFAB) m/z (relative intensity) 495 (M^+ + H, 27), 461 (25), 399 (32); HRFAB calcd for $C_{29}H_{34}O_5S_1$ (+H): 495.2205, found 495.2215.

11β-[α-[*N*-[2-[*N*-[2′-Methyl-2′-[(triphenylmethyl)thio]propyl]amino]ethyl]-*N*-[2′-methyl-2′-[(triphenylmethyl)thio]propyl]amino]-*p*-tolyl]-17α-propynyl-17β-hydroxy-4,9-estradien-3-one (11β-BAT II estradiene, C13). A solution of BAT II (1.5 g, 2.12 mmol) and steroid **C12** (0.5 g, 1.01 mmol) in 10 mL of 1,2-dichloroethane was stirred at 80 °C for 2 h. While still at 80 °C, the solvent was evaporated under a stream of nitrogen. The resulting thick brown-orange oil was cooled to room temperature. Product isolation (1 N NaOH, CH_2Cl_2, $MgSO_4$) and purification (flash chromatography, 1/1 EtOAc/hexane, required two or more separate columns) gave **C13** (0.71 g, 63%) as a glass. The product runs as a streak with a median R_f = 0.30 on silica TLC and follows directly behind a prominent yellow band: ^{1}H NMR ($CDCl_3$) δ 7.02–7.61 (m, 34 H, Ar-H), 5.74 (s, 1 H, 4-CH), 4.45 (d, br, 1 H, J = 6.73 Hz, 11-CH), 3.43 (s, br, 2 H, $ArCH_2N$), 1.90 (s, 3 H, $C{\equiv}CCH_3$), 0.95 (s, 6 H, $C(CH_3)_2$), 0.94 (s, 6 H, $C(CH_3)_2$), 0.44 (s, 3 H, 18-CH_3); MS (LRFAB) m/z (relative intensity) 1119 (M^+ + H, 40), 877 (8), 633 (15), 559 (17), 244 (100). HRFAB calcd for $C_{76}H_{82}O_2N_2S_2$ (+H) 1119.5896, found 1119.5879.

General S-Deprotection Reaction. Exemplified by the deprotection of **C13** to form **C14**, the following method is completely general and was used to deprotect all of the steroid–BAT chelators.

A homogeneous mixture containing $AgNO_3$ (58.5 mg, 0.345 mmol), pyridine (30 μL, 0.37 mmol), and 1 mL of EtOH was added to a 65 °C solution of steroid **C13** (193 mg, 0.172 mmol) dissolved in 2 mL of 2/1 EtOAc/EtOH. The reaction mixture was stirred at 65 °C for 45 min, reduced to one-third of its volume, and then cooled to room temperature. With stirring, 20 mL of Et_2O was added, causing the disilver salt to precipitate. The precipitate was collected by filtration over Celite. As the precipitate could not be separated from the Celite pad, the inseparable mixture of Celite and precipitate was dried. The dried Celite/precipitate mixture was stirred for 30 min in a solution of 15 mL of acetone and 0.6 mL of 6 N HCl. Product isolation (aqueous saturated $NaHCO_3$, EtOAc, $MgSO_4$) gave 133 mg of **C14** as a crude off-white, amorphous solid. The crude product was used in this form for the next reaction sequence. **A3** and **B5** were produced in an analogous manner and afforded similar yields of crude product.

21-[*N*-[2-[*N*-(2′-Methyl-2′-mercaptopropyl)amino]ethyl]-*N*-(2′-methyl-2′-mercaptopropyl)amino]progesterone (21-BAT I progesterone, A3): MS (LRFAB) m/z (relative intensity) 549 (M^+ + H, 100), 531 (20), 515 (18), 461 (10); HRFAB calcd for $C_{31}H_{52}O_2N_2S_2$ (**H**) 549.3548, found 549.3551.

13β-Ethyl-17α-[3-[*N*-[2′-[*N*-(2″-methyl-2″-mercaptopropyl)amino]ethyl]-*N*-(2″-methyl-2″-mercaptopropyl)amino]propynyl]-17β-hydroxy-4-gonen-3-one (17α-BAT I norgestrel, B5): MS (LRFAB) m/z (relative intensity) 561 (M^+ + H, 100), 527 (8), 325 (2); HRFAB calcd for $C_{32}H_{52}O_2N_2S_2$ (+H) 561.3548, found 561.3542.

11β-[α-[*N*-[2-[*N*-(2′-Methyl-2′-mercaptopropyl)amino]ethyl]-*N*-(2′-methyl-2′-mercaptopropyl)amino]-*p*-tolyl]-17α-propynyl-17β-hydroxy-4,9-estradien-3-one (11β-BAT I estradiene, C14). Crude **C14** was synthesized by the $AgNO_3$ reaction described above. This material was used for the Re-insertion reaction: MS (LRFAB) m/z (relative intensity) 635 (M^+ + H, 25), 460 (5), 279 (8); HRFAB calcd for $C_{38}H_{54}O_2N_2S_2$ (+H) 635.3705, found 635.3722.

Pure **C14**, suitable for RBA determinations, was obtained by the $Hg(OAc)_2$ method described to form **D8** from **D7** (65% yield): ^{1}H NMR for **C14** ($CDCl_3$, 300 MHz) δ 7.21 (AB q, 4 H, $\Delta\delta$ = 0.161, J = 8.04 Hz, Ar-H), 5.78 (s, 1 H, 4-CH), 4.43 (d, br, 1 H, J = 6.75 Hz, 11-CH), 3.71 (s, 2 H, $ArCH_2N$), 3.08 (s, br, 3 H, SH and NH), 1.90 (s, 3 H, $C{\equiv}CCH_3$), 1.347 (s, 6 H, $C(CH_3)_2$), 1.333 (s, 3 H, $C(CH_3)(CH_3)$), 1.325 (s, 3 H, $C(CH_3)(CH_3)$), 0.50 (s, 3 H, 18-CH_3).

General ReO Insertion Reaction. Exemplified by ReO insertion into **A3** to form **A4**, the following method is completely general and was used to form all the steroid–BAT Re chelates.

Steroid **A3** (102 mg, 0.19 mmol) and oxotrichlorobis(triphenylphosphine)rhenium(V) (155 mg, 0.19 mmol) were dissolved in 1.90 mL (1.90 mmol) of 1 N methanolic NaOAc. The reaction mixture was heated at reflux for 45 min and then allowed to cool to room temperature. Product isolation (H_2O, EtOAc, $MgSO_4$) gave a green oil.

[21-[*N*-[2-[*N*-(2′-Methyl-2′-mercaptopropyl)amino]ethyl]-*N*-(2′-methyl-2′-mercaptopropyl)amino]progesteronato(4−)]oxorhenium(V) (21-N_2S_2 Re Chelate, A4). Pure product (diastereomeric mixture of **A4syn1,2**) was obtained as a glass (29%) after two separate silica flash columns (1/1 EtOAc/hexane). The syn (purple) diastereomeric pair were the only desired products isolated. The diastereomers were inseparable by HPLC: ^{1}H NMR ($CDCl_3$, 300 MHz) δ 5.74 (s, 1 H, 4-CH), 4.78/4.77 (AB q, 2 H, $\Delta\delta$ = 0.133/0.206, J = 19.29/19.22 Hz, $COCH_2N$, 1/1 diastereomeric ratio), 4.05–4.18 (m, 1 H, $NCHHCH_2N$), 3.91–3.98 (m, 1 H, $NCHHCH_2N$), 3.90 (d, 1 H, J = 10.97 Hz, amide-$NCHHC(CH_3)_2$, diastereomers displaced by 5.9 Hz), 3.65 (d, 1 H, J = 13.35 Hz, amine-$NCHHC(CH_3)_2$), 3.61 (d, 1 H, J = 10.97 Hz, amide-$NCHHC(CH_3)_2$), 3.22–3.33 (m, 1 H, $NCHHCH_2N$), 2.89–2.98 (m, 1 H, $NCHHCH_2N$), 2.63 (d, 1 H, J = 13.35 Hz, amine-$NCHHC(CH_3)_2$), 1.91 (s, 3 H, $C(CH_3)(CH_3)$), 1.70 (s, 3 H, $C(CH_3)(CH_3)$, diastereomers displaced by 6.7 Hz), 1.58 (s, 3 H, $C(CH_3)(CH_3)$, diastereomers displaced by 19.9 Hz), 1.47 (s, 3 H, $C(CH_3)(CH_3)$), 1.19 (s, 3 H, 18-CH_3, diastereomers displaced by 2.4 Hz), 0.77 (s, 3 H, 19-CH_3, diastereomers displaced by 2.4 Hz); IR (solution, $CHCl_3$) 1708 (20-ketone), 1664 (3-ketone), 938 cm^{-1} (Re=O); MS (LRFAB) m/z (relative intensity) 749 (M^+ + H (Re = 187), 100), 732 (3), 549 (8), 419 (12), 279 (11); HRFAB calcd for $C_{31}H_{49}O_3N_2S_2$Re (+H) 749.2821, found 749.2822.

[13β-Ethyl-17β-hydroxy-17α-[3-[*N*-[2-[*N*-(2′-methyl-2′-mercaptopropyl)amino]ethyl]-*N*-(2′-methyl-2′-mercaptopropyl)amino]propynyl]-4-gonen-3-onato(4−)]oxorhenium(V) (17α-N_2S_2 Re Chelate, B6). Pure product (**B6**) was obtained as a glass (40%) after two separate silica flash columns using 1/1 EtOAc/hexane as the eluent in the first column and 3/2/1 Et_2O/CH_2Cl_2/hexane as the eluent in the second column. Syn (**B6syn1**, **B6syn2**) and anti (**B6anti1**, **B6anti2**) diastereomeric pairs were obtained in a 4/1 (syn/anti) ratio. The diastereomers in each diastereomeric pair were inseparable by HPLC.

Analysis for syn diastereomer mixture **B6syn1,2**: ^{1}H NMR ($CDCl_3$, 300 MHz) δ 5.85 (s, 1 H, 4-CH), 4.652/4.655 (AB q, 2 H, $\Delta\delta$ = 0.091/0.118, J = 17.67/17.80 Hz, $C{\equiv}CCH_2N$, 1/1 diastereomeric mixture), 4.21 (ddd, 1 H,

J = 4.30, 9.36, 12.91 Hz, NC*H*HCH$_2$N), 3.74 (AB q, 2 H, $\Delta\delta$ = 0.263, J = 11.07 Hz, amide-NC*H*$_2$C(CH$_3$)$_2$), 3.70/3.61 (ddd, 1 H, J = 3.59/3.80, 3.59/3.80, 4.30/4.30 Hz, NC*H*HCH$_2$N, 1/1 diastereomeric mixture), 3.45/3.49 (d, 1 H, J = 12.69/12.62 Hz, amine-NC*H*HC(CH$_3$)$_2$, 1/1 diastereomeric mixture), 3.28–3.37 (m, 1 H, NC*H*HCH$_2$N), 1.90 (s, 3 H, C(C*H*$_3$)CH$_3$), 1.74 (s, 3 H, C(C*H*$_3$)CH$_3$), 1.62 (s, 3 H, C(C*H*$_3$)(CH$_3$)), 1.46 (s, 3 H, C(C*H*$_3$)(CH$_3$)), 1.03 (t, 3 H, J = 7.33 Hz, 18-CH$_2$C*H*$_3$); IR (solution, CHCl$_3$) 3420 (br, OH), 1663 (3-ketone), 938 cm^{-1} (Re=O); MS (LRFAB) m/z (relative intensity) 761 (M$^+$ + H (Re = 187), 33), 433 (11), 279 (37); HRFAB calcd for C$_{32}$H$_{49}$O$_3$N$_2$S$_2$Re (+H) 761.2815, found 761.2806.

Analysis for anti diastereomer mixture **B6anti1,2**: ^{1}H NMR (CDCl$_3$, 300 MHz) δ 5.85 (s, 1 H, 4-CH), 4.11 (d, 1 H, J = 12.00 Hz, amide-NC*H*HC(CH$_3$)$_2$, diastereomers displaced by 1 Hz), 4.02–4.18 (m, 1 H, NC*H*HCH$_2$N), 3.52–3.89 (m, 4 H, amine-NC*H*HC(CH$_3$)$_2$ and NC*H*HC*H*$_2$N), 3.38 (AB q, 2 H, $\Delta\delta$ = 0.209, J = 10.87 Hz, C≡CCH$_2$N), 3.11 (d, 1 H, J = 12.00 Hz, amide-NC*H*HC(CH$_3$)$_2$, diastereomers displaced by 1 Hz), 1.90 (s, 3 H, C(C*H*$_3$)(CH$_3$)), 1.86 (s, 3 H, C(C*H*$_3$)(CH$_3$), diastereomers displaced by 1.6 Hz), 1.66 (s, 3 H, C(C*H*$_3$)(CH$_3$)), 1.40 (s, 3 H, C(C*H*$_3$)(CH$_3$)), 1.02 (t, 3 H, J = 6.71 Hz, 18-CH$_2$C*H*$_3$, diastereomers displaced by 1 Hz); IR (solution, CHCl$_3$) 3420 (br, OH), 1663 (3-ketone), 947 cm^{-1} (Re=O). MS (LRFAB) m/z (relative intensity) 761 (M$^+$ + H (Re = 187), 42), 743 (25), 613 (10), 461 (9); HRFAB calcd for C$_{32}$H$_{49}$O$_3$N$_2$S$_2$Re (+H) 761.2821, found 761.2813.

[17β-Hydroxy-11β-[α-[*N*-[2-[*N*-(2′-methyl-2′-mercaptopropyl)amino]ethyl]-*N*-(2′-methyl-2′-mercaptopropyl)amino]-*p*-tolyl]-17α-propynyl-4,9-estradien-3-onato(4-)]oxorhenium(V) (11β-N$_2$S$_2$Re Chelate, C15). Pure product (**C15**) was obtained as a glass (45%) after two separate silica flash columns (2/1 EtOAc/hexane). Syn (purple) and anti (orange) diastereomeric pairs were obtained in a 10/1 (syn/anti) ratio. The anti diastereomers **C15anti1** and **C15anti2** were separable by HPLC whereas the syn diastereomers **C15syn1** and **C15syn2** were not separable by HPLC:

Analysis for syn diastereomer mixture **C15syn1,2**: ^{1}H NMR (CDCl$_3$, 300 MHz) δ 7.352/7.350 (AB q, 4 H, $\Delta\delta$ = 0.055/0.049, J = 8.04/8.04 Hz, Ar-H, 1/1 diastereomeric ratio), 5.80 (s, 1 H, 4-CH), 4.965/4.963 (AB q, 2 H, $\Delta\delta$ = 0.517/0.524, J = 14.30/14.30 Hz, ArCH$_2$N, 1/1 diastereomeric ratio), 4.48–4.56 (m, 2 H, NC*H*HCH$_2$N and 11-C*H*), 3.79 (AB q, 2 H, $\Delta\delta$ = 0.402, J = 10.99 Hz, amide-NC*H*$_2$C(CH$_3$)$_2$), 3.36–3.44 (m, 2 H, NC*H*HCH$_2$N and amine-NC*H*HC(CH$_3$)$_2$), 3.25 (ddd, 1 H, J = 5.21, 12.90, <1 Hz, NC*H*HCH$_2$N), 1.92 (s, 3 H, C(C*H*$_3$)(CH$_3$)), 1.91 (s, 3 H, C(C*H*$_3$)(CH$_3$)), 1.90 (s, 3 H, C≡CCH$_3$), 1.62 (s, 3 H, C(C*H*$_3$)(CH$_3$)), 1.53 (s, 3 H, C(C*H*$_3$)(CH$_3$)), 0.48 (s, 3 H, 18-CH$_3$, diastereomers displaced by 2.1 Hz); IR (solution, CHCl$_3$) 3420 (br, OH), 1655 (3-ketone), 941 cm^{-1} (Re=O); MS (LRFAB) m/z (relative intensity) 835 (M$^+$ + H (Re = 187), 55), 435 (22), 399 (14), 275 (10), 249 (10); HRFAB calcd for C$_{38}$H$_{51}$O$_3$N$_2$S$_2$Re (+H) 835.2977, found 835.2956. Anal. Calcd for C$_{38}$H$_{51}$O$_3$N$_2$S$_2$Re: C, 54.71; H, 6.16; N, 3.36; S, 7.69. Found: C, 54.92; H, 6.44; N, 3.16; S, 7.49.

Analysis for anti diastereomer **C15anti1**: ^{1}H NMR (CDCl$_3$, 300 MHz) δ 7.24 (AB q, 4 H, $\Delta\delta$ = 0.039, J = 8.25 Hz, Ar-H), 5.80 (s, 1 H, 4-CH), 4.45 (d, br, 1 H, J = 7.12 Hz, 11-CH), 4.09 (ddd, 1 H, J = 6.45, 12.45, <1 Hz, NC*H*HCH$_2$N), 3.99 (d, 1 H, J = 13.08 Hz, amide-NC*H*HC(CH$_3$)$_2$), 3.90 (ddd, 1 H, J = 4.87, 11.82, 12.45 Hz, NC*H*HCH$_2$N), 3.81 (d, 1 H, J = 14.45 Hz, amine-NC*H*HC(CH$_3$)$_2$), 3.52–3.60 (m, 1 H, NC*H*HCH$_2$N), 3.47 (ddd, 1 H, J = 4.69, 11.82, <1 Hz, NC*H*HCH$_2$N), 3.39 (AB q, 2 H, $\Delta\delta$ = 0.399, J = 11.00 Hz, ArCH$_2$N), 3.03 (d, 1 H, J = 13.08 Hz, amide-NC*H*HC(CH$_3$)$_2$), 2.13 (s, 3 H, C(C*H*$_3$)(CH$_3$)), 1.94 (s, 3 H, C(C*H*$_3$)(CH$_3$)), 1.91 (s, 3 H, C≡CCH$_3$), 1.69 (s, 3 H, C(C*H*$_3$)(CH$_3$)), 1.43 (s, 3 H, C(C*H*$_3$)(CH$_3$)), 0.46 (s, 3 H, 18-CH$_3$); IR (solution, CHCl$_3$) 1655 (3-ketone), 953 cm^{-1} (Re=O); MS (LRFAB) m/z (relative intensity) 835 (M$^+$ + H (Re = 187), 19), 435 (12), 399 (5), 279 (8); HRFAB calcd for C$_{38}$H$_{51}$O$_3$N$_2$S$_2$Re (+H) 835.2977, found 835.2953.

Analysis for anti diastereomer **C15anti2**: ^{1}H NMR (CDCl$_3$, 300 MHz) δ 7.25 (AB q, 4 H, $\Delta\delta$ = 0.045, J = 8.24 Hz, Ar-H), 5.80 (s, 1 H, 4-CH), 4.45 (d, br, 1 H, J = 7.03 Hz, 11-CH), 4.09 (ddd, 1 H, J = 5.98, 12.54, <1 Hz, NC*H*HCH$_2$N), 3.98 (d, 1 H, J = 13.09 Hz, amide-NC*H*HC(CH$_3$)$_2$), 3.88–3.95 (m, 1 H, NC*H*HCH$_2$N), 3.81 (d, 1 H, J = 14.46 Hz, amine-NC*H*HC(CH$_3$)$_2$), 3.52–3.60 (m, 1 H, NC*H*HCH$_2$N), 3.49 (ddd, 1 H, J = 4.92, 11.96, <1 Hz, NC*H*HCH$_2$N), 3.38 (AB q, 2 H, $\Delta\delta$ = 0.401, J = 11.05 Hz, ArCH$_2$N), 3.03 (d, 1 H, J = 13.09 Hz, amide-NC*H*HC(CH$_3$)$_2$), 2.14 (s, 3 H, C(C*H*$_3$)(CH$_3$)), 1.94 (s, 3 H, C(C*H*$_3$)(CH$_3$)), 1.91 (s, 3 H, C≡CCH$_3$), 1.69 (s, 3 H, C(C*H*$_3$)(CH$_3$)), 1.42 (s, 3 H, C(C*H*$_3$)(CH$_3$)), 0.46 (s, 3 H, 18-CH$_3$); IR (solution, CHCl$_3$) 1655 (3-ketone), 951 cm^{-1} (Re=O); MS (LRFAB) m/z (relative intensity) 835 (M$^+$ + H (Re = 187), 35), 435 (19), 399 (10), 275 (10), 249 (5); HRFAB calcd for C$_{38}$H$_{51}$O$_3$N$_2$S$_2$Re (+H) 835.2977, found 835.2956.

Pregnane 16α,17α-Series (D). 2-[(Triphenylmethyl)thio]ethylamine (5). Triphenylmethanol (11.45 g, 44 mmol) was added to a stirring solution containing 2-aminoethanethiol hydrochloride (5 g, 44 mmol) and 40 mL of trifluoroacetic acid. The resulting brown solution was stirred for 30 min and then the solvent was evaporated under reduced pressure. Product isolation (2.5 N NaOH, EtOAc, K$_2$CO$_3$) and recrystallization from Et$_2$O afforded a quantitative yield of **5** as a solid: mp 94–95 °C; ^{1}H NMR (CDCl$_3$) δ 7.15–7.55 (m, 15 H, ArH), 2.60 (t, 2 H, J = 8.0 Hz, NCH$_2$), 2.32 (t, 2 H, J = 8.0 Hz, SCH$_2$), 1.08 (s, br, 2 H, NH$_2$). Anal. Calcd for C$_{21}$H$_{21}$N$_1$S$_1$: C, 78.95; H, 6.62; N, 4.39. Found: C, 78.94; H, 6.64; N, 4.34.

***N*-[2-[(Triphenylmethyl)thio]ethyl]bromoacetamide (6).** To a −16 °C solution containing bromoacetyl bromide (2.3 g, 11.4 mmol) and 5 mL of CH$_2$Cl$_2$ was added **5** (3 g, 9.4 mmol) and Et$_3$N (0.94 g, 9.34 mmol) dissolved in 15 mL of CH$_2$Cl$_2$. The reaction mixture was then allowed to warm room temperature. Product isolation (H$_2$O, CH$_2$Cl$_2$, 10% NaHCO$_3$, 1 N HCl, MgSO$_4$) and recrystallization from Et$_2$O/hexane afforded 3.1 g (70.5%) of **6** as a solid: mp 130–132 °C; ^{1}H NMR (CDCl$_3$) δ 7.15–7.55 (m, 15 H, ArH), 6.60 (s, br, 1 H, NH), 3.80 (s, 2 H, BrCH$_2$), 3.10 (dt, 2 H, J_d = 8.0, J_t = 8.0 Hz, NCH$_2$), 2.43 (t, 2 H, J = 8.0 Hz, SCH$_2$). Anal. Calcd for C$_{23}$H$_{22}$NOSBr: C, 62.73; H, 5.04; N, 3.18; S, 7.28; Br, 18.14. Found: C, 62.80; H, 5.03; N, 3.18; S, 7.26; Br, 18.07.

3β-Hydroxy-*N*-methylpregnano[16α,17α-*d*]isoxazolidin-20-one (D4). A solution containing **D3** (1 g, 3.15 mmol), *N*-methylhydroxylamine hydrochloride (0.53 g, 6.3 mmol), (iPr)$_2$NH (1.1 mL, 7.89 mmol), paraformaldehyde (0.19 g, 6.3 mmol), and 40 mL of EtOH was heated to reflux for 10 h and cooled to room temperature, and then the solvent was evaporated under reduced pressure. Product isolation (H$_2$O, CH$_2$Cl$_2$, brine, Na$_2$SO$_4$) and purification (flash chromatography, 1/1 EtOAc/hexane) gave 0.52 g (44%) of **D4** as a solid: mp 197–198 °C; ^{1}H NMR (CDCl$_3$) δ 3.54–3.66 (m, 1 H, 3-CH), 3.44–3.50 (m, 2 H, NCH$_2$), 2.66 (s, 3 H, NCH$_3$), 2.20 (s, 3 H, 21-CH$_3$), 0.80 (s, 3 H, 19-CH$_3$), 0.61 (s, 3 H, 18-CH$_3$); MS (LRFAB) m/z (relative intensity) 376 (M$^+$ + H, 100), 358 (11), 515

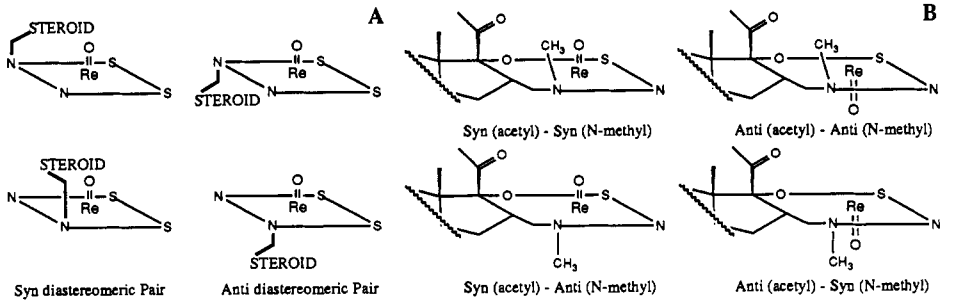
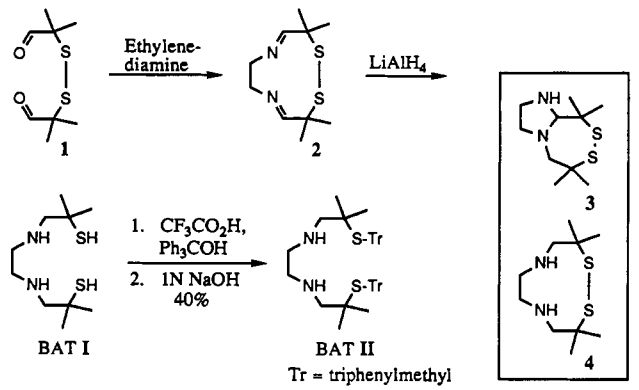


Figure 1. Possible diastereomers for N_2S_2 and N_2OS complexes.

Scheme I



(18), 332 (7). Anal. Calcd for $C_{23}H_{37}O_3N_1$: C, 73.56; H, 9.93; N, 3.72. Found: C, 73.44; H, 9.90; N, 3.67.

16α-(2′-Azapropyl)-3β,17α-dihydroxy-5α-pregnan-20-one (D5). A solution containing **D4** (0.40 g, 1.06 mmol), 4 mL of 55% hydrazine hydrate, and 5 mL of EtOH was heated at reflux for 15 h. After such time, a small amount of Raney nickel W-2 was added and heating continued for two additional hours. Two 1-mL portions of hydrazine hydrate were added during this additional 2-h time period. After cooling to room temperature, the Raney nickel was separated from the solution by filtration through a Celite pad and then the solvent was evaporated under reduced pressure. The resulting residue was heated at reflux for 10 h in a solution of 8 mL of EtOH, 8 mL of 1.2 N HCl, and 1 mL of acetone. Product isolation (aqueous 10% NH_4OH, EtOAc, brine, Na_2SO_4) and recrystallization from CH_2Cl_2/Et_2O gave 0.30 g (75%) of **D5** as a solid: mp 196–197 °C: ^1H NMR ($CDCl_3$) δ 3.55–3.65 (m, 1 H, 3-CH), 3.04–3.20 (m, 1 H), 2.52–2.72 (m, 2 H, NCH_2), 2.32 (s, 3 H, NCH_3), 2.20 (s, 3 H, 21-CH_3), 0.80 (s, 3 H, 19-CH_3), 0.60 (s, 3 H, 18-CH_3); MS (LRFAB) m/z (relative intensity) 378 (M^+ + H, 100), 360 (5), 252 (17); HRFAB calcd for $C_{23}H_{39}O_3N_1$ (+H) 378.3016, found 378.3012.

16α-[2′-[*N*-[2″-[(Triphenylmethyl)thio]ethyl]-acetamido]-2′-azapropyl]-3β,17α-dihydroxy-5α-pregnan-20-one (D6). Compound **D5** (1.0 g, 2.12 mmol) and (*i*-Pr)$_2$(Et)N (1 mL, 5.3 mmol) were added to a stirring solution of **6** (0.4 g, 1.06 mmol) in 4 mL of THF. The reaction mixture was stirred for 15 h. Product isolation (H_2O, CH_2Cl_2, brine, Na_2SO_4) and purification (flash chromatography, 2/1 EtOAc/hexane) gave 0.75 g (96%) of **D6** as a solid: mp 203–205 °C; ^1H NMR ($CDCl_3$, 200 MHz) δ 7.24–7.44 (m, 15 H, ArH), 6.0 (t, 1 H, J = 6.0 Hz, NH), 3.59 (m, 1 H, 3-CH), 3.08–3.25 (m, 4 H), 2.89 (AB q, 2 H, Δδ = 0.297, J = 15.4 Hz, $COCH_2N$), 2.42 (t, 2 H, J = 6.6 Hz, SCH_2), 2.19 (s, 3 H, 21-CH_3), 2.13 (s, 3 H, NCH_3), 0.79 (s, 3 H, 19-CH_3), 0.67 (s, 3 H, 18-CH_3); MS (LRFAB) m/z (relative intensity) 737 (M^+ + H, 20), 495 (7), 390 (10), 243 (80); HRFAB calcd for $C_{46}H_{60}O_4N_2S$ (+H) 737.4352, found 737.4351.

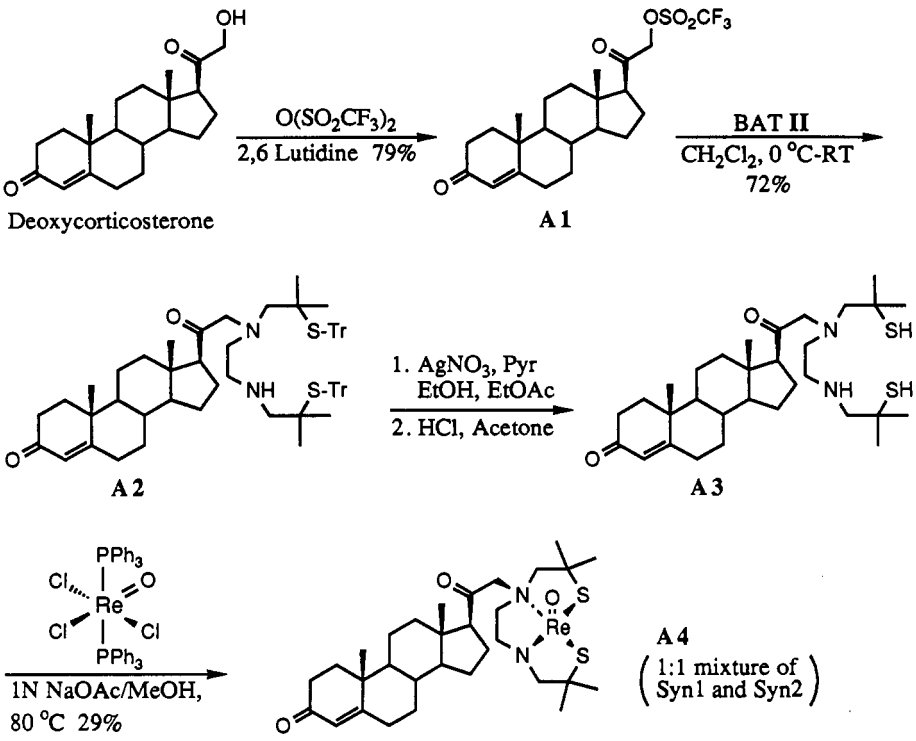
16α-[2′-[*N*-[2″-[(Triphenylmethyl)thio]ethyl]-acetamido]-2′-azapropyl]-17α-hydroxy-5α-pregnane-3,20-dione (D7). A solution containing *N*-methylmorpholine *N*-oxide (0.13 g, 1.1 mmol) and 5 mL of CH_2Cl_2 was dried over $MgSO_4$ and filtered. **D6** was dissolved in the filtrate and then (nPr)$_4$$NRuO_4$ (10 mg, 0.03 mmol) was added in one portion. After stirring for 1 h, the dark solution was evaporated under reduced pressure and purified (flash chromatography, 1/1 EtOAc/hexane) to give 0.25 g (63%) of **D7** as a solid: mp 108–110 °C; ^1H NMR ($CDCl_3$, 200 MHz) δ 5.85–5.93 (m, 1 H, NH), 3.00–3.25 (m, 4 H), 2.90 (AB q, 2 H, Δδ = 0.309, J = 16.0 Hz, $COCH_2N$), 2.21 (s, 3 H, 21-CH_3), 2.13 (s, 3 H, NCH_3), 1.0 (s, 3 H, 19-CH_3), 0.71 (s, 3 H, 18-CH_3); MS (LRFAB) m/z (relative intensity) 735 (M^+ + H, 52), 645 (7), 388 (48), 243 (100); HRFAB calcd for $C_{46}H_{58}O_4N_2S$ (+H) 735.4196, found 735.4189.

16α-[2′-[*N*-(2″-Mercaptoethyl)acetamido]-2′-azapropyl]-17α-hydroxy-5α-pregnane-3,20-dione (D8). A homogeneous solution containing $Hg(OAc)_2$ (0.20 g, 0.62 mmol) and 3 mL of EtOH was added to a warm solution of **D7** (0.33 g, 0.45 mmol) dissolved in 10 mL of 1/1 EtOAc/EtOH. The reaction mixture was stirred at reflux for 30 min, cooled to room temperature, and then treated with excess hydrogen sulfide. The resulting brown precipitate was filtered with a Celite pad and the filtrate was evaporated under reduced pressure. The residue obtained from the filtrate was purified (flash chromatography, 20/1 CH_2Cl_2/*i*PrOH) to give 0.17 g (76%) of **D8** as a glass: ^1H NMR ($CDCl_3$, 200 MHz) δ 6.44 (s, br, 1 H, NH), 5.09 (s, br, 1 H, SH), 3.37–3.58 (m, 2 H), 3.10–3.30 (m, 2 H), 3.02 (AB q, 2 H, Δδ = 0.317, J = 15.0 Hz, $COCH_2N$), 2.69 (dt, 2 H, J_t = 8.1 Hz, J_d = 6.3 Hz, SCH_2), 2.28 (s, 3 H, 21-CH_3), 2.20 (s, 3 H, NCH_3), 1.0 (s, 3 H, 19-CH_3), 0.73 (s, 3 H, 18-CH_3); MS (LRFAB) m/z (relative intensity) 493 (M^+ + H, 100), 388 (35), 278 (9); HRFAB calcd for $C_{27}H_{44}O_4N_2S$ (+H) 493.3100, found 493.3099.

16α-[2′-[*N*-(2″-Mercaptoethyl)acetamido]-2′-azapropyl]-3β,17α-dihydroxy-5α-pregnan-20-one (D9). Compound **D9** was obtained as a glass in 88.7% yield from **D6** by using the method described for the synthesis of **D8**: ^1H NMR ($CDCl_3$, 200 MHz) δ 6.55 (s, br, 1 H, NH), 3.55–3.69 (m, 1 H, 3-CH), 3.39–3.55 (m, 2 H), 3.10–3.29 (m, 2 H), 3.02 (AB q, 2 H, Δδ = 0.295, J = 15.7 Hz, $COCH_2N$), 2.69 (dt, 2 H, J_t = 8.7 Hz, J_d = 6.3 Hz, SCH_2), 2.69 (m, 2 H), 2.26 (s, 3 H, 21-CH_3), 2.19 (s, 3 H, NCH_3), 0.80 (s, 3 H, 19-CH_3), 0.71 (s, 3 H, 18-CH_3); MS (LRFAB) m/z (relative intensity) 495 (M^+ + H, 82), 477 (10), 390 (30); HRFAB calcd for $C_{27}H_{44}O_4N_2S$ (+H) 495.3271, found 495.3264.

[17α-Hydroxy-16α-[2′-[*N*-(2″-mercaptoethyl)acetamido]-2′-azapropyl]-5α-pregnan-3,20-dionato(4−)]-oxorhenium(V) (D10). To a stirring suspension of oxotrichlorobis(triphenylphosphine)rhenium(V) (0.06 g, 0.072 mmol) in 3 mL of anhydrous THF was added (*i*Pr)$_2$(Et)N (0.053 g, 0.3 mmol). The mixture was allowed to darken,

Scheme II



and then 1 mL of CH_3CN, **D8** (0.03 g, 0.06 mmol) in 1 mL THF, and pyridine (0.025 mL, 0.3 mmol) were added. The reaction mixture was heated to reflux for 2 h and then the solvent was evaporated by allowing a stream of N_2 to pass over the surface. Purification (flash chromatography, 100/3 CH_2Cl_2/*i*PrOH) gave 0.13 g (62%) of **D10** as an amorphous solid: mp 205 °C dec; ^1H NMR ($CDCl_3$, 200 MHz) δ 4.39 (dd, 1 H, J = 5.5, 13.0 Hz), 3.94 (AB q, 2 H, $\Delta\delta$ = 0.201, J = 14.6 Hz, $COCH_2N$), 3.69 (dd, 1 H, J = 5.0, 11.6 Hz), 3.17 (dt, 2 H, J_d = 5.5, J_t = 12.4 Hz), 3.0 (s, 3 H, 21-CH_3), 2.80 (s, 3 H, NCH_3), 1.11 (s, 3 H, 19-CH_3), 0.97 (s, 3 H, 18-CH_3); MS (LREI, 70 eV) m/z (relative intensity) 692 (M^+ (Re = 187), 20), 649 (25), 631 (10), 446 (10), 249 (20), 44 (100); HREI calcd for $C_{27}H_{41}O_5N_2SRe$ 692.2293, found 692.2287.

[3β,17α-Dihydroxy-16α-[2′-[*N*-(2″-mercaptoethyl)-acetamido]-2′-azapropyl]-5α-pregnan-20-onato(4−)]-oxorhenium)(V) (D11). Compound **D11** was obtained as an amorphous solid in 70% yield from **D9** by using the method described for the synthesis of **D10**: mp 220 °C dec; ^1H NMR ($CDCl_3$, 200 MHz) δ 4.38 (dd, 1 H, J = 6.0, 13.0 Hz), 3.94 (AB q, 2 H, $\Delta\delta$ = 0.357, J = 14.7 Hz, $COCH_2N$), 3.55–3.60 (m, 1 H, 3-CH), 3.65 (dd, 1 H, J = 5.0, 12.0 Hz), 3.20 (dt, 2 H, J_d = 5.6, J_t = 12.3 Hz), 3.0 (s, 3 H, 21-CH_3), 2.80 (s, 3 H, NCH_3), 1.08 (s, 3 H, 19-CH_3), 0.77 (s, 3 H, 18-CH_3); MS (LRFAB) m/z (relative intensity) 695 (M^+ + H (Re = 187), 20), 461 (5), 279 (60); HRFAB calcd for $C_{27}H_{43}O_5N_2SRe$ (+H) 695.2529, found 695.2522.

RESULTS

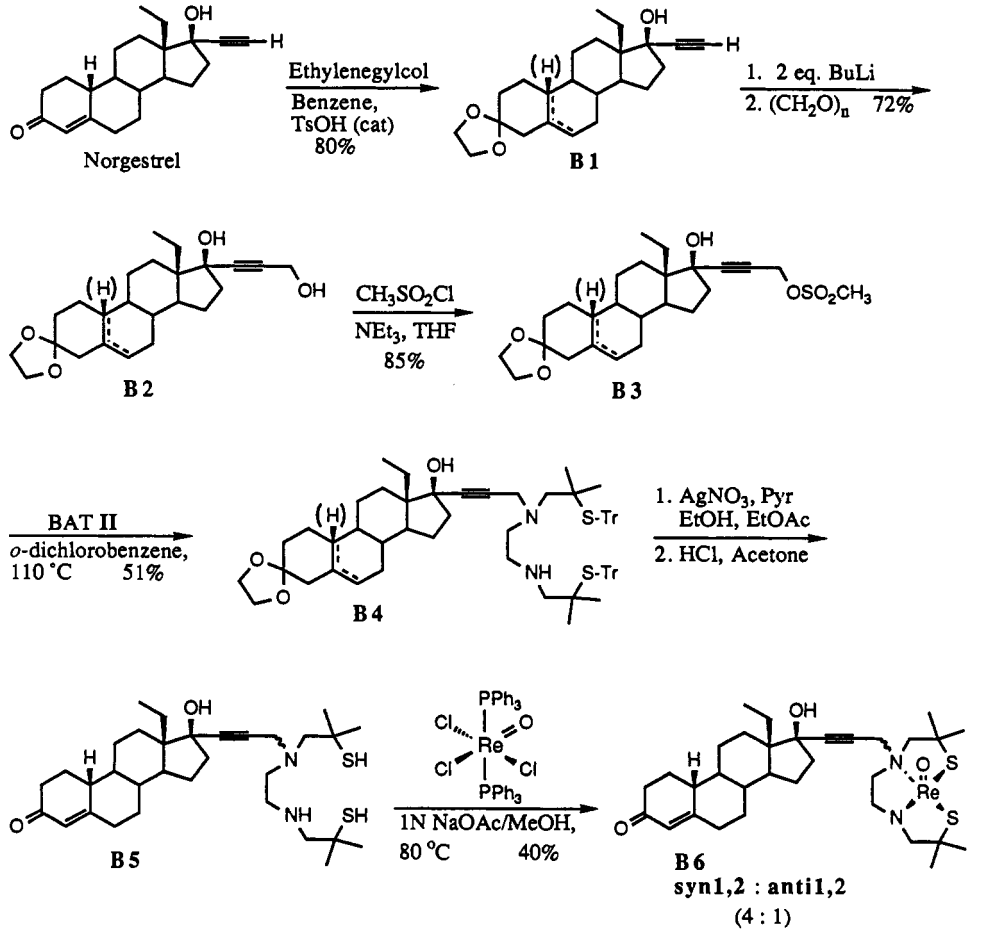
Chemical Synthesis. General. Attachment of the N_2S_2 chelate system to the 21-, 17α-, or 11β-position of the various progestins was achieved by the mono-N-alkylation of a trityl S-protected N_2S_2 chelator by a reactive steroid derivative (α-keto triflate, propargyl mesylate, or benzyl mesylate). The second type of chelate system, the N_2OS chelate, was integrated into the 16α,17α-positions of the steroid skeleton by a key 1,3-dipolar cycloaddition reaction on a 16-dehydroprogestin in which two of the four chelating heteroatoms were introduced. The rhenium(V)–oxo core (Re^VO) was introduced into the various chelators through ligand exchange with dioxo(tetrapyridine)rhenium(V) chloride or oxotrichlorobis(triphenylphosphine)rhenium(V) in basic medium. We found that in situ reduction (using acidic $SnCl_2$) of perrhenate (*21*) in the presence of the chelator gave lower insertion yields than use of the Re(V) species.

Insertion of the ReO core can result in the creation of four diastereomeric products for each N_2S_2 (Figure 1, panel A) or N_2OS (Figure 1, panel B) system. For the N_2OS system, these products are differentiated by the sidedness (relative to the N_2OS plane) of the steroid face and the *N*-methyl moiety compared to the rhenium–oxo atom. In our hands, only one of these N_2OS diastereomers was isolated; the other three diastereomers were apparently not formed in perceptible yield. For the N_2S_2 system, all representative diastereomers were isolated and are denoted as the syn and anti diastereomeric pairs. The terms syn and anti are defined by the orientation of the steroid substituent and the rhenium–oxo atom relative to the N_2S_2 plane. The syn diastereomeric pair, which was always obtained in higher yield than the anti pair, is consistently purple, whereas the anti diastereomeric pair is orange; this is true whether in solution or in the solid state.

The N_2S_2 and N_2OS rhenium chelates can be safety stored in a closed container under ambient conditions for months. A caveat to this statement is that air oxidation does occur to a certain extent; therefore care must be taken when storing small amounts of the rhenium chelates, such is the case when working with tracer levels of ^{186}Re (*22*). The lone pair electrons of the heteroatoms in these complexes appear to be completely involved in bonding; this is apparent from the complexes relatively nonpolar behavior on TLC. In contrast, the precursor N_2S_2 uncomplexed systems are much more polar and run on TLC only in high polarity solvents and then with streaking.

The rhenium chelates give characteristic NMR patterns due to the constrained system and the anisotropy caused by the ReO core. Syn and anti N_2S_2 systems are easily discernable by NMR through the work of Lever et al.,

Scheme III



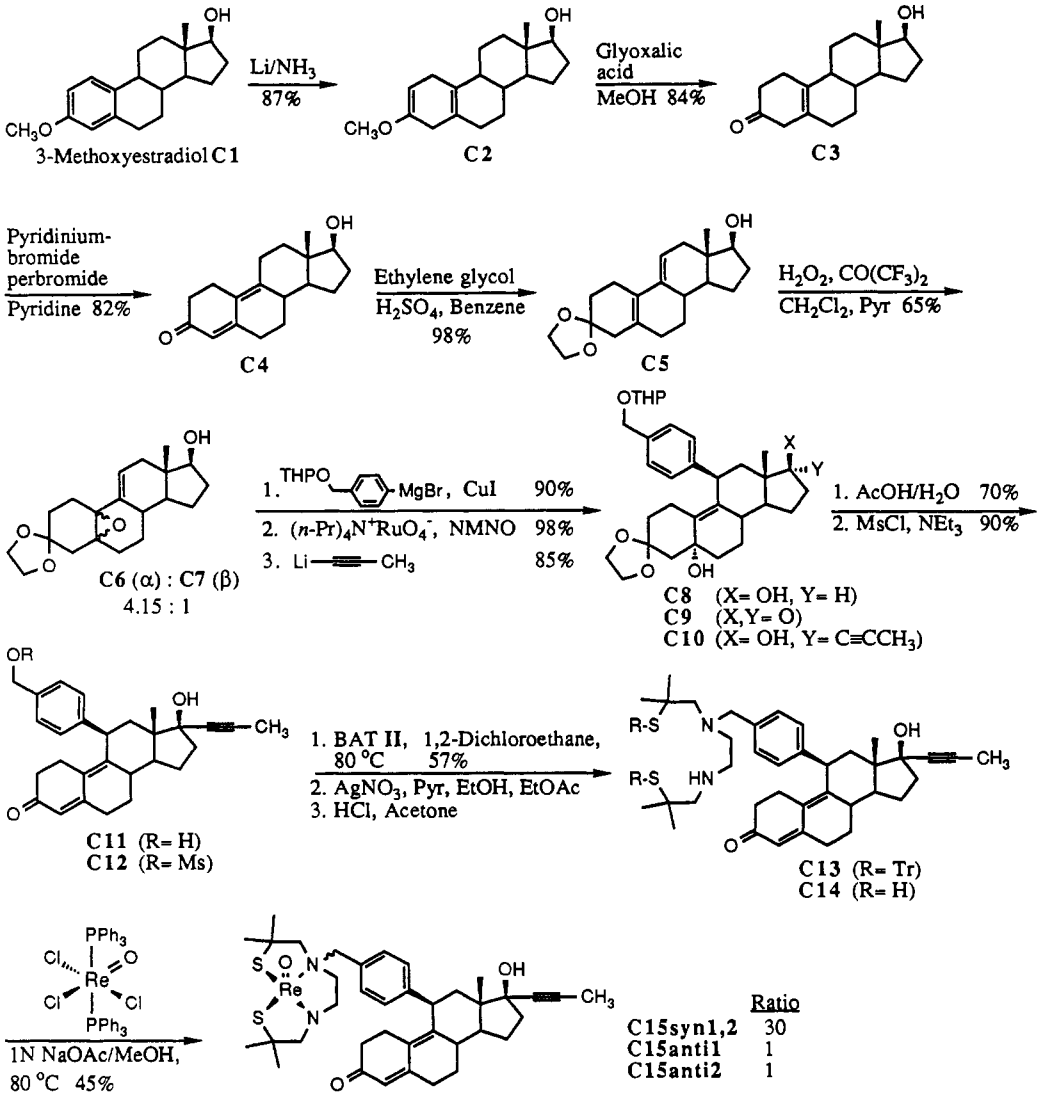
(*21*), which correlates NMR patterns with rhenium N_2S_2 chelate X-ray structures. Of particular note is the chemical shift of the hydrogens on the methylene carbon that links the steroid to the chelate moiety. Linker methylene hydrogens in the anti position are δ 1.2–1.6 upfield relative to linker methylene hydrogens in the syn position. Another diagnostic feature in our N_2S_2 chelate systems is that the rhenium–oxo IR bond stretch for the syn diastereomers is consistently lower (938–941 cm^{-1}) than that of the anti diastereomers (947–953 cm^{-1}).

Synthesis of the Trityl S-Protected BAT II. The synthesis of trityl S-protected BAT II is shown in Scheme I. Aldehyde 1 and diimine 2 are prepared by procedures similar to those of D'Amico and Corbin (*16, 17*). Although diimine 2 could exist as three distinct double bond isomers (trans–trans, cis–trans, and cis–cis), gas chromatographic and NMR analysis indicate that the isolable product is a single isomer. The fact that only one coupling constant of 6.3 Hz is seen for the four hydrogens on the unsubstituted ethylene portion of the molecule gives evidence for C-2 symmetry. Monte Carlo molecular modeling studies using the program Macromodel (*23*) predict that the trans–trans conformation is, by far, the lowest energy structure of the three possible double bond isomers. Coupling constants of 4.8 and 11.0 Hz were calculated from the minimized structures for the ethylene hydrogens on the trans–trans and cis–cis conformations, respectively; the calculated trans–trans coupling constant of 4.8 Hz is close in value to the actual measured coupling constant of 6.3 Hz. These data strongly imply that diimine 2 is in the trans–trans conformation as depicted in Scheme I.

Vigorous reduction of diimine 2 using lithium aluminum hydride (*17*) affords BAT I in nearly quantitative yield. Cyclic products can be obtained when diimine 2 is treated with sodium borohydride in EtOH (*3b*), which reduces only one imine and results in the bicyclo[5.3.0]decane system 3, or sodium cyanoborohydride in acidic MeOH, which reduces both imines and results in the cyclic 10-membered diamine disulfide (4). In order to assure clean N-alkylation in the steroid linking step, BAT I was trityl S-protected in the form of BAT II. Purification of BAT II (or any derivative of BAT II) is difficult due to its noncrystalline nature and its polar and basic character. Silica gel flash chromatography of BAT II and its derivatives results in extensive streaking; therefore, successive column runs, sometimes employing a different eluent for each run, are necessary.

21-BAT-Substituted Progesterone. The synthesis of the 21-substituted progesterone **A4** is shown in Scheme II. Linkage of the steroid skeleton with the N_2S_2 chelator system was accomplished by allowing a two-fold excess of BAT II to react with 21-trifloxyprogesterone (**A1**) at low temperature. Other less reactive derivatives (21-chloro, 21-mesyloxy, and 21-tresyloxyprogesterone) required higher temperatures for alkylation and gave side reactions such as dialkylation and disulfide formation. After purification via a series of silica gel flash columns, **A2** was S-deprotected by using silver nitrate in ethanol (*24*), and the resulting 21-BAT I conjugate (**A3**) was carried on to the ReO-insertion step without extensive purification. The 21-N_2S_2 Re chelate **A4** was formed in a ligand-exchange reaction in which **A3** was allowed to react with oxotrichlorobis(triphenylphosphine)rhenium(V) (*25*) in a refluxing, basic methanolic medium. The syn diastereomeric pair (the diastereomers were inseparable by HPLC) was

Scheme IV

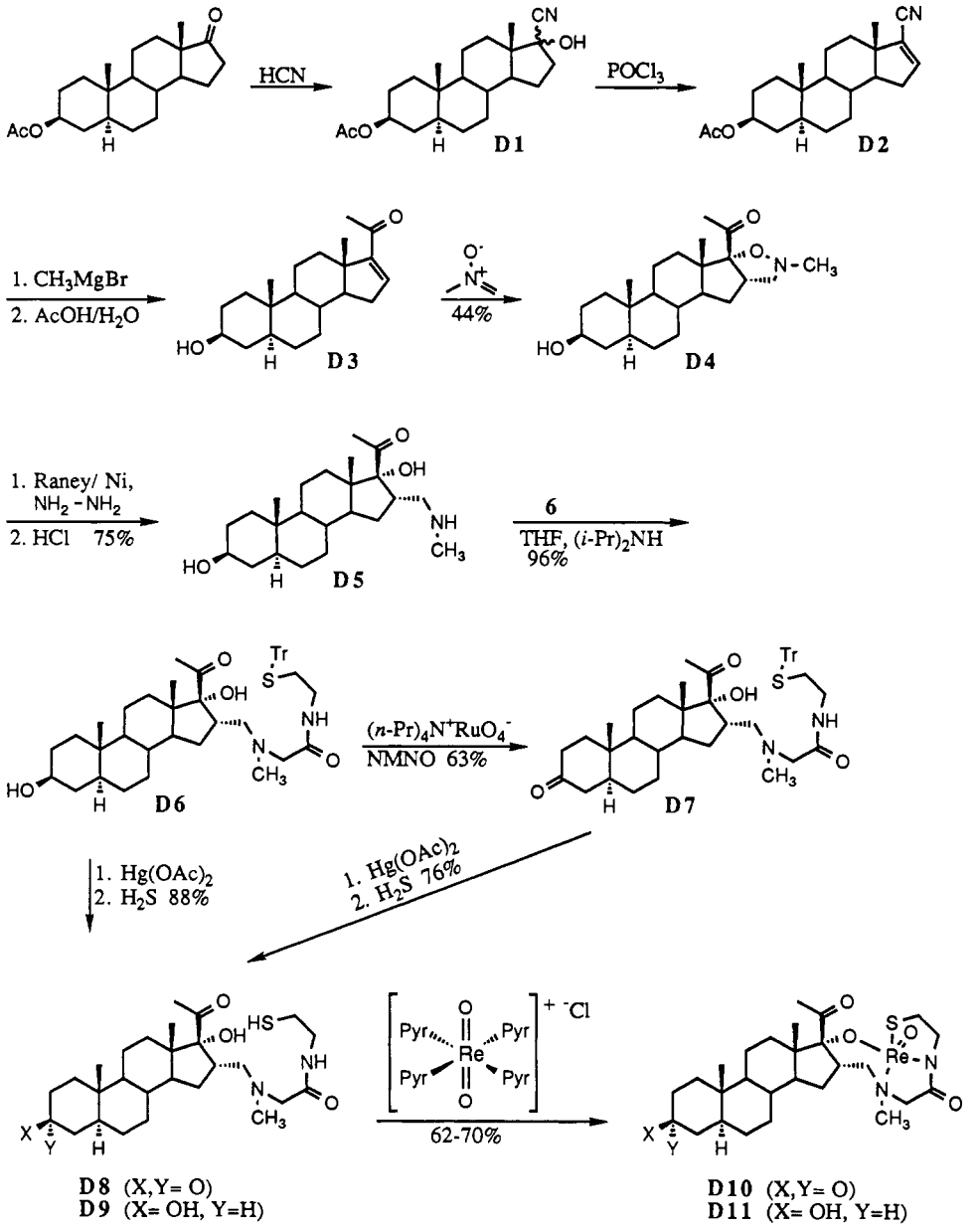


obtained from the reaction; the anti pair was not formed in perceptible yield.

17α-BAT-Substituted Norgestrel. This system is derived from the potent synthetic progestin norgestrel, the homologue of ethynyl nortestosterone. The synthesis of 17α-N_2S_2 Re chelate **B6** is shown in Scheme III. To elaborate the 17α-side chain for attachment of the N_2S_2 chelator, the dianion of 3,3-(ethylenedioxy)norgestrel (**B1**) was treated with paraformaldehyde to form propargylic alcohol **B2**, which was converted into the corresponding mesylate **B3**. Reaction of **B3** with a 2-fold excess of BAT II required rather vigorous conditions (110 °C), producing BAT II–steroid conjugate **B4** in 51% yield, together with several byproducts (dialkylation, disulfide formation, and decomposition). The more reactive propargyl triflate proved to be too unstable and could not be isolated. All of the protecting groups on **B4** were removed, and the ReO core was inserted by the method described for the 21-substituted series. A syn and anti diastereomeric pair were obtained in a 4/1 ratio, respectively. Although the syn pair was separated from anti pair, neither pair could be separated into its individual diastereomers.

11β-BAT-Substituted Progestin. This system is related to the antiprogestin RU486 (RU 38486, mefipristone), and our route to the steroidal framework, shown in Scheme IV, is based on the strategy developed by Roussel Uclaf (*26*). The crystalline diene-3-one **C4** was prepared in gram quantities in 56% overall yield from estradiol 3-methyl ether, by Birch reduction (*18*), decomposition of the resulting enol ether (*18*), and then bromination–debromination (*19*). Double bond migration to the 5,10- and 9,11-positions through ketalization (**C5**) prepared the system for selective epoxidation using H_2O_2 and hexafluoroacetone. This afforded 5α,10α-epoxide **C6** and 5β,-10β-epoxide **C7** in a 4.15/1 ratio, respectively, as determined by NMR analysis. Although facial selectivity was improved by the use of iron phthalocyanine–*N*-methylmorpholine *N*-oxide as the epoxidizing reagent (*27*), it was more than offset by a loss in regioselectivity. A 6/1 α/β-mixture of **C6** was achieved after a single purification of the H_2O_2 reaction product; further purification was unnecessary since complete separation of isomers was readily achieved after the next reaction. Copper-catalyzed addition of the functionalized phenyl Grignard reagent to the allylic epoxide system proceeded in an anti-S_N2' sense, directing the aryl group to the 11β-position. The 11β-aryl product (**C8**) was identified by a characteristic high-field resonance of the C-18 methyl group (^{1}H NMR δ 0.35), due to shielding by the aromatic ring. The 17α-propyne moiety was introduced by oxidation of **C8** to the 17-ketone (**C9**) followed by addition of 1-propynyllithium. Tetrapropylammonium perruthenate–*N*-methylmorpholine *N*-oxide proved to be an excellent oxidant, as it is compatible with acid-sensitive protecting groups; PDC was slower and less efficient (80%). Treatment of **C10** with acetic acid deprotected the benzyl alcohol and 3-keto moieties and

Scheme V



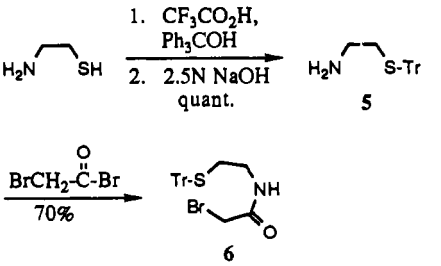
D8 (X,Y= O)
D9 (X= OH, Y=H)

D10 (X,Y= O)
D11 (X= OH, Y=H)

dehydrated the A-ring to form dienone **C11**, which was then converted to the mesylate **C12**. Reaction between benzyl mesylate **C12** and a 2-fold excess of BAT II required elevated temperature. The resulting BAT II–steroid conjugate **C13** was S-deprotected, and the ReO core was inserted by the method described for the 21-substituted series. Syn and anti diastereomeric pairs, obtained in a 15/1 ratio, were separated by column chromatography. The anti pair could be further separated into its individual diastereomers by HPLC, whereas the syn pair was not separable.

16α,17α-Substituted System. The synthesis of the 16α,17α-substituted progestin is shown in Scheme V. 16-Dehydropregnan-3β-ol **D3** was prepared from 3β-acetoxy-5α-androstane-17-one by standard methods: cyanohydrin formation, dehydration and addition of methyl Grignard reagent (*20*). The 16α,17α-functionality, ultimately used to generate the rhenium-chelating system, was introduced by a 1,3-dipolar cycloaddition of *N*-methylmethyliminium *N*-oxide on 3β-hydroxy-16-dehydro-5α-pregnan-20-one (**D3**) to produce isoxazolidine **D4** in 44% yield. Scission of the N–O bond in **D4** by treatment with Raney nickel in excess hydrazine was followed by treatment with

Scheme VI



1 N HCl to hydrolyze the resulting 20-hydrazone. The final two heteroatoms of the chelator were added to the steroidal amino alcohol **D5** by alkylation with bromoamide **6** (obtained by acylation of 2-[(triphenylmethyl)-thio]ethylamine (**5**) with bromoacetyl bromide, Scheme VI) to give protected chelator **D6**. Oxidation at C-3 with tetrapropylammonium perruthenate–*N*-methylmorpholine *N*-oxide gave the corresponding 3-keto system **D7**. S-Deprotection of **D6** and **D7** was accomplished by treatment with mercuric acetate, followed by protonation of the resulting steroidal mercury salt with hydrogen

Table I. Binding Affinity of Progesterone Systems for the Progesterone Receptor[a]

compound	% RBA[b]	compound	% RBA[b]
R5020	645		
	C-21 Series		
progesterone	100	21-[(methylsulfonyl)oxy]-progesterone	3[c]
21-chloroprogesterone	11[c]	**A4syn1,2** (Re chelate)	0.03
	17α-Series		
norgestrel	426	**B6anti1,2** (Re chelate)	1.8
B6syn1,2 (Re chelate)	0.06		
	11β-Series		
C11 (benzyl alcohol)	97	**C15syn1,2** (Re chelate)	161
C12 (benzyl mesylate)	107	**C15anti1** (Re chelate)	283
C14 (11β-BAT I estradiene)	68	**C15anti2** (Re chelate)	64
	16α,17α-Series		
D8 (3-keto)	0.14	**D10** (3-keto) (Re chelate)	0.10
D9 (3-hydroxy)	0.03	**D11** (3-hydroxy) (Re chelate)	0.05

[a] Relative binding affinities were determined by a competitive radiometric binding assay, using uterine cytosol from estrogen-primed immature rats as a source of receptor, tritium-labeled R5020 as tracer, and charcoal dextran as adsorbant of free tracer, as described previously (*28*). [b] RBA = relative binding affinity. Association constant as a percent of the affinity of progesterone. Although R5020 was used as the tracer, binding affinities are expressed relative to the affinity of progesterone. [c] Katzenellenbogen, unpublished.

sulfide, to afford the N_2OS steroid chelators **D8** and **D9**. We tried to affect ReO insertion through the use of oxotrichlorobis(triphenylphosphine)rhenium(V), but the reagent was not reactive enough for this system. However, ligand exchange did occur when **D8** and **D9** were treated with dioxo(tetrapyridine)rhenium(V) chloride in refluxing THF; the 16α,17α-N_2OS Re chelates **D10** and **D11** were formed in 62% and 70% yield, respectively. In each case, only one of the four possible diastereomers of the 16α,17α-N_2OS Re chelates was isolated; the other diastereomers appear not to form in perceptible yield. We do not know which diastereomer we have obtained.

Attempts to place an N_2S_2 chelate system off the 16α,17α-position were unsuccessful. We were successful in forming [16α,17α-*c*]pyrazoline-fused progesterone by a 1,3-dipolar cycloaddition of diazomethane to Δ^{16}-progesterone, but subsequent reduction using a variety of methods was unsuccessful due to decomposition and the reoxidation of potentially useful reaction products.

Receptor Binding Affinity. The binding affinity of the oxo–rhenium complexes and a number of precursors for the progesterone system are listed in Table I. These values were determined through a competitive radiometric binding assay using estrogen-primed rat uterine cytosol as a source of receptor, tritium-labeled R5020 as tracer, and dextran-coated charcoal as adsorbent for free tracer; the experimental details have been published elsewhere (*28*). None of the 21-, 17α-, and 16α,17α-analogues we developed display a binding affinity that warrants further study. The progesterone receptor does not tolerate the amount and/or type of bulk added to these areas. One observation of note in the 17α-steroid–chelates is that although their binding affinity is low, the anti diastereomeric pair binds noticeably better than the syn pair.

The 11β-analogues, on the other hand, display remarkably high binding affinity for the progesterone receptor. The high relative binding affinity of the 11β-N_2S_2 Re chelates (**C15**) demonstrates that a bulky metal chelate can be incorporated into a steroid with retention of very favorable receptor binding. In fact, chelates **C15anti1** and **C15syn1,2** have an affinity for the progesterone receptor that is greater than that of the two benzyloxy precursors **C11** and **C12**. One of the anti diastereomers and the syn pair have affinities that actually exceed that of progesterone. This could mean that the added lipophilic bulk is stabilizing the binding interaction or that one or more of the heteroatoms on the chelate is involved in some type of hydrogen bonding or polar interaction with the receptor.

The chelator 11β-BAT I estradiene (without ReO) has a binding affinity less than two of the three 11β-Re chelates and equal to the third. So, it seems that reducing the conformational space of the BAT system through metal chelation has a beneficial effect on binding. Since the Re chelates only decompose about 6% per hour in the rat uterine cytosol preparations used in the binding affinity measurements (*22*), these results point out that the binding we measure is not that of the regenerated chelators. In fact, we proved conclusively, through the use of ^{186}Re radiolabeling, that the 11β-N_2S_2 Re chelates were indeed binding (with the N_2S_2 oxorhenium system intact) to the progesterone receptor (*22*).

The syn diastereomeric pair of **C15** has a binding affinity that is about the average of the two anti diastereomers, but because the syn pair was inseparable by HPLC, we have no first hand information on the individual diastereomers. It is interesting that **C15anti1** and **C15anti2** show a significant (4.5-fold) difference in binding affinity; this means that even in these bulky systems, subtle changes in structure can have a noticeable effect on binding interactions. Modifications in the chelate structure such as deleting the *gem*-dimethyl groups or adding oxo functions (to make the molecule less lipophilic) might further increase the relative binding affinity of these steroid–chelates and could also serve to lessen their nonspecific binding. Extending the linker chain between steroid and chelator should also affect the binding in some way.

DISCUSSION

We have prepared the first steroid conjugates of an N_2S_2 or N_2OS metal-chelate system and formed their corresponding oxo–rhenium complexes. We chose to prepare these complexes in the progestin system because the progesterone receptor is known to bind a number of hormone analogues bearing other large substituents (*11–14*, *29*), and we patterned the design of these conjugates to place the bulky metal chelate at these sites. Nevertheless, the metal complex is far more bulky than the substituents in the previously known sysetms, so it is not surprising that in three of the four series, the oxo–rhenium complexes had low affinity for the receptor. The 11β-substituted system, patterned after the antiprogestin RU486, furnished three species, two are pure diastereomers (both anti) and the third a mixture (syn) as yet inseparable. The one pure diastereomer and the mixture had remarkably high affinity for the progesterone receptor, exceeding that of progesterone itself.

There has been relatively little work done on the synthesis of steroid hormone analogues labeled with metals. The most extensive investigations are those of Jaouen and Vessieres, who have prepared arene–chromium tricarbonyl and ferrocenyl complexes of estradiol derivatives (*30*) and the antiprogestin RU486 (*31*) and complexes of ethynyl steroids with $Mo_2Cp_2(CO)_4$ and $Co_2(CO)_6$ (*31*). Several of these metal complexes retain high receptor

binding affinity, and they have been used as receptor tracers in conjunction with FT-IR. Nevertheless, it appears that it would be difficult to prepare these compounds labeled with a metal radioisotope, at high specific activity. There are two brief reports of neuroreceptor ligands labeled with technetium-99m. Ballinger (*32*) prepared a technetium tris(dithiocarbamate) derivative of spiperone. Not surprisingly, this bulky trimer showed negligible affinity for the dopamine D2 receptor. More recently Lever (*33*) has prepared a technetium–N_2S_2 analogue of quinuclidinyl benzylate (QNB), where the metal complex replaces the benzylate portion. The affinity of this conjugate ligand for the muscarinic acetyl choline receptor is in the micromolar range, compared to the nanomolar affinity of QNB itself; the extent of nonspecific binding is also very great.

While the high receptor binding affinity of rhenium complex **C15** that we have prepared is encouraging and is a prerequisite for further development of these and similar systems as in vivo diagnostic imaging agents for progesterone-receptor-positive breast tumors, one must not lose sight of other critical issues in this development. First, their preparation must be adapted to synthesis at the tracer level, either with radioisotopes of rhenium or with technetium-99m. In general, it has proved more difficult to prepare rhenium than technetium complexes, but tracer-scale syntheses of related compounds have been achieved with both metals. More uncertain, however, is how these complex steroid derivatives will behave in terms of their nonreceptor interactions; that is, will they undergo adsorption, distribution, cell uptake, and metabolism in a manner and at rates that will enable them to be useful as in vivo imaging agents. We have found with other steroid diagnostics that the extent of nonreceptor, nonspecific binding (*1*, *7b*) and the timely clearance of activity levels from nontarget areas (*7b*) can be critical in obtaining adequate target to nontarget contrast for imaging. The behavior of these bulky sterol metal conjugates in this regard is totally unknown.

ACKNOWLEDGMENT

We are grateful for support of this research through grants from the Department of Energy (DOE DE FG02 86ER60401, to J.A.K.) and (DOE DE FG02 86ER60460, partial support to A.D.). Preliminary experiments on systems related to the progestin complex **D10** were performed by Reinhard J. Ambros, and Aimee Reed provided skillful assistance.

LITERATURE CITED

(1) (a) Katzenellenbogen, J. A., Heiman, D. F., Senderoff, S. G., McElvany, K. D., Landvatter, S. W., Carlson, K. E., Goswami, R., and Lloyd, J. E. (1982) Estrogen Receptor-Based Agents for Imaging Breast Tumors: Binding Selectivity as a Basis for Design and Optimization. In *Applications of Nuclear and Radiochemistry* (N. Morcos, and R. M. Lambrecht, Eds.) pp 311–323, Pergamon Press, New York. (b) Katzenellenbogen, J. A., Heiman, D. F., Carlson, K. E., and Lloyd, J. E. (1982) *In Vivo* and *In Vitro* Steroid Receptor Assays in the Design of Estrogen Pharmaceuticals in *Receptor Binding Radiotracers* (W. C. Eckelman, Ed.) Vol. 1, Chapter 6, pp 93–126, CRC Press, Boca Raton, FL. (c) Katzenellenbogen, J. A. The Pharmacology of Steroid Radiopharmaceuticals: Specific and Non-Specific Binding and Uptake Selectivity. In *The Chemistry and Pharmacology of Radiopharmaceuticals* (A. Nunn, Ed.) in press, M. Dekker, New York. (d) Brandes, S. J., and Katzenellenbogen, J. A. (1988) Fundamental Considerations in the Design of Fluorine-18 Labeled Progestins and Androgens as Imaging Agents for Receptor-Positive Tumors of the Breast and Prostate. *Nucl Med. Biol. (Int. J. Radiat. Appl. Instrum., Part B) 15*, 53–67.

(2) (a) Muenze, R. and Berger, R. (1987) Technetium Generators and Kits. *Radiochim. Acta 41* (2–3), 97–101. (b) Boyd, R. E. (1987) Technetium Generators: Status and Prospects. *Radiochim. Acta 41* (2–3), 59–63.

(3) (a) Kung, H. F., Guo, Y. Z., Chi, C., Billings, J., Subramanyam, V., and Calabrese, J. C. (1989) New Brain Perfusion Imaging Agents Based on Technetium-99m Bis(aminoethanethiol) Complexes: Stereoisomers and Biodistribution. *J. Med. Chem. 32* (2), 433–437. (b) Baidoo, K. E., and Lever, S. Z. (1990) Synthesis of a Diamine Dithiol Bifunctional Chelating Agent for Incorporation of Technetium-99m into Biomolecules. *Bioconjugate Chem. 1* (2), 132–137. (c) Epps, L. A., Burns, H. D., Lever, S. Z., Goldfarb, H. W., and Wagner, H. N., Jr. (1987) Brain Imaging Agents: Synthesis and Characterization of (N-Piperidinylethyl) Hexamethyl Diaminodithiolate Oxo Technetium(V) Complexes. *Appl. Radiat. Isot. 38* (8), 661–664. (d) Cheesman, E. H., Blanchette, M. A., Ganey, M. V., Mejeu, L. J., Miller, S. J., and Watson, A. D. (1988) Technetium-99m ECD: Ester-Derivatized Diamine-Dithiol Tc Complexes for Imaging Brain Perfusion. *J. Nucl. Med. 29*, 788.

(4) Bryson, N., Dewan, J. C., Lister-James, J., Jones, A., and Davison, A. (1988) Neutral Technetium(V) Complexes with Amide–Thiol–Thioether Chelating Ligands. *Inorg. Chem. 27*, 2154–2161.

(5) Troutner, D. E., Volkert, W. A., Hoffman, T. J., and Holmes, R. A. (1984) A Neutral Lipophilic Complex of ^{99m}Tc with a Mutidentate Amine Oxime. *Int. J. Appl. Radiat. Isot. 35* (6), 467–470.

(6) Narra, R. K., Nunn, A. D., Kuczynski, B. L., Feld, T., Wedeking, P., and Eckelman, W. C. (1989) A Neutral Technetium-99m Complex for Myocardial Imaging. *J. Nucl. Med. 30* (11), 1830–1837.

(7) (a) Kiesewetter, D. O., Kilbourn, M. R., Landvatter, S. W., Heiman, D. F., and Katzenellenbogen, J. A., Welch, M. J. (1984) Preparation of Four Fluorine-18 Labeled Estrogens and their Selective Uptake in Target Tissues of Immature Rats. *J. Nucl. Med. 25*, 1212–1221. (b) Pomper, M. G., VanBrocklin, H., Thieme, A. M., Thomas, R. D., Kiesewetter, D. O., Carlson, K. E., Mathias, C. J., Welch, M. J., and Katzenellenbogen, J. A. (1990) Methoxy-, 11β-Ethyl-, and 17α-Ethynyl-substituted 16α-Fluoroestradiols: Receptor-Based Imaging Agents with Enhanced Uptake Efficiency and Selectivity. *J. Med. Chem. 33*, 3143–3155.

(8) (a) Katzenellenbogen, J. A., Senderoff, S. G., McElvany, K. D., O'Brien, H. A., Jr., and Welch, M. J. (1981) [^{77}Br]-16α-Bromoestradiol-17β: A High Specific-Activity Gamma-Emitting Tracer with Uptake in Rat Uterus and Induced Mammary Tumors. *J. Nucl. Med. 22*, 42–47. (b) Katzenellenbogen, J. A., McElvany, K. D., Senderoff, S. G., Carlson, K. E., Landvatter, S. W., and Welch, M. J. (1982) 16α-[^{77}-Br]-Bromo-11β-methoxyestradiol-17β. A Gamma-Emitting Estrogen Imaging Agent with High Uptake and Retention by Target Organs. *J. Nucl. Med. 23*, 411–419.

(9) (a) McElvany, K. D., Carlson, K. E., Welch, M. J., Senderoff, S. G., and Katzenellenbogen, J. A. (1982) In Vivo Comparison of 16α-[^{77}Br]-Bromoestradiol-17β and 16α-[^{125}I]-Iodoestradiol-17β. *J. Nucl. Med. 23*, 420–424. (b) Hanson, R. N., and Franke, L. A. (1984) Preparation and Evaluation of 17α-[^{125}I]Iodovinyl-11β-methoxyestradiol as a Highly Selective Radioligand for Tissues Containing Estrogen Receptors: Concise Communication. *J. Nucl. Med. 25* (9), 998–1002. (c) Jagoda, E. M., Gibson, R. E., Goodgold, H., Ferreira, N., Francis, B. E., Reba, R. C., Rzeszotarski, W. J., and Eckelman, W. C. (1984) 17α-[I-125]Iodovinyl-11β-methoxyestradiol: In Vivo and In Vitro Properties of a High-Affinity Estrogen-Receptor Radiopharmaceutical. *J. Nucl. Med. 25* (4), 472–477. (d) Hochberg, R. B., Hoyte, R. M., Rosner, W. (1985) *E*-17α-(2-[^{125}I]iodovinyl)-19-nortestosterone: The Synthesis of a Gamma-Emitting Ligand for the Progesterone Receptor. *Endocrinology (Baltimore) 117* (6), 2550–2552.

(10) (a) Katzenellenbogen, J. A., Carlson, K. E., Heiman, D. F., and Goswami, R. (1980) Receptor-Binding Radiopharmaceuticals for Imaging Breast Tumors: Estrogen Receptor Inter-

actions and Selectivity of Tissue Uptake of Halogenated Estrogen Analogs. *J. Nucl. Med. 21*, 550–558. (b) Heiman, D. F., Senderoff, S. G., Katzenellenbogen, J. A., and Neeley, R. J. (1980) Estrogen Receptor-Based Imaging Agents. 1. Synthesis and Receptor Binding Affinity of Some Aromatic and D-Ring Halogenated Estrogens. *J. Med. Chem. 23*, 994–1002. (c) Goswami, R., Harsy, S. G., Heiman, D. F., and Katzenellenbogen, J. A. (1980) Estrogen Receptor-Based Imaging Agents. 2. The Synthesis and Receptor Binding Affinity of Side-Chain Halogenated Hexestrol Derivatives. *J. Med. Chem. 23*, 1002–1008. (d) Fevig, T. L., Mao, M. K., and Katzenellenbogen, J. A. (1988) Estrogen Receptor Binding Tolerance of 16α-Substituted Estradiol Derivatives. *Steroids 51* 471–497.

(11) (a) Djerassi, C., and Konopelski, J. P. (1980) Synthesis and Biochemical Screening of Phenylselenium-Substituted Steroid Hormones. *J. Med. Chem. 23*, 722–726. (b) Surcouf, E., Lepicard, G., Mornon, J. P., Ojasoo, T., Raynaud, J. P. (1983) Additional Conformational Data for the Mapping of the Progesterone Binding Site: Crystal Structures of 21-(Phenylseleno)-progesterone and 17α-(Phenylseleno)progesterone. *J. Med. Chem. 26*, 1320–1323.

(12) (a) Salman, M., Stotter, P. L., and Chamness, G. (1989) Iodine-125-labeled Ligand for the Progesterone Receptor: 17α-(6′-iodohex-1′-ynyl)-19-nortestosterone. *J. Steroid Biochem. 33* (1), 25–31. (b) Salman, M., Ruiz, A., Stotter, P. L., and Chamness, G. (1987) A Progesterone Receptor Affinity-Chromatography Reagent: 17-Hexynylnortestosterone-Sepharose. *J. Steroid Biochem. 26* (3), 283–291.

(13) Fried, J., Sabo, E. F., Grabowich, P., Lerner, L. J., Kessler, W. B., Brennan, D. M., and Borman, A. (1961) Progestationally Active Acetals and Ketals of 16α,17α-Dihydroxyprogesterone. *Chem. Ind.* 465–466.

(14) (a) Carlson, K. E., Coppey, M., Magdelenat, H., and Katzenellenbogen, J. A. (1989) Receptor Binding of NBD-Labeled Fluorescent Estrogens and Progestins in Whole Cells and Cell-Free Preparations. *J. Steroid Biochem. 32*, 345–355. (b) Belanger, A., Philibert, D., and Teutsch, G. (1981) Regio and Stereospecific Synthesis of 11β-Substituted 19-Norsteroids: Influence of 11β-Substitution on Progesterone Receptor Affinity. *Steroids 37* (4), 361–382.

(15) Still, W. C., Kahn, M., and Mitra, A. (1978) Rapid Chromatographic Technique for Preparative Separations with Moderate Resolution. *J. Org. Chem. 43*, 2923–2925.

(16) D'Amico, J. J., and Dahl, W. E. (1975) Novel Synthesis of Aminoethanethiols. *J. Org. Chem. 40* (9), 1224–1227.

(17) Corbin, J. L., and Work, D. E. (1976) 1-Alkyl- (or aryl-) amino-2-methylpropane-2-thiols. Some Bi- and Tetradentate Nitrogen-Sulfur Ligands from Schiff's Base Disulfides. *J. Org. Chem.* 41 (3), 489–491.

(18) Wilds, A. L., and Nelson, N. A. (1953) The Facile Synthesis of 19-Nortestosterone and 19-Norandrostenedione from Estrone. *J. Am. Chem. Soc. 75*, 5366–5369.

(19) Perelman, M., Farkas, E., Forefeld, E. J., Kraal, R. J., and Rapala, R. T. (1960) A New Class of Active Steroids: The 19-Nor-$\Delta^{4,9}$-3-ketosteroids. *J. Am. Chem. Soc. 82*, 2402–2403.

(20) Garraffo, H. M., and Gros, E. G. (1982) Synthesis of [20-^{14}C]-3β-Hydroxy-5β-pregnan-20-one. *J. Labelled Compd. Radiopharm. 19* (1), 149–150.

(21) Mahmood, A., Baidoo, K. E., and Lever, S. Z. (1990) Stereoisomers of Neutral Oxotechnetium(V) and Oxorhenium-(V) Complexes. *Technetium in Chemistry and Nuclear Medicine* (M. Nicolini, G. Bandoli, and U. Mazzi, Eds.) Vol. 3, pp 119–124, Cortina International, Verona.

(22) DiZio, J. P., Anderson, C. J., Davison, A., Ehrhardt, G. J., Welch, M. J., and Katzenellenbogen, J. A. Technetium and Rhenium Labeled Progestins: Synthesis, Receptor Binding and In Vivo Distribution of an 11β-substituted Progestin Labeled with Technetium-99 and -99m and Rhenium-186, in preparation.

(23) Chang, G., Guida, W. C., and Still, W. C. (1989) An Internal Coordinate Monte Carlo Method for Searching Conformational Space. *J. Am. Chem. Soc. 111*, 4379–4386.

(24) Hiskey, R. G., Tomishige, M., and Igeta, H. (1966) Sulfur-Containing Polypeptides. II. Selective Removal of S-Protective Groups from Some L-Cysteinyl-L-cysteine Derivatives. *J. Org. Chem. 31*, 1188–1192.

(25) Parshall, G. W., Shive, L. W., and Cotton, F. A. (1977) Phosphine Complexes of Rhenium: Trichlorooxobis(triphenylphosphine)-Rhenium(V). *Inorg. Syn. 17*, 110–111.

(26) (a) Teutsch, G., and Belanger, A. (1979) Regio and Stereospecific Synthesis of 11β-Substituted 19-Norsteroids. *Tetrahedron Lett. 22*, 2051–2054. (b) Teutsch, G., Belanger, A., Philibert, D., and Tournemine, C. (1982) Synthesis of 11-Vinyl-19-Norsteroids as Potent Progestins. *Steroids 39* (6), 607–615. (c) Ottow, E., Beier, S., Elger, W., Henderson, D., Neef, G., and Weichert, R. (1984) Synthesis of Ent-17-(Prop-1-ynyl-17β-Hydroxy-11β-(4-*N,N*-dimethylamino))-Phenyl)-4,9-Estradien-3-one, The Antipode of RU-38486. *Steroids 44* (6), 519–530. (d) Neef, G. (1986) Anti-Progestins—A New Approach to Contraception. *Trends in Medicinal Chemistry, Proceedings of the Ninth International Symposium on Medicinal Chemistry, Berlin 1986* (E. Mutschler, and E. Winterfeldt, Ed.) pp 565–579, VCH, Berlin.

(27) Rhode, R., Neef, G., Sauer, G., and Wiechert, R. (1985) Stereoselective Epoxidation of 5(10), 9(11)-estradienes. *Tetrahedron Lett. 26* (17), 2069–2072.

(28) Brandes, S. J., and Katzenellenbogen, J. A. (1987) Fluorinated Androgens and Progestins: Molecular Probes for Androgen and Progesterone Receptors with Potential Use in Positron Emission Tomography. *Mol. Pharmacol. 32*, 391–403.

(29) Raynaud, J. P., and Ojasoo, T. (1986) Receptor Binding as a Tool in the Development of Selective New Bioactive Steroids and Nonsteroids. *Innovative Approaches in Drug Research* (A. F. Harms, Ed.) pp 47–72, Elsevier Science Publishers B. V., Amsterdam.

(30) (a) Vessieres, A., Top, S., Ismail, A. A., Butler, I. S., Louer, M., and Jaouen, G. (1988) Organometallic Estrogens: Synthesis, Interaction with Lamb Uterine Estrogen Receptor, and Detection by Infrared Spectroscopy. *Biochemistry 27*, 6659–6666. (b) Vessieres, A., Vaillant, C., Groselle, M., Vichard, D., and Jaouen, G. (1990) Affinity Labeling of Estradiol Receptor by Ferrocenyl Tagging of Estradiol 17α-Position. *J. Chem. Soc., Chem. Commun.* 837–839.

(31) Jaouen, G., and Vessieres, A. (1989) The Use of High Affinity Binding Bioligands Modified by Transition Metal Carbonyl Moieties. *Pure Appl. Chem. 61* (3), 565–572.

(32) Ballinger, J. R., Gulenchyn, K. Y., and Hassan, M. N. (1989) Technetium-99m Spiperone Dithiocarbamate: A Potential Radiopharmaceutical for Dopamine Receptor Imaging with SPECT. *Appl. Radiat. Isot. 40* (6), 547–549.

(33) Lever, S. Z., and Wagner, H. N. (1990) The Status and Future of Technetium-99m Radiopharmaceuticals. *Technetium* and Rhenium in Chemistry and Nuclear Medicine (M. Nicolini, G. Bandoli, and V. Mazzi, Eds.) Vol. 3, pp 648–659, Cortina International, Verona.

Reversed-Phase High-Pressure Liquid Chromatographic Tryptic Peptide Mapping for the Comparison and Study of Monoclonal Antibodies

Geoffrey F. Lee† and D. C. Anderson*

Biochemistry Department, NeoRx Corporation, Seattle, Washington 98119. Received February 4, 1991

We have examined and optimized several parameters to generate efficient, high-resolution, high-information tryptic peptide maps of monoclonal antibodies and their Fab fragments, without separating the H and L chains, using reversed-phase high-pressure liquid chromatography. Use of a high protease-to-substrate ratio with optimized digestion time and HPLC gradient conditions led to a reproducible mapping of the reduced, carboxymethylated Fab fragments of two antibodies. The technique was then used to screen Fab lots for batch-to-batch consistency, and for examining the effect of 10 mM cysteine on papain cleavage of whole antibody. The technique was modified by labeling cysteine with chromophoric analogues of iodoacetamide instead of radiolabeled iodoacetamide, resulting in a three-dimensional peptide map. With multiwavelength detection, this consisted of simultaneous observation of all chromophores at 214 nm, those with aromatic residues at 280 nm, and those with cysteine at 422 nm, without collecting and counting each peak to identify cysteine-containing peptides.

INTRODUCTION

Proteins and protein conjugates produced for use in human pharmaceutical products are closely scrutinized by the United States Food and Drug Administration to meet stringent quality control criteria, including lot-to-lot consistency. Many laboratories use peptide mapping on reversed-phase high-pressure liquid chromatography (RP-HPLC) columns as a key analytical tool to characterize the primary structure of their protein products (*1–5*) and to thereby determine primary structural consistency in serially produced lots. The use of peptide mapping of recombinant tissue plasminogen activator (rt-PA) has been published (*1*, *2*), and it is increasingly evident that peptide mapping is becoming a standard test for guaranteeing primary structure consistency (*6*). A single amino acid difference in an rt-PA variant was identified by tryptic mapping (*2*), and Chloupek and colleagues have identified glycosylated and cysteine-containing peptides of rt-PA using this technique (*1*). This method should be applicable to a similar analysis of purified, defined conjugates constructed with proteolytically inert moieties such as drugs or carbohydrate carriers attached to the protein.

Monoclonal antibodies (mAbs) and their conjugates are of significant interest in biotechnology for use as imaging and therapeutic agents. Many companies have products in development which use mAbs for the screening and treatment of cancer, toxic shock, graft versus host disease, and cardiovascular illnesses. These complex glycoproteins and their fragments need to be examined for constancy of primary structure. We report here on the development of high-resolution RP-HPLC tryptic peptide mapping for the analysis of proteolytically derived Fab fragments from two monoclonal antibodies and additional mapping studies on one of the precursor whole antibodies. The effects of digestion time and protease-to-substrate ratio, as well as the effect of HPLC gradient slope on map resolution were investigated. We also report on studies of the reproducibility of the mapping assay, and on the lot-to-lot comparison of Fab fragments produced by papain digestion in the presence or absence of cysteine as a reducing agent. Results from this experiment are relevant to explaining the effect of cysteine in enhancing the yield of papain-mediated production of Fab fragments. To avoid the process of radiolabeling cysteine with reagents such as iodoacetic acid, which requires the collection and counting of individual peaks from the peptide map, cysteine-containing peptides were identified with a chromophoric labeling reagent.

EXPERIMENTAL PROCEDURES

Antibodies and Reagents. Two IgG2b antibodies with melanoma (*7*) and pancarcinoma (*8*) reactivities (designated NRML-05 and NRLU-10, respectively) were used. Fab fragments of these antibodies were generated by using immobilized papain on agarose beads (*9*). Each antibody and Fab fragment was purified by ion-exchange chromatography to a single peak. For lots that had been frozen, their purity was checked on the analytical scale by anion-exchange HPLC on a Synchrom strong-anion-exchange column; each Fab fragment and whole antibody used here gave a single peak under isocratic elution conditions.

Iodoacetic acid (IAA), tris(hydroxymethyl)aminomethane (Tris) buffer, and calcium chloride ($CaCl_2$) were purchased from Sigma Chemical Co. (St. Louis, MO). Hydrochloric acid was from J. T. Baker (Phillipsburg, NJ). Urea was from EM Sciences (Cherry Hill, NJ), and 2-mercaptoethanol (electrophoresis grade) was from Bio-Rad Laboratories (Richmond, CA). Lucifer yellow iodoacetamide (LYIA) was from Molecular Probes, Inc. (Eugene, OR). HPLC-grade water and acetonitrile were from Burdick & Jackson (Muskegon, MI) or J. T. Baker. HPLC-grade trifluoroacetic acid (TFA) was from Pierce Chemical Co. (Rockford, IL). [^{14}C]Iodoacetate (1.25 mg, 50 μCi) was from ICN (Irvine, CA).

Equipment. A Hewlett-Packard (Palo Alto, CA) HP-1090M chromatography system, equipped with column oven, diode-array detector, and autosampler, was used for mapping digests. Vydac 4.1 × 250 mm C_{18} reversed-phase columns (300 Å pores, 5 μm particles) and C_{18} guard column cartridges obtained from Alltech Associates (Deerfield, IL) were used. A Varian DMS 100 dual-beam spectro-

* Author to whom correspondence should be addressed: Somatogen Inc., 5797 Central Ave., Boulder, CO 80301.

† Current address: Department of Biochemistry and Biophysics, Washington State University, Pullman, WA 99164.

1043-1802/91/2902-0367$02.50/0 © 1991 American Chemical Society

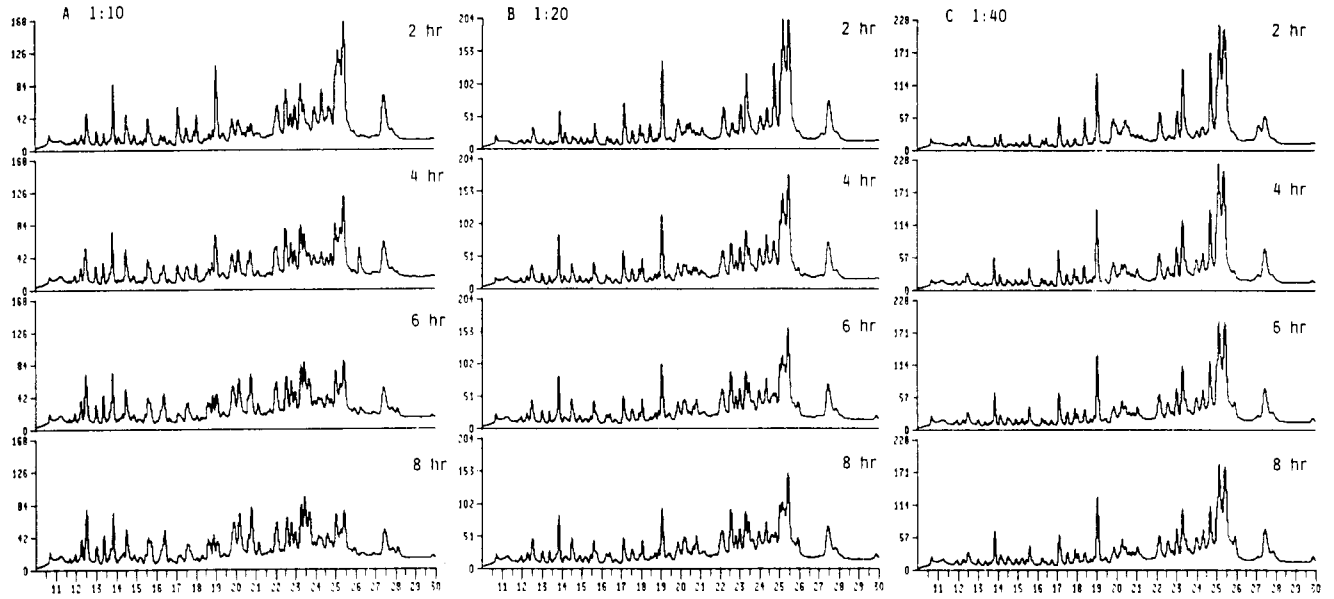


Figure 1. Peptide maps showing optimization of digestion time and protease to substrate ratio using NRML-05 Fab. S-carboxymethylation used iodoacetate. The eluting gradient was from 100% A (water + 0.05% TFA) to 60% B (acetonitrile + 0.05% TFA) from 5 to 35 min. The flow rate was 1 mL/min and the oven temperature was 40 °C. Twenty-five microliters (0.65 nmol) of antibody was injected. Different columns of the graphs list the different initial protease to substrate ratios: (A) 1:10; (B) 1:20; (C) 1:40. The rows of the graphs list different digestion times: (1) 2, (2) 4, (3) 6, (4) 8 h. The X axis of individual maps gives the retention time in minutes, the Y axis milli absorbance units (mAU) at 214 nm.

photometer was used for protein A_{280} measurements. Integration of HPLC peak areas and calculation of peak retention times was done with standard ChemStation software supplied by Hewlett-Packard. The baselines for the peaks were assigned by using the macro THINKING.G, supplied by Dr. Tom Keel (Hewlett-Packard), which constructed the peak baselines by drawing a straight line from valley to valley of each peak.

Sample Preparation. Reduction of antibody chains and alkylation of cysteines were performed by using modifications of the method of Crestfield et al. (*10*). Antibody (10 mg/mL) in degassed chain-separation buffer [0.1 M Tris, 0.1 or 0.01 M dithiothreitol (DTT), and 6 M urea, pH 8.0] was incubated for 1 h at 60 °C under argon to effect reduction of disulfide bonds. For NRLU-10 whole and Fab antibodies the DTT concentration was 10 mM, whereas for the more stable NRML-05 Fab, 100 mM DTT was used to reduce disulfide bonds. A 2-fold molar thiol excess of alkylating agent (iodoacetate or LYIA) was then added to the reaction, and the mixture was incubated in the dark for another hour at 60 °C with constant stirring. 2-Mercaptoethanol was then added to quench excess alkylating agent. The antibody preparation was then dialyzed, or buffer exchanged by ultrafiltration, into digestion buffer (0.1 M Tris, 10 mM $CaCl_2$, 6 M urea, pH 8.0), and the protein concentration was determined from absorbance measurements at 280 nm. LYIA (97.2% pure by RP-HPLC) alone absorbed strongly at 280 nm, causing overestimation of protein concentration for antibodies treated with these agents. To circumvent this problem, we S-carboxymethylated an additional antibody sample with IAA as a control and assumed that its A_{280} protein concentration was similar to that of the LYIA-labeled samples.

Tryptic Digestion. After chain reduction and alkylation of cysteines, antibodies were diluted to 2 mg/mL in digestion buffer and then digested with trypsin (TPCK-treated, type XIII, Sigma Chemical Co., St. Louis, MO) at 37 °C with constant stirring. The protease-to-substrate ratios used varied by experiment (see the text for details). After 2 h, a second equal-volume aliquot of trypsin was added, and incubation continued at 37 °C. The digestion was terminated by the addition of $^1/_{10}$ volume 1 M HCl.

Peptide Mapping. Peptide digests (25 μL, 0.65 nmol) were separated with water + 0.05% TFA (buffer A) to acetonitrile + 0.05% TFA (buffer B) linear gradients (see text for exact gradients used) at 1 mL/min and 40 °C. The diode-array detector was set to gather absorption signals at 214 and 280 nm in all experiments (detection of peptide bonds and aromatic amino acids, respectively), and also at 422 nm when the chromophoric labeling agent lucifer yellow iodoacetamide was used.

The reproducibility of each peak retention time and area was calculated by using the coefficient of variation (*11*), which was calculated from the standard deviation σ and the mean value from n analyses, X_n, as $(\sigma/X_n) \times 100\%$. This assumed a normal (Gaussian) error distribution.

RESULTS

Optimization of Map Resolution. Effect of Digestion Conditions. Whole antibody and Fab fragments were both analyzed with respect to the effect of digestion time and protease-to-substrate ratio on map resolution. The general protocol involved reduction of antibody chains, S-carboxymethylation of cysteines with iodoacetate, and digestion of antibody chains at 1:10, 1:20, and 1:40 (w/w) initial protease to substrate ratios, followed by sampling of digests at 2, 4, 6, 8, and 24 h and separation of peptides by HPLC on C_{18} columns using gradients of 2% buffer B/min. Figure 1 shows a matrix of mapping results for the Fab fragment of the anti-melanoma antibody, NRML-05. Although the maps changed over time and protease to substrate ratio, there were time periods where the number, position, and height of peaks changed little at a given ratio by visual examination. We defined optimal digestion conditions as being the combination of protease to substrate ratio and time span at which few peaks changed and where the number of peaks was at a maximum. For NRML-05 Fab, this combination was achieved at a 1:10 (w/w) protease to substrate ratio at 6 h (Figure 1).

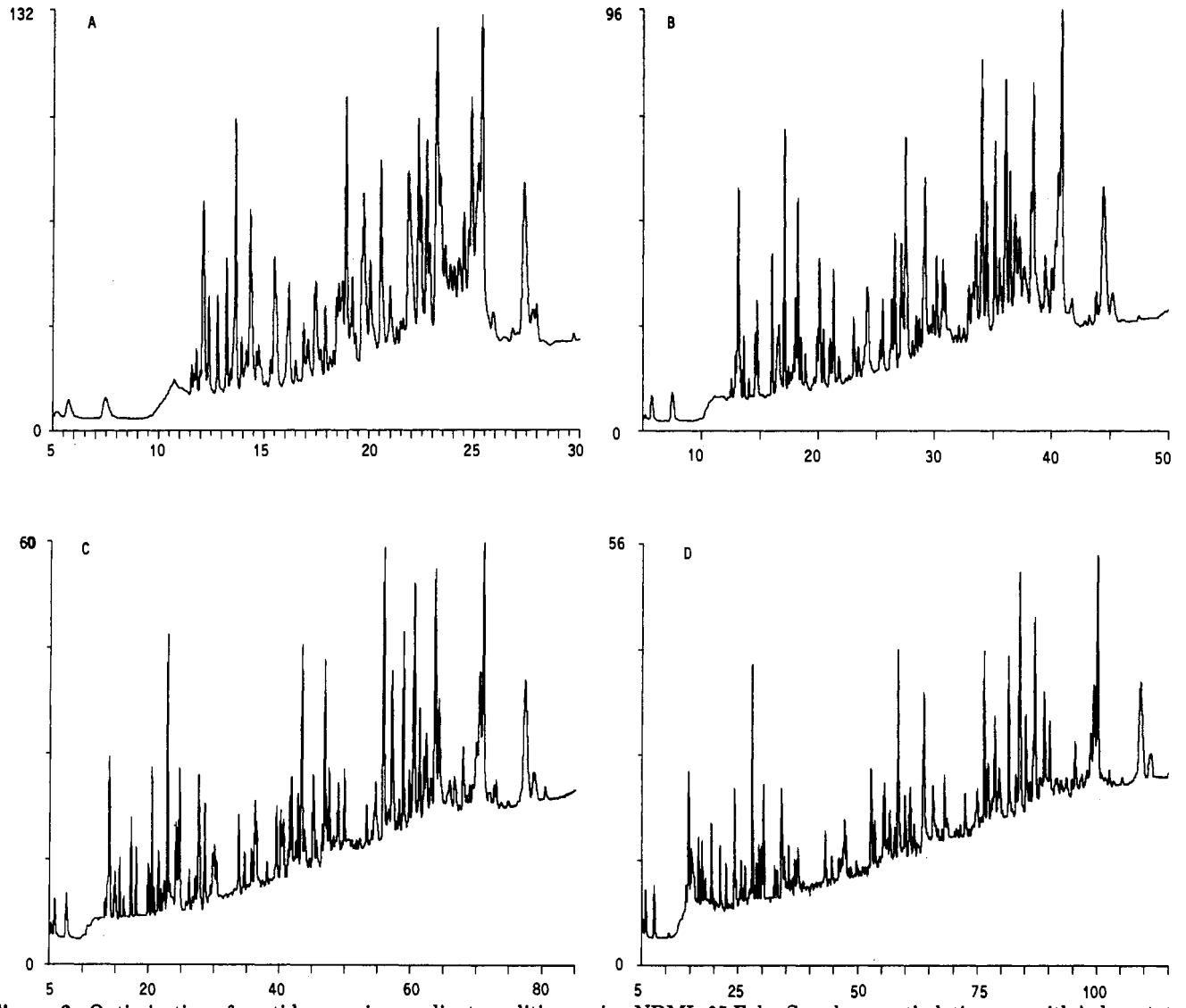


Figure 2. Optimization of peptide mapping gradient conditions using NRML-05 Fab. S-carboxymethylation was with iodoacetate. Digestion was for 6 h at a 1:10 initial protease to substrate ratio, and 25 μL (0.65 nmol) of antibody was injected. The *X* axes of individual maps give retention time in minutes, the Y axes milli absorbance units (mAU) at 214 nm. Gradients were (A) 2.0% B/min over 30 min, (B) 1.0% B/min over 60 min, (C) 0.5% B/min over 120 min, and (D) 0.33% B/min over 180 min. The flow rate was 1 mL/min and the oven temperature was 40 °C.

For NRLU-10, both whole and Fab, digestion at a 1:10 ratio for 5 h produced the best results (data not shown). These data show that trypsin is active on these substrates in 6 M urea at 37 °C.

Due to the high protease to substrate ratio used here, trypsin was checked for autolysis. A trypsin solution was mapped that had been incubated without substrate for 5–6 h at 37 °C in digestion buffer at concentrations duplicating the 1:10 and 1:5 protease to substrate ratios. No additional peaks were generated in the presence of the 10 mM calcium used here.

Effect of HPLC Gradient Slope. Due to the large number of peaks expected, the gradient slope was optimized by running aliquots from a single digest. The digestion was performed at an optimal protease to substrate ratio and optimal time for a limit digest. HPLC gradient slopes which were tested ranged from 0.33 to 2.0% buffer B/min at a flow rate of 1 mL/min and a column temperature of 40 °C. Previous tryptic maps have used gradients as low as 0.22% B/min (*12*). Decreasing gradient slope (and lengthening gradient time) from 2.0 to 0.5% B/min enhanced gradient resolution as measured visually by the number and sharpness of peaks for all tested antibodies. Figure 2 illustrates this effect with NRML-05 Fab antibody fragments. With the highest gradient slope conditions (2%/min), the mapping generated about 66 peaks. Reduction of the gradient slope to 1% B/min increased the number of peaks by 7 to ca. 73, and further reduction of the slope to 0.5% B/min increased the number of peaks to ca. 89. Decreasing the slope to 0.33% B/min, however, did little to improve resolution, although the peaks appeared slightly more dispersed in time.

This pattern of increasing peak number with decreasing gradient slope also occurred in the optimization of NRLU-10 Fab and whole antibody maps (Figure 3). As the slope decreased from 2% to 1% to 0.5% B/min, the number of Fab peaks increased from 53 to 60 to 69, while the number of peaks generated from whole antibody went from 58 to 73 to 89. All of the peaks from each sample were eluted from the column by the time the gradient reached 40% acetonitrile. The optimized HPLC slope was thus determined to be one where buffer B went from 0 to 40% in 80 min after an initial 5 min at 100% buffer A.

Peptide Map Reproducibility and Comparison of Antibody Lots. The reproducibility of our procedure was checked since more peaks than predicted by the

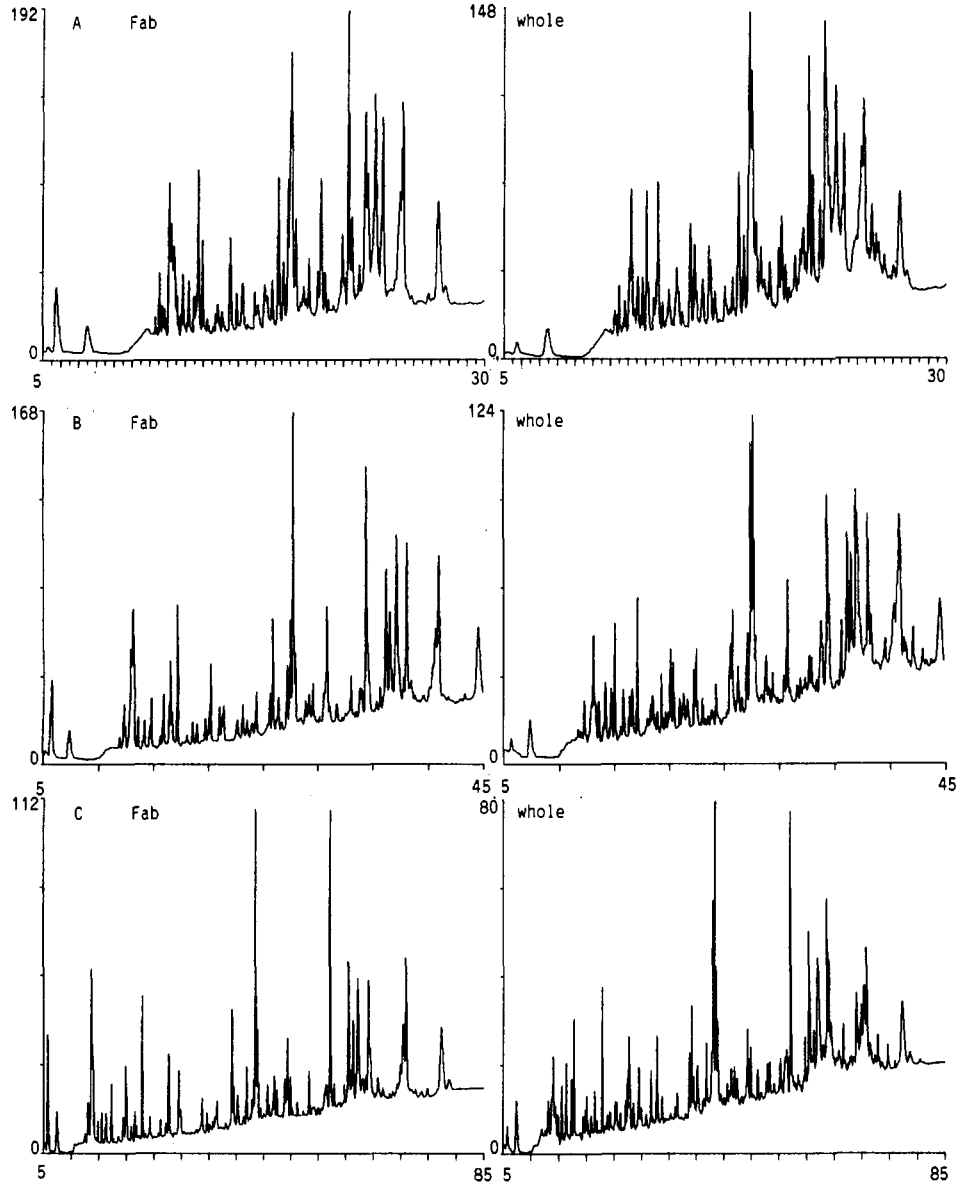


Figure 3. Optimization of peptide mapping gradient conditions using the NRLU-10 whole antibody and Fab fragment. S-carboxymethylation was with iodoacetate, digestion was for 5 h at 1:10 initial protease to substrate ratio and 25 μL (0.65 nmol) of antibody was injected. The *X* axis of individual maps gives retention time in minutes, the *Y* axis milli absorbance units (mAU) at 214 nm. Gradients were (A) 2.0% B/min over 30 min, (B) 1.0% B/min over 60 min, and (C) 0.5% B/min over 120 min. The flow rate was 1 mL/min, and the oven temperature was 40 °C.

consensus (Lys + Arg) content of IgG2b were observed. About 35–37 peaks were expected for the Fab fragments, and about 63–65 were expected for the whole antibodies. These numbers are estimates since the sequences of only the Fv regions of these antibodies are known. Multiple consecutive mapping runs of a single digest under optimized conditions appeared identical with one another at both 214 or 280 nm (data not shown). Two samples from one vial of antibody which were simultaneously digested and mapped also appeared to give visually identical maps.

The reproducibility of the tryptic mapping procedure and of NRLU-10 Fab production was also examined more quantitatively. Under optimized conditions for digestion and mapping, several lots of NRLU-10 Fab were compared. Two of the lots of Fab (E and F, the latter produced by a second manufacturer) were produced by using papain in the absence of cysteine, while four other lots (A–D) were produced by using 10 mM cysteine as a reducing agent. Cysteine has been found in the past to increase the yield of Fab produced from while IgG1 antibodies by preactivating papain (*13*), and we have noticed this effect for these IgG2b antibodies as well (data not shown). Samples of these lots were subjected to the optimized reduction, S-carboxymethylation, digestion, and mapping procedures. The peptide maps of the six lots tested appeared to be very similar at both 214 nm (Figure 4A) and at 280 nm (Figure 4B). In only one case, lot F, was a difference seen: the enhanced appearance of a very small peak eluting at 78 min that was not present to as large an extent in any other sample.

The coefficient of variation was calculated for lots A–F for the retention times and peak areas of the 35 largest peaks observed at 214 nm, approximately the number of peaks expected from the tryptic digest. This coefficient ranged from 0.0051 to 0.23% with an average of 0.037% for retention times of maps from the six lots. For the corresponding peak areas, the coefficient of variation ranged from 2.6 to 20.4% with an average of 10.7%. Thus the peak positions were highly reproducible, while the areas were somewhat less so. This may be due in part to difficulties in reproducibly assigning parameters important

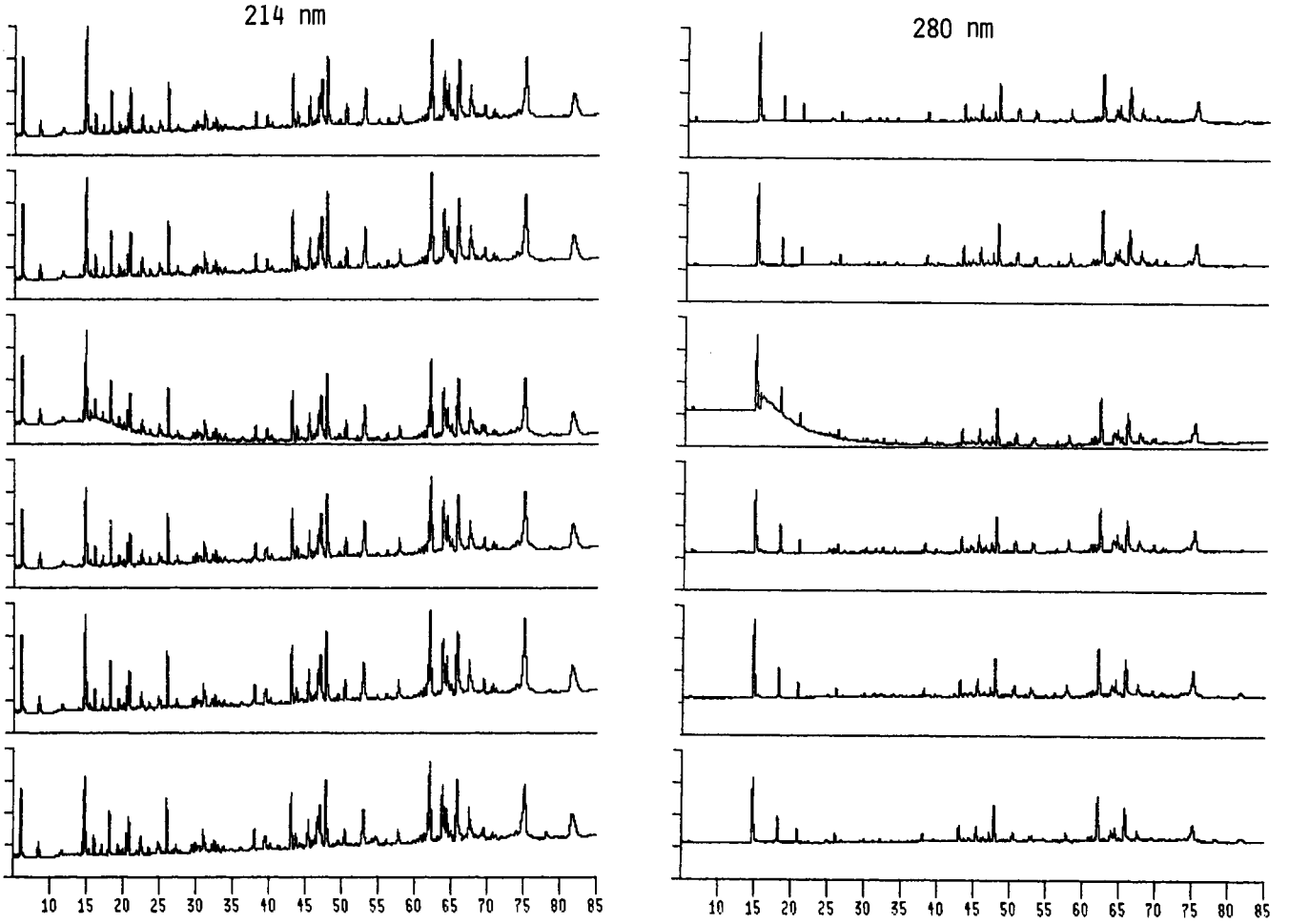


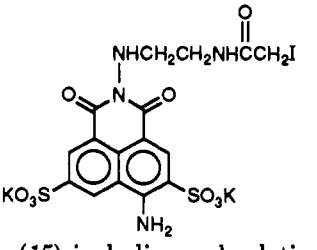
Figure 4. Comparison of peptide maps of six different lots of NRLU-10 Fab. Samples were S-carboxymethylated with iodoacetate and then digested for 5 h at an initial 1:10 protease to substrate ratio. Injections were 25 μL (0.65 nmol) of antibody, the gradient was 0.5% B/min over 80 min, and the flow rate was 1 mL/min at 40 °C. The *X* axis gives retention time in minutes, the *Y* axis milli absorbance units (mAU) at 214 nm (left) or at 280 nm (right). Rows 1 and 2 have lots A–F listed from top to bottom.

for integration of the HPLC chromatogram such as the baseline for each peak.

The coefficient of variation in the retention times and areas was also calculated for lots A–D. For peak retention times and areas, this coefficient ranged from 0.0040 to 0.28% with an average of 0.044%, and from 2.40 to 29.0% with an average value of 10.8%, respectively. On the basis of the similarities of the average values for the coefficients of variation for lots A–F vs lots A–D as well as the visual similarities of the tryptic maps, there appears to be little difference between NRLU-10 Fab prepared in the presence or absence of cysteine during digestion by papain. Similar results were obtained when several lots of NRML-05 Fab were compared to one another, with lower resolution 2.0% B/min gradients (data not shown).

Identification of Cysteine-Containing Peptides. Cysteine-containing peptides were identified by substituting lucifer yellow iodoacetamide, a highly water soluble chromophoric analogue of iodoacetamide, for iodoacetic acid in the labeling procedure (see Experimental Procedures).

This and similar haloacetyl compounds react most rapidly with thiols between pH 7 and 8, and significant reactivity with amines begins to occur at pH values higher than about 8.5 (*14*). To avoid potential additional reaction with lysines, histidines, or methionines, the stoichiometric excess over the expected number of cysteines in both the heavy and light chains was kept low (*14*). Numerous such iodoacetyl chromophores have been used as thiol-



specific reagents (*15*), including such relatively apolar ones as 2-(bromoacetamido)-4-nitrophenol (*16*). The labeled protein was digested and mapped under optimized conditions. Detection of LYIA-labeled peptides was accomplished by monitoring elution at 422 nm simultaneously with 214 and 280 nm wavelengths by using a photo-diode array detector. NRLU-10 Fab labeled with LYIA gave high-resolution maps containing ca. 70 peaks at 214 nm (Figure 5; column A), and 9–12 major peaks at 422 nm (Figure 5; column B). The large peak at 16 min in the 422-nm maps coelutes with free LYIA.

A comparison of several lots of NRLU-10 Fab labeled with LYIA (Figure 5) showed that the maps appeared very similar at both 214 and 422 nm as would be expected on the basis of the similarity of maps of IAA-labeled Fabs. The reproducibility of the elution times and peak areas (from four different lots) of the 422-nm map was estimated by calculating the coefficient of variation as before. For the areas from the 10 largest peaks other than the free LYIA peak, the coefficient of variation ranged from 0.045

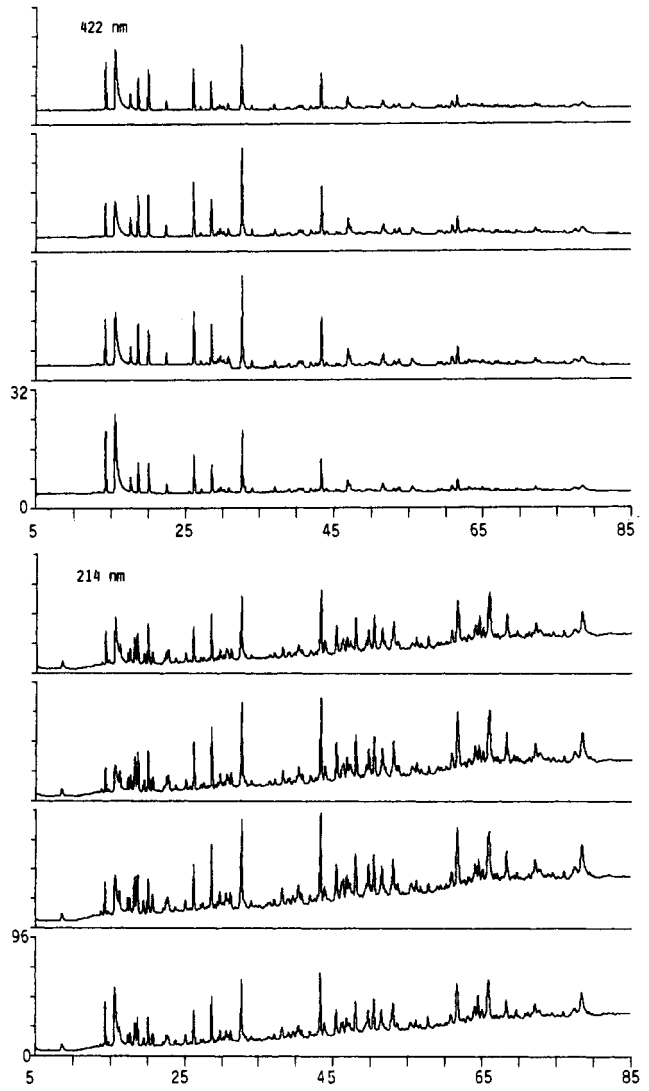


Figure 5. Comparison of peptide maps of four lots of NRLU-10. The Fab fragment was labeled with lucifer yellow iodoacetamide and then digested for 5 h at an initial 1:10 protease to substrate ratio. Injections were 25 μL (0.65 nmol) of labeled antibody, the gradient was 0.5% B/min over 80 min, and the flow rate was 1 mL/min at 40 °C. The *X* axis gives retention time in minutes, the *Y* axis milli absorbance units (mAU) at 214 nm (bottom) and 422 nm (top). Free lucifer yellow iodoacetamide elutes at ca. 16 min in these chromatograms.

to 0.38% with an average value of 0.23%. This coefficient ranged from 9.6 to 26% with an average value of 18% for the areas of these peaks. Thus the peak retention times for the 422-nm map were highly reproducible while the peak areas were less reproducible. These maps appeared to be different from those labeled with IAA (Figure 6A). This is not unexpected, since the LYIA-labeled peptides may shift to earlier retention times with the addition of charged groups present on the chromophoric label. Direct comparison of 214 and 422-nm signals (Figure 6B) indicated the peaks that are expected to contain cysteine. Papain-produced mouse IgG_{2b} Fab fragments are expected to contain 10 cysteines (*9*, *17–18*), and NRLU-10 has an additional cysteine in a heavy chain hypervariable loop (unpublished data). The number of major peaks (*9–12*) thus agrees well with the expected number (*11*) of cysteine-containing peptides generated by tryptic digestion of this mouse IgG2b Fab fragment.

In a separate experiment, NRLU-10 Fab was reacted with a 2-fold excess of [^{14}C]iodoacetate under standard conditions with and without a prior reaction (and subsequent ultrafiltration to remove excess free reagent) with a 2-fold excess of LYIA. Only 12% of the control 82 800 cpm were incorporated, suggesting that LYIA competes with iodoacetate for labeling these antibody chains.

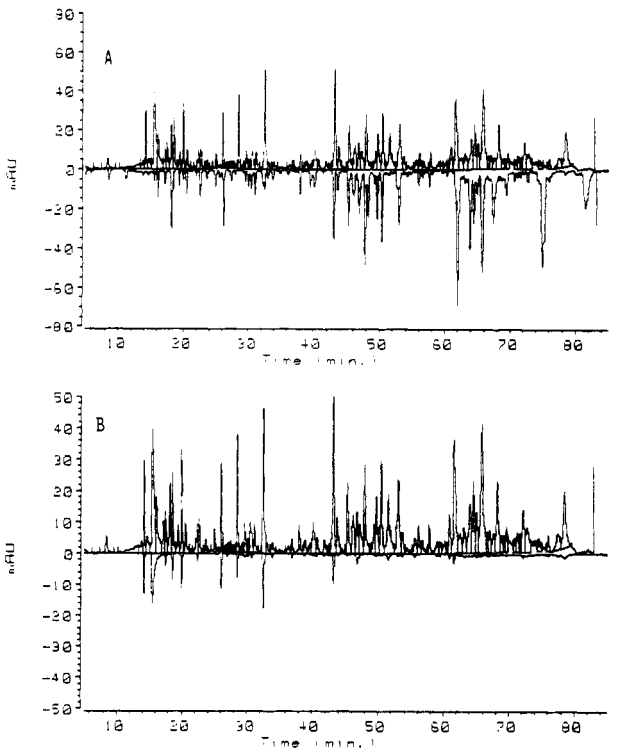


Figure 6. (A) Comparison of peptide maps of IAA- and LYIA-labeled samples from one lot of NRLU-10 Fab at 214 nm, with the IAA map inverted. (B) Comparison of peptide maps of LYIA-labeled sample at 214 and 422 nm, with the latter map inverted. In both cases, the gradient was 0.5% B/min over 80 min, the flow rate was 1 mL/min at 40 °C. The *X* axis shows retention time in minutes, the *Y* axis milli absorbance units.

DISCUSSION

In this paper we have examined the application of tryptic peptide mapping techniques to two IgG2b monoclonal antibodies and their Fab fragments which have gone through Phase III clinical trails as ^{99m}Tc-labeled imaging agents for melanoma and small cell lung cancer. This technique should be useful for quality assurance groups to monitor batches of incoming whole antibody and processed Fab fragments for consistency and to monitor different production techniques to identify those which may modify residues of the final product.

One of our goals was to develop a reproducible procedure generating a large number of peptide fragments to facilitate a detailed comparison of different antibody lots. On the basis of estimation of the reproducibility by the coefficient of variation, this has been achieved for the map of NRLU-10 Fab alkylated by either iodoacetic acid or by lucifer yellow iodoacetamide. Due to their larger coefficient of variation, the peak areas appear in general to contain more variability than the peak retention times with the HPLC hardware and integration algorithms used here. The peak retention times appear to be remarkably consistent from run to run, with one standard deviation of the elution time of a NRLU-10 Fab eluting after 40 min, typically in the range of 1 s. This may be due in part to the use of a precise automated injection system, reliable microbore HPLC pumps, a good algorithm for peak detection, and a flow-cell volume (ca. 7 μL) which is less than the volume of a narrow peak (ca. 200 μL).

A single substitution of a norleucine for the N-terminal methionine in a bovine somatotropin 17-mer tryptic peptide has been shown to result in a 30–40 s increase in this peptide's 53-min retention time (*19*). This suggests that any change in the amino acid composition of a specific peptide might be detectable by an altered peak retention time (as well as the appearance of a new peak) in our system. Factors derived from the tryptic digest itself, from the properties of the generated peptides such as solubility or susceptibility to different reactions, and perhaps from the peak integration protocol, may limit the reproducibility of the peak areas. With an HPLC system such as that used here, the most sensitive way to detect changes in the final antibody may be detection of changes in the peak retention times.

Consensus sequences exist for the mouse κ light chain and γ 2b heavy chains (*17, 18, 20*). By including the known Fv-region sequences of the two antibodies used here, we expect that 35 tryptic sites exist in the NRML-05 Fab fragment, that 37 exist in the NRLU-10 Fab fragment, and that an additional 28 sites (excluding peptides resulting from adjacent basic residues) exist in the Fc region of the heavy chain. Including minor peaks, at the highest resolution our maps contained 83–89 peaks (Fab fragments) or ca. 89 peaks (NRLU-10 whole antibody), suggesting that either incomplete digestion or overdigestion may have occurred.

Incomplete digestion is known to occur with other proteins, for example at Arg-Pro or Lys-Pro bonds (*1*). Since high levels of urea (6 M) were used to solubilize the denatured alkylated chains, and since trypsin is thought to be less active at higher levels of urea (*23*), this may occur here as well. The facts that we obtain distinct and reproducible tryptic maps of different antibodies and that control experiments with trypsin alone show no evidence of autolysis (due perhaps to the 10 mM calcium added for its suppression (*21*) suggest that trypsin is in fact proteolytically active on these substrates. Further, conditions were developed so that this would be a limit digest, and little change was seen in the map for NRLU-10 Fab after 6 h. Thus incomplete digestion is perhaps not the only explanation for the number of peaks seen here.

Due to the high 1:10 enzyme:substrate weight ratio employed here [1:100 is normally used (*21*)], it could be argued that an overdigestion is responsible for the observed number of peaks. For example, trypsin is known to cleave at chymotryptic sites (*1, 21*), and this could generate extra fragments. It is also possible that the high urea levels result in a loss of the normal specificity of trypsin for cleavage on the C-terminal side of Lys or Arg. However LYIA-labeled maps of NRLU-10 Fab contain close to the expected number of 11 peaks, thus trypsin appears to retain significant specificity. Other possible reasons for the observation of extra peaks could include the presence of glycosylated residues known to occur in IgG2b antibodies (*22*). Without the N-terminal sequences of a number of the peaks generated in these tryptic maps, we cannot at present distinguish these possibilities. In spite of the number of peaks observed, the maps appear reproducible both upon multiple injections or upon mapping of different antibody lots.

Besides their previous use for sequence comparisons of antibodies or individual antibody chains (*21, 24, 25*), we have used tryptic maps here to examine modifications in the papain fragmentation procedure used to produce Fab fragments. The Fab peptide maps compared here with and without 10 mM cysteine appear essentially identical, suggesting that the papain cleavage sites, located in the hinge region in the sequence (*24*), have probably not changed in the presence of cysteine. Although this has not been seen by Parham for other IgG2b antibodies (*13*), one or more of the hinge region disulfides, all three of which are within about 16 residues of the papain cleavage sites, may be reduced, with a concomitant improvement of the substrate properties of the antibody.

In order to facilitate the detection of cysteine-containing peptides, we have used lucifer yellow iodoacetamide as an analogue of iodoacetate to react with cysteines and thus label cysteine-containing peptides. This approach is similar to the use of other chromophores to label cysteine, such as DTNB or 4-vinylpyridine (*17*). The advantages of the chromophore used here are that it is highly water-soluble and has an absorption band with an extinction coefficient of 13 000 M^{-1} cm^{-1} at 426 nm (*15*), which is separate from the bands at 214 or 280 nm. Lucifer yellow iodoacetamide is also strongly fluorescent, which should if necessary allow a more sensitive detection of these peptides. We have used the LYIA alkylation of cysteines to replace the carboxymethylation by iodoacetate which may prevent the refolding of very stable disulfide-containing proteins such as antibodies before trypsinization. Due to the appearance of a lucifer yellow labeled tryptic map of similar complexity to that generated after S-carboxymethylation, alkylation with lucifer yellow iodoacetamide appears to be as successful as iodoacetate in preventing this refolding of the reduced H and L chains.

Results presented here demonstrate the reproducibility of mAb scale-up production runs and fragmentation processes, and the utility of three-wavelength data collection for rapid mapping of cysteine-containing proteins. Additional dimensions might be added to these maps, for example by specific labeling of arginines with 1-pyreneglyoxal or 7-(diethylamino)coumarin-3-glyoxal (*22*), or by labeling aspartates and glutamates with chromophoric carboxylate-specific reagents. Application to the characterization of immunoconjugates can also be envisioned wherein the number and type of modified residues, which alter the chromatographic properties of the peptides produced, can be identified after isolation and sequencing.

ACKNOWLEDGMENT

We acknowledge Dr. Alan Fritzberg for his support of this work, numerous helpful suggestions, and careful reading of the manuscript, and John Reno for suggesting a comparison of the Fab fragments produced in the presence and absence of cysteine.

LITERATURE CITED

(1) Chloupek, R. C., Harris, R. J., Leonard, C. K., Keck, R. G., Keyt, B. A., Spellman, M. W., Jones, A. J. S., and Hancock, W. S. (1989) *J. Chromatog. 463*, 375–396.

(2) Garnick, R. L., Solli, N. J., and Papa, P. A. (1988) *Anal. Chem. 60*, 2546–2557.

(3) Hartman, P. A., Stodola, J. D., Harbour, G. C., and Hoogerheide, J. G. (1986) *J. Chromatogr. 360*, 385–395.

(4) Harris, R. J., Chamow, S. M., Gregory, T. J., and Spellman, M. W. (1990) *Eur. J. Biochem. 188*, 291–300.

(5) Kohr, W. J., Keck, R., and Harkins, R. N. (1982) *Anal. Biochem. 122*, 348–359.

(6) Hancock, W. S. (1986) *Chromatogr. Forum 1*, 57–59.

(7) Woodhouse, C. S., Bordonaro, J. P., Beaumier, P. L., and Morgan, A. C. (1990) In *Human Melanoma, from Basic Research to Clinical Application* (S. Ferrone, et al., Eds.) pp 413–429, Springer-Verlag, New York.

(8) Varki, N. M., Reisfeld, R. A., and Walker, L. E. (1984) *Cancer Res. 44*, 681–687.

(9) Parham, P. (1986) In *Handbook of Experimental Immunology, Volume 1, Immunochemistry* (D. M. Weir, Ed.) Chapter 14, Blackwell Scientific Publications, London.
(10) Crestfield, A. M., Moore, S., and Stein, W. H. (1963) *J. Biol. Chem. 238*, 622–627.
(11) Bendat, J. S., and Piersol, A. G. (1986) *Random Data, Analysis and Measurement Procedures*, 2nd ed., pp 252–256, John Wiley and Sons, New York.
(12) Ebert, R. F., and Schmelzer, C. H. (1988) *J. Chromatogr. 443*, 309–316.
(13) Parham, P. (1983) *J. Immunol. 131*, 2895.
(14) Means, G. R., and Feeney, R. E. (1971) *Chemical Modification of Proteins*, p 105, Holden-Day, San Francisco.
(15) Haugland, R. P. (1989) *Molecular Probes Handbook of Fluorescent Probes and Research Chemicals*, Molecular Probes, Inc., Eugene, OR.
(16) Gardner, J. A., and Matthews, K. S. (1987) *Anal. Biochem. 167*, 140–144.
(17) Kabat, E. A., Wu, T. T., and Bilofsky, H. (1979) *Sequences of Immunoglobulin Chains*, U.S. Dept. of Health, Education and Welfare, Public Health Service, National Institutes of Health, Washington, DC.
(18) Kabat, E. A., Wu, T. T., Bilofsky, H., Reid-Miller, M., and Perry, H. (1983) *Sequences of Proteins of Immunological Interest*, U.S. Dept. of Health and Human Services, Public Health Service, National Institutes of Health, Washington, DC.
(19) Violand, B. N., Siegel, N. R., Bogosian, G., Workman, W. E., and Kane, J. F. (1989) In *Techniques in Protein Chemistry* (T. E. Hugli, Ed.) pp 315–326, Academic Press, San Diego.
(20) These sequences were taken from the PIR protein sequence data bank (release 14) and Genbank release 59.0 (Intelligenetics Inc., Mountain View, CA).
(21) Allen, G. (1981) *Sequencing of Proteins and Peptides*, p 54 ff, North-Holland, Amsterdam.
(22) Burton, D. R. (1985) *Mol. Immunol. 22*, 161–206.
(23) Stone, K. S., LoPresti, M. B., Crawford, J. M., de Angelis, R., and Williams, K. R. (1989) in *A Practical Guide to Protein and Peptide Purification for Microsequencing* (P. Matsudaira, Ed.), pp 31–47.4, Academic Press, San Diego.
(24) Kratzin, H., Yang, C., Krusche, J. U., and Hilschmann, N. (1980) *Hoppe-Seyler's Z. Physiol. Chem. 361*, 1591–1598.
(25) Yang, C. Y., Pauly, E., Kratzin, H., and N. Hilschmann (1981) *Hoppe-Seyler's Z. Physiol. Chem. 362*, 1131–1146.
(26) Hiratsuka, D. (1987) *J. Biochem. 101*, 1457.

Registry No. Lucifer yellow iodoacetamide, 135760-52-0.

TECHNICAL NOTE

Nuclear Targeting of a Viral-Cointernalized Protein by a Short Signal Sequence from Human Retinoic Acid Receptors

François Hamy,† Philippe Verwaerde,‡ Nicole Helbecque,† Pierre Formstecher,§ and Jean-Pierre Hénichart*,†

INSERM U16, INSERM U233, Laboratoire de Biochimie Structurale, Faculté de Médecine, Place de Verdun, 59045 Lille Cedex, France. Received December 14, 1990

The synthesis of a putative nuclear localization signal from the human retinoic acid receptor is described. Its ability to target a carrier protein to the nucleus is demonstrated following microinjection or a new technique of cell internalization in the presence of adenovirus 3.

INTRODUCTION

Eucaryotic cells contain different sets of proteins, either nuclear or cytoplasmic, which are all synthesized in the cytoplasm. Mature polypeptides destined to the nuclear compartment of the cell must subsequently migrate to the nucleus (*1*). This involves mechanism(s) of transport, implying passage through pore complexes of the nuclear envelope. The phenomenon occurs in a fundamentally different manner from transport of proteins into mitochondria or endoplasmic reticulum due to the nature of nuclear pores which act as large aqueous channels ca. 9 nm in diameter (*2*). Two mechanisms of nuclear localization are commonly considered (*3*). Small proteins (MW < 50 kDa) freely diffuse into the nucleus with subsequent retention of nuclear proteins by binding to a nondiffusible substrate. On the other hand, access of the majority of large proteins to the nucleus requires that they participate in a specific interaction with a cellular component involved in transport of proteins to the nucleus.

A short peptidic sequence of the protein has been shown to be implied in the nuclear transfer. Experimental evidence for this was first provided by intracellular injection experiments with nucleoplasmin (*4*). The precise signal sequences of a number of nuclear proteins have been determined, the best characterized one being that of simian virus 40 large T-antigen.

In the present study we describe the synthesis of a short basic amino acid tract occurring in the sequences of the various forms of the retinoic acid receptor, recently deduced from their cloned cDNAs isolated from human (*5–10*) and mouse (*11*). The peptide (Asp-Arg-Asn-Lys_4-Glu) was chemically cross-linked to bovine serum albumin (BSA). This sequence, distinct from SV40 T-antigen was shown to be a new nuclear localization signal (NLS) sequence since it can direct a normally cytoplasmic BSA to the nucleus.

The comparison between two techniques (microinjection/viral cointernalization) for introducing the complex in the cytoplasm of cultured cells demonstrates the practical utility for membrane transcytosis using the original technique of viral cointernalization. This later technique could be a very important contribution to the study of intracellular biochemistry.

EXPERIMENTAL PROCEDURES

Peptide Synthesis. The peptide Cys-Gly-Tyr-Gly-Asp-Arg-Asn-Lys-Lys-Lys-Lys-Glu was synthesized on a LKB Biolynx peptide synthesizer using Fmoc–amino acid chemistry (*12*) on a Wang resin to give a free carboxyl at the C-terminus (*13*). After cleavage from the resin and deprotection using aqueous trifluoroacetic acid, the peptide was purified by high-performance liquid chromatography on a C18 column eluted by 20% aqueous acetonitrile. The major peak (82%) was collected and lyophilized. Purity was assessed by the presence of a single peak by analytical reversed-phase high-pressure liquid chromatography, the correct amino acid composition (Gly, 2.06; Cys, 1.68; Tyr, 1.035; Asx, 1.88; Arg, 1.02; Lys, 4.02; Glu, 0.96), and the presence of the predicted parent ion by fast atom bombardment mass spectroscopy (M^+ = 1425.6).

Peptide–Protein Conjugation. The synthetic peptide was conjugated to bovine serum albumin (BSA) with a bifunctional cross-linking reagent, *m*-maleimidobenzoic acid succinimido ester (MBS), according to the method of Lerner (*14*). For activating BSA, 5.0 mg of BSA in 0.05 M phosphate buffer, pH 7.0, was reacted with MBS dissolved in tetrahydrofuran at a molar ratio of 1:40 BSA:MBS. The solution was stirred for 30 min at room temperature. Unreacted MBS was removed by dialysis against distilled water for one night at 4 °C. Purified peptide (2 mg) was added to 2 mg of MBS-activated BSA in 2 mL of 0.05 M phosphate buffer, pH 7.0. The solution was stirred for 3 h at room temperature and the final product was isolated by dialysis against water for 48 h at 4 °C.

A sample was examined by sodium dodecyl sulfate–polyacrylamide gel electrophoresis (5–30%) to visualize an increase in molecular weight due to the addition of peptide to the protein. A more accurate estimate of the average degree of conjugation was determined by amino acid analysis (three measurements). The increase in the ratios of residues contained in the peptide to those that were absent was used to calculate the ratio of the peptide to BSA in the conjugated sample.

Microinjection. MCF 7 and HeLa S3 cells were grown in Dulbeco medium (GIBCO Laboratories, Grand Island, NY) on No. 2 cover slips which had been premarked to identify and localize injection sites. About 150 cells of each kind were microinjected per assay in the growth

* Author to whom correspondence should be addressed.
† INSERM U16.
‡ INSERM U233.
§ Laboratoire de Biochimie Structurale.

1043-1802/91/2902-0375$02.50/0 © 1991 American Chemical Society

medium at 23 °C by the method of Graessmann and Graessmann (*15*) with a Leitz micromanipulator. Glass needles were femtotips (Eppendorf, Hamburg, Germany), the internal diameter of which was estimated to be 0.5 μm. Approximately 100 cells were injected. After injection cells were returned to a CO_2 incubator for 1 and 2 h.

Viral Cointernalization. The adenovirus serotype 3 (subgroup B) was produced in suspension-grown KB cells. Adenovirons were extracted and purified in CsCl gradients, as previously described (*16*) and the virus titers were determined and expressed as fluorescent focus units (FFU). MCF 7 and HeLa S3 cell monolayers were infected with adenovirus 3 suspensions (300 FFU/cell) in Dulbeco medium including BSA or peptide–BSA at 1 mg/mL. After several incubation times at 37 °C (20, 40, 60, 120 min), cells were prepared for immunofluorescence.

Immunofluorescence. Soon after incubation cells were harvested for immunofluorescence according to the method of Langranger et al. (*17*). Cells were washed three times in phosphate-buffered saline (PBS), pH 7.4, fixed in cold methanol (95% in PBS) (4 °C) for 5 min and washed again in four changes of PBS (pH 7.4). Cells were then fixed in paraformaldehyde (3%, final) and glutaraldehyde (0.05%, final) in PBS (pH 7.4) for 20 min, washed in solution A (5 mM Pipes, 5 mM $MgCl_2$, 2 mM ETGA, in PBS, pH 6.1) and incubated for 10 min in 0.1 M glycine in solution A at room temperature. Subsequently cells were permeabilized with Triton X100, 5% in solution A for 5 min, washed in solution A, and incubated in normal rabbit IgG (0.5% in PBS, pH 7.4) for 16 h at 4 °C. BSA was detected by indirect immunofluorescence using goat anti BSA IgG (Sigma, St. Louis, MO), internalized fluorescent macromolecules were examined with an Olympus BH-2 microscope (excitation wavelength at 530–560 nm, edge filter at 580 nm). Photomicrographs were taken with a Kodak citachrome film (400 Asa).

RESULTS

Conjugation of the Synthetic Peptide to a Carrier Protein. A dodecamer synthetic peptide was synthesized which contains the eight amino acid core sequence Asp-Arg-Asn-Lys-Lys-Lys-Lys-Glu from hRAR (human retinoic acid receptor) that is supposed to act as nuclear localization signal. The sequence Cys-Gly-Tyr-Gly was added to the amino terminal as a spacer containing a cysteinyl residue for ease of coupling to a carrier protein (*18*). It was coupled to BSA chosen as carrier protein because of its widespread use in similar studies. Coupling was made by using the MBS procedure (*14*). The coupling ratios were estimated by two methods: amino acid analysis and estimation of the increase in apparent molecular weight of BSA (67 000 → 72–74 000) by retardation of mobility by sodium dodecyl sulfate–polyacrylamide gel electrophoresis and coomassie staining. Both data gave an average ratio of 4.2 peptides per carrier molecule.

Cell Internalization of the Peptide–BSA Conjugate. Microinjection of BSA alone (Figure 1B) shows immunofluorescence in the cytoplasm and a relatively dark nucleus: very little if any nuclear transport without the signal peptide attached. With the signal attached, cells exhibit bright nuclei, but the cytoplasms were never completely depleted, even 2 h after microinjection. These data suggest that this peptide from hRARs is a nuclear localization signal but not as strong as those observed in the literature. The same results were observed for the same time (2 h) and shorter times (40 and 50 min) following cointernalization (data not shown). Though it seems clear that viral cointernalization works to get the fluorescence into the cytoplasm, results were not as clear, essentially because of leakage of control BSA on the surface of the nucleus probably due to the mechanism of action of adenovirus 3.

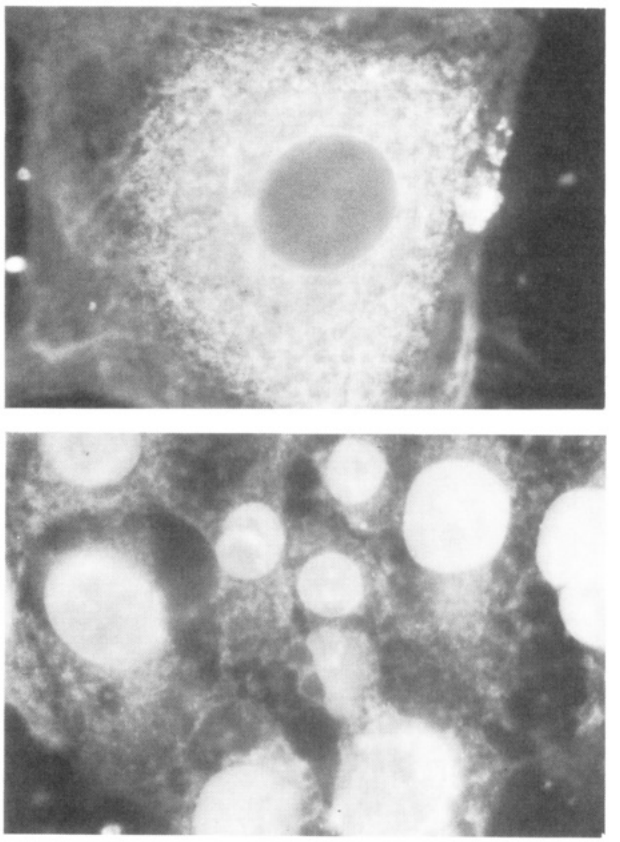


Figure 1. Subcellular localization of microinjected BSA (A, top) and peptide–BSA conjugate (B, bottom) in HeLa S3 cells. Proteins were visualized by indirect immunofluorescence staining as described in the Experimental Procedures. (The results shown are representative of more than 50 cells positive for nuclear localization.)

The choice of adenovirus 3 (Ad3) was directed by the fact that this DNA virus has a slow infection process (early viral RNA synthesis occurs about 3 h after infection (*19*)). Moreover, events such as membrane and cytoskeleton reorganization, which normally arise at early times after adenovirus infection, are less important with adenovirus 3 (e.g. processing of vimentin is hardly, if at all, induced by Ad3 serotype) (*20*). Therefore biochemical activities of the virus do not a priori interfere with nuclear translocation that arises between 20 and 30 min after the protein enters the cytoplasm (kinetics data from ref 21). Secondly endocytosis vesicles including adenovirus 3 develop until the formation of an endosome, the content of which is poured in the vicinity of nuclear pores.

DISCUSSION

The problem of the existence of specific targeting signals for the nuclear import of proteins has been the subject of many studies during the last decade (*22*). The demonstration of the presence in retinoic acid receptors of such a signal sequence led us to bring into play different methodologies. The first of them concerned the introduction of the protein, bearing several copies of the basic sequence, into the cytoplasm. Among the numerous ways of introducing proteins into the cytoplasm of cultured cells (*23*), we first selected microinjection because of its widespread use in this kind of study, though the traumatism caused by the glass needle immediately triggers

Table I. Comparison of Amino Acid Sequences of Putative Nuclear Localization Signals in the Steroid/Thyroid Hormone Receptor Superfamily, SV40 Large T-Antigen, and *Xenopus laevis* Nucleoplasmin and Lamin L1[a]

protein	sequence and position of its first amino acid	receptor domain	experimental arguments for nuclear localization signal activity
SV 40 large T-antigen	P K K K R K V		+
X. laevis nucleoplasmin	Q A K K K K L		+
X. laevis L1	K G K R K R I		+
retinoic acid receptors	(α) 162 (β) 155 R N K K K K E (γ) 164	hinge (+14)	+
thyroid hormone receptors	(α) 142 R E R R R K E	hinge (+27)	
	(β) 191 R E K R R R E	hinge (+27)	
	(α) 130 K R V A K R K L	hinge (+15)	
	(β) 179 K R L A K R K L	hinge (+15)	
vitamin D receptor	102 R K R E M I L K R K	hinge (+18)	
glucocorticoid receptor	491 R K T K K K I K	hinge (+10)	+
progesterone receptor	637 R K F K K F N K	hinge (+10)	+
estrogen receptor	256 R K D R R G G R	hinge (+11)	

[a] The sequences are reported for human T3 receptors α (*31*) and β (*32*), vitamin D receptor (*33*), glucocorticoid receptor (*34*), progesterone receptor (*35*), and estrogen receptor (*36, 37*). These sequences are highly conserved among species for a given receptor (ref 6 and references cited therein). Numbers in parentheses indicate the distance of the sequence from the last conserved cystein in the DNA binding domain (*38*). Basic amino acids are underlined. Signal sequences of *X. laevis* nucleoplasmin and lamin L1 were found in ref 27.

different sorts of metabolic reactions to repair damages to the integrity of the membrane. Therefore, to make an attempt at being more physiological, we used viral cointernalization, a phenomenon based on the early permeabilization of cells to proteins by animal viruses. Evidence for cointernalization was first described by Otero (*24*). Cell infection by a virus first involves fixation of a viral particle on the external side of the host-cell membrane. Subsequently the viral particle internalization occurs, accompanied by an entry of extracellular medium among which are macromolecules such as proteins. This method presents many advantages since (i) it is more physiological (for short times) than others like microinjection, (ii) close to the totality of cells are infected, and (iii) it is easy to carry out even for kinetic studies and for suspended cells.

In the case of the steroid/thyroid hormone receptor superfamily, experiments conducted either on the glucocorticoid (*25*) or on the progesterone (*26*) receptors suggest the existence of at least two nuclear localization signals. One of them is responsible for hormone-dependent nuclear uptake. The other, constitutively active and located at the C-terminus of the DNA-binding region, consists of a small basic sequence similar to other nuclear localization signals characterized in many proteins. Such motifs are present in the hinge region of all steroid receptor superfamily (Table I). However, none of the consensus proposed for the nuclear localization signals, either in the case of steroid hormone receptors (*26*) or of various nuclear proteins (*27*), can account for the diversity of the potential nuclear localization signals found in the steroid/thyroid receptors superfamily. Our demonstration that the particular sequence found in the retinoic acid receptors is effectively able to target to the nucleus a nonnuclear protein is the first one in this field. However, the peptide corresponding to this sequence is a relative weak nuclear location signal (no total nuclear immunofluorescence was observed for 4.2 peptides/BSA after 2 h) and further work will be required to understand how this signal works in its natural context. Mutagenesis experiments might address this question. In addition, it could be thought that other sequences of the protein are also involved in its nuclear localization. In particular, a recent study (*28*) has pointed out that, in several but not in all nuclear proteins containing a SV40-like motif, there are two conserved basic amino acids 10 residues before the signal. The spacer can sometimes be longer (e.g. 11 residues in the estrogen receptor). In the case of hRARs, 12 residues separate a highly conserved lysyl residue in the superfamily from the NLS.

Though the initial site for signal recognition has not been defined, recent results (*29, 30*) suggest that nuclear import may be a receptor-mediated process. If this hypothesis reflects a step of the actual mechanism of protein import into the nucleus, the nuclear localization signal must then be implicated in protein–protein interactions. In this case its conformational flexibility might play a critical role too. The presumed nuclear localization signal sequence from hRARs corresponds to a sequence localized in a region of the receptors which has a predicted helical conformation. In fact, the association basic amino acid sequence/helix-predicted region is conserved in the hinge region of each member from the steroid/thyroid receptors superfamily, and preliminary results indicate that the corresponding synthetic peptides share a similar surrounding-induced behavior with those from hRAR (work in progress). A generalization in that field of sequence/conformational behavior should lead to the conception of a simplified nuclear localization vector agent providing a tool for nuclear vectorization of diverse molecules.

ACKNOWLEDGMENT

This work was financially supported by INSERM and the Association pour la Recherche contre le Cancer (No. 6932). F.H. and P.V. are allocataires of the Ministère de la Recherche et de la Technologie.

LITERATURE CITED

(1) Dingwall, C., and Laskey, R. A. (1986) Protein import into the cell nucleus. *Annu. Rev. Cell. Biol. 2*, 367–370.

(2) Gerace, L., and Burke, B. (1988) Functional organization of the nuclear envelope. *Annu. Rev. Cell. Biol. 4*, 335–375.

(3) Newmeyer, D. D., and Forbes, D. J. (1988) Nuclear import can be separated into distinct steps: in vitro nuclear pore binding and translocation. *Cell 52*, 641–653.

(4) Dingwall, C., Schoolnick, S. V., and Laskey, R. A. (1982) A polypeptide domain that specifies migration of nucleoplasmin into the nucleus. *Cell 30*, 449–458.

(5) Benbrook, D., Lenhardt, E., and Pfahl, M. (1988) A new retinoic acid receptor identified from a hepatocellular carcinoma. *Nature 333*, 669–672.

(6) Brand, N., Petkovich, M., Krust, A., Chambon, P., De Thé, H., Marchio, A., Tiollais, P., and Dejean, A. (1988) Identification of a second retinoic acid receptor. *Nature 332*, 850–853.
(7) De Thé, H., Marchio, A., Tiollais, P., and Dejean, A. (1989) Differential expression and ligand regulation of the retinoic acid receptor α and β genes. *EMBO J. 8*, 429–433.
(8) Giguère, V., Ong, E. S., Segui, P., and Evans, R. M. (1987) Identification of a receptor for the morphogen retinoic acid. *Nature 330*, 624–629.
(9) Krust, A., Kastner, P., Petkovich, M., Zelent, A., and Chambon, P. (1989) A third human retinoic acid receptor: hRAR. *Proc. Natl. Acad. Sci. U.S.A. 86*, 5310–5314.
(10) Petkovich, M., Brand, N. J., Krust, A., and Chambon, P. (1987) A human retinoic acid receptor which belongs to the family of nuclear receptors. *Nature 330*, 444–450.
(11) Zelent, A., Krust, A., Petkovich, M., Kastner, P., and Chambon, P. (1989) Cloning of murine α and β retinoic acid receptors and a novel receptor γ predominently expressed in skin. *Nature 339*, 714–717.
(12) Sabatier, J. M., Teissier-Rochat, M., Granier, C., Van Rietschoten, J., Pedroso, E., Grandas, A., Albericio, F., and Giralt, E. (1987) Convergent solid phase synthesis VI: Synthesis by the Fmoc-procedure with a modified protocol of two protected segments, sequence 15–17 and 18–31 of the neurotoxin II of the scorpion *Androctonus australis* Hector. *Tetrahedron 43*, 5973–5980.
(13) Wang, S. S. (1973) pAlkoxy alcohol resin for solid phase synthesis of protected peptide fragments. *J. Am. Chem. Soc. 95*, 1328–1333.
(14) Lerner, R. A., Green, N., Alexander, H., Liu, F. T., Sutliffe, J. G., and Shinnick, T. M. (1981) Chemically synthesized peptides predicted from the nucleotide sequence of the hepatitis B virus genome elicit antibodies reactive with the native envelope protein of dane particle. *Proc. Natl. Acad. Sci. U.S.A. 78*, 3403–3407.
(15) Graessmann, M., and Graessmann, A. (1976) "Early" simian-virus 40 specific RNA contains information for tumor antigen formation and chromatin replication. *Proc. Natl. Acad. Sci. U.S.A. 73*, 366–370.
(16) D'Halluin, J. C., Milleville, M., Boulanger, P. A., and Martin, G. R. (1978) Temperature-sensitive mutant of adenovirus type 2 blocked in virion assembly: accumulation of light intermediate particles. *J. Virol. 26*, 344–356.
(17) Langranger, G., De Mey, J., Moeemans, M., Daneels, G., De Brabander, M., and Small, J. V. (1984) Ultrastructural localization of α-actinin and filamin in cultured cells with the immunogold staining (IGS) method. *J. Cell. Biol. 99*, 1324–1334.
(18) Lanford, R. D., Kanda, P., and Kennedy, R. C. (1986) Induction of nuclear transport with a synthetic peptide homologous to the SV40 T antigen transport signal. *Cell 46*, 575–582.
(19) Flint, B. J. (1986) Regulation of adenovirus mRNA formation. *Adv. Virus Res. 31*, 169–228.
(20) Belin, M. T., and Boulanger, P. (1987) Processing of vimentin occurs during the early stages of adenovirus infection. *J. Virol. 61*, 2559–2566.
(21) Richardson, W. D., Mills, A. D., Dilworth, S. M., Laskey, R. A., and Dingwall, C. (1988) Nuclear protein migration involves two steps: rapid binding at the nuclear envelope followed by slower translocation through nuclear pores. *Cell 52*, 655–664.
(22) Silver, P. A. (1991) How proteins enter the nucleus. *Cell 64*, 489–497.
(23) Richardson, W. D. (1988) Introducing proteins into cultured animal cells. *J. Cell. Sci. 91*, 319–322.
(24) Otero, M. J., and Carrasco, L. (1987) Proteins are co-internalized with virion particles during early infection. *Virology 160*, 75–80.
(25) Picard, D., and Yamamoto, K. R. (1987) Two signals mediate hormone dependent nuclear localization of glucocorticoid receptor. *EMBO J. 6*, 3333–3340.
(26) Guiochon-Mantel, A., Loosfelt, H., Lescop, P., Sar, S., Atger, M., Perrot-Applanat, M., and Milgrom, E. (1989) Mechanisms of nuclear localization of the progesterone receptor: evidence for interaction between dimers. *Cell 57*, 1147–1154.
(27) Chelsky, D., Ralph, R., and Jonak, G. (1989) Sequence requirements for synthetic peptides mediated translocation to the nucleus. *Mol. Cell. Biol. 9*, 2487–2492.
(28) Robbins, J., Dilworth, S. M., Laskey, R. A., and Dingwall, C. (1991) Two interdependent basic domains in nucleoplasmin nuclear targeting sequence: Identification of a class of bipartite nuclear targeting sequence. *Cell 64*, 615–623.
(29) Adam, S. A., Lobl, T. J., Mitchell, M. A., and Gerace, L. (1989) Identification of specific binding proteins for a nuclear location sequence. *Nature 337*, 276–279.
(30) Yamasaki, L., Kanida, P., and Lanford, R. E. (1989) Identification of four nuclear transport signal-binding proteins that interact with diverse transport signals. *Mol. Cell. Biol. 9*, 3028–3036.
(31) Benbrook, D. (1987) A novel thyroid hormone receptor encoded by a cDNA clone from a human testis library. *Science 238*, 788–791.
(32) Weinberger, C., Thompson, C. C., Ong, E. S., Lebo, R., Gruol, D. J., and Evans, R. M. (1986) The c-erb-A gene encodes a thyroid hormone receptor. *Nature 324*, 641–646.
(33) Walters, M. R., Hungiker, W., and Norman, A. W. (1981) 1,25-Dihydroxyvitamin D_3 receptors. *Trends Biochem. Sci. 6*, 268–271.
(34) Hollenberg, S. M., Weinberger, C., Ong, E. S., Cerelli, G., Oro, A., Lebo, R., Thompson, E. B., Rosenfeld, M. G., and Evans, R. M. (1985) Primary structure and expression of a functional human glucocorticoid receptor cDNA. *Nature 318*, 635–641.
(35) Misrahi, M., Atger, M., D'Auriol, L., Loosfelt, H., Meriel, C., Friedlansky, F., Guiochon-Mantel, A., Galibert, F., and Milgrom, E. (1987) Complete amino acid sequence of the human progesterone receptor deduced from cloned cDNA. *Biochem. Biophys. Res. Commun. 143*, 740–748.
(36) Green, S., Walter, P., Kumar, V., Krust, A., Bornet, J. M., Argos, P., and Chambon, P. (1986) Human oestrogen cDNA: sequence, expression and homology to v-erb-A. *Nature 320*, 134–139.
(37) Greene, G. L., Gilna, P., Waterfield, M., Baker, A., Hort, Y., and Shine, J. (1986) Sequence and expression of human estrogen receptor complementary DNA. *Science 231*, 1150–1154.
(38) Evans, R. M. (1988) The steroid and thyroid hormone receptor superfamily. *Science 240*, 889–895.

Registry No. Cys-Gly-Tyr-Gly-Asp-Arg-$(Lys)_4$-Glu, 135929-31-6; retinoic acid, 302-79-4.

Bioconjugate Chemistry

NOVEMBER/DECEMBER 1991
Volume 2, Number 6

© Copyright 1991 by the American Chemical Society

REVIEW

DNA Recognition by Intercalator–Minor-Groove Binder Hybrid Molecules

Christian Bailly and Jean-Pierre Hénichart*

INSERM Unité 16, Place de Verdun, 59045 Lille, France. Received January 29, 1991

Recently many research efforts have been aimed at targeting specific sequences in DNA with synthetic ligands with the idea of designing both drugs and molecular probes for DNA polymorphism. The selective inhibition of transcription from particular sequences by the specific targeting of a ligand, in other words the control of gene expression, has become a very attractive and productive research area (*1*).

Many groups have spelled out a strategy to reach this objective with the common and ultimate goal to design agents which can effectively read DNA in a manner analogous to regulatory proteins. Among the various proposed approaches, oligonucleotides able to recognize DNA via the formation of triple helices (*2–9*) appear to be by far the most sequence-specific agents able to read DNA with an extreme fidelity. However, if their utility as tools for molecular biology is indisputable, they are not yet pharmacologically useful. Binding mostly to homopurine–homopyrimidine sequences of duplex, low ability to penetrate the cells, or sensitivity to cellular nucleases are examples of problems encountered with these ligands. Changes in the anomeric configuration of nucleotides (*10, 11*) and/or combination of the oligonucleotide with a DNA carrier or chelating agent (*10–23*) represent elegant extensions of this approach which might lead to the development of more efficient compounds. These oligonucleotides bind to the major groove of DNA (*24*) because of the greater width of the major over the minor groove in B-DNA (*25*). Also, they are directly able to compete with DNA-binding proteins. Most protein–DNA (*26–31*) complexes characterized to date involve major-groove contacts. However, minor-groove protein–DNA contacts conferring sequence specific binding are also reported (*32–36*).

In parallel to this oligonucleotide-based approach, low molecular weight agents which would be able to fit isohelically in the minor groove of DNA have been designed and are now known to be endowed with sequence specific recognition properties (*37*). Isohelical sequence-reading drug polymers, initially called "isolexins" (*38*), are currently the subject of a great deal of work to evaluate their real potential in terms of compounds of biological interest. They show promise even if their usefulness as efficient anticancer or antiviral drugs is not yet definitively proved.

Difficulties in these studies arise from the need to correlate changes in sequence specificity to the nature and location of particular substituents introduced into a drug molecule. Put another way, the problem lies in the interpretation of the relationships between structure and DNA binding. In their extensive studies of the sequence-specific DNA binding properties of minor-groove binders, Lown (*39*), Dervan (*40*), and their collaborators, by reference to the pioneer computer analysis study of Goodsell and Dickerson (*38*), have in part achieved this distinction by comparing the binding specificity of homologous compounds in which the overall balance between AT/GC selectivity could be controlled (more or less) by judicious substitutions with H bond donor or acceptor heteroatoms. The expected GC recognition should involve a specific hydrogen bond between a heteroatom of the ligand and the 2-amino groups of guanine bases protruding into the minor groove. In this way, they have succeeded in identifying sites of the well-known naturally occurring oligopeptides netropsin and distamycin (Figure 1), where substitution may alter their high AT specificity and enhance their GC acceptance without change to their mode of binding.

These efforts, which led to the synthesis of "lexitropsins", or sequence-reading oligopeptides structurally related to netropsin (*41, 42*), are still going on with the aim to design pure GC-specific minor-groove binders and drugs able to recognize a portion of DNA of definite sequence. The rational structural modification of natural DNA-sequence-selective agents has evidenced the importance of several

1043-1802/91/2902-0379$02.50/0 © 1991 American Chemical Society

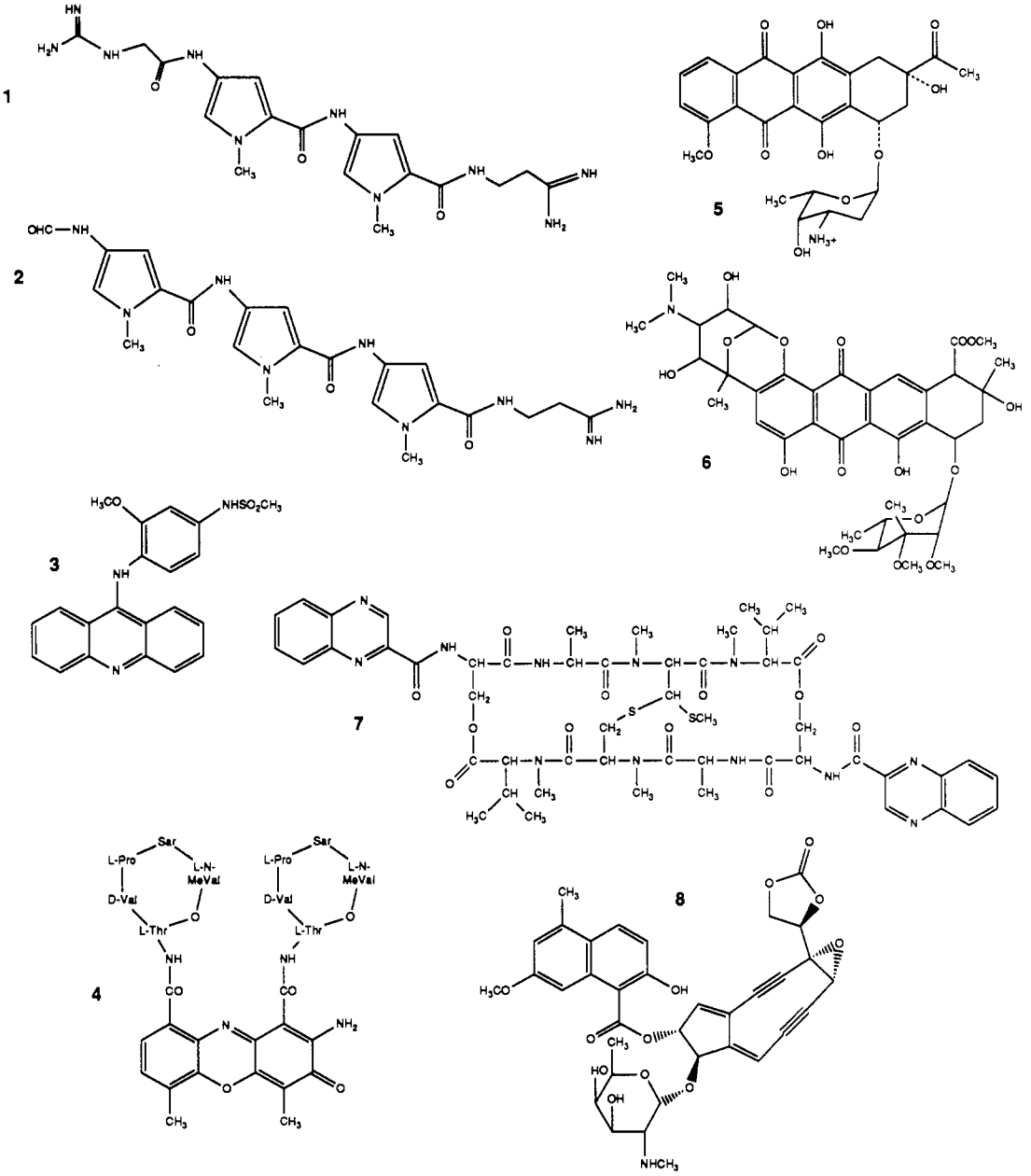


Figure 1. Structure of netropsin (1), distamycin (2), amsacrine (3), actinomycin D (4), daunomycin (5), nogalamycin (6), echinomycin (7), and neocarzinostatin chromophore (8).

of the structural, stereochemical, conformational, and electrostatic factors necessary for a better understanding and control of drug–DNA molecular-recognition processes. However, we must admit that to date the success of converting from an AT word to a word that will also tolerate GC with less binding affinity for AT is obvious but still limited. The significance of hydrogen bonds between the ligands and DNA for determination of sequence specificity could be overestimated. Geometrical and electrostatic factors must be considered more carefully. The distribution of the electrostatic potential in B-DNA favors the minor groove of AT sequences over the minor groove of GC sequences (*43*, *44*). The narrowness of the minor groove in AT-rich regions, compared with the markedly wider minor groove in GC-rich regions, suggests an explanation for the marked AT selectivity almost invariably observed with netropsin analogues (*45*). Minor-groove binders seem to recognize potential binding sites more by the shapes of the DNA than by the specific sequence that is contained in the site. The DNA flexibility will also be an important feature to consider. Because of the inherently lower flexibility of GC-rich regions (*46*), the design of GC recognition elements will require extremely accurate matching of groove and ligands surfaces, whereas a much cruder match may suffice for AT recognition (*47*). Considering the notions of geometrical fitting, hydrogen-bonding capabilities, and the overall electronic properties of the interacting species, a new generation of isolexins was recently proposed. A significant increase both in GC specificity and in DNA binding energy is expected by replacing the amide linkage between the *N*-methylpyrrole units of netropsin by C=C double bonds (yielding the so called "vinylexins") (*48*). The success of such an endeavour may ultimately open the road to the creation of drugs able to read DNA fragments of any proposed base sequences.

An alternative and complementary approach to the oligonucleotide and lexitropsin efforts is the design of ligands of mixed modes of binding. Indeed, many minor-groove binders such as netropsin, distamycin, DAPI [which can also intercalate (*49*, *50*)], berenil, and Hoechst 33258 bind DNA with a powerful AT specificity (*51–60*). A marked

lack of binding to AT-rich sequences is observed with many intercalators [such as ethidium (*61*) and different anthraquinones (*62*) or benzophenanthridines (*63*)], some of which exhibiting a more pronounced GC selectivity [ellipticine (*64, 65*) and acridine derivatives (*66*)]. It should, however, be pointed out here that GC-specific minor-groove binders [such as chromomycin A_3 (*52, 67–70*) and mithramycin (*67, 71–77*)] as well as AT-selective intercalators (*78*) exist. With this in mind, an apparently simple way to associate AT and GC specificities lies in the design of hybrid molecules combining a potentially intercalating heteropolyaromatic moiety with a peptidic or pseudopeptidic groove-binding entity. The aims of such a strategy include increasing intrinsic drug potency as well as controlling the pattern of DNA-sequence-specific recognition. The intricate shape of such hybrid molecules—which we name "combilexins" by analogy with the "lexitropsins"—would provide opportunities for binding in several distinct orientations and modes along the helix.

This interesting and original approach, first introduced by Krivtsora et al. (*79*) and Dervan (*80*) is simple only in appearance because, apart from the complex chemical aspect, the approach is further complicated by drug-induced DNA conformational changes. Indeed, theoretical and experimental studies have both clearly shown that binding to DNA, whatever the nature of the implied process, results in an adaptation of the DNA conformation to that of the ligand and vice versa. In attempting the design of hybrid ligands, it must be kept in mind that intercalators and minor-groove binders affect the DNA backbone conformation in very different ways (*25*) and that the susceptibility of DNA to such changes may vary with the nature of the targeted sequence. Minor-groove binding results in the removal of the ordered water molecules located in AT-rich regions (*81–83*) [a network termed the spine of hydration (*84, 85*)]. Only slight changes in the gross DNA structure was observed, typified by a maximal 2-Å widening of the minor groove, a bending of the helix by 8° per drug molecule, and an unwinding and stiffening of the DNA helix in some extent (*81, 82, 86–89*). In contrast, in order to produce the binding site, intercalators involve a large-scale local structural change such as large unwinding, stiffening, and lengthening of the DNA sugar–phosphate backbone by 3.4 Å per drug molecule. Long-range DNA structural distortions remote from the site of intercalation are also frequently observed, extending over at least four to five base pairs (*90*).

Footprinting studies confirm that intercalation jointly results in sequence-dependent structural changes [probably an increased width of the minor groove (*91*)] in regions surrounding the binding sites and that these can be cooperatively propagated over several turns of the DNA helix (deduced from DNAase I hypersensitivity at these sites). Detailed studies, using echinomycin (*92–96*) and actinomycin D (*51, 97–100*), clearly show that such effects propagate most efficiently through sequences that are relatively unstable to helix melting, such as $d(AT)_n$, i.e. at favored binding sites for minor-groove binders. Therefore, to design a minor-groove binder–intercalator hybrid is thus a challenge, but it is known that DNA can accept two types of binding in a very close proximity (*51, 101–103*).

The scope of this review is not to cover all studies which have been devoted to the development of ligands of mixed modes of binding, but to focus mainly on the design of minor-groove binder–intercalator hybrid molecules and on the binding of these synthetic drugs to nucleic acids. Moreover, it would appear simplistic to design drugs with the expectation that chemotherapeutic selectivity will be improved by virtue of only an increase in sequence selectivity. A direct correlation between DNA-sequence selectivity and antitumor activity has not yet been evidenced. It is at best a hypothesis yet to be tested. Associated factors, such as modulation of topoisomerase activity and cellular uptake, should also be taken into account for the rational design of hybrid ligands. Before discussing the DNA binding properties of recently designed netropsin–intercalator combilexins, it is worth remembering that this new topic has its origin in natural drugs.

NATURALLY OCCURRING HYBRID MOLECULES

Nature provides examples of drugs whose binding to DNA simultaneously implicates various processes. Such is the case for actinomycin D (Figure 1), a natural antitumor agent which consists of a phenoxazone disubstituted by cyclic pentapeptides. Intercalation of actinomycin (*90, 104, 105*) occurs preferentially at some, but not at all, GpC sequences (*51–53, 97–99*) with the cyclic peptides fitting above and below the intercalating ring in the minor groove, each covering three base pairs [strong binding was also shown to occur at non-GpC sites (*106*)]. The symmetrically disposed peptides actively participate in the GC-specific recognition process through hydrogen-bonding interactions between the N-3 atoms and 2-amino groups of the guanines and the amide groups of the threonine residues (*107, 108*). Because of these sequence-specific peptide–DNA interactions, intercalation of the phenoxazone between GC base pairs is strongly preferred only if the 5′-flanking base is a pyrimidine and the 3′-flanking base is not a cytosine (*109*). This mode of binding was used for the rational design of the first intercalator–minor-groove binder hybrid molecule (vide infra).

Such a bimodal binding process has been found in the interaction with DNA of different natural antitumor anthracyclines, typified by daunomycin and doxorubicin (Figure 1). The elucidation of the detailed interaction between these two related drugs and a short DNA duplex by X-ray diffraction analysis (*110–113*) has definitely demonstrated that while the chromophore intercalates CpG steps, the glycan moiety lies in the minor groove. The sugar forms several bonds with DNA and so greatly contributes to the stability of the complex. But its binding is also important in terms of sequence specificity. Solution (*114, 115*), crystallographic (*110–113*), and theoretical studies (*116, 117*) have converged to show that daunomycin preferentially recognizes triplet sequences, 5′-ACG and 5′-TCG being the most preferred. The chromophore intercalates between the CG base pair and the sugar moiety interacts with A or T through several key hydrogen bonds (for comprehensive reviews see refs 118 and 119).

A considerable number of DNA-binding natural products contain carbohydrate residues that are likely to serve as DNA recognition elements. The molecular architecture is even more complicated with another natural anthracycline, nogalamycin (Figure 1), which differs from doxorubicin and daunomycin in that it contains two sugar moieties attached to the chromophore. The binding of nogalamycin to DNA consists of the combination of intercalation of the anthracycline ring and groove binding of the sugar moieties (*120–124*). The nogalose is lying in the minor groove, and the positively charged aminoglucose is lying in the major groove, with the two sugars pointing on the same side of the aglycon ring. Studies on the sequence-specific binding of this compound have not revealed any strongly preferred triplet sequences for nogalamycin binding, as determined for doxorubicin. Foot-

printing experiments (*125*) have demonstrated that its binding sites are located in regions of alternating purine–pyrimidine sequences, most commonly associated to the dinucleotide steps TpG (CpA) and GpT (ApC). Assuming that the drug preferentially intercalates between GpC steps and taking into account the footprinting data, triplet sequences in which a GC dinucleotide is juxtaposed to an A or T residue may certainly provide strong binding sites for nogalamycin. A similar bimodal binding process has been recently evidenced with the anthracycline antibiotic arugomycin (*126*).

Another example of natural drugs presenting these binding characteristics concerns the quinoxaline antibiotics. Quinoxaline antibiotics are a family of antitumor drugs, of which echinomycin (Figure 1) is the best-known member, and in which two quinoxaline-2-carboxylic acid chromophores are attached to a cross-bridged cyclic octapeptide dilactone containing both L- and D-amino acids. This group of compounds include triostin (*127–129*) and synthetic analogues (*130–133*), which have the common properties with echinomycin to bisintercalate with DNA placing the peptide ring into the minor groove. [It should be noted that bisintercalation can also occur through the major groove, as it was demonstrated with the synthetic molecule ditercalinium (*134–136*).] Here again specific hydrogen bonds between the peptide ring and DNA bases are determinant for sequence specific recognition by the drug (for recent and comprehensive reviews, see refs 58, 133, 137, and 138).

The models of echinomycin and triostin A bound to DNA provide instructive examples of drug-induced DNA polymorphism. On the basis of crystallographic data, Wang, Rich, and co-workers (*127–129*) have shown that when the two quinoxalines of triostin A intercalate between the two distal GC base pairs of the DNA hexamer d(CGTACG)$_2$, the central AT bases are paired through Hoogsteen hydrogen bonds (a pairing arrangement where the purines adopt a syn conformation). In solution, the existence of Hoogsteen base pairs in DNA upon binding of echinomycin or triostin A remains controversial. Thus unusual base pairing, first observed in the crystalline state, has been also detected by NMR studies of echinomycin complexed to small oligonucleotides and appears to be highly dependent on the temperature and the DNA sequence. For example, Hoogsteen base pairs have been found in d(GCGC)$_2$ (*68*), d(ACGT)$_2$ (*139*), and d(ACGTACGT)$_2$ (*140*, *141*) complexes but not with d(TCGA)$_2$– and d(TCGATCGA)$_2$–echinomycin complexes. With the octamer of d(ACGTACGT)$_2$, Hoogsteen pairs are formed in the presence of echinomycin with the two terminal and the central AT base pairs at low temperature. But at physiological temperature, only the terminal AT pairs remains Hoogsteen paired while the central ones are converted to either an open or a Watson–Crick base-paired state (*140*). Therefore, if the echinomycin-induced Hoogsteen base pairs seem to appear as an artefact of crystallization, the question is yet not definitively resolved. However, NMR (*68*, *139–141*) and footprinting (*93–96*) studies concur in finding that the binding of echinomycin does not necessarily implicate Hoogsteen pairs. Whatever the exact conformation of the central AT base pairs between the two CpG intercalation sites, clearly the drug induces large changes in DNA conformation which allows close packing of the peptide portion of the molecule in the minor groove against the newly shaped DNA helix, thereby stabilizing the complex via close van der Waals contacts. This example illustrates the fact that the high degree of DNA distortions induced by intercalating agents can be useful and can serve for adjacent minor-groove binding.

Thus actinomycin, doxorubicin, daunomycin, nogalamycin, and the quinoxaline antibiotics are many examples of drugs whose binding to short DNA sequences implicates two processes, intercalation and groove binding simultaneously and in close proximity. Both processes contribute to the affinity and sequence-specific recognition. As a last example (and the list is not exhaustive) supporting this conclusion, we can mention two natural alkylating agents of the enediyne family, dynemicin A (*142*) and neocarzinostatin (Figure 1) (*143*, *144*). They bind DNA by intercalation of their chromophore (naphtoate for neocarzinostatin and anthraquinone for dynemicin), placing their reactive enediyne containing bicyclic core moiety in the minor groove in a suitable position for selective DNA cleavage (these two compounds are primarily DNA-strand cleavers by free-radical mechanism). All these natural compounds could provide models for the rational design of ligands exhibiting mixed modes of binding.

ACRIDINE-LINKED OLIGOPYRROLECARBOXAMIDES

The DNA Target. The two naturally occurring oligopeptides, netropsin and distamycin, are the most frequently used compounds for the synthesis of hybrid molecules. The molecular basis governing their selectivity has been well-elucidated (*81*, *82*, *86*, *145–151*). Their binding, almost exclusively at AT-rich sites, is stabilized by a combination of hydrogen-bonding, van der Waals, and electrostatic interactions. On the other hand, acridines can be considered as the archetype of the intercalators. This heterocycle is not only the first model compound used for the discovery of the intercalation process (*152*, *153*), but because of its synthetic accessibility, it is also certainly the most extensively used intercalator for the design of anticancer drugs (*154–156*). Studies on acridine derivatives have culminated with the synthesis of amsacrine (Figure 1), an anilinoaminoacridine derivative particularly active in the treatment of acute leukemia (*157–160*). Acridines, and amsacrine in particular, are still subject to considerable attention and more efficient analogues are in clinical trials (*161*, *162*).

The first example of acridine-linked netropsin bifunctional mixed ligands was reported by Eliadis et al. (*163*). In the described molecules, the nature of the aliphatic spacer was found to be crucial for the affinities of the hybrid compounds to DNA. The optimum fit was obtained with a butyroyl chain between the 9-amino group of acridine and the 3-amino group of the N-terminal methylpyrrole of distamycin. Although the intercalation of the acridine chromophore and the minor-groove binding of the oligopyrrolecarboxamide part have been demonstrated, footprinting experiments only reveal identical binding site sizes and locations for netropsin and netropsin–acridine hybrids. Only the preference of the pyrrolamide residues for AT-rich regions was shown (*163*).

The influence of the intercalative moiety was clearly shown with other acridine-linked oligopeptide carboxamides. These molecules were built using a combination of the natural antitumor agents distamycin or netropsin and the anilinoacridine chromophore related to the synthetic antileukemic drug amsacrine (*164*). Apart from its evident pharmacological interest, the model of amsacrine was also attractive in our case since it had been postulated (*165*, *166*) that intercalation of the acridine ring was accompanied by minor-groove binding of the adjacent anilino ring [this model has been recently

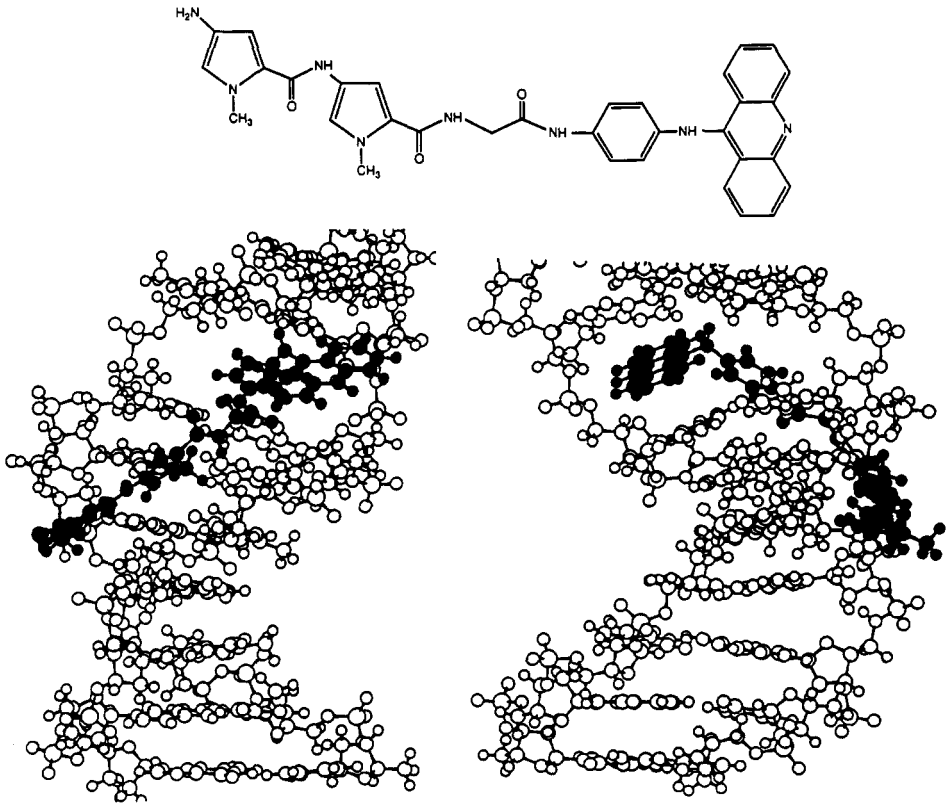


Figure 2. Structure of the netropsin–acridine hybrid compound NetGA. Computer-generated depiction of the binding of NetGA to DNA. The left view shows the minor-groove binding of the bis-pyrrole moiety and the aniline. On the right view, the drug–DNA complex has been rotated in space to focus on the intercalation of the acridine.

questioned and major-groove binding of the aniline is proposed (*167, 168*)]. Based on this assumption, it seemed very interesting to covalently tether netropsin to acridine through attachment on the anilino ring. However CPK models showed that direct linkage of netropsin to the aniline was disfavorable for DNA binding and that a linker was required. The choice of a linker connecting the recognition elements may be a critical design feature with regard to simultaneous binding of all moieties (*80*), so we elaborated a first series of netropsin–acridine hybrid molecules in which the two parts were linked by a glycine connector (*164*). This short tether should provide a frame for anchoring the minor groove moiety in the proper orientation. Their DNA-binding properties were determined using a wide range of biochemical and physicochemical techniques (*164, 169*). Binding data were found to be consistent with a model in which the acridine nucleus occupies an intercalation site and the netropsin or distamycin residue lies in the DNA minor groove.

One of these pseudopeptides, named NetGA (Figure 2), was studied in detail for its DNA-sequence specificity. Complementary strand MPE–Fe(II) footprinting showed that NetGA binds to 5′-AAAT. It is interesting to note that both types of netropsin–acridine ligands [i.e. using aminoacridine (*163*) and anilinoacridine (*169*)] concur in finding that protected sites are of the strict AT type. Regions of enhanced cleavage by MPE, particularly at GC-rich sequences, were observed adjacent to and even remote from the binding site. It is interesting to note that NetGA exhibits a strict preference for AAAT dominated by the oligopeptide moiety at high concentration of ligand and reveals evidence for intercalation of the acridine moiety at lower concentration. Intercalation of the acridine part of NetGA is influenced by the netropsin part. Linear dichroism measurements revealed an insertion of the acridine into the DNA helix with a tilt of about 20° relative to the plane of the DNA base pairs, higher than that measured for the acridine alone and reflecting the influence of the netropsin moiety. Nevertheless, the short spacer glycinyl, in spite of its relative rigidity, was apparently not an obstacle for the binding of the two parts of the molecules. This was further supported by a molecular modeling study which shows not only that minor-groove binding of the netropsin part and intercalation of the acridine can effectively occur simultaneously but also that this bimodal binding process induces a local distortion of the DNA helix near the intercalation site. An energy-minimized model of the NetGA–DNA complex is presented in Figure 2.

Thus the hybrid molecule NetGA interacts with DNA in a well-defined geometry at specific sequences. On the unique basis of DNA specificity, the intercalating moiety of the drug could appear to be useless since the hybrid drug is essentially AT selective as the netropsin half of the hybrid. However, the intercalating chromophore provides a better anchorage of the drug to the DNA helix. At low drug to DNA ratio, the affinity of NetGA for DNA (K_a = 9.1×10^5 M^{-1}) is approximately 3-fold larger than that of netropsin ($K_a = 2.9 \times 10^5$ M^{-1}) (*169*). This also suggests that the two parts of the molecule are bound to DNA. Thus, the intercalating part of NetGA efficiently compensates the absence of the amidine and guanidine side chains of netropsin.

Increase in DNA-sequence specificity would possibly not directly result in an improved antitumor activity. This is borne out by the observation that drugs such as daunomycin, nogalamycin, or echinomycin (Figure 1) exhibit noticeable sequence selectivity but they have therapeutic selectivity beyond what would be expected, based upon mere consideration of DNA-binding specificity. Thus other receptors are determinant (*170*). Future design of DNA-binding ligands will demand a more careful con-

sideration of other cellular targets. In particular there are now clear indications that topoisomerases, among other DNA-binding proteins, represent preferred targets for a large number of anticancer drug acting at the DNA level.

The Topoisomerase Target. Briefly it is worth remembering that topoisomerases are enzymes that alter DNA topology. The two major distinctions between type I and type II topoisomerases are single- versus double-stranded-DNA cleavage and the energy requirement of type II enzymes (for a more precise definition see refs 171–176). Topoisomerases are extremely relevant in the area of human cancers and viral diseases, as these enzymes are privileged targets for a variety of antineoplastic and antiviral agents (*177–186*). These enzymes now appear as one of the most promising target for the design of more active antitumor drugs.

Topoisomerase II introduces a transient double-strand break in the DNA and forms a protein–DNA complex referred to as the cleavable complex. Certain intercalating agents, *m*-AMSA and some related acridines in particular (*187–196*), trap the enzyme at this stage, stabilizing the cleavable complex and thus preventing the restoration of intact DNA structure.

The molecular basis for the design of topoisomerase poisons are yet to be elucidated. However, the most satisfying model to account for the effects of intercalating agents would be able to distinguish between the two functional domains in the drug (*197*). With amsacrine, it is highly suspected that the acridine ring would represent the DNA binding domain and that the aniline would allow the interaction with the topoisomerase II (*198*). Modifications of the protein-binding domain have already been correlated with altered biological properties of the tested ligands. Also it may be interesting to introduce on the aniline ring another substituent known for its capability to interact with the topoisomerases.

In this perspective, the choice of a minor-groove-binding ligand is perfectly justified. Indeed certain minor-groove binders are also to impede the catalytic activity of topoisomerases I (*199*, *200*) and II (*201–203*). Beside the alteration in topoisomerase activity, the effects of minor-groove binders on other DNA-reactive enzymes have been reported (*204–206*). With this in mind, the combination of minor-groove binders and intercalators could be potentially useful as topoisomerase-mediated antitumor agents. Such hybrid drugs would thus be able to target both a DNA sequence (*sequence specificity*) and a DNA conformation which is a consequence of protein–DNA interaction. At present it is not definitively proved that the topoisomerase poisons directly interact with the enzyme. The modulation of the catalytic activity of the enzyme may simply result from ligand-induced DNA structural changes without physical interaction with the proteins. Combilexins, because of their bifunctional mode of binding to DNA, would probably induce particular constraints of the helix structure and thus they could provide interesting tools for the modulation of the topoisomerase activities. For example, the curvature of the DNA upon hybrid-ligand binding may contribute to targeting the topoisomerase I to particular sites (*207*). Thus, in this area too, the design of hybrid ligands offers stimulating opportunites.

Before reaching the DNA target, the drug has to enter the cell easily, to join the nucleus and to bind DNA associated with histones in a nucleosomal structure. The highly ordered structures of DNA in vivo may alter the drug accessibility to DNA, although the drug-targeted DNA is generally believed to be in its nucleosome-free transcriptionally active form. Needless to say, many problems have to be solved to direct the drug selectively toward cancer cells. The intricacy of the mechanism of tumor proliferation significantly increases the complexity of the drug-design problem. It is thus obvious that any chemical strategy, as efficient as it can be, cannot address all the problems simultaneously. However, efforts must be made to consider different putative targets whenever possible.

Cellular Uptake. With hybrid compounds and in particular with longer ligands, the problem of cellular transport will emerge. Poor ability to penetrate the cells is one of the major problems encountered with oligonucleotide-based DNA probes. Therefore, a cellular transport program has to be considered in addition to the DNA-binding unit strategy currently in use. This problem can be addressed through the design of hybrid ligands.

Netropsin exhibits rather slow kinetics of cell penetration and only a moderate amount of drug can be recovered in the nucleus (*208*). On the other hand, acridine derivatives rapidly enter the cells and efficiently accumulate in the nucleus rather than in the cytoplasm (*209*). For this supplementary reason, the coupling of a minor-groove entity to an intercalating chromophore appears extremely interesting. It was effectively shown that the hybrid NetGA penetrates very rapidly into the cell and preferentially concentrates into the nucleus rather than in the cytoplasm. The vector for the nucleus was found to be the acridine chromophore (*210*).

DNA-sequence-specific targeting, modulation of topoisomerase activity, and rapid cellular uptake are complementary effects observed with the netropsin–acridine hybrid molecules. Each half of the molecule has a defined function (sequence specificity by the groove-binding moiety and nuclear targeting by the intercalating moiety). Therefore, with judicious combination, synergistic effects could be expected. Of course the model compound NetGA needs various improvements, essentially to increase its affinity and specificity for definite duplex sequences and to elevate its antitumor activity to a clinically useful level. An approach to reach these two objectives might be to combine netropsin or distamycin entities with very active amsacrine analogues. We are currently examining this possibility. Another way might consist of combining other intercalators with different groove-binding drugs which would lead to efficient synergistic effects. The last section of this article briefly summarizes the recent advances into this subject which undoubtedly shows promise and merits further development.

OTHER GROOVE BINDER–INTERCALATOR HYBRID LIGANDS

Netropsin and distamycin have been subjected to extensive studies aimed at modulating their DNA sequence recognition properties. These modifications include deletion, substitution (*211–217*), or increase in the number of *N*-methylpyrrole units by polymerization of units (*218–221*) or coupling of fragments (*222–229*). In addition, the pyrrole ring has been replaced by other heterocycles such as imidazole (*230–239*), thiazole (*240–245*), furan (*246*), thiophene (*247*), pyridine (*248*), and other heterocycles (*249–256*). Groove-binding entities have also been attached to alkylating agents (*257–264*) or nonintercalating compounds such as metal chelates (*265–267*) and amino acids (*268*).

Similarly, intercalators have been condensed with a variety of agents such as alkylating (*269–282*) or metal-complexing agents (*283–292*), amino acids and peptides

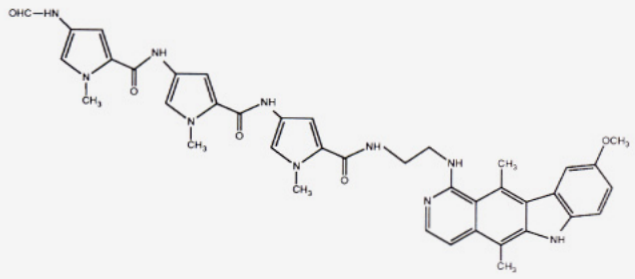


Figure 3. Structure of the distamycin–ellipticine hybrid compound.

(*293–297*), and photoreactive groups (*298* and references cited therein). But to date, very few studies have been devoted to the design of netropsin–intercalator conjugates and, to our knowledge, none to the synthesis of intercalator–minor-groove binder conjugates containing a minor-groove binder other than netropsin.

As already mentioned above, the first hybrid molecule of this class (*79*, *80*) consisted of an actinomycin-like molecule in which two distamycin moieties sandwiched a phenoxazone ring. This hybrid molecule, named "distactin", was shown to span over 10 base pairs. The existence of such a large binding site supported the conclusion that the drug was able to bind DNA by intercalation of its chromophore between a GC step, ideally placing the two distamycin moieties above and below the site of intercalation, presumably in the minor groove, exactly as actinomycin does. Shorter binding sites, consistent with a binding of only one distamycin part to AT-rich sequences, were also located. Even if its biological properties were never reported, this pioneer hybrid model was extremely interesting with respect to its DNA-binding properties and has provided guidelines for the design of other ligands of this class.

Very recently we examined the DNA-binding ability of a distamycin–ellipticine hybrid compound (Figure 3). This agent was built by linking the AT-specific agent distamycin to an ellipticine derivative endowed with marked GC-selective recognition properties (*65*). By means of several complementary spectroscopic techniques, it was clearly demonstrated that the drug intercalates and wedges in the minor groove simultaneously (Figure 4). Its propensity to read DNA sequences was analyzed by DNAase I footprinting experiments. These analyses gave conflicting results compared to those obtained with the acridine-linked netropsin molecules (*163*, *169*) described above. Indeed, with the acridine–netropsin combilexins, the binding sites were confined to AT-rich sequences while, with the distamycin–ellipticine ligand, binding sites mainly consisting of GC-rich sequences were protected from cleavage by DNAase I. This distamycin–ellipticine hybrid compound retains the specificity of the ellipticine moiety alone (*65*). Thus in this case, as in triostin and other related structures, intercalation appears to be the crucial element.

This demonstrates that depending on the nature of the coupled drugs and of the DNA sequences, one or the other of the two binding modes can predominate. An identical situation was recently exposed with an oxazolopyridocarbazole (OPC)–netropsin hybrid (OPC derivatives can be considered as ellipticine analogues) where intercalation and groove binding would be both implicated at AT-rich sequences and where intercalative binding only would be involved at GC-rich sequences (*299*). Here again, while spectroscopic analysis supported the involvement of the two DNA binding modes, footprinting experiments failed to exhibit the complementary effects expected from the coupling of a GC-selective intercalator to a powerful AT-specific groove binder.

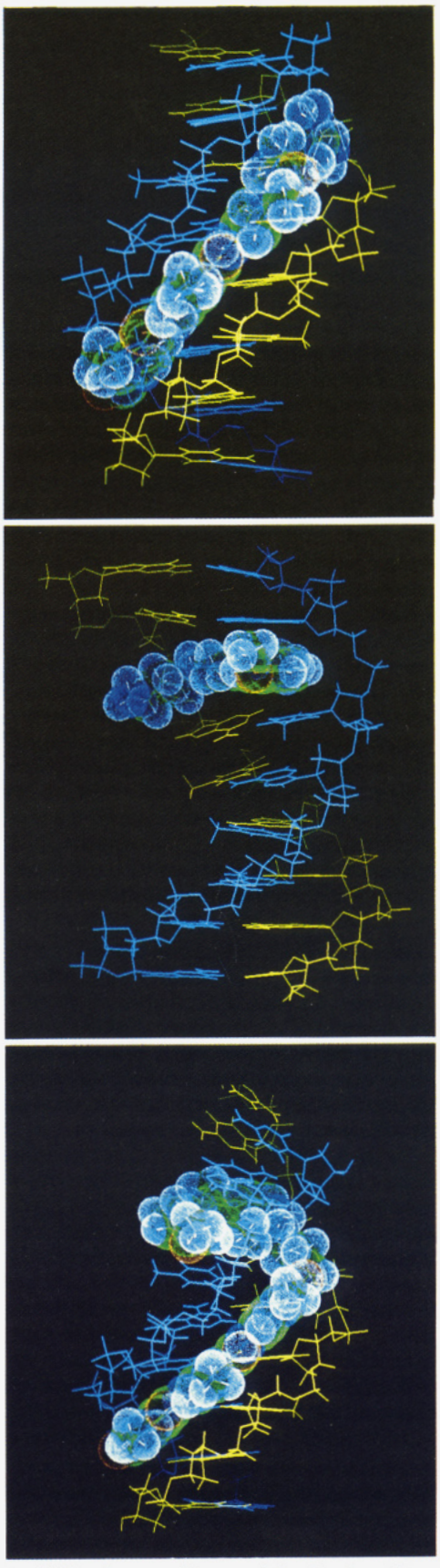


Figure 4. Molecular graphics models showing (from top to bottom) the minor-groove binding of distamycin, the intercalation of ellipticine, and the simultaneous minor-groove binding and intercalation of the distamycin–ellipticine hybrid ligand. Models were constructed using the Jumna package software (by Dr. J. S. Sun).

CONCLUSION

To date our knowledge of the sequence-dependent variation in DNA structure (*300*) and the structural perturbation produced by simultaneous intercalation and groove binding is incomplete and does not allow a full understanding of the subject. It is too early to propose any guidelines for the design of hybrid molecules. With the present state of knowledge, the actual determinant (groove binding or intercalation) for retention of the sequence specificity is not very clear and more extensive analysis for dissociating the two effects is required. The manner in which the two halves of the molecule need to be linked awaits molecular modeling studies and more accurate physical measurements.

Whatever the chemical strategies adopted to decipher and ultimately to control sequence-specific DNA recognition (i.e. triple helix, lexitropsin, and combilexin) it will be necessary to combine our knowledge of the sequence dependence of DNA flexibility and of the ligand-induced DNA structural deformation. Unfortunately, it must also be admitted that the design of ligands capable of attaining sufficient sequence specificity to bind a DNA sites critical for a cell is still a purely conjectural idea and only a small part of the overall problem. Many equally important questions remain to be answered. Inhibition of the DNA repair system, development of a cell-specific delivery system, cellular drug resistance, drug distribution, toxicity, etc., are other topics capable of adding further complexity to this picture. Interdisciplinary approaches are essential.

Many studies, many compounds, and hence much time will be necessary before we may perfectly control the targeting to definite DNA sequences with agents combining different DNA-binding processes. This new topic is a real challenge far from being solved, and during this time, cancer and viral diseases are still booming. But this approach has the merit of being highly rational and as such should deservedly be retained, developed, and improved and hopefully might lead to the discovery of tumor-active compounds.

ACKNOWLEDGMENT

This work has received the financial support from the INSERM and the Association pour la Recherche contre le Cancer. The authors express their gratitude to Dr. J. S. Sun for his invaluable molecular modeling analysis and to E. Sayers for advice.

LITERATURE CITED

(1) Nielsen, P. E. (1991) Sequence-selective DNA recognition by synthetic ligands. *Bioconjugate Chem. 2*, 1–12.

(2) Lyamichev, V. I., Mirkin, S. M., Frank-Kamenetskii, M. D., and Cantor, C. R. (1988) A stable complex between homopyrimidine oligomers and the homologous regions of duplex DNAs. *Nucleic Acids Res. 16*, 2165–2178.

(3) François, J. C., Saison-Behmoaras, T., and Hélène, C. (1988) Sequence-specific recognition of the major groove of DNA by oligodeoxynucleotides via triple helix formation. Footprinting studies. *Nucleic Acids Res. 16*, 11431–11440.

(4) Povsic, T. J., and Dervan, P. B. (1989) Triple helix formation by oligonucleotides on DNA extended to the physiological pH range. *J. Am. Chem. Soc. 111*, 3059–3061.

(5) Griffin, L. C., and Dervan, P. B. (1989) Recognition of thymine-adenine base pairs by guanine in a pyrimidine triple helix motif. *Science 245*, 967–971.

(6) Umemoto, K., Sarma, M. H., Gupta, G., Luo, J., and Sarma, R. H. (1990) Structure and stability of a DNA triple helix in solution: NMR studies on $d(T)_6 \cdot d(A)_6 \cdot d(T)_6$ and its complex with a minor groove binder drug. *J. Am. Chem. Soc. 112*, 4539–4545.

(7) Strobel, S. A., and Dervan, P. B. (1991) Single-site enzymatic cleavage of yeast genomic DNA mediated by triple helix formation. *Nature 350*, 172–174.

(8) Beal, P. A., and Dervan, P. B. (1991) Second structural motif for recognition of DNA by oligonucleotide-directed triple-helix formation. *Science 251*, 1360–1363.

(9) Pilch, D. S., Levenson, C., and Shafer, R. H. (1991) Structure, stability, and thermodynamics of a short intermolecular purine–purine–pyrimidine triple helix. *Biochemistry 30*, 6081–6087.

(10) Le Doan, T., Perrouault, L., Praseuth, D., Habhoub, N., Decout, J. L., Thuong, N. T., Lhomme, J., and Hélène, C. (1987) Sequence-specific recognition, photocrosslinking and cleavage of the DNA double helix by an [α]-thymidylate covalently linked to an azidoproflavine derivative. *Nucleic Acids Res. 15*, 7749–7760.

(11) Praseuth, D., Perrouault, L., Le Doan, T., Chassignol, M., Thuong, N., and Hélène, C. (1988) Sequence-specific binding and photocrosslinking of α and β oligodeoxy nucleotides to the major groove of DNA via triple helix formation. *Proc. Natl. Acad. Sci. U.S.A. 85*, 1349–1353.

(12) Moser, H. E., and Dervan, P. B. (1987) Sequence-specific cleavage of double helical DNA by triple helix formation. *Science 238*, 645–650.

(13) Boidot-Forget, M., Chassignol, M., Takasugi, M., Thuong, N. T., and Hélène, C. (1988) Site-specific cleavage of single-stranded and double-stranded DNA sequences by oligodeoxynucleotides covalently linked to an intercalating agent and an EDTA–Fe chelate. *Gene 72*, 361–371.

(14) François, J. C., Saison-Behmoaras, T., Chassignol, M., Thuong, N. T., and Hélène, C. (1988) Sequence-targeted cleavage of single- and double-stranded DNA by oligothymidylates covalently linked to 1,10-phenanthroline. *J. Biol. Chem. 264*, 5891–5898.

(15) Perrouault, L., Asseline, U., Rivalle, C., Thuong, N. T., Bisagni, E., Giovannangeli, C., Le Doan, T., and Hélène, C. (1988) Sequence-specific artificial photo-induced endonucleases based on triple helix-forming oligonucleotides. *Nature 344*, 358–360.

(16) Strobel, S. A., Moser, H. E., and Dervan, P. B. (1988) Double-strand cleavage of genomic DNA at a single site by triple-helix formation. *J. Am. Chem. Soc. 110*, 7927–7929.

(17) Vlassov, V. V., Gaidamakov, S. A., Zarytova, V. F., Knorre, D. G., Levina, A. S., Nikonova, A. A., Podust, L. M., and Fedorova, O. S. (1988) Sequence-specific chemical modification of double-stranded DNA with alkylating oligodeoxyribonucleotide derivatives. *Gene 72*, 313–322.

(18) Sun, J. S., François, J. C., Montenay-Garestier, T., Saison-Behmoaras, T., Roig, V., Thuong, N. T., and Hélène, C. (1989) Sequence-specific intercalating agents: Intercalation at specific sequences on duplex DNA via major groove recognition by oligonucleotide-intercalator conjugates. *Proc. Natl. Acad. Sci. U.S.A. 86*, 9198–9202.

(19) François, J. C., Saison-Behmoaras, T., Barbier, C., Chassignol, M., Thuong, N. T., Hélène, C. (1989) Sequence-specific recognition and cleavage of duplex DNA via triple-helix formation by oligonucleotides covalently linked to a phenanthroline–copper chelate. *Proc. Natl. Acad. Sci. U.S.A. 86*, 9702–9706.

(20) Corey, D. R., Pei, D., and Schultz, P. G. (1989) Sequence-specific hydrolysis of duplex DNA by an oligonucleotide-directed nuclease. *J. Am. Chem. Soc. 111*, 8523–8525.

(21) Povsic, T. J., and Dervan, P. B. (1990) Sequence-specific alkylation of double-helical DNA by oligonucleotide-directed triple-helix formation. *J. Am. Chem. Soc. 112*, 9428–9430.

(22) Pei, D., Corey, D. R., and Schultz, P. G. (1990) Site-specific cleavage of duplex DNA by a semisynthetic nuclease via triple-helix formation. *Proc. Natl. Acad. Sci. U.S.A. 87*, 9858–9862.

(23) Collier, D. A., Thuong, N. T., and Hélène, C. (1991) Sequence-specific bifunctional DNA ligands based on triple-helix-forming oligonucleotides inhibit restriction enzyme cleavage under physiological conditions. *J. Am. Chem. Soc. 113*, 1457–1458.

(24) Wells, R. D., Collier, D. A., Hanvey, J. C., Shimizu, M., and Wohlrab, F. (1988) The chemistry and biology of unusual DNA structures adopted by oligopurine–oligopyrimidine sequences. *FASEB J. 2*, 2939–2949.

(25) Neidle, S., Pearl, L. H., and Skelly, J. V. (1987) DNA structure and perturbation by drug binding. *Biochem. J. 243*, 1–13.

(26) Ohlendorf, D. H., Anderson, W. F., Fisher, R. G., Takeda, Y., and Matthews, B. W. (1982) The molecular basis of DNA–protein recognition inferred from the structure of cro repressor. *Nature 298*, 718–723.

(27) Pabo, C. O., and Saver, R. T. (1984) Protein–DNA recognition. *Ann. Rev. Biochem. 53*, 293–321.

(28) Ollis, D. L., and White, S. W. (1987) Structural basis of protein-nucleic acid interactions. *Chem. Rev. 87*, 981–995.

(29) Schleif, R. (1987) DNA binding by proteins. *Science 241*, 1182–1187.

(30) Travers, A. A. (1989) DNA conformation and protein binding. *Annu. Rev. Biochem. 58*, 427–452.

(31) Brennan, R. G., and Matthews, B. W. (1989) Structural basis of DNA–protein recognition. *Trends Biol. Sci. 14*, 286–290.

(32) Sluka, J. P., Horwath, S. J., Glasgow, A. C., Simon, M. I., and Dervan, P. B. (1990) Importance of minor groove contacts for recognition of DNA by the binding domain of Hin recombinase. *Biochemistry 29*, 6551–6561.

(33) Segers, A., Wyns, L., and Lasters, I. (1991) A model for histone H5-DNA interaction: simultaneous minor and major groove binding. *Biochem. Biophys. Res. Commun. 174*, 898–902.

(34) Churchill, M. E. A., and Travers, A. A. (1991) Protein motifs that recognize structural features of DNA. *Trends Biol. Sci. 16*, 92–97.

(35) Friedman, D. I. (1988) Integration host factor: A protein for all reasons. *Cell 55*, 545–554.

(36) Bonnefoy, E., and Rouviere-Yaniv, J. (1991) HU and IHF, two homologous histone-like proteins of *Escherichia coli*, form different protein–DNA complexes with short DNA fragments. *EMBO J. 10*, 687–696.

(37) Zimmer, C., and Wahnert, U. (1986) Non-intercalating DNA-binding ligands: Specificity of the interaction and there use as tools in biophysical, biochemical and biological investigations of the genetic material. *Prog. Biophys. Mol. Biol. 47*, 31–112.

(38) Goodsell, D., and Dickerson, R. E. (1986) Isohelical analysis of DNA groove-binding drugs. *J. Mol. Biol. 29*, 727–733.

(39) Zimmer, C., Luck, G., Burckhardt, G., Krowicki, K., and Lown, J. W. (1986) The molecular mechanism of interaction of non-intercalative groove binding antitumor drugs with DNA. *Molecular Mechanisms of Carcinogenic and Antitumor Activity* (C. Chagas, and B. Pullman, Eds.) pp 339–363, Adenine Press, New York.

(40) Dervan, P. B. (1986) Design of synthetic sequence specific DNA binding molecules. *Molecular Mechanisms of Carcinogenic and Antitumor Activity* (C, Chagas, and B. Pullman, Eds.) pp 365–384, Adenine Press, New York.

(41) Lown, J. W. (1988) Lexitropsins: rational design of DNA sequence reading agents as novel anti-cancer agents and potential cellular probes. *Anti-Cancer Drug Des. 3*, 25–40.

(42) Lown, J. W. (1989) Synthetic chemistry of naturally occuring oligopeptide antibiotics and related lexitropsins. *Org. Prep. Proc. Int. 21*, 1–46.

(43) Zakrzewska, K., Lavery, R., and Pullman, B. (1983) Theoretical studies of the selective binding to DNA of two non-intercalating ligands: netropsin and SN 18071. *Nucleic Acids Res. 11*, 8825–8839.

(44) Zakrzewska, K., and Pullman, B. (1983) A theoretical evaluation of the effect of netropsin binding on the reactivity of DNA towards alkylating agents. *Nucleic Acids Res. 11*, 8841–8845.

(45) Gago, F., Reynolds, C. A., and Richards, W. G. (1989) The binding of non intercalative drugs to alternating DNA sequences. *Mol. Pharmacol. 35*, 232–241.

(46) Drew, H. R., and Travers, A. A. (1984) DNA structural variations in the E. coli *tyr* T promoter. *Cell 37*, 491–502.

(47) Laughton, C. A., Jenkins, T. C., Fox, K. R., and Neidle, S. (1990) Interaction of berenil with the *tyrT* DNA sequence studied by footprinting and molecular modelling. Implications for the design of sequence-specific DNA recognition agents. *Nucleic Acids Res. 18*, 4479–4488.

(48) Zakrzewska, K., Randrianarivelina, M., and Pullman, B. (1988) Drug recognition of DNA. Proposal for GC minor groove specific ligands: Vinylexins. *J. Biomol. Struct. Dyn. 6*, 331–344.

(49) Wilson, W. D., Tanious, F. A., Barton, H. J., Strekowski, L., and Boykin, D. W. (1989) Binding of 4′-6-diamidino-2-phenylindole (DAPI) to GC and mixed sequences in DNA: Intercalation of a classical groove-binding molecules. *J. Am. Chem. Soc. 111*, 5008–5010.

(50) Wilson, W. D., Tanious, F. A., Barton, H. J., Jones, R. L., Fox, K. R., Wydra, R. L., and Strekowski, L. (1990) DNA sequence dependent binding modes of 4′,6-diamidino-2-phenylindole (DAPI). *Biochemistry 29*, 8452–8461.

(51) Lane, M. J., Dabrowiak, J. C., and Vournakis, J. N. (1983) Sequence specificity of actinomycin D and netropsin binding to pBR322 DNA analyzed by protection from DNase I. *Proc. Natl. Acad. Sci. U.S.A. 80*, 3260–3264.

(52) Van Dyke, M. W., and Dervan, P. B. (1983) Methidiumpropyl-EDTA-Fe(II) and DNAase I footprinting report different small molecule binding site sizes on DNA. *Nucleic Acids Res. 11*, 5555–5567.

(53) Van Dyke, M. W., Hertzberg, R. P., and Dervan, P. B. (1983) Map of distamycin, netropsin, and actinomycin binding sites on heterogeneous DNA: DNA cleavage-inhibition patterns with methidiumpropyl-EDTA-Fe(II). *Proc. Natl. Acad. Sci. U.S.A. 79*, 5470–5474.

(54) Harshman, K. D., and Dervan, P. B. (1985) Molecular recognition of B-DNA by Hoescht 33258. *Nucleic Acids Res. 13*, 4825–4835.

(55) Portugal, J., and Waring, M. J. (1987) Comparison of binding sites in DNA for berenil, netropsin and distamycin. A footprinting study. *Eur. J. Biochem. 167*, 281–289.

(56) Portugal, J., and Waring, M. J. (1987) Hydroxyl radical footprinting of the sequence-selective binding of netropsin and distamycin to DNA. *FEBS Lett. 225*, 195–200.

(57) Fox, K. R., and Waring, M. J. (1987) The use of micrococcal nuclease as a probe for drug-binding sites on DNA. *Biochim. Biophys. Acta 909*, 145–155.

(58) Ward, B., Rehfuss, R., and Dabrowiak, J. C. (1987) Quantitative footprinting analysis of the netropsin–DNA interaction. *J. Biomol. Struct. Dyn. 4*, 685–695.

(59) Portugal, J., and Waring, M. J. (1988) Assignment of DNA binding sites for 4′,6-diamidine-2-phenylindole and bisbenzimide (Hoechst 33258). A comparative footprinting study. *Biochim. Biophys. Acta 949*, 158–168.

(60) Churchill, M. E. A., Hayes, J. J., and Tullius, T. D. (1990) Detection of drug binding to DNA by hydroxyl radical footprinting. Relationship of distamycin binding sites to DNA structure and positioned nucleosomes on 5S RNA genes of xenopus. *Biochemistry 29*, 6043–6050.

(61) Fox, K. R., and Waring, M. J. (1987) Footprinting at low temperature: Evidence that ethidium and other simple intercalators can discriminate between different nucleotide sequences. *Nucleic Acids Res. 15*, 491–507.

(62) Fox, K. R., Waring, M. J., Brown, J. R., and Neidle, S. (1986) DNA sequence preferences for anti-cancer drug mitoxanthrone and related anthraquinones revealed by DNasel footprinting. *FEBS Lett. 202*, 289–294.

(63) Bajaj, N. P. S., McLean, M. J., Waring, M. J., and Smekal, E. (1990) Sequence-selective pH-dependent binding to DNA of benzophenanthridine alkaloids. *J. Mol. Recognit. 3*, 48–54.

(64) Schwaller, M. A., Aubard, J., Auclair, C., Paoletti, C., and Dodin, G. (1989) The GC base-pair preference of 2-*N*-methyl 9-hydroxyellipticinium. *Eur. J. Biochem. 181*, 129–134.

(65) Bailly, C., OhUigin, C., Rivalle, C., Bisagni, E., Hénichart, J. P., and Waring, M. J. (1990) Sequence-selective binding of an ellipticine derivative to DNA. *Nucleic Acids Res. 18*, 6283–6291.

(66) Bailly, C., Denny, W. A., Mellor, L. E., Wakelin, L. P. G., and Waring, M. J. Sequence-specificity of the binding of antitumor amsacrine-4-carboxamides to DNA studied by DNAase I footprinting. *Biochemistry*, submitted.

(67) Van Dyke, M. W., Dervan, P. B. (1983) Chromomycin, mithramycin, and olivomycin binding sites on heterogeneous deoxiribonucleic acid. Footprinting with (methidiumpropyl-EDTA)iron(II). *Biochemistry 22*, 2373–2377.

(68) Gao, X., and Patel, D. J. (1989) Antitumor drug-DNA interactions: NMR studies of echinomycin and chromomycin complexes. *Q. Rev. Biophys. 22*, 93–138.
(69) Gao, X., and Patel, D. J. (1989) Chromomycin dimer-DNA oligomere complexes. Sequence selectivity and divalent cation specificity. *Biochemistry 29*, 10940–10956.
(70) Sakaguchi, R., Katahira, M., Kyogoku, Y., and Fujii, S. (1991) An NMR study on the conformation of a deoxyribonucleotide duplex, $d(GGGGCCCC)_2$, and its complex with chromomycin. *J. Biochem. 109*, 317–327.
(71) Banville, D. L., Keniry, M. A., and Shafer, R. H. (1990) NMR investigation of mithramycin A binding to $d(ATGCAT)_2$: A comparative study with chromomycin A3. *Biochemistry 29*, 9294–9304.
(72) Fox, K. R., and Howarth, N. R. (1985) Investigations into the sequence-selective binding of mithramycin and related ligands to DNA. *Nucleic Acids Res. 13*, 8695–8714.
(73) Sarker, M., and Chen, F. M. (1989) Binding of mithramycin to DNA in the presence of second drugs. *Biochemistry 28*, 6651–6657.
(74) Cons, B. M. G., and Fox, K. R. (1989) Interaction of mithramycin with metal ions and DNA. *Biochem. Biophys. Res. Commun. 160*, 517–524.
(75) Cons, B. M. G., and Fox, K. R. (1989) High resolution hydroxyl radical footprinting of the binding of mithramycin and related antibiotics to DNA. *Nucleic Acids Res. 17*, 5447–5459.
(76) Cons, B. M. G., and Fox, K. R. (1990) Footprinting studies of sequence recognition by mithramycin. *Anti-Cancer Drug Des. 5*, 93–97.
(77) Cons, B. M. G., and Fox, K. R. (1991) Effects of the antitumor antibiotic mithramycin on the structure of repetitive DNA regions adjacent to its GC-rich binding site. *Biochemistry 30*, 6314–6321.
(78) Wilson, W. D., Wang, Y. H., Kusuma, S., Chandrasekaran, S., Yang, N. C., and Boykin, D. W. (1985) Binding strength and specificity in DNA interactions: the design of AT specific intercalators. *J. Am. Chem. Soc. 107*, 4989–4995.
(79) Krivtsora, M. A., Moroshkina, E. B., and Glibin, E. (1984) DNA interaction with low molecular weight ligands with different structures. III. Complexes of DNA with distactins. *Mol. Biol. 18*, 950–956.
(80) Dervan, P. B. (1986) Design of sequence-specific DNA-binding molecules. *Science 232*, 464–471.
(81) Kopka, M. L., Yoon, C., Goodsell, D., Pjura, P., and Dickerson, R. E. (1985) The molecular origin of DNA-drug specificit in netropsin and distamycin. *Proc. Natl. Acad. Sci. U.S.A. 82*, 1376–1380.
(82) Kopka, M. L., Yoon, C., Goodsell, D., Pjura, P., and Dickerson, R. E. (1985) Binding of an antitumor drug to DNA: Netropsin and $CGCGAATT^{Br}CGCG$. *J. Mol. Biol. 183*, 553–563.
(83) Patel, D. J., and Shapiro, L. (1986) Sequence-dependent recognition of DNA duplexes. *J. Biol. Chem. 261*, 1230–1240.
(84) Dickerson, R. E., and Drew, H. R. (1981) Structure of a B-DNA dodecamer. II. Influence of base sequence on helix structure. *J. Mol. Biol. 149*, 761–786.
(85) Drew, H. R., and Dickerson, R. E. (1981) Structure of a B-DNA dodecamer. III. Geometry of hydration. *J. Mol. Biol. 151*, 535–556.
(86) Klevit, R. E., Wemmer, D. E., and Reid, B. R. (1986) ^1H NMR studies on the interaction between distamycin A and a symmetrical DNA dodecamer. *Biochemistry 25*, 3296–3303.
(87) Carrondo, M. A. A., de C. T., Coll, M., Aymami, J., Wang, A. H. J., Van der Marel, G. A., Van Boom, J. H., and Rich, A. (1989) Binding of a Hoechst dye to d(CGCGATATCGCG) and its influence on the conformation of the DNA fragment. *Biochemistry 28*, 7849–7859.
(88) Pjura, P. E., Grzeskoniak, K., and Dickerson, R. E. (1987) Binding of Hoechst 33258 to the minor groove of B-DNA. *J. Mol. Biol. 197*, 257–271.
(89) Larsen, T. A., Goodsell, D. S., Cascio, D., Grezeskowiak, K., and Dickerson, R. E. (1989) The structure of DAPI bound to DNA. *J. Biomol. Struct. Dyn. 7*, 477–491.
(90) Neidle, S., and Abraham, Z. (1984) Structural and sequence-dependent aspects of drug intercalation into nucleic acids. *CRC Crit. Rev. Biochem. 17*, 73–121.
(91) Fox, K. R., and Waring, M. J. (1984) DNA structural variations produced by actinomycin and distamycin as revealed by DNAase I footprinting. *Nucleic Acids Res. 12*, 9271–9285.
(92) Low, C. M. L., Drew, H. R., and Waring, M. J. (1984) Sequence-specific binding of echinomycin to DNA: evidence for conformational changes affecting flanking sequences. *Nucleic Acids Res. 12*, 4865–4879.
(93) Portugal, J., Fox, K. R., McLean, M. J., Richenberg, J. L., and Waring, M. J. (1988) Diethyl pyrocarbonate can detect a modified DNA structure induced by the binding of quinoxaline antibiotics. *Nucleic Acids Res. 16*, 3655–43670.
(94) McLean, M. J., and Waring, M. J. (1988) Chemical probes reveal no evidence of Hoogsteen base pairing in complexes formed between echinomycin and DNA in solution. *J. Mol. Recog. 1*, 138–151.
(95) McLean, M. J., Seela, F., and Waring, M. J. (1989) Echinomycin-induced hypersensitivity to osmium tetroxide of DNA fragments incapable of forming Hoogsteen base pairs. *Proc. Natl. Acad. Sci. U.S.A. 86*, 9687–9691.
(96) Fox, K. R., and Kentebe, E. (1990) Echinomycin binding to the sequence CG(AT)nCG alters the structure of the central AT region. *Nucleic Acids Res. 18*, 1957–1963.
(97) Lane, M. J., LaPlante, S. R., Rehfuss, R. P., Borer, P. N., and Cantor, C. R. (1987) Actinomycin D facilitates transition of AT domains in molecules of sequence $(AT)_nAGCT(AT)_n$ to a DNAse I detectable alternating structure. *Nucleic Acids Res. 15*, 839–852.
(98) Huang, Y. Q., Rehfuss, R. P., LaPlante, S. R., Boudreau, E., Borer, P. N., and Lane, M. J. (1988) Actinomycin D induced DNase I cleavage enhancement caused by sequence specific propagation of an altered DNA structure. *Nucleic Acids Res. 16*, 11125–11137.
(99) Bishop, K. D., Borer, P. N., Huang, Y. Q., and Lane, M. J. (1991) Actinomycin D induced DNase I hypersensitivity and asymmetric structure transmission in a DNA hexadecamer. *Nucleic Acids Res. 19*, 871–875.
(100) Waterloh, K., and Fox, K. R. (1991) The effects of actinomycin on the structure of $dA_n{\cdot}dT_n$ and $(dA\text{-}dT)_n$ regions surrounding its GC binding site. *J. Biol. Chem. 266*, 6381–6388.
(101) Wartell, R. M., Larson, J. E., and Wells, R. D. (1975) The compatibility of netropsin and actinomycin binding to natural deoxyribonucleic acid. *J. Biol. Chem. 250*, 2698–2702.
(102) Patel, D. J., Pardi, A., and Itakura, K. (1982) DNA conformation, dynamics, and interactions in solution. *Science 216*, 581–590.
(103) Patel, D. J., Kozlowski, S. A., Rice, J. A., Broka, C., and Itakura, K. (1981) Mutual interaction between adjacent dG·dC actinomycin binding sites and dA·dT netropsin binding sites on the self-complementary d(CGCGAATTCGCG) duplex in solution. *Proc. Natl. Acad. Sci. U.S.A. 78*, 7281–7284.
(104) Takusagawa, F., Dabrow, M., Neidle, S., and Berman, H. M. (1982) The structure of a pseudo intercalated complex between actinomycin and the DNA binding sequence d(GpC). *Nature 296*, 466–469.
(105) Brown, S. C., Mullis, K., Levenson, C., and Shafer, R. H. (1984) Aqueous solution structure of an intercalated actinomycin D-dATGCAT complex by two-dimensional and one-dimensional proton NMR. *Biochemistry 23*, 403–408.
(106) Snyder, J. G., Hartman, N. G., Langlois D'Estantoit, B., Kennard, O., Remeta, D. P., and Breslauer, K. J. (1989) Binding of actinomycin D to DNA: Evidence for a nonclassical high-affinity binding mode that does not require GpC sites. *Proc. Natl. Acad. Sci. U.S.A. 86*, 3968–3972.
(107) Scott, E. V., Zon, G., Marzilli, L. G., and Wilson, W. D. (1988) 2D NMR investigation of the binding of the anticancer drug actinomycin D to duplexed dATCGCGAT: Conformational features of the unique 2:1 adduct. *Biochemistry 27*, 7940–7951.
(108) Scott, E. V., Jones, R. L., Banville, D. L., Zon, G., Marzilli, L. G., and Wilson, W. D. (1988) ^1H and ^{31}P NMR investigations of actinomycin D binding selectivity with oligodeoxyribonucleotides containing multiple adjacent d(GC) sites. *Biochemistry 27*, 915–923.
(109) Rill, R. L., Marsch, G. A., and Graves, D. E. (1989) 7-Azidoactinomycin D: a photoaffinity probe of the sequence spec-

ificity of DNA binding by actinomycin D. *J. Biomol. Struct. Dyn. 7*, 591–605.
(110) Quigley, G. J., Wang, A. H. J., Ughetto, G., Van der Marel, G. A., Van Boom, J. H., and Rich, A. (1980) Molecular structure of an anticancer drug–DNA complex: Daunomycin plus d(CpGpTpApCpG). *Proc. Natl. Acad. Sci. U.S.A. 77*, 7204–7208.
(111) Wang, A. H. J., Ughetto, G., Quigley, G. J., and Rich, A. (1987) Interactions between an anthracycline antibiotic and DNA: Molecular structure of daunomycin complexed to d(CpGpTpApCpG) at 1.2-Å resolution. *Biochemistry 26*, 1152–1163.
(112) Holbrook, S. R., Wang, A. H. J., Rich, A., and Kim, S. H. (1988) Local mobility of nucleic acids as determined from crystallographic data. III. A daunomycin–DNA complex. *J. Mol. Biol. 199*, 349–357.
(113) Frederick, C. A., Williams, L. D., Ughetto, G., van der Marel, G. A., van Boom, J. H., Rich, A., and Wang, A. H. J. (1990) Structural comparison of anticancer drug–DNA complexes: Adriamycin and daunomycin. *Biochemistry 29*, 2538–2549.
(114) Chaires, J. B., Fox, K. R., Herrera, J. E., Britt, M., and Waring, M. J. (1987) Site and sequence specificity of the daunomycin–DNA interaction. *Biochemistry 26*, 8227–8236.
(115) Chaires, J. B., Herrera, J. E., and Waring, M. J. (1990) Preferential binding of daunomycin to 5′A/TCG and 5′A/TGC sequences revealed by footprinting titration experiments. *Biochemistry 29*, 6145–6153.
(116) Gresh, N., Pullman, B., and Arcamone, F. (1985) A theoretical investigation on the sequence selective binding of daunomycin to double-stranded polynucleotides. *J. Biomol. Struct. Dyn. 3*, 445–466.
(117) Gresh, N., Pullman, B., Arcamone, F., Menozzi, M., and Tonani, R. (1989) Joint experimental and theoretical investigation of the comparative DNA binding affinities of intercalating anthracycline derivatives. *Mol. Pharmacol. 35*, 251–256.
(118) Chaires, J. B. (1990) Biophysical chemistry of the daunomycin–DNA interaction. *Biophys. Chem. 35*, 191–202.
(119) Chaires, J. B. (1990) Daunomycin binding to DNA: from the macroscopic to the microscopic. *Molecular Basis of Specificity in Nucleic Acid–Drug Interactions* (B. Pullman, and J. Jortner, Eds.) pp 225–245, Kluwer Academic Publishers, Dordrecht, Netherlands.
(120) Searle, M. S., Hall, J. G., Denny, W. A., and Wakelin, L. P. G. (1988) NMR studies of the interactions of the antibiotic nogalamycin with the hexadeoxyribonucleotide duplex d(5′-GCATGC)$_2$. *Biochemistry 27*, 4340–4349.
(121) Liaw, Y. C., Gao, Y. G., Robinson, H., Van der Marel, G. A., van Boom, J. H., and Wang, A. H. J. (1989) Antitumor drug nogalamycin binds DNA in both grooves simultaneously: Molecular structure of nogalamycin–DNA complex. *Biochemistry 28*, 9913–9918.
(122) Gao, Y. G., Liaw, Y. C., Robinson, H., and Wang, A. H. J. (1990) Binding of the antitumor drug nogalamycin and its derivatives to DNA: structural comparison. *Biochemistry 29*, 10307–10316.
(123) Williams, L. D., Egli, M., Gao, Q., Bash, P., Van der Marel, G. A., Van Boom, J. H., Rich, A., and Frederick, C. A. (1990) Structure of nogalamycin bound to a DNA hexamer. *Proc. Natl. Acad. Sci. U.S.A. 87*, 2225–2229.
(124) Egli, M., Williams, L. D., Frederick, C. A., and Rich, A. (1991) DNA–nogalamycin interactions. *Biochemistry 30*, 1364–1372.
(125) Fox, K. R., and Waring, M. J. (1986) Nucleotide sequence binding preferences of nogalamycin investigated by DNAase I footprinting. *Biochemistry 25*, 4349–4356.
(126) Searle, M., Bicknell, W., Wakelin, L. P. G., and Denny, W. A. (1991) Anthracycline antibiotic arugomycin binds in both grooves of the DNA helix simultaneously: An NMR and molecular modelling study. *Nucleic Acids Res. 19*, 2897–2906.
(127) Wang, A. H. J., Ughetto, G., Quigley, G. J., Hakoshima, T., Van der Marel, G. A., Van Boom, J. H., and Rich, A. (1984) The molecular structure of a DNA–Triostin A complex. *Science 225*, 1115–1121.
(128) Ughetto, G., Wang, A. H. J., Quigley, G. J., Van der Marel, G. A., Van Boom, J. H., and Rich, A. (1985) A comparison of the structure of echinomycin and triostin A complexed to a DNA fragment. *Nucleic Acids Res. 13*, 2305–2323.
(129) Quigley, G. J., Ughetto, G., Van der Marel, G. A., Van Boom, J. H., Wang, A. H. J., and Rich, A. (1986) Non-Watson-Crick G·C and A·T base pairs in a DNA–antibiotic complex. *Science 232*, 1255–1258.
(130) Bernier, J. L., Hénichart, J. P., and Catteau, J. P. (1981) Design, synthesis and DNA-binding capacity of a new peptidic bifunctional intercalating agent. *Biochem. J. 199*, 479–484.
(131) Helbecque, N., Bernier, J. L., and Hénichart, J. P. (1985) Design of a new DNA-polyintercalating drug, a bisacridinyl peptidic analogue of Triostin A. *Biochem. J. 225*, 829–832.
(132) Viswamitra, M. A., Kennard, O., Cruse, W. B. T., Egert, E., Sheldrick, G. M., Jones, P. G., Waring, M. J., Wakelin, L. P. G., and Olsen, R. K. (1981) Structure of TANDEM and its implication for bifunctional intercalation into DNA. *Nature 289*, 817–819.
(133) Wakelin, L. P. G. (1986) Polyfunctional DNA intercalating agents. *Med. Res. Rev. 6*, 275–340.
(134) Delbarre, A., Delepierre, M., D'Estaintot, B. L., Igolen, J., and Roques, B. P. (1987) Bisintercalation of ditercalinium into a d(CGCG) minihelix: Structure and dynamic aspects—A 400 MHz NMR study. *Biopolymers 26*, 1001–1033.
(135) Delbarre, A., Delepierre, M., Garbay, C., Igolen, J., Le Pecq, J. B., and Roques, B. P. (1987) Geometry of the antitumor drug ditercalinium bis intercalated into d(CpGpCpG)$_2$ by ^{1}H NMR. *Proc. Natl. Acad. Sci. U.S.A. 84*, 2155–2159.
(136) Maroun, R. C., and Roques, J. B. (1991) Induction of DNA bending by bifunctional intercalating agents of the 7H-pyridocarbazole family. *Biophys. Chem. 39*, 45–56.
(137) Waring, M. J. (1986) Recognition of DNA by quinoxaline antibiotics. *Molecular Mechanisms of Carcinogenic and Antitumor Activity* (C. Chagas, B. Pullman, Eds.) pp 317–337, Adenine Press, New York.
(138) Waring, M. J. (1990) The molecular basis of specific recognition between echinomycin and DNA. *Molecular Basis of Specificity in Nucleic Acid–Drug Interactions* (B. Pullman, and J. Jortner, Eds.) pp 225–245, Kluwer Academic Publishers, Dordrecht, Netherlands.
(139) Gao, X., and Patel, D. J. (1988) NMR studies of echinomycin bisintercalation complexes with d(A1-C2-G3-T4) and d(T1-C2-G3-A4) duplexes in aqueous solution: Sequence-dependent formation of Hoogsteen A1·T4 and Watson–Crick T1·A4 base pairs flanking the bisintercalation site. *Biochemistry 27*, 1744–1751.
(140) Gilbert, D. A., van der Marel, G. A., van Boom, J. H., and Feigon, J. (1989) Unstable Hoogsteen base pairs adjacent to echinomycin binding sites within a DNA duplex. *Proc. Natl. Acad. Sci. U.S.A. 86*, 3006–3010.
(141) Gilbert, D. E., and Feigon, J. (1991) The DNA sequence at echinomycin binding sites determines the structural changes induced by drug binding: NMR studies of echinomycin binding to [d(ACGTACGT)]$_2$ and [d(TCGATCGA)]$_2$. *Biochemistry 30*, 2483–2494.
(142) Sugiura, Y., Shiraki, T., Konishi, M., and Oki, T. (1990) DNA intercalation and cleavage of an antitumor antibiotic dynemicin that contains anthracycline and enediyne cores. *Proc. Natl. Acad. Sci. U.S.A. 87*, 3831–3835.
(143) Dasgupta, D., and Goldberg, I. H. (1986) Mode of reversible binding of neocarzinostatin chromophore to DNA: Base sequence dependency of binding. *Nucleic Acid Res. 14*, 1089–1105.
(144) Lee, S. H., and Goldberg, I. H. (1989) Sequence-specific, strand-selective, and directional binding of neocarzinostatin chromophore to oligodeoxyribonucleotides. *Biochemistry 28*, 1019–1026.
(145) Patel, D. J. (1982) Antibiotic–DNA interactions: intermolecular nuclear Overhauser effects in the netropsin-d(CGCGAATTCGCG) complex in solution. *Proc. Natl. Acad. Sci. U.S.A. 79*, 6424–6428.
(146) Marky, L. A., and Breslauer, K. J. (1987) Origins of netropsin binding affinity and specificity: Correlation of thermodynamic and structural data. *Proc. Natl. Acad. Sci. U.S.A. 84*, 4359–4363.
(147) Coll, M., Aymami, J., Van der Marel, G. A., Van Boom, J. H., Rich, A., and Wang, A. H. J. (1989) Molecular structure

of the netropsin–d(CGCGATATCGCG) complex: DNA conformation in an alternating AT segment. *Biochemistry 28*, 310–320.
(148) Pelton, J. G., and Wemmer, D. E. (1990) Binding modes of distamycin A with d(CGCAAATTTGCG)$_2$ determined by two-dimensional NMR. *J. Am. Chem. Soc. 112*, 1393–1399.
(149) Caldwell, J., and Kollman, P. A. (1986) A molecular mechanical study of netropsin–DNA interactions. *Biopolymers 25*, 249–266.
(150) Coll, M., Frederick, C. A., Wang, A. H. J., and Rich, A. (1987) A bifurcated hydrogen bonded conformation in the d(A·T) base pairs of the DNA dodecamer of d(CGCAATTGCG) and its complex with distamycin. *Proc. Natl. Acad. Sci. U.S.A. 84*, 8385–8389.
(151) Boehncke, K., Nonella, M., Schulten, K., and Wang, A. H. J. (1991) Molecular dynamics investigation of the interaction between DNA and distamycin. *Biochemistry 30*, 5465–5475.
(152) Lerman, L. S. (1961) Structural considerations in the interaction of DNA and acridines. *J. Mol. Biol. 3*, 18–30.
(153) Lerman, L. S. (1963) The structure of the DNA–acridine complex. *Proc. Natl. Acad. Sci. U.S.A. 49*, 94–105.
(154) Denny, W. A., Baguley, B. C., Cain, B. F., and Waring, M. J. (1983) Antitumour acridines. *Molecular Aspects of Anticancer Drug Action* (S. Neidle, and M. J. Waring, Eds.) pp 1–34, Verlag Chemie, Sutton, England.
(155) Denny, W. A. (1990) DNA-intercalating ligands as anticancer drugs: Prospects for future design. *Anti-Cancer Drug. Des. 4*, 241–263.
(156) Baguley, B. C. (1991) DNA intercalating anti-tumour agents. *Anti-Cancer Drug. Des. 6*, 1–35.
(157) Arlin, Z. (1983) Current status of amsacrine combination chemotherapy programs in acute leukemia. *Cancer Treat. Rep. 67*, 969–970.
(158) Louie, A. C., and Issell, B. F. (1985) Amsacrine (AMSA)—A clinical review. *J. Clin. Oncol. 3*, 562–592.
(159) Zittoun, R. (1985) *m*-AMSA: A review of clinical data. *Eur. J. Cancer Clin. Oncol. 21*, 649–653.
(160) Cassileth, P. A., and Gale, R. P. (1986) Amsacrine: A review. *Leukemia Res. 10*, 1257–1265.
(161) Leopold, W. R., III, Corbett, T. H., Griswold, D. P., Plowman, J., and Baguley, B. C. (1987) Experimental antitumor activity of the amsacrine analogue CI-921. *J. Natl. Cancer Inst. 79*, 343–349.
(162) Hardy, J. R., Harvey, V. J., Paxton, J. W., Evans, P., Smith, S., Grove, W., Grillo-Lopex, A. J., and Baguley, B. C. (1988) A phase I trial of the amsacrine analog 9-[[2-methoxy-4-[(methylsulfonyl)amino]phenyl]amino]-*N*,5-dimethyl-4-acridinecarboxamide (CI-921). *Cancer Res. 48*, 6593–6596.
(163) Eliadis, A., Phillips, D. R., Reiss, J. A., and Skorobogaty, A. (1988) The synthesis and DNA footprinting of acridine-linked netropsin and distamycin bifunctional mixed ligands. *J. Chem. Soc., Chem. Commun.* 1049–1052.
(164) Bailly, C., Pommery, N., Houssin, R., and Hénichart, J. P. (1989) Design, synthesis, DNA binding and biological activity of a series of DNA minor-groove-binding intercalating drugs. *J. Pharm. Sci. 78*, 910–917.
(165) Denny, W. A., Atwell, G. J., and Baguley, B. C. (1983) Potential antitumor agents. 39. Anilino ring geometry of amsacrine and derivatives: Relationship to DNA binding and antitumor activity. *J. Med. Chem. 26*, 1625–1630.
(166) Chen, K. X., Gresh, N., and Pullman, B. (1988) Energetics and stereochemistry of DNA complexation with the antitumor AT specific intercalators tilorane and *m*-AMSA. *Nucleic Acids Res. 16*, 3061–3073.
(167) Denny, W. A., and Wakelin, L. P. G. (1986) Kinetic and equilibrium studies of the interaction of amsacrine and anilino ring-substituted analogues with DNA. *Cancer Res. 46*, 1717–1721.
(168) Wakelin, L. P. G., Chetcuti, P., and Denny, W. A. (1990) Kinetic and equilibrium binding studies of amsacrine-4-carboxamides: a class of asymmetrical DNA-intercalating agents which bind by threading through the DNA helix. *J. Med. Chem. 33*, 2039–2044.
(169) Bailly, C., Helbecque, N., Hénichart, J. P., Colson, P., Houssier, C., Rao, K. E., Shea, R. G., and Lown, J. W. (1990) Molecular recognition between oligopeptides and nucleic acids. DNA sequence specificity and binding properties of an acridine-linked netropsin hybrid ligand. *J. Mol. Recognit. 3*, 26–35.
(170) Hurley, L. H. (1989) DNA and associated targets for drug design. *J. Med. Chem. 32*, 2027–2033.
(171) Gellert, M. (1981) DNA topoisomerases. *Annu. Rev. Biochem. 50*, 879–910.
(172) Liu, L. F. (1983) DNA topoisomerases–enzymes that catalyse the breaking and rejoining of DNA. *Crit. Rev. Biochem. 15*, 1–24.
(173) Wang, J. C. (1985) DNA topoisomerases. *Annu. Rev. Biochem. 54*, 665–697.
(174) Maxwell, A., and Gellert, M. (1986) Mechanistic aspects of DNA topoisomerases. *Adv. Protein Chem. 38*, 69–107.
(175) Wang, J. C. (1987) Recent studies of DNA topoisomerases. *Biochim. Biophys. Acta 909*, 1–9.
(176) Sutcliffe, J. A., Gootz, T. D., and Barrett, J. F. (1989) Biochemical characteristics and physiological significance of major DNA topoisomerases. *Antimicrob. Agents Chemother. 33*, 2027–2033.
(177) Ross, W. E. (1985) DNA topoisomerases as targets for cancer therapy. *Biochem. Pharmacol. 34*, 4191–4195.
(178) Lock, R. B., and Ross, W. E. (1987) DNA topoisomerases in cancer therapy. *Anti-Cancer Drug Des. 2*, 151–164.
(179) Kohn, K. W., Pommier, Y., Kerrigan, D., Markovits, J., and Covey, J. M. (1987) Topoisomerase II as a target of anticancer drug action in mammalian cells. *Natl. Cancer Inst. Monogr. 4*, 61–71.
(180) Glisson, B. S., and Ross, W. E. (1987) DNA topoisomerase II: a primer on the enzyme and its unique role as a multidrug in cancer chemotherapy. *Pharmacol. Ther. 32*, 89–106.
(181) Drlica, K., and Franco, R. J. (1988) Inhibitors of DNA topoisomerases. *Biochemistry 27*, 2253–2259.
(182) D'Arpa, P., and Liu, L. F. (1989) Topoisomerase-targeting antitumor drugs. *Biochim. Biophys. Acta 989*, 163–177.
(183) Liu, L. F. (1989) DNA topoisomerase poisons as antitumor drugs. *Annu. Rev. Biochem. 58*, 351–375.
(184) Zwelling, L. A. (1989) Topoisomerase II as a target of antileukemia drugs: A review of controversial areas. *Hum. Pathol. 3*, 101–112.
(185) Kreuzer, K. N. (1989) DNA topoisomerases as potential targets of antiviral action. *Pharm. Ther. 43*, 377–395.
(186) Zunino, F., and Capranico, G. (1990) DNA topoisomerase II as the primary target of anti-tumor anthracyclines. *Anti-Cancer Drug Des. 5*, 307–317.
(187) Pommier, Y., Mattern, M. R., Scharwtz, R. E., Zwelling, L. A., and Kohn, K. N. (1984) Changes in deoxyribonucleic acid linking number due to treatment of mammalian cells with the intercalating agents 4′-(9-acridinylamino)methanesulfon-*m*-anisidide. *Biochemistry 23*, 2927–2932.
(188) Nelson, E. M., Tewey, K. M., and Liu, L. F. (1984) Mechanism of antitumor drug action. Poisoning of mammalian DNA topoisomerase II on DNA by 4′-(9-acridinylamino)methanesulfon-*m*-anisidide. *Proc. Natl. Acad. Sci. U.S.A. 81*, 1361–1365.
(189) Marshall, B., and Ralph, R. K. (1985) The mechanism of action of mAMSA. *Adv. Cancer Res. 44*, 267–293.
(190) Pommier, Y., Schwartz, R. E., Zwelling, L. A., and Kohn, K. W. (1985) Effects of DNA intercalating agents on topoisomerase II induced DNA strand cleavage in isolated mammalian cell nuclei. *Biochemistry 24*, 6406–6410.
(191) Pommier, Y., Minford, J. K., Schwartz, R. E., Zwelling, L. A., and Kohn, K. W. (1985) Effects of the DNA intercalators 4′-(9-acridinylamino)methanesulfon-*m*-anisidide and 2-methyl-9-hydroxyellipticinium on topoisomerase II mediated DNA strand cleavage and strand passage. *Biochemistry 24*, 6410–6416.
(192) Rowe, T. C., Chen, G. L., Hsiang, Y. H., and Liu, L. F. (1986) DNA damage by antitumor acridines mediated by mammalian DNA topoisomerase II. *Cancer Res. 46*, 2021–2026.
(193) Pommier, Y., Covey, J., Kerrigan, D., Mattes, W., Markovits, J., and Kohn, K. W. (1987) Role of DNA intercalation in the inhibition of purified mouse leukemia-(L1210) DNA topoisomerase II by amino-9-acridines. *Biochem. Pharmacol. 36*, 3477–3486.

(194) Covey, J. M., Kohn, K. W., Kerrigan, D., Tilchen, E. J., and Pommier, Y. (1988) Topoisomerase II-mediated DNA damage produced by 4'-(9-acridinylamino)methanesulfon-*m*-anisidide and related acridines in L1210 cells and isolated nuclei: Relation to cytotoxicity. *Cancer Res. 48*, 860–865.

(195) Fox, M. E., and Smith, P. J. (1990) Long term inhibition of DNA synthesis and the persistence of trapped topoisomerase II complexes in determining the toxicity of the antitumor DNA intercalators m-AMSA and mitoxantrone. *Cancer Res. 50*, 5813–5818.

(196) Finlay, G. J., Wilson, W. R., and Baguley, B. C. (1989) Chemoprotection by 9-aminoacridine derivatives against the cytotoxicity of topoisomerase II-directed drugs. *Eur. J. Cancer Clin. Oncol. 25*, 1695–1701.

(197) Chow, K. C., MacDonald, T. L., and Ross, W. E. (1989) DNA binding by epipodophyllotoxins and N-acyl anthracyclines: Implications for mechanism of topoisomerase II inhibition. *Mol. Pharmacol. 34*, 467–473.

(198) Baguley, B. C., Holdaway, K. M., and Fray, L. M. (1990) Design of DNA intercalators to overcome topoisomerase II-mediated multidrug resistance. *J. Natl. Cancer Inst. 82*, 399–402.

(199) McHugh, M., Woynarowski, J. M., Sigmund, R. D., and Beerman, T. A. (1989) Effect of minor groove binding drugs on mammalian topoisomerase I activity. *Biochem. Pharmacol. 38*, 2323–2328.

(200) McHugh, M., Sigmund, R. D., and Beerman, T. A. (1990) Effect of minor groove binding drugs on camptothecin-induced DNA lesions in L1210 nuclei. *Biochem. Pharmacol. 39*, 707–714.

(201) Fesen, M., and Pommier, Y. (1989) Mammalian topoisomerase II activity is modulated by the DNA minor groove binder distamycin in simian virus 40 DNA. *J. Biol. Chem. 264*, 11354–11359.

(202) Woynarowski, J. M., McHugh, M., Sigmund, R. D., and Beerman, T. A. (1989) Modulation of topoisomerase II catalytic activity by DNA minor groove binding agents distamycin, Hoechst 33258, and 4',6-diamidine-2-phenylindole. *Mol. Pharmacol. 35*, 177–182.

(203) Woynarowski, J. M., Sigmund, R. D., and Beerman, T. A. (1989) DNA minor groove binding agents interfere with topoisomerase II mediated lesions induced by epipodophyllotoxin derivative VM-26 and acridine derivative m-AMSA in nuclei from L1210 cells. *Biochemistry 28*, 3850–3855.

(204) Shishedo, K., Sakaguchi, R., and Nosoh, Y. (1984) Enhancement of S1 nuclease-susceptibility of negatively superhelical DNA by netropsin. *Biochem. Biophys. Res. Commun. 124*, 388–392.

(205) Bruzik, J. P., Auble, D. T., and DeHaseth, P . L. (1987) Specific activation of transcription initiation by the sequence specific DNA-binding agents distamycin A and netropsin. *Biochemistry 26*, 950–956.

(206) Straney, D. C., and Crothers, D. M. (1987) Effect of drug–DNA interactions upon transcription initiation at the *lac* promoter. *Biochemistry 26*, 1987–1995.

(207) Krogh, S., Mortensen, U. H., Westergaard, O., and Bonven, B. (1991) Eukaryotic topoisomerase I-DNA interaction is stabilized by helix curvature. *Nucleic Acids Res. 19*, 1235–1241.

(208) Bailly, C., Catteau, J. P., Hénichart, J. P., Reszka, K., Shea, R. G., Krowicki, K., and Lown, J. W. (1989) Subcellular distribution of a nitroxide spin-labeled netropsin in living KB cells. *Biochem. Pharmacol. 38*, 1625–1630.

(209) Lemay, P., Bernier, J. L., Hénichart, J. P., and Catteau, J. P. (1983) Subcellular distribution of nitroxide spin-labelled 9-aminoacridine in living KB cells. *Biochem. Biophys. Res. Commun. 111*, 1074–1081.

(210) Bailly, C., and Hénichart, J. P. (1990) Subcellular distribution of a nitroxide spin-labeled netropsine-acridine hybrid in living KB cells. Electron spin resonance study. *Biochem. Biophys. Res. Commun. 167*, 798–806.

(211) Bialer, M., Yagen, B., Mechoulam, R., and Becker, Y. (1980) Structure–activity relationships of pyrrole amidine antiviral antibiotics III. Preparation of distamycin and congocidine derivatives based on 2,5-disubstituted pyrroles. *J. Pharm. Sci. 69*, 1334–1338.

(212) Bialer, M., Yagen, B., and Mechoulam, R. (1980) Structure–activity relationships of pyrrole amidine antiviral antibiotics II. Preparation of mono- and tripyrrole derivatives of congocidine. *J. Med. Chem. 23*, 1144–1148.

(213) Gendler, P. L., and Rapoport, H. (1981) Permethyl analogue of the pyrrolic antibiotic distamycin A. *J. Med. Chem. 24*, 33–38.

(214) Grehn, L., Ragnarsson, U., and Datema, R. (1983) Synthesis and antiviral activity of distamycin A analogues: Substitutions on the different pyrrole nitrogens and in the amidine function. *J. Med. Chem. 26*, 1042–1049.

(215) Grehn, L., Ragnarsson, U., and Datema, R. (1986) Structure–activity relationships in distamycin A analogues: effect of alkyl groups on the pyrrole nitrogen at the non-amidine end of the molecule combined with methyl elimination in the following ring. *Acta Chem. Scand. 40*, 145–151.

(216) Lee, M., Krowicki, K., Hartley, J. A., Pon, R. T., and Lown, J. W. (1988) Molecular recognition between oligopeptides and nucleic acids: Influence of van der Waals contacts in determining the 3'-terminus of DNA sequences read by monocationic lexitropsins. *J. Am. Chem. Soc. 110*, 3641–3649.

(217) Wang, A. H. J., Cottens, S., Dervan, P. B., and Yesinowski, J. P., van der Marel, G. A., and van Boom, J. H. (1989) Interactions between a symmetrical minor groove binding compound and DNA oligonucleotides; ^{1}H and ^{19}F NMR studies. *J. Biomol. Struct. Dyn. 7*, 101–117.

(218) Grokhovsky, S. L., Zhuze, A. L., and Gottikh, B. P. (1975) DNA base pair specific ligands. I. Synthesis of distamycin A and its analogs with different number of *N*-methyl and *N*-propylpyrrole residues. *Bioorgan. Khim. 1*, 1616–1623.

(219) Schultz, P. G., and Dervan, P. B. (1983) Distamycin and penta-*N*-methylpyrrole-carboxamide binding sites on native DNA, a comparison of methidiumpropyl-EDTA-iron(II) footprinting and DNA affinity cleaving. *J. Biomol. Struct. Dyn. 1*, 1133–1140.

(220) Schultz, P. G., and Dervan, P. B. (1983) Sequence-specific double-strand cleavage of DNA by penta-*N*-methylpyrrolecarboxamide-EDTA-Fe(II). *Proc. Natl. Acad. Sci. U.S.A. 80*, 6834–6837.

(221) Youngquist, R. S., and Dervan, P. B. (1985) Sequence specific recognition of B-DNA by oligo(*N*-methylpyrrole carboxamides). *Proc. Natl. Acad. Sci. U.S.A. 82*, 2565–2569.

(222) Khorlin, A. A., Krylov, A. S., Grokhovsky, S. L., Zhuze, A. L., Zasedatelev, A. S., Gursky, G. V., and Gottikh, B. P. (1980) A new type of AT-specific ligand constructed of two netropsin-like molecules. *FEBS Lett. 118*, 311–314.

(223) Schultz, P. G., and Dervan, P. B. (1983) Sequence-specific double-strand cleavage of DNA by bis(EDTA-distamycin-Fe^{II}) and EDTA-bis(distamycin)Fe^{II}. *J. Am. Chem. Soc. 105*, 7748–7750.

(224) Youngquist, R. S., and Dervan, P. B. (1985) Sequence-specific recognition of B-DNA by bis(EDTA-distamycin)fumaramide. *J. Am. Chem. Soc. 107*, 5528–5529.

(225) Youngquist, R. S., and Dervan, P. B. (1987) A synthetic peptide binds 16 base pairs of A,T double helical DNA. *J. Am. Chem. Soc. 109*, 7564–7566.

(226) Lown, J. W., Krowicki, K., Balzarini, J., Newman, R. A., and De Clercq, E. (1989) Novel linked antiviral and antitumor agents related to netropsin and distamycin: Synthesis and biological evaluation. *J. Med. Chem. 32*, 2368–2375.

(227) Kissinger, K. L., Dabrowiak, J. C., and Lown, J. W. (1990) Molecular recognition between oligopeptides and nucleic acids: DNA binding specificity of a series of bis-netropsin analogues deduced from footprinting analysis. *Chem. Res. Toxicol. 3*, 162–168.

(228) Rao, K. E., Zimmermann, J., and Lown, J. W. (1991) Sequence-selective DNA binding by linked bis-*N*-methylpyrrole dipeptides: An analysis by MPE footprinting and force field calculations. *J. Org. Chem. 56*, 786–797.

(229) Lown, J. W. (1990) Molecular mechanisms of DNA sequence recognition by groove binding ligands: Biochemical and biological consequences. *Molecular Basis of Specificity in Nucleic Acid–Drug Interactions* (B. Pullman, and J. Jortner, Eds.) pp 103–122, Kluwer Academic Publishers, Dordrecht, Netherlands.

(230) Lown, J. W., Krowicki, K., Balzarini, J., and De Clercq, E. (1986) Structure–activity relationship of novel oligopeptide

antiviral and antitumor agents related to netropsin and distamycin. *J. Med. Chem. 29*, 1210–1214.
(231) Lown, J. W., Krowicki, K., Bhat, U. G., Skorobogaty, A., Ward, B., and Dabrowiak, J. C. (1986) Molecular recognition between oligopeptides and nucleic acids: Novel imidazole-containing oligopeptides related to netropsin that exhibit altered DNA sequence specificity. *Biochemistry 25*, 7408–7416.
(232) Krowicki, K., and Lown, J. W. (1987) Synthesis of novel imidazole-containing DNA minor groove binding oligopeptides related to the antiviral antibiotic netropsin. *J. Org. Chem. 52*, 3493–3501.
(233) Kissinger, K. L., Krowicki, K., Dabrowiak, J. C., and Lown, J. W. (1987) Molecular recognition between oligopeptides and nucleic acids: Monocationic imidazole lexitropsins that display enhanced GC sequence dependent DNA binding. *Biochemistry 26*, 5590–5595.
(234) Lee, M., Hartley, J. A., Pon, R. T., Krowicki, K., and Lown, J. W. (1988) Sequence specific molecular recognition by a monocationic lexitropsin of the decadeoxyribonucleotide d(CATGGCCATG)$_2$: Structural and dynamic aspects deduced from high field ^{1}H-NMR studies. *Nucleic Acids Res. 16*, 665–684.
(235) Lee, M., Chang, D. K., Hartley, J. A., Pon, R. T., Krowicki, K., and Lown, J. W. (1988) Structural and dynamic aspects of binding of a prototype lexitropsin to the decadeoxyribonucleotide d(CGCAATTGCG)$_2$ deduced from high resolution ^{1}H NMR studies. *Biochemistry, 27*, 445–455.
(236) Lee, M., Coulter, D. M., Pon, R. T., Krowicki, K., and Lown, J. W. (1988) Sequence specific molecular recognition and binding of a monocationic bis-imidazole lexitropsin to the decadeoxyribonucleotide d[(GATCCGTATG):(CATACGGATC)]: Structural and dynamic aspects of intermolecular exchange studied by ^{1}H-NMR. *J. Biomol. Struct. Dyn. 5*, 1059–1087.
(237) Lee, M., Pon, R. T., Krowicki, K., and Lown, J. W. (1988) Structural and dynamic aspects of the sequence specific binding of netropsin and its bis-imidazole analogue on the decadeoxyribonucleotide d(CGCAATTGCG)$_2$. *J. Biomol. Struct. Dyn. 5*, 939–949.
(238) Burckhardt, G., Luck, G., Zimmer, C., Störl, J., Krowicki, K., and Lown, J. W. (1989) Variation of DNA sequence specificity of DNA–oligopeptide binding ligands related to netropsin: imidazole-containing lexitropsins. *Biochim. Biophys. Acta 1009*, 11–18.
(239) Randrianarivelo, M., Zakrzewska, K., and Pullman, B. (1989) Theoretical modeling of DNA–monocationic lexitropsin complexation: Influence of ligand binding on DNA curvature. *J. Biomol. Struct. Dyn. 6*, 769–779.
(240) Bailly, C., Houssin, R., Bernier, J. L., and Hénichart, J. P. (1988) Depsipeptide analogs of the antitumor drug distamycin containing thiazole amino acids residues. *Tetrahedron 44*, 5833–5843.
(241) Plouvier, B., Houssin, R., Bailly, C., and Hénichart, J. P. (1989) Synthesis and DNA-binding study of a thiazole-containing analog of netropsin. *J. Heterocycl. Chem. 26*, 1643–1647.
(242) Kumar, S., Jaseja, M., Zimmermann, J., Yadagiri, B., Pon, R. T., Sapse, A. M., and Lown, J. W. (1990) Molecular recognition and binding of a GC site-avoiding thiazole–lexitropsin to the decadeoxyribonucleotide d-(CGCAATTGCG)$_2$: ^{1}H-NMR evidence for thiazole intercalation. *J. Biomol. Struct. Dyn. 8*, 99–121.
(243) Rao, K. E., Shea, R. G., Yadagiri, B., and Lown, J. W. (1990) Molecular recognition between oligopeptides and nucleic acids: DNA sequence specificity and binding properties of thiazole-lexitropsins incorporating the concepts of base site acceptance and avoidance. *Anti-Cancer Drug Des. 5*, 3–20.
(244) Rao, K. E., Bathini, Y., and Lown, J. W. (1990) Synthesis of novel thiazole containing DNA minor groove binding oligopeptides related to the antibiotic distamycin. *J. Org. Chem. 55*, 728–737.
(245) Plouvier, B., Bailly, C., Houssin, R., and Hénichart, J. P. (1991) Synthesis of two new thiazole-containing oligopeptides as potential DNA minor groove binding analogs of netropsin. *Heterocycles 32*, 693–701.
(246) Lee, M., Krowicki, K., Shea, R. G., Lown, J. W., and Pon, R. T. (1991) Molecular recognition between oligopeptides and nucleic acids: Specificity of binding of a monocationic bisfuran lexitropsin to DNA deduced from footprinting and ^{1}H-NMR studies. *J. Mol. Recogit. 2*, 84–93.
(247) Jones, D. H., and Wooldridge, R. H. (1968) Amidines and guanidines related to congocidine. Part IV. Thiophene, pyridine, and benzene analogues. *J. Chem. Soc.* 550–554.
(248) Wade, W. S., and Dervan, P. B. (1987) Alteration of the sequence specificity of distamycin on DNA by replacement of an N-methylpyrrole carboxamide with pyridine-2-carboxamide. *J. Am. Chem. Soc. 109*, 1574–1575.
(249) Braithwaite, A. W., and Baguley, B. C. (1980) Existence of an extended series of antitumor compounds which bind to deoxyribonucleic acid by nonintercalative means. *Biochemistry 19*, 1101–1106.
(250) Baguley, B. C. (1982) Non intercalative DNA-binding antitumour compounds. *Mol. Cell. Biochem. 43*, 167–181.
(251) Rajagopalan, M., Ayyer, J., and Sasisekharan, V. (1985) Interaction of non-intercalative drugs with DNA: Distamycin analogues. *J. Biosci. 7*, 27–32.
(252) Dasgupta, D., Rajagopalan, M., and Sasisekharan, V. (1986) DNA-binding characteristics of a synthetic analogue of distamycin. *Biochem. Biophys. Res. Commun. 140*, 626–631.
(253) Dasgupta, D., Parrack, P., and Sasisekharan, V. (1987) Interaction of synthetic analogues of distamycin with poly(dA-dT): Role of the conjugated *N*-methylpyrrole system. *Biochemistry 26*, 6381–6386.
(254) Parrack, P., Dasgupta, D., Ayyer, J., and Sasisekharan, V. (1987) Interaction of synthetic analogs of distamycin with DNA. Role of the conjugated N-methylpyrrole system in specificity of binding. *FEBS Lett. 212*, 297–301.
(255) Rao, K. E., Dasgupta, D., and Sasisekharan, V. (1988) Interaction of a synthetic analogues of distamycin and netropsin with nucleic acids. Does curvature of ligand play a role in distamycin–DNA interactions? *Biochemistry 27*, 3018–3024.
(256) Arcamone, F. A., Lazzari, E., Menozzi, M., Soranzo, C., and Verini, M. A. (1989) Synthesis, DNA binding and antiviral activity of distamycin analogues containing different heterocyclic moities. *Anti-Cancer Drug Des. 1*, 235–244.
(257) Arcamone, F. A., Animati, F., Barbieri, B., Configliacchi, E., D'Alesio, R., Geroni, C., Giulani, F. C., Lazzari, E., Menozzi, M., Mongelli, N., Penco, S., and Verini, M. A. (1989) Synthesis, DNA-binding properties, and antitumor activity of novel distamycin derivatives. *J. Med. Chem. 32*, 774–778.
(258) Baker, B. F., and Dervan, P. B. (1985) Sequence-specific cleavage of double-helical DNA. *N*-bromoacetyldistamycin. *J. Am. Chem. Soc. 107*, 8266–8268.
(259) Baker, B. F., and Dervan, P. B. (1989) Sequence-specific cleavage of DNA by *N*-bromoacetyldistamycin. Product and kinetic analyses. *J. Am. Chem. Soc. 111*, 2700–2712.
(260) Krowicki, K., Balzarini, J., De Clercq, E., Newman, R. A., and Lown, J. W. (1988) Novel DNA groove binding alkylators: design, synthesis, and biological evaluation. *J. Med. Chem. 31*, 341–345.
(261) Church, K. M., Wurdeman, R. L., Zhang, Y., and Gold, B. (1990) *N*-(2-chloroethyl)-*N*-nitrosoureas bound to nonionic and monocationic lexitropsin dipeptides. Synthesis, DNA affinity binding characteristics, and reactions with ^{32}P-end-labeled DNA. *Biochemistry 29*, 6827–6838.
(262) Broggini, M., Erba, E., Ponti, M., Ballinari, D., Geroni, C., Spreafico, F., and D'Incalci, M. (1991) Selective DNA interaction of the novel distamycin derivative FCE 24517. *Cancer Res. 51*, 199–204.
(263) Grokhovsky, S. L., and Zubarev, V. E. (1991) Sequence-specific cleavage of double-stranded DNA caused by X-ray ionization of the platinum atom in the Pt–bis-netropsin–DNA complex. *Nucleic Acids Res. 19*, 257–264.
(264) Gravatt, G. L., Baguley, B. C., Wilson, W. R., and Denny, W. A. (1991) DNA-directed alkylating agents. 4. 4-anilinoquinoline-based minor groove directed aniline mustards. *J. Med. Chem. 34*, 1552–1560.
(265) Schultz, P. G., Taylor, J. S., and Dervan, P. B. (1982) Design and synthesis of a sequence-specific DNA cleaving molecule. (distamycin–EDTA)iron(II). *J. Am. Chem. Soc. 104*, 6861–6863.
(266) Taylor, J. S., Schultz, P. G., and Dervan, P. B. (1984) DNA affinity cleaving. Sequence specific cleavage of DNA by dis-

tamycin-EDTA·Fe(II) and EDTA-distamycin·Fe(II). *Tetrahydron 40*, 457-465.
(267) Otsuka, M., Masuda, T., Haupt, A., Ohno, M., Shiraki, T., Sugiura, Y., and Maeda, K. (1990) Man-designed bleomycin with altered sequence specificity in DNA cleavage. *J. Am. Chem. Soc. 112*, 838-845.
(268) Debart, F., Perigaud, C., Gosselin, G., Mrani, D., Rayner, B., Le Ber, P., Auclair, C., Balzarini, J., De Clercq, E., Paoletti, C., and Imbach, J. L. (1989) Synthesis, DNA binding, and biological evaluation of synthetic precursors and novel analogues of netropsin. *J. Med. Chem. 32*, 1074-1083.
(269) Bowler, B. E., Hollis, L. S., and Lippard, S. J. (1984) Synthesis and DNA binding and photonicking properties of acridine orange linked by a polymethylene tether to (1,2-diaminoethane)dichloroplatinium(II). *J. Am. Chem. Soc. 106*, 6102-6104.
(270) Bowler, B. E., Ahmed, K. J., Sundquist, W. I., Hollis, L. S., Whang, E. E., and Lippard, S. J. (1989) Synthesis and DNA-binding properties of (1,2-diaminoethane) platinum(II) complexes linked to the DNA intercalator acridine orange by trimethylene and hexamethylene chains. *J. Am. Chem. Soc. 111*, 1299-1306.
(271) Koyama, M., Kelly, T. R., and Watanabe, K. A. (1988) Novel type of potential anticancer agents derived from chrysophanol and emodin. Some structure-activity relationship studies. *J. Med. Chem. 31*, 383-384.
(272) Koyama, M., Takahashi, K., Chou, T. C., Darzynkiewicz, Z., Kapucinski, J., Kelly, T. R., and Watanabe, K. A. (1989) Intercalating agents with covalent bond forming capability. A novel type of potential anticancer agents. 2. Derivatives of chrysophanol and emodin. *J. Med. Chem. 32*, 1594-1599.
(273) Ferguson, L. R., Gourdie, T. A., Valu, and Denny, W. A. (1989) Bacterial mutagenicity studies of DNA-intercalating aniline mustard: An insight into the mode of action of a novel class of antitumour drugs. *Anti-Cancer Drug Des. 4*, 209-219.
(274) Gourdie, T. A., Valu, K. K., Gravatt, G. L., Boritzki, T. J., Baguley, B. C., Wakelin, L. P. G., Wilson, W. R., Woodgate, P. D., and Denny, W. A. (1990) DNA-directed alkylating agents. 1. Structure-activity relationships for acridine-linked aniline mustards: consequences of varying the reactivity of the mustard. *J. Med. Chem. 33*, 1177-1186.
(275) Palmer, B. D., Lee, H. H., Johnson, P., Baguley, B. C., Wicklam, G., Wakelin, L. P. G., McFadyen, W. D., and Denny, W. A. (1990) DNA-directed alkylating agents. 2. Synthesis and biological activity of platinum complexes linked to 9-anilinoacridine. *J. Med. Chem. 33*, 3008-3014.
(276) Valu, K. K., Gourdie, T. A., Boritzki, T. J., Gravatt, G. L., Baguley, B. C., Wilson, W. R., Wakelin, L. P. G., Woodgate, P. D., and Denny, W. A. (1990) DNA-directed alkylating agents. 3. Structure-activity relationships for acridine-linked aniline mustards: Consequences of varying the length of the linker chain. *J. Med. Chem. 33*, 3014-3019.
(277) Prakash, A. S., Denny, W. A., Gourdie, T. A., Valu, K. K., Woodgate, P. D., and Wakelin, L. P. G. (1990) DNA-directed alkylating ligands as potential antitumor agents: Sequence specificity of alkylation by intercalating aniline mustards. *Biochemistry 29*, 9799-9807.
(278) Prakash, A. S., Denny, W. A., and Wakelin, L. P. G. (1990) Differences in sequence selectivity of DNA alkylation by isomeric intercalating aniline mustards. *Chem.-Biol. Interact. 76*, 241-248.
(279) Gourdie, T. A., Prakash, A. S., Wakelin, L. P. G., Woodgate, P. D., and Denny, W. A. (1991) Synthesis and evaluation of DNA-targeted spatially separated bis(aniline mustards) as potential alkylating agents with enhanced DNA cross-linking capability. *J. Med. Chem. 34*, 240-248.
(280) Wickham, G., Prakash, A. S., Wakelin, L. P. G., and McFadyen, W. D. (1991) DNA-binding properties and antitumour activity of monofunctional alkylating groups attached to the DNA-intercalating chromophore phenanthridine: *n*-Bromoalkylphenanthridinium bromides. *Biochim. Biophys. Acta 1073*, 528-537.
(281) Farquhar, D., Newman, R. A., Zuckerman, J. E., and Anderson, B. S. (1991) Doxorubicin analogues incorporating chemically reactive substituents. *J. Med. Chem. 34*, 561-564.
(282) Gibson, D., Gean, K. F., Ben-Shoshan, R., Ramu, A., Ringel, I., and Katzhendler, J. (1991) Preparation, characterization, and anticancer activity of a series of *cis*-$PtCl_2$ complexes linked to anthraquinone intercalators. *J. Med. Chem. 34*, 414-420.
(283) Hertzberg, R. P., and Dervan, P. B. (1982) Cleavage of double helical DNA by (methidium propyl-EDTA)iron(II). *J. Am. Chem. Soc. 104*, 313-315.
(284) Hertzberg, R. P., and Dervan, P. B. (1984) Cleavage of DNA with methidiumpropyl-EDTA-iron(II): Reaction conditions and product analyses. *Biochemistry 23*, 3934-3945.
(285) Lown, J. W., and Joshua, A. V. (1982) Bleomycin models. Haemin-acridines which bind to DNA and cause oxygen-dependent scission. *J. Chem. Soc., Chem. Commun.* 1298-1300.
(286) Hashimoto, Y., Iijima, H., Nozaki, Y., and Shudo, K. (1986) Functional analogues of bleomycin: DNA cleavage by bleomycin and hemin-intercalators. *Biochemistry 25*, 5103-5110.
(287) Lown, J. W., Sondhi, S. M., Ong, C. W., Skorobogaty, A., Kishikawa, H., and Dabrowiak, J. C. (1986) Deoxyribonucleic acid cleavage specificity of a series of acridine- and acodazole-iron porphyrins as functional bleomycin models. *Biochemistry 25*, 5111-5117.
(288) Bailly, C., Bernier, J. L., Houssin, R., Helbecque, N., and Hénichart, J. P. (1987) Design of two metal-chelating, DNA-binding models. Molecular combinations of bleomycin and amsacrine anti-tumour drugs. *Anti-Cancer Drug Des. 1*, 303-312.
(289) Bailly, C., Kenani, A., Helbecque, N., Bernier, J. L., Houssin, R., and Hénichart, J. P. (1988) DNA-binding and DNA cleaving properties of a synthetic model AGAGLU related to the antitumour drugs AMSA and bleomycin. *Biochem. Biophys. Res. Commun. 152*, 695-702.
(290) Hosseini, M. W., Blacker, A. J., and Lehn, J. M. (1990) Multiple molecular recognition and catalysis. A multifunctional anion receptor bearing an anion binding site, an intercalating group, and a catalytic site for nucleotide binding and hydrolysis. *J. Am. Chem. Soc. 112*, 3896-3904.
(291) Ding, L., Etemad-Moghadam, G., and Meunier, B. (1990) Oxidative cleavage of DNA mediated by hybrid metalloporphyrin-ellipticine molecules and functionalized metalloporphyrin precursors. *Biochemistry 29*, 7868-7875.
(292) Ding, L., Etemad-Moghadam, G., Cros, S., Auclair, C., and Meunier, B. (1991) Syntheses and in vitro evaluation of water soluble "cationic metalloporphyrin-ellipticine" molecules having a high affinity for DNA. *J. Med. Chem. 34*, 900-906.
(293) Hénichart, J. P., Bernier, J. L., and Catteau, J. P. (1982) Interaction of 4-(9-acridinylamino)aniline and derivatives with DNA. *Hoppe-Seyler's Z. Physiol. Chem. 363*, 835-841.
(294) Karup, G., Meldal, M., Nielsen, P. E., and Buchardt, O. (1988) 9-Acridinylpeptides and 9-acridinyl-4-nitrophenylsulfonylpeptides. Synthesis, binding to DNA, and photoinduced DNA cleavage. *Int. J. Pept. Protein Res. 32*, 331-343.
(295) Larsen, A. K., Paoletti, J., Belehradek, J., Jr., and Paoletti, C. (1986) Uptake, cytofluorescence, and cytotoxicity of oxazolopyrido carbazoles (amino acid-ellipticine conjugates) in murine sarcoma cells. *Cancer Res. 46*, 5236-5240.
(296) Morier-Teissier, E., Bailly, C., Bernier, J. L., Houssin, R., Helbecque, N., Catteau, J. P., Colson, P., Houssier, C., and Hénichart, J. P. (1989) Synthesis, biological activity and DNA interaction of anilinoacridine and bithiazole peptide derivatives related to the antitumor drugs m-amsa and bleomycin. *Anti-Cancer Drug Des. 4*, 37-52.
(297) Morier-Teissier, E., Bernier, J. L., Lohez, M., Catteau, J. P., Hénichart, J. P. (1990) Free radical production and DNA cleavage by copper chelating peptide-anthraquinones. *Anti-Cancer Drug Des. 5*, 291-305.
(298) Nielsen, P. E. (1990) Chemical and photochemical probing of DNA complexes. *J. Mol. Recognit. 3*, 1-25.
(299) Subra, F., Carteau, S., Pager, J., Paoletti, J., Paoletti, C., Auclair, C., Mrani, D., Gosselin, G., and Imbach, J. L. (1991) Bis(pyrrolecarboxamide) linked to intercalating chromophore oxazolopyridocarbazole (OPC): Selective binding to DNA and polynucleotides. *Biochemistry 30*, 1642-1650.
(300) Shakked, Z., and Rabinovich, D. (1986) The effect of the base sequence on the fine structure of the DNA double helix. *Prog. Biophys. Mol. Biol. 47*, 159-195.

ARTICLES

Proton Magnetic Relaxation of Manganese(II) Tetrakis(4-sulfophenyl)porphine Ion in Water

Griselda Hernández[†,‡] and Robert G. Bryant*[,§]

Department of Biophysics and Department of Chemistry, University of Rochester, Rochester, New York 14642.
Received May 13, 1991

Water proton nuclear magnetic spin–lattice relaxation rates are reported as a function of magnetic field strength for aqueous solutions of manganese tetrakis(4-sulfophenyl)porphine complexes. The manganese(III) complex displays relaxation that is remarkably independent of temperature at low magnetic field and a magnetic field dependence that is characteristic of the electron spin relaxation rates, making a contribution to the correlation time that dominates the electron-nuclear coupling. The manganese(II) complex is much more effective in relaxing water protons, but the usual models of first coordination sphere and outer-sphere relaxation fail to account for the magnitude and the magnetic field dependence of the relaxation rates. The data suggest that the delocalization of the electron density into the ligand system provides an increase in the effectiveness of what may be called the outer-sphere paths for water proton relaxation.

Magnetic relaxation provides a means for controlling the information content of a nuclear magnetic resonance image, sharpening anatomic detail, or decreasing image acquisition time (*1–4*). Manganese compounds are among the more effective agents for increasing nuclear spin–lattice relaxation rates because they generally have relatively long electron spin–lattice relaxation times, which are crucial to the development of high nuclear spin–lattice relaxation rates. Manganese–porphyrin compounds have been of particular interest because, in addition to good nuclear spin relaxation efficiency (*5, 6*), they have been found to localize differentially in tissues and provide enhanced image contrast in tumors (*7–10*).

Manganese tetrakis(4-sulfophenyl)porphine complexes, $Mn(TPPS_4)$, are well-characterized compounds that are soluble in water. The aqueous chemistry of manganese–porphyrins is somewhat complicated because the metal center as well as the ligand periphery provide sites for acid–base chemistry, and the complex may participate in several redox equilibria (*11*). The manganese(III) complex is stable in air, is reported to have two coordinated water molecules, has been characterized magnetically, and is effective in vivo as a contrast agent (*5–10*). The manganese(II) complex is accessible by reduction, which shifts the acid–base equilibria associated with the complex. An ionization is reported at pH values of about 12, which is thought to involve the formation of an oxo species. The formation of the hydroxo species from the aquo species is difficult to detect because of metal dissociation at low pH. The UV–visible spectrum of the manganese(II) complex changes little from pH 7 to 11, suggesting that the coordination sphere suffers no ionization over this range. A reasonable assumption is that this pH range supports the hydroxo species, which places one proton at the metal center.

The magnetic field dependence of the water proton relaxation in aqueous $[Mn(III)(TPPS_4)]^{3-}$ solutions is unusual in that it is somewhat similar to manganese(II) ion coordinated to a macromolecule (*6, 12*), however, the manganese(III) is a d^4 ion with lower electronic symmetry than the d^5 ion, the consequence of which is generally short electron relaxation times that limit the relaxation efficiency of the complex (*13*). We explore here the magnetic relaxation properties of the $[Mn(II)TPPS_4]^{4-}$ complexes in which the manganese is formally a d^5 ion that may have higher electronic symmetry that results in a longer electron relaxation time and higher water proton relaxation efficiency.

EXPERIMENTAL PROCEDURES

The $Mn(III)TPPS_4$ complex was obtained as the sodium salt from Porphyrin Products, Inc. (Logan, UT), $Na_2S_2O_4$ was from Sigma Chemical Co. (St. Louis, MO), and stock solutions were prepared in 50 mM HEPES buffer. $[Mn(III)TPPS_4]^{3-}$ was reduced with a 50-fold molar excess of dithionite over porphyrin under a nitrogen atmosphere (*14*). $[Mn(II)TPPS_4]^{4-}$ and $[Mn(III)TPPS_4]^{3-}$ were identified spectrophotometrically by their absorption bands at 436 and 469 nm, respectively, with molar extinction coefficients of 342×10^3 and 95×10^3 M^{-1} cm^{-1}, respectively (*11*). The nuclear magnetic relaxation rates were measured over a range of magnetic field strengths corresponding to proton Larmor frequencies between 0.01 and 30 MHz using a field-cycling spectrometer described elsewhere (*15, 16*). This instrument switches the current in a copper solenoidal magnet to vary the field according to a program that initially polarizes the spins at a high field and then switches to the magnetic field of interest (measure field) for a variable delay time, after which it switches to a resonance field corresponding to a proton Larmor frequency of 7.25 MHz, where the remaining magnetization is measured by numerically integrating a spin echo or a free induction

* Address correspondence to Robert G. Bryant, Biophysics Department, University of Rochester Medical Center, Rochester, NY 14642.
† Department of Chemistry.
‡ Present address: Department of Chemistry, University of California, Davis, CA 95616.
§ Department of Biophysics.

1043-1802/91/2902-0394$02.50/0 © 1991 American Chemical Society

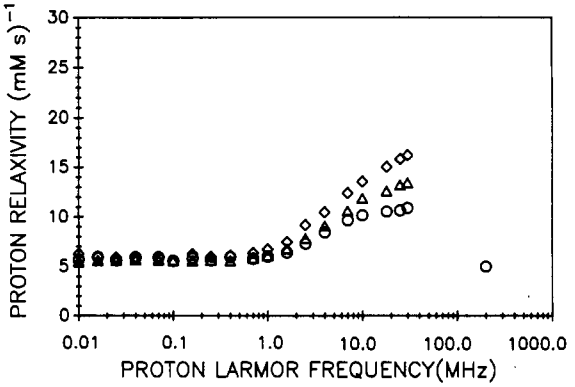


Figure 1. The water proton nuclear spin–lattice relaxation rate per millimole of $[Mn(III)TPPS_4]^{3-}$ at pH 7 plotted against the magnetic field strength expressed as the proton Larmor frequency: (◇) 278 K, (△) 288 K, (○) 298 K.

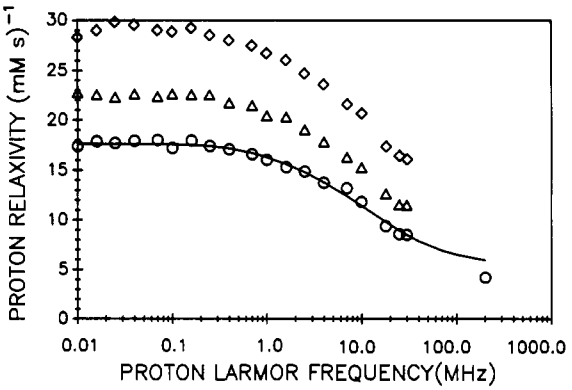


Figure 2. The water proton nuclear spin–lattice relaxation rate per millimole of $[Mn(II)TPPS_4]^{4-}$ at pH 7 plotted against the magnetic field strength expressed as the proton Larmor frequency: (◇) 278 K, (△) 288 K, (○) 298 K. The solid line was computed using a sum of contributions from translational and first coordination sphere contributions with the following parameters: rotational correlation time of 500 ps, manganese–proton distance of 3.3 Å, first coordination sphere exchange time of 10 μs, low field electron relaxation time of 1 ns, distance of closest approach of water protons to the paramagnetic center of 1.9 Å, and water diffusion ceofficient in the vicinity of the paramagnetic center of 0.9 $cm^2\ s^{-1}$.

decay. Samples are contained in Pyrex test tubes sealed with both a rubber stopper and a Teflon screw cap. The sample chamber of the magnet system is bathed in recirculating perchloroethylene that is thermostated using a Neslab RTE-8 temperature controller. Typically 32 points are taken on the magnetization decay curve and fitted to a single exponential using software developed in this laboratory by Dr. Cathy C. Lester (17). The magnetic relaxation dispersion plots are generated by changing the measure field over the range of interest.

RESULTS AND DISCUSSION

Both the manganese(II) and manganese(III) complexes are high spin. The EPR spectrum of the manganese(III) complex is broad while the manganese(II) complex spectrum is narrower, consistent with a longer electron relaxation time (*11*). This feature is supported by the magnetic relaxation dispersion profiles for water protons shown in Figures 1 and 2.

Proton magnetic relaxation data for the aqueous manganese(III) complex has been reported by Koenig and coworkers (*12*). The data in Figure 1 are very similar. We note that for the manganese(III) complex, the water proton relaxation rate increases with increasing magnetic field strength, which is a clear indication that the electron relaxation rate makes a dominant contribution to the effective correlation time for the electron-nuclear coupling. That is, the correlation time, τ_c, may be written as

$$\frac{1}{\tau_c} = \frac{1}{\tau_{rot}} + \frac{1}{\tau_{ex}} + \frac{1}{\tau_e} \qquad (1)$$

where τ_{rot} is the rotational correlation time, τ_{ex} the mean residence time of the observed water proton at the paramagnetic center, and τ_e the electron relaxation time. Of these contributions, only the electron relaxation rate is a function of the magnetic field strength. The electron relaxation rate decreases with increasing magnetic field strength. The consequence is that when the electron relaxation dominates the low magnetic field nuclear relaxation rate, the observed water proton relaxation rate increases with increasing magnetic field strength. The water proton relaxation rates shown in Figure 1 are practically independent of temperature over the range studied, which implies that either there are compensating changes in the contributions to eq 1 or the electron spin relaxation rate is independent of temperature. In either case, it is clear that over the range studied, the temperature dependence of the water proton relaxation rate is weaker than could be described by an activation law with an activation energy appropriate for the usual transport properties in water such as translation or rotation.

Reduction of the Mn(III) complex to the Mn(II) compound changes the water proton relaxation profile profoundly; the low field relaxation rates are considerably greater, the relaxation rate decreases with increasing magnetic field strength, and the water proton relaxation rate decreases with increasing temperature at all magnetic field strengths measured. The high relaxation rate may be caused by an increased number of labile protons at the metal site, but as discussed above, the manganese(II) complex is expected to have a hydroxide ion coordinated to the metal or at most a water molecule (*18*).

The dipolar contribution to the paramagnetically induced relaxation of water protons caused by hexaaquomanganese(II) ion at 298 K may be attributed almost entirely to first coordination effects and is ca. 1.6 $s^{-1}\ mM^{-1}$ of coordinated water molecule protons (*12, 19*). The increase in relaxation efficiency upon reduction and the change in the temperature dependence imply that the electron relaxation rate makes a much smaller contribution if any to the effective correlation time for the electron–nuclear coupling. The first coordination sphere contribution to relaxation should, therefore, be controlled by rotational motions of the complex. Compared with the hexaaquomanganese(II) ion, the porphyrin complex is much larger. Though no precise value of the rotational correlation time has been reported, estimates are reported that suggest the correlation time for rotation of the porphyrin complex is larger than that for the aquo ion by as much as a factor of 10 (*20, 21*). With the assumption that we have either an aquo complex with two protons in the first coordination sphere of the manganese(II) or the hydroxo complex with one, the low magnetic field relaxivity is in the range from 8 to 17 s^{-1} per mM of coordinated water protons at 298 K. Thus, the magnitude of relaxation rate per proton is consistent with the dipolar part of the aquo ion, scaled by the anticipated changes in the rotational correlation time.

For a first coordination sphere dipole–dipole contribution to account for the high relaxation rate, the rotational correlation time for the complex must be on the order of 10 times that for the hexaaquamanganese(II) ion as

mentioned. In this case, the inflection point in the relaxation dispersion curve should be at about 0.8 MHz, which is much lower than that shown in Figure 2. Therefore, there must be additional important contributions to the relaxation rate besides the first coordination sphere dipole–dipole contribution. This assertion is supported by the observation that the relaxation dispersion relaxation profile is broader than predicted by the Lorentzian shapes associated with first coordination sphere effects. Broad non-Lorentzian dispersion profiles are characteristic of outer-sphere or diffusional contributions to relaxation.

The absence of a clear bimodal dispersion curve makes it somewhat difficult to separate the contributions from the first coordination sphere exchange of water molecules and an outer-sphere contribution. We use the theory developed by Freed and co-workers for outer-sphere relaxation caused by relative translation of the interacting magnetic moments (*22–24*)

$$1/T_1 = (32\pi/405)\gamma_I^2\gamma_S^2\hbar^2S(S+1)(N_a/1000) \times ([S]/bD) \times \{j_2(\omega_S - \omega_I)\} + 3j_1(\omega_I) + 6j_2(\omega_S + \omega_I) \quad (2)$$

with the spectral density function $j_k(\omega)$:

$$j_k(\omega) = \mathrm{Re}\{(1 + s/4)/(1 + s + 4s^2/9 + s^3/9)\} \quad (3)$$

$$s = b\{(i\omega + (T_k^s)^{-1})/D\}^{1/2} \quad (4)$$

where γ_I and γ_S are the proton and electron magnetogyric ratios respectively, ω_I and ω_S are the nuclear and the electron Larmor frequencies, $\hbar$ is Planck's constant divided by 2π, S is the electron spin, N_a is Avogadro's number, the square brackets indicate molar concentration, b is the distance of closest approach between the centers of the interacting magnetic moments, and D is the relative translational diffusion constant, i.e., the sum of the water and porphyrin complex diffusion constants, Re means real part of, and T_k^s is the electron relaxation time with k = 1, 2. The first coordination sphere contribution may be modeled using the dipolar part of the Solomon, Bloembergen, and Morgan equations

$$(1/T_{1m}) = \{(2/15)\gamma_I^2\gamma_s^2\hbar^2S(S+1)/r^6\}\{3\tau_{c1}/(1 + \omega_I^2\tau_{c1}^2) + 7\tau_{c2}/(1 + \omega_s^2\tau_{c2}^2)\} \quad (5)$$

where r is the distance from the metal center of a hydrated ion to a proton of hydration, and the correlation times are given by eq 1 (*13*).

The solid line in Figure 2 was computed using eq 5 and 2 with a rotational correlation time of 500 ps and an intermoment distance of 3.3 Å, and then the parameters of eqs 2–4 were adjusted to provide reasonable agreement with the data. This procedure yields a relative translational diffusion coefficient of 0.9 $cm^2\ s^{-1}$, which is within a factor of 2 of that in bulk water (*25*). The distance of closest approach of the water protons to the metal center, a parameter that adjusts the magnitude of the low magnetic field relaxation rate, is 1.9 Å, which is muct too short to be reasonable.

Both parts of this computation rest on the assumption that the effective electron magnetic moment may be approximated as a point dipole, which is usually a fair assumption for simple complexes (26–29). However, the observation of large contact chemical shifts in porphyrin systems like those studied here suggest that the electrons may be delocalized significantly (*30*). If electron delocalization is significant, then the distance parameters that enter eqs 2–5 do not have a clear meaning, but it is intuitively reasonable that a greater number of water molecules may efficiently sense the paramagnetic center simultaneously, increasing the outer-sphere contribution as a consequence. This observation suggests a strategy for controlling outer sphere relaxation efficiency that represents a new opportunity for relaxation control in low molecular weight and macromolecular systems.

In summary, we have shown that the reduction of the $[Mn(III)TPPS_4]^{3-}$ complex to form the electronically more symmetric $[Mn(II)TPPS_4]^{4-}$ complex leads to considerable increases in the effectiveness of the metal center to relax water protons, particularly at low magnetic field strengths. Further, the water relaxation rate in solutions of the manganese(II) complex is not accounted for by the usual first coordination sphere arguments or by standard treatments of outer-sphere relaxation unless delocalization of the electron spin is considered. This result raises the interesting possibility that the ability of a paramagnetic agent to relax water protons could be markedly enhanced if the electron spin density is well-delocalized into the ligand system. It would, therefore, seem possible to maintain high relaxation efficiency even if the first coordination sphere positions make minor contributions to the final proton relaxation rate.

LITERATURE CITED

(1) Lauterbur, P. C., Dias, M. H. M., and Rudin, A. M. (1978) In *Frontiers of Biological Energies, Vol. 1. Electrons to Tissues*, pp 752–259, Academic Press, New York.

(2) Brash, R. C. (1983) Methods of contrast enhancement for NMR imaging and potential applications. *Radiology 147*, 781.

(3) Wolf, G. L., Joseph, P. M., and Goldstein, E. J. (1986) Optimal pulsing sequences for MR contrast agents. *Am. J. Radiol. 147*, 367.

(4) Koenig, S. H., Spiller, M., Brown, R. D., III, and Wolf, G. (1986) Magnetic field dependence (NMRD profile) of $1/T_1$ of rabbit kidney medulla and urine after intravenous injection of Gd(DTPA). *Invest. Radiol. 21*, 697.

(5) Chen, C.-W., Cohen, J. S., Meyers, C. E., and Sohn, M. (1984) Paramagnetic metalloporphyrins as potential contrast agents in NMR imaging. *FEBS Lett. 168*, 70.

(6) Lyon, R. C., Faustino, P. J., Cohen, J. S., Katz, A., Mornex, F., Colcher, D., Baglin, C., and Koenig, S. H. (1987) Tissue distribution and stability of metalloporphyrin MRI contrast agents. *Magn. Reson. Med. 4*, 24.

(7) Furmanski, P., and Longley, C. (1988) Metalloporphyrin enhancement of magnetic resonance images of human tumor xenografts in nude mice. *Cancer Res. 48*, 4604.

(8) Fiel, R. J., Musser, D. A., Mark, E. H., Mazurchuk, R., and Alletto, J. J. (1990) A comparative study of manganese *meso*-sulfonatophenylporphyrins: contrast enhancing agents for tumors. *Magn. Reson. Imaging 8*, 255.

(9) Ogan, M. D., Revel, D., and Brasch, R. C. (1987) Metalloporphyrin contrast enhancement of tumors in magnetic resonance imaging. A study of human carcinoma, lymphoma, and fibrosarcoma in mice. *Invest. Radiol. 22*, 822.

(10) Fiel, R. J., Button, T. M., Gilani, S., Mark, E. H., Musser, D. A., Henkelman, R. M., Bronskill, M. J., and van Heteren, J. G. (1987) Enhancement by manganese(III)$TPPS_4$ in a model tumor system. *Magn. Reson. Imaging 5*, 199.

(11) Harriman, A., and Porter, G. J. (1979) Photochemistry of manganese porphyrins. *J. Chem. Soc., Faraday Trans. 2 75*, 1532.

(12) Koenig, S. H., Brown, R. D., III, and Spiller, M. (1987) The anomalous relaxivity of $Mn^{3+}(TPPS_4)$. *Magn. Reson. Med. 4*, 252.

(13) Bertini, I., and Luchinat, C. (1986) *NMR of Paramagnetic Molecules in Biological Systems*; Benjamin Cummings, Menlo Park, CA.

(14) Hambright, P., and Chock, P. B. (1974) Metal porphyrin interactions. IV. Electron-transfer kinetics between dithionite and manganese(III) and cobalt(III) porphyrins. *Inorg. Chem. 13*, 3029.
(15) Hernandez, G. H., Brittain, H. G., Tweedle, M. F., and Bryant, R. G. (1990) Nuclear magnetic relaxation in aqueous solutions of Gd(HEDTA) complex. *Inorg. Chem. 29*, 985.
(16) Lester, C. C., and Bryant, R. G. (1991) Magnetically coupled paramagnetic relaxation agents. *Magn. Reson. Med.*, in press.
(17) C. C. Lester, (1990) Nuclear magnetic relaxation studies of water in paramagnetic and heterogeneous systems. Ph.D. Thesis, University of Rochester, Rochester, NY.
(18) Gonzalez, B., Kouba, S. Y., Reed, C. A., Kirner, J. F., and Scheidt, R. (1975) Manganese(II) porphyrins. Synthesis, structures and preference for five coordination. *J. Am. Chem. Soc. 97*, 3247.
(19) Koenig, S. H., Baglin, C., Brown, R. D., III, and Brewer, C. F. (1984) Magnetic field dependence of solvent proton relaxation induced by Gd^{3+} and Mn^{2+} complexes. *Magn. Reson. Med. 1*, 496.
(20) La Mar, G. N., and Walker, F. A. (1973) Proton nuclear magnetic resonance line widths and spin relaxation in paramagnetic metalloporphyrins of chromium(III), manganese(II),and iron(III). *J. Am. Chem. Soc. 95*, 6950.
(21) Pitt, D. A., and Smyth, C. P. (1959) Microwave absorption and molecular structure in liquids. XXVI. The dielectric relaxation times of two large oblate ellipsoidal molecules in benzene solution. *J. Phys. Chem. 63*, 582.
(22) Hubbard, P. S. (1966) Theory of electron-nuclear Overhauser effects in liquids containing free radicals. *Proc. R. Soc. London, Ser. A 291*, 582.
(23) Hwant, L., and Freed, J. H. (1985) Dynamic effects of pair correlation functions on spin relaxation by translational diffusion in liquids. *J. Chem. Phys. 63*, 4017.
(24) Freed, J. (1978) Dynamic effects of pair correlation functions on spin relaxation by translational diffusion in liquids, II. Finite jumps and independent T_1 processes. *J. Chem. Phys. 68*, 4034.
(25) Kell, G. S. (1972) Thermodynamic and transport properties of fluid water. In *Water: A Comprehensive Treatise* (F. Franks, Ed.) Vol. 1, p 363, Plenum Press: New York.
(26) Waysbort, D., and Navon, G. (1978) The effect of spin delocalization on the proton magnetic relaxation in transition metal hexaaquo ions. *J. Chem. Phys. 68*, 3074.
(27) Gottlieb, H. P. W., Barfield, M., and Doddrell, D. M. (1977) An electron spin density matrix description of nuclear spin–lattice relaxation in paramagnetic molecules. *J. Chem. Phys. 67*, 3785.
(28) Doddreel, D. M., Healy, P. C., and Bendall, M. R. (1978) Ligand centered proton and carbon electron–nuclear dipolar relaxation in a Ni(II) complex. Breakdown of the Solomon–Bloembergen equation. *J. Magn. Reson. 29*, 163.
(29) Nordenskiold, L., Laaksonen, A., and Kowalewski, J. (1982) Applicability of the Solomon–Bloembergen equations to the study of the paramagnetic transition-metal–water complexes. An ab initio SCF-MO study. *J. Am. Chem. Soc. 104*, 379.
(30) Unger, S. W., Jui, T., and La Mar, G. N. (1985) Proton NMR dipolar relaxation by delocalized spin density in low spin ferric porphyrin complexes. *J. Magn. Reson. 61*, 448.

Registry No. $[Mn(II)(TPPS_4)]^{4-}$, 71112-30-6; $[Mn(III)(TPPS_4)]^{3-}$, 88992-32-9; water, 7732-18-5.

Interaction of Doxorubicin with Lipid Systems

Jordi Hernández, Antoni Martí, and Joan Estelrich*

Unitat de Fisicoquímica, Facultat de Farmàcia, Universitat de Barcelona, 08028-Barcelona, Catalonia, Spain.
Received May 15, 1991

The action of doxorubicin, a cancer chemotherapeutic agent, on liposomes of dipalmitoylphosphatidylcholine obtained by extrusion, with or without cholesterol, and on monolayers of the same composition, was determined by photon correlation spectroscopy, penetration kinetics, and adsorption isotherms. Doxorubicin produced a wider vesicle distribution in both of liposomes, but liposomes containing cholesterol underwent an increase of mean diameter as well as polydispersity. In contrast, films containing cholesterol showed least interaction with the drug. Since both lipids are neutral, any interaction must be primarily hydrophobic.

INTRODUCTION

Doxorubicin hydrochloride (DXR) is a cancer chemotherapeutic agent with an anthracycline structure, which consists of an aglycon, adriamycinone, combined with an amino sugar, daunosamine. A pharmaceutical form which contains lactose as an excipient, is manufactured by Farmitalia (Milan, Italy) and sold under the trademark of Adriamycin.

Doxorubicin interacts widely with some membrane models such as lipid bilayers and liposomes (1-12). The affinity of DXR of liposomal membranes which bear no net charge is moderate. This interaction is believed to be dominated by forces other than ionic ones, since the affinity is only slightly dependent on the concentration of metal ions in the solution (2). In any case, an electrostatic interaction is observed between the ammonium group of DXR and the phosphate group of neutral phospholipids (8). In contrast, DXR interacts strongly with positively or negatively charged liposomes. However, binding of DXR to charged vesicles is not strictly dependent on electrostatic interactions, because the binding characteristics of a DXR derivative, daunorubicin, which presents a comparable basicity, were totally different from those of DXR (10). Therefore, DXR binding to the lipid bilayers appears to be dominated by hydrophobic interactions, although it is not clear where DXR is localized in the lipid bilayer.

In energy-transfer experiments it has been observed that anthracyclines interact preferentially with the hydrophobic core of lipid bilayers, while from measurements of circular dichroism, two different binding sites of DXR with lipids have been described. In the first one, the dihydroanthraquinone moiety lies outside the lipid bilayer, and in the second, it is embedded in the bilayer. The localization of DXR in membranes depends on the molecular packing of the lipid. In this way, DXR can penetrate a monolayer at low surface pressure but is squeezed out from the monolayer above a surface pressure of 23 $mN \cdot m^{-1}$. For this reason, DXR does not readily penetrate natural membranes, since they present a tight lipid molecular packing. The lateral surface pressure of red-cell membrane ranges from 31 to 35 $mN \cdot m^{-1}$ and this corresponds to a lateral pressure of a monolayer higher than 25 $mN \cdot m^{-1}$ (11).

On the basis of NMR studies, other authors have suggested that phospholipid bilayers become more fluid upon interaction with DXR and that the latter binds with the same affinity to liposomes of various compositions (6).

The aim of this study is to determine the influence of DXR on a planar membrane model, namely lipid monolayers, formed by neutral lipids and to compare this effect with the action of DXR on liposomes of the same composition as a model of curved bilayer. This is an aspect that can contribute to a better understanding of the drug–membrane interactions.

EXPERIMENTAL PROCEDURE[1]

Chemicals. L-α-Dipalmitoylphosphatidylcholine (DPPC), specified as 99% pure, and cholesterol (CHOL), type 99+% pure, were purchased from Sigma. Doxorubicin hydrochloride used in monolayers was purchased from Sigma and that used for liposome preparation was a gift of Farmitalia-Carlo Erba (Barcelona, Spain). Organic solvents (chloroform, *n*-hexane, and ethanol) obtained from Merck were without surface-active impurities. Water was double-distilled, the last time in presence of potassium permanganate, in borosilicate apparatus, and then purified through a Mill-Q system (Millipore).

Preparation of Liposomes. Liposomes of DPPC (or DPPC and CHOL at equal molar ratio) were obtained by the extrusion method (13). Briefly, 40 μmol of DPPC or DPPC and CHOL were dissolved in chloroform. The solution was dried under a stream of dry nitrogen and then lyophilized. Lipids were rehydrated in 7 mL of 145 mM NaCl, 10 mM Tris (pH 7.4) buffer solution containing DXR at 2 mM concentration. Hence, the molar ratio between lipid and DXR was 2.88. The multilamellar vesicles produced above were extruded seven times through polycarbonate membrane filters of variable pore size (Nucleopore) using nitrogen pressures of up 55×10^5 $N \cdot m^{-2}$. Unbound DXR was separated from bound DXR to liposomes by means of gel-filtration chromatography. Aliquots of 0.5 mL were applied on a column (30 × 0.9 cm i.d.) filled with Sephadex G-50 (Pharmacia LKB). The elution was carried out with the Tris buffer at a flow rate of 27.72 $mL/cm^2 \cdot h$.

Monolayer Technique. Films of DPPC or DPPC:CHOL (1:1, molar ratio) dissolved in *n*-hexane–ethanol were spread over the subphase of a Teflon trough filled

* Author to whom correspondence should be addressed.

[1] Abbreviations used: CHOL, cholesterol; DPPC, L-α-dipalmitoylphosphatidylcholine; DXR, doxorubicin hydrochloride; NMR, nuclear magnetic resonance; SUVs, small unilamellar vesicles; T_m, transition temperature.

1043-1802/91/2902-0398$02.50/0 © 1991 American Chemical Society

Table I. Influence of Doxorubicin on Liposome Size

liposome composition	filter pore size, nm	mean diameter, nm ± SD	polydispersity
DPPC	200	161.5 ± 41.9	0.064
DPPC	100	112.9 ± 23.1	0.041
DPPC	50	77.4 ± 22.2	0.077
DPPC + DXR	200	166.9 ± 83.0	0.201
DPPC + DXR	100	115.4 ± 58.7	0.207
DPPC + DXR	50	84.3 ± 39.1	0.179
DPPC:CHOL	200	184.5 ± 66.4	0.116
DPPC:CHOL	100	120.5 ± 30.7	0.082
DPPC:CHOL	50	111.2 ± 46.0	0.147
DPPC:CHOL + DXR	200	585.1 ± 744.0	0.679
DPPC:CHOL + DXR	100	169.8 ± 114.3	0.318
DPPC:CHOL + DXR	50	128.0 ± 57.4	0.169

with 10 mM Tris and 145 mM NaCl buffer (pH 7.4) solution. Compression isotherms were measured using an electromicrobalance (Sartorius A-120-S) based on the Wilhelmy method and coupled to a chart recorder to give a continuous reading of force on the dipping plate. The dimensions of the Teflon trough were 28.4 × 17.45 × 0.625 cm. Compression started at least 30 min after spreading and the compression rate was of 5 Å^2/molecule per min. For each experiment, buffer surface tension was first measured. DXR in the above solution was injected into the aqueous subphase beneath the lipid film and the subphase solution was stirred well by a magnetic stirrer (1 min). The final concentration of DXR in the bulk was 10 or 20 nM. Penetration kinetics were performed by spreading the necessary amount of DPPC to obtain monolayers of an initial pressure of 5 or 10 mN·m^{-1}. The area of the Teflon trough was 124 cm^2. Different volumes of DXR solution were injected into the subphase with a Hamilton syringe to attain DXR concentrations in the range of 10–40 nM. In kinetic assays, agitation in the subphase was maintained by two magnetic Teflon stirrer bars turning at 250 rpm. All data reported here are the average of three measurements. The temperature was kept at 24 ± 1 °C. The accuracy of the surface tension measurements was ±0.25 mN·m^{-1}.

Photon Correlation Spectroscopy (PCS). Fluctuations in scattered light intensity generated by the diffusion of vesicles in solution were analyzed. Analysis of the intensity fluctuations using a multichannel digital correlator allowed the mean diameter of vesicles to be obtained. PCS was performed in an Autosizer IIc photon correlation spectrometer (Malvern Instruments) consisting of a 5-mW, 632.8-nm, helium–neon laser irradiating the scattering cell placed inside a temperature-regulated enclosure. Data acquisition was via a Malvern 7032-N, 72-channel multibit correlator. Experimental conditions were temperature, 25.0 °C; reference angle, 90°; viscosity, 0.899 × 10^{-3} Pa·s; refractive index, 1.330.

Two principle methods can be used for data analysis. Assuming a log-normal size distribution of particles, the method of cumulant analysis (*14*) is available, while for broad monomodal distributions (polydisperse systems) the model independent analysis, which does not assume any particular form of the distribution, is used.

RESULTS AND DISCUSSION

Influence of DXR on Size of Liposomes. Size and polydispersity of liposomes obtained by extrusion and the influence of DXR on these parameters are shown in Table I. Mean diameters with their standard deviation and polydispersity were determined by PCS using the cumulants method and Gaussian analysis for mean diameter and standard deviation determinations, respectively. Polydispersity values are within the range of 0–1. Values of polydispersity ≤0.100 correspond to monodisperse population. As can be observed, DXR barely altered the mean diameter of DPPC liposomes, although it enhanced the standard deviation and the polydispersity. So, we can conclude that the presence of DXR in such liposomes results in wider vesicle distribution. On the contrary, the action on DXR on mixed liposomes produced an increase both in size and polydispersity. It is clear that the largest liposomes were those most affected, while liposomes extruded through filters with 50-nm pores underwent a variation like that observed in DPPC liposomes.

These variations in size and polydispersity can be explained by means of aggregation and fusion processes, although the main mechanism is the fusion, since determinations of size by photon correlation spectroscopy at 50 °C (temperature above the T_m of DPPC) afford us values similar to those obtained at 25 °C. As in SUVs, the T_m is always lower than in pure lipid; we have determined the variations in size of DPPC liposomes at temperatures ranging from 20 to 50 °C and we have checked that DPPC liposomes extruded through a 0.1-μm porous membrane show the minimal size and polydispersity at 33–34 °C; at this temperature, size parameters remained high. In the absence of DXR, a homogeneous vesicle population is obtained, but when DXR is present in the rehydratation buffer, the thermodynamically metastable vesicle suspension becomes less stable and the aggregation processes are now more likely to be due to the DXR charge. Aggregates of vesicles may fuse to form larger vesicles and small micelles. Liposomes which contains CHOL show, indeed, a larger average size. The presence of CHOL in DPPC liposomes produces a slight increase in *z* average diameter when it is present at equal molar ratio, but the increase is bigger if the ratio is 1.6:1 (DPPC:CHOL). (Liposomes of this composition and extruded by a 100-nm membrane filter have a mean diameter of 146 ± 54.) As the packing constraints of bilayer vesicles are determined by both the entropy of the system and the molecular geometry and as the latter is measured by a critical packing parameter that relates the optimal cross-sectional molecular area, the hydrocarbon chain volume and the maximal hydrophobic length (*15*), the insertion of DXR in the bilayer will modify these parameters and, thus, the vesicles will be of different sizes.

Increase in bilayer fluidity (*6*) or aggregation and fusion of small unilamellar liposomes of DPPC has been observed elsewhere (*16*).

Given that mixing the freeze-dried lipid and DXR can be close to an equilibrium because the lipid molecules will incorporate DXR molecules rather easily when they are forming liposomes, we mixed a liposome and a DXR solution and checked the vesicle size variation at several time intervals in order to rule out the localization of DXR being a consequence of the codispersion of DXR and lipids. Under these conditions, DXR also produced the modification of both polydispersity and *z* average diameter within vesicles. The aggregation process is fast (30 s after the last extrusion the size increase can be monitored by photon correlation spectroscopy) for the first 30 min and it becomes slower. Table II exhibits the variation in size 30 min after the mixing.

Measurements of Penetration Kinetics. Initially we determined the adsorption kinetics of DXR to the air–water interface in the absence of the lipid monolayer. DXR concentrations ranging from 10 to 100 nM were injected into the subphase. Above 90 nM the increase in surface pressure presented a plateau (steady state), but anyway,

Table II. Influence of Incubation of DXR on Size and Polydispersity of Liposomes

membrane pore, nm	liposome composition[a] DPPC	DPPC + DXR	DPPC:CHOL	DPPC:CHOL + DXR
50	92.4 (0.100)	100.4 (0.356)	91.7 (0.099)	113.6 (0.319)
100	116.1 (0.061)	117.4 (0.189)	126.5 (0.102)	203.9 (0.617)
200	188.0 (0.089)	251.3 (0.386)	168.8 (0.072)	221.0 (0.636)

[a] Values show the *z* average diameter (nm) and the polydispersity (in brackets) 30 min after the incubation.

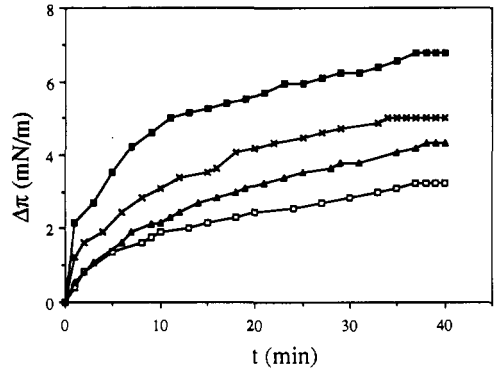


Figure 1. Variation in surface pressure for the interaction of doxorubicin at four concentrations (□, 10 nM; ▲, 20 nM; ×, 30 nM; and ■, 40 nM) with dipalmitoylphosphatidylcholine monolayer. Subphase buffer: 145 mM NaCl, 10 mM Tris-HCl (pH 7.4). The initial surface pressure of the film was 5 mN·m^{-1}.

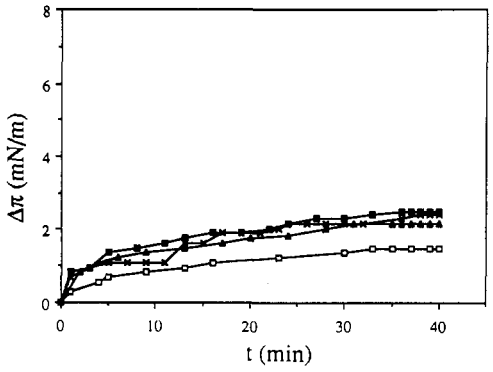


Figure 2. Variation in surface pressure for the interaction of doxorubicin at four concentrations with dipalmitoylphosphatidylcholine monolayer. The initial surface pressure of the film was 10 mN·m^{-1} (for conditions, see caption of Figure 1).

the increase never exceeded 0.96 mN·m^{-1}. This plateau was reached in 15–20 min.

In Figures 1–4 the registered increase in surface pressure of lipid monolayers produced by solutions of DXR at 10–20 nM concentration range are drawn as a function of time. Previously, it has been checked that a DPPC or DPPC/CHOL monolayer alone does not exhibit any change in its surface pressure over the period of 40 min. Figures 1 and 2 refer to DPPC monolayers at initial surface pressure (π_i) of 5 and 10 mN·m^{-1}, respectively. As in the surface activity experiments, an increase in surface pressure ($\Delta\pi$) of a lipid monolayer is taken to indicate an interaction of the substance present in the subphase with the lipid film. It can be established from these plots that the greater the concentration, the greater the interaction obtained. But at identical drug concentration, the increase obtained was significantly greater when a more expanded monolayer was employed. So, a 6.77 mN·m^{-1} increase in surface pressure was observed at π_i = 5 mN·m^{-1}, whereas

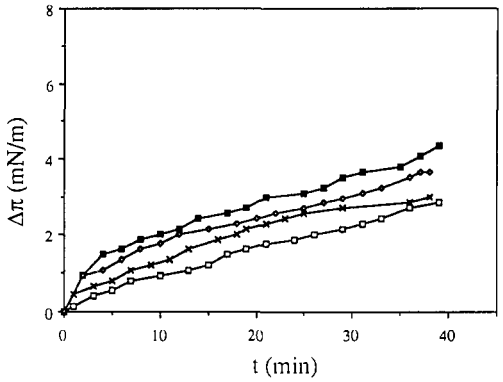


Figure 3. Variation in surface pressure for the interaction of doxorubicin at four concentrations with dipalmitoylphosphatidylcholine cholesterol monolayer. The initial surface pressure of the film was 5 mN·m^{-1} (for conditions, see caption of Figure 1).

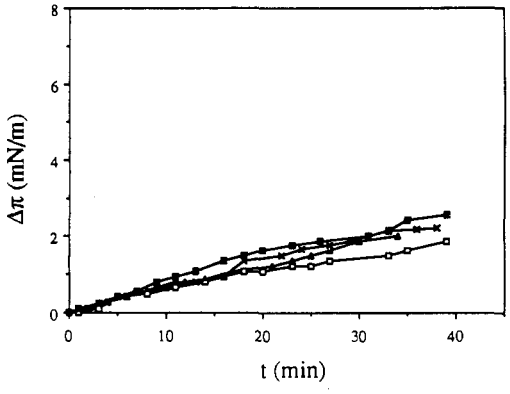


Figure 4. Variation in surface pressure for the interaction of doxorubicin at four concentrations with dipalmitoylphosphatidylcholine cholesterol monolayer. The initial surface pressure of the film was 10 mN·m^{-1} (for conditions, see caption of Figure 1).

at π_i = 10 mN·m^{-1} it was 2.49. Thus, the drug–lipid interaction is highly dependent on the initial pressure of the monolayer being lower for more compressed monolayers. At surface pressures from 20 to 40 mN·m^{-1}, this increase is progressively abolished and can be accounted for by a partial exclusion of DXR from monolayer at high pressures.

Figures 3 and 4 show the effect of DXR on DPPC:CHOL monolayers. It can be observed that the interaction with such lipids layers followed a similar pattern, although the curves were closer to each other than in DPPC monolayers and they seem to lead to constant values. An important difference between the two kinds of lipids layers was the time necessary to reach the steady state. Thus, monolayers of DPPC presented a plateau about 35 min after the injection of DXR into the subphase, while DPPC:CHOL monolayers needed much longer to uptake DXR. Thus, saturation values $\Delta\pi$ for DPPC:CHOL may be higher than the DPPC ones. Unfortunately, incubation times longer than 35 min alter monolayer properties and it was not possible to check the DXR incorporation after this time.

Measurements of Compression Isotherms. Measurements of the surface pressure–area (π–A) of DPPC films are shown in Figure 5. The compression isotherms were characteristic of lipids in the liquid-expanded state. From this figure it is clear that the adsorption of DXR to the lipid film produced a less condensed monolayer. This finding, which is a consequence of the drug–lipid interaction, was more evident at a surface pressure of 10

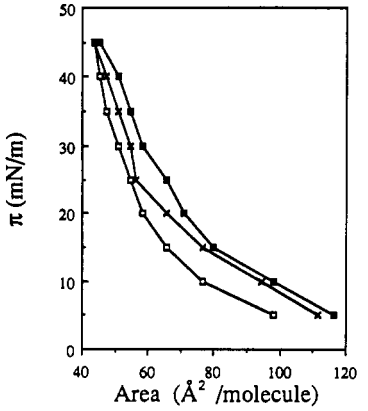


Figure 5. Surface pressure–molecular area isotherms for adsorbed films of doxorubicin at the dipalmitoylphosphatidylcholine–water (Tris buffer, pH 7.4) interface. Concentration of doxorubicin (nM): □, 0; ×, 10; ■, 20.

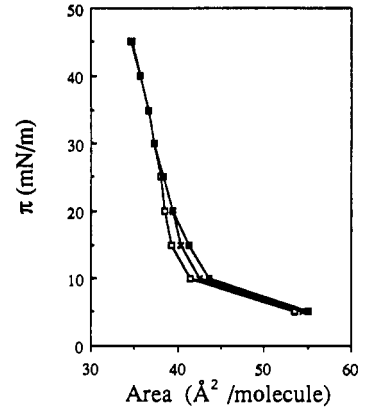


Figure 6. Surface pressure–molecular area isotherms for adsorbed films of doxorubicin at the dipalmitoylphosphatidylcholine:cholesterol–water (Tris buffer, pH 7.4) interface (for conditions, see caption of Figure 5).

$mN \cdot m^{-1}$. At this pressure, which corresponds to the expanded–condensed liquid-phase transition of pure DPPC monolayers, the area/molecule was nearly 77 Å², while in the presence of 10 and 20 nM DXR it rose to 95 and 99 Å², respectively. However, the three curves tended to collapse at similar π (45 $mN \cdot m^{-1}$), corresponding to the limiting molecular area of 44 ± 1 Å²/molecule. Such values are in good agreement with those described elsewhere (*17*).

In contrast, the effect of DXR on mixed films was almost insignificant (Figure 6). In this case, isotherms were parallel from 5 to 20 $mN \cdot m^{-1}$ surface pressure, and at higher surface pressure the isotherms were superimposable. So, the amount of DXR incorporated appears to be small. Nevertheless, it must be borne in mind that DPPC:CHOL membranes are much harder than DPPC membranes and, for this reason, it is logical to suppose that the uptake of the molecules from the water phase is considerably slow. The stiffness of the DPPC:CHOL is evident from Figures 5 and 6; the onset of the π–A curve for DPPC:CHOL is very steep. Moreover, with such mixed films it is not possible to observe the effect of the interaction at the surface pressure of the phase transition, because it is eliminated when the cholesterol mole fraction in a mixed film is higher than 0.23 (*18*).

To sum up, we may conclude that both methods, monolayer technique and photon correlation spectroscopy, show that DXR interacts with the lipid systems used. So, the effect of DXR on liposomes involves the vesicle distribution becoming broader in DPPC liposomes. With DPPC:CHOL liposomes, not only was the distribution wider but the average diameter also increases. DXR is believed to induce fusion and aggregation. It is also important to notice that the extension of this effect varies with the liposome curvature.

On the other hand, results from penetration kinetics and compression isotherms also indicate a interaction between DXR and monolayers. The binding of water-soluble substances, such as DXR, to a lipid monolayer may be due to hydrophobic interactions for noncharged and partially hydrophobic chains of the molecule, and to electrostatic interactions for polar or ionizable groups. DXR in the hydrochloride form contains a charged tertiary amine and can establish electrostatic interactions, but due to its structure it can also behave as a hydrophobic substance and penetrate into the hydrophobic core of the lipid layer. In this way, a weak insertion of the planar anthracenic part of anthracycline into the lipidic leaflet has been observed (*10*). This insertion into the hydrocarbon region explains that the apparent area occupied is higher in the presence of DXR, as well as the enhancement of liposome size. Furthermore, as both lipids DPPC and CHOL, are neutral, the main kind of interaction between DXR and such lipids must be primarily hydrophobic.

Finally, it is important to remark on the apparently opposite effect of CHOL in liposomes in comparison to monolayers. So, while the interaction was greater in liposomes containing CHOL, mixed monolayers experienced the minimum disturbance in their ordered configuration. Bearing in mind that the interaction between lipid and DXR has been only observed in monolayers at low initial surface pressures and, on the other hand, at room temperature, liposomal lipids are in the gel state and, consequently, the lateral surface pressure is high, it is difficult to make a comparison between the two lipids systems as far as the DXR interaction is concerned.

ACKNOWLEDGMENT

This research was supported in part by the CICYT (No. 86-0484) (Spain). We thank Robyn Rycroft for his help in translation to the English version.

LITERATURE CITED

(1) Goldman, R., Facchinetti, T., Bach, D., Raz, A., and Shinitzky, M. (1978) A differential interaction of daunomycin, adriamycin and their derivatives with human erythrocytes and phospholipid bilayers. *Biochim. Biophys. Acta 512*, 254–269.

(2) Karczmar, G. S., and Tritton, T. R (1979) The interaction of adryamicin with small unilamellar vesicle liposomes. A fluorescence study. *Biochim. Biophys. Acta 557*, 306–319.

(3) Crommelin, D. J. A., Slaats, N., and van Blois, L. (1983) Preparation and characterization of doxorubicin-containing liposomes: I. Influence of liposome charge and pH of hydration medium on loading capacity and particle size. *Int. J. Pharm. 16*, 79–92.

(4) Burke, T. G., and Tritton, T. R. (1984) Ligand self-association at the surface of liposomes: a complication during equilibrium-binding studies. *Anal. Biochem. 143*, 135–140.

(5) Burke, T. G., and Tritton, T. R. (1985) Structural basis of anthracycline selectivity for unilamellar phosphatidylcholine vesicles: an equilibrium binding study. *Biochemistry 24*, 1768–1770.

(6) Burke, T. G., and Tritton, T. R. (1985) Location and dynamics of anthracyclines bound to unilamellar phosphatidylcholine vesicles. *Biochemistry 24*, 5972–5980.

(7) Griffin, E., Vanderkooi, J., Maniara, G., and Erecinska, M. (1986) Anthracycline binding to synthetic and natural membranes. A study using resonance energy transfer. *Biochemistry 25*, 7875–7880.

(8) Giuliani, A. M., Boicelli, C. A., De-Angelis, L., Giomini, M., Giustini, M., and Trotta, E. (1988) Doxorubicin interactions with neutral phospholipids: An infrared and thermal analysis study. *Stud. Biophys. 123*, 45–52.
(9) Nicolay, K., Sautereau, A. M., Tocanne, J. F., Brasseur, R., Huart, P., Ruysschaert, J. M., and de Kruijff, B. (1988) A comparative model membrane study on estructural effects of membrane-active positively charged anti-tumor drugs. *Biochim. Biophys. Acta 940*, 197–208.
(10) Henry-Toulme, N. Stefanska, B., Borowski, E., and Bolard, J. (1988) Structural basis for the binding of antitumor anthracycline antibiotics to model membrane: Circular dichroism studies. *Mol. Pharmacol. 33*, 574–579.
(11) Dupou-Cézanne, L., Sautereau, A. M., and Tocanne, J. F. (1989) Localization of adryamicin in model and natural membranes. *Eur. J. Biochem. 18*, 695–702.
(12) Wolf, F. A. de, Maliepaard, M., van Dorsten, F., Berghuis, I., Nocolay, K., and de Kruijff, B. (1991) Comparable interaction of doxorubicin with various acidic phospholipids results in changes of lipid order and dynamics. *Biochim. Biophys. Acta 1096*, 67–80.
(13) Mayer, L. D., Hope, M. J., and Cullis, P. R. (1986) Vesicles of variable sizes produced by a rapid extrusion procedure. *Biochim. Biophys. Acta 858*, 161–168.
(14) Koppel, D. E. (1972) Analysis of macromolecular polydispersity in intensity correlation spectroscopy: The method of cumulants. *J. Chem. Phys. 57*, 4814–4820.
(15) Maggio, B., Albert, J., and Yu, R. K. (1988) Thermodynamic–geometric correlations for the morphology of self-assembled structures of glycosphingolipids and their mixtures with dipalmitoylphosphatidylcholine. *Biochim. Biophys. Acta 945*, 145–160.
(16) Constantinides, P. P., Tritton, T. T., and Sartorelli, A. C. (1988) Interaction of adryamicin with single and multibilayer dipalmitoylphosphatidylcholine vesicles: spin-labeling and calorimetric study. *J. Liposome Res. 1*, 35–62.
(17) von Tscharner, V., and McConnell, H. M. (1981) An alternative view of phospholipid phase behavior at the air–water interface. *Biophys. J. 36*, 409–419.
(18) Cadenhead, D. A., and Kellner, M. J. (1976) The miscibility of dipalmitoylphosphatidylcholine and cholesterol in monolayers. *J. Colloid Interface Sci. 57*, 224–227.

A Novel Technique to Assay Adducts of DNA Induced by Anticancer Agent *cis*-Diamminedichloroplatinum(II)

Minoti Sharma,* Rama Jain, and Thomas V. Isac

Department of Biophysics, Roswell Park Cancer Institute, Buffalo, New York 14263. Received May 20, 1991

The dideoxynucleotides d(pGpG) and d(pApG) and the tetradeoxynucleotide d(CpTpApG) were synthesized in solution phase by a modified phosphotriester technique and reacted with the anticancer agent *cis*-diamminedichloroplatinum(II) (cisplatin). The major products were isolated by HPLC and characterized by NMR and mass spectrometry as cross-link adducts of cisplatin with the neighboring purine bases. The cross-link adducts of d(pGpG) and d(pApG) were dansylated through a 5′-phosphoramidate linkage with ethylenediammine. The labeling efficiency of the adducts was quantitative as in the case of the normal dinucleotides. The modified tetramer was digested with nuclease P_1. The excised adduct was enriched by HPLC and labeled with dansyl chloride. The analysis of the postlabeled adduct by HPCL, using a fluorescence detector, detected a peak with retention time corresponding to that of the dansylated *cis*-Pt$(NH_3)_2$d(pApG). Cochromatography with the authentic marker confirmed the identification. The same overall procedure was used to assay calf thymus DNA exposed to cisplatin. The major adducts were identified as *cis*-Pt$(NH_3)_2$d(pGpG) and *cis*-Pt$(NH_3)_2$d(pApG). The quantitative labeling efficiency of platinum adducts combined with highly sensitive fluorescence detection technique (subfemtomol) suggests that fluorescence postlabeling assay could be a novel approach for real-time analysis of DNA modification induced by platinated drugs in biological system.

INTRODUCTION

cis-Diamminedichloroplatinum(II) (cisplatin) is a widely used chemotherapeutic agent that is effective against ovarian, testicular, and other tumors (*1–3*). It is now generally accepted that the antineoplastic activity of the drug is based on its interaction with genomic DNA (*4*). Analysis of cisplatin-modified DNA shows two major adducts, *cis*-Pt$(NH_3)_2$d(pGpG) and *cis*-Pt$(NH_3)_2$d(pApG), both derived from intrastrand cross-link of cisplatin and neighboring nucleobases (*5*). It is interesting that, in the latter adduct, deoxyadenosine is always the 5′-nucleotide. Investigations of these adducts by NMR spectroscopy reveal that cisplatin is bound to the purine base at the N-7-position. Interstrand cross-links are relatively minor lesions (*6, 7*).

The study of the molecular basis of the anticancer agent requires not only the detection but also identification and reliable quantitation of the various adducts derived from exposure of DNA to the agent. Correlation between the presence of specific cisplatin adducts in DNA from nucleated blood cells and clinical response could permit a predictive assay of the effectiveness of the agent for individual patient. Therefore, the need for a highly sensitive and straight-forward assay which would allow the detection, identification, and quantification of the level of adducts distribution in exposed DNA cannot be overstated. Large quantities of material ($\geq 10^8$ cells) are needed for reliable determination of cisplatin adducts by atomic absorption spectroscopy (AAS) (*8*). This precludes many investigations on clinical material. The use of radiolabeled Pt compounds (*9*) is not suitable for human experimentation. A series of in vitro and in vivo studies were performed to characterize DNA damage recognized by an antiserum elicited against DNA modified with cisplatin. Adducts determined by cisplatin–DNA enzyme linked immunosorbent assay (ELISA) in blood cell DNA have been shown to correlate well with positive clinical outcome in testicular and ovarian cancer patients receiving platinum-drug-based chemotherapy (*10, 11*). However, with human samples, the characterization of the DNA damage recognized by an antiserum elicited against cisplatin-modified DNA measured a variable fraction of the total DNA-bound Pt determined by AAS study (*12*). The cisplatin–DNA antiserum has primary specificity for a three-dimensional lesion formed by intrastrand Pt–GG and Pt–AG adducts of DNA and oligomers but does not recognize adducts obtained from digested DNA. A variety of factors that affect a specific region of DNA could possibly influence what is recognized by the antibody. Recently, Tilby et al. reported highly sensitive detection of DNA modification (1 Pt adduct/10^6 bases) induced by cisplatin and carboplatin [*cis*-diammine(1,1-cyclobutanedicarboxylato)platinum(II)] in both in vitro and in vivo using monoclonal antibody (*13*). But the immunoassay does not permit the resolution of the various DNA adducts formed by these agents. Fichtinger-Schepman et al. reported immunochemical quantitation of *cis*-Pt$(NH_3)_2$d(pGpG) but not *cis*-Pt$(NH_3)_2$d(pApG) after analytical separation of the modified DNA digest by FPLC on Mono Q anion-exchange column (*5, 14*). The ^{32}P-postlabeling technique introduced by Randerath et al. (*15*) has been a powerful tool for chromatographic resolution of low-level DNA adducts in experimental animal and human using only 1–5 μg of DNA digest. The successful application of this technique depends, however, on the efficiency of the radiolabeling of the modified substrates with [γ-^{32}P]ATP and polynucleotide kinase. The major cisplatin–DNA adduct has been reported recently to be phosphorylated only with an efficiency of 0.1% of the corresponding dinucleotide (*16*). This low level of phosphorylation does not appear encouraging for quantitative determination requiring a high sensitivity. We have developed a novel technique to assay DNA damage by combining enzymatic digestion of the modified DNA with fluorescence postlabeling (*17*). The fluorescent label is introduced chemically and the procedure, therefore, does not suffer from the vagaries of the enzymatic labeling. We observed that the two major intrastrand *cis*-Pt$(NH_3)_2$ adducts of d(pGpG) and d(pApG) are labeled with dansyl chloride with the same efficiency as their normal counterparts. The

* To whom correspondence should be addressed.

1043-1802/91/2902-0403$02.50/0 © 1991 American Chemical Society

labeling efficiency was determined by previously published procedures (*17, 18*). This report describes the fluorescence postlabeling assay of cisplatin-modified DNA model d(CTAG) and calf thymus DNA.

EXPERIMENTAL PROCEDURES

Protected mononucleotide phosphotriesters and protected nucleosides were obtained from Gallard Schesinger Biochemicals. Calf thymus DNA, dansyl chloride, bovine pancrease DNAse I, and nuclease P_1 from *Penecilium citriums* were purchased from Sigma. Cisplatin was obtained from Fulka.

The syntheses of d(GpG), d(ApG), and d(CpTpApG) were carried out in solution phase by a modified phosphotriester technique previously reported (*19*). The dinucleoside monophosphates were 5′-phosphorylated by a facile chemical procedure previously described (*17*). The cisplatin adducts of the di- and tetradeoxynucleotides were prepared by reacting 2 OD units of the nucleotide in 50 μL of sodium phosphate buffer (4 mM, pH 6) with 50 μL of cisplatin in water (1 mg/mL). The reaction was allowed to proceed at room temperature for 16 h. The products from the large-scale reactions were isolated by reverse-phase HPLC (C18, 5 μm, 10 mm × 25 cm) using a linear gradient of 0–20% acetonitrile in 0.1 M ammonium acetate buffer. The isolated products were desalted in the same system using a linear gradient of 0–100% methanol in water.

Calf thymus DNA was reacted with cisplatin and the modified DNA was degraded enzymatically following reported procedures (*5*). The modified tetramer (2 OD units) was degraded by nuclease P_1 (20 μg) at 37 °C in 100 μL of sodium acetate buffer (0.1 M, pH 5.5) containing 0.2 mM $ZnCl_2$.

The FAB mass spectra and the ^1H NMR measurements were done with Finnigan MAT 90 and Bruker WP200 spectrometers, respectively. The HPLC conditions used for the various analyses have been described in the figure legends. The authentic markers and the various fractions collected from the digests were labeled with dansyl chloride following reported procedures (*17, 18*).

RESULTS AND DISCUSSION

The major platinated adducts from the reactions of cisplatin with d(pGpG) and d(pApG) were isolated in 90% and 70% yields, respectively. The adducts were characterized by FAB mass spectrometry and ^1H NMR. Although a matrix of triethanolamine facilitated the formation of deprotonated nucleotides during negative-ion FAB mass spectrometry, platinated nucleotides showed poor solubility in this matrix. An equal volume mixture of triethanolamine and glycerol was superior to either pure triethanolamine or pure glycerol for the platinated nucleotide. The observed molecular ions $(M-H)^-$ at m/z 901 and 886 for the platinated dinucleotide adducts supported the expected molecular weights for *cis*-Pt$(NH_3)_2$d(pGpG) and *cis*-Pt$(NH_2)_2$d(pApG), respectively. The negative-ion mass spectrum of the monoplatinated tetradeoxynucleotide d(CpTpApG) contained fragment ions indicative of the oligonucleotide sequence and location of platination (Figure 1). The molecular ion $(M-H)^-$ at m/z 1400 agreed with the expected molecular weight for the tetramer containing the cross-link *cis*-Pt$(NH_3)_2$d(pApG) adduct. The molecular ion region of each platinated adduct was characterized by multiple isotope peaks due largely to isotopes of platinum (*20*).

The ^1H NMR spectra of both the adducts were in agreement with the reported results (*5*). Having been

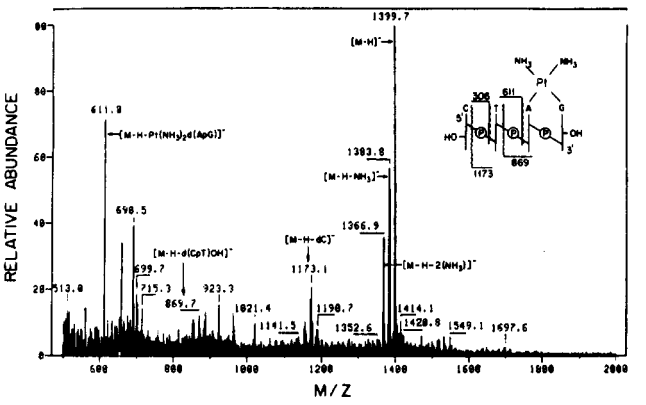


Figure 1. Negative-ion FAB mass spectrum of monoplatinated adduct of d(CTAG) with cisplatin.

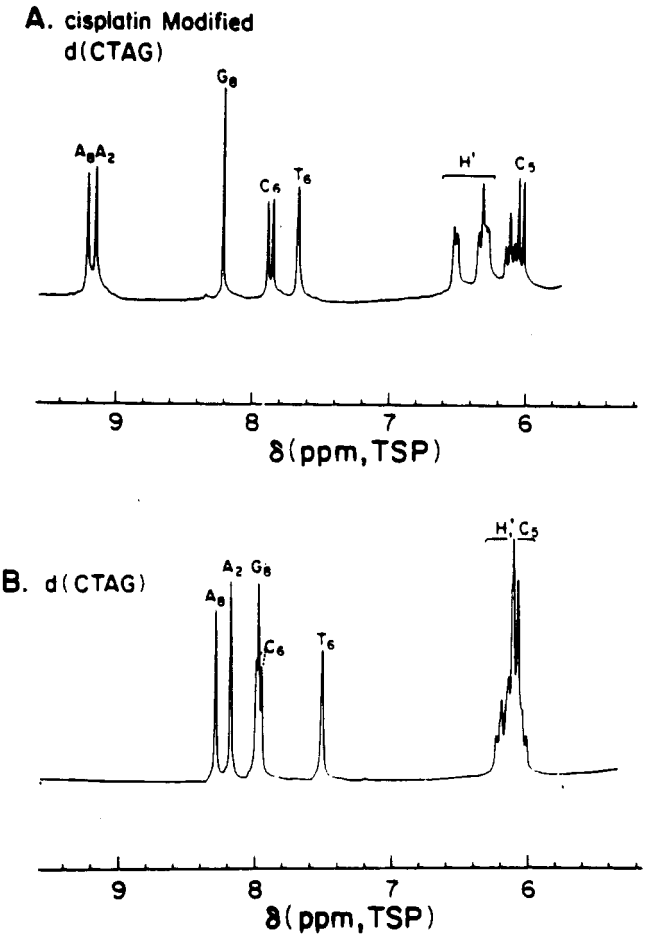


Figure 2. Low-field resonances of 200-MHz ^1H NMR spectra of (A) cisplatin-modified d(CTAG) and (B) d(CTAG). Solutions were 10 mM base in D_2O, pH 6.0 (uncorrected), and referenced to TSP.

characterized, the dinucleotide adducts served to identify the same lesions from DNA exposed to cisplatin. The downfield resonances of the ^1H NMR spectra of the tetradeoxynucleotide d(CTAG), before and after reaction with cisplatin, are shown in Figure 2. The integrated intensity of all the protons are in agreement with 1:1 ratio of the four nucleobases in both the spectra. In general, the chemical shifts of the nonexchangeable base protons have been reported to move downfield upon binding of the platinum compound to the nucleobases (*21*). As shown in Figure 2, the chemical shifts of both AH-8 and AH-2 protons showed a significant downfield shift from 8.28 and 8.17 ppm before modification to 9.20 and 9.14 ppm, respectively, after modification. The GH-8 proton and

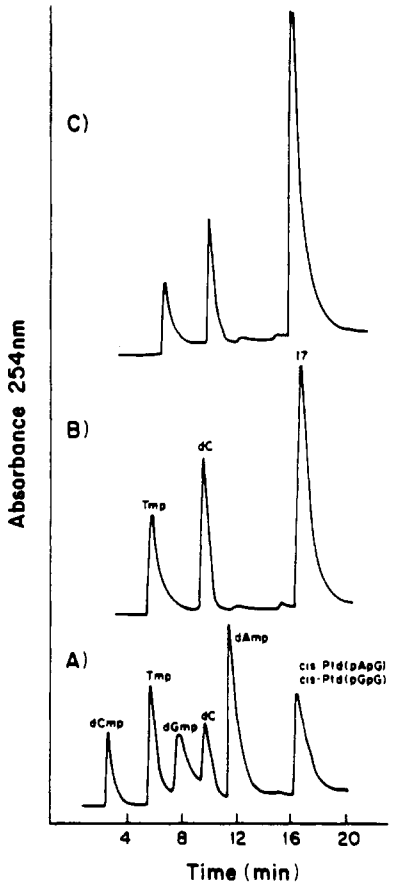


Figure 3. HPLC elution profiles in a Radial-Pak LC cartridge 8MBC18 (10 μm, 8 mm × 10 cm) eluted with a linear gradient of 0–20% acetonitrile in 0.1 M ammonium acetate buffer. (A) A mixture of dCmp, Tmp, dGmp, dAmp, dC, *cis*-Pt(NH_3)$_2$d(pGpG), and *cis*-Pt(NH_3)$_2$d(pApG), (B) nuclease P_1 digest of platinated d(CTAG), and (C) cochromatography of nuclease P_1 digest of platinated d(CTAG) with *cis*-Pt(NH_3)$_2$d(pApG).

the TH-6 proton also showed downfield shift of 0.24 and 0.10 ppm, respectively, after modification. The CH-5 and CH-6 protons of the self-complementary tetramer, on the other hand, showed upfield shifts suggesting increased shielding of these protons by the aromatic rings of the cross-linked purine bases after modification.

Figure 3B shows HPLC analysis of the nuclease P_1 digest of the platinated d(CpTpApG). The profile contains peaks due to Tmp and dC along with an unknown at 17 min. Nuclease P_1 has been reported to excise bulky adducts from modified DNA as 5′-phosphorylated dinucleotide whereas the normal nucleotides are released as 5′-monophosphates (*22*). The peak at 17 min in profile B was identified as *cis*-Pt(NH_3)$_2$d(pApG) by cochromatography with the authentic marker (see profile 3C). Profile 3A shows the analysis of a mixture of four normal nucleotides, dC, and the two authentic markers *cis*-Pt(NH_3)$_2$d(pGpG) and *cis*-Pt(NH_3)$_2$d(pApG). The markers, although well resolved from the normal nucleotides, coelute under the HPLC condition used in the Figure 3. The DNA model d(CpTpApG) lacks two adjacent guanine residues. Therefore, the conclusion drawn from the cochromatographic analysis shown in profile C is valid for the identification of the peak at 17 min in profile B. Thus the nuclease P_1 digestion study supports the spectroscopic data in showing that the cisplatin reacted DNA model contains the cross-link adduct *cis*-Pt(NH_3)$_2$d(pApG).

The peak at 17 min in profile B was collected, lyophilized, and dansylated. HPLC analysis of the postlabeled sample using fluorescence detection showed a peak at 36

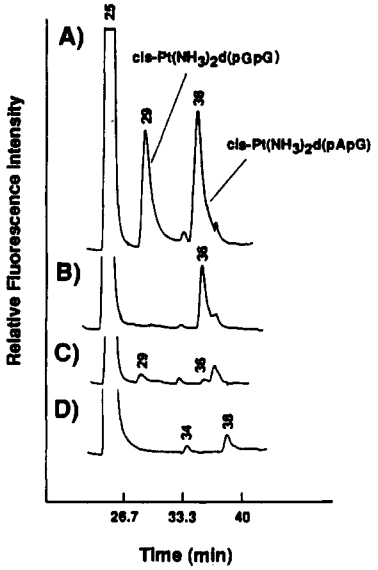


Figure 4. HPLC elution profiles of dansylated nucleotides generated with a reversed-phase C18 column (5 μm, 4.6 mm × 25 cm) eluted with a 30-min linear gradient of 15–20% acetonitrile in 0.1 ammonium acetate buffer and detected with a fluorescent detector (excitation 340 nm, emission 520 nm): (A) *cis*-Pt(NH_3)$_2$d(pGpG) at 29 min and *cis*-Pt(NH_3)$_2$d(pApG) at 36 min, (B) nuclease P_1 digested adduct from platinated d(CTAG), (C) nuclease P_1 digested adduct from platinated calf thymus DNA, and (D) nuclease P_1 digested DNA control.

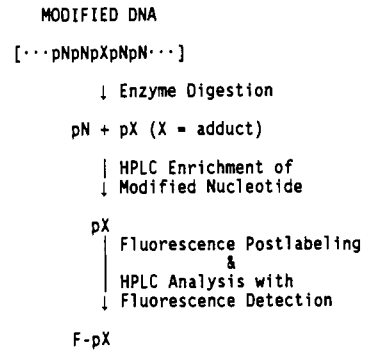


Figure 5. Scheme of fluorescence postlabeling assay for DNA damage; F denotes fluorescence label.

min (Figure 4B) which coeluted with dansyl-labeled authentic marker *cis*-Pt(NH_3)$_2$d(pApG) (the results not shown). Profile A in the Figure 4 shows the HPLC analysis of the dansyl-labeled markers *cis*-Pt(NH_3)$_2$d(pGpG) and *cis*-Pt(NH_3)$_2$d(pApG). These two markers, which coeluted prior to the labeling (Figure 3A), resolve well after dansylation.

The detection and identification of the adduct from cisplatin reacted DNA model study having been achieved, the fluorescence postlabeling technique was extended to assay damage induced by cisplatin in calf thymus DNA. Figure 5 outlines the steps involved in the fluorescence postlabeling assay.

Calf thymus DNA was modified with cisplatin and resulted in a total input drug/nucleotide ratio in solution of 0.055. The modified DNA (20 μg) was digested with DNAse I and nuclease P_1 to excise the adducts. The normal nucleotides were released as 5′-monophosphates. A same-size sample of untreated DNA was also processed simultaneously as a control. The digests were filtered in a centrifugal ultrafree microunit with 10 000 NMWL polysulfone membrane. The filtrates were fractionated by HPLC using the same condition as described in the model study (see Figure 3). The HPLC profiles from the

digests showed only the normal nucleotides. Calculation of the peak area of each nucleotide multiplied by the response factor (area/nmol) of the corresponding standard nucleotide showed that the digestion efficiency of the modified DNA was 75% of the control value. A fraction was collected from each treated and control DNA digest corresponding to the retention time of the authentic markers as shown in the profile A in Figure 3. Collection of such a fraction from the treated DNA samples, prior to labeling, enriches both the adducts from the normal nucleotides. The collected fractions were lyophilized and dansylated. HPLC analysis (Figure 4) showed that the profile C from the modified postlabeled sample had two peaks in addition to those present in the control (profile D in Figure 4). The peaks at 29 and 36 min in profile C were identified as *cis*-Pt$(NH_3)_2$d(pGpG) and *cis*-Pt-$(NH_3)_2$d(pApG) respectively by cochromatography with the dansylated authentic markers (results not shown). We observed that in cisplatin-modified calf thymus DNA, the area of the d(pGpG) adduct is twice the area of the d(pApG) adduct. The cross-link adducts constituted nearly 90% of total platinum bound to DNA. A similar observation has been reported for cisplatin-modified salmon sperm DNA using FPLC of the DNA digest followed by measurement of platinum content by AAS (*5*). The artifactual peaks at 34 and 38 min shown in the control profile D are also present in profiles A–C. The large peak at 25 min is due to excess labeling reagent.

The profiles shown in Figure 4C,D correspond to the analysis from 5-μg DNA digests. Recently we have developed an analytical system for fluorescence postlabeling assay by combining microbore HPLC with laser-induced fluorescence detection (*18*). The preliminary investigation shows that the new system has a subfemtomole detection limit and is 4 orders of magnitude more sensitive than the conventional system used in the current study (*23*). The present report, though preliminary, suggests that fluorescence postlabeling assay could be a novel approach in correlating clinical outcome with the efficacy of those drugs that bind covalently with DNA resulting in molecular lesions.

ACKNOWLEDGMENT

Supported in part by National Cancer Institute Grant CA46896.

LITERATURE CITED

(1) Harder, H. C., and Rosenberg, B. (1970) Inhibitory effects of anti-tumor platinum compounds on DNA, RNA and protein synthesis in mammalian cells in vitro. *Int. J. Cancer 6*, 207–216.

(2) Rosecweig, M., Von Hoff, D. D., Slavik, M., and Muggia, F. M. (1977) Cis-diamminedichloroplatinum(II): A new anticancer drug. *Ann. Int. Med. 86*, 803–812.

(3) Gottlieb, J. A., and Drewinko, B. (1975) Review of the current clinical status of platinum coordination compounds in cancer chemotherapy. *Cancer Chemother. Rep. 59*, 621–628.

(4) Roberts, J. J. (1981) Mechanism of action of anti-tumor platinum coordination compounds. *Molecular Actions and Targets for Cancer Chemotherapeutic Agents* (A. C. Sartorelli, J. S. Lazo, and J. R. Bertino, Eds.) pp 17–43, Academic Press, New York.

(5) Fichtinger-Schepman, A. M. J., Van der Veer, J. L., den Hartog, J. H. J., Lohman, P. H. M., and Reedijk, J. (1985) Adducts of the antitumor drug *cis*-diamminedichloroplatinum(II) with DNA: Formation, identification, and quantitation. *Biochemistry 24*, 707–713.

(6) Lemaire, M-A., Schwartz, A. M., Rahmouni, A. R., and Leng, M. (1991) Interstrand cross-links are preferentially formed at the d(GC) sites in the reaction between *cis*-diamminedichloroplatinum(II) and DNA. *Proc. Natl. Acad. Sci. U.S.A. 88*, 1982–1985.

(7) Hopkins, P. B., Millard, T. J., Woo, J., Weidner, M. F., Kirchner, J. J., Sigurdsson, S. T., and Raucher, S. (1991) Sequence preferences of DNA interstrand cross-linking agents: Importance of minimal DNA structural reorganization in the cross-linking reaction of merchlorethamine, cisplatin, and mitomycin C. *Tetrahedron 47*, 2475–2489.

(8) Fichtinger-Schepman, A. M. J., Lohman, P. H. M., and Reedijk, J. (1982) Detection and quantitation of adducts formed upon interaction of *cis*-diamminedichloroplatinum(II) with DNA by ion-exchange chromatography after enzymatic degradation. *Nucleic Acids Res. 10*, 5345–5356.

(9) Eastman, A. (1983) Characterization of the adducts produced in DNA by *cis*-diamminedichloroplatinum(II). *Biochemistry 22*, 3927–3933.

(10) Reed, E., Ozols, F., Tarone, R., Stuart, H. Y., and Poirier, M. C. (1988) The measurement of cisplatin–DNA adduct levels in testilcular cancer patients. *Carcinogenesis 9*, 1909–1911.

(11) Reed, E., Litterst, C. L., Thill, C. C., Yuspa, S. H., and Poirier, M. C. (1987) Platinum-DNA adducts in leukocyte correlate with disease response in ovarian cancer patients receiving platinum-based chemotherapy. *Proc. Natl. Acad. Sci. U.S.A. 84*, 5024–5028.

(12) Reed, E., Gupta-Burt, S., Litterst, C. L., and Poirier, M. C. (1990) Characterization of the DNA damage recognized by an antiserum elicited against *cis*-diamminedichloroplatinum(II)-modified DNA. *Carcinogenesis 11*, 2117–2121.

(13) Tilby, M. J., Johnson, C., Knox, R. J., Cordell, J., Roberts, J. J., and Dean, C. J. (1991) Sensitive detection of DNA modifications induced by cisplatin and carboplatin in vitro and in vivo using a monoclonal antibody. *Cancer Res. 51*, 123–129.

(14) Fichtinger-Schepman, A. M. J., Baan, R. A., Luiten-Schuite, A., Van Dijk, M., and Lohman, P. H. M. (1985) Immunochemical quantitation of adducts induced in DNA by *cis*-diamminedichloroplatinum(II) and analysis of adduct-related DNA-unwinding. *Chem.-Biol. Interact. 55*, 275–288.

(15) Randerath, K., Reddy, M. Y., and Gupta, R. C. (1981) ^{32}P-postlabeling test for DNA damage. *Proc. Natl. Acad. Sci. U.S.A. 78*, 6126–6129.

(16) Hemminki, K., Peltonin, K., and Mustonin, R. (1990) ^{32}P-postlabeling of 7-methyl-dGmp, ring-opened 7-methyl-dGmp and platinated d(GpGp). *Chem.-Biol. Interact. 74*, 45–54.

(17) Kelman, D. J., Lilga, K. T., and Sharma, M. (1988) Synthesis and application of fluorescent labeled nucleotides to assay DNA damage. *Chem.-Biol. Interact. 66*, 85–100.

(18) Sharma, M., and Freund, H. G. (1991) Development of laser-induced fluorescence detection to assay DNA damage. In *Optical Methods for Ultrasensitive Detection and Analysis: Techniques and Applications* (B. L. Fearey, Ed.) Proc. SPIE 1435, pp 280–291, SPIE, Bellingham, WA.

(19) Sharma, M., and Box, H. C. (1985) Synthesis, modification with *N*-acetoxy-2-acetylaminofluorene and physicochemical studies of DNA model compound d(TACGTA). *Chem.-Biol. Interact. 56*, 73–88.

(20) Martin, L. B., III, Schverner, A. F., and van Breeman, R. B. (1991) Characterization of cisplatin adducts of oligonucleotides by fast atom bombardment mass spectrometry. *Anal. Biochem. 193*, 6–15.

(21) Caradonna, J. P., and Lippard, S. J. (1982) The antitumor drug *cis*-[Pt$(NH_3)_2$Cl2] forms an intrastrand d(GpG) cross-link upon reaction with [d(ApGpGpCpCpT)]$_2$. *J. Am. Chem. Soc. 104*, 5793–5795.

(22) Randerath, K., Randerath, E., Danna, T. F., Van Golen, K. L., and Putnam, K. L. (1989) A new sensitive ^{32}P-postlabeling assay based on the specific enzymatic conversion of bulky DNA lesions to radiolabeled dinucleotides and nucleoside monophosphates. *Carcinogenesis 10*, 1231–1239.

(23) Sharma, M. (1991) A new technique to assay DNA damage using microbore HPLC with laser-induced fluorescence detector. The Pittsburgh Conference, Chicago, IL, March 4–8, Abstracts 072.

Technetium Labeling of Monoclonal Antibodies with Functionalized BATOs: 2. $TcCl(DMG)_3CPITC$ Labeling of B72.3 and NP-4 Whole Antibodies and NP-4 $F(ab')_2$

K. E. Linder, M. D. Wen, D. P. Nowotnik,* K. Ramalingam, R. M. Sharkey,† F. Yost, R. K. Narra, A. D. Nunn, and W. C. Eckelman

The Bristol-Myers Squibb Pharmaceutical Research Institute, One Squibb Drive, New Brunswick, New Jersey 08903, and Center for Molecular Medicine and Immunology, 5 Bruce Street, Newark, New Jersey 07103. Received May 30, 1991

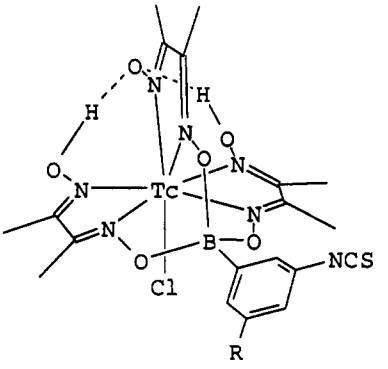
BATO (boronic acid adduct of technetium dioximes) complexes, $TcCl(dioxime)_3BR$, were prepared in which the boron substituent (R) was the protein-reactive 2-carboxy-4-phenyl isothiocyanate (CPITC). The ^{99}Tc complexes, where the dioxime was either dimethylglyoxime (DMG) or cyclohexanedione dioxime (CDO), were prepared and characterized. The ^{99m}Tc complex $TcCl(DMG)_3CPITC$ was prepared from a freeze-dried kit and used to label B72.3 (anti-TAG.72) and NP-4 (anti-CEA) whole antibodies, and the NP-4 $F(ab')_2$ fragment. SDS–PAGE electrophoresis indicated that the labeling reagent was strongly bound to antibody. The labeled antibodies displayed high binding to affinity columns and good tumor uptake in GW39 tumor-bearing mice.

INTRODUCTION

In a previous publication (*1*), we described the preparation and protein-labeling application of a BATO (boronic acid adduct of technetium dioximes) complex functionalized with an isothiocyanato group. BATOs are seven-coordinate Tc(III) complexes, prepared by the low pH/100 °C template reaction of a vicinal dioxime, a boronic acid, and pertechnetate (TcO_4^-) in the presence of the reducing agent $SnCl_2$ (*2*, *3*). The ease of synthesis of BATOs from relatively simple components permitted the study of biodistribution of a large number of these neutral, lipophilic technetium complexes (*4*). Two were selected for clinical evaluation as myocardial and cerebral perfusion tracers (*5*, *6*).

Addition of isothiocyanate (a functional group known to be effective in linking bifunctional chelating agents to proteins (*7*, *8*)) to the boronic acid "cap" of a BATO transformed the chelate into a protein-labeling reagent (*1*). The reagent $TcCl(DMG)_3PITC$ (Figure 1) formed a stable link (presumed to be a substituted thiourea, by reaction of the isothiocyanate with the ϵ-amino group of lysine groups in the protein) to the monoclonal antibody B72.3. Use of a preformed chelate such as a BATO is the preferred method for technetium labeling of antibodies as it eliminates the possibility of nonspecific binding of the radiotracer and, as a result, should provide a radiopharmaceutical with high in vivo stability (*9*, *10*). However, the low water solubility of this reagent necessitated that protein-labeling reactions be conducted in 10% aqueous DMSO. As the potential of this reagent for routine protein labeling might be increased through an improvement in water solubility, we set out to prepare and study a more water-soluble derivative of this reagent, one which contained a carboxylate group. In this paper, we describe the synthesis and characterization of the new reagent $TcCl(DMG)_3CPITC$ (Figure 1) and the use of this reagent in labeling B72.3 and NP-4 whole antibodies and NP-4 $F(ab')_2$ fragments. The biodistributions of these ^{99m}Tc-labeled proteins in normal and tumor-bearing mice are also described here.

† Center for Molecular Medicine and Immunology (CMMI).



$TcCl(DMG)_3PITC$ R = H
$TcCl(DMG)_3CPITC$ R = COOH

Figure 1. Structures of the BATO PITC labeling reagents.

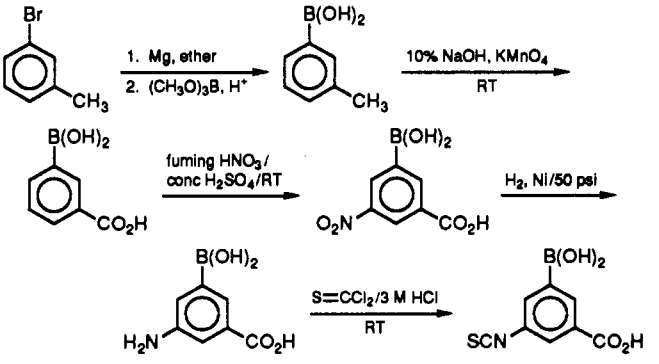


Figure 2. Synthesis of $(OH)_2B$-CPITC.

EXPERIMENTAL PROCEDURES

Materials and Reagents. Dimethylglyoxime (DMG) (Eastern Chemicals), glycine (Aldrich), and stannous chloride (MCB) were used as received. The boronic acid 3-carboxy-5-isothiocyanatophenylboronic acid [$(OH)_2B$-CPITC] was synthesized by the five-step process shown in Figure 2. Details of the synthesis of $(OH)_2B$-CPITC are reported elsewhere (*11*). The complexes $^{99}TcCl(DMG)_3$ and $^{99}Tc(DMG)_3(\mu\text{-}OH)SnCl_3$ were prepared as described previously (*3*). $^{99m}TcO_4^-$ in saline solution was obtained from an E.R. Squibb Minitec Generator. Freeze-dried

1043-1802/91/2902-0407$02.50/0 © 1991 American Chemical Society

kits for the preparation of the tris-dioxime complexes $^{99m}TcCl(DMG)_3$ and $^{99m}TcCl(CDO)_3$ were manufactured as described previously (*1*). All other chemicals were of reagent grade and were used as received. All solvents were of either HPLC or reagent grade (except acetonitrile, which was pesticide grade) and were used as received. All water used in these studies was obtained from a Millipore Milli-Q water purification unit.

B72.3 monoclonal antibody (Lot #3-178-870107, 2.81 mg/mL) was purchased from Damon Biotech. NP-4 $F(ab')_2$ fragment and NP-4 monoclonal antibody were obtained from CMMI (NP-4 is a murine IgG_1 monoclonal antibody that recognizes a CEA specific epitope (*12*)). PRP-1 resin (12–20 μm) was purchased from Alltech Associates. Sep-Pak Lite C_{18} cartridges were purchased from Waters Associates. Most reagents and standards used in the SDS–polyacrylamide gel electrophoresis were purchased from Bio-Rad. Phast gel blue, 10–15% gradient gel, and SDS buffer strips were purchased from Pharmacia. Buffers used in the study were prepared as described previously (*1*).

A TAG-72–Reacti-Gel affinity column in a RAININ Leur-lock column, with a 2.5-mL bed volume, was prepared in-house (*1*). A CEA–Affi-Gel-10 affinity column was prepared using CEA extracted from GW-39 human colonic tumor xenograft (*13*).

Analysis of the Labeling Reagents. HPLC separations were made using a Spectra Physics Model SP8700 HPLC system equipped with an ISCO V^4 UV/visible detector and a radiometric detector, dual-pen recorder, and fraction collector. The outputs from the radiation detector and spectrophotometer (set at 280 or 450 nm) were integrated by a SP4270 integrator. The data were stored and reprocessed using LABNET software. Analyses were carried out on either a 15-cm Nucleosil column (Alltech), using a mobile phase of acetonitrile/0.1 M citric acid (pH 2.3) and a flow rate of 1.5 mL/min, or on a Hamilton PRP-1 column, using a mobile phase of acetonitrile/0.1 M NH_4OAc (pH 4.6) and a flow rate of 2 mL/min.

Fast-atom-bombardment mass spectra were obtained on a VG-ZAB-2F spectrometer, from a matrix of CH_2Cl_2/thioglycerol. Infrared spectra were obtained on a Sirius 100 FT-IR spectrometer as KBr pellets. Proton NMR data (250 MHz) were obtained with a JEOL-GX-250 spectrometer. UV/visible spectra were measured using a Hewlett-Packard 8451A photodiode-array spectrophotometer. Elemental analyses were performed by the Squibb Microanalytical Department.

Analysis of the Labeled Antibodies. HPLC methods involving the TSK-SWG3000 column (Phenomenex), the 1-cm ISRP precolumn (Alltech Associates), and a combined ISRP/TSK-SWG3000 column, Phast SDS-PAGE electrophoresis, and affinity chromatography using a TAG-72-affinity column were described previously (*1*). Affinity chromatography on NP-4-labeled materials was conducted on a CEA-affinity column (*13*), using the methods described previously for the TAG-72 affinity column (*1*). Rat serum stability studies on HPLC-purified $TcCl(DMG)_3$CPITC-labeled B72.3 were carried out as described previously for $TcCl(DMG)_3$PITC-labeled B72.3 (*1*). A control sample was prepared by incubating $TcCl(DMG)_3$CPITC in PBS buffer in the absence of antibody. Both samples were incubated at 37 °C. Each sample was then evaluated by both gel electrophoresis and ISRP-TSK HPLC at 1 h after incubation.

A Phast SDS–PAGE electrophoresis system (Pharmacia) was used for the characterization of ^{99m}Tc-labeled antibodies and antibody fragments using 10–15% gradient gels and the reagents, buffers, separation protocols, and development methods recommended by the manufacturer.

Synthesis of Tc Complexes. *Synthesis of $^{99}TcCl(DMG)_3$CPITC from $TcCl(DMG)_3$.* To $^{99}TcCl(DMG)_3$ (23.8 mg, 0.049 mmol) in 3 mL of CH_3CN was added 3 drops of 1 M HCl and 11.5 mg (0.051 mmol) of $(OH)_2$B–CPITC. The reaction mixture was heated at 50 °C with stirring for 15 min. It was then treated with an equal volume of 1 M HCl and cooled to room temperature. The resulting red-orange precipitate was isolated by suction filtration, washed with 15 mL of 1 M HCl, and dried in vacuo to yield 25 mg (75.6%) of relatively pure product. Recrystallization from a small volume of CH_3CN/1 M HCl yielded analytically pure needles, isolated as a 1.5-hydrate. Anal. Calcd for $C_{20}H_{24}N_7BClO_8STc \cdot 1.5H_2O$: C, 34.57; H, 3.92; N, 14.11. Found: C, 34.76; H, 3.90; N, 13.90.

Synthesis of $^{99}TcCl(DMG)_3$CPITC from $Tc(DMG)_3(\mu\text{-}OH)SnCl_3$. To $^{99}Tc(DMG)_3(\mu\text{-}OH)SnCl_3$ (84 mg, 0.114 mmol), dissolved in 15 mL of CH_3CN, was added boronic acid $(OH)_2$B-CPITC (30 mg, 0.136 mmol), followed by 1.5 mL of 3 M HCl. The reaction mixture was heated with stirring at 50 °C for 30 min. The warm solution was then treated with 40 mL of 1 M HCl and cooled to room temperature. The resulting red-orange precipitate was isolated by suction filtration, washed with 15 mL of 1 M HCl and H_2O, and dried in vacuo to yield 58 mg (76%) of desired product. Following recrystallization from CH_3CN/1 M HCl, the material thus isolated was identical to that prepared as above, as determined by TLC and HPLC (Nucleosil system, 65/35 CH_3CN/0.1 M citric acid, t_R = 2.85 min).

Synthesis of $^{99m}TcCl(DMG)_3$CPITC from $^{99m}TcO_4^-$. Samples of the ^{99m}Tc complex were prepared by adding $(OH)_2$B-CPITC (3 mg) in ethanol (50 μL) and $^{99m}TcO_4^-$/saline (1.0 mL, 25 mCi) to a freeze-dried tris-DMG kit. The kit was heated to 70 °C for 5 min, cooled to room temperature, and passed through a Waters Associates Sep-Pak Lite C_{18} cartridge. The Sep-Pak cartridge was washed with 1 mL of saline and 2 mL of 25/75 EtOH/saline. The complex was eluted from the resin by treatment with 1 mL of 100% EtOH. Analysis of the reaction mixture, using the Nucleosil system above, showed the reaction mixture radiochemical purity (RCP) to be 28%. The purified material had an RCP of 60–65%.

Synthesis of $^{99}TcCl(CDO)_3$CPITC from $TcCl(CDO)_3$. To 4.0 mg of $TcCl(CDO)_3$, dissolved in 3 mL of ACN, was added 1.5 mg of $(OH)_2$B–CPITC and 3 drops of 3 M HCl. The solution was heated gently for 20 min and monitored by HPLC at 280 nm (Nucleosil system, 60/40 ACN/0.1 M citric acid. During this time, $TcCl(CDO)_3$ (t_R = 5.0 min) and the boronic acid (t_R = 1.66 min) both disappeared, and a peak at t_R = 8.0 min formed. The UV/visible spectrum of this reaction mixture in acetonitrile indicated that a BATO complex had formed (maxima at 276, 386, and 466 nm). When analyzed by FAB mass spectroscopy, a strong molecular ion at the expected mass of $TcCl(CDO)_3$CPITC (*m/e* 745/747) was observed in both positive and negative modes.

Synthesis of $^{99m}TcCl(CDO)_3$CPITC. Method I: from $^{99m}TcO_4^-$. To a freeze-dried tris CDO kit was added $(OH)_2$B–CPITC (3 mg) in ethanol (50 μL) and $^{99m}TcO_4^-$/saline (1.0 mL, 25 mCi). The kit was heated at 70 °C for 5 min and purified on a Waters Sep Pak Lite C-18 cartridge as described above for $^{99m}TcCl(DMG)_3$CPITC. The RCP of the reaction mixture before purification was 15%; after purification the RCP was 67%.

Method II: from $^{99m}TcCl(CDO)_3$. A sample of ^{99m}TcCl-

$(CDO)_3$ was prepared by adding 24 mCi of TcO_4^- in 1 mL of saline to a freeze-dried kit containing CDO. After heating at 100 °C for 5 min, the RCP of $^{99m}TcCl(CDO)_3$ was 92%. To this kit was added $(OH)_2$B-CPITC (2.4 mg) in ethanol (50 μL). The mixture was heated for 15 min at 100 °C to give $^{99m}TcCl(CDO)_3$CPITC in 49% yield. After purification as described above, the RCP was 74%.

Method III: from $^{99m}TcCl(CDO)_3$. A sample of $^{99m}TcCl(CDO)_3$ was prepared as described in method II above. After heating at 100 °C for 5 min, the RCP of $^{99m}TcCl(CDO)_3$ was 92%. The $TcCl(CDO)_3$ was isolated, and kit components were removed, by purification on Hamilton PRP-1 resin. The kit contents were drawn up into a needle-hub of resin and then rinsed with 1 mL of saline, 1 mL of 25/75 EtOH/saline, 1 mL of H_2O, and 1 mL of EtOH. The ethanol fraction contained 17 mCi of $TcCl(CDO)_3$ (RCP = 86.6%). Half of the ethanol fraction was added to a vial that contained 1.5 mg of $(OH)_2$B-CPITC and 50 μL of 1 N HCl. This kit was heated for 5 min at 100 °C and then reanalyzed by HPLC as described above. The yield of $TcCl(CDO)_3$CPITC prepared by this method was 82% (94% yield based on the purity of starting $TcCl(CDO)_3$. Sep-Pak Lite purification as described above did not increase the RCP.

The Effects of pH, Temperature, and Heating Time on the RCP of $^{99m}TcCl(DMG)_3$CPITC. $^{99m}TcCl(DMG)_3$CPITC was prepared by adding $(OH)_2$B-CPITC (3 mg) in ethanol (50 μL) and $^{99m}TcO_4^-$ (1.0 mL, 20–30 mCi) to a freeze-dried kit containing DMG. The effects of heating temperature (70–100 °C), heating time (5–50 min), and pH (2.0–4.0) on the RCP of the labeling reagent were evaluated as was described for $TcCl(DMG)_3$PITC in ref 1.

Studies of the Reactivity of the NCS Group. *Reaction of $(OH)_2$B-PITC and $(OH)_2$B-CPITC with Glycine.* Equimolar solutions of $(OH)_2$B-PITC (*1*) and $(OH)_2$B-CPITC were made by dissolving 4.80 mg (0.0268 mmol) or 6.00 mg (0.0269 mmol) of ligand, respectively, in 4.0 mL of EtOH. An 0.01385 M glycine solution was prepared by dissolving 10.4 mg of glycine in 10.0 mL of 0.1 M sodium phosphate buffer (pH 9.5). All three solutions were brought to 37 °C. At $t = 0$, 1 mL of boronic acid solution (0.0067 mmol) was added to 4 mL of glycine solution (0.0553 mmol, 8.3-fold excess). The mixture was incubated at 37 °C. At 5 min-intervals, 25-μL aliquots from both reaction mixtures were removed and analyzed by HPLC, using a Nucleosil C8 column and CH_3CN/0.1 M citric acid mobile phase at 1.5 mL/min. The solvent ratio for samples from the reaction with $(HO)_2$B–PITC was 40/60, while, for the $(OH)_2$B–CPITC reaction, a 30/70 CH_3CN/citric acid mixture was used. The disappearance of the boronic acid was determined by the change in area under the boronic acid peak at 290 nm.

Hydrolysis of $^{99}TcCl(DMG)_3CPITC$ to $^{99}TcOH(DMG)_3CPITC$. A sample of 10 mg of $^{99}TcCl(DMG)_3$CPITC was dissolved in 5 mL of CH_3CN and 5 mL of 0.1 M sodium phosphate buffer (pH 9.5). The apparent pH of this mixture was 9.0 on wet E. Merck narrow-range pH paper. The solution was incubated at 37 °C (±1 °C) for 100 min. During this time, the color of the reaction mixture changed from red-orange to yellow-orange. Aliquots of the reaction were analyzed by HPLC on a Nucleosil column that was eluted with 65/35 CH_3CN/0.1 M citric acid at a flow rate of 1.5 mL/min. $TcCl(DMG)_3CPITC$ (t_R = 2.89 min) was cleanly converted to a more polar complex ($TcOH(DMG)_3CPITC$) at t_R = 1.86 min, as detected by absorbance at 280 nm.

After 70 min, an aliquot of the mixture was acidified to pH 1.0, by treatment with 2 drops of concentrated HCl. The original color returned immediately. HPLC analysis of this solution showed almost full conversion back to starting material.

Aqueous Solubility of $^{99m}TcCl(DMG)_3CPITC$. $^{99m}TcCl(DMG)_3CPITC$ was prepared by heating at 100 °C for 5 min and purified as described above. The purified labeling reagent in ethanol was divided into three 300-μL aliquots. Each sample was dried under a stream of N_2. An aliquot of 100 μL of EtOH, 100 μL of 0.1 M sodium phosphate buffer (pH 9.5), or 5 μL of DMSO in 95 μL of pH 9.5 phosphate buffer was added to the dried ^{99m}Tc complex. The samples were then incubated at room temperature for 2 h, after adding an additional 100 μL of phosphate buffer (pH 9.5) to each vial. The sample in each vial was transferred into a separate test tube after incubation. The radioactivity recovered in the test tube and the radioactivity remaining in the vial were determined with a dose calibrator. The percent recovery was calculated as radioactivity recovered/(radioactivity recovered + radioactivity remaining in the vial).

General Procedure for Labeling of Monoclonal Antibodies and Fragments with $^{99m}TcCl(DMG)_3$CPITC. A 300-μL aliquot of the purified $^{99m}TcCl(DMG)_3$CPITC solution in ethanol was dried under a stream of N_2 and 100 μL of the antibody or antibody fragment (10 mg/mL in 0.1 M sodium phosphate buffer, pH 9.5) was added to the dried ^{99m}Tc complex. The reaction mixture was incubated at 37 °C for 2 h. The ^{99m}Tc labeled antibody was then purified using an ISRP-TSK HPLC system, as described previously (*1*).

Biodistribution Studies. *In Normal Mice.* The biodistributions of $^{99m}TcCl(DMG)_3$CPITC and of $^{99m}TcCl(DMG)_3$CPITC-labeled B72.3 whole antibody, -labeled NP4 $F(ab')_2$, and -labeled NP4 whole antibody were evaluated in normal mice (n = 4 or 5/study). Mice were injected iv with about 1 μCi (100 μL) of either the ^{99m}Tc complex or the ^{99m}Tc-labeled antibody and sacrificed at 1 or 24 h after injection. Organs of interest were taken, weighed, and assayed for radioactivity. The percent injected dose/organ and percent injected dose/gram of tissue were determined.

In Tumor-Bearing Mice. GW39 tumors (*14*, *15*) were grown serially in nude mice by inoculation with 0.2 mL of a 10% tumor suspension. The suspension was prepared by mincing an established tumor and then passing this preparation through a 40-mesh wire screen to obtain a uniform cell suspension.

After 14 days, 10–20 μCi of labeled antibody (B72.3, NP-4, or NP-4 $F(ab')_2$ fragment) was administered via tail vein injection. Mice (n = 4–8 for each time point) were dissected at 1 or 24 h after injection. For the studies with Tc-labeled B72.3, a sample of ^{131}I–B72.3 (prepared by chloramine T iodination) (*16*) was injected into another group of tumor-bearing mice as a control. The percent injected dose/organ and percent injected dose/gram of tissue were determined.

RESULTS AND DISCUSSION

Synthesis and Characterization of ^{99}Tc Complexes. As was the case for $TcCl(DMG)_3$PITC (*1*), $^{99}TcCl(DMG)_3$CPITC can be prepared in good yield from either $TcCl(DMG)_3$ or $Tc(DMG)_3(\mu\text{-}OH)SnCl_3$. $^{99}TcCl(CDO)_3$-CPITC was prepared quantitatively from $TcCl(CDO)_3$. These compounds are expected to have a structure that is quite similar to our first-generation protein-labeling reagent, $TcCl(DMG)_3$B-PITC, which was characterized by X-ray crystal structure analysis (*1*). All analytical data

Table I. HPLC Retention Times for $TcCl(DMG)_3CPITC$ and Important Side Products

complex	column[a]	solvent ratio	buffer pH	t_R, min
$TcCl(DMG)_3CPITC$	PRP-1	40/60	4.6	13.0
$TcCl(DMG)_3CPITC$	PRP-1	40/60	5.1	2.2–2.5[1]
$TcCl(DMG)_3CPITC$	PRP-1	65/35	4.6	3.1–3.5[1]
$TcCl(DMG)_3CPITC$	PRP-1	50/50	4.6	6.2–10[1]
$TcCl(DMG)_3CPITC$	C_8	65/35	2.3	2.85
$TcOH(DMG)_3CPITC$	PRP-1	50/50	4.6	1.45
$TcOH(DMG)_3CPITC$	C_8	65/35	2.3	1.85
$TcCl(DMG)_3$	PRP-1	50/50	4.6	6.8
$TcCl(DMG)_3$	C_8	60/40	2.3	2.67

[a] For the PRP-1 system, the mobile phase solvent mixture is ACN/0.1 M NH_4OAc at 2 mL/min. Note (*1*): the retention time is variable using this buffer, being highly dependent upon the pH of the mobile phase. For the Nucleosil C_8 system, the mobile phase is ACN/0.1 M citric acid, at 1.5 mL/min.

on the $^{99}TcCl(dioxime)_3CPITC$ complexes suggests that this similarity exists.

The ^1H NMR spectrum of $TcCl(DMG)_3CPITC$ is as expected. Phenyl resonances for the trisubstituted phenyl boron cap are seen at 7.2–7.8 ppm. The methyl resonances for the two equivalent dimethylglyoxime ligands and the one unique ligand fall between 2.2 and 2.4 ppm. The two oxime protons (O- -H- -O), which are seen at 15.1 ppm in the spectrum of the PITC complex, are not seen in the spectrum of the CPITC compound, nor is a peak for the carboxylic acid proton (COOH). However, the large water peak in this spectrum (the complex was isolated as a hydrate) suggests that the disappearance of these resonances is due to exchange with water.

The FAB +/− mass spectra of $^{99}TcCl(DMG)_3CPITC$ show strong molecular ion peaks at m/z 668/670 $(M + H)^+$ or 666/668 $(M - H)^-$ in the positive and negative modes, respectively. Losses observed from these ions parallel fragmentation patterns observed previously in the spectra of several other BATO complexes (*17*). The infrared spectrum of $TcCl(DMG)_3CPITC$ contains a pronounced peak at about 2100 cm^{-1} due to the NCS group; strong carboxylate absorptions are seen at 3440 (vs) and 1720 cm^{-1} (m).

The retention time of $TcCl(DMG)_3CPITC$ on reversed-phase HPLC is very sensitive to the buffer pH (Table I). Changing buffer pH from 4.6 to 5.1 results in a change in the HPLC retention time from 13 to 2.5 min. This is consistent with a large change in the degree of ionization of the carboxylic acid functionality on the boronic acid cap, from primarily free acid at pH 4.6 to partially deprotonated form at pH 5.1. Coinjection studies with $^{99}TcCl(DMG)_3CPITC$ and $^{99m}TcCl(DMG)_3CPITC$ were carried out in several HPLC systems (the systems shown in Table I). Coelution of the two compounds was noted in all cases.

Synthesis of ^{99m}Tc Complexes. When the $^{99m}TcCl(dioxime)_3CPITC$ complexes were prepared directly from pertechnetate, yields were very poor (<30%). This stands in sharp contrast to reactions which form BATO complexes that do not contain the NCS group, where yields of >90% are regularly obtained (*6*, *18*). Attempts to improve the yield of the CPITC complexes by varying pH, temperature, and reaction time were relatively unsuccessful. Although these factors had an effect on yield that was similar to those reported previously for the PITC complex, the optimum yield obtained for $^{99m}TcCl(DMG)_3CPITC$ was only 28% when heated at 100 °C for 5 min at pH 2.0. At longer reaction times, considerable degradation of the labeling reagent was seen (Figure 3). Under similar

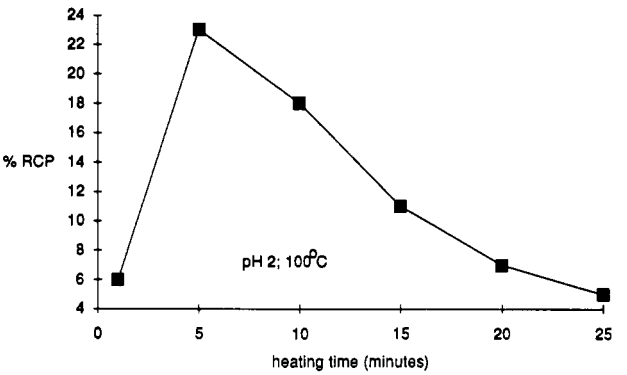


Figure 3. The influence of reaction time on the RCP of $^{99m}TcCl(DMG)_3CPITC$ (pH = 2.0 at 100 °C).

Table II. Comparison of the Recovery of $^{99m}TcCl(DMG)_3PITC$ and $^{99m}TcCl(DMG)_3CPITC$

activity dissolved in	% recovery from vial[a]	
	$TcCl(DMG)_3$-PITC	$TcCl(DMG)_3$-CPITC
50% EtOH/50% PO_4^- buffer	20	92.6
5% DMSO/95% PO_4^- buffer	59	90
100% PO_4^- buffer	10	89

[a] Percent recovery from vial following a 1-h incubation at 37 °C in the specified solvent.

conditions, the yield of $^{99m}TcCl(CDO)_3CPITC$ was only 15% at 5 min, when prepared directly from pertechnetate.

The yield of $^{99}TcCl(DMG)_3CPITC$ was also low when prepared directly from $^{99}TcO_4^-$, but good when prepared from either of the intermediates in BATO formation (*3*), $Tc(dioxime)_3(\mu\text{-}OH)SnCl_3$ or $TcCl(dioxime)_3$. These trends led us to consider whether kit components were responsible for the poor radiochemical yields of the ^{99m}Tc protein-labeling reagents when prepared directly from pertechnetate. A study was conducted in which the BATO precursor $^{99m}TcCl(CDO)_3$ was prepared from a kit, and then the boronic acid cap was added to the reaction mixture. The yield in this reaction (method II) was increased to 49% (compared to a 15% yield when prepared directly from pertechnetate).

When the $^{99m}TcCl(CDO)_3$ was isolated from all kit components by solid-phase extraction and then mixed with boronic acid at pH 2.0 (method III), the desired BATO complex could be prepared in 82% yield (equivalent to 94% conversion based on purity of $^{99m}TcCl(CDO)_3$ starting material). Thus, it is clear that one of the kit components, and not low pH or heating, is responsible for the poor yield of these protein-labeling reagents when prepared directly from TcO_4^-. The implication is that the protein-labeling BATOs can be made in a reasonable overall yield (50–60%) from $^{99m}TcO_4^-$, but that this improvement in yield is achieved through an additional solid-phase purification step.

Aqueous Solubility of $^{99m}TcCl(DMG)_3CPITC$. Addition of a carboxyl group to the PITC cap was intended to improve the water solubility of the protein-labeling reagent above that previously observed with $^{99m}TcCl(dioxime)_3PITC$. This appears to have been achieved. The solubilities of $^{99m}TcCl(DMG)_3PITC$ and $TcCl(DMG)_3CPITC$ in a variety of solvents are compared in Table II. Of note is the fact that after a 1-h incubation of $^{99m}TcCl(dioxime)_3PITC$ in phosphate buffer, recovery was only 10% (the remainder remaining adhered to the vial wall), compared with 89% recovery for $^{99m}TcCl(dioxime)_3CPITC$. Thus, protein labeling with the CPITC

reagent may be conducted without the addition of an organic modifier to solubilize the reagent. The carboxylic acid substituent is presumably in the ionized form at the pH (9.0) at which protein labeling occurs, creating a complex with a net 1- charge. This conclusion is drawn from HPLC data, where it is observed that complex retention time varies significantly in the pH range 4.6–5.0, indicating that the apparent pK_a of the carboxylic acid is close to this range (*19–21*).

The presence of an ionized group on the phenyl ring is expected to alter the reactivity of the isothiocyanate electrophile toward proteins (compared with PITC, the ligand without a carboxylate group), although the meta orientation of carboxylate to isothiocyanate should minimize this effect (*22*). For this reason, various studies were undertaken to examine the reactivity of CPITC compared to that of PITC.

Hydrolysis of Labeling Reagent in the Absence of Protein: ^{99}TcCl(DMG)$_3$CPITC to ^{99}TcOH(DMG)$_3$-CPITC. Hydrolysis of ^{99}TcCl(DMG)$_3$CPITC at pH 9.5/37 °C gave a 95% yield of a more polar product, accompanied by a color change from red-orange to yellow-orange. However, on treatment with HCl (pH = 1.0), the original color of the reaction mixture returned immediately. HPLC analysis of the acidified solution showed almost full conversion back to ^{99}TcCl(DMG)$_3$CPITC. These results indicate that hydrolysis of the NCS group did not occur under these conditions, as NCS hydrolysis to the amine is not reversible under the conditions used. The reaction observed is consistent with the product of hydrolysis being TcOH(DMG)$_3$CPITC, where the axial chloride ligand has been replaced a hydroxide. Chloro/hydroxy exchange in BATOs is known (*23*) to occur at a rate that is consistent with the time course observed.

Similar results were observed with both ^{99m}TcCl(DMG)$_3$PITC and ^{99m}TcCl(DMG)$_3$CPITC. Both complexes were hydrolyzed in pH 9.5 phosphate buffer (10% DMSO) to more polar products within 2 h. The HPLC retention time of the hydrolysis product of ^{99m}TcCl(DMG)$_3$CPITC was identical to that of authentic ^{99}TcOH(DMG)$_3$CPITC. Based on these results, we expect that chloro/hydroxy exchange to form ^{99m}TcOH(DMG)$_3$CPITC also occurs in protein labeling reaction mixtures. However, the nature of the axial ligand on the BATO is unlikely to have much influence on the performance of a derivatized BATO as a protein-labeling reagent (except to improve solubility; hydroxy BATOs are much less lipophilic than their chloro analogues (*24*)). The significant result is that little hydrolysis of the isothiocyanate group takes place under protein-labeling conditions for either reagent.

Reactions of PITC and CPITC Reagents with Glycine and Antibodies. When the boronic acids (OH)$_2$B-PITC and (OH)$_2$B-CPITC were incubated with glycine under identical conditions, coupling of the NCS group on the boronic acid and glycine occured and both boronic acids disappeared (Figure 4). The reaction half-lives were 18 min for (OH)$_2$B-PITC and 22.8 min for (OH)$_2$B-CPITC, indicating similar reactivity toward amines. This result indicates that all other things being equal, the PITC and CPITC reagents should be equally reactive toward proteins. However, in the labeling of B72.3 antibody, the BATO with the water-solubilizing carboxylate function proved to be markedly superior. On the basis of five experiments, the antibody labeling yield is higher for ^{99m}TcCl(DMG)$_3$CPITC than it is for ^{99m}TcCl(DMG)$_3$PITC (32.4%, compared to 7.5%). These yields are lower than that observed for reaction with glycine, presumably due to the lower concentration of antibody (0.2 mM) compared

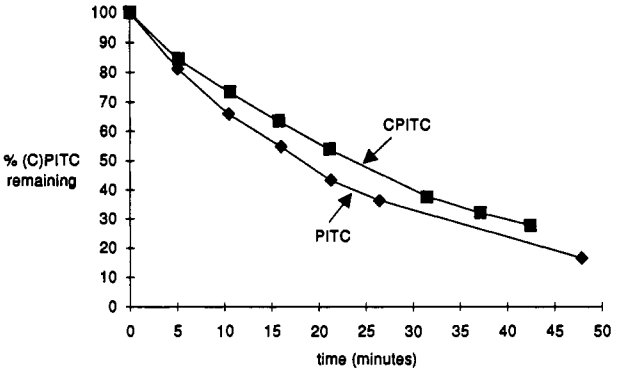


Figure 4. Graph showing the disappearance of the isothiocyanate reagents on reaction of (HO)$_2$B-PITC and (HO)$_2$B-CPITC with glycine.

to glycine (10 mM) and the lower accessibility of the reagent to protein ϵ-amino lysine groups compared to the amine group on glycine. We have shown previously (*1*) that there is no binding of BATO to protein using a BATO complex which did not contain an isothiocyanate group, so that these protein binding yields should reflect specific binding only.

Following isolation of the labeled antibodies by HPLC, it was found that both protein recovery and immunoreactivity of the product were also slightly better for B72.3 labeled with ^{99m}TcCl(DMG)$_3$CPITC than with ^{99m}TcCl(DMG)$_3$PITC (71.4% and 67% protein recovery and 72% and 60% binding to TAG-72 affinity columns, respectively).

Labeling studies with ^{99m}TcCl(DMG)$_3$CPITC were then extended to examine the radiolabeling of the NP-4 whole antibody, and the NP-4 F(ab')$_2$ fragment. Percent incorporation of radiolabel, protein recovery, and immunoreactivity results are given in Table III. NP-4 is an anti-CEA IgG, which has been compared previously to B72.3 in the nude mouse model (*25*). The radiolabeling yields and protein recoveries for NP-4 whole antibody were similar to those obtained for B72.3. Immunoreactivity studies on isolated NP-4 labeled with ^{99m}TcCl(DMG)$_3$-CPITC showed little binding to a TAG-72 affinity column (which contains an irrelevant antigen that does not bind to NP-4), but >90% binding to a CEA affinity column (Table III).

The labeling efficiency and protein recovery of NP-4 F(ab')$_2$ labeled with ^{99m}TcCl(DMG)$_3$CPITC were lower than for the whole antibody. As the concentration of NP-4 antibody and its F(ab')$_2$ fragment were similar in these labeling experiments, the reason for this difference is uncertain at this time.

Characterization of Labeled Antibodies. As in our previous study (*1*), the stability of the link between label and antibody was demonstrated by SDS–PAGE. Under nonreducing conditions, 90.6% (B72.3) and 82% (NP-4 whole antibody) of the radioactivity was found to be associated with antibody. Reduction with β-mercaptoethanol resulted in significant loss of the label, observed as activity at the dye front in gels that were not subjected to the stain/destain protocol (destaining washes this dye-front activity away).

F(ab')$_2$ fragments, under nonreducing conditions, migrate in SDS–PAGE to a single band at 100 kDa; 88% of total radioactivity was associated with this fraction in the nonreduced labeled fragment. When reduced with β-mercaptoethanol, F(ab')$_2$ fragments give a doublet of bands at 25 kDa on SDS–PAGE. The lower band of the doublet corresponds to the light chain, while the higher band is the amine-terminal portion of the cleaved heavy chain

Table III. Radiolabeling of B72.3 and NP-4 with ^{99m}TcCl(DMG)$_3$CPITC: Yield and Characterization of Products

a. Yield and Immunoreactivity (Affinity Column)

protein	% labeling	% protein recovery	% immunoreactivity
B72.3 whole antibody	32	71	72[a]
NP-4 whole antibody	26	75	6[a]
			96[b]
NP-4 F(ab')$_2$	15	43	93[b]

b. SDS-PAGE

protein		unreduced: % bound to whole mAb	reduced with β-mercaptoethanol: % bound to the heavy chain	% bound to the light chain
B72.3 whole mAb[a]	gel not stained	90.6	35.7	8.5
	gel stained/destained	97	84	10.2
NP-4 whole mAb	gel not stained	82	18	9
	gel stained/destained	96	64	18
NP-4 F(ab')$_2$	gel not stained	88		43[c]
	gel stained/destained	80		83[c]

[a] Binding to the TAG-72 affinity column (irrelevant antigen for NP-4 antibody). [b] Binding to the CEA affinity column. [c] Light chain plus NH_2-terminal portion of the cleaved heavy chain (F_d).

Table IV. Comparison of the Biodistribution of ^{99m}TcCl(DMG)$_3$PITC, ^{99m}TcCl(DMG)$_3$CPITC, and Whole B72.3 Labeled with These Reagents, in Normal Mice

Distribution of Labeling Reagents in Normal Mice

	% ID/g in tissue							
	^{99m}TcCl(DMG)$_3$PITC, n = 5				^{99m}TcCl(DMG)$_3$CPITC, n = 4			
	1 h	SD	24 h	SD	1 h	SD	24 h	SD
blood	0.42	0.24	2.29	1.12	7.43	4.82	2.85	1.20
heart	4.33	3.14	0.67	0.21	1.84	0.35	1.54	1.40
lungs	3.52	1.38	1.00	0.34	2.78	1.04	1.05	0.31
brain	0.99	0.39	0.11	0.11	0.32	0.14	0.12	0.02
liver	1.03	0.18	3.62	0.24	4.92	1.20	0.98	0.10
spleen					1.37	0.53	0.63	0.26
GI	11.0	1.16	1.80	0.66	22.20	1.10	0.32	0.06
kidneys	42.49	0.98	0.12	0.15	2.83	0.32	1.06	0.16
muscle	2.23	0.98	0.21	0.15	1.31	1.15	0.33	0.26

Distribution of Tc(C)PITC-Labeled B72.3 in Normal Mice

	% ID/g in tissue							
	^{99m}TcCl(DMG)$_3$PITC-B72.3, n = 5				^{99m}TcCl(DMG)$_3$CPITC-B72.3, n = 4			
	1 h	SD	24 h	SD	1 h	SD	24 h	SD
blood	30.33	5.12	13.09	1.95	29.61	5.50	13.37	1.44
heart	6.90	2.10	3.51	1.35	7.14	1.07	6.27	2.02
lungs	8.57	3.29	4.39	1.48	13.15	2.86	4.99	1.39
brain	1.06	1.06	0.51	0.51	1.02	0.74	0.57	0.09
liver	8.19	0.87	4.19	0.34	8.06	0.69	5.63	1.14
spleen			2.31	0.29	4.50	0.79	4.83	2.17
GI	2.44	0.16	2.91	0.41	2.59	0.24	1.79	0.57
kidneys	5.61	1.28	2.76	0.56	6.17	0.78	4.48	0.83
muscle	1.00	0.24	2.36	0.78	1.45	0.18	1.92	0.80

(F_d) (*26*). Only 43% of the original activity remains bound to these reduced fragments.

Serum Stability of B72.3 Labeled with ^{99m}TcCl(DMG)$_3$CPITC. The stability of the radiolabel in serum was demonstrated by incubation of B72.3 labeled with ^{99m}TcCl(DMG)$_3$CPITC in rat serum; no loss of label was observed after 1 h in serum. Only one radioactive component, coincident with the radiolabeled monomer, could be detected on analysis of the labeled antibody in rat serum (1 h at 37 °C) by ISRP-TSK HPLC. By electrophoresis, 96.1% of total radioactivity in rat serum was associated with the whole antibody fragment. No activity was found to be bound to any serum component. In a control study, in which B72.3-labeled with ^{99m}TcCl(DMG)$_3$CPITC was incubated in buffer for 1 h, 96.2% of the radioactivity was associated with the protein monomer.

Biodistributions. Biodistribution data are given in Tables IV–VI. Table IV provides a comparison of the biodistributions in normal mice of the labeling reagents ^{99m}TcCl(DMG)$_3$PITC and ^{99m}TcCl(DMG)$_3$CPITC and of whole B72.3 labeled with these reagents. Data on the biodistributions of B72.3 in GW39 tumor-bearing mice, labeled with either ^{99m}TcCl(DMG)$_3$CPITC or ^{131}I, are given in Table V. Biodistribution data on TcCl(DMG)$_3$CPITC-labeled NP-4 (whole antibody and F(ab')$_2$ fragment) in normal and GW39 tumor-bearing mice are given in Table VI.

The biodistribution of the labeling reagents ^{99m}TcCl(DMG)$_3$PITC and ^{99m}TcCl(DMG)$_3$CPITC are very different from one another. In normal mice, the neutral PITC complex shows rapid clearance through the kidneys; the anionic CPITC compound appears to clear through the GI system. In contrast, the normal mouse distributions of B72.3 labeled with these two reagents are quite similar to one another, and very different from that of either labeling reagent. Both Tc reagents have less than 3% ID/g in blood at 24 h. When the antibody B72.3 is labeled with either compound, blood values (30 and 13% ID/g at

Table V. Comparison of the Biodistributions in GW39 Tumor-Bearing Mice of B72.3 Labeled with either ^{99m}TcCl(DMG)$_3$CPITC or ^{131}I

	% ID/g in tissues at times in tumor-bearing mice, n = 5							
	^{99m}Tc-B72.3				^{131}I-B72.3			
	1 h	SD	24 h	SD	1 h	SD	24 h	SD
blood	30.66	3.36	15.84	2.26	25.96	7.32	18.98	2.71
liver	9.05	0.72	6.13	1.23	7.80	1.17	5.50	1.13
GI	4.47	0.52	3.31	0.30	2.04	0.43	1.45	0.18
stomach	2.51	1.95	1.60	0.34	2.46	0.72	4.47	1.12
kidneys	10.49	3.70	5.17	0.87	11.19	6.66	6.26	1.03
urine	7.88	0.90	6.50	3.64	8.45	4.89	4.28	1.70
spleen	7.70	1.08	3.82	1.10	8.57	3.17	5.11	1.51
muscle	1.37	0.24	1.46	0.32	1.33	0.44	2.16	0.32
bone	2.91	0.59	1.91	0.41	3.43	1.21	2.63	0.48
thyroid	8.94	3.43	4.79	2.04	27.65	12.10	45.95	14.67
tumor	2.48	0.75	10.47	3.79	3.10	1.41	18.20	8.36

Table VI. Biodistribution of Labeled NP-4 (Whole Antibody and F(ab')$_2$ Fragment) in Normal and GW39 Tumor-Bearing Mice

	% ID/g in tissue							
	normal mice				tumor-bearing mice			
	^{99m}Tc-NP4-F(ab')$_2$		^{99m}Tc-NP4		^{99m}Tc-NP4-F(ab')$_2$		^{99m}Tc-NP4	
	1 h	24 h	1 h	24 h	2 h	24 h	2 h	24 h
blood	24.3	2.9	27.5	17.0	29.4	6.2	21.0	11.5
heart	3.4	1.7	6.3	4.0				
lungs	5.9	1.9	8.3	5.1	10.9	3.8	10.5	5.4
kidneys	7.8	5.8	4.9	3.9	17.7	18.0	7.1	3.5
liver	3.3	1.0	8.1	5.2	8.0	3.3	5.8	4.3
tumor					4.0	10.5	1.8	16.6
	n = 5	n = 5	n = 5	n = 5	n = 4	n = 8	n = 6	n = 6

1 and 24 h, respectively) are dramatically higher than those observed for the labeling reagents themselves. These high blood values are in keeping with the slow blood clearance that is expected for a labeled antibody.

These data strongly suggest that the link between the labeling reagents and protein is strong and that substantial loss of label does not occur. This is substantiated by a comparison of the biodistributions in tumor-bearing mice of B72.3 labeled with either ^{131}I or TcCl(DMG)$_3$CPITC (Table V). There are no significant differences in the organ distributions of the two labeled proteins, except that the GI values are slightly higher for the Tc-labeled protein and the thyroid values are substantially higher for the iodinated antibody. Tumor uptake for the iodine-labeled B72.3 was higher, but not significantly so. Substantial variation in % ID/g in the tumors was seen, with the highest % ID seen in the smallest tumors. This pattern has been noted previously by others (*27–29*).

The biodistribution of TcCl(DMG)$_3$CPITC-labeled NP-4 in both normal and tumor-bearing (nude) mice was also performed. NP-4 is a monoclonal antibody that is specific for carcinoembryonic antigen (CEA) and which, unlike some B72.3 monoclonals, does not significantly complex to circulating blood CEA. The tumor uptake of Tc-CPITC-labeled B72.3 and NP-4 were similar at 24 h (10.5 ± 3.8% vs 16.6 ± 5.8% ID/g, respectively), but because blood values for labeled NP-4 were lower at 24 h, the tumor to blood ratio was improved from 0.7 to 1.7.

Because imaging at such low tumor to blood ratios is not feasible, and because the short half-life of ^{99m}Tc precludes imaging at later times, we have also briefly explored the use of F(ab')$_2$ fragments labeled with TcCl(DMG)$_3$CPITC. It is well-known that blood clearance for such fragments is much faster than that observed with whole antibodies (*9*). As shown in Table VI, blood clearance for the Tc-labeled fragment was significantly faster than that of whole NP-4. However, absolute tumor uptake was also somewhat lowered, so an improvement in tumor to blood ratios was not noted at 24 h. Significant activity was, as expected, found in the kidneys when Tc-labeled NP-4 fragment was used.

The distributions observed above are those expected of radiolabeled antibodies and are very different from those of the labeling reagent itself, suggesting again that the Tc–protein linkage in these BATO-labeled antibodies is a stable one. However, despite the fact that the BATO labeling reagent TcCl(DMG)$_3$CPITC can be prepared in good yield, and incorporation of the CPITC complex into proteins was substantially improved over that seen with our previous PITC reagent (30% vs 7.5% labeling), the overall yield of Tc-labeled protein is still disappointingly low. It appears that the reactivity of the isothiocyanate group toward amines under the protein-labeling conditions used may not be sufficient. Further work should probably focus on the use of other, more reactive linking groups.

ACKNOWLEDGMENT

We thank Lillian Belnavis, Mary Ann Homack, and Christine Hood for technical assistance with the biodistribution studies in normal mice at Bristol-Myers Squibb and Rosarito Aninipot for technical assistance with the biodistribution studies in tumor-bearing mice at CMMI.

LITERATURE CITED

(1) Linder, K. E., Wen, M. D., Nowotnik, D. P., Malley, M. F., Gougoutas, J. Z., Nunn, A. D., and Eckelman, W. C. (1991) Technetium-labeling of monoclonal antibodies with functionalized BATOs: 1. TcCl(DMG)$_3$PITC. *Bioconjugate Chem. 2*, 160–170.

(2) Treher, E. N., Francesconi, L. C., Gougoutas, J. Z., Malley, M. F., and Nunn, A. D. (1989) Monocapped tris(dioxime) complexes of technetium(III): Synthesis and structural characterization of TcX(dioxime)$_3$B-R (X = Cl,Br; dioxime = dimethylglyoxime, cyclohexanedione dioxime; R = CH_3, C_4H_9). *Inorg. Chem. 28*, 3411–3416.

(3) Linder, K. E., Malley, M. F., Gougoutas, J. Z., Unger, S. E., and Nunn, A. D. (1990) Neutral, seven-coordinate dioxime complexes of technetium(III): synthesis and characterization. *Inorg. Chem. 29*, 2428–2434.
(4) Nunn, A. D., Feld, T., and Narra, R. K. (1990) Quantitative structure distribution relationships (QSDRs) of BATOs. *Technetium and Rhenium in Chemistry and Nuclear Medicine 3* (M. Nicolini, G. Bandoli, and U. Mazzi, Eds.) pp 399–404, Cortina International, Verona, Italy.
(5) Zielonka, J. S., Cannon, P., Johnson, L., Seldin, D., Bellinger, R. L., Chua, E., Coleman, R. E., Reba, R. C., Wasserman, A., Drane, W., Williams, C., Goris, M. L., Leppo, J. A., Aktar, R., Bamrah, V. S., and Krubsack, A. J. (1990) Multicenter trial of ^{99m}Tc-Teboroxime (Cardiotec): A new myocardial perfusion agent. *Nuklearmedizin* 211–212.
(6) Narra, R. K., Nunn, A. D., Kuczynski, B. L., Di Rocco, R. J., Feld, T., Silva, D. A., and Eckelman, W. C. (1990) A neutral lipophilic technetium-99m complex for regional cerebral blood flow imaging. *J. Nucl. Med. 31*, 1370–1377.
(7) Mirzadeh, S., Brechbiel, M. W., Atcher, R. W., and Gansow, O. A. (1990) Radiometal labeling of immunoproteins: Covalent linkage of 2-(4-isothiocyanatobenzyl)diethylenetriaminepentaacetic acid ligands to immunoglobulin. *Bioconjugate Chem. 1*, 59–65 (and references therein).
(8) Meares, C. F. (1986) Chelating agents for the binding of metal ions to antibodies. *Nucl. Med. Biol. 13*, 311–318.
(9) Eckelman, W. C. (1990) Development of radiochemically pure antibodies. *Cancer Res. 50*, 780s–782s.
(10) Fritzberg, A. R., Abrams, P. G., Beaumier, P. L., Kasina, S., Morgan, A. C., Rao, T. N., Reno, J. M., Sanderson, J. A., Srinivasan, A., Wilbur, D. S., and Vanderheyden, J.-L. (1988) Specific and stable labeling of antibodies with technetium-99m with a diamide dithiolate chelating agent. *Proc. Natl. Acad. Sci. U.S.A. 85*, 4025–4029.
(11) Ramalingam, K., and Nowotnik, D. P. Synthesis of phenylisothiocyanate boronic acids: Bifunctional reagents for labeling of monoclonal antibodies with technetium-99m. *Org. Prep. Proc. Int.*, in press.
(12) Primus, F. J., Newell, K. D., Blue, A., and Goldenberg, D. M. (1983) Immunological heterogeneity of carcinoembryonic antigen: Antigenic determinants on carcinoembryonic antigen distinguished by monoclonal antibodies. *Cancer Res. 43*, 686–692.
(13) Tu, Y. Y., Primus, F. J., Shochat, D., and Goldenberg, D. M. (1988) Purification and characterization of carcinoembryonic antigen from GW-39, a xenografted human colonic tumor system. *Tumor Biol. 9*, 212–220.
(14) Goldenberg, D. M., Witte, S., and Elster, K. (1966) GW-39: A new human tumor serially transplantable in the golden hamster. *Transplantation 4*, 760–763.
(15) Goldenberg, D. M., and Hansen, H. J. (1972) Carcinoembryonic antigen present in human colonic neoplasms serially propagated in hamsters. *Science 175*, 1117–1118.
(16) Weadock, K. S., Sharkey, R. M., Varga, D. C., and Goldenberg, D. M. (1990) Evaluation of a remote radioiodination system for radioimmunotherapy. *J. Nucl. Med. 31*, 508–511.
(17) Unger, S. E., McCormick, T. J., Treher, E. N., and Nunn, A. D. (1987) Comparison of desorption ionization methods for the analysis of neutral seven-coordinate technetium radiopharmaceuticals. *Anal. Chem. 59*, 1145–1149.
(18) Narra, R. K., Nunn, A. D., Kuczynski, B. L., Feld, T., Wedeking, P., and Eckelman, W. C. (1989) A neutral technetium-99m complex for myocardial imaging. *J. Nucl. Med. 30*, 1830–1837.
(19) Horvath, C., Melander, W., and Molnar, I. (1977) Liquid chromatography of ionogenic substances with nonpolar stationary phases. *Anal. Chem. 49*, 142–154.
(20) Fritzberg, A. R., and Nunn, A. D. (1986) Radio-HPLC: Application to organics and metal chelate chemistry. *Analytical and Chromatographic Techniques in Radiopharmaceutical Chemistry* (D. M. Wieland, M. C. Tobes, and T. J. Mangner, Eds.) pp 183–212, Springer-Verlag, New York.
(21) Stylli, C., and Theobald, A. E. (1987) Determination of ionisation constants of radiopharmaceuticals in mixed solvents by HPLC. *Int. J. Appl. Radiat. Isot. 38*, 701–708.
(22) Solomons, T. W. G. (1990) *Fundamentals of Organic Chemistry*. J. Wiley & Sons, Inc., New York.
(23) Jurisson, S., Hirth, W., Linder, K., Di Rocco, R. J., Narra, R. K., Nowotnik, D. P., and Nunn, A. D. (1991) Chloro→hydroxy substitution on technetium BATO (TcCl(dioxime)$_3$BR) complexes. *Nucl. Med. Biol. 18*, 735–744.
(24) Feld, T., and Nunn, A. D. (1989) A chromatographic method for the measurement of the lipophilicity of lipophilic technetium complexes. *J. Lab. Compds. Radiopharm. 26*, 274–276.
(25) Sharkey, R. M., Gold, D. V., Aninipot, R., Vagg, R., Ballance, C., Newman, E. S., Ostella, F., Hansen, H. J., and Goldenberg, D. M. (1991) Comparison of tumor targeting in nude mice by murine monoclonal antibodies directed against different human colorectal cancer antigens. *Cancer Res. 50*, 828–834.
(26) Weir, D. M., Herzenberg, L. A., Blackwell, C. B., and Herzenberg, L. A., Eds. (1980) *Handbook of Experimental Immunology. 1. Immunochemistry*. Blackwell Scientific Publications, Oxford, UK.
(27) Cheung, N.-K. V., Neely, J. E., Landmeier, B., Nelson, D., and Miraldi, F. (1987) Targeting of ganglioside G_{D2} monoclonal antibody to neuroblastoma. *J. Nucl. Med. 28*, 1577–1583.
(28) Chatal, J. F., Saccavini, J. C., Gestin, J. F., Thredrez, P., Curtet, C., Kremer, M., Guerreau, D., Nolibe, D., Fumoleau, P., and Guillard, Y. (1989) Biodistribution of indium-111-labeled OC125 monoclonal antibody intraperitoneally injected into patients operated on for ovarian carcinomas. *Cancer Res. 49*, 3087–3094.
(29) Murray, J. L., Mujoo, K., Wilmanns, C., Mansfield, P., Wilbur, D. S., and Rosenblum, M. G. (1991) Variables influencing tumor uptake of anti-melanoma monoclonal antibodies radioiodinated using para-iodobenzoyl (PIB) conjugate. *J. Nucl. Med. 32*, 279–287.

Registry No. ^{99}TcCl(DMG)$_3$, 127709-21-1; (OH)$_2$B-CPITC, 136537-21-8; ^{99}TcCl(DMG)$_3$CPITC, 136537-22-9; ^{99}Tc(DMG)$_3$(μ-OH)SnCl$_3$, 127686-39-9; ^{99m}TcO$_4^-$, 23288-61-1; ^{99}TcCl(CDO)$_3$CPITC, 136537-23-0; ^{99}TcCl(CDO)$_3$, 127686-41-3; ^{99}TcOH(DMG)$_3$CPITC, 136586-68-0; (OH)$_2$B-PITC, 133887-74-8; glycine, 56-40-6.

Antibody Labeling with Copper-67 Using the Bifunctional Macrocycle 4-[(1,4,8,11-Tetraazacyclotetradec-1-yl)methyl]benzoic Acid

Peter M. Smith-Jones,† Raimund Fridrich,‡ Thomas A. Kaden,§ Ilse Novak-Hofer,† Karl Siebold,‡ Daniel Tschudin,‡ and Helmut R. Maecke*,‡

Radiopharmacy Division, Paul Scherrer Institut, Wuerenlingen, Switzerland, Institut für Anorganische Chemie der Universität Basel, Basel, Switzerland, and Department of Nuclear Medicine, University Hospital Basel, Petersgraben 4, 4031 Basel, Switzerland. Received July 24, 1991

The high kinetic stability of the Cu^{2+} complex of the chelator 4-[(1,4,8,11-tetraazacyclotetradec-1-yl)-methyl]benzoic acid was demonstrated at physiological pH as well as under acidic conditions. The chelating agent was conjugated to AB35, a monoclonal antibody directed against CEA, without a significant loss of immunoreactivity. The conjugate could, under optimal labeling conditions, be labeled with ^{67}Cu in acetate buffer with a full occupancy of ligands within 20 min. This radiolabeled conjugate showed no transfer of radiocopper to serum proteins in human serum over 7 days. The biodistribution in tumor-bearing mice was measured and compared to that of iodinated AB35. Tumor uptake was high with 15 ± 3% ID (injected dose)/g after 24 h and 32 ± 7% ID/g after 96 h for the ^{67}Cu-labeled antibody and 13 ± 4% ID/g after 24 h and 14 ± 2% ID/g after 96 h for the ^{125}I-labeled antibody. Whereas radioactivity in normal organs decreased with time after 24 h, increased residence time was shown up to 4 days with the ^{67}Cu-labeled AB35.

Radiolabeled monoclonal antibodies show promise as specific agents for cancer diagnosis and therapy (*1–4*). The most commonly used radioisotopes for antibody labeling are those of iodine (*5*). They have several drawbacks, e.g. logistical problems, the need of having labeling units for the iodination of the antibodies, etc. Furthermore, the in vivo deiodination process leads to the incorporation of iodine into both the thyroid and the stomach; it also appears to be responsible for short residence times of the radiolabel on or in the tumor cell because of antibody processing. Radiometals have the potential to overcome these problems if they can be stably bound to the antibody with preservation of its immunoreactivity (*6, 7*). Higher flexibility in terms of labeling is also possible because this may be performed by simply mixing of the radioisotope, in an appropriate buffer, with the antibody conjugated to a suitable bifunctional ligand (*8*). Among the metallic radionuclides for therapy, ^{67}Cu is one of the more promising because of a 61.9-h half-life, which is ideal in terms of the residence time of antibodies on tumors and in terms of dose rate. It releases β-particles as well as γ-emissions of 93 and 184 keV which allow easy biodistribution studies and tumor imaging in patients. Furthermore, ^{64}Cu is a positron emitter with the potential of accurate dose assessment, three dimensional-representation of tumors, and high resolution. The properties of these two copper radionuclides are summarized in Table I.

In order to utilize $^{67}Cu^{2+}$, a kinetically labile radiometal, one has to incorporate it into a bifunctional ligand which ensures that the metal ion remains bound to the carrier antibody under physiological conditions. Moreover, the chelator must be covalently bound to the protein.

We have previously studied the covalent attachment of the Cu^{2+} complex of the functionalized macrocyclic ligand 4-[(1,4,8,11-tetraazacyclotetradec-1-yl)methyl]benzoic acid (CPTA, Figure 1) to simple amines as model compounds and to bovine serum albumin (*9*). Furthermore, we showed that the ^{64}Cu complex can be attached to the antibody b-12 using the preconjugation labeling approach without significant loss of immunoreactivity (*10*).

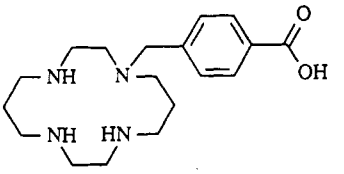


Figure 1. Structure of 4-[(1,4,8,11-tetraazacyclotetradec-1-yl)-methyl]benzoic acid (CTPA).

Table I. Properties of Copper Radionuclides

properties	^{64}Cu	^{67}Cu
half-life, h	12.9	61.9
decay modes	β^- (39.6%)	β^- (100%)
	EC (45.0%)	
	β^+ (19.3%)	
β-energies, keV		
β^-	573 (40%)	395 (51%)
		484 (28%)
		577 (20%)
β^+	654 (19%)	
γ-energies, keV	511 (39%)	91 (6%)
	1346 (0.6%)	93 (35%)
		185 (45%)
		300 (0.6%)

In continuation of these studies, we present new studies with the same ligand in the postconjugation labeling approach with the antibody AB35, which is directed against CEA producing cells (*11*).

Bifunctional macrocyclic ligands have been used before as a means to synthesize ^{67}Cu- and/or ^{64}Cu-labeled antibodies (*12, 13*). Most advanced is the use of the excellent copper chelator 6-(*p*-nitrobenzyl)-TETA,[1] a bifunctional carboxymethylated cyclam-14 derivative (*14*). The high stability of the copper chelate under physiological conditions has been demonstrated and attributed to its high kinetic stability. The chelate has been tested bound to the LYM-1 antibody in tumor-bearing mice with good success. Macrocyclic amines are known to form Cu^{2+}

† Paul Scherrer Institute.
‡ University Hospital Basel.
§ Institut für Anorganische Chemie der Universität Basel.

[1] TETA, 1,4,8,11-tetraazacyclotetradecane-*N,N',N'',N'''*-tetraacetic acid.

1043-1802/91/2902-0415$02.50/0 © 1991 American Chemical Society

complexes which are kinetically more stable than polyamino polycarboxylates (*15*). Two bifunctional derivatives of cyclam-14 conjugated to antibodies have also been tested by two different groups (*12*, *16*). The aim of this study was to demonstrate the feasibility of a kit formulation with our simple bifunctional macrocycle and to compare this radiopharmaceutical with the corresponding iodinated antibody in tumor-bearing mice.

EXPERIMENTAL PROCEDURES

Materials and Methods. All reagents and solvents were obtained from commercial sources and were used without further purification. Copper stock solutions were prepared from $CuSO_4 \cdot 5H_2O$. The concentration was determined by volumetric titration with Na_2EDTA and murexid as indicator (*17*). Sephadex G-50 was used for gel filtration, and HPLC on the labeled antibody and antibody chelator conjugates was done on a Hewlett-Packard HPLC system (Model 1050) and a Waters 30-cm TSK 3000 column with a 5-cm TSK 125 precolumn. UV studies were performed with a Perkin-Elmer Lambda 2 UV spectrophotometer coupled to a Compaq 386 computer and PEXIS software (Perkin-Elmer). Radioactive fractions were measured with an automated Packard well counter and a manual Picker ionization chamber depending on the activities involved. Both detectors were calibrated with ^{67}Cu sources whose activities were determined by γ-ray spectroscopy with a HPGe detector. Radiochromatograms of either TLC or gel chromatography were analyzed using a Berthold TLC linear analyzer coupled to a IBM PC-XT, using a Chroma software (Berthold).

Polyacrylamide SDS gel electrophoresis was done according to Lämmli (*18*) on a LKB 2001 electrophoresis chamber and a Biowerk power supply with Tris buffer (0.375 M, pH 8.3) at 300 V. The protein bands were visualized using Coomassie Brilliant Blue staining. Ultra filtration was done using 10 kDa Omegacell filters (Filtron Technology Corp.) and/or 30 kDa Mini Cent filters (Bio-Rad Laboratories).

The bifunctional macrocycle 4-[(1,4,8,11-tetraazacyclotetradec-1-yl)methyl]benzoic acid tetrahydrochloride (CPTA) (Figure 1) was synthesized as described earlier (*19*). Three batches of ^{67}Cu were obtained, two from Los Alamos Scientific Laboratory (Los Alamos, NM) (39 μCi $^{67}Cu/\mu g$ Cu and 1.6 mCi/μg of Cu in 2 M HCl) and another from Brookhaven National Laboratory (Upton, NY) (0.77 mCi $^{67}Cu/\mu g$ of Cu in 0.1 M HCl). Zn^{2+} impurities were removed by using cation-exchange chromatography (1.5-mL column AG1-X8, 100–200 mesh). The monoclonal antibody used in this study was the IgG1 AB35, which is a murine anti-CEA antibody and was originally prepared as described by Haskell et al. (*11*).

Stability of Cu–CPTA in Aqueous Solution and Human Serum. The Cu^{2+} complex of CPTA was synthesized as described earlier (*9*) and isolated as a perchlorate salt. A 5 mM stock solution (I = 1.0, KNO_3) was prepared. The reaction was started by mixing this solution with 1.0 M HNO_3, 0.1 M HNO_3, or 5×10^{-2} M EDTA (pH 7.3, I = 1.0, KNO_3). The decay of the complex was followed spectrophotometrically at 37 °C. Spectra were taken at different time intervals up to 7 days. The stability in human serum was determined by mixing 7.5 μL of a 6.6 mM solution of CPTA at pH 5 (0.1 M NaOAc) with 0.5 μL of a 6 μM $^{67}CuCl_2$ stock solution (610 μCi/mL, 1.6 mCi/μg), and the mixture diluted to 38 μL (0.1 M NaOAc, pH 5). After 2 h at 37 °C the mixture was mixed into 1.3 mL of sterile human serum and incubated up to 8 days at 37 °C in a chamber maintained at 5% CO_2 and 95% air.

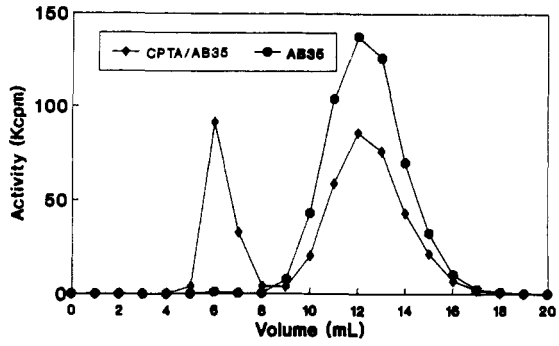


Figure 2. G-50 gel filtration elution curve of EDTA removal of nonspecifically bound ^{67}Cu with both the CPTA–AB35 conjugate and unmodified AB35. The protein peak has an elution maximum at 6 mL and $^{67}Cu(EDTA)^{2-}$ has an elution maximum at 12 mL.

After appropriate intervals, 100-μL samples were taken and subjected to gel filtration. The relative amounts of both CPTA and protein-bound radiocopper were determined by gel-filtration chromatography on a Sephadex G-50 column (19 × 1 cm) using Tris buffer (0.1 M, pH 7).

Conjugation Chemistry. A mixture of 30.6 mg of ligand, 75.3 mg of *N*-ethyl-*N'*-[3-(diethylamino)propyl]-carbodiimide dihydrochloride and 16.2 mg of *N*-hydroxysuccinimide was dissolved in 2.2 mL of phosphate buffer (0.1 M, pH 7). The reaction was allowed to proceed for 1 h at room temperature before being further diluted to 4.4 mL with phosphate buffer. Three portions of 550 μL of AB35 (3.33 mg/mL, 0.1 M Tris buffer, pH 7) were reacted with 8.2, 24.6, and 73.8 μL of the above mixture. After 2 h at room temperature the protein was recovered by ultrafiltration and buffer changed to 0.1 M sodium acetate (pH 5.5). The protein fractions were then filtered using a 0.22-μm filter, and an aliquot was assayed using the absorbance at 276 nm. The absorption at this wavelength was determined to be 1 AU for 1 mg/mL.

In a second experiment three portions of 500 μL of AB35 (3.33 mg/mL, 0.1 M phosphate buffer, pH 7.0) were reacted with 20, 40, and 80 μL of the above mixture. A further two portions of 250 μL of AB35 solution were reacted with 80 and 160 μL of the ligand/activated ester mixture. After 1 h at room temperature the ligand-conjugated protein was recovered by ultrafiltration and the buffer changed to 0.1 M acetate (pH 5.5).

Quantitating the Number of Copper Binding Sites. Ten- or 100-μg portions of modified antibody were incubated with a known excess of a standardized solution of $CuSO_4$ (0.1 M NaOAc, pH 5.5), containing tracer amounts of ^{67}Cu, at 37 °C. Incubation times varied between 20 min and 24 h. Following incubation, the excess copper was complexed with EDTA (50 mM, pH 5.5) at room temperature for 10 min. The mixtures obtained were then separated on a G-50 column (19 × 1 cm) or on a TSK 3000 column (30 cm), using either 0.1 M PBS (pH 7.0 with 0.5% BSA) or 0.1 M PBS (pH 7.0), depending on the concentration of antibody. One-milliliter fractions of the eluate were collected and counted in an automatic well counter. A typical elution profile is shown in Figure 2. The number of macrocyclic ligands attached to the antibody was determined by relative amount of activity recorded in protein fractions and calculated as follows:

$$\text{number of ligands} = \frac{\text{activity in protein fraction} \times \text{moles of Cu}}{\text{total activity} \times \text{moles of AB 35}}$$

As we found slight differences in the calculated number of copper binding sites depending on the separation

method (G-50 or TSK 3000 column), all further experiments were done on HPLC-purified labeled immunoconjugates.

Several ligand binding site assays were performed using a 50 times excess of zinc with respect to copper to ascertain if there is a need to purify ^{67}Cu from any zinc present in commercial supplies.

Radiolabeling of CPTA-AB35 Conjugate. Five hundred microliters of CPTA-AB35 conjugate (1.36 binding sites, 1.62 mg/mL in 0.1 M NaOAc, pH 5.5) was mixed with 60 μL of ^{67}Cu stock solution and incubated for 1 h at room temperature. Following complexation, 100 μL of 50 mM Na_2EDTA (in 0.1 M NaOAc, pH 5.5) was added to chelate unspecifically bound ^{67}Cu. After 5 min the reaction mixture was loaded onto a TSK 3000 column (8 × 300 mm, 8 × 50 mm precolumn). The radiolabeled conjugate was eluted with 0.1 M PBS (pH 7.3) at 1 mL/min. The first peak corresponding to a 300–400 kDa molecular mass was rejected and only part of the main peak collected. In total, 284 μg of labeled AB35, with an activity of 71.3 μCi, was recovered in a 1.2-mL volume.

The second coupling experiment afforded five fractions of modified AB35. They were incubated with 3–5 times the amount of ^{67}Cu solution relative to the number of available CPTA binding sites in a 0.1 M acetate buffer (pH 5.5) for 30 min at room temperature. The same purification procedure was followed as described above to yield 41% of protein.

Iodination of AB35. One hundred micrograms of AB35 was labeled with ^{125}I (0.5 mCi/18.5 MBq) using 20 μg of Iodogen (Pierce) in 300 μL of PBS for 15 min on ice according to the manufacturer's protocol. Labeled mAb was purified over a Sephadex G10 column (PD 10, Pharmacia).

In Vitro Cell-Binding Tests. Titer curves of AB35–CPTA conjugates were compared with underivatized AB35 by binding various concentrations of mAb's to a fixed number of cells (0.5 × 10^6/well) for 16 h at 37 °C. After removal of unbound mAb, bound mAb was detected by a second incubation of ^{125}I-labeled goat anti-mouse antibody (^{125}I-GAM, Bio-Rad) for 2 h. After incubation cells were washed with PBS/HSA, dissolved in 0.5 mL of 1 N NaOH, and counted in a γ-counter.

Immunoreactivity of radiolabeled AB35 was determined by cell-binding assays with the CEA-producing LoVo (human colon adeno carcinoma) cell line (American Type Culture Collection). Cells were seeded in 24-well microtiter plates (maximally 2 × 10^6 cells/well) and allowed to attach for 1 h at 37 °C. The medium (Minimal Eagles Medium containing 10% fetal calf serum) was then taken off; plates were dried for 3 days at room temperature in a laminar-flow hood and could then be stored at 4 °C for at least 6 months. Before use, plates were presaturated for 60 min at 37 °C with 0.5 mL/well of PBS containing 0.5% HSA. Binding of ^{125}I- or ^{67}Cu-labeled AB35 was measured by incubating 10^5 cpm of labeled mAb in 0.5 mL of PBS-HSA for 16 h at 37 °C. Plates were then washed three times with 0.5 mL of ice-cold PBS-HSA. Cells were dissolved in 0.5 mL of 1 N NaOH and radioactivity was counted in a γ-counter. Nonspecific binding was determined in separate wells by addition of 10 μg of unlabeled mAb to the labeled preparations and was subtracted. Immunoreactivity of radiolabeled mAb was determined by binding to increasing numbers of cells and analysis of saturation curves by the method of Lindmo (*20*).

Stability Studies of ^{67}Cu–CPTA–AB35 in PBS Buffer and Human Serum. The stability of the ^{67}Cu-labeled AB35–CPTA conjugate was determined by copper exchange between the immunoconjugate and free Cu^{2+}. The ^{67}Cu–CPTA–AB35 conjugate (143 pM in PBS, pH 7.3, 4.5 Cu atoms per AB35) was treated with a 50 times excess of cold Cu^{2+}. The solution was maintained at 37 °C, and 500-μL aliquots were removed at intervals over a 5-day period. The removed solutions were immediately treated with 500 μL of a 50 mM EDTA solution allowed to stand for 5 min and subject to analysis on a G-50 column (19 × 1 cm) using 0.1 M PBS (pH 7.3).

Table II. Stability of Cu–CPTA Complex from Spectrophotometric Data

time, days	% dissociation of Cu–CPTA complex		
	50 mM EDTA[a]	50 mM HNO_3	500 mM HNO_3
0	0	0	0
0.07	0	0	1.5
0.28	0	0	
0.69	0.7		14.7
2.78		2.8	36.7
6.94	0.7	6.9	

[a] The optical density change of measurements in EDTA is within experimental error.

The stability of the radiocopper-labeled conjugate was studied in vitro by using human serum at 37 °C and in vivo by analyzing blood samples reserved from sacrificed mice by size-exclusion HPLC and SDS gel electrophoresis. In the former case samples were prepared by mixing 10 μL of ^{67}Cu-labeled AB35 with 1 mL of human serum and incubating the mixture in a 5% CO_2, 95% air environment for up to 7 days. In the latter case samples of murine serum was recovered from the animals and 100-μL samples were analyzed by SDS gel electrophoresis.

Animal Biodistribution Studies. Nude mice (strain ZH ICR nu/nu, Institut für Versuchstierforschung) were subcutaneously injected with 5 × 10^6 LoVo cells (suspended in Minimal Eagles Medium containing 10% fetal calf serum) into the right and left flank. After 1 week, tumors of 20–300 mg were produced. The mice were then injected either with 10 μg of iodinated AB35 (5 mCi of ^{125}I/mg) or 20 μg of ^{67}Cu-labeled AB35 (250–500 μCi/mg) by means of an intravenous tail injection. The animals were counted in a well counter at regular time intervals after injection until sacrifice. The animals were sacrificed between 1 and 4 days after injection and were dissected directly after sacrifice. The various organs were removed, rinsed in saline, blotted, weighed, and counted in an automated well counter. The uptake of radioactivity by organs was calculated as percent injected dose per gram tissue. At least three animals were used for every time point.

Imaging Studies. Prior to sacrifice, the mice, previously injected with the ^{67}Cu-labeled Ab35, were anesthesized for imaging studies by intraperitoneal injection of Nembutal. They were subsequently imaged, at several time points, with a Picker γ-camera interfaced to a VAX computer. A low-energy collimator was used and the 20% window centered at 180 keV; 30 000 counts were collected.

RESULTS

Stability of Cu–CPTA in Aqueous Solution and Human Serum. The stability of Cu–CPTA was studied spectrophotometrically at pH 7.3 and 37 °C with excess EDTA. Within 7 days no spectral change could be observed, indicating extremely high kinetic stability of the complex (Table II). Even at low pH in 0.05 M HNO_3 only 7% of the complex dissociated within 7 days. Significant dissociation only occurs in 0.5 M HNO_3 with around 37% after 3 days.

The same high kinetic stability of the complex is found in human serum with less than 0.1% of radioactive $^{67}Cu^{2+}$

Scheme I

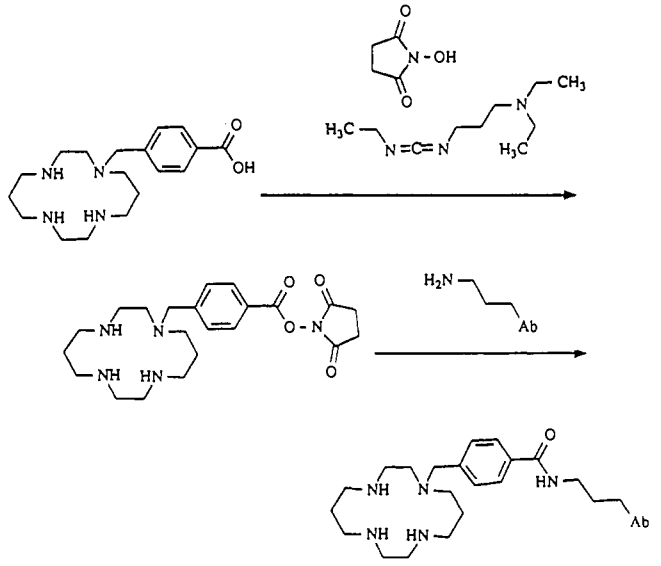


Table III. Properties of mAb35–CPTA Conjugate

reaction ratio ligand:AB35	% immunoreactivity of CPTA–AB35[a]	ratio CPTA:AB35	% immunoreactivity of ^{67}Cu–CPTA–AB35[b]	^{67}Cu ratio heavy:light chain
51:1	>90	4.5	80–100	2.14
102:1	>90	4.5	80–100	1.95
204:1	>90	5.4	80–100	1.96
408:1	>90	5.6	80–100	1.89

[a] Immunoreactivity as determined by the Sandwich assay. [b] Immunoreactivity as determined by the Lindmo procedure (*20*).

transferred to serum proteins within the time period of 8 days (data not shown).

Conjugation Chemistry. The reaction scheme for conjugation of the ligand to AB35 is outlined in Scheme I. As shown before activation of the carboxylate group of CPTA can be done with a mixture of *N*-ethyl-*N'*-[3-(diethylamino)propyl]carbodiimide and *N*-hydroxysuccinimide (*9*). This affords a conjugate with 1.36 chelators per antibody when conjugation is done in Tris buffer under the conditions described. This conjugate showed preserved immunoreactivity and was used in the first of two in vivo experiments in tumor-bearing nude mice. Buffer exchange to PBS afforded chelator to antibody ratios of up to 5.6, depending on reagent ratios (Table III).

Radiolabeling and Quantitation of Binding Sites. Since all unlabeled immunoconjugates exhibited a high immunoreactivity, they were used for further experiments without further purification. For critical applications (a secondary immunoreactivity test and the animal experiment) the radiolabeled conjugate was purified by HPLC.

The number of binding sites per antibody was determined by excessive reaction with a known concentration of Cu^{2+} tracered with radiocopper. Copper complexation to the AB35–CPTA conjugate was done in acetate buffer (pH 5.5). It is fast and complete within 20 min. No further increase of protein-bound copper was observed after this time and up to 24 h.

The labeling experiment in the presence of a 50 times excess of Zn^{2+} showed a slight reduction of copper incorporation to 80% of the theoretical labeling yield within 30 min, indicating rather high selectivity of the bifunctional macrocycle for Cu^{2+}. Thus it may be possible to avoid time-consuming purification of the radiocopper solutions.

In several blank runs using unmodified AB35, the unspecific binding of copper was low, demonstrating the

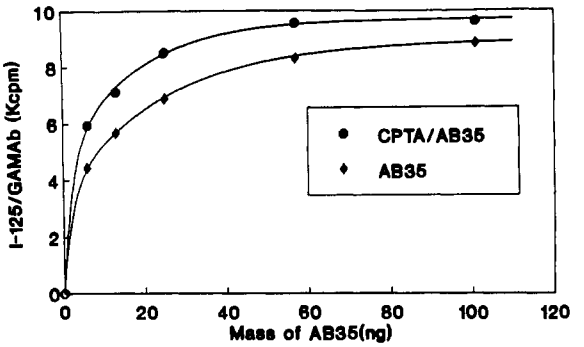


Figure 3. Typical immunoreactivity binding curves for CPTA–AB35 conjugate and unmodified AB35. The CPTA–AB35 conjugate has an average of 4.5 chelators per antibody.

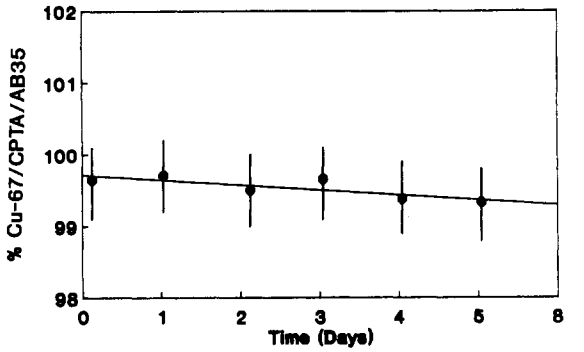


Figure 4. Exchange studies of ^{67}Cu–CTPA-AB35 with a 50-fold excess of cold copper in phosphate buffer, pH 7.0. The pseudo-first-order rate constant is estimated to be 6.7×10^{-4} day^{-1}.

effectiveness of the EDTA complexation of excess copper. Figure 2 shows typical G50 separation runs for the ^{67}Cu–CPTA–AB35 conjugate and AB35 incubated with $^{67}Cu^{2+}$.

SDS gel electrophoresis of the HPLC-purified antibody showed approximately a 2:1 ratio for the distribution of activity of the heavy and light chains, respectively. There was a slight trend for light chain labeling at the higher reaction ratios (Table III).

Iodination. Yield for iodination were typically between 90 and 100%. Specific activity of the iodinated antibody was 5 mCi/mg.

In Vitro Cell-Binding Test. The unlabeled immunoconjugates were tested for immunoreactivity with the described Sandwich assay and compared to unmodified antibody. A typical binding curve can be seen from Figure 3. The immunoreactivity of different conjugates is shown in Table III. Conjugation of up to 5.6 ligands per antibody did not impair the biological integrity to an appreciable extent. The binding assay showed binding of ca. 90% of modified AB35 to the plated LoVo cells if compared to the unmodified antibody.

The immunoreactivity of the radiolabeled antibody measured according to Lindmo (*20*) was 85 ± 15% (Table III) and in accordance with the unlabeled conjugates. The immunoreactivity of the radioiodinated antibody was 90 ± 10%.

Stability Studies of ^{67}Cu–CPTA–AB35 in PBS Buffer and Human Serum. Exchange measurement in phosphate buffer (pH 7) of the radiocopper-labeled conjugate and excess cold copper gave an apparent half-life of copper exchange of >1000 days (Figure 4). This is consistent with the in vitro stability of Cu–CPTA toward excess EDTA and in human serum toward serum albumin. The labeled conjugate proved also to be unchanged after incubation in human serum (data not shown).

Animal Biodistribution Studies. Animal experiments were done with a conjugate having 1.36 chelators

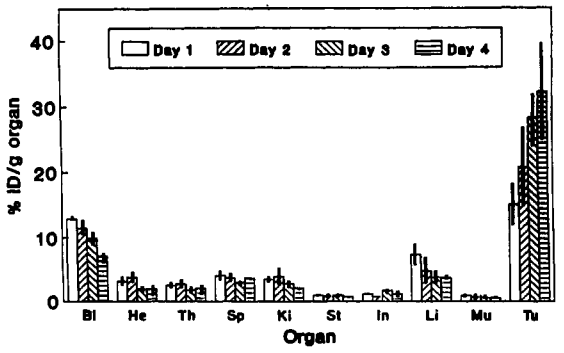


Figure 5. Biodistribution data for ^{67}Cu–CPTA–AB35 in 12 tumor-bearing nude mice. Mice were injected with 20 μg of ^{67}Cu–CPTA–AB35 containing either 1.3 or 4.5 CPTA groups per antibody. Data are means ± SD of three animals. No significant variations were observed between the two different radiolabeled conjugates. Bl = blood, He = heart, Th = thyroid, Sp = spleen, Ki = kidney, St = stomach, In = intestines, Li = liver, Mu = muscle, Tu = tumor.

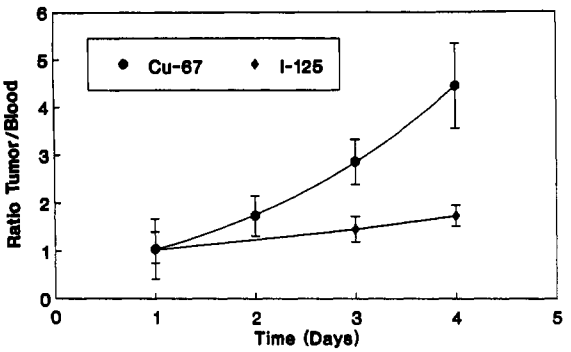


Figure 6. Tumor to blood accumulation rates for ^{125}I–AB35 and ^{67}Cu–CPTA–AB35 in tumor-bearing nude mice. Data are means ± SD of two animals (^{125}I–AB35) and of three animals (^{67}Cu–AB35).

per mAb35 and a second experiment with 4.5 chelators per antibody.

The biodistribution in tumor-bearing mice with ^{67}Cu–CPTA–AB35 was followed up to 4 days. Figure 5 shows the organ distribution of the combined experiments with conjugates having 1.36 and 4.5 chelators per antibody. There was no significant biological variation in the in vitro or in vivo behavior of the two conjugates. The amount of radioactivity increases in tumors whereas the activity in normal organs decreases with time after 24 h. The liver activity is surprisingly low with 7.3% ID/g after 24 h and is decreasing with a time constant similar to that of the blood activity, indicating that most of the liver activity corresponds to blood-pool activity. Liver activity in two normal mice measured 2 h postinjection was found to be 12% ID/g liver.

The tumor to blood ratio is given in Figure 6. The comparative biodistribution of ^{125}I-labeled and ^{67}Cu-labeled antibody is shown in Figure 7 and 8. The data are given for days 1 and 4.

The whole-body clearance of both the iodinated and radiocopper-labeled antibody is shown in Figure 9. Assuming a first-order excretion, the two data sets give respective half-lives of 120 and 210 h.

Serum studies using SDS gel electrophoresis showed that the circulating Cu–CPTA–AB35 conjugates remain intact with time in vivo (data not shown).

Imaging Studies. Due to the favorable γ-energy of the isotope, good γ-camera images could be obtained. A typical image is shown in Figure 10. The picture was taken 100 h postinjection (animal A) and 102 h postinjection

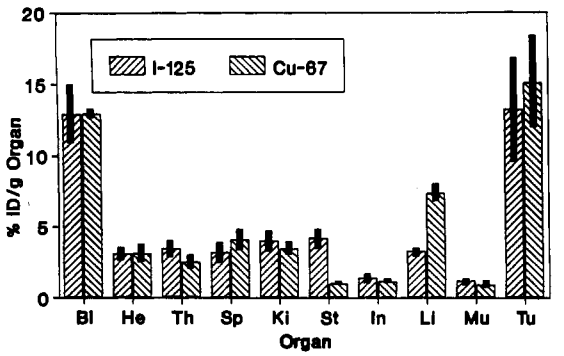


Figure 7. Biodistribution data for radiolabeled AB35 in tumor-bearing nude mice 1 day postinjection. Mice were injected with either 10 μg of ^{125}I–AB35 (5 mCi/mg) or 20 μg of ^{67}Cu–CPTA–AB35 (250–500 μCi/mg). See Figure 5 for legend.

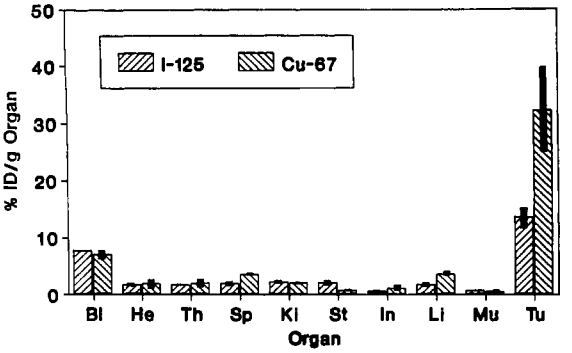


Figure 8. Biodistribution data for radiolabeled AB35 in tumor-bearing nude mice 4 days postinjection. Injection was as in Figure 7. See Figure 5 for legend.

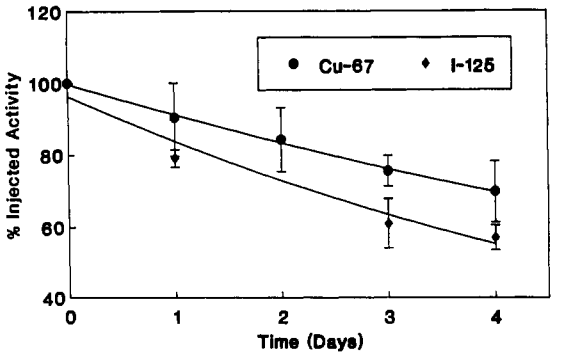


Figure 9. Whole-body retention of both ^{125}I–AB35 and ^{67}Cu–CPTA–AB35 in tumor-bearing nude mice. Apparent biological half-lives of 120 and 210 h were observed for the respective ^{125}I- and ^{67}Cu-labeled antibodies.

(animal B). The tumor masses of A were ca. 34 and 150 mg. In the smaller tumor ca. 1500 cpm/mg were measured after excision, whereas the larger tumor measured about 1400 cpm/mg. The tumors of animal B weighed ca. 215 mg (left) and 100 mg (right) with around 1650 and 1700 cpm/mg. The figure represents photographs of unprocessed images.

DISCUSSION

Copper-67 is one of the attractive radiometals for radioimmunotherapy; it has abundant β-particles, and the γ-energy of 184 keV is suitable for imaging studies (Table I). The maximum β-energy of 0.57 MeV is close to the corresponding energy of ^{131}I and appears to be suitable for the treatment of small tumors and metastases. Because of the similarity in β-energy, a comparative biodistribution study with an iodinated and copper-labeled immunoconjugate appeared especially interesting to us. The

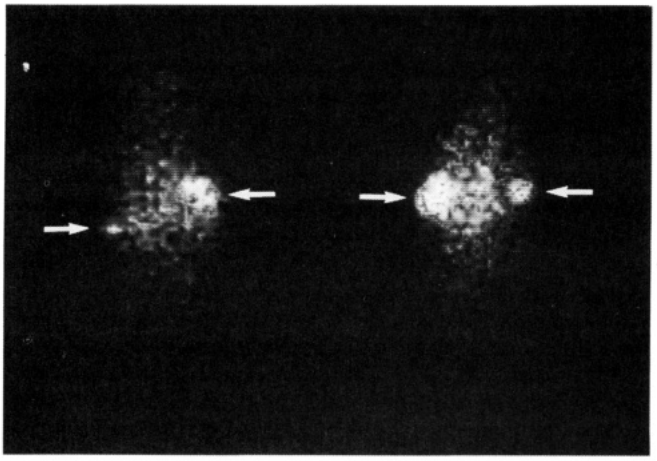


Figure 10. Anterior γ-camera images of two nude mice bearing LoVo tumors 4 days postinjection of ^{67}Cu–CTPA–AB35 with two tumors each (arrows) ranging between 34 and 215 mg. Mice were injected with 20 μg of ^{67}Cu-labeled AB35 (500 μCi/mg).

use of the metallic radionuclide allows the preparation of an instant kit and avoids complicated in-house labor with the iodination. An instant kit procedure affords the use of bifunctional chelators which can be attached to the protein in advance; the conjugate can be purified and stored.

Thirteen- and 14-membered tetraazamacrocycles are known to form kinetically inert, well-defined complexes with Cu^{2+} (*21*, *22*). Our choice was 4-[(1,4,8,11-tetraazacyclotetradec-1-yl)methyl]benzoic acid as bifunctional ligand. The synthesis is done very simply in one step and can be done in 1 day, yielding gram amounts. We reported in a previous publication that the ligand can be conjugated to simple amines, bovine serum albumin, and a monoclonal antibody against a mucinelike carcinoma–associated antigen using activated ester methods and the prelabeling approach (*9*, *10*). In these experiments the Cu^{2+} protects the amino groups on the macrocycle to prevent dimerization or polymerization of the ligand and allows exclusive reaction with the exogeneous amines. In the uncomplexed ligand some degree of intermolecular reaction is expected in addition to the reaction of the activated ester with the ϵ-amino group of the lysine side chains. However since the macrocycle carries two protons around pH 7 (*19*), this may provide efficient enough protection to avoid extensive polymerization of the ligand. This appears indeed to be the case, conjugation occurs mildly and the biological integrity of the antibody is preserved.

The fast rate of copper complexation by both the CPTA ligand and the protein–CPTA conjugate may be explained by disturbed symmetry of the tetraazamacrocycle due to alkylation of one nitrogen. This same activation of ligand toward complexation was found with the very rigid porphyrins if one nitrogen is substituted with a benzyl group (*23*).

The fast rate of complexation is of particular importance since this can lead to reliable cold kit preparations of a predefined quality, i.e. immunoreactivity and number of binding sites. Excess copper can be removed easily after labeling by use of a small gel-filtration column.

Despite the N-functionalization of the ligand, the Cu^{2+} complex exhibits high stability. It is totally inert in human serum and toward excess EDTA at pH 7.3. Only in strong acid has significant decay been shown.

Moreover, the ligand appears to have remarkable selectivity for Cu^{2+} over Zn^{2+}. The presence of large excess of Zn^{2+} had a minor effect on the labeling yield. This fact may facilitate the radiochemical manipulation of radiocopper solution and render time-consuming removal of Zn^{2+} contaminations unnecessary. Any chemical separation performed on the initial ^{67}Cu solution will ultimately add more carrier copper, the amount depending on the purity of reagents. Comparative kinetic studies of the respective metal complexation rates are in progress.

The low pH used for labeling avoids $Cu(OH)_2$ colloid formation, moreover it removes the risk of high unspecific labeling of the protein due to efficient protonation of the amino groups of the antibody.

The distribution of the macrocycle at the antibody is random and the biological integrity is preserved after conjugation and labeling. Similar data were reported with somewhat analogous systems by other groups. Franz et al. (*16*) report antibody labeling with a 1-(3-aminopropyl)-4-methyl derivative of cyclam-14. They report preserved immunoreactivity but significant levels of nonspecifically bound copper even after chasing of copper with 1 mM EDTA. It is our impression that this is only due to higher pH than necessary for the labeling and chasing step.

Parker's group (*12*, *13*) uses a C-functionalized cyclam-14 macrocycle to label the B 72.3 antibody. With only about 0.25 chelators per antibody high immunoreactivity was shown, but labeling efficiency is only 33%. The labeled conjugate was tested in healthy mice and showed reasonable biodistribution and high in vivo stability.

Most advanced as to chemical characterization of a ^{67}Cu chelate and in vivo studies is the work of Meares' group (*14*) with the bifunctional chelator 6-(*p*-nitrobenzyl)-TETA, a C-functionalized tetra-N-carboxymethylated derivative of cyclam-14. The Cu^{2+} complex was characterized by X-ray crystal structure (*24*) and high kinetic stability of the chelate in human serum was demonstrated. The macrocyclic tetra-*N*-acetate was clearly superior to the usual chelators EDTA and DTPA (*15*). The *p*-(bromoacetamido)benzyl-TETA was conjugated to Lym-1 and stably labeled with ^{67}Cu under preservation of immunoreactivity. The radiopharmaceutical showed excellent biodistribution in RAJI tumor-bearing mice (*14*) and is now used in patients (*25*).

The biodistribution data of our copper-labeled conjugates clearly show high tumor uptake and decreasing activity in all organs with time after 24 h, except in tumors. Most important is the extended residence time of radioactivity on the tumor if compared to radioiodinated antibody.

Moreover, the liver activity is low and its time course is favorable and decreases with time at approximately the same extent as it disappears from blood. This indicates that processing and handling of the radionuclide and the chelate is more favorable than in the case of antibodies labeled with ^{111}In and ^{90}Y using bifunctional polyamino polycarboxylates like DTPA and EDTA. This may be due to the extreme kinetic stability of the ^{67}Cu/CPTA complex and/or the ease of hydrolysis of the peptide bond formed in the conjugation process.

ACKNOWLEDGMENT

This work was supported by the Swiss National Science Foundation (Grant No. 31-27739.89), the "Regionale Krebsliga beider Basel", and Roche Research Foundation. The expert technical help of R. Stolz, D. Tschudin, N. Ulmer, and L. Siegfried-Hertli is gratefully acknowledged.

LITERATURE CITED

(1) Rainsburry, R. M., Westwood, J. H., Coombes, R. C., Neville, A. M., Ott, R. J., Kalirai, T. S., McCready, V. R., and Gazet, J. C. (1983) Location of Metastatic Breast Carcinoma

by a Monoclonal Antibody Chelate Labeled with Indium-111. *Lancet* 934–938.
(2) Carrasquillo, J. A., Bunn, P. A., Keenan, A. M., Reynolds, J. C., Schroff, R. W, Foon, K. A., Ming-Hus, S., Gazdar, A. F., Mushine, J. L., Oldham, R. K., Perentesis, P., Horowitz, M., Eddy, J., James, P., and Larson, S. (1986) Radioimmunodetection of Cutaneous T-Cell Lymphoma with 111-In-Labeled T 101 Monoclonal Antibody. *N. Engl. J. Med. 315*, 673–680.
(3) Macklis, R. M., Kinsey, B. M., Kassis, A. I., Ferrara, J. L. M., Atcher, R. W., Hines, J. J., Coleman, C. N., Adelstein, S. J., Burakoff, S. J. (1988) Radioimmunotherapy with Alpha-Particle-Emitting Immunoconjugates. *Science 240*, 1024–1026.
(4) Baldwin, R. W., and Byers, V. S. (1986) Monoclonal Antibodies in Cancer Treatment. *Lancet* 603–605.
(5) Mach, J. P., Crarrel, S., Forni, M., Ritschard, J., Donath, A., and Alberto, P. (1980) Tumor Localization of Radiolabelled Antibodies against Carcinoembryonic Antigen in Patients with Carcinoma. *N. Engl. J. Med. 303*, 5–9.
(6) Brechbiel, M. W., Gansow, O. A., Atcher, R. W., Schlom, J., Esteban, J., Simpson, D. E., and Colcher, D. (1986) Synthesis of 1-(*p*-isothiocyanatobenzyl) derivatives of DTPA and EDTA. Antibody labeling and tumor imaging studies. *Inorg. Chem. 25*, 2772–2781.
(7) Meares, C. F., McCall, M. J., Reardan, D. T., Goodwin, D. A., Diamanti, C. I., and McTigue, M. (1984) Conjugation of Antibodies with Bifunctional Chelating Agents: Isothiocyanate and Bromoacetamide Reagents, Methods of Analysis, and Subsequent Addition of Metal Ions. *Anal. Biochem. 142*, 68–78.
(8) Hnatowich, D. J., Layne, U. U., Childs, R. I., Lateigne, D., Davis, M. A., Griffin, T. W., and Doherty, P. W. (1983) Radioactive labeling of antibody: a simple and efficient method. *Science 220*, 613–615.
(9) Studer, M., Kaden, Th. A., and Maecke, H. R. (1990) Reactivity Studies of the Pendant Carboxylic Group in a Macrocyclic Cu^{2+} Complex Towards Amide Formation and Its Use as a Protein-Labelling Agent. *Helv. Chim. Acta 73*, 149–153.
(10) Maecke, H. R., Kaden, T., Riesen, A., Ritter, W., and Studer, M. (1989) Some aspects of Antibody Labeling with Metallic Radionuclides. *Int. J. Cancer Suppl. 2, 59*, 307.
(11) Haskell, C. M., Buchegger, F., Schreyer, M., Carrel, S., and Mach, J. P. (1983) Monoclonal Antibodies to Carcinoembryonic Antigen: Ionic Strength as a Factor in the Selection of Antibodies for Immunoscintigraphy. *Cancer Res. 43*, 3857–3864.
(12) Morphy, J. R., Parker, D., Alexander, R., Bains, A., Carne, A. F., Eaton, M. A. W., Harrison, A., Millican, A., Phipps, A., Rhind, S. K., Titmas, R., and Weatherby, D. (1988) Antibody Labelling with Functionalised Cyclam Macrocycles. *J. Chem. Soc., Chem. Commun.* 156–157.
(13) Morphy, J. R., Parker, D., Kataky, R., Eaton, M. A. W., Harrison, A., Millican, A., Phipps, A., and Walker, C. (1989) Towards Tumor Targeting with Copper-radiolabelled Macrocycle-Antibody Conjugates. *J. Chem. Soc., Chem. Commun.* 792–794.
(14) Desphande, S. V., DeNardo, S. J., Meares, C. F., McCall, M. J., Adams, G. P., Moi, M. K., and DeNardo, G. L. (1988) Copper-67-labeled Monoclonal Antibody Lym-1, a Potential Radiopharmaceutical for Cancer Therapy: Labeling and Biodistribution in RAJI Tumored Mice. *J. Nucl. Med. 29*, 217–225.
(15) Cole, W. C., DeNardo, S. J., Meares, C. F., McCall, M. J., DeNardo, G. L., Epstein, A. L., O'Brien, H. A., and Moi, M. K. (1987) Comparative Serum Stability of Radiochelates for Antibody Radiopharmaceuticals. *J. Nucl. Med. 28*, 83–90.
(16) Franz, J., Freeman, G. M., Barefield, E. K., Volkert, W. A., Ehrhardt, G. J., and Holmes, R. A. (1987) Labelling of Antibodies with ^{64}Cu Using a Conjugate Containing a Macrocyclic Amine Chelating Agent. *Int. J. Radiat. Appl. Instrum. Part B 14*, No. 5, 479–484.
(17) Schwarzenbach, G. (1957) *Die komplexometrische Titration*, Verlag F. Enke, Stuttgart.
(18) Lämmli, U. (1970) Cleavage of Structural Proteins During the Assembly of the Head of Bacteriophage T4. *Nature 227*, 680–681.
(19) Studer, M., and Kaden, Th. A. (1986) One-Step Synthesis of Mono-N-substituted Azamacrocycles with a Carboxylic Group in the Side-Chain, and Their Complexes with Cu^{2+} and Ni^{2+}. *Helv. Chim. Acta 69*, 2081–2086.
(20) Lindmo, T., Boven, E., Cuttitta, F., Fedorko, J., and Bunn, P. A., Jr. (1984) Determination of the immunoreactive fraction of radiolabelled monoclonal antibodies by linear extrapolation to binding at infinite antigen excess. *J. Immunol. Methods 72*, 77–89.
(21) Leugger, A. P., Hertli, L., and Kaden, Th. A. (1978) Metal Complexes with Macrocyclic Ligands. XI), Ring Size Effect on the Complexation Rates with Transition Metal Ions. *Helv. Chim. Acta 61*, 2296–2306.
(22) Lindoy, L. F. (1989) *The Chemistry of Macrocyclic Ligand Complexes*, Cambridge University Press, Cambridge.
(23) Mercer-Smith, J. A., Roberts, J. C., Figard, S. D., and Lavellee, D. K. (1988) The development of copper-67-labeled porphyrin-antibody conjugates. *Targeted Diagnosis and Therapy*, Vol. 1, pp 317–323, Marcel Dekker, New York.
(24) Moi, M. K., Yanuck, M., Desphande, S. V., Hope, H., DeNardo, S. J., and Meares, C. F. (1987) X-ray Crystal Structure of a Macrocyclic Copper Chelate Stable Enough for Use in Living Systems: Copper(II) Dihydrogen 6-(*p*-Nitrobenzyl)-1,4,8,11-tetraazacyclotetradecane-1,4,8,11-tetraacetate. *Inorg. Chem. 26*, 3458–3463.
(25) DeNardo, G., De Nardo, S. J., Kukis, D., Diril, H., Suey, C., and Meares, C. F. (1991) Strategies for Enhancement of Radioimmunotherapy. *Nucl. Med. Biol. 13*, 359–362.

Effect of Structural Variations in Cholesteryl-Conjugated Oligonucleotides on Inhibitory Activity toward HIV-1

Firdous Farooqui,† Prem S. Sarin,‡ Daisy Sun,§ and Robert L. Letsinger*,†

Department of Chemistry and Department of Biochemistry, Molecular and Cell Biology, Northwestern University, Evanston, Illinois 60208-3113, Department of Biochemistry and Molecular Biology, George Washington University Medical Center, 2300 I Street, NW, Washington, D.C. 20037, and Laboratory of Tumor Cell Biology, National Cancer Institute, Bethesda, Maryland 20892. Received August 5, 1991

A number of oligonucleotide analogues containing internucleoside phosphorothioate linkages and a covalently attached cholesteryl residue was synthesized and tested for activity against HIV-1 in cultures of Molt3 cells. Structural features important for high antiviral activity are the presence of a cholesteryl moiety, a run of terminal phosphorothioate groups, and the presence of nucleoside residues. An increase in length of the tether between cholesteryl and phosphorus from six to 14 atoms has no significant effect on antiviral activity, and up to one-half of the internucleoside links in a cholesteryl-conjugated phosphorothioate oligomer and one-third of the internucleoside links in a nonconjugated phosphorothioate can be replaced with phosphodiester links without much change in antiviral activity. However, replacement of nucleoside units in the oligomers by a simple analogue ($-OCH_2CH_2CH_2O-$) yields inactive or very weakly active compounds, even in the presence of a cholesteryl group. Dose–response patterns for assays in which cholesteryl-conjugated oligomers are added to test cells either simultaneously or subsequently to viral infection are similar for homooligomer derivatives and for oligomers containing "antisense" sequences, suggesting a similarity in mode of action for the two classes of oligomers in this system.

INTRODUCTION

Phosphorothioate oligonucleotide analogues are effective inhibitors of replication of HIV-1 in cell culture (*1–3*). Considerable evidence indicates that they may function in either a sequence independent mode (*1*) or a sequence specific mode (*4, 5*), depending on the sequence and stage of infection when the oligomer is applied. The anti-HIV activity of both the phosphorothioate analogues and normal phosphodiester oligonucleotides is enhanced when cholesterol is conjugated near the 3′ (*6*) or 5′ (*7*) terminus. This enhancement is particularly pronounced for short oligomers.

To gain further information on the relation of structure to the antiviral activity of cholesteryl-conjugated oligonucleotides we have prepared and examined compounds with changes in the phosphodiester/phosphorothioate ratio, the nucleotide sequence, the length of the oligomer, the length of the tether to cholesteryl, the nucleoside/phosphorothioate ratio, and the number of cholesteryl groups. The structures are shown in Table I. In conjunction with assays involving successive as well as simultaneous addition of virus and phosphorothioate oligomer to the test cells, this study serves to define more clearly the structural requirements for anti-HIV activity in this system.

EXPERIMENTAL PROCEDURES

General Procedures. High-performance liquid chromatography (HPLC) was carried out with a C-18 reversed-phase column (5 μm Hypersil ODS; 100 × 2.1 mm) on a Hewlett-Packard 1090 chromatograph using aqueous 0.03 M triethylammonium acetate (pH 7.3) and an acetonitrile gradient (1%/min increase in acetonitrile; 0.5 mL/min flow rate). Thin-layer chromatography (TLC) was carried out with Brinkman silica gel plates using *n*-propyl alcohol/ammonium hydroxide/water (55/10/35 v/v/v). Polyacrylamide gel electrophoresis (PAGE) was carried out with denaturing cross-linked 20% gels (bisacrylamide/acrylamide 1/28.4, w/w; 1 × 140 × 170 mm) at 400 V. Nucleotide bands were visualized by UV shadowing and by staining with methylene blue (0.02%). Migration distances are reported relative to bromophenol blue.

For the enzyme digests a sample of the oligonucleotide (1 A_{260} unit in doubly distilled water) was warmed at 37 °C for 5 h with 15 μL of snake venom phosphodiesterase I (Sigma, 2 mg/mL), 8 μL of calf liver alkaline phosphatase (Boehringer Mannheim, 102 μL/510 μg), and 150 μL of buffer (32 mM Tris·HCl and 12 mM in magnesium chloride, pH 7.5). The solution was heated at 70–75 °C for 5 min, cooled, diluted with 100 μL of water, and subjected to HPLC.

Oligomer Synthesis. Phosphorothioate and cholesteryl-conjugated phosphorothioate oligonucleotide analogues (compounds **1**, **2**, **4**, **6–15**, Table I) were prepared using hydrogen phosphonate chemistry (*8*), with oxidation with sulfur to form internucleoside phosphorothioate links (*2*) and oxidation with carbon tetrachloride in the presence of the appropriate [[(cholesteryloxy)carbonyl]amino]alkylamine to form the phosphoramidate links (*6*). Typically, the first coupling and attachment of a tethered cholesteryl group was carried out manually in a syringe, starting with 1 μmol of the designated 3′-terminal nucleoside anchored to a controlled pore glass (CPG) support. The derivatized support was then transferred to a DNA synthesizer (Milligen Biosearch 8600) for automated synthesis. Following oxidation with sulfur, the solid support was removed and treated with concentrated ammonium hydroxide at 55 °C for 5 h; then the solution was concentrated and the oligomer was isolated by reversed-phase HPLC. The anucleosidic oligomers (X compounds, Table I) were prepared in the same manner as the oligonucleotide derivatives by using DMT-$OCH_2CH_2CH_2OPH(O)(O^-)$ in place of nucleoside hydrogen phosphonate reagents. They were isolated in yields of 30–35%.

† Northwestern University.
‡ George Washington University Medical Center.
§ National Cancer Institute.

1043-1802/91/2902-0422$02.50/0 © 1991 American Chemical Society

Table I. Phosphorothioate Oligodeoxyribonucleotide Derivatives[a]

		HPLC t_R,[b] min	TLC R_f[c]	PAGE R_m[d]	$ID_{50(de\ novo)}$,[e] μM
1	GTGTCTCCCCTTCT T	17.2	1.10	0.76	1.4
2	GTGTCTCCCCTTC T*T	44.6	1.14	0.68	0.2
3	GTGTCTC CCCTTCT*T	43.5	1.14	0.70	0.3
4	ACACCCAATTCTGAAAATG G	16.8	1.10	0.67	1
5	ACACCC AATTCTGAAAATG G	14.9	1.07	0.66	0.7
6	ACACCCAATTCTGAAAAT G*G	40.2	1.13	0.64	0.1
7	CTCGCACCCATCTCTCTC C*T	42.7	1.29	0.60	0.02
8	CCCCCCCCCCCCCCCCCCC C	18.4	1.11	0.76	>3
9	CCCCCCCCCCCCCCCCCC C*C	42.3	1.15	0.67	0.03
10	GTGTCTCCCCTTCTTCCTGCC A*T	41.1	1.23	0.62	0.01
11	AGTCATTGGTCTTAAAGGTACCTGA G*G	36.5	0.80	0.49	0.05
12	CCCCCCCC C*C	46.2	1.14	0.94	~3
13	CCCCCCCC C#C	56.3	1.50	0.92	~3
14	CCCCCC C*C C*C	62.5	1.45	[f]	~2[g]
15	TTTTTTTT T#T	55.2	2.05	0.73	~4
16	XXXXXXXX X*C	46.3	1.34	1.0	inactive[h]
17	XXXXXXXX X*T	44.6	1.65	1.08	inactive[h]
18	XXXXXXXXXXXXX X*T	34.8	1.06	1.45	inactive[i]

[a] Abbreviations: underlined nucleotide units have 3′-phosphorothioate links; An asterisk indicates a O=PNH(CH_2)$_2$NHCOO–cholesteryl link; A pound sign indicates a O=PNH(CH_2)$_{10}$NHCOO–cholesteryl link; X represents that –O(CH_2)$_3$O– has replaced a nucleoside unit. [b] Elution time (see the experimental section for conditions). [c] R_f relative to dpT. [d] R_m relative to bromophenol blue. [e] Concentration of oligomer that leads to 50% inhibition, averaged for inhibition of syncytia and cells testing positive for P17 and P24 viral proteins. [f] Did not migrate in the gel. [g] Lethal to the cells at concentrations of 4 μM or higher. [h] Inactive at concentrations up to at least 50 μM. [i] Inactive at 25 μM and below; at 50 μM, inactive in P17 and P24 tests, but active in inhibiting syncytia.

ACACCC AATTCTGAAAATGG (Oligomer 5). DMT(*p,p′*-dimethoxytrityl)-ibdG-CPG (30 mg, 1 μmol nucleoside) in a glass tight syringe was extended six nucleoside units in accord with the formula, using hydrogen phosphonate chemistry (*8*); then the support-bound intermediate was oxidized with sulfur (1 mL of 0.2 M sulfur in carbon disulfide/triethylamine 9/1, v/v; 2 h), washed twice with methylene chloride, and treated with 3% DCA in methylene chloride to remove the DMT group. The next nucleoside hydrogen phosphonate block (seven nucleoside units) was constructed using the hydrogen phosphonate protocol (*8*), but oxidation of the block was effected with carbon tetrachloride/methanol/triethylamine (8/1/1, v/v/v; 30 min) to generate internucleoside methyl phosphotriesters. Following washing (methylene chloride) and detritylation (3% DCA), the remaining nucleoside phosphorothioate block was built by the procedure used for the first phosphorothioate block. At the end, following oxidation with sulfur, the support-bound oligomer was treated with 1 mL of a solution of thiophenol/dioxane/triethylamine (1/2/1, v/v/v; 1 h) to convert the triesters to phosphodiesters; when the oligomer was cleaved from the support with concentrated ammonium hydroxide (6 h, 55 °C). Evaporation and HPLC afforded the DMT–oligomer, which was detritylated (80% aqueous acetic acid) and rechromatographed (HPLC). See Table I and Results for properties.

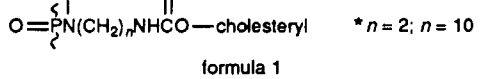
3-[(*p,p′*-Dimethoxytrityl)oxy]-1-propanol. A mixture of *p,p′*-dimethoxytrityl chloride (5.06 g) and 1,3-propanediol (5.7 g) in pyridine (25 mL) was stirred overnight at room temperature. Concentration, dilution with water, extraction with chloroform, concentration of the chloroform layer, and chromatography of the residue on a silica gel column (hexane; elution with 30% ethyl acetate in hexane) yielded 3.1 g (56%) of the title compound as a viscous oil: IR (Nujol) 3588–3224 (s) cm^{-1}; ^1H NMR ($CDCl_3$) 1.85 (p, 2 H, $-CH_2-$), 2.21 (t, 1 H, OH), 3.28 (t, 2 H, $-CH_2O-$), 3.76 (t, 2 H, $-CH_2O-$), 3.79 (s, 6 H, OCH_3), 6.82–7.43 (m, 13 H, aromatic H) ppm; FAB mass spectrum, *m/e* 441 (M^+).

3-[(*p,p′*-Dimethoxytrityl)oxy]propyl Hydrogen Phosphonate Triethylammonium Salt. To a solution of imidazole (6.7 g, 98 mmol) in acetonitrile (100 mL) at ice-bath temperature was added dropwise with stirring first phosphorus trichloride (3.0 mL, 30 mmol), then triethylamine (14.6 mL, 104 mmol), and, after 15 min, 3-[(*p,p′*-dimethoxytrityl)oxy]-1-propanol (2.6 g, 6.9 mmol) in dry acetonitrile (100 mL). The ice bath was removed and the solution stirred for 2 h, at which time TLC indicated complete conversion of the starting alcohol to a new product with lower mobility. Water was added and stirring continued for another 30 min; then the solution was evaporated under reduced pressure and extracted with chloroform. Purification by silica gel chromatography afforded 2.0 g (62%) of the title compound; mp 132–135 °C after recrystallization from ethyl acetate/hexane; ^1H NMR ($CDCl_3$) 1.22 (t, 9 H, Et_3N), 1.91 (p, 2 H, $-CH_2-$), 2.93 (q, 6 H, Et_3N), 3.13 (t, 2 H, $-CH_2O-$), 3.72 (s, 6 H, OCH_3), 3.97 (t, 2 H, $-OCH_2-$), 6.7–7.4 (m, 13 H, aromatic H), 6.05 and 7.57 (d of H–P, J = 612 Hz) ppm; ^{31}P NMR ($CDCl_3$, with 85% H_3PO_4 as reference) 4.56 (J = 620 Hz) ppm.

Assay for Inhibition by HIV-1. Assays for inhibition of HIV-1 in both de novo and postinfection experiments were carried out by the procedure described previously (*5*).

RESULTS AND DISCUSSION

Oligomers. Phosphorothioate oligonucleotides were prepared using conventional chemistry. Cholesteryl was linked via a phosphoramidate bond with either a six-atom tether (formula 1, *) or a 14-atom tether (formula 1, #),



formula 1

as indicated in Table I. An HPLC profile for the products obtained in the synthesis of compound **10** is shown in Figure 1.

For preparation of oligomer **3**, nucleoside methyl phosphoramidite reagents (*10*) were employed to generate methyl triesters at sites destined to be phosphodiesters. The rest of the chain was constructed using nucleoside hydrogen phosphonate reagents; then the hydrogen phosphonate groups were oxidized with sulfur, and methyl phosphotriesters groups were converted to phosphodiesters

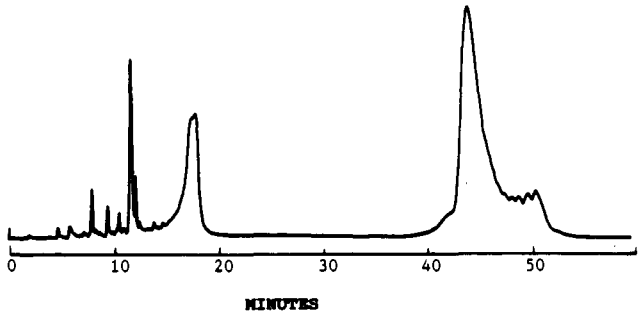


Figure 1. Profile for HPLC of crude reaction product from preparation of GTGTCTCCCCTTCTTCCTGC T*T (compound **10**); C-18 Dionex RP column (200 × 4.6 mm) with 0.03 M triethylammonium acetate (pH 7.4) and an acetonitrile gradient (1%/min increase in MeCN, 0.5 mL/min flow rate). A cut of the major peak eluting at 44 min was collected.

by thiophenoxide. That the final oligomer indeed contained phosphodiester links was confirmed by treating it with a commercial sample of snake venom phosphodiesterase and alkaline phosphatase. In accord with the proposed structure, the oligomer was converted to dC, dT, a residual nondegradable phosphorothioate fragment, and the cholesteryl-conjugated dinucleoside phosphate derivative (T*T). These products eluted on C-18 HPLC (200-mm column) at 6.0, 9.0, 17.9, and 90.0 min, respectively. By contrast, compound **2**, which had only phosphorothioate internucleoside links, was not degraded under the same conditions.

Since iodine/water oxidizes internucleoside phosphorothioates, affording phosphodiesters, an alternative oxidative procedure was employed in the synthesis of compound **5**, which has a run of phosphodiesters on the 5′-side of phosphorothioate links. Following synthesis of a phosphorothioate segment (AAAATGG -CPG), a block of nucleoside hydrogen phosphonates was constructed and converted to a block of nucleoside methyl phosphotriester units by oxidation with carbon tetrachloride/methanol/triethylamine. The chain was then extended to give the final nucleoside phosphorothioate block in the usual way. Phosphodiester links were obtained by deblocking the methyl phosphotriesters with thiophenoxide. As in the case of **3**, compound **5** hydrolyzed on treatment with snake venom phosphodiesterase and alkaline phosphatase to nucleosides (dC, dT, dG, and dI[1]) and fragments corresponding to the phosphorothioate oligonucleotide blocks.

Compounds **16** and **18** are lipophilic, anionic analogues of phosphorothioate oligonucleotides in which nucleoside units have been replaced by a three-carbon diol fragment, $-OCH_2CH_2CH_2O-$. These oligomers were prepared to see whether nucleoside units per se play a significant role in the activity of the cholesteryl-conjugated polymers. A terminal nucleoside was retained to facilitate characterization and monitoring.

De Novo Inhibition. In these tests a culture of Molt-3 cells was treated simultaneously with virus and the oligomeric inhibitor. After 4 days syncytia were counted and the fraction of cells testing positive for the p17 or p24 viral protein was determined. Except where noted in Table I, the oligomers were nontoxic to the cells at the relevant concentrations ($LD_{50} > 100$ μg/mL).

The three assays were self-consistent for de novo tests on a given compound. A dose-dependent response was found in all cases, and at high oligomer concentrations, inhibition was complete in these in vitro tests. Representative data for two of the oligomers (compounds **2** and **3**) are shown in Figure 2.

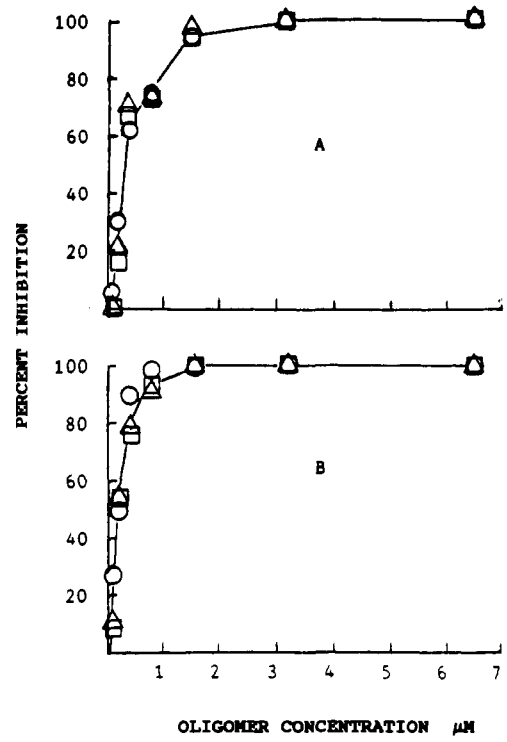


Figure 2. Inhibition of HIV-1 by cholesteryl-conjugated oligomers in de novo tests (simultaneous addition of oligomer and virus): A, CTGTCTC CCCTTCT*T (compound **3**); and B, CTGTCTCCCCTTC T*T (compound **2**). Monitored by syncytia, ○; P17, □; and P24, △.

As shown in Table I, a variety of cholesteryl-conjugated phosphorothioates proved to be effective inhibitors. In agreement with previous observations (*6*, *7*), the cholesteryl derivatives are more active than the nonconjugated counterparts (compare **1** and **2**, **4** and **6**, and **8** and **9** in Table I), and modified oligomers in the 20–28mer range are more active than shorter ones (compare **10** and **2**, **9** and **12**). Sequence as well as length of the oligomer appears to play a role. Thus 20mer **7** is more active than 20mer **6**, and 23mer **10** is more active than 28mer **11**. Compounds **6**, **7**, **10**, and **11** are complementary to segments of viral genes for the *tat* splice site, the packaging site, *rev*, and *nef*, respectively. However, it is significant that the activity of the cholesteryl modified homo-dC-20mer (compound **9**; $ID_{50} = 0.03$ μM) is comparable to that for 20mers with "antisense" sequences ($ID_{50} = 0.02$–0.1). Even homodecamers **12**–**14** exhibit some activity ($ID_{50} \approx 3$–4 μM; see also ref 7). It therefore appears that the high anti-HIV activity of the cholesteryl-modified oligomers observed in these de novo tests stems from a process other than antisense inhibition. The cholesteryl group probably enhances the "non-sequence-specific" process operative for simple phosphorothioate derivatives (*1*, *4*).

Oligomer **5**, in which a block with seven phosphodiester links is flanked by two oligonucleotide blocks containing six phosphorothioate links, was found to be as effective in inhibiting HIV as oligomer **4**, in which all links are phosphorothioate. This result is interesting since unmodified oligonucleotides are much weaker inhibitors of HIV than phosphorothioate derivatives with the same sequence (*4*, *5*). It is consistent with the suggestion that the superiority of the phosphorothioates reflects the resistance of these analogues to degradation by intracellular exo-

[1] dA was converted to dI by a contaminant in the commercial enzymes, as demonstrated by a control experiment carried out under the same conditions with dA and the enzymes.

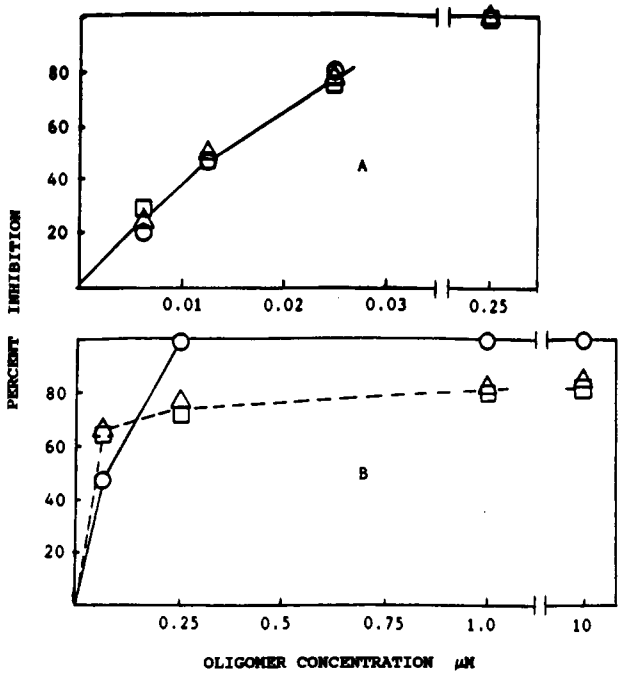


Figure 3. Inhibition of HIV-1 by GTGTCTCCCCT-TCTTCCTGCC A*T (compound **10**) in A, de novo assays; and B, postinfection assays (oligomer added 24 h after viral infection). Monitored by syncytia, ○; P17, □; and P24, △.

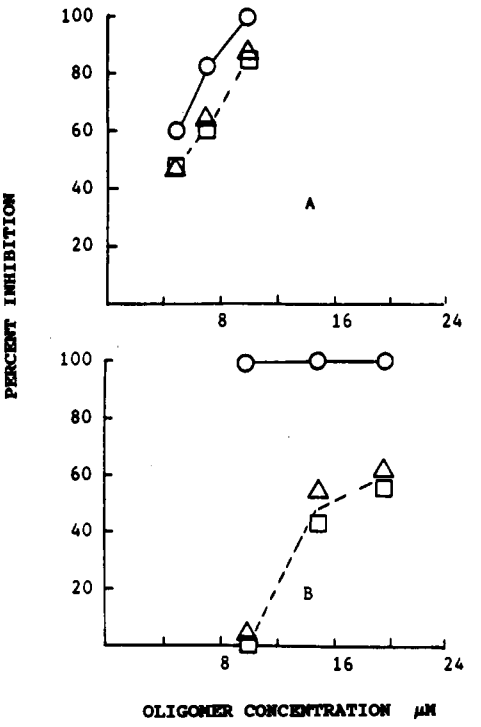


Figure 4. Inhibition of HIV-1 by TTTTTTTT T#T (compound **15**) in A, de novo assays; and B, postinfection assays (oligomer added 24 h after viral infection). Monitored by syncytia, ○; P17, □; and P24, △.

nucleases (*3*). Similarly, replacement of several phosphorothioate links by phosphodiester groups in a cholesteryl-conjugated derivative did not significantly reduce antiviral activity as measured in these tests (compare compounds **2** and **3** in Table I and Figure 2).

Compounds **12** and **13** differ in the length of the methylene chain in the diamine linking cholesteryl to the oligonucleotide, compound **2** having a two-carbon chain and compound **3** a 10-carbon chain. The data in Table I show that this change in the tether does not alter activity of the compounds in the de novo tests significantly.

Incorporation of two cholesteryl groups near the 3′-terminus of a dC-10mer (compound **14**) affords an oligomer that, though still active against HIV, is toxic to the host Molt-3 cells. This compound is also unique in that it does not migrate on gel electrophoresis under the conditions used for the other compounds in Table I, suggestive of aggregation of the short, doubly substituted oligomer in the aqueous medium.

Oligomers **16**–**18**, analogues that contain cholesteryl and multiple phosphorothioate groups but only one nucleoside unit, are ineffective as inhibitors of HIV-1 (Table I). We therefore conclude that the nucleoside components, as well as the phosphorothioate and cholesteryl groups, contribute to the antiviral property of the highly active oligonucleotide derivatives listed in Table I.

Postinfection Inhibition Studies. The antiviral properties of a phosphorothioate oligonucleotide depend on the stage of infection of the host cells at the time the oligonucleotide is administered (*4*, *5*). To characterize further the activity of cholesteryl-modified compounds, we carried out a series of tests in which cells were exposed to free virus for 24 h before addition of the oligonucleotide inhibitor. About 20% of the cells were infected during this period. The modified oligonucleotides were then added, and after incubation for another 72 h, the cultures were assayed for formation of syncytia and for presence of cells exhibiting P17 and P24 viral proteins.

In these tests the cholesteryl-conjugated phosphorothioate oligonucleotide derivatives exhibit similar patterns in the inhibition versus dose plots, although the activities of individual inhibitors vary markedly. Typical curves are presented in Figures 3 and 4, which show data for the most active compound tested (compound **10**, in part complementary to the *rev* gene) and for a weak inhibitor (compound **15**, modified oligo-dT-10mer). In general, values for percent inhibition as measured by syncytia in the postinfection experiments are similar to the values obtained in the de novo tests, and proceed to 100% at higher concentrations. In contrast, the plots for percent inhibition versus oligomer concentration, measured by the tests for P17 and P24, level off near 80% inhibition. These results indicate that the cholesteryl-modified phosphorothioate derivatives inhibit infection of Molt3 cells by both free virus particles and viral-infected cells. The similarity in the dose–response patterns observed for "antisense" oligomers and for homonucleotide derivatives is consistant with the view that both classes of compounds are functioning here in a similar manner. It is quite possible, of course, that a sequence-specific mode of inhibition can operate for the antisense compounds but is largely masked in these assays by a competing process that is not dependent on specific nucleotide sequences.

ACKNOWLEDGMENT

This work was supported by the National Cooperative Drug Discovery Group for the treatment of AIDS, Grant U OI AI24846 from the National Cancer Institute and the National Institute of Allergy and Infectious Diseases.

LITERATURE CITED

(1) Matsukura, M., Shinozuka, K., Zon, G., Mitsuya, H., Reitz, M., Cohen, J. S., and Broder, S. (1987) Phosphorothioate analogs of oligodeoxynucleotides: Inhibitors of replication and cytopathic effects of human immunodeficiency virus. *Proc. Natl. Acad. Sci. U.S.A. 84*, 7706–7710.

(2) Agrawal, S., Goodchild, J., Civeira, M. P., Thornton, A. H., Sarin, P. S., and Zamecnik, P. C. (1988) Oligodeoxynucleoside

phosphoramidates and phosphorothioates as inhibitors of human immunodeficiency virus. *Proc. Natl. Acad. Sci. U.S.A. 85*, 7079–7083.

(3) Agrawal, S., and Sarin, P. S. (1991) Antisense Oligonucleotides; Gene Regulation and Chemotherapy of AIDS. *Adv. Drug Del. Res. 6*, 251–270.

(4) Matsukura, M., Zon, G., Shinozuka, K., Robert-Guroff, M., Shimada, T., Stein, C. A., Mitsuya, H., and Wong-Staal, F. (1989) Regulation of viral expression of human immunodeficiency virus in vitro by an antisense phosphorothioate oligodeoxynucleotide against rev (art/trs) in chronically infected cells. *Proc. Natl. Acad. Sci. U.S.A 86*, 4244–4248.

(5) Agrawal, S., Ikeuchi, T., Sun, D., Sarin, P. S., Konopka, A., Maizel, J., and Zamecnik, P. C. (1989) Inhibition of human immunodeficiency virus in early infected and chronically infected cells by antisense oligodeoxynucleotides and their phosphorothioate analogues. *Proc. Natl. Acad. Sci. U.S.A. 86*, 7790–7794.

(6) Letsinger, R. L., Zhang, G., Sun, D. K., Ikeuchi, T., and Sarin, P. S. (1989) Cholesteryl-conjugated oligonucleotides: Synthesis, properties, and activity as inhibitors of replication of human immunodeficiency virus in cell culture. *Proc. Natl. Acad. Sci. U.S.A. 86*, 6553–6556.

(7) Stein, C. A., Pal, R., DeVico, A. L., Hoke, G., Mumbauer, S., Kinstler, O., Sarngadharan, M. G., and Letsinger, R. L. (1991) Mode of action of 5′-linked cholesteryl phosphorothioate oligodeoxynucleotides in inhibiting syncytia formation and infection by HIV-1 and HIV-2 in vitro. *Biochemistry 30*, 2439–2444.

(8) Froehler, B. C., Ng, P. G., and Matteucci, M. D. (1986) Synthesis of DNA via deoxynucleoside H-phosphonate intermediates. *Nucleic Acids Res. 14*, 5399–5407.

(9) Froehler, B. C. (1988) Deoxynucleoside H-phosphonate diester intermediates in the synthesis of internucleotide phosphate analogues. *Tetrahedron Lett. 27*, 5575–5579.

(10) Caruthers, M. H., Barone, A. D., Beaucage, S. L., Dodds, D. R., Fisher, E. F., McBride, L. J., Matteucci, M., Stabinsky, Z., and Tang, J.-Y. (1987) Chemical synthesis of deoxyoligonucleotides by the phosphoramidite method. *Methods Enzymol. 154*, 287–293.

A Novel Heterobifunctional Linker for Formyl to Thiol Coupling

Ned D. Heindel,*,†,‡ Huiru Zhao,† Roger A. Egolf,§ Chien-Hsing Chang,∥ Keith J. Schray,† Jacqueline G. Emrich,‡ Joanne P. McLaughlin,‡ and David V. Woo‡

Department of Chemistry, Lehigh University, Bethlehem, Pennsylvania 18015, Immunomedics, Warren, New Jersey 07060, Pennsylvania State University, Fogelsville, Pennsylvania 18051, and Department of Radiation Oncology and Nuclear Medicine, Hahnemann University, Philadelphia, Pennsylvania 19102.
Received August 6, 1991

A maleimide hydrazide has been synthesized as a heterobifunctional cross-linking agent for thiol to formyl coupling. This linker has been applied to the coupling of the monoclonal antibody 17-1A, or an Fab′ derived therefrom, to polyaldehyde dextran onto which the antineoplastic agent ellipticine has been attached. High binding avidities for the unshed antigen on the SW1116 colorectal tumor cell are retained in these drug–dextran–linker–antibody conjugates.

INTRODUCTION

Heterobifunctional cross-linking reagents are being increasingly employed for their regiospecificity in coupling toxins, chemotherapeutics, or chelates to antibodies for targeted delivery (*1–3*). Frequently, the differential side chain reactivities of the two diverse termini in the cross-linker enable the coupling to be carried out in a stepwise manner which allows for purification/characterization of an intermediate before assembly of the final conjugate. Often such bifunctional reagents involve a maleimido or a thiol group on the linker–drug side to the couple to thiols on the antibody via thioether or disulfide bonds (*4, 5*). Generally, the more stable thioether linkage is to be preferred to overcome the susceptibility of the disulfide bond to cleavage by endogenous thiols.

Recently, the considerable advantages (ease of synthesis, minimal oligomerization, hydrolytic stability) inherent in hydrazide-to-carbonyl couplings have been noted (*6, 7*). We have synthesized prosthetic radioiodinated hydrazides and chemotherapeutic pharmaceutical hydrazides and demonstrated their facile conversion to stable drug–carrier conjugates (*8, 9*). Similarly, we and others have shown that conjugation of pharmaceuticals to functionalized dextrans, with subsequent attachment of a minimal number of such drug–dextran chains to an antibody, not only enhances the metabolic stability of the drug itself but often leads to a pharmaceutical–dextran–antibody conjugate with higher retained binding avidity than would be possible if an equal number of drugs were directly linked to the IgG (*10, 11*).

EXPERIMENTAL PROCEDURES

Materials. Clinical-grade dextran (40 kDa) was supplied by Pharmachem Corp. (Bethlehem, PA). The monoclonal antibodies 17-1A and ^{125}I-17-1A were provided by Centocor (Malvern, PA). All other chemicals were of the highest purity commercial grade. Combustion analyses were supplied by Quantitative Technologies (Bound Brook, NJ). ^{1}H NMR spectra were recorded in the indicated solvents on a JEOL FX90Q spectrophotometer. Melting points were obtained in capillaries on a Thomas-Hoover apparatus and are reported uncorrected. Ultraviolet–visible spectra were recorded on a Perkin-Elmer Lambda-5 spectrophotometer. Infrared spectra were obtained as 1% KBr pellets on a Perkin-Elmer Model 1470 spectrophotometer.

Syntheses. Maleimidoacetic Acid Hydrazide Hydrochloride (1). A freshly prepared solution of 3.00 g (11.9 mmol) of maleimidoacetic acid *N*-succinimidyl ester (*12*), 1.62 g (12.3 mmol) of *tert*-butyl carbazate, and 9.0 mL of anhydrous acetonitrile was stirred at 22 °C for 6 h. The reaction mixture was then diluted with 375 mL of ethyl acetate and washed successively with 2 × 100 mL each of saturated aqueous sodium bicarbonate, 0.1 N hydrochloric acid, and saturated aqueous sodium chloride. The organic layer was dried over calcium sulfate and evaporated in vacuo to yield maleimidoacetic acid (*tert*-butyloxycarbonyl)hydrazide as a thick yellow oil. While this hydrazide precursor could be stored in this form it could also be converted to a stable but hygroscopic hydrochloride by agitation with 39 mL of anhydrous 2 M hydrogen chloride in 50 mL of 1,4-dioxane at ambient temperature for 40 min. Addition of 200 mL of hexane precipitated the tan hydrochloride which was recrystallized from 2-propanol/hexane to yield 1.62 g (55% yield) of yellow-white crystals of the title compound, mp 135–150 °C dec. The product crystallized with 0.5 mol of 1,4-dioxane, confirmed by both NMR and elemental analysis, which could not be removed by vacuum drying without substantial decomposition: IR (KBr) 3450, 1395, 3080, 1710, 1675, and 1655 cm^{-1}; ^{1}H NMR (DMSO-d_6) δ 3.58 (s, 4 H, 0.5 O(CH_2CH_2)$_2$O), 4.24 (s, 2 H, CH_2CO), and 7.19 ppm (s, 2 H, -CH=CH-). Anal. Calcd for $C_6H_7N_3O_3$·HCl·0.5O(CH_2CH_2)$_2$O: C, 38.49; H, 4.85; N, 16.83. Found: C, 38.25; H, 4.99; N, 16.61.

Maleimidoacetic Acid Benzylidenehydrazide (2a). A solution of 0.200 g (0.800 mmol) of 1, 0.103 g (0.972 mmol) of benzaldehyde, and 0.133 g (0.972 mmol) of sodium acetate was prepared in 2 mL of water and after brief agitation the product precipitated directly. To insure completeness of reaction the mixture was warmed in a beaker of boiling water for 5 min, cooled in an ice bath, and filtered. The product was washed on the filter with 5 mL of ice water and dried in vacuo to yield 0.198 g (96% yield) of **2a**: mp 181–184 °C; IR (KBr) 3470, 3196, 3099, and 1688 (br) cm^{-1}; ^{1}H NMR (DMSO-d_6) δ 4.60 (s, 2 H, CH_2CO), 7.18 (s, 2 H, -CH=CH-), 7.37–7.80 (m, 5 H, C_5H_5), 8.02 (s, 1 H, CH=N), and 10.6 (br s, 1 H, NH). Anal. Calcd for $C_{13}H_{11}N_3O_3$: C, 60.64; H, 4.31; N, 16.41. Found: C, 60.50; H, 4.43; N, 16.16.

Model Conjugation of L-Cysteine to Maleimidoacetic Acid Benzylidenehydrazide. Preparation of 3a.

* To whom requests for reprints should be addressed at Lehigh University.
† Lehigh University.
‡ Hahnemann University.
§ Pennsylvania State University, Allentown Campus.
∥ Immunomedics.

1043-1802/91/2902-0427$02.50/0 © 1991 American Chemical Society

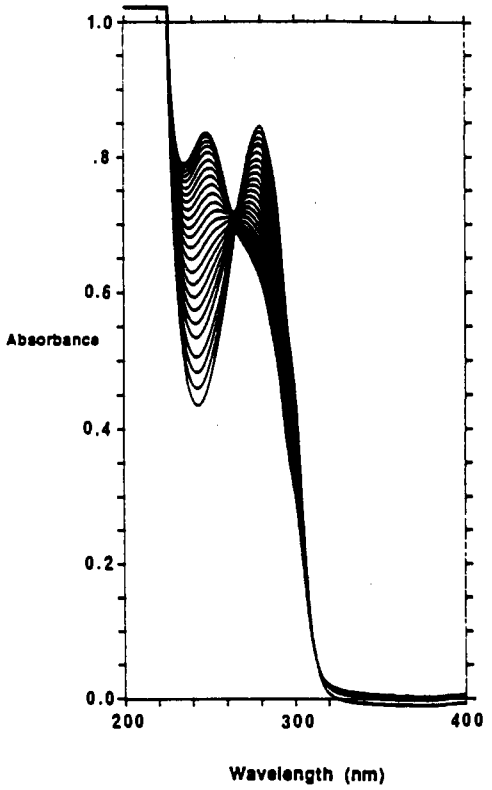


Figure 1. Isobestic behavior in the conjugation of cysteine to **2a**.

The reaction of **2a** and L-cysteine was carried out under pseudo-first-order conditions with UV monitoring in thermostated cells at 25.0 °C at both pH 5.2 and 7.4. The requisite hydrazone, **2a** (1.35 mg), was dissolved in 100 mL of pH 5.2 phosphate buffer (alternatively, 100 mL of pH 7.4 phosphate buffer), 900 μL of this solution was placed in a quartz UV cell, and 100 μL of a 50 mM solution of L-cysteine, also prepared in the same phosphate buffer, was added. The spectrum between 200 and 400 nm was repetitively scanned at hourly intervals for 24 h vs a buffer blank (see Figure 1). Effective concentrations in the reaction medium for UV scanning were 47.2 μM **2** and 5 mM L-cysteine. Under similar reaction conditions in 5 mL of pH 5.2 buffer, equimolar quantities (0.33 mmol) of L-cysteine and **2a** (dissolved in 5 mL of ethanol) were stirred at ambient temperature for 24 h and provided 0.065 g or 46% yield of **3a**: mp 200–203 °C (from ethanol); ^{1}H NMR (DMSO-d_6) δ 2.52 (2 H, CHCH_2CO, overlaps signal from DMSO), 3.30 (2 H, CH_2S), 4.20 (1 H, CHCH_2S), 4.51 (2 H, CH_2CON), 7.2–7.9 (m, 5 H, C_6H_5), and 8.11 ppm (s, 1 H, N=CH). Anal. Calcd for $C_{16}H_{18}N_4O_5S$: N, 14.81. Found: N, 15.14.

Conjugation of 1 to Ellipticinium Hydrazide–Dextran. A polyaldehyde dextran (PAD) was prepared as indicated by periodate oxidation of a 40-kDa dextran (*13*). Analysis revealed 0.36 formyl residues per glucose unit (ca. 80 formyls/dextran) (*11*). This PAD was linked to the chemotherapeutic drug ellipticine as described previously via a hydrazide side-chain analogue [2-(5-hydrazino-5-oxopentyl)ellipticinium bromide] (see Figure 2) to yield a purified conjugate (PAD–EH) with 9 mol of drug/mol of polymer (*14*). A dried sample of this conjugate (0.028 g or 49 μmol of formyl residues) was incubated for 24 h with 4.61 × 10^{-3} g (23 μmol) of **1** in 30 mL of 10 mM phosphate buffer (pH 3), charged to a Bio-Gel P-60 column, and eluted with 10 mM phosphate buffer (pH 5.3) to separate conjugate from unbound **1**. The product fraction was cut by monitoring the absorbance at 305 nm of the eluting material. This conjugate (PAD–EH–1) was lyophilized and dried to constant weight in vacuo. The number of attached maleimide residues was determined by the standard method and found to be 19 per dextran (*15*). This drug–dextran–linker conjugate was employed in two forms in subsequent couplings to the antibody and its fragments, one form in which free formyl and CH=N linkages were reduced by treatment with sodium borohydride and one form in which no reduction was utilized.

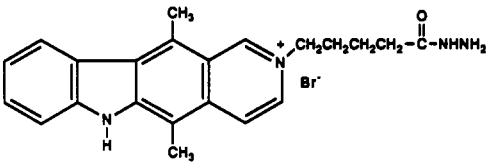


Figure 2. Structure of 2-(5-hydrazino-5-oxopentyl)ellipticinium bromide.

Coupling to mAb 17-1A at Reduced Interchain Disulfides. The published technique for the use of dithiothreitol (0.99 M, 0.10 mL) in partial reduction of interchain disulfides in the monoclonal antibody 17-1A (57.7 μM, 0.4 mL) and subsequent purification of the IgG-SH was employed as indicated (*16*). Available thiol content was determined as 1.7 ± 0.3/antibody (*18*). The drug–dextran–maleimide linker conjugate PAD–EH–1 and the thiol-activated 17-1A were solubilized in a minimum volume of 10 mM phosphate-buffered saline (pH 5.3) at a molar ratio of 84 ellipticine equivalents per IgG (equivalent to 9 mol of the drug–dextran–maleimide linker conjugate/mol of 17-1A) and incubated at either 37 °C for 3 h or, alternatively, 4 °C for 24 h. Purification of this conjugate, **3b**, was effected on Bio-Gel P-150 with elution by eluting buffer (50 mM sodium citrate, 0.1 N sodium chloride, and 1 mM EDTA at pH 8.0) at the calibrated volume fraction for the antibody conjugate. The number of ellipticines per antibody was determined as 4.0 ± 0.2 by a difference UV assay, a technique reported previously by our group, reading at 280 and 305 nm by reference to calibrated standard curves (*18*). The ellipticine–dextran–17-1A triple component conjugate eluted at 6.8 min when injected onto a Du Pont Bioseries GF-250 column (25 cm × 9.4 mm i.d.) packed with Zorbax PSM 150 and mounted on a Perkin-Elmer Series 2 HPLC. The mobile phase was 10 mM PBS (pH 7.4) and the flow rate was 1.0 mL/min with UV monitoring at 280 nm. Unmodified 17-1A was retained much longer and did not commence elution till >7 min.

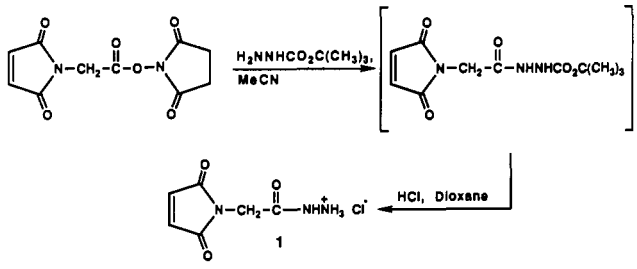
Coupling to 17-1A Fab′. The Fab′ fraction of 17-1A was prepared and purified as reported in our previous study (*19*). This Fab′-SH was used immediately in coupling with the drug–dextran–maleimide or PAD–EH–1 linker conjugate as outlined above. Purification was effected on a Bio-Gel P-60 + P-100 column with the standard eluting buffer. The product, **3c**, was collected in accord with molecular weight standards above 45 kDa and concentrated 10-fold against a mini concentrator membrane. Drug load, determined by the dual wavelength method, was 4 per Fab′.

Evaluation of Cell Binding of the Modified Conjugates. Immunoreactivities of the conjugates **3b** and **3c** were determined by RIA against SW1116 colorectal tumor cells using ^{125}I–17-1A standard as has been discussed previously (*18*).

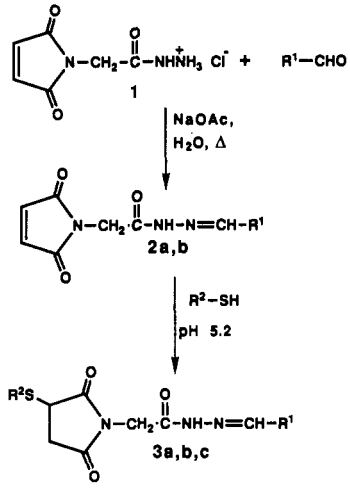
RESULTS AND DISCUSSION

Several unsuccessful synthetic approaches to maleimidocarboxy hydrazides such as **1** were employed before a successful method (Scheme I) was discovered. Although it is well-established that (methoxycarbonyl)maleimide

Scheme I. Synthesis of the Linker



Scheme II. Use of Linker To Bridge Thiols to Formyls



Compound	R1	R2
2a	phenyl	
2b	ellipticinium hydrazide dextran	
3a	phenyl	L-cysteine
3b	ellipticinium hydrazide dextran	IgG
3c	ellipticinium hydrazide dextran	Fab'

or NMCM can be condensed with amine nucleophiles (*4*), its reaction with either hydrazine or *tert*-butyl carbazate even at 4 °C gave intractable oils. Similarly, hydrazine or carbazates with maleimidoacetic acid methyl ester produced red-brown gums. ^{1}H NMR inspections of these oily materials showed loss of the typical maleimide vinyl proton resonance at 7.2 ppm and implicated competitive Michael addition of the hydrazine or carbazate to the double bond. At equimolar concentrations, and without application of heat, maleimidoacetic acid *N*-succinimidyl ester and *tert*-butyl carbazate react smoothly to give the stable maleimidoacetic acid (*tert*-butyloxycarbonyl)hydrazide, which can readily be cleaved to **1** in anhydrous HCl. The hydrochloride salt is stable for months; the free base cannot be stored.

As employed herein, the heterobifunctional linker **1** was first reacted with the aldehydic function, benzaldehyde in a model study of drug–polyaldehyde dextran in immunoconjugate preparations, at pH's of 3–5 to facilitate inactivation by protonation of potentially competing amine groups (see Scheme II). This purified conjugate was subsequently condensed with the requisite thiol. The model investigation on addition of the cysteine thiol to **2a** showed that coupling occurs cleanly at pH 5.2 with the smooth conversion of the major 280-nm maleimide absorption into a new chromophore at 247 nm (Figure 1). A single product was obtained which was identified as **3a**. The same cysteine-to-linker condensation attempted on **2a** at pH 7.4 showed no isobestic behavior, gave a complicated UV spectrum (peaks and shoulders at 224, 235, and 278 nm), and did not yield a single, clean product. Maleoyl groups are known to be susceptible to basic hydrolysis above pH 7.0 (*20*).

Exploring the utility of **1** in immunoconjugate syntheses we utilized a PAD–ellipticine previously described, the fifth conjugate listed in Table I of ref 15. This drug–formyl polymer unit or PAD–EH was condensed with the linker **1** to give a conjugate containing nine ellipticines and 19 maleimide hydrazones bounded to the 40-kDa PAD backbone (PAD–EH–1). This three-component conjugate (ellipticine–dextran–linker) was subsequently used as the standard polymer for attachment to the antibody with and without prereduction of its excess CHO moieties. One would expect that, if the dextran–drug–linker contained available formyl residues, then—even if the coupling were carried out at acidic pH—some lysines in the antibody might cross couple to CHO's in competition with the regiospecific linkage of hinge-region thiol to maleimide.

Our recent work on immunotargeted chemotherapy has employed the monoclonal antibody 17-1A, which recognizes a nonshed membrane receptor on colon carcinoma and which has precedent for use in delivering toxin moieties (*9*, *18*). In this report we have used that antibody and its Fab' fragment to test the utility of linker **1** in coupling drug–dextran polymers to immunocarriers.

In condensations with an induced thiol created by partial reduction of disulfides in 17-1A, similar drug loads of 4 ellipticines/IgG were prepared in the three immunoconjugates synthesized herein, although the resulting conjugate structures were obviously of widely differing character. When no prereduction of formyls was performed or when the amount of $NaBH_4$ was regulated to reduce 50% of the formyls, conjugates of ellipticine–PAD–linker with 17-1A were obtained that had binding avidities to SW1116 cells of only 13–16%. However, when excess $NaBH_4$ was used to reduce all the formyls in the ellipticine–PAD and thereby insure regiospecific thiol to maleimide coupling, the dextran conjugate to 17-1A retained 81–87% binding avidity.

The standard ellipticine–PAD–maleimide linker was also condensed with the Fab' of 17-1A to give a conjugate with an average of 4 drugs/Fab'. The binding avidity of this conjugate to the SW1116 colorectal tumor cells was 100%, equal to that of unmodified 17-1A. Studies of direct drug linking to monoclonal antibodies 17-1A and 19-9 have shown that these two antibodies are remarkably sensitive to loss of binding avidity with drug load, a factor which severely limits their utility in immunochemotherapy (*18*, *21*). Even with as few as 4 drug molecules/antibody attached directly and randomly onto the protein backbone, only 40–50% binding avidity remains. The drug–dextran–linker-antibody systems reported herein, although obviously only in the initial stage of development, show retention of both regiospecificity and higher tumor cell binding avidity than our previously reported direct drug-to-antibody conjugates.

ACKNOWLEDGMENT

This project was supported by a grant to N.D.H. from the W. W. Smith Charitable Trust and by fellowship support to H.Z. from the Quaker Chemical Foundation. We acknowledge the assistance and advice of Drs. David J. Shealy and Jeffrey A. Mattis of Centocor Corp. (Malvern, PA).

LITERATURE CITED

(1) Ghose, T., and Blair, A. H. (1987) The design of cytotoxic agent antibody conjugates. *CRC Crit. Rev. Ther. Drug Carrier Syst. 3*, 300–301.

(2) Mueller, B. M., Wrasidlo, W. A., and Reisfeld, R. A. (1990) Antibody conjugates with morpholinodoxorubicin and acid-cleavable linkers. *Bioconjugate Chem. 1*, 325–330.
(3) Imai, N., Kometani, T., Crocker, P. J., Bowdan, J. B., Demir, A., Dwyer, L. D., Mann, D. M., Vanaman, T. C., and Watt, D. S. (1990) Photoaffinity heterobifunctional cross-linking reagents based on *N*-(azidobenzoyl)tyrosines. *Bioconjugate Chem. 1*, 138–143.
(4) Arano, Y., Matsushima, H., Tagawa, M., Koizumi, M., Endo, K., Konishi, J., and Yokoyama, A. (1991) A novel bifunctional metabolizable linker for the conjugation of antibodies with radionuclides. *Bioconjugate Chem. 2*, 71–76.
(5) Ghosh, S. S., Hao, P. M., McCue, A. W., and Chappelle, H. L. (1990) Use of maleimide–thiol coupling chemistry for efficient synthesis of oligonucleotide–enzyme conjugate hybridization probes. *Bioconjugate Chem. 1*, 71–76.
(6) O'Shannessy, D. J. (1988) Hydrazides as specific reagents for the labeling of glycoproteins. *ISBT Commun. 3*, 4–6.
(7) Wilchek, M., and Bayer, E. A. (1987) Labeling glycoconjugates with hydrazide reagents. *Methods Enzymol. 138*, 429.
(8) Heindel, N. D., and Van Dort, M. (1985) Prosthetic group radioiodination at "no carrier added" level of carbonyl containing molecules. *J. Org. Chem. 50*, 1988–1990.
(9) Heindel, N. D., Van Dongen, J. M. A. M., Fitzpatrick, D. A., Mease, B. A., and Schray, K. J. (1987) Macromolecular attachment as a metabolic stabilizer for a labile radiosensitizer. *J. Pharm. Sci. 76*, 384–386.
(10) Hurwitz, E., Kashi, R., Arnon, R., Wilchek, M., and Sela, M. (1985) The covalent linking of two nucleotide analogues to antibodies. *J. Med. Chem. 28*, 137–140.
(11) Zhao, H., and Heindel, N. D. (1991) Determination of degree of substitution of formyl groups in polyaldehyde dextran. *Pharm. Res. 8*, 400–402.
(12) Keller, O., and Rudinger, J. (1975) Preparation and some properties of maleimido acids and maleoyl derivatives of peptides. *Helv. Chim. Acta 58* 531–541.
(13) Bernstein, A., Hurwitz, E., Maron, R., Arnon, R., Sela, M., and Wilchek, M. (1978) Higher tumor efficacy of daunomycin linked to dextran. *J. Natl. Cancer Inst. 60*, 379–383.
(14) Heindel, N. D., Zhao, H., Leiby, J., VanDongen, J. M., Lacey, C. J., Lima, D. A., Shabsoug, B., and Buzby, J. H. (1990) Hydrazide pharmaceuticals as conjugates to polyaldehyde dextran: syntheses, characterization, and stability. *Bioconjugate Chem. 1*, 77–82.
(15) Grassetti, D. R., and Murray, J. R. (1967) Determination of sulfhydryl groups with 2,2′- or 4,4′-dithiodipyridine. *Arch. Biochem. Biophys. 119*, 41.
(16) de Rosario, R. B., Wahl, R. L., Brocchini, S. J., Lawton, R. G., and Smith, R. H. (1990) Sulfhydryl site-specific cross-linking and labeling of monoclonal antibodies by a fluorescent equilibrium transfer alkylation cross-link reagent. *Bioconjugate Chem. 1*, 51–59.
(17) Riddles, P. W., Blakely, R. L., and Zerner, B. (1979) Ellman's reagent: 5,5′-dithiobis(2-nitrobenzoic acid)—A reexamination. *Anal. Biochem. 94*, 75–81.
(18) Pierce, D. L., Heindel, N. D., Schray, K. J., Jetter, M. M., Emrich, J. G., and Woo, D. V. (1990) Misonidazole conjugates of the colorectal tumor associated monoclonal 17-1A. *Bioconjugate Chem. 1*, 314–318.
(19) Bender, R. A., Nau, E. A., Burton, J., Zhao, H., Abel, J. H., and Heindel, N. D. Effect of whole IgG antibody versus antibody fragments on endocytosis. *Pharma. Res.*, submitted.
(20) Yoshitake, S., Yamada, T., Ishikawa, E., and Masseyeff, R. (1979) Conjugation of glucose antibodies using *N*-hydroxysuccinimide ester of *N*-(4-carboxycyclohexylmethyl)maleimide. *Eur. J. Biochem. 101*, 395–399.
(21) Borlinghaus, K. P., Fitzpatrick, D. A., Heindel, N. D., Mattis, J. A., Mease, B. A., Schray, K. J., Shealy, D. J., Walton, H. L., and Woo, D. V. (1987) Radiosensitizer conjugation to the carcinoma 19-9 monoclonal antibody. *Cancer Res. 47*, 4071–4075.

Photooxidation of Oligodeoxynucleotides by UO_2^{2+} [1]

Aubrey R. Hill, Jr. and Leslie E. Orgel*

The Salk Institute for Biological Studies, P.O. Box 85800, San Diego, California 92186-5800.
Received June 28, 1991

Photooxidation and consequent cleavage of oligodeoxynucleotides by the uranyl ion is greatly enhanced in the presence of a terminal 5'- or 3'-phosphate group. This enhanced cleavage is confined to nearby phosphodiester bonds in the case of a 5'-phosphate, but is less localized in the case of a 3'-phosphate. Several attempts to use a complementary oligodeoxynucleotide to direct a uranyl "warhead" against an oligodeoxynucleotide target were unsuccessful. Our results are most easily explained if we suppose that uranyl ions form coordination complexes with terminal phosphates and that, on photoexcitation, coordinated uranyl ions extract a hydrogen atom from the CH bond of a nearby deoxyribose residue.

INTRODUCTION

Photochemical oxidation of polydeoxynucleotides by uranyl ions (UO_2^{2+}) has recently been introduced as a method of footprinting DNA (Nielsen et al., 1988; Jeppesen & Nielsen, 1989). In the absence of associated proteins, the efficiency of cleavage of backbone phosphodiester bonds is similar for single- and double-stranded DNA and is insensitive to base sequence. The binding of protein to internal sequences of double-stranded DNA protects some regions of the DNA from cleavage and, in addition, can induce extensive cleavage at specific sites close to the protein.

Photochemical oxidation of alcohols by UO_2^{2+} involves direct attack of the excited ion on the alcohol (Rabinowitch & Belford, 1964) while other similar footprinting methods depend on the production of diffusible radicals (Hertzberg & Dervan, 1984). It seemed interesting, therefore, to explore in detail the oxidation of short oligodeoxynucleotides by UO_2^{2+}.

EXPERIMENTAL PROCEDURES

Materials. Reagent-grade chemicals were used throughout. Uranyl nitrate hexahydrate was purchased from Mallinckrodt; adenosine 5'-[γ-^{32}P]triphosphate, triethylammonium salt (~3000 Ci/mmol), and cytidine 5'-[α-^{32}P]triphosphate, triethylammonium salt (~3000 Ci/mmol), were from Amersham; alkaline phosphatase from calf intestine (molecular biology quality) was from Boehringer Mannheim Biochemicals; T4 polynucleotide kinase was from New England Biolabs; terminal deoxynucleotidyl transferase was from Pharmacia LKB Biotechnology; and phosphodiesterase I, type VII, was from Sigma Chemical Co. The following oligodeoxynucleotides were synthesized on an automated DNA synthesizer and purified by HPLC on RPC-5 at pH 12 using a perchlorate gradient as previously described (Bridson and Orgel, 1980).

N_{11}: d$^{5'}$[CAC CCA ACT CG]$^{3'}$

N_{16}: d$^{5'}$[CAC AAT TCC ACA CAA C]$^{3'}$

N_{37}: d$^{5'}$[TCG TAT GTT GTG TGG AAT TGT GAG CGG ATA ACA ATT T]$^{3'}$

Methods. Gel electrophoresis was carried out on 0.75 mm thick 20% polyacrylamide denaturing gels cast and run in 1× TBE buffer. Conversion of oligodeoxynucleotides to 5'-[^{32}P]phosphates was carried out using T4 polynucleotide kinase (Chu & Orgel, 1985). Conversion of oligodeoxynucleotides to 3'-[^{32}P]phosphates was achieved by adding a single ^{32}P-labeled C residue with terminal deoxynucleotidyl transferase (Deng & Wu, 1983), purifying by HPLC, and then carrying out oxidation-elimination (Weith & Gilham, 1967). Hydrolysis of oligodeoxynucleotides with venom phosphodiesterase was carried out in 10 mM Tris buffer at pH 7.5.

Irradiations were performed at room temperature using Philips TL40W/03 fluorescent lamps with Super Actinic Radiation ($\lambda \approx 420$ nm, 30-nm band width). Solutions were sterilized by filtration through 0.2 μm filters. Reactions were carried out in sterilized 0.65-mL presiliconized, RNase-free microfuge tubes (National Scientific) irradiated from below at a distance of 4 in. from the light source. Reaction volumes were usually 10 μL, and the concentration of oligodeoxynucleotides was in the range of 1-10 nM. Solutions of uranyl nitrate were prepared frequently, since they tend to decompose on storage even in the dark. The compositions of the reaction mixtures are indicated in the legends to the figures.

RESULTS AND DISCUSSION

Preliminary experiments with 5'-[^{32}P]-N_{37} showed that, in the absence of complexing anions, the rate of photooxidation of oligodeoxynucleotides and the nature of the photoproducts depends in a complicated way on the concentration of the UO_2^{2+} ion. In Figure 1 we illustrate a typical series of experiments using a range of UO_2^{2+} concentrations from 0.4 to 250 μM. At the higher concentrations of UO_2^{2+} the reaction is relatively inefficient. The regular ladder of bands (lanes 1 and 2) suggests that all internucleotide bonds are attacked at a comparable rate. When the UO_2^{2+} concentration is reduced (lanes 3 and 4), the reaction becomes much more efficient and the nature of the products changes—most of the cleavage occurs close to the 5'-end of the oligomer. At even lower

[1] Abbreviations used: HPLC, high-performance liquid chromatography; TBE, Tris/borate/EDTA buffer, pH 8.0; pN is the 5'-phosphate of the nucleoside N; pN_{11} is the 5'-phosphate of the oligodeoxynucleotide N_{11}; $N_{11}p$ is the 3'-phosphate of the oligodeoxynucleotide N_{11}; $N_{11}prC$ is the oligonucleotide obtained by adding one riboC residue to the 3'-terminus of the oligodeoxynucleotide N_{11}. Corresponding derivatives of other oligodeoxynucleotides are represented in a similar way.

* Corresponding author.

1043-1802/91/2902-0431$02.50/0 © 1991 American Chemical Society

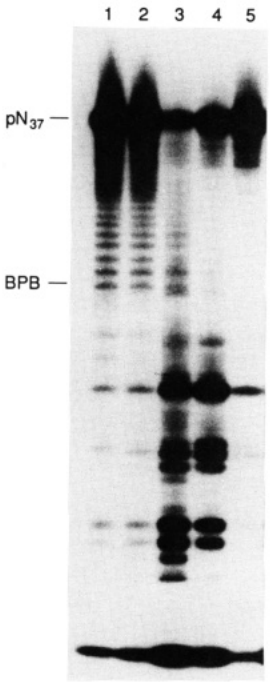


Figure 1. Autoradiogram of a 20% denaturing gel showing concentration-dependence of the photooxidation of 5′-[^{32}P]-N_{37} by UO_2^{2+} in 10 mM Tris·HCl (pH 7.5) after a 2-h irradiation. UO_2^{2+} concentrations are as follows: lane 1, 250 μM; lane 2, 50 μM; lane 3, 10 μM; lane 4, 2 μM; lane 5, 0.4 μM.

concentrations of UO_2^{2+}, the same pattern of products is obtained, but the reaction is slower (lane 5). The unusual concentration dependence that we observe is presumably due to the formation of polynuclear complexes.

The addition of complexing agents including inorganic phosphate, inorganic polyphosphates, nucleoside monophosphates, and nucleoside polyphosphates to reaction mixtures containing high concentrations of UO_2^{2+} leads to a change in the pattern of products qualitatively similar to that observed on lowering the concentration of UO_2^{2+}. The nature of the complexing agents, however, significantly and reproducibly influences the relative amounts of different products. A typical experiment using 5′-[^{32}P]-N_{11} as substrate and a variety of complexing agents is illustrated in Figure 2. These findings are consistent with the work of Jeppesen and Nielsen (1989), who noted that the addition of citrate, a ligand that chelates the UO_2^{2+} ion, leads to efficient photochemistry. We adopted their protocol and used a solution containing 10 mM Tris·HCl (pH 7.5), 0.25 mM UO_2^{2+}, and 0.25 mM citrate (pH 7.5) unless otherwise noted.

The time course of the photooxidation of 5′-[^{32}P]-N_{37} in the presence of citrate is illustrated in Figure 3, lanes 1–6. Extensive destruction occurs after only 5 min to give labeled inorganic phosphate and low molecular weight labeled phosphate-containing products. The corresponding reaction in the presence of uridine 5′-monophosphate is illustrated in Figure 3, lanes 7–12. Decomposition is slower and the pattern of products is slightly different. Since low molecular weight products are already present after short irradiation times, they must be formed by a single cleavage close to the labeled 5′-phosphate group and not as a result of extensive random degradation.

The chemical nature of the ^{32}P-labeled photoproducts released from a 5′-[^{32}P]-oligodeoxynucleotide cannot be determined from experiments of the kind described here, since the amounts of material photolyzed are very small. However, an estimate of the molecular sizes can be obtained using gel electrophoresis.

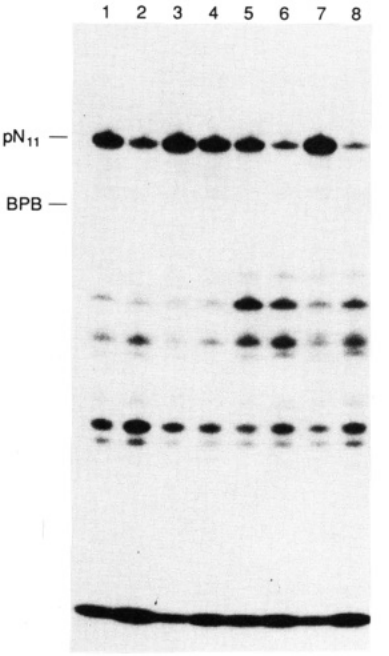


Figure 2. Autoradiogram of a 20% denaturing gel showing the effect of complexing agents on the photooxidation of 5′-[^{32}P]-N_{11} after a 2-h irradiation in 10 mM Tris·HCl (pH 7.5) with 0.25 mM UO_2^{2+} and 0.25 mM complexing agent. Complexing agents are as follows: lane 1, pA; lane 2, pC; lane 3, pG; lane 4, pU; lane 5, ADP; lane 6, CDP; lane 7, GDP; lane 8, UDP.

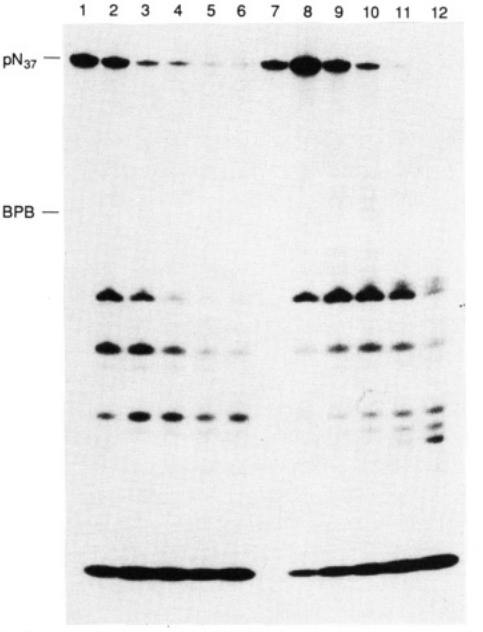


Figure 3. Autoradiogram of a 20% denaturing gel showing time-dependence of photolysis of 5′-[^{32}P]-N_{37} in the presence of citrate or pU in 10 mM Tris·HCl (pH 7.5) with 0.25 mM UO_2^{2+} and 0.25 mM citrate (lanes 1–6) or 0.25 mM pU (lanes 7–12). Irradiation times: lanes 1 and 7, time 0; lanes 2 and 8, 5 min; lanes 3 and 9, 15 min; lanes 4 and 10, 30 min; lanes 5 and 11, 60 min; lanes 6 and 12, 120 min.

The fastest moving band seen on gels (for example in Figure 1) is shown to be inorganic phosphate by comparison with authentic material. In lanes 2 and 3 of Figure 4 we compare the ladder obtained by venom phosphodiesterase digestion of 5′-[^{32}P]-N_{11} with the pattern of products obtained by the UO_2^{2+} photooxidation of the same oligomer (lane 4). One of the three major organic photolysis products moves faster than pC, one moves at about the same speed, and one moves somewhat slower, but still substantially faster than pCpA. Presumably the fastest

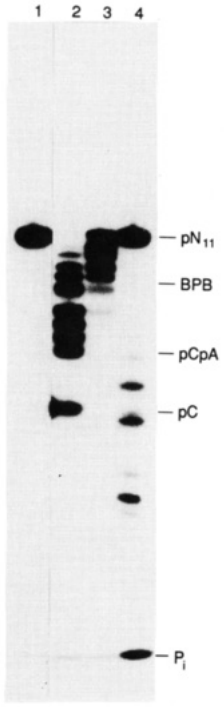


Figure 4. Autoradiogram of a 20% denaturing gel showing the comparison of products formed by venom phosphodiesterase treatment of 5′-[^{32}P]-N_{11} with those formed by UO_2^{2+} photooxidation. Lane 1, 5′-[^{32}P]-N_{11}, 10 mM Tris·HCl (pH 7.5); lane 2, same as lane 1 but incubated for 15 min with 1×10^{-6} units of enzyme at 37 °C; lane 3, same as lane 2 but with 2×10^{-7} units of enzyme; lane 4, 10 mM Tris·HCl (pH 7.5), 0.25 mM UO_2^{2+}, 0.25 mM citrate, 5-min irradiation.

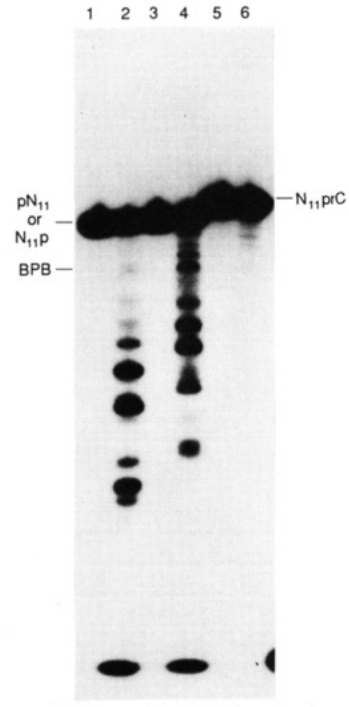


Figure 5. Autoradiogram of a 20% denaturing gel showing the photolysis of pN_{11} (lanes 1 and 2), $N_{11}p$ (lanes 3 and 4), and $N_{11}prC$ (lanes 5 and 6) by UO_2^{2+} after a 5-min irradiation. Lanes 1, 3, and 5, 10 mM Tris·HCl (pH 7.5); lanes 2, 4, and 6, 10 mM Tris·HCl (pH 7.5), 0.25 mM UO_2^{2+}, and 0.25 mM citrate.

moving band corresponds to pCp or a bis-monophosphate related to pCp. The band with intermediate mobility probably corresponds to a monophosphate of C. The slowest moving band is either a derivative of pC or a dimer related to pCpAp. It seems clear that the major products of photolysis of pN_{11} are no longer than dimers, and hence that photooxidation occurs very close to the 5′-terminus.

The patterns of labeled products obtained from pN_{11} (Figure 4, lane 4) and pN_{37} (Figure 1) are similar. Three strong bands are visible on the gel, corresponding to short oligodeoxynucleotides and very little material closer to the starting material. The results obtained with 5′-[^{32}P]-N_{16} are somewhat different (data not shown). In addition to the characteristic strong bands corresponding to short oligomers, which coincide exactly with those obtained from 5′-[^{32}P]-N_{11} since the 5′-terminal residues are C followed by A in each case, there is a substantial production of material of intermediate molecular weight.

The experiments described above strongly suggest that the UO_2^{2+} associates specifically with the terminal 5′-phosphate group of each of the oligomers pN_{11}, pN_{16}, and pN_{37} and then photooxidizes residues close to the 5′-terminus of the nucleotide, thus releasing labeled inorganic phosphate and short labeled oligodeoxynucleotides and their oxidation products. In addition, some complexing must occur at an internal site on pN_{16} to account for the production of longer oligodeoxynucleotide photoproducts from that oligomer. To test this hypothesis we synthesized and photooxidized 3′-phosphate-labeled oligodeoxynucleotides.

The results of the experiments using terminally radiolabeled 5′-[^{32}P]-N_{11}, N_{11}-3′-[^{32}P], and N_{11}-[^{32}P]-rC are shown in Figure 5. $N_{11}prC$, which does not contain a phosphomonoester group, is not significantly photolyzed under our standard conditions (lane 6). $N_{11}p$, on the other hand, undergoes extensive breakdown to give a complex pattern of products, including a substantial amount of material of intermediate molecular weight (lane 4). In this behavior it differs significantly from pN_{11}, which gives shorter products predominantly (lane 2). This experiment strongly suggests that a terminal phosphomonoester provides a complexing site for UO_2^{2+} and consequently greatly increases the efficiency of photooxidation. It also suggests that, while a 5′-phosphate directs oxidation to close-by sugar residues, a 3′-phosphate enhances less localized oxidation.

The products of photooxidation of $N_{16}p$ and $N_{16}prC$ were generally consistent with this interpretation (data not shown). The oxidation of $N_{16}prC$ yielded few short products, but substantial amounts of longer oligomers, again suggesting that there is a coordination site for UO_2^{2+} somewhere in the interior of the molecule. $N_{16}p$ gave the most complicated pattern of products that we have seen, presumably because there are two coordination sites, one at the 3′-terminus and one internal, and each produces cleavage at a substantial number of different internucleotide bonds.

We carried out many experiments attempting to use the 5′-[^{32}P]-37mer as target and a derivative of the complementary oligomer pN_{16} as an antisense reagent to direct a UO_2^{2+} "warhead" to internal sites on the target (Figure 6). None of these experiments succeeded; the oxidation of the 37mer produced the same pattern of products whether it was free in solution or hybridized to a 16mer carrying a complexing group at its 5′-terminus. (See caption to Figure 6 for a list of the complexing groups used.) We confirmed in independent experiments that pN_{16} hybridizes to 5′-[^{32}P]-37mer under the conditions of our experiments.

The photooxidation of alcohols by UO_2^{2+} has been studied extensively (Rabinowitch & Belford, 1964). The reaction is initiated by the transfer of a hydrogen atom from a carbon atom of the alcohol to one of the O atoms

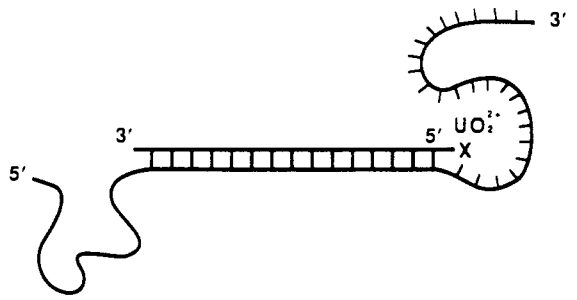


Figure 6. Conformation that we anticipated for an oligodeoxynucleotide target and a complementary oligomer carrying a UO_2^{2+} "warhead" attached to a coordinating group X. The complexing groups X used unsuccessfully in this study were inorganic phosphate, cystamine, ethylenediaminetetraacetic acid, diethylenetriaminepentaacetic acid, ethylenediamine, pentaethylenehexamine.

of the UO_2^{2+} ion. Our results suggest that UO_2^{2+} attached to a 5'-terminal phosphate group attacks the terminal sugar residue to liberate inorganic phosphate or attacks one of the two terminal sugar residues to liberate mono- and possibly dinucleotide derivatives. Coordination of a second phosphate-containing molecule such as uridine 5'-monophosphate to the UO_2^{2+} ion somewhat changes the conformation of the 5'-terminus of the oligodeoxynucleotide and hence alters the proportion of different oxidation products that are formed. A UO_2^{2+} ion attached to a phosphate ion at the 3'-end of an oligodeoxynucleotide acts less discriminatingly by attacking residues more distant along the backbone.

Sequence-dependent cleavage due to attachment of the UO_2^{2+} ion to internal sequences in the oligodeoxynucleotide is suggested by our findings with pN_{16}. Highly specific cleavage of DNA in the neighborhood of a bound RNA polymerase molecule has been reported. It presumably arises in the same way, that is by coordination of a UO_2^{2+} ion to a region of the nucleic acid molecule that, influenced by the bound protein, forms an unusually strong coordination site for the UO_2^{2+} ion (Jeppesen & Nielsen, 1989). It is not clear whether coordination is to backbone phosphodiester groups, bases, or both.

ACKNOWLEDGMENT

This work was supported by Grant No. GM13435-23 from The National Institutes of Health. We thank Sylvia Bailey for manuscript preparation.

LITERATURE CITED

Bridson, P. K., and Orgel, L. E. (1980) Catalysis of accurate poly(C)-directed synthesis of 3'-5'-linked oligoguanylates by Zn^{2+}. *J. Mol. Biol. 144*, 567–577.

Chu, B. C. F., and Orgel, L. E. (1985) Nonenzymatic sequence-specific cleavage of single-stranded DNA, *Proc. Natl. Acad. Sci., U.S.A. 82*, 963–967.

Deng, G-r., and Wu, R. (1983) Terminal transferase: use in the tailing of DNA and for *in vitro* mutagenesis. In *Methods in Enzymology* (R. Wu, L. Grossman, and K. Moldave, Eds.) Vol. 100, pp 96–116, Academic Press, New York.

Hertzberg, R. P., and Dervan, P. B. (1984) Cleavage of DNA with methidiumpropyl-EDTA-iron(II): Reaction conditions and product analyses. *Biochemistry 23*, 3934–3945.

Jeppesen, C., and Nielsen, P. E. (1989) Uranyl mediated photofootprinting reveals strong *E. coli* RNA polymerase-DNA backbone contacts in the +10 region of the *Deo*P1 promoter open complex. *Nucleic Acids Res. 17*, 4947–4956.

Nielsen, P. E., Jeppesen, C., and Buchardt, O. (1988) Uranyl salts as photochemical agents for cleavage of DNA and probing of protein–DNA contacts. *FEBS Lett. 235*, 122–124.

Rabinowitch, E., and Belford, R. L. (1964) *Spectroscopy and Photochemistry of Uranyl Compounds*, The Macmillan Company, New York.

Weith, H. L., and Gilham, P. T. (1967) Structural analysis of polynucleotides by sequential base elimination. The sequence of the terminal decanucleotide fragment of the ribonucleic acid from bacteriophage f2. *J. Am. Chem. Soc. 89*, 5473–5474.

Preparation and in Vivo Evaluation of an *N*-(*p*-[^{125}I]Iodophenethyl)maleimide-Antibody Conjugate

Mark D. Hylarides,* D. Scott Wilbur,† Michael W. Reed, Stephen W. Hadley, Joan R. Schroeder, and Leah M. Grant

NeoRx Corporation, 410 West Harrison Street, Seattle, Washington 98119. Received May 20, 1991

Protein sulfhydryl reactive *N*-(4-[^{125}I]iodophenethyl)maleimide (IPEM, **5**) was obtained from *N*-[4-(tri-*n*-butylstannyl)phenethyl]maleimide in 59–100% radiochemical yield. Conjugation of **5** to NR-ML-05 Fab, a murine anti-melanoma antibody Fab fragment that had been previously reduced with dithiothreitol (DTT), was effected in an average of 85% yield. Results from in vitro chemical challenges and serum stability studies on the IPEM conjugate of NR-ML-05 Fab (**6**) indicated a stable covalent attachment of the radioiodine. A biodistribution study of the IPEM conjugate in tumor-bearing athymic nude mice showed lack of significant accumulation of radioiodine in the thyroid and stomach which was an indication of in vivo stability. The observed uptake in tumor was consistant with that obtained for Chloramine-T- or *p*-iodobenzoate-labeled NR-ML-05 Fab conjugates.

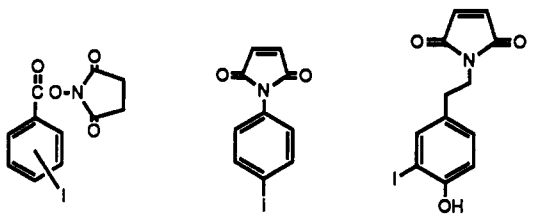
INTRODUCTION

Several different labeling procedures have been reported for the radioiodination of antibodies, however, direct labeling procedures using NaI with Chloramine-T or Iodogen as oxidants have been used most extensively (*1*). Radioiodination of antibodies using these direct labeling procedures results in the attachment of radioiodine to a phenolic tyrosine residue (*2*). Under certain circumstances, preservation of underivatized tyrosine residues, which may be present in the binding region of antibodies, was shown to be critical to maintain high antibody immunoreactivity after radioiodination (*3*). Additionally, radioiodinated antibodies prepared by direct methods frequently show extensive deiodination in vivo, resulting in undesirable accumulation of radioiodine in the thyroid and stomach (*4*).

Protein radioiodination acylating reagents such as the Bolton–Hunter reagent (*5*) and Wood's reagent (*6*) have been developed as alternatives to direct labeling so that the protein to be radiolabeled is not subjected to harsh oxidizing conditions. More recently, similar acylating reagents designed to improve the in vivo stability of the carbon–radioiodine bond, *N*-succinimidyl *p*-iodobenzoate (PIB, **1a**) (*7*) and *N*-succinimidyl *m*-iodobenzoate (**1b**) (*8*), have been developed (Chart I). In these reagents, the radioiodine is attached to a nonactivated (nonphenolic) aromatic ring of the protein-reactive molecule. Site-specific radioiodination of either reagent is accomplished by an iododestannylation reaction of the organotin precursor. Conjugation of **1a** or **1b** to protein is then accomplished by reaction with protein lysine residues at pH 8–10 to form an amide bond.

As an alternative to acylation of protein lysine residues, maleimide derivatives have also been used extensively for protein modification. Maleimide derivatives selectively react with protein sulfhydryls at pH 6–8 (*9*, *10*) and have demonstrated good utility as cross-linking and general conjugating reagents (*11*, *12*). For our applications, radioiodinated maleimide analogues were envisaged as potential reagents for labeling proteins containing a free sulfhydryl group. In particular, these types of reagents

Chart I



1a para-iodobenzoate (PIB) **2** **3**

1b meta-iodobenzoate

could be useful for labeling pH sensitive proteins or proteins containing unavailable or modified lysine residues.

The preparation of *N*-(*p*-[^{125}I]iodophenyl)maleimide (**2**) from an arylmercuric derivative followed by protein conjugation was initially reported by Srivastava et al. (*13*, *14*). Preparation of **2** from an aryltin precursor and subsequent conjugation to antibody was later described (*15*). In the phenethyl series, preparation and protein conjugation of *N*-(3-[^{125}I]iodo-4-hydroxyphenethyl)maleimide (**3**) using a direct radioiodination procedure was reported starting with *N*-(4-hydroxyphenethyl)maleimide (*16*). In all instances, the minimal thyroid uptake of radioiodine observed in vivo for the resultant protein conjugates was indicative of good in vivo stability.

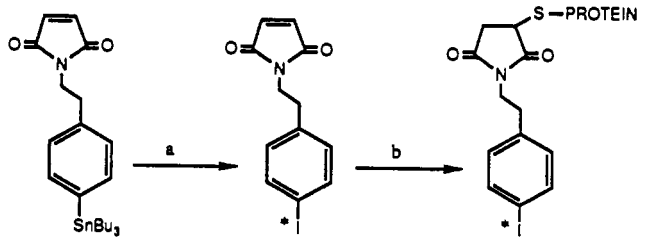
We anticipated that an aryltin phenethylmaleimide would be easier to prepare and potentially show better long-term stability than the corresponding *N*-phenylmaleimide derivative. Therefore, using the analogous synthetic route established for preparation of **2** from an aryltin precursor, we investigated the preparation of aryltin phenethylmaleimide **4**. Reported herein is a study of the feasibility of using *N*-(4-[^{125}I]iodophenethyl)maleimide (IPEM, **5**) as reagent for protein labeling. To accomplish this, aryltin phenethylmaleimide **4** was prepared and radioiodinated to produce **5**. The labeled product was subsequently conjugated to a Fab fragment of NR-ML-05,[1] a murine anti-melanoma monoclonal antibody (Scheme I). Prior to the conjugation step, the antibody fragment had been reduced with DTT to generate reactive protein

† Department of Radiation Oncology, RC-08, University of Washington Medical Center, 1959 N.E. Pacific St., Seattle, WA 98195.

[1] NR-ML-05 is a murine IgG_{2b} monoclonal antibody that recognizes a 250-kDa proteoglyan antigen expressed by melanoma cells.

1043-1802/91/2902-0435$02.50/0 © 1991 American Chemical Society

Scheme I. Preparation and Conjugation of 5 to Protein[a]



4 5 6

[a] Reagents: (a) NCS, Na*I; (b) protein-SH, pH 6.2.

thiols. Radiolabeling conditions were established such that efficient conjugation of 5 to protein could occur without an intermediate purification step. A biodistribution study was carried out to evaluate the IPEM conjugate 6 in nude mice bearing a human melanoma xenograft.

EXPERIMENTAL PROCEDURES

General Procedure. All reagents used were reagent grade or better and were used as purchased. 4-Bromophenethylamine and hexabutylditin were obtained from Alpha Products. All other reagents were obtained from Aldrich Chemical Co. Solvents for HPLC analysis were obtained as HPLC grade (Baxter) and filtered (0.45 μm) prior to use. For the gradient HPLC analysis, pure solvents were mixed with a minimum of 2% of the opposing solvent and degassed prior to use. Phosphate-buffered saline (PBS) was purchased from Gibco Labs as Dulbecco's phosphate-buffered saline. Iodine-125 was obtained from NEN/Du Pont in a 0.1 N NaOH solution at 17 Ci/mg.

Nuclear magnetic resonance spectra were obtained on a Varian Gemini-200 200-MHz instrument. The chemical shifts are expressed as ppm using tetramethylsilane or $CDCl_3$ as internal references. IR spectra were obtained on a Perkin-Elmer 1310 infrared spectrophotometer. Mass spectral data were obtained on a VG 7070H mass spectrometer using fast atom bombardment (Fab^+) or chemical ionization (CI) in conjunction with a direct-insert probe.

High-performance liquid chromatography (HPLC) was conducted with a SpectraPhysics Model 8800 gradient pumping system, Beckman Model 160 UV detector, Beckman Model 170 radioisotope detector, and Rheodyne Model 7125 injector. Spectrophotometric analysis of the HPLC effluant was performed by UV detection at 254 nm. Radiometric analyses of the effluant was achieved by NaI scintillation optimized for the isotope used. Integration and plotting of the chromatograms was accomplished using a Dynamic Solutions Maxima 820 computer workstation. Reversed-phase HPLC chromatography was carried out using a Whatman Partisphere (4.6 mm × 12.5 cm) C-18 column using a gradient solvent system at a flow rate of 1.0 mL/min. Solvent A in the gradient was 98% acetonitrile with 2% of a 1% HOAc/water solution. Solvent B was 10% acetonitrile in a 90% solution of 1% HOAc/water solution. After 2 min at 50% A, the gradient was increased to 98% A over 8 min and held at 98% A for 10 min. The gradient was then decreased to the original 50% A over a 5-min period. Size-exclusion HPLC was performed on a Du Pont Zorbax Bio-Series GF-250 (9.4 mm × 24 cm) column eluting with 0.2 M sodium phosphate, pH 6.8, at a flow rate of 1.0 mL/min.

Instant thin-layer chromatography (ITLC) was performed on silica gel impregnated glass-fiber strips (Gelman), eluting with 4:1 MeOH/water solution. Radiochemical purity of the antibody conjugates was calculated based on the percent of counts remaining at the origin versus counts which eluted with the solvent front. Radioactive samples were counted in a dose calibrator for microcuries or larger quantities or in a γ-counter for smaller quantities.

Synthesis of *N*-(4-Bromophenethyl)phthalimide (8). To a solution of 4-bromophenethylamine (7; 5.0 g, 25 mmol) in 100 mL of ethyl ether was added 3.7 g (25 mmol) of phthalic anhydride as a solid. An additional 50 mL of ethyl ether was added to ensure efficient stirring as the product precipitated. After 1 h of stirring, the white solid (7.83 g) was isolated by vacuum filtration and washed repeatedly with 20 mL of cold ethyl ether. A 3.0-g portion of the solid intermediate was suspended in 25 mL of glacial acetic acid and heated at 65 °C for 2 h, after which the solution was allowed to stand overnight at room temperature. The resultant white needles were isolated and washed thoroughly with cold acetic acid to yield 2.5 g (79% yield) of 8. Mp = 208–210 °C. ^1H NMR ($CDCl_3$): 2.95 (t, 2 H, J = 4 Hz), 3.90 (t, 2 H, J = 4 Hz), 7.12 (d, 2 H, J = 4 Hz), 7.39 (d, 2 H, J = 4 Hz), 7.72 (m, 2 H), 7.85 (m, 2 H). ^{13}C NMR ($CDCl_3$): 33.97, 38.76, 120.65, 123.38, 130.70, 131.77, 132.11, 134.11, 137.07, 168.33. Anal. Calcd for $C_{16}H_{12}NO_2Br$: C, 58.18; H, 3.64; N, 4.24. Found: C, 58.00; H, 3.32; N, 4.04.

Synthesis of *N*-[4-(Tri-*n*-butylstannyl)phenethyl]phthalimide (9). To a solution of 6.0 g (18.2 mmol) of 8 in 150 mL of dry toluene was added 31.6 g (54.5 mmol) of hexabutylditin and 0.21 g (0.18 mmol) of tetrakis(triphenylphosphine)palladium(0) catalyst. The resultant solution was refluxed under N_2 for 48 h. An additional 0.15 g of palladium catalyst was added after the reaction had proceeded for 6 h. After the mixture had cooled to room temperature, most of the solvent was removed under reduced pressure and the resultant dark slurry was chromatographed by flash chromatography (silica gel 60) on a 2 × 40 cm column using 1:9 ethyl acetate/hexane as the eluting solvent. After removal of the solvents under reduced pressure, 9.3 g (95% yield) of 9 was isolated as a pale yellow oil. ^1H NMR ($CDCl_3$): 0.75–1.70 (m, 27 H), 2.95 (t, 2 H, J = 8 Hz), 3.90 (2 H, J = 8 Hz), 7.25 (d, 2 H, J = 8 Hz), 7.4 (d, 2 H, J = 8 Hz), 7.7 (m, 2 H), 7.8 (m, 2 H). ^{13}C NMR ($CDCl_3$): 9.71, 13.85, 27.57, 29.30, 34.85, 39.49, 123.67, 128.99, 132.68, 134.39, 137.23, 138.16, 140.32, 168.78. MS (CI, direct probe): m/z isotope cluster at 480–488 (M + H − 57 [butane]).

Synthesis of 4-(Tri-*n*-butylstannyl)phenethylamine (10). To a solution of 5.7 g (10.5 mmol) of 9 in 55 mL of methanol was added 1.0 mL (31.6 mmol) anhydrous hydrazine. The pale yellow solution was stirred at room temperature for 18 h followed by removal of the phthalhydrazine byproduct by vacuum filtration. The filtrate was concentrated and stirred with 150 mL of ether and 100 mL of 2.5 N NaOH until the solid dissolved. The organic layer was isolated and washed again with 2.5 N NaOH and saturated NaCl solution and dried over anhydrous K_2CO_3. After removal of the solvent under reduced pressure, the liquid residue was purified by Kugelrohr distillation (150 °C, 10 mmHg) to give 3.42 g (79% yield) of the title compound as a colorless liquid. ^1H NMR ($CDCl_3$): 0.76–1.65 (m, 27 H), 2.70 (t, 2 H, J = 6.8 Hz), 2.95 (t, 2 H, J = 6.8 Hz), 7.18 (d, 2 H, J = 8 Hz), 7.40 (d, 2 H, J = 8 Hz). ^{13}C NMR ($CDCl_3$): 9.71, 13.81, 27.58, 29.31, 40.28, 43.73, 129.06, 137.15, 139.60, 139.94. MS (CI, direct probe): m/z isotope cluster at 408–416 (M + H), 350–358 (M + H − 57 [butyl]).

Synthesis of *N*-[4-(Tri-*n*-butylstannyl)phenethyl]maleimide (4). To a stirred solution of 148 mg (0.36 mmol)

of **10** in 10 mL ether was added 43 mg (0.44 mmol) of maleic anhydride. After the reaction mixture was allowed to stir overnight, the solvent was removed under reduced pressure, affording a white solid. Acetic anhydride (10 mL) and 0.12 g (1.26 mmol) of KOAc were combined with 155 mg of the white solid, and the mixture was stirred at 90 °C in a water bath for 1 h followed by standing at room temperature for 15 h. The reaction mixture was dissolved in 30 mL of ether and then washed with 3 × 30 mL of water and once with 30 mL of 5% Na_2CO_3. The organic phase was dried over anhydrous Na_2SO_4 and filtered, and the solvents were removed under reduced pressure to afford 127 mg (85% yield) of crude maleimide. A 30-mg portion was further purified by silica gel (deactivated with triethylamine) flash chromatography by elution with 5:95 ethyl acetate/hexane to provide 14 mg of pure **4**. ^1H NMR ($CDCl_3$): 0.75–1.70 (m, 27 H), 2.7 (t, 2 H, J = 6 Hz), 2.9 (t, 2 H, J = 6 Hz), 6.9 (s, 2 H), 7.2 (d, 2 H, J = 7.8 Hz), 7.4 (d, 2 H, J = 7.6 Hz). ^{13}C NMR ($CDCl_3$): 10.0, 14.2, 27.9, 28.0, 35.0, 39.0, 128.3, 134.8, 138.3, 140.7, 171.5. MS (CI, direct probe): m/z isotope cluster at 487–492 (M + H), 431–437 (M + H − 57 [butyl]). Anal. Calcd for $C_{24}H_{37}NO_2Sn$: C, 58.78; H, 7.77; N, 2.86. Found: C, 58.50; H, 7.94; N, 2.49.

Synthesis of *N*-(4-Iodophenethyl)maleimide (5a). To 14.5 mg (0.03 mmol) of **4** in 10 mL of 1:4 HOAc/isopropyl alcohol (IPA) were added 4.59 mg (0.03 mmol) NaI and 12.4 mg (.09 mmol) *N*-chlorosuccinimide (NCS) as solids. After the addition of another 10 mL of IPA, the yellow solution was heated at 70 °C for 5 min and then allowed to stir at room temperature for 15 h, which yielded a clear colorless solution. After removal of the solvents under reduced pressure, 25 mL of CH_2Cl_2 and 25 mL of water were added. The organic phase was washed with 3 × 25 mL of water and dried over anhydrous Na_2SO_4, and solvents were removed under reduced pressure. The crude material was purified by silica gel chromatography by elution with 1:9 ethyl acetate/hexane to yield 4.0 mg of the title compound as a white solid. Mp = 98–99 °C. ^1H NMR ($CDCl_3$): 2.85 (t, 2 H, J = 7.4 Hz), 3.74 (t, 2 H, J = 7.4 Hz), 6.67 (s, 2 H), 6.95 (d, 2 H, J = 8.4 Hz), 7.60 (d, 2 H, J = 8.2 Hz). ^{13}C NMR ($CDCl_3$): 34.54, 39.31, 113.14, 131.72, 134.95, 138.53, 162.80. MS (CI, direct probe): 327 (M^+ + H), 202 (M^+ + H − 127). Anal. Calcd for $C_{12}H_{10}NO_2I$: C, 44.04; H, 3.06; N, 4.28. Found: C, 44.16, H, 3.04, N, 4.00.

Synthesis of *N*-(4-[^{125}I]Iodophenethyl)maleimide (IPEM, 5). To a solution of 10 μg (0.02 μmol) of **4** in 22 μL of 1% acetic acid/methanol was added 3.0 μL (1.5 mCi) of $Na^{125}I$. Immediately following, 6 μL of a 0.5 mg/mL solution of NCS in MeOH was added. After 15 min the reaction was quenched by the addition of 3 μL of $NaHSO_3$ solution (0.72 mg/mL in H_2O). Analysis by HPLC showed the desired compound **5**, eluting at 10.4 min, which represented a 59–100% radiochemical yield. Radioiodinated **5** in MeOH was directly conjugated to DTT-reduced NR-ML-05 Fab.

Preparation of [^{125}I]IPEM–NR-ML-05 Fab Conjugate (6). To a solution of 3.4 mg of NR-ML-05 Fab in 0.35 mL of PBS, pH 7.4, was added 2.7 mg of dithiothreitol (DTT). The solution, at a final concentration of 50 mM DTT, was incubated at 37 °C for 2 h. The excess DTT was removed from the solution by gel filtration (Pharmacia, PD-10) using degassed 0.2 M sodium phosphate buffer, pH 6.2. The reduced Fab which eluted from the column was kept at 5 °C and used within 15 min of purification.

To the methanolic solution of **5** was added 0.52 mL (0.5 mg) of DTT-treated Fab in pH 6.2 buffer. After 20 min, the sample was purified by gel filtration (Pharmacia PD-10), eluting with PBS to give the radioiodinated protein in a overall 50–85% radiochemical yield, based on an average conjugation yield of 85%. The radiochemical purity of **6**, as assessed by ITLC, generally exceeded 99% protein bound. The IPEM conjugate used for the biodistribution study was obtained with a specific activity of 0.45 mCi/mg Fab. Radiometric analysis of the conjugate by HPLC size exclusion (Zorbax GF-250) showed only the desired monomeric species at a retention time of 9.3 min.

Chemical Challenge Experiments. To test tubes containing 50 μL of either 0.1 M DTT, 0.1 M *N*-acetylcysteine, 12% TCA, 6 M urea, or 0.1 M NaOH was added 25 μL (14 μg) of labeled protein. After mixing, the solutions were incubated at 37 °C for 3 days. Aliquots were periodically removed and analyzed by ITLC (80% MeOH).

Serum Stability. Samples of freshly isolated human serum were filtered through 0.2-μm filters and placed in sterile capped culture tubes. Approximately 15 μg (25 μL) of labeled protein was added to each 0.5-mL serum sample. The samples were lightly vortexed and incubated at 37 °C for 24 h. Samples were periodically removed and analyzed by ITLC using 4:1 acetonitrile/H_2O as the eluting solvent.

Immunoreactivity Assessment. The immunoreactivities of the radioiodinated antibodies were determined from a cell-binding assay using a fixed labeled antibody concentration and a varied number of antigen positive cells as previously described (*7*, *17*, *18*).

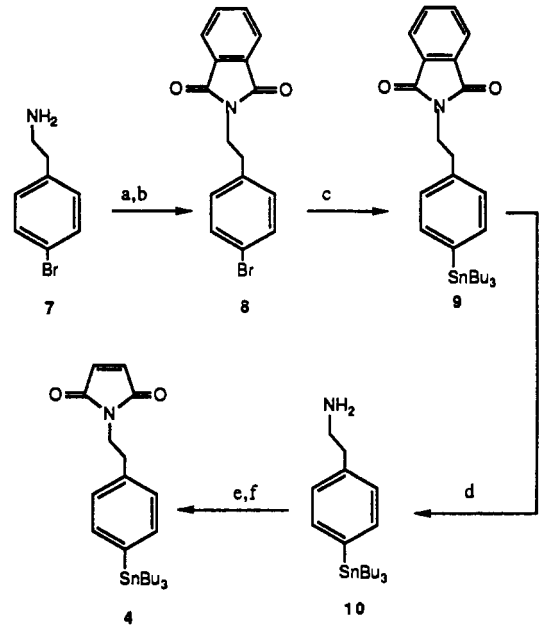
Biodistribution Studies. Female athymic mice (nu/nu) were obtained from Simonsen Laboratories, Inc. (Gilroy, CA) and were used at 10–12 weeks of age. Tumor xenografts were produced by subcutaneous implantation of 2.5 × 10^6 FEM-X cultured human melanoma tumor cells. The tumors were grown for 7–10 days before use.

The biodistribution study was conducted by injection of 5 μg of [^{125}I]-**5** in 100 μL of PBS intravenously via the lateral tail vein. The animals were sacrificed by cervical dislocation at 4 and 20 h postinjection. Blood samples were obtained by retroorbital bleeding. Syringes were weighed before and after injection to determine the volume of conjugate injected. The activity per unit volume was calculated from standards. The animals were weighed (19.5 ± 2.7 g, n = 8) and marked for identification in all experiments. Ten different tissues were evaluated: blood, tumor, muscle (thighs), lung, liver, spleen, stomach, neck including thyroid (the major portion of the muscle from the front of the neck), kidney (both), and intestine. The excised tissues were blotted, weighed, and counted in a γ-counter. Summarized data include mean ± SD of percent injected dose per gram.

RESULTS

Chemistry. The desired aryltin maleimide precursor **4** was prepared from *p*-bromophenethylamine (**7**) (Scheme II). The amine was converted to phthalimide **8** by treatment with phthalic anhydride followed by cyclization of the intermediate acid with acetic acid. Phthalimide **8** was subjected to a palladium-catalyzed metal–halogen exchange reaction with hexabutylditin and tetrakis(triphenylphosphine)palladium(0) catalyst, generating the aryltin phthalimide adduct **9** in 53% yield. Removal of the phthalimide protecting group of **9** by treatment with methanolic hydrazine afforded *p*-(tri-*n*-butylstannyl)phenethylamine (**10**). The phthalimide functionality proved to be an excellent protecting group for preparation of **10**. Following the metal–halogen exchange

Scheme II. Synthesis of Aryltin Phenethylmaleimide Intermediate 4[a]



[a] Reagents: (a) phthalic anhydride, Et_2O; (b) HOAc; (c) Bu_6Sn_2, Pd(0) catalyst, toluene; (d) NH_2NH_2, MeOH; (e) maleic anhydride, Et_2O; (f) Ac_2O, HOAc.

reaction, removal of the phthalimide group in the presence of the tri-*n*-butylstannyl group with methanolic hydrazine to regenerate the amine was a facile and high-yield reaction.

Maleimide **4** was prepared from **10** in 33% yield by reaction with maleic anhydride followed by cyclization of the intermediate maleimic acid with acetic anhydride/sodium acetate. The maleimide was routinely stored at 4 °C under nitrogen prior to use.

Radioiodination of **4** at no-carrier-added levels of ^{125}I using NCS as the oxidant for iodide in 1% HOAc/MeOH provided radiochemical yields of **5** ranging from 59 to 100%, depending on the batch of **4** used. Following the radioiodination, a stoichiometric amount of $NaHSO_3$ (based on NCS) was added to quench the reaction. The addition of reductant ensured that the antibody to be added was not exposed to electrophilic iodine or oxidant during the conjugation step. Solutions of **5** were found to be stable to radiochemical decomposition over a period of 6 days, as assessed by HPLC.

Conjugation of **5** to the reduced antibody Fab fragment at pH 6.2 proceeded in an average 85% radiochemical efficiency within 20 min. No labeled conjugate was obtained when nonreduced antibody was treated with **5** under the same conditions. HPLC and ITLC analysis of the labeled conjugate over a period of 7 days indicated excellent radiochemical stability.

In Vitro Analysis. Chemical challenge studies were conducted to quantitate the extent of noncovalent (nonspecific) binding of radioiodinated small molecular weight species to the antibody fragment. Exposure to chemical reagents including 12% TCA, 6 M urea, 0.1 M *N*-acetylcysteine, and 0.1 M DTT, over a 24-h period, resulted in no loss of radioactivity from the antibody. Treatment of the conjugate with 0.1 N NaOH for 24 h resulted in 80% loss of radioactivity from the protein. Serum stability data was obtained for the IPEM conjugate by incubation with human serum at 37 °C for 24 h. Similar to the chemical challenge studies, less than 5% loss of radioiodine from the antibody was observed.

Table I. Tissue Distribution of Radioiodine at 4 and 20 h Postinjection of IPEM–NR-ML-05 Fab Conjugate [^{125}I]-6[a]

	% injected dose/g	
tissue	4 h	20 h
blood	3.01 ± 0.27	0.45 ± 0.07
tumor	3.08 ± 0.28	1.24 ± 0.06
muscle	0.72 ± 0.10	0.05 ± 0.01
bone	0.48 ± 0.03	0.07 ± 0.01
lung	2.12 ± 0.21	0.44 ± 0.14
liver	1.51 ± 0.36	0.16 ± 0.03
spleen	0.81 ± 0.06	0.16 ± 0.02
stomach	0.78 ± 0.21	0.05 ± 0.10
neck	1.08 ± 0.17	0.21 ± 0.11
kidney	12.21 ± 1.82	0.97 ± 0.16
intestine	1.34 ± 0.27	0.15 ± 0.10

[a] Results were obtained from $n = 4$ mice per time point and are tabulated as mean ± SD of the % injected dose/g. The specific activity and radiochemical purity for [^{125}I]-**6** was 0.45 μCi/μg and 99.2%. Tumor weights were 0.24 g ± 0.08 g.

The immunoreactivity of the IPEM conjugate was assessed by a radiolabeled cell binding assay prior to injection into animals. The extent of antigen binding of the IPEM conjugate, as measured by percent counts bound, was shown to be comparable to that obtained for the standard PIB NR-ML-05 Fab conjugate (*7*) (79% and 72%, respectively).

Biodistribution. A biodistribution study of the IPEM conjugate was conducted to assess its in vivo distribution and stability by quantitating the accumulation of radioiodine in various tissues at 4 and 20 h. These results are summarized in Table I.

DISCUSSION

The simplicity of the overall protein radiolabeling procedure becomes especially critical when many routine labelings are performed or when high levels of radioiodine are used. For this reason, an aryltin organometallic was chosen as a synthetic precursor since compounds containing this functionality generally undergo very rapid and efficient electrophilic iodination reactions (*19*, *20*).

The key intermediate, *N*-[4-(tri-*n*-butylstannyl)phenethyl]maleimide (**4**) was prepared by a four-step synthesis starting with commercially available 4-bromophenethylamine. No-carrier-added radioiodination of **4** using NaI and NCS as an oxidant proceeded in 59–100% radiochemical yield within 15 min. Although the kinetics of the radioiodination reaction have not been determined, it is likely that it was completed within a shorter time. The facile metal–halogen exchange reaction observed was consistent with earlier comparative iodo–destannylation reactions performed in our laboratory (*21*).

Reactive thiols for the conjugation reaction were generated on NR-ML-05 Fab by reduction with DTT (*22*). Use of DTT as a reducing agent in our laboratory typically has resulted in reduced intact antibodies or antibody fragments which contain 5% or less of aggregated species. When other sulfhydryl-generating agents such as *N*-succinimidyl *S*-acetylthioacetate (SATA) (*23*) or *N*-succinimidyl 3-(2-pyridyldithio)propionate (SPDP) (*24*) were investigated as alternate means of generating reactive thiols, higher percentages of aggregated material were consistently observed. Spectrophotometric analysis of the sulfhydryl content of DTT-reduced Fab using a DTNB [5,5′-dithiobis(2-nitrobenzoic acid)] assay (*25*) showed an average of 2 equiv of thiol/equiv of Fab after purification by size exclusion. If the purified reduced antibody was allowed to stand at room temperature, rapid reoxidation of the reactive thiols occurred. To minimize this oxidation,

purified DTT-reduced Fab was prepared using N_2 sparged buffers, kept cold, and used immediately after preparation.

Conjugation of **5** to DTT-treated NR-ML-05 Fab was performed at pH 6.2 to ensure that reaction was with free protein sulfhydyls in preference to amines. The covalent nature of the iodine attachment was confirmed by the good stability of the protein-iodine bond to in vitro chemical challenges.

Biodistribution of the IPEM conjugate in tumor-bearing nude mice (Table I) showed minimal accumulations of radioactivity in most normal organs evaluated at the 20-h time point. The kidney showed significant uptake at 4 h but cleared rapidly over the 20-h period and appears to be the primary route of excretion of intact conjugate or resultant metabolites. Thyroid uptake at 4 h (1.0% ID/g) diminished to 0.2% ID/g at 20 h. These values are similar to those obtained for PIB NR-ML-05 Fab conjugates in two previous studies (*7*, *26*). The percent loss of radioactivity from the thyroid from 4 to 20 h closely parallels that of other nontarget organs, which is suggestive of general clearance from the vasculature. In contrast, earlier studies have shown substantially higher accumulations of radioactivity in thyroid (2–10% ID/g at 20 h) using radioiodinated NR-ML-05 Fab prepared by a direct labeling method (*7*, *26*). The comparatively low uptake in thyroid observed for the IPEM conjugate is indicative of negligible in vivo deiodination.

Radioactivity levels in tumor at 20 h for the IPEM conjugate (1.24% ID/g) is consistent with that obtained for PIB and chloramine-T labeled NR-ML-05 Fab conjugates (1.47–2.19% ID/g and 1.27–1.63% ID/g, respectively). Therefore, the extent of tumor uptake observed for the IPEM conjugate is likely to be characteristic of the antibody fragment rather than a result of damage to the antibody that might have occurred during the labeling procedure.

On the basis of previous studies, PIB conjugates of Fab fragments have been shown to be metabolized to corresponding lysine adducts that are rapidly excreted in the urine (*27*). Although we have not characterized the metabolites of the IPEM conjugate, their biodistribution properties appear to be similar to PIB metabolites in the melanoma tumor model.

In conclusion, we have demonstrated that radioiodinated (iodophenethyl)maleimide (IPEM) can be prepared in good radiochemical yield from an aryltin precursor. Without purification, the labeled compound can be covalently conjugated to a DTT reduced antibody Fab fragment. The resultant IPEM conjugate showed negligible in vivo deiodination, consistent with that reported for the corresponding PIB conjugates. The IPEM conjugate retained biological immunoreactivity in vitro as measured by cell binding assays and in vivo as assessed by tumor retention.

Radioiodinated (iodophenethyl)maleimide **5** shows promise as general protein labeling reagent and could be applied to the preparation of labeled antibody conjugates for the detection and/or therapy of cancer.

ACKNOWLEDGMENT

We thank Don Axworthy, Dr. Mary Ann Gray, and Dr. Paul L. Beaumier for conducting the biodistribution studies. Also, we thank the NIH for the partial financial support of these studies through SBIR Contracts, N43-CM-57759 and N43-CM-67759.

LITERATURE CITED

(1) Regoeczi, E. (1984) Methods of Protein Iodination. In *Iodine Labeled Plasma Proteins*, Vol. I, pp 35–102, CRC Press Inc., Boca Raton, FL.

(2) Krohn, K. A., Knight, L. C., Harwig, J. F., and Welch, M. J. (1977) Differences in the Site of Iodination of Proteins Following Four Methods of Radioiodination. *Biochim. Biophys. Acta 490*, 497–505.

(3) Hadley, S. W., Berninger, R. W., and Wilbur, D. S. Antibody Radioiodination Using Purified *N*-Succinimidyl-*para*-[^{131}I]-iodobenzoate. A Mild Method for Radioiodination of Sensitive Antibodies. Manuscript in preparation.

(4) Engler, D., and Burger, A. G. (1984) The Deiodination of the Iodothyroxins and Their Derivatives in Man. *Endocr. Rev. 5*, 151–184.

(5) Bolton, A. E., and Hunter, W. M. (1973) The Labeling of Proteins to High Specific Radioactivity by Conjugation to an ^{125}I-Containing Acylating Agent. Applications to the Radioimmunoassay. *Biochem. J. 133*, 529–539.

(6) Wood, F. T., Wu, M. M., and Gerhart, J. C. (1975) The Radioactive Labeling of Proteins with an Iodinated Amidination Reagent. *Anal. Biochem. 69*, 339–349.

(7) Wilbur, D. S., Hadley, S. W., Hylarides, M. D., Abrams, P. G., Beaumier, P. A., Morgan, A. C., Reno, J. M., and Fritzberg, A. R. (1989) Development of a Stable Radioiodinating Reagent to Label Monoclonal Antibodies for Radiotherapy of Cancer. *J. Nucl. Med. 30*, 216–226.

(8) Zalutski, M. R., and Narula, A. S. (1988) Radiohalogenation of a Monoclonal Antibody Using an *N*-Succinimidyl 3-(Tri-*n*-butyl)stannyl Benzoate Intermediate. *Cancer Res. 48*, 1446.

(9) Gregory, J. D. (1955) The Stability of *N*-ethylmaleimide and Its Reaction with Sulfhydryl Groups. *J. Am. Chem. Soc. 77*, 3922–3.

(10) Smyth, D. G. (1964) Reactions of *N*-Ethylmaleimide with Peptides and Amino Acids. *Biochem. J. 91*, 589–595.

(11) Partis, M. D., Griffiths, D. G., Roberts, G. C., and Beechey, R. B. (1983) Cross Linking of Proteins by ω-Maleimido Alkanoyl *N*-Hydroxysuccinimido Esters. *J. Protein Chem. 2*, 263–277.

(12) Martin, F. J., and Papahadjopoulos, D. (1982) Irreversible Coupling of Immunoglobulin Fragments to Preformed Vesicles. *J. Biol. Chem. 257*, 286–288.

(13) Srivastava, P. C., Knapp, F. F., Karl, D. W., and Mills, D. C. B. (1986) *N*-(*p*-Iodophenyl)maleimide. A New Radioiodinated Thiol Reagent with Selective Effects on Platelet Membrane Functions. *J. Nucl. Med. 27*, abstract, 1046.

(14) Srivastava, P. C., Kanpp, F. F., Allred, J. F., and Buchsbaum, D. J., (1989) Evaluation of *N*-(*p*-[^{125}I]Iodophenyl)maleimide for Labeling Monoclonal Antibodies. *J. Labelled Compd. 26*, 296–298.

(15) Wilbur, D. S., Hylarides, M. D., Hadley, S. W., Schroeder, J., and Fritzberg, A. R. (1989) A General Approach to Radiohalogenation of Proteins. Radiohalogenation of Organometallic Intermediates Containing Protein Reactive Substituents. *J. Labelled Compd. 26*, 316–318.

(16) Srivastava, P. C., Allred, J. F., Lambert, C. R., and Kennel, S. J. (1990) No-Carrier Added Preparation of a New Radioiodinated Maleimide as a Potentially Attractive Radioimmunoconjugator with Low *In Vivo* Deiodination. *J. Nucl. Med. 31*, abstract, 906.

(17) Lindmo, T., Boven, E., Cuttitta, F., Fedorko, J., and Bunn, P. A., Jr. (1984) Determination of the Immunoreactive Fraction of Radiolabeled Monoclonal Antibodies by Linear Extrapolation to Infinite Antigen Excess. *J. Immunol. Methods 72*, 77–89.

(18) Beaumier, P. L., Neuzil, D., Yang, H. M., Noll, E. A., Kishore, R., Eary, J. F., Krohn, K. A., Nelp, W. B., Hellstrom, K. E., and Hellstrom, I. (1986) Immunoreactivity Assay for Labeled Anti-melanoma Monoclonal Antibodies. *J. Nucl. Med. 27*, 824–828.

(19) Adam, M. J., Ruth, T. J., Homma, Y., and Pate, B. D. (1985) Radiobromination of Aromatic Compounds by Cleavage of Aryl Tin Bonds. *Int. J. Appl. Radiat. Isot. 36*, 935–937.

(20) Seitz, D. E., Tonnesen, G. L., Hellman, S., and Adelstein, S. J. (1980) Iododestannylation. Position-specific Synthesis of Iodotamoxifin. *J. Organomet. Chem. 186*, C33–36.
(21) Hylarides, M. D., Wilbur, D. S., Hadley, S. W., and Fritzberg, A. R. (1989) Synthesis and Iodination of Methyl 4-tri-*n*-butylstannylbenzoate, *p*-(methoxycarbonyl)phenylmercuric chloride, and *p*-(methoxycarbonyl)phenylboronic acid. *J. Organomet. Chem. 367*, 259–265.
(22) Cleland, W. W. (1964) Dithiothreitol, a New Protective Reagent for SH Groups. *Biochemistry 3*, 480–482.
(23) Duncan, R. J., Weston, P. D., and Wrigglesworth, R. (1983) A New Reagent Which May Be Used To Introduce Sulfhydryl Groups into Proteins and Its Use in the Preparation of Conjugates for Immunoassay. *Anal. Biochem. 132*, 68–73.
(24) Carlsson, J., Drevin, H., and Axen, R. (1978) Protein Thiolation and Reversible Protein–Protein Conjugation, *N*-Succinimidyl 3-(2-Pyridyldithio)propionate, a New Heterobifunctional Reagent. *Biochem. J. 173*, 723–737.
(25) Kastenschmidt, L. L., Kastenschmidt, J., and Helmreich, E. (1968) Subunit Interactions and Their Relationship to the Allosteric Properties of Rabbit Muscle Phosphorylase b. *Biochemistry 7*, 3590–3608.
(26) Hadley, S. W., and Wilbur, D. S. (1990) Evaluation of Iodovinyl Antibody Conjugates: Comparison with a *p*-Iodobenzoyl Conjugate and Direct Radioiodination. *Bioconjugate Chem. 1*, 154–161.
(27) Axworthy, D. B., Vanderheyden, J. L., Wilbur, D. S., Hadley, S. W., Hylarides, M. D., Wahl, R. L., Hanelin, L., and Fritzberg, A. R. (1989) Urinary Metabolites of I-131 and Re-186 Radiolabeled Conjugates of Monoclonal Antibodies and Fragments in Patients. *J. Nucl. Med. 30*, 793.

A Novel Biotinylated Adenylate Analogue Derived from Pyrazolo[3,4-*d*]pyrimidine for Labeling DNA Probes

Charles R. Petrie,* A. David Adams, Michael Stamm, Jeffery Van Ness, Susan M. Watanabe, and Rich B. Meyer, Jr.

MicroProbe Corporation, 1725 220th St SE, No 104, Bothell, Washington 98021. Received August 26, 1991

A novel dATP analogue, 3-[5-[(*N*-biotinyl-6-amiocaproyl)amino]pentyl]-1-(2-deoxy-β-D-*erythro*-pentofuranosyl)-1*H*-pyrazolo[3,4-*d*]pyrimidin-4-amine 5′-triphosphate (**9**, bio-13-dAPPTP), which is modified at the 3-position with a flexible linker arm bearing a terminal biotin moiety, has been synthesized. This nucleotide is readily incorporated into DNA probes by nick translation. These probes hybridize to complementary targets as well as probes labeled with bio-dUTP, as judged by slot blot. When incorporated into oligonucleotides, they do not cause the loss of hybridization efficiency that an N-6-substituted adenine nucleotide does when incorporated into the same sites in the oligonucleotide.

INTRODUCTION

Nucleic acid hybridization has become a powerful tool in genetic research, biomedical research, and clinical diagnostics. Typically, radiolabeled nucleic acid probes are hybridized to a DNA or RNA sample that has been directly or indirectly immobilized on a solid support. Because of the inconveniences in using radioisotopes (e.g. potential health hazards, disposal problems, and the inherent instability associated with the radioisotope), efforts are being made to develop nonisotopic means of labeling nucleic acid.

Most currently used procedures for nonisotopic labeling of nucleic acid involve the incoroporation of a biotin moiety into the nucleic acid probe. The high binding affinity of biotin for avidin and streptavidin is well-documented in the literature and has found widespread use. Langer et al. (*1*), Brigati et al. (*2*), and Nelson et al. (*3*) have described the labeling of nucleic acids with pyrimidine nucleotide triphosphates substituted at the 5-position of the heterocycle with an alkyl chain bearing a terminal biotin (i.e. bio-11-dUTP, **11**; Chart I). These modified nucleotides can be incorporated into the probe using DNA or RNA polymerases. Gebeyehu et al. (*4*) have shown that N-6-substituted deoxyadenosine and N-4-substituted deoxycytidine triphosphates can also be used to label DNA with biotin. Transamination of cytidine residues has also been reported as a means of biotinylating nucleic acids (*5*). A photoactivatable biotinylation reagent has also been used to label nucleic acid (*6*); however, the site of biotinylation is unknown. Recently, Dattagupta et al. (*7*) described the biotinylation of nucleic acid using a biotinylated angelicin derivative in a photochemical labeling reaction.

We have been interested in using a derivatized purine nucleotide bearing a biotin as a means of labeling DNA probes without severly affecting the T_m of the duplex formed by the labeled probe and its target. This could serve the purpose of allowing more label incorporation (when used with the commercially available pyrimidine nucleotide) and of establishing the optimal structural parameters for the placement of labels in the probes. The only published procedure for incorporating a biotinylated purine into nucleic acid utilized an N-6-substituted deoxyadenosine triphosphate (*4*). However, Gebeyehu et al. (*4*) showed that the $C_0t_{1/2}$ (time taken for half the probe to reanneal at a given concentration) was significantly reduced for probes containing N-6-substituted adenine. Presumably, the reduced rate of reannealing was due to attachment of the biotin to an H-bonding site (N-6) of the nucleotide.

Recently, Seela and Driller (*8*) synthesized oligodeoxynucleotides containing 8-aza-7-deaza-2′-deoxyguanosine (6-amino-1-(2-deoxy-β-D-*erythro*-pentofuranosyl)-1*H*-pyrazolo[3,4-*d*]pyrimidin-4-one) and showed that the T_m was increased as compared to those of unmodified oligodeoxynucleotides.

In the present paper we report the synthesis of a representative of a novel class of derivatized purine deoxynucleotide analogues, the 3-substituted pyrazolo[3,4-*d*]-pyrimidin-4-amine deoxyribonucleotides. The use of this nucleotide, bio-13-dAPPTP (**9**), for enzymatic labeling of DNA and colorimetric detection of hybridization on slot blots is also described. Bio-13-dAPPTP (**9**) and the commercially available N-6-substituted deoxyadenosine nucleotide (biotin-7-dATP, **10**; Chart I) were incorporated into a short oligonucleotide by a primer extension reaction to study the effect of the nucleotide incorporation on the T_m.

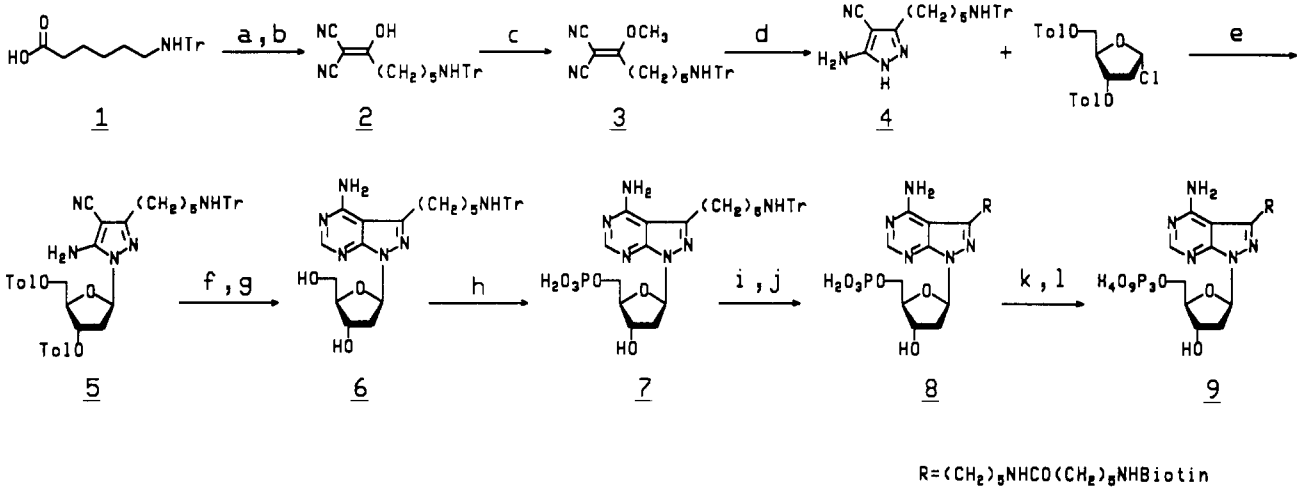
EXPERIMENTAL PROCEDURES

Unless otherwise specified, all reagents used in the syntheses were purchased from Aldrich Chemical Co. *N*-Biotinyl-6-aminocaproic acid N-succinimide ester, 5-bromo-4-chloroindoyl 3-phosphate, nitro blue tetrazolium, and bio-11-dUTP were from Sigma Chemical Co. Biotin-7-dATP was purchased from Bethesda Research Laboratories. Radionucleotides were purchased from ICN Radiochemicals. Nucleotides used for polymerase reactions were from Pharmacia. DNase was purchased from ICN Pharmaceuticals, DNA polymerase I and Sequenase II (genetically engineered T7 DNA polymerase) were from US Biochemicals. 10X-DP consists of 1 M Tris, pH 7.5 (20 mL), 0.5 M DTT (80 μL), 1 M $MgCl_2$ (2.8 mL), and H_2O (17 mL); SDS/FW is 0.09 M sodium chloride, 50 mM Tris (pH 7.6), 25 mM EDTA, and 0.1% SDS; TNTG is 100 mM Tris (pH 7.5), 100 mM sodium chloride, 0.5% Triton X-100, and 1.0% liquid gelatin; TMNZ is 100 mM Tris (pH 8.5), 50 mM magnesium chloride, 100 mM sodium chloride, and 0.1 mM zinc chloride; AP (alkaline phosphatase) substrate solution is 1 mM 5-bromo-4-chloroindoyl 3-phosphate, 1 mM nitro blue tetrazolium, and 0.01% Tween 20 in TMNZ.

Melting points were determined on a Mel-Temp melting point apparatus and are uncorrected. Nuclear magnetic

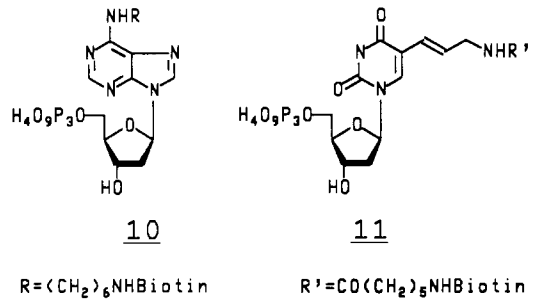
1043-1802/91/2902-0441$02.50/0 © 1991 American Chemical Society

Scheme I[a]



[a] (a) *i*-BuOCOCl/Et_3N/0 °C; (b) $(CN)_2CH_2/Et_3N$; (c) CH_2N_2; (d) NH_2NH_2/MeOH; (e) NaH/CH_3CN; (f) $(EtO)_2CHOAc$; (g) NH_3/MeOH; (h) $POCl_3/(MeO)_3PO$; (i) EtOH/cyclohexadiene/$Pd(OH)_2$/carbon; (j) biotinyl-$NH(CH_2)_5CONHS$; (k) CDI/DMF; (l) $(Bu_3NH^+)_4(O_3POPO_3^{4-})$.

Chart I. Schematic Representation of Bio-7-dATP (10) and Bio-11-dUTP (11)



resonance (NMR) spectra were obtained at 300 MHz on a Varian VXR-300 spectrometer. The chemical shift values are expressed in δ values (parts per million) relative to tetramethylsilane as an internal standard. Infrared spectra (IR) were recorded on a Perkin-Elmer 783 spectrophotometer. Ultraviolet spectra (UV) were recorded on a Beckman DU-40 spectrophotometer. Elemental analyses were performed by Robertson Laboratories. Thin-layer chromatography was run on silica gel 60 F-254 (EM Reagents) aluminum-backed plates. EM Reagents silica gel (230–400 mesh) was used for flash column chromatography (*9*), using 50 mm × 20 cm columns. Components were detected on TLC by UV light and with 5% H_2SO_4 in MeOH spray followed by heating. Evaporations were carried out under reduced pressure with a bath temperature below 30 °C.

***N*-Trityl-6-aminocaproic Acid (1).** 6-Aminocaproic acid (26 g, 0.2 mmol) was dissolved in dichloromethane (200 mL) by the addition of triethylamine (100 mL). Trityl chloride (120 g, 0.45 mmol) was added and the solution stirred for 36 h. The resulting solution was washed with 1 N HCl (500 mL) and the organic layer evaporated to dryness. The residue was suspended in 2-propanol/1 N NaOH (300 mL/100 mL) and refluxed for 3 h. The solution was evaporated to a thick syrup and added to dichloromethane (500 mL). Water (500 mL) was added and the aqueous layer adjusted to pH 2–3 with concentrated HCl. The phases were separated, and the organic layer was dried over sodium sulfate and evaporated to dryness. The residue was suspended in 2-propanol (250 mL), heated to reflux, cooled, and filtered to give 43.5 g (58%) of 1. Recrystallization from water gave analytically pure material: mp 126–127 °C. Anal. Calcd for $C_{25}H_{27}NO_2 \cdot 2.5H_2O$: C, 71.74; H, 7.71; N, 3.35; Found: C, 71.43; H, 7.53; N, 3.14.

***N*-Trityl-2-[(5-aminopentyl)hydroxymethylene]-malononitrile (2).** To a dichloromethane solution (500 mL) of 1 (20.0 g, 53 mmol) and triethylamine (20 mL) cooled in an ice/water bath was added dropwise over 30 min isobutyl chloroformate (8.3 mL, 64 mmol). After stirring for 2 h in an ice/water bath, freshly distilled malononitrile (4.2 g, 64 mmol) was added all at once. The solution was stirred for 2 h in an ice/water bath followed by stirring for 2 h at ambient temperature. The dichloromethane solution was washed with ice-cold 2 N HCl (300 mL) and the biphasic mixture filtered to remove product (13.2 g). The phases were separated, and the organic layer was dried and evaporated to a thick syrup. The syrup was covered with dichloromethane and on standing deposited fine crystals of product. The crystals were filtered and dried to give 6.3 g for a total yield of 19.5 g (87%): mp 167–170 °C dec; IR (KBr) 2170, 2190 (CN), 1710 (C=O), 1610 (C=COH) cm^{-1}. Anal. Calcd for $C_{28}H_{27}N_3O \cdot 0.5H_2O$: C, 78.11; H, 6.56; N, 9.76; Found: C, 78.26; H, 6.66; N, 9.33.

***N*-Trityl-2-[(5-aminopentyl)methoxymethylene]-malononitrile (3).** A suspension of **2** (13 g, 31 mmol) in ether/dichloromethane (900 mL/100 mL), cooled in an ice/water bath, was treated with a freshly prepared ethereal solution (300 mL) of diazomethane (from 50 mmol of Diazald). The solution was stirred for 6 h and then neutralized with acetic acid (10 mL). The solution was evaporated to dryness and the residue chromatographed on silica gel using dichloromethane/acetone (4/1) as the eluent. Fractions containing product were pooled and evaporated to a syrup. The syrup was triturated with dichloromethane to induce crystallization. The crystals were filtered and dried to give 8.3 g (61%) of chromatographically pure **3**: mp 105–106 °C; IR (KBr) 2220 (CN) cm^{-1}.

5-Amino-3-(*N*-trityl-5-aminopentyl)pyrazole-4-carbonitrile (4). To a methanol solution (100 mL) of **3** (7.0 g, 16 mmol) in an ice/water bath was added hydrazine monohydrate (7.8 mL, 160 mmol) dropwise over 15 min. After stirring for 30 min in an ice/water bath the solution was evaporated to dryness. The residue was suspended in cold methanol and filtered to give 7.1 g (100%) of **4** after drying. An analytical sample was prepared by recrystallization from water: mp 126–127 °C; ^1H NMR

($CDCl_3$) δ 7.60–7.10 (15 H, m, trityl arom H), 4.11 (2 H, s, NH_2), 2.64 (2 H, t, $(CH_2)_4CH_2NHTr$, J = 7.5 Hz), 2.13 (2 H, t, $CH_2(CH_2)_4NHTr$, J = 7.5 Hz), 1.7–1.3 (6 H, 3 m, $CH_2(CH_2)_3CH_2NHTr$); IR (KBr) 2220 (CN) cm^{-1}. Anal. Calcd for $C_{28}H_{29}N_5 \cdot 0.75H_2O$: C, 74.89; H, 6.85; N, 15.59; Found: C, 74.96; H, 6.77; N, 15.59.

5-Amino-1-(2-deoxy-3,5-di-*O*-toluoyl-β-D-*erythro*-pentofuranosyl)-3-(*N*-trityl-5-aminopentyl)pyrazole-4-carbonitrile (5). An ice-cold acetonitrile solution (250 mL) of **4** (3.5 g, 8 mmol) was treated with sodium hydride (60% dispersion in oil, 384 mg, 9.6 mmol) and stirred for 30 min at 0–4 °C. 1-Chloro-1,2-dideoxy-3,5-di-*O*-toluoyl-ribofuranose (3.5 g) was added and the solution stirred for 1 h at 0–4 °C. The solution was poured into a saturated solution of sodium bicarbonate (200 mL) and extracted with dichloromethane (3 × 100 mL). The organic layer was dried over anhydrous sodium sulfate and evaporated to dryness. The residue was flash chromatographed on silica gel using toluene/ethyl acetate (5/1) as eluent. Two major products were isolated and identified as the N-1 (**5**) (R_f = 0.25) and N-2 (R_f = 0.31) isomers in 57% (3.6 g) and 20% (1.2 g) yields, respectively. An additional 1 g of the N-2-isomer contaminated with a small amount of the N-1-isomer was also collected. The overall yield of glycosylated material was 5.8 g (92%). The N-1-isomer, **5**, was used without further purification: ^1H NMR ($CDCl_3$) δ 7.90–7.1 (23H, m, arom, H), 6.01 (1 H, t, H-1′, J = 6.40 Hz), 5.66 (1, H, m, H-4′), 4.6–4.4 (3 H, m, H-3′ + H-4′), 3.31–2.56 (2 H, m, H-2′$_{a,b}$), 2.43 + 2.41 (6 H, 2 s, 2 × CH_3), 2.5–1.2 (10 H, m, $(CH_2)_5$); N-2-isomer: ^1H NMR ($CDCl_3$) δ 7.90–7.1 (23 H, m, arom H), 5.97 (1 H, t, H-1′, J = 5.86 Hz), 5.80 (1 H, m, H-4′), 4.6–4.4 (3 H, m, H-3′ + H-4′), 3.35–2.50 (2 H, m, H-2′$_{a,b}$), 2.43 + 2.41 (6 H, 2 s, 2 × CH_3), 2.81–1.2 (10 H, m, $(CH_2)_5$).

1-(2-Deoxy-β-D-*erythro*-pentofuranosyl)-3-(*N*-trityl-5-aminopentyl)-1*H*-pyrazolo[3,4-*d*]pyrimidin-4-amine (6). To a toluene (100 mL) solution of **5** (3.5 g, 4.4 mmol) was added diethoxymethyl acetate (1.1 mL, 6.7 mmol). The solution was kept at 80–90 °C for 5 h and then evaporated to a syrup. The syrup was dissolved in dichloromethane (10 mL) and added to ice-cold methanolic ammonia (100 mL) in a glass pressure bottle. After 2 days at ambient temperature the contents of the bottle were evaporated to dryness. The residue was dissolved in methanol and adjusted to "pH 8" (using moist pH paper as indicator) with freshly prepared sodium methoxide to complete the deprotection. After stirring overnight the solution was treated with Dowex-50 H^+ resin, filtered, and evaporated to dryness. The residue was dissolved in MeOH (25 mL) and adsorbed onto silica gel (10 g) and loaded onto the top of a silica gel column. The column was eluted using acetone/hexane (3/2) as eluent to give 2.0 g (77%) of analytically pure **6**: ^1H NMR (DMSO-d_6) δ 8.14 (1 H, s, H-6) 7.40–7.10 (15 H, m, trityl arom H), 6.49 (1 H, t, H-1′, J = 6.60 Hz), 5.24 (1 H, d, 3′-OH), 4.82 (1 H, t, 5′-OH), 4.42 (1 H, m, H-4′) + other sugar and side-chain protons; UV λ_{max} (pH 1) 257 nm (ε 5300), (pH 7) 258 (ε 12 600), 274 (ε 11 500), (pH 11) 257 (ε 9500), 277 (ε 8400). Anal. Calcd for $C_{34}H_{38}N_6O_3 \cdot 0.25H_2O$; C, 70.02; H, 6.65; N, 14.41; Found: C, 69.95; H, 6.39; N, 14.62.

1-(2-Deoxy-β-D-*erythro*-pentofuranosyl)-3-(*N*-trityl-5-aminopentyl)-1*H*-pyrazolo[3,4-*d*]pyrimidin-4-amine 5′-Monophosphate (7). To an ice-cold solution of **6** (1.15 g, 2 mmol) in trimethyl phosphate (25 mL) was added phosphoryl chloride (225 μL, 2.4 mmol) and the solution was kept at 0–4 °C. The reaction was monitored by reversed-phase HPLC using a linear gradient from 0 to 100% acetonitrile in water over 25 min. After stirring for 5 h, an additional aliquot of phosphoryl chloride (50 μL) was added and the solution stirred another 5 h while being warmed to room temperature. The solution was poured into 0.1 M sodium bicarbonate (200 mL) and kept in the cold overnight. The solution was then extracted with ether and the aqueous layer lyophilized. The residue was dissolved in water (5 mL) and purified by reversed-phase HPLC using a 22 mm × 50 cm C18 column. The column was equilibrated in 0.5 M ammonium bicarbonate and eluted with a gradient of 0–100% acetonitrile over 20 min. Fractions containing the desired material were pooled and lyophilized to give 530 mg (56%) of chromatographically pure nucleotide. This material was used without further purification.

3-[5-[(*N*-Biotinyl-6-aminocaproyl)amino]pentyl]-1-(2-deoxy-β-D-*erythro*-pentofuranosyl)-1*H*-pyrazolo-[3,4-*d*]pyrimidin-4-amine 5′-Monophosphate (8). To a solution of **7** (530 mg) in 70% ethanol (200 mL) were added palladium hydroxide on carbon (400 mg) and cyclohexadiene (10 mL). The resulting mixture was refluxed for 72 h [additional amounts of palladium hydroxide on carbon (400 mg) and cyclohexadiene (10 mL) were added at 6 and 12 h], filtered, and evaporated to dryness. The residue was washed with dichloromethane, dissolved in DMF/H_2O (25 mL/5 mL) containing triethylamine (150 μL), and treated with N-succinimidyl 6-(biotinylamino)-caproate (450 mg). After stirring for 72 h the reaction mixture was evaporated to dryness and suspended in hot 2-propanol to remove *N*-hydroxysuccinimide and 6-(biotinylamino)caproic acid. The residue was filtered and dried to give 485 mg of analytically pure **8**: UV λ_{max} (pH 1) 253 nm (ε 7900), (pH 7 + pH 11) 258 (ε 8250), 274 (ε 8650). Anal. Calcd for $C_{31}H_{50}N_9O_9PS \cdot NH_3 2.0H_2O$: C, 46.03; H, 7.10; N, 17.32; S, 3.96; Found: C, 46.35; H, 6.82; N, 17.33; S, 3.86.

3-[5-[(*N*-Biotinyl-6-aminocaproyl)amino]pentyl]-1-(2-deoxy-β-D-*erythro*-pentofuranosyl)-1*H*-pyrazolo-[3,4-*d*]pyrimidin-4-amine 5′-Triphosphate (9). Monophosphate **8** (350 mg, 0.43 mmol) was dissolved in DMF with the addition of tributylamine (500 μL). 1,1′-Carbonyldiimidazole (350 mg, 2.0 mmol) was added and the solution was stirred at ambient temperature for 18 h. The solution was treated with methanol (1.5 mL) and after stirring for 30 min tributylammonium pyrophosphate (750 mg in 0.5 mL in DMF) was added. After stirring for 10 h another aliquot of tributylammonium pyrophosphate was added and the solution stirred overnight. The reaction mixture was evaporated to dryness and the residue dissolved in H_2O and applied to the top of a Sephadex-DEAE-A25 (HCO_3^- form, 3 cm i.d. × 10 cm) column equilibrated in water. The column was washed with H_2O (100 mL) followed by a linear gradient from H_2O (1 L) to 1.5 M ammonium bicarbonate (1 L) at 2 mL/min; 10-mL fractions were collected. Fractions 90–125 were pooled and lyophilized. The residue was dissolved in concentrated ammonium hydroxide (100 mL) and kept at 50 °C in a glass pressure bottle for 18 h to remove *N*-4-acyl groups. The ammonium hydroxide solution was lyophilized to give 525 mg of chromatographically pure **9**: UV λ_{max} (pH 1) 253 nm (ε 7900), (pH 7 + pH 11) 258 (ε 8200), 274 (ε 8700).

3-(*N*-Trityl-5-aminopentyl)-1*H*-pyrazolo[3,4-*d*]pyrimidin-4-amine. A mixture of **4** (4.36 g, 10 mmol) and formamidine acetate (5.20 g, 50 mmol) in 2-propanol (100 mL) was heated at reflux for 3 h, after which additional formamidine acetate (5.20 g, 50 mmol) was added. The mixture was refluxed another 3 h. The reaction mixture was cooled to room temperature and evaporated to dryness. The residue was suspended in H_2O and extracted with

EtOAc (3 × 200 mL). The organic layer was dried (Na_2SO_4), filtered, and evaporated to dryness to give 2.52 g of analytically pure **10**. The aqueous layer was reextracted with EtOAc (3 × 200 mL), dried (Na_2SO_4), filtered, and evaporated to dryness to give another 1.73 g. The total yield was 4.25 g (95%) of an amorphous, chromatographically pure solid: ^{1}H NMR (DMSO-d_6) δ 12.90 (1 H, s, NH), 8.10 (1 H, s, H-6), 7.5–7.1 (15 H, m, trityl arom H), 2.9–1.3 (10 H, m, side chain H). UV λ_{max} (pH 1), 257 nm (ϵ 7100), (pH 7) 257 (ϵ 8800), 277 (ϵ 7400), (pH 11) 260 (ϵ 11 600), 278 (ϵ 10 000).

Preparation of Biotinylated DNA. Probe DNA, which was complementary to the human papillomavirus type 16 (HPV-16) genome, was prepared from recombinant inserts in a pBluescript cloning vector (i.e. pHPV-16 is a genomic sequence of human papillomavirus type 16 inserted into pBluescript). The probe DNA was then biotinylated by a nick-translation reaction (*1*).

Nick-Translation Reaction. To an ice-cold mixture of 10X-DP (4 μL), pHPV-16 (2 μL, 2.16 mg/mL), nucleotide mix (6 μL, 2 mM each of dGTP, dCTP, TTP, and bio-13-dAPPTP), and H_2O was added DNase (1 μL, 4 μg/mL) and DNA polymerase I (2.4 μL, 8 units/μL). The reaction mixture was incubated at 16 °C for 1 h. The DNA was purified by gel filtration on NAP-25 columns (Pharmacia). For comparison, probe was also prepared as above using a nucleotide mix of dATP, dGTP, dCTP,m and bio-11-dUTP.

Hybridization of Slot Blot Assays. Target DNA (pHPV-16 at 1.0, 0.10, 0.01, and 0.00 μg/slot, with each slot also containing 1 μg of salmon sperm DNA as a control for nonspecific binding) was denatured and slotted onto nitrocellulose filters which were then baked at 80 °C. The slotted target nucleic acids were hybridized to biotinylated probe (200 ng/mL) in hybridization solution (5 mL) for 24 h at room temperature. The filters were washed with SDS/FW (3 × 50 mL) and then incubated for 30 min in a TNTG solution of streptavidin/alkaline phosphatase (*10*) conjugate (2 μg/mL) at room temperature. After being washed three times (5 min per wash) in TMNZ at room temperature, the filters were incubated in AP substrate solution for about 60 min at 37 °C.

Preparation of Biotinylated Oligonucleotides. A ^{32}P-labeled (prepared using polynucleotide kinase (*11*)) 15-mer primer, 5′-GGATTGACAGATTGA-3′, was extended using its 21-mer complement, 3′-CCTAACTGTCTAACTCTCGAGAAA-5′, as the template. A single biotinylated nucleotide was incorporated into the 24-mer product 5′-GGATTGACAGATTGAGA*GCTCTTT-3′. Three biotins were incorporated into an 18-mer, 5′-ACTCCTACGGGA*GGCA*GCA*G-3′, by extending the ^{32}P-labeled 9-mer primer 5′-ACTCCTACG-3′ and using 3′-TGAGGATGCCCTCCGTCGTC-5′ as the template.

Primer Extension Reaction. To an ice-cold mixture of 10X-DP (9.6 μL), ^{32}P-labeled primer (10 μL, 8 pmol), cold primer (6.4 μL, 292 pmol), template (1.8 μL, 600 pmol), nucleotide mix (3 μL, 10 mM each of dGTP, dCTP, TTP, and either bio-13-dAPPTP, bio-7-dATP, or dATP), and H_2O (70 μL) was added T7 DNA polymerase (2.0 μL, 13 units/μL). The reaction mixtures were incubated at 37 °C for 28 h. Aliquots (4 μL) were taken at 0.25, 1, 4, 16, and 24 h, quenched by heating at 90 °C for 1 min, and then run on a 20% acrylamide, 7 M urea, 1 × TBE denaturing gel at 50 °C.

T_m Studies. ^{32}P-Labeled oligonucleotide (5 ng) from the primer extension reactions was heated to 80 °C to denature the product from the template. The biotinylated products were hybridized in 300-μL volumes at ambient temperature for 30 min with the appropriate template covalently immobilized on $^3/_{32}$ in. nylon beads (*12*). The beads were then washed three times with 1 mL of the 3 M GuSCN hybridization solution, three times with SDS/FW, and then once more with the respective hybridization solution. The beads were then placed in a 15 °C water bath in 300 μL of 3 M GuSCN hybridization solution. The T_m was determined as follows: The temperature of the water bath was raised in 5 °C intervals, the beads were equilibrated at the new temperature for 5 min, the solution was decanted into a scintillation vial, and then fresh hybridization solution was added to the beads. This process was repeated until the temperature reached 80 °C. Radioactivity was determined by scintillation counting.

To calculate the T_m, cumulative counts eluted at each temperature were plotted against temperature, and the temperature at which 50% of the ^{32}P-labeled oligonucleotide had melted off of the beads was taken as the T_m.

RESULTS AND DISCUSSION

Synthesis. The synthesis of 3-aminoalkyl-substituted 4-amino-1*H*-pyrazolo[3,4-*d*]pyrimidine deoxyribosides was approached by the ring closure of the preformed ditoluoyl-blocked pyrazole deoxyriboside. A modification of the method of Kobayashi et al. (*13*) was used to synthesize **4**. Treatment of 6-aminocaproic acid with trityl chloride in dichloromethane and triethylamine followed by hydrolysis of the trityl ester gave a good yield of *N*-trityl-6-aminocaproic acid (1). The carboxylic acid was activated with isobutyl chloroformate to give the mixed anhydride, which was treated with malononitrile to give enol **2** in high yield. Methylation of the enol with diazomethane followed by ring closure with hydrazine gave **4**. The heterocycle was directly glycosylated using the sodium salt procedure (*14*) to give a 2/1 mixture of what was later determined to be the N-1- (**5**) and N-2-isomers. Pyrazole nucleoside **5**, with the lower R_f, was treated with diethoxymethyl acetate and then simultaneously cyclized and deprotected with methanolic ammonia to yield **6**. A comparison of the UV spectra of **6** at pH 1, 7, and 11 with those of the parent heterocycle (formed by ring closure of the unribosylated pyrazole **4** with formamidine acetate), showed that they were identical, confirming the assignment of the site of glycosylation (*15*). Nucleoside **6**, with the alkylamine blocked with a trityl group, was phosphorylated using $POCl_3$ in trimethyl phosphate as described by Yoshikawa et al. (*16*). The resulting monophosphate was detritylated by catalytic hydrogenation and biotinylated with 6-(biotinamino)caproic acid *N*-succinimide ester. Triphosphate **9** was then obtained using the Hoard–Ott procedure (*17*). This procedure results in the acylation of the N-4-position, presumably via reaction of the exocyclic amine with carbonyldiimidazole, forming the methyl carbamate after treatment with MeOH. That the N-4-position had been modified was evidenced by a bathochromic shift in the UV spectra at pH 1, 7, and 11 (*18*). The N-4 modification was readily removed by treatment with concentrated ammonium hydroxide.

Nick-Translation Reactions. Bio-13-dAPPTP and bio-11-dUTP were each incorporated into pHPV-16 DNA by *Escherichia coli* DNA polymerase I in a standard nick-transition reaction (*1*). Biotinylated probe prepared with either bio-13-dAPPTP or bio-11-dUTP could detect 0.5 pg of target nucleic acid in a slot blot assay with a 1-h substrate development. P_1-Nuclease digestion of the labeled nucleic acid (labeled using either bio-13-dAPPTP or bio-11-dUTP as substrate) followed by HPLC analysis

Table I. T_m Values of Oligonucletides Containing Modified Adenine Bases

oligonucleotide[a]	biotinylated nucleotide (X)	T_m,[b] °C
5′-GGATTGACAGATTGAGXGCTCTTT-3′	bio-13-dAPP	31.5
5′-GGATTGACAGATTGAGXGCTCTTT-3′	bio-7-dA	30
5′-GGATTGACAGATTGAGXGCTCTTT-3′	dA	32.5
5′-ACTCCTACGGGXGGCXGCXG-3′	bio-13-dAPP	36
5′-ACTCCTACGGGXGGCXGCXG-3′	bio-7-dA	30
5′-ACTCCTACGGGXGGCXGCXG-3′	dA	40

[a] Modified adenine nucleotides are shown as X. [b] Average of three determinations (standard deviation < 0.5 °C).

of the monophosphates showed that the biotinylated nucleotide accounted for approximately 5% of the total nucleotide pool. These two results would indicate that the ability of the two biotinylated nucleoside triphosphates to serve as DNA polymerase I substrates is comparable, as is the ability of the resultant probes to hybridize to complementary strands.

Primer Extension Reactions. Bio-13-dAPPTP, bio-7-dATP, and dATP were compared in two primer extension reactions using T7 DNA polymerase (Sequenase II) that has been genetically engineered to have no exonuclease. In both sets of primer extension reactions, the reactions using dATP, bio-7-dATP, and bio-13-dAPPTP proceeded to completion in 0.25, 4, and 16 h, respectively. The difference in reactivity between the bio-7-dATP and the bio-13-dAPPTP may be due to steric effects by the larger sidearm on the bio-13-dAPPTP. A similar effect was observed by Gebeyehu et al. (*4*) in which the bio-7-dATP was a much better substrate than those biotinylated dATP analogues having much longer sidearms. Others have also observed (*19*) that reduction of the double bond in the side arm of bio-11-dUTP and reduction of the triple bond in the alkynyl substituted pyrimidine and 7-deazapurine nucleotides significantly inhibits their function as substrates in certain DNA polymerase reactions. The nature of the sidearm and the ability of these nucleotides to function as a substrate also appears to be dependent on the enzyme used. For example, we have found that bio-13-dAPPTP is efficiently used by both DNA polymerase I and the Klenow fragment. In contrast, 7-deazapurine nucleotides containing a fully saturated sidearm are substrates for DNA polymerase I but are poor substrates for the Klenow fragment (*19*). We have also found that Taq polymerase can readily incorporate 5-aminopropyl-dUTP (the nonbiotinylated precursor to bio-11-dUTP) but poorly utilizes bio-11-dUPT and does not utilize bio-13-dAPPTP at all.

Melting Temperatures (T_m). The products from the extension reactions were hybridized to immobilized template and the melting temperatures (T_m) were determined (Table I). The introduction of our bio-13-dAPP-modified nucleotides into the oligonucleotides reduced the T_m ~1 °C for each biotin incorporated. However, the T_m for the oligonucleotides containing the bio-7-dA was significantly lower (~3 °C/biotin incorporated) than the bio-13-dAPP-labeled oligonucleotide. This might be expected since the introduction of a linker arm at the H-bonding position at N-6 of the bio-7-dATP should perturb the stability of hybrid into which it is incorporated. Judging from this data, it would appear that the probes containing the 3-substituted pyrazolopyrimidines can hybridize more efficiently to complements.

CONCLUSIONS

The novel biotinylated dATP analogue reported here also shown to be a substrate for DNA polymerase I and T7 DNA polymerase, and could be used in the preparation of biotinylated DNA probes for nucleic acid hybridization assays. The biotin-labeled nucleic acid was shown to efficiently hybridize to complementary DNA on slot blots and could detect subpicogram quantities of target nucleic acid. The incorporated nucleotide was shown to have a minimal effect on the T_m of a hybrid formed between the biotinylated oligonucleotide and its complement. This is in contrast to the commercially available, bio-7-dATP, which was shown to more dramatically reduce the T_m of oligonucleotides into which it is incorporated. The new reagent is especially useful for applications in nonisotopic diagnostic kits utilizing DNA probe hybridization.

ACKNOWLEDGMENT

This work was supported by Grants R01 CA40336 and R44 CA45905 from the NIH, NCI, USPHS. We thank Drs. Howard Gamper and Dennis Schwartz for useful discussions.

LITERATURE CITED

(1) Langer, P. R., Waldrop, A. A., and Ward, D. C. (1981) Enzymatic Synthesis of biotin-labeled polynucleotides: Novel nucleic acid affinity probes. *Proc. Natl. Acad. Sci. U.S.A. 78*, 6633–6637.

(2) Brigati, D. J., Myerson, D., Leary, J. J., Spalholz, B., Travis, S. Z., Fong, C. K. Y., Hsiung, G. D., and Ward, D. C. (1983) Detection of viral genomes in cultured cells and paraffin-embedded tissue sections using biotin-labeled hybridization probes. *Virology 126*, 32–50.

(3) Nelson, P. S., Bahl, C., and Gibbons, I. (1986) Convenient preparation of a new C-5 biotinylated dUTP derivative. *Nucleosides Nucleotides 5*, 233–241.

(4) Gebeyehu, G., Rao, P. Y., SooChan, P., Simms, D. A., and Klevan, L. (1987) Novel biotinylated nucleotide-analogs for labeling and colorimetric detection of DNA. *Nucleic Acids. Res. 15*, 4513–4534.

(5) Viscidi, R. P., Connelly, C. J., and Yolken, R. H. (1986) Novel chemical method for the preparation of nucleic acid for non-isotopic hybridization. *J. Clin. Microbiol. 23*, 311–317.

(6) Forster, A. C., McInnes, J. L., Skingle, D. C., and Symons, R. H. (1985) Non-radioactive hybridization probes prepared by the chemical labeling of DNA and RNA with a novel reagent, photobiotin. *Nucleic Acids Res. 13*, 745–761.

(7) Albarella, J. P., Minegar, R. L., Patterson, W. L., Dattagupta, N., and Carlson, E. (1989) "Monoadduct forming photochemical reagents for labeling nucleic acids for hybridization. *Nucleic Acids Res. 17*, 4293–4308.

(8) Seela, F., and Driller, H. (1989) Alternating d(G-C)$_3$ and d(C-G)$_3$ hexanucleotides containing 7-deaza-2′-deoxyguanosine or 8-aza-7-deaza-2′-deoxyguanosine in place of dG. *Nucleic Acids Res. 17*, 901–910.

(9) Still, W. C., Kahn, M., and Mitra, A. (1978) Rapid chromatographic technique for preparative separations with moderate resolution. *J. Org. Chem. 43*, 2923–2925.

(10) The alkaline phosphatase/streptavidin conjugate was prepared in-house by proprietary methods.

(11) Sambrook, J., Fritsch, E. F., and Maniatis, T. (1989) *Molecular Cloning: A Laboratory Manual*, 2nd ed. (N. Irwin, Ed.) Cold Spring Harbor Laboratory Press, Cold Spring Harbor, NY.

(12) Van Ness, J., Kalbfleisch, S., Petrie, C. R., Reed, M. W.; Tabone, J., and Vermeulen, N. M. J. (1991) A versatile solid support system for oligonucleotide probe-based hybridization assays. *Nucleic Acids Res. 19*, 3345–3350.

(13) Kobayashi, S. (1973) The synthesis and xanthine oxidase inhibitory activity of pyrazolo[3,4-*d*]pyrimidines. *Chem. Pharm. Bull. 21*, 941–951.

(14) Kazimierczuk, Z., Cottam, H. B., Revankar, G. R., and Robins, R. K. (1984) Synthesis of 2′-deoxytubercidin, 2′-deoxyadenosine, and related 2′-deoxynucleosides via a direct stereospecific sodium salt glycosylation procedure. *J. Am. Chem. Soc. 106*, 6379–6384.

(15) Earl, R. A., Pugmire, R. J., Revankar, G. R., and Townsend, L. B. (1975) A chemical and carbon-13 nuclear magnetic resonance reinvestigation of the N-methyl isomers obtained by direct methylation of 5-amino-3,4-dicyanopyrazole and the synthesis of certain pyrazolo[3,4-*d*]pyrimidines. *J. Org. Chem. 40*, 1822–1828.

(16) Yoshikawa, M., Kato, T., and Takenishi, T. (1967) A novel method for phosphorylation of nucleosides to 5′-nucleotides. *Tetrahedron Lett. 50*, 5065–5067.

(17) Hoard, D. E., and Ott, D. G. (1965) Conversion of mono- and oligodeoxyribonucleotides to 5′-triphosphates. *J. Am. Chem. Soc. 87*, 1785–1788.

(18) Hecht, S. M., Frye, R. B., Werner, D., Fukui, T., and Hawrelak, S. D. (1976) Synthesis and biological activity of pyrazolo[3,4-*d*]pyrimidine nucleosides related to tubercidin, toyocamycin, and sangivamycin. *Biochemistry 15* (5), 1005–1015.

(19) Du Pont Co., Instrument Systems, technical service department.

Generation of 5-Fluorouracil from 5-Fluorocytosine by Monoclonal Antibody–Cytosine Deaminase Conjugates

Peter D. Senter,* Peter C. D. Su, Tohoru Katsuragi,† Takuo Sakai,† Wesley L. Cosand, Ingegerd Hellström, and Karl Erik Hellström

Oncogen Division of the Bristol-Myers Squibb Pharmaceutical Research Institute, 3005 First Avenue, Seattle, Washington 98121, and University of Osaka Prefecture, College of Agriculture, Mozuumemachi, Sakai, Osaka, 591 Japan. Received June 24, 1991

Cytosine deaminase (CDase) catalyzes the conversion of cytosine to uracil and is also able to convert the clinically used antifungal agent 5-fluorocytosine (5FC) into the anticancer drug 5-fluorouracil (5FU). The enzyme was purified from bakers' yeast in a six-step procedure. Studies indicated that bakers' yeast CDase had a molecular weight of approximately 32 kDa and was composed of two subunits of equal molecular weights. Monoclonal antibodies were covalently attached to CDase, forming conjugates that could bind to antigens on tumor cell surfaces. The combination of L6-CDase and 5FC was equivalent in cytotoxic activity to 5FU when tested against the H2981 human lung adenocarcinoma cell line (L6 positive, 1F5 negative). 5FC alone was noncytotoxic. The activation of 5FC was immunologically specific since 1F5-CDase did not enhance 5FC activity.

INTRODUCTION

Many of the drugs that are utilized in cancer chemotherapy have dose-limiting side effects that can lead to the destruction of nontarget tissues (*1*). As a result, much effort has been directed toward the discovery of pharmacologically inactive anticancer drug precursors (prodrugs) that can be activated by enzymes or physiological conditions preferentially found in cancer cells and tumor masses (*2–4*). For example, prodrugs have been developed to take advantage of the hypoxic nature of solid tumors (*5–7*), or the presence in some tumors of high levels of enzymes such as plasminogen activator (*8*). Unfortunately, progress in the development of such anticancer prodrugs for the clinic has been hindered by the lack of a suitable target for drug activation that is abundantly present within tumors compared to normal tissues.

We (*9–12*) and others (*13*, *14*) have recently described approaches to prodrug activation in which monoclonal antibodies (mAbs)[1] that bind to tumor-associated antigens are used to localize enzymes at tumor masses. The enzymes are selected for their abilities to convert prodrugs into active anticancer drugs. mAbs have been covalently attached to enzymes such as alkaline phosphatase (*10*, *11*), carboxypeptidase G2 (*13*), penicillin amidase (*12*), and β-lactamase (*14*) for the activation of a wide range of prodrugs. Significant antitumor activities have been reported.

One of the uncertainties surrounding the prodrug substrates for mAb–enzyme conjugates is that nothing is known about their pharmacological properties and toxicities in humans. Because of this, there may be advantages in utilizing anticancer prodrugs that have well-understood clinical properties. This paper describes the conversion of the clinically used antifungal agent 5-fluorocytosine (5FC) into the known antitumor drug 5-fluorouracil (5FU) by mAb–cytosine deaminase (mAb–CDase) conjugates. The properties of both CDase and mAb–CDase conjugates, and the in vitro activities of mAb–CDase in combination with 5FC, are presented.

EXPERIMENTAL PROCEDURES

Materials. The antibodies used were L6 (IgG2a), which binds to an antigen on human carcinomas (*15*), and 1F5 (IgG2a), which binds to the CD20 antigen on normal and neoplastic B-cells (*16*). The cell line H2981 was established at Oncogen from a human lung adenocarcinoma. Fluorescence activated cell sorter analysis indicates that L6 binds strongly to H2981 cells, whereas 1F5 shows very weak binding.

Purification of CDase. CDase was purified from Fleishmann's compressed bakers' yeast using procedures related to those of Katsuragi and co-workers (*17*). All steps in the purification were carried out at 4 °C. The enzyme activity was determined with cytosine or 5FC at 3 mM in phosphate-buffered saline (PBS) at 37 °C as described earlier (*18*). Solutions of the enzyme were added, and the course of reaction was monitored spectrophotometrically on aliquots that were quenched with 0.1 N HCl. The millimolar concentrations of the drugs were calculated as follows: $[5FC] = 0.119 \times A_{290} - 0.025 \times A_{255}$; $[5FU] = 0.185 \times A_{255} - 0.049 \times A_{290}$; $[\text{cytosine}] = 0.110 \times A_{280} - 0.024 \times A_{250}$; $[\text{uracil}] = 0.158 \times A_{250} - 0.049 \times A_{280}$. One unit of enzyme activity is defined as 1 μmol of 5FU formed/min at 37 °C. Protein concentrations were measured using the BCA assay available from Pierce (Rockford, IL). The step-by-step results of the purification are shown in Table I.

Step 1. Preparation of Yeast Autolysate. Bakers' yeast (2.25 kg) was mixed with ethyl acetate (225 mL) and stirred for 30 min. To this was added 2.25 L of 50 mM potassium phosphate buffer at pH 7.2 containing 15% $(NH_4)_2SO_4$, 5 mM EDTA, and 0.1 mM dithiothreitol (DTT). The mixture was stirred for 3 days and the pH was adjusted daily to pH 7.2 with solid tris(hydroxymethyl)aminomethane (Tris). The cell debris was removed by centrifugation at 17700*g* for 15 min.

Step 2. Ammonium Sulfate Fractionation. Protein was precipitated from the supernatant of step 1 by

* Author to whom correspondence should be addressed at Oncogen.

† University of Osaka Prefecture.

[1] Abbreviations used: 5FC, 5-fluorocytosine; 5FU, 5-fluorouracil; CDase, cytosine deaminase; DTT, dithiothreitol; EDTA, ethylenediaminetetraacetic acid; mAb, monoclonal antibody; PBS, phosphate-buffered saline, pH 7.2; SDS–PAGE, sodium dodecyl sulfate polyacrylamide gel electrophoresis; Tris, tris(hydroxymethyl)aminomethane.

1043-1802/91/2902-0447$02.50/0 © 1991 American Chemical Society

Table I. Purification of CDase from 2.25 kg of Bakers' Yeast

step	total protein[a] (mg)	total activity[b] (units)	specific activity (units/mg)	fold purification
1. cell-free extract	120000	1750	0.014	1
2. $(NH_4)_2SO_4$	36000	1270	0.035	2.5
3. Q-Sepharose	4200	685	0.16	11.4
4. G-75 Sephadex	184	648	3.5	250
5. octyl-Sepharose	20	495	25	1800
6. G-75-Sephadex	6	394	67	4800

[a] Protein concentration determined using a BCA assay (Pierce). [b] One unit of enzyme activity is defined as 1 μmol 5FU formed/min at 37 °C.

adjusting the EDTA concentration to 5 mM and adding $(NH_4)_2SO_4$ to a final concentration of 70% saturation. After 16 h, the precipitate was collected by centrifugation. The pellet was dissolved in 1.5 L of 50 mM potassium phosphate at pH 7.2 containing 5 mM EDTA and 0.1 mM DTT, and dialysis against this buffer was allowed to proceed overnight. Additional $(NH_4)_2SO_4$ was added to reach 50% saturation. After 1 h, the precipitate was centrifuged and additional $(NH_4)_2SO_4$ was added to the supernatant so that the final concentration of $(NH_4)_2SO_4$ was 73% saturation. The precipitate was collected, dissolved in 1 L of 20 mM Tris buffer at pH 8.0 containing 0.1 mM DTT, and dialyzed extensively with this buffer.

Step 3. Anion-Exchange Chromatography. The dialysate from step 2 (1.5 L) was applied to a 4.8 × 25 cm Q-Sepharose (Pharmacia) column equilibrated with 20 mM Tris containing 0.1 mM DTT at pH 8.0. The column was washed with 900 mL of 20 mM Tris containing 0.1 mM DTT, and the enzyme was eluted with a linear gradient (1 L each) of 0–0.3 M KCl in the above buffer. The fractions containing CDase activity were pooled and concentrated to approximately 20 mL by ultrafiltration (Amicon, PM-30 filter).

Step 4. Gel-Permeation Chromatography. The CDase from step 3 was applied to a G-75 Sephadex column (2.5 × 100 cm) and eluted with PBS containing 0.1 mM DTT. The fractions containing CDase activity were pooled and then dialyzed against 4 L of 100 mM potassium phosphate buffer containing 1.8 M $(NH_4)_2SO_4$ at pH 7.0.

Step 5. Hydrophobic Interaction Chromatography. The material from step 4 was applied to a 2.5 × 15 cm octyl-Sepharose (Pharmacia) column equilibrated with 100 mM potassium phosphate containing 1.8 M $(NH_4)_2SO_4$ at pH 7.0. The enzyme was eluted with a linear gradient (300 mL each) of 1.8–0 M $(NH_4)_2SO_4$ in 100 mM potassium phosphate at pH 7.0. The fractions containing CDase activity were combined and concentrated by ultrafiltration (Amicon, YM-5 filter).

Step 6. Gel-Permeation Chromatography. A final gel filtration of the material from step 5 on G-75 Sephadex using PBS as eluant was performed as described in step 4. The purified enzyme was concentrated by ultrafiltration and stored at −70 °C.

Preparation of mAb–CDase Conjugates. To a solution of CDase (2 mL at 1.5 mg/mL) in 100 mM sodium phosphate at pH 7 was added 100 μL of succinimidyl 4-(*N*-maleimidomethyl)cyclohexane-1-carboxylate (Pierce, 20 mM in DMF). After 30 min at 30 °C, the protein was separated from low molecular weight materials on a G-25 Sephadex column that was eluted with 40 mM sodium phosphate containing 500 mM NaCl at pH 7.2.

Thiol groups were introduced into the mAbs, L6 and 1F5 (1–2 thiols/protein molecule), as previously described (*10*). The maleimide- and thiol-modified proteins were combined immediately following preparation and characterization in a 1:1 molar ratio and allowed to stand at 4 °C overnight. The conjugates were purified by gel filtration on S-300 Sepharose (Pharmacia) at 4 °C using PBS as eluant. Fractions were monitored at 280 nm and for CDase activity as previously described. Those fractions consisting mainly of 1:1 mAb–CDase adducts by sodium dodecyl sulfate polyacrylamide gel electrophoresis (SDS–PAGE) were combined, concentrated by ultrafiltration (Amicon, PM-30 filter), and sterile filtered. At 4 °C the conjugates thus prepared were stable and showed no loss of enzyme activity after several weeks.

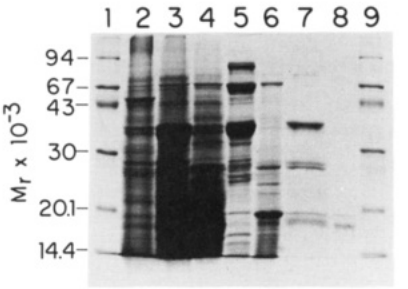


Figure 1. Composition of proteins (as determined on a 14% SDS–PAGE gel under nonreducing conditions) during CDase purification. Lanes 1 and 9, molecular weight standards; lane 2, autolysis supernatant (step 1, Table I); lane 3, 70% $(NH_4)_2SO_4$ precipitation (step 2, Table I); lane 4, 50–73% $(NH_4)_2SO_4$ precipitation (step 2, Table I); lane 5, Q-Sepharose chromatography (step 3, Table I); lane 6, G-75 Sephadex chromatography (step 4, Table I); lane 7, octyl-Sepharose chromatography (step 5, Table I); lane 8, G-75 Sephadex chromatography (step 6, Table I).

In Vitro Cytotoxicity Assays. H2981 cells in medium (Iscoves' modified Dulbeco's medium with 10% v/v fetal calf serum, 200 units/mL penicillin, 100 μg/mL streptomycin, and 2 mM glutamine) were plated into 96-well microtiter plates at 10 000 cells/well and allowed to adhere overnight at 37 °C. The cells were washed, and conjugate was added (100 μL at 10 μg/mL containing 10 unit/mg CDase activity) in medium. After 30 min at 4 °C, the cells were washed four times, and 0.15 mL of leucine-free RPMI media containing dilutions of 5FC was added to each of the wells. 5FU was added to cells untreated with conjugate. After 18 h at 37 °C, the cells were pulsed with [^{3}H]leucine (1 μCi in 50 μL of leucine-free RPMI), and incubation at 37 °C was continued for 6 h. The cells were frozen at −70 °C, thawed, and harvested onto glass fiber disks. The filters were counted on a Beckman 3701 scintillation counter.

RESULTS

Purification and Characterization of CDase. The six-step procedure used for the purification of CDase is shown in Table I. Starting from 2.25 kg of bakers' yeast, 6 mg of a highly purified preparation of CDase was obtained. This represents a 4800-fold purification, and a 22% overall recovery of enzyme activity.

SDS–PAGE analysis (nonreducing) of the protein sample obtained during enzyme purification is shown in Figure 1. Two distinct protein bands at 17 and 19 kDa were observed for the purified protein sample (lane 8) in a ratio of approximately 4:1. Complete separation of these two proteins has been achieved by reversed-phase HPLC (H. Marquardt, unpublished results). Analyses of the purified proteins indicated that the major band at 17 kDa possesses the CDase activity.

The molecular weight of CDase was determined, under nondenaturing conditions, by application of the purified

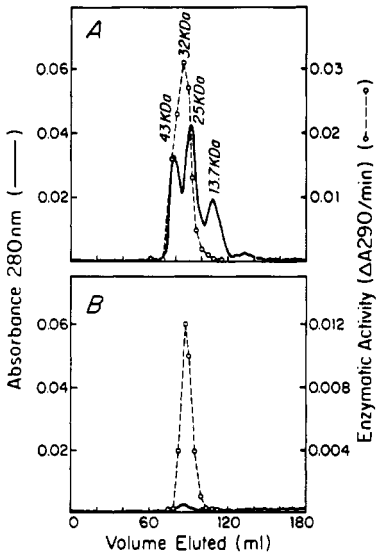


Figure 2. Elution of CDase off of G-50 Sephadex (1.5 × 100 cm). (A) 27 units of CDase (from step 6, Table I) was mixed with 2 mg each of ribonuclease A and ovalbumin and 1 mg of chymotrypsinogen A and eluted with PBS. Fractions were monitored at 280 nm, to determine total protein content, and at 290 nm using the CDase assay with 5FC as a substrate. (B) Elution of CDase off of the same G-50 Sephadex column without the calibration standards.

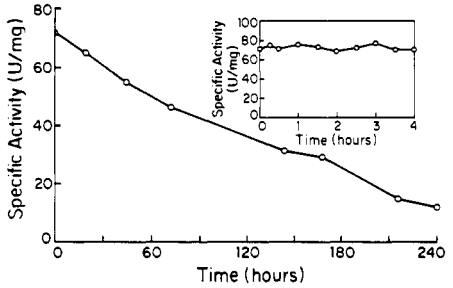


Figure 3. Stability of CDase at 37 °C. Purified CDase (from step 6, Table I) in PBS (0.04 mg/mL) containing protease-free BSA (1 mg/mL) was incubated at 37 °C in a polypropylene tube. At various intervals, the CDase activity was determined using 10 μL of the enzyme solution.

enzyme (lane 8, Figure 1) to a G-50 Sephadex column along with other calibration proteins (Figure 2). Fractions were monitored at 280 nm to measure total protein as well as for CDase activity using 5FC as a substrate. CDase activity was centered at 32 kDa, or approximately twice the molecular weight observed by SDS-PAGE (Figure 1). This is consistent with the purified enzyme existing in a dimeric noncovalently associated form, but does not rule out the possibility that a disulfide bond between the two chains was broken by reducing agents during purification. Under nondenaturing conditions, purified CDase contained no detectable free thiol groups. Prolonged storage (8 months at 4 °C in PBS) did not alter the enzyme's activity or composition by SDS-PAGE.

The stability of the CDase activity in the preparation (after step 6, Table I) was determined in PBS at pH 7.2. Using 5FC as a substrate, a slow decrease in enzyme activity was observed upon prolonged incubation at 37 °C (Figure 3). Under these conditions, the enzyme lost half of its activity after 5.2 days. There was no apparent loss of CDase activity in the first 4 h of incubation (Figure 3, inset).

CDase Immunoconjugates. Immunoconjugates of CDase (from step 4 in Table I) were prepared with the mAbs L6 (*15*) and 1F5 (*16*) using chemistry described

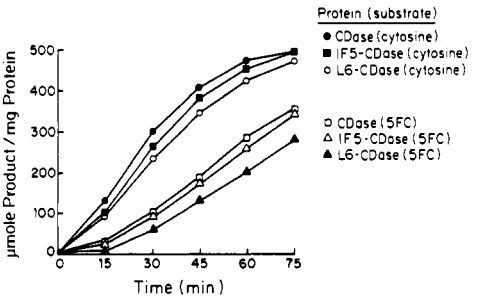


Figure 4. Activity of CDase and mAb-CDase conjugates using cytosine and 5FC (3 mM in PBS at 23 °C) as substrates. The free CDase solutions contained 5 μg/mL total protein from step 4, Table I. The protein concentrations in the mAb-CDase conjugates were corrected using the factor 35 kDa/195 kDa, which represents the proportion of CDase in the conjugate.

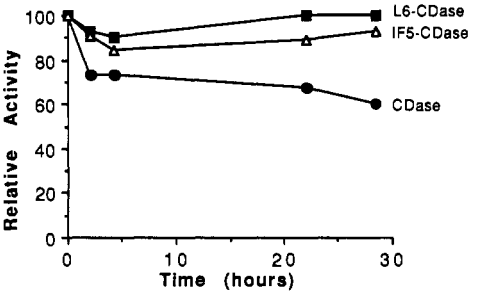


Figure 5. Stability of CDase and mAb-CDase conjugates at 37 °C. The conjugates and CDase (from step 4, Table I) in PBS were incubated at 37 °C. At various intervals, the CDase activity was determined on aliquots as described in the experimental section.

earlier for the preparation of alkaline phosphatase conjugates (*10*). Stable thioether bonds between the two proteins were formed by combining mAbs and CDase that were modified with thiols and maleimides, respectively. The crude conjugate preparations were purified by gel filtration and characterized by SDS-PAGE, CDase activity, and binding to cell surface antigens on human H2981 lung adenocarcinoma cells. Yields using this conjugation procedure are consistently around 20%. The remaining protein consists of high molecular weight aggregates, unconjugated material, and mixed fractions.

Fluorescence activated cell sorter analysis indicated that L6 bound strongly to the H2981 cells and that antigen saturation occurred at ca. 10 μg/mL. At this concentration, the L6-CDase/L6 linear fluorescence equivalence ratio was 120/158, indicating that the conjugate bound 82% as efficiently as the unmodified mAb. At a subsaturating concentration (1 μg/mL), the ratio was 67/75, again indicating good binding activity for the L6-CDase conjugate. 1F5-CDase showed no detectable binding up to an antibody concentration of 10 μg/mL.

Both the free enzyme and the mAb-CDase conjugates were capable of converting 5FC into 5FU and cytosine into uracil (Figure 4). The rates of product formation catalyzed by the conjugates were approximately equal to that with free CDase. Thus, there was no apparent loss in enzyme activity as a result of conjugation. The finding that the activity was somewhat lower with 5FC than with cytosine is consistent with what has been observed with CDase from *Escherichia coli* (*18*).

The stability of CDase activity in the mAb-CDase conjugates was compared to that of free CDase at 37 °C in PBS. After 29 h, the conjugates lost very little activity and under these conditions they were at least as active as the free enzyme (Figure 5). The thermal stability of CDase is not lost as a result of conjugation.

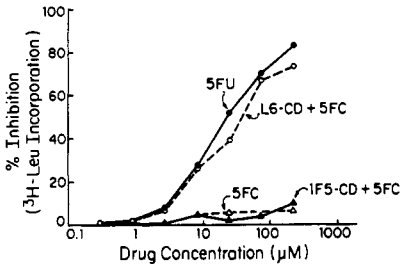


Figure 6. In vitro cytotoxicity of 5FC, 5FU, and mAb–CDase plus 5FC against H2981 cells.

In Vitro Cytotoxicity. The cytotoxic effects of 5FC, 5FU, and combinations of the mAb–CDase conjugates with 5FC were determined by measuring the incorporation of [^{3}H]leucine into the protein of H2981 cells (Figure 6). 5FU (IC_{50} = 20 μM) was much more cytotoxic than 5FC (noncytotoxic up to 200 mM). The combination of L6-CDase and 5FC proved to be as cytotoxic as 5FU. The nonbinding conjugate 1F5–CDase did not enhance the activity of 5FC.

DISCUSSION

5FU and its deoxyribonucleoside derivative are used extensively in the treatment of metastatic cancer, either as single agents or in combination chemotherapy (*19*). The drugs are toxic and frequently cause leukopenia and gastrointestinal disorders (*20*). In contrast, 5FC is lacking in antineoplastic activity and is used in humans for the treatment of fungal infections (*21*). This activity is most likely due to the conversion of the noncytotoxic prodrug 5FC into 5FU by the CDase present in the fungal cells, but not in mammalian cells (*22, 23*).

Localized generation of 5FU from 5FC has been achieved by surgically implanting encapsulated CDase into subcutaneous tumors growing in rats followed by intraperitoneal treatment with 5FC (*22*). This approach was designed to minimize the toxic effects of systemically administered 5FU and to improve the activity of the drug by generating it directly at the tumor. Considerable antitumor activity for the immobilized enzyme-5FC combination was observed. For the treatment of cancers that are widely disseminated, or surgically inaccessible, we felt that a more suitable strategy for localized 5FU generation would be to deliver CDase with mAbs that bind to tumor-associated antigens.

The physical properties of CDase from various organisms have been shown to differ significantly in molecular weights, stabilities, activities, and subunit compositions. The thermostable CDase enzymes from *Salmonella typhimurium* (*24*) and *E. coli* (*18*) have molecular weights above 200 kDa and are composed of several subunits. On the other hand, bakers' yeast CDase has been reported as having a molecular weight of 32–41 kDa based on gel filtration (*17, 25*), SDS–PAGE (*26*), and amino acid analysis (*26*). Immunoconjugates of bakers' yeast CDase were therefore expected to have sufficiently low molecular weights to allow for good penetration into tumors.

The CDase isolated, according to the procedures indicated in Table I, displays properties that distinguish it from previously isolated CDase enzymes from bakers' yeast. Gel filtration (Figure 2) indicated that the enzyme had a molecular weight of approximately 32 kDa, but SDS–PAGE displayed a single band at 17 kDa corresponding to CDase activity. Based on these observations, it appears that the purified CDase isolated here is dimeric and that each of the subunits has molecular weights of 17 kDa. In addition, although previous reports indicate bakers' yeast CDase to be thermolabile (*17, 23, 27*), the enzyme purified according to the methods described in this work has considerable stability at 37 °C (Figure 3). Enzyme thermostability is a necessary feature for in vivo applications of this targeting strategy, because there may be several days between the administrations of conjugate and prodrug (*10, 11, 13*).

From the in vitro data presented in Figure 5, it is evident that 5FU is formed from 5FC in an immunologically specific manner by L6–CDase that is bound to cell-surface antigens. These studies provide the basis of current studies involving the in vivo activities of mAb–CDase conjugates.

ACKNOWLEDGMENT

We wish to thank David Hirschberg for performing the cytotoxicity assays, Peter Linsley for valuable discussions, and Ana Wieman for preparing the manuscript.

LITERATURE CITED

(1) Zubrod, C. G. (1982) Principles of Chemotherapy. *Cancer Medicine* (J. F. Holland, and E. Frei, Eds.) pp 627–632, Lea, and Febiger, Philadelphia.

(2) Wilman, D. E. V. (1986) Prodrugs in cancer chemotherapy. *Biochem. Soc. Trans. 14*, 375–382.

(3) Denny, W. A. (1988) New directions in the design, and evaluation of anti-cancer drugs. *Drug Des. Delivery 3*, 99–124.

(4) Conners, T. A. (1986) Prodrugs in cancer chemotherapy. *Xenobiotica 16*, 975–988.

(5) Ross, W. C. J., and Warwick, G. P. (1955) Reduction of cytotoxic compounds by hydrazine and by the xanthine oxidase system. *Nature 176*, 298–299.

(6) Senter, P. D., Pearce, W. E., and Greenfield, R. S. (1990) Development of a drug-release strategy based on the reductive fragmentation of benzyl carbamate disulfides. *J. Org. Chem. 55*, 2975–2978.

(7) Kennedy, K. A. (1987) Hypoxic cells as specific drug targets for chemotherapy. *Anti-Cancer Drug Des. 2*, 181–194.

(8) Chakravarty, P. K., Carl, P. L., Weber, M. J., and Katzenellenbogen, J. A. (1983) Plasmin-activated prodrugs for cancer chemotherapy. Synthesis and biological activity of peptidylacivicin and peptidylphenylenediamine mustard. *J. Med. Chem. 26*, 633–638.

(9) Senter, P. D. (1990) Activation of prodrugs by antibody–enzyme conjugates: A new approach to cancer therapy. *FASEB J. 4*, 188–193.

(10) Senter, P. D., Saulnier, M. G., Schreiber, G. J., Hirschberg, D. L., Brown, J. P., Hellstrom, I., and Hellstrom, K. E. (1988) Anti-tumor effects of antibody–alkaline phosphatase conjugates in combination with etoposide phosphate. *Proc. Natl. Acad. Sci. U.S.A. 85*, 4842–4846.

(11) Senter, P. D., Schreiber, G. J., Hirschberg, D. L., Ashe, S. A., Hellstrom, K. E., and Hellstrom, I. (1989) Enhancement of the in vitro and in vivo antitumor activities of phosphorylated mitomycin c and etoposide derivatives by monoclonal antibody-alkaline phosphatase conjugates. *Cancer Res. 49*, 5789–5792.

(12) Kerr, D. E., Senter, P. D., Burnett, W. V., Hirschberg, D. L., Hellstrom, I., and Hellstrom, K. E. (1990) Antibody–penicillin-V-amidase conjugates kill antigen-positive tumor cells when combined with doxorubicin phenoxyacetamide. *Cancer Immunol. Immunother. 31*, 202–206.

(13) Bagshawe, K. D., Springer, C. J., Searle, F., Antoniw, P., Sharma, S. K., Melton, R. G., and Sherwood, R. F. (1988) A cytotoxic agent can be generated selectively at cancer sites. *Br. J. Cancer 58*, 700–703.

(14) Shepherd, T. A., Jungheim, L. N., Meyer, D. L., and Starling, J. J. (1991) A novel targeted delivery system utilizing a cephalosporin–oncolytic prodrug activated by an antibody β-lactamase conjugate for the treatment of cancer. *Bioorg. Med. Chem. Lett. 1*, 21–26.

(15) Hellstrom, I., Horn, D., Linsley, P. S., Brown, J. P., Brankovan, V., and Hellstrom, K. E. (1986) Monoclonal antibodies raised against human lung carcinoma. *Cancer Res. 46*, 3917–3923.
(16) Clark, E. A., Shu, G., and Ledbetter, J. A. (1985) Role of the Bp35 cell surface polypeptide in human B cell activation. *Proc. Natl. Acad. Sci. U.S.A. 82*, 1766–1770.
(17) Katsuragi, T., Sonoda, T., Matsumoto, K., Sakai, T., and Tonomura, K. (1989) Purification and some properties of cytosine deaminase from bakers' yeast. *Agric. Biol. Chem. 53*, 1313–1319.
(18) Katsuragi, T., Sakai, T., Matsumoto, K., and Tonomura, K. (1986) Cytosine deaminase from *Escherichia coli*—production, purification, and some characteristics. *Agric. Biol. Chem. 50*, 1721–1730.
(19) Heidelberger, C. (1975) Fluorinated Pyrimidines and Their Nucleosides. *Handb. Exp. Pharmacol. 38*, 193–231.
(20) Heidelberger, C. (1982) Pyrimidine and pyrimidine nucleoside antimetabolites. *Cancer Medicine* (J. F. Holland, and E. Frei, Eds.) pp 801–824, Lea and Febiger, Philadelphia.
(21) Steer, P. L., Marks, M. I., Klite, P. D., and Eickhoff, T. C. (1972) 5-Fluorocytosine: An oral antifungal compound. A report on clinical and laboratory experience. *Ann. Intern. Med. 76*, 15–22.
(22) Nishiyama, T., Kawamura, Y., Kawamoto, K., Matsumura, H., Yamamoto, N., Ito, T., Ohyama, A.; Katsuragi, T., and Sakai, T. (1985) Antineoplastic effects in rats of 5-fluorocytosine in combination with cytosine deaminase capsules. *Cancer Res. 45*, 1753–1761.
(23) Kream, J., and Chargaff, E. (1952) On the cytosine deaminase of yeast. *J. Am. Chem. Soc. 74*, 5157–5160.
(24) West, T. P., Shanley, M. S., and O'Donovan, G. A. (1982) Purification and some properties of cytosine deaminase from *Salmonella typhimurium*. *Biochim. Biophys. Acta 149*, 1171–1174.
(25) Ipata, P. L., Marmocchi, F., Magni, G., Felicioli, R., and Polidoro, G. (1971) Bakers' yeast cytosine deaminase. Some enzymic properties and allosteric inhibition by nucleosides and nucleotides. *Biochemistry 10*, 4270–4276.
(26) Yergatian, S., Lee, J. B., Geisow, M. J., and Ireson, J. C. (1977) Cytosine deaminase: Structural modification studies. *Experientia 33*, 1570–1571.
(27) Katsuragi, T., Sakai, T., and Tonomura, K. (1987) Implantable enzyme capsules for cancer chemotherapy from bakers' yeast cytosine deaminase immobilized on epoxy-acrylic resin and urethane prepolymer. *Appl. Biochem. Biotechnol. 16*, 61–69.

Registry No. 5FC, 2022-85-7; 5FU, 51-21-8; CDase, 9025-05-2.

The Covalent Attachment of Multiple Fluorophores to DNA Containing Phosphorothioate Diesters Results in Highly Sensitive Detection of Single-Stranded DNA

Nancy E. Conway and Larry W. McLaughlin*

Department of Chemistry, Boston College, 140 Commonwealth Avenue, Chestnut Hill, Massachusetts 02167.
Received May 6, 1991

DNA fragments containing multiple internucleotidic phosphorothioate diesters, prepared by either chemical or enzymatic syntheses, are amenable to labeling with the fluorophore monobromobimane. With the incorporation of phosphorothioate diesters at each internucleotidic site, multiple fluorophores, ideally one for each nucleotide residue, can be covalently attached to the DNA fragment. The presence of multiple labels can be expected to interfere with analysis techniques, such as polyacrylamide gel electrophoresis. To avoid such problems, the fluorophores are introduced in a "postassay" fashion, that is, while the fragments are still embedded within the gel matrix. The detection limit (to the naked eye) for multiply labeled single-stranded DNA containing hundreds of base residues is in the low femtomole range. DNA containing >1000 base residues can be visualized in some cases in the subfemtomole range without the use of sophisticated electronic instrumentation.

INTRODUCTION

The detection of single-stranded DNA fragments resulting from procedures such as DNA sequencing has commonly relied upon the use of radioisotopes (^{32}P and ^{35}S) in conjunction with autoradiography (*1*). Such radioisotopic techniques have become common for the visualization of the DNA fragments present in a sequencing ladder obtained after polyacrylamide gel electrophoresis. However, the use of radioisotopes is complicated by problems related to their storage and disposal as well as the health hazards arising from exposure to atomic emissions. Fluorescent, rather than radioisotopic, labeling techniques avoid these problems, but are themselves often limited by their sensitivity to detection (at least in the absence of sophisticated lasers, electronics, and computers).

Many fluorescent labeling procedures reported to date have relied upon the introduction of a single fluorophore at one termini of the DNA fragment using a variety of chemical or enzymatic techniques (*2*). This approach is conceptually similar to radioisotopic end labeling, but typically requires the use of lasers and sophisticated electronic detection systems to locate the nucleic acid containing the fluorophore at femtomole or subfemtomole levels. Nevertheless, several DNA sequencing techniques have been developed that rely upon the detection of nucleic acid fragments carrying a single fluorophore (*3–5*).

The incorporation of multiple fluorophores or other nonradioactive labels into nucleic acids has the potential to significantly enhance the detection limit for suitably labeled fragments by increasing the amount of signal present for a given quantity of nucleic acid. Two approaches are commonly used to incorporate multiple residues. (i) A modified nucleotide is synthesized that carries the fluorophore of interest or a functional group amenable to fluorescent labeling. Multiple fluorophores can be introduced into the DNA fragment as often as the modified nucleotide is inserted into the sequence. This has been very successful for biotin-based detection systems (*6–8*). (ii) An appropriate multifunctional linker is attached to the terminus of the nucleic acid to provide several sites for attachment of the fluorophores. Several related studies have been recently reported (*8–12*). Both approaches will enhance the detection limit of the DNA, but are complicated by the necessity of synthesizing the modified nucleoside or multifunctional linker. Additionally, while enhanced detection sensitivity should be available with biological macromolecules containing multiple fluorophores, the expected increases in sensitivity can be complicated by quenching effects. In such cases, an increase in the number of fluorophores does not always result in a corresponding increase in measured fluorescence intensity (see, for example, ref 10). This observation suggests that nonradiative mechanisms for relaxation of the excited state can be present, or even predominate, with the close association of multiple fluorophores. Appropriate spacing of the fluorophores may reduce nonradiative relaxation processes and be advantageous in enhancing the sensitivity of detection.

In the present paper, we examine an approach to the fluorescent labeling of nucleic acids in which the fluorophores are attached to the internucleotidic phosphorus residues of DNA fragments containing phosphorothioate diesters. This approach allows the incorporation of multiple fluorophores into the DNA, ideally one fluorophore for each nucleotide residue containing a phosphorothioate diester while spacing the fluorophores at roughly equal distances throughout the fragment. So that the covalent attachment of fluorophores does not alter the characteristics of the DNA, for example its electrophoretic mobility during assays such as polyacrylamide gel electrophoresis, the labels are introduced "postassay"—that is, after completion of electrophoretic analysis. In this procedure the DNA fragments are covalently labeled with the fluorophore while they remain embedded within the polyacrylamide gel matrix.

EXPERIMENTAL PROCEDURES

Materials. Monobromobimane was obtained from Calbiochem (San Diego, CA) under the name Thiolyte reagent or from Molecular Probes (Eugene, OR). [α-^{35}S]dATP was obtained from New England Nuclear (Billerica, MA). M13mp18 DNA, DNA polymerase I, T4 DNA ligase, and the restriction endonucleases *Hpa*II and *Ava*I were products of New England Biolabs (Beverly, MA), while

1043-1802/91/2902-0452$02.50/0 © 1991 American Chemical Society

Sequenase was obtained from U.S. Biochemical Corporation (Cleveland, OH). The 2'-deoxynucleoside 5'-*O*-(1-thiotriphosphates) were obtained from Amersham (Arlington Heights, IL). Polyacrylamide gels were destained with a KS-10 shaker from BEA-Enprotech Corp. (Hyde Park, MA), and the fluorescent bands containing DNA were viewed on a transilluminator, Model TL-33 (λ_{max} = 366 nm), manufactured by UVP, Inc. (San Gabriel, CA). Fluorescence in solution was measured with a Perkin-Elmer (Norwalk, CT) fluorescence spectrophotometer, Model 650-10S. The radioactivity was measured with an LKB Wallac RackBeta liquid scintillation counter (Uppsala, Sweden). Oligodeoxynucleotides were synthesized on an Applied Biosystems (Foster City, CA) 381A DNA synthesizer.

Methods. *Chemical DNA Synthesis.* DNA fragments containing phosphorothioate diesters were prepared using phosphoramidite DNA synthesis techniques in which the iodine/water/THF/lutidine oxidation was replaced by sulfur/carbon disulfide/lutidine (*13*, *14*). Using this approach, DNA could be prepared containing phosphorothioates at every internucleotidic site, or prepared as a mixture of derivatives with some sites containing phosphate diesters and others containing phosphorothioate diesters.

Enzymatic DNA Synthesis. M13mp18 DNA was converted to the replicative form (RF) as follows. The template DNA (2.5 μg) and universal primer (0.1 μg) were annealed in 25 μL of buffer containing 100 mM NaCl, 20 mM $MgCl_2$, and 100 mM Tris-HCl (pH 8.0) by heating the mixture to 56 °C for 15 min followed by slow cooling to ambient temperature. The final 50-μL reaction containing dATP, dGTP, dCTP, dTTP (500 μM each), ATP (1 mM), DNA polymerase I (*Escherichia coli*, 10 units), and T4 DNA ligase (10 units) was incubated overnight at 16 °C. Substitution of the appropriate dNTPαS derivative(s) for the corresponding dNTP(s) essentially as described by Taylor (*16*) allowed the enzymatic incorporation of phosphorothioate diesters in place of phosphodiesters. For internal standardization, [α-^{35}S]dATP (1.4 Ci/mmol) was employed in some experiments in the elongation reaction.

Polyacrylamide Gel Electrophoresis. Gel electrophoresis was performed on 20 × 20 × 0.075 cm or 34 × 42 × 0.075 cm gels of 6% acrylamide, 0.6% bis(acrylamide), 3 mM Na_2EDTA, 7 M urea, and 50 mM Tris-borate (pH 8.3).

Fluorescent Labeling of DNA Embedded within Polyacrylamide Gels. Postassay labeling was performed both in the presence and in the absence of 7 M urea. The DNA was fixed in the gel by soaking it in 10% aqueous acetic acid for 10 min. The gel was then transferred to a 4 mM solution of monobromobimane in 50% aqueous acetonitrile and allowed to react overnight (18 hours) in the dark.

Visualization of Labeled DNA. The gel was removed from the monobromobimane solution and destained by shaking in 50% aqueous acetonitrile for 1–4 h. The destaining period appeared necessary because of minor reactions with the gel components and monobromobimane. Following a brief treatment (5 min) in 60% aqueous dimethylformamide, the DNA was viewed on a standard long-wavelength ultraviolet transilluminator at 366 nm. To quantify the results, the fluorescent bands of DNA were cut out of the gel and the amount of DNA present in the gel was determined by scintillation counting.

Labeling and Isolation of a 15-mer Containing Three Phosphorothioate Diesters. After postassay fluorescent labeling (described above) with monobromobimane, the 5'-^{32}P end-labeled 15-mer was electroeluted for 2 h from a 20% polyacrylamide gel into dialysis tubing containing 0.5 × TBE buffer. The solution was evaporated to dryness, redissolved in 1 mL of distilled water, and desalted using a column of Sephadex G-10. The DNA fragment was collected, evaporated to dryness, and redissolved in 3 mL of 5 mM KH_2PO_4 (pH 4.5). The fluorescence of the solution was measured and the concentration of the 15-mer determined by scintillation counting. The fluorescence as a function of concentration of the phosphorothioate diesters was plotted on the standard bimane-labeled Tp(s)T curve.

Preparation of DNA Restriction Fragments Containing Phosphorothioate Diesters. M13mp18 DNA was converted to the RF form as described above. Substitution of the appropriate dNTPαS derivative(s) for the corresponding dNTP(s) allowed the enzymatic incorporation of phosphorothioate diesters in place of phosphodiesters. Restriction digests with *Ava*I were performed as follows. The *Ava*I reaction mixture contained RF M13mp18 DNA, 100 mM NaCl, 20 mM $MgCl_2$, and 100 mM Tris-HCl (pH 8.0). The reaction was initiated by the addition of the enzyme and incubated at 37 °C for 4 h.

Generation of DNA Sequencing Ladders Containing Phosphorothioate Diesters. In a 15-μL mixture, M13mp18 single-stranded DNA (2.5 μg) and universal primer (60 ng) were annealed in buffer containing 40 mM Tris-HCl (pH 7.5), 10 mM $MgCl_2$, and 50 mM NaCl by heating the mixture to 65 °C followed by slow cooling to ambient temperature. To the annealed mixture were added 2 μL of the dCTP mix (2 μM each of dATPαS, dGTPαS, dTTPαS) and 6 units of Sequenase to give a total volume of 20 μL. The reaction was incubated for 10 min at 37 °C followed by the addition of 5 μL of A,G,C, or T mix that contained a final concentration of 300 μM dNTPαS and 3 μM ddNTP. After 10 min the reaction was stopped by the addition of 5 μL of formamide dye (deionized formamide, 20 mM Na_2EDTA, 0.03% bromophenol blue, and 0.03% xylene cyanol).

RESULTS

We have previously described (*13*) the alkylation of phosphorothioate diesters as a simple method to introduce a large number of fluorophores into a DNA sequence already embedded within a gel matrix. In the present paper we have extended these studies to show that long fragments of DNA containing phosphorothioate diesters can be visualized at subfemtomole ($<10^{-15}$ mol) levels using this technique. The covalent attachment of fluorophores to the DNA as described here exploits the simple and straight forward substitution of a sulfur atom for a nonbridging oxygen at the internucleotidic phosphorus residue. DNA containing phosphorothioate diesters can be generated by chemical (*14*, *15*) and enzymatic (*16*, *17*) techniques, and these residues are amenable to alkylation reactions (*18*, *19*) and can be used as sites for the incorporation of fluorophores (*13*, *19*).

The alkylation of a negatively charged phosphorothioate diester by the fluorophore yields a neutral phosphorothioate triester (see Figure 1). With efficient labeling of the internucleotidic phosphorus residues, the DNA fragment increases in molecular weight and loses most (if not all) of its anionic character. DNA fragments labeled in this fashion are unlikely to migrate under the influence of an electric field in a gel matrix. In fact, DNA fragments modified in this manner will not exhibit many properties that are similar to native sequences.

This difficulty can be overcome by the "postassay" labeling of the phosphorothioate DNA. With this procedure, the label is introduced after the assay of interest, such as gel electrophoresis. This approach relies upon efficient labeling of the DNA fragments while they are still embedded within the polyacrylamide gel matrix. In

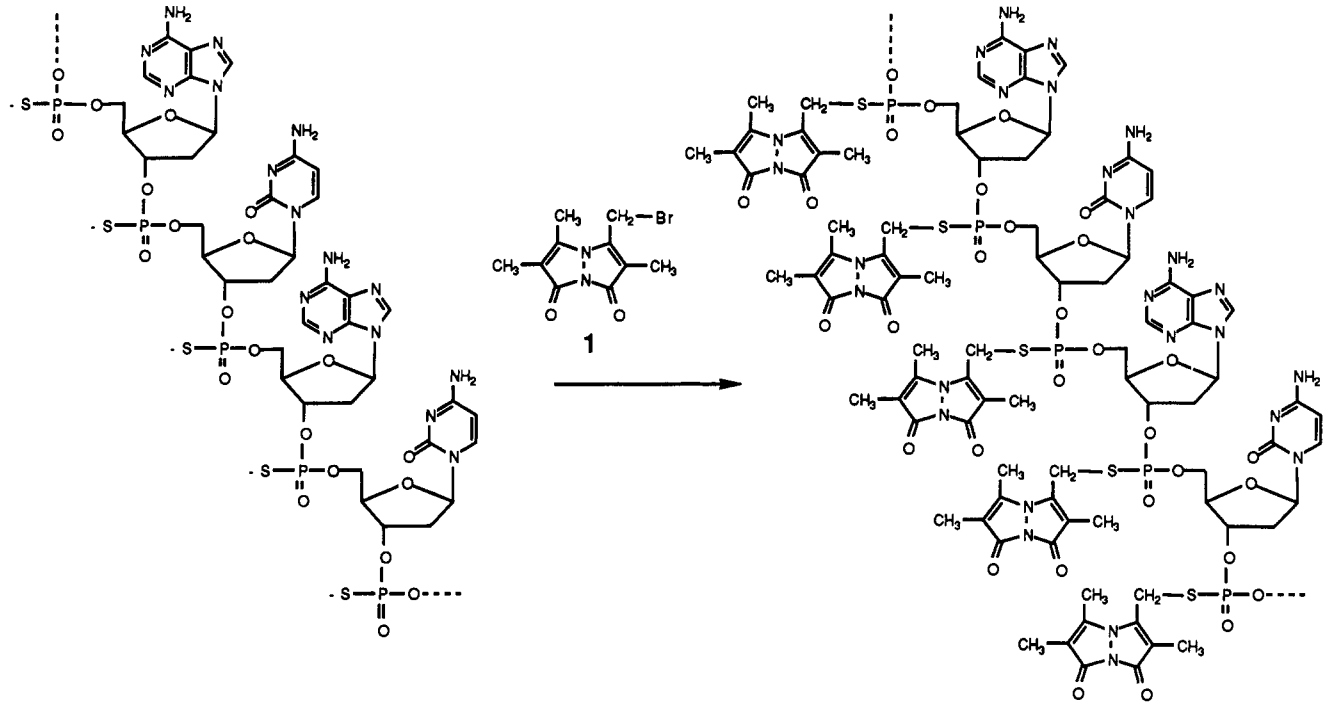


Figure 1. The covalent attachment of multiple fluorophores to single-stranded DNA using internucleotidic phosphorothioate diesters.

order for efficient labeling to occur within the DNA matrix and result in highly sensitive detection of DNA, the "ideal" fluorophore should possess several properties: (i) small molecular size to facilitate diffusion through the polyacrylamide matrix to the embedded DNA, (ii) solubility in aqueous or largely aqueous solutions compatible with the water-based polyacrylamide gel matrix, (iii) fluorescence properties only present (or dramatically enhanced) upon alkylation of the DNA. This will maximize the dection of the labeled DNA in the presence of a gel matrix saturated with unreacted fluorophore, and (iv) excitation maximum removed from the absorbance maximum of DNA.

Although these properties are all important for effective labeling of DNA fragments embedded within the polyacrylamide gel matrix, the most unusual requirement is that the unreacted fluorophore exhibits an extremely low quantum yield, while the labeled DNA exhibits a very high quantum yield. The fluorophore that best meets this requirement, as well as the others noted, is monobromobimane 1 (Figure 1).

Monobromobimane exhibits an excitation maximum of 390 nm and an emission maximum of 450 nm. The quantum yield (vs quinine sulfate) for the bromo derivative is <0.001 and this value increases to 0.33 upon alkylation of a sulfur residue (*20*). Monobromobimane is the fluorophore used exclusively in the present studies.

Labeling of Matrix-Bound DNA. After electrophoretic separation of a restriction digest of phosphorothioate-containing DNA (see Experimental Procedures) on a polyacrylamide gel, the gel was soaked overnight in a 4 mM solution of monobromobimane in 50% aqueous acetonitrile. After labeling of the DNA fragments, the gel was washed briefly in 50% aqueous acetonitrile followed by a brief treatment in 50% aqueous DMF. The fluorescent bands could be clearly visualized by placing the gel on a long-wave (366 nm) transilluminator. Although the DNA was brightly fluorescent, indicating that it had been labeled, we could not immediately determine the efficiency of the labeling procedure. Quantitative labeling of each phosphorothioate diester within a given fragment requires that the fluorophore is capable of labeling adjacent phosphorothioate diesters without significant steric interference. To examine the labeling efficiency, we had previously used a 21-mer containing 20 phosphorothioate diesters that was radioactively end-labeled (using [^{32}P]-ATP) for internal standardization, resolved by PAGE, and subsequently labeled with monobromobimane (*13*). However, we were completely unsuccessful in isolating the labeled DNA from the gel by electrophoresis, capillary action, or liquid extraction of the crushed gel, for further analysis. This difficulty in itself suggested that the 21-mer has lost much of its anionic character, presumably due to the efficient labeling of the phosphorothioate diesters.

We additionally prepared a 15-mer that contained three internal adjacent phosphorothioate diesters and 11 phosphate diesters. The radioisotopic end-labeled 15-mer could be electrophoretically extracted from the gel after monobromobimane labeling since 11 of the phosphorus residues remained as charged diesters. We could then quantitatively measure the fluorescence of various isolated samples using a spectrofluorimeter. We compared the fluorescence of three isolated samples of the labeled 15-mer with that obtained from varying concentrations of the labeled dTp(s)T dimer containing a single monobromobimane label (Figure 2). In each case the quantity of 15-mer present (determined from the radioactive end label) was measured and plotted according to the total concentration of phosphorothioate diesters (three times the 15-mer concentration) and compared with the standard curve generated from the labeled dTp(s)T samples. For each of the three samples, the fluorescence measured for the 15-mer was equal to the fluorescence observed for 3 times the same quantity of labeled dimer (Figure 2).

Detection of DNA Labeled with Multiple Fluorophores. We have examined the sensitivity of detection by the naked eye of a variety of DNA fragments prepared by chemical or enzymatic synthesis. The limit of visibility for the dTp(s)T dimer containing a single fluorophore was approximately 20 pmol. Increasing the number of sites amenable to labeling to three (present in the 15-mer described above) decreased the level of visible DNA to 7 pmol. The 21-mer containing 20 phosphorothioate di-

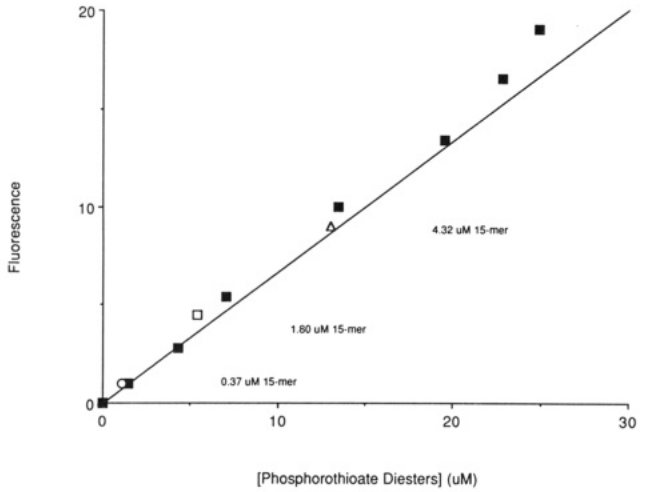


Figure 2. Plot of fluorescence vs the concentration of phosphorothioate diesters available for labeling. The standard curve represents varying concentrations of bimane-labeled dTp(s)T (■). The fluorescence for three different samples of a 15-mer containing three phosphorothioates have been added to this plot. Sample A (△) contains the labeled 15-mer at a concentration of 4.32 μM (or a phosphorothioate diester concentration of 12.96 μM). Sample B (□) contains the labeled 15-mer at a concentration of 1.80 μM (or a phosphorothioate diester concentration of 5.40 μM). Sample C (○) contains the labeled 15-mer at a concentration of 0.37 μM (or a concentration of phosphorothioate diesters of 1.11 μM).

esters could be detected in gels at a level of approximately 1 pmol. Longer fragments containing hundreds of phosphorothioate diesters were prepared using a M13mp18 single-stranded template and the α-thio-2′-deoxynucleotide triphosphates (dNTPαS). Fragments of known length could be excised from the polymerization product using an appropriate restriction endonuclease. Radioisotopic labeling at known specific activity was done to determine the amount of DNA present. The *Ava*I restriction endonuclease produced two restriction fragments of 422 bp and 6828 bp. The number of available labeling sites in these fragments could be varied by using one, two, or three dNTPαS derivatives in conjunction with native dNTPs. For example, the 422-mer prepared with dATPαS, dTTP, dCTP, and dGTP contained 101 phosphorothioate diesters while the 6828 base pair fragment contained approximately 1700 labeling sites. The limit of detection was observed to be approximately 30 fmol (30×10^{-15} mol) for the 422-mer and approximately 2 fmol for the 6828 base pair fragment (see Figure 3). In each lane of Figure 3, the quantity of the 422 and 6828 base residue fragment should be identical since they were both obtained from a simple restriction digest. However, at the higher fragment concentrations (lanes 1–3, Figure 3) the amount 422-mer in the gel matrix always exceeded the amount of the larger fragment. For example, in lane 1, scintillation counting indicated 271 fmol of the small fragment but only 146 fmol of the large fragment. This may reflect less efficient entry into the 6% polyacrylamide gel by the larger fragment. As the quantity of DNA added to the gel decreased (lanes 4–7, Figure 3), both fragments were present in identical amounts as expected.

By comparison, the values obtained for the 422-mer prepared using two (dATPαS and dTTPαS) or three (dATPαS, dTTPαS, and dGTPαS) phosphorothioate derivatives were 21 and 10 fmol, respectively. Similarly, with two and three dNTPαS derivatives, the level of detection of the 6828 residue fragment was 1 and 0.5 fmol, respectively. For all fragments studied, the quantity of DNA that could be detected was inversely proportional to the number of labeling sites present (Figure 4).

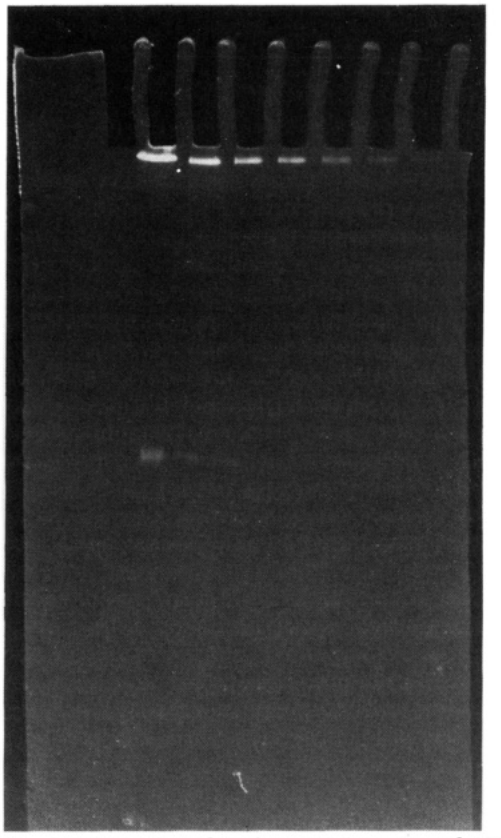


Figure 3. A polyacrylamide gel containing 422 and 6828 base residue fragments obtained from an *Ava*I digest of M13mp18 DNA that was converted to the RF form using dATPαS (including some [α-^{35}S]dATP), dTTP, dGTP, dCTP (this generates 101 sites for labeling in the 422-mer and approximately 1700 sites in the larger fragment) and *E. coli* DNA polymerase. After electrophoretic resolution, the fragments were labeled with monobromobimane, visualized using a long-wave (366 nm) transilluminator, and photographed through a sharp-cutoff filter. The quantities of DNA present in each lane (based on scintillation counting of the excised bands) were (6828-mer/422-mer) as follows (left to right): lane 1, 146 fmol/271 fmol; lane 2, 51 fmol/68 fmol; lane 3, 26 fmol/37 fmol; lane 4, 17 fmol/19 fmol; lane 5, 9 fmol/9 fmol; lane 6, 5 fmol/5 fmol; lane 7, 2 fmol/3 fmol.

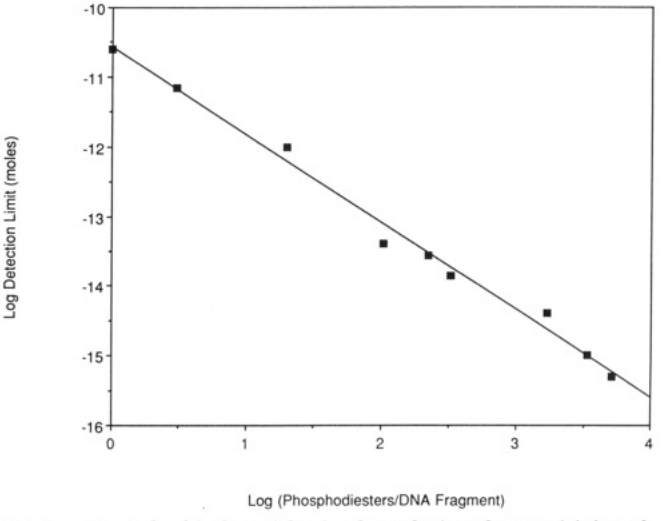


Figure 4. A double-logarithmic plot relating the sensitivity of detection and the number of phosphorothioates present for a series of DNA fragments.

DNA Sequencing Ladders. On the basis of the data plotted in Figure 4, DNA fragments of approximately 200–400 bases in length and containing the same number of phosphorothioate diesters should be visible after labeling with monobromobimane in the 10–20 fmol level. This

detection limit is within approximately 1 order of magnitude of that typically present in a radioisotopically labeled DNA sequencing ladder (each sequencing band contains approximately 1 fmol of DNA). We have altered the conditions commonly used for Sanger dideoxy sequencing to increase the amount of DNA present in the sequencing ladder in order to judge the effectiveness of labeling the DNA fragments with multiple bimane labels. Unfortunately, with high concentrations of DNA, the resolution of the sequencing ladder deteriorated. Under optimal conditions, we could generate sequencing ladders with acceptable resolution (based on autoradiography) that contained approximately 5 fmol of DNA per band. The quantity of DNA present was determined from radiolabeling of the sequencing reactions to known specific activity (*21*). Labeling of these sequencing ladders resulted in gels that exhibited significant fluorescence in the sequencing lanes, some bands were clearly visible, but the fluorescence intensity of all the labeled DNA bands present in the gel was not sufficient for accurate interpretation of the sequences.

DISCUSSION

Phosphorothioate diesters can be incorporated into DNA fragments by chemical or enzymatic syntheses with only minor procedural changes. The use of phosphorothioate diesters in this manner provides a simple and rapid technique for the generation of multiple nucleophilic sites within a DNA fragment that are amendable to alkylation by fluorophores. The number of fluorophores that can be incorporated into a DNA fragment is directly proportional to the number of base residues present in the fragment.

Labeling by the described procedure requires that the fluorophore saturate the gel matrix. After the labeling reaction is complete, it is necessary that the fluorophore be completely removed from the gel, or that the quantum yield for the unreacted fluorophore be substantially less than that of the labeled DNA. The latter possibility is conceptually similar to ethidium bromide labeling of double-stranded DNA. With ethidium bromide labeling the gel is also saturated with the fluorophore, but the quantum yield of the intercalated fluorophore increases dramatically in comparison to that of the free fluorophore. The nonfluorescent character of monobromobimane has been explained in terms of a facile isomerization that occurs in the excited state (*22*) and results in nonradiative relaxation processes. However, upon alkylation of an appropriate nucleophile, such as the phosphorothioate diester, the fluorescence quantum yield of the bimane derivative increases by greater than 2 orders of magnitude (*20*). This unusual property is advantageous in the present "postassay" labeling procedure since it is not necessary to remove completely the unreacted bimane from the polyacrylamide gel prior to visualization of the labeled fragments.

Labeling of the phosphorothioate diesters produces neutral triesters. DNA containing phosphorus residues, present largely as the neutral triesters, is exceedingly difficult to remove from the gel matrix for additional analysis. For the 15-mer containing three adjacent phosphorothioates, the labeled DNA could be isolated from the gel by electrophoretic elution since eleven of the internucleotidic phosphorus residues were present as charged phosphate diesters. Examination of the fluorescence characteristics of this fragment (Figure 2) suggests that adjacent phosphorothioate diesters can be labeled with a high degree of efficiency by monobromobimane while they remain embedded within the polyacrylamide gel matrix. The analysis of a similar labeling experiment with a 21-mer containing 20 phosphorothioate diesters failed because of the inability to isolate the DNA from the polyacrylamide gel. But this difficulty suggests that the fluorescent labeling has probably occurred with a high degree of efficiency (if not nearly quantitative).

We have previously shown that fragments such as the 422-mer (Figure 3) can be visualized in the low femtomole range. However, Figure 3 also illustrates that increasing the number of labeling sites to provide for thousands of covalently bound fluorophores allows visualization in the subfemtomole range. For example, lane 3 (Figure 3) contains 37 fmol of the 422-mer (with 101 labeling sites) and it is just visible to the naked eye. By comparison, the longer fragment (6828 residues) containing approximately 1700 labeling sites is just visible at a level about 17-fold lower (2 fmol). The generation of this fragment with three dNTPαS derivatives and a single phosphate (and the restriction site) further lowered this level to approximately 0.5 fmol.

It is difficult to quantitate the extent of the labeling reaction within the gel matrix for samples containing hundreds or thousands of base residues. Yet the direct correlation observed between the number of potential labeling sites (phosphorothioate diesters) and the level of detection (Figure 4) that can be clearly observed for the two different sized fragments in Figure 3 suggests that highly efficiently labeling of the diesters has occurred.

The direct correlation between the detection limit (or emitted irradiation) and the number of labeled sites was unexpected. It has been more commonly reported that an increase in the number of fluorophores attached to a biological macromolecule results in a decrease in the corresponding quantum yield for each fluorophore (*10*). This has been interpreted to result from a higher frequency of nonradiative mechanisms for relaxation of the excited state; presumably either a higher number of collisions between excited fluorophores results or other nonradiative mechanisms (e.g., dipole–dipole interactions) for energy transfer account for relaxation of the excited state (*23*). However, the labeling of adjacent phosphorus residues as described in the present report resulted in essentially a consistent quantum yield for each individual fluorophore. This produced a linear increase in fluorescence intensity for a corresponding increase in the number of fluorophores, and this increase in fluorescence was consistent for a large change in the total number of fluorophores (over 3 orders of magnitude; see Figure 4). The absolute detection sensitivities observed agree with such a correlation. For example, we have estimated that one bimane molecule [labeled dTp(s)T] can be visualized at a level of approximately 20 pmol. More bimane molecules can be attached to longer DNA fragments, but it is likely that the total quantity of bimane necessary to be visualized within the gel matrix by the naked eye remains near the 20-pmol level. Thus, the 6828 base residue fragment prepared from two sulfur-containing triphosphate residues has (with efficient labeling) approximately 3400 bimane molecules. One femtomole of a fragment with 3400 fluorophores (roughly the limit of detection for this fragment) would then contain between 3 and 4 pmol of bimane, and this is roughly the predicted value. By a similar calculation, 21 fmol of the 422-mer containing 202 labeling sites contains between 4 and 5 pmol of bimane, also approximating the predicted value.

The level of visualization of single-stranded DNA by monobromobimane labeling compares favorably with the level of visualization observed for ethidium bromide detection of double-stranded DNA. The detection limit for ethidium bromide labeling is typically 10 ng of double-stranded DNA. For a fragment containing 422 base pairs, the 10-ng limit corresponds to approximately 40 fmol of

DNA. On the basis of the present results with varying numbers of labeling sites, a 422 base residue fragment with fluorophores at each internucleotidic linkage should be visible to the naked eye at a level of approximately 5–7 fmol. This corresponds to approximately 1 ng of DNA.

One potentially valuable application for highly sensitive fluorescent labeling of single-stranded DNA is that of DNA sequencing. The individual bands present in a polyacrylamide-generated sequencing ladder typically contain approximately 1 fmol of DNA. Recently reported fluorescence-based DNA sequencing techniques rely upon the introduction of a single terminal fluorophore for detection of the generated fragments (*3–5*). With laser excitation and sophisticated electronic detection systems, DNA fragments can be detected in subfemtomole quantities. The present labeling procedure has to date relied solely upon excitation with a simple transilluminator and visualization with the naked eye (in combination with photography) to detect the labeled DNA fragments. But, by optimizing the labeling reaction such that hundreds of fluorophores can be efficiently and easily incorporated into the DNA fragments of interest, we can detect fragments containing hundreds of fluorophores (i.e., the 422-mer) at low femtomole quantities (10–20 fmol) by this relatively simple detection system. A slightly more sophisticated excitation/detection system that would enhance fluorescence detection by approximately 1 order of magnitude should be sufficient to allow efficient nonradioactive DNA sequencing by the "postassay" labeling procedures described in this paper.

CONCLUSIONS

Bimane labels can be incorporated into nucleic acid fragments at multiple sites using phosphorothioate diesters. DNA labeled in this manner can be detected with high sensitivity (to the naked eye) using a simple longwave transilluminator. The detection limit correlates well with the potential number of bimane labels present, and the experiments indicate that over the range examined (1–5100 labeling sites) a corresponding decrease in the amount of detectable DNA was observed. Fragments containing from 200 to 400 base residues, which would be commonly present in DNA sequencing ladders, can be visualized with the naked eye at the low femtomole level (10–20 fmol). This sensitivity to detection of bimane-labeled sequencing ladders is not sufficient at present to allow unaided determination of the DNA sequence, but the use of relatively simple detection systems should easily provide the approximately 1 order of magnitude increase in detection limit required for effective reading of the sequencing ladder.

ACKNOWLEDGMENT

This work was supported by a grant from the National Institutes of Health (GM 37065). L.W.M. is the recipient of an American Cancer Society Faculty Research Award.

LITERATURE CITED

(1) Sanger, F., Nicklen, S., and Coulson, A. R. (1977) DNA Sequencing With Chain-Terminating Inhibitors. *Proc. Natl. Acad. Sci. U.S.A. 74*, 5463–5467.

(2) Goodchild, J. (1989) Conjugates of Oligonucleotides and Modified Oligonucleotides: A Review of Their Synthesis and Properties. *Bioconjugate Chem. 1*, 165–187.

(3) Smith, L. M., Sanders, J. Z., Kaiser, R. J., Hughes, P., Dodd, C., Connell, C. R., Heiner, C., Kent, S. B. H., and Hood, L. E. (1986) Fluorescence Detection in Automated DNA Sequence Analysis. *Nature 321*, 674–679.

(4) Prober, J. M., Trainor, G. L., Dam, R. J., Hobbs, F. W., Robertson, C. W., Zagursky, R. J., Cocuzza, A. J., Jensen, M. A., and Baumeister, K. (1987) A System for Rapid DNA Sequencing with Fluorescent Chain-Terminating Dideoxynucleotides. *Science 238*, 336–341.

(5) Ansorge, W., Sproat, B. S., Stegemann, J., and Schwager, C. (1986) A Non-Radioactive Automated Method for DNA Sequence Determination. *J. Biochem. Biophys. Methods 13*, 315–323.

(6) Langer, P. R., Waldrop, A. A., and Ward, D. C. (1981) Enzymatic Synthesis of Biotin-Labeled Polynucleotides: Novel Nucleic Acid Affinity Probes. *Proc. Natl. Acad. Sci. U.S.A. 78*, 6633–6637.

(7) Leary, J. J., Brigati, D. J., and Ward, D. C. (1981) Rapid and Sensitive Colorimetric Method for Visualizing Biotin-Labeled DNA Probes Hybridized to DNA or RNA Immobilized on Nitrocellulose: Bio-blots. *Proc. Natl. Acad. Sci. U.S.A. 80*, 4045–4049.

(8) Kempe, T., Sundquist, W. I., Chow, F., and Hu, S.-L. (1985) Chemical and Enzymatic Biotin Labelling of Oligodeoxyribonucleotides. *Nucleic Acids Res. 13*, 45–47.

(9) Nelson, P. S., Sherman-Gold, R., and Leon, R. (1989) A New and Versatile Reagent for Incorporation of Multiple Primary Amines into Synthetic Oligonucleotides. *Nucleic Acids Res. 17*, 7179–7186.

(10) Haralambidis, J., Angus, K., Poconall, S., Duncan, L., Chai, M., and Tregear, G. W. (1990) The Preparation of Polyamide-Oligonucleotide Probes Containing Multiple Non-Radiative Labels. *Nucleic Acids Res. 18*, 501–505.

(11) Misiura, K., Duirrant, I., Evans, M. R., and Gait, M. J. (1990) Biotinyl and Phosphotyrosinyl Phosphoramidite Derivatives Useful in the Incorporation of Multiple Reporter Groups on Synthetic Oligonucleotides. *Nucleic Acids Res. 18*, 4345–4354.

(12) Tang, J. Y., and Agrawal, S. (1990) Incorporation of Multiple Reporter Groups on Synthetic Oligonucleotides. *Nucleic Acids Res. 18*, 6461.

(13) Hodges, R. R., Conway, N. E., and McLaughlin, L. W. (1989) "Post-Assay" Covalent Labeling of Phosphorothioate-Containing Nucleic Acids with Multiple Fluorophores. *Biochemistry 28*, 261–267.

(14) Connolly, B. A., Potter, B. V. L., Eckstein, F., Pingoud, A., and Grotjahn, L. (1984) Synthesis and Characterization of an Octanucleotide Containing the *Eco*RI Recognition Sequence with a Phosphorothioate Group at the Cleavage Site. *Biochemistry 23*, 3443–3453.

(15) Stec, W. J., Zon, G., Egan, W., and Stec, B. (1984) Automated Solid Phase Synthesis, Separation and Stereochemistry of Phosphorothioate Analogues of Oligodeoxyribonucleotides. *J. Am. Chem. Soc. 106*, 6077–6079.

(16) Potter, B. V. L., and Eckstein, F. (1984) Cleavage of Phosphorothioate-Substituted DNA by Restriction Endonuclease. *J. Biol. Chem. 259*, 14243–14248.

(17) Taylor, J. W., Schmidt, W., Cosstick, R., Okruszek, A., and Eckstein, F. (1985) The Use of Phosphorothioate-Modified DNA in Restriction Enzyme Reactions to Prepare Nicked DNA. *Nucleic Acids Res. 13*, 8749–8764.

(18) Gish, G., and Eckstein, E. (1988) DNA and RNA Sequencing Determination Based on Phosphorothioate Chemistry. *Science 240*, 1520–1522.

(19) Fidanza, J., and McLaughlin, L. W. (1989) Introduction of Reporter Groups at Specific Sites in DNA Containing Phosphorothioate Diesters. *J. Am. Chem. Soc. 111*, 9117–9119.

(20) Kosower, N. S., Kosower, E. M., Newton, G. L., and Ranney, H. M. (1979) Bimane Fluorescent Labels: Labeling of Normal Human Red Cells Under Physiological Conditions. *Proc. Natl. Acad. Sci. U.S.A. 76*, 3382–3386.

(21) Tsang, T. C., and Bentley, D. R. (1988) An Improved Sequencing Method Using Sequenase That Is Independent of Template Concentration. *Nucleic Acids Res. 16*, 6238.

(22) Kosower, E. M., Pazhenchevsky, B., Dodiuk, H., Kanety, H., and Faust, D. (1981) Bimanes. 6. Reactive Halogen Derivatives of *syn-* and *anti*-1,5-Diazabicyclo[3.3.0]octadienediones (9,10-Dioxabimanes). *J. Org. Chem. 46*, 1666–1673.

(23) Morawetz, H. (1988) Studies of Synthetic Polymers by Nonradiative Energy Transfer. *Science 240*, 172–176.

Registry No. Monobromobimane, 71418-44-5.

TECHNICAL NOTES

Synthesis of N^{α}-(*tert*-Butoxycarbonyl)-N^{ϵ}-[*N*-(bromoacetyl)-β-alanyl]-L-lysine: Its Use in Peptide Synthesis for Placing a Bromoacetyl Cross-Linking Function at Any Desired Sequence Position

John K. Inman,*,† Patricia F. Highet,† Nelly Kolodny,‡ and Frank A. Robey‡

Bioorganic Chemistry Section, Laboratory of Immunology, National Institute of Allergy and Infectious Diseases, and the Peptide and Immunochemistry Unit, Laboratory of Cellular Development and Oncology, National Institute of Dental Research, National Institutes of Health, Bethesda, Maryland 20892. Received July 12, 1991

A new amino acid derivative, N^{α}-(*tert*-butoxycarbonyl)-N^{ϵ}-[*N*-(bromoacetyl)-β-alanyl]-L-lysine (BBAL), has been synthesized as a reagent to be used in solid-phase peptide synthesis for introducing a side-chain bromoacetyl group at any desired position in a peptide sequence. The bromoacetyl group subsequently serves as a sulfhydryl-selective cross-linking function for the preparation of cyclic peptides, peptide conjugates, and polymers. BBAL is synthesized by condensation of *N*-bromoacetyl-β-alanine with N^{α}-Boc-L-lysine and is a white powder which is readily stored, weighed, and used with a peptide synthesizer, programmed for N^{α}-Boc amino acid derivatives. BBAL residues are stable to final HF deprotection/cleavage. BBAL peptides can be directly coupled to other molecules or surfaces which possess free sulfhydryl groups by forming stable thioether linkages. Peptides containing both BBAL and cysteine residues can be self-coupled to produce either cyclic molecules or linear peptide polymers, also linked through thioether bonds. Products made with BBAL peptides may be characterized by amino acid analysis of acid hydrolyzates by quantification of β-alanine, which separates from natural amino acids in suitable analytical systems. Where sulfhydryl groups on coupling partners arise from cysteine residues, *S*-(carboxymethyl)cysteine in acid hydrolyzates may also be assayed for this purpose. Examples are given of the use of BBAL in preparing peptide polymers and a peptide conjugate with bovine albumin to serve as immunogens or model vaccine components.

INTRODUCTION

Conjugates of synthetic peptides with proteins, other peptides, polymers (soluble/insoluble; natural/synthetic), and surfaces of special materials are being employed increasingly in biomedical research and biotechnology. Applications of peptide conjugates include the preparation of immunogens (including synthetic vaccines) for raising antibodies to selected portions of protein antigens (*1–4*), affinity adsorbents, immunoassay components, and cell-adhesion surfaces (*5*, *6*).

The locus of attachment of a peptide to its conjugate partner may have a major influence on the biological activity or performance of the conjugate (*7–9*). Strategies for cross-linking a peptide through a single, selected locus are often complicated by the presence of more than one amino or carboxyl group, and the need to protect (then deprotect) amino groups if a carboxyl function is to be activated. Peptides can be more or less selectively derivatized through their N-terminal amino groups by means of acylation reactions in slightly acidic media and/or with use of certain types of reagents, such as symmetrical anhydrides (*10*). However, if one wishes to synthesize a peptide in order to prepare a conjugate, planning the synthesis for this purpose can prove very advantageous. For example, some workers have introduced a reactive cysteine residue at the desired position for heteroligation (*11*, *12*); Drijfhout et al. (*13*) completed a sequence on a solid support with an N-terminal *S*-acetylmercaptoacetyl group. The deprotected peptide was treated with hydroxylamine to remove the *S*-acetyl group and then joined through its N-terminal sulfhydryl group to a conjugate partner bearing an SH-selective electrophilic function (e.g., an N-substituted maleimide or an α-haloacetyl moiety) by means of a very stable thioether linkage (*12*, *13*).

Strategy considerations may show preference to placing sulfhydryl groups on the conjugate partner (or using those already present) and coupling it to Cys peptides by means of less stable disulfide bonds. The coupling can be effected through an activating group, such as *S*-[(3-nitro-2-pyridyl)-sulfenyl] (Npys),[1] previously placed on a cysteine side chain (*14–16*). A Cys(Npys) residue, introduced in solid-phase peptide synthesis (SPPS), will remain intact during trifluoroacetic acid (TFA) or HF cleavage steps.

For an alternative approach, the peptide synthesis program could be modified in order to introduce an SH-selective electrophile somewhere in the sequence, again allowing use of stable thioether cross-linkages. Lindner and Robey (*17*) described the incorporation of N-terminal

* Address correspondence to John K. Inman, Ph.D., NIAID-LI, Bldg 10, Room 11N311, National Institutes of Health, Bethesda, MD 20892.
† National Institute of Allergy and Infectious Diseases.
‡ National Institute of Dental Research.

[1] Abbreviations used: Npys, *S*-[(3-nitro-2-pyridyl)sulfenyl]; SPPS, solid-phase peptide synthesis; TFA, trifluoroacetic acid, BBAL, N^{α}-(*tert*-butoxycarbonyl)-N^{ϵ}-[*N*-(bromoacetyl)-β-alanyl]-L-lysine; SDS–PAGE, sodium dodecyl sulfate–polyacrylamide gel electrophoresis; CMC, *S*-(carboxymethyl)cysteine; BSA, bovine serum albumin; Bu_3P, tri-*n*-butylphosphine; SBAP, succinimidyl 3-(bromoacetamido)propionate; DMF, *N*,*N*-dimethylformamide; DCE, 1,2-dichloroethane; HOBt, 1-hydroxybenzotriazole; DCC, *N*,*N*′-dicyclohexylcarbodiimide.

Not subject to U.S. Copyright. Published 1991 by American Chemical Society

(chloroacetyl)glycylglycyl groups in the last cycle of an automated SPPS. Subsequently, Robey and Fields (*18*) and Kolodny and Robey (*19*) described a similar method for introducing the more reactive bromoacetyl group at the N-termini of peptides made by SPPS. Using this approach, these authors have prepared many useful immunogens either as peptide–protein conjugates or as self-polymers of peptides that contain both a cysteine residue and an N-terminal bromoacetyl group.

The main limitation to the above approach is lack of flexibility in choosing the site for an α-haloacetyl group. To our knowledge, there has not yet been reported a method for introducing an SH-selective alkylating function at *any* desired position in a peptide that is being synthesized sequentially. Accordingly, we designed and synthesized a new Boc-amino acid derivative, N^{α}-(*tert*-butoxycarbonyl)-N^{ϵ}-[*N*-(bromoacetyl)-β-alanyl]-L-lysine (BBAL). With this compound, one can introduce the bromoacetyl cross-linking function at the N- or C-terminus or at any intermediate position of a synthetic peptide that is being prepared by automated SPPS programs employing temporary N^{α}-Boc protection and final HF-induced deprotection and cleavage. Coupling of these peptides to thiol-bearing carriers can be readily accomplished by mixing the components in a neutral or slightly alkaline buffered medium. The ensuing peptide–carrier conjugates may be quantitatively characterized by means of the β-alanine liberated upon acid hydrolysis of a sample. If coreactant groups are cysteine sulfhydryls, *S*-(carboxymethyl)-cysteine (CMC) also appears in the hydrolyzate (*19*). The β-alanine residue places additional spacing in the cross-link and appears to be a necessary part of the structure of BBAL that results in its being a stable solid that can be conveniently stored, weighed, and dispensed for synthesizer operations.

EXPERIMENTAL PROCEDURES

Materials and Methods. Reagent-grade chemicals and solvents used in the synthesis were obtained from Fisher Scientific (Pittsburgh, PA). β-Alanine and *N*-hydroxysuccinimide were purchased from Sigma Chemical Co. (St. Louis, MO). The latter reagent was recrystallized once from ethyl acetate. *N*,*N*′-Diisopropylcarbodiimide was obtained from Aldrich Chemical Co. (Milwaukee, WI); bromoacetyl bromide was ordered from Fluka (Ronkonkoma, NY); N^{α}-Boc-L-lysine was obtained from Vega Biochemicals (Tucson, AZ).

With the exception of BBAL, all reagents used for the automated synthesis of peptides were purchased from Applied Biosystems, Inc. (Foster City, CA). Sodium dodecyl sulfate–polyacrylamide gel electrophoresis (SDS–PAGE) was performed on the peptide polymers with the gel electrophoresis system sold by Novex (Encinitas, CA). This system provided the materials required to run gels by the method of Laemmli (*20*). Two amino acid analysis systems were used as described by the manufacturers for the analyses of products that were made using BBAL: Amino Quant by Hewlett-Packard, Inc. (Gaithersburg, MD) and Picotag by Waters Associates (Millipore Corp., Milford, MA). CMC and bovine serum albumin (BSA) were from Sigma Chemical Co., and tri-*n*-butylphosphine (Bu_3P) was purchased from Aldrich Chemical Co.

NMR spectra for ^1H and ^{13}C were obtained on a Varian XL200 spectrometer at 200 and 50 MHz, respectively. Typically, solutions of 10 mM concentration yielded spectra after the collection of 64 free induction decays for ^1H (digital resolution of 0.3 Hz) and 60 000 free induction decays for ^{13}C (digital resolution of 1 Hz). Assignments were based on published spectra and known substituent effects (*21*).

***N*-(Bromoacetyl)-β-alanine.** A solution of β-alanine (53.5 g, 0.60 mol) in 600 mL of water was cooled to 5 °C with an ice–alcohol bath. Bromoacetyl bromide (60.0 mL as 95% pure, 0.66 mol) was added under efficient stirring at such a rate as to maintain the temperature below 12 °C. Concurrently, 5 M NaOH was added at a rate needed to keep the pH near 7. These conditions were maintained for 45 min after completing addition of the bromoacetyl bromide. Because the latter reagent is a highly toxic irritant, the above operation was carried out in a hood. The pH of the reaction mixture was then adjusted to 1.9–2.0 using 48% HBr, and its volume was reduced in a rotary evaporator to ca. 150 mL using a 60 °C bath and aspirator vacuum. The heavy precipitate of NaBr was removed by suction filtration and washed with ca. 15 mL of water.

The filtrate was treated with a small volume of water to dissolve newly precipitated NaBr and then shaken once with hexane–ethyl ether 1:1 v/v (450 mL), once with ethyl ether (450 mL), and four times with ethyl acetate–ethyl ether 1:5 v/v (450 mL each time). The first upper phase (rich in bromoacetic acid) and final lower phase were discarded. The next five upper phases were pooled, filtered through Whatman #1 paper, and rotary evaporated to remove solvent.

The residue was dried under vacuum and crystallized from hot ethyl acetate (81 mL) by addition of hexane (about 12 mL) and cooling to 4 °C. The dried product (31.4 g) was similarly recrystallized from ethyl acetate (69 mL) plus hexane (15 mL) and dried under vacuum/$CaCl_2$: yield, 30.0 g (23.8%); mp 88.5–91 °C [lit. (*22*) mp 80–81 °C]; ^1H NMR (DMSO-d_6) δ 2.43 (t, 2 H, α), 3.26 (q, 2 H, β), 3.84 (s, 2 H, α′), 8.32 (br, N*H*), 12.20 (br, COOH); ^{13}C NMR (DMSO-d_6) δ 29.31 (α′), 33.4 (α), 35.2 (β), 165.91 (Ac C=O), 172.6 (Ala C=O). Anal. Calcd for $C_5H_8BrNO_3$: C, 28.59; H, 3.84; N, 6.67; Br, 38.05. Found: C, 28.67; H, 3.97; N, 6.64; Br, 38.40.

Succinimidyl 3-(Bromoacetamido)propionate (SBAP). To a solution of *N*-(bromoacetyl)-β-alanine (21.00 g, 100 mmol) and *N*-hydroxysuccinimide (13.01 g, 113 mmol) in 2-propanol (280 mL) at room temperature was added 1,3-diisopropylcarbodiimide (16.0 mL, 101 mmol). After 8–10 min, oily precipitation of the product began, and the walls of the container were scratched to induce crystallization. The mixture was allowed to stand for 1 h at room temperature and overnight at 4 °C. The crystals were collected, washed with 2-propanol (30 mL), and redissolved in 2-propanol (200 mL brought to reflux). After an overnight stand at 4 °C, the crystals were collected, washed with 2-propanol then hexane, and dried under vacuum/$CaCl_2$: yield, 22.9 g (74.6%); mp 107–110.5 °C [lit. (*23*) mp 104–106 °C]; ^1H NMR (DMSO-d_6) δ 2.80 (s, 4 H, α″), 2.82 (t, 2 H, α), 3.64 (q, 2 H, β), 3.82 (s, 2 H, α′), 7.03 (br, N*H*); ^{13}C NMR ($CDCl_3$) δ 25.62 (α″), 28.67 (α′), 31.39 (α), 35.65 (β), 166.20 (Ac C=O), 167.30, 169.06 (C=O, s). Anal. Calcd for $C_9H_{11}BrN_2O_5$: C, 35.20; H, 3.61; N, 9.12; Br, 26.02. Found: C, 35.74; H, 3.83; N, 9.20; Br, 26.12.

***N*$^{\alpha}$-(*tert*-Butoxycarbonyl)-*N*$^{\epsilon}$-[*N*-(bromoacetyl)-β-alanyl]-L-lysine (BBAL).** N^{α}-Boc-L-lysine (17.73 g, 72 mmol) was ground to a fine powder and suspended in *N*,*N*-dimethylformamide (DMF) (600 mL). SBAP (18.43 g, 60.0 mmol) was added to the suspension in five portions at 10-min intervals. The reaction mixture was stirred for 2 h at room temperature, allowed to stand overnight at 4 °C, filtered, and rotary evaporated to remove DMF (bath 30 °C, pump vacuum). The residue was shaken with a

mixture of ethyl acetate (960 mL), 1-butanol (240 mL), and aqueous 0.2 M $KHSO_4$ (300 mL). The upper phase was shaken twice with 0.2 M $KHSO_4$ (300 and 150 mL, respectively), filtered (Whatman #1 paper), and rotary evaporated to remove solvent (32 °C bath, pump vacuum). Vacuum was applied (for at least 2 h) to purge the last traces of solvent. The oily residue was dissolved in 1,2-dichloroethane (DCE) (400 mL) by gentle warming and swirling. The solution was slowly cooled to 15–20 °C during which time the product initially precipitated as an oil but was induced to crystallize by scratching. After an overnight stand (4 °C), the product was collected, washed (3 × 36-mL portions of DCE), and dried in vacuum/$CaCl_2$: yield, 17.3 g (65.8%), mp 117–122 °C dec; ^1H NMR (DMSO-d_6) δ 1.34 (s, 9 H, α'''), 1.5 (m, 6 H, β, γ, δ), 2.22 (t, 2 H, α'), 3.02 (q, imp), 3.50 (m, ϵ, β', imp), 3.82 (s + m, α + α' + imp's), 6.95 (d, Lys-α-N*H*), 7.82 (t, NH), 8.24 (t, N*H*); ^{13}C NMR (DMSO-d_6) δ 22.96 (γ), 28.13 (CH_3), 28.60 (β), 29.40 (α''), 30.41 (α'), 34.80 (δ), 35.75 (β'), 38.17 (ϵ), 53.36 (α), 61.32 (imp, $HOCH_2CON$?), 77.90 [$OC(CH_3)_3$], 155.50 (carbamate C=O), 165.81 (($BrCH_2C$=O), 169.83, 174.08 (C=O's). Anal. Calcd for $C_{16}H_{28}BrN_3O_6$: C, 43.84; H, 6.44; N, 9.59; Br, 18.23; Cl, 0. Found: C, 43.79; H, 6.61; N, 9.51; Br, 18.32; Cl, 0.38.

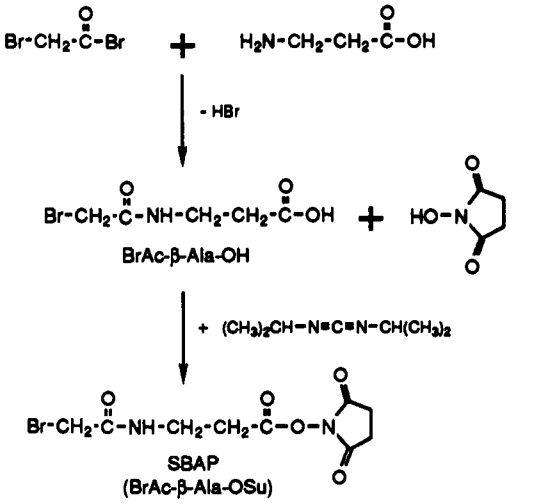
Synthesis of BBAL-Containing Peptides. The various BBAL-containing peptides were synthesized using an automated solid-phase peptide synthesizer (Model 430A, Applied Biosystems, Inc., Foster City, CA) that is based on the original Boc/Bzl solid-phase peptide synthesis procedures described in 1963 by Merrifield (*24*). For introducing BBAL residues into peptides at any desired position along the chain, the same double coupling cycles for asparagine that are preprogrammed into the instrument were found to be most suitable when peptides were synthesized on a 0.5-mmol scale, the larger of the two scales that are preprogrammed for the Model 430A. The reason for this is that BBAL is very soluble in DMF, but sparingly soluble in CH_2Cl_2, and the asparagine coupling steps of the Model 430A employ 1-hydroxybenzotriazole (HOBt) ester formation in DMF.

Briefly, the synthesis first involved the following: A mixture of BBAL and HOBt was made by dissolving 2.0 mmol BBAL in a solution containing 2.0 mmol HOBt in 4.0 mL of DMF and 0.3 mL of CH_2Cl_2. The BBAL–HOBt mixture was added to 4.0 mL of 0.5 M *N,N'*-dicyclohexylcarbodiimide (DCC) in CH_2Cl_2. This mixture was agitated by bubbling with N_2 over a period of at least 30 min at 25 °C. The dicyclohexylurea byproduct, which precipitated during the formation of the BBAL-OBt ester, was filtered off, and the ester in the filtrate was reacted with a free amine on the PAM resin to give the BBAL PAM-coupled product. *t*-Boc was removed from the coupled BBAL in the next cycle with TFA in CH_2Cl_2 using the manufacturer's preprogrammed protocol.

Following the synthesis, the peptide was deprotected and released from the PAM resin using a standard HF deprotection method as described by Robey and Fields (*18*) for preparing N-terminally bromoacetylated peptides. The only scavenger used was anisole. As mentioned previously (*18*), sulfur-containing scavengers such as thiophenol or thioanisole were avoided as a precautionary measure.

Synthesis of Peptide Polymers Using BBAL. Peptide polymers prepared with the use of BBAL have been synthesized as candidate immunogens (F. A. Robey, unpublished results). These polymerized peptides were all assembled by following the same procedure detailed previously for making peptide polymers coupled head-to-tail with cysteine at the peptide's C-terminus and bromoacetyl at the N-terminus (*18*). For polymers involving the use of synthetic peptides containing BBAL, the peptide is designed to contain cysteine at any desired position and BBAL at any other position. The BBAL, Cys-containing peptide was dissolved in 0.5 M phosphate buffer, pH 7.2, at a concentration of 20 mg/mL. The polymer was formed generally within 3 h at ambient temperatures, but we routinely allowed the mixture to stir overnight. The mixture was then dialyzed and lyophilized as detailed previously (*18*).

Scheme I

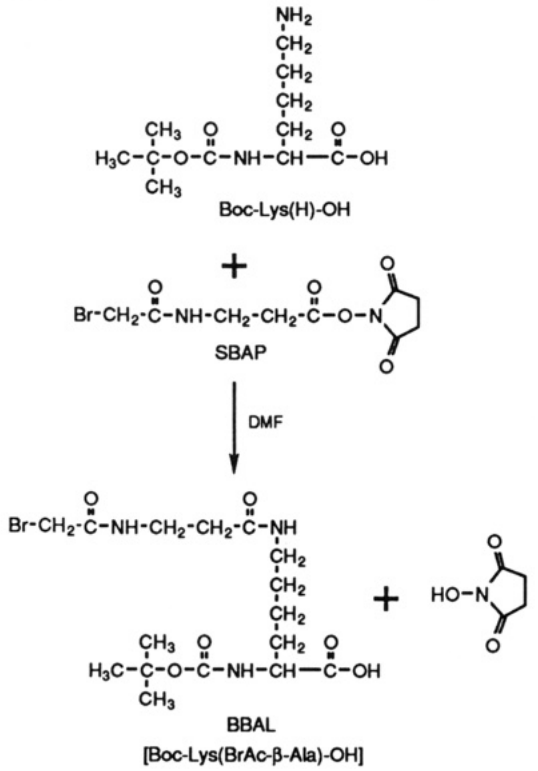


Coupling BBAL-Containing Peptides to Bovine Serum Albumin (BSA). Synthetic peptides were coupled to BSA following the same procedure outlined by Kolodny and Robey (*19*) for coupling N-terminal bromoacetyl peptides to BSA: To 30 mg of BSA dissolved in 5 mL of 0.1 M $NaHCO_3$ was added 0.2 mL of a 0.7 M solution of Bu_3P in 2-propanol, and the reaction mixture was stirred for 30 min at room temperature. Then, 30 mg of the BBAL-containing peptide was added, and the reaction mixture was continuously stirred for 1 h. The entire 6 mL of the conjugation reaction mixture was dialyzed for 12 h at 4 °C against a 6-L batch of 0.1 M NH_4HCO_3 and then against three changes of the same solution over a 2-day period. The conjugates were then obtained in powder form by lyophilization.

RESULTS

The synthesis of BBAL was accomplished in three stages as shown in Schemes I and II. First, *N*-(bromoacetyl)-β-alanine was prepared by a procedure similar to the ones reported by Yamada et al. (*22*) and Zaitsu et al. (*23*) (Scheme I, first reaction). The product was adequately separated from bromoacetic acid, resulting from hydrolysis of excess bromoacetyl bromide, by a series of extractions that obviated the need for an adsorption chromatography step. The product was purified by two crystallizations from ethyl acetate–hexane, rather than from tetrahydrofuran–isopropyl ether, and gave a melting point about 10 °C higher than that reported by Yamada et al. (*22*). This acid was converted to its *N*-hydroxysuccinimide active ester, SBAP (Scheme I, second reaction), by a technically facile approach whereby the product itself crystallized from the reaction mixture rather than a urea byproduct: Coupling was accomplished with *N,N'*-diisopropylcarbodiimide in 2-propanol instead of with DCC in a less polar solvent as is commonly done (*23*). The synthesis of BBAL was carried out conveniently and

Scheme II



cleanly with SBAP and commercially available N^{α}-Boc-L-lysine (Scheme II).

During the course of developing the above synthesis, alternative reagents and solvents were tried. Preliminary examination of products by NMR or MS often revealed significant exchange of Br with Cl in the bromoacetyl moiety whenever Cl was present in the system (data not given). This problem was especially severe when bromoacetyl chloride was used and extractions were conducted over aqueous NaCl, suggesting an ionic mechanism for the halogen exchange. All Cl-containing reagents were then eliminated from use except 1,2-dichloroethane used to crystallize BBAL, since it and dichloromethane were the only solvents that we found from which the final solidification and purification of BBAL could be achieved. The Cl content of BBAL, crystallized once from dichloroethane, was 0.38% (4.7 mol %), but it increased to 1.1% (13.6 mol %) following recrystallization from the same solvent.

A simpler analogue of BBAL, N^{α}-(*tert*-butoxycarbonyl)-N^{ϵ}-(bromoacetyl)-L-lysine, was prepared by three different routes, each leading to a noncrystallizable, vitreous product (data not given). The method deemed most satisfactory for yielding a pure product was the one that paralleled the BBAL synthesis reported above wherein SBAP was substituted with *N*-succinimidyl bromoacetate, prepared as described by Bernatowicz and Matsueda (*12*).

BBAL can be used effectively in strategies for polymerizing synthetic peptides. For example, the peptides can be polymerized "tail-to tail" if both cysteine and BBAL have been placed in the C-terminal region of the peptide monomers and if they are subjected to conditions that favor reaction of a thiol group of one molecule with a bromoacetyl moiety on another one, etc. The monomer peptides are thus joined through stable thioether linkages. The result of one such experiment is shown by the SDS–PAGE run presented in Figure 1. Molecular masses as high as 30 kDa are observable in the mixture of polymer sizes. Other peptides have been polymerized in like manner to yield polymer components with molecular masses exceeding 30 kDa (results not shown). In general, we have found that the size distribution of the peptide polymers depends in part on the solubility and size of the peptide monomers; the greater the solubility, the higher is the degree of polymerization.

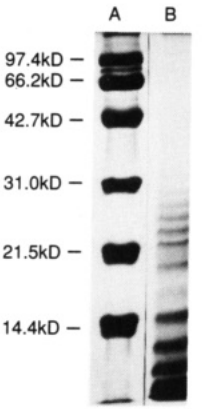


Figure 1. SDS–PAGE run of a peptide polymer obtained by intermolecular cross-linking of a BBAL-containing peptide with itself through a coexisting cysteine residue. Lane A shows the molecular weight standards; lane B shows the synthetic peptide polymer having the monomer sequence Lys-Ser-Ile-Arg-Ile-Gln-Arg-Gly-Pro-Gly-Arg-Val-Ile-Tyr-Cys-BBAL-NH_2. The gel was stained with Coomassie Brilliant Blue R250.

Although we have not investigated cyclization in detail, there appears to be a tendency for peptides to cyclize that have four to six amino acid residues between the bromoacetyl-bearing and Cys residues (unpublished observations). Therefore, the recommendation for optimal polymerization (greatest number of repeat units) is to use peptide monomers with more than six interstitial residues, preferably ones with 15–20 such residues. The sequence of the peptide used in the experiment illustrated by Figure 1 is given in the caption.

Synthetic peptides containing BBAL, but not cysteine, are readily conjugated with carriers bearing reactive sulfhydryl groups. Peptide-carrier conjugates are commonly used as immunogens or test antigens. We have employed BSA as a carrier following reduction of some of its cystine disulfide bonds with Bu_3P (*25*) in order to release multiple thiol groups as conjugation sites (see the Experimental Procedures and ref 19). Two systems of amino acid analysis were used in this study to evaluate the number of BBAL peptides conjugated to modified BSA. The Picotag chromatogram of Figure 2 clearly shows a measurable amount of CMC from the hydrolysis of Gly-Arg-Gly-Glu-Pro-Thr-BBAL linked to reduced BSA. The amino acid standard chromatogram containing CMC in the Picotag system and the calculation to quantify the CMC were presented previously (*19*).

The Picotag amino acid analysis system could not be used to quantify the β-alanine that is also formed from the acid hydrolysis of BBAL–peptide-derived structures. β-Alanine elutes at the same position as histidine (ca. 4.2–4.5 min), and thus the two components cannot be distinguished. A value for β-alanine could be obtained by Picotag if the sample undergoing analysis contained no histidine.

The second amino acid analysis system that we employed was Amino Quant. The 1-nmol standard chromatogram, containing 1 nmol of β-alanine, is shown in Figure 3. It is clear from examining this chromatogram that the β-alanine peak (designated Beta-ALA) is completely resolved from the nearest amino acids (threonine and alanine). Shown in Figure 4 is the Amino Quant chromatogram of

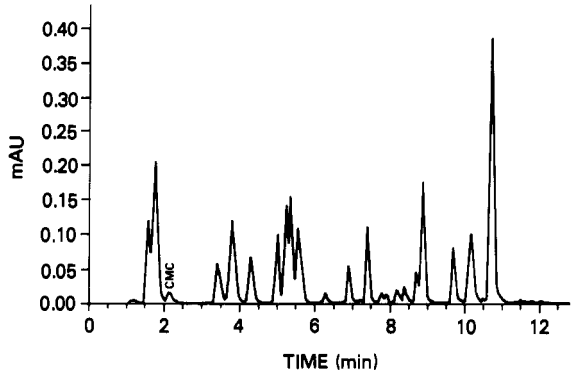


Figure 2. A Picotag chromatogram of the acid hydrolyzate of the conjugate (Gly-Arg-Gly-Glu-Pro-Thr-BBAL)$_n$–BSA. The conjugate was formed by reaction of the BBAL peptide with Bu_3P-reduced BSA as detailed under Experimental Procedures and in ref 19. CMC is cleanly resolved, allowing the measurement of BBAL peptide covalently coupled to BSA. β-Alanine, which also results from hydrolysis of the conjugate, overlaps the histidine peak and therefore cannot be assayed using the standard conditions for analysis in the Picotag system.

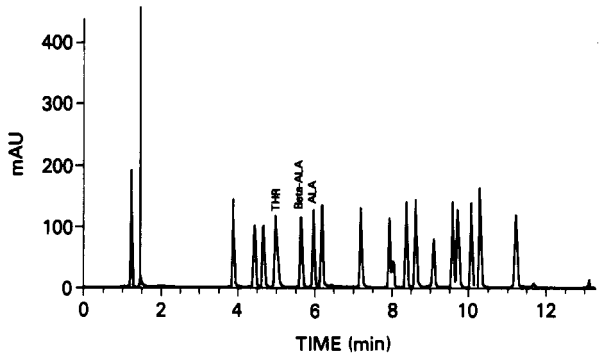


Figure 3. Chromatogram for a 1-nmol amino acid standard spiked with β-alanine, using the Amino Quant system. β-Alanine is cleanly resolved from the adjacent amino acids, Thr and Ala, and thus, is used to quantitate directly the amount of BBAL-containing peptide conjugated to a protein. The naturally occurring amino acids from the carrier protein are likely to mask all other amino acids in the synthetic peptide. CMC, readily detected with the Picotag system, cannot be measured from a typical Amino Quant run because it elutes with the acidic amino acids (not shown).

the acid hydrolyzate of the same peptide–BSA conjugate described in Figure 2. Again, the β-alanine peak is cleanly baseline-resolved from the other amino acids. Thus, Figures 2 and 4 demonstrate the unique versatility of conjugating peptides to cysteine residues of a protein carrier; more than one amino acid marker can be used to quantify the amount of peptide coupled to the carrier protein.

DISCUSSION

We have described in this paper the synthesis and characterization of a new compound, BBAL, that provides the peptide chemist with a novel means for building peptides that contain a residue bearing a thiol-reactive side chain at any desired location in the sequence. With this capability, he/she is able to prepare specific peptide components of biological response modifiers that can be readily attached to other molecular species or specialized surfaces through stable thioether bonds. The locus of attachment of peptide epitopes and thus their orientation and biological activity will be uniform and controlled by design. Furthermore, peptides synthesized with both BBAL and Cys residues may be cyclized or self-polymerized.

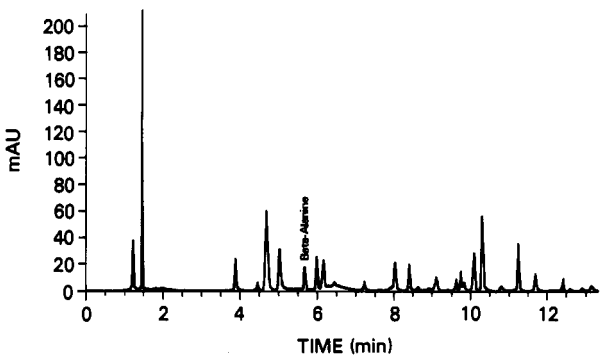


Figure 4. Amino Quant analysis of the hydrolyzate from the same peptide–BSA conjugate described in the Figure 2 caption. The β-alanine peak is clearly displayed in this system.

The first two stages of the synthesis of BBAL yielded a reagent, *N*-succinimidyl 3-(bromoacetamido)propionate (SBAP) (Scheme I) that provided a direct and convenient means for preparing BBAL from commercially available N^{α}-Boc-L-lysine (Scheme II). The conditions for the synthesis of SBAP and BBAL were developed with the goal of allowing easy scale up. It was pointed out by Zaitsu et al. (*23*) that SBAP itself has the properties of a generally useful heterobifunctional cross-linking reagent. The method for synthesis of this compound that has been detailed in this report should prove easier to carry out on lab or pilot scale than the one previously described (*22*, *23*).

Attempts to prepare other functionally equivalent analogues of BBAL [e.g., Boc-Lys(BrAc)-OH and Boc-Orn(BrAc-β-Ala)-OH] resulted in products that could not be obtained in solid form, placing a practical constraint on their use and rendering them more difficult to purify on a large scale. The intended characteristics of our reagent were (1) possession of three functional groups, bromoacetyl, Boc-amine, and free carboxyl, and (2) that it be a stable, crystalline solid. BBAL met these demands, and the β-alanine residue incorporated into its structure provided four atoms of additional spacing in the side-chain linkage function plus an acid-stable marker (β-alanine) for analysis of conjugate composition.

BBAL has been successfully employed with a standard solid-phase synthesis program based on N^{α}-Boc temporary protection, benzyl-type side-chain protection and final HF deprotection/cleavage. In this type of system, there is the possibility of some nucleophilic attack at the α-bromo carbon atom of BBAL side chains by HOBt or freshly liberated α-amino groups following TFA cleavage and alkalinization steps. We have observed minor amounts of byproducts that may have resulted from this side reaction; however, it would be feasible to remove these impurities if they should enter into and impair functioning of the end product. Although we have not tried using BBAL with methods based on N^{α}-Fmoc protection, it seems to us that its use might not be feasible anywhere except at the N-terminal position because of the expected reaction of bromoacetyl groups with the nucleophilic Fmoc cleavage reagent (e.g., piperidine).

The bromoacetyl group, like the somewhat less reactive chloroacetyl moiety, survives HF cleavage conditions (*17*, *18*), while the iodoacetamido function does not (F. A. Robey, unpublished observation). The selectivity of bromoacetamido groups for sulfhydryl anions in neutral or slightly alkaline media is comparable to that of iodoacetamido and may be significantly greater than that of maleimido groups (*12*).

A large number of practical applications can be envisaged

wherein a substance such as BBAL, incorporated into synthetic peptides, could play a critical role. In the case of synthetic peptide vaccine candidates, linear polymerization of peptides appears to enhance immunogenicity (*17*, *18*, *26*). BBAL, Cys peptide polymerizations may be directed in "tail-to-tail", "head-to-tail", or "head-to-head" modes by virtue of the independence allowed in positioning the functional residues in the monomer epitope. Used as immunogens, the resulting polymers gave rise to significantly different immune responses (F. A. Robey, unpublished observations). Cyclic peptides may be favored by autoreaction of BBAL, Cys peptides in very dilute solution. These looped peptides may form the basis of epitopes that better imitate those of the native protein (*27*). Potentially useful peptide conjugates with many types of molecules, polymers, or surfaces may be made from BBAL peptides. For example, conjugates can be prepared with oriented peptide epitopes attached to immunogen carriers, adsorbents, immunoassay materials, or surfaces of medical prostheses. These products should have clearly defined biological responses and distinct properties made possible by the flexible and uniform positioning of cross-linking loci.

ACKNOWLEDGMENT

We express our gratitude to Dr. Robert J. Highet of the National Heart Lung and Blood Institute, National Institutes of Health, for the NMR analyses and interpretation of the spectra. We also thank Allison Murphey for valuable technical assistance and recognize the excellent service of Galbraith Laboratories, Inc., Knoxville, TN, where the elemental analyses were performed.

LITERATURE CITED

(1) Lerner, R. A. (1982) Tapping the immunological repertoire to produce antibodies of predetermined specificity. *Nature 299*, 592–596.

(2) Zavala, F., Tam, J. P., Hollingdale, M. R., Cochrane, A. H., Quakyi, I., Nussenzweig, R. S., and Nussenzweig, V. (1985) Rationale for development of a synthetic vaccine against *Plasmodium falciparum* malaria. *Science 228*, 1436–1440.

(3) Tam, J. P. (1988) Synthetic peptide vaccine design: Synthesis and properties of a high-density multiple antigenic peptide system. *Proc. Natl. Acad. Sci. U.S.A. 85*, 5409–5413.

(4) Milich, D. R. (1989) Synthetic T and B cell recognition sites. *Adv. Immunol. 45*, 195–282.

(5) Massia, S. P., and Hubbell, J. A. (1990) Covalent surface immobilization of Arg-Gly-Asp- and Tyr-Ile-Gly-Ser-Arg-containing peptides to obtain well-defined cell-adhesive substrates. *Anal. Biochem. 187*, 292–301.

(6) Brandley, B. K., and Schnaar, R. L. (1988) Covalent attachment of an Arg-Gly-Asp sequence to derivatizable polyacrylamide surfaces: Support of fibroblast adhesion and long-term growth. *Anal. Biochem. 172*, 270–278.

(7) Dyrberg, T., and Oldstone, M. B. A. (1986) Peptides as antigens. Importance of orientation. *J. Exp. Med. 164*, 1344–1349.

(8) Schaaper, W. M. M., Lankhof, H., Puijk, W. C., and Meloen, R. H. (1989) Manipulation of antipeptide immune response by varying the coupling of the peptide with the carrier protein. *Mol. Immunol. 26*, 81-85.

(9) Golvano, J., Lasarte, J. J., Sarobe, P., Gullón, A., Prieto, J., and Borrás-Cuesta, F. (1990) Polarity of immunogens: Implications for vaccine design. *Eur. J. Immunol. 20*, 2363–2366.

(10) Wetzel, R., Halualani, R., Stults, J. T., and Quan, C. (1990) A general method for highly selective cross-linking of unprotected polypeptides via pH-controlled modification of N-terminal α-amino groups. *Bioconjugate Chem. 1*, 114–122.

(11) Green, N., Alexander, H., Olson, A., Sutcliffe, J. G., and Lerner, R. A. (1982) Immunogenic structure of the influenza virus hemagglutinin. *Cell 28*, 477–487.

(12) Bernatowicz, M. S., and Matsueda, G. R. (1986) Preparation of peptide–protein immunogens using *N*-succinimidyl bromoacetate as a heterobifunctional crosslinking reagent. *Anal. Biochem. 155*, 95–102.

(13) Drijfhout, J. W., Bloemhoff, W., Poolman, J. T., and Hoogerhout, P. (1990) Solid-phase synthesis and applications of *N*-(*S*-acetylmercaptoacetyl) peptides. *Anal. Biochem. 187*, 349–354.

(14) Bernatowicz, M. S., Matsueda, R., and Matsueda, G. R. (1986) Preparation of Boc-[*S*-(3-nitro-2-pyridinesulfenyl)]-cysteine and its use for unsymmetrical disulfide bond formation. *Int. J. Pept. Protein Res. 28*, 107–112.

(15) Drijfhout, J. W., Perdijk, E. W., Weijer, W. J., and Bloemhoff, W. (1988) Controlled peptide-protein conjugation by means of 3-nitro-2-pyridinesulfenyl protection-activation. *Int. J. Pept. Protein Res. 32*, 161–166.

(16) Ponsati, B., Giralt, E., and Andreu, D. (1989) A synthetic strategy for simultaneous purification–conjugation of antigenic peptides. *Anal. Biochem. 181*, 389–395.

(17) Lindner, W., and Robey, F. A. (1987) Automated synthesis and use of *N*-chloroacetyl-modified peptides for the preparation of synthetic peptide polymers and peptide–protein immunogens. *Int. J. Pept. Protein Res. 30*, 794–800.

(18) Robey, F. A., and Fields, R. L. (1989) Automated synthesis of *N*-bromoacetyl-modified peptides for the preparation of synthetic peptide polymers, peptide–protein conjugates, and cyclic peptides. *Anal. Biochem. 177*, 373–377.

(19) Kolodny, N., and Robey, F. A. (1990) Conjugation of synthetic peptides to proteins: Quantitation from *S*-carboxymethylcysteine released upon acid hydrolysis. *Anal. Biochem. 187*, 136–140.

(20) Laemmli, U. K. (1970) Cleavage of structural proteins during the assembly of the head of bacteriophage T4. *Nature 227*, 680–685.

(21) Kalinowski, H.-O., Berger, S., and Braun, S. (1988) *Carbon-13 NMR Spectroscopy*, John Wiley & Sons, New York.

(22) Yamada, H., Uozumi, F., Ishikawa, A., and Imoto, T. (1984) Nature of the binding site around and reactivity of histidine-15 in lysozyme. *J. Biochem. 95*, 503–510.

(23) Zaitsu, K., Ohnishi, M., Hosoya, H., Sugimoto, H., and Ohkura, Y. (1987) New heterobifunctional cross-linking reagents for protein conjugation, *N*-(bromoacetamido-*n*-alkanoyloxy)succinimides. *Chem. Pharm. Bull. 35*, 1991–1997.

(24) Merrifield, R. B. (1963) Solid phase peptide synthesis. I. The synthesis of a tetrapeptide. *J. Am. Chem. Soc. 85*, 2149–2154.

(25) Rüegg, U. Th., and Rudinger, J. (1977) Reductive cleavage of cystine disulfides with tributylphosphine. *Methods Enzymol. 47*, 111–116.

(26) Borras–Cuesta, F., Fedon, Y., and Petit-Camurdan, A. (1988) Enhancement of peptide immunogenicity by linear polymerization. *Eur. J. Immunol. 18*, 199–202.

(27) Jemmerson, R., and Hutchinson, R. M. (1990) Fine manipulation of antibody affinity for synthetic epitopes by altering peptide structure: antibody binding to looped peptides. *Eur. J. Immunol. 20*, 579–585.

Preparation of Oligonucleotide–Peptide Conjugates

Ching-Hsuan Tung, M. Jonathan Rudolph, and Stanley Stein*

Center for Advanced Biotechnology and Medicine, and Chemistry Department, Rutgers University, 679 Hoes Lane, Piscataway, New Jersey 08854. Received August 9, 1991

A procedure for preparing oligonucleotide–peptide conjugates is presented. It is based on appending a maleimide group to the oligonucleotide for selective coupling to the thiol side chain of a cysteine residue in the peptide. A convenient chromatographic purification procedure, based on Fmoc-on/Fmoc-off, is described.

Conjugates of oligonucleotides with peptides having specific functions can be useful for various applications. Examples include the use of a nuclear transport signal peptide to direct intracellular trafficking (*1*), a hydrophobic peptide (*2*) or polylysine (*3*) to increase cell penetrability, and polylysine to provide multiple attachment sites for nonradioactive reporting probes (*4*, *5*). The tripeptide Gly-Gly-His has been demonstrated to be a metal chelator which can bind Cu(II) or Ni(II) (*6*, *7*). This tripeptide has been conjugated to the N-terminus of the DNA-binding domain of the protein *Hin* recombinase. In the presence of Cu(II) or Ni(II) and a free-radical source, there is a sequence-specific cleavage of DNA via an oxidative degradation mechanism. Attachment of this tripeptide to an oligonucleotide might, therefore, provide a type of restriction enzyme based on sequence-specific hybridization.

Synthesizing peptide–oligonucleotide conjugates directly on solid-phase peptide and DNA synthesizers has been reported (*2*, *4*). Unfortunately, the purine bases of adenine and guanine are labile to acidic conditions. Peptide amide bonds, as well as side chains of certain amino acids, can be partially hydrolyzed under alkaline conditions. Therefore, complete solid-phase synthesis of these conjugates on either a peptide synthesizer or a DNA synthesizer might be unsatisfactory due to side reactions during coupling cycles or cleavage from the solid support (*1*). Postsynthesis conjugation is an alternative.

A convenient and specific approach for conjugating an oligonucleotide to a peptide utilizes the reaction of a maleimide group with a thiol group. Similar conjugations of peptides or proteins through disulfide linkage have been reported (*8–10*). In our procedure, a primary, aliphatic amino group is incorporated at the 5′-terminus of the oligonucleotide at the last cycle of automated synthesis. The oligonucleotide is cleaved from the support and purified, and then a maleimide group is appended to the amino group. A residue of cysteine, which has a side-chain thiol, may be placed at any position in the peptide during its synthesis. The peptide is, likewise, cleaved and purified. The maleimidyl oligonucleotide is then reacted in solution with the peptide. This approach differs from the recently published methods in which a thiol group is incorporated into the synthetic oligonucleotide (*1*, *11*). That requires a more complicated thiolation step or detriylation step, and places the readily oxidizable thiol on the oligonucleotide, which is the limiting reagent for the final conjugation reaction. An additional feature of our process is the facile purification of the final product by two steps of chromatography of the Fmoc-on and Fmoc-off conjugates.

The peptide amide (Fmoc-Gly-Gly-His-Cys-NH_2) in Scheme I was synthesized on the PAL support by Fmoc chemistry in a MilliGen/Biosearch Model Excell peptide synthesizer (Burlington, MA). After synthesis, the peptide with the last Fmoc group left on was cleaved from the solid support with 5 mL of TFA/anisole (95/5) and the solid support was removed by filtration. The filtrate was evaporated to near dryness under a stream of dry nitrogen and then precipitated from ethyl ether. The precipitate was collected by filtration and stored at room temperature. This peptide was used without further purification. Cysteine-containing peptides in the solid form are stable toward oxidation (*12*).

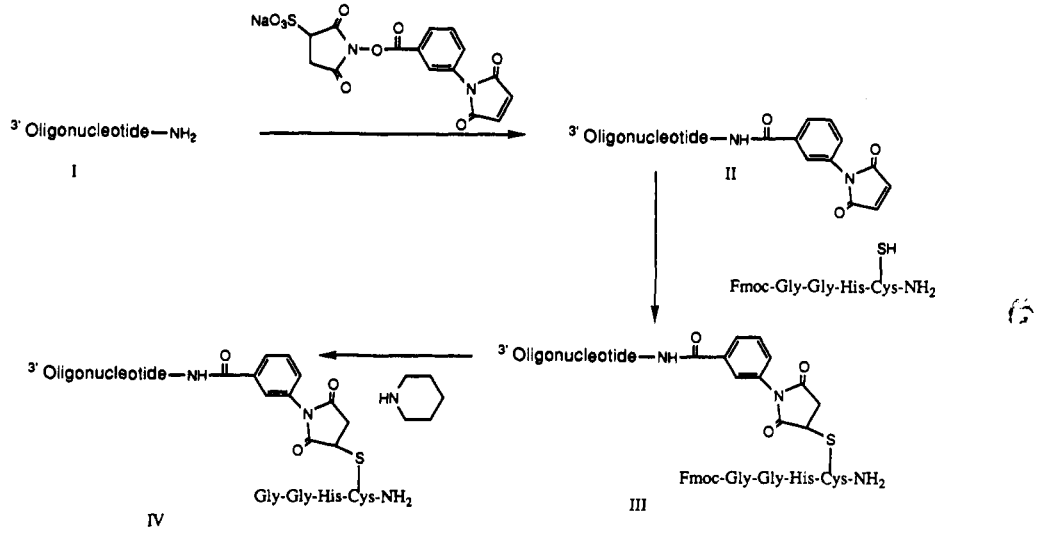
The oligonucleotide used in these studies was an amino-linked 15-mer with the sequence of 5′ TAC TTG GGT-TGG CTT 3′, which was synthesized by phosphoramidite methodology using a Model 380B DNA synthesizer (Applied Biosystems, Foster City, CA). A hexanolamine linker was coupled to the 5′-end of the 15-mer on the synthesizer.

3-Maleimidobenzoic acid sulfosuccinimido ester (Sulfo-MBS) (2 mg) (Pierce; Rockford, IL) and purified amino-linked oligonucleotide I (4 OD, A_{260}) were incubated in sodium bicarbonate solution (0.1 M, 100 μL) for 30 min. The unreacted Sulfo-MBS and some byproducts were removed by anion-exchange chromatography. The chromatographic separations were performed on a Nucleogen 60-7 DEAE column (4 × 125 mm). Mobile phase A was 60% 20 mM NaOAc (pH 6.5) and 40% acetonitrile, and mobile phase B was mobile phase A containing 0.7 M LiCl. The gradient was 100% isocratic A for 10 min, 100% A to 88% A for 20 min, and 88% A to 50% A in 1 min. The eluent at 34 min was collected. The collected portion was then desalted by reverse-phase chromatography (Figure 1B). The chromatogram was quite clean, since the byproducts and unreacted Sulfo-MBS had been removed by ion-exchange purification. Multiple peaks are commonly observed for derivatized oligonucleotides (*13*). All the peaks from 19 to 23 min were examined using the photodiode-array detector, and a UV spectrum characteristic of DNA was observed for each single peak. All peaks between 19 and 23 min were pooled and dried under vacuum, giving a 70% yield (2.8 OD, A_{260}).

Fmoc-Gly-Gly-His-Cys-NH_2 (3 mg) and maleimidobenzoyl oligonucleotide II (2.8 OD, A_{260}) were allowed to react in phosphate buffer (0.1 M, pH 6.6, 200 μL) and acetonitrile (100 μL) overnight. The reaction mixture was purified by reverse-phase chromatography. Because of the hydrophobicity of the Fmoc group, all the peaks between 19 and 23 min had disappeared, and a new broad peak was seen at 34 min (Figure 1C). Excess, unreacted peptide appeared at 42 min. Fmoc–peptide–oligonucleotide III was collected and dried under vacuum to give an 86% yield (2.4 OD, A_{260}).

1043-1802/91/2902-0464$02.50/0 © 1991 American Chemical Society

Scheme I. Synthetic Scheme of Peptide–Oligonucleotide Preparation



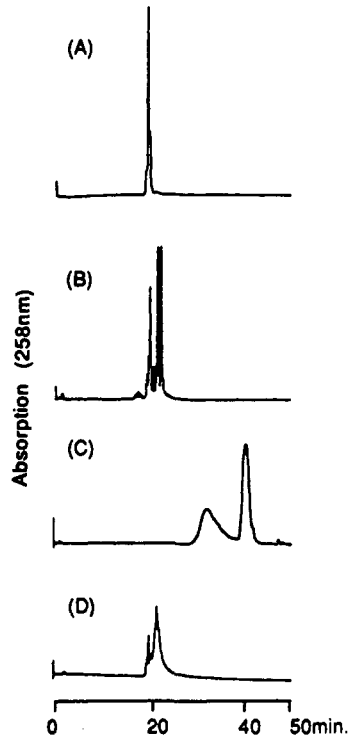


Figure 1. Reverse-phase HPLC chromatogram: (A) amino-linked oligonucleotide I, (B) maleimidyl oligonucleotide II; (C) Fmoc-on peptide–oligonucleotide III; (D) Fmoc-off peptide–oligonucleotide IV. Reverse-phase separation was done on an EM LiChrospher 100RP-18, 5-μm column (4 × 125 mm). Mobile phase A was 95% 0.1 M TEAA buffer (pH 7.0) and 5% acetonitrile, and mobile phase B was 5% 0.1 M TEAA buffer (pH 7.0) and 95% acetonitrile. The gradient was 100% A for 5 min, 100% A to 50% A in 50 min. The flow rate was 1 mL/min.

The Fmoc group on the peptide–oligonucleotide conjugate was removed by treatment with piperidine/water (1:1, 100 μL) for 10 min. The piperidine solution was removed under vacuum. The residue was purified by reverse-phase chromatography. The major peak had shifted to 21 min (Figure 1D). The yield for this step was 88% (2.1 OD, A_{260}). The overall yield of this conjugation was 53%. The collected final product IV was identified by amino acid analysis. The ratio of Gly:His was 70:30, and cysteine was not measured.

Herein, we successfully coupled a metal-chelate peptide to an oligonucleotide through Sulfo-MBS. By Fmoc-on and Fmoc-off two-step purification, the product was easily prepared and purified. Further studies aimed at sequence-specific cleavage are in progress.

LITERATURE CITED

(1) Eritja, R., Pons, A., Escarceller, M., Giralt, E., and Albericio, F. (1991) Synthesis of defined peptide-oligonucleotide hybrids containing a nuclear transport signal sequence. *Tetrahedron 47*, 4113–4120.

(2) Juby, C. D., Richardson, C. D., and Brousseau, R. (1991) Facile preparation of 3'oligonucleotide-peptide conjugates. *Tetrahedron Lett. 32*, 879–882.

(3) Leonetti, J.-P., Degols, G., and Lebleu, B. (1990) Biological activity of oligonucleotide-poly(L-lysine) conjugates: mechanism of cell uptake. *Bioconjugate Chem. 1*, 149–153.

(4) Haralambidis, J., Duncan, L., and Tregear, G. W. (1987) The solid phase synthesis of oligonucleotides containing a 3'-peptide moiety. *Tetrahedron Lett. 28*, 5199–5202.

(5) Haralambidis, J., Duncan, L., Angus, K., and Tregear, G. W. (1990) The synthesis of polyamide–oligonucleotide conjugate molecules. *Nucleic Acids Res. 18*, 493–499.

(6) Mack, D. P., Iverson, B. L., and Dervan, P. B. (1988) Design and chemical synthesis of a sequence-specific DNA-cleaving protein. *J. Am. Chem. Soc. 110*, 7572–7574.

(7) Mack, D. P., and Dervan, P. B. (1990) Nickel-mediated sequence-specific oxidative cleavage of DNA by a designed metalloprotein. *J. Am. Chem. Soc. 112*, 4604–4606.

(8) Gaur, P. K., Sharma, P., and Gupta, K. C. (1989) A simple method for the introduction of thiol group at 5'-termini of oligodeoxynucleotides. *Nucleic Acids Res. 17*, 4404.

(9) Zuckermann, R., Corey, D., and Schultz, P. (1987) Efficient methods for attachment of thiol specific probes to the 3'-ends of synthetic oligodeoxyribonucleotides. *Nucleic Acids Res. 15*, 5305–5321.

(10) Chu, B. C. F., and Orgel, L. E. (1988) Ligation of oligonucleotides to nucleic acids or proteins via disulfide bonds. *Nucleic Acids Res. 16*, 3671–3691.

(11) Ghosh, S. S., Kao, P. M., McCue, A. W., and Chappelle, H. L. (1990) Use of maleimide–thiol coupling chemistry for efficient syntheses of oligonucleotide–enzyme conjugate hybridization probes. *Bioconjugate Chem. 1*, 71–76.

(12) Tsao, J., Lin, X., Lackland, H., Tous, G., Wu, Y., and Stein, S. (1991) Internally standardized amino acid analysis for determining peptide/carrier protein coupling ratio. *Anal. Biochem. 197*, 137–142.

(13) Agrawal, S., and Zamecnik, P. C. (1990) Site specific functionalization of oligonucleotides for attaching two different reporter groups. *Nucleic Acids Res. 18*, 5419–5423.

Biotinylated Granulocyte/Macrophage Colony-Stimulating Factor Analogues: Effect of Linkage Chemistry on Activity and Binding

Timothy P. Angelotti,*,† Michael F. Clarke,‡ Marc A. Longino,§ and Stephen G. Emerson‡

Department of Pharmacology, Department of Internal Medicine, Division of Hematology and Oncology, and Department of Radiology, University of Michigan Medical School, Ann Arbor, Michigan 48109.
Received July 18, 1991

Biotinylated granulocyte/macrophage colony-stimulating factor (GM-CSF) analogues with different linkage chemistries and levels of conjugated biotin were synthesized by reacting recombinant human GM-CSF with sulfosuccinimidyl 6-biotinamidohexanoate or biotin hydrazide/1-[3-(dimethylamino)-propyl]-3-ethylcarbodiimide. These chemically reactive forms of biotin produced derivatives biotinylated at amine or carboxyl groups, respectively. Amine-derivatized analogues of 1.2 and 3.8 mol of biotin/mol of protein (N^1-bGM-CSF and N^4-bGM-CSF) and a carboxyl-modified analogue of 4.6 mol of biotin/mol of protein (C^5-bGM-CSF) were synthesized. These analogues were compared to determine the effect of biotinylation on biological activity and GM-CSF receptor binding characteristics. The biotinylated proteins migrated with the same molecular weight as the native, unmodified protein as determined by SDS-PAGE and could be detected by Western blotting with alkaline phosphatase conjugated streptavidin, thus demonstrating the biotin linkage. All three analogues retained full agonist activity relative to the native protein (EC_{50} = 10–15 pM) when assayed for the stimulation of human bone marrow progenitor cell growth. Cell surface GM-CSF receptor binding was characterized by the binding of the analogues to human neutrophils, with detection by fluorescein-conjugated avidin and fluorescence-activated cell sorting. The N-bGM-CSFs demonstrated GM-CSF receptor specific binding that was displaceable by excess underivatized protein, with the detected fluorescence signal decreasing with increasing biotin to protein molar ratio. In contrast, C^5-bGM-CSF binding above background fluorescence could not be detected using this system, suggesting that this derivative could bind to and activate the receptor, but not simultaneously bind fluorescein-conjugated avidin. The amine-derivatized biotinylated GM-CSF analogues retained biological activity, could specifically label cell surface receptors, and may be useful nonradioactive probes with which to study GM-CSF receptor cytochemistry and receptor modulation by flow cytometry.

INTRODUCTION

Human granulocyte/macrophage colony-stimulating factor (GM-CSF[1]) is a pleiotropic glycoprotein cytokine that exerts effects on both immature and mature hematopoietic cells. It stimulates not only proliferation and maturation of myeloid progenitor cells but also enhances several physiological functions of mature myeloid-derived cells, including the priming of neutrophil respiratory bursts and antibody-dependent cell-mediated cytotoxicity, and macrophage tumoricidal activity (reviewed in ref 1). Cloning of the cDNA encoding human GM-CSF (*2*) has made it possible to purify the recombinant protein for study of its in vitro and in vivo effects. Milligram quantities of the pure protein now can be obtained for chemical modification, and the development of such derivatives has greatly enhanced the characterization of the biochemistry and physiology of this gr· ·th factor. Radioiodinated recombinant GM-CSF has been synthesized by many laboratories and utilized to understand the complex interactions of GM-CSF with its cell surface receptor (*3–6*). Recent cloning of the receptor cDNAs suggests that the low affinity form of the receptor is composed of a single subunit that can be converted to a high-affinity state upon interaction with a second 120-kDa protein (*6*, *7*). It is not completely clear, though, which affinity state of the receptor mediates which physiological functions. Radioiodinated GM-CSF has been a useful tool with which to investigate ligand–receptor interactions, but its utility is mostly limited to cell surface and solubilized receptor studies (*8*).

By taking advantage of the high affinity of biotin for avidin or streptavidin (*9*, *10*), development of biotin-conjugated protein ligands has enabled many investigators to expand the study of receptors to other functions beyond receptor binding kinetics. These include postreceptor binding events (including receptor internalization), receptor biochemistry, and isolation of viable receptor expressing cells (*11–17*). Radiolabeled ligands are not generally applicable to the study of these events. Recent advances in biotin-conjugation reagents for protein modification at specific amino acid and carboxylate residues (*18*) have enabled researchers to use biotinylated proteins as tools with which to study how the protein structure effects its function. For some proteins, such as β-nerve growth factor, interleukin-1α or -β, parathyroid hormone, and erythropoietin, modification of the protein at specific

* To whom reprint requests should be addressed at Department of Pharmacology, 6322 Medical Science I, University of Michigan Medical School, Ann Arbor, MI 48109-0626.
† Department of Pharmacology.
‡ Department of Internal Medicine.
§ Department of Radiology.

[1] Abbreviations: GM-CSF, granulocyte/macrophage colony-stimulating factor; rhGM-CSF, recombinant human GM-CSF; sulfo-NHS-biotin, sulfosuccinimidyl 6-biotinamidohexanoate; EDAC, 1-[3-(dimethylamino)propyl]-3-ethylcarbodiimide; IMDM, Iscove's Modified Dulbecco's Medium; FBS, fetal bovine serum; HABA, 4-hydroxyazobenzene-2′-carboxylic acid; MES, 2-morpholinoethanesulfonic acid; SDS–PAGE, sodium dodecyl sulfate polyacrylamide gel electrophoresis; kDa, kilodalton; BCIP, 5-bromo-4-chloro-3-indolyl phosphate; NBT, nitroblue tetrazolium; cpm, counts per minute; FITC–avidin, fluorescein-conjugated avidin; PBS, Dulbecco's phosphate-buffered saline (pH = 7.4): Na_2PO_4 (4.3 mM), KH_2PO_4 (1.4 mM), KCl (2.7 mM), and NaCl (137 mM).

1043-1802/91/2902-0466$02.50/0 © 1991 American Chemical Society

lysine residues resulted in inactivation of the protein (*14*, *15*, *17*, *19*, *20*), suggesting a role for these amino acid residues in receptor binding or maintenance of protein tertiary structure.

We wished to develop a biologically active and chemically stable biotinylated GM-CSF analogue for use in flow cytometric analysis of receptors expressed on cells at low levels. By conjugation of GM-CSF to biotin using different specific amino acid linkage chemistries, we also sought to investigate the role of specific basic and acidic residues on biological activity and binding. In this paper, we describe the synthesis of three biotinylated derivatives of GM-CSF modified at amine- or carboxyl-containing residues. We demonstrated that modification of human GM-CSF with approximately one or four biotins at amine residues or five biotins at carboxyl residues does not diminish biological activity as assessed by the stimulation of enriched bone marrow progenitor cell growth. Detection of the amine-modified derivatives bound to neutrophils using fluoroscein-conjugated avidin (FITC–avidin) and flow cytometry diminished with increasing biotin content. In contrast, the binding of the carboxyl-modified GM-CSF was not perceptible with this system, suggesting that the biotin-modified residues are hidden from detection upon receptor binding or that the protein was not uniformly derivatized using this linkage chemistry.

EXPERIMENTAL PROCEDURES

Materials. Yeast- and CHO-derived recombinant human GM-CSF (rhGM-CSF) were the generous gifts of Dr. Steven Gillis (Immunex, Seattle, WA) and Dr. Steven C. Clark (Genetics Institute, Cambridge, MA), respectively. Chemicals used in these experiments were obtained from the following sources: sulfosuccinimidyl 6-biotinamidohexanoate (sulfo-NHS-biotin) and 1-[3-dimethylamino)propyl]-3-ethylcarbodiimide (EDAC), Pierce Chemical Co. (Rockford, IL); *d*-biotin, Research Organics, Inc. (Cleveland, OH); biotin (long arm) hydrazide, avidin D, and fluorescein-conjugated avidin DCS (cell sorter grade), Vector Laboratories (Burlingame, CA); biotinylated and nonbiotinylated low molecular weight protein markers, Bio-Rad, Inc. (Richmond, CA); streptavidin-conjugated alkaline phosphatase and Iscove's Modified Dulbecco's Medium (IMDM), Gibco-BRL (Gaithersburg, MD); fetal bovine serum, Hyclone Laboratories Inc. (Logan, UT); [^{3}H]thymidine, NEN/Du Pont (Bannockburn, IL); Ficoll Hypaque, Pharmacia Fine Chemicals (Piscataway, NJ); and 4-hydroxyazobenzene-2′-carboxylic acid (HABA), 2-morpholinoethanesulfonic acid (MES), Coomassie Brilliant Blue R250, and all other chemicals, Sigma Chemicals (St. Louis, MO).

Cell Source. Peripheral blood granulocytes and bone marrow were obtained following informed consent from normal donors under a protocol approved by the University of Michigan Human Investigation Committee.

Protein Concentration. Protein concentration was assayed in duplicate using the BCA Protein Assay Kit (Pierce Chemical Co.) according to the manufacturer's instructions using bovine serum albumin as the standard (*21*).

Biotin Assay. The biotin content of the GM-CSF derivatives was determined colorimetrically using the 4-hydroxyazobenzene-2′-carboxylic acid (HABA) dye-based method of Green (*22*). In this assay, HABA bound to avidin in solution is displaced by added *d*-biotin or biotin-derivatized proteins, and the decrease in the absorption at 500 nm (absorption maxima for the avidin–HABA complex) is measured spectrophotometrically. A standard curve was created by plotting the measured change in absorbance against the final concentration of *d*-biotin added to the cuvette; sequential 2 μL-aliquots of stock *d*-biotin solutions were added. Biotin derivatized protein solutions were assayed in 20 μL-aliquots. Volumetric changes due to the addition of the biotin or biotin-derivatized GM-CSF solutions were taken into account when calculating the concentrations of biotin. The detectable range of biotin was 0.30–30.0 nmol/20-μL aliquot.

Dialysis of rhGM-CSF. The yeast-derived rhGM-CSF (Immunex) was formulated in a mannitol/sucrose/Tris buffered solution. Before any chemical reactions could be performed, the Tris buffer (a primary amine) had to be exchanged with a nonprimary amine containing buffer. This was accomplished by dialyzing 500 μg of rhGM-CSF in 1 mL of mannitol/sucrose/Tris buffer against PBS with a Microdialyzer System 500 (Pierce Chemical Co.), according to the maufacturer's instructions. Briefly, the protein solution was dialyzed in three separate aliquots at 4 °C using the bulk flow method, with complete PBS buffer exchanges every hour for the first 5 h, followed by a final 12-h dialysis. The protein recovery was 75.7% or 378 μg of rhGM-CSF.

Biotinylation of GM-CSF via Amine Groups. A fresh 12.5 mM solution of sulfo-NHS-biotin was made in PBS (7.00 mg/10.0 mL). Aliquots were added to four 1.5-mL microcentrifuge tubes containing 60 μg (3.0 nmol) of rhGM-CSF (approximate M_r = 20 kDa, including variable glycosylation) at molar ratios of 1:1, 2:1, 5:1, and 15:1 of sulfo-NHS-biotin:rhGM-CSF in a final volume of 250 μL of PBS (pH = 7.4). The reactions were incubated at 23 °C for 3 h with periodic mixing. Unincorporated sulfo-NHS-biotin was removed by dialysis against PBS using the Microdialyzer as described above. Protein and biotin concentrations for each reaction were determined for duplicate 20-μL aliquots as described above. Protein recovery exceeded 90% in all reactions.

Biotinylation of GM-CSF via Carboxyl Groups. Two 60-μg aliquots (3.0 nmol) of rhGM-CSF in PBS, were adjusted to pH = 5.0–6.0 by the addition of 25 μL of 300 mM 2-morpholinoethanesulfonic acid (MES) in PBS and placed in 1.5-mL microcentrifuge tubes. Biotin hydrazide was dissolved immediately before use, in dimethylformamide at a concentration of 80 mM (3.0 mg/100 μL), diluted 1:10 with the same solvent, and added to the tubes containing the rhGM-CSF at a 20:1 molar excess of biotin hydrazide to GM-CSF. The coupling reagent EDAC was also dissolved at 80 mM in PBS (15.3 mg/1.0 mL) and added to the biotin hydrazide/GM-CSF reaction vials at a 20:1 and 200:1 molar ratio (EDAC:GM-CSF). The reaction volumes were brought up to 250 μL with the addition of PBS; the final concentration of DMF was 10% v/v. The mixtures were incubated overnight at 23 °C with gentle shaking on a vortex apparatus. The next morning, precipitated material was removed by centrifugation for 10 min at 16 000 rpm. The supernatants were dialyzed as described above to remove the unincorporated chemical reagents, and 20-μL aliquots were assayed for protein and biotin content as before. All proteins were stored at 4 °C.

Polyacrylamide Gel Electrophoresis. Native and biotinylated GM-CSFs were analyzed by denaturing sodium dodecyl sulfate polyacrylamide gel electrophoresis (SDS-PAGE) as described previously by Laemmli (*23*). Samples of nonbiotinylated low molecular weight markers ($^1/_{20}$ dilution of stock solution from Bio-Rad), native CHO-derived GM-CSF, and biotin-derivatized GM-CSF (4.0 μg each) were boiled in sample buffer containing dithiothre-

Table I. Summary of GM-CSF Biotinylation Reactions

reaction chemisty[a]	reagent:proton ratio[b]	biotin:protein ratio final product[c]	name
sulfo-NHS-biotin	1:1	<1.0:1[d]	
sulfo-NHS-biotin	2:1	<1.0:1	
sulfo-NHS-biotin	5:1	1.2 ± 0.3:1	N^1-bGM-CSF
sulfo-NHS-biotin	15:1	3.8 ± 0.8:1	N^4-bGM-CSF
biotin hydrazide/EDAC	20:1/20:1	4.6 ± 0.3:1	C^5-bGM-CSF
biotin hydrazide/EDAC	20:1/200:1	N/A[e]	

[a] Sulfo-NHS-biotin and biotin hydrazide/EDAC are reactive with primary amine and carboxyl group containing amino acid residues, respectively. [b] The reagent:protein ratio is relative to 3.0 nmol of rhGM-CSF reacted, as described in Experimental Procedures. [c] the biotin content was determined twice for each protein sample and the ratio (nmol of biotin:nmol of protein) is presented as the average ± SEM:1. [d] A biotin:protein ratio of <1.0:1 represents a biotin content that was less than the minimum level of detection for the assay as described in Experimental Procedures. Such samples were not studied further and hence not named. [e] The protein in this reaction precipitated out of solution. See Results for a further description.

itol and loaded on a 3.5%/12% polyacrylamide stacking/running gel. The gel was run at a constant current of 20 mA for 6 h and maintained at 20 °C with a circulating water bath. The gel was stained with Coomassie Brilliant Blue R250, dried under vacuum, and photographed.

Western Blot Analysis. Western blot analysis was performed on a parallel SDS-PAGE gel containing instead a $^1/_{10}$ dilution of biotinylated low molecular weight marker stock solution and 1.5–3.0 μg of native or biotinylated GM-CSFs. Electrophoretic transfer of proteins onto Immobilon (Millipore, Bedford, MA) was performed using a Bio-Rad Transblot apparatus, as described by Towbin et al. (*24*). Briefly, the gel and Immobilon membrane (prewetted with 100% methanol) were equilibrated for 30 min in transfer buffer containing 192 mM glycine, 25 mM Tris-HCl (pH = 8.3), and 20% methanol, and the proteins transferred with a 100 mA/30 V current for 3 or 6 h at 4 °C. The blot was blocked, washed, and blotted with streptavidin-conjugated alkaline phosphatase at a 1:3000 dilution, and bands were stained with 5-bromo-4-chloro-3-indolyl phosphate and nitroblue tetrazolium (BCIP/NBT) using the Alkaline Phosphatase Conjugate Substrate Kit (Bio-Rad) according to the manufacturer's instructions.

Biological Assay of GM-CSF Activity. GM-CSF derivatives were assayed for the stimulation of bone marrow progenitor cell proliferation by the measurement of [^{3}H]thymidine incorporation into genomic DNA. Human bone marrow progenitor cells were enriched by Ficoll Hypaque gradient centrifugation, selective adherence, and negative antibody panning (*25*) and plated at 100 000 per well (96-well microtiter plate) in 50 μL of IMDM supplemented with 10% fetal bovine serum (FBS). Native and biotinylated GM-CSFs were sterilized by centrifugation through 0.22 μm cellulose acetate filters (low protein binding) using a Spin-X microcentrifuge filter insert (Costar, Cambridge, MA), and the recovered proteins were diluted with IMDM/10% FBS. One hundred percent recovery of the proteins was assumed. Plated cells were treated with vehicle or increasing concentration of native or derivatized GM-CSF at final concentrations of 1.0, 5.0, 10.0, 50.0, 100.0, 500.0, and 1000.0 pM in a final volume of 100 μL per well. The assays were run in quadruplicate for each concentration of native or biotinylated GM-CSF. Cells were placed in 5% CO_2 incubator at 37 °C for 4 days. One microcurie of [^{3}H]thymidine (20.0 Ci/mmol) in 25 μL of IMDM/10% FBS was then added per well. After a 6-h incubation at 37 °C, cells were harvested onto GF-C glass-fiber filters (Whatman, Clifton, NJ) using a Cambridge Technology PhD Harvester (Cambridge, MA), washed extensively with water and ethanol, and dried overnight, and [^{3}H]thymidine incorporation into DNA was measured by scintillation counting. Background [^{3}H]thymidine incorporation in the absence of added growth factor was subtracted from each data point (approximately 25% of maximum cpm incorporated) and the net cpm incorporated at each concentration of GM-CSF or analogue was averaged. EC_{50} values were calculated using the GraphPAD Inplot computer program (GraphPAD Software Inc, San Diego, CA).

Neutrophil Binding Assay. Human peripheral blood neutrophils were isolated from 30 mL of whole blood by sedimentation with 3% dextran in 0.9% saline and centrifugation of the upper layer over Ficoll Hypaque at 1800 rpm for 30 min at 16 °C. The pellet, containing red blood cells and neutrophils, was treated with two rounds of hypotonic lysis. Briefly, the RBCs were selectively lysed by the addition of 10.0 mL of 0.2% saline for 20 s, followed by dilution with 10.0 mL of 1.6% saline (0.9% saline final concentration), and centrifuged at 1400 rpm for 10 min and repeated. Ninety-five percent pure neutrophils were recovered. An aliquot of 1×10^6 neutrophils was incubated with 4 nM biotinylated GM-CSF derivative in the absence or presence of 200 nM native GM-CSF for 2 h at 37 °C in 250 μL of binding buffer (*3*), containing NaN_3 to prevent receptor internalization. Cells were washed twice by centrifugation in PBS and fixed in 3.5% formaldehyde/PBS for 45 min at 23 °C. Cells were washed twice again in PBS, resuspended in 250 μL of binding buffer, and labeled with 8 mg/mL fluorescein-conjugated avidin (FITC-avidin) in the presence or absence of 4000 nM biotin at 37 °C for 20 min. Cells were washed again as above, and cell surface binding was analyzed on an EPIC_C flow cytometer (Coulter Instruments, Hialeah, FL). Cell-associated fluorescence was monitored at an excitation wavelength of 488 nm, with a water-cooled argon laser at 200 mW. Analysis of GM-CSF receptor binding to a population of cells identified by forward- and right-angle light scatter properties was performed using an EPICS Easy 88 computer workstation. The percent of specific positive cells was calculated by subtracting the percent of positive cells in the presence of 50-fold molar excess of the nonbiotinylated GM-CSF from the percent of total positive cells in the absence of nonderivatized GM-CSF. Only cells with the highest granularity and size were analyzed. Autofluorescence was removed by use of a filter. For most experiments 5–10 000 events were collected.

RESULTS

Synthesis of Biotinylated GM-CSF Derivatives. Conjugation of rhGM-CSF with the amine group specific reagent sulfo-NHS-biotin was performed at four different ratios of chemical reagent to protein (see Table I). This particular biotin reagent was chosen because it was water soluble, thus allowing the reaction to be performed in an aqueous solution without organic solvents that may denature the protein, and because it has a six-carbon spacer arm between the biotin and the reactive group. Significant

incorporation of biotin (above the minimal level of detection) only occurred at the two highest ratios of reagent to protein attempted, 5:1 and 15:1. These reactions produced derivatives with 1.2 and 3.8 nmol of biotin/nmol of protein and were given the names N^1-bGM-CSF and N^4-bGM-CSF, respectively. The other reaction products were not studied further. In all cases, the product yield after dialysis was approximately 90% or greater.

The conditions for the coupling of biotin hydrazide to carboxyl-containing amino acid residues via EDAC (a carbodiimide coupling reagent) was first worked out using the protein transferrin, following previously published guidelines (*26*). These trial experiments were performed to minimize the loss of the more costly GM-CSF. Transferrin has a similar content of glutamic and aspartic acid residues as GM-CSF and was readily available in large quantities for optimization of the reaction conditions. Reactions were carried out as described in Experimental Procedures with 20, 200, and 2000:1 molar ratios of biotin hydrazide and EDAC to protein. Each reagent was varied independently. Biotin content was determined, and samples were analyzed by Western blot analysis (data not shown). It was determined that a 20:1 ratio of biotin hydrazide with a 20 or 200:1 ratio of EDAC to transferrin afforded product with a significant level of biotin incorporation and minimal amount of protein cross-linkage and precipitation. Thus these conditions were used for the coupling of biotin hydrazide to carboxyl-containing amino acid residues of GM-CSF. Long-chain biotin hydrazide was also used to provide a six-carbon spacer arm for the protein attachment. Coupling of biotin hydrazide and EDAC at equivalent 20:1 ratios to protein produced a biotinylated derivative with an incorporation of 4.6 nmol of biotin/nmol of protein (see Table I). The protein recovery after dialysis was 91% and the protein was named C^5-bGM-CSF. Coupling with EDAC at a 200:1 molar ratio instead caused significant precipitation of the protein. The precipitate was pelleted by centrifugation and the supernatant was dialyzed as described. Protein and biotin determinations on the dialyzed supernatant and pellet were performed. Only 15% of the initial protein was found in the supernatant; the remainder was in the pellet, most likely in a cross-linked form (data not shown). Though the supernatant contained some biotinylated GM-CSF, there was not enough present for all of the remaining assays and hence it was not studied further.

The determination of biotin content by the HABA dye binding assay required that the biotin moiety be accessible to avidin in solution. Both biotin reagents used had a six-carbon spacer arm inserted between the biotin molecule and the reactive group, to allow for maximal interaction. Therefore, the biotin content determined for each derivative may underestimate the level of biotin incorporation, since not all biotin moieties present on the protein may be able to bind avidin in solution due to steric hindrance around the molecule. It was also possible that the biotin measured in the dialyzed, final product was the biotin reagent and not protein-conjugated biotin. To test for this possibility, 60 nmol of biotin hydrazide and sulfo-NHS-biotin in 250 μL of their appropriate reaction buffers were dialyzed in parallel with the protein reactions. Twenty-microliter aliquots were assayed for biotin as described, and the amount of biotin reagent remaining after dialysis was beneath the limit of detection (<0.30 nmol/20 μL, data not shown). Hence, we believe that the biotin content determined for each derivative represents the actual amount of biotin conjugated to protein.

SDS–PAGE and Western Blot Analysis. The biotinylated GM-CSF derivatives migrated as single broad bands on SDS–PAGE at approximately 20 kDa (Figure 1, lanes 2–4). The molecular weight of the proteins was in good agreement with the manufacturer's specifications (Immunex). The conjugates were coelectrophoresed with a sample of CHO cell derived rhGM-CSF (Genetics Institute, lane 1), which migrated as a more diffuse band of 25–32 kDa due to differential glycosylation (*27*). This alternately produced rhGM-CSF was analyzed by SDS–PAGE since we had utilized all of the yeast-derived protein for the various synthetic reactions and because future characterization of biological activity and receptor binding of the derivatives would be made using this protein as the control. The purity of all protein samples was estimated to be >95%. The faster rate of migration of C^5-bGM-CSF when compared to N^1- and N^4-bGM-CSFs may be due to changes in the protein structure upon addition of the biotin moieties to the carboxyl groups. Also, the band appeared to be spread across a slighter larger range of molecular weights, suggesting that the derivatization of the protein may not be uniform, in contrast to the N^1- and N^4-bGM-CSFs, which migrated as sharper bands.

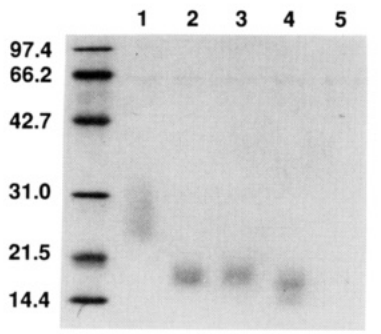


Figure 1. SDS–PAGE of native and biotinylated GM-CSF proteins run under reducing conditions and visualized with Coomassie Blue R250 staining. A 4.0-μg sample of recombinant human GM-CSF or biotinylated analogue was run per lane: lane 1, native GM-CSF (Genetics Institute, CHO cell derived); lane 2, N^1-bGM-CSF; lane 3, N^4-bGM-CSF; lane 4, C^5-bGM-CSF; lane 5, SDS–PAGE sample buffer control. Relative positions of coelectrophoresed low molecular weight markers (Bio-Rad), in kilodaltons, are shown at the far left. The protein band at approximately 66 kDa is an artifact of the SDS–PAGE sample buffer, as it is also present in the control lane (lane 5). The artifact is most likely due to the presence of dithiothreitol used as a reducing agent, since substitution with β-mercaptoethanol removed the band (data not shown).

To verify that the derivatized GM-CSFs actually were conjugated to biotin, polyacrylamide gels containing the proteins were transferred to Immobilon membrane and the proteins detected by blotting with alkaline phosphatase conjugated streptavidin and staining with BCIP/NBT. In Figure 2A, it is evident that the proteins in lanes 2–4 contain biotin and that these bands comigrated with the 20-kDa proteins stained with Coomassie Blue R250 (Figure 1). Native GM-CSF (lane 1) and the control buffer lane (lane 5) did not stain, as expected. The higher molecular weight of N^4-bGM-CSF (lane 3) relative to N^1-bGM-CSF (Lane 2) due to the addition of 2 or 3 more biotin moieties is evident. Each conjugated biotin with its six-carbon spacer arm added 355 Da to the molecular weight. Two other bands are clearly present in lanes 2 and 3 at approximately 40 and 65 kDa. The relative amounts of each protein were less than 5% of the total protein in the lane and they were not visible on the Coomassie stained gel. The 65-kDa protein is most likely human serum albumin that was added to the rhGM-CSF formulation and subsequently biotinylated, while the 40-kDa band may represent dimerization of the biotin-conjugated GM-CSFs.

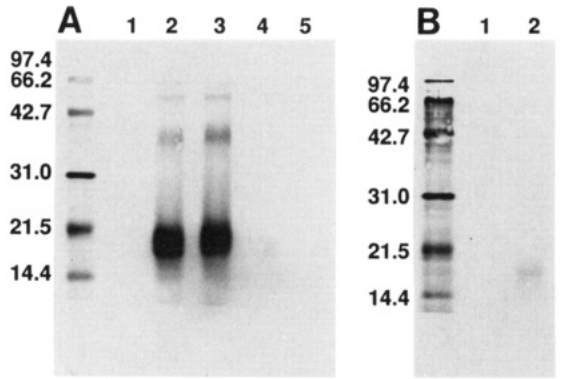


Figure 2. Western blot analysis of biotinylated GM-CSF analogues. Protein samples were run under reducing conditions in 12% polyacrylamide gels and transferred to Immobilon membrane by electroblot transfer for either (A) 3 h or (B) 6 h. Biotinylated proteins were detected with streptavidin-conjugated alkaline phosphatase and BCIP/NBT staining as described in Experimental Procedures. A: lane 1, native GM-CSF (Genetics Institute, CHO cell derived); lane 2, N^1-bGM-CSF; lane 3, N^4-bGM-CSF; lane 4, C^5-bGM-CSF; lane 5, SDS-PAGE sample buffer control. B: lane 1 as in A; lane 2, C^5-bGM-CSF. Relative positions of coelectrophoresed biotinylated low molecular weight markers (Bio-Rad), in kilodaltons, are shown at the far left of each blot. A 1.5-μg sample of each protein was loaded per lane except for C^5-bGM-CSF, where 3.0 μg was loaded. Blots A and B were stained for 50 and 120 min, respectively.

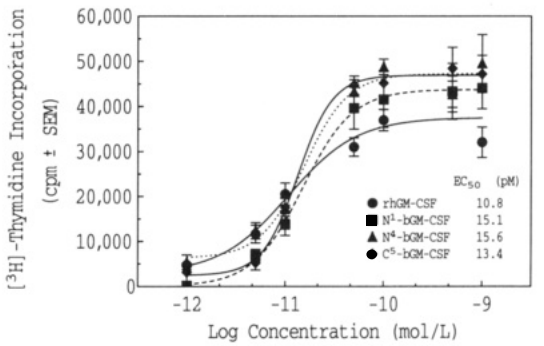


Figure 3. Stimulation of [^{3}H]thymidine incorporation into replicating DNA of enriched bone marrow progenitor cells by native GM-CSF (Genetics Institute) and biotinylated GM-CSF derivatives. 1×10^5 cells were plated per well in a 96-well microtiter plate in medium supplemented with increasing concentration of colony-stimulating factor. After 4 days of growth, cells were pulse-labeled for 6 h with 1 μCi [^{3}H]thymidine, and radioactive DNA was isolated onto glass-fiber filters with a cell harvester and counted in scintillation fluid. [^{3}H]Thymidine incorporation in the absence of added colony stimulating factor (12 292 ± 340 cpm) was subtracted from each data point. Each point represents the mean of four determinations ± standard error of the mean as described in Experimental Procedures. The EC_{50} values were calculated using the GraphPAD Inplot computer program.

The amino-derivatized analogues stained quite nicely after 50 min of exposure to substrate, but the carboxyl-derivatized analogue (lane 4) did not. It was noted that C^5-bGM-CSF did not transfer as well as either N^1- or N^4-bGM-CSF to either nitrocellulose or Immobilon membranes (data not shown). Thus this sample was run on a polyacrylamide gel again, but transferred to Immobilon for 6 h instead of 3 h and stained with substrate for 120 min instead of 50 min (Figure 2B). The biotin-derivatized protein is more apparent in this blot (lane 2). The loss of negatively charged residues in C^5-bGM-CSF would likely decrease its rate of transfer from the polyacrylamide gel to the Immobilon, thus accounting for the light staining of the band. Notice that the 40- and 65-kD bands present in Figure 2A (lane 2 and 3) are not present in either blot (Figure 2A, lane 4, and Figure 2B, lane 2), even with the increased substrate incubation time, suggesting that a possible incomplete transfer of the carboxy-modified proteins may have occurred. The lower intensity of the GM-CSF band relative to the other conjugates may also reflect a decreased accessibility of biotin to the streptavidin probe, when conjugated to GM-CSF with this linkage chemistry.

Effect of Biotinylation on Biological Activity. The biotin-conjugated GM-CSF derivatives were tested along with native GM-CSF (CHO cell derived) for biological activity in a bone marrow progenitor cell growth assay (Figure 3). GM-CSF added to enriched bone marrow cells causes the proliferation of the myeloid stem and progenitor cells which was detected by measuring DNA synthesis with a radioactive tracer. All three biotinylated GM-CSFs retained full biological activity when compared to native GM-CSF, with EC_{50} values of 10.8, 15.1, 15.6, and 13.4 pM for native GM-CSF, N^1-, N^4-, and C^5-bGM-CSF, respectively. All protein stimulated similar maximum levels of [^{3}H]thymidine incorporation. Thus it appears that derivatization of GM-CSF at amine or carboxyl residues did not effect biological activity.

Flow Cytometric Analysis of GM-CSF Receptors. Peripheral blood neutrophils possess approximately 80–500 high affinity binding sites (K_d of 17–51 pM) on their cell surface (*4*, *5*). This low level of high-affinity receptors is similar to that seen on many other myeloid-derived cells and cell lines (*3*–*5*), thus making neutrophils a good model cell system with which to study cell surface binding of GM-CSF. GM-CSF receptors were detected by binding the biotinylated derivatives to freshly purified neutrophils at saturating concentrations (4 nM) as described by Park et al. (*3*). Bound biotin-conjugated GM-CSF was detected by subsequent binding of FITC-avidin and separation of fluorescent cells by flow cytometric analysis. Figure 4A–C depicts the fluorescent profiles of the specific binding of the derivatives N^1-bGM-CSF, N^4-bGM-CSF, and C^5-bGM-CSF, respectively. Binding was done in the absence (profile I) and presence of 50-fold molar excess of native GM-CSF (profile II). Profile III depicts the nonspecific binding of FITC–avidin to neutrophils (bound biotinylated protein detected with FITC–avidin in the presence of a 1000-fold molar excess of *d*-biotin).

The results, comparing profile I to III, show that the binding of N^1-bGM-CSF (A) caused a 5–10-fold shift to increasing fluorescence intensities of stained cells and that the binding of C^5-bGM-CSF (C) exhibited no such rightward shift. The majority of the N^1-bGM-CSF staining could be competitively inhibited by excess native, non-biotinylated GM-CSF (profile II). The incomplete reversal of this fluorescence shift has been seen in other such experiments using biotinylated proteins coupled with FITC–avidin detection (*14*, *17*). The proportion of cells in Figure 4A that demonstrate specific fluorescent staining is approximately 10%, but the noticeable shift of the complete curve and retention of the skewed Gaussian distribution suggest that all cells are in fact staining. The low proportion of specific staining and the shape of the fluorescence profile may reflect heterogeneity of the number of GM-CSF receptors on the surface of individual cells. Binding of N^4-bGM-CSF under similar conditions (B) also demonstrated specific fluorescent staining, but with a smaller rightward shift of profile I. This data suggests that increasing amine derivatization of GM-CSF, while retaining full biological activity, may possibly alter the equilibrium binding conditions for the receptor. The inability to detect the bound C^5-bGM-CSF, when it was shown to possess full biological activity, suggests that the

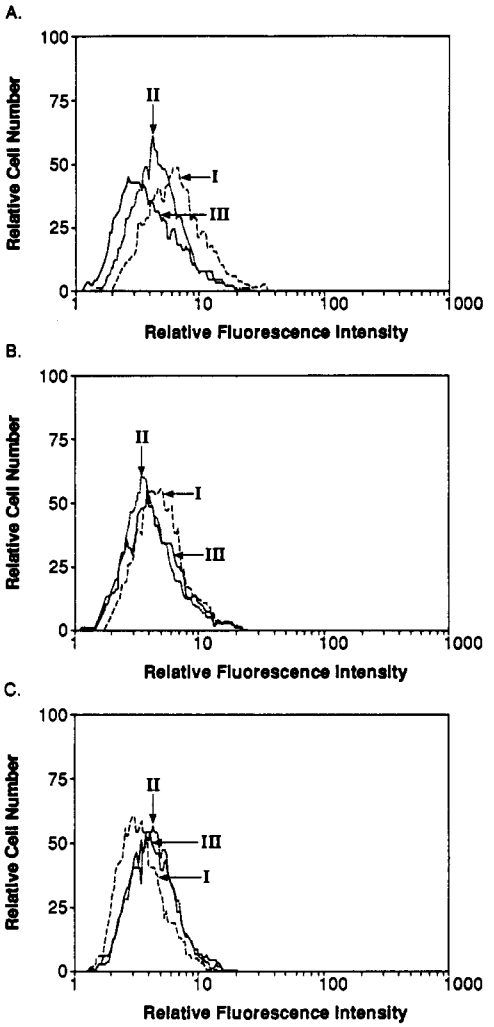


Figure 4. Flow cytometric analysis of human neutrophils stained with saturating concentrations (4 nM) of N^1-bGM-CSF (A), N^4-bGM-CSF (B), or C^5-bGM-CSF (C): (I) bGM-CSF bound alone followed by FITC–avidin (8 μg/mL); (II) bGM-CSF coincubated with a 50-fold excess of native GM-CSF followed by FITC–avidin; (III) bGM-CSF followed by FITC–avidin with a 1000-fold excess of *d*-biotin. Staining of neutrophils alone with FITC–avidin produced a fluorescence profile which was superimposable with curve III (data not shown). Relative fluorescence intensity and relative cell number are in arbitrary units.

biotin moieties conjugated to the carboxyl groups are either not accessible to FITC–avidin, when bound to the receptor, or the protein is not uniformly labeled with biotin and the biotin-conjugated fractions is too small to be detected by this method.

DISCUSSION

Chemical modification of proteins is a powerful technique for elucidating the function of a protein from its structure. By modifying the protein with various molecular "tags" (e.g. ^{125}I, a cross-linking reagent, or biotin), one can create new tools with which to study protein–protein interactions. We have synthesized three analogues of GM-CSF biotinylated at amine- and carboxyl-containing amino acid residues and have demonstrated their utility as receptor probes. All three derivatives retained full biological activity as assessed by their ability to stimulate bone marrow progenitor cell growth with concentration–response relationships similar to native GM-CSF. However, the different biotin conjugation chemistries utilized in the synthetic reactions differentially affected the ability of fluorescein-conjugated avidin and flow cytometry to detect cell surface receptor binding on neutrophils.

Derivatization of rhGM-CSF at lysyl residues (or possibly the N-terminal amino group) by sulfo-NHS-biotin, followed by dialysis to remove unincorporated reagent, proved to be a relatively simple method with which to biotinylate the protein. By varying the ratio of reagent to protein, derivatives with increasing numbers of biotin molecules conjugated per molecule of GM-CSF were synthesized. The two amino derivatized GM-CSF analogues characterized in this report had 1.2 and 3.8 nmol of biotin/nmol of protein (N^1-bGM-CSF and N^4-bGM-CSF, respectively) and were produced using a 5:1 and 15:1 ratio of reagent to protein, respectively. The total number of primary amine containing amino acid residues in rhGM-CSF is seven, six lysine residues and the N-terminal alanine residue of the mature protein (*2*), and thus the upper limit of biotin conjugation probably would be approached at much higher biotin ratios. At lower ratios than 5:1, the product had less than one molecule of biotin per protein. Direct evidence for the conjugation of biotin to the protein was provided by the Western blot analysis (Figure 2A). Though the blot was purposely overstained to detect the existence of the potential dimeric products at 40 kDa, both proteins stained with roughly similar intensities. Most likely, not all of the biotin moieties attached to N^4-bGM-CSF were available for binding to the streptavidin probe, hence it stained with similar intensity as N^1-bGM-CSF. Thus the higher ratio of biotin to protein in the final product may not prove to be advantageous for use as a receptor probe.

The carboxyl-conjugate C^5-bGM-CSF was obtained by reacting GM-CSF with biotin hydrazide and EDAC (a carbodiimide coupling reagent) at equal 20:1 ratios of reagent to protein, resulting in the incorporation of approximately five biotin molecules per molecule of protein. This level of derivatization is low relative to the total number of carboxyl-containing amino acid residues found in the mature protein (13 glutamic acids, four aspartic acids, and the α-carboxyl group of the C-terminal glutamic acid residue). The use of higher ratios of the coupling reagent caused the precipitation of the protein presumably due to cross-linkage. Interestingly, the C^5-bGM-CSF analogue stained poorly on Western blots compared to the amine conjugates (Figure 2A,B). The biotin content determination (Table I) was performed on the final dialyzed product in parallel with dialyzed control biotin solutions, to rule out possible carry over of the biotin reagent in the analysis. One possible explanation for the high level of biotin incorporation in the protein with poor Western blot staining would be the loss of negative charges on GM-CSF by biotinylation at carboxyl residues, which would decrease the rate of transfer of the protein to the membrane during the electroblot procedure. Another potential contributing factor could be the difference between avidin, used for the biotin determination, and streptavidin, used for the blot. The biotin binding site on avidin is located approximately 9 Å beneath the surface of the molecule while the streptavidin biotin binding site is located deep within a β-barrel (*9*, *28*); thus the probes may differ in their ability to interact with the biotin conjugated on C^5-bGM-CSF. All derivatives synthesized had a six-carbon spacer arm between the biotin moiety and the protein. No conjugates were synthesized with a shorter or longer spacer, but incorporation of more carbon residues most likely would have enhanced, not decreased, detection of the biotinylated GM-CSF after receptor binding, by decreasing steric hindrance.

All of the chemical modifications made to rhGM-CSF did not affect its biological activity, as seen in Figure 3.

The three derivatives had similar EC_{50} values, and thus specific activities, and similar intrinsic activities as native GM-CSF. Unlike erythropoietin and β-nerve growth factor (*19*, *20*), amine derivatization does not inactivate this protein. This finding has been demonstrated before when it was shown that similar chemical modification of amine groups of GM-CSF with the ^{125}I-labeled Bolton–Hunter reagent also retained full biological activity (*5*). This suggests that the modified lysine or N-terminal alanine residues are not necessary for receptor binding or biological activity. But like β-nerve growth factor, carbodiimide coupling of GM-CSF at carboxyl-containing amino acids also did not affect biological activity (*19*).

Detection of the cell surface binding of the biotinylated GM-CSF molecules to neutrophils by FITC–avidin resulted in an adequately strong fluorescence signal despite the low receptor numbers on these cells (*3–5*). The extent of detection with this protocol differed though, depending upon the nature and extent of the chemical modification. Both N^1- and N^4-bGM-CSF could be detected after binding to the receptor, while the C^5-bGM-CSF analogue was not observable. This result suggests that the biotin moieties attached via amine-containing residues are free of the active site of GM-CSF and far enough away to allow access to the avidin probe. It was noticed that the binding of the N^4-bGM-CSF did not produce as intense a FITC–avidin staining of the cell population as the monoderivatized analogue. It is doubtful that the presence of more biotin moieties on the protein could somehow interfere with the ability of FITC–avidin to bind, since steric hindrance would limit the attachment of only one or possibly two FITC–avidin molecules to the biotinylated GM-CSF after binding to its receptor. Each biotin molecule can bind only one molecule of FITC–avidin. The initial binding of the ligand was done at equilibrium at 37 °C as determined for ^{125}I-labeled GM-CSF (*3*), but these conditions may not apply for the biotinylated GM-CSFs and hence account for the decreased fluorescence profile shift of N^4-bGM-CSF seen in Figure 4B. The inability of FITC–avidin to detect C^5-bGM-CSF bound to the cell surface receptor could have also occurred due to a change in the equilibrium binding conditions, although the inaccessibility of the conjugated biotins may be a possible explanation as reflected in the Western blots. Though these biotin molecules did not interfere with activity, they may be near the active site of GM-CSF so that after receptor binding they are inaccessible to FITC–avidin. The use of a preformed $N^{1,4}$-/C^5-bGM-CSF/FITC–avidin complex for the binding may enhance the detection of receptor binding as was seen for biotinylated interleukin-1β (*17*).

rhGM-CSF could be modified directly with fluorescein at amine residues using the same reaction chemistry and conditions as described above using fluorescein–NHS. A low level of incorporation would probably produce a conjugate with similar chemical and biological properties as N^1-bGM-CSF. One disadvantage of using this conjugate over N^1-bGM-CSF/FITC–avidin to detect receptor expression is that the fluorescence may be quenched by neighboring group effects of the growth factor or receptor. Second, since the FITC–avidin has a 4:1 ratio of fluorescein to protein, it amplifies the fluorescence signal and further enhances the detection of low level receptor expression.

The poor Western blot staining, full biological activity, and lack of fluorescein-conjugated avidin detected cell surface receptor binding seen for the C^5-bGM-CSF derivative could be explained by nonuniform labeling of the protein during its synthesis. A preparation of carboxy-modified protein that contained a large amount of slightly biotinylated GM-CSF and a small percentage of highly modified GM-CSF could exhibit full biological activity, yet not stain with fluorescein-conjugated avidin. The poor Western blot of the analogue most likely would be due to the poor transfer of the carboxy-derivatized protein from the gel to the membrane, as described earlier. Analysis of the percent of final GM-CSF product that was biotinylated by binding to avidin agarose for instance, would not determine the uniformity of the label but only the extent of the labeling reaction. Due to the small amounts of derivatized proteins synthesized, this assay was not performed. Though the same arguments concerning the extent of the biotinylation reactions hold true for the amino derivatized GM-CSF analogues, their intense Western blot staining, full biological activity, and cell surface binding suggest that their reaction conditions produce a more uniformly labeled product.

On the basis of these findings, a few general comments can be made concerning the interaction of GM-CSF with its receptor. Two recent papers using independent methods have localized a region of the GM-CSF protein necessary for binding to its receptor and hence activity. By producing murine-human hybrid GM-CSF proteins with spliced cDNA constructs, Kaushansky et al. delineated two potential α-helical regions important for human GM-CSF receptor binding (amino acids 21–31 and 78–94 of the mature protein) (*29*). Kanakura et al. used neutralization of GM-CSF with monoclonal antibodies coupled with synthetic peptide mapping of the antibody binding sites to identify the second potential α-helix as being important for GM-CSF receptor binding, along with amino acid residues 40–77 and 110–127 (*30*). If these regions are important for receptor binding, then they are likely to be found on the outside of the molecule and this positioning would tend to make them also available for modification by chemical reagents. Though the exact location of biotin on the amine-derivatized analogues is not known, it seems unlikely that it occurred at Lys^{85} since this would place it in the middle of the second α-helix delineated by Kaushansky et al. Alternatively, if it did occur at this residue, then it must not be necessary for receptor binding. Also, the locations of four of the remaining five lysyl residues of the mature protein occur in the regions of amino acids 40–77 and 110–127 (Lys^{53}, Lys^{62}, Lys^{64}, and Lys^{111}), suggesting that either these sites are less important than the amino acid region 78–94 for receptor binding or the actual active portion of these sites is smaller. Since cells bound with N^1-bGM-CSF or N^4-bGM-CSF can be detected by the subsequent binding of FITC–avidin, these biotin-modified residues must not lie at the interface of the ligand and receptor, again suggesting that the lysyl residues found outside of the described α-helix most likely do not lie within the actual receptor binding site. The carboxyl-modified analogue, C^5-bGM-CSF, had full activity, yet it could not be detected when bound to the cell surface GM-CSF receptor by FITC–avidin. If this analogue is uniformly conjugated with a high ratio of biotin to protein, these results would suggest that these modified residues may lie either near but not at the interface of ligand and receptor or within the folded GM-CSF molecule and that they are inaccessible to FITC–avidin while bound to the receptor, but not when they are in solution as during the biotin/HABA assay.

Previous work characterizing the GM-CSF receptor has relied upon the radioiodination of the protein at tyrosine residues to produce a tool with which to study receptor kinetics and modulation. In some reports, this modification reduced the biological activity of the protein (*3*).

Preparation of fully active radioiodinated GM-CSF is possible (*4*, *5*), but the resultant protein is biologically unstable due to autolysis from the high levels of γ-emitting isotope in the preparation. It also has a short radioactive half-life relative to β-emitters such as ^{3}H and ^{14}C, which are more commonly employed for receptor binding assays. The reported development of N^{1}-bGM-CSF as an alternative ligand is advantageous for several reasons. First, this ligand possesses high biological activity when compared to the native protein. Second, the ligand is biologically stable for at least 1 month when stored at 4 °C and probably longer when stored at −20 °C. Third, the biotin-conjugate linkage to GM-CSF is chemically stable and will not cause radioautolysis of the protein, as ^{125}I labeling does. Fourth, this low-level linkage of biotin to GM-CSF through amine-containing residues allows for specific receptor binding, as assessed by its displacement by a 50-fold excess of unmodified GM-CSF. Finally, numerous covalently modified streptavidin and avidin probes for detection of biotin-labeled proteins are presently available, each with its own particular utility in the study of receptor biochemistry and physiology (*31*). For example, ultrastructural studies of the mechanism of receptor internalization and the intracellular fate of internalized interleukin-2 have been performed with the use of colloidal-gold-conjugated streptavidin and biotinylated interleukin-2 (*11*). Also, biotin-conjugated insulin, erythropoietin, and interleukin-2 have been used to partially purify their respective receptors without the need for chemical cross-linking of the ligand to the receptor (*12*, *13*, *32*). Cell surface binding of biotinylated ligands to their respective receptors coupled with detection by fluoroscein-conjugated avidin or streptavidin has made it possible to study receptor modulation on single cell populations by flow cytometry and to fractionate receptor bearing cells from nonreceptor bearing cells (*14–17*). We have already shown that N^{1}-bGM-CSF can be used to identify receptor-bearing cells with FITC–avidin and flow cytometry and we anticipate that it will be a useful, nonradiative tool with which to study many questions concerning GM-CSF receptor structure and function.

ACKNOWLEDGMENT

T.P.A. is a recipient of a Pharmaceutical Manufacturers Association Foundation Predoctoral Fellowship. This work was supported by National Institutes of Health Grant CA-46657 (M.F.C. and S.G.E). We wish to thank Clair Rogers for performing the flow cytometric analyses and Mark Gerhardt for assistance with the GraphPAD and flow cytometry plots.

LITERATURE CITED

(1) Gasson, J. (1990) Molecular physiology of granulocyte-macrophage colony-stimulating factor. *Blood 77*, 1131–1145.

(2) Wong, G. G., Witek, J. S., Temple, P. A., Wilkens, K. M., Leary, A. C., Luxenberg, D. P., Jones, S. S., Brown, E. L., Kay, R. M., Orr, E. C., Shoemaker, C., Golde, D. W., Kaufman, R. J., Hewick, R. M., Wang, E. A., and Clark, S. C. (1985) Human GM-CSF: Molecular cloning of the complementary DNA and purification of the natural and recombinant proteins. *Science 228*, 810–815.

(3) Park, L. S., Friend, D., Gillis, S., and Urdal, D. (1986) Characterization of the cell surface receptor for human granulocyte/macrophage colony-stimulating factor. *J. Exp. Med. 164*, 251–262.

(4) Gasson, J. C., Kaufman, S. E., Weisbart, R. H., Tomonaga, M., and Golde, G. W. (1986) High-affinity binding of granulocyte-macrophage colony-stimulating factor to normal and leukemic human myeloid cells. *Proc. Natl. Acad. Sci. U.S.A. 83*, 669–673.

(5) DiPersio, J., Billing, P., Kaufman, S., Eghtesady, P., Williams, R. E., and Gasson, J. C. (1988) Characterization of the human granulocyte-macrophage colony-stimulating factor receptor. *J. Biol. Chem. 263*, 1834–1841.

(6) Hayashida, K., Kitamura, T., Gorman, D. M., Arai, K. I., Yokota, T., and Miyajima, A. (1990) Molecular cloning of a second subunit of the receptor for human granulocyte macrophage colony-stimulating factor (GM-CSF)—Reconstitution of a high-affinity GM-CSF receptor. *Proc. Natl. Acad. Sci. U.S.A. 87*, 9655–9659.

(7) Gearing, D. P., King, J. A., Gough, N. M., and Nicola, N. A. (1989) Expression cloning of a receptor for human granulocyte-macrophage colony-stimulating factor. *EMBO J. 8*, 3667–3676.

(8) DiPersio, J. F., Hedvat, C., Ford, C. F., Golde, D. W., and Gasson, J. C. (1991) Characterization of the soluble human granulocyte-macrophage colony-stimulating factor receptor complex. *J. Biol. Chem. 266*, 279–286.

(9) Green, N. M. (1975) Avidin. *Advances in Protein Chemistry* (C. B. Anfinsen, J. T. Edsall, and F. M. Richards, Eds.) pp 85–133, Academic Press, New York.

(10) Chalet, L., and Wolf, K. J. (1964) The properties of streptavidin, a biotin-binding protein produced by *Streptomyces*. *Arch. Biochem. Biophys. 106*, 1–5.

(11) Peters, D. K., and Norback, D. H. (1990) Binding and internalization of biotinylated interleukin-2 in human lymphocytes. *Blood 76*, 96–104.

(12) Wognum, A. W., Lansdorp, P. M., Humphries, R. K., and Krystal, G. (1990) Detection and isolation of the erythropoietin receptor using biotinylated erythropoietin. *Blood 76*, 697–705.

(13) Foxwell, B. M. J., Taylor, D., Greiner, B., Mihatsch, M. J., Olivieri, V., and Ryffel, B. (1988) Biotinylated recombinant interleukin-2. *J. Immunol. Methods 113*, 221–229.

(14) Newman, W., Beall, L. D., Levine, M. A., Cone, J. L., Randhawa, Z. I., and Bertolini, D. R. (1989) Biotinylated parathyroid hormone as a probe for the parathyroid hormone receptor. *J. Biol. Chem. 264*, 16359–16366.

(15) Abou-Samra, A. B., Freeman, M., Jüppner, H., Uneno, S., and Segre, G. V. (1990) Characterization of fully active biotinylated parathyroid hormone analogs. *J. Biol. Chem. 265*, 58–62.

(16) Newman, W., Beall, L. D., Bertolini, D. R., and Cone, J. L. (1989) Modulation of TGF-β type 1 receptor: Flow cytometric detection with biotinylated TGF-β. *J. Cell Physiol. 141*, 170–180.

(17) Chollet, A., Bonefoy, J. Y., and Odermatt, N. (1990) Preparation, application and biological characterization of interleukin-1β mutant protein biotinylated at a single site. *J. Immunol. Methods 127*, 179–185.

(18) Billingsley, M. L., Pennypacker, K. R., Hoover, C. G., and Kincaid, R. L. (1987) Biotinylated proteins as probes of protein structure and protein–protein interactions. *Biotechniques 5*, 22–31.

(19) Rosenberg, M. B., Hawrot, E., and Breakefield, X. O. (1986) Receptor binding activities of biotinylated derivatives of β-Nerve Growth Factor. *J. Neurochem. 46*, 641–648.

(20) Wojchowski, D. M., and Caslake, L. (1989) Biotinylated recombinant human erythropoietins: Bioactivity and utility as receptor ligand. *Blood 74*, 952–958.

(21) Smith, P. K., Krohn, R. I., Hermanson, G. T., Mallia, A. K., Gartner, F. H., Provenzano, M. D., Fujimoto, E. K., Goeke, N. M., Olson, B. J., and Klenk, D. C. (1985) Measurement of protein using bicinchoninic acid. *Anal. Biochem. 150*, 76–85.

(22) Green, N. M. (1970) Spectrophotometric determination of avidin and biotin. *Methods Enzymol. 18A*, 418–424.

(23) Laemmli, U. K. (1970) Cleavage of structural proteins during the assembly of the head of bacteriophage T4. *Nature 227*, 680–685.

(24) Towbin, H., Staehelin, T., and Gordon, J. (1979) Electrophoretic transfer of proteins from polyacrylamide gels to nitrocellulose sheets: procedure and some applications. *Proc. Natl. Acad. Sci. U.S.A. 76*, 4350–4354.

(25) Sieff, C. A., Emerson, S. G., Mufson, A., Gesner, T. G., and Nathan, D. G. (1986) Dependence of highly enriched human

bone marrow progenitors on hemopoietic growth factors and their response to recombinant erythropoietin. *J. Clin. Invest. 77*, 74–81.

(26) Yamada, H., Imoto, T., Fujita, K., Okazaki, K., and Motomura, M. (1981) Selective modification of aspartic acid-101 in lysozyme by carbodiimide reaction. *Biochemistry 20*, 4836–4842.

(27) Cebon, J., Nicola, N., Ward, M., Gardner, I., Dempsey, P., Layton, J., Dührsen, U., Burgess, A. W., Nice, E., and Morstyn, G. (1990) Granulocyte-macrophage colony-stimulating factor from human lymphocytes: The effect of glycosylation on receptor binding and biological activity. *J. Biol. Chem. 265*, 4483–4491.

(28) Weber, P. C., Ohlendorf, D. H., Wendoloski, J. J., and Saleme, F. R. (1989) Structural origins of high-affinity biotin binding to streptavidin. *Science 243*, 85–88.

(29) Kaushansky, K., Shoemaker, S. G., Alfaro, S., and Brown, C. (1989) Hematopoietic activity of granulocyte/macrophage colony-stimulating factor is dependent upon two distinct regions of the molecule: Functional analysis based upon the activities of interspecies hybrid growth factors. *Proc. Natl. Acad. Sci. U.S.A. 86*, 1213–1217.

(30) Kanakura, Y., Cannistra, S. A., Brown, C. B., Nakamura, M., Seelig, G. F., Prosise, W. W., Hawkins, J. C., Kaushansky, K., and Griffin, J. D. (1991) Identification of functionally distinct domains of human granulocyte-macrophage colony-stimulating factor using monoclonal antibodies. *Blood 77*, 1033–1043.

(31) Wilchek, M., and Bayer, E. A., Eds. (1990) Avidin-Biotin Technology. *Methods in Enzymology*, Vol. 184, Academic Press, Inc., New York.

(32) Finn, F. M., Titus, G., Horstman, D., and Hofmann, K. (1984) Avidin–biotin affinity chromatography: application to the isolation of human placental insulin receptor. *Proc. Natl. Acad. Sci. U.S.A. 81*, 7328–7332.

Registry No. GM-CSF, 83869-56-1.